Contents

Natural Resources Canada
Ressources naturelles Canada

Geological Survey of Canada
Bulletin 608

Geological synthesis of Baffin Island (Nunavut) and the Labrador–Baffin Seaway

Edited by
L.T. Dafoe and N. Bingham-Koslowski

2022

Canada

Geological Survey of Canada
Bulletin 608

Geological synthesis of Baffin Island (Nunavut) and the Labrador–Baffin Seaway

Edited by
L.T. Dafoe and N. Bingham-Koslowski

2022

© Her Majesty the Queen in Right of Canada, as represented by the Minister of Natural Resources, 2022

ISSN 2560-7219
ISBN 978-0-660-30386-4
Catalogue No. M42-608E-PDF
Permanent link: https://doi.org/10.4095/314542

A copy of this publication is also available for reference in depository libraries across Canada through access to the Depository Services Program's Web site at http://dsp-psd.pwgsc.gc.ca.

This publication is available for free download through GEOSCAN (https://geoscan.nrcan.gc.ca).

Recommended citation

Dafoe, L.T. and Bingham-Koslowski, N. (ed.), 2022. Geological synthesis of Baffin Island (Nunavut) and the Labrador–Baffin Seaway; Geological Survey of Canada, Bulletin 608, 2 .zip files. https://doi.org/10.4095/314542

Cover illustration
View of Southwind Fiord, Nunavut from the deck of the *CCGS Hudson*. Photograph by A. Normandeau. NRCan photo 2022-182

Editors

L.T. Dafoe (lynn.dafoe@nrcan-rncan.gc.ca)
Geological Survey of Canada
1 Challenger Drive
P.O. Box 1006
Dartmouth, Nova Scotia
B2Y 4A2

N. Bingham-Koslowski (nikole.bingham-koslowski@nrcan-rncan.gc.ca)
Geological Survey of Canada
601 Booth Street
Ottawa, Ontario
K1A 0E8

Correction date:

Information contained in this publication or product may be reproduced, in part or in whole, and by any means, for personal or public non-commercial purposes, without charge or further permission, unless otherwise specified.

You are asked to:
- exercise due diligence in ensuring the accuracy of the materials reproduced;
- indicate the complete title of the materials reproduced, and the name of the author organization; and
- indicate that the reproduction is a copy of an official work that is published by Natural Resources Canada (NRCan) and that the reproduction has not been produced in affiliation with, or with the endorsement of, NRCan.

Commercial reproduction and distribution is prohibited except with written permission from NRCan. For more information, contact NRCan at copyright-droitdauteur@nrcan-rncan.gc.ca.

CONTENTS

Introduction and summary

N. Bingham-Koslowski[1*], L.T. Dafoe[2], M.R. St-Onge[1], E.C. Turner[3], J.W. Haggart[4], U. Gregersen[5], C.E. Keen[2], A.L. Bent[6], and J.C. Harrison[1]

Bingham-Koslowski, N., Dafoe, L.T., St-Onge, M.R., Turner, E.C., Haggart, J.W., Gregersen, U., Keen, C.E., Bent, A.L., and Harrison, J.C., 2022. Introduction and summary; in *Geological synthesis of Baffin Island (Nunavut) and the Labrador–Baffin Seaway, (ed.) L.T. Dafoe and N. Bingham-Koslowski; Geological Survey of Canada, Bulletin 608, p. 1–11. https://doi.org/10.4095/321823*

Abstract: The papers contained in this bulletin provide a comprehensive summary and updated understanding of the onshore geology and evolution of Baffin Island, the Labrador–Baffin Seaway, and surrounding onshore regions. This introductory paper summarizes and links the geological and tectonic events that took place to develop the craton and subsequent Proterozoic to Cenozoic sedimentary basins. Specifically, the Precambrian and Paleozoic geology of Baffin Island and localized occurrences underlying the adjacent Labrador–Baffin Seaway, the Mesozoic to Cenozoic stratigraphy and rift history that records the opening and evolution of the Labrador–Baffin Seaway, the seismicity of the region, as well as both the mineral (Baffin Island) and hydrocarbon (onshore and offshore) resource potential are discussed.

[1]Geological Survey of Canada, 601 Booth Street, Ottawa, Ontario K1A 0E8
[2]Geological Survey of Canada, 1 Challenger Drive, P.O. Box 1006, Dartmouth, Nova Scotia B2Y 4A2
[3]Harquail School of Earth Sciences, Laurentian University, Sudbury, Ontario P3E 2C6
[4]Geological Survey of Canada, 1500-605 Robson Street, Vancouver, British Columbia V6B 5J3
[5]Geological Survey of Denmark and Greenland (GEUS), Øster Voldgade 10, DK-1350, Copenhagen K, Denmark
[6]Canadian Hazards Information Service, 930 Carling Avenue, Ottawa, Ontario K1A 0Y3
*Corresponding author: N. Bingham-Koslowski (email: Nikole.Bingham-Koslowski@nrcan-rncan.gc.ca)

OVERVIEW

Situated between the northeastern margin of Canada and western Greenland lies a vast region comprising the Labrador–Baffin Seaway and its onshore margins, including Baffin Island, Bylot Island, and West Greenland (Fig. 1). The associated geology of this region records numerous successive tectonic events, beginning with the assembly of cratons in the Paleoproterozoic to form the Laurentian portion of the supercontinent Nuna (St-Onge et al., 2009). Localized extension in the Mesoproterozoic formed the Bylot basins on northern Baffin Island and beneath northern Baffin Bay, as well as in surrounding onshore areas (Fahrig et al., 1981). During the early Paleozoic, sedimentary platform successions accumulated following the breakup of the supercontinent Rodinia (Bell and Howie, 1990). Deposition ceased with the closing of Paleozoic seaways and the formation of the supercontinent Pangea. Subsequently, Pangea underwent extension in the Labrador–Baffin Seaway region starting in the Early Cretaceous (Roest and Srivastava, 1989). This resulted in the eventual separation of Greenland from the paleo–North American Plate beginning in the Maastrichtian and developing regionally in the Paleocene before seafloor spreading ended in the late Paleogene (Oakey and Chalmers, 2012; Keen et al., 2018a, b). This rifting and seafloor spreading resulted in the formation of the Labrador–Baffin Seaway, a region that includes the Labrador Sea, Davis Strait, and Baffin Bay, and consists of several major offshore basins, as well as localized onshore basins.

Gaining new insights into local and regional aspects of the complex geological history of the Labrador–Baffin Seaway and its onshore margins was addressed within the Geo-mapping for Energy and Minerals (GEM) program led by the Geological Survey of Canada (GSC). The aim of the two-phased program (GEM-1 from 2008 to 2013 and GEM-2 from 2013 to 2020) was to promote sustainable economic advancement in Canada's North by providing geoscience knowledge for decision making related to land-use and resource development. The GEM-2 program had six regions of interest in Canada's North, with the focus of this particular geological synthesis on the study region that included Baffin Island (Nunavut) and the Labrador–Baffin Seaway. Within this study region, scientific research conducted under the GEM-2 program included onshore field-based studies on Baffin and Bylot islands by GSC scientists and their external collaborators to further understand the Precambrian bedrock geology (and associated mineral potential) and the Mesozoic–Cenozoic stratigraphic successions. In addition to these field-based studies, offshore research within the Labrador–Baffin Seaway involved comprehensive compilations of existing data, combined with modern techniques and new analyses to study the Paleozoic stratigraphic history and Mesozoic–Cenozoic stratigraphic and rift history. The culmination of the GEM-2 scientific work, in conjunction with essential contributions from collaborators, results derived from the GEM-1 program, and knowledge from pre-existing studies, has led to the development of this GSC Bulletin.

The papers included in this volume comprise detailed synopses of previous geological and geophysical knowledge, as well as novel insights from a regional perspective for the offshore subsurface of the Labrador–Baffin Seaway and the onshore successions and bedrock of Baffin Island, Bylot Island, and the Nuussuaq Basin, thus providing a comprehensive, updated overview of the geology and tectonic history of the area. The geology of the region is addressed within six informal subregions defined in this bulletin (Baffin Island, western Baffin Bay, Bylot Island, the Labrador margin and central Labrador Sea, western Davis Strait, and the West Greenland margin; Fig. 1), with contributions grouped into three parts: Precambrian and lower Paleozoic geology; Mesozoic to Cenozoic geology and Recent seismicity; and resources. The first part includes a synopsis of the Archean, Paleoproterozoic, Mesoproterozoic, and lower Paleozoic geology of Baffin Island, as well as offshore occurrences of lower Paleozoic rocks in the Labrador–Baffin Seaway. The Mesozoic to Cenozoic geology of part two relates to the rifting and opening of the Labrador–Baffin Seaway and includes papers addressing the associated stratigraphic successions found onshore and offshore in the subregions. The stratigraphic and tectonic evolution of the conjugate margins as a whole, and the Recent seismicity encountered in the offshore and surrounding onshore areas, are also discussed. The third part, resources, details known and potentially economically significant mineral resources on Baffin Island and hydrocarbon resources in the Labrador–Baffin Seaway and onshore West Greenland.

PRECAMBRIAN AND LOWER PALEOZOIC GEOLOGY

Baffin Island is underlain by accreted Archean and Paleoproterozoic structural domains, including the northern Rae Craton and the southern Meta Incognita microcontinent. Rocks of these domains are overlain locally on northern Baffin Island by Mesoproterozoic rocks of the Borden Basin. Lower Paleozoic platform successions cover parts of northern and southern Baffin Island, and are present offshore in western Davis Strait and along the Labrador margin.

Archean and Paleoproterozoic cratonic rocks

An overview of geological investigations on Baffin Island, from Martin Frobisher's trans-Atlantic voyages, completed during the second half of the 16th century (Hogarth et al., 1994), through to the recent Geological Survey of Canada (GSC) Geo-mapping for Energy and Minerals (GEM) North Baffin Island Bedrock Mapping activity (Saumur et al., 2018) is presented in St-Onge et al. (this volume). The main Archean and Paleoproterozoic structural domains of Baffin Island and a synthesis of their assembly during a period of global continental aggregation in the middle Paleoproterozoic is also provided.

From north to south, four structural domains are recognized. The first is the eastern upper-plate Rae Craton, which comprises Archean basement orthogneiss, felsic plutonic rocks, and supracrustal packages (Skipton et al., 2017), unconformably overlain along its southern margin by middle Paleoproterozoic supracrustal cover (Piling Group; Wodicka et al., 2014) and stratigraphically similar units of the Hoare Bay Group on Cumberland Peninsula (Sanborn-Barrie et al., 2017). A middle Paleoproterozoic felsic plutonic suite (Qikiqtarjuaq plutonic suite; Rayner et al., 2012) intrudes both the cratonic basement and supracrustal cover strata. The second structural domain includes Archean to middle Paleoproterozoic metaplutonic gneissic units and middle Paleoproterozoic tectonostratigraphic cover units (Lake Harbour Group; Jackson and Taylor, 1972), collectively termed the 'Meta Incognita microcontinent' by St-Onge et al. (2000), which represents crust rifted from either the Rae Craton or the Superior Craton, or is exotic to both (St-Onge et al., 2016). The third structural domain comprises middle Paleoproterozoic, dominantly monzogranitic to granodioritic orthogneiss, interpreted as a deformed arc-magmatic terrane (Narsajuaq terrane; Scott, 1997; Wodicka and Scott, 1997; Thériault et al., 2001; St-Onge et al., 2009). The fourth structural domain consists of Archean tonalitic to granitic orthogneiss, interpreted as the northern continuation of the lower-plate Superior Craton crystalline basement, and associated middle Paleoproterozoic continental margin supracrustal cover (Povungnituk Group; St-Onge et al., 1996).

These four structural domains were progressively accreted from north to south across a series of south- and north-dipping crustal sutures during long-lived deformation associated with the Himalayan-scale Trans-Hudson Orogen. The oldest of these sutures, the 'Baffin suture,' is proposed to have resulted from accretion of the Meta Incognita microcontinent to the Rae Craton at ca. 1880–1865 Ma (St-Onge et al., 2006). To the south, the 'Soper River suture' records the accretion of the Narsajuaq arc-magmatic terrane to the composite Rae-Meta Incognita continental margin between ca. 1845 Ma and ca. 1842 Ma (Scott, 1997; Dunphy and Ludden, 1998). The youngest suture, the 'Bergeron suture', formed during terminal collision of the Superior Craton with the Churchill plate (or peri-Churchill collage) between ca. 1820 Ma and ca. 1795 Ma (Wodicka and Scott, 1997; Scott and Wodicka, 1998).

Mesoproterozoic Borden Basin

Knowledge of the late Mesoproterozoic Borden Basin, on northern Baffin Island, summarized in Turner (this volume), derives from GSC mapping in the 1970s (e.g. Jackson and Iannelli, 1981; Scott and de Kemp, 1998) in conjunction with subsequent university-based studies. The Borden Basin, one of the four Bylot basins (Fahrig et al.,

Figure 1. Extent of the Geological Synthesis of Baffin Island (Nunavut) and the Labrador–Baffin Seaway study region depicting the six informal subregions. Note that the geology in the international waters between the Canadian and Greenland (Denmark) exclusive economic zones (EEZs) is described in conjunction with the associated Canadian subregions (the Labrador margin and central Labrador Sea, and Western Davis Strait). Additional projection information: Central Meridian = 60°W, Standard Parallels = 65°W, 75°W, and Latitude of Origin: = 65°N.

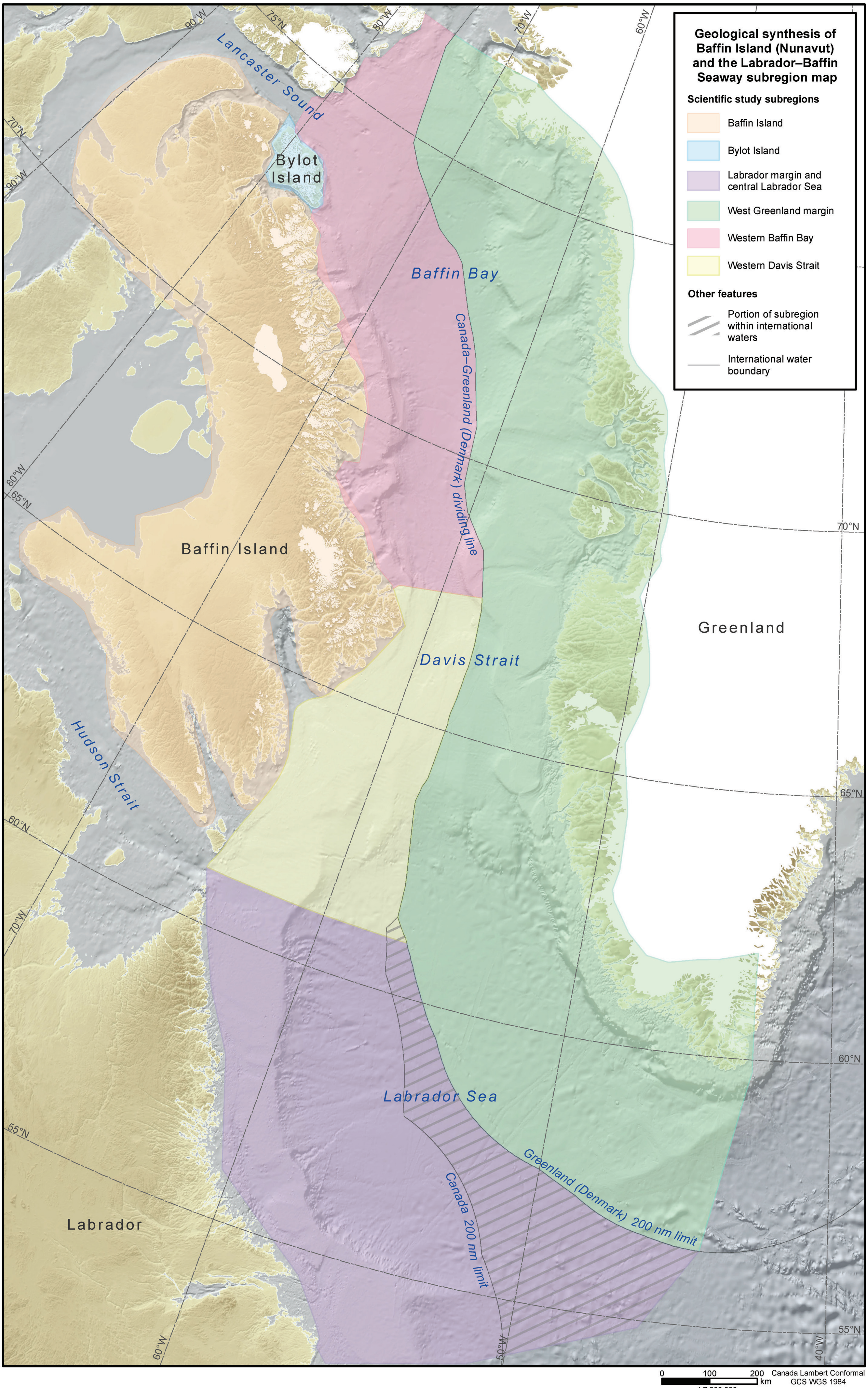
Geological synthesis of Baffin Island (Nunavut) and the Labrador–Baffin Seaway subregion map
Scientific study subregions
Baffin Island
Bylot Island
Labrador margin and central Labrador Sea
West Greenland margin
Western Baffin Bay
Western Davis Strait
Other features
Portion of subregion within international waters
International water boundary
Lancaster Sound
Bylot Island
Baffin Bay
Canada–Greenland (Denmark) dividing line
Baffin Island
Davis Strait
Greenland
Hudson Strait
Labrador Sea
Greenland (Denmark) 200 nm limit
Canada 200 nm limit
Labrador
90°W
80°W
70°W
60°W
50°W
40°W
75°N
70°N
65°N
60°N
55°N
0 100 200 km
1:7 500 000
Canada Lambert Conformal
GCS WGS 1984

1981), contains approximately 6 km of Bylot Supergroup strata overlying the Rae Craton; its stratigraphy is best known from the Milne Inlet Graben.

Turner (this volume) presents detailed lithological descriptions, depositional paleoenvironments, and an overview of the tectonostratigraphic evolution of the Bylot Supergroup. Initially, subaqueous basalt of the Nauyat Formation and overlying marine sandstone of the Adams Sound Formation record deposition in a regional sag basin (Long and Turner, 2012; Turner et al., 2016). Pronounced rifts then developed, within which diverse, coeval successions accumulated: debris fans at the margins (Fabricius Fiord Formation; Jackson and Iannelli, 1981; Scott and de Kemp, 1998); deep-water black shale (upper Arctic Bay Formation; Turner and Kamber, 2012); deep-water carbonate seep-mounds (Ikpiarjuk Formation; Turner, 2009; Hahn and Turner, 2017); and a southeastern prograding carbonate ramp (Iqqittuq Formation; Turner, 2009). Geochemical evidence suggests that the Fabricius Fiord, upper Arctic Bay, Ikpiarjuk, and Iqqittuq formations accumulated in lacustrine environments (Hahn et al., 2015; Gibson et al., 2019).

Exposure of Ikpiarjuk Formation mound tops was accompanied by abrupt changes in the basin-floor settings, with accumulation of shallow-marine carbonate to the southeast (Angmaat Formation) and contemporaneous anoxic laminite to the northwest (Nanisivik Formation), separated by a tectonic platform rim characterized by tepee cycles (Turner, 2009). Pronounced differential uplift, tilting, and exposure produced an unconformity with hundreds of metres of relief, with subsequent flooding depositing muddy carbonate ramp strata (Victor Bay Formation; Turner, 2011). A second major episode of differential uplift resulted in local karstification (Victor Bay Formation), with drowning elsewhere (Athole Point Formation; Sherman et al., 2002). An episode of tectonic instability led to deposition of local conglomerate and sandstone of the lowermost Strathcona Sound Formation that was followed by an upward-shallowing marine succession of siltstone and sandstone (Strathcona Sound, Aqigilik, and Sinasiuvik formations; Turner et al., 2016).

Geochronological constraints on accumulation of the Bylot Supergroup are sparse (*see* Turner, this volume), with deposition of the Bylot Supergroup occurring between 1267 Ma and 723 Ma (LeCheminant and Heaman, 1989; Heaman et al., 1992; Pehrsson and Buchan, 1999; Denyszyn et al., 2009). The basal basalt is inferred to be related to the ca 1270 Ma Mackenzie igneous event, but no direct evidence for its age is yet available. Shale units in the middle of the succession have late Mesoproterozoic (U-Th-Pb, Re-Os) depositional ages (Turner and Kamber, 2012; Gibson et al., 2018). Detrital zircon crystals derived from the Grenville Orogen are found in the uppermost formations, limiting their depositional age to less than 1.14 Ga (Rainbird et al., 2012; Turner et al., 2016). A synopsis of the metallogeny of the Borden Basin is also provided by Turner (this volume). The Milne Inlet Graben contains numerous carbonate-hosted Zn-Pb showings (e.g. Nanisivik ore-body) the distribution of which is stratigraphically and structurally controlled (Sangster, 1998; Scott and de Kemp, 1998; Turner, 2011).

Lower Paleozoic stratigraphy

Geographically discontinuous lower Paleozoic strata are present within the Labrador–Baffin Seaway, and also occur in outcrop on Baffin Island. The rifting of the supercontinent Pangea, and synchronous opening of the Labrador Sea and Baffin Bay in the Early Cretaceous resulted in the extensive erosion of Paleozoic deposits in the region, which now exist as isolated erosional remnants along the Labrador margin and in western Davis Strait (Moir, 1989; Bell and Howie, 1990). Paleozoic rocks also outcrop on Baffin Island where they can form laterally extensive deposits (e.g. Trettin, 1965a, b, 1969, 1975). An overview of the lower Paleozoic strata from these regions, including lithological descriptions, updated biostratigraphical information, and paleoenvironmental interpretations is presented in Bingham-Koslowski, Zhang, and McCartney (this volume). Additionally, maps detailing the distribution of lower Paleozoic strata are included for the Labrador margin, the southeastern Baffin Shelf (as mapped in Dafoe, DesRoches, and Williams, this volume), and onshore Baffin Island.

Lower Paleozoic strata within the Labrador–Baffin Seaway are composed predominantly of carbonate rocks (Bell and Howie, 1990; Bingham-Koslowski, 2018, 2019), with no formal formations recognized. Middle to Upper Ordovician strata are known from wells on the southern Labrador Shelf, where they were initially deposited in an epeiric sea and now locally form basement rock to the younger synrift and post-rift strata that characterize the Hopedale Basin (Bell and Howie, 1990). Ordovician rocks from the western Davis Strait region are known only from shallow seabed drill cores collected by the GSC in the 1970s (Jansa, 1976; MacLean et al., 1977; Bell and Howie, 1990). The extent of the lower Paleozoic in western Davis Strait is refined through seismic mapping in Dafoe, DesRoches, and Williams (this volume). Lower Paleozoic strata outcrop in three main regions on Baffin Island: Brodeur Peninsula, northwestern Baffin Island, and southern Baffin Island. The lower Paleozoic sequence on Baffin Island is primarily composed of Ordovician carbonate rocks, with localized occurrences of Cambrian clastic and Silurian carbonate rocks. The lower Paleozoic of Baffin Island has been previously subdivided into nine formal units (e.g. Blackadar, 1956; Lemon and Blackadar, 1963; Sanford and Grant, 1990, 2000) that are summarized and refined in Bingham-Koslowski, Zhang, and McCartney (this volume).

Bingham-Koslowski, Zhang, and McCartney (this volume) further discuss possible correlations of lower Paleozoic strata between onshore Baffin Island and offshore southeastern Baffin Shelf. Based on the distribution of the strata, biostratigraphic and lithostratigraphic differences, as well as the absence of lower Paleozoic strata in wells from the northern Labrador margin and western Davis Strait, the authors of this paper informally subdivide the lower Paleozoic into two unrelated, depositional subsets: a northern area, that includes onshore and offshore Baffin Island and a southern region, encompassing offshore Labrador.

MESOZOIC TO CENOZOIC GEOLOGY AND RECENT SEISMICITY

Mesozoic to Cenozoic stratigraphy

The tectonic evolution of the Labrador–Baffin Seaway, which began in the Early Cretaceous, resulted in the development of thick Mesozoic to Cenozoic successions within sedimentary basins. Whereas strata are distributed widely within offshore basins, few onshore correlatives of these offshore strata exist along the Canadian margin. Onshore exposures of Cretaceous to Paleogene strata are preserved in the Cape Dyer area of east-central Baffin Island and also on Bylot Island (Fig. 1) and adjacent areas of northern Baffin Island. Haggart et al. (this volume) summarize the historical research on these strata, specifically the lithostratigraphy and biostratigraphy of the successions. The distribution and geographic extent of the onshore Cretaceous to Paleogene strata were first elucidated during GSC mapping programs in the 1960s and 1970s (Jackson and Davidson, 1975; Jackson et al., 1975, 1979; Jackson and Morgan, 1978). Stratigraphic studies undertaken subsequently by the GSC and others (e.g. Miall et al., 1980; Ioannides, 1986; Sparkes, 1989; Waterfield, 1989; Benham and Burden, 1990; Burden and Langille, 1990, 1991; Wiseman, 1991) led to definition of the sedimentary facies that are present in the onshore successions, and also provided preliminary age assignments. Dating and correlation of onshore strata relies principally on palynology, as the strata are depauperate with respect to well preserved molluscan fossils, and interstratified tuff deposits are absent. The onshore strata include an abundance of sandstone and lesser mudstone and conglomerate deposits that were interpreted, on sedimentological grounds, to record a variety of nonmarine, nearshore-marine, and deep-water paleoenvironments.

Despite lacking an overall comprehensive assessment of the regional distribution and facies relationships, the studies of the 1970s and 1980s established the framework of the Cretaceous to Paleogene successions in the onshore areas bounding western Baffin Bay. Key contributions from these studies, discussed by Haggart et al. (this volume), include: the association of rift-related sedimentary and volcanic strata in the Cape Dyer area (Burden and Langille, 1990) with regional Paleogene volcanism centred within Davis Strait; the stratigraphic affinity of Upper Cretaceous strata of Bylot Island and vicinity with the Kanguk succession of Sverdrup Basin (Miall et al., 1980); and the proposition that the Cretaceous to Paleogene succession of the Bylot Island region was deposited in two distinct depocentres—Eclipse and North Bylot troughs (Miall et al., 1980; Benham and Burden, 1990), with Benham and Burden (1990) proposing a significantly divergent stratigraphic history between the two depocentres in the Cenozoic. No comprehensive stratigraphic framework for the Cretaceous to Paleogene strata of the Bylot Island region has been developed from these studies, however, and the depositional settings of some stratigraphic units remain unresolved. Furthermore, the necessity for detailed palynostratigraphy to correlate the clastic successions of the onshore was recognized (Ioannides, 1986; Sparkes, 1989; Waterfield, 1989; Wiseman, 1991). Palynological studies in the region have not yet resulted in a formal biostratigraphic scheme for the onshore strata, but have demonstrated the challenge of differentiating Quaternary from older Cenozoic, and even Mesozoic, strata due to reworking (Burden and Holloway, 1985; Newman, 1987).

As defined in this bulletin, the Canadian portion of the Labrador–Baffin Seaway is divided into three informal subregions (Fig. 1), each of which contain prominent sedimentary basins: 1) the Labrador margin and central Labrador Sea, including the Hopedale Basin and the southern part of the Saglek Basin; 2) the western Davis Strait region, which encompasses the northern part of the Saglek Basin, the Cumberland Basin, and the western part of the Lady Franklin Basin; and 3) the western Baffin Bay area, which contains the Scott and Buchan grabens and the Lady Ann Basin. Coeval basins also developed on the West Greenland margin, with thick Cenozoic strata blanketing the central regions of the Labrador Sea and Baffin Bay, primarily underlain by oceanic crust.

The Mesozoic to Cenozoic offshore stratigraphic successions of the Canadian portion of the Labrador–Baffin Seaway have been studied since the 1970s through evidence from exploration wells, seabed samples of bedrock, an ODP corehole, and the cumulative acquisition of an extensive seismic reflection data set. Five significant discoveries of hydrocarbons were made within the Hopedale Basin (*see* Bingham-Koslowski, McCartney, and Bojesen-Koefoed, this volume), resulting in a comparatively high concentration of data sets (i.e. seismic profiles and exploration wells) for offshore Labrador. Accordingly, the lithostratigraphic framework for the offshore Canadian portion of the seaway is derived primarily from the Labrador margin. The lithostratigraphic units first proposed for this margin by Umpleby (1979) and modified by McWhae et al. (1980) include the: Alexis, Bjarni, Markland (Freydis Member), Gudrid, Cartwright, Kenamu (Brown Mudstone and Leif members), Mokami, and Saglek formations. This framework was expanded upon by Balkwill (1987), Bell (1989), Balkwill and McMillan (1990), and Dickie et al. (2011), and is further refined or adapted in three papers: Dafoe, Dickie, Williams, and McCartney (this volume) for the Labrador margin and central Labrador Sea; Dafoe, DesRoches, and Williams (this volume) for the western Davis Strait region; and Dafoe, Dickie, and Williams (this volume) for western Baffin Bay.

In these three papers, pre-rift basement rocks are described along the Canadian margin for each of the three subregions (Labrador margin and central Labrador Sea, western Davis Strait, and western Baffin Bay), and identified locally where data exist to constrain their distribution. The Mesozoic to Cenozoic synrift and postrift stratigraphy is also described and the distribution of these units is mapped based on the available data sets. Updated ages, as determined biostratigraphically, are presented, in addition to refinements to the paleoenvironmental interpretations. The type sections, which were derived from wells along the Labrador margin, are shown and discussed. Key results from the three papers include refinements to the age of the Bjarni Formation and the overlying Markland Formation and associated Freydis Member sandstone units. The age of the overlying Gudrid Formation is also more clearly defined, as is its shallow-marine origin. The lithostratigraphic picks in the three wells on the southeast Baffin Shelf are redefined based on new age constraints and seismic correlations. Seabed samples of bedrock in the western Davis Strait region and along the Baffin Shelf are also incorporated into the lithostratigraphic framework. They show good agreement with the Labrador margin stratigraphy in terms of their age and paleoenvironmental interpretation, and help constrain seismic mapping.

Also presented in the three papers for the Canadian margin is a seismic stratigraphic framework based on the lithostratigraphy of the Labrador margin as shown on key seismic reflection profiles across each of the three regions. Newly compiled distribution maps are also included for three key intervals: Cretaceous, lower Cenozoic, and upper Cenozoic. Pre-rift basement rocks are mapped along the platform and as localized highs, with major faults delineated. Seismic interpretation and well correlations enabled mapping of the distribution of Cretaceous rocks, as well as associated Early Cretaceous volcanic rocks and the seaward extent of the Lower Cretaceous Bjarni Formation for parts of the Labrador margin. The extent of the lower Cenozoic interval (Paleocene through middle Miocene section) is mapped, in addition to the distribution of volcanic (magma-rich) margins, related volcanic units (such as inner flows), and volcanic cover (mostly located within the Davis Strait region). The upper Cenozoic interval, from middle Miocene through Pleistocene, is also shown in each of the three papers, in addition to regions in which Quaternary sedimentation dominates the succession. Significant new results from this work include a new understanding of the extent of Cretaceous strata offshore Labrador and in the Canadian portion of the Lady Franklin Basin. Farther north, the Cretaceous interval in the Scott Graben on the Baffin Shelf is interpreted to contain a thin Lower Cretaceous section and a thick Upper Cretaceous section, similar to successions encountered in parts of the southern Saglek Basin and Melville Bay Graben (offshore West Greenland). New age constraints from the ODP Site 645 corehole help to refine mapping of key seismic horizons in the upper Cenozoic interval for western Baffin Bay. In western Davis Strait, a new structural map includes basement highs, volcanic highs, and faults, providing a major refinement to the understanding of the region's geology.

A summary of the onshore and offshore stratigraphy along the conjugate West Greenland margin of the Labrador–Baffin Seaway, and the margin's tectonic evolution, is presented by Gregersen et al. (this volume). This margin contains numerous sedimentary basins and structures dating back to the Proterozoic (Dam et al., 2009; Henriksen et al., 2009; St-Onge et al., 2009; Gregersen, 2014; Gregersen et al., 2019), but the main focus of Gregersen et al. (this volume) is the Cretaceous to Cenozoic successions related to the opening of the seaway. An understanding of the onshore geology for the West Greenland margin has developed over the past century, driven by numerous mapping and field expeditions (e.g. Dam et al., 2009; Henriksen et al., 2009). Offshore studies did not begin until the 1970s and have expanded with the cumulative acquisition of seismic data and the drilling of exploration and scientific wells (Christiansen, 2011). Gregersen et al. (this volume) present a geological synopsis that incorporates basin evolution, lithostratigraphy, biostratigraphy, seismic stratigraphy, tectonostratigraphy, and studies of volcanic rocks, as well as crustal structure with interpretations based on seismic reflection surveys, seismic refraction data, well and outcrop data, seabed samples, magnetic and gravity data, and stratigraphic compilations.

The West Greenland margin is subdivided by Gregersen et al. (this volume) into southern, central, and northern regions, and an overview of the basins in each region is provided with a primary focus on the Cretaceous and Paleogene successions. Cretaceous to Paleocene sedimentary successions, with overlying volcanic rocks, are well known from outcrops and wells in the Nuussuaq Basin of central West Greenland (Dam et al., 2009). The sedimentary basins of the offshore West Greenland margin are underlain by continental crust to the east, and Cenozoic basins to the west are underlain by a crustal transition zone to oceanic crust.

A description of the stratigraphy and geological evolution of the basins in each region is presented and six tectonostratigraphic phases are recognized: pre-rift and early extension (pre-Cretaceous), early rift (Early to middle Cretaceous), subsidence and rifting (middle Cretaceous to early Campanian), late rift (Campanian to Early Paleocene), drift (Paleocene to Eocene), and post-drift (post-Eocene). In their tectonostratigraphic summary, Gregersen et al. (this volume) further correlate and compare the West Greenland margin with the conjugate Canadian margin.

The Mesozoic to Cenozoic stratigraphy of the entire Labrador–Baffin Seaway is discussed as a whole in Dafoe, Williams et al. (this volume). The biostratigraphic framework from Nøhr-Hansen et al. (2016) forms an important basis for understanding the age of the successions and correlations between regions. This framework consists of a palynostratigraphic events chart based on first and last occurrences, as well as peak abundances of dinoflagellate cysts, spores and pollen, and the freshwater fern *Azolla* from samples across the region, allowing for refinement of the stratigraphic columns along the margins. Dafoe, Williams et al. (this volume) use the seismic stratigraphic framework from Gregersen et al. (2013, 2018, 2019, this volume; units H through A from oldest to youngest), with adaptations for the Canadian margin (Dafoe, Dickie, Williams, and McCartney, this volume), to compare the development of Cretaceous and younger stratigraphic successions along the seaway. This includes regional stratigraphic distribution maps compiled from several papers in this bulletin, as well as conjugate margin profiles showing correlations of the seismic units across the region. This work demonstrates the correlation and nature of major seismic horizons, with some horizons displaying lateral variation from unconformable to conformable elsewhere. Growth faulting is well developed in the Lower Cretaceous (unit G), and the Upper Cretaceous (unit F) is generally seismically transparent regionally, indicating deposition of marine shale units. The Cenozoic interval (units E through A) shows variation in thickness across the seaway and is partly influenced by major basement highs such as the Davis Strait High. Clinoform progradation is typical in units C, B, and A on the margins of the seaway. The paleoclimate and paleoceanography of the region is also summarized by Dafoe, Williams et al. (this volume) in light of these more recent results.

Mesozoic to Cenozoic rift history

The timing and geometry of the large-scale plate motions that created the Labrador–Baffin Seaway have been of interest, and the subject of controversy, since the earliest days of continental-drift theory (e.g. Taylor, 1910). Keen et al. (this volume) report on geophysical studies within Baffin Bay, Davis Strait, and the Labrador Sea; their interpretations have been central to understanding the basic elements of Mesozoic-Cenozoic plate motions, and the consequent lithospheric rifting processes. The focus of this paper is primarily on the rifted continental margins surrounding the deep oceanic regions formed by seafloor spreading.

Keen et al. (this volume) present updated maps of gravity and magnetic anomalies for the entire seaway. Such data have been critical in determining the seafloor spreading history of the ocean basins (Srivastava, 1978; Roest and Srivastava, 1989; Oakey and Chalmers, 2012), and in delineating linkages between onshore and offshore features. Previous interpretations show that the onset of seafloor spreading was diachronous, starting first in the central Labrador Sea (ca. 69 Ma) and slightly later regionally within the seaway (ca. 62 Ma). Two stages of seafloor spreading are identified and are distinguished by a change in the direction of plate motions in the latest Paleocene. Spreading ceased near the Eocene–Oligocene boundary (Oakey and Chalmers, 2012). These results are somewhat controversial and are still being refined, mainly through combining geological and geophysical data sets over the entire Labrador–Baffin Seaway and adjacent regions (e.g. Oakey and Chalmers, 2012).

A synthesis of recent (Funck et al., 2007, 2012; Suckro et al., 2012, 2013; Altenbernd et al., 2014, 2015) and older seismic refraction results in Keen et al. (this volume) show a variety of structural styles, which can be distilled into two main types of rifted margin: 1) magma-poor margins with hyperextended zones, serpentinized, and possibly exhumed mantle, and proto-oceanic crust (e.g. Chian et al., 1995; Keen et al., 2018a); and 2) magma-rich margins with thick zones of igneous crust, possibly overlying older, magma-poor margins in some regions (Keen et al., 2012, 2018b). Based on the seismic refraction observations and gravity modelling, crustal thinning and subsidence are highly asymmetric across the conjugate margins (Welford and Hall, 2013; Welford et al., 2018). The magma-rich margins appear to be centred on the Davis Strait region, where Paleocene to Eocene volcanic rocks are mapped both onshore and offshore (e.g. Clarke, 1970; Larsen et al., 2009), possibly reflecting the influence of a ‘hot spot’, or mantle plume (Storey et al., 2007). The cause of this magmatism is still disputed (Peace et al., 2017; Clarke and Beutel, 2020). In addition to crustal-scale observations, Keen et al. (this volume) present new maps showing the distribution of sedimentary rocks throughout the region; these maps are derived from multichannel seismic reflection data tied to exploration wells. The maps demonstrate the great thicknesses (over 10 km) of strata deposited on the continental margins, and the distribution of these syn-rift and younger sediments can be correlated with the nature and style of rifting and subsidence.

Keen et al. (this volume) use their mapping to update the landward limit of oceanic crust and the extent of offshore sedimentary basins. They further employ previously derived timing and poles of rotation for Greenland relative to North America (Hosseinpour et al., 2013) to reconstruct the positions of the continents through time, from the present day to the pre-rift closure of the continents. Large-offset transform faults in Davis Strait and Baffin Bay resulted in hundreds of kilometres of displacement between conjugate margins of the seaway. Plate velocities, estimated in this and previous studies, show a rapid increase during the Campanian, which may indicate a rapid decrease in the strength of the continental lithosphere, as previously suggested by Brune et al. (2016). On closure, the Precambrian terranes and their boundaries on land exhibit a good fit between Greenland and North America.

Many of the large-scale, crustal and sedimentary features described for the rifted margins of the Labrador–Baffin Seaway are similar to those of other rifted margins globally. One might have expected the cold, thick cratonic lithosphere of the region to have responded differently to rifting; this raises questions for future studies.

Seismicity

Seismic hazard maps for Canada (Earthquakes Canada, 2018) and Greenland (Voss et al., 2007) indicate moderate to high hazard levels for Baffin Bay, the Labrador Sea, and adjacent onshore regions. As outlined in Bent and Voss (this volume), studying earthquakes in the Labrador–Baffin Seaway is challenging despite the relatively high seismicity rates, primarily due to the remoteness and vastness of the region. There is no knowledge of earthquake activity in the Labrador–Baffin Seaway prior to 1933, when a magnitude 7.4 earthquake occurred in Baffin Bay (Bent, 2002). With improved instrumentation, increased seismograph coverage in the North, real-time data sharing between Canada and Denmark (Greenland), and modern analytical techniques, the knowledge and understanding of earthquakes in the Labrador–Baffin region is improving. Bent and Voss (this volume) present a summary of the seismicity of the Labrador–Baffin Seaway and adjacent onshore regions, including synopses of earthquake monitoring in the area, regions of high seismic activity, focal mechanisms for the largest earthquakes recorded from the region, and the processes that may be involved with earthquake generation in the area.

Seismicity in the Labrador Sea appears to be associated to the extinct seafloor spreading ridge and oceanic fracture zones in that region (*see* Keen et al., this volume), but it has been difficult to find a comparable link between seismicity and structure in Baffin Bay. Research focusing on Baffin Bay from the 1970s to early 2000s (e.g. Basham et al., 1977; Bent, 2002) found no correlation between earthquake activity in Baffin Bay and either mapped structures (i.e. faults) or geophysical anomalies. Despite a further two decades of earthquake monitoring with improved instrumentation, during which time new structural maps of Baffin Bay were developed, a correlation between structure and seismicity remains elusive.

Focal mechanism (fault plane) solutions can now be determined for many more Labrador–Baffin earthquakes than in the past. Bent and Voss (this volume) demonstrate that focal mechanism solutions for the Labrador–Baffin Seaway show a mix of faulting styles, predominantly strike-slip and thrust. Orientations of regional stress axes exhibit more consistency than the faulting style, suggesting that seismic activity is occurring on existing structures in response to the current stress field. The possibility that glacial isostatic adjustment may be a triggering mechanism for earthquakes in the Labrador–Baffin region remains tantalizing, but efforts to model a correlation, except at a broad regional scale, have led to equivocal results (e.g. James and Schamehorn, 2016).

RESOURCES

Minerals

Mineral resources of Baffin Island include iron (e.g. Mary River Group), kimberlite-hosted diamonds (e.g. the Chidliak deposit), carbonate-hosted zinc and lead deposits (e.g. the Nanisivik deposit), nickel, copper, platinum-group elements, uranium, thorium, gemstones (sapphire, spinel, and lapis lazuli), carving stone, and coal. Harrison et al. (this volume) present an overview of the known and prospective types of minerals from Baffin Island and include an updated map of the island depicting the location and types of resources in conjunction with the geology.

Iron deposits in the Neoarchean Mary River Group (2.83 Ga; 2.76–2.72 Ga) include the Mary River 1–4 deposits of northern Baffin Island, which contain 586 Mt of 66% Fe (G.H. Wahl, R. Gharapetian, J.E. Jackson, V. Khera, and G.G. Wortman, unpub. report, 2011; Iannelli et al., 2013b). Other iron-formation prospects in the larger Mary River district include: Glacier Lake, Turner River, North Cockburn River, North Rowley River, Cockburn-Rowley, southeast Rowley, North Isortoq, South Isortoq, and Eqe Bay (Iannelli et al., 2013a; Campbell and MacLeod, 2014). In addition, base- and precious-metal occurrences are widespread, often occurring in mafic–ultramafic sills or in the Paleoproterozoic Lake Harbour Group near Kimmirut on southern Baffin Island (Vande Guchte, 1998; Vande Guchte and Gray, 1999). Commodities in anomalous concentrations include nickel, copper, palladium, platinum, and locally gold, silver, and zinc. In the Mesoproterozoic Borden Basin, the Nanisivik and Ikpiarjuk formations (Turner, 2011; *see* Turner, this volume) host the Nanisivik deposit, a Mississippi Valley-type (MVT) deposit that consists of 9.0% Zn, 0.9% Pb, and 41 ppm Ag.

A diamond-rich kimberlite, dated to 156.7–138.9 Ma (Heaman et al., 2015), occurs as sheets and small pipes at Chidliak on Hall Peninsula. The host rock is composed of magmatic kimberlite with xenoliths of eclogite and peridotite, as well as pyrope garnet, chrome diopside, and olivine phenocrysts up to 10 cm across (J. Pell, unpub. report, 2008).

Carving stones are an important mineral resource to Northern communities and descriptions of known deposits are provided in Harrison et al. (this volume). At least 32 carving stone localities are known, consisting of serpentinite, marble, serpentinized marble, and soapstone. Notable deposits include marble and serpentinite near

Arctic Bay (Beauregard and Ell, 2015), serpentinite east of Cape Dorset (Steenkamp et al., 2014), marble and ultramafic rocks west of Kimmirut (Elgin, 2017), pink marble near Clyde River (Beauregard et al., 2013), soapstone near Mary River (Beauregard et al., 2013), and serpentinite and soapstone southwest of Pangnirtung (Steenkamp et al., 2015).

Coal is another important resource with the first documented occurrence on Baffin Island by McMillan (1910). Coal occurs in the Cretaceous to Paleogene Eclipse Trough of Bylot Island and northwestern Baffin Island (Miall et al., 1980), and exposures near Pond Inlet have been excavated for local use.

Hydrocarbons

The stratigraphic and tectonic history of the Labrador–Baffin Seaway has resulted in all hydrocarbon system elements being present locally throughout the region, driving hydrocarbon exploration efforts since the 1960s (e.g. Bell and Campbell, 1990; Christiansen, 2011). Despite exploration activities, which are still ongoing on the Labrador margin, no commercial quantities of hydrocarbons have been identified. Furthermore, an indefinite moratorium was decreed by the Canadian federal government in 2016, subject to review every five years, halting the issuing of any new exploration licences in Canadian Arctic waters (Government of Canada, 2018). As of July 2021, new oil and gas exploration activities have also been suspended along the west Greenland margin (both onshore and offshore).

Bingham-Koslowski, McCartney, and Bojesen-Koefoed (this volume) address hydrocarbon resources in the Labrador–Baffin Seaway by subregion: 1) the Labrador margin; 2) western Davis Strait and the southeast Baffin Shelf; 3) northeast Baffin Shelf and western Baffin Bay; and 4) the West Greenland margin (both onshore and offshore). The history of hydrocarbon exploration in the Labrador–Baffin Seaway, as well as any previous hydrocarbon assessments conducted in the region (e.g. McWhae et al., 1980; Nantais, 1984; Harrison et al., 2011; MacLean et al., 2014; Carey et al., 2020) are discussed. No formal hydrocarbon assessments have been conducted in the western Davis Strait and southeastern Baffin Shelf areas; however, a Significant Discovery Licence was awarded at Hekja O-71 (western Davis Strait) based on a gas show, and the northeast Baffin Shelf and entire Baffin Bay area have been assessed a 50% chance of having at least one oil accumulation greater than 1 billion barrels of oil (Gautier et al., 2011). Bingham-Koslowski, McCartney, and Bojesen-Koefoed (this volume) further present known and predicted hydrocarbon system elements from each area and summarize the hydrocarbon potential of the subregions. A synopsis of the five oil types from onshore oil seeps along the West Greenland margin (Bojesen-Koefoed et al., 1999; Bojesen-Koefoed, 2011), indicators of the presence of multiple hydrocarbon systems, is also included.

Bingham-Koslowski, McCartney, and Bojesen-Koefoed (this volume) review the presence of known and potential hydrocarbon slicks and seeps along the Canadian margin of the Labrador–Baffin Seaway. Numerous potential oil slicks have been identified in the region based on visual observations and using synthetic aperture radar images (e.g. Budkewitsch et al., 2013; Decker et al., 2013); however, the majority of these cannot be correlated definitively with seafloor hydrocarbon seeps. Previous hydrocarbon slick studies, along with possible seafloor seep evidence, are discussed; only the slick located off Scott Inlet (northwestern Baffin Bay) has a proven, natural, seafloor seep origin (Grant et al., 1986). The presence of this definitive hydrocarbon seep along with other direct hydrocarbon indicators observed in exploration wells, provide proof that multiple working hydrocarbon systems exist in the Labrador–Baffin Seaway.

ACKNOWLEDGMENTS

The authors would like to thank Dawn Kellett and Rob Fensome for reviewing this paper, as well as Leith MacLeod for producing the map figure. In regards to the GSC Bulletin 608 as a whole, the authors recognize that this work is the result of a collaborative undertaking led by the GSC as part of the GEM-2 program. The Geological Survey of Denmark and Greenland (GEUS) was a major contributor to this volume, in addition to key contributions provided by other partner organizations including: the Canada–Nunavut Geoscience Office, the Canadian Hazards Information Service, Laurentian University, Memorial University of Newfoundland, Polar Knowledge Canada, Université du Québec à Montréal, the University of Cambridge, and the Yukon Geological Survey. Accordingly, the authors of this paper would like to thank all of the other contributors who helped make this publication possible: Kimberley Bell (GSC), Jørgen A. Bojesen-Koefoed (GEUS), Elliott Burden (Memorial University of Newfoundland), Lisel Currie (GSC), Gregers Dam (GEUS), Sonya Dehler (GSC), Kevin DesRoches (GSC), Kate Dickie (GSC), Rob Fensome (GSC), Thomas Funck (GEUS), John R. Hopper (GEUS), Jussi Hovikoski (GEUS), Jon R. Ineson (GEUS), Paul C. Knutz (GEUS), Lotte M. Larsen (GEUS), Tannis McCartney (GSC), Henrik Nøhr-Hansen (GEUS), Gunver K. Pedersen (GEUS), Nicole Rayner (GSC), Mary Sanborn-Barrie (GSC), Benoit M. Saumur (Université du Québec à Montréal), Dave J. Scott (Polar Knowledge Canada), Nina Skaarup (GEUS), Diane R. Skipton (Yukon Geological Survey), Peter Voss (GEUS), Kim Welford (Memorial University of Newfoundland), Owen M. Weller (University of Cambridge), Graham Williams (GSC), Natasha Wodicka (GSC), and Shunxin Zhang (Canada-Nunavut Geoscience Office). In addition, the authors are grateful to the GEM-2 project management and co-ordination team for supporting the component research projects and this synthesis publication (Michel Plouffe, Natalie Shea, Marlene Francis, Paul Wozniak, and Rosemarie Khoun). The authors would also like to thank the numerous internal and external reviewers that were involved with the publication of this bulletin; their feedback has greatly improved the quality of work presented within. Thanks are owed for all of the GIS support that was provided by the various GSC offices, and specifically to Leith MacLeod who oversaw the compilation of the metadata for the bulletin and generated maps for many of the papers in this volume. Thank you to the GSC publications team for co-ordination, scientific editing, and layout of the papers in this bulletin, particularly Evelyn Inglis, Natalie Morisset, Alison Weatherston, Paul Champagne, Liam Boudreau, and Marie-France Dufour, who were closely involved with this particular GEM-2 volume. The authors would also like to acknowledge the GEM-2 engagement team, especially Kate Clark, who helped communicate the synthesis initiative and the science that comprises it to Northern communities.

REFERENCES

Altenbernd, T., Jokat, W., Heyde, I., and Damm, V., 2014. A crustal model for northern Melville Bay, Baffin Bay; Journal of Geophysical Research: Solid Earth, v. 119, no. 12, p. 8610–8632. https://doi.org/10.1002/2014JB011559

Altenbernd, T., Jokat, W., Heyde, I., and Damm, V., 2015. Geophysical evidence for the extent of crustal types and the type of margin along a profile in the northeastern Baffin Bay; Journal of Geophysical Research: Solid Earth, v. 120, no. 11, p. 7337–7360. https://doi.org/10.1002/2015JB012307

Balkwill, H.R., 1987. Labrador basin: structural and stratigraphic style; *in* Sedimentary Basins and Basin-Forming Mechanisms, (ed.) C. Beaumont and A.J. Tankard; Canadian Society of Petroleum Geologists Memoir, v. 12, p. 17–43.

Balkwill, H.R. and McMillan, N.J., 1990. Mesozoic-Cenozoic geology of the Labrador Shelf; *in* Chapter 7 of Geology of the Continental Margin of Eastern Canada, (ed.) M.J. Keen and G.L. Williams; Geological Survey of Canada, Geology of Canada, no. 2, p. 295–324 (*also* Geological Society of America, The Geology of North America, v. I-1, p. 295–324). https://doi.org/10.4095/132708

Basham, P.W., Forsyth, D.A., and Wetmiller, R.J., 1977. The seismicity of northern Canada; Canadian Journal of Earth Sciences, v. 14, p. 1646–1667. https://doi.org/10.1139/e77-140

Beauregard, M.A. and Ell, J., 2015. Nunavut Carving Stone Deposit Evaluation Program: 2015 fieldwork at Rankin Inlet, Cumberland Sound and Arctic Bay, Nunavut; *in* Summary of Activities 2015; Canada-Nunavut Geoscience Office, p. 183–192.

Beauregard, M.A., Ell, J., Pikor, R.K., and Ham, L.J., 2013. Nunavut Carving Stone Evaluation Program (2010-2013): third year results; *in* Summary of Activities 2012; Canada-Nunavut Geoscience Office, p. 151–162.

Bell, J.S., 1989. Labrador Sea. East Coast Basin Atlas Series; Geological Survey of Canada, 135 p. https://doi.org/10.4095/127152

Bell, J.S. and Campbell, G.R., 1990. Petroleum Resources; Chapter 12 *in* Geology of the Continental Margin of Eastern Canada, (ed.) M.J. Keen and G.L. Williams; Geological Survey of Canada, Geology of Canada, no. 2, p. 677–720 (*also* Geological Society of America, The Geology of North America, v. I-1, p. 677–720). https://doi.org/10.4095/132720

Bell, J.S. and Howie, R.D., 1990. Paleozoic geology; Chapter 4 *in* Geology of the Continental Margin of Eastern Canada, (ed.) M.J. Keen and G.L. Williams; Geological Survey of Canada, Geology of Canada, no. 2, p. 141–165 (*also* Geological Society of America, The Geology of North America, v. I-1, p. 141–165). https://doi.org/10.4095/132700

Benham, P.H. and Burden, E.T., 1990. Stratigraphy of Cretaceous–Tertiary rocks of North Bylot Trough, Bylot Island, N.W.T.; *in* Current Research, Part D; Geological Survey of Canada, Paper 90-1D, p. 179–185. https://doi.org/10.4095/131353

Bent, A.L., 2002. The 1933 Ms 7.3 Baffin Bay earthquake: strike-slip faulting along the northeastern Canadian passive margin; Geophysical Journal International, v. 150, no. 3, p. 724–736. https://doi.org/10.1046/j.1365-246X.2002.01722.x

Bingham-Koslowski, N., 2018. Descriptions of drill cores and thin sections from lower Paleozoic strata, southeastern Baffin Island shelf, Nunavut; Geological Survey of Canada, Open File 8409, 80 p. https://doi.org/10.4095/308354

Bingham-Koslowski, N., 2019. Description of Paleozoic cores and thin sections from the Gudrid H-55, Roberval K-92, Indian Harbour M-52, and Freydis B-87 wells, offshore Labrador (Newfoundland and Labrador); Geological Survey of Canada, Open File 8543, 142 p. https://doi.org/10.4095/313573

Blackadar, R.H., 1956. Geological reconnaissance of Admiralty Inlet, Baffin Island, Arctic Archipelago, Northwest Territories; Geological Survey of Canada, Paper 55-6, 25 p. https://doi.org/10.4095/101291

Bojesen-Koefoed, J.A., 2011. West Greenland petroleum systems: an overview of source rocks and oil seepages and their implications for offshore petroleum exploration; Danmarks og Grønlands Geologiske Undersøgelse Rapport, 2011/42, 49 p.

Bojesen-Koefoed, J.A., Christiansen, F.G., Nytoft, H.P., and Pedersen, A.K., 1999. Oil seepage onshore West Greenland: evidence of multiple source rocks and oil mixing; *in* Petroleum Geology of Northwest Europe: Proceedings of the 5th Conference, (ed.) A.J. Fleet and S.A.R. Boldy; Geological Society, London, p. 305–314. https://doi.org/10.1144/0050305

Brune, S., Williams, S.E., Butterworth, N.P., and Müller, R.D., 2016. Abrupt plate accelerations shape rifted continental margins; Nature, v. 536, p. 201–204. https://doi.org/10.1038/nature18319

Budkewitsch, P., Pavlic, G., Oakey, G., Jauer, C., and Decker, V., 2013. Reconnaissance mapping of suspect oil seep occurrences in Baffin Bay and Davis Strait using satellite radar: preliminary results; Geological Survey of Canada, Open File 7068, 1 .zip file. https://doi.org/10.4095/292280

Burden, E. and Holloway, D., 1985. Palynology and age of the Scott Inlet inliers of Baffin Island (Northwest Territories); Canadian Journal of Earth Sciences, v. 22, p. 1542–1545. https://doi.org/10.1139/e85-160

Burden, E.T. and Langille, A.B., 1990. Stratigraphy and sedimentology of Cretaceous and Paleocene strata in half-grabens on the southeast coast of Baffin Island, Northwest Territories; Bulletin of Canadian Petroleum Geology, v. 38, no. 2, p. 185–196.

Burden, E.T. and Langille, A.B., 1991. Palynology of Cretaceous and Tertiary strata, northeast Baffin Island, Northwest Territories, Canada: implications for the history of rifting in Baffin Bay; Palynology, v. 15, p. 91–114. https://doi.org/10.1080/01916122.1991.9989392

Campbell, H. and MacLeod, M., 2014. Mary River project: 2013 exploration program highlights rand outline of 2014 program; Nunavut Mining Symposium PowerPoint Presentation [Baffinland Iron Mines Corporation]. <https://www.nunavutminingsymposium.ca/2014-presentations> [accessed January 18, 2017]

Carey, J.S., McCartney, T., Hanna, M.C., Lister, C., and Keng, L.E., 2020. Qualitative petroleum resource assessment of the Labrador margin; Geological Survey of Canada, Open File 8535, 104 p. https://doi.org/10.4095/326017

Chian, D., Louden, K.E., and Reid, I., 1995. Crustal structure of the Labrador Sea conjugate margin and implications for the formation of nonvolcanic continental margins; Journal of Geophysical Research, v. 100, no. B12, p. 24239–24253. https://doi.org/10.1029/95JB02162

Christiansen, F.G., 2011. Greenland petroleum exploration: history, breakthroughs in understanding and future challenges; *in* Artic Petroleum Geology, (ed.) A.M. Spencer, A.F. Embry, D.L. Gautier, A.V. Stoupakova, and K. Sørensen; Geological Society of London, Memoirs, v. 35, p. 647–661. https://doi.org/10.1144/M35.42

Clarke, D.B., 1970. Tertiary basalts in Baffin Bay: possible primary magma from the mantle; Contributions to Mineralogy and Petrology, v. 25, p. 203–224. https://doi.org/10.1007/BF00371131

Clarke, D.B. and Beutel, E.K., 2020. Davis Strait Paleocene picrites: products of a plume or plates?; Earth-Science Reviews, v. 206, art. no. 102770. https://doi.org/10.1016/j.earscirev.2019.01.012

Dam, G., Pedersen, G.K., Sønderholm, M., Midtgaard, H., Larsen, L.M., Nøhr-Hansen, H., and Pedersen, A.K., 2009. Lithostratigraphy of the Cretaceous-Paleocene Nuussuaq Group, Nuussuaq Basin, West Greenland; Geological Survey of Denmark and Greenland Bulletin, v. 19, 171 p. https://doi.org/10.34194/geusb.v19.4886

Decker, V., Budkewitsch, P., and Tang, W., 2013. Database of suspect oil seeps in the marine environment of Baffin Bay and Davis Strait, Nunavut, identified from a survey of RADARSAT-2 data; Geological Survey of Canada, Open File 7404, 12 p. https://doi.org/10.4095/292761

Denyszyn, S.W., Davis, D.W., and Halls, H.C., 2009. Paleomagnetism and U-Pb geochronology of the Clarence Head dikes, Arctic Canada: orthogonal emplacement of mafic dikes in a large igneous province; Canadian Journal of Earth Sciences, v. 46, p. 155–167. https://doi.org/10.1139/E09-011

Dickie, K., Keen, C.E., Williams, G.L., and Dehler, S.A., 2011. Tectonostratigraphic evolution of the Labrador margin, Atlantic Canada; Marine and Petroleum Geology, v. 28, p. 1663–1675. https://doi.org/10.1016/j.marpetgeo.2011.05.009

Dunphy, J.M. and Ludden, J.N., 1998. Petrological and geochemical characteristics of a Paleoproterozoic magmatic arc (Narsajuaq Terrane, Ungava Orogen, Canada) and comparisons to Superior Province granitoids; Precambrian Research, v. 91, p. 109–142. https://doi.org/10.1016/S0301-9268(98)00041-2

Earthquakes Canada, 2018. Simplified seismic hazard map for Canada, the provinces and territories. <https://www.earthquakescanada.nrcan.gc.ca/hazard-alea/simphaz-en.php> [accessed March 4, 2020].

Elgin, R.A., 2017. Status and implications of reserves at carving stone quarries within the Qikiqtaaluk Region of Nunavut; *in* Summary of Activities 2017; Canada-Nunavut Geoscience Office, p. 151–158.

Fahrig, W.F., Christie, K.W., and Jones, D.L., 1981. Paleomagnetism of the Bylot basins: evidence for Mackenzie continental tensional tectonics; Geological Survey of Canada, Paper 81-10, p. 303–312. https://doi.org/10.4095/109368

Funck, T., Jackson, H.R., Louden, K.E., and Klingelhöfer, F., 2007. Seismic study of the transform-rifted margin in Davis Strait between Baffin Island (Canada) and Greenland: what happens when a plume meets a transform; Journal of Geophysical Research, v. 112, no. B4, 22 p. https://doi.org/10.1029/2006JB004308

Funck, T., Gohl, K., Damm, V., and Heyde, I., 2012. Tectonic evolution of southern Baffin Bay and Davis Strait: results from a seismic refraction transect between Canada and Greenland; Journal of Geophysical Research, v. 117, no. B4, 24 p. https://doi.org/10.1029/2011JB009110

Gautier, D.L., Bird, K.J., Charpentier, R.R., Grantz, A., Houseknecht, D.W., Klett, T.R., Moore, T.E., Pitman, J.K., Schenk, C.J., Schuenemeyer, J.H., Sørensen, K., Tennyson, M.E., Valin, Z.C., and Wandrey, C.J., 2011. Oil and gas resource potential north of the Arctic Circle; Chapter 9 *in* Arctic Petroleum Geology, (ed.) A.M. Spencer, A.F. Embry, D.L. Gautier, A.V. Stoupakova, and K. Sørensen; Geological Society of London, Memoirs, v. 35, p. 151–161. https://doi.org/10.1144/M35.9

Gibson, T.M., Shih, P.M., Cumming, V.M., Fischer, W.W., Crockford, P.W., Hodgskiss, M.S.W., Worndle, S., Creaser, R., Rainbird, R.H., Skulski, T.M., and Halverson, G.P., 2018. Precise age of *Bangiomorpha pubescens* dates the origin of eukaryotic photosynthesis; Geology, v. 46, p. 135–138. https://doi.org/10.1130/G39829.1

Gibson, T.M., Worndle, S., Crockford, P.W., Bui, T.H., Creaser, R.A., and Halverson, G.P., 2019. Radiogenic isotope chemostratigraphy reveals marine and nonmarine depositional environments in the late Mesoproterozoic Borden Basin, Arctic Canada; Geological Society of America Bulletin, v. 131, no. 11-12, p. 1965–1978. https://doi.org/10.1130/B35060.1

Government of Canada, 2018. Arctic offshore oil and gas. <www.rcaanc-cirnac.gc.ca/eng/1535571547022/1538586415269> [accessed May 23, 2019]

Grant, A.C., Levy, E.M., Lee, K., and Moffat, J.D., 1986. Pisces IV research submersible finds oil on Baffin Shelf; *in* Current Research, Part A; Geological Survey of Canada, Paper 86-1A, p. 65–69. https://doi.org/10.4095/120351

Gregersen, U., 2014. The West Greenland continental margin; *in* Tectonostratigraphic Atlas of the North-East Atlantic region, (ed.) J.R. Hopper, T. Funck, M. Stoker, U. Árting, G. Peron-Pinvidic, H. Dorrnenbal, and C. Gaina; Geological Survey of Denmark and Greenland, Copenhagen, Denmark, p. 321–325.

Gregersen, U., Hopper, J.R., and Knutz, P.C., 2013. Basin seismic stratigraphy and aspects of prospectivity in the NE Baffin Bay, northwest Greenland; Marine and Petroleum Geology, v. 46, p. 1–18. https://doi.org/10.1016/j.marpetgeo.2013.05.013

Gregersen, U., Andersen, M.S., Nøhr-Hansen, H., Sheldon, E., Kokfelt, T.F., Olivarius, M., Knudsen, C., Jakobsen, K.G., and Adolfssen, J.S., 2018. New subsurface mapping offshore southern West Greenland using geophysical and geological data; Geological Survey of Denmark and Greenland Bulletin, v. 41, p. 57–62. https://doi.org/10.34194/geusb.v41.4342

Gregersen, U., Knutz, P.C., Nøhr-Hansen, H., Sheldon, E., and Hopper, J.R., 2019. Tectonostratigraphy and evolution of the West Greenland continental margin; Bulletin of the Geological Society of Denmark, v. 67, p. 1–21. https://doi.org/10.37570/bgsd-2019-67-01

Hahn, K.E. and Turner, E.C., 2017. Composition and history of giant lacustrine carbonate seep mounds, Mesoproterozoic Borden Basin, Arctic Canada; Precambrian Research, v. 293, p. 150–173. https://doi.org/10.1016/j.precamres.2017.03.009

Hahn, K., Turner, E.C., Babechuk, M.G., and Kamber, B.S., 2015. Deep-water seep-related carbonate mounds in a Mesoproterozoic alkaline lake, Borden Basin (Nunavut, Canada); Precambrian Research, v. 271, p. 173–197. https://doi.org/10.1016/j.precamres.2015.09.025

Harrison, J.C., Brent, T.A., and Oakey, G.N., 2011. Baffin Fan and its inverted rift system of Arctic eastern Canada: stratigraphy, tectonics and petroleum resource potential; Chapter 40 *in* Arctic Petroleum Geology, (ed.) A.M. Spencer, A.F. Embry, D.L. Gautier, A.V. Stoupakova, and K. Sørensen; Geological Society of London, Memoirs, v. 35, p. 595–626. https://doi.org/10.1144/M35.40

Heaman, L.M., LeCheminant, A.N., and Rainbird, R.H., 1992. Nature and timing of Franklin igneous events, Canada: implications for a Late Proterozoic mantle plume and the breakup of Laurentia; Earth and Planetary Science Letters, v. 109, p. 117–131. https://doi.org/10.1016/0012-821X(92)90078-A

Heaman, L.M., Pell, J., Gruetter, H.S., and Creaser, R.A., 2015. U-Pb geochronology and Sr/Nd isotope compositions of groundmass perovskite from the newly discovered Jurassic Chidliak kimberlite field, Baffin Island, Canada; Earth and Planetary Science Letters, v. 415, p. 183–199. https://doi.org/10.1016/j.epsl.2014.12.056

Henriksen, N., Higgins, A.K., Kalsbeek, F., and Pulvertaft, T.C., 2009. Greenland from Archean to Quaternary. Descriptive text to the 1995 Geological map of Greenland 1:2 500 000, 2nd edition; Geological Survey of Denmark and Greenland Bulletin, v. 18, 126 p. https://doi.org/10.34194/geusb.v18.4993

Hogarth, D.D., Boreham, P.W., and Mitchell, J.G., 1994. Martin Frobisher's northwest venture, 1576-1581: mines, minerals & metallurgy; Canadian Museum of Civilization, Mercury Series, Directorate paper no. 7, 181 p.

Hosseinpour, M., Muller, R.D., Williams, S.E., and Whittaker, J.M., 2013. Full-fit reconstruction of the Labrador Sea and Baffin Bay; Solid Earth, v. 4, p. 461–479. https://doi.org/10.5194/se-4-461-2013

Iannelli, T., Robatian, M., Breckon, S., Campbell, H., Dao, P., and MacLeod, M., 2013a. Baffinland–Assessment Report: rock sampling, prospecting, geological mapping and geophysical surveying; report prepared for Indian and Northern Affairs Canada, Assessment Report #085816. <https://nunavutgeoscience.ca/gateway/browseA.php> [accessed April 25, 2022]

Iannelli, T., Robatian, M., Breckon, S., Campbell, H., Dao, P., and MacLeod, M., 2013b. Baffinland–Assessment Report: rock sampling, prospecting, geological mapping, and geophysical surveying; report prepared for Indian and Northern Affairs Canada, Assessment Report #085823. <https://nunavutgeoscience.ca/gateway/browseA.php> [accessed April 25, 2022]

Ioannides, N.S., 1986. Dinoflagellate cysts from Upper Cretaceous-Lower Tertiary sections, Bylot and Devon islands, Arctic Archipelago; Geological Survey of Canada, Bulletin 371, 99 p. https://doi.org/10.4095/123641

Jackson, G.D. and Davidson, A., 1975. Geology, Bylot Island, District of Franklin; Geological Survey of Canada, Map 1397A, scale 1:250 000. https://doi.org/10.4095/109007

Jackson, G.D. and Iannelli, T.R., 1981. Rift-related cyclic sedimentation in the Neohelikian Borden Basin, northern Baffin Island; Geological Survey of Canada, Paper 81-10, p. 269–302. https://doi.org/10.4095/109369

Jackson, G.D. and Morgan, W.C., 1978. Geology, Conn Lake, District of Franklin; Geological Survey of Canada, Map 1458A, scale 1:250 000. https://doi.org/10.4095/109162

Jackson, G.D. and Taylor, F.C., 1972. Correlation of major Aphebian rock units in the northeastern Canadian Shield; Canadian Journal of Earth Sciences, v. 9, p. 1650–1669. https://doi.org/10.1139/e72-146

Jackson, G.D., Davidson, A., and Morgan, W.C., 1975. Geology of the Pond Inlet map-area, Baffin Island, District of Franklin (38A, 38B, part of 48A); Geological Survey of Canada, Paper 74-25, 33 p. https://doi.org/10.4095/102498

Jackson, G.D., Morgan, W.C., and Davidson, A., 1979. Geology, Buchan Gulf-Scott Inlet, District of Franklin; Geological Survey of Canada, Map 1449A, scale 1:250 000. https://doi.org/10.4095/109159

James, T.S. and Schamehorn, T.D., 2016. A comparison of seismicity to the crustal deformation predicted by a glacial isostatic adjustment model in northern Canada and western Greenland; Geological Survey of Canada, Open File 8106, 18 p. https://doi.org/10.4095/299098

Jansa, L.F., 1976. Lower Paleozoic radiolarian-bearing limestones from the Baffin Island shelf; *in* Report of Activities, Part B; Geological Survey of Canada, Paper 76-1B, p. 99–105. https://doi.org/10.4095/104085

Keen, C.E., Dickie, K., and Dehler, S.A., 2012. The volcanic margins of the northern Labrador Sea: insights to the rifting process; Tectonics, v. 31, no. 1, 13 p. https://doi.org/10.1029/2011TC002985

Keen, C.E., Dickie, K., and Dafoe, L.T., 2018a. Structural characteristics of the ocean-continent transition along the rifted continental margin, offshore central Labrador; Marine and Petroleum Geology, v. 89, no. 2, p. 443–463. https://doi.org/10.1016/j.marpetgeo.2017.10.012

Keen, C.E., Dickie, K., and Dafoe, L.T., 2018b. Structural evolution of the rifted margin off northern Labrador: the role of hyper-extension and magmatism; Tectonics, v. 37, no. 7, p. 1955–1972. https://doi.org/10.1029/2017TC004924

Larsen, L.M., Heaman, L.M., Creaser, R.A., Duncan, R.A., Frei, R., and Hutchison, M., 2009. Tectonomagmatic events during stretching and basin formation in the Labrador Sea and the Davis Strait: evidence from age and composition of Mesozoic to Palaeogene dyke swarms in West Greenland; Journal of the Geological Society, v. 166, no. 6, p. 999–1012. https://doi.org/10.1144/0016-76492009-038

LeCheminant, A.N. and Heaman, L.M., 1989. Mackenzie igneous events, Canada: middle Proterozoic hotspot magmatism associated with ocean opening; Earth and Planetary Science Letters, v. 96, p. 38–48. https://doi.org/10.1016/0012-821X(89)90122-2

Lemon, R.R.H. and Blackadar, R.G., 1963. Admiralty Inlet area, Baffin Island, District of Franklin; Geological Survey of Canada, Memoir 328, 84 p. https://doi.org/10.4095/108031

Long, D.G.F. and Turner, E.C., 2012. Tectonic, sedimentary and metallogenic re-evaluation of basal strata in the Mesoproterozoic Bylot basins (NU): are unconformity-type U concentrations a realistic expectation; Precambrian Research, v. 214-215, p. 192–209. https://doi.org/10.1016/j.precamres.2011.11.005

MacLean, B., Jansa, L.F., Falconer, R.K.H., and Srivastava, S.P., 1977. Ordovician strata on the southeastern Baffin Island shelf revealed by shallow drilling; Canadian Journal of Earth Sciences, v. 14, p. 1925–1939. https://doi.org/10.1139/e77-163

MacLean, B., Williams, G., and Zhang, S., 2014. New insights into the stratigraphy and petroleum potential of the Baffin Shelf's Cretaceous rocks; Bulletin of Canadian Petroleum Geology, v. 62, no. 4, p. 289–310. https://doi.org/10.2113/gscpgbull.62.4.289

McMillan, J.G., 1910. Geologist's report on the Arctic Expedition, 1908–1909; *in* Cruise of the Arctic 1908-1909, (ed.) J.E. Bernier; Government Printing Bureau, Ottawa, Ontario, 529 p.

McWhae, J.R.H., Elie, R., Laughton, K.C., and Gunther, P.R., 1980. Stratigraphy and petroleum prospects of the Labrador Shelf; Bulletin of Canadian Petroleum Geology, v. 28, p. 460–488.

Miall, A.D., Balkwill, H.R., and Hopkins, W.S., Jr., 1980. Cretaceous and tertiary sediments of Eclipse trough, Bylot Island area, Arctic Canada, and their regional setting; Geological Survey of Canada, Paper 79-23, 20 p. https://doi.org/10.4095/102162

Moir, P.S., 1989. Lithostratigraphy Labrador Sea: review and type sections; *in* East Coast Basin Atlas Series, Labrador Sea, (ed.) J.S. Bell; Geological Survey of Canada, p. 26–27. https://doi.org/10.4095/127166

Nantais, P., 1984. Regional hydrocarbon potential of the Labrador Shelf; Geological Survey of Canada, Open File 1197, 50 p. https://doi.org/10.4095/130015

Newman, L.A., 1987. Quaternary stratigraphy of the Scott Lowland, Baffin Island, Northwest Territories; B.Sc. thesis, Memorial University of Newfoundland, St. John's, Newfoundland and Labrador, 53 p.

Nøhr-Hansen, H., Williams, G.L., and Fensome, R.A., 2016. Biostratigraphic correlation of the western and eastern margins of the Labrador–Baffin Seaway and implications for the regional geology; Geological Survey of Denmark and Greenland Bulletin, v. 37, 74 p. https://doi.org/10.34194/geusb.v37.4356

Oakey, G.N. and Chalmers, J.A., 2012. A new model for the Paleogene motion of Greenland relative to North America: plate reconstructions of the Davis Strait and Nares Strait regions between Canada and Greenland; Journal of Geophysical Research, v. 117, no. B10, 28 p. https://doi.org/10.1029/2011JB008942

Peace, A.L., Foulger, G.R., Schiffer, C., and McCaffrey, K.J.W., 2017. Evolution of Labrador Sea-Baffin Bay: plate or plume processes?; Geoscience Canada, v. 44, p. 91–102. https://doi.org/10.12789/geocanj.2017.44.120

Pehrsson, S.J. and Buchan, K.L., 1999. Borden dykes of Baffin Island, N.W.T.: a Franklin U-Pb baddeleyite age and a paleomagnetic interpretation; Canadian Journal of Earth Sciences, v. 36, p. 65–73. https://doi.org/10.1139/e98-091

Rainbird, R., Cawood, P., and Gehrels, G.E., 2012. The Great Grenvillian sedimentation episode: record of supercontinent Rodinia's assembly; *in* Recent Advances in Tectonics of Sedimentary Basins, (ed.) C. Busby and A. Azor; Blackwell Publishing Ltd., Oxford, United Kingdom, p. 583–601. https://doi.org/10.1002/9781444347166.ch29

Rayner, N.M., Sanborn-Barrie, M., Young, M.D., and Whalen, J.B., 2012. U-Pb ages of Archean basement and Paleoproterozoic plutonic rocks, southern Cumberland Peninsula, eastern Baffin Island, Nunavut; Geological Survey of Canada, Current Research 2012-8, 28 p. https://doi.org/10.4095/291401

Roest, W.R. and Srivastava, S.P., 1989. Sea-floor spreading in the Labrador Sea: a new reconstruction; Geology, v. 17, no. 11, p. 1000–1003. https://doi.org/10.1130/0091-7613(1989)017%3c1000:SFSITL%3e2.3.CO%3b2

Sanborn-Barrie, M., Thrane, K., Wodicka, N., and Rayner, N., 2017. The Laurentia - West Greenland connection at 1.9 Ga: New insights from the Rinkian fold belt; Gondwana Research, v. 51, p. 289–309. https://doi.org/10.1016/j.gr.2017.07.002

Sanford, B.V. and Grant, A.C., 1990. New findings relating to the stratigraphy and structure of the Hudson Platform; *in* Current Research, Part D; Geological Survey of Canada, Paper 90-1D, p. 17–30. https://doi.org/10.4095/131335

Sanford, B.V. and Grant, A.C., 2000. Geological framework of the Ordovician system in the southeast Arctic Platform, Nunavut; *in* Geology and Paleontology of the Southeast Arctic Platform and Southern Baffin Island, Nunavut, (ed.) A.D. McCracken and T.E. Bolton; Geological Survey of Canada, Bulletin 557, p. 13–38. https://doi.org/10.4095/211845

Sangster, D.F., 1998. Mineral deposits compilation and metallogenic domains, northern Baffin Island and northern Melville Peninsula, Northwest Territories; Geological Survey of Canada, Open File 3635, scale 1:1 000 000. https://doi.org/10.4095/210026

Saumur, B.M., Skipton, D.R., St-Onge, M.R., Bros, E.R., Acosta-Gongora, P., Kelly, C.J., Morin, A., O'Brien, M.E., Johnston, S.T., and Weller, O.M., 2018. Precambrian geology of the surroundings of Steensby Inlet and western Barnes Ice Cap (parts of NTS 37E, 37F, 37G), Baffin Island, Nunavut; *in* Summary of Activities 2018; Canada-Nunavut Geoscience Office, p. 29–46.

Scott, D.J., 1997. Geology, U-Pb, and Pb-Pb geochronology of the Lake Harbour area, southern Baffin Island: Implications for the Paleoproterozoic tectonic evolution of northeastern Laurentia; Canadian Journal of Earth Sciences, v. 34, p. 140–155. https://doi.org/10.1139/e17-012

Scott, D.J. and de Kemp, E.A., 1998. Bedrock geology compilation, northern Baffin Island and northern Melville Peninsula; Geological Survey of Canada, Open File 3633, scale 1:500 000. https://doi.org/10.4095/210024

Scott, D.J. and Wodicka, N.A., 1998. Second report on the U-Pb geochronology of southern Baffin Island, Northwest Territories; *in* Current Research 1998-F; Geological Survey of Canada, p. 47–57. https://doi.org/10.4095/210055

Sherman, A.G., James, N.P., and Narbonne, G.M., 2002. Evidence for reversal of basin polarity during carbonate ramp development in the Mesoproterozoic Borden Basin, Baffin Island; Canadian Journal of Earth Sciences, v. 39, p. 519–538. https://doi.org/10.1139/e01-089

Skipton, D.R., Saumur, B.M., St-Onge, M.R., Wodicka, N., Bros, E.R., Morin, A., Brouillette, P., Weller, O.M., and Johnston, S.T., 2017. Precambrian bedrock geology of the Pond Inlet-Mary River area, northern Baffin Island; *in* Summary of Activities 2018; Canada-Nunavut Geoscience Office, p. 49–67.

Sparkes, K.E., 1989. Stratigraphy and terrestrial palynology of Late Cretaceous Eclipse Group strata, Bylot Island, Northwest Territories, Canada; B.Sc. thesis, Memorial University of Newfoundland, St. John's, Newfoundland and Labrador, 195 p.

Srivastava, S.P., 1978. Evolution of the Labrador Sea and its bearing on the early evolution of the North Atlantic; Geophysical Journal International, v. 52, p. 313–357. https://doi.org/10.1111/j.1365-246X.1978.tb04235.x

St-Onge, M.R., Hanmer, S., and Scott, D.J., 1996. Geology of the Meta Incognita Peninsula, south Baffin Island, Northwest Territories: tectonostratigraphic units and regional correlations; *in* Current Research 1996-C; Geological Survey of Canada, p. 63–72. https://doi.org/10.4095/207444

St-Onge, M.R., Scott, D.J., and Lucas, S.B., 2000. Early partitioning of Quebec: microcontinent formation in the Paleoproterozoic; Geology, v. 28, p. 323–326. https://doi.org/10.1130/0091-7613(2000)28%3c323:EPOQMF%3e2.0.CO%3b2

St-Onge, M.R., Searle, M.P., and Wodicka, N., 2006. Trans-Hudson Orogen of North America and Himalaya-Karakoram-Tibetan Orogen of Asia: structural and thermal characteristics of the lower and upper plates; Tectonics, v. 25, no. 4, 22 p. https://doi.org/10.1029/2005TC001907

St-Onge, M.R., Van Gool, J.A.M., Garde, A.A., and Scott, D.J., 2009. Correlation of Archaean and Palaeoproterozoic units between northeastern Canada and western Greenland: constraining the pre-collisional upper plate accretionary history of the Trans-Hudson orogen; Geological Society of London, Special Publications, v. 318, p. 193–235. https://doi.org/10.1144/SP318.7

St-Onge, M.R., Weller, O.M., and Rayner, N.M., 2016. 2016 report of activities for completing the regional bedrock mapping of the southern half of Baffin Island: GEM 2 Baffin Project; Geological Survey of Canada, Open File 8118, 11 p. https://doi.org/10.4095/299195

Steenkamp, H.M., Pizzo-Lyall, M., Wallace, C.J., Beauregard, M.A., and Dyck, B.J., 2014. Geology, history and site-management planning of the Kangiqsukutaaq carving stone quarry, southern Baffin Island; *in* Summary of Activities 2013; Canada-Nunavut Geoscience Office, p. 193–200.

Steenkamp, H.M., Beauregard, M.A., and Mate, D.J., 2015. Carving stone and mineral resource potential of the Opingivik deposit, southern Baffin Island; *in* Summary of Activities 2014; Canada-Nunavut Geoscience Office, p. 153–162.

Storey, M., Duncan, R.A., and Tegner, C., 2007. Timing and duration of volcanism in the North Atlantic Igneous Province: implications for geodynamics and links to the Iceland hotspot; Chemical Geology, v. 241, no. 3-4, p. 264–281. https://doi.org/10.1016/j.chemgeo.2007.01.016

Suckro, S.K., Gohl, K., Funck, T., Heyde, I., Ehrhardt, A., Schreckenberger, B., Gerlings, J., Damm, V., and Jokat, W., 2012. The crustal structure of southern Baffin Bay: implications from a seismic refraction experiment; Geophysical Journal International, v. 190, no. 1, p. 37–58. https://doi.org/10.1111/j.1365-246X.2012.05477.x

Suckro, S.K., Gohl, K., Funck, T., Heyde, I., Schreckenberger, B., Gerlings, J., and Damm, V., 2013. The Davis Strait crust—a transform margin between two oceanic basins; Geophysical Journal International, v. 193, no. 1, p. 78–97. https://doi.org/10.1093/gji/ggs126

Taylor, F.B., 1910. Bearing of the Tertiary mountain belt on the origin of the Earth's plan; Geological Society of America Bulletin, v. 21, p. 179–226. https://doi.org/10.1130/GSAB-21-179

Thériault, R.J., St-Onge, M.R., and Scott, D.J., 2001. Nd isotopic and geochemical signature of the Paleoproterozoic Trans-Hudson Orogen, southern Baffin Island, Canada: implications for the evolution of eastern Laurentia; Precambrian Research, v. 108, p. 113–138. https://doi.org/10.1016/S0301-9268(00)00159-5

Trettin, H.P., 1965a. Middle Ordovician to Middle Silurian carbonate cycle, Brodeur Peninsula, northwestern Baffin Island; Bulletin of Canadian Petroleum Geology, v. 13, p. 155–180.

Trettin, H.P., 1965b. Lower Paleozoic sediments of northwestern Baffin Island, District of Franklin; Geological Survey of Canada, Paper 64-47, 28 p. https://doi.org/10.4095/101000

Trettin, H.P., 1969. Lower Paleozoic sediments of northwestern Baffin Island; Geological Survey of Canada, Bulletin 157, 70 p. https://doi.org/10.4095/102249

Trettin, H.P., 1975. Investigations of Lower Paleozoic geology, Foxe Basin, northeastern Melville Peninsula, and parts of northwestern and central Baffin Island; Geological Survey of Canada, Bulletin 251, 177 p. https://doi.org/10.4095/103973

Turner, E.C., 2009. Mesoproterozoic carbonate systems in the Borden Basin, Nunavut; Canadian Journal of Earth Sciences, v. 46, p. 915–938. https://doi.org/10.1139/E09-062

Turner, E.C., 2011. Structural and stratigraphic controls on carbonate-hosted base-metal mineralization in the Mesoproterozoic Borden Basin (Nanisivik District), Nunavut; Economic Geology and the Bulletin of the Society of Economic Geologists, v. 106, p. 1197–1223. https://doi.org/10.2113/econgeo.106.7.1197

Turner, E.C. and Kamber, B.S., 2012. Arctic Bay Formation, Borden Basin, Nunavut (Canada): Basin evolution, black shale base-metal potential and dissolved metal systematics in the Mesoproterozoic ocean; Precambrian Research, v. 208–211, p. 1–18. https://doi.org/10.1016/j.precamres.2012.03.006

Turner, E.C., Long, D.G.F., Rainbird, R.H., Petrus, J.A., and Rayner, N.M., 2016. Late Mesoproterozoic rifting in Arctic Canada during Rodinia assembly: impactogens, trans-continental far-field stress, and zinc mineralisation; Terra Nova, v. 28, p. 188–194. https://doi.org/10.1111/ter.12207

Umpleby, D.C., 1979. Geology of the Labrador Shelf; Geological Survey of Canada, Paper 79-13, 40 p. https://doi.org/10.4095/105927

Vande Guchte, M.J., 1998. Geological, geochemical and geophysical report on the Incognito joint venture project [Rubicon Minerals Corp.]; Aboriginal Affairs and Northern Development Canada, Assessment Report 084053. <https://nunavutgeoscience.ca/gateway/browseA.php> [accessed April 25, 2022]

Vande Guchte, M.J. and Gray, M.J., 1999. Geological, geochemical and diamond drilling report on the Incognito joint venture project, 1997 exploration program [Rubicon Minerals Corp.]; Aboriginal Affairs and Northern Development Canada, Assessment Report 084168. <https://nunavutgeoscience.ca/gateway/browseA.php> [accessed April 25, 2022]

Voss, P., Poulsen, S.K., Simonsen, S.B., and Gregersen, S., 2007. Seismic hazard assessment of Greenland; Geological Survey of Denmark and Greenland Bulletin, v. 13, p. 57–60. https://doi.org/10.34194/geusb.v13.4976

Waterfield, J.J., 1989. Stratigraphy, sedimentology and palynology of Cretaceous and Tertiary strata, southwest Bylot Island, Northwest Territories, Canada; M.Sc. thesis, Memorial University of Newfoundland, St. John's, Newfoundland and Labrador, 260 p.

Welford, J.K. and Hall, J., 2013. Lithospheric structure of the Labrador Sea from constrained 3-D gravity inversion; Geophysical Journal International, v. 195, no. 2, p. 767–784. https://doi.org/10.1093/gji/ggt296

Welford, J.K., Peace, A.L., Geng, M., Dehler, S.A., and Dickie, K., 2018. Crustal structure of Baffin Bay from constrained three-dimensional gravity inversion and deformable plate tectonic models; Geophysical Journal International, v. 214, p. 1281–1300. https://doi.org/10.1093/gji/ggy193

Wiseman, T.R., 1991. Sedimentology of the Maastrichtian, Pond Inlet Formation (channelized turbidite system), Bylot Island, Northwest Territories, Canada; B.Sc. thesis, Memorial University of Newfoundland, St. John's, Newfoundland and Labrador, 133 p.

Wodicka, N. and Scott, D.J., 1997. A preliminary report on the U-Pb geochronology of the Meta Incognita Peninsula, southern Baffin Island, Northwest Territories; *in* Current Research 1997-C; Geological Survey of Canada, p. 167–178. https://doi.org/10.4095/208642

Wodicka, N., St-Onge, M.R., Corrigan, D., Scott, D.J., and Whalen, J.B., 2014. Did a proto-ocean basin form along the southeastern Rae cratonic margin? Evidence from U-Pb geochronology, geochemistry (Sm-Nd and whole-rock), and stratigraphy of the Paleoproterozoic Piling Group, northern Canada; Geological Society of America Bulletin, v. 126, p. 1625–1653. https://doi.org/10.1130/B31028.1

Contents

Introduction et sommaire

N. Bingham-Koslowski[1*], L.T. Dafoe[2], M.R. St-Onge[1], E.C. Turner[3], J.W. Haggart[4], U. Gregersen[5], C.E. Keen[2], A.L. Bent[6] et J.C. Harrison[1]

Bingham-Koslowski, N., Dafoe, L.T., St-Onge, M.R., Turner, E.C., Haggart, J.W., Gregersen, U., Keen, C.E., Bent, A.L. et Harrison, J.C., 2022. Introduction et sommaire; in *Geological synthesis of Baffin Island (Nunavut) and the Labrador–Baffin Seaway, (éd.) L.T. Dafoe et N. Bingham-Koslowski; Commission géologique du Canada, Bulletin 608, p. 13–24. https://doi.org/10.4095/330002*

Résumé : Les articles contenus dans le présent bulletin offrent un résumé complet et une mise à jour de nos connaissances de la géologie côtière et de l'évolution de l'île de Baffin, du bras de mer Labrador-Baffin et des régions côtières environnantes. Cet article d'introduction résume et relie les événements géologiques et tectoniques qui ont contribué à l'évolution du craton et des bassins sédimentaires subséquents s'échelonnant du Protérozoïque au Cénozoïque. Plus précisément, nous examinons la géologie du Précambrien et du Paléozoïque de l'île de Baffin et celle d'occurrences localisées de roches de ces âges dans le sous-sol du bras de mer Labrador-Baffin adjacent, la stratigraphie du Mésozoïque au Cénozoïque ainsi que l'histoire du rift qui rend compte de l'ouverture et de l'évolution du bras de mer Labrador-Baffin, la sismicité de la région, ainsi que le potentiel en ressources minérales (île de Baffin) et en hydrocarbures (à terre et en mer).

[1]Commission géologique du Canada, 601, rue Booth, Ottawa (Ontario) K1A 0E8
[2]Commission géologique du Canada, 1 Challenger Drive, P.O. Box 1006, Dartmouth (Nouvelle-Écosse) B2Y 4A2
[3]École des sciences de la Terre Harquail, Université Laurentienne, Sudbury (Ontario) P3E 2C6
[4]Commission géologique du Canada, 1500-605 Robson Street, Vancouver (Colombie-Britannique) V6B 5J3
[5]Geological Survey of Denmark and Greenland (GEUS), Øster Voldgade 10, DK-1350, Copenhague K, Danemark
[6]Service canadien d'information sur les risques, 930, avenue Carling, Ottawa (Ontario) K1A 0Y3
*Auteur correspondant : N. Bingham-Koslowski (courriel : Nikole.Bingham-Koslowski@nrcan-rncan.gc.ca)

VUE D’ENSEMBLE

Entre la marge nord-est du Canada et l’ouest du Groenland se trouve une vaste région comprenant le bras de mer Labrador-Baffin et ses marges côtières, qui comprennent entre autres l’île de Baffin, l’île Bylot et l’ouest du Groenland (fig. 1). La géologie propre à cette région témoigne de nombreux événements tectoniques successifs, à commencer par l’assemblage de cratons au Paléoprotérozoïque pour former la partie laurentienne du supercontinent Nuna (St-Onge et al., 2009). Une déformation par extension localisée au Mésoprotérozoïque a créé les bassins de Bylot qui s’étendent au nord de l’île de Baffin et se prolongent sous la partie nord de la baie de Baffin ainsi que dans les zones côtières environnantes (Fahrig et al., 1981). Au début du Paléozoïque, des successions sédimentaires de plate-forme se sont accumulées après la rupture du supercontinent Rodinie (Bell et Howie, 1990). La sédimentation a cessé avec la fermeture des bras de mer du Paléozoïque et la formation du supercontinent Pangée. Par la suite, la Pangée a été soumise à une déformation par extension dans la région du bras de mer Labrador-Baffin à partir du Crétacé précoce (Roest et Srivastava, 1989). Il en a résulté une séparation éventuelle du Groenland de la paléoplaque nord-américaine, créant une ouverture qui a pris naissance au Maastrichtien et s’est étendue à l’échelle régionale à partir du Paléocène jusqu’à ce que l’expansion des fonds marins cesse à la fin du Paléogène (Oakey et Chalmers, 2012; Keen et al., 2018a, b). Ce rifting et l’expansion des fonds marins ont entraîné la formation du bras de mer Labrador-Baffin, une région qui comprend la mer du Labrador, le détroit de Davis et la baie de Baffin et qui renferme plusieurs grands bassins extracôtiers, ainsi que des bassins localisés en milieu terrestre.

Le programme Géocartographie de l’énergie et des minéraux (GEM), dirigé par la Commission géologique du Canada (CGC), a permis d’obtenir de nouveaux renseignements sur les aspects locaux et régionaux de l’histoire géologique complexe du bras de mer Labrador-Baffin et de ses marges côtières. Le programme en deux phases (GEM-1, de 2008 à 2013, et GEM-2, de 2013 à 2020) visait à promouvoir l’avancement économique durable dans le Nord du Canada en fournissant des connaissances géoscientifiques pour la prise de décisions liées à l’utilisation des terres et à la mise en valeur des ressources. Le programme GEM-2 comportait six régions d’intérêt dans le Nord du Canada, et la présente synthèse géologique se concentre sur la région d’étude qui comprend l’île de Baffin (Nunavut) et le bras de mer Labrador-Baffin. Dans cette région d’étude, les recherches scientifiques menées dans le cadre du programme GEM-2 comprenaient des études sur le terrain dans les îles de Baffin et Bylot effectuées par des scientifiques de la CGC et leurs collaborateurs externes pour mieux comprendre la géologie du socle rocheux précambrien (et le potentiel minéral qui s’y rattache) ainsi que les successions stratigraphiques du Mésozoïque au Cénozoïque. En plus de ces études sur le terrain, la recherche au large des côtes dans le bras de mer Labrador-Baffin a nécessité la compilation complète des données existantes, combinée à l’utilisation de techniques modernes et à la réalisation de nouvelles analyses pour étudier l’histoire stratigraphique du Paléozoïque ainsi que l’histoire du rifting et de la stratigraphie du Mésozoïque au Cénozoïque. Les travaux scientifiques du programme GEM-2, combinés aux contributions essentielles des collaborateurs, aux résultats dérivés du programme GEM-1 et aux connaissances issues d’études préexistantes, ont mené à l’élaboration du présent bulletin de la CGC.

Les articles inclus dans ce volume comprennent des résumés détaillés des connaissances géologiques et géophysiques antérieures, ainsi que de nouvelles connaissances suivant une approche régionale sur le sous-sol extracôtier du bras de mer Labrador-Baffin et sur les successions côtières et le socle rocheux de l’île de Baffin, de l’île Bylot et du bassin de Nuussuaq, offrant ainsi un aperçu complet et actualisé de la géologie et de l’histoire tectonique de la région. La géologie de la région est abordée sous l’angle de six sous-régions informelles définies dans le présent bulletin (île de Baffin, baie de Baffin occidentale, île Bylot, marge du Labrador et mer du Labrador centrale, détroit de Davis occidental et marge ouest du Groenland; fig. 1), les contributions étant regroupées en trois parties : géologie du Précambrien et du Paléozoïque inférieur; géologie du Mésozoïque au Cénozoïque et sismicité récente; et ressources. La première partie comprend un synopsis de la géologie de l’Archéen, du Paléoprotérozoïque, du Mésoprotérozoïque et du Paléozoïque inférieur de l’île de Baffin, ainsi que des occurrences extracôtières de roches du Paléozoïque inférieur dans le bras de mer Labrador-Baffin. La géologie du Mésozoïque au Cénozoïque de la deuxième partie a trait au rifting et à l’ouverture du bras de mer Labrador-Baffin et comprend des articles portant sur les successions stratigraphiques s’y rattachant qui se trouvent dans les sous-régions, à terre et au large des côtes. L’évolution stratigraphique et tectonique des marges conjuguées dans leur ensemble, ainsi que la sismicité récente observée dans les zones extracôtières et côtières environnantes sont également abordées. La troisième partie, sur les ressources, expose en détail les ressources minérales connues et potentiellement importantes sur le plan économique dans l’île de Baffin et les ressources en hydrocarbures dans le bras de mer Labrador-Baffin et sur la côte ouest du Groenland.

GÉOLOGIE DU PRÉCAMBRIEN ET DU PALÉOZOÏQUE INFÉRIEUR

L’île de Baffin repose sur des domaines structuraux accrétés de l’Archéen et du Paléoprotérozoïque, dont la partie nord du craton de Rae et la partie sud du microcontinent Meta Incognita. Les roches de ces domaines sont recouvertes localement dans le nord de l’île de Baffin par des roches mésoprotérozoïques du bassin de Borden. Les successions de plate-forme du Paléozoïque inférieur couvrent des parties du nord et du sud de l’île de Baffin et sont présentes au large des côtes dans le détroit de Davis occidental et le long de la marge du Labrador.

Roches cratoniques de l’Archéen et du Paléoprotérozoïque

L’article de St-Onge et al. (le présent volume) offre un aperçu des études géologiques menées dans l’île de Baffin, depuis les voyages transatlantiques de Martin Frobisher effectués pendant la deuxième moitié du XVIe siècle (Hogarth et al., 1994) jusqu’à la récente activité de cartographie du substratum rocheux du nord de l’île de Baffin (Saumur et al., 2018) du programme Géocartographie de l’énergie et des minéraux (GEM) de la Commission géologique du Canada (CGC). On y présente également les principaux domaines structuraux de l’Archéen et du Paléoprotérozoïque de l’île de Baffin et une synthèse de leur assemblage pendant une période d’agrégation continentale planétaire au Paléoprotérozoïque moyen.

Du nord au sud, quatre domaines structuraux sont reconnus. Le premier, constituant la partie orientale de la plaque supérieure, est le craton de Rae, qui comprend des orthogneiss, des roches plutoniques felsiques et des ensembles de roches supracrustales du socle archéen (Skipton et al., 2017), que surmontent en discordance le long de sa marge sud une couverture de roches supracrustales du Paléoprotérozoïque moyen (Groupe de Piling; Wodicka et al., 2014) et des unités semblables sur le plan stratigraphique du Groupe de Hoare Bay dans la péninsule Cumberland (Sanborn-Barrie et al., 2017). Une suite plutonique felsique du Paléoprotérozoïque moyen (suite plutonique de Qikiqtarjuaq; Rayner et al., 2012) recoupe à la fois le socle cratonique et les strates de la couverture de roches supracrustales. Le deuxième domaine structural comprend des unités métaplutoniques gneissiques de l’Archéen au Paléoprotérozoïque moyen et des unités tectonostratigraphiques de couverture du Paléoprotérozoïque moyen (Groupe de Lake Harbour; Jackson et Taylor, 1972), collectivement regroupées sous l’appellation « microcontinent Meta Incognita » par St-Onge et al. (2000), qui représente de la croûte dérivée par rifting du craton de Rae ou du craton du lac Supérieur, ou est allochtone par rapport à ces deux cratons (St-Onge et al., 2016). Le troisième domaine structural comprend surtout des orthogneiss monzogranitiques à granodioritiques du Paléoprotérozoïque moyen, et correspondrait, selon les interprétations, à un terrane d’arc magmatique déformé (terrane de Narsajuaq; Scott, 1997; Wodicka et Scott, 1997; Thériault et al., 2001; St-Onge et al., 2009). Le quatrième domaine structural est constitué d’orthogneiss tonalitiques à granitiques de l’Archéen, qui correspondraient au prolongement nord du socle cristallin du craton du lac Supérieur de la plaque inférieure, et de la couverture de roches supracrustales de marge continentale associée du Paléoprotérozoïque moyen (Groupe de Povungnituk; St-Onge et al., 1996).

Figure 1. Étendue couverte par la synthèse géologique du présent volume montrant les six sous-régions informelles. Il est à noter que la géologie du secteur situé en eaux internationales entre les zones économiques exclusives (ZEE) du Canada et du Groenland (Danemark) est décrite en liaison avec celle des sous-régions canadiennes associées (la marge du Labrador et la mer du Labrador centrale, et le détroit de Davis occidental). Renseignements supplémentaires sur la projection : méridien central = 60° W, parallèles de référence = 65° N, 75° N et latitude d’origine = 65° N.

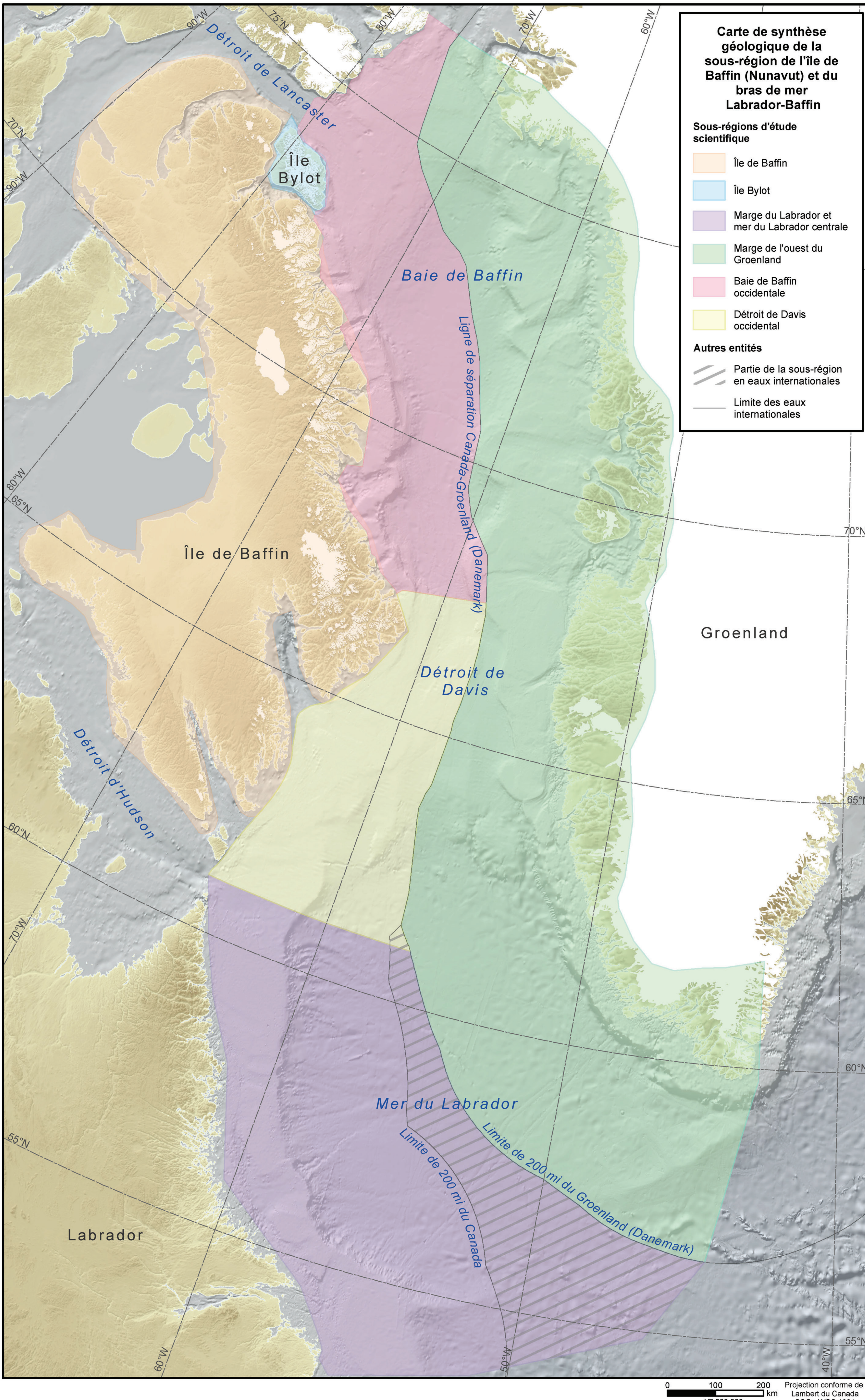
Carte de synthèse géologique de la sous-région de l'île de Baffin (Nunavut) et du bras de mer Labrador-Baffin
Sous-régions d'étude scientifique
Île de Baffin
Île Bylot
Marge du Labrador et mer du Labrador centrale
Marge de l'ouest du Groenland
Baie de Baffin occidentale
Détroit de Davis occidental
Autres entités
Partie de la sous-région en eaux internationales
Limite des eaux internationales
Détroit de Lancaster
Île Bylot
Baie de Baffin
Ligne de séparation Canada-Groenland (Danemark)
Île de Baffin
Groenland
Détroit de Davis
Détroit d'Hudson
Mer du Labrador
Limite de 200 mi du Groenland (Danemark)
Limite de 200 mi du Canada
Labrador
75°N
70°N
65°N
60°N
55°N
90°W
80°W
70°W
60°W
50°W
40°W
0
100
200
km
1/7 500 000
Projection conforme de Lambert du Canada
SCG : WGS 1984

Ces quatre domaines structuraux se sont accrétés progressivement du nord au sud à travers une série de sutures crustales inclinées vers le nord ou le sud, pendant une déformation de longue durée associée à la formation de l'orogène trans-hudsonien d'échelle himalayenne. La plus ancienne de ces sutures, la « suture de Baffin », serait le résultat de l'accrétion du microcontinent Meta Incognita au craton de Rae vers 1880-1865 Ma (St-Onge et al., 2006). Au sud de celle-ci, la « suture de Soper River » rend compte de l'accrétion du terrane d'arc magmatique de Narsajuaq à la marge continentale composite Rae-Meta Incognita entre 1845 Ma et 1842 Ma environ (Scott, 1997; Dunphy et Ludden, 1998). La plus récente suture, la « suture de Bergeron », a été formée lors de la collision terminale du craton du lac Supérieur avec la plaque de Churchill (ou collage péri-Churchill) entre 1820 Ma et 1795 Ma environ (Wodicka et Scott, 1997; Scott et Wodicka, 1998).

Bassin de Borden du Mésoprotérozoïque

Les connaissances sur le bassin de Borden du Mésoprotérozoïque tardif, dans le nord de l'île de Baffin, qui sont résumées dans Turner (le présent volume), proviennent de la cartographie géologique réalisée par la CGC dans les années 1970 (p. ex., Jackson et Iannelli, 1981; Scott et de Kemp, 1998) de concert avec des études universitaires subséquentes. Le bassin de Borden, l'un des quatre bassins de Bylot (Fahrig et al., 1981), contient environ 6 km de strates du Supergroupe de Bylot qui recouvrent le craton de Rae; sa stratigraphie est surtout connue d'après le graben de Milne Inlet.

Turner (le présent volume) présente des descriptions lithologiques détaillées, les paléoenvironnements sédimentaires et un aperçu de l'évolution tectonostratigraphique du Supergroupe de Bylot. Au départ, les basaltes subaquatiques de la Formation de Nauyat et les grès marins sus-jacents de la Formation d'Adams Sound rendent compte d'une accumulation dans un bassin d'affaissement régional (Long et Turner, 2012; Turner et al., 2016). Des rifts prononcés se sont ensuite formés, à l'intérieur desquels diverses successions contemporaines les unes des autres se sont accumulées : des cônes de débris sur les marges (Formation de Fabricius Fiord; Jackson et Iannelli, 1981; Scott et de Kemp, 1998); des shales noirs d'eau profonde (partie supérieure de la Formation d'Arctic Bay; Turner et Kamber, 2012); des monticules-suintements carbonatés d'eau profonde (Formation d'Ikpiarjuk; Turner, 2009; Hahn et Turner, 2017); et une rampe carbonatée à progradation dirigée vers le sud-est (Formation d'Iqqittuq; Turner, 2009). Les données géochimiques portent à croire que la Formation de Fabricius Fiord, la partie supérieure de la Formation d'Arctic Bay, ainsi que les formations d'Ikpiarjuk et d'Iqqittuq se sont accumulées dans des milieux lacustres (Hahn et al., 2015; Gibson et al., 2019).

L'exposition du sommet des monticules de la Formation d'Ikpiarjuk a été accompagnée de changements abrupts dans les milieux du fond du bassin, avec l'accumulation de roches carbonatées en milieu marin peu profond au sud-est (Formation d'Angmaat) au même moment que se déposaient des laminites anoxiques au nord-ouest (Formation de Nanisivik), les deux milieux étant séparés par un rebord de plate-forme tectonique caractérisé par des cycles de roches carbonatées à figures de tepee (Turner, 2009). Un soulèvement différentiel prononcé, un basculement et une exposition ont produit une discordance présentant un relief de centaines de mètres et un ennoyage subséquent a donné lieu au dépôt de strates de boue carbonatée dans un milieu de rampe (Formation de Victor Bay; Turner, 2011). Un second important épisode de soulèvement différentiel a entraîné une karstification locale (Formation de Victor Bay), avec ennoyage ailleurs (Formation d'Athole Point; Sherman et al., 2002). Un épisode d'instabilité tectonique a entraîné le dépôt local de conglomérat et de grès (partie basale de la Formation de Strathcona Sound), suivi de l'accumulation d'une succession marine de siltite et de grès à profondeur de dépôt décroissante vers le haut (formations de Strathcona Sound, d'Aqigilik et de Sinasiuvik; Turner et al., 2016).

Les contraintes géochronologiques quant à l'accumulation du Supergroupe de Bylot sont rares (*voir* Turner, le présent volume), le dépôt du Supergroupe de Bylot ayant eu lieu entre 1267 Ma et 723 Ma (LeCheminant et Heaman, 1989; Heaman et al., 1992; Pehrsson et Buchan, 1999; Denyszyn et al., 2009). On suppose que le basalte basal est lié à l'événement igné de Mackenzie vers 1270 Ma, mais aucune preuve directe de son âge n'est encore disponible. Des unités de shale au milieu de la succession présentent des âges sédimentaires (U-Th-Pb, Re-Os) du Mésoprotérozoïque tardif (Turner et Kamber, 2012; Gibson et al., 2018). Des cristaux de zircon détritiques provenant de l'orogène de Grenville sont présents dans les formations sommitales, ce qui limite l'âge de leur dépôt à moins de 1,14 Ga (Rainbird et al., 2012; Turner et al., 2016). Un résumé de la métallogénie du bassin de Borden est également fourni par Turner (le présent volume). Le graben de Milne Inlet contient de nombreux indices de Zn-Pb dans des roches carbonatées (p. ex., corps minéralisé de Nanisivik) dont la distribution révèle un contrôle stratigraphique et structural (Sangster, 1998; Scott et de Kemp, 1998; Turner, 2011).

Stratigraphie du Paléozoïque inférieur

Des strates du Paléozoïque inférieur discontinues sur le plan géographique sont présentes dans le bras de mer Labrador-Baffin, ainsi que dans des affleurements de l'île de Baffin. Le rifting du supercontinent Pangée et l'ouverture synchrone de la mer du Labrador et de la baie de Baffin au Crétacé précoce ont entraîné une importante érosion des dépôts du Paléozoïque dans la région, lesquels n'existent maintenant que sous forme de lambeaux d'érosion isolés le long de la marge du Labrador et dans le détroit de Davis occidental (Moir, 1989; Bell et Howie, 1990). Des roches du Paléozoïque affleurent également dans l'île de Baffin, où elles peuvent former des dépôts étendus latéralement (p. ex., Trettin, 1965a, b, 1969, 1975). Un aperçu des strates du Paléozoïque inférieur de ces régions, comprenant entre autres des descriptions lithologiques, des renseignements biostratigraphiques mis à jour et des interprétations paléoenvironnementales, est présenté dans Bingham-Koslowski, Zhang et McCartney (le présent volume). De plus, des cartes offrant une vue détaillée de la répartition des strates du Paléozoïque inférieur sont incluses pour la marge du Labrador, la partie sud-est de la plate-forme continentale de Baffin (d'après la cartographie présentée dans Dafoe, Desroches et Williams, le présent volume) et la région côtière de l'île de Baffin.

Les strates du Paléozoïque inférieur du bras de mer Labrador-Baffin sont composées principalement de roches carbonatées (Bell et Howie, 1990; Bingham-Koslowski, 2018, 2019), pour lesquelles aucune formation formelle n'a été reconnue. Nos connaissances des strates de l'Ordovicien moyen et supérieur proviennent de puits situés dans le sud de la plate-forme continentale du Labrador, où elles se sont à l'origine déposées dans une mer épicontinentale et forment maintenant par endroits le socle rocheux sur lequel reposent les strates syn-rift et post-rift plus récentes qui caractérisent le bassin de Hopedale (Bell et Howie, 1990). Les roches de l'Ordovicien de la région du détroit de Davis occidental sont connues uniquement d'après des carottes de forages peu profonds du fond marin recueillies par la CGC dans les années 1970 (Jansa, 1976; MacLean et al., 1977; Bell et Howie, 1990). L'étendue de la succession du Paléozoïque inférieur dans le détroit de Davis occidental est affinée par une cartographie sismique dans Dafoe, Desroches et Williams (le présent volume). Des strates du Paléozoïque inférieur affleurent dans trois régions principales de l'île de Baffin : la péninsule Brodeur, le nord-ouest de l'île de Baffin et le sud de l'île de Baffin. La séquence du Paléozoïque inférieur dans l'île de Baffin est principalement composée de roches carbonatées de l'Ordovicien, avec des occurrences localisées de roches détritiques du Cambrien et de roches carbonatées du Silurien. Le Paléozoïque inférieur de l'île de Baffin a été subdivisé antérieurement en neuf unités formelles (p. ex., Blackadar, 1956; Lemon et Blackadar, 1963; Sanford et Grant, 1990, 2000) qui sont résumées et précisées dans Bingham-Koslowski, Zhang et McCartney (le présent volume).

Bingham-Koslowski, Zhang et McCartney (le présent volume) analysent plus à fond les corrélations possibles des strates du Paléozoïque inférieur entre la côte de l'île de Baffin et la zone extracôtière de la partie sud-est de la plate-forme continentale de Baffin. Selon la répartition des strates, les différences biostratigraphiques et lithostratigraphiques ainsi que l'absence de strates du Paléozoïque inférieur dans les puits de la partie nord de la marge du Labrador et du détroit de Davis occidental, les auteurs de cet article subdivisent de façon informelle le Paléozoïque inférieur en deux sous-ensembles de dépôts non reliés, soit : une région nord, qui comprend les régions côtières et extracôtières de l'île de Baffin, et une région sud, qui comprend la zone extracôtière du Labrador.

GÉOLOGIE DU MÉSOZOÏQUE AU CÉNOZOÏQUE ET SISMICITÉ RÉCENTE

Stratigraphie du Mésozoïque au Cénozoïque

L'évolution tectonique du bras de mer Labrador-Baffin, qui a commencé au Crétacé précoce, a entraîné l'accumulation d'épaisses successions du Mésozoïque au Cénozoïque dans des bassins sédimentaires. Bien que les strates soient largement réparties dans les bassins extracôtiers, il existe peu d'unités corrélatives de ces strates extracôtières en milieu terrestre le long de la marge canadienne. Des affleurements des strates du Crétacé au Paléogène en milieu terrestre sont conservées dans la région du cap Dyer du centre est de l'île de Baffin, ainsi que dans l'île Bylot (fig. 1) et dans les zones adjacentes du nord de l'île de Baffin. Haggart et al. (le présent volume) résument la recherche historique sur ces strates, en particulier la lithostratigraphie et la biostratigraphie des successions. La répartition et l'étendue géographique des strates côtières du Crétacé au Paléogène ont été élucidées pour la première fois lors des programmes de cartographie de la CGC dans les années 1960 et 1970 (Jackson et Davidson, 1975; Jackson et al., 1975, 1979; Jackson et Morgan, 1978). Des études stratigraphiques entreprises par la CGC et d'autres par la suite (p. ex., Miall et al., 1980; Ioannides, 1986; Sparkes, 1989; Waterfield, 1989; Benham et Burden, 1990; Burden et Langille, 1990, 1991; Wiseman, 1991) ont mené à la définition des faciès sédimentaires présents dans les successions côtières, et a également fourni des attributions d'âge préliminaires. La datation et la corrélation des strates côtières reposent principalement sur la palynologie, car les strates sont appauvries en ce qui a trait aux fossiles de mollusques bien conservés, et elles ne contiennent pas de dépôts de tuf interstratifiés. Les strates côtières comprennent une abondance de grès et en moindre quantité des dépôts de mudstone et de conglomérat qui témoigneraient, selon les interprétations fondées sur des considérations sédimentologiques, d'une variété de paléoenvironnements non marins, littoraux-marins et d'eau profonde.

En dépit de l'absence d'une évaluation d'ensemble de la répartition régionale et des relations faciologiques de ces strates, les études des années 1970 et 1980 ont établi le cadre des successions du Crétacé au Paléogène dans les zones côtières entourant la baie de Baffin occidentale. Les principales contributions de ces études, analysées par Haggart et al. (le présent volume), comprennent : l'association de strates sédimentaires et volcaniques liées au rift dans la région du cap Dyer (Burden et Langille, 1990) avec un volcanisme régional du Paléogène centré dans le détroit de Davis; l'affinité stratigraphique des strates du Crétacé supérieur de l'île Bylot et des environs avec la succession de Kanguk du bassin de Sverdrup (Miall et al., 1980); et la proposition selon laquelle la succession du Crétacé au Paléogène de la région de l'île Bylot s'est déposée dans deux dépocentres distincts - les cuvettes d'Eclipse et de North Bylot (Miall et al., 1980; Benham et Burden, 1990), où Benham et Burden (1990) proposent des histoires stratigraphiques fortement divergentes entre les deux dépocentres au Cénozoïque. Aucun cadre stratigraphique complet pour les strates du Crétacé au Paléogène de la région de l'île Bylot n'a toutefois été élaboré à partir de ces études, et les milieux de dépôt de certaines unités stratigraphiques ne sont toujours pas résolus. De plus, on a reconnu la nécessité d'une palynostratigraphie détaillée pour corréler les successions détritiques de la côte (Ioannides, 1986; Sparkes, 1989; Waterfield, 1989; Wiseman, 1991). Les études palynologiques menées dans la région n'ont pas encore abouti à un schéma biostratigraphique formel pour les strates côtières, mais elles ont démontré la difficulté de différencier les strates quaternaires des strates plus anciennes du Cénozoïque, et même du Mésozoïque, en raison d'un remaniement (Burden et Holloway, 1985; Newman, 1987).

Telle qu'elle est définie dans le présent bulletin, la partie canadienne du bras de mer Labrador-Baffin est divisée en trois sous-régions informelles (fig. 1), chacune renfermant des bassins sédimentaires importants : 1) la marge du Labrador et la mer du Labrador centrale, y compris le bassin de Hopedale et la partie sud du bassin de Saglek; 2) la région du détroit de Davis occidental, qui comprend la partie nord du bassin de Saglek, le bassin de Cumberland et la partie ouest du bassin de Lady Franklin; 3) la baie de Baffin occidentale, où se trouvent les grabens de Scott et de Buchan et le bassin de Lady Ann. Des bassins du même âge ont également été formés sur la marge de l'ouest du Groenland, d'épaisses strates du Cénozoïque recouvrant les régions centrales de la mer du Labrador et de la baie de Baffin, qui reposent principalement sur de la croûte océanique.

Les successions stratigraphiques extracôtières de la partie canadienne du bras de mer Labrador-Baffin du Mésozoïque au Cénozoïque ont été étudiées depuis les années 1970 à l'aide de données probantes provenant de puits d'exploration, d'échantillons du substratum rocheux du fond marin, d'un trou carotté du Programme de sondage des fonds marin et de l'acquisition cumulée d'un ensemble considérable de données de sismique-réflexion. Cinq importantes découvertes d'hydrocarbures ont été faites dans le bassin de Hopedale (*voir* Bingham-Koslowski, McCartney et Bojesen-Koefoed, le présent volume), ce qui a donné lieu à une concentration relativement élevée d'ensembles de données (p. ex., profils sismiques et puits d'exploration) pour la zone extracôtière du Labrador. Par conséquent, le cadre lithostratigraphique de la partie canadienne de la zone extracôtière du bras de mer a été établi principalement à partir de la marge du Labrador. Les unités lithostratigraphiques qui ont d'abord été proposées pour cette marge par Umpleby (1979) et modifiées par McWhae et al. (1980) comprennent les formations d'Alexis, de Bjarni, de Markland (Membre de Freydis), de Gudrid, de Cartwright, de Kenamu (membres de Brown Mudstone et de Leif), de Mokami et de Saglek. Ce cadre a été élargi par Balkwill (1987), Bell (1989), Balkwill et McMillan (1990) et Dickie et al. (2011), et il a été peaufiné ou adapté dans trois articles : Dafoe, Dickie, Williams et McCartney (le présent volume) pour la marge du Labrador et la mer du Labrador centrale; Dafoe, Desroches et Williams (le présent volume) pour la région du détroit de Davis occidental; et Dafoe, Dickie et Williams (le présent volume) pour la baie de Baffin occidentale.

Dans ces trois articles, les roches du socle pré-rift sont décrites le long de la marge canadienne pour chacune des trois sous-régions (marge du Labrador et mer du Labrador centrale; détroit de Davis occidental; et baie de Baffin occidentale) et identifiées localement là où des données existent pour délimiter leur répartition. La stratigraphie syn-rift et post-rift du Mésozoïque au Cénozoïque est également décrite, et la répartition de ces unités est cartographiée en fonction des ensembles de données disponibles. Des âges mis à jour, déterminés de façon biostratigraphique, sont présentés, en plus des améliorations apportées aux interprétations paléoenvironnementales. Les coupes-types, établies dans des puits le long de la marge du Labrador, sont présentées et analysées. Les principaux résultats de ces trois articles comprennent des précisions à l'âge de la Formation de Bjarni et de la Formation de Markland sus-jacente ainsi que des unités de grès associées du Membre de Freydis. L'âge de la Formation de Gudrid sus-jacente est également défini plus clairement, tout comme son origine en milieu marin peu profond. Les sélections lithostratigraphiques dans les trois puits du sud-est de la plate-forme continentale de Baffin sont redéfinies en fonction de nouvelles contraintes d'âge et de corrélations sismiques. Des échantillons du substratum rocheux du fond marin dans le détroit de Davis occidental et le long de la plate-forme continentale de Baffin sont également incorporés dans le cadre lithostratigraphique. Ils sont en bon accord avec la stratigraphie de la marge du Labrador pour ce qui est de leur âge et de leur interprétation paléoenvironnementale, et ils aident à encadrer la cartographie sismique.

Les trois articles sur la marge canadienne présentent également un cadre sismostratigraphique fondé sur la lithostratigraphie de la marge du Labrador, tel qu'illustré dans des profils de sismique-réflexion clés de chacune des trois régions. Des cartes de répartition nouvellement compilées sont également incluses pour trois intervalles clés : Crétacé, Cénozoïque inférieur et Cénozoïque supérieur. Des cartes des roches du socle pré-rift le long de la plate-forme et dans des hauteurs localisées sont aussi présentées dans lesquelles les failles majeures sont délimitées. L'interprétation sismique et les corrélations entre les puits ont permis de cartographier la répartition des roches du Crétacé, ainsi que des roches volcaniques associées du Crétacé précoce, de même que l'étendue vers le large de la Formation de Bjarni du Crétacé inférieur pour certaines parties de la marge du Labrador. L'étendue de l'intervalle du Cénozoïque inférieur (coupe du Paléocène jusqu'au Miocène moyen) est cartographiée, en plus de la répartition des marges volcaniques (riches en magma), des unités volcaniques apparentées (comme les coulées internes) et de la couverture volcanique (principalement dans la région du détroit de Davis). L'intervalle du Cénozoïque supérieur, du Miocène moyen jusqu'au Pléistocène, est également indiqué dans chacun des trois articles, en plus des régions dans lesquelles la sédimentation du Quaternaire a fourni la composante dominante de la succession. Les nouveaux résultats importants de ces travaux comprennent une nouvelle compréhension de l'étendue des strates du Crétacé au large du Labrador et dans la partie canadienne du bassin de Lady Franklin. Plus au nord, l'intervalle crétacé du graben de Scott dans la plate-forme continentale de Baffin contiendrait, selon les interprétations, une mince coupe du Crétacé inférieur et une épaisse coupe du Crétacé supérieur, de façon analogue à ce que l'on observe dans les successions de certaines secteurs de la partie sud du bassin de Saglek et du graben de Melville Bay (au large de l'ouest du Groenland). De nouvelles contraintes d'âge offertes par un trou de forage carotté au site 645 du Programme de sondage des fonds marins aident à préciser le tracé cartographique d'horizons sismiques clés dans l'intervalle du Cénozoïque supérieur de la baie de Baffin occidentale. Dans le détroit de Davis occidental, une nouvelle carte structurale comprend des hauteurs du socle, des sommets volcaniques et des failles, ce qui permet de mieux comprendre la géologie de la région.

Gregersen et al. (le présent volume) présentent un résumé de la stratigraphie côtière et extracôtière le long de la marge conjuguée du bras de mer Labrador-Baffin de l'ouest du Groenland, ainsi que de l'évolution tectonique de cette marge. Cette marge renferme de nombreux bassins sédimentaires et structures datant du Protérozoïque (Dam et al., 2009; Henriksen et al., 2009; St-Onge et al., 2009; Gregersen, 2014; Gregersen et al., 2019), mais le principal centre d'intérêt de Gregersen et al. (le présent volume) concerne les successions du Crétacé au Cénozoïque liées à l'ouverture du bras de mer. Une compréhension de la géologie côtière de la marge de l'ouest du Groenland s'est développée au cours du dernier siècle, grâce à de nombreuses expéditions de cartographie et de travaux sur le terrain (p. ex., Dam et al., 2009; Henriksen et al., 2009). Les études en zone extracôtière n'ont commencé qu'au cours des années 1970 et se sont étendues avec l'acquisition cumulée de données sismiques et le forage de puits d'exploration et de puits scientifiques (Christiansen, 2011). Gregersen et al. (le présent volume) présentent un résumé géologique qui intègre l'évolution du bassin, la lithostratigraphie, la biostratigraphie, la sismostratigraphie, la tectonostratigraphie et les études des roches volcaniques, ainsi que la structure de la croûte terrestre à des interprétations fondées sur des levés de sismique-réflexion, des données de sismique-réfraction, des données sur des puits et des affleurements, des échantillons du fond marin, des données magnétiques et gravimétriques, ainsi que des compilations stratigraphiques.

La marge de l'ouest du Groenland est subdivisée par Gregersen et al. (le présent volume) en régions sud, centrale et nord, et une vue d'ensemble des bassins de chaque région est fournie avec un accent particulier sur les successions du Crétacé et du Paléogène. Les successions sédimentaires du Crétacé au Paléocène, avec les roches volcaniques sus-jacentes, sont bien connues en affleurements et dans les puits dans le bassin de Nuussuaq dans l'ouest du Groenland Central (Dam et al., 2009). Les bassins sédimentaires en milieu extracôtier de la marge de l'ouest du Groenland reposent sur une croûte continentale à l'est, et les bassins du Cénozoïque à l'ouest reposent sur une zone de transition crustale à la croûte océanique.

Une description de la stratigraphie et de l'évolution géologique des bassins dans chaque région est présentée, et six phases tectonostratigraphiques sont reconnues, soit pré-rift et distension précoce (pré-Crétacé), rift précoce (Crétacé précoce et moyen), subsidence et rifting (du Crétacé moyen au Campanien précoce), rift tardif (du Campanien au Paléocène précoce), dérive (du Paléocène à l'Éocène) et post-dérive (post-Éocène). Dans leur résumé tectonostratigraphique, Gregersen et al. (le présent volume) établissent en outre une corrélation et comparent la marge de l'ouest du Groenland à la marge canadienne conjuguée.

La stratigraphie du Mésozoïque au Cénozoïque de l'entièreté du bras de mer Labrador-Baffin est examinée dans son ensemble dans Dafoe, Williams et al. (le présent volume). Le cadre biostratigraphique de Nøhr-Hansen et al. (2016) constitue une base importante pour comprendre l'âge des successions et les corrélations entre les régions. Ce cadre est constitué d'un tableau des événements palynostratigraphiques basé sur les premières et les dernières occurrences, ainsi que sur les pointes d'abondance de kystes de dinoflagellés, de spores et de pollens, et de la fougère d'eau douce *Azolla* provenant d'échantillons de toute la région, ce qui permet d'améliorer la précision des colonnes stratigraphiques le long des marges. Dafoe, Williams et al. (le présent volume) utilisent le cadre sismostratigraphique de Gregersen et al. (2013, 2018, 2019, le présent volume; unités H à A, de la plus ancienne à la plus récente), avec adaptations pour la marge canadienne (Dafoe, Dickie, Williams et McCartney, le présent volume), pour comparer l'évolution des successions stratigraphiques du Crétacé et de temps plus récents le long du bras de mer. Cela comprend des cartes de répartition stratigraphique régionale compilées à partir de plusieurs articles du présent bulletin, ainsi que des profils des marges conjuguées montrant les corrélations entre les unités sismiques de toute la région. Ces travaux démontrent la corrélation et la nature des principaux horizons sismiques, certains horizons affichent des variations latérales, passant d'une discordance à une concordance ailleurs. Les failles synsédimentaires sont bien développées dans le Crétacé inférieur (unité G), et le Crétacé supérieur (unité F) est généralement transparent sur le plan sismique à l'échelle régionale, ce qui indique le dépôt d'unités de shale marin. L'intervalle du Cénozoïque (unités E à A) montre une variation d'épaisseur dans l'ensemble du bras de mer, qui est en partie influencée par l'existence d'importantes hauteurs du socle, comme la hauteur du détroit de Davis. La progradation de clinoformes est typique dans les unités C, B et A sur les marges du bras de mer. Le paléoclimat et la paléo-océanographie de la région sont également résumés par Dafoe, Williams et al. (le présent volume) à la lumière de ces résultats plus récents.

Histoire du rift du Mésozoïque au Cénozoïque

La chronologie et la géométrie des mouvements de plaques à grande échelle qui ont créé le bras de mer Labrador-Baffin ont suscité l'intérêt et la controverse depuis les premiers jours de la théorie de la dérive des continents (p. ex., Taylor, 1910). Keen et al. (le présent volume) rendent compte des études géophysiques dans la baie de Baffin, le détroit de Davis et la mer du Labrador; leurs interprétations ont été essentielles pour comprendre les éléments de base des mouvements des plaques au Mésozoïque-Cénozoïque, ainsi que les processus de rifting lithosphérique qui en découlent. Cet article porte principalement sur les marges continentales de divergence entourant les régions océaniques profondes formées par l'expansion des fonds marins.

Keen et al. (le présent volume) présentent des cartes à jour des anomalies magnétiques et gravimétriques pour l'ensemble du bras de mer. De telles données ont joué un rôle essentiel dans la détermination de l'historique de l'expansion des fonds marins des bassins océaniques (Srivastava, 1978; Roest et Srivastava, 1989; Oakey et Chalmers, 2012), ainsi que dans la détermination des liens entre les entités côtières et extracôtières. Les interprétations antérieures montrent que le début de l'expansion des fonds marins était diachronique, commençant d'abord dans la mer du Labrador centrale (vers 69 Ma) et un peu plus tard à l'échelle régionale dans le bras de mer (vers 62 Ma). Deux stades d'expansion des fonds marins sont reconnus et se distinguent par un changement de direction dans les mouvements des plaques au Paléocène terminal. L'expansion a cessé près de la limite Éocène-Oligocène (Oakey et Chalmers, 2012). Ces résultats sont quelque peu controversés et continuent d'être peaufinés, principalement en combinant des ensembles de données géologiques et géophysiques sur l'ensemble du bras de mer Labrador-Baffin et les régions adjacentes (p. ex., Oakey et Chalmers, 2012).

Une synthèse des résultats récents (Funck et al., 2007, 2012; Suckro et al., 2012, 2013; Altenbernd et al., 2014, 2015) et plus anciens relatifs à la sismique-réfraction présentée par Keen et al. (le présent volume) fait état d'une variété de styles structuraux, qui peuvent être regroupés en deux principaux types de marges de divergence : 1) des marges pauvres en magma présentant des zones d'hyperextension, un manteau serpentinisé, peut-être exhumé, et une protocroûte océanique (p. ex., Chian et al., 1995; Keen et al., 2018a); et 2) des marges riches en magma avec des zones épaisses de croûte ignée, qui peuvent surmonter dans certaines régions des marges plus anciennes pauvres en magma (Keen et al., 2012, 2018b). D'après les observations de sismique-réfraction et la modélisation gravimétrique, l'amincissement crustal et la subsidence sont hautement asymétriques d'une marge conjuguée à l'autre (Welford et Hall, 2013; Welford et al., 2018). Les marges riches en magma semblent être centrées sur la région du détroit de Davis, où des roches volcaniques du Paléocène à l'Éocène ont été relevées à la fois en zone côtière et en zone extracôtière (p. ex., Clarke, 1970; Larsen et al., 2009), reflétant peut-être l'influence d'un « point chaud », ou panache mantellique (Storey et al., 2007). La cause de ce magmatisme fait toujours l'objet de débats (Peace et al., 2017; Clarke et Beutel, 2020). En plus des observations à l'échelle de la croûte, Keen et al. (le présent volume) présentent de nouvelles cartes montrant la répartition des roches sédimentaires dans la région; ces cartes sont dérivées de données obtenues par sismique-réflexion multicanal et calées sur des puits d'exploration. Les cartes montrent la grande épaisseur (plus de 10 km) des strates déposées sur les marges continentales, et la répartition de ces sédiments syn-rift et plus récents peut être corrélée avec la nature et le style du rifting et de la subsidence.

Keen et al. (le présent volume) utilisent leur cartographie pour mettre à jour la limite côté terre de la croûte océanique et l'étendue des bassins sédimentaires au large des côtes. Ils utilisent en outre la chronologie et les pôles de la rotation du Groenland par rapport à l'Amérique du Nord provenant de travaux antérieurs (Hosseinpour et al., 2013) afin de reconstituer les positions des continents au fil du temps, depuis l'époque actuelle jusqu'au regroupement des continents avant le rifting. Les failles transformantes à grand décalage dans le détroit de Davis et la baie de Baffin ont entraîné des centaines de kilomètres de déplacement entre les marges conjuguées du bras de mer. Les vitesses des plaques, estimées dans cette étude et d'autres antérieures, montrent une augmentation rapide pendant le Campanien, ce qui peut indiquer une diminution rapide de la résistance de la lithosphère continentale, comme l'ont suggérée précédemment Brune et al. (2016). Si l'on procède à une fermeture du domaine océanique, on constate que les terranes précambriens et leurs limites terrestres présentent une bonne correspondance entre le Groenland et l'Amérique du Nord.

Bon nombre des entités crustales et sédimentaires à grande échelle décrites pour les marges de divergence du bras de mer Labrador-Baffin sont semblables à celles d'autres marges de divergence à l'échelle planétaire. On aurait pu s'attendre à ce que la lithosphère cratonique, froide et épaisse, de la région ait réagi différemment au rifting, ce qui soulève des questions pour les études futures.

Sismicité

Les cartes de l'aléa sismique pour le Canada (Earthquakes Canada, 2018) et le Groenland (Voss et al., 2007) indiquent des niveaux d'aléa allant de modérés à élevés pour la baie de Baffin, la mer du Labrador et les régions côtières adjacentes. Comme il est indiqué dans Bent et Voss (le présent volume), l'étude des séismes dans le bras de mer Labrador-Baffin présente des défis malgré les taux de sismicité relativement élevés, principalement en raison de l'éloignement et de l'immensité de la région. On ne connaît pas l'activité sismique dans le bras de mer Labrador-Baffin avant 1933, année où un tremblement de terre de magnitude 7,4 s'est produit dans la baie de Baffin (Bent, 2002). Grâce à l'amélioration de l'instrumentation, à l'augmentation de la couverture sismographique dans le Nord, à la mise en commun des données en temps réel entre le Canada et le Danemark (Groenland) et aux techniques d'analyse modernes, notre connaissance et notre compréhension des tremblements de terre dans la région de Labrador-Baffin s'améliorent. Bent et Voss (le présent volume) présentent une vue d'ensemble de la sismicité du bras de mer Labrador-Baffin et des régions côtières adjacentes, qui comprend des résumés portant sur la surveillance des séismes dans la région, les secteurs où l'activité sismique est élevée, les mécanismes au foyer des plus grands séismes enregistrés dans la région, et les processus qui peuvent être impliqués dans la génération de séismes dans la région.

Dans la mer du Labrador, la sismicité semble être associée à la dorsale d'expansion des fonds marins éteinte et aux zones de fracture océaniques dans cette région (*voir* Keen et al., le présent volume), mais il a été difficile de trouver un lien comparable dans la baie de Baffin entre la sismicité et la structure. Les recherches portant sur la baie de Baffin, des années 1970 au début des années 2000 (p. ex., Basham et al., 1977; Bent, 2002), n'ont révélé aucune corrélation entre l'activité sismique dans la baie de Baffin et les structures cartographiées (c.-à-d. les failles) ou les anomalies géophysiques. Malgré deux autres décennies de surveillance sismique avec des instruments améliorés, au cours desquelles de nouvelles cartes structurales de la baie de Baffin ont été élaborées, une corrélation entre la structure et la sismicité demeure difficile à établir.

Les solutions des mécanismes au foyer (plan de faille) peuvent maintenant être déterminées pour beaucoup plus de séismes de la région de Labrador-Baffin que par le passé. Bent et Voss (le présent volume) montrent que les solutions des mécanismes au foyer pour le bras de mer Labrador-Baffin révèlent un mélange de styles de failles, principalement de coulissage et de chevauchement. Les orientations des axes de contraintes à l'échelle régionale sont plus cohérentes que les styles des failles, ce qui donne à penser que l'activité sismique touche des structures existantes en réponse au champ des contraintes actuel. La possibilité que l'ajustement isostatique glaciaire soit un mécanisme déclencheur de séismes dans la région de Labrador-Baffin demeure attirante, mais les efforts déployés pour modéliser une corrélation, sauf à une vaste échelle régionale, ont livré des résultats équivoques (p. ex., James et Schamehorn, 2016).

RESSOURCES

Minéraux

Les ressources minérales de l'île de Baffin comprennent du fer (p. ex., Groupe de Mary River), des diamants dans de la kimberlite (p. ex., le gisement de Chidliak), des gisements de zinc et de plomb dans des roches carbonatées (p. ex., le gisement de Nanisivik), du nickel, du cuivre, des éléments du groupe du platine, de l'uranium, du thorium, des gemmes (saphir, spinelle et lapis-lazuli), de la pierre à sculpter et du charbon. Harrison et al. (le présent volume) présentent un aperçu des types de minéraux connus et potentiels de l'île de Baffin et incluent une carte à jour de l'île illustrant l'emplacement et les types de ressources sur un fond géologique.

Les gisements de fer présents dans le Groupe de Mary River du Néoarchéen (2,83 Ga; 2,76-2,72 Ga) comprennent les gisements n^{os} 1-4 de Mary River dans le nord de l'île de Baffin, qui contiennent 586 Mt de minerai à 66 % de Fe (G.H. Wahl, R. Gharapetian, J.E. Jackson, V Khera et G.G. Wortman, rapport inédit, 2011; Iannelli et al., 2013b). Dans le grand district de Mary River, on relève d'autres prospects dans des formations de fer dont les suivants : Glacier Lake, Turner River, North Cockburn River, North Rowley River, Cockburn-Rowley, southeast Rowley, North Isortoq, South Isortoq et Eqe Bay (Iannelli et al., 2013a; Campbell et MacLeod, 2014). De plus, des indices de métaux communs et de métaux précieux sont répandus et se trouvent fréquemment dans des filons-couches de composition mafique-ultramafique ou dans des unités du Groupe de Lake Harbour du Paléoprotérozoïque près de Kimmirut, dans le sud de l'île de Baffin (Vande Guchte, 1998; Vande Guchte et Gray, 1999). Les matières premières présentes en concentrations anomales comprennent le nickel, le cuivre, le palladium, le platine et, par endroits, l'or, l'argent et le zinc. Dans le bassin de Borden du Mésoprotérozoïque, les formations de Nanisivik et d'Ikpiarjuk (Turner, 2011; *voir* Turner, le présent volume) abritent le gisement de Nanisivik, un gisement de type Mississippi-Valley qui présente des teneurs de 9,0 % de Zn, 0,9 % de Pb et 41 ppm de Ag.

Une kimberlite riche en diamants, datée de 156,7 à 138,9 Ma (Heaman et al., 2015), est présente sous forme de feuillets et de petites cheminées à Chidliak, dans la péninsule Hall. La roche hôte est composée de kimberlite magmatique renfermant des xénolites d'éclogite et de péridotite, ainsi que des phénocristaux de grenat pyrope, de diopside chromifère et d'olivine, d'un diamètre pouvant atteindre 10 cm (J. Pell, rapport inédit, 2008).

La pierre à sculpter est une ressource minérale importante pour les collectivités du Nord, et les gisements connus sont décrits dans Harrison et al. (le présent volume). Au moins 32 emplacements de pierre à sculpter sont connus, et on y trouve de la serpentinite, du marbre, du marbre serpentinisé et de la pierre à savon. Les dépôts notables comprennent du marbre et de la serpentinite près d'Arctic Bay (Beauregard et Ell, 2015), de la serpentinite à l'est du cap Dorset (Steenkamp et al., 2014), du marbre et des roches de composition ultramafique à l'ouest de Kimmirut (Elgin, 2017), du marbre rose près de Clyde River (Beauregard et al., 2013), de la pierre à savon près de la rivière Mary (Beauregard et al., 2013), ainsi que de la serpentinite et de la pierre à savon au sud-ouest de Pangnirtung (Steenkamp et al., 2015).

Le charbon est une autre ressource importante où la première occurrence documentée dans l'île de Baffin a été faite par McMillan (1910). Le charbon est présent dans la cuvette d'Eclipse du Crétacé au Paléogène, qui s'étend à l'île Bylot et au nord-ouest de l'île de Baffin (Miall et al., 1980), et des affleurements près de Pond Inlet ont été excavés pour une utilisation locale.

Hydrocarbures

L'histoire stratigraphique et tectonique du bras de mer Labrador-Baffin a fait en sorte que tous les éléments d'un système pétrolier sont présents, par endroits, dans toute la région, ce qui a stimulé les activités d'exploration des hydrocarbures depuis les années 1960 (p. ex., Bell et Campbell, 1990; Christiansen, 2011). Malgré les activités d'exploration qui sont toujours en cours sur la marge du Labrador, aucune quantité commerciale d'hydrocarbures n'a été identifiée. De plus, un moratoire d'une durée indéterminée a été décrété par le gouvernement fédéral du Canada en 2016, sous réserve d'un examen tous les cinq ans, interrompant la délivrance de tout nouveau permis d'exploration dans les eaux de l'Arctique canadien (Government of Canada, 2018). Depuis juillet 2021, toutes nouvelles activités d'exploration pétrolière et gazière ont également été suspendues le long de la marge du Groenland (à terre et en mer).

Bingham-Koslowski, McCartney et Bojesen-Koefoed (le présent volume) traitent des ressources en hydrocarbures dans le bras de mer Labrador-Baffin par sous-région : 1) la marge du Labrador; 2) le détroit de Davis occidental et la partie sud-est de la plate-forme continentale de Baffin; 3) la partie nord-est de la plate-forme contnentale de Baffin et la baie de Baffin occidentale; et 4) la marge de l'ouest du Groenland (à terre et en mer). L'historique de l'exploration des hydrocarbures dans le bras de mer Labrador-Baffin, ainsi que toute évaluation antérieure des hydrocarbures effectuée dans la région (p. ex., McWhae et al., 1980; Nantais, 1984; Harrison et al., 2011; MacLean et al., 2014; Carey et al., 2020) sont examinés. Aucune évaluation officielle des hydrocarbures n'a été effectuée dans le détroit de Davis occidental et la partie sud-est de la plate-forme continentale de Baffin; toutefois, une attestation de découverte importante a été accordée au puits Hekja O-71 (détroit de Davis occidental) pour un indice de gaz, et on a évalué à 50 % la probabilité qu'il y ait au moins une accumulation de pétrole de plus de 1 milliard de barils dans la partie nord-est de la plate-forme continentale de Baffin et dans l'ensemble de la baie de Baffin (Gautier et al., 2011). Bingham-Koslowski, McCartney et Bojesen-Koefoed (le présent volume) présentent en outre des éléments connus et anticipés d'un système pétrolier pour chaque secteur et résument le potentiel en hydrocarbures des sous-régions. On y trouve aussi un résumé des cinq types de pétrole provenant de suintements en milieu terrestre le long de la marge de l'ouest du Groenland (Bojesen-Koefoed et al., 1999; Bojesen-Koefoed, 2011), qui révèlent l'existence de multiples systèmes pétroliers.

Bingham-Koslowski, McCartney et Bojesen-Koefoed (le présent volume) examinent la présence de suintements et de nappes d'hydrocarbures connus et potentiels le long de la marge canadienne du bras de mer Labrador-Baffin. De nombreuses nappes de pétrole potentielles ont été identifiées dans la région à partir d'observations visuelles et à l'aide d'images obtenues par radar à synthèse d'ouverture (p. ex., Budkewitsch et al., 2013; Decker et al., 2013); cependant, la majorité d'entre elles ne peuvent être corrélées de façon définitive avec des suintements d'hydrocarbures sur le fond marin. Les études antérieures sur les nappes d'hydrocarbures, ainsi que les preuves possibles de suintement sur le fond marin, sont examinées; seule la nappe située au large de l'inlet Scott (nord-ouest de la baie de Baffin) a une origine prouvée, naturelle, de suintement sur le fond marin (Grant et al., 1986). La présence irréfutable de ce suintement d'hydrocarbures ainsi que d'autres indicateurs directs d'hydrocarbures observés dans des puits d'exploration prouvent l'existence de multiples systèmes pétroliers actifs dans le bras de mer Labrador-Baffin.

REMERCIEMENTS

Les auteurs aimeraient remercier Dawn Kellett et Rob Fensome d'avoir examiné cet article, ainsi que Leith MacLeod d'avoir produit la carte de la figure 1. En ce qui concerne le Bulletin 608 de la CGC dans son ensemble, les auteurs tiennent à souligner que cet ouvrage est le résultat d'une entreprise de collaboration dirigée par la CGC dans le cadre du programme GEM-2. Le Geological Survey of Denmark and Greenland (Service géologique du Danemark et du Groenland; GEUS) a grandement contribué au présent volume, et des contributions clés ont été fournies par d'autres organismes partenaires, dont les suivantes : le Bureau géoscientifique Canada-Nunavut, le Service canadien d'information sur les risques, l'Université Laurentienne, l'Université Memorial de Terre-Neuve, Savoir polaire Canada, l'Université du Québec à Montréal, l'Université de Cambridge et la Commission géologique du Yukon. Par conséquent, les auteurs de cet article tiennent à remercier tous les autres collaborateurs qui ont contribué à rendre cette publication possible : Kimberley Bell (CGC), Jørgen A. Bojesen-Koefoed (GEUS), Elliott Burden (Université Memorial de Terre-Neuve), Lisel Currie (CGC), Gregers Dam (GEUS), Sonya Dehler (CGC), Kevin Desroches (CGC), Kate Dickie (CGC), Rob Fensome (CGC), Thomas Funck (GEUS), John R. Hopper (GEUS), Jussi Hovikoski (GEUS), Jon R. Ineson (GEUS), Paul C. Knutz (GEUS), Lotte M. Larsen (GEUS), Tannis McCartney (CGC), Henrik Nøhr-Hansen (GEUS), Gunver K. Pedersen (GEUS), Nicole Rayner (CGC), Mary Sanborn-Barrie (CGC), Benoit M. Saumur (Université du Québec à Montréal), Dave J. Scott (Savoir polaire Canada), Nina Skaarup (GEUS), Diane R. Skipton (Commission géologique du Yukon), Peter Voss (GEUS), Kim Welford (Université Memorial de Terre-Neuve), Owen M. Weller (Université de Cambridge), Graham Williams (CGC), Natasha Wodicka (CGC) et Shunxin Zhang (Bureau géoscientifique Canada-Nunavut). De plus, les auteurs sont reconnaissants à l'équipe de gestion et de coordination du projet GEM-2 d'avoir soutenu les projets de recherche de ce volet du programme et la réalisation de cette publication de synthèse (Michel Plouffe, Natalie Shea, Marlene Francis, Paul Wozniak et Rosemarie Khoun). Les auteurs aimeraient également remercier les nombreux examinateurs internes et externes qui ont participé à la publication de ce bulletin; leurs commentaires ont grandement amélioré la qualité des travaux présentés. Nous sommes très reconnaissants de tout le soutien offert par les di-vers bureaux de la CGC en matière de SIG et tenons à remercier plus particulièrement Leith MacLeod, qui a supervisé la compilation des métadonnées pour le bulletin et l'élaboration des cartes de bon nombre des articles du présent volume. Merci à l'équipe des publications de la CGC pour la coordination, la révision scientifique et la mise en page des articles de ce bulletin, en particulier Evelyn Inglis, Natalie Morisset, Alison Weatherston, Paul Champagne, Liam Boudreau et Marie-France Dufour, qui ont participé activement à ce volume de GEM-2. Les auteurs aimeraient également remercier l'équipe de mobilisation de GEM-2, en particulier Kate Clark, qui a aidé à communiquer l'initiative de synthèse et la science qui la compose aux communautés du Nord.

RÉFÉRENCES

Altenbernd, T., Jokat, W., Heyde, I. et Damm, V., 2014. A crustal model for northern Melville Bay, Baffin Bay; Journal of Geophysical Research: Solid Earth, v. 119, no. 12, p. 8610–8632. https://doi.org/10.1002/2014JB011559

Altenbernd, T., Jokat, W., Heyde, I. et Damm, V., 2015. Geophysical evidence for the extent of crustal types and the type of margin along a profile in the northeastern Baffin Bay; Journal of Geophysical Research: Solid Earth, v. 120, no. 11, p. 7337–7360. https://doi.org/10.1002/2015JB012307

Balkwill, H.R., 1987. Labrador basin: structural and stratigraphic style; *in* Sedimentary Basins and Basin-Forming Mechanisms, (ed.) C. Beaumont and A.J. Tankard; Canadian Society of Petroleum Geologists Memoir, v. 12, p. 17–43.

Balkwill, H.R. et McMillan, N.J., 1990. Mesozoic-Cenozoic geology of the Labrador Shelf; *in* Chapter 7 of Geology of the Continental Margin of Eastern Canada, (ed.) M.J. Keen and G.L. Williams; Geological Survey of Canada, Geology of Canada, no. 2, p. 295–324 (*also* Geological Society of America, The Geology of North America, v. I-1, p. 295–324). https://doi.org/10.4095/132708

Basham, P.W., Forsyth, D.A. et Wetmiller, R.J., 1977. The seismicity of northern Canada; Canadian Journal of Earth Sciences, v. 14, p. 1646–1667. https://doi.org/10.1139/e77-140

Beauregard, M.A. et Ell, J., 2015. Nunavut Carving Stone Deposit Evaluation Program: 2015 fieldwork at Rankin Inlet, Cumberland Sound and Arctic Bay, Nunavut; *in* Summary of Activities 2015; Canada-Nunavut Geoscience Office, p. 183–192.

Beauregard, M.A., Ell, J., Pikor, R.K. et Ham, L.J., 2013. Nunavut Carving Stone Evaluation Program (2010-2013): third year results; *in* Summary of Activities 2012; Canada-Nunavut Geoscience Office, p. 151–162.

Bell, J.S., 1989. Labrador Sea. East Coast Basin Atlas Series; Geological Survey of Canada, 135 p. https://doi.org/10.4095/127152

Bell, J.S. et Campbell, G.R., 1990. Petroleum Resources; Chapter 12 *in* Geology of the Continental Margin of Eastern Canada, (ed.) M.J. Keen and G.L. Williams; Geological Survey of Canada, Geology of Canada, no. 2, p. 677–720 (*also* Geological Society of America, The Geology of North America, v. I-1, p. 677–720). https://doi.org/10.4095/132720

Bell, J.S. et Howie, R.D., 1990. Paleozoic geology; Chapter 4 *in* Geology of the Continental Margin of Eastern Canada, (ed.) M.J. Keen and G.L. Williams; Geological Survey of Canada, Geology of Canada, no. 2, p. 141–165 (*also* Geological Society of America, The Geology of North America, v. I-1, p. 141–165). https://doi.org/10.4095/132700

Benham, P.H. et Burden, E.T., 1990. Stratigraphy of Cretaceous–Tertiary rocks of North Bylot Trough, Bylot Island, N.W.T.; *in* Current Research, Part D; Geological Survey of Canada, Paper 90-1D, p. 179–185. https://doi.org/10.4095/131353

Bent, A.L., 2002. The 1933 Ms 7.3 Baffin Bay earthquake: strike-slip faulting along the northeastern Canadian passive margin; Geophysical Journal International, v. 150, no. 3, p. 724–736. https://doi.org/10.1046/j.1365-246X.2002.01722.x

Bingham-Koslowski, N., 2018. Descriptions of drill cores and thin sections from lower Paleozoic strata, southeastern Baffin Island shelf, Nunavut; Geological Survey of Canada, Open File 8409, 80 p. https://doi.org/10.4095/308354

Bingham-Koslowski, N., 2019. Description of Paleozoic cores and thin sections from the Gudrid H-55, Roberval K-92, Indian Harbour M-52, and Freydis B-87 wells, offshore Labrador (Newfoundland and Labrador); Geological Survey of Canada, Open File 8543, 142 p. https://doi.org/10.4095/313573

Blackadar, R.H., 1956. Geological reconnaissance of Admiralty Inlet, Baffin Island, Arctic Archipelago, Northwest Territories; Geological Survey of Canada, Paper 55-6, 25 p. https://doi.org/10.4095/101291

Bojesen-Koefoed, J.A., 2011. West Greenland petroleum systems: an overview of source rocks and oil seepages and their implications for offshore petroleum exploration; Danmarks og Grønlands Geologiske Undersøgelse Rapport, 2011/42, 49 p.

Bojesen-Koefoed, J.A., Christiansen, F.G., Nytoft, H.P. et Pedersen, A.K., 1999. Oil seepage onshore West Greenland: evidence of multiple source rocks and oil mixing; *in* Petroleum Geology of Northwest Europe: Proceedings of the 5th Conference, (ed.) A.J. Fleet and S.A.R. Boldy; Geological Society, London, p. 305–314. https://doi.org/10.1144/0050305

Brune, S., Williams, S.E., Butterworth, N.P. et Müller, R.D., 2016. Abrupt plate accelerations shape rifted continental margins; Nature, v. 536, p. 201–204. https://doi.org/10.1038/nature18319

Budkewitsch, P., Pavlic, G., Oakey, G., Jauer, C. et Decker, V., 2013. Reconnaissance mapping of suspect oil seep occurrences in Baffin Bay and Davis Strait using satellite radar: preliminary results; Geological Survey of Canada, Open File 7068, 1 .zip file. https://doi.org/10.4095/292280

Burden, E. et Holloway, D., 1985. Palynology and age of the Scott Inlet inliers of Baffin Island (Northwest Territories); Canadian Journal of Earth Sciences, v. 22, p. 1542–1545. https://doi.org/10.1139/e85-160

Burden, E.T. et Langille, A.B., 1990. Stratigraphy and sedimentology of Cretaceous and Paleocene strata in half-grabens on the southeast coast of Baffin Island, Northwest Territories; Bulletin of Canadian Petroleum Geology, v. 38, no. 2, p. 185–196.

Burden, E.T. et Langille, A.B., 1991. Palynology of Cretaceous and Tertiary strata, northeast Baffin Island, Northwest Territories, Canada: implications for the history of rifting in Baffin Bay; Palynology, v. 15, p. 91–114. https://doi.org/10.1080/01916122.1991.9989392

Campbell, H. et MacLeod, M., 2014. Mary River project: 2013 exploration program highlights and outline of 2014 program; Nunavut Mining Symposium PowerPoint Presentation [Baffinland Iron Mines Corporation]. <https://www.nunavutminingsymposium.ca/2014-presentations> [consulté le 18 janvier 2017]

Carey, J.S., McCartney, T., Hanna, M.C., Lister, C., and Keng, L.E., 2020. Qualitative petroleum resource assessment of the Labrador margin; Geological Survey of Canada, Open File 8535, 104 p. https://doi.org/10.4095/326017

Chian, D., Louden, K.E. et Reid, I., 1995. Crustal structure of the Labrador Sea conjugate margin and implications for the formation of nonvolcanic continental margins; Journal of Geophysical Research, v. 100, no. B12, p. 24239–24253. https://doi.org/10.1029/95JB02162

Christiansen, F.G., 2011. Greenland petroleum exploration: history, breakthroughs in understanding and future challenges; *in* Artic Petroleum Geology, (ed.) A.M. Spencer, A.F. Embry, D.L. Gautier, A.V. Stoupakova, and K. Sørensen; Geological Society of London, Memoirs, v. 35, p. 647–661. https://doi.org/10.1144/M35.42

Clarke, D.B., 1970. Tertiary basalts in Baffin Bay: possible primary magma from the mantle; Contributions to Mineralogy and Petrology, v. 25, p. 203–224. https://doi.org/10.1007/BF00371131

Clarke, D.B. et Beutel, E.K., 2020. Davis Strait Paleocene picrites: products of a plume or plates?; Earth-Science Reviews, v. 206, art. no. 102770. https://doi.org/10.1016/j.earscirev.2019.01.012

Dam, G., Pedersen, G.K., Sønderholm, M., Midtgaard, H., Larsen, L.M., Nøhr-Hansen, H. et Pedersen, A.K., 2009. Lithostratigraphy of the Cretaceous-Paleocene Nuussuaq Group, Nuussuaq Basin, West Greenland; Geological Survey of Denmark and Greenland Bulletin, v. 19, 171 p. https://doi.org/10.34194/geusb.v19.4886

Decker, V., Budkewitsch, P. et Tang, W., 2013. Database of suspect oil seeps in the marine environment of Baffin Bay and Davis Strait, Nunavut, identified from a survey of RADARSAT-2 data; Geological Survey of Canada, Open File 7404, 12 p. https://doi.org/10.4095/292761

Denyszyn, S.W., Davis, D.W. et Halls, H.C., 2009. Paleomagnetism and U-Pb geochronology of the Clarence Head dikes, Arctic Canada: orthogonal emplacement of mafic dikes in a large igneous province; Canadian Journal of Earth Sciences, v. 46, p. 155–167. https://doi.org/10.1139/E09-011

Dickie, K., Keen, C.E., Williams, G.L. et Dehler, S.A., 2011. Tectonostratigraphic evolution of the Labrador margin, Atlantic Canada; Marine and Petroleum Geology, v. 28, p. 1663–1675. https://doi.org/10.1016/j.marpetgeo.2011.05.009

Dunphy, J.M. et Ludden, J.N., 1998. Petrological and geochemical characteristics of a Paleoproterozoic magmatic arc (Narsajuaq Terrane, Ungava Orogen, Canada) and comparisons to Superior Province granitoids; Precambrian Research, v. 91, p. 109–142. https://doi.org/10.1016/S0301-9268(98)00041-2

Earthquakes Canada, 2018. Simplified seismic hazard map for Canada, the provinces and territories. <https://www.earthquakescanada.nrcan.gc.ca/hazard-alea/simphaz-en.php> [consulté le 4 mars 2020].

Elgin, R.A., 2017. Status and implications of reserves at carving stone quarries within the Qikiqtaaluk Region of Nunavut; *in* Summary of Activities 2017; Canada-Nunavut Geoscience Office, p. 151–158.

Fahrig, W.F., Christie, K.W. et Jones, D.L., 1981. Paleomagnetism of the Bylot basins: evidence for Mackenzie continental tensional tectonics; Geological Survey of Canada, Paper 81-10, p. 303–312. https://doi.org/10.4095/109368

Funck, T., Jackson, H.R., Louden, K.E. et Klingelhöfer, F., 2007. Seismic study of the transform-rifted margin in Davis Strait between Baffin Island (Canada) and Greenland: what happens when a plume meets a transform; Journal of Geophysical Research, v. 112, no. B4, 22 p. https://doi.org/10.1029/2006JB004308

Funck, T., Gohl, K., Damm, V. et Heyde, I., 2012. Tectonic evolution of southern Baffin Bay and Davis Strait: results from a seismic refraction transect between Canada and Greenland; Journal of Geophysical Research, v. 117, no. B4, 24 p. https://doi.org/10.1029/2011JB009110

Gautier, D.L., Bird, K.J., Charpentier, R.R., Grantz, A., Houseknecht, D.W., Klett, T.R., Moore, T.E., Pitman, J.K., Schenk, C.J., Schuenemeyer, J.H., Sørensen, K., Tennyson, M.E., Valin, Z.C. et Wandrey, C.J., 2011. Oil and gas resource potential north of the Arctic Circle; Chapter 9 *in* Arctic Petroleum Geology, (ed.) A.M. Spencer, A.F. Embry, D.L. Gautier, A.V. Stoupakova, and K. Sørensen; Geological Society of London, Memoirs, v. 35, p. 151–161. https://doi.org/10.1144/M35.9

Gibson, T.M., Shih, P.M., Cumming, V.M., Fischer, W.W., Crockford, P.W., Hodgskiss, M.S.W., Worndle, S., Creaser, R., Rainbird, R.H., Skulski, T.M. et Halverson, G.P., 2018. Precise age of *Bangiomorpha pubescens* dates the origin of eukaryotic photosynthesis; Geology, v. 46, p. 135–138. https://doi.org/10.1130/G39829.1

Gibson, T.M., Worndle, S., Crockford, P.W., Bui, T.H., Creaser, R.A. et Halverson, G.P., 2019. Radiogenic isotope chemostratigraphy reveals marine and nonmarine depositional environments in the late Mesoproterozoic Borden Basin, Arctic Canada; Geological Society of America Bulletin, v. 131, no. 11-12, p. 1965–1978. https://doi.org/10.1130/B35060.1

Government of Canada, 2018. Arctic offshore oil and gas. <www.rcaanc-cirnac.gc.ca/eng/1535571547022/1538586415269> [consulté le 23 mai 2019]

Grant, A.C., Levy, E.M., Lee, K. et Moffat, J.D., 1986. Pisces IV research submersible finds oil on Baffin Shelf; *in* Current Research, Part A; Geological Survey of Canada, Paper 86-1A, p. 65–69. https://doi.org/10.4095/120351

Gregersen, U., 2014. The West Greenland continental margin; *in* Tectonostratigraphic Atlas of the North-East Atlantic region, (ed.) J.R. Hopper, T. Funck, M. Stoker, U. Árting, G. Peron-Pinvidic, H. Dornenbal, and C. Gaina; Geological Survey of Denmark and Greenland, Copenhagen, Denmark, p. 321–325.

Gregersen, U., Hopper, J.R. et Knutz, P.C., 2013. Basin seismic stratigraphy and aspects of prospectivity in the NE Baffin Bay, northwest Greenland; Marine and Petroleum Geology, v. 46, p. 1–18. https://doi.org/10.1016/j.marpetgeo.2013.05.013

Gregersen, U., Andersen, M.S., Nøhr-Hansen, H., Sheldon, E., Kokfelt, T.F., Olivarius, M., Knudsen, C., Jakobsen, K.G. et Adolfssen, J.S., 2018. New subsurface mapping offshore southern West Greenland using geophysical and geological data; Geological Survey of Denmark and Greenland Bulletin, v. 41, p. 57–62. https://doi.org/10.34194/geusb.v41.4342

Gregersen, U., Knutz, P.C., Nøhr-Hansen, H., Sheldon, E. et Hopper, J.R., 2019. Tectonostratigraphy and evolution of the West Greenland continental margin; Bulletin of the Geological Society of Denmark, v. 67, p. 1–21. https://doi.org/10.37570/bgsd-2019-67-01

Hahn, K.E. et Turner, E.C., 2017. Composition and history of giant lacustrine carbonate seep mounds, Mesoproterozoic Borden Basin, Arctic Canada; Precambrian Research, v. 293, p. 150–173. https://doi.org/10.1016/j.precamres.2017.03.009

Hahn, K., Turner, E.C., Babechuk, M.G. et Kamber, B.S., 2015. Deep-water seep-related carbonate mounds in a Mesoproterozoic alkaline lake, Borden Basin (Nunavut, Canada); Precambrian Research, v. 271, p. 173–197. https://doi.org/10.1016/j.precamres.2015.09.025

Harrison, J.C., Brent, T.A. et Oakey, G.N., 2011. Baffin Fan and its inverted rift system of Arctic eastern Canada: stratigraphy, tectonics and petroleum resource potential; Chapter 40 *in* Arctic Petroleum Geology, (ed.) A.M. Spencer, A.F. Embry, D.L. Gautier, A.V. Stoupakova, and K. Sørensen; Geological Society of London, Memoirs, v. 35, p. 595–626. https://doi.org/10.1144/M35.40

Heaman, L.M., LeCheminant, A.N. et Rainbird, R.H., 1992. Nature and timing of Franklin igneous events, Canada: implications for a Late Proterozoic mantle plume and the breakup of Laurentia; Earth and Planetary Science Letters, v. 109, p. 117–131. https://doi.org/10.1016/0012-821X(92)90078-A

Heaman, L.M., Pell, J., Gruetter, H.S. et Creaser, R.A., 2015. U-Pb geochronology and Sr/Nd isotope compositions of groundmass perovskite from the newly discovered Jurassic Chidliak kimberlite field, Baffin Island, Canada; Earth and Planetary Science Letters, v. 415, p. 183–199. https://doi.org/10.1016/j.epsl.2014.12.056

Henriksen, N., Higgins, A.K., Kalsbeek, F. et Pulvertaft, T.C., 2009. Greenland from Archean to Quaternary. Descriptive text to the 1995 Geological map of Greenland 1:2 500 000, 2nd edition; Geological Survey of Denmark and Greenland Bulletin, v. 18, 126 p. https://doi.org/10.34194/geusb.v18.4993

Hogarth, D.D., Boreham, P.W. et Mitchell, J.G., 1994. Martin Frobisher's northwest venture, 1576-1581: mines, minerals & metallurgy; Canadian Museum of Civilization, Mercury Series, Directorate paper no. 7, 181 p.

Hosseinpour, M., Muller, R.D., Williams, S.E. et Whittaker, J.M., 2013. Full-fit reconstruction of the Labrador Sea and Baffin Bay; Solid Earth, v. 4, p. 461–479. https://doi.org/10.5194/se-4-461-2013

Iannelli, T., Robatian, M., Breckon, S., Campbell, H., Dao, P. et MacLeod, M., 2013a. Baffinland–Assessment Report: rock sampling, prospecting, geological mapping and geophysical surveying; report prepared for Indian and Northern Affairs Canada, Assessment Report #085816. <https://nunavutgeoscience.ca/gateway/browseA.php> [consulté le 25 avril 2022]

Iannelli, T., Robatian, M., Breckon, S., Campbell, H., Dao, P. et MacLeod, M., 2013b. Baffinland–Assessment Report: rock sampling, prospecting, geological mapping, and geophysical surveying; report prepared for Indian and Northern Affairs Canada, Assessment Report #085823. <https://nunavutgeoscience.ca/gateway/browseA.php> [consulté le 25 avril 2022]

Ioannides, N.S., 1986. Dinoflagellate cysts from Upper Cretaceous-Lower Tertiary sections, Bylot and Devon islands, Arctic Archipelago; Geological Survey of Canada, Bulletin 371, 99 p. https://doi.org/10.4095/123641

Jackson, G.D. et Davidson, A., 1975. Geology, Bylot Island, District of Franklin; Geological Survey of Canada, Map 1397A, scale 1:250 000. https://doi.org/10.4095/109007

Jackson, G.D. et Iannelli, T.R., 1981. Rift-related cyclic sedimentation in the Neohelikian Borden Basin, northern Baffin Island; Geological Survey of Canada, Paper 81-10, p. 269–302. https://doi.org/10.4095/109369

Jackson, G.D. et Morgan, W.C., 1978. Geology, Conn Lake, District of Franklin; Geological Survey of Canada, Map 1458A, scale 1:250 000. https://doi.org/10.4095/109162

Jackson, G.D. et Taylor, F.C., 1972. Correlation of major Aphebian rock units in the northeastern Canadian Shield; Canadian Journal of Earth Sciences, v. 9, p. 1650–1669. https://doi.org/10.1139/e72-146

Jackson, G.D., Davidson, A. et Morgan, W.C., 1975. Geology of the Pond Inlet map-area, Baffin Island, District of Franklin (38A, 38B, part of 48A); Geological Survey of Canada, Paper 74-25, 33 p. https://doi.org/10.4095/102498

Jackson, G.D., Morgan, W.C. et Davidson, A., 1979. Geology, Buchan Gulf-Scott Inlet, District of Franklin; Geological Survey of Canada, Map 1449A, scale 1:250 000. https://doi.org/10.4095/109159

James, T.S. et Schamehorn, T.D., 2016. A comparison of seismicity to the crustal deformation predicted by a glacial isostatic adjustment model in northern Canada and western Greenland; Geological Survey of Canada, Open File 8106, 18 p. https://doi.org/10.4095/299098

Jansa, L.F., 1976. Lower Paleozoic radiolarian-bearing limestones from the Baffin Island shelf; *in* Report of Activities, Part B; Geological Survey of Canada, Paper 76-1B, p. 99–105. https://doi.org/10.4095/104085

Keen, C.E., Dickie, K. et Dehler, S.A., 2012. The volcanic margins of the northern Labrador Sea: insights to the rifting process; Tectonics, v. 31, no. 1, 13 p. https://doi.org/10.1029/2011TC002985

Keen, C.E., Dickie, K. et Dafoe, L.T., 2018a. Structural characteristics of the ocean-continent transition along the rifted continental margin, offshore central Labrador; Marine and Petroleum Geology, v. 89, no. 2, p. 443–463. https://doi.org/10.1016/j.marpetgeo.2017.10.012

Keen, C.E., Dickie, K. et Dafoe, L.T., 2018b. Structural evolution of the rifted margin off northern Labrador: the role of hyper-extension and magmatism; Tectonics, v. 37, no. 7, p. 1955–1972. https://doi.org/10.1029/2017TC004924

Larsen, L.M., Heaman, L.M., Creaser, R.A., Duncan, R.A., Frei, R. et Hutchison, M., 2009. Tectonomagmatic events during stretching and basin formation in the Labrador Sea and the Davis Strait: evidence from age and composition of Mesozoic to Palaeogene dyke swarms in West Greenland; Journal of the Geological Society, v. 166, no. 6, p. 999–1012. https://doi.org/10.1144/0016-76492009-038

LeCheminant, A.N. et Heaman, L.M., 1989. Mackenzie igneous events, Canada: middle Proterozoic hotspot magmatism associated with ocean opening; Earth and Planetary Science Letters, v. 96, p. 38–48. https://doi.org/10.1016/0012-821X(89)90122-2

Lemon, R.R.H. et Blackadar, R.G., 1963. Admiralty Inlet area, Baffin Island, District of Franklin; Geological Survey of Canada, Memoir 328, 84 p. https://doi.org/10.4095/108031

Long, D.G.F. et Turner, E.C., 2012. Tectonic, sedimentary and metallogenic re-evaluation of basal strata in the Mesoproterozoic Bylot basins (NU): are unconformity-type U concentrations a realistic expectation; Precambrian Research, v. 214-215, p. 192–209. https://doi.org/10.1016/j.precamres.2011.11.005

MacLean, B., Jansa, L.F., Falconer, R.K.H. et Srivastava, S.P., 1977. Ordovician strata on the southeastern Baffin Island shelf revealed by shallow drilling; Canadian Journal of Earth Sciences, v. 14, p. 1925–1939. https://doi.org/10.1139/e77-163

MacLean, B., Williams, G. et Zhang, S., 2014. New insights into the stratigraphy and petroleum potential of the Baffin Shelf's Cretaceous rocks; Bulletin of Canadian Petroleum Geology, v. 62, no. 4, p. 289–310. https://doi.org/10.2113/gscpgbull.62.4.289

McMillan, J.G., 1910. Geologist's report on the Arctic Expedition, 1908–1909; *in* Cruise of the Arctic 1908-1909, (ed.) J.E. Bernier; Government Printing Bureau, Ottawa, Ontario, 529 p.

McWhae, J.R.H., Elie, R., Laughton, K.C. et Gunther, P.R., 1980. Stratigraphy and petroleum prospects of the Labrador Shelf; Bulletin of Canadian Petroleum Geology, v. 28, p. 460–488.

Miall, A.D., Balkwill, H.R. et Hopkins, W.S., Jr., 1980. Cretaceous and tertiary sediments of Eclipse trough, Bylot Island area, Arctic Canada, and their regional setting; Geological Survey of Canada, Paper 79-23, 20 p. https://doi.org/10.4095/102162

Moir, P.S., 1989. Lithostratigraphy Labrador Sea: review and type sections; *in* East Coast Basin Atlas Series, Labrador Sea, (ed.) J.S. Bell; Geological Survey of Canada, p. 26–27. https://doi.org/10.4095/127166

Nantais, P., 1984. Regional hydrocarbon potential of the Labrador Shelf; Geological Survey of Canada, Open File 1197, 50 p. https://doi.org/10.4095/130015

Newman, L.A., 1987. Quaternary stratigraphy of the Scott Lowland, Baffin Island, Northwest Territories; B.Sc. thesis, Memorial University of Newfoundland, St. John's, Newfoundland and Labrador, 53 p.

Nøhr-Hansen, H., Williams, G.L. et Fensome, R.A., 2016. Biostratigraphic correlation of the western and eastern margins of the Labrador–Baffin Seaway and implications for the regional geology; Geological Survey of Denmark and Greenland Bulletin, v. 37, 74 p. https://doi.org/10.34194/geusb.v37.4356

Oakey, G.N. et Chalmers, J.A., 2012. A new model for the Paleogene motion of Greenland relative to North America: plate reconstructions of the Davis Strait and Nares Strait regions between Canada and Greenland; Journal of Geophysical Research, v. 117, no. B10, 28 p. https://doi.org/10.1029/2011JB008942

Peace, A.L., Foulger, G.R., Schiffer, C. et McCaffrey, K.J.W., 2017. Evolution of Labrador Sea-Baffin Bay: plate or plume processes?; Geoscience Canada, v. 44, p. 91–102. https://doi.org/10.12789/geocanj.2017.44.120

Pehrsson, S.J. et Buchan, K.L., 1999. Borden dykes of Baffin Island, N.W.T.: a Franklin U-Pb baddeleyite age and a paleomagnetic interpretation; Canadian Journal of Earth Sciences, v. 36, p. 65–73. https://doi.org/10.1139/e98-091

Rainbird, R., Cawood, P. et Gehrels, G.E., 2012. The Great Grenvillian sedimentation episode: record of supercontinent Rodinia's assembly; *in* Recent Advances in Tectonics of Sedimentary Basins, (ed.) C. Busby and A. Azor; Blackwell Publishing Ltd., Oxford, United Kingdom, p. 583–601. https://doi.org/10.1002/9781444347166.ch29

Rayner, N.M., Sanborn-Barrie, M., Young, M.D. et Whalen, J.B., 2012. U-Pb ages of Archean basement and Paleoproterozoic plutonic rocks, southern Cumberland Peninsula, eastern Baffin Island, Nunavut; Geological Survey of Canada, Current Research 2012-8, 28 p. https://doi.org/10.4095/291401

Roest, W.R. et Srivastava, S.P., 1989. Sea-floor spreading in the Labrador Sea: a new reconstruction; Geology, v. 17, no. 11, p. 1000–1003. https://doi.org/10.1130/0091-7613(1989)017%3c1000:SFSITL%3e2.3.CO%3b2

Sanborn-Barrie, M., Thrane, K., Wodicka, N. et Rayner, N., 2017. The Laurentia - West Greenland connection at 1.9 Ga: New insights from the Rinkian fold belt; Gondwana Research, v. 51, p. 289–309. https://doi.org/10.1016/j.gr.2017.07.002

Sanford, B.V. et Grant, A.C., 1990. New findings relating to the stratigraphy and structure of the Hudson Platform; *in* Current Research, Part D; Geological Survey of Canada, Paper 90-1D, p. 17–30. https://doi.org/10.4095/131335

Sanford, B.V. et Grant, A.C., 2000. Geological framework of the Ordovician system in the southeast Arctic Platform, Nunavut; *in* Geology and Paleontology of the Southeast Arctic Platform and Southern Baffin Island, Nunavut, (ed.) A.D. McCracken and T.E. Bolton; Geological Survey of Canada, Bulletin 557, p. 13–38. https://doi.org/10.4095/211845

Sangster, D.F., 1998. Mineral deposits compilation and metallogenic domains, northern Baffin Island and northern Melville Peninsula, Northwest Territories; Geological Survey of Canada, Open File 3635, scale 1:1 000 000. https://doi.org/10.4095/210026

Saumur, B.M., Skipton, D.R., St-Onge, M.R., Bros, E.R., Acosta-Gongora, P., Kelly, C.J., Morin, A., O'Brien, M.E., Johnston, S.T et Weller, O.M., 2018. Precambrian geology of the surroundings of Steensby Inlet and western Barnes Ice Cap (parts of NTS 37E, 37F, 37G), Baffin Island, Nunavut; *in* Summary of Activities 2018; Canada-Nunavut Geoscience Office, p. 29–46.

Scott, D.J., 1997. Geology, U-Pb, and Pb-Pb geochronology of the Lake Harbour area, southern Baffin Island: Implications for the Paleoproterozoic tectonic evolution of northeastern Laurentia; Canadian Journal of Earth Sciences, v. 34, p. 140–155. https://doi.org/10.1139/e17-012

Scott, D.J. et de Kemp, E.A., 1998. Bedrock geology compilation, northern Baffin Island and northern Melville Peninsula; Geological Survey of Canada, Open File 3633, scale 1:500 000. https://doi.org/10.4095/210024

Scott, D.J. et Wodicka, N.A., 1998. Second report on the U-Pb geochronology of southern Baffin Island, Northwest Territories; *in* Current Research 1998-F; Geological Survey of Canada, p. 47–57. https://doi.org/10.4095/210055

Sherman, A.G., James, N.P. et Narbonne, G.M., 2002. Evidence for reversal of basin polarity during carbonate ramp development in the Mesoproterozoic Borden Basin, Baffin Island; Canadian Journal of Earth Sciences, v. 39, p. 519–538. https://doi.org/10.1139/e01-089

Skipton, D.R., Saumur, B.M., St-Onge, M.R., Wodicka, N., Bros, E.R., Morin, A., Brouillette, P., Weller, O.M. et Johnston, S.T., 2017. Precambrian bedrock geology of the Pond Inlet-Mary River area, northern Baffin Island; *in* Summary of Activities 2018; Canada-Nunavut Geoscience Office, p. 49–67.

Sparkes, K.E., 1989. Stratigraphy and terrestrial palynology of Late Cretaceous Eclipse Group strata, Bylot Island, Northwest Territories, Canada; B.Sc. thesis, Memorial University of Newfoundland, St. John's, Newfoundland and Labrador, 195 p.

Srivastava, S.P., 1978. Evolution of the Labrador Sea and its bearing on the early evolution of the North Atlantic; Geophysical Journal International, v. 52, p. 313–357. https://doi.org/10.1111/j.1365-246X.1978.tb04235.x

St-Onge, M.R., Hanmer, S. et Scott, D.J., 1996. Geology of the Meta Incognita Peninsula, south Baffin Island, Northwest Territories: tectonostratigraphic units and regional correlations; *in* Current Research 1996-C; Geological Survey of Canada, p. 63–72. https://doi.org/10.4095/207444

St-Onge, M.R., Scott, D.J. et Lucas, S.B., 2000. Early partitioning of Quebec: microcontinent formation in the Paleoproterozoic; Geology, v. 28, p. 323–326. https://doi.org/10.1130/0091-7613(2000)28%3c323:EPOQMF%3e2.0.CO%3b2

St-Onge, M.R., Searle, M.P. et Wodicka, N., 2006. Trans-Hudson Orogen of North America and Himalaya-Karakoram-Tibetan Orogen of Asia: structural and thermal characteristics of the lower and upper plates; Tectonics, v. 25, no. 4, 22 p. https://doi.org/10.1029/2005TC001907

St-Onge, M.R., Van Gool, J.A.M., Garde, A.A. et Scott, D.J., 2009. Correlation of Archaean and Palaeoproterozoic units between northeastern Canada and western Greenland: constraining the pre-collisional upper plate accretionary history of the Trans-Hudson orogen; Geological Society of London, Special Publications, v. 318, p. 193–235. https://doi.org/10.1144/SP318.7

St-Onge, M.R., Weller, O.M. et Rayner, N.M., 2016. 2016 report of activities for completing the regional bedrock mapping of the southern half of Baffin Island: GEM 2 Baffin Project; Geological Survey of Canada, Open File 8118, 11 p. https://doi.org/10.4095/299195

Steenkamp, H.M., Pizzo-Lyall, M., Wallace, C.J., Beauregard, M.A. et Dyck, B.J., 2014. Geology, history and site-management planning of the Kangiqsukutaaq carving stone quarry, southern Baffin Island; *in* Summary of Activities 2013; Canada-Nunavut Geoscience Office, p. 193–200.

Steenkamp, H.M., Beauregard, M.A. et Mate, D.J., 2015. Carving stone and mineral resource potential of the Opingivik deposit, southern Baffin Island; *in* Summary of Activities 2014; Canada-Nunavut Geoscience Office, p. 153–162.

Storey, M., Duncan, R.A. et Tegner, C., 2007. Timing and duration of volcanism in the North Atlantic Igneous Province: implications for geodynamics and links to the Iceland hotspot; Chemical Geology, v. 241, no. 3-4, p. 264–281. https://doi.org/10.1016/j.chemgeo.2007.01.016

Suckro, S.K., Gohl, K., Funck, T., Heyde, I., Ehrhardt, A., Schreckenberger, B., Gerlings, J., Damm, V. et Jokat, W., 2012. The crustal structure of southern Baffin Bay: implications from a seismic refraction experiment; Geophysical Journal International, v. 190, no. 1, p. 37–58. https://doi.org/10.1111/j.1365-246X.2012.05477.x

Suckro, S.K., Gohl, K., Funck, T., Heyde, I., Schreckenberger, B., Gerlings, J. et Damm, V., 2013. The Davis Strait crust—a transform margin between two oceanic basins; Geophysical Journal International, v. 193, no. 1, p. 78–97. https://doi.org/10.1093/gji/ggs126

Taylor, F.B., 1910. Bearing of the Tertiary mountain belt on the origin of the Earth's plan; Geological Society of America Bulletin, v. 21, p. 179–226. https://doi.org/10.1130/GSAB-21-179

Thériault, R.J., St-Onge, M.R. et Scott, D.J., 2001. Nd isotopic and geochemical signature of the Paleoproterozoic Trans-Hudson Orogen, southern Baffin Island, Canada: implications for the evolution of eastern Laurentia; Precambrian Research, v. 108, p. 113–138. https://doi.org/10.1016/S0301-9268(00)00159-5

Trettin, H.P., 1965a. Middle Ordovician to Middle Silurian carbonate cycle, Brodeur Peninsula, northwestern Baffin Island; Bulletin of Canadian Petroleum Geology, v. 13, p. 155–180.

Trettin, H.P., 1965b. Lower Paleozoic sediments of northwestern Baffin Island, District of Franklin; Geological Survey of Canada, Paper 64-47, 28 p. https://doi.org/10.4095/101000

Trettin, H.P., 1969. Lower Paleozoic sediments of northwestern Baffin Island; Geological Survey of Canada, Bulletin 157, 70 p. https://doi.org/10.4095/102249

Trettin, H.P., 1975. Investigations of Lower Paleozoic geology, Foxe Basin, northeastern Melville Peninsula, and parts of northwestern and central Baffin Island; Geological Survey of Canada, Bulletin 251, 177 p. https://doi.org/10.4095/103973

Turner, E.C., 2009. Mesoproterozoic carbonate systems in the Borden Basin, Nunavut; Canadian Journal of Earth Sciences, v. 46, p. 915–938. https://doi.org/10.1139/E09-062

Turner, E.C., 2011. Structural and stratigraphic controls on carbonate-hosted base-metal mineralization in the Mesoproterozoic Borden Basin (Nanisivik District), Nunavut; Economic Geology and the Bulletin of the Society of Economic Geologists, v. 106, p. 1197–1223. https://doi.org/10.2113/econgeo.106.7.1197

Turner, E.C. et Kamber, B.S., 2012. Arctic Bay Formation, Borden Basin, Nunavut (Canada): Basin evolution, black shale base-metal potential and dissolved metal systematics in the Mesoproterozoic ocean; Precambrian Research, v. 208–211, p. 1–18. https://doi.org/10.1016/j.precamres.2012.03.006

Turner, E.C., Long, D.G.F., Rainbird, R.H., Petrus, J.A. et Rayner, N.M., 2016. Late Mesoproterozoic rifting in Arctic Canada during Rodinia assembly: impactogens, trans-continental far-field stress, and zinc mineralisation; Terra Nova, v. 28, p. 188–194. https://doi.org/10.1111/ter.12207

Umpleby, D.C., 1979. Geology of the Labrador Shelf; Geological Survey of Canada, Paper 79-13, 40 p. https://doi.org/10.4095/105927

Vande Guchte, M.J., 1998. Geological, geochemical and geophysical report on the Incognito joint venture project [Rubicon Minerals Corp.]; Aboriginal Affairs and Northern Development Canada, Assessment Report 084053. <https://nunavutgeoscience.ca/gateway/browseA.php> [consulté le 25 avril 2022]

Vande Guchte, M.J. et Gray, M.J., 1999. Geological, geochemical and diamond drilling report on the Incognito joint venture project, 1997 exploration program [Rubicon Minerals Corp.]; Aboriginal Affairs and Northern Development Canada, Assessment Report 084168. <https://nunavutgeoscience.ca/gateway/browseA.php> [consulté le 25 avril 2022]

Voss, P., Poulsen, S.K., Simonsen, S.B. et Gregersen, S., 2007. Seismic hazard assessment of Greenland; Geological Survey of Denmark and Greenland Bulletin, v. 13, p. 57–60. https://doi.org/10.34194/geusb.v13.4976

Waterfield, J.J., 1989. Stratigraphy, sedimentology and palynology of Cretaceous and Tertiary strata, southwest Bylot Island, Northwest Territories, Canada; M.Sc. thesis, Memorial University of Newfoundland, St. John's, Newfoundland and Labrador, 260 p.

Welford, J.K. et Hall, J., 2013. Lithospheric structure of the Labrador Sea from constrained 3-D gravity inversion; Geophysical Journal International, v. 195, no. 2, p. 767–784. https://doi.org/10.1093/gji/ggt296

Welford, J.K., Peace, A.L., Geng, M., Dehler, S.A. et Dickie, K., 2018. Crustal structure of Baffin Bay from constrained three-dimensional gravity inversion and deformable plate tectonic models; Geophysical Journal International, v. 214, p. 1281–1300. https://doi.org/10.1093/gji/ggy193

Wiseman, T.R., 1991. Sedimentology of the Maastrichtian, Pond Inlet Formation (channelized turbidite system), Bylot Island, Northwest Territories, Canada; B.Sc. thesis, Memorial University of Newfoundland, St. John's, Newfoundland and Labrador, 133 p.

Wodicka, N. et Scott, D.J., 1997. A preliminary report on the U-Pb geochronology of the Meta Incognita Peninsula, southern Baffin Island, Northwest Territories; *in* Current Research 1997-C; Geological Survey of Canada, p. 167–178. https://doi.org/10.4095/208642

Wodicka, N., St-Onge, M.R., Corrigan, D., Scott, D.J. et Whalen, J.B., 2014. Did a proto-ocean basin form along the southeastern Rae cratonic margin? Evidence from U-Pb geochronology, geochemistry (Sm-Nd and whole-rock), and stratigraphy of the Paleoproterozoic Piling Group, northern Canada; Geological Society of America Bulletin, v. 126, p. 1625–1653. https://doi.org/10.1130/B31028.1

Archean and Paleoproterozoic cratonic rocks of Baffin Island

M.R. St-Onge[1]*, D.J. Scott[2], N. Rayner[1], M. Sanborn-Barrie[1], D.R. Skipton[3], B.M. Saumur[4], N. Wodicka[1], and O.M. Weller[5]

St-Onge, M.R., Scott, D.J., Rayner, N., Sanborn-Barrie, M., Skipton, D.R., Saumur, B.M., Wodicka, N., and Weller, O.M., 2022. Archean and Paleoproterozoic cratonic rocks of Baffin Island; in *Geological synthesis of Baffin Island (Nunavut) and the Labrador–Baffin Seaway, (ed.) L.T. Dafoe and N. Bingham-Koslowski; Geological Survey of Canada, Bulletin 608, p. 25–53. https://doi.org/10.4095/321824*

Abstract: Archean and Paleoproterozoic cratonic rocks of Baffin Island define four stacked structural levels that are juxtaposed within the middle Paleoproterozoic Trans-Hudson Orogen. From north to south, and highest to lowest structural level, these comprise: 1) the Archean Rae Craton, unconformably overlain along its southern margin by middle Paleoproterozoic supracrustal cover (Piling Group) and stratigraphically similar units of the Hoare Bay Group on Cumberland Peninsula; 2) Archean to middle Paleoproterozoic metaplutonic units and middle Paleoproterozoic metasedimentary cover (Lake Harbour Group), collectively termed the 'Meta Incognita microcontinent'; 3) middle Paleoproterozoic orthogneiss, interpreted as a deformed arc–magmatic terrane (Narsajuaq terrane) or alternatively as Narsajuaq-age intrusions emplaced in the Meta Incognita microcontinent; and 4) Archean orthogneiss, interpreted as the northern continuation of the lower-plate Superior Craton, and associated middle Paleoproterozoic continental-margin supracrustal cover (Povungnituk Group).

Résumé : Les roches cratoniques de l'Archéen et du Paléoprotérozoïque de l'île de Baffin définissent un empilement de quatre niveaux structuraux qui sont juxtaposés dans l'orogène trans-hudsonien du Paléoprotérozoïque moyen. Du nord au sud, et du plus haut au plus bas niveau structural, ceux-ci comprennent : 1) le craton de Rae de l'Archéen, recouvert en discordance le long de sa marge sud par des roches supracrustales de couverture du Paléoprotérozoïque moyen (Groupe de Piling) et des unités stratigraphiquement semblables du Groupe de Hoare Bay dans la péninsule Cumberland; 2) des unités métaplutoniques de l'Archéen au Paléoprotérozoïque moyen et des roches métasédimentaires de couverture du Paléoprotérozoïque moyen (Groupe de Harbour Lake), collectivement dénommées « microcontinent de Meta Incognita »; 3) des orthogneiss du Paléoprotérozoïque moyen, qui correspondraient à un terrane d'arc magmatique déformé (terrane de Narsajuaq) ou à des intrusions d'âge Narsajuaq mises en place dans le microcontinent de Meta Incognita; et 4) des orthogneiss de l'Archéen, qui constitueraient le prolongement nord du craton du lac Supérieur (plaque inférieure), et des roches supracrustales de couverture de la marge continentale associée du Paléoprotérozoïque moyen (Groupe de Povungnituk).

[1]Geological Survey of Canada, 601 Booth Street, Ottawa, Ontario K1A 0E8
[2]Polar Knowledge Canada, 170 Laurier Avenue West, Ottawa, Ontario K1P 5V5
[3]Yukon Geological Survey, Government of Yukon, Box 2703, Whitehorse, Yukon Y1A 2C6
[4]Université du Québec à Montréal, 201, avenue du Président-Kennedy, Montréal, Quebec H2X 3Y7
[5]Department of Earth Sciences, University of Cambridge, Cambridge, United Kingdom
*Corresponding author: M.R. St-Onge (email: marc.st-onge@nrcan-rncan.gc.ca)

PREVIOUS WORK

Although Martin Frobisher's second and third voyages in 1577 and 1578, directed as they were to searching for gold, had a geological connotation (Hogarth et al., 1994), geological investigation of Baffin Island properly began with fossils recovered at Silliman's Fossil Mount (Fig. 1) by C.F. Hall in 1861; this collection indicated the existence of Ordovician strata and the affinities of these strata to North American sections (Hall, 1865; Miller et al., 1954). In 1885, R. Bell of the Geological Survey of Canada (GSC) made a brief examination of the area around Amadjuak Bay on the southern coast of Baffin Island (Fig. 1; Bell, 1885) and, in 1897, he carried out a coastal reconnaissance between Big Island and Chorkbak Inlet (Fig. 1; Bell, 1901).

In 1926–1927, L.J. Weeks and M.H. Haycock built Canada's first Arctic research station and overwintered in Pangnirtung (Fig. 1). They carried out studies around the head of Cumberland Sound and west from Nettilling Fiord to Nettilling Lake (Fig. 1; Weeks, 1928a, b). In 1927, the Putnam Baffin Island Expedition explored the northern coast of Foxe Peninsula and traversed inland from Bowman Bay to Putnam Highland, documenting part of the extensive Paleozoic cover between Amadjuak Lake and Foxe Basin (Fig. 1; Putnam, 1928).

Reconnaissance geological investigations of southern Baffin Island by the GSC resumed in 1949 when Y.O. Fortier and W.L. Davison examined the coast of Meta Incognita Peninsula, and in addition made four traverses across the peninsula. Davison continued the coastal studies in 1950 and 1951, and carried out detailed mapping near Kimmirut (Fig. 1; Davison, 1959a). In 1950, he mapped the northern shore of Frobisher Bay and the eastern coast of Hall Peninsula as far north as Cape St. David (Fig. 1). The following season, he continued coastal mapping west from Kimmirut to Chorkbak Inlet (Fig. 1; Davison, 1959b), while G.C. Riley carried out geological investigations along the shores of Cumberland Sound to Cape St. David (Fig. 1; Riley, 1959). Studies of the northern shore of Hudson Strait were continued in 1952 under the direction of Y.O. Fortier, and the shoreline was mapped between Chorkbak Inlet and the former community of Nuwata (Fig. 1), on western Foxe Peninsula.

Low-grade iron deposits discovered on southern Baffin Island during the preceding work were staked in 1956–1957 by Ultra Shawkey Mines Ltd. Interest in the economic possibilities of southern Baffin Island led the GSC to undertake more detailed work and, in 1958, R.G. Blackadar commenced mapping at a scale of 1 inch to 4 miles. He mapped the Mingo Lake and Macdonald Island map areas between 1958 and 1960 (Blackadar, 1959, 1960, 1961, 1967a, b,) and the Andrew Gordon Bay and Cory Bay map areas in 1961 and 1964 (Blackadar, 1962, 1967c).

Reconnaissance mapping of Baffin Island south of latitude 66°N was completed in 1965 during 'Operation Amadjuak', a fixed-wing- and helicopter-supported project. Bedrock mapping was carried out across eighteen 1:250 000 NTS map areas and these data, together with those derived from published and unpublished GSC maps, were compiled into three regional bedrock maps published at 1:506 880 scale by Blackadar (1967c, d, e). This was followed by a series of helicopter-borne operations in central Baffin Island (e.g. Morgan, 1983; Henderson, 1985). Bedrock mapping at 1:50 000 scale was conducted by the GSC in 1994 across a 2800 km^2 area centred on Eqe Bay (Fig. 1), west-central Baffin Island. Mapping results, geochronological and geochemical data were presented in Bethune and Scammell (1997, 2003a, b). Subsequently, modern geoscience knowledge has been provided by field campaigns featuring helicopter-assisted foot traverses in: 1) southern Baffin Island (1995–1997; green shading in Fig. 1); 2) central Baffin Island (2000–2002; orange shading in Fig. 1); 3) southwestern Baffin Island (2006; yellow shading in Fig. 1); 4) Cumberland Peninsula (2009–2011; pale pink shading in Fig. 1); 5) Hall Peninsula (2012–2014; blue shading in Fig. 1); 6) Meta Incognita Peninsula (2014; purple shading in Fig. 1); and 7) in the Clearwater Fiord–Sylvia

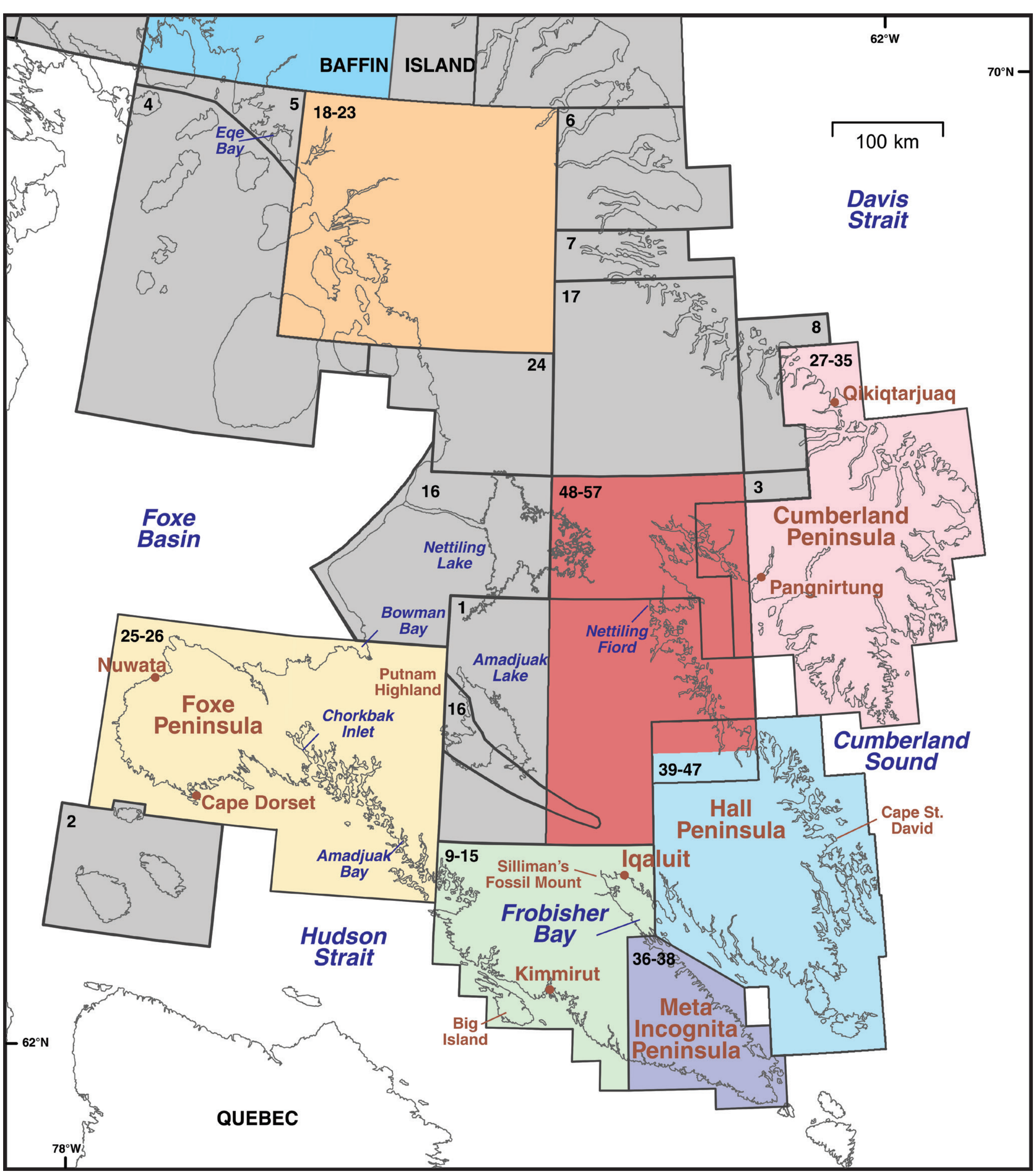

Figure 1. Summary of bedrock mapping campaigns undertaken south of latitude 70°N on Baffin Island, Nunavut. Bold numbers denote map references in chronological order, which are listed in Appendix A. Coloured shading highlights areas where field campaigns were conducted, as described in the text.

Grinnell Lake area (2015; pale red shading in Fig. 1). The latter project effectively completed the framework bedrock mapping of southern Baffin Island (Weller et al., 2015; St-Onge et al., 2016).

North of latitude 70°N, reconnaissance geological mapping was conducted by G.D. Jackson and R.G. Blackadar in 1965–1968 as part of two bedrock mapping operations on northern Baffin Island (Fig. 2; Blackadar et al., 1968a–h; Jackson and Davidson, 1975a, b; Jackson and Morgan, 1978; Jackson et al., 1979; Jackson, 1984). Mapping involved helicopter traverses with stops spaced approximately 8 km apart, supplemented by more detailed targeted work to examine the stratigraphy of supracrustal rocks, including exposures in the Mary River area (Fig. 2), where Archean greenstone belts host world-class iron deposits. In 1987, a bedrock geological map of Borden Peninsula was published (Fig. 2; Jackson and Sangster, 1987) and, in 1988, a geological map focused on the Mesoproterozoic Fury and Hecla Group was released (Fig. 2; Chandler, 1988). Jackson et al. (1975) and Jackson (2000) presented a summary of the bedrock geology of northern Baffin Island, including descriptions of lithological units and preliminary accounts of metamorphism, deformation and economic mineralization. Detailed sketch maps of the iron-bearing Mary River Group were subsequently released (Jackson, 2006).

In 2003–2005, the Canada-Nunavut Geoscience Office completed targeted bedrock mapping as a subcomponent of the 2003–2005 North Baffin project, in which surficial geology was the primary focus. Resulting 1:50 000 scale maps were published in Young et al. (2004), together with an interpreted structural–stratigraphic framework. More recently, targeted and 1:100 000 scale bedrock mapping was conducted under the Geo-mapping for Energy and Minerals program North Baffin Island Bedrock Mapping activity (2017–2018; blue shading in Fig. 2) to bring bedrock mapping and geoscience knowledge to an equal level with that achieved on southern Baffin Island (e.g. St-Onge et al., 2015c; Weller et al., 2015).

The geological and tectonic synthesis of the Archean and Paleoproterozoic cratonic units of Baffin Island presented in this paper relies in part on original field observations and descriptions of rock formations that have been previously published by the co-authors in several field reports. Chief amongst these are the following publications, to which the reader is referred for further information: St-Onge et al. (2015b, c), Weller et al. (2015), Skipton et al. (2017), and Saumur et al. (2018).

TECTONIC FRAMEWORK

Baffin Island forms part of the northeastern (Quebec–Baffin) segment of the Trans-Hudson Orogen (THO), which is a collisional/accretionary orogenic belt that extends in a broad arcuate corridor from northeastern to south-central North America (Hoffman, 1988; Lewry and Collerson, 1990). The THO formed during the final phase of growth of the Nuna supercontinent, and *sensu lato* records closure of the Manikewan Ocean between the lower Superior and upper Churchill plates from ca. 1.92 to 1.80 Ga. In detail, the northeastern THO is a composite collision zone that comprises tectonostratigraphic assemblages accumulated on, or accreted to, the northern margin of the lower-plate Archean Superior Craton and involved a series of short-duration tectonothermal events, which encompass specific accretionary phases within the much larger orogenic system during 120 Ma of gradual ocean-basin closure (St-Onge et al., 2006, 2007, 2009; Corrigan et al., 2009; Corrigan, 2012; Weller and

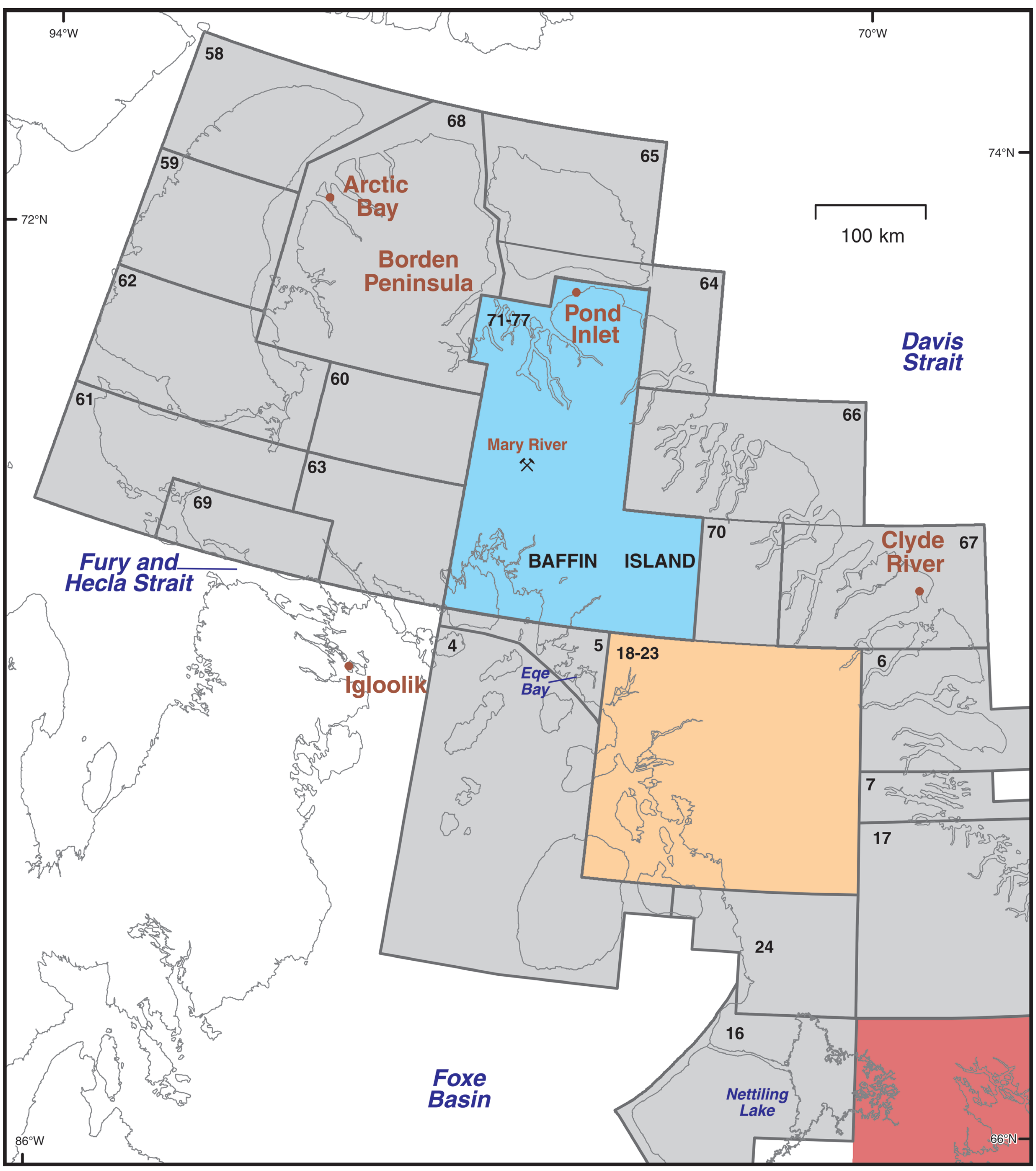

Figure 2. Summary of bedrock mapping campaigns undertaken north of latitude 70°N on Baffin Island, Nunavut. Bold numbers denote map references in chronological order, which are listed in Appendix A. Coloured shading highlights areas where field campaigns were conducted, as described in the text.

St-Onge, 2017). Four orogen-scale stacked structural levels have been identified in the eastern THO (Fig. 3). From north to south, and highest to lowest structural level, these comprise:

- Level 4 – The eastern Rae Craton (Bethune and Scammell, 2003a; Skipton et al., 2017; Saumur et al., 2018), consisting of Archean basement orthogneiss, felsic plutonic rocks and supracrustal packages, unconformably overlain along its southern margin by middle Paleoproterozoic supracrustal cover (Piling Group; Partin et al., 2014a; Wodicka et al., 2014) and stratigraphically similar units of the Hoare Bay Group on Cumberland Peninsula (Sanborn-Barrie et al., 2017). A middle Paleoproterozoic felsic plutonic suite (Qikiqtarjuaq plutonic suite; Sanborn-Barrie et al., 2011, 2013; Rayner et al., 2012) intrudes both the cratonic basement and supracrustal cover strata.
- Level 3 – Archean to middle Paleoproterozoic gneissic and metaplutonic units and middle Paleoproterozoic metasedimentary cover units (Lake Harbour Group; Jackson and Taylor, 1972), collectively termed the 'Meta Incognita microcontinent' by St-Onge et al. (2000a), which represents crust rifted from the Rae Craton, or the Superior Craton, or that is exotic to both.
- Level 2 – Middle Paleoproterozoic, dominantly monzogranitic to granodioritic orthogneiss, interpreted as a deformed arc-magmatic terrane (Narsajuaq terrane; Scott, 1997; Wodicka and Scott, 1997; Thériault et al., 2001; St-Onge et al., 2009) or alternatively as Narsajuaq-age intrusions emplaced in Level 3 (Corrigan et al. 2009).
- Level 1 – Archean tonalitic to granitic orthogneiss, interpreted as the northern continuation of the lower-plate Superior Craton crystalline basement, and associated middle Paleoproterozoic continental-margin supracrustal cover (Povungnituk Group; St-Onge et al., 1996).

Levels 3 and 4 are intruded by the Qikiqtarjuaq plutonic suite (Sanborn-Barrie et al., 2011, 2013; Rayner et al., 2012), dated between ca. 1896 and 1886 Ma (Rayner, 2017), and the Cumberland batholith, which comprises various granitoid phases dated at ca. 1865 to 1845 Ma (Whalen et al., 2010; Rayner, 2015, 2017). The Cumberland batholith has been interpreted as an Andean-type batholith (St-Onge et al., 2009), or as the result of postcollisional lithospheric delamination and mantle upwelling (Whalen et al., 2010). Level 4 is unconformably overlain by the Mesoproterozoic sedimentary and volcanic units of the Borden and Fury and Hecla basins (Chandler, 1988; Jackson, 2000). All levels are cut by ca. 720 Ma basaltic dykes of the Franklin swarm, which were emplaced during plume magmatism associated with the breakup of the Rodinia Supercontinent (Heaman et al., 1992). Levels 3 and 4 are unconformably overlain by Cambro–Ordovician clastic and carbonate sedimentary strata (Blackadar, 1967e; Blackadar et al., 1968a–h), whereas Level 4 is also unconformably overlain by Cretaceous sandstone (Jackson and Davidson, 1975b; Jackson et al., 1975) and Paleocene volcanic and sedimentary strata (Clarke and Upton, 1971).

The four structural levels were progressively accreted from north to south across a series of, in part, cryptic crustal sutures during long-lived deformation associated with the THO. The oldest of these sutures, the Level 3–4 'Baffin suture' (Fig. 3), is proposed to have resulted from accretion of the Meta Incognita microcontinent to the Rae Craton between 1915 ± 8 Ma (the youngest, most precise maximum age constraint for the Piling Group; Wodicka et al., 2014) and 1896 ± 8 Ma (the oldest dated phase of the Qikiqtarjuaq plutonic suite; Rayner 2017). Evidence of this suture is relatively sparse due to postaccretion magmatism engulfing the putative suture zone but includes the presence of distinct and opposite-facing, shelf-to-basin stratigraphic sequences (St-Onge et al., 2009; Weller et al., 2015). To the north of the proposed suture lies the stratigraphically south-facing Piling Group, which comprises a continental-margin sequence, characterized by basal shallow-marine

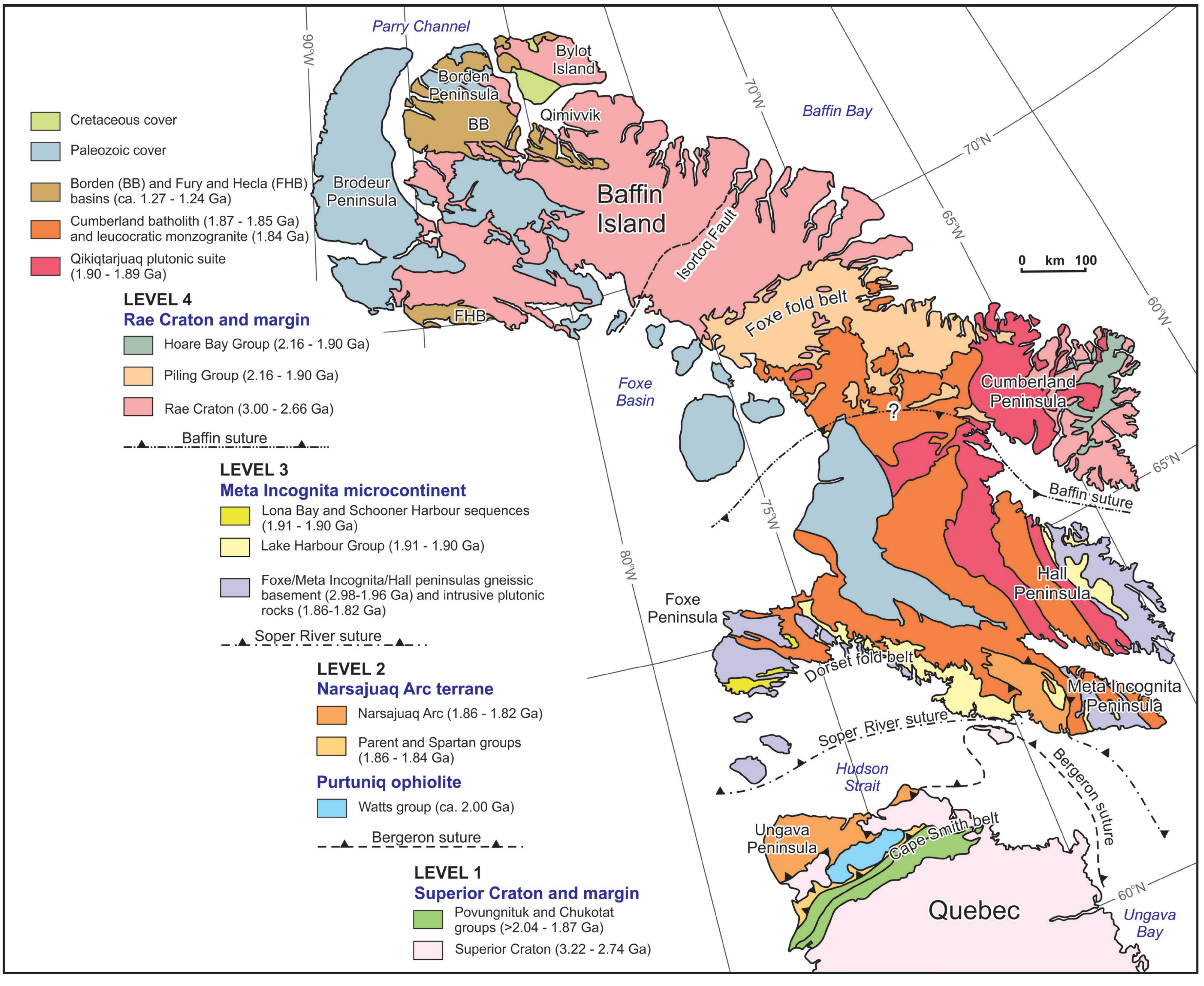

Figure 3. Simplified geological terrane map of the Quebec–Baffin segment of the Trans-Hudson Orogen (*modified from* St-Onge et al., 2007; Weller et al., 2015; Rayner, 2017), showing the four structural levels and three sutures that characterize the middle Paleoproterozoic assembly of Baffin Island. The map provides a regional tectonic context for the principal Archean and Paleoproterozoic tectonostratigraphic assemblages of Baffin Island.

continental-margin clastic and carbonate-platform strata, overlain by a volcano-sedimentary rift package that includes iron-formation, and capped by deep-water turbidites (Partin et al., 2014a; Wodicka et al., 2014). To the south of the proposed suture lies the Lake Harbour Group, which grades basinward to the north and comprises a clastic–carbonate continental-margin sequence (Scott et al., 1997, 2002a). Stratigraphic differences with the Piling Group include the presence of a basal orthoquartzite and the absence of iron-formation and greywacke. Further evidence for the proposed suture includes north-verging thrust imbrication of Piling Group strata in Level 4 (Corrigan et al., 2001, 2009; Scott et al., 2002b, 2003), as well as thrust imbrication of basement-cover panels in Level 3 that predate emplacement of the Cumberland batholith (St-Onge et al., 2007).

The Level 2–3 'Soper River suture' (Fig. 3) records the accretion of the Narsajuaq magmatic arc to the composite Rae–Meta Incognita continental margin. Formation of the suture is bracketed between 1845 ± 2 Ma, the age of the youngest intra-oceanic phase in the arc (Dunphy and Ludden, 1998), and 1842 +5/-3 Ma, the age of the oldest Andean-type phase of the Narsajuaq Arc (Scott, 1997). Deformation in the hanging wall of the Soper River suture is both extensive and penetrative, and manifest as a regional synmetamorphic amphibolite- to granulite-facies metamorphic foliation (St-Onge et al., 2007).

The Level 1–2 'Bergeron suture' (Fig. 3) formed during terminal collision of the Superior Craton with the amalgamated mosaic of upper-plate terranes (collectively the Churchill plate or peri-Churchill collage) and is bracketed between 1820 +4/-3 Ma, the age of the youngest dated plutonic unit in the hanging wall of the suture (Scott and Wodicka, 1998), and 1795 ± 2 Ma, the age of an undeformed dyke that crosscuts the suture (Wodicka and Scott, 1997). This event resulted in localized retrograde amphibolite-facies metamorphism of granulite-facies rocks in the upper plate of the collision on southern Baffin Island, specifically along reactivated segments of the Soper River suture and associated fluid-infiltration zones (St-Onge et al., 2000b).

ARCHEAN RAE CRATON (LEVEL 4)

On Baffin Island, the Rae Craton comprises 2901 ± 3 to 2706 ± 3 Ma granodioritic to monzogranitic orthogneiss and temporally distinct volcano-sedimentary sequences, namely the 2833 ± 3 to 2731 ± 6 Ma Meso- to Neoarchean Mary River Group and the younger ca. 2740 to 2725 Ma Neoarchean Eqe Bay and Isortoq greenstone belts, all of which are intruded by 2731 ± 3 to 2658 +16/-14 Ma granodioritic to monzogranitic and rare tonalitic plutonic rocks (Fig. 4; Jackson et al., 1990; Scott and de Kemp, 1999; Jackson, 2000; Wodicka et al., 2002b; Bethune and Scammell, 2003a; Scott et al., 2003; Young et al., 2004, 2007; Johns and Young, 2006; Skipton et al., 2019). The Archean units of northern Baffin Island have been correlated with the Prince Albert and Repulse Bay blocks (or north Rae Domain) of the Rae Craton, the latter extending from central Nunavut to at least northern Baffin Island (Jackson and Berman, 2000; Pehrsson et al., 2011, 2013; Snyder et al., 2013; St-Onge et al., 2015a). In their type area west of Foxe Basin, the correlative Prince Albert and Repulse Bay blocks are characterized by ca. 2.97–2.60 Ga granite-greenstone belts with isotopic evidence of Eo- to Mesoarchean cratonic basement (e.g. Wodicka et al., 2011; Corrigan et al., 2013; LaFlamme et al., 2014).

On northern Baffin Island, the Archean crust of the Rae Craton is truncated by the Isortoq Fault (Jackson, 2000) and unconformably overlain by the Paleoproterozoic Piling Group (Fig. 4). Both fault and cover have been interpreted as corresponding to the northern margin of the ca. 1.92–1.80 Ma Himalayan-scale accretionary/collisional THO (St-Onge et al., 2002). The Isortoq Fault is considered to record northwest-directed thrusting of the Piling Group and underlying crystalline basement over Archean crust of northern Baffin Island at ca. 1850–1820 Ma (Jackson, 2000; Jackson and Berman, 2000; Bethune and Scammell, 2003b; Saumur et al., 2018).

Paleoproterozoic felsic plutonic rocks, ranging in age from 1897 +7/-4 to ca. 1805 Ma and including the northernmost components of the Cumberland batholith, intrude the Piling Group and Rae Craton rocks (*see below*; Jackson et al., 1990; Henderson and Henderson, 1994; Wodicka and Scott, 1997; Scott and Wodicka, 1998; Scott, 1999; Wodicka et al., 2002b, 2014; Bethune and Scammell, 2003b; Gagné et al., 2009; Whalen et al., 2010).

Archean basement gneiss

Archean basement orthogneiss of the Rae Craton on Baffin Island (Fig. 4) mainly comprises granodiorite, tonalite, and monzogranite. Crystallization ages for units interpreted as basement to the Mary River Group (*see* 'Mary River Group' section), east and north of Mary River (Fig. 4), are 2851 +20/-17 Ma for a tonalite gneiss (Jackson et al., 1990), ca. 2900 Ma for a granodiorite gneiss (Young et al., 2007; M. Young, unpub. data, 2007), and 2901 ± 3 Ma for a

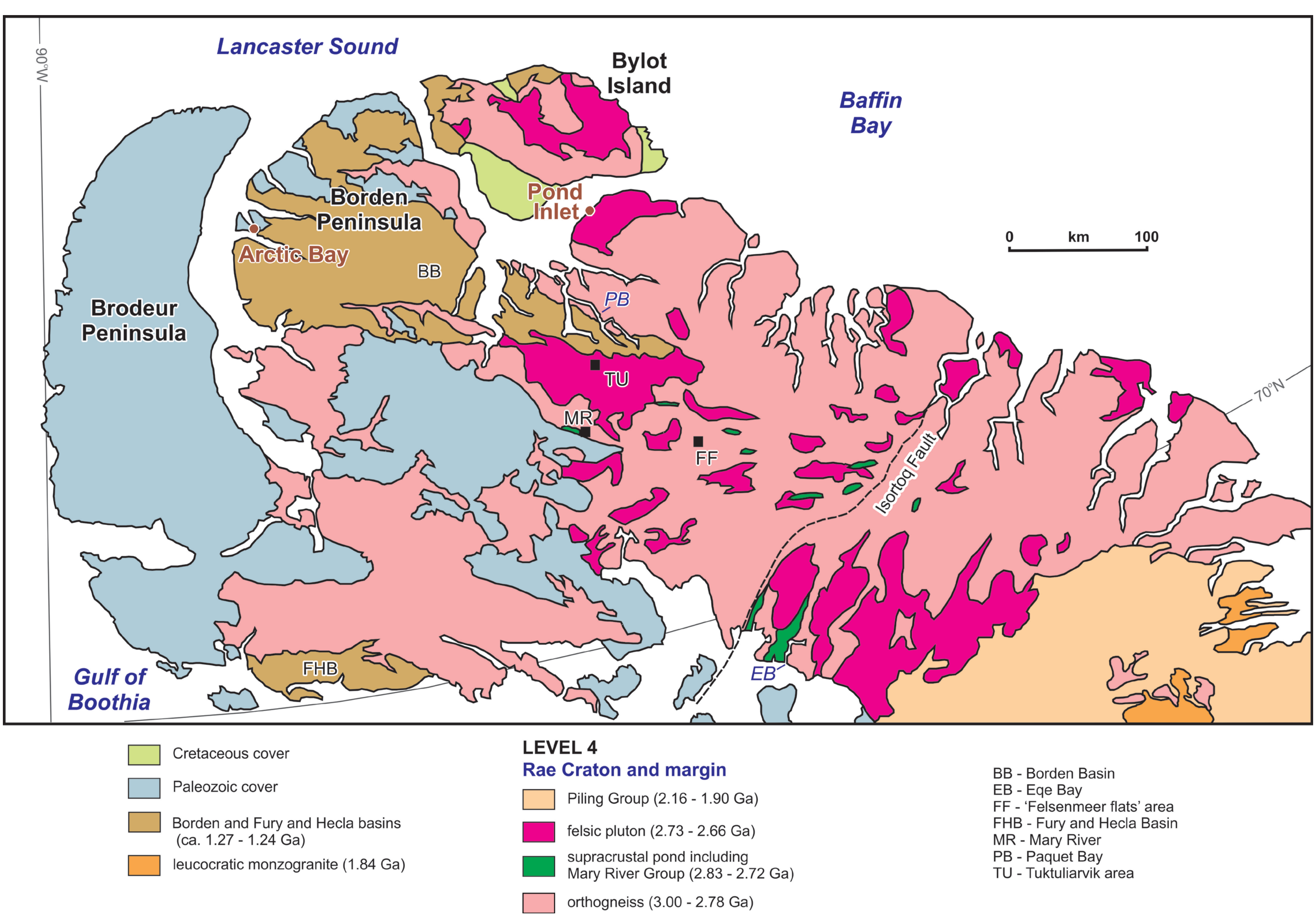

Figure 4. Geology of the Archean Rae Craton on northern Baffin Island (*after* Harrison et al., in press).

K-feldspar-phyric granodiorite (Skipton et al., 2019). These ages are within the 3000–2775 ± 2 Ma range of protolith ages for basement gneiss from the Eqe Bay area (Fig. 4; Bethune and Scammell, 2003a) to the south.

Granodiorite–tonalite–monzogranite gneiss

Gneissic units in the Rae Craton are characteristically foliated and medium grained, with compositional banding on a 1–10 cm scale (Fig. 5a). Mafic bands contain a biotite±hornblende±magnetite assemblage, whereas felsic bands mainly consist of plagioclase–quartz±K-feldspar. The gneiss commonly contains enclaves or bands of quartz diorite, diorite, gabbro and, less commonly, hornblendite, which are oriented parallel to foliation and layering (Fig. 5a, b). The centimetre-scale gneissosity defined by alternating mafic- and felsic-rich bands is generally accompanied by decimetre- to metre-scale compositional banding resulting from the transposition of different rock types.

Mary River Group

The Mary River Group comprises mafic metavolcanic rocks with intervening strata of siliciclastic units, banded iron-formation, felsic to intermediate metavolcanic rocks and ultramafic sills/volcanic rocks. Existing U–Pb data indicate at least two temporally distinct volcanic episodes. North of the type locality at Mary River (Fig. 4), Skipton et al. (2019) documented ages of 2833 ± 3 Ma and 2829 ± 5 Ma for felsic–intermediate volcanism, whereas they reported a considerably younger crystallization age of 2731 ± 6 Ma for a dacite north of the 'Felsenmeer flats' area (Fig. 4). In the Eqe Bay and Isortoq greenstone belts in the Eqe Bay area (Fig. 4), intermediate–felsic volcanism occurred between ca. 2740 and 2725 Ma (Bethune and Scammell, 2003a).

In general, the stratigraphy of the Neoarchean Mary River Group comprises a lower section of dominantly mafic metavolcanic rocks with lesser psammite±quartzite, overlain by iron-formation, and an upper sequence of psammite±quartzite and felsic–intermediate metavolcanic rocks with minor mafic metavolcanic units. Ultramafic rocks form low-volume, discontinuous layers at various stratigraphic levels (Jackson, 2000; Young et al., 2004; Johns and Young, 2006; Bros and Johnston, 2017; Skipton et al., 2017; Saumur et al., 2018).

Mafic metavolcanic (and subvolcanic) rocks

Mafic metavolcanic rocks are fine- to medium-grained and contain hornblende-plagioclase±actinolite±clinopyroxene±magnetite±biotite±quartz±garnet±chlorite±epidote assemblages. The rocks are typically equigranular or characterized by hornblende, or plagioclase, that forms medium-grained crystals within a fine-grained matrix. Compositional banding is common, defined by alternating mafic and felsic layers 5–50 mm thick that may reflect primary layering. Relict volcanic textures occur locally, including fine-grained plagioclase-rich clasts or coarse-grained hornblende/clinopyroxene pods within a fine-grained mafic matrix, or layered bomb- or lens-shaped mafic clasts (Fig. 5c, d). In rare cases, mafic volcanic deposits contain thin layers of fine-grained carbonate (Fig. 5d). Fine- to medium-grained mafic rocks that lack definitive volcanic textures may represent thick flows or shallow subvolcanic intrusions.

Banded iron-formation

The Mary River Group hosts Neoarchean oxide- and silicate-facies banded iron-formation. Iron-formation is typically 3–10 m thick, concordant with volcano-sedimentary layering and locally forms bodies that can be more than 100 m thick and extend for tens of kilometres along strike (MacLeod, 2012). The group hosts nine high-grade iron deposits that are currently tenured to Baffinland Iron Mines Corporation, most notably the Deposit No. 1 mine at Mary River (Fig. 4). The high-grade iron ore is interpreted to have formed from banded iron-formation that underwent pervasive desilicification resulting from circulation of hot, alkaline brine (MacLeod, 2012). The deposits are described in detail in a number of studies (Jackson, 2000, 2006; Young et al., 2004; MacLeod, 2012).

The oxide-facies banded iron-formation is characterized by 0.1–3 cm scale banding of magnetite(±hematite) and chert (Fig. 5e), with local occurrences of massive magnetite beds up to 10 m thick. Silicate-facies banded iron-formation is less common and comprises alternating bands of quartz, magnetite, and cummingtonite-grunerite±garnet that are 0.1–3 cm thick (Fig. 5f). Whereas some banded iron-formations have orange and/or purple gossanous weathering, most weather dark grey, grey-blue or dark brown. Outside the banded iron-formation, isolated ironstone layers are relatively common within mafic and ultramafic volcanic units, forming centimetre- to decimetre-scale bands of granular magnetite±hematite.

Andesite and rhyolite

Intermediate rocks are less common than mafic units in the Mary River Group. Although they contain higher proportions of plagioclase and quartz, intermediate volcanic and subvolcanic rocks have the same metamorphic mineral assemblages and similar textures as their mafic counterparts, described above.

Rhyolite is overlain by banded iron-formation and underlain by psammite in the Tuktuliarvik area (Fig. 4). The rhyolite is aphanitic apart from fine-grained muscovite and millimetre-scale quartz bands, which are parallel to compositional banding defined by alternating pale yellow and cream-coloured bands up to 1 cm thick.

Ultramafic rocks

Ultramafic rocks form a relatively minor component of the Mary River Group, and recent field observations (Skipton et al., 2017; Saumur et al., 2018) suggest that they are not as spatially extensive as indicated by previous studies (e.g. Davidson et al., 1979). Ultramafic rocks, which form discontinuous layers, typically comprise aligned orthopyroxene phenocrysts within a beige or light grey to black, fine-grained to aphanitic groundmass, suggesting a subvolcanic or volcanic origin (i.e. komatiite). Spinifex texture, diagnostic of quenched komatiitic flow sequences, was not observed, possibly owing to extensive recrystallization and/or deformation. In places, ultramafic rocks form medium- to coarse-grained intrusive bodies that contain clinopyroxene ±orthopyroxene±hornblende±olivine.

Psammite, quartzite, semipelite, pelite

Concordant with volcanic strata, siliciclastic sequences are mostly up to approximately 10 m thick (hundreds of metres thick at Tuktuliarvik; Fig. 4). Muscovite±biotite psammite is most common. Quartzite contains muscovite±biotite±garnet and is in sharp contact with (structurally) underlying monzogranite. Pelite and semipelite contain chlorite-muscovite-biotite±garnet±staurolite±magnetite, with staurolite locally forming porphyroblasts up to 7 cm long. Garnet is euhedral and typically 0.5–1 cm in size, reaching 5 cm locally.

Plutonic rocks

Quartzofeldspathic intrusions include foliated to massive quartz monzonite–granodiorite–monzogranite (±K-feldspar or plagioclase megacrysts) and aplitic to pegmatitic syenite dykes. An age of 2709 +4/-3 Ma is reported for monzogranite near Paquet Bay (Fig. 4; Jackson et al., 1990), whereas an age of 2731 ± 3 Ma is documented for a monzogranite east of Mary River (Fig. 4; Skipton et al., 2019). Further south, six calcalkaline granite–granodiorite intrusions near Eqe Bay (Fig. 4) yielded similar ages ranging from ca. 2726 to 2714 Ma, and thus appear in part contemporaneous with, and to outlast, the younger phase of Mary River Group volcanism (Bethune and Scammell, 2003a).

Monzogranite–granodiorite

Medium-grained biotite±hornblende±magnetite monzogranite–granodiorite (Fig. 5g) is widespread in the Rae Craton of Baffin Island. Plutons are homogeneous and typically weakly foliated, but range from massive to strongly foliated, and can occur as L- or L>S-tectonite. Potassium-feldspar megacrysts (±1.5 cm) occur in some localities. The intrusions locally contain enclaves of diorite or gabbro, and rarely enclaves (<1 m to 10–20 m) of fine-grained, foliated, mafic volcanic rocks interpreted as Mary River Group. Weakly foliated monzogranite is observed to cut granodiorite gneiss in several localities.

Feldspar-megacrystic monzogranite to granodiorite intrusions form 1–10 km scale plutons and are characterized by euhedral, weakly compositionally zoned megacrysts (2–5 cm) of either K-feldspar or plagioclase feldspar within a medium- to coarse-grained groundmass. Mafic minerals include biotite+hornblende+magnetite. The plutons locally exhibit a weak tectonic lineation or foliation, but are typically massive due to their coarse grain size and low proportion of mafic minerals. Megacrysts are locally aligned, potentially indicative of primary magmatic flow.

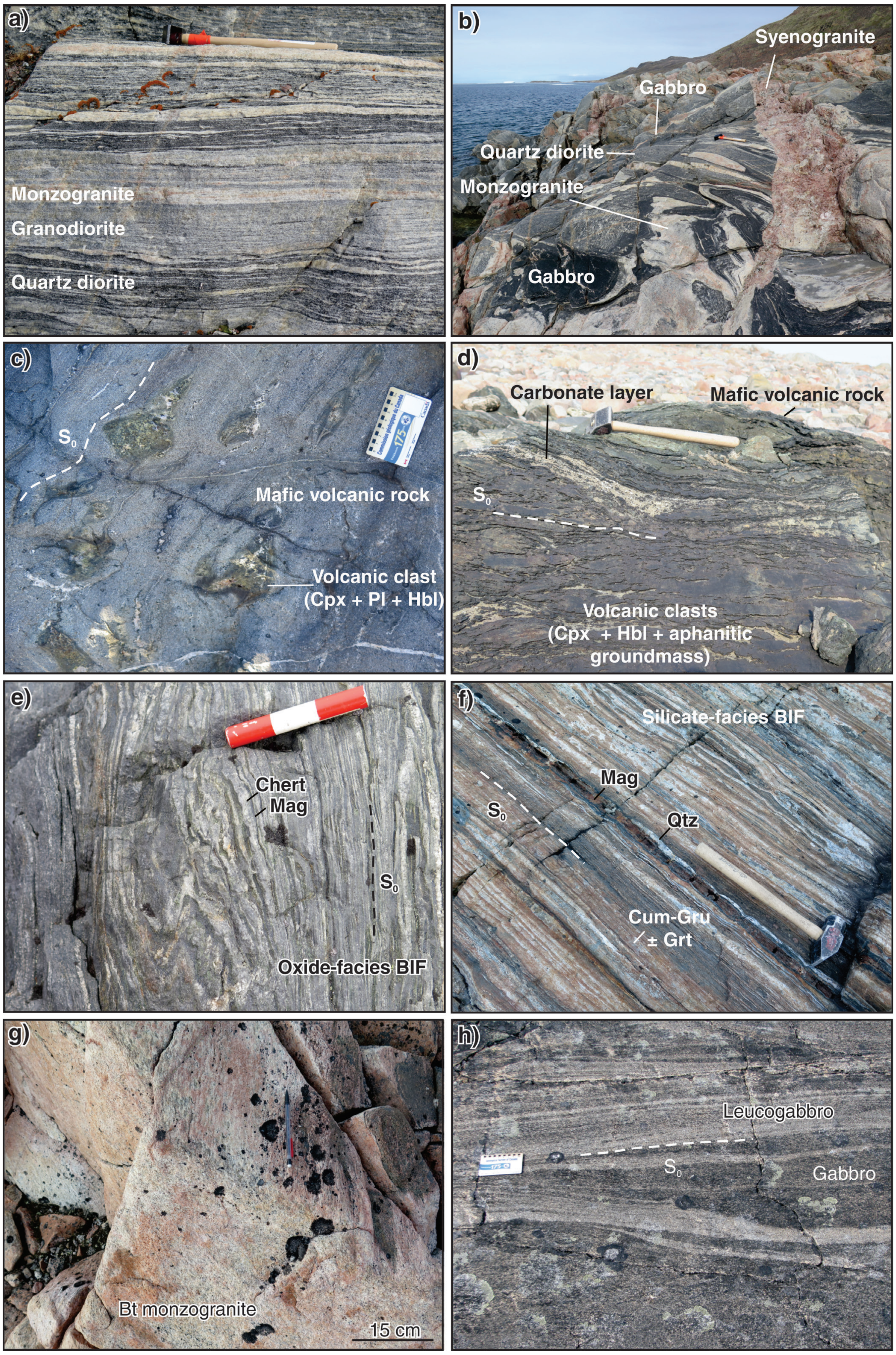

Figure 5. Rae Craton basement gneiss and Mary River Group strata, northern Baffin Island (*modified from* Skipton et al., 2017). **a)** Gneiss composed of granodiorite with bands of quartz diorite and monzogranite (hammer for scale). Photograph by D.R. Skipton. NRCan photo 2018-338. **b)** Gneiss composed of quartz diorite with monzogranite bands and gabbro enclaves/bands; folded and boudinaged gneissic bands are crosscut by a pegmatitic syenogranite dyke (hammer for scale). Photograph by D.R. Skipton. NRCan photo 2018-339. **c)** Mafic metavolcanic rock preserving volcanic layering (S_0) composed of a fine-grained matrix and pods of coarse-grained clinopyroxene (Cpx), plagioclase (Pl) and hornblende (Hbl), interpreted as volcanic clasts (scale bar = 7 cm). Photograph by D.R. Skipton. NRCan photo 2018-340. **d)** Clinopyroxene (Cpx)–hornblende (Hbl)-bearing mafic metavolcaniclastic rock with layers of fine-grained carbonate (± crystalline calcite) and volcanic layering (S_0) (hammer for scale). Photograph by E.R. Bros. NRCan photo 2018-341. **e)** Oxide-facies banded iron-formation near the Tuktuliarvik area (Fig. 4), composed of alternating layers (S_0) of magnetite (Mag) and chert (scale marker is 8 cm long). Photograph by D.R. Skipton. NRCan photo 2018-342. **f)** Silicate-facies banded iron formation in the Tuktuliarvik area (Fig. 4), consisting of alternating layers (S_0) of quartz (Qtz), magnetite (Mag) and cummingtonite (Cum)–grunerite (Gru)±garnet (Grt) (hammer for scale). Photograph by D.R. Skipton. NRCan photo 2018-343. **g)** Homogeneous biotite (Bt) monzogranite. Photograph by B.M. Saumur. NRCan photo 2018-344. **h)** Gabbro and leucograbbro layers (S_0) within a layered mafic–ultramafic intrusion (scale bar = 7 cm). Photograph by M.R. St-Onge. NRCan photo 2018-345. Mineral abbreviations after Whitney and Evans (2010).

Syenogranite

The youngest documented felsic plutonic phase comprises coarse-grained to pegmatitic, massive biotite±magnetite syenogranite dykes, 5 cm to 3 m wide. The dykes intrude the granodiorite–tonalite–monzogranite gneiss (Fig. 5b), monzogranite–granodiorite intrusions, and rarely the Mary River Group, including the banded iron-formation. Hornblende or clinopyroxene occurs locally in pegmatitic syenogranite dykes that cut hornblende-bearing plutonic units or mafic enclaves.

Diorite, gabbro, and hornblendite enclaves

Medium-grained hornblende±biotite±clinopyroxene diorite and gabbro enclaves occur within granodiorite–tonalite–monzogranite gneiss (commonly forming bands; Fig. 5a, b) and monzogranite–granodiorite intrusions; medium- to coarse-grained hornblendite enclaves are less common. Enclaves are generally foliated, less than 1 m in size, comprise less than 10% of outcrop volume and are oriented parallel to the tectonic fabrics in the host rocks.

Layered mafic–ultramafic bodies

Mafic–ultramafic intrusions comprise 100 to 500 m thick layers of gabbro/diorite with hornblende clinopyroxenite and/or websterite. Within gabbroic portions, primary decimetre-scale, rhythmic compositional layering is defined by varying proportions of plagioclase and clinopyroxene (or hornblende after clinopyroxene), producing alternating bands of leucogabbro and gabbro (Fig. 5h). Layering is irregular along strike, exhibiting truncations and layer-scale deformation that possibly reflect dynamic magmatic conditions.

PALEOPROTEROZOIC SOUTHERN MARGIN OF THE RAE CRATON (LEVEL 4)

The Paleoproterozoic Piling Group on central Baffin Island (Fig. 6) comprises shallow-water siliciclastic–carbonate strata, mafic–ultramafic volcanic rocks, and deep-water basinal strata (e.g. Morgan et al., 1976; Henderson et al., 1979; Henderson and Tippett, 1980; Tippett, 1985; Jackson, 2000; Corrigan et al., 2001; Scott et al., 2002b, 2003; St-Onge et al., 2005; Partin et al., 2014a; Wodicka et al., 2014). The shallow-water strata and volcanic rocks are generally regarded as having accumulated as a result of regional crustal extension along the southeastern margin of the Archean Rae Craton (e.g. Rainbird et al., 2010), followed by deposition of the deep-water strata in a foreland or proto-ocean basin (Partin et al., 2014a; Wodicka et al., 2014). Subsequently, all stratigraphic units were deformed and metamorphosed during the ca. 1.92–1.80 Ga Trans-Hudson Orogeny (Corrigan et al., 2001; Scott et al., 2002b; St-Onge et al., 2006; Gagné et al., 2009). The Piling Group (Fig. 6) forms part of an extensive cover sequence on the Rae Craton, with stratigraphic correlatives extending from the western Churchill Province on mainland Nunavut (e.g. Penrhyn, Amer, Ketyet River, Chantrey, and Montresor groups; Jackson and Taylor, 1972; Taylor, 1982; Rainbird et al., 2010), across Baffin Island (Hoare Bay Group; St-Onge et al., 2009), to western Greenland (Karrat and Anap nunâ groups; Escher and Pulvertaft, 1976; Henderson and Pulvertaft, 1987; Garde and Steenfelt, 1999).

Piling Group

The Piling Group is divided into five formations (Morgan, 1983; Tippett, 1985), which comprise, in ascending stratigraphic order, the Dewar Lakes, Flint Lake, Bravo Lake, Astarte River, and Longstaff Bluff formations (Fig. 6, 7).

Dewar Lakes formation

The Dewar Lakes formation can be subdivided into three members (Scott et al., 2003), the lowest of which comprises thinly bedded, muscovite-rich quartzite, grey- to pink-weathering psammite, and feldspathic quartzite (Fig. 7a). The overlying, and by far the most widespread, middle member comprises medium to thickly bedded sillimanite±muscovite-rich quartzite (Fig. 7b) characterized by dominantly southward-directed cross-stratification. The upper member comprises thin beds of quartzite to psammite and rusty semipelite to pelite (Fig. 7c). The overall thickness of the Dewar Lakes formation varies significantly from less than 1 m to locally over 1000 m. Thickness variability may reflect primary sedimentary depocentres (Tippett, 1985; Jackson, 2000; Scott et al., 2003). Basal quartzite and rare psammite of the lower Dewar Lakes formation are in stratigraphic (locally reworked) unconformable contact with underlying Archean orthogneissic and plutonic rocks, and the formation is interpreted as a clastic sheet deposited on Rae cratonic basement. The dominance of quartz over feldspar and the presence of rock fragments throughout the formation suggest a relatively high degree of sedimentological

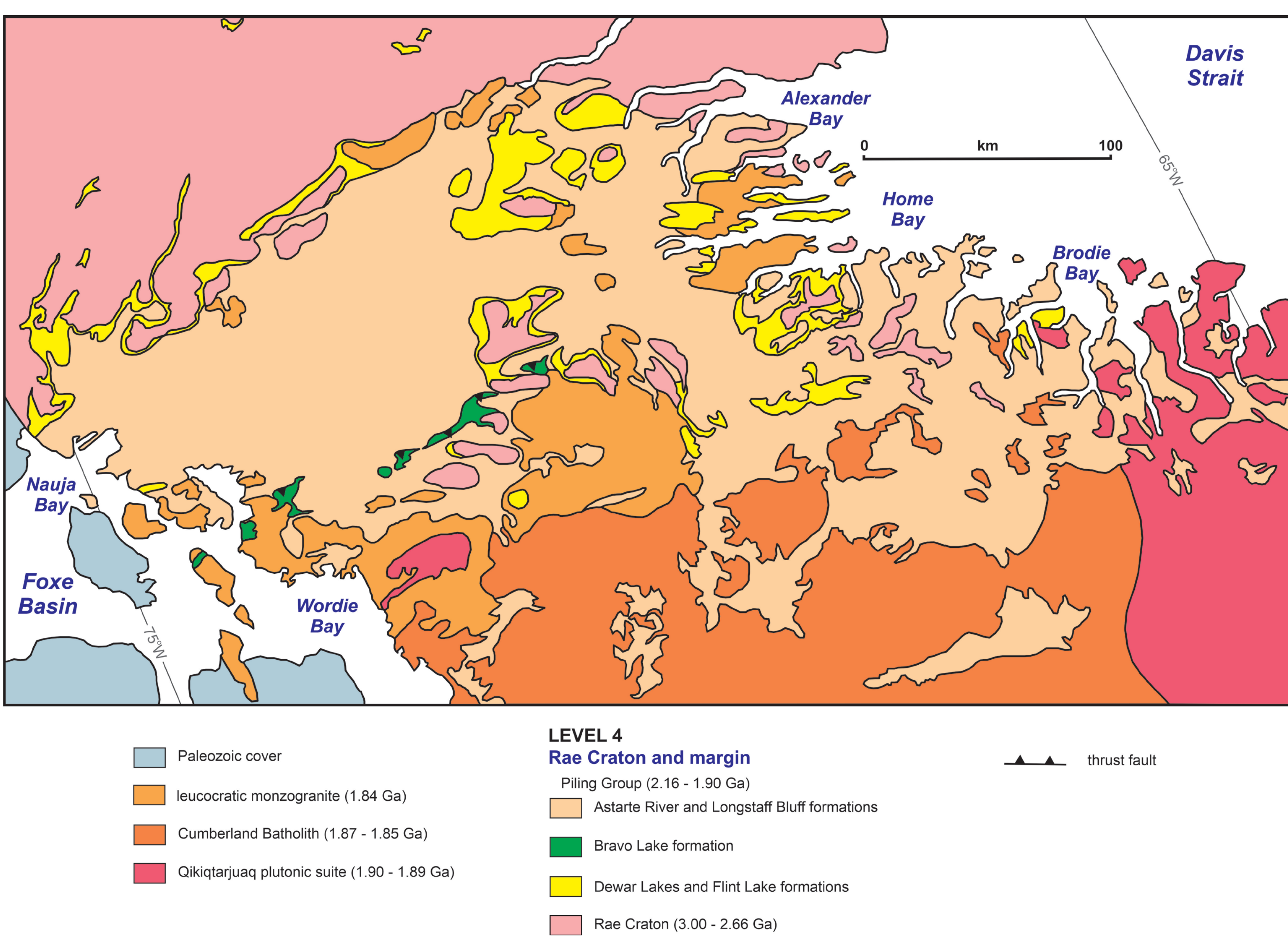

Figure 6. Geology of the Paleoproterozoic Piling Group on central Baffin Island (*after* Harrison et al., in press).

maturity (Tippett, 1985). Most of the Dewar Lakes formation was likely deposited in a shallow marine environment (e.g. Tippett, 1985; de Kemp et al., 2002a, b).

Flint Lake formation

White- to grey-weathering dolostone, marble, and calc-silicate strata of the Flint Lake formation (Fig. 7d) interlayered with lesser semipelite, pelite, quartzite, iron-formation, and chert, stratigraphically overlie the upper member of the Dewar Lakes formation (Morgan et al., 1976; Corrigan et al., 2001; Scott et al., 2002b; St-Onge et al., 2005). The exposed thickness of this formation varies considerably both along and across strike, from several metres to 500–1000 m (Fig. 6). The overall decrease in carbonate material toward the south led Scott et al. (2002b, 2003) to suggest that the Flint Lake formation originally formed a relatively narrow (75–100 km wide) south-facing carbonate shelf adjacent and parallel to the southeastern edge of the Rae Craton, with significant along-strike variation in primary thickness.

Bravo Lake formation

The Bravo Lake formation forms a nearly continuous, 120 km long, east-trending mafic volcanic belt in the southern part of the Piling structural basin (Fig. 6). Like the Flint Lake formation, it conformably overlies the siliciclastic rocks of the upper Dewar Lakes formation, which suggests that the lithologically distinct carbonate and volcanic sequences occupy an equivalent stratigraphic position within the Piling Group (de Kemp et al., 2002a, b; Scott et al., 2003). Based on lithostratigraphic and structural considerations, the Bravo Lake formation, and in places the Dewar Lakes formation, are interpreted to have been tectonically juxtaposed against the younger Longstaff Bluff formation across a north- to northwest-directed thrust fault (Fig. 6; Tippett, 1985; Corrigan et al., 2001; de Kemp et al., 2002a, b; Stacey and Pattison, 2003). The Bravo Lake formation has an estimated thickness of 1.0–2.5 km and can be subdivided into two sequences (Modeland and Francis, 2003, 2004; Johns et al., 2006).

The lower sequence is dominated by pillowed, subalkaline, tholeiitic to picritic basaltic flows (Fig. 7e) and volcaniclastic rocks with iron-formation and rare intrusive mafic to ultramafic sills. The upper sequence comprises volcaniclastic rocks and mostly alkaline basaltic flows intruded by numerous ultramafic to mafic alkaline sills (Fig. 7f) and locally abundant partially sheeted dykes at its base. A succession of siliciclastic rocks 10 to 300 m thick, including quartzite, semipelite, pelite, and calcsilicate, separates the two sequences and represents a key regional stratigraphic marker. The mafic magmas range in composition from tholeiitic in the lower sequence to dominantly alkaline in the upper sequence, strikingly similar to that of modern ocean-island basalt suites (e.g. Modeland and Francis, 2004; Partin et al., 2014a). Detailed mapping suggests that the mafic–ultramafic volcanism occurred in a low-energy, shallow submarine environment (de Kemp et al., 2002a, b; Johns et al., 2006). Based on its stratigraphic setting and chemical composition, the Bravo Lake formation is interpreted to have formed in a rift setting (i.e. intracontinental rift or incipient oceanic rift; Jackson, 2000; Johns et al., 2006; Corrigan et al., 2009; Wodicka et al., 2014) or foredeep

Figure 7. Piling Group strata, central Baffin Island. **a)** Thinly bedded psammite and quartzite, lower member of the Dewar Lakes formation (hammer for scale). Photograph by M.R. St-Onge. NRCan photo 2018-350. **b)** Thick-bedded quartzite, middle member of the Dewar Lakes formation (location of hammer for scale indicated with arrow). Photograph by M.R. St-Onge. NRCan photo 2018-351. **c)** Thinly bedded psammite and quartzite of the upper member of the Dewar Lakes formation (hammer for scale). Photograph by M.R. St-Onge. NRCan photo 2018-352. **d)** Dolomitic marble (light) and calcsilicate rocks (dark) of the Flint Lake formation (nose of helicopter for scale). Photograph by M.R. St-Onge. NRCan photo 2018-353. **e)** Pillowed, subalkaline, tholeiitic to picritic basaltic flows, lower sequence of Bravo Lake formation (hammer for scale). Photograph by M.R. St-Onge. NRCan photo 2018-354. **f)** Alkaline basaltic flows intruded by ultramafic to mafic alkaline sills, upper sequence of Bravo Lake formation (hammer for scale). Photograph by M.R. St-Onge. NRCan photo 2018-355.

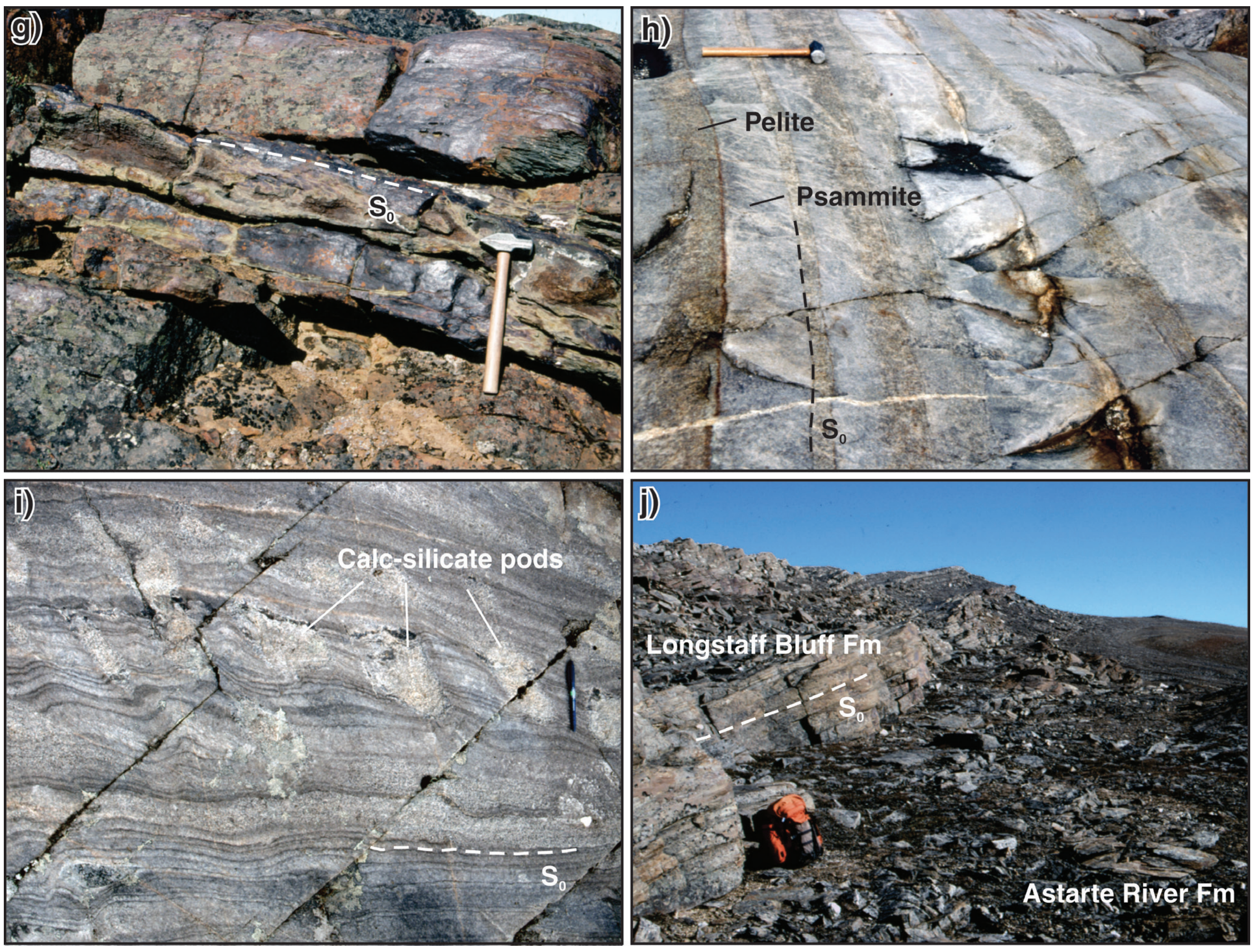

Figure 7. (cont.) g) Rusty, thinly bedded pelite, semipelite and ironstone of the Astarte River formation (hammer for scale). Photograph by M.R. St-Onge. NRCan photo 2018-356. **h)** Psammite-pelite beds of the Longstaff Bluff formation displaying normally graded bedding, with stratigraphic tops to the right (hammer for scale). Photograph by M.R. St-Onge. NRCan photo 2018-357. **i)** Calc-silicate pods in the Longstaff Bluff formation, interpreted as metamorphosed carbonate concretions (pen for scale). Photograph by M.R. St-Onge. NRCan photo 2018-358. **j)** Ledge-forming psammite–semipelite turbidite of the Longstaff Bluff formation (Fm) on the left overlying rusty pelite of the Astarte River formation on the right (backpack for scale). Photograph by M.R. St-Onge. NRCan photo 2018-359.

setting (Partin et al., 2014a), underlain by variably enriched mantle (Modeland and Francis, 2004). The structural trends of the sheeted dykes within the upper sequence indicate offset rifting within strike-slip pull-apart basins (Johns et al., 2006). Scattered mafic sills occur within the underlying Dewar Lakes formation and Archean basement, and the overlying Longstaff Bluff formation (Tippett, 1985; St-Onge et al., 2005). These rocks show a close geochemical correspondence with mafic–ultramafic rocks from the Bravo Lake formation, indicating a potential cogenetic relationship (Tippett, 1984, 1985; Gladstone and Francis, 2003) and suggesting that, in part, Bravo Lake magmatism continued after deposition of the Longstaff Bluff formation.

Astarte River formation

Rusty-weathering graphitic pelite, semipelite, and minor sulphide-facies iron-formation of the Astarte River formation (Fig. 7g) directly overlie carbonate rocks of the Flint Lake formation in the northwest, siliciclastic rocks of the Dewar Lakes formation in the central part of the Piling structural basin, and mafic volcanic rocks of the Bravo Lake formation in the south (Fig. 6; Scott et al., 2003). This sulphide-rich (pyrite-pyrrhotite) sequence is estimated to be over 500 m thick and marks a relatively abrupt transition from shallow-water sedimentation and volcanism to deep-water sedimentation, suggesting the onset of a tectonic process that rapidly increased rates of subsidence and led to drowning of the Flint Lake carbonate platform.

Longstaff Bluff formation

The Longstaff Bluff formation, the uppermost stratigraphic component of the Piling Group (Fig. 6), is a 3–5 km thick, monotonous succession of feldspathic psammite and greywacke, subordinate semipelite, and rare pelite interpreted as turbidite (e.g. Henderson et al., 1979; Henderson and Tippett, 1980; Tippett, 1985; Jackson, 2000; Scott et al., 2002b). These rocks are distinguished from the quartz-rich rocks of the Dewar Lakes formation by their greater mica content (notably biotite) and the dominance of plagioclase relative to K-feldspar (Tippett, 1985). Primary sedimentary features are best preserved in the dominantly low-metamorphic-grade area and type locality for the Longstaff Bluff formation northeast of Nauja Bay (Fig. 6). In this region, individual psammite beds display normally graded bedding (Fig. 7h), generally indicating an upright sequence. Other primary structures such as crossbeds, scours, and ripples are less common (Forester and Gray, 1966; Morgan et al., 1975; Jackson, 2000; Scott et al., 2003; St-Onge et al., 2005). Paleocurrents measured from these structures in the middle and upper parts of the Longstaff Bluff formation indicate an apparent east–west sediment transport. The composition of the turbiditic rocks (e.g. euhedral feldspar crystals and crystal fragments, blue quartz, and mafic minerals) suggests derivation from, at least in part, a volcanic source area (Jackson, 2000; Corrigan et al., 2001; Scott et al., 2002b). Calc-silicate pods (Fig. 7i), interpreted as metamorphosed carbonate concretions, are ubiquitous. According to most workers, the Longstaff Bluff formation is considered to extend as migmatitic metasedimentary rocks south of the Bravo Lake formation (Fig. 6; e.g. Tippett, 1985; Henderson and Henderson, 1994; St-Onge et al. 2005).

Field relationships indicate that Longstaff Bluff turbiditic beds stratigraphically overlie both rusty pelite of the Astarte River formation (Fig. 7j) and volcanic rocks of the Bravo Lake formation. The character of the better preserved northern Longstaff Bluff formation, including the generally fine-grained nature of the turbiditic rocks, the dominance of normal-graded bedding, and the lateral continuity in bedding thicknesses, combine to suggest that the bedded strata represent distal-facies turbidite (e.g. Henderson and Tippett, 1980) deposited on the suprafan lobe portion of an outer submarine fan (Tippett, 1985). Most workers have suggested that the deep-water deposits signal a dramatic change in tectonic conditions, with the clastic detritus originating in a foreland, molasse-type basin and/or a fragmented proto-ocean basin (e.g. Jackson, 2000; Corrigan et al., 2001, 2009; Scott et al., 2003; St-Onge et al., 2005; Partin et al., 2014a; Wodicka et al., 2014). Wodicka et al. (2014) have specifically suggested a two-component source with possible input from the Snowbird tectonic zone to the west and the Bravo Lake formation more locally.

Piling Group age constraints

The U-Pb zircon and carbon-isotope chemostratigraphy data presented by Partin et al. (2014a) and Wodicka et al. (2014) provide important insights into the depositional ages of principal sedimentary units of the Piling Group and the timing of Bravo Lake formation mafic–ultramafic volcanism and sill emplacement. The youngest detrital zircon grains from samples collected in the lower, middle, and upper members of the Dewar Lakes formation have yielded highly variable, but progressively younger, maximum ages of deposition of ca. 2725 Ma, 2719 ± 22 Ma, 2312 ± 23 Ma, and 2159 ± 16 Ma, respectively (Wodicka et al., 2014). The youngest U-Pb zircon age from adjacent basement rocks (2658 +16/-14 Ma; St-Onge et al.,

2009) provides the current best maximum age for the onset of lowermost Piling Group sedimentation. However, the true age of basin formation and onset of shallow-water sedimentation could be considerably younger, particularly given that the youngest detrital zircon grains in passive-margin or cratonic successions, which typically lack evidence for contemporaneous igneous activity, may be tens to hundreds of millions of years older than the time of sediment accumulation (e.g. Cawood and Nemchin, 2001; Bradley, 2008).

In the overlying Flint Lake formation, $\delta^{13}C$ values suggest formation of the carbonate platform after ca. 2.06 Ga (Partin et al., 2014a). The chemostratigraphic age constraints are consistent with the maximum age constraint of 2.16 Ga for the upper Dewar Lakes formation.

Field relationships, geochemistry, and age constraints suggest that magmatic activity related to the Bravo Lake formation occurred over a period of approximately100 Ma. Two indirect lines of evidence indicate that tholeiitic to picritic volcanism within the lower Bravo Lake sequence may have commenced as early as ca. 1980 Ma. A 1979 ± 13 Ma anhedral zircon fragment in a trachyte dyke (Wodicka et al., 2014) could represent a xenocryst incorporated into the trachytic melt during ascent through the lower Bravo Lake formation volcanic pile. Similarly, 1980 ± 11 Ma detrital zircon grains within quartzose semipelite, taken from a channel near the base of the lower Bravo Lake formation, could be derived from erosion of adjacent lava flows or volcaniclastic rocks (Wodicka et al., 2014). Upper Bravo Lake formation magmatism is constrained at or before 1923 ± 15 Ma (Wodicka et al., 2014), the age of the upper Bravo Lake trachyte dyke with a synvolcanic origin (Johns et al., 2006). A maximum depositional age of 1940 ± 28 Ma for a lithic metawacke from the upper Bravo Lake formation (Partin et al., 2014a) is consistent with this interpretation. The youngest magmatism possibly related to the Bravo Lake formation, consisting of highly differentiated sills, occurred at 1897 +10/-5 Ma (Wodicka et al., 2014) and 1883.3 ± 4.7 Ma (Henderson and Parrish, 1992), following deposition of the Longstaff Bluff formation.

Five Longstaff Bluff formation detrital zircon samples have yielded maximum ages of deposition of 1964 ± 9 Ma and 1931 ± 4 Ma for samples located in the high-grade area south of the Bravo Lake formation (i.e. southern Longstaff Bluff formation), and 1923 ± 7 Ma, 1915 ± 8 Ma and 1883 ± 38 Ma for samples taken north of the volcanic belt (i.e. northern Longstaff Bluff formation; Partin et al., 2014a; Wodicka et al., 2014), with the differences in ages possibly indicating diachronous deposition between the northern and southern parts of the Longstaff Bluff formation. Minimum age constraints are obtained from a 1897 +7/-4 Ma rapakivi-textured, K-feldspar megacrystic monzogranite intrusive into the southern turbiditic strata (Fig. 6; Wodicka et al., 2014), a unit possibly correlative (Sanborn-Barrie et al., 2017) with the Qikiqtarjuaq plutonic suite of Rayner et al. (2012) and Sanborn-Barrie et al. (2013), and from in situ ages of 1878 ± 25 Ma and 1875 ± 31 Ma for metamorphic monazite growth in northern deposits of the Longstaff Bluff formation (Gagné et al., 2009).

Hoare Bay Group

The Hoare Bay Group (Jackson, 1971, 1998) is a Paleoproterozoic supracrustal sequence exposed on central Cumberland Peninsula, eastern Baffin Island (Fig. 8). Traditionally, the group has been correlated with, and interpreted as, a deep-water equivalent of the Piling Group of central Baffin Island (Fig. 6; Jackson and Taylor, 1972; St-Onge et al., 2006). Recent bedrock mapping on Cumberland Peninsula (Sanborn-Barrie and Young, 2011; Sanborn-Barrie et al., 2013a) has further highlighted the broad lithological similarities between the Hoare Bay and Piling groups, as well as differences in the chemistry of the volcanic units; published regional syntheses (e.g. St-Onge et al., 2009) have suggested both groups may also broadly correlate with the Karrat and Anap nunâ groups of West Greenland (Hamilton, 2014).

The Hoare Bay Group is a clastic-dominated succession, the lower part of which consists of pelite, semipelite and psammite, minor orthoquartzite, marble and calc-silicate, and ultramafic–mafic volcanic and intrusive rocks. The middle part of the group, the focus of study by Keim et al. (2011) and Keim (2012), is composed of ultramafic–mafic volcanic rocks and their intrusive equivalents (Totnes Road formation) and overlain by a sequence dominated by iron-formation (Clephane Bay formation). Psammite, semipelite, and minor ultramafic–mafic volcanic and intrusive rocks comprise the upper part of the Hoare Bay Group (Hamilton, 2014).

Lower Hoare Bay Group

The lower Hoare Bay Group comprises staurolite, andalusite- and sillimanite-bearing pelite and semipelite interlayered with lesser quartzite (Fig. 9a), psammite, and siliceous marble (Hamilton, 2014). Lithological layering occurs at a millimetre- to decimetre-scale. Lenticular hornblendite bodies that locally crosscut the compositional layering in the pelitic host rocks are interpreted as feeder dykes and sills to one of three overlying ultramafic–mafic volcanic units (Mackay, 2011; Keim, 2012; Whalen et al., 2012), which locally preserve a pyroclastic texture with lapilli- and bomb-sized fragments. Massive varieties occasionally contain plagioclase-rich, millimetre-wide varioles (Hamilton, 2014).

Middle Hoare Bay Group

Stratigraphically above the uppermost pelite of the lower Hoare Bay Group, a sharp contact defines the base of the Totnes Road formation (Keim, 2012). In the type Totnes Road locality (Fig. 8), the formation comprises plagioclase-hornblende schist and gneiss,

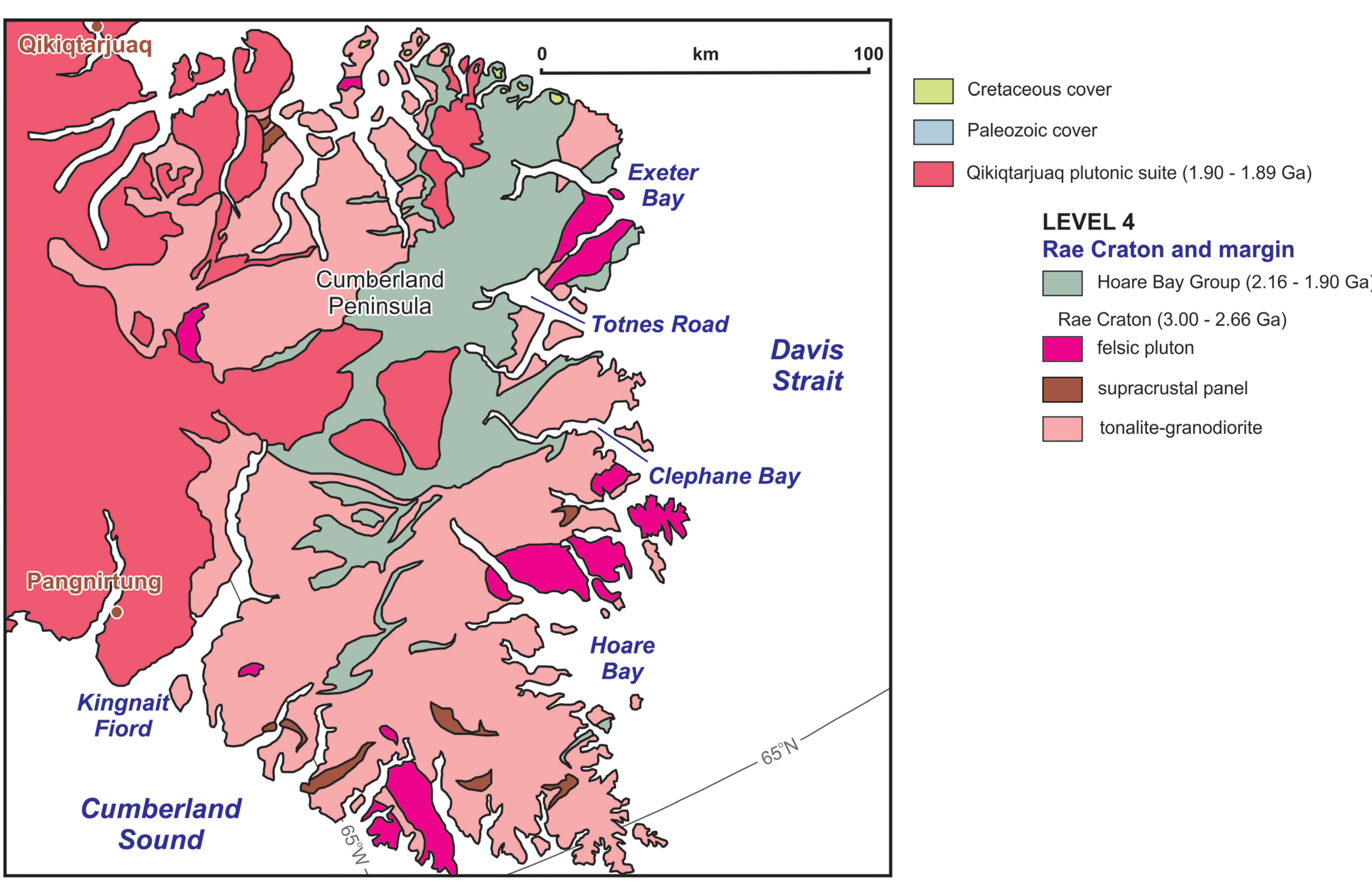

Figure 8. Geology of the Paleoproterozoic Hoare Bay Group on Cumberland Peninsula, eastern Baffin Island (*after* Harrison et al., in press).

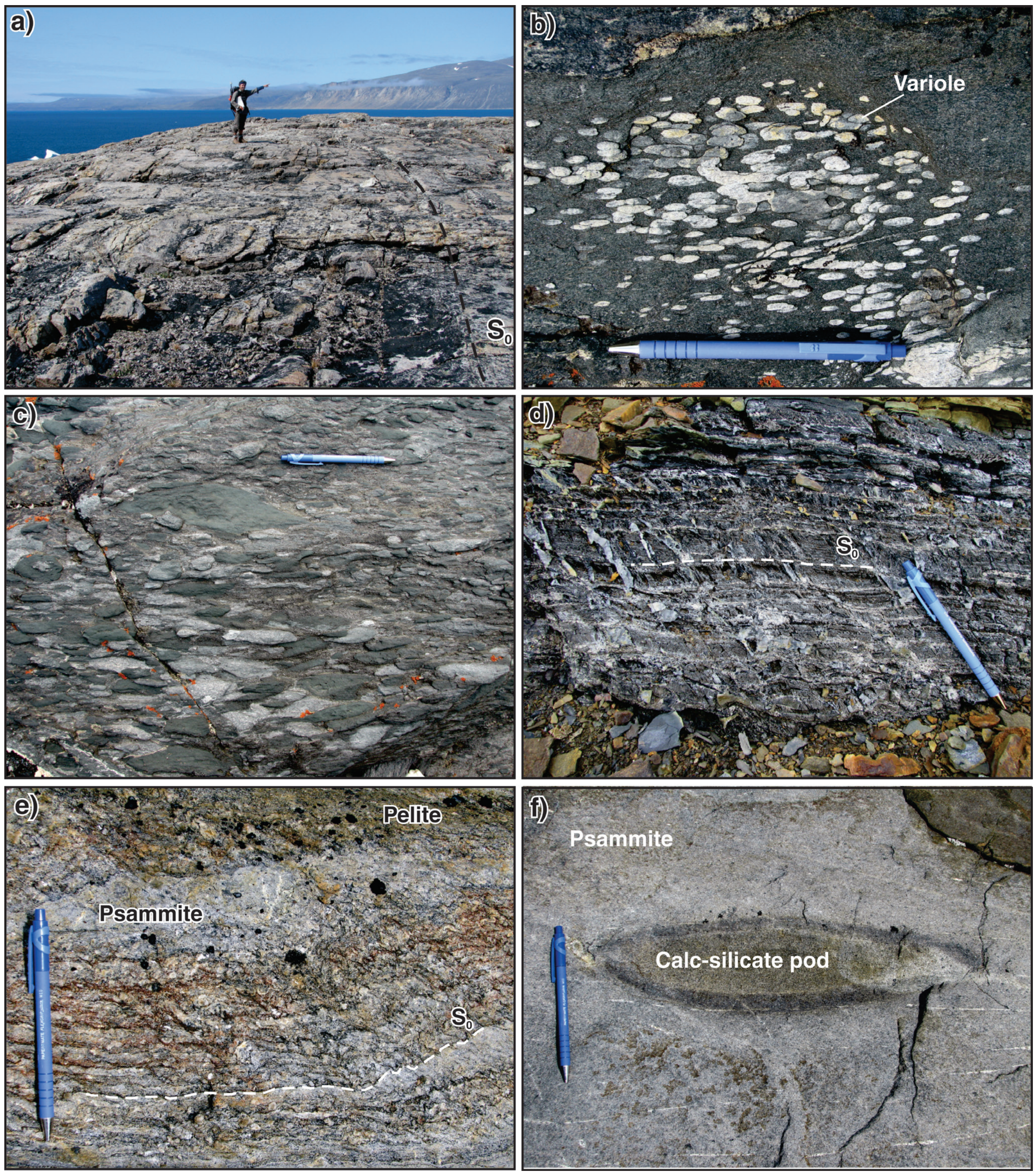

Figure 9. Hoare Bay Group strata, Cumberland Peninsula, eastern Baffin Island. **a)** Orthoquartzite, lower Hoare Bay Group (geologist for scale). Photograph by M.R. St-Onge. NRCan photo 2018-360. **b)** Plagioclase-rich varioles 2–4 mm wide in tholeiitic basalt of the Totnes Road formation, middle Hoare Bay Group (pen for scale). Photograph by M.R. St-Onge. NRCan photo 2018-361. **c)** Pyroclastic unit with lapilli- and bomb-sized fragments, Totnes Road formation, middle Hoare Bay Group (pen for scale). Photograph by M.R. St-Onge. NRCan photo 2018-362. **d)** Graphite-rich shale with millimetre-scale bedding laminae and high-angle axial-planar cleavage (parallel to pen for scale), Clephane Bay formation, middle Hoare Bay Group. Photograph by M.R. St-Onge. NRCan photo 2018-363. **e)** Interbedded pelite and psammite, upper Hoare Bay Group (pen for scale). Photograph by M.R. St-Onge. NRCan photo 2018-364. **f)** Calc-silicate concretion, upper Hoare Bay Group (pen for scale). Photograph by M.R. St-Onge. NRCan photo 2018-365.

locally with clinopyroxene. Some layers are characterized by millimetre-wide, plagioclase-rich varioles (Fig. 9b), whereas others have a fragmental texture (Fig. 9c). Chemical analyses of the volcanic rocks suggest that they comprise Karasjok-type komatiite, komatiitic basalt, and tholeiitic basalt (Keim et al., 2011; Keim, 2012).

Several types of iron-formation, collectively referred to as the 'Clephane Bay formation' (Keim, 2012), overlie the Totnes Road formation. Silicate-facies iron-formation is represented by garnet-quartz-grunerite±magnetite layers (Storey, 2012), whereas sulphide-facies iron-formation is gossanous, recessively weathering, pyrite- and graphite-rich, and contains quartz, grunerite, and garnet in various proportions. Oxide-facies iron-formation (quartz and magnetite) can be layered on a millimetre to centimetre scale. The iron-formation is associated with graphite-rich shale and biotite-muscovite-bearing pelite (Fig. 9d; Sanborn-Barrie and Young, 2011; Sanborn-Barrie et al., 2011, 2013a; Keim et al., 2011; Keim, 2012).

Upper Hoare Bay Group

The upper Hoare Bay Group consists of a thick package of biotite±muscovite semipelite and psammite (Fig. 9e). Layering is on the centimetre- to decimetre-scale, graded bedding has been observed, and the strata are interpreted as metamorphosed wacke (Hamilton, 2014). Locally, the turbiditic beds contain elongated pods of calc-silicate that are interpreted as metamorphosed calcareous strata and concretions (Fig. 9f).

Hoare Bay Group age constraints

On eastern Baffin Island, the lowermost quartz-rich rocks of the Hoare Bay Group were initially derived from 2.99 to 2.71 Ga Archean sources (Fig. 8; Sanborn-Barrie et al., 2017), similar in age to underlying or nearby basement rocks (Rayner et al., 2012). Overlying upper Hoare Bay Group psammitic–semipelitic rocks were derived from both Archean (2.80–2.69 Ga) and Paleoproterozoic (1.99–1.97 Ga) sources (Sanborn-Barrie et al., 2017).

In contrast to the middle–upper (or northern) Longstaff Bluff formation of the Piling Group, clastic rocks of the Hoare Bay Group lack detrital peaks of ca. 2.58–2.55 Ga and 1.92 Ga (Wodicka et al., 2014), with the youngest detrital zircon grains consistently establishing a maximum depositional age of 1.96 Ga (Sanborn-Barrie et al., 2017). The absence of a 1.92 Ga detrital peak in the Hoare Bay succession, may reflect diachronous deposition, with sedimentation in eastern Baffin Island predating that to the northwest. The influx of Paleoproterozoic detritus into the Hoare Bay basin after 1.96 Ga points to uplift and exhumation of an extensive belt of 1.99 to 1.97 Ga plutonic rocks potentially corresponding to either the Taltson and Thelon magmatic zones (van Breemen et al., 1987, 1992; McDonough et al., 2000) to the west, 1.99 to 1.98 Ga orthogneiss of the Prudhoe Land complex in West Greenland (Nutman et al., 2008) to the north, or both (Sanborn-Barrie et al., 2017).

Qikiqtarjuaq plutonic suite

Both the Archean basement gneiss of the southeastern Rae Craton and the overlying Paleoproterozoic cover strata of the Hoare Bay Group are cut by foliated, locally K-feldspar-phyric granodiorite± monzogranite±quartz diorite plutons that form a plutonic belt exposed between Pangnirtung and Qikiqtarjuaq (Fig. 8). This plutonic belt, which forms the spectacular peaks of the Auyuittuq National Park and was designated the 'Qikiqtarjuaq plutonic suite' by Sanborn-Barrie et al. (2011, 2013) and Rayner et al. (2012), seems to extend across the Baffin suture into the Meta Incognita microcontinent (Rayner, 2017; Fig. 3). Seven samples from this belt have yielded similar crystallization ages between 1896 and 1886 Ma, including:

- a biotite-hornblende-magnetite monzogranite near Pangnirtung (Fig. 8) and a biotite-hornblende-garnet granodiorite exposed 50 km northeast of Pangnirtung dated at 1894 ± 5 Ma and 1889 ± 3 Ma, respectively (Rayner et al., 2012)
- three samples of orthopyroxene-bearing monzogranite from the head, and west, of Cumberland Sound (Fig. 10) with crystallization ages between 1896 ± 8 Ma and 1887 ± 4 Ma (Rayner, 2017)
- two fine-grained biotite monzogranite samples exposed west of Nettilling Fiord (Fig. 1) with crystallization ages of 1891 ± 7 Ma and 1886 ± 5 Ma (Rayner, 2017). An orthopyroxene-bearing tonalite from further south on Hall Peninsula (Fig. 10), dated by Scott (1999) at 1890 +3/-2 Ma, might also belong to the Qikiqtarjuaq plutonic suite. The ages for the plutonic suite are distinctly older than those for the ca. 1865–1845 Ma Cumberland batholith (Whalen et al., 2010; Rayner, 2015, 2017) described below.

ARCHEAN TO PALEOPROTEROZOIC META INCOGNITA MICROCONTINENT (LEVEL 3)

The Meta Incognita microcontinent or terrane (St-Onge et al., 2000a), which includes much of southern Baffin Island (Fig. 10), is considered to have accreted to the southern Rae Craton between 1915 ± 8 Ma (the youngest, most precise maximum age constraint for the Piling Group; Wodicka et al., 2014) and 1896 ± 8 Ma (the oldest dated phase of the Qikiqtarjuaq plutonic suite; Rayner 2017). The microcontinent comprises: 1) a clastic–carbonate-shelf succession (Lake Harbour Group) and its crystalline basement; 2) an overlying micaceous quartzite succession (Blandford Bay assemblage); 3) a western feldspathic quartzite-dominated clastic sequence (Lona Bay sequence); 4) a mafic volcanic sequence (Schooner Harbour sequence); and 5) an extensive suite of quartz diorite to monzogranitic plutons (Cumberland batholith) that intrude both the platformal strata and underlying crystalline basement. Orthogneiss samples from the stratigraphic basement to the Lake Harbour Group have yielded Archean ages between 3019 ± 5 and 2701 ± 2 Ma (Scott, 1998, 1999; Rayner, 2014, 2015; From et al., 2015), and a Paleoproterozoic age of 1950 +6/-4 Ma (Scott and Wodicka, 1998). A 2310 ± 3 Ma granitic clast from a conglomerate with primitive mantle $\delta^{18}O$ values and positive εHf values, and interpreted to have derived from the Meta Incognita microcontinent, provides additional evidence for Paleoproterozoic juvenile crust (Partin et al., 2014b). Plutons of the Cumberland batholith have yielded ages between 1865 ± 10 and 1845 ± 19 Ma (Jackson et al., 1990; Wodicka and Scott, 1997; Scott and Wodicka, 1998; Scott, 1999, Whalen et al., 2010; Rayner, 2015, 2017).

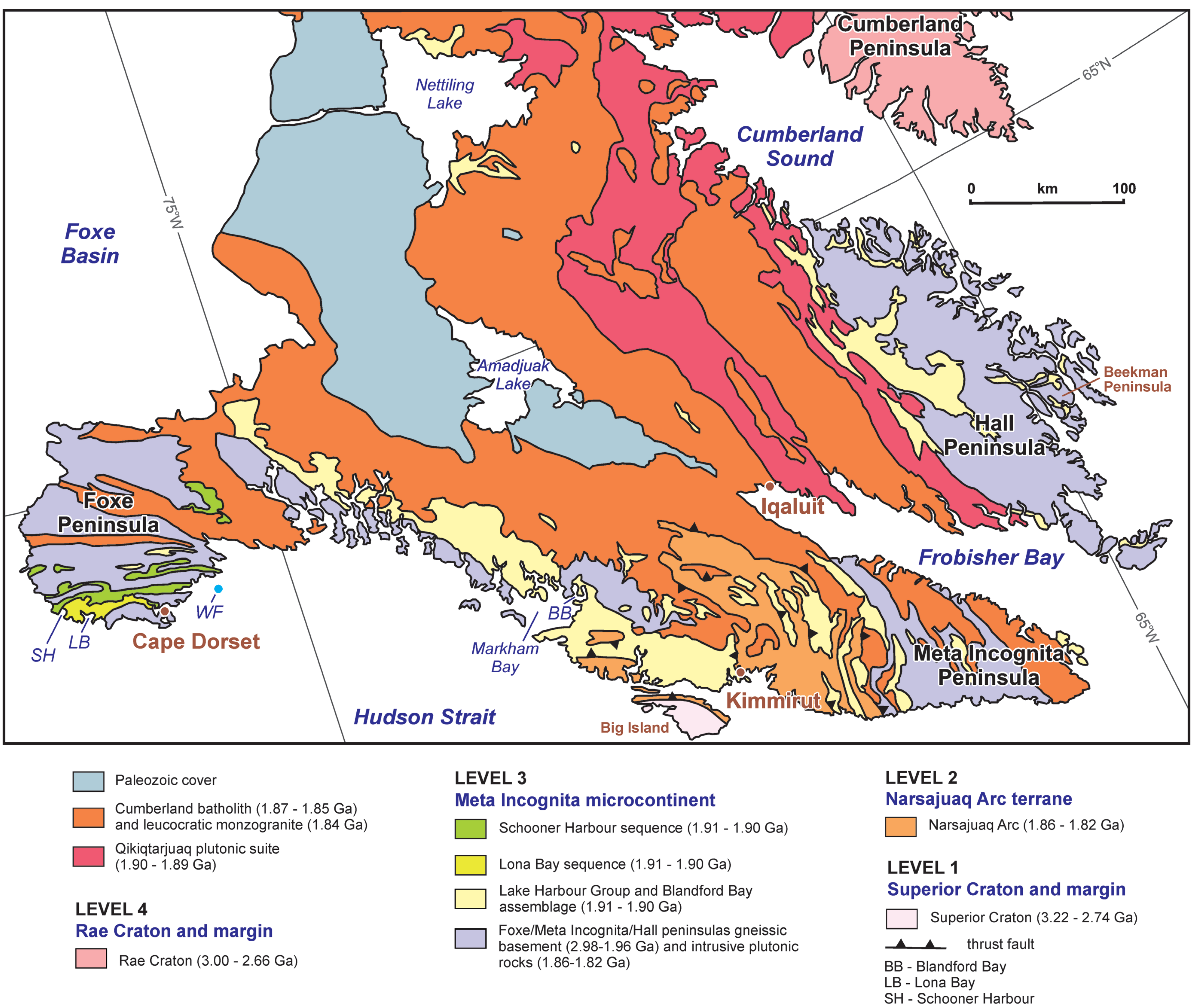

Figure 10. Geology of the Meta Incognita microcontinent, Narsajuaq Arc terrane, and the Superior Craton, southern Baffin Island (*after* Harrison et al., in press).

Basement orthogneiss

The basement gneiss exposed on Hall Peninsula (Fig. 10) comprises a complex assortment of polydeformed and polymetamorphosed plutonic rocks collectively termed the 'Archean orthogneiss complex' (From et al., 2013). The complex and similar units on Meta Incognita Peninsula and Foxe Peninsula (Fig. 10) are composed mostly of gneissic to migmatitic orthopyroxene-biotite±hornblende tonalite to porphyroclastic monzogranite with subsidiary components of well foliated to relatively massive biotite syenogranite, and boudinaged and discontinuous layers of hornblende-orthopyroxene-clinopyroxene diorite to quartz diorite (Fig. 11a; Blackadar, 1967c, d, e; Sanborn-Barrie et al., 2008; From et al., 2014; Steenkamp and St-Onge, 2014; St-Onge et al., 2015c).

Based on lithological similarities, overlying cover sequences, geochronological constraints and aeromagnetic characteristics, different cratonic correlations have been proposed for the basement gneiss of the Meta Incognita microcontinent. These include correlations with the Rae Craton of northern Baffin Island (Fig. 4) and western Greenland (Hoffman, 1988), gneiss underlying the Core Zone in northeastern Quebec (St-Onge et al., 2009), the Aasiaat domain of central western Greenland (Hollis et al., 2006a, b; Thrane and Connelly, 2006; St-Onge et al., 2009), and/or the Nain Craton of northern Labrador (Scott, 1999; Connelly, 2001; Wardle et al., 2002). Alternatively, the basement gneiss of Meta Incognita microcontinent may represent a unique and distinct crustal component (Whalen et al., 2010).

Lake Harbour Group

Quartzite, marble, psammite and semipelite mapped on the eastern and western peninsulas of southern Baffin Island are lithologically similar to the metasedimentary strata of the contiguous Lake Harbour Group in its type locality of Kimmirut (Fig. 10; St-Onge et al., 1996, 1998; Scott et al., 1997). Two lithologically and geographically distinct sequences can be recognized. Over much of southern Baffin Island, the Lake Harbour Group is composed of quartzite, garnetiferous psammite, minor semipelite and pelite, structurally overlain by laterally continuous to boudinaged bands of pale grey to white marble and calc-silicate rocks ('Kimmirut sequence'; Scott et al., 1997). In contrast, extensive garnetiferous psammite interlayered with pelite and/or semipelite, with less than 5% marble and calc silicate rocks ('Markham Bay sequence'; Scott et al., 1997), is exposed on the eastern islands and bluffs of Meta Incognita Peninsula, as well as in the Markham Bay area (Fig. 10). Both sequences are cut by generally concordant sheets of mafic to ultramafic rocks (Frobisher suite; Liikane et al., 2015).

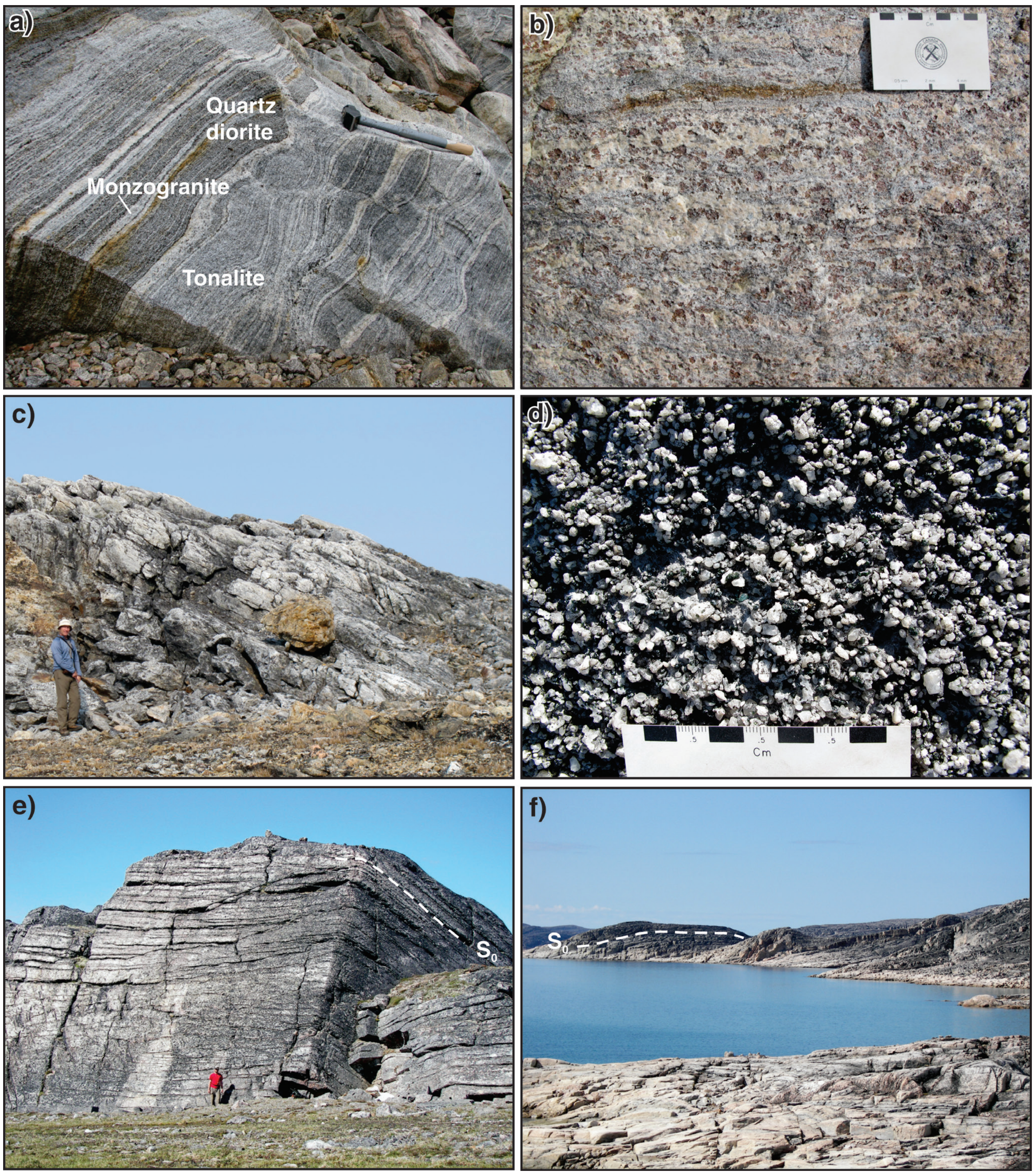

Figure 11. Hall Peninsula gneiss, Lake Harbour Group, Blandford Bay assemblage, Lona Bay sequence and Schooner Harbour sequence strata, Frobisher suite sills, southern Baffin Island (*modified in part from* St-Onge, 2015b, c). **a)** Gneissic orthopyroxene-biotite±hornblende tonalite with subsidiary components of relatively massive biotite syenogranite, and boudinaged and discontinuous layers of hornblende-orthopyroxene-clinopyroxene diorite to quartz diorite, Archean orthogneiss complex, Hall Peninsula (hammer for scale). Photograph by M.R. St-Onge. NRCan photo 2018-366. **b)** Garnet-sillimanite-biotite-leucosome psammite, Lake Harbour Group, Meta Incognita Peninsula (pen for scale). Photograph by M.R. St-Onge. NRCan photo 2018-367. **c)** Shallowly dipping, well-layered, garnet-bearing orthoquartzite, Lake Harbour Group, Meta Incognita Peninsula (geologist for scale). Photograph by D.R. Skipton. NRCan photo 2018-368. **d)** Diopside-phlogopite-spinel-apatite-quartz calcareous grit, Lake Harbour Group, Meta Incognita Peninsula. Photograph by M.R. St-Onge. NRCan photo 2018-369. **e)** Light to dark grey-weathering feldspathic quartzite, Blandford Bay assemblage, Blandford Bay (geologist for scale). Photograph by M.R. St-Onge. NRCan photo 2018-370. **f)** Cream- to buff-weathering, well-bedded, arenaceous quartzite of the Lona Bay sequence, Foxe Peninsula (width of field of view is 1 km). Photograph by M.R. St-Onge. NRCan photo 2018-371.

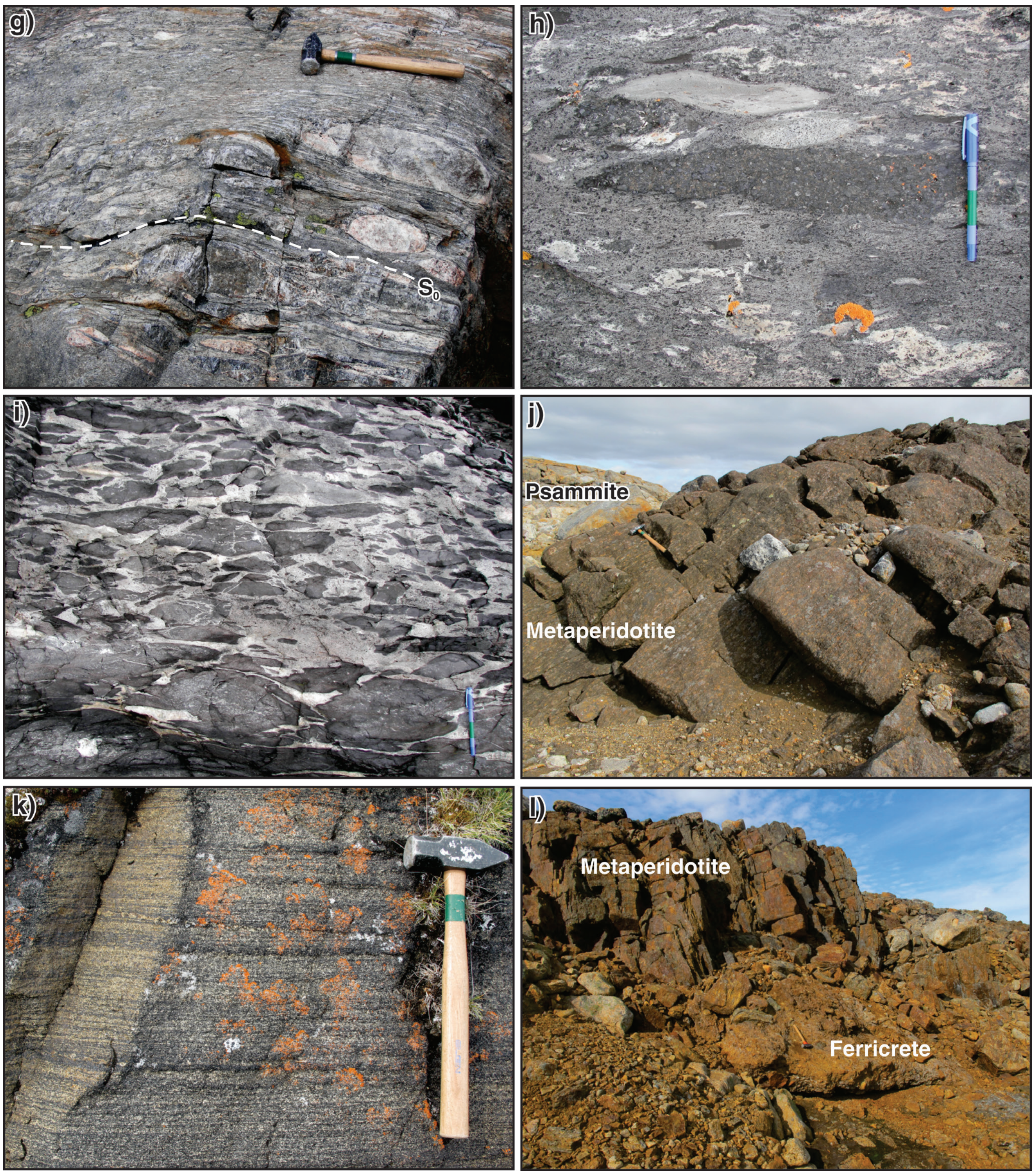

Figure 11. (cont.) g) Intraformational conglomeratic horizons, upper Lona Bay sequence, Foxe Peninsula (hammer for scale). Photograph by M.R. St-Onge. NRCan photo 2018-372. **h)** Primary fragmental textures in a mafic to intermediate lapilli tuff, Schooner Harbour sequence, Foxe Peninsula (pen for scale). Photograph by M.R. St-Onge. NRCan photo 2018-373. **i)** Mafic lithic fragments within an intermediate matrix in a pyroclastic layer of the Schooner Harbour sequence, Foxe Peninsula (hammer for scale). Photograph by M.R. St-Onge. NRCan photo 2018-374. **j)** Layered metaperidotite sill (Frobisher suite) emplaced in Lake Harbour Group psammite, Meta Incognita Peninsula (hammer for scale). Photograph by M.R. St-Onge. NRCan photo 2018-375. **k)** Layered metagabbro sill (Frobisher suite), Blandford Bay (hammer for scale), with rhythmic layering defined by variations in the modal amount of clinopyroxene, hornblende, and plagioclase. Photograph by M.R. St-Onge. NRCan photo 2018-376. **l)** Ferricrete below a metaperidotite sill (Frobisher suite), Meta Incognita Peninsula (hammer for scale). Photograph by M.R. St-Onge. NRCan photo 2018-377.

Psammite, quartzite, semipelite and pelite

Compositional layers within psammite range from centimetres to tens of centimetres in thickness and can be traced for up to tens of metres along strike. They are generally defined by variations in the modal abundance of quartz, plagioclase, biotite, garnet, sillimanite, cordierite and granitic melt (Fig. 11b). Garnet-sillimanite pelite typically occurs as thin layers within garnet-biotite semipelite, the latter subordinate within the psammite. Psammite and semipelite are generally rusty weathering due to trace amounts of disseminated graphite, pyrite and chalcopyrite.

Quartzite occurs as discrete layers (Fig. 11c) several metres to several hundred metres thick. The layers compositionally range from orthoquartzite to feldspathic quartzite, commonly contain graphite±garnet±sillimanite and are strongly recrystallized. Primary sedimentary features were not observed. White leucogranite, rich in lilac garnet and sillimanite, is a ubiquitous constituent cutting the siliciclastic package, generally occurring as concordant layers or pods <0.5 m thick, but locally several tens of metres thick.

Marble and calc-silicate

Calcareous rocks are medium to coarse grained, locally with compositional layering defined by varied modal proportions of calcite, forsterite, humite, diopside, tremolite, phlogopite, spinel, apatite and, rarely, wollastonite. Individual layers range from centimetres to metres in thickness and can be traced for tens of metres along strike. Calc-silicate rocks are commonly interlayered with siliciclastic rocks and generally associated with marble. Locally, the calcareous strata include layers of calcareous grit with abundant 1–2 mm detrital quartz grains (Fig. 11d). Thicknesses of calcareous units typically range from several decametres to about 1 km north of Kimmirut (Fig. 10). Individual marble units can be traced from 5 to 25 km along strike. No primary structures were observed in the calcareous rocks.

Blandford Bay assemblage

In the Blandford Bay area (Fig. 10), rocks of the Blandford Bay assemblage are found disconformably overlying those of the Lake Harbour Group (Scott et al., 1997).

Pelite

Rusty-weathering pelite is thinly bedded and commonly forms sections several hundreds of metres thick. Garnet, sillimanite, disseminated pyrite and minor chalcopyrite are found throughout. Compositionally graded beds are observed locally and comprise coarser psammitic bases that pass into pelitic tops, consistent with turbidite deposits. A gradational contact separates this unit from overlying feldspathic quartzite.

Feldspathic quartzite

Light to dark grey-weathering feldspathic quartzite, typically medium- to coarse-grained, forms the dominant siliciclastic component of the Blandford Bay assemblage (Fig. 11e). Homogeneous sections up to 500 m thick are common and form prominent ridges with individual beds generally 10–20 cm thick but reaching up to 2 m in thickness. Wave-washed exposures of dominantly massive and subordinate planar-laminated quartzite on the northern shore of Blandford Bay display well-developed upright crossbedding.

Lona Bay sequence

A succession of relatively homogeneous arenaceous rocks is exposed on southwestern Foxe Peninsula, in the southern part of Baffin Island. This sequence, informally designated the 'Lona Bay sequence' (Fig. 10; Sanborn-Barrie et al., 2008), consists of cream- to buff-weathering quartzose rocks that are typically well bedded (Fig. 11f). In general, beds 10 to 30 cm thick are highlighted by variations in grain size, cross-stratification, and distribution of metamorphic porphyroblasts. Although locally these rocks consist of muscovite with porphyroblastic texture, their aluminous character is more typically reflected by the occurrence of white-weathering, 0.5–2 cm long knots of sillimanite±muscovite±K-feldspar±magnetite (faserkiesel texture). The Lona Bay sequence primarily forms a broad, open antiform defined by shallow, west-dipping beds exposed at Schooner Harbour in the west (Fig. 10), and shallow east-dipping beds east of Lona Bay. Toward the stratigraphic top of the exposed sequence, several conglomeratic horizons (Fig. 11 g), ranging from 20 cm to 1 m in thickness, are interbedded with the arenaceous rocks. These horizons are believed to be intraformational with respect to the upper Lona Bay sequence.

On southeastern Foxe Peninsula, arenaceous rocks including muscovitic quartzite overlie semipelite and marble strata interpreted as middle to upper Lake Harbour Group. The arenaceous rocks are oriented in the same direction as the Lona Bay sequence and have been correlated with it based on composition, texture, and creamy weathering. If the correlation is correct and the contact relationships are stratigraphic rather than tectonic, it suggests that the Lona Bay sequence is younger than the Lake Harbour Group and may disconformably overlie it (Sanborn-Barrie et al., 2008).

Schooner Harbour sequence

A heterogeneous volcanic-rock-bearing supracrustal belt that structurally overlies the arenaceous strata of the Lona Bay sequence extends across southern Foxe Peninsula for approximately 100 km, from Schooner Harbour in the west, to the West Foxe Islands in the east. Kilometre-scale belts of amphibolite also occur north and northeast of this main corridor. All the above was designated the 'Schooner Harbour sequence' by Sanborn-Barrie et al. (2008) based on exposures of low-grade, well-preserved volcanic rock in the vicinity of Schooner Harbour (Fig. 10). Volcanic units are mainly of basaltic to andesitic composition and include lapilli tuff (Fig. 11h) and variolitic strata. Heterogenous units characterized by epidote-rich layers and lenses are widespread throughout the Schooner Harbour sequence. Extrusive rocks of ultramafic composition are exposed along the coast near Schooner Harbour, where brilliant green-weathering rocks with a subtle fragmental texture appear to represent komatiitic lapilli stone. Inland, silver green-weathering chlorite schist interlayered with fine-grained basalt and psammite is interpreted as a highly strained and hydrated ultramafic horizon (Sanborn-Barrie et al., 2008). Rocks of andesitic composition exposed on the West Foxe Islands (Fig. 10) comprise a well bedded pyroclastic sequence that commonly shows normal grading of lithic fragments (Fig. 11i). At this locality, both matrix and fragments are commonly pyroxene-phyric. Rare, thin, cream-weathered siliceous units may represent a minor component of flow-banded rhyolite, or chert.

Low in the exposed Schooner Harbour sequence, clastic rocks associated with the volcanic units include fine-grained pelite, slate, and schist that contain medium-pressure staurolite-andalusite-garnet assemblages (Smye et al., 2009). White-weathering orthoquartzite occurs as 1 m thick horizons that alternate with amphibolite, with more psammitic units upsection. Polymictic conglomerate with flattened pebbles of granite, foliated tonalite, quartzite, and psammite is also present as discontinuous horizons generally less than 1 m thick. Beds containing clasts of variolitic basalt provide evidence of a proximal erosion event occurring during accumulation of the Schooner Harbour sequence (Sanborn-Barrie et al., 2008).

Age constraints for Meta Incognita microcontinent cover sequences

Five recent mapping campaigns on southern Baffin Island (Fig. 1) have documented that the composition, association, and context of metasedimentary rocks southwest of Cumberland Sound (Weller et al., 2015), on the adjacent Hall Peninsula (e.g. Rayner et al., 2012; Steenkamp et al., 2016), on eastern Meta Incognita Peninsula (St-Onge et al. 2015c), on western Meta Incognita Peninsula (Scott et al., 2002a), and in the Markham Bay–Cape Dorset area (Scott et al., 2002a; Sanborn-Barrie et al., 2008) are similar and can be correlated with the type Lake Harbour Group assemblage in the Kimmirut area of western Meta Incognita Peninsula (St-Onge et al., 1996; Scott et al., 1997, 2002a).

A subset of Lake Harbour Group quartzite samples from eastern Hall and Meta Incognita peninsulas (Fig. 10), interpreted as locally derived basal sedimentary rocks, preserved mostly Archean detrital ages. Significant modes have been documented at 2.92, 2.85–2.80, 2.78–2.77, 2.72, and 2.68–2.67 Ga, and minor ones at 3.30–3.20 Ga (Scott et al., 2002a; Rayner, 2014, 2015). Two samples also contain minor Paleoproterozoic detritus, one of which provides a maximum depositional age of 2010 ± 19 Ma for the basal Lake Harbour Group (Wodicka et al., 2008).

Siliciclastic and carbonate samples from stratigraphically higher levels of the Lake Harbour Group yield dominantly Paleoproterozoic detritus but tend to fall into one of two provenance-profile types. The first type is characterized by detrital zircon grains yielding distinctive age peaks at 2.60–2.50, 2.40–2.30, 2.20, 2.14–2.08, 1.97–1.95 and 1.93–1.91 Ga (Scott et al., 2002a; Rayner, 2014, 2015, 2017). Older Archean detritus generally defines subordinate peaks, except for one sample from Beekman Peninsula (Fig. 10) immediately east of Hall Peninsula, which contains significant secondary populations yielding ages between 2.95 and 2.55 Ga (Rayner, 2014). Overall, the detritus from the first provenance-profile type is inferred to be sourced from local underlying Meta Incognita microcontinent basement (Wodicka et al., 2010; Rayner, 2017). In contrast, the detritus in the second provenance-profile type is almost exclusively Paleoproterozoic in age, with dominant peaks between 2.10 and 1.87 Ga (Scott et al., 2002a, Rayner, 2014, 2015, 2017). The psammite- and quartzite-rich rocks of the second type define a belt from Cumberland Sound to the eastern tip of Meta Incognita Peninsula and share many similarities with the Tasiuyak paragneiss of northern Labrador (e.g. Scott et al., 2002a).

The maximum age of deposition of the first and second provenance-profile types in the Lake Harbour Group is very similar at 1906 ± 9 and 1907 ± 9 Ma, respectively (Rayner, 2014). The intrusive Frobisher suite, with an estimated age of ca. 1900 Ma (and possibly as old as 1922 ± 12 Ma; Liikane et al., 2015), provides a minimum age constraint for the clastic–carbonate-shelf succession.

Feldspathic quartzite of the Blandford Bay assemblage contains detritus of exclusively Archean age, in contrast to the Paleoproterozoic detritus of the stratigraphically underlying Lake Harbour Group. Scott et al. (2002a) showed a dominant mode at 2.86 Ga, and subordinate peaks at 3.64, 3.02 and 2.76 Ga. Nevertheless, as rocks of the Blandford Bay assemblage depositionally overlie those of the Lake Harbour Group, the assemblage is also constrained by a maximum age of 1906 ± 9 Ma (Scott et al., 2002a; Rayner, 2014).

Volcanic units of the Schooner Harbour sequence (Fig. 10) could not be dated successfully owing to the absence of igneous zircon, but detrital zircon populations from clastic rocks show major peaks at ca. 2.69, 2.62, 2.41, 2.31 and 2.10 Ga, and define a maximum depositional age of 2099 ± 5 Ma (Wodicka et al., 2010).

Frobisher suite

Generally concordant sheets of medium- to coarse-grained, massive to weakly foliated peridotite, pyroxenite, layered peridotite-gabbro, and homogeneous gabbro occur within the Lake Harbour Group, the Blandford Bay assemblage and the lower part of the Schooner Harbour sequence (Fig. 10; St-Onge et al., 1996, 1998, 2015b; Scott et al., 1997; Sanborn-Barrie et al., 2008; MacKay and Ansdell, 2014; Steenkamp et al., 2014). These mafic to ultramafic rocks are collectively designated the 'Frobisher suite' by Liikane et al. (2015). Individual units are typically 10 to 100 m thick, although some reach a few hundred metres in thickness and extend up to several kilometres along strike. They are dark green- to reddish-brown-weathering resistive units that form prominent ridges relative to adjacent supracrustal host rocks (Fig. 11j). Metagabbroic textures and compositional layering at the centimetre to metre scale defined by variations in modal abundance of clinopyroxene, orthopyroxene, hornblende, and plagioclase are commonly preserved in the mafic bodies (Fig. 11k). The concordant nature, tabular shape, and sharp contacts of these bodies all indicate they are sills. Ultramafic bodies, either clinopyroxene-orthopyroxene±hornblende metapyroxenite or olivine-clinopyroxene-orthopyroxene metaperidotite, are common. In numerous localities, the ultramafic rocks are compositionally layered with many sills containing disseminated sulphide, some associated with a ferricrete, which consists of medium to coarse clastic sediment cemented by an iron oxy-hydroxide (Fig. 11l). A full field description of the mafic and ultramafic rocks on southern Baffin Island is provided in St-Onge et al. (2015b) and Liikane et al. (2015).

The occurrence of the ultramafic to mafic sills emplaced in the sedimentary units of the Lake Harbour Group and lower Schooner Harbour sequence suggests that the intrusive units may represent hypabyssal feeders to the mafic to ultramafic Schooner Harbour volcanic sequence (Sanborn-Barrie et al., 2008).

The layered mafic–ultramafic sills define a magmatic suite that characterizes the whole of the Meta Incognita microcontinent, as exposed on southern Baffin Island (Liikane et al., 2015). The size and distribution of the mantle-derived rocks suggest that they are the product of a major large igneous province event with a study of the petrology, geochemistry, and associated mineralization presented in Liikane (2017). A sample of Frobisher suite leucogabbro from south-central Meta Incognita Peninsula has yielded an igneous zircon crystallization age of 1922 ± 12 Ma (Liikane et al., 2015).

Cumberland batholith

The southern Rae Craton, the Piling Group cover sequence, and the crystalline and supracrustal units of Meta Incognita microcontinent are cut by plutonic rocks of the Cumberland batholith (Fig. 6, 10). The batholith is dominated by granitic phases dated between 1865 ± 10 and 1845 ± 19 Ma (Jackson et al., 1990; Wodicka and Scott, 1997; Scott and Wodicka, 1998; Scott, 1999; Whalen et al., 2010; Rayner, 2015, 2017) and has been interpreted as an Andean-type batholith (St-Onge et al., 2009), or as the result of postcollisional lithospheric delamination and mantle upwelling (Whalen et al., 2010).

Coarse-grained to pegmatitic, kilometre-scale, layered clinopyroxene-biotite-magnetite±hornblende gabbro (Fig. 12a) forms one of the older recognized plutonic suites within the batholith (Weller et al., 2015) and can include metre-scale lenses of clinopyroxene-bearing anorthosite. Quartz diorite dated at 1865 ± 9 Ma (Rayner, 2017) occurs as fine-grained, dark-weathering, massive to foliated units (Fig. 12b) containing the assemblage biotite-clinopyroxene-orthopyroxene±hornblende.

Well-foliated biotite±orthopyroxene±magnetite±hornblende±garnet monzogranite is dominant and underlies large parts of south-central Baffin Island. These rocks are typically medium grained, tan to pink weathering and equigranular, alternating between magnetite-rich and magnetite-free domains (Weller et al., 2015). A sample of biotite monzogranite collected from the eastern end of Meta Incognita Peninsula was dated at 1865 ± 10 Ma by Rayner (2015). White-weathering, massive to foliated, fine- to medium-grained garnet-biotite±magnetite monzogranite dated at 1853 ± 8 Ma (Rayner, 2017) forms plutons and dykes that are intrusive into the biotite monzogranite, as well as the coarse-grained K-feldspar megacrystic monzogranite of the Qikiqtarjuaq plutonic suite (Fig. 12c). Garnet is present as abundant burgundy phenocrysts 2 to 30 mm across, frequently in association with biotite.

Dykes of garnet-sillimanite leucogranite (1852 ± 11 Ma; Rayner, 2017) cut the garnet-biotite monzogranite. The dykes are typically fine grained, with 1 to 5 mm lilac garnet phenocrysts and mats of sillimanite. The presence of sillimanite suggests that the leucogranite is derived from muscovite-dehydration melting of metasedimentary units (e.g. Weller et al., 2015), rather than being a highly fractionated component of the plutonic suite.

Pink- to orange-weathering, medium- to coarse-grained, massive to foliated biotite±orthopyroxene±magnetite±garnet monzogranite, with distinctive K-feldspar megacrysts (Fig. 12d), occurs throughout large parts of southern Baffin Island. Potassium-feldspar phenocrysts form augen up to 10 cm wide and locally display rapakivi textures (ovoid alkali feldspar mantled by plagioclase feldspar). Megacrystic monzogranite from Meta Incognita Peninsula was dated by Rayner (2015) at 1845 ± 19 Ma.

PALEOPROTEROZOIC NARSAJUAQ ARC TERRANE (LEVEL 2)

The Narsajuaq Arc terrane is considered to be represented by two temporally and petrologically distinct magmatic suites: an older intraoceanic suite exposed on the Ungava Peninsula of northern Quebec (Fig. 3) and a younger Andean-margin-type suite (Dunphy and Ludden, 1998), exposed both in northern Quebec and southern Baffin Island (Fig. 10). The older suite includes calc-alkaline layered

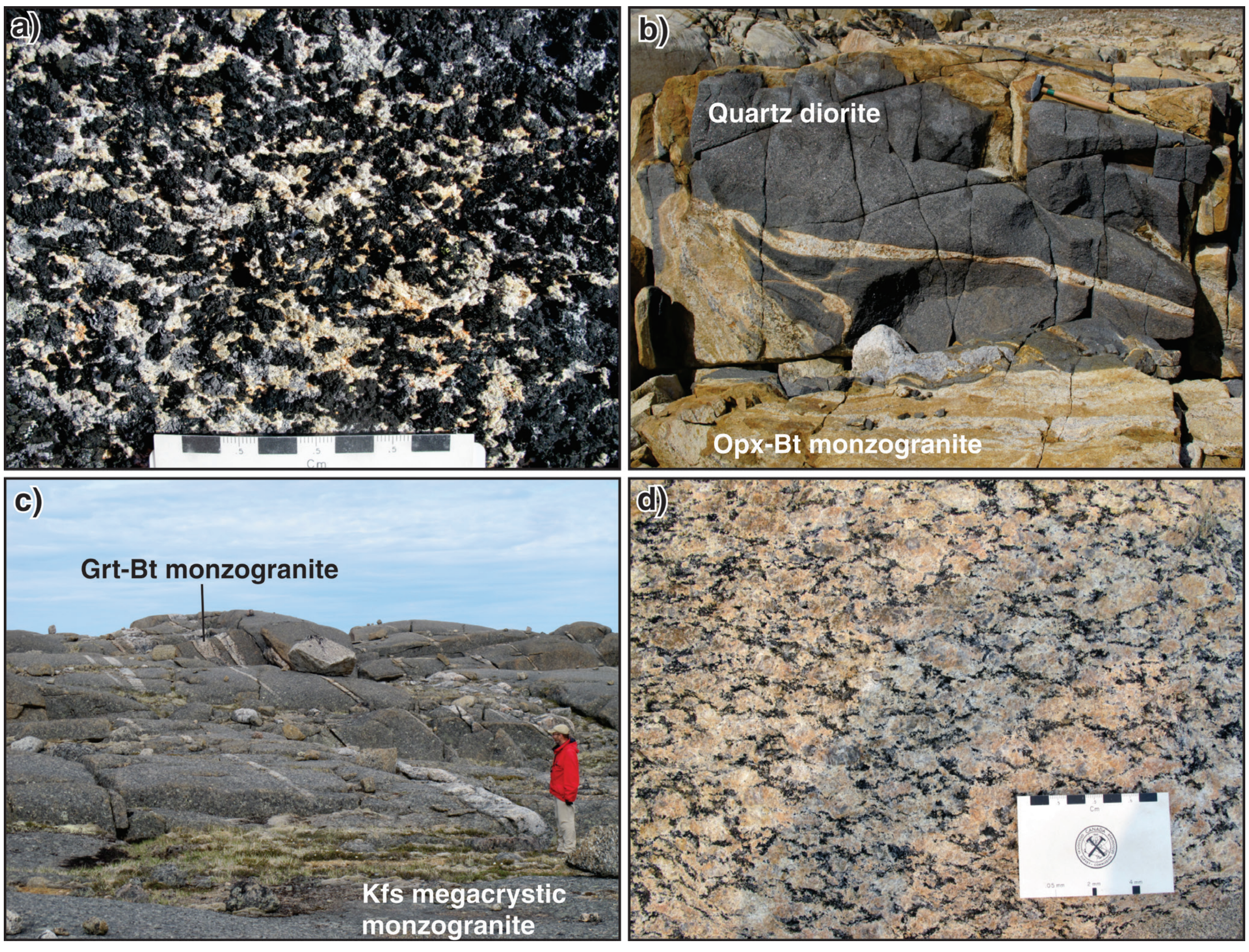

Figure 12. Plutonic suites of the Cumberland batholith, southern Baffin Island (*modified from* Weller et al., 2015). **a)** Clinopyroxene-biotite-magnetite±hornblende gabbro, Cumberland Sound region. Photograph by M.R. St-Onge. NRCan photo 2018-378. **b)** Enclave of quartz diorite in orthopyroxene-biotite monzogranite, Meta Incognita Peninsula (hammer for scale). Photograph by M.R. St-Onge. NRCan photo 2018-379. **c)** dykes of garnet-biotite±magnetite monzogranite emplaced in K-feldspar megacrystic monzogranite of the Qikiqtarjuaq plutonic suite, Cumberland Sound region (geologist for scale). Photograph by B.J. Dyck. NRCan photo 2018-380. **d)** Coarse-grained, massive biotite±orthopyroxene±magnetite±garnet monzogranite, with distinctive K-feldspar megacrysts, Meta Incognita Peninsula. Photograph by M.R. St-Onge. NRCan photo 2018-381.

diorite-tonalite gneiss (Fig. 13a), and tholeiitic to calc-alkaline basaltic andesite (Fig. 13b) to rhyolite, dated between 1863 ± 2 Ma and 1845 ± 2 Ma (St-Onge et al., 1992; Machado et al., 1993; R.R. Parrish, unpub. data, 1989). The older magmatic suite is interpreted as an island-arc assemblage built on Paleoproterozoic oceanic crust and a sliver of Archean continental crust (Thériault et al., 2001). The younger suite comprises crosscutting, foliated to massive, monzodiorite to granite plutons dated between 1842 +5/-3 Ma and 1820 +4/-3 Ma (Fig. 3; Machado et al., 1993; Scott, 1997; Scott and Wodicka, 1998; Rayner, 2017; R.R. Parrish, unpub. data, 1989) and interpreted as having been emplaced in a continental-margin arc setting (Dunphy and Ludden, 1998; Thériault et al., 2001).

Crosscutting field relationships (St-Onge et al., 1998) indicate that the oldest unit of the younger magmatic suite of Narsajuaq Arc on southern Baffin Island is a layered, fine- to medium-grained, grey to buff orthopyroxene-biotite±hornblende±garnet tonalitic orthogneiss with subordinate grey orthopyroxene-biotite±hornblende granodiorite layers, and pink monzogranite sheets and veins (Fig. 13c). Lenses, layers and locally discordant dykes of dark hornblende-biotite-clinopyroxene±orthopyroxene quartz diorite, up to several metres thick, commonly form an integral component of the orthogneiss. The tonalitic, granodioritic, and quartz dioritic components are cut by concordant to discordant veins of medium-grained orthopyroxene-biotite±hornblende monzogranite and by rare coarse-grained hornblende-biotite±orthopyroxene syenogranite. Grey anorthosite layers up to several tens of metres thick and over 1 km in strike length also occur.

Large areas of Narsajuaq Arc (Fig. 10) on southern Baffin Island are underlain by medium-grained, gneissic to massive orthopyroxene-biotite±hornblende monzogranite (Fig. 13d) that intrudes the layered tonalite-monzogranite gneiss described above. Coarse-grained and locally megacrystic layers can reach 100 m in thickness. A hornblende-clinopyroxene-orthopyroxene-biotite quartz diorite phase is common.

ARCHEAN SUPERIOR CRATON AND ITS PALEOPROTEROZOIC NORTHERN MARGIN (LEVEL 1)

In northern Quebec (Fig. 3), the Archean Superior Craton predominantly comprises felsic orthogneiss and biotite-hornblende±orthopyroxene plutonic units (Fig. 14a) ranging in age between 3220 +32/-23 Ma and 2554 ± 5 Ma (Machado et al., 1989; Mortensen and Percival, 1989; Parrish, 1989; St-Onge et al., 1992; Scott and St-Onge, 1995; Wodicka and Scott, 1997; R.R. Parrish, pers. comm., 1994). Unconformably overlying the felsic basement is a suite of parautochthonous basal clastic sedimentary strata (Fig. 14b), carbonatitic volcaniclastic rock, continental tholeiitic flood basalt (Fig. 14c) and rhyolite (Povungnituk Group, Fig. 3) associated with initial Paleoproterozoic rifting of the northern Superior Craton and yielding ages between 2038 +4/-2 Ma and 1958.6 +3.1/-2.7 Ma (Parrish, 1989; Machado et al., 1993; Kastek et al., 2018). In the Ungava Peninsula of northern Quebec (Fig. 3), a younger succession of predominantly Mg-rich komatiitic to tholeiitic basalt (Chukotat Group; Fig. 14d) accumulated during renewed rifting along the northern continental margin (St-Onge et al., 2000a). The Chukotat Group disconformably overlies the initial rift sedimentary and volcanic rocks and is dated between 1887 +37/-11 Ma and 1870 ± 4 Ma (Fig. 3; Wodicka et al., 2002a; R.R. Parrish, unpub. data, 1989). The ages of the younger volcanic succession indicate that approximately 150 Ma elapsed between the onset of initial continental rifting and the subsequent renewed rifting event (St-Onge et al. 2000a).

On Big Island, just south of Baffin Island (Fig. 10), orthogneiss dated at 2875 +9/-7 Ma (Wodicka and Scott, 1997) and associated clastic rocks containing detrital zircons ranging in age between 3.15 and 2.54 Ga, with distinct modes at 2.79, 2.73, and 2.69 Ga (Scott et al., 2002a), are correlated with the Archean Superior Craton and the Povungnituk Group clastic rift sequence, respectively (St-Onge et al., 1996; Scott et al., 2002a).

PALEOPROTEROZOIC OROGENIC BELTS AND PLATE GEOMETRIES

Within Baffin Island, the constituent Archean cratons, attendant Paleoproterozoic cover sequences, microcontinental blocks, and continental magmatic arcs, as described above, were assembled during a period of global amalgamation that occurred between ca. 1.9 and 1.8 Ga (St-Onge et al., 2009). Documentation of the geometry, age, structural evolution, magmatic context, and metamorphic framework of the intervening deformation zones and orogenic belts allows the relative upper plate versus lower plate geometry to be established in each case (Fig. 3). This in turn allows the tectonic evolution of Baffin Island during the Paleoproterozoic to be modelled as a series

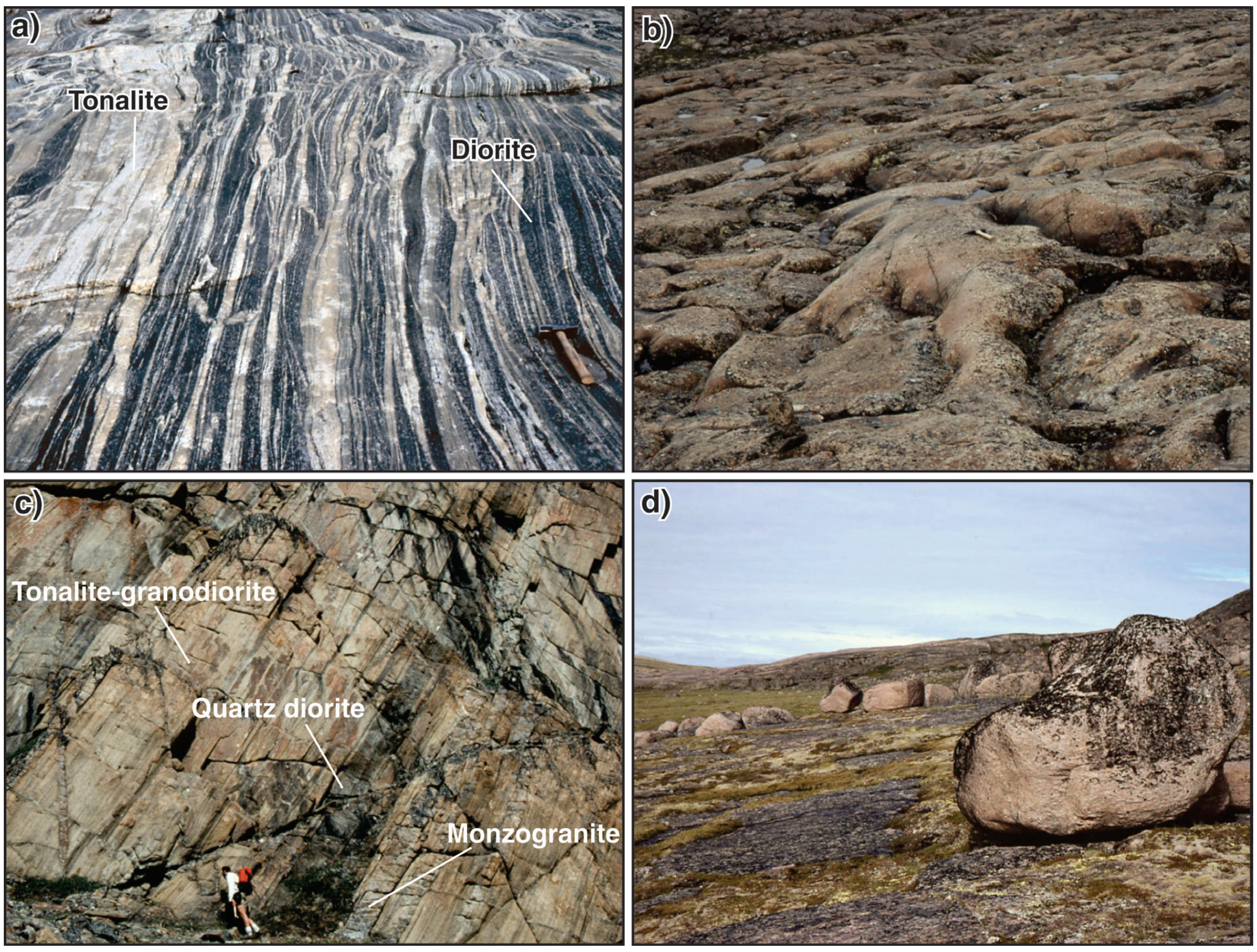

Figure 13. Magmatic components of Narsajuaq Arc terrane, northern Quebec and southern Baffin Island. **a)** Calc-alkaline layered diorite-tonalite gneiss, older suite of Narsajuaq Arc terrane, Ungava Peninsula, Quebec (hammer for scale). Photograph by M.R. St-Onge. NRCan photo 2018-382. **b)** Calc-alkaline basaltic andesite, older suite of Narsajuaq Arc terrane, Ungava Peninsula, Quebec (hammer for scale). Photograph by M.R. St-Onge. NRCan photo 2018-383. **c)** Tonalite–granodiorite gneiss with quartz diorite layers and crosscutting monzogranite dykes, younger suite of Narsajuaq Arc terrane, southern Baffin Island (geologist for scale). Photograph by M.R. St-Onge. NRCan photo 2018-384. **d)** Massive monzogranite, younger suite of Narsajuaq Arc terrane, southern Baffin Island (height of boulder on right is 2 m). Photograph by M.R. St-Onge. NRCan photo 2018-385.

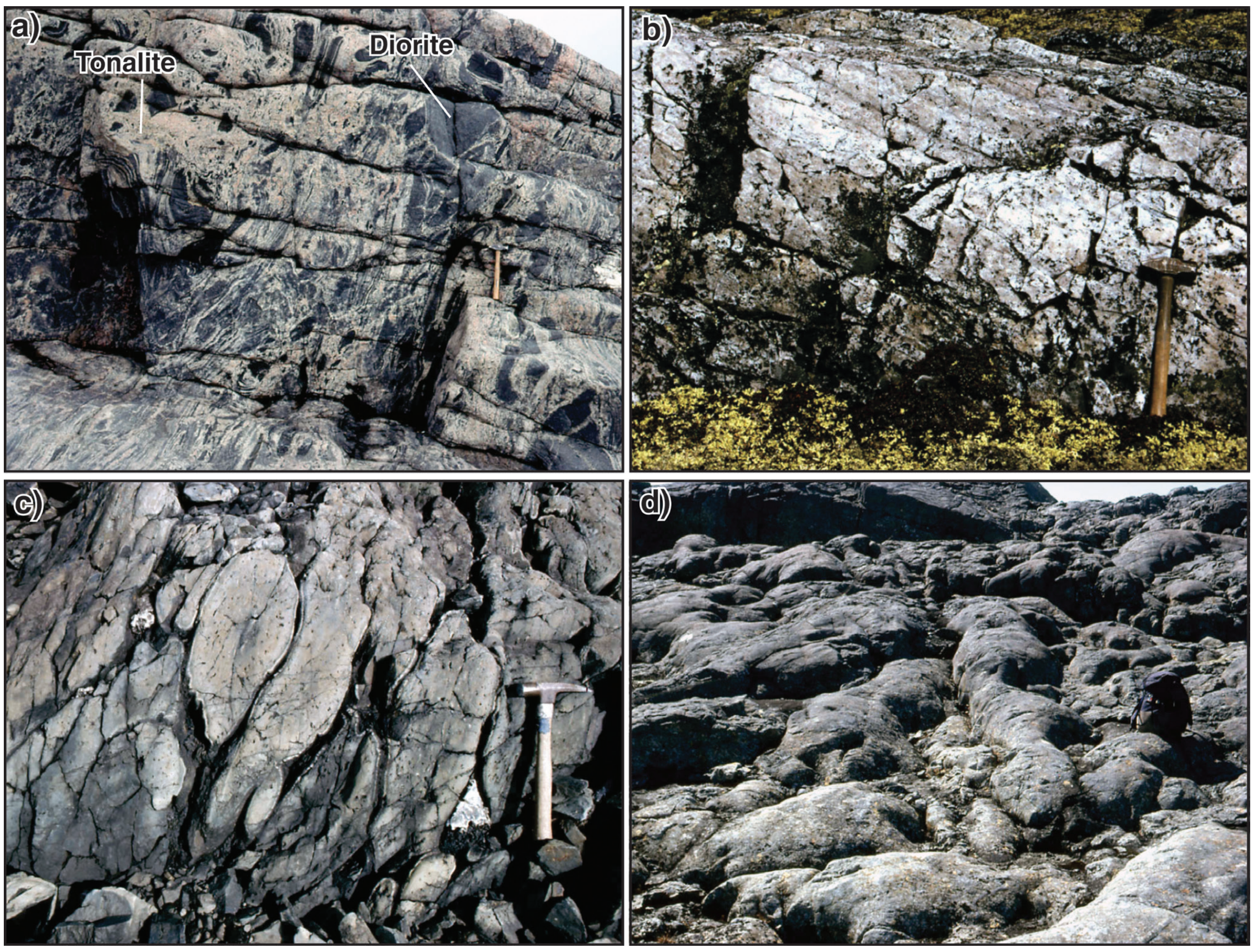

Figure 14. Superior Craton basement and cover units, northern Quebec and southern Baffin Island. **a)** Archean biotite-hornblende+orthopyroxene tonalite with abundant diorite enclaves, Superior Craton, northern Quebec (hammer for scale). Photograph by M.R. St-Onge. NRCan photo 2018-386. **b)** Shallowly-dipping, Paleoproterozoic basal quartzite, Povungnituk Group, southern Baffin Island (hammer for scale). Photograph by M.R. St-Onge. NRCan photo 2018-387. **c)** Paleoproterozoic pillowed basalt in a continental tholeiite flow, Povungnituk Group, northern Quebec (hammer for scale). Photograph by M.R. St-Onge. NRCan photo 2018-388. **d)** Lava pillows and tubes of Mg-rich komatiitic basalt, Chukotat Group, northern Quebec (backpack for scale). Photograph by M.R. St-Onge. NRCan photo 2018-389.

of cumulative accretion–collision events contributing to the southerly growth (present co-ordinates) of the Nuna Supercontinent culminating at ca. 1.8 Ga.

Qimivvik crustal shortening

Deformation along the northern margin of the Rae Craton in the Qimivvik area of northern Baffin Island (Fig. 3) is characterized by southwest-vergent crustal shortening that juxtaposed Archean crystalline basement over cover strata, potentially due to thrust faulting (Skipton et al., 2017). The peak metamorphic assemblage in pelite contains garnet, sillimanite, cordierite±K-feldspar, and foliation is defined by aligned biotite and compositional banding. Pelite hosts foliation-parallel leucogranite layers that are consistent with mica dehydration melting and peak metamorphism at upper-amphibolite- to granulite-facies conditions. Southwest-vergent folding of leucogranite layers suggests that peak metamorphism conditions were associated with pre- to synductile deformation. However, cliff exposures also reveal subvertical leucogranite dykes that stem from the leucogranite melt network within the pelitic metasedimentary rocks, and which crosscut the contact with the overlying basement orthogneiss. Preliminary in situ U-Pb ages of monazite in pelitic metasedimentary units indicate a protracted tectonometamorphic history: garnet cores contain ca. 2.5 Ga monazite inclusions, whereas matrix monazite is dominantly ca. 1.9 Ga, including foliation-parallel grains, locally with partial ca. 1.8 Ga rims (D. Skipton, pers. comm., 2018).

Foxe fold belt

Deformation along the southern margin of the Rae Craton within the Foxe fold belt of central Baffin Island (Fig. 3) is characterized by early north-verging, thin-skinned imbrication and tight intrafolial isoclinal folding of the Piling Group, followed by northeast-trending upright folding of both Paleoproterozoic cover and Archaean basement, and subsequent open northwest-trending, thick-skinned crossfolding (Scott et al., 2003). Metamorphic grade increases from greenschist facies at higher structural levels to granulite facies at lower structural levels and in proximity to the plutonic units of the Qikiqtarjuaq plutonic suite (Gagné et al., 2009; Wodicka et al., 2014).

The proposed Baffin suture (St-Onge et al., 2006) separating the Archaean Rae Craton and its flanking, southern Palaeoproterozoic continental-margin sedimentary and volcanic sequences (Piling and Hoare Bay groups) from accreted tectonic elements to the south (Meta Incognita microcontinent and associated Lake Harbour Group) trends east from the Foxe Basin to the head of Cumberland Sound (Fig. 3). Closing across the proposed suture is thought to postdate 1915 ± 8 Ma (the youngest, most precise maximum age constraint for the Piling Group; Wodicka et al., 2014) and predate emplacement of the 1896 ± 8 Ma to 1886 ± 5 Ma Qikiqtarjuaq plutonic suite (Rayner, 2017). Engulfment of the cryptic suture zone by younger, voluminous granitic plutons precludes any direct constraints on the polarity of the Baffin suture (St-Onge et al., 2009; Weller et al., 2015), although Corrigan et al. (2009) have presented arguments for a north-directed sense of vergence.

Dorset fold belt

Convergence between the southern margin of the Meta Incognita microcontinent and crustal domains to the south led to development of the Dorset fold belt and formation of the north-dipping Soper River suture (Fig. 3). Closing of the suture is bracketed between 1845 ± 2 Ma, the age of the youngest unit associated with the intra-oceanic phase of the accreted Narsajuaq Arc (Fig. 3; Dunphy and Ludden, 1998) and 1842 +5/-3 Ma (Scott, 1997), the age of the oldest plutonic unit of the continental-margin arc phase of the Narsajuaq Arc (St-Onge et al., 2007).

Deformation in the Dorset fold belt includes:

- structural repetition and truncation of distinct tectonostratigraphic units yielding an overall south-southwest-verging ramp-flat fault geometry (Scott et al., 1997)
- associated tight to isoclinal folding during south- to southwest-directed deformation (Sanborn-Barrie et al., 2008)
- development of a penetrative granulite-facies compositional fabric
- formation of ribbon mylonites and transposition of crosscutting intrusive units into parallelism in the vicinity of the Soper River suture
- later, open crossfolding and localized dextral transcurrent shearing oriented northwest–southeast.

Syntectonic granulite-facies regional metamorphism associated with emplacement of the Cumberland batholith and closure of the Soper River suture is bracketed between ca. 1849 and 1835 Ma (St-Onge et al., 2007).

The south- to southwest-verging thrusting and folding documented within the Dorset fold belt and the location of the Cumberland batholith continental-margin arc rocks in the northern hanging wall of the suture suggest that the Meta Incognita microcontinent occupied an upper plate position with respect to the Narsajuaq Arc to the south (Fig. 3) during convergence across the Soper River suture.

Cape Smith belt

Within the Cape Smith belt of northern Quebec and southernmost Baffin Island (Fig. 3), parautochthonous sedimentary and volcanic strata along the northern margin of the Superior Craton are imbricated by thrust faults above a regional basal décollement (Lucas, 1989; St-Onge et al., 2001). Fault displacement was in a southerly direction, with thin-skinned imbrication and associated folding occurring in a piggyback sequence toward the southern foreland. Thrust deformation was initiated after 1870 ± 4 Ma, the age of the youngest unit within the parautochthonous Superior Craton cover sequence.

A distinct suite of late or 'out-of-sequence' thrust faults that postdate the thin-skinned structures re-imbricate the cover units of the Superior Craton (Lucas, 1989). These younger south-verging structures are thick-skinned (involving both crystalline basement and Palaeoproterozoic cover units) and are collisional in origin as they can be linked to the terrane boundary faults of the Narsajuaq Arc terrane and Purtuniq ophiolite in northern Quebec (Fig. 3; St-Onge et al., 2001). The late faults truncate the metamorphic isograds within the Cape Smith belt and thus must postdate 1820 +4/-3 to 1815 ± 4 Ma (Bégin, 1992). They predate the age of emplacement of postkinematic syenite plugs and syenogranite dykes at 1795 ± 2 to 1758.2 ± 1.2 Ma (St-Onge et al., 2006).

Regional, Barrovian-style, kyanite–sillimanite-grade metamorphism is associated with early thin-skinned thrusting of cover units along the northern margin of the Superior Craton (Bégin, 1992). Metamorphism is bracketed between 1820 +4/-3 and 1815 ± 4 Ma and is interpreted as a consequence of the relaxation of isotherms in the tectonically thickened thrust belt (St-Onge and Lucas, 1991).

A south-verging tectonic boundary or crustal suture (Bergeron suture; Fig. 3) separates the northern Superior margin strata from allochthonous crustal elements to the north (St-Onge et al., 1999, 2001). Associated with, and sitting in the hanging wall of, the Bergeron suture are the crustal components of an obducted 1998 ± 2 Ma ophiolite (Watts group; Parrish, 1989; Scott et al., 1992, 1999), as well as the plutonic, volcanic, and sedimentary components of the Narsajuaq Arc (described above). Preservation of the ophiolite and the higher structural levels it represents within the Cape Smith belt is entirely a function of the late- to postcollisional, crustal-scale, orogen-parallel folding and orogen-perpendicular crossfolding that characterize the southern margin of the Trans-Hudson Orogen in northern Quebec (Lucas and Byrne, 1992). Closure of the Bergeron suture, and collision of the accreted terrane with the Superior Craton, is bracketed between 1820 +4/-3 Ma (youngest component of the Narsajuaq Arc) and 1795 ± 2 Ma (the age of an undeformed crosscutting syenogranite pegmatite dyke) (St-Onge et al., 2006).

The architecture of the foreland thin- to thick-skinned thrust–fold belt, the geometry of the Bergeron suture, the regional Barrovian metamorphism developed within the Cape Smith belt, as well as the recent documentation of high-pressure eclogite in the crystalline basement footwall (Weller and St-Onge, 2017) corroborate the lower plate position of the Superior Craton during its collision with the accreted terranes to the north (Fig. 3).

CONCLUSIONS

Documentation of the Archean and Paleoproterozoic bedrock units and structures on Baffin Island as synthesized in this paper allows identification of an internally consistent, north-to-south sequence of accretionary and collisional tectonic events during the Paleoproterozoic (Fig. 3). These tectonic events (itemized below) first resulted in the growth of a composite upper-plate domain around the crustal nucleus represented by the Rae Craton. Initial assembly of the upper-plate (Churchill) domain was then followed by collision with the southern, lower-plate Superior Craton, which resulted in the terminal collisional phase of the Trans-Hudson Orogeny and significantly added to the landmass of the emerging Laurentian Craton.

Based on available tectonostratigraphic, structural, and geochronological data for Baffin Island, the tectonic events that characterize the accretionary–collisional growth of northeast Laurentia during the middle Paleoproterozoic are as follows (Fig. 3):

- deformation along the northern margin of the Rae Craton at ca. 1.90 Ga (Qimivvik area)
- accumulation of a stratigraphically south-facing, rift- to continental-margin sequence in a fragmented proto-ocean basin setting developed along the southern margin of the Rae Craton between ca. 2.16 and 1.91 Ga
- north–south convergence and accretion of the Meta Incognita microcontinent to the southern margin of the Rae Craton across the Baffin suture between ca. 1.91 and 1.90 Ga (Foxe fold belt)
- accretion of the Narsajuaq Arc terrane to the southern margin of the growing Churchill Domain at ca. 1.845 Ga (Dorset fold belt)
- collision of the lower plate Superior Craton with the composite upper-plate Churchill Domain between ca. 1.82 and 1.795 Ga (Cape Smith belt)

ACKNOWLEDGMENTS

The first author would like to thank the following Geological Survey of Canada and Canada Centre for Remote Sensing colleagues: D. Boerner, P. Brouillette, P. Budkewitsch, D. Corrigan, E. de Kemp, L. Dredge, A. Ford, K. Ford, S. Hanmer, J. Harris, P. Harrison, B. Harvey, D. Hodgson, O. Ijewliw, A. Jones, R. Knight, T. Little, S. Lucas, T. Lynds, A. Morin, T. Peterson, N. Rayner, M. Sanborn-Barrie, B. Saumur, D. Skipton, D. Snyder, J. Spratt, R. Thériault, V. Tschirhart, N. Wodicka; Canada-Nunavut Geoscience Office colleagues: C. Gilbert, D. James, D. Mate, H. Steenkamp, D. Scott; university colleagues: K. Ansdell (University of Saskatchewan), D. Carmichael (Queen's University), D. Francis (McGill University), R. Jamieson (Dalhousie University), H. Helmstaedt (Queen's University), S. Johnston (University of Alberta), D. Pattison (University of Calgary), D. Schneider (University of Ottawa), O. Weller (University of Cambridge), J. White (University of New Brunswick), M. Young (Dalhousie University); and university and college student field assistants: M. Allen, M. Appaqaq, F. Berniolles, E. Bros, G. Brown, J. Butler, T. Chadwick, J. Chakungal, D. Copeland, K. Dubach, B. Dyck, S. Evans, R. From, S. Gagné, J. Gladstone, C. Herd, R. Hinanik, C. Hogue, B. Hrabi, C. Huebert, H. Iyerak, S. Johns, R. Keiser, D. Liikane, C. Mackay, A. Markey, T. Milton, S. McMullen, S. Modelland, S. Noble-Nowdluk, L. Piper, J. Rae, J. Robillard, T. Rowe, J. Ruechel, I. Russell, B. Sharp, A. Simmons, A. Smye, J. Stacey, E. Turner, and C. Yakymchuk, who have all contributed greatly over the past 25 years to the understanding of the Archean and Paleoproterozoic stratigraphy, structure, and tectonic evolution of Baffin Island.

The authors gratefully acknowledge the careful reviews of this contribution by David Corrigan and Christopher Harrison.

REFERENCES

Bégin, N.J., 1992. Contrasting mineral isograd sequences in metabasites of the Cape Smith Belt, northern Quebec, Canada: three new bathograds for mafic rocks; Journal of Metamorphic Geology, v. 10, p. 685–704. https://doi.org/10.1111/j.1525-1314.1992.tb00115.x

Bell, R., 1885. Observations on the geology, zoology and botany of Hudson's Strait and Bay, made in 1885; Geological Survey of Canada, Annual Report v. 1, pt. DD, 32 p. https://doi.org/10.4095/297069

Bell, R., 1901. Report of an exploration on the northern side of Hudson Strait; Geological Survey of Canada, Annual Report v. 11 (1898), pt. M, 46 p. https://doi.org/10.4095/297002

Bethune, K.M. and Scammell, R.J., 1997. Precambrian geology, Koch Island area (part of NTS 37C), District of Franklin, Northwest Territories; Geological Survey of Canada, Open File 3391, scale 1:50 000. https://doi.org/10.4095/208509

Bethune, K.M. and Scammell, R.J., 2003a. Geology, geochronology, and geochemistry of Archean rocks in the Eqe Bay area, north-central Baffin Island, Canada: constraints on the depositional and tectonic history of the Mary River Group of northeastern Rae Province; Canadian Journal of Earth Sciences, v. 40, no. 8, p. 1137–1167. https://doi.org/10.1139/e03-028

Bethune, K.M. and Scammell, R.J., 2003b. Distinguishing between Archean and Paleoproterozoic tectonism, and evolution of the Isortoq fault zone, Eqe Bay area, north-central Baffin Island, Canada; Canadian Journal of Earth Sciences, v. 40, no. 8, p. 1111–1135. https://doi.org/10.1139/e03-040

Blackadar, R.G., 1959. Cape Dorset, Baffin Island, District of Franklin, Northwest Territories; Geological Survey of Canada, Preliminary Map 11–1959, scale 1:126 720. https://doi.org/10.4095/108525

Blackadar, R.G., 1960. Hobart Island, Baffin Island, District of Franklin, Northwest Territories; Geological Survey of Canada, Preliminary Map 55–1959, scale 1:253 440. https://doi.org/10.4095/108650

Blackadar, R.G., 1961. Mingo Lake, Baffin Island, District of Franklin, Northwest Territories; Geological Survey of Canada, Preliminary Map 43–1960, scale 1:253 440. https://doi.org/10.4095/108736

Blackadar, R.G., 1962. Geology, Andrew Gordon Bay–Cory Bay, Baffin Island, District of Franklin; Geological Survey of Canada, Preliminary Map 5–1962, scale 1:253 440. https://doi.org/10.4095/108797

Blackadar, R.G., 1967a. Geology, Mingo Lake–Macdonald Island, Baffin Island, District of Franklin; Geological Survey of Canada, Map 1185A, scale 1:253 440. https://doi.org/10.4095/107493

Blackadar, R.G., 1967b. Geology of Mingo Lake–Macdonald Island map area, Baffin Island, District of Franklin; Geological Survey of Canada, Memoir 345, 54 p. https://doi.org/10.4095/100532

Blackadar, R.G., 1967c. Geology, Foxe Peninsula, District of Franklin; Geological Survey of Canada, Preliminary Map 16–1966, scale 1:506 880. https://doi.org/10.4095/108489

Blackadar, R.G., 1967d. Geology, Cumberland Sound, District of Franklin; Geological Survey of Canada, Preliminary Map 17–1966, scale 1:506 880. https://doi.org/10.4095/108490

Blackadar, R.G., 1967e. Geology, Frobisher Bay, District of Franklin; Geological Survey of Canada, Preliminary Map 18–1966, scale 1:506 880. https://doi.org/10.4095/108491

Blackadar, R.G., Davison, W.L., and Trettin, H.P., 1968a. Geology, Milne Inlet, District of Franklin; Geological Survey of Canada, Map 1235A, scale 1:253 440. https://doi.org/10.4095/107494

Blackadar, R.G., Davison, W.L., and Trettin, H.P., 1968b. Geology, Navy Board Inlet, District of Franklin; Geological Survey of Canada, Map 1236A, scale 1:253 440. https://doi.org/10.4095/107498

Blackadar, R.G., Davison, W.L., and Trettin, H.P., 1968c. Geology, Arctic Bay–Cape Clarence, District of Franklin; Geological Survey of Canada, Map 1237A, scale 1:253 440. https://doi.org/10.4095/107330

Blackadar, R.G., Davison, W.L., and Trettin, H.P., 1968d. Geology, Moffet Inlet–Fitzgerald Bay, District of Franklin; Geological Survey of Canada, Map 1238A, scale 1:253 440. https://doi.org/10.4095/107497

Blackadar, R.G., Davison, W.L., and Trettin, H.P., 1968e. Geology, Phillips Creek, District of Franklin; Geological Survey of Canada, Map 1239A, scale 1:253 440. https://doi.org/10.4095/107510

Blackadar, R.G., Davison, W.L., and Trettin, H.P., 1968f. Geology, Agu Bay–Easter Cape, District of Franklin; Geological Survey of Canada, Map 1240A, scale 1:253 440. https://doi.org/10.4095/107336

Blackadar, R.G., Davison, W.L., and Trettin, H.P., 1968g. Geology, Berlinguet Inlet–Bourassa Bay, District of Franklin; Geological Survey of Canada, Map 1241A, scale 1:253 440. https://doi.org/10.4095/107412

Blackadar, R.G., Davison, W.L., and Trettin, H.P., 1968h. Geology, Erichsen Lake area, District of Franklin; Geological Survey of Canada, Map 1242A, scale 1:253 440. https://doi.org/10.4095/108947

Bradley, D.C., 2008. Passive margins through earth history; Earth-Science Reviews, v. 91, p. 1–26. https://doi.org/10.1016/j.earscirev.2008.08.001

Bros, E.R. and Johnston, S.T., 2017. Field observations of the Mary River Group south of Tay Sound, northern Baffin Island, Nunavut: stratigraphy and structure of supracrustal sequences and surrounding plutonic suites; *in* Summary of activities 2017, Canada-Nunavut Geoscience Office, p. 69–79.

Cawood, P.A. and Nemchin, A.A., 2001. Paleogeographic development of the east Laurentian margin: constraints from U-Pb dating of detrital zircons in the Newfoundland Appalachians; Geological Society of America Bulletin, v. 113, p. 1234–1246. https://doi.org/10.1130/00167606(2001)113

Chandler, F.W., 1988. Geology of the late Precambrian Fury and Hecla Group, northwest Baffin Island, District of Franklin; Geological Survey of Canada, Bulletin 370, 30 p. https://doi.org/10.4095/126938

Clarke, D.B. and Upton, B.G.J., 1971. Tertiary basalts of Baffin Island: field relations and tectonic setting; Canadian Journal of Earth Sciences, v. 8, p. 248–258. https://doi.org/10.1139/e71-025

Connelly, J.N., 2001. Constraining the timing of metamorphism: U-Pb and Sm-Nd ages from a transect across the northern Torngat Orogen, Labrador, Canada; The Journal of Geology, v. 109, p. 57–77. https://doi.org/10.1086/317965

Corrigan, D., 2012. Paleoproterozoic crustal evolution and tectonic processes: insights from the LITHOPROBE program in the Trans-Hudson Orogen, Canada; *in* Tectonic Styles in Canada: the LITHOPROBE perspective, (ed.) J.A. Percival, F.A. Cook, and R.M. Clowes; Geological Association of Canada, Special Paper 49, p. 237–284.

Corrigan, D., Scott, D.J., and St-Onge, M.R., 2001. Geology of the northern margin of the Trans-Hudson Orogen (Foxe Fold Belt), central Baffin Island, Nunavut; Geological Survey of Canada, Current Research 2001-C23, 27 p. https://doi.org/10.4095/212249

Corrigan, D., Pehrsson, S., Wodicka, N., and de Kemp, E., 2009. The Palaeoproterozoic Trans-Hudson Orogen: a prototype of modern accretionary processes; Ancient orogens and modern analogues, (ed.) J.B. Murphy, J.D. Keppie, and A.J. Hynes; Geological Society, Special Publication 327, p. 457–479. https://doi.org/10.1144/SP327.19

Corrigan, D., Nadeau, L., Brouillette, P., Wodicka, N., Houlé, M.G., Tremblay, T., Machado, G., and Keating, P., 2013. Overview of the GEM Multiple Metals-Melville Peninsula project, central Melville Peninsula, Nunavut; Geological Survey of Canada, Current Research 2013–19, 21 p. https://doi.org/10.4095/292862

Davidson, A., Jackson, G.D., and Morgan, W.C., 1979. Geology, Icebound Lake, District of Franklin; Geological Survey of Canada, Map 1451A, scale 1:250 000. https://doi.org/10.4095/109161

Davison, W.L., 1959a. Lake Harbour, Baffin Island, District of Franklin, Northwest Territories; Geological Survey of Canada, Preliminary Map 29–1958, scale 1: 63 360. https://doi.org/10.4095/108520

Davison, W.L., 1959b. Foxe Peninsula, eastern part, Baffin Island, District of Franklin, Northwest Territories; Geological Survey of Canada, Preliminary Map 4–1959, scale 1:253 440. https://doi.org/10.4095/108511

de Kemp, E.A., Sherwin, T., Ryder, I., Davies, A., and Snyder, D., 2002a. Detailed stratigraphic, structural, and three-dimensional mapping of the basal surface of the Paleoproterozoic Bravo Lake Formation, Nadluardjuk Lake area, Central Baffin Island, Nunavut, Canada; Geological Survey of Canada, Current Research 2002-C18, 10 p. https://doi.org/10.4095/213195

de Kemp, E.A., Sherwin, T., Ryder, I., Davies, A., and Snyder, D., 2002b. Paleoproterozoic geology, Nadluardjuk Lake area, central Baffin Island, Nunavut; Geological Survey of Canada, Open File 4168, scale 1:15 000. https://doi.org/10.4095/213475

Dunphy, J.M. and Ludden, J.N., 1998. Petrological and geochemical characteristics of a Paleoproterozoic magmatic arc (Narsajuaq Terrane, Ungava Orogen, Canada) and comparisons to Superior Province granitoids; Precambrian Research, v. 91, p. 109–142. https://doi.org/10.1016/S0301-9268(98)00041-2

Escher, A. and Pulvertaft, T.C.R., 1976. Rinkian mobile belt of West Greenland; *in* Geology of Greenland, (ed.) A. Escher and W.S. Watt; Grønlands geologiske Undersøgelse, Copenhagen, p. 104–119.

Forester, W. and Gray, N., 1966. Geological studies on Baffin Island; *in* Field report, north-central Baffin Island, (ed.) O.H. Løken; Department of Energy, Mines and Resources, Geographical Branch, p. 93–96.

From, R.E., Camacho, A.L., and St-Onge, M.R., 2013. Preliminary observations on the nature and origin of the eastern orthogneiss complex of southern Hall Peninsula, Baffin Island, Nunavut; *in* Summary of activities 2012, Canada-Nunavut Geoscience Office, p. 43–54.

From, R.E., St-Onge, M.R., and Camacho, A.L., 2014. Preliminary characterization of the Archean orthogneiss complex of Hall Peninsula, Baffin Island, Nunavut; *in* Summary of activities 2013, Canada-Nunavut Geoscience Office, p. 53–62.

From, R.E., Rayner, N.M., and Camacho, A., 2015. Archean magmatism and metamorphism of eastern Hall Peninsula, southern Baffin Island, Nunavut; *in* Summary of activities 2015, Canada-Nunavut Geoscience Office, p. 73–88.

Gagné, S., Jamieson, R.A., MacKay, R., Wodicka, N., and Corrigan, D., 2009. Texture, composition, and age variations in monazite from the lower amphibolite to the granulite facies, Longstaff Bluff Formation, Baffin Island, Canada: Canadian Mineralogist, v. 47, p. 847–869. https://doi.org/10.3749/canmin.47.4.847

Garde, A.A. and Steenfelt, A., 1999. Precambrian geology of Nuussuaq and the area north-east of Disko Bugt, West Greenland; *in* Precambrian geology of the Disko Bugt region, West Greenland, (ed.) F. Kalsbeek; Geology of Greenland Survey, Bulletin 181, p. 6–40.

Gladstone, J. and Francis, D., 2003. The origin of basaltic intrusions within the Longstaff Bluff formation, central Baffin Island, Nunavut; Joint Central Baffin/Committee Bay Workshop; Geological Association of Canada (Geological Survey of Canada), Program with Abstracts, v. 1, p. 22.

Hall, C.F., 1865. Arctic researches, and life among the Esquimaux: being the narrative of an expedition in search of Sir John Franklin, in the years 1860, 1861, and 1862; Harper & Brothers, New York, New York, 595 p.

Hamilton, B.M., 2014. A detailed description of the Hoare Bay group and Paleoproterozoic plutonic rocks near Mischief Glacier and Clephane Bay, Cumberland Peninsula, Baffin Island, Nunavut; Geological Survey of Canada, Current Research 2014–3, 23 p. https://doi.org/10.4095/293891

Harrison, J.C., St-Onge, M.R., Paul, D., and Brodaric, B., in press. Geology of Canada (north of 60); Geological Survey of Canada, Canadian Geoscience Map 293, scale 1:3 000 000.

Heaman, L.M., LeCheminant, A.N., and Rainbird, R.H., 1992. Nature and timing of Franklin igneous events, Canada: implications for a Late Proterozoic mantle plume and the break-up of Laurentia; Earth and Planetary Science Letters, v. 109, p. 117–131. https://doi.org/10.1016/0012-821X(92)90078-A

Henderson, J.R., 1985. Geology, McBeth Fiord–Cape Henry Kater, District of Franklin; Geological Survey of Canada, Map 1605A, scale 1:250 000. https://doi.org/10.4095/120467

Henderson, J.R. and Parrish, R.R., 1992. Geochronology and structural geology of the Early Proterozoic Foxe–Rinkian Orogen, Baffin Island, NWT; Geological Survey of Canada, Current Activities Forum 1992, Program with Abstracts, p. 12.

Henderson, G. and Pulvertaft, T.C.R., 1987. The lithostratigraphy and structure of a Lower Proterozoic dome and nappe complex, Geological map of Greenland, scale 1:100 000, Mârmorilik 71–V.2 Syd, Nûgâtsiaq 71 V.2 Nord, and Pangnertôq 72 V.2 Syd; Grønlands Geologiske Undersøgelse, descriptive text, 72 p.

Henderson, J.R. and Tippett, C.R., 1980. Foxe Fold Belt in eastern Baffin Island, District of Franklin; *in* Current research, Part A; Geological Survey of Canada, Paper 80–1A, p. 147–152. https://doi.org/10.4095/106195

Henderson, J.R., Henderson, M.N., Grott, J., Heijke, P., Falardeau, F., Perreault, S., and Derome, I., 1994. Geology, Dewar Lakes area, central Baffin Island, District of Franklin, Northwest Territories (parts of 27 B and 37 A); Geological Survey of Canada, Open File 2924, scale 1:100 000. https://doi.org/10.4095/194767

Henderson, J.R., Shaw, D., Mazurski, M., Henderson, M., Green, R., and Brisbin, D., 1979. Geology of part of Foxe Fold Belt, central Baffin Island, District of Franklin; *in* Current research, Part A; Geological Survey of Canada, Paper 79–1A, p. 95–99. https://doi.org/10.4095/104833

Hoffman, P.F., 1988. United Plates of America, the birth of a craton: Early Proterozoic assembly and growth of Laurentia; Annual Review of Earth and Planetary Sciences, v. 16, p. 543–603. https://doi.org/10.1146/annurev.ea.16.050188.002551

Hogarth, D.D., Boreham, P.W., and Mitchell, J.G., 1994. Martin Frobisher's northwest venture, 1576–1581: mines, minerals & metallurgy; Canadian Museum of Civilization, Mercury Series, Directorate paper no. 7, 181 p.

Hollis, J.A., Frei, D., Van Gool, J.A.M., Garde, A.A., and Persson, M., 2006a. Using zircon geochronology to resolve the Archaean geology of southern West Greenland; Geological Survey of Denmark and Greenland, Bulletin no. 10, p. 49–52.

Hollis, J.A., Keiding, M., Stensgaard, B.M., Van Gool, J.A.M., and Garde, A.A., 2006b. Evolution of Neoarchaean supracrustal belts at the northern margin of the North Atlantic Craton, West Greenland; *in* Precambrian crustal evolution and Cretaceous–Palaeogene faulting in West Greenland, (ed.) A.A. Garde and F. Kalsbeek; Geological Survey of Denmark and Greenland, Bulletin no. 11, p. 9–31.

Jackson, G.D., 1971. Operation Penny Highlands, south-central Baffin Island; *in* Report of activities, Part A; Geological Survey of Canada, Paper 71–1A, p. 138–140. https://doi.org/10.4095/105595

Jackson, G.D., 1984. Geology, Clyde River, District of Franklin; Geological Survey of Canada, Map 1582A, scale 1:250 000. https://doi.org/10.4095/119788

Jackson, G.D., 1998. Geology, Okoa Bay–Padloping Island area, District of Franklin, Northwest Territories; Geological Survey of Canada, Open File 3532, scale 1:250 000. https://doi.org/10.4095/209911

Jackson, G.D., 2000. Geology of the Clyde–Cockburn Land map area, north-central Baffin Island, Nunavut; Geological Survey of Canada, Memoir 440, 316 p. https://doi.org/10.4095/211268

Jackson, G.D., 2006. Field data, NTS 37G/5 and G/6, northern Baffin Island, Nunavut, Canada; Geological Survey of Canada, Open File 5317, scale 1:50 000. https://doi.org/10.4095/222169

Jackson, G.D. and Berman, R.G., 2000. Precambrian metamorphic and tectonic evolution of northern Baffin Island, Nunavut, Canada; Canadian Mineralogist, v. 38, p. 399–421. https://doi.org/10.2113/gscanmin.38.2.399

Jackson, G.D. and Davidson, A., 1975a. Geology, Pond Inlet and Nova Zembla Island, District of Franklin; Geological Survey of Canada, Map 1396A, scale 1:250 000. https://doi.org/10.4095/109005

Jackson, G.D. and Davidson, A., 1975b. Geology, Bylot Island, District of Franklin; Geological Survey of Canada, Map 1397A, scale 1:250 000. https://doi.org/10.4095/109007

Jackson, G.D. and Morgan, W.C., 1978. Geology, Conn Lake, District of Franklin; Geological Survey of Canada, Map 1458A, scale 1:250 000. https://doi.org/10.4095/109162

Jackson, G.D. and Sangster, D.F., 1987. Geology and resource potential of a proposed national park, Bylot Island and northwestern Baffin Island, Northwest Territories; Geological Survey of Canada, Paper 87–17, 31 p. https://doi.org/10.4095/122369

Jackson, G.D. and Taylor, F.C., 1972. Correlation of major Aphebian rock units in the northeastern Canadian Shield; Canadian Journal of Earth Sciences, v. 9, p. 1650–1669. https://doi.org/10.1139/e72-146

Jackson, G.D., Davidson, A., and Morgan, W.C., 1975. Geology of the Pond Inlet map-area, Baffin Island, District of Franklin (38A, 38B, part of 48A); Geological Survey of Canada, Paper 74–25, 33 p. https://doi.org/10.4095/102498

Jackson, G.D., Morgan, W.C., and Davidson, A., 1979. Geology, Buchan Gulf–Scott Inlet, District of Franklin; Geological Survey of Canada, Map 1449A, scale 1:250 000. https://doi.org/10.4095/109159

Jackson, G.D., Hunt, P.A., Loveridge, W.D., and Parrish, R.R., 1990. Reconnaissance geochronology of Baffin Island, N.W.T; *in* Radiogenic age and isotopic studies: report 3; Geological Survey of Canada, Paper 89–2, p. 123–148. https://doi.org/10.4095/129079

Johns, S.M. and Young, M.D., 2006. Bedrock geology and economic potential of the Archean Mary River group, northern Baffin Island, Nunavut; Geological Survey of Canada, Current Research 2006-C5, 13 p. https://doi.org/10.4095/222954

Johns, S.M., Helmstaedt, H.H., and Kyser, T.K., 2006. Paleoproterozoic submarine intrabasinal rifting, Baffin Island, Nunavut, Canada: volcanic structure and geochemistry of the Bravo Lake Formation; Canadian Journal of Earth Sciences, v. 43, p. 593–616. https://doi.org/10.1139/e06-009

Kastek, N., Ernst, R.E., Cousens, B.L., Kamo, S.L., Bleeker, W., Söderlund, U., Baragar, W.R.A., and Sylvester, P., 2018. U-Pb geochronology and geochemistry of the Povungnituk Group of the Cape Smith Belt: part of a craton-scale circa 2.0 Ga Minto–Povungnituk Large Igneous Province, northern Superior Craton; Lithos, v. 320–321, p. 315–331. https://doi.org/10.1016/j.lithos.2018.09.026

Keim, R.D., 2012. Stratigraphy, petrology and geochemistry of the North Touak–Cape Dyer volcanic belt, and implications for the tectonic setting of the Paleoproterozoic Hoare Bay Group, eastern Baffin Island; M.Sc. thesis, University of Saskatchewan, Saskatoon, Saskatchewan, 124 p.

Keim, R.D., Sanborn-Barrie, M., Ansdell, K., and Young, M.D., 2011. Totnes Road metavolcanic rocks: a fragmental Ti-enriched komatiitic volcanic suite on Cumberland Peninsula, Baffin Island, Nunavut; Geological Survey of Canada, Current Research 2011–13, 18 p. https://doi.org/10.4095/289072

LaFlamme, C., McFarlane, C.R.M., and Corrigan, D., 2014. U–Pb, Lu-Hf and REE in zircon from 3.2 to 2.6 Ga Archean gneisses of the Repulse Bay block, Melville Peninsula, Nunavut; Precambrian Research, v. 252, p. 223–239. https://doi.org/10.1016/j.precamres.2014.07.012

Lewry, J.F. and Colleron, K.D., 1990. The Trans-Hudson Orogen; extent, subdivision, and problems; *in* The Early Proterozoic Trans-Hudson Orogen of North America, (ed.) J.F. Lewry and M.R. Stauffer; Geological Association of Canada, Special Paper 37, p. 1–14.

Liikane, D.A., 2017. Geochemical, isotopic, and mineralogical characterization of the Frobisher suite mafic–ultramafic sills, southern Baffin Island, Nunavut, with implications for mineral potential; M.Sc. thesis, Carleton University, Ottawa, Ontario, 437 p.

Liikane, D.A., St-Onge, M.R., Kjarsgaard, B.A., Rayner, N.M., Ernst, R.E., and Kastek, N., 2015. Frobisher suite mafic, ultramafic and layered mafic–ultramafic sills, southern Baffin Island, Nunavut; *in* Summary of activities 2015, Canada-Nunavut Geoscience Office, p. 21–32.

Lucas, S.B., 1989. Structural evolution of the Cape Smith thrust belt and the role of out-of-sequence faulting in the thickening of mountain belts; Tectonics, v. 8, p. 655–676. https://doi.org/10.1029/TC008i004p00655

Lucas, S.B. and Byrne, T., 1992. Footwall involvement during arc–continent collision, Ungava Orogen, northern Canada; Journal of the Geological Society, v. 149, p. 237–248. https://doi.org/10.1144/gsjgs.149.2.0237

Machado, N., Goulet, N., and Gariépy, C., 1989. U-Pb geochronology of reactivated Archean basement and of Hudsonian metamorphism in the northern Labrador Trough; Canadian Journal of Earth Sciences, v. 26, p. 1–15. https://doi.org/10.1139/e89-001

Machado, N., David, J., Scott, D.J., Lamothe, D., Philippe, S., and Gariépy, C., 1993. U-Pb geochronology of the western Cape Smith Belt, Canada: new insights on the age of initial rifting and arc magmatism; Precambrian Research, v. 63, p. 211–223. https://doi.org/10.1016/0301-9268(93)90034-Y

Mackay, C., 2011. Petrographic and geochemical study of the origin of "spotted" dykes and their relationship to the North Touak–Cape Dyer volcanic belt: Cumberland Peninsula, Baffin Island; B.Sc. thesis, University of Saskatchewan, Saskatoon, Saskatchewan, 29 p.

MacKay, C.B. and Ansdell, K.M., 2014. Geochemical study of mafic and ultramafic rocks from southern Hall Peninsula, Baffin Island, Nunavut; *in* Summary of activities 2013, Canada-Nunavut Geoscience Office, p. 85–92.

MacLeod, M.E., 2012. Metallogenic setting of high-grade iron ores, Mary River District, north Baffin Island, Nunavut; M.Sc. thesis, University of Western Ontario, London, Ontario, 285 p.

McDonough, M.R., McNicoll, V.J., Schetselaar, E.M., and Grover, T.W., 2000. Geochronological and kinematic constraints on crustal shortening and escape in a two-sided oblique-slip collisional and magmatic orogen, Paleoproterozoic Taltson magmatic zone, northeastern Alberta; Canadian Journal of Earth Sciences, v. 37, p. 1549–1573. https://doi.org/10.1139/e00-089

Miller, A.K., Youngquist, W., and Collinson, C., 1954. Ordovician cephalopod fauna of Baffin Island; Geological Society of America, Memoir 62, 234 p.

Modeland, S.J. and Francis, D., 2003. Paleoproterozoic alkaline magmatism of the Bravo Lake formation on central Baffin Island; Geological Association of Canada-Mineralogical Association of Canada-Society of Economic Geologists, Joint Annual Meeting, Vancouver, May 25–28, 2003, Abstracts, v. 28, p. 115.

Modeland, S.J. and Francis, D., 2004. Implications of high field-strength element anomalies in Paleoproterozoic mafic alkaline magmas of central Baffin Island; Eos, Transactions American Geophysical Union, 28–31 May 2004, Montreal, Joint Assembly Supplement, v. 85, no. 17, Abstract V14A-03.

Morgan, W.C., 1983. Geology, Lake Gillian, District of Franklin; Geological Survey of Canada, Map 1560A, scale 1:250 000. https://doi.org/10.4095/127057

Morgan, W.C., Bourne, J., Herd, R.K., Pickett, J.W., and Tippett, C.R., 1975. Geology of the Foxe Fold Belt, Baffin Island, District of Franklin; *in* Current research, Part A; Geological Survey of Canada, Paper 75–1A, p. 343–347. https://doi.org/10.4095/104561

Morgan, W.C., Okulitch, A.V., and Thompson, P.H., 1976. Stratigraphy, structure and metamorphism of the west half of the Foxe Fold Belt, Baffin Island; *in* Current research, Part B; Geological Survey of Canada, Paper 76–1B, p. 387–391. https://doi.org/10.4095/104230

Mortensen, J.K. and Percival, J.A., 1989. Reconnaissance U-Pb zircon and monazite geochronology of the Lac Clairambault area, Ashuanipi complex, Quebec; *in* Radiogenic age and isotopic studies: report 1; Geological Survey of Canada, Paper 87–2, p. 135–142. https://doi.org/10.4095/122758

Nutman, A.P., Dawes, P.R., Kalsbeek, F., and Hamilton, M.A., 2008. Palaeoproterozoic and Archaean gneiss complexes in northern Greenland: Palaeoproterozoic terrane assembly in the High Arctic; Precambrian Research, v. 161, p. 419–451. https://doi.org/10.1016/j.precamres.2007.09.006

Parrish, R.R., 1989. U-Pb geochronology of the Cape Smith Belt and Sugluk block, northern Quebec; Geoscience Canada, v. 16, p. 126–130.

Partin, C.A., Bekker, A., Corrigan, D., Modeland, S.J., Francis, D., and Davis, D.W., 2014a. Revised age and correlation of the Paleoproterozoic Penrhyn and Piling groups of Arctic Canada; Geological Association of Canada-Mineralogical Association of Canada Joint Annual Meeting, Fredericton, May 21–23, 2014, Abstracts, v. 37, p. 213–214.

Partin, C.A., Bekker, A., Sylvester, P.J., Wodicka, N., Stern, R.A., Chacko, T., and Heaman, L., 2014b. Filling in the juvenile magmatic gap: evidence for uninterrupted Paleoproterozoic plate tectonics; Earth and Planetary Science Letters, v. 388, p. 123–133. https://doi.org/10.1016/j.epsl.2013.11.041

Pehrsson, S., Jefferson, C., Corrigan, D., Sanborn-Barrie, M., Berman, R., and Peterson, T., 2011. Unravelling the mineral potential of the Churchill province; Prospectors and Developers Association of Canada, Annual Convention, Toronto, Ontario, March 4–7, 2011, CD-ROM (abstract).

Pehrsson, S.J., Berman, R.G., Eglington, B., and Rainbird, R., 2013. Two Neoarchean supercontinents revisited: the case for a Rae family of cratons; Precambrian Research, v. 232, p. 27–43. https://doi.org/10.1016/j.precamres.2013.02.005

Putnam, G.P., 1928. The Putnam Baffin Island Expedition; Geographical Review, v. 18, no. 1, p. 1–40. https://doi.org/10.2307/208761

Rainbird, R.H., Davis, W.J., Pehrsson, S.J., Wodicka, N., Rayner, N., and Skulski, T., 2010. Early Paleoproterozoic supracrustal assemblages of the Rae domain, Nunavut, Canada: intracratonic basin development during supercontinent break-up and assembly; Precambrian Research, v. 181, p. 167–186. https://doi.org/10.1016/j.precamres.2010.06.005

Rayner, N.M., 2014. New U-Pb geochronological results from Hall Peninsula, Baffin Island, Nunavut; *in* Summary of activities 2013, Canada-Nunavut Geoscience Office, p. 39–52.

Rayner, N.M., 2015. New (2013–2014) U-Pb geochronological results from northern Hall Peninsula, southern Baffin Island, Nunavut; *in* Summary of activities 2014, Canada-Nunavut Geoscience Office, p. 31–44.

Rayner, N.M., 2017. U-Pb zircon geochronology constraints on timing of plutonism and sedimentary provenance from the Clearwater Fiord–Sylvia Grinnell Lake area, southern Baffin Island, Nunavut; Geological Survey of Canada, Open File 8204, 32 p. https://doi.org/10.4095/299720

Rayner, N.M., Sanborn-Barrie, M., Young, M.D., and Whalen, J.B., 2012. U-Pb ages of Archean basement and Paleoproterozoic plutonic rocks, southern Cumberland Peninsula, eastern Baffin Island, Nunavut; Geological Survey of Canada, Current Research 2012–8, 28 p. https://doi.org/10.4095/291401

Riley, G.C., 1959. Cumberland Sound, Baffin Island, District of Franklin, Northwest Territories; Geological Survey of Canada, Map 1061A, scale 1:506 880. https://doi.org/10.4095/107415

Sanborn-Barrie, M. and Young, M., 2011. Bulk compositional data for sulfidic and gossanous rocks from Cumberland Peninsula, Baffin Island, Nunavut; Geological Survey of Canada, Open File 6916, 11 p. https://doi.org/10.4095/288710

Sanborn-Barrie, M. and Young, M., 2013. Geology, Qikiqtarjuaq, Nunavut; Geological Survey of Canada, Canadian Geoscience Map 39 (preliminary edition), scale 1:100 000. https://doi.org/10.4095/292016

Sanborn-Barrie, M., St-Onge, M.R., Young, M.D., and James, D.T., 2008. Bedrock geology of southwestern Baffin Island, Nunavut: expanding the tectonostratigraphic framework with relevance to mineral resources; Geological Survey of Canada, Paper 2008–6, 16 p. https://doi.org/10.4095/225179

Sanborn-Barrie, M., Young, M., Whalen, J., James, D., and St-Onge, M.R., 2011. Geology Touak Fiord, Nunavut; Geological Survey of Canada, Canadian Geoscience Map 3 (second preliminary edition), scale 1:100 000. https://doi.org/10.4095/288931

Sanborn-Barrie, M., Young, M., Keim, R., and Hamilton, B., 2013. Geology, Sunneshine Fiord, Baffin Island, Nunavut; Geological Survey of Canada, Canadian Geoscience Map 6, (preliminary edition), scale 1:100 000. https://doi.org/10.4095/288931

Sanborn-Barrie, M., Thrane, K., Wodicka, N., and Rayner, N., 2017. The Laurentia–West Greenland connection at 1.9 Ga: new insights from the Rinkian fold belt; Gondwana Research, v. 51, p. 289–309. https://doi.org/10.1016/j.gr.2017.07.002

Saumur, B.M., Skipton, D.R., St-Onge, M.R., Bros, E.R., Acosta-Gongora, P., Kelly, C.J., Morin, A., O'Brien, M.E., Johnston, S.T., and Weller, O.M., 2018. Precambrian geology of the surroundings of Steensby Inlet and western Barnes Ice Cap (parts of NTS 37E, 37F, 37G), Baffin Island, Nunavut; *in* Summary of activities 2018; Canada-Nunavut Geoscience Office, p. 29–46.

Scott, D.J., 1997. Geology, U-Pb, and Pb-Pb geochronology of the Lake Harbour area, southern Baffin Island: implications for the Paleoproterozoic tectonic evolution of northeastern Laurentia; Canadian Journal of Earth Sciences, v. 34, p. 140–155. https://doi.org/10.1139/e17-012

Scott, D.J., 1998. U-Pb ages of Archean crust in the southeast arm of the Rae Province, southeastern Ungava Bay, Quebec; *in* Radiogenic age and isotopic studies: report 11; Geological Survey of Canada, Current Research 1998-F, p. 41–45. https://doi.org/10.4095/210054

Scott, D.J., 1999. U-Pb geochronology of the eastern Hall Peninsula, southern Baffin Island, Canada: a northern link between the Archean of West Greenland and the Paleoproterozoic Torngat Orogen of northern Labrador; Precambrian Research, v. 93, p. 5–26. https://doi.org/10.1016/S0301-9268(98)00095-3

Scott, D.J. and de Kemp, E.A., 1999. An overview of the bedrock geology of northern Baffin Island and the northern Melville Peninsula, Northwest Territories (Nunavut); *in* North Baffin Partnership Project: summary of investigations, (ed.) D.G. Richardson; Geological Survey of Canada, Open File 3637, p. 5–21. https://doi.org/10.4095/210287

Scott, D.J. and St-Onge, M.R., 1995. Constraints on Pb closure temperature in titanite based on rocks from the Ungava orogen, Canada: implications for U-Pb geochronology and P-T-t path determinations; Geology, v. 23, p. 1123–1126. https://doi.org/10.1130/0091-7613(1995)023%3c1123:COPCTI%3e2.3.CO%3b2

Scott, D.J. and Wodicka, N.A., 1998. A second report on the U-Pb geochronology of southern Baffin Island, Northwest Territories; *in* Radiogenic age and isotopic studies: report 11; Geological Survey of Canada, Current Research 1998-F, p. 47–57. https://doi.org/10.4095/210055

Scott, D.J., Helmstaedt, H., and Bickle, M.J., 1992. Purtuniq ophiolite, Cape Smith belt, northern Quebec, Canada: a reconstructed section of Early Proterozoic oceanic crust; Geology, v. 20, p. 173–176. https://doi.org/10.1130/0091-7613(1992)020%3c0173:POCSBN%3e2.3.CO%3b2

Scott, D.J., St-Onge, M.R., Wodicka, N., and Hanmer, S., 1997. Geology of the Markham Bay–Crooks Inlet area, southern Baffin Island, Northwest Territories; *in* Current research 1997-C; Geological Survey of Canada, p. 157–166. https://doi.org/10.4095/208641

Scott, D.J., St-Onge, M.R., Lucas, S.B., and Helmstaedt, H., 1999. The 2.00 Ga Purtuniq ophiolite, Cape Smith Belt, Canada: MORB-like crust intruded by OIB-like magmatism; Ofioliti, v. 24, p. 199–215.

Scott, D.J., Stern, R.A., St-Onge, M.R., and McMullen, S.M., 2002a. U-Pb geochronology of detrital zircons in metasedimentary rocks from southern Baffin Island: implications for the Paleoproterozoic tectonic evolution of northeastern Laurentia; Canadian Journal of Earth Sciences, v. 39, no. 5, p. 611–623. https://doi.org/10.1139/e01-093

Scott, D.J., St-Onge, M.R., and Corrigan, D., 2002b. Geology of the Paleoproterozoic Piling Group and underlying Archean gneiss, central Baffin Island, Nunavut; Geological Survey of Canada, Current Research 2002-C17, 10 p. https://doi.org/10.4095/213194

Scott, D.J., St-Onge, M.R., and Corrigan, D., 2003. Geology of the Archean Rae Craton and Mary River Group and the Paleoproterozoic Piling Group, central Baffin Island, Nunavut; Geological Survey of Canada, Current Research 2003-C26, 12 p. https://doi.org/10.4095/214208

Skipton, D.R., Saumur, B.M., St-Onge, M.R., Wodicka, N., Bros, E.R., Morin, A., Brouillette, P., Weller, O.M., and Johnston, S.T., 2017. Precambrian bedrock geology of the Pond Inlet–Mary River area, northern Baffin Island, Nunavut; *in* Summary of activities 2017, Canada-Nunavut Geoscience Office, p. 49–67.

Skipton, D.R., Wodicka, N., McNicoll, V., Saumur, B.M., St-Onge, M.R., and Young, M.D., 2019. U-Pb zircon geochronology of Archean greenstone belts (Mary River Group) and surrounding Archean to Paleoproterozoic rocks, northern Baffin Island, Nunavut; Geological Survey of Canada, Open File 8585, 43 p. https://doi.org/10.4095/314938

Smye, A.J., St-Onge, M.R., and Waters, D.J., 2009. Contrasting metamorphic pressure-temperature histories within the Trans-Hudson Orogen's hinterland, southwest Baffin Island, Nunavut; Geological Survey of Canada, Current Research 2009–6, 21 p. https://doi.org/10.4095/247603

Snyder, D.B., Berman, R.G., Kendall, J.-M., and Sanborn-Barrie, M., 2013. Seismic anisotropy and mantle structure of the Rae craton, central Canada, from joint interpretation of SKS splitting and receiver functions; Precambrian Research, v. 232, p. 189–208. https://doi.org/10.1016/j.precamres.2012.03.003

St-Onge, M.R. and Lucas, S.B., 1991. Evolution of regional metamorphism in the Cape Smith Trust Belt (northern Quebec, Canada): interaction of tectonic and thermal processes; Journal of Metamorphic Geology, v. 9, p. 515–534. https://doi.org/10.1111/j.1525-1314.1991.tb00545.x

St-Onge, M.R., Lucas, S.B., and Parrish, R.R., 1992. Terrane accretion in the internal zone of the Ungava Orogen, northern Quebec, Part 1: tectonostratigraphic assemblages and their tectonic implications; Canadian Journal of Earth Sciences, v. 29, p. 746–764. https://doi.org/10.1139/e92-064

St-Onge, M.R., Hanmer, S., and Scott, D.J., 1996. Geology of the Meta Incognita Peninsula, south Baffin Island, Northwest Territories: tectonostratigraphic units and regional correlations; *in* Current research 1996-C; Geological Survey of Canada, p. 63–72. https://doi.org/10.4095/207444

St-Onge, M.R., Scott, D.J., Wodicka, N., and Lucas, S.B., 1998. Geology of the McKellar Bay–Wight Inlet–Frobisher Bay area, southern Baffin Island, Northwest Territories; *in* Current research 1998-C; Geological Survey of Canada, p. 43–53. https://doi.org/10.4095/209512

St-Onge, M.R., Lucas, S.B., Scott, D.J., and Wodicka, N., 1999. Upper and lower plate juxtaposition, deformation and metamorphism during crustal convergence, Trans-Hudson Orogen (Quebec–Baffin segment), Canada; Precambrian Research, v. 93, p. 27–49. https://doi.org/10.1016/S0301-9268(98)00096-5

St-Onge, M.R., Scott, D.J., and Lucas, S.B., 2000a. Early partitioning of Quebec: microcontinent formation in the Paleoproterozoic; Geology, v. 28, p. 323–326. https://doi.org/10.1130/0091-7613(2000)28%3c323:EPOQMF%3e2.0.CO%3b2

St-Onge, M.R., Wodicka, N., and Lucas, S.B., 2000b. Granulite- and amphibolite-facies metamorphism in a convergent-plate-margin setting: synthesis of the Quebec–Baffin segment of the Trans-Hudson Orogen; Canadian Mineralogist, v. 38, p. 379–398. https://doi.org/10.2113/gscanmin.38.2.379

St-Onge, M.R., Scott, D.J., and Wodicka, N., 2001. Terrane boundaries within Trans-Hudson Orogen (Quebec–Baffin segment), Canada: changing structural and metamorphic character from foreland to hinterland; Precambrian Research, v. 107, p. 75–91. https://doi.org/10.1016/S0301-9268(00)00155-8

St-Onge, M.R., Scott, D.J., and Wodicka, N., 2002. Review of crustal architecture and evolution in the Ungava Peninsula–Baffin Island area: connection to the LITHOPROBE ECSOOT transect; Canadian Journal of Earth Sciences, v. 39, p. 589–610. https://doi.org/10.1139/e02-022

St-Onge, M.R., Scott, D.J., Corrigan, D., and Wodicka, N., 2005. Geology, central Baffin Island, Nunavut; Geological Survey of Canada, Maps 2077A to 2082A, scale 1:100 000. https://doi.org/10.4095/221054 and https://doi.org/10.4095/221091 to https://doi.org/10.4095/221095

St-Onge, M.R., Searle, M.P., and Wodicka, N., 2006. Trans-Hudson Orogen of North America and Himalaya–Karakoram–Tibetan Orogen of Asia: structural and thermal characteristics of the lower and upper plates; Tectonics, v. 25, TC4006, 22 p. https://doi.org/10.1029/2005TC001907

St-Onge, M.R., Wodicka, N., and Ijewliw, O., 2007. Polymetamorphic evolution of the Trans-Hudson Orogen, Baffin Island, Canada: integration of petrological, structural and geochronological data; Journal of Petrology, v. 48, p. 271–302. https://doi.org/10.1093/petrology/egl060

St-Onge, M.R., Van Gool, J.A.M., Garde, A.A., and Scott, D.J., 2009. Correlation of Archaean and Palaeoproterozoic units between northeastern Canada and western Greenland: constraining the pre-collisional upper plate accretionary history of the Trans-Hudson orogen; *in* Earth accretionary systems in space and time, (ed.) P.A. Cawood and A. Kroner; Geological Society of London, Special Publications, v. 318, p. 193–235. https://doi.org/10.1144/SP318.7

St-Onge, M.R., Harrison, J.C., Paul, D., Tella, S., Brent, T.A., Jauer, C.D., and Maclean, B.C., 2015a: Tectonic map of Arctic Canada; Geological Survey of Canada, Canadian Geoscience Map 187 (preliminary edition), scale 1:4 000 000. https://doi.org/10.4095/295945

St-Onge, M.R., Rayner, N.M., Liikane, D., and Chadwick, T., 2015b. Mafic, ultramafic and layered mafic–ultramafic sills, Meta Incognita Peninsula, southern Baffin Island, Nunavut; *in* Summary of activities 2014, Canada-Nunavut Geoscience Office, p. 11–16.

St-Onge, M.R., Rayner, N.M., Steenkamp, H.M., and Skipton, D.R., 2015c. Bedrock mapping of eastern Meta Incognita Peninsula, southern Baffin Island, Nunavut; *in* Summary of activities 2014, Canada-Nunavut Geoscience Office, p. 105–118.

St-Onge, M.R., Weller, O.M., and Rayner, N.M., 2016. 2016 report of activities for completing the regional bedrock mapping of the southern half of Baffin Island: GEM 2 Baffin Project; Geological Survey of Canada, Open File 8118, 11 p. https://doi.org/10.4095/299195

Stacey, J.R. and Pattison, D.R.M., 2003. Stratigraphy, structure, and petrology of a representative klippe of the Bravo Lake Formation, Piling Group, central Baffin Island, Nunavut; Geological Survey of Canada, Current Research 2003-C13, 11 p. https://doi.org/10.4095/214195

Steenkamp, H.M. and St-Onge, M.R., 2014. Overview of the 2013 regional bedrock mapping program on northern Hall Peninsula, Baffin Island, Nunavut; *in* Summary of activities 2013, Canada-Nunavut Geoscience Office, p. 27–38.

Steenkamp, H.M., Bros, E.R., and St-Onge, M.R., 2014. Altered ultramafic and layered mafic–ultramafic intrusions: new economic and carving stone potential on northern Hall Peninsula, Baffin Island, Nunavut; *in* Summary of activities 2013, Canada-Nunavut Geoscience Office, p. 11–20.

Steenkamp, H.M., Gilbert, C., St-Onge, M.R., 2016. Geology, Beekman Peninsula (south), Baffin Island, Nunavut, NTS 25P (south) and 15-M (part); Geological Survey of Canada, Canadian Geoscience Map 267 (preliminary edition); Canada- Nunavut Geoscience Office, Open File 2016-04, scale 1:100 000. https://doi.org/10.4095/297351

Storey, E., 2012. Characterization of silicate-facies meta-iron formation from Cumberland Peninsula, Baffin Island, Canada; B.Sc. thesis, University of Calgary, Calgary, Alberta, 109 p.

Taylor, F.C., 1982. Precambrian geology of the Canadian North borderlands; *in* Geology of the North Atlantic Borderlands, (ed.) J.W. Kerr, A.J. Fergusson, and L.C. Machan; Canadian Society of Petroleum Geologists, Memoir no. 7, p. 11–30.

Thériault, R.J., St-Onge, M.R., and Scott, D.J., 2001. Nd isotopic and geochemical signature of the Paleoproterozoic Trans-Hudson Orogen, southern Baffin Island, Canada: implications for the evolution of eastern Laurentia; Precambrian Research, v. 108, p. 113–138. https://doi.org/10.1016/S0301-9268(00)00159-5

Thrane, K. and Connelly, J.N., 2006. Zircon geochronology from the Kangaatsiaq–Qasigiannguit region, the northern part of the 1.9–1.8 Ga Nagssugtoqidian orogen, West Greenland; Geological Survey of Denmark and Greenland, Bulletin no. 11, p. 87–99.

Tippett, C.R., 1984. Supplementary data concerning “Geology of a transect through the southern margin of the Foxe Fold Belt, central Baffin Island, District of Franklin”; Geological Survey of Canada, Open File 1111, 84 p. https://doi.org/10.4095/129946

Tippett, C.R., 1985. Geology of a transect through the southern margin of the Foxe Fold Belt, central Baffin Island, District of Franklin; Geological Survey of Canada, Open File 1110, 77 p. https://doi.org/10.4095/129953

van Breemen, O., Henderson, J.B., Loveridge, W.D., and Thompson, P.H., 1987. U-Pb zircon and monazite geochronology and zircon morphology of granulites and a granite from the Thelon tectonic zone, Healey Lake and Artillery Lake map areas, N.W.T.; *in* Current research, Part A; Geological Survey of Canada, Paper 87–1A, p. 783–801. https://doi.org/10.4095/122484

van Breemen, O., Bostock, H.H., and Loveridge, W.D., 1992. Geochronology of granites along the margin of the northern Taltson magmatic zone and western Rae Province, Northwest Territories; *in* Radiogenic age and isotopic studies: report 5; Geological Survey of Canada, Current Research 91–2, p. 17–24. https://doi.org/10.4095/132907

Wardle, R.J., James, D.T., Scott, D.J., and Hall, J., 2002. The southeastern Churchill Province: synthesis of a Palaeoproterozoic transpressional orogeny; Canadian Journal of Earth Sciences, v. 39, p. 639–663. https://doi.org/10.1139/e02-004

Weeks, L.J., 1928a. Head of Cumberland Sound and route to Nettilling Lake, Baffin Island; Geological Survey of Canada, Map 219A, scale 1:506 880. https://doi.org/10.4095/107406

Weeks, L.J., 1928b. Cumberland Sound area, Baffin Island; Geological Survey of Canada, Summary Report 1927, pt. C, p. 83–95. https://doi.org/10.4095/297953

Weller, O.M. and St-Onge, M.R., 2017. Record of modern-style plate tectonics in the Palaeoproterozoic Trans-Hudson orogen; Nature Geoscience, v. 10, p. 305–311. https://doi.org/10.1038/ngeo2904

Weller, O.M., Dyck, B.J., St-Onge, M.R., Rayner, N.M., and Tschirhart, V., 2015. Completing the bedrock mapping of southern Baffin Island, Nunavut: plutonic suites and regional stratigraphy; *in* Summary of activities 2015, Canada-Nunavut Geoscience Office, p. 33–48.

Whalen, J.B., Wodicka, N., Taylor, B.E., and Jackson, G.D., 2010. Cumberland batholith, Trans-Hudson Orogen, Canada: petrogenesis and implications for Paleoproterozoic crustal and orogenic processes; Lithos, v. 117, p. 99–118. https://doi.org/10.1016/j.lithos.2010.02.008

Whalen, J.B., Sanborn-Barrie, M., and Young, M., 2012. Geochemical data from Archean and Paleoproterozoic plutonic and volcanic rocks of Cumberland Peninsula, eastern Baffin Island, Nunavut; Geological Survey of Canada, Open File 6933, 15 p. https://doi.org/10.4095/291453

Whitney, D.L., and Evans, B.W., 2010, Abbreviations for names of rock-forming minerals; The American Mineralogist, v. 95, p. 185–187. https://doi.org/10.2138/am.2010.3371

Wodicka, N. and Scott, D.J., 1997. A preliminary report on the U-Pb geochronology of the Meta Incognita Peninsula, southern Baffin Island, Northwest Territories; *in* Current research 1997-C; Geological Survey of Canada, p. 167–178. https://doi.org/10.4095/208642

Wodicka, N., Madore, L., Larbi, Y., and Vicker, P., 2002a. Géochronologie U-Pb de filons-couches mafiques de la Ceinture de Cape Smith et de la Fosse du Labrador; *in* 23e Séminaire d'information sur la recherche géologique, Ministère des Ressources naturelles du Québec, Programme et résumés, DV 2002–10, p. 48.

Wodicka, N., St-Onge, M.R., Scott, D.J., and Corrigan, D., 2002b. Preliminary report on the U-Pb geochronology of the northern margin of the Trans-Hudson Orogen, central Baffin Island; *in* Radiogenic age and isotopic studies: report 15 (ed.) R.A. Stern; Geological Survey of Canada, Current Research 2002-F7, 12 p. https://doi.org/10.4095/213623

Wodicka, N., St-Onge, M.R., and Whalen, J.B., 2008. Characteristics of two opposing continental margin successions in northeast Laurentia; Geochimica et Cosmochimica Acta, Goldschmidt Conference Abstracts 2008, v. 72, A1030.

Wodicka, N., Whalen, J.B., St-Onge, M.R., and Corrigan, D., 2010. Meta Incognita microcontinent revisited: insights from U-Pb geochronology and Nd isotopes; Geological Association of Canada-Mineralogical Association of Canada, GeoCanada 2010 Conference, Calgary, May 10–14, 2010, Abstracts, v. 35.

Wodicka, N., Corrigan, D., Nadeau, L., and Erdmann, S., 2011. New U-Pb geochronological results from Melville Peninsula: unravelling the Archean and Early Paleoproterozoic magmatic history of the north-central Rae craton; Geological Association of Canada-Mineralogical Association of Canada Annual Meeting, Ottawa, May 25–27, 2011, Abstracts, v. 34, p. 236.

Wodicka, N., St-Onge, M.R., Corrigan, D., Scott, D.J., and Whalen, J.B., 2014. Did a proto-ocean basin form along the southeastern Rae cratonic margin? Evidence from U-Pb geochronology, geochemistry (Sm-Nd and whole-rock), and stratigraphy of the Paleoproterozoic Piling Group, northern Canada; Geological Society of America Bulletin, v. 126, p. 1625–1653. https://doi.org/10.1130/B31028.1

Young, M.D., Sandeman, H., Berniolles, F., and Gertzbein, P.M., 2004. A preliminary stratigraphic and structural geology framework of the Archean Mary River Group, northern Baffin Island, Nunavut; Geological Survey of Canada, Current Research 2004-C1, 14 p. https://doi.org/10.4095/215376

Young, M., Sandeman, H., Creaser, R., and James, D., 2007. Meso- to Neoarchean crustal growth and recycling on northern Baffin Island and correlation of Rae Province rocks across mainland Nunavut and Greenland; Geological Association of Canada-Mineralogical Association of Canada, Yellowknife, May 23–25, 2007, Program with Abstracts, v. 32, p. 89.

APPENDIX A – MAP REFERENCES IN FIGURES 1 AND 2

1. Blackadar, R.G., 1967. Geology, Cumberland Sound, District of Franklin; Geological Survey of Canada, Preliminary Map 17-1966, scale 1:506 880. https://doi.org/10.4095/108490
2. Blackadar, R.G., 1970. Nottingham, Salisbury, and Mill Islands, District of Franklin; Geological Survey of Canada, Map 1205A, scale 1:250 000. https://doi.org/10.4095/109212
3. Jackson, G.D., 1971. Operation Penny Highlands, south-central Baffin Island; in Report of activities, Part A; Geological Survey of Canada, Paper 71-1 A, p. 138–140. https://doi.org/10.4095/105595
4. Trettin, H.P., 1975. Geology, Lower Paleozoic geology, central and eastern parts of Foxe Basin and Baird Peninsula, Baffin Island; Geological Survey of Canada, Map 1406A, scale 1:500 000. https://doi.org/10.4095/109081
5. Morgan,W.C., 1982. Geology, Koch Island, District of Franklin; Geological Survey of Canada, Map 1535A, scale 1:250 000. https://doi.org/10.4095/127056
6. Henderson, J.R., 1985a. Geology, McBeth Fiord–Cape Henry Kater, District of Franklin; Geological Survey of Canada, Map 1605A, scale 1:250 000. https://doi.org/10.4095/120467
7. Henderson, J.R., 1985b. Geology, Ekalugad Fiord–Home Bay, District of Franklin; Geological Survey of Canada, Map 1606A, scale 1:250 000. https://doi.org/10.4095/120468
8. Jackson, G.D., 1998. Geology, Okoa Bay Padloping Island area, District of Franklin, Northwest Territories; Geological Survey of Canada, Open File 3532, scale 1:250 000. https://doi.org/10.4095/209911
9. St-Onge, M.R., Scott, D.J., and Wodicka, N., 1999a. Geology, Frobisher Bay, Nunavut; Geological Survey of Canada, Map 1979A, scale 1:100 000. https://doi.org/10.4095/210833
10. St-Onge, M.R., Scott, D.J., and Wodicka, N., 1999b. Geology, Hidden Bay, Nunavut; Geological Survey of Canada, Map 1980A, scale 1:100 000. https://doi.org/10.4095/210835
11. St-Onge, M.R., Scott, D.J., and Wodicka, N., 1999c. Geology, McKellar Bay, Nunavut; Geological Survey of Canada, Map 1981A, scale 1:100 000. https://doi.org/10.4095/210836
12. St-Onge, M.R., Scott, D.J., and Wodicka, N., 1999d. Geology, Wright Inlet, Nunavut; Geological Survey of Canada, Map 1982A, scale 1:100 000. https://doi.org/10.4095/210840
13. St-Onge, M.R., Scott, D.J., and Wodicka, N., 1999e. Geology, Blandford Bay, Nunavut; Geological Survey of Canada, Map 1983A, scale 1:100 000. https://doi.org/10.4095/210837
14. St-Onge, M.R., Scott, D.J., and Wodicka, N., 1999f. Geology, Crooks Inlet, Nunavut; Geological Survey of Canada, Map 1984A, scale 1:100 000. https://doi.org/10.4095/210838
15. St-Onge, M.R., Scott, D.J., and Wodicka, N., 1999g. Geology, White Strait, Nunavut; Geological Survey of Canada, Map 1985A, scale 1:100 000. https://doi.org/10.4095/210839
16. Sanford, B.V. and Grant, A.C., 2000. Geological framework of the Ordovician system in the southeast Arctic platform, Nunavut; *in* Geology and paleontology of the southeast Arctic Platform and southern Baffin Island, Nunavut, (ed.) A.D. McCracken and T.E. Bolton; Geological Survey of Canada, Bulletin 557, p. 13–38. https://doi.org/10.4095/211845
17. Jackson, G.D., 2002. Geology, Isurtuq River–Nedlukseak Fiord, Nunavut; Geological Survey of Canada, Open File 4259, scale 1:250 000. https://doi.org/10.4095/213304
18. St-Onge, M.R., Scott, D.J., Corrigan, D., and Wodicka, N., 2005a. Geology, Ikpik Bay, Baffin Island, Nunavut; Geological Survey of Canada, Map 2077A, scale 1:100 000. https://doi.org/10.4095/221054
19. St-Onge, M.R., Scott, D.J., Corrigan, D., and Wodicka, N., 2005b. Geology, Flyway Lake, Baffin Island, Nunavut; Geological Survey of Canada, Map 2078A, scale 1:100 000. https://doi.org/10.4095/221091
20. St-Onge, M.R., Scott, D.J., Corrigan, D., and Wodicka, N., 2005c. Geology, Clyde River, Baffin Island, Nunavut; Geological Survey of Canada, Map 2079A, scale 1:100 000. https://doi.org/10.4095/221092
21. St-Onge, M.R., Scott, D.J., Corrigan, D., and Wodicka, N., 2005d. Geology, Piling Bay, Baffin Island, Nunavut; Geological Survey of Canada, Map 2080A, scale 1:100 000. https://doi.org/10.4095/221093
22. St-Onge, M.R., Scott, D.J., Corrigan, D., and Wodicka, N., 2005e. Geology, Straits Bay, Baffin Island, Nunavut; Geological Survey of Canada, Map 2081A, scale 1:100 000. https://doi.org/10.4095/221094
23. St-Onge, M.R., Scott, D.J., Corrigan, D., and Wodicka, N., 2005f. Geology, Dewar Lakes, Baffin Island, Nunavut; Geological Survey of Canada, Map 2082A, scale 1:100 000. https://doi.org/10.4095/221095
24. Jackson, G.D., 2006. Geology, Hantzsch River area, Baffin Island, Nunavut; Geological Survey of Canada, Open File 4202, scale 1:250 000. https://doi.org/10.4095/221809
25. St-Onge, M.R., Sanborn-Barrie, M., and Young, M., 2007a. Geology, Mingo Lake, Baffin Island, Nunavut; Geological Survey of Canada, Open File 5433, scale 1:250 000. https://doi.org/10.4095/224163
26. St-Onge, M.R., Sanborn-Barrie, M., and Young, M., 2007b. Geology, Foxe Peninsula, Baffin Island, Nunavut; Geological Survey of Canada, Open File 5434, scale 1:250 000. https://doi.org/10.4095/224222
27. Sanborn-Barrie, M., Young, M., Whalen, J., and James, D., 2011a. Geology, Ujuktuk Fiord, Nunavut; Geological Survey of Canada, Canadian Geoscience Map 1, (second preliminary edition), scale 1:100 000. https://doi.org/10.4095/289237
28. Sanborn-Barrie, M., Young, M., and Whalen, J., 2011b. Geology, Kingnait Fiord, Nunavut; Geological Survey of Canada, Canadian Geoscience Map 2, (second preliminary edition), scale 1:100 000. https://doi.org/10.4095/289238
29. Sanborn-Barrie, M., Young, M., Whalen, J., James, D., and St-Onge, M.R., 2011c. Geology, Touak Fiord, Nunavut; Geological Survey of Canada, Canadian Geoscience Map 3 (second preliminary edition), scale 1:100 000. https://doi.org/10.4095/289239
30. Sanborn-Barrie, M. and Young, M., 2013a. Geology, Circle Lake, Nunavut; Geological Survey of Canada, Canadian Geoscience Map 5 (preliminary edition), scale 1:100 000. https://doi.org/10.4095/288929
31. Sanborn-Barrie, M., Young, M., Keim, R., and Hamilton, B.M., 2013b. Geology, Sunneshine Fiord, Baffin Island, Nunavut; Geological Survey of Canada, Canadian Geoscience Map 6 (preliminary edition), scale 1:100 000. https://doi.org/10.4095/288931
32. Sanborn-Barrie, M. and Young, M., 2013c. Geology, Padle Fiord, Baffin Island, Nunavut; Geological Survey of Canada, Canadian Geoscience Map 37 (preliminary edition), scale 1:100 000. https://doi.org/10.4095/292014
33. Sanborn-Barrie, M. and Young, M., 2013d. Geology, Durban Harbour, Baffin Island, Nunavut; Geological Survey of Canada, Canadian Geoscience Map 38 (preliminary edition), scale 1:100 000. https://doi.org/10.4095/292015
34. Sanborn-Barrie, M. and Young, M., 2013e. Geology, Qikiqtarjuaq, Baffin Island, Nunavut; Geological Survey of Canada, Canadian Geoscience Map 39 (preliminary edition), scale 1:100 000. https://doi.org/10.4095/292016
35. Jackson, G.D. and Sanborn-Barrie, M., 2014. Geology, Pangnirtung Fiord, Baffin Island, Nunavut; Geological Survey of Canada, Canadian Geoscience Map 4 (preliminary edition), scale 1:100 000. https://doi.org/10.4095/288928
36. St-Onge, M.R., Rayner, N.M., Steenkamp, H.M., and Gilbert, C., 2015a. Geology, Terra Nivea, Baffin Island, Nunavut; Geological Survey of Canada, Canadian Geoscience Map 215E (preliminary); Canada-Nunavut Geoscience Office, Open File Map2015-02E, scale 1:100 000. https://doi.org/10.4095/296104
37. St-Onge, M.R., Rayner, N.M., Steenkamp, H.M., and Gilbert, C., 2015b. Geology, Pritzler Harbour, Baffin Island, Nunavut; Geological Survey of Canada, Canadian Geoscience Map 216E (preliminary edition); Canada-Nunavut Geoscience Office, Open File Map 2015-03E, scale 1:100 000. https://doi.org/10.4095/296109

38. St-Onge, M.R., Rayner, N.M., Steenkamp, H.M., and Gilbert, C., 2015c. Geology, Grinnell Glacier, Baffin Island, Nunavut; Geological Survey of Canada, Canadian Geoscience Map 217E (preliminary edition); Canada-Nunavut Geoscience Office, Open File Map 2015-04E, scale 1:100 000. https://doi.org/10.4095/296111

39. Steenkamp, H.M., Gilbert, C., and St-Onge, M.R., 2016a. Geology, Loks Land, Baffin Island, Nunavut, NTS 25I (part); Geological Survey of Canada, Canadian Geoscience Map 264 (preliminary edition); Canada-Nunavut Geoscience Office, Open File Map 2016-01, scale 1:100 000. https://doi.org/10.4095/297344

40. Steenkamp, H.M., Gilbert, C., and St-Onge, M.R., 2016b. Geology, Ward Inlet (south), Baffin Island, Nunavut, NTS 25O (south) and 25-J (part); Geological Survey of Canada, Canadian Geoscience Map 266 (preliminary edition); Canada-Nunavut Geoscience Office, Open File Map 2016-02, scale 1:100 000. https://doi.org/10.4095/297349

41. Steenkamp, H.M., Gilbert, C., and St-Onge, M.R., 2016c. Geology, Ward Inlet (north), Baffin Island, Nunavut, NTS 25O (north); Geological Survey of Canada, Canadian Geoscience Map 265 (preliminary edition); Canada-Nunavut Geoscience Office, Open File Map 2016-03, scale 1:100 000. https://doi.org/10.4095/297348

42. Steenkamp, H.M., Gilbert, C., St-Onge, M.R., 2016d. Geology, Beekman Peninsula (south), Baffin Island, Nunavut, NTS 25P (south) and 15M (part); Geological Survey of Canada, Canadian Geoscience Map 267 (preliminary edition); Canada-Nunavut Geoscience Office, Open File Map 2016-04, scale 1:100 000. https://doi.org/10.4095/297351

43. Steenkamp, H.M., Gilbert, C., and St-Onge, M.R., 2016e. Geology, Beekman Peninsula (north), Baffin Island, Nunavut, NTS 25P (north) and 15M (part); Geological Survey of Canada, Canadian Geoscience Map 268 (preliminary edition); Canada-Nunavut Geoscience Office, Open File Map 2016-05, scale 1:100 000. https://doi.org/10.4095/297352

44. Steenkamp, H.M., Gilbert, C., and St-Onge, M.R., 2016f. Geology, Leybourne Islands (south), Baffin Island, Nunavut, NTS 26A (south); Geological Survey of Canada, Canadian Geoscience Map 269 (preliminary edition); Canada-Nunavut Geoscience Office, Open File Map 2016-06, scale 1:100 000. https://doi.org/10.4095/297353

45. Steenkamp, H.M., Gilbert, C., and St-Onge, M.R., 2016g. Geology, Leybourne Islands (north), Baffin Island, Nunavut, NTS 26A (north); Geological Survey of Canada, Canadian Geoscience Map 271 (preliminary edition); Canada-Nunavut Geoscience Office, Open File Map 2016-07, scale 1:100 000. https://doi.org/10.4095/297355

46. Steenkamp, H.M., Gilbert, C., and St-Onge, M.R., 2016h. Geology, Chidliak Bay (south), Baffin Island, Nunavut, NTS 26B (south); Geological Survey of Canada, Canadian Geoscience Map 272 (preliminary edition); Canada-Nunavut Geoscience Office, Open File Map 2016-08, scale 1:100 000. https://doi.org/10.4095/297357

47. Steenkamp, H.M., Gilbert, C., and St-Onge, M.R., 2016i. Geology, Chidliak Bay (north), Baffin Island, NTS 26B (north); Geological Survey of Canada, Canadian Geoscience Map 270 (preliminary edition); Canada-Nunavut Geoscience Office, Open File Map 2016-09, scale 1:100 000. https://doi.org/10.4095/297354

48. St-Onge, M.R., Weller, O.M., Dyck, B.J., Rayner, N.M., Chadwick T., and Liikane, D., 2016a. Geology, Sylvia Grinnell Lake (north), Baffin Island, Nunavut; Geological Survey of Canada, Canadian Geoscience Map 253E (preliminary edition); Canada-Nunavut Geoscience Office, Open File Map 2016-10E, scale 1:100 000. https://doi.org/10.4095/297592

49. St-Onge, M.R., Weller, O.M., Dyck, B.J., Rayner, N.M., Chadwick T., and Liikane, D., 2016b. Geology, Sylvia Grinnell Lake (south), Baffin Island, Nunavut; Geological Survey of Canada, Canadian Geoscience Map 254E (preliminary edition); Canada-Nunavut Geoscience Office, Open File Map 2016-11E, scale 1:100 000. https://doi.org/10.4095/297593

50. St-Onge, M.R., Weller, O.M., Dyck, B.J., Rayner, N.M., Chadwick T., and Liikane, D., 2016c. Geology, Amittok Lake (north), Baffin Island, Nunavut; Geological Survey of Canada, Canadian Geoscience Map 255E (preliminary edition); Canada-Nunavut Geoscience Office, Open File Map 2016-12E, scale 1:100 000. https://doi.org/10.4095/297790

51. St-Onge, M.R., Weller, O.M., Dyck, B.J., Rayner, N.M., Chadwick T., and Liikane, D., 2016d. Geology, Amittok Lake (south), Baffin Island, Nunavut; Geological Survey of Canada, Canadian Geoscience Map 256E (preliminary edition); Canada-Nunavut Geoscience Office, Open File Map 2016-13E, scale 1:100 000. https://doi.org/10.4095/297791

52. St-Onge, M.R., Weller, O.M., Dyck, B.J., Rayner, N.M., Chadwick T., and Liikane, D., 2016e. Geology, Clearwater Fiord (north), Baffin Island, Nunavut; Geological Survey of Canada, Canadian Geoscience Map 257E (preliminary edition); Canada-Nunavut Geoscience Office, Open File Map 2016-14E, scale 1:100 000. https://doi.org/10.4095/297792

53. St-Onge, M.R., Weller, O.M., Dyck, B.J., Rayner, N.M., Chadwick T., and Liikane, D., 2016f. Geology, Clearwater Fiord (south), Baffin Island, Nunavut; Geological Survey of Canada, Canadian Geoscience Map 258E (preliminary edition); Canada-Nunavut Geoscience Office, Open File Map 2016-15E, scale 1:100 000. https://doi.org/10.4095/297793

54. St-Onge, M.R., Weller, O.M., Dyck, B.J., Rayner, N.M., Chadwick T., and Liikane, D., 2016g. Geology, McKeand River (north), Baffin Island, Nunavut; Geological Survey of Canada, Canadian Geoscience Map 259E (preliminary edition); Canada-Nunavut Geoscience Office, Open File Map 2016-16E, scale 1:100 000. https://doi.org/10.4095/297594

55. St-Onge, M.R., Weller, O.M., Dyck, B.J., Rayner, N.M., Chadwick T., and Liikane, D., 2016h. Geology, McKeand River (south), Baffin Island, Nunavut; Geological Survey of Canada, Canadian Geoscience Map 260E (preliminary edition); Canada-Nunavut Geoscience Office, Open File Map 2016-17E, scale 1:100 000. https://doi.org/10.4095/297595

56. St-Onge, M.R., Weller, O.M., Dyck, B.J., Rayner, N.M., Chadwick T., and Liikane, D., 2016i. Geology, Irvine Inlet (north), Baffin Island, Nunavut; Geological Survey of Canada, Canadian Geoscience Map 261E (preliminary edition); Canada-Nunavut Geoscience Office, Open File Map 2016-18E, scale 1:100 000. https://doi.org/10.4095/297794

57. St-Onge, M.R., Weller, O.M., Dyck, B.J., Rayner, N.M., Chadwick T., and Liikane, D., 2016j. Geology, Irvine Inlet (south), Baffin Island, Nunavut; Geological Survey of Canada, Canadian Geoscience Map 262E (preliminary edition); Canada-Nunavut Geoscience Office, Open File Map 2016-19E, scale 1:100 000. https://doi.org/10.4095/297795

58. Blackadar, R.G., Davison, W.L., and Trettin, H.P., 1968a. Geology, Arctic Bay–Cape Clarence, District of Franklin; Geological Survey of Canada, Map 1237A, scale 1:253 440. https://doi.org/10.4095/107330

59. Blackadar, R.G., Davison, W.L., and Trettin, H.P., 1968b. Geology, Moffet Inlet–Fitzgerald Bay, District of Franklin; Geological Survey of Canada, Map 1238A, scale 1:253 440. https://doi.org/10.4095/107497

60. Blackadar, R.G., Davison, W.L., and Trettin, H.P., 1968c. Geology, Phillips Creek, District of Franklin; Geological Survey of Canada, Map 1239A, scale 1:253 440. https://doi.org/10.4095/107510

61. Blackadar, R.G., Davison, W.L., and Trettin, H.P., 1968d. Geology, Agu Bay–Easter Cape, District of Franklin; Geological Survey of Canada, Map 1240A, scale 1:253 440. https://doi.org/10.4095/107336

62. Blackadar, R.G., Davison, W.L., and Trettin, H.P., 1968e. Geology, Berlinguet Inlet–Bourassa Bay, District of Franklin; Geological Survey of Canada, Map 1241A, scale 1:253 440. https://doi.org/10.4095/107412

63. Blackadar, R.G., Davison, W.L., and Trettin, H.P., 1968f. Geology, Erichsen Lake, District of Franklin; Geological Survey of Canada, Map 1242A, scale 1:253 440. https://doi.org/10.4095/108947

64. Jackson, G.D. and Davidson, A., 1975a. Geology, Pond Inlet and Nova Zembla Island, District of Franklin; Geological Survey of Canada, Map 1396A, scale 1:250 000. https://doi.org/10.4095/109005

65. Jackson, G.D. and Davidson, A., 1975b. Geology, Bylot Island, District of Franklin; Geological Survey of Canada, Map 1397A, scale 1:250 000. https://doi.org/10.4095/109007

66. Jackson, G.D., Morgan, W.C., and Davidson, A., 1979. Geology, Buchan Gulf–Scott Island, District of Franklin; Geological Survey of Canada, Map 1449A, scale 1:250 000. https://doi.org/10.4095/109159

67. Jackson, G.D., 1984. Geology, Clyde River, District of Franklin; Geological Survey of Canada, Map 1582A, scale 1:250 000. https://doi.org/10.4095/119788

68. Jackson, G.D, and Sangster, D.F., 1987. Geology and resource potential of a proposed national park, Bylot Island and northwest Baffin Island, Northwest Territories; Geological Survey of Canada, Paper 87-17, 31 p. https://doi.org/10.4095/122369

69. Chandler, F.W., 1988. Geology of the late Precambrian Fury and Hecla Group, northwest Baffin Island, District of Franklin; Geological Survey of Canada, Bulletin 370, p. https://doi.org/10.4095/126938

70. Jackson, G.D. and Morgan, W.C., 1979. Geology, Conn Lake, District of Franklin; Geological Survey of Canada, Map 1458A, scale 1:250 000. https://doi.org/10.4095/109162

71. Skipton, D.R., Saumur, B.M., St-Onge, M.R., Wodicka, N., Bros, E.R., Currie, L.D., Weller, O.M., and Haggart, J.W., 2018. Bedrock geology, Pond Inlet, Nunavut, part of NTS 38-B; Geological Survey of Canada, Canadian Geoscience Map 347, scale 1:100 000. https://doi.org/10.4095/306578

72. Saumur, B.M., Skipton, D.R., St-Onge, M.R., Wodicka, N., Bros, E.R., and Weller, O.M., 2018. Bedrock geology, Mumiksaa–Milne Inlet, Nunavut, parts of NTS 38-B and 48-A; Geological Survey of Canada, Canadian Geoscience Map 348, scale 1:100 000. https://doi.org/10.4095/306579

73. Saumur, B.M., Skipton, D.R., St-Onge, M.R., Jackson, G.D., Wodicka, N., Bros, E.R., and Weller, O.M., in press. Geology, Angijurjuk–Mary River (37G west), Nunavut; Geological Survey of Canada, Canadian Geoscience Map 403, scale 1:100 000.

74. Skipton, D.R., Saumur, B.M., St-Onge, M.R., Bros, E.R., and Weller, O.M.,in press. Geology, Ravn River (37G east), Nunavut; Geological Survey of Canada, Canadian Geoscience Map 405, scale 1:100 000.

75. Saumur, B.M., Skipton, D.R., Zhang, S., St-Onge, M.R., Bros, E.R., Acosta-Gongora, P., Kelly, C.J., O'Brien, M.E., Weller, O.M., and Johnston, S.T., in press. Geology, Nina Bang Lake (37F west), Nunavut; Geological Survey of Canada, Canadian Geoscience Map 404, scale 1:100 000.

76. Skipton, D.R., Saumur, B.M., St-Onge, M.R., Bros, E.R., Acosta-Gongora, P., Kelly, C.J., O'Brien, M.E., Johnston, S.T., and Weller, O.M., in press. Geology, Rowley River–Isortoq River (37F east), Nunavut; Geological Survey of Canada, Canadian Geoscience Map 406, scale 1:100 000.

77. Skipton, D.R., Saumur, B.M., St-Onge, M.R., Bros, E.R., Acosta-Gongora, P., Kelly, C.J., O'Brien, M.E., Weller, O.M., and Johnston, S.T., in press. Geology, Barnes Ice Cap Northwest (37E west), Nunavut; Geological Survey of Canada, Canadian Geoscience Map 402, scale 1:100 000.

Contents

Mesoproterozoic Borden Basin, northern Baffin Island

E.C. Turner[1*]

Turner, E.C., 2022. Mesoproterozoic Borden Basin, northern Baffin Island; in *Geological synthesis of Baffin Island (Nunavut) and the Labrador–Baffin Seaway, (ed.) L.T. Dafoe and N. Bingham-Koslowski; Geological Survey of Canada, Bulletin 608, p. 55-77. https://doi.org/10.4095/321825*

Abstract: The unmetamorphosed and nearly undeformed late Mesoproterozoic Borden Basin on northern Baffin Island exhibits sag, rift, and foreland-basin–like phases. A thin, partly subaqueous basal basalt is overlain by mature shallow-marine quartz arenite, upward-deepening siltstone and shale (marking the beginning of rifting), a complex suite of rift-delineated carbonate units containing two dramatic internal unconformities, and a flysch-molasse–like succession containing evidence of sediment derivation from the Grenville Orogen. Geochronological data indicate that deposition of most of the succession took place ca. 1100 to 1050 Ma. One of the carbonate intervals, Nanisivik Formation, is the main host of regional Zn-Pb showings including the past-producing Nanisivik orebody, which formed in the late Mesoproterozoic from low-temperature fluids, and which was emplaced under strong structural and stratigraphic controls. Minimal postdepositional deformation is limited to the emplacement of mafic dykes ca. 720 Ma and repeated reactivation of basement-rooted normal faults.

Résumé : Situé dans le nord de l'île de Baffin, le bassin de Borden est une entité non métamorphisée et presque non déformée du Mésoprotérozoïque tardif qui présente des phases de bassin d'affaissement, de rift et d'une structure s'apparentant à un bassin d'avant-pays. Une mince couche basale de basalte, en partie subaquatique, est surmontée de quartzarénite mature de milieu marin peu profond, d'une succcession de siltstone et de shale témoignant d'un approfondissement du milieu de dépôt vers le haut (marquant le début du rifting), d'une série complexe d'unités carbonatées circonscrites au rift qui renferme deux spectaculaires discordances internes, et d'une succession d'aspect flysch-molasse contenant des preuves d'une source de sédiments située dans l'orogène de Grenville. Les données géochronologiques indiquent que le dépôt de la plus grande partie de la succession s'est déroulé de 1100 à 1050 Ma environ. Un des intervalles carbonatés, la Formation de Nanisivik, est la principale unité encaissante des indices de Zn-Pb observés à l'échelle régionale ainsi que du gisement de Nanisivik, autrefois exploité, qui a été formé au Mésoprotérozoïque tardif par des fluides de basse température, et dont la mise en place a été régie par de forts contrôles structuraux et stratigraphiques. Une déformation postsédimentaire minimale est limitée à la mise en place de dykes mafiques, à environ 720 Ma, et à la réactivation répétée de failles normales enracinées dans le socle.

[1]Harquail School of Earth Sciences, Laurentian University, Sudbury, Ontario P3E 2C6
*Corresponding author: E.C. Turner (email: eturner@laurentian.ca)

INTRODUCTION

The Borden Basin contains siliciclastic, carbonate, and volcanic strata of the late Mesoproterozoic Bylot Supergroup, an approximately 6 km thick succession of unmetamorphosed and little-deformed strata that nonconformably overlies Archean to Paleoproterozoic crystalline basement on northernmost Baffin Island (Fig. 1). These strata were deposited in sag, rift, and foreland-basin–like settings approximately 1.1 Ga, are crosscut by mafic Franklin dykes (ca. 720 Ma), and are overlain by flat-lying Paleozoic strata of the Franklinian passive margin as well as locally by Cretaceous to Cenozoic strata.

The earliest work undertaken to establish the regional geology of the Borden Basin, undertaken in 1954 (by dog-team; Blackadar, 1956; Lemon and Blackadar, 1963) and in 1963 (aircraft-supported Operation Admiralty; Blackadar, 1970), established the stratigraphy of the basin, interpreted it as rift-related, and identified the rich base-metal endowment of part of the succession. A Geological Survey of Canada (GSC) mapping campaign (Operation Borden) took place from 1977 to 1984 (Jackson and Iannelli, 1981; Scott and deKemp, 1998) with the intent of providing a comprehensive account of the bedrock geology and its stratigraphy. Independent research has since focused on refining and modernizing the understanding of the tectonostratigraphic evolution, depositional paleoenvironments, geochronology, paleobiology, and metallogeny of the basin. Recent GSC mapping (2017) on north Baffin Island included the southeasternmost part of the Milne Inlet Graben (Saumur et al., 2018a, b).

The Borden Basin is one of the four Bylot basins (Fig. 1; Fahrig et al., 1981), a group of seemingly related, rift-influenced basins (Aston-Hunting Basin, Somerset Island; Fury and Hecla Basin, Baffin Island; Thule Basin, east-central Ellesmere Island and nearby parts of Greenland; and Borden Basin, northern Baffin Island). In the Borden Basin, the Bylot Supergroup fills three northwest-widening paleograbens up to 250 km long (Fig. 1; Milne Inlet, Eclipse, and North Bylot troughs) and is separated by basement horsts, which conspicuously span the geological map of northern Baffin Island (Scott and deKemp, 1998). Of these, the Milne Inlet Graben is the largest and best exposed, and it is there that most stratigraphic work and mineral exploration have been focused.

General structure

Map expression of the Bylot Supergroup (Scott and deKemp, 1998) includes two types of areal coverage (Fig. 1). 1) Conspicuous, northwest-widening, narrow triangles on the geological map of the Borden Peninsula, Bylot Island, and nearby areas, extend southeastward to Kanajuqtuuq (Paquet Bay), define the three grabens of the Borden Basin (Milne Inlet, Eclipse, and North Bylot troughs), and are occupied by strata of the middle and upper part of the supergroup (upper Arctic Bay Formation and above). 2) Broad areas surrounding the paleograbens and directly overlying basement are thinly covered by lowermost strata of the Bylot Supergroup (Nauyat to lower Arctic Bay formations). These map patterns are compatible with tectonostratigraphic work that interprets an early, broad sag basin (Nauyat and Adams Sound formations; Long and Turner, 2012) followed by rift-delimited sedimentation (Arctic Bay through Victor Bay formations; Turner and Kamber, 2012; Turner et al., 2016), and then foreland-basin–like accumulation (Sherman et al., 2002; Turner et al., 2016).

Crosscutting Franklin dykes were emplaced into pre-existing basement-rooted structures that also crosscut Bylot Supergroup strata ca. 720 Ma (Heaman et al., 1992). The basin has been minimally deformed or metamorphosed. The deep-seated normal faults involved in graben development were repeatedly reactivated during Mesoproterozoic sedimentation and in the time since then (Jackson and Cumming, 1981; Turner, 2011), producing local fault-related folding.

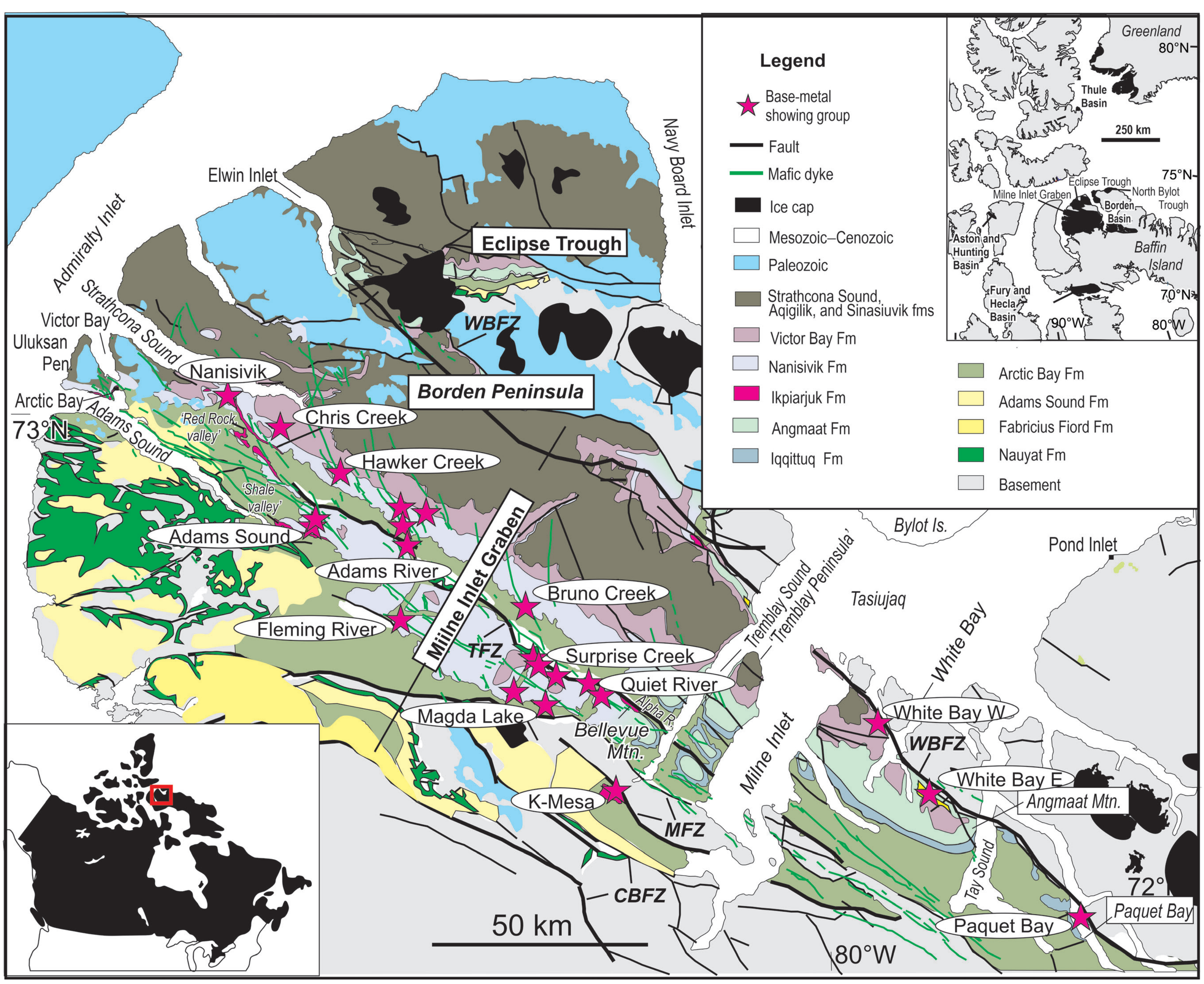

Figure 1. a) Simplified geology of the Borden Basin, after Scott and deKemp (1998) as *modified by* Turner (2009; 2011). **b)** Location of Bylot basins. WBFZ = White Bay Fault Zone; TFZ = Tikirarjuaq Fault Zone; MFZ = Magda Fault Zone; CBFZ = Central Baffin Fault Zone.

STRATIGRAPHY AND DEPOSITIONAL PALEOENVIRONMENTS

Early geological fieldwork (Blackadar, 1956, 1970; Lemon and Blackadar, 1963) produced a general understanding of the bedrock geology of northern Baffin Island, and established a stratigraphic scheme (Fig. 2a) containing eight formations and two groups (Eqalulik and Uluksan), many of which lacked a designated type section or type area. Results of a GSC mapping campaign in the 1970s yielded an amended stratigraphic scheme (Fig. 2b) that designated nine formations and three groups (Eqalulik, Uluksan, and Nunatsiaq groups; Jackson and Iannelli, 1981). Fahrig et al. (1981) highlighted the inferred relationships among seemingly similarly aged strata in separate basins of the Bylot basins group, on Somerset Island (Aston-Hunting Basin), elsewhere on northern Baffin Island (Fury and Hecla Basin), and on Ellesmere Island and northwestern Greenland (Thule Basin). Knight and Jackson (1994) produced an updated stratigraphy for the uppermost siliciclastic units of the Bylot Supergroup (Elwin subgroup; Fig. 2c). Stratigraphic work by scientists outside the GSC starting in the 1990s yielded a refined stratigraphic scheme and understanding of the geological history of the basin (Fig. 2c) based on a modern understanding of Proterozoic lithofacies and environments (Sherman et al., 2000, 2001; Turner, 2009, 2011; Turner and Kamber, 2012; Long and Turner, 2012; Hahn et al., 2015, 2018; Hahn and Turner, 2017), rigorous documentation of unconformities in the succession (Sherman et al., 2002; Turner, 2009, 2011), transformative new geochronological data (Turner and Kamber, 2012; Turner et al., 2016; Gibson et al., 2018), and geochemical and isotopic evidence (Hahn et al., 2015; Gibson et al., 2019)

The currently accepted stratigraphy of the Bylot Supergroup (Fig. 2c), based on its best exposed and best mineralized area, the Milne Inlet Graben, consists of units established or described in Blackadar (1956, 1970), Lemon and Blackadar (1963), Jackson and Iannelli (1981), Knight and Jackson (1994), Sherman et al. (2000, 2001, 2002), and Turner (2009, 2011), and internal unconformities described in Sherman et al. (2002), Turner (2009, 2011), and Turner et al. (2016). The basic stratigraphy appears to be applicable in the other two grabens of the Borden Basin, with local nuances (Jackson and Davidson, 1978).

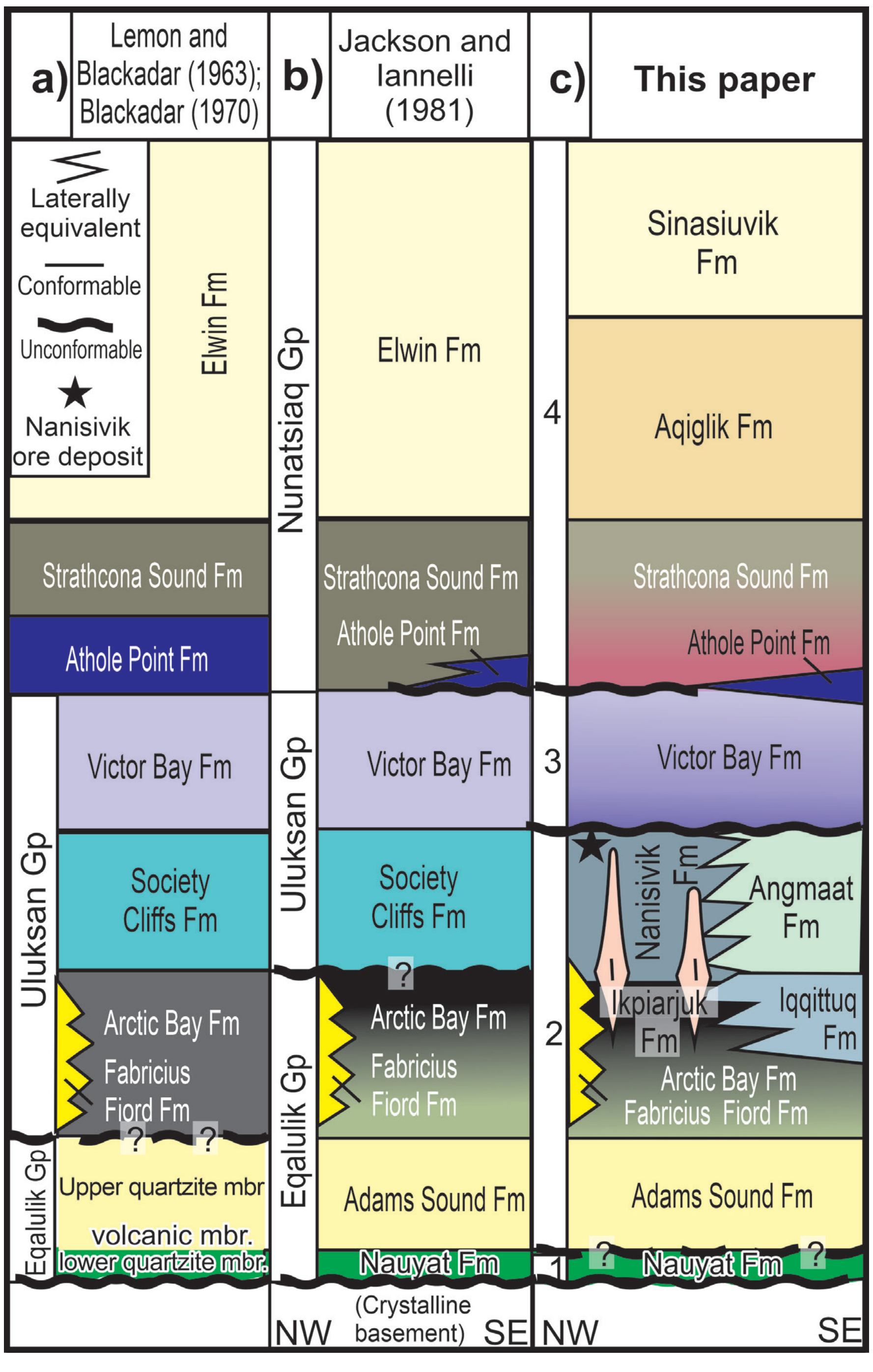

Figure 2. a), **b)** Previous and **c)** current lithostratigraphic nomenclature for the Borden Basin. Gradational colour fills indicate units in which the composition changes stratigraphically. Numbers 1 to 4 indicate group-scale stratigraphically coherent intervals separated by unconformities.

The undated basal unit, the Nauyat Formation (interval 1), is of uncertain affinity; originally assumed to be related to the Mackenzie igneous event (ca. 1270 Ma; Fahrig et al., 1981; Dostal et al., 1989), it could be younger, based on geochronological constraints discussed below. The remainder of the succession forms three further stratigraphically coherent intervals (intervals 2–4) separated by two dramatic, well documented unconformities: Adams Sound to Angmaat-Nanisivik formations; Victor Bay and Athole Point formations; and Strathcona Sound to Sinasiuvik formations. The four depositionally coherent intervals (Fig. 2) are not compatible with any of the previously established groups (Blackadar, 1956, 1970; Lemon and Blackadar, 1963; Jackson and Iannelli, 1981), because 1) it is unclear whether the Adams Sound Formation is temporally related to the Nauyat Formation (collectively forming the Eqalulik Group), 2) the carbonate-dominated Uluksan Group (consisting of the abandoned Society Cliffs Formation and the Victor Bay Formation) is now known to be interrupted by a substantial unconformity (Turner, 2009, 2011), and 3) the southeastern Athole Point Formation is now known to be time-equivalent to the northwestern unconformity on the Victor Bay Formation, not laterally equivalent to the lower Strathcona Sound Formation within the Nunatsiaq Group (Sherman et al., 2002). The complex tectonostratigraphic history of the succession has begun to be deciphered (e.g. Turner et al., 2016), but further stratigraphic revisions and refinements may be required. All Bylot Supergroup strata are crosscut by Franklin dykes (Fig. 3), which are a conspicuous part of the geology of the basin.

The formations of the Bylot Supergroup are outlined below, and typical exposures illustrated (for those units that outcrop well). Owing to the variable vintage and type of work previously undertaken on each formation, the type and detail of the descriptions vary. Rock photos are figured only for those units that are dominated by unusual lithofacies, not extensively figured or described in previous publications, or important to the distribution of base-metal concentrations.

Nauyat Formation

The Nauyat Formation (Blackadar, 1956; no type section) is up to about 400 m thick in widespread exposures south of Adams Sound, and thins eastward to zero near Tremblay Sound. It nonconformably overlies Rae Province basement and consists of continental tholeiitic basalt and intercalated sandstone. This formation has been assumed to be affiliated with the ca. 1270 Ma Mackenzie igneous event based on paleomagnetic data (Fahrig et al., 1981) and geochemistry (Dostal et al., 1989). This unit (Fig. 4) consists of a locally exposed lower cross-bedded sandstone- and conglomerate-dominated unit (up to 200 m thick) with minor amygdaloidal basalt flows, and an upper unit, 0 to 430 m thick, dominated by basalt flows that are 2 to 60 m thick, containing intercalated sandstone and siltstone, stromatolitic carbonate, ferroan carbonate mudstone, and chert (Jackson and Iannelli, 1981). Pillows and flow-top breccia are rare (Jackson and Iannelli, 1981).

Although some workers interpreted the succession as subaerial and rift-related (Dostal et al., 1989), the presence of stromatolitic carbonate interflow deposits, intercalated sandstone interpreted as marine, and sand injectites and peperites, suggests that at least some of the succession was deposited subaqueously (Long and Turner, 2012). Together with the geographic distribution of the formation, which is not delimited by rift location, these characteristics point to a sag-like basin interpretation for the oldest strata of the Bylot Supergroup rather than subaerial volcanism associated with thermal doming and rifting (Nauyat and Adams Sound formations; Long and Turner, 2012; Turner et al., 2016). Whether the absence of basalt from the eastern part of the basin was the product of nondeposition or postdepositional erosion has not been determined. The Nauyat Formation has never been dated directly; given recent advances in dating the deposition of units higher in the stratigraphy of the supergroup (Turner and Kamber, 2012; Turner et al., 2016; Gibson et al. 2018), the presumed Mackenzie age of the basalt not yet been verified.

Adams Sound Formation

The Adams Sound Formation (Fig. 4, 5; Blackadar, 1956; up to 610 m thick; no designated type section) consists of crossbedded quartz arenite with minor conglomerate and siltstone intervals, with widespread exposure across Borden Peninsula and east to Paquet Bay; regional variation is detailed by Jackson and Iannelli (1981). Whether the sharp basal contact is conformable with Nauyat Formation basalt is unclear. Long and Turner (2012) describe the

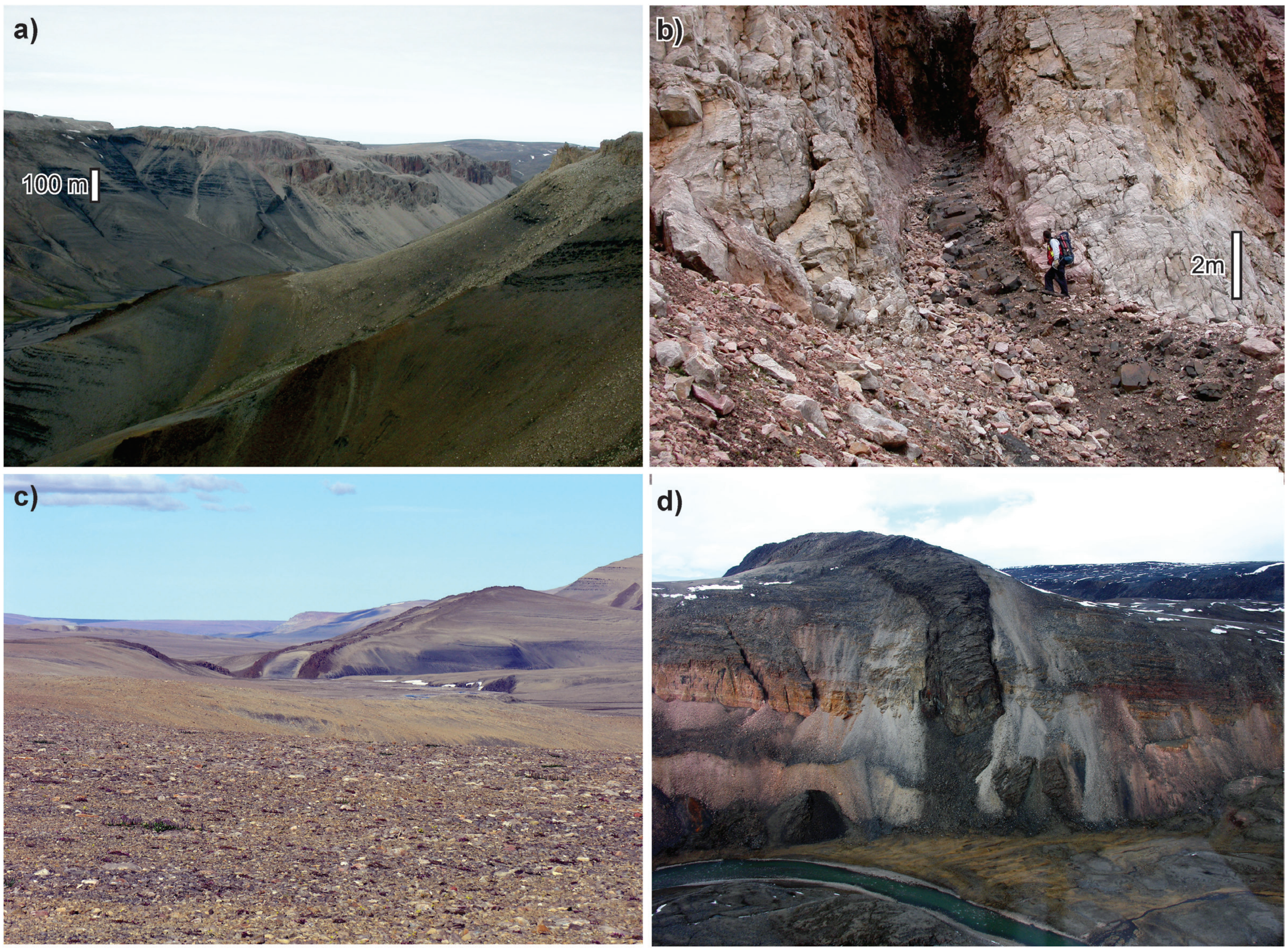

Figure 3. Exposure of presumed Franklin dykes (ca. 723 Ma) in the Milne Inlet Graben. **a)** Multiple dykes cut through Arctic Bay Formation black shale and Ikpiarjuk Formation dolostone (cliff). NRCan photo 2019-532. **b)** Close-up of a dyke crosscutting the Ikpiarjuk Formation in 3a; person for scale. NRCan photo 2019-533. **c)** Parallel dykes crosscut Victor Bay shale near showing #9 of Sangster (1998); note narrow zones of bleached country rock. Distance between dykes is about 400 m. NRCan photo 2019-534. **d)** Resistantly weathering dyke (estimated width about 75 m) crosscuts Adams Sound Formation near Adams Sound. NRCan photo 2019-535. All photographs by E.C. Turner.

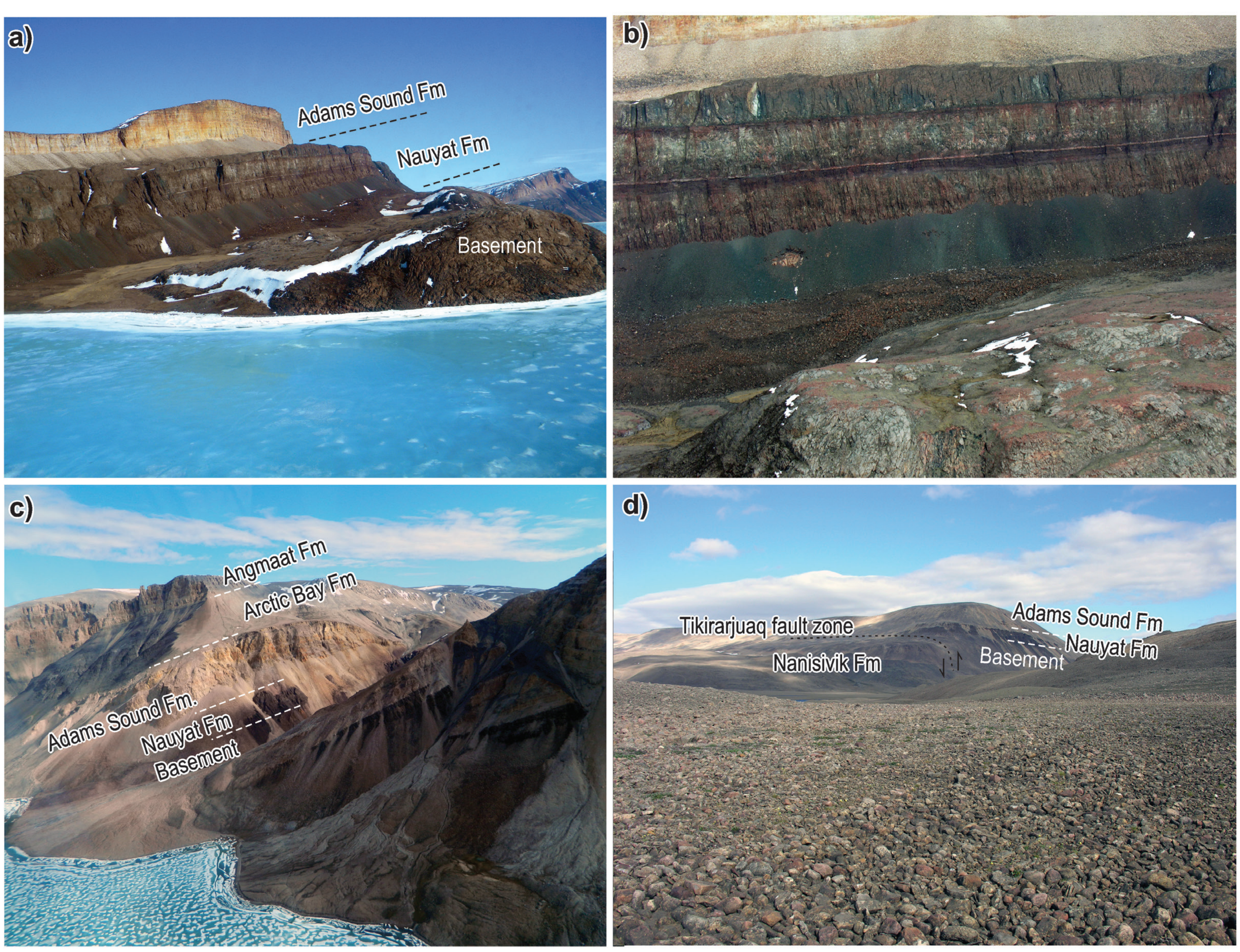

Figure 4. Exposures of the Nauyat Formation. **a)** Exposure on north side of Adams Sound; Nauyat Formation is approximately 80 m thick. NRCan photo 2019-536. **b)** Close-up of area in 4a showing basement rocks in foreground overlain by at least three flows with different alteration and weathering characteristics, separated by thin interflow strata. Nauyat Formation (dark layers in middle) approximately 80 m thick. NRCan photo 2019-537. **c)** Nauyat Formation exposure on east side of Elwin Inlet is estimated to be 50 m thick. NRCan photo 2019-538. **d)** Nauyat Formation exposure at Surprise Creek (central Borden Peninsula) is approximately 35 m thick. The Nanisivik Formation contains multiple copper and zinc showings adjacent to the Tikirarjuaq Fault Zone. NRCan photo 2019-539. All photographs by E.C. Turner.

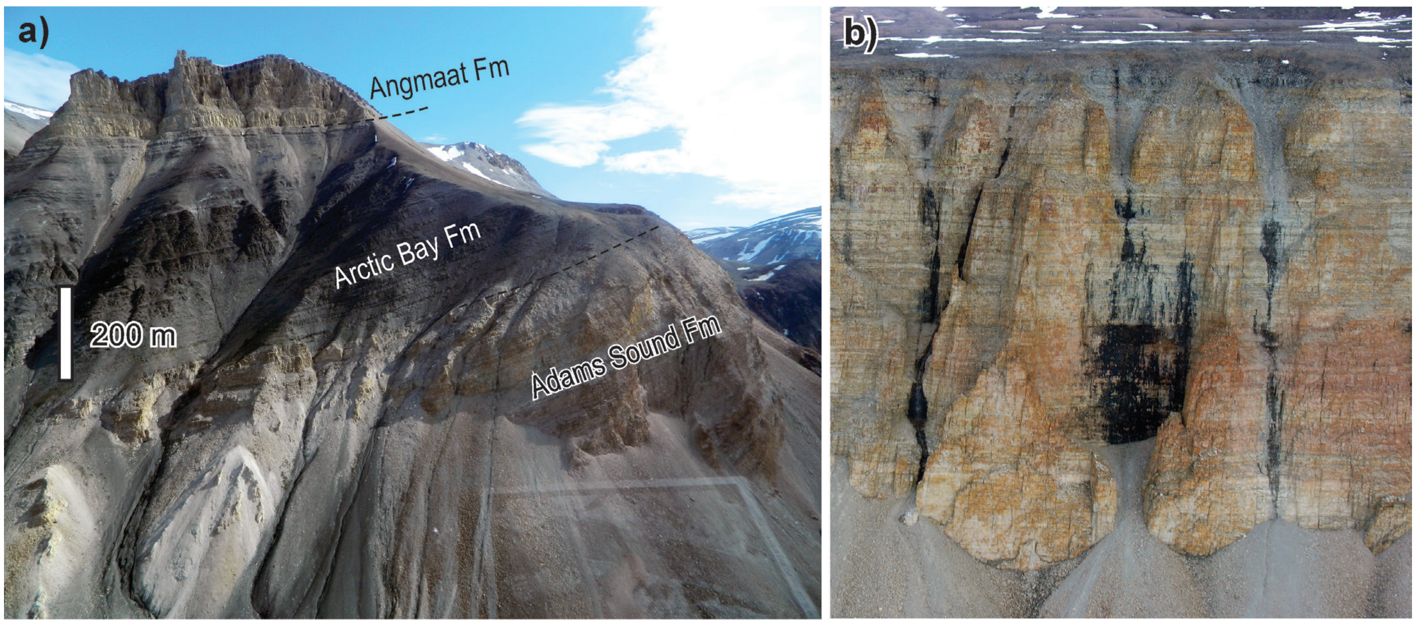

Figure 5. Typical exposures of the Adams Sound Formation. **a)** Adams Sound, Arctic Bay, and Angmaat formations on east side of Elwin Inlet. NRCan photo 2019-540. **b)** An approximately 100 m high sea cliff on the north side of Adams Sound exhibiting typical flat and continuous bedding of the Adams Sound Formation. NRCan photo 2019-541. All photographs by E.C. Turner.

noncyclic, tabular-layered succession as dominated by trough- and planar-crossbedded sandstone interpreted as large sandwave complexes, and planar-laminated sandstone, with local pebbly units.

Although part of the succession may have been deposited in fluvial environments (Jackson and Iannelli, 1981), the formation is dominated by marine characteristics (Fig. 5; Long and Turner, 2012). Together with the geographic distribution of the formation, which is not delineated by rift location, this evidence includes paleocurrents that indicate deposition on a storm- and tide-influenced shallow-marine shelf in an epicratonic sag basin that show no influence of the later developed grabens. Paleomagnetic data were interpreted to indicate a depositional age of ca. 1220 Ma (Fahrig et al., 1981).

Arctic Bay Formation

The Arctic Bay Formation (Fig. 6; Blackadar, 1956; up to more than 600 m thick; original, but atypical type section at Arctic Bay (Blackadar, 1970)) encompasses a fining-upward sandstone-to-shale succession up to 800 m thick that sharply, but conformably overlies the Adams Sound Formation. Decametre-scale coarsening-upward sandstone-siltstone cycles in the lower part of the formation gradually pass upward by fining and thinning of cycles into noncyclic, drab siltstone-shale in the southeastern part of the graben, but into black shale (up to 200 m thick) in the western part of the basin (Jackson and Iannelli, 1981; Turner and Kamber, 2012). The sandstone units exhibit hummocky cross-stratification, syneresis cracks, and ripple crosslamination. The western black shale unit that is the uppermost part of the formation on Borden Peninsula (northwestern part of the graben) is time-equivalent to the Iqqittuq Formation in the southeast, rather than to drab siltstone of the upper Arctic Bay Formation in the southeast (Fig. 2; Turner, 2009; Turner and Kamber, 2012), and is also temporally equivalent to deep-water carbonate mounds of the Ikpiarjuk Formation (Turner, 2004; Hahn et al., 2015; Hahn and Turner, 2017). A contact formerly interpreted at the contact of the Arctic Bay Formation black shale and overlying intraclastic carbonate rocks west of Tremblay Sound (Geldsetzer, 1973; Jackson and Iannelli, 1981) is now known to record the local nucleation and rapid expansion of very large deep-water carbonate mounds and their flanking debris (Ikpiarjuk Formation) over surrounding, coeval deep-water black shale, without any exposure or hiatus (Turner, 2009). Geochronological data (U-Pb-Th; Re-Os) indicate a depositional age in the range of ca. 1020–1100 Ma for the black shale unit (1092 ± 59 Ma, U-Pb-Th whole-rock black shale, Turner and Kamber, 2012; 1048 ± 12 Ma, Re-Os black shale, Gibson et al., 2018).

The lower Arctic Bay Formation is interpreted as a northwest-deepening and overall fining- and deepening-upward cyclic shallow-marine ramp. The upper Arctic Bay Formation (black shale; of significant thickness only in the northwest) is interpreted as a restricted, starved, anoxic lacustrine basin with local deep-water mounds (Ikpiarjuk Formation; Turner and Kamber, 2012; Hahn et al., 2015) centred over syndepositionally active subaqueous normal faults, an adjacent shallow-marine carbonate ramp to the southeast (Iqqittuq Formation), graben-margin fan deltas at the southern margin of the graben (Fabricius Fiord Formation), and normal fault activity on the basin floor producing local deep-water paleotopography and sediment remobilization (Turner and Kamber, 2012). The black shale is now thermally overmature, but nonetheless retains significant organic carbon, and would originally have been extremely organic-rich (Turner and Kamber, 2012; Fustic et al., 2017). The stratigraphic configuration of the black shale unit and related strata strongly resembles that of oil-shale deposits in Phanerozoic lacustrine rocks (Fustic et al., 2017). Although the black shale has been reported to be rusty (sulphidic; Jackson and Iannelli, 1981), and trace-element geochemistry allows for a sulphidic interpretation of bottom-water conditions (Turner and Kamber, 2012), controversy remains over the interpretation of the depositional conditions of this unit and its basin-water chemistry (Hahn et al., 2015; Gibson et al., 2019).

Fabricius Fiord Formation

The Fabricius Fiord Formation (Blackdar, 1970; type section near Fabricius Fiord) occupies an exposure belt about 30 km long, 8 km wide, and up to 2000 m thick parallel to the Central Borden Fault Zone, as well as isolated areas of similar material adjacent to graben-bounding faults elsewhere (Scott and deKemp, 1998). This unit typically consists of a thin (10–20 m) lower interval of interlayered quartz arenite, siltstone, and black shale (FF1); overlain by a thick interval (to more than 800 m) of decametre-scale shale to quartz arenite cycles (FF2); a thick interval (to more than 800 m) of subarkose and conglomerate (FF3); and an interval approximately 100 to 200 m thick of arkose, microbial and intraclastic carbonate, and conglomerate (Fig. 7; Jackson and Iannelli, 1981). Of limited areal extent, but substantial thickness (up to more than 2000 m), this formation was deposited in graben-margin fan deltas on the southern border of the Milne Inlet Graben and as small areas of similar material near graben margins elsewhere in the basin (Jackson and Iannelli, 1981; Scott and deKemp, 1998). This unit is laterally and temporally equivalent to the Arctic Bay Formation, Iqqittuq Formation, Ikpiarjuk Formation, and lower Angmaat and Nanisivik formations (Jackson and Iannelli, 1981; Turner, 2009; Turner and Kamber, 2012; Turner et al., 2016).

Iqqittuq Formation

The Iqqittuq Formation (Fig. 8; Turner, 2009; type section west side of Tay Sound) is one of four carbonate formations subdivided from the now-abandoned Society Cliffs Formation (Lemon and Blackadar, 1963; Geldsetzer, 1973); it is the lower, southeastern part of the former Society Cliffs Formation. This formation consists of noncyclic dolostone and minor siliciclastic units (brightly coloured mudstone to sandstone in vicinity of graben-margin faults) as well as minor evaporitic units (Jackson and Iannelli, 1981; Saumur et al., 2018b) that locally reach substantial thickness on Bylot Island (Jackson and Cumming, 1981). The carbonate components of this formation are characterized by low-energy, shallow-subtidal features such as molar-tooth carbonate mudstone and rare stromatolites southeast of 'Tremblay peninsula' (informal name), but centimetrically layered carbonate mudstone, intraclast rudstone, and graded layers of fine-grained carbonate with slump folds, interlayered with dark grey to black shale northwestward from Tremblay Sound. In all locations, the base of the formation is gradational with underlying mudstone-shale of the lower Arctic Bay Formation.

The carbonate components of this formation prograde and thin northwestward to zero at Bellevue Mountain on the Borden Peninsula, depicting a northwest-prograding and -deepening carbonate ramp that passed laterally, on eastern Borden Peninsula, to coeval black shale of the upper Arctic Bay Formation (Fig. 2; Turner, 2009). Owing to its

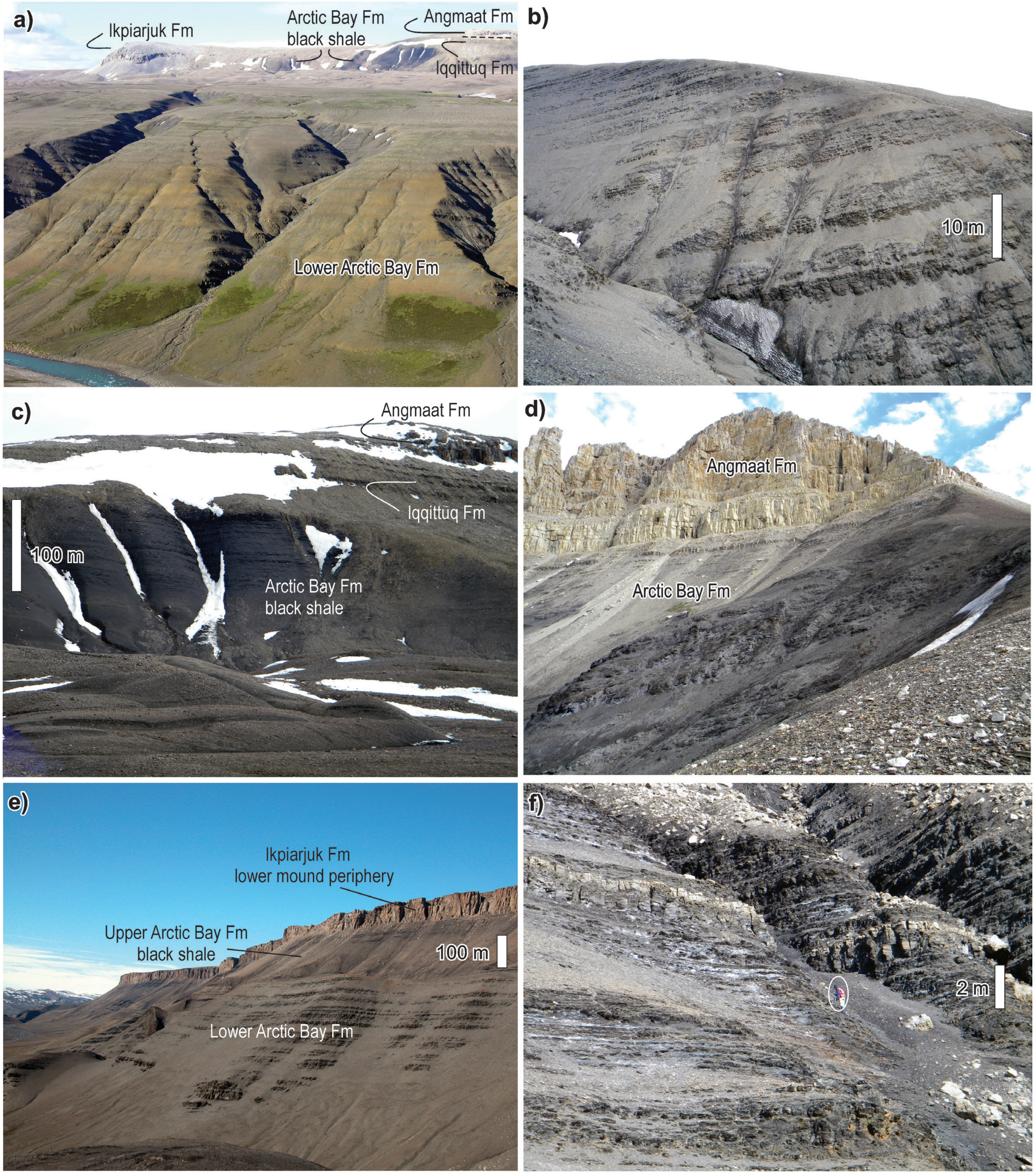

Figure 6. Typical exposures of the Arctic Bay Formation. **a)** Fining-upward decametre-scale cycles of lower Arctic Bay Formation in lower part of Alpha River valley, overlain by upper Arctic Bay Formation black shale and its lateral equivalents, the Iqqittuq and Ikpiarjuk formations. Vertical thickness of strata incised by canyons in foreground is approximately 500 m. NRCan photo 2019-542. **b)** A closer view of cycles in left creek figured in 6a. NRCan photo 2019-543. **c)** A closer view of stratigraphic relations among Arctic Bay, Iqqittuq, and Angmaat formations in upper right of 6a. NRCan photo 2019-544. **d)** Arctic Bay and Angmaat formations on east side of Elwin Inlet; Amgmaat Formation cliffs are about 200 m high. NRCan photo 2019-545. **e)** Arctic Bay and Ikpiarjuk formations at 'Shale valley'; black shale interval is about 150 m thick. NRCan photo 2019-546. **f)** Upper part of the lower Arctic Bay Formation at 'Shale valley'; person (circled) for scale. NRCan photo 2019-547. All photographs by E.C. Turner.

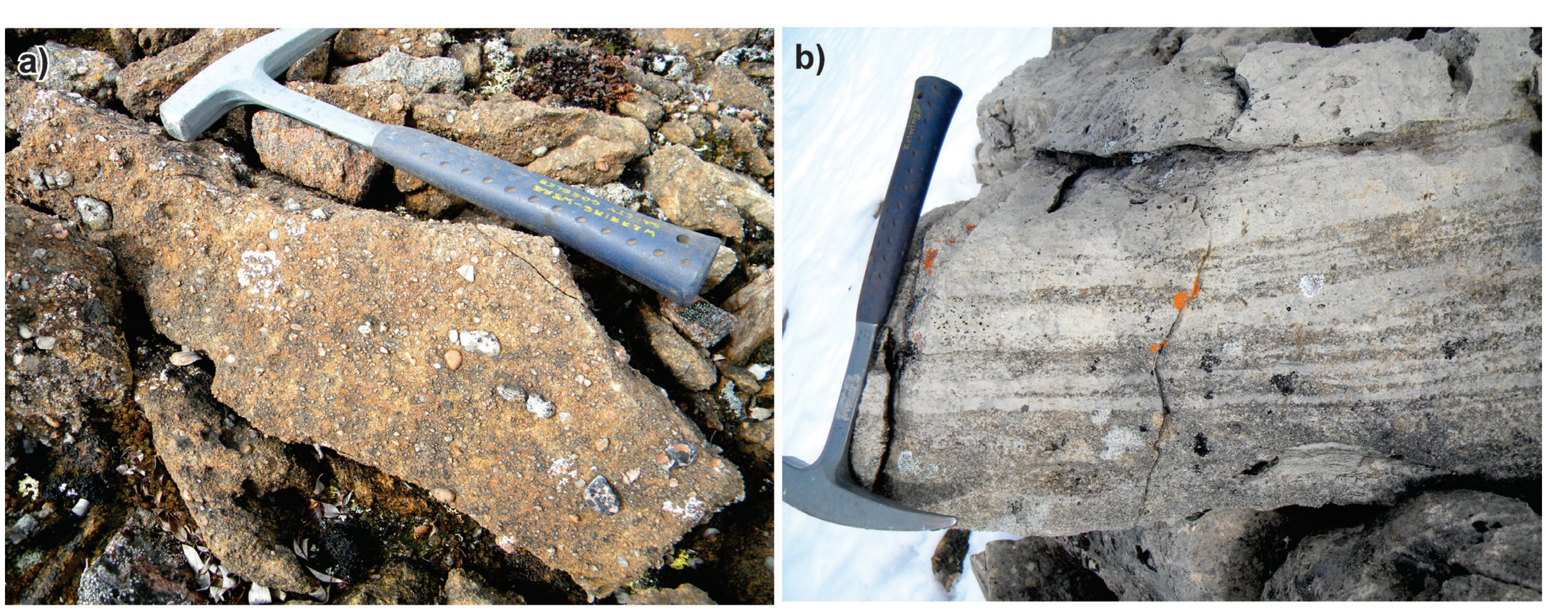

Figure 7. Characteristics of the Fabricius Fiord Formation. **a)** Float of quartzose dolowacke. Hammer is 32 cm long. NRCan photo 2019-548. **b)** Float of quartzose dolostone. Hammer is 32 cm long. NRCan photo 2019-549. All photographs by E.C. Turner.

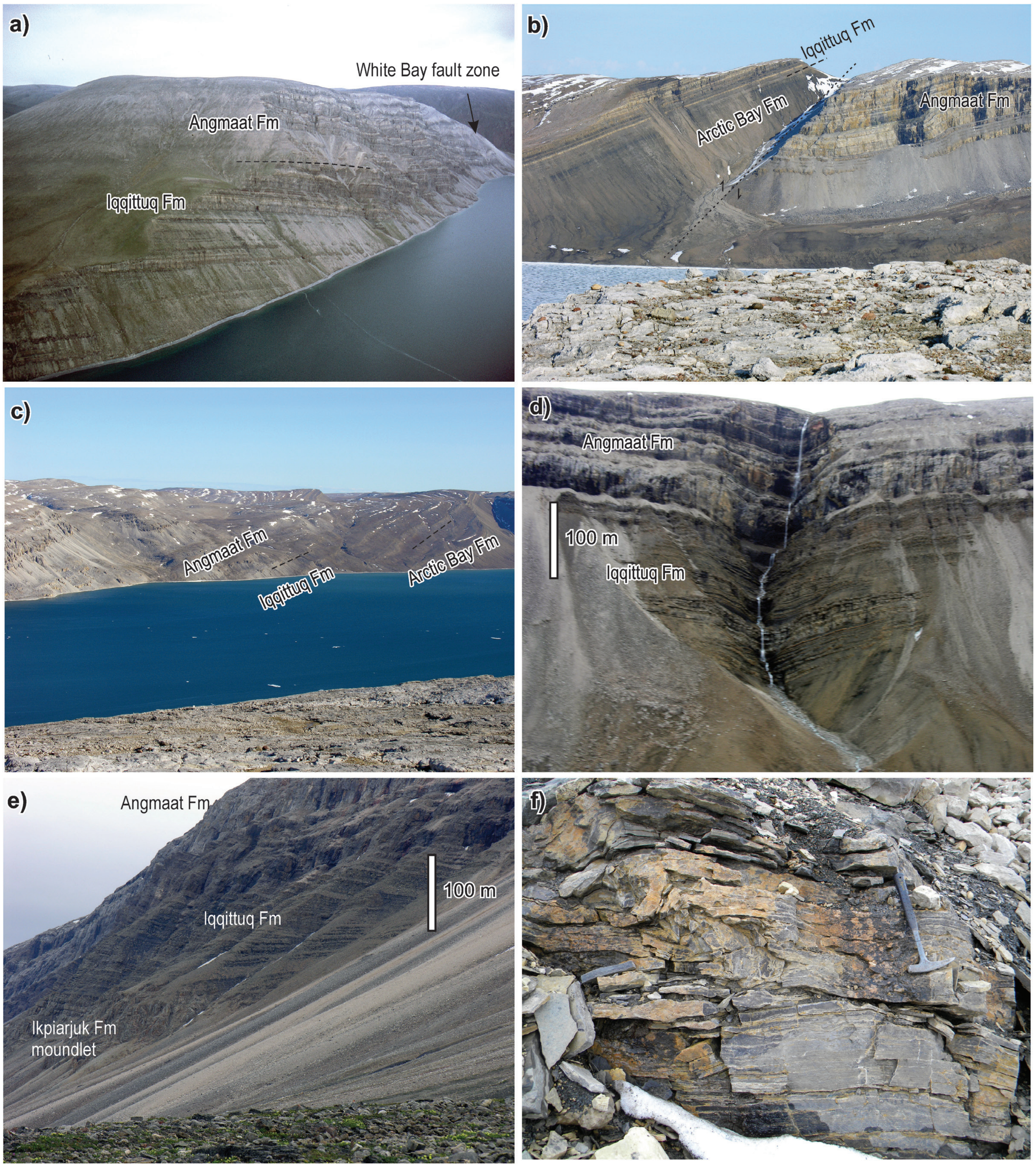

Figure 8. Exposures of the Iqqittuq Formation. **a)** Noncyclic Iqqittuq Formation and cyclic Angmaat Formation (type section) on west side of Tay Sound. Cliff is about 400 m high. NRCan photo 2019-550. **b)** Base of Iqqittuq Formation at its type section on west side of 'Tremblay peninsula'. Exposure is about 400 m high. NRCan photo 2019-551. **c)** Type section of Iqqittuq Formation (outer ramp), west side of 'Tremblay peninsula'. Exposures are about 400 m high. NRCan photo 2019-552. **d)** Iqqittuq Formation (outer ramp to slope) on south side of Alpha River. NRCan photo 2019-553. **e)** Iqqittuq Formation (slope) just east of Bellevue Mountain. NRCan photo 2019-554. **f)** Slope-facies soft-sediment fold in outermost Iqqittuq Formation east of Alpha River mouth. Hammer is 32 cm long. NRCan photo 2019-555. All photographs by E.C. Turner.

temporal and geometric equivalence to the Arctic Bay and Ikpiarjuk formations (Turner, 2009), this formation must also be interpreted as lacustrine, an interpretation supported by geochemical evidence (Gibson et al., 2019).

Ikpiarjuk Formation

The Ikpiarjuk Formation ((Fig. 9, 10; Turner, 2009; type section in cliffs west of Ikpiarjuk (Arctic Bay); reference section at Bellevue Mountain) consists of large, deep-water carbonate mounds (kilometres in diameter; hundreds of metres thick) dispersed within black shale of the upper Arctic Bay Formation across Borden Peninsula, in the immediate vicinity of generally northwest-trending, syndepositionally active intragraben faults (Turner, 2004; Hahn et al., 2015; Hahn and Turner, 2017); the mounds are time-equivalent to Arctic Bay Formation black shale and to the Iqqittuq Formation carbonate ramp in southeastern Milne Inlet Graben. The mounds exhibit subtle textures, indicating both benthic microbial carbonate precipitation (thrombolitic clots) and pelagic carbonate mud precipitation (Hahn and Turner, 2017), as well as a diverse range of early and late diagenetic cements filling original porosity in the microbial framework (Hahn et al., 2018). As shown by mound-flank relationships with enclosing strata (boulder- to pebble-grade debris interfingered with black shale at lower mound flanks), the mounds expanded rapidly after their nucleation and developed pronounced topographic relief above the contemporaneous basin floor, which persisted after they had ceased to accumulate; sand- to pebble-grade debris continued to be shed from defunct mounds during deposition of the overlying Nanisivik Formation. In some cases, paleotopographic relief of the mounds was fully erased only by erosion during the exposure interval postdating the deposion of the Nanisivik Formation. Ikpiarjuk Formation mounds are patchily present across the Borden Peninsula, including beneath the orebody at the Nanisivik mine, and compose much of the thickness of the original type section of the abandoned Society Cliffs Formation west of the hamlet of Arctic Bay (Ikpiarjuk; Lemon and Blackadar, 1963).

Geochemical (rare-earth element plus yttrium; REE+Y) characteristics of the benthic and pelagic carbonate precipitates suggest lacustrine rather than marine deposition, and precipitation as a result of mixing between anoxic, alkaline lacustrine bottom water and local basin-floor seep fluid. The seep fluid is inferred to have vented along syndepositionally active, northwest-trending graben-floor normal faults (Turner, 2004, 2009; Hahn et al., 2015; Hahn and Turner, 2017) that compartmentalized the bottom-water of the graben into

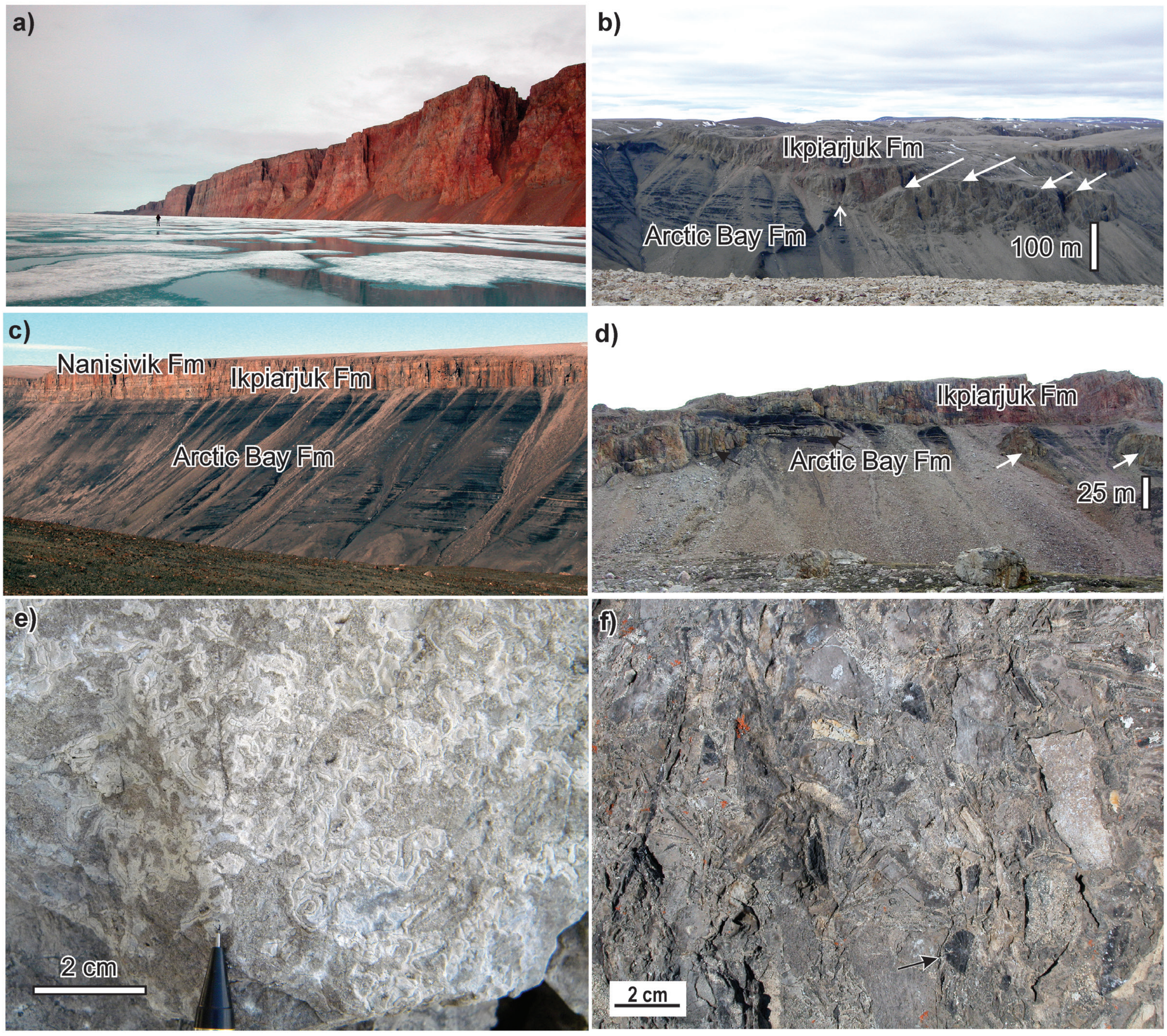

Figure 9. Exposures of the Ikpiarjuk Formation. **a)** Type section west of Ikpiarjuk (Arctic Bay) is about 250 m thick and goes up the cleft on right side of image; person for scale. NRCan photo 2019-556. **b)** Exposure on southwest side of 'Red Rock valley' shows crude clinoform-like surfaces (slanted arrows) associated with expansion of mound dolostone over surrounding black shale of upper Arctic Bay Formation. Leftmost white arrow indicates dyke shown in Figures 3a and b. NRCan photo 2019-557. **c)** Lower part of cliff above Arctic Bay Formation at 'Shale valley' (total about 60 m thick) consists of massive intraclast rudstone of mound-derived, shaly, and Nanisivik Formation clasts; upper part is Nanisivik Formation. NRCan photo 2019-558. **d)** Isolated small mounds (arrowed) embedded in shaly outermost Iqqittuq Formation underlying main mound exposure at K-Mesa (south of Tremblay Sound). NRCan photo 2019-559. **e)** Thrombolitic mound fabric of Ikpiarjuk Formation at K-Mesa mound (south of Tremblay Sound). NRCan photo 2019-560. **f)** Intraclast rudstone of lower mound flank facies at 'Shale valley' (as in 9c) contains pale mound-derived clasts, dark brown, platy dolostone clasts (Nanisivik Formation), and dark grey clasts (arrow) that are resedimented concretions from lower Nanisivik Formation. NRCan photo 2019-561. All Photographs by E.C. Turner.

geochemically isolated zones. If this interpretation is accurate, a lacustrine interpretation must also apply to the coeval, laterally equivalent upper Arctic Bay Formation black shale (Turner and Kamber, 2012; Fustic et al., 2017) as well as the Iqqittuq Formation carbonate ramp, an interpretation supported (Gibson et al., 2019) using radiogenic isotope evidence.

Angmaat Formation

The Angmaat Formation (Fig. 11; Turner, 2009; type section west side of Tay Sound; reference section west side of 'Tremblay peninsula') is a conspicuously cyclic shallow-marine carbonate succession up to 800 m thick present southeast of easternmost Borden Peninsula in the Milne Inlet Graben and in northern Borden Peninsula and Bylot Island (Fig. 1). East of 'Tremblay peninsula', the decametre-scale cycles consist of carbonate mudstone, pseudomorphed seafloor aragonite fans, abiogenic 'stromatolites', tepees, and minor gypsite (Jackson and Cumming, 1981; Kah et al., 1999; Turner, 2009, 2011), whereas on 'Tremblay peninsula', the formation consists of ooid-tepee cycles defining the margin of a carbonate platform (Turner, 2009). This formation is the only carbonate unit in the Bylot Supergroup that has truly 'platformal' characteristics, and even those have been interpreted as possibly of tectonic rather than autogenic origin (Turner, 2009). The Angmaat Formation is laterally and temporally equivalent to the Nanisivik Formation, passing northwest to the Nanisivik Formation on the easternmost Borden Peninsula; it is geometrically laterally equivalent to parts of some Ikpiarjuk Formation relict topography carbonate mounds, although the deposition of the mounds predated accumulation of the Angmaat Formation. A dramatic unconformity separates the Angmaat and Nanisivik formations from the overlying Victor Bay Formation (Turner, 2011); the unconformity is characterized by subtle angularity and pronounced paleotopographic relief (minimum 250 m).

Nanisivik Formation

The Nanisivik Formation (Fig. 12, 13, 14, 15; Turner, 2009; type section in Alpha River valley) is the northwestern, upper part of the abandoned Society Cliffs Formation; it is extremely important as the main host of base-metal mineralization in the Borden Basin and at Nanisivik in particular. The basal contact of Nanisivik Formation with underlying black shale of the upper Arctic Bay Formation is abrupt, but conformable, and locally includes a thin interval of debris shed from the margins of Ikpiarjuk Formation carbonate mounds, Arctic Bay Formation shale clasts, and reworked basal Nanisivik Formation clasts (e.g. 'Shale valley' (informal name)). The generally poorly exposed Nanisivik Formation nowhere provides a complete stratigraphic section; the description of Turner (2009) was based on outcrop for the lower part of the formation and core for the upper part; widespread felsenmeer indicates that the essential characteristics of the formation are consistently present throughout its full thickness. The formation consists entirely of millimetre-scale to submillimetre-scale laminated dark brown–weathering dolostone containing nonstratiform, cement- and locally sediment-filled synsedimentary

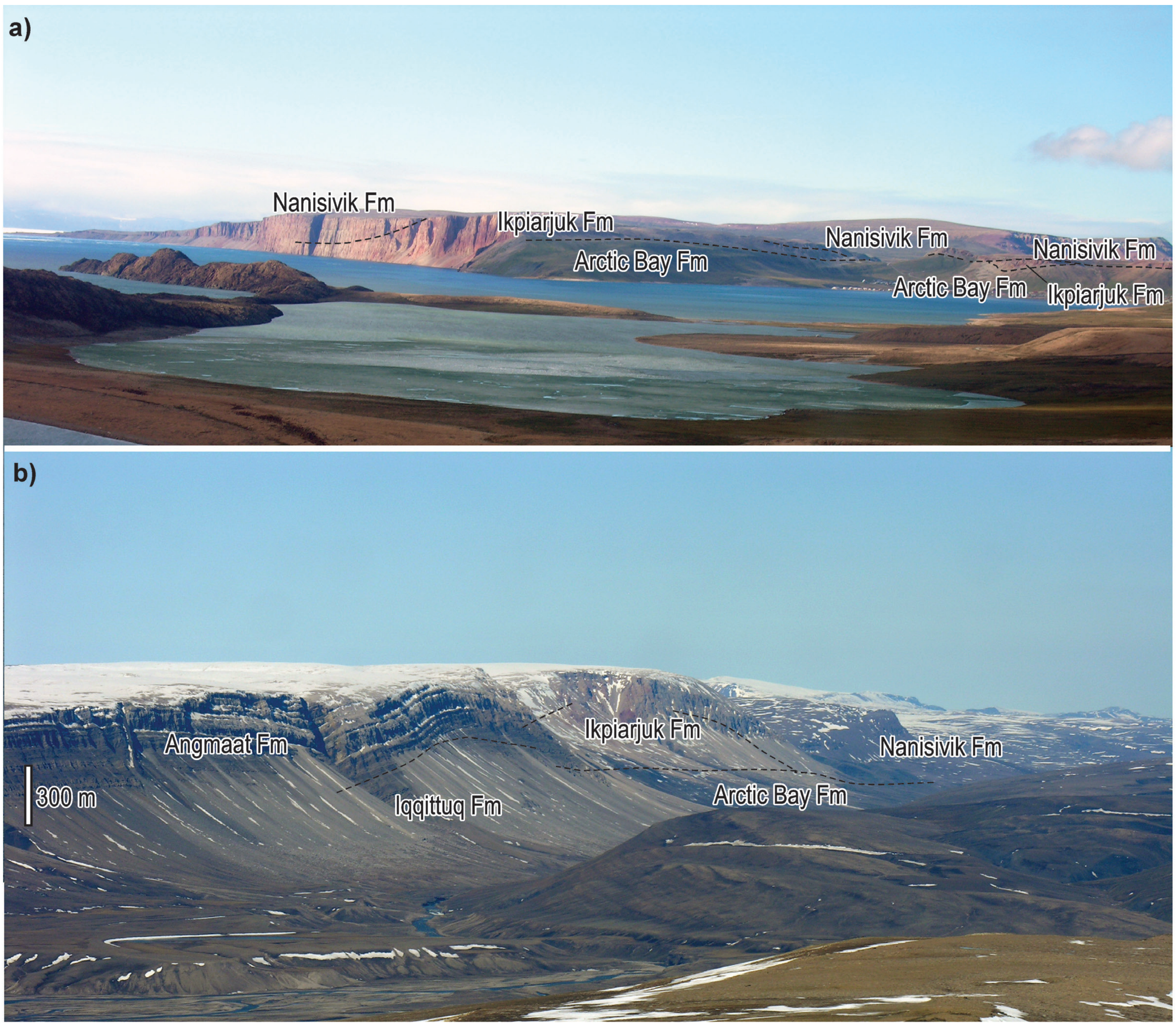

Figure 10. Geometric relationship of the Ikpiarjuk Formation with its stratigraphic neighbours. **a)** Arctic Bay townsite is on Arctic Bay Formation black shale, but cliffs of Ikpiarjuk Formation and Nanisivik Formation perch above town. Red sea cliffs are 250 m high. NRCan photo 2019-562. **b)** Complex geometric relationships among the Arctic Bay, Iqqittuq, Angmaat, Ikpiarjuk, and Nanisivik formations at Bellevue Mountain. NRCan photo 2019-563. All photographs by E.C. Turner.

and later breccia units. Soft-sediment folds, and chaotic to graded beds of laminite-intraclast rudstone, are interpreted as creep folds and resedimentation as debrite and turbidite units, respectively. Locally common in the basal 100 m of the formation in the vicinity of northwest-trending intragraben faults are: soft-sediment folds (creep folds), chaotic to graded beds of laminite-intraclast rudstone (debrite and turbidite units), and lenses of sand-grade mixed carbonate and terrigenous material. These features are interpreted as material shed from syndepositionally active seafloor fault blocks (Turner, 2003, 2004, 2009). In the vicinity of Ikpiarjuk Formation mounds (e.g. 'Red Rock valley' (informal name)), mounds contribute to the Nanisivik Formation in two ways: the basal few metres to tens of metres of the Nanisivik Formation consist of debris shed from mounds, commonly mixed with shale clasts (Arctic Bay Formation) and brown dololaminite clasts (Nanisivik Formation); and a substantial thickness of the upper part of the Nanisivik Formation consists of wedges of pale, sand- to pebble-grade debris shed down the flanks of the defunct mounds, interfingering with dark Nanisivik Formation dololaminite. Although local evidence of basin-floor topography during deposition of the lowermost Nanisivik Formation is common, and local residual paleotopography of defunct Ikpiarjuk Formation mounds is associated with mound-flank debrite units in the upper part of the formation, there is no sedimentary evidence for a regional slope at any level of the formation (Turner, 2009, 2011). The Nanisivik Formation commonly emits a bituminous odour when freshly broken. Its abrupt upper contact with overlying shale of the lowermost Victor Bay Formation is unconformable, and although the contact is generally covered, core shows that the basal metre consists of angular clasts of reworked Nanisivik Formation embedded in black shale (Fig. 16e). At a map scale, the upper contact of the Nanisivik Formation is undulatory, with relief of at least 250 m; the undulatory surface is locally offset by small grabens filled with lowermost Victor Bay Formation shale, which produced a stratigraphic-structural phenomenon controlled the distribution of mineralization at Nanisivik and at least one other major showing (Turner, 2011).

The abrupt, conformable basal contact is interpreted to record a sudden, probably tectonically influenced change in basin conditions from sediment-starved, organic-rich, anoxic black shale to sediment-starved, organic-lean, anoxic pelagic carbonate, perhaps as the preceding lacustrine system was breached and a partial marine connection was re-established. Localized soft-sediment deformation and siliciclastic sediment-gravity deposits interfingered with dololaminite in the lower approximate 100 m of the formation attest to localized paleotopographic relief on the basin floor and residual tectonic instability in the vicinity of northwest-trending intragraben faults (Turner, 2003, 2009) during deposition of the earliest part of the Nanisivik Formation. Local contribution of Ikpiarjuk Formation mound clasts at the formation base and in the upper part of the formation indicate that their relief persisted during Nanisivik Formation deposition. This monotonous, noncyclic formation contains no evidence of a hydrodynamic position above storm wave-base or of benthic microbial communities; it is interpreted as a deep-water laminite deposited on a regionally flat basin floor as a result of water-column carbonate precipitation with periodic (perhaps annual) influxes of minute amounts of eolianterrigenous clastic material that define the characteristic lamination of the formation (Turner, 2009). Although the basin floor of the northwestern Milne Inlet Graben was low-energy, subphotic, regionally flat, and anoxic, its configuration, which was at least partly restricted and apparently had small fetch, produced seemingly 'deep'-water, low-energy, subphotic conditions in what was comparatively 'shallow' water adjacent to the Angmaat Formation carbonate platform. Distinctive, noncyclic lithofacies of the Nanisivik Formation interfinger with lithofacies of the decametre-scale cyclic lower Angmaat Formation in outcrop on 'Tremblay peninsula', attesting to the contemporaneity of these two paleoenvironmentally contrasting units.The upper contact of the Nanisivik Formation is a dramatic subaerial unconformity with paleotopographic relief of at least 250 m, produced by uplift, exposure, and tilting to the northeast. Previous interpretations of Nanisivik Formation dololaminite attributed its pervasive lamination to carbonate deposition in shallow subtidal microbial mats (Geldsetzer, 1973; Jackson and Iannelli, 1981), and its synsedimentary brecciation to deep karstification (Geldsetzer, 1973); these conclusions have since

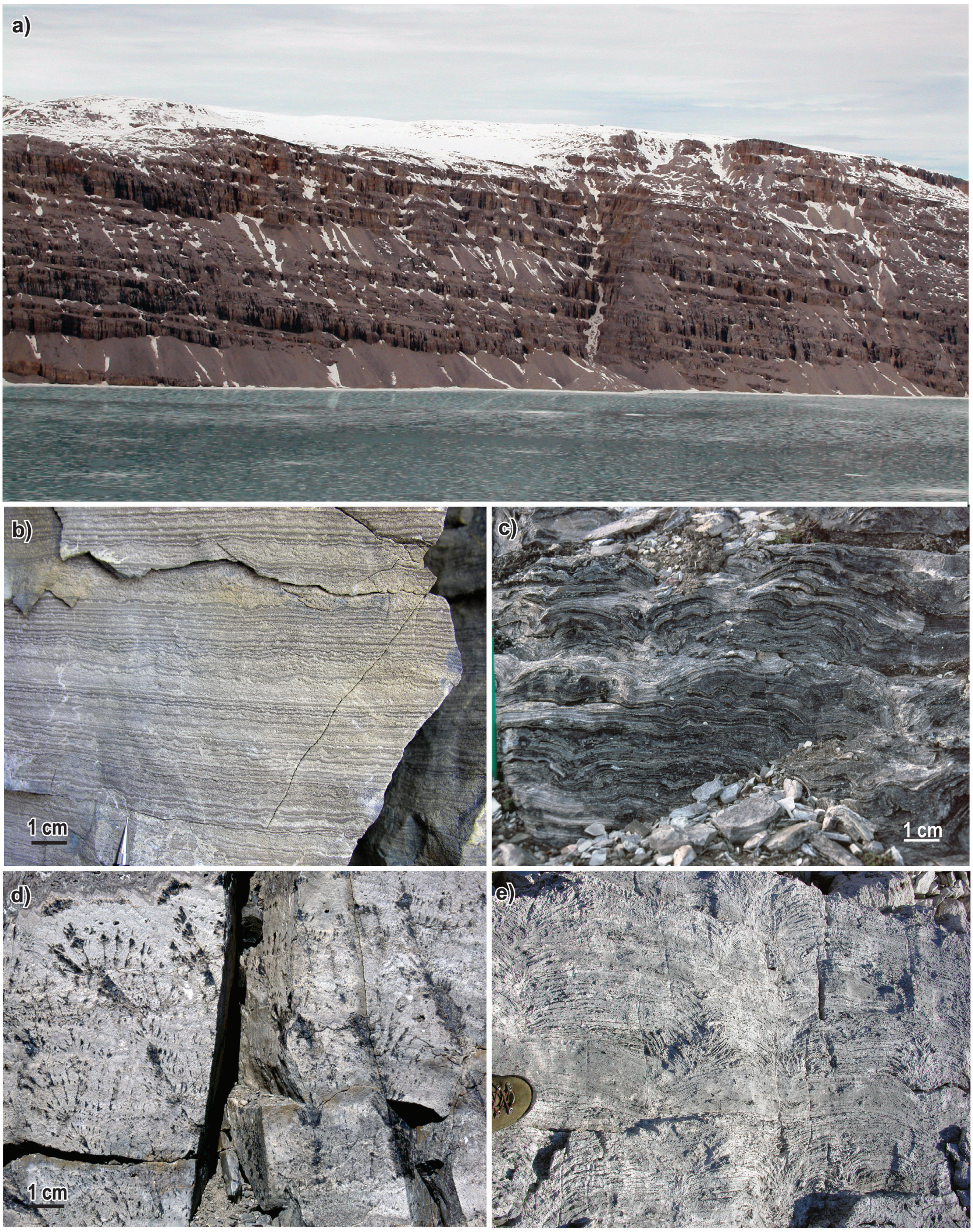

Figure 11. Exposures and lithofacies of the Angmaat Formation. **a)** Angmaat Formation cycles on west side of Tremblay Sound; cliff is about 400 m high. NRCan photo 2019-564. **b)** Subtidal microbial laminite of lower cycle halves in platform interior. NRCan photo 2019-565. **c)** Silicified isopachous seafloor precipitates ('abiogenic stromatolites') are ubiquitous in platform interior (Angmaat Mountain). NRCan photo 2019-566. **d)** Lightly silicified aragonite dendrites in platform interior (Angmaat Mountain). NRCan photo 2019-567. **e)** Tepees of upper halves of platform margin cycles (Tremblay Sound; boot for scale is 10 cm wide). NRCan photo 2019-568. All photographs by E.C. Turner.

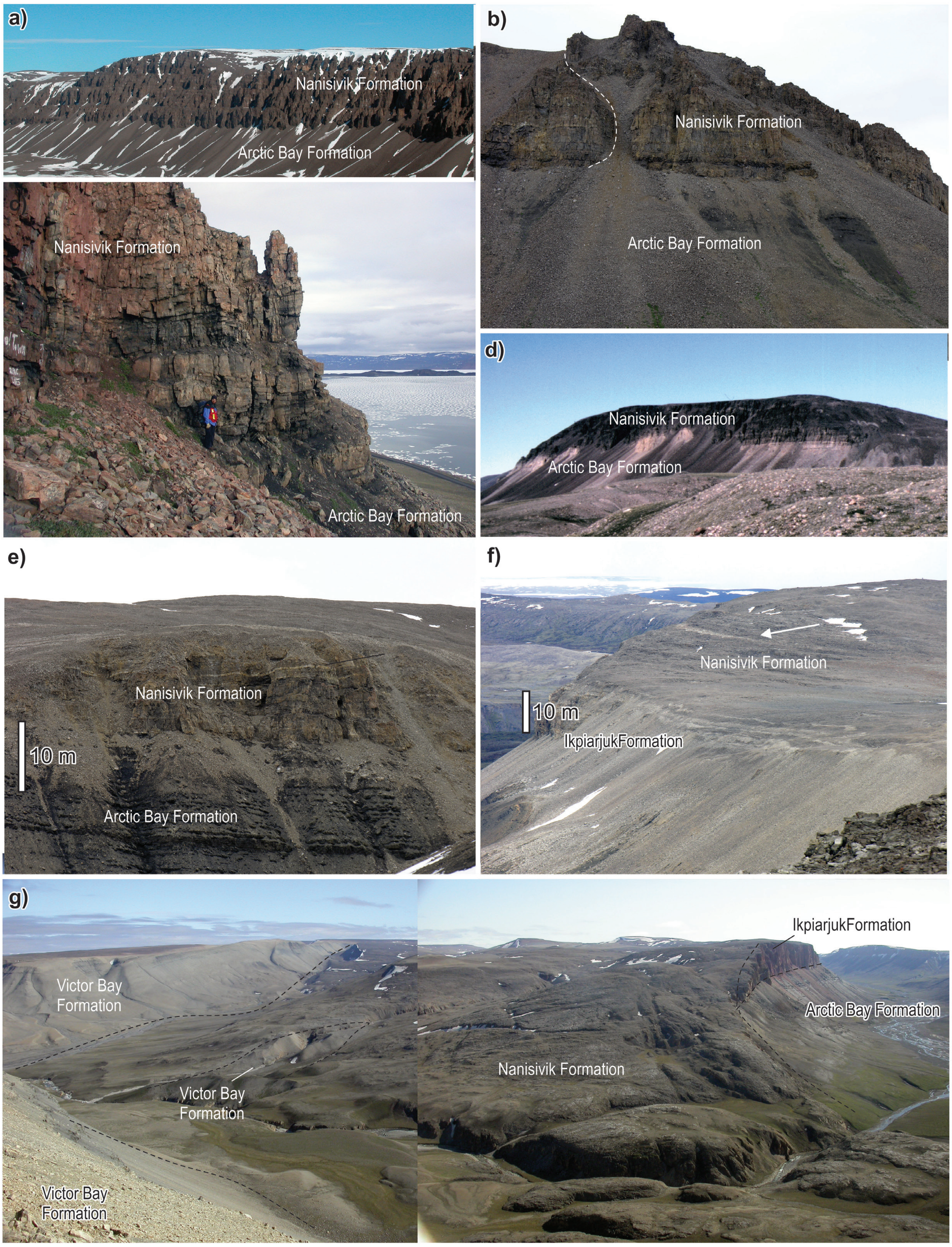

Figure 12. Exposures of the Nanisivik Formation. **a)** Typical dark-weathering exposures of Nanisivik Formation in upper Alpha River valley; about 125 m thick. NRCan photo 2019-569 **b)** Type section (dashed line) of Nanisivik Formation spans only the lowermost 100 m of the formation owing to generally poor exposure. NRCan photo 2019-570. **c)** Basal contact of Nanisivik Formation above Arctic Bay townsite, is gradational by interfingering. Person for scale is 2 m tall. NRCan photo 2019-571. **d)** Locally, the basal few metres of the Nanisivik Formation consist of distal mound facies of the Ikpiarjuk Formation, as seen here at Magda Lake. Exposure is about 100 m thick. NRCan photo 2019-572. **e)**, **f)** The lowermost Nanisivik Formation locally contains thin wedges of coarse siliciclastic dolowacke (arrow). NRCan photo 2019-573, 2019-574. **g)** Relationships among Nanisivik Formation and its stratigraphic neighbours at 'Red Rock valley'–Chris Creek area (view to southeast), highlighting the pinching out of Ikpiarjuk Formation and irregular, unconformable contact of Nanisivik and Victor Bay formations. field of view is 5 km wide. NRCan photo 2019-575, 2019-576. All photographs by E.C. Turner.

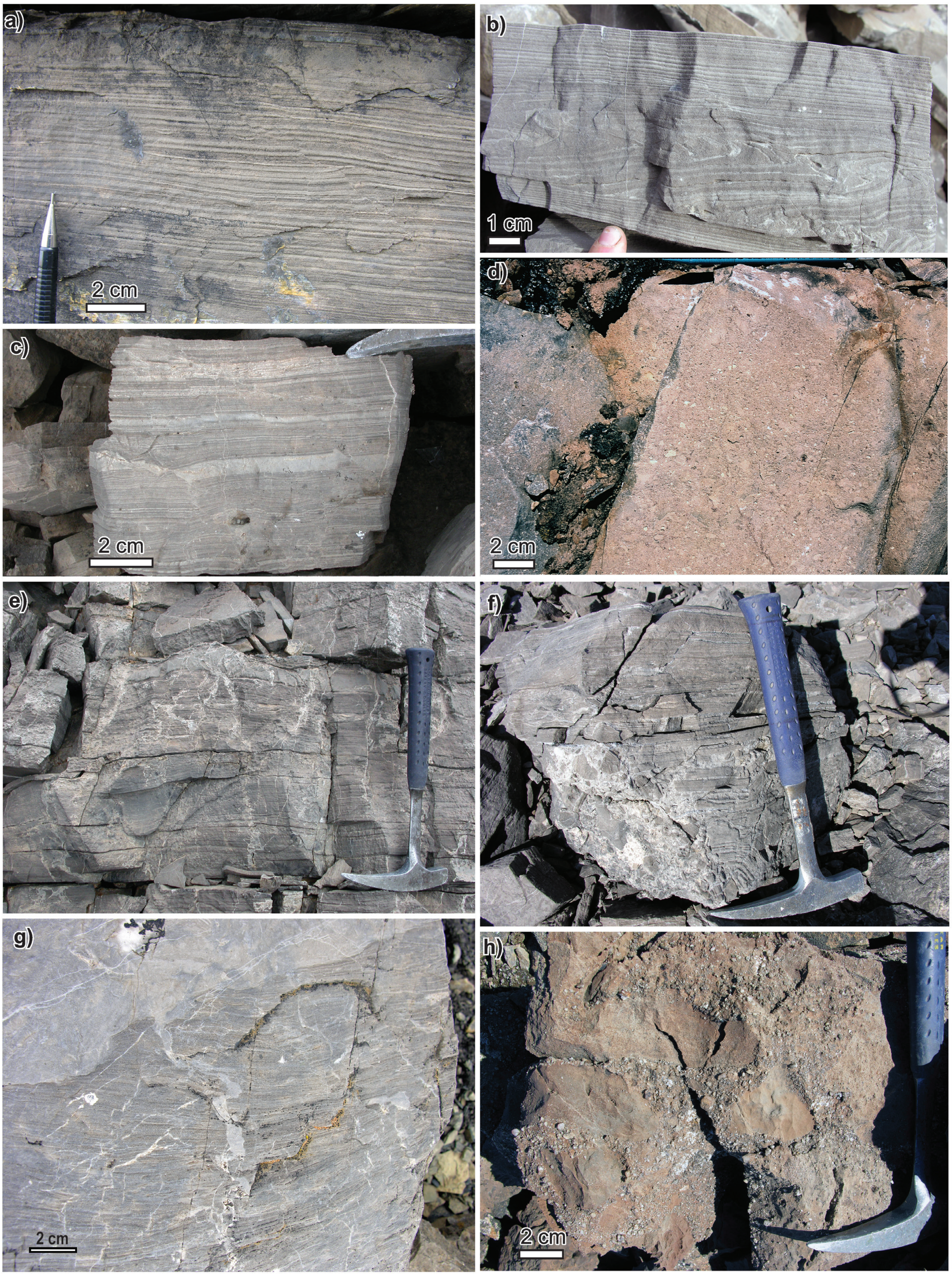

Figure 13. Lithofacies of the Nanisivik Formation. **a)** Typical lithofacies of the Nanisivik Formation is brown submillimetre-scale laminated dolostone. NRCan photo 2019-577. **b)** Near the base of the formation, soft-sediment folds are common. NRCan photo 2019-578. **c)** Healed synsedimentary microfaults are locally common. NRCan photo 2019-579. **d)** At the flanks of upper Ikpiarjuk Formation, mounds are thick wedges of granule- to pebble-grade carbonate debris that interfinger with Nanisivik Formation dololaminite. NRCan photo 2019-580. **e)** Several generations of crackle breccia are commonly present; syndepositional, diagenetic, and mineralization-related breccia types can be difficult to distinguish in the field when they are all occluded by dolospar; hammer is 32 cm long. NRCan photo 2019-581. **f)** Local rubble breccia fabric is variously interpreted as early (synsedimentary) or late. Hammer is 32 cm long. NRCan photo 2019-582. **g)** Locally, breccia interstices are filled with dolomudstone, indicating that breccia fracture systems had formed in lithified laminate whereas dolomud remained unlithified and could infiltrate the voids. NRCan photo 2019-583. **h)** In the vicinity of terrigenous debrite wedges, breccia interstices are filled with terrigenous dolowacke, indicating that lithification and brecciation of dolostone took place under minimal burial. NRCan photo 2019-584. All photographs by E.C. Turner.

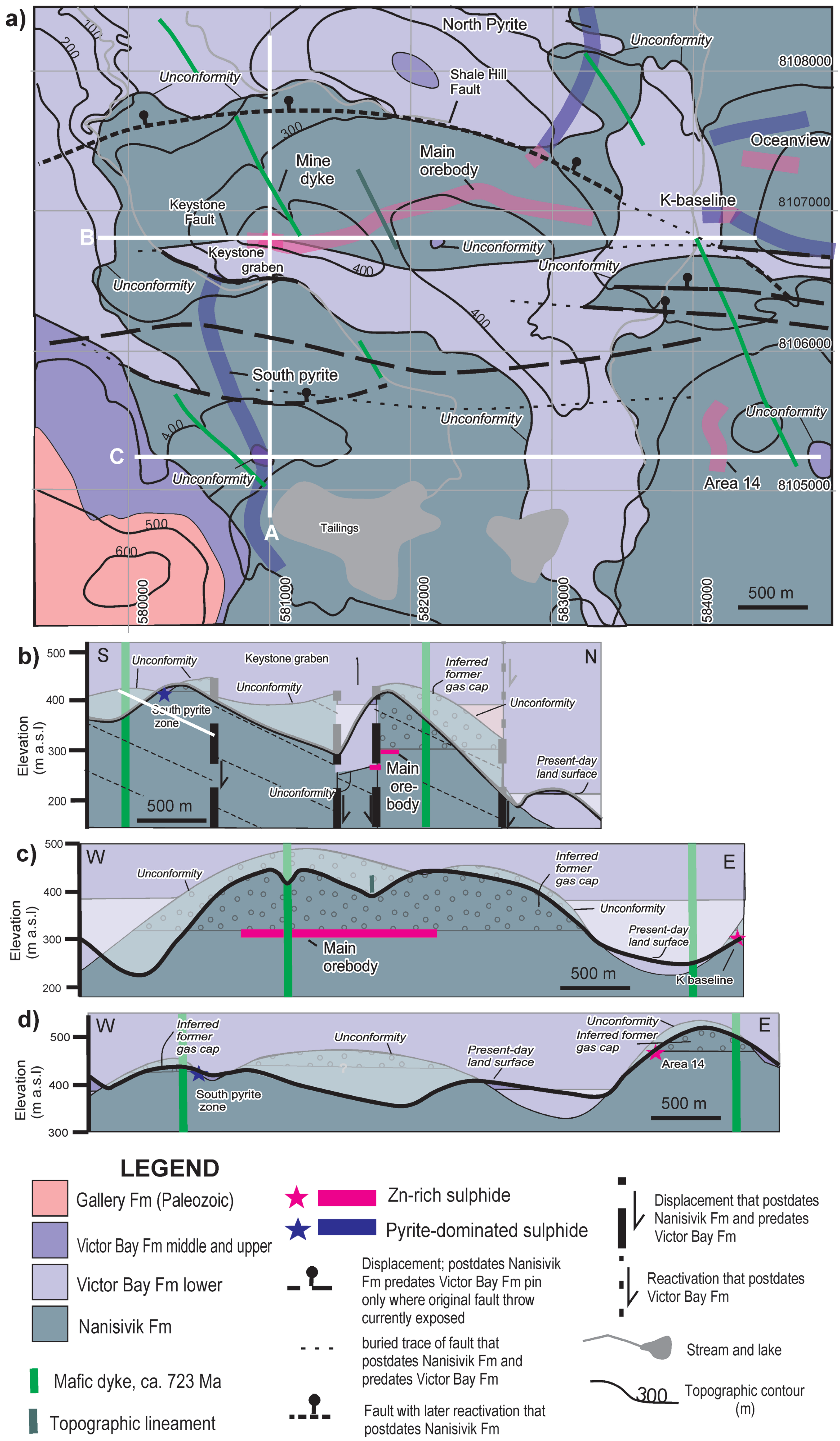

Figure 14. Geological map and cross-sections of the Nanisivik area illustrating undulatory unconformity between Nanisivik and lower Victor Bay formations, incremental filling of minor grabens formed after the unconformity by successive parts of the lower Victor Bay Formation, and the stratigraphically and structurally constrained position of the Nanisivik orebody. *After* Turner (2011).

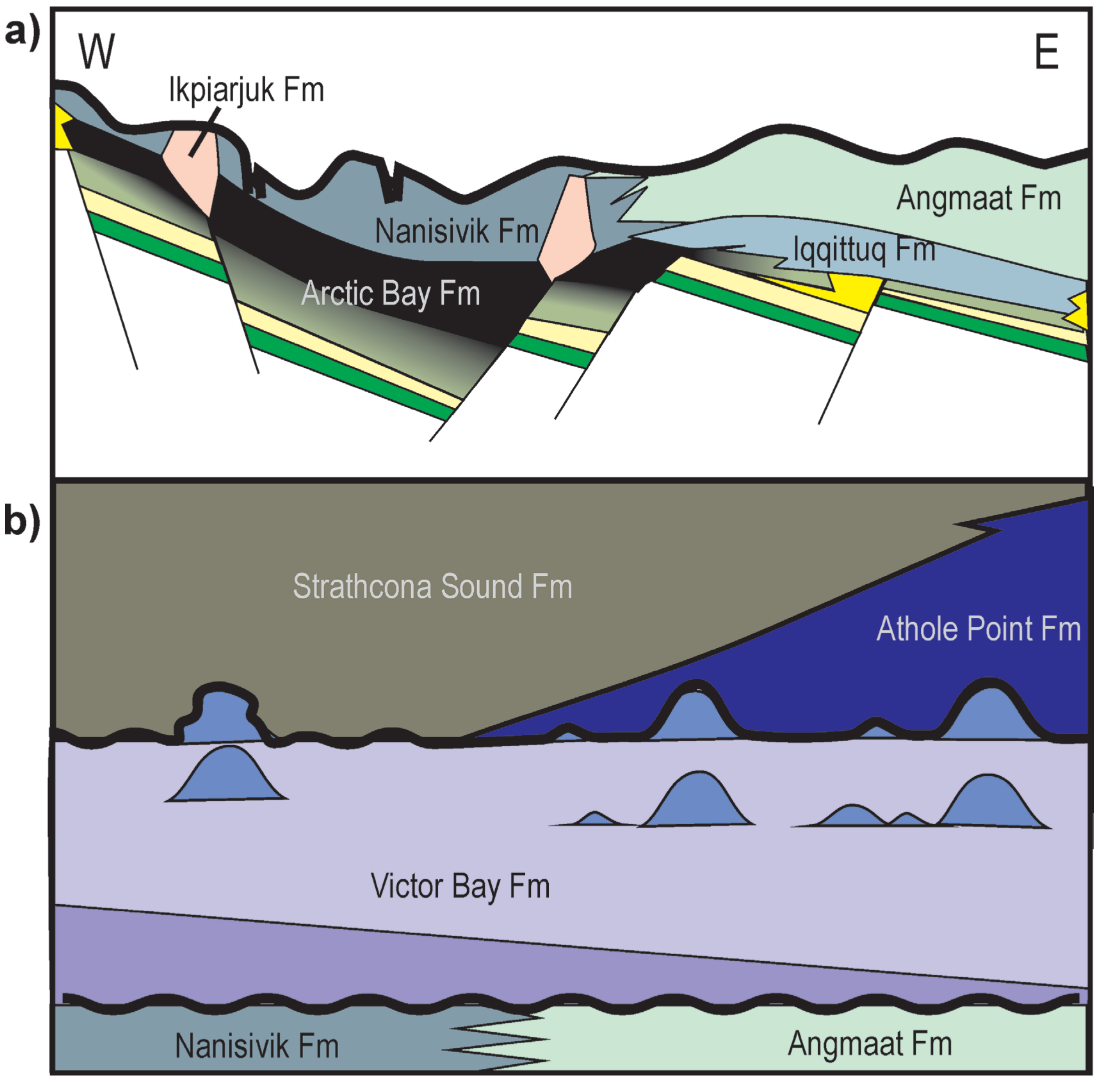

Figure 15. Diagrammatic cross-sections to illustrate two important internal unconformities (thick, wavy black lines) of the Bylot Supergroup. **a)** The unconformity at the top of the Nanisivik Formation and the laterally equivalent Angmaat Formation was produced by uplift and tilting to the northeast, and developed erosional topography of hundreds of metres as well as minor normal faulting postdating the unconformity (*after* Turner et al., 2016). **b)** The unconformity at the top of the Victor Bay Formation was produced by uplift in the west and contemporaneous subsidence in the east, producing karstification of the Victor Bay Formation in the west, but drowning of the Victor Bay Formation (recorded by overlying Athole Point Formation) in the east (*after* Sherman et al., 2002). Victor Bay Formation locally thins to zero in the west (at Elwin Inlet and Victor Bay; not depicted in this diagram).

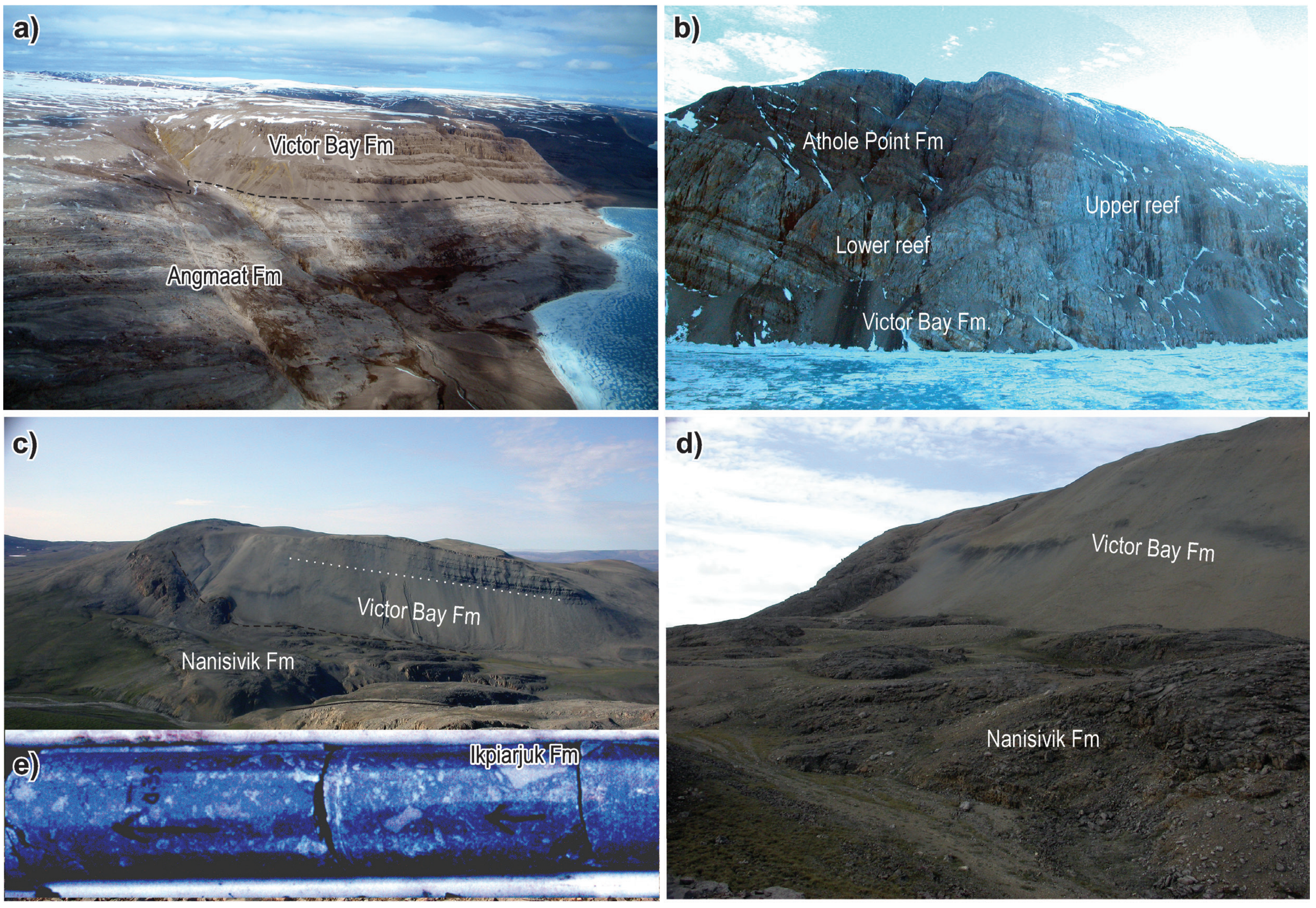

Figure 16. Exposures of the Victor Bay Formation. **a)** Unconformable contact of Angmaat Formation platform-rimming tepee cycles with basal shale of the Victor Bay Formation on west side of Tremblay Sound. Sea cliffs are approximately 400 m high. NRCan photo 2019-585. **b)** A Victor Bay Formation reef is flanked by Athole Point Formation at White Bay (eastern part of Milne Inlet Graben). Exposure is approximately 300 m high. NRCan photo 2019-586. **c)** Victor Bay Formation sharply overlies irregular unconformity surface atop Nanisivik Formation at 'Red Rock valley'. Victor Bay Formation strata in this exposure are approximately 150 m thick. NRCan photo 2019-587. **d)** Close view of 16c showing exhumed irregularity of top of Nanisivik Formation and sharp contact with basal Victor Bay Formation shale. Victor Bay Formation strata in this exposure are approximately 150 m thick. NRCan photo 2019-588. **e)** Part of Nanisivik mine exploration core 98-03, from north side of Strathcona Sound, showing base of Victor Bay Formation containing angular clasts of Nanisivik Formation dolostone. This important contact is never naturally exposed because it is always covered by shale of the overlying basal Victor Bay Formation. Stratigraphic up is to left; core is approximately 5 cm in diameter. NRCan photo 2019-589. All photographs by E.C. Turner.

been disproven on the basis of extensive field, petrographic, and analytical evidence, described above, depicting a subphotic, anoxic, low-energy, subaqueous depositional environment, lacking evidence of evaporite minerals, syndepositional exposure surfaces, or meteoric karstification associated with the upper surface of the formation.

The extremely variable preserved thickness of the formation (0 to (inferred) more than 500 m; Jackson and Iannelli, 1981) is a function of the presence or absence of underlying mound lithofacies of the Ikpiarjuk Formation (Nanisivik Formation dololaminite flanks, encloses, and locally thinly overlies the defunct upper parts of mounds); geographic location within syndepositional subgrabens of the basin system, which subsided differentially during Nanisivik Formation deposition; and location relative to paleotopographic highs and lows of the subaerial, erosional landscape that developed after deposition of the Nanisivik and Angmaat formations, but prior to deposition of the Victor Bay Formation.

The upper contact of the Nanisivik Formation, like that of the Angmaat Formation, is a regionally irregular, angular unconformity, as demonstrated by field mapping (Fig. 12, 14, 15; Turner, 2011). Although the unconformity surface is broadly undulatory, reflecting a hilly exposure surfact postdating Nanisivik Formation deposition, there is little to no evidence of karstic dissolution below the unconformity surface. This observation is compatible with other roughly contemporaneous evidence of aridity (e.g. evaporate units in the Iqqittuq Formation and seafloor precipitates in the Angmaat Formation; negligible delivery of siliciclastic material beyond graben margins in both Angmaat and Nanisivik formations).

The Nanisivik Formation hosts the past-producing Nanisivik Zn deposit and most of the known Zn-Pb showings in the Borden Basin, in specific stratigraphic positions (*see* below; Turner, 2011).

Victor Bay Formation

The Victor Bay Formation (Fig. 16; Blackadar, 1956) has a problematic original type section, at the head of Victor Bay, where no Victor Bay Formation strata are present. This formation is interpreted as a west-deepening, low-energy, decametre-scale cyclic, prograding muddy carbonate ramp (Sherman et al., 2000, 2001) characterized by normal marine features such as molar-tooth carbonate mudstone, centimetre-scale bedded and laminated carbonate mudstone, carbonate-clast rudstone, and stromatolite reefs. Its basal unit commonly consists of dark shale, but in the vicinity of recently active normal faults (northwestern part of Milne Inlet Graben), this earliest deposited component of the formation is absent on horsts, but present in adjacent grabens (Turner, 2011). Large stromatolite reefs (Narbonne and James, 1996; Sherman et al., 2000, 2002) are locally present, notably at the head of Strathcona Sound and near White Bay. The exposure area of the formation spans central Borden Peninsula (centre of Milne Inlet Graben), suggesting that the rift geometry that initially developed during deposition of the Arctic Bay Formation persisted until the end of Victor Bay deposition. Deposition of the Victor Bay Formation has been dated at 1046 ± 16 Ma (Re-Os; Gibson et al., 2018)

In the northwestern part of the Milne Inlet Graben, the Victor Bay Formation, including its reefs, is truncated by a karstified unconformity that resulted from an episode of differential uplift (west) and subsidence (central and east; Sherman et al., 2002). In the western part of both the Eclipse Trough (Fig. 15), and the Milne Inlet Graben, the Victor Bay Formation was completely removed during this episode of differential uplift, such that the Angmaat Formation or Nanisivik Formation is overlain by the Strathcona Sound Formation. This revised history resolves the puzzlement of earlier workers over the apparent absence of Victor Bay Formation in some westernmost locations (Blackadar, 1970; Geldsetzer, 1973); the seeming indistinguishability of Victor Bay Formation carbonate lithofacies from those of underlying strata in some locations (where in fact Victor Bay Formation is absent); and the difficulty of picking its upper formational contact in some northwestern areas, where slope carbonate–intraclast rudstone units of the Victor Bay Formation must be distinguished from unrelated carbonate-clast conglomerate units of basal Strathcona Sound Formation (Lemon and Blackadar, 1963; Blackadar, 1970). The previous confusion also highlights the complete absence of the Victor Bay Formation at its type locality: siliciclastic intervals containing carbonate-clast conglomerate beds (both Nanisivik and Victor Bay lithologies) and siltstone ascribed to the Victor Bay Formation at Victor Bay belong instead to the lowermost Strathcona Sound Formation, and directly overlie Nanisivik Formation dololaminite. The presence of lower Victor Bay Formation shale above the undulatory, locally block-faulted, unconformity that postdates Nanisivik Formation is critical to the development of Nanisivik-type sulphide bodies, because it acted as a permeability barrier (Fig. 14; Turner, 2011).

The history of the Victor Bay Formation started with flooding of low areas in an erosionally hilly, exposed region with local small grabens and horsts; widespread, poorly interlinked, sediment-starved low areas were sites of black shale accumulation (Turner, 2011). This earliest episode in Victor Bay Formation deposition has been interpreted as lacustrine (Gibson et al., 2019). Gradual development of a marine-connected, low-energy carbonate ramp ensued, with inner-ramp (molar-tooth carbonate mudstone; stromatolite reefs) and outer-ramp to slope (northwestern ribbon carbonate mudstone and associated intraclast rudstone) zones (Sherman et al., 2000, 2001) and local very large reefs (Narbonne and James 1996). Although the presence of decametre-scale cycles suggests glacioeustatic forcing (Sherman et al., 2001), an interpretation that should also apply to the thick cycles of Angmaat Formation (Turner, 2009), no glaciation is known in the late Mesoproterozoic. Compression and tilting caused uplift, erosion, and karstification in the western end of the graben, producing one of the two major unconformities in the Bylot Supergroup, but deepening and continued carbonate deposition in the central and eastern parts (Fig. 15; Sherman et al., 2002). Complete removal of Victor Bay Formation strata took place locally in the northwestern Milne Inlet Graben (e.g. at Victor Bay and Elwin Inlet); locally, resedimented carbonate clasts derived from the Victor Bay Formation are preserved in the lowermost Strathcona Sound Formation, for example at Victor Bay, where no Victor Bay Formation strata are preserved.

Athole Point Formation

The Athole Point Formation (Fig. 16b; Blackadar, 1970; no designated type section) is a 0 to approximately 585 m thick succession of thin-bedded, mixed carbonate mudstone and fine-grained, calcareous siliciclastic rocks present southeast of eastern Borden Peninsula. The formation conformably overlies upper Victor Bay Formation strata in an area (central to southeastern Milne Inlet Graben) where syndepositional tilting produced pronounced deepening as opposed to uplift and exposure (as in northwestern Milne Inlet Graben; Sherman et al., 2002). Although carbonate-clast debrite units are locally present at the base of the formation, it is otherwise dominated by calciturbidite-like graded beds and intraclast rudstone, with local shallow-water features such as microbialites (Jackson and Iannelli, 1981). The upper contact of the formation with the Strathcona Sound Formation is described as gradational. Sherman et al. (2002) interpreted this formation to record tilting and reversal of basin polarity (eastward deepening accompanied by western exposure, which contrasts with westward deepening that prevailed through most of the underlying stratigraphic units) as a result of an unknown far-field stress.

Strathcona Sound Formation

The Strathcona Sound Formation (Fig. 17; Blackadar, 1956; Lemon and Blackadar, 1963; no designated type section) is a thick (as much as 900 m; Jackson and Iannelli, 1981), coarsening-upward siliciclastic succession exposed across central and northern Borden Peninsula (Fig. 1). This unit conformably overlies the Athole Point Formation where the latter is present, and otherwise unconformably overlies the Victor Bay Formation (or Angmaat Formation, where Victor Bay Formation strata are completely absent; Fig. 15, 17a); its contact relationship with the Athole Point Formation is characterized as gradational (Jackson and Iannelli, 1981). Jackson and Iannelli (1981) described an array of six interfingering lithofacies assemblages composing six mappable members (SS1–SS6) that have complex geographic distributions related to their respective proximity to syndepositionally active normal and reverse faults. The lower members of the formation locally contain carbonate-clast conglomerate units and olistolith units shed from exposed, uplifted areas of underlying carbonate formations, as well as stromatolitic carbonate, but much of the formation is dominated by dark green-grey- and red-weathering graded siltstone beds of all scales, locally with carbonate-boulder talus deposits in the lower part of the formation, and by graded arkose, wacke, and conglomerate beds in the upper part (Jackson and Iannelli, 1981). Paleocurrent data exhibit no predominant transport direction.

The sedimentological information from the six contrasting members of the Strathcona Sound Formation collectively points to a complex array of alluvial, supratidal, intertidal, lacustrine, shallow-subtidal, and slope environments that developed under an unstable tectonic regime (Jackson and Iannelli, 1981). The formation was interpreted by Jackson and Iannelli (1981) to record the accumulation of alluvial fan complexes and associated shallow-marine sediment on the northern margin of the Milne Inlet

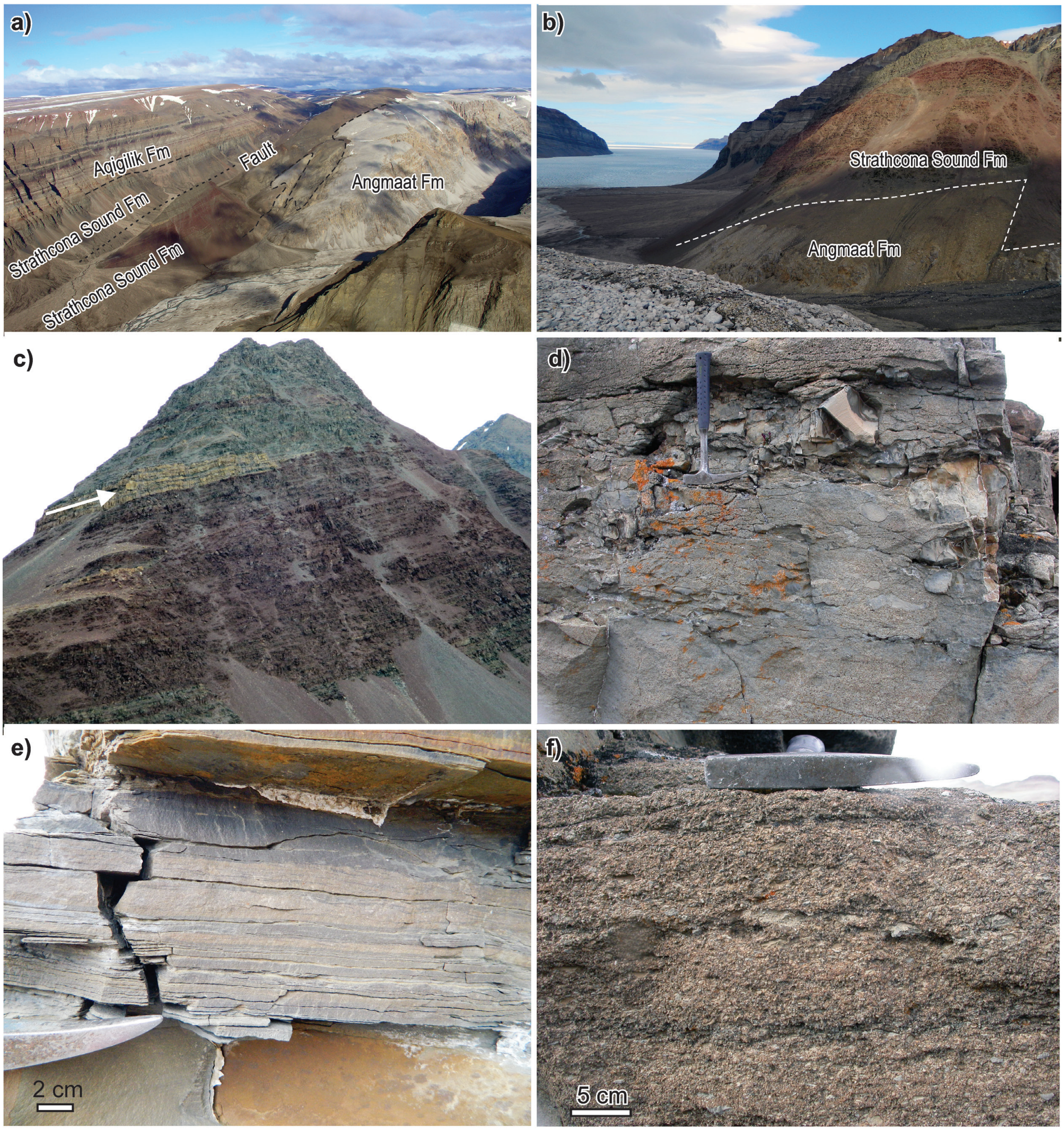

Figure 17. Exposures and lithofacies of the Strathcona Sound Formation. **a)** Strathcona Sound Formation unconformably overlies Angmaat Formation on east side of Elwin Inlet. Field of view is approximately 3 km wide. NRCan photo 2019-590. **b)** Unconformable basal contact of Strathcona Sound Formation on Angmaat Formation at Elwin Inlet. Exposure in foreground is approximately 200 m high. NRCan photo 2019-591. **c)** Lower Strathcona Sound Formation with wedge of dolostone cobbles (arrow) shed from irregular unconformity surface at Elwin Inlet. Exposure is approximately 100 m thick. NRCan photo 2019-592. **d)** Wedge of cobble-sized dolostone debris interfingers with lower Strathcona Sound Formation siltstone at Elwin Inlet. Hammer is 32 cm long. NRCan photo 2019-593. **e)** Typical thin, subtly graded beds of very fine-grained sandstone-siltstone in the upper Strathcona Sound Formation at Elwin Inlet. NRCan photo 2019-594. **f)** Basal Strathcona Sound Formation at Victor Bay consists of carbonate-clast conglomerate with sandy matrix, together with various siltstone units and dolomitic sandstone. NRCan photo 2019-595. All photographs by E.C. Turner.

Graben during uplift of the adjacent Navy Board High. In contrast, Knight and Jackson (1994) and Sherman et al. (2002) interpreted the formation to record locally complex faulting, pronounced deepening, and flysch-like sedimentation in response to inferred east-directed compression and basin inversion that terminated deposition of the Victor Bay Formation, together with renewed siliciclastic delivery after a lengthy episode of carbonate and shale deposition under arid conditions.

On the basis of detrital zircon geochronology and evidence of deep-water deposition in central Borden Peninsula, Turner et al. (2016) interpreted this formation to contain a terrigenous detrital component derived in part from the rising Grenville Orogen some 2000 km away, into a remote yet foreland-basin–like setting to which the newly developed, distant siliciclastic source delivered material first in deeper water (Strathcona Sound Formation), but then in progressively shallower marine environments (uppermost formations of the Bylot Supergroup). Although delivery of substantial terrigenous clastic material, some of it from a great distance, probably requires fluvial transport, no evidence of fluvial deposition has been noted in the Strathcona Sound Formation. Paleomagnetic data initially suggested a depositional age of ca. 1200 Ma (Fahrig et al., 1981), but this date is not compatible with more recent geochronological results for deposition of the older Arctic Bay and Victor Bay formations (Turner and Kamber, 2012; Gibson et al., 2018).

Aqigilik Formation

The Aqigilik Formation (Fig. 18; Knight and Jackson, 1994; type section north side of Elwin Inlet; up to 450 m thick), was established by subdivision of the Elwin Formation of Lemon and Blackadar (1963; type section at Elwin Inlet) into the Aqigilik and Sinasiuvik formations (Elwin Subgroup). This formation conformably overlies the Strathcona Sound Formation and is exposed only on northern Borden Peninsula. It consists of a diverse array of interlayered, thin-bedded units dominated by variably coloured quartz arenite and red siltstone, and includes minor dolostone, with abundant planar- and crosslamination, desiccation cracks, ripples, and local halite casts. Knight and Jackson (1994) established five members (AQ1–AQ5) and interpreted a succession of marine, braided fluvial, shoreface, and lagoonal environments, with sediment delivery predominantly from the west.

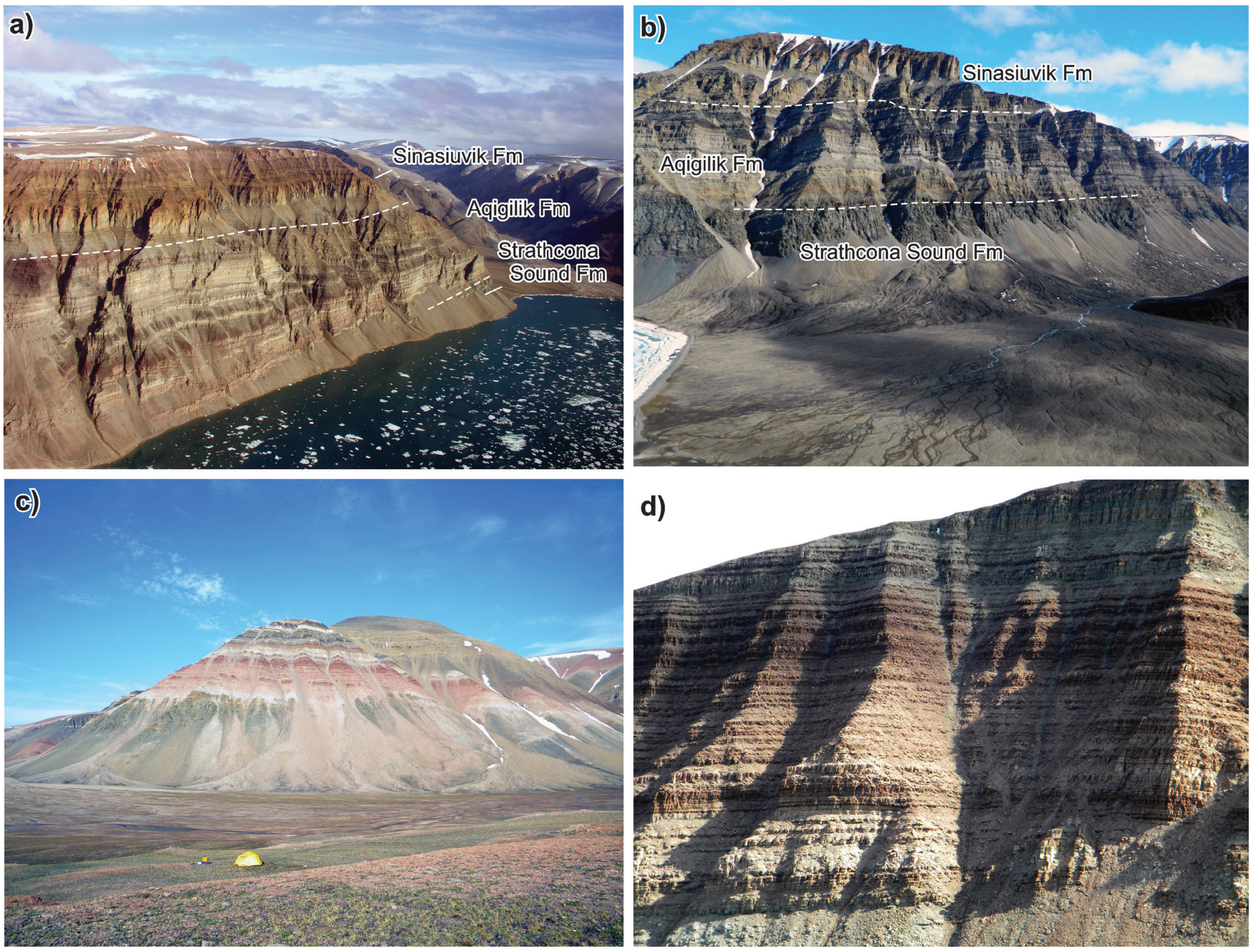

Figure 18. Exposures of the Aqigilik and Sinasiuvik formations. **a)** Type sections of Aqigilik and Sinasiuvik formations on east side of Elwin Inlet. Sea cliffs are 600 m high. NRCan photo 2019-596. **b)** Contact relationships among Strathcona Sound, Aqigilik, and Sinasiuvik formations, east side of Elwin Inlet. Exposure is approximately 600 m high. NRCan photo 2019-597. **c)** Aqigilik Formation exposure, Charles Yorke River (central Borden Peninsula). Hill in centre is approximately 400 m high. NRCan photo 2019-598. **d)** Typical tabular, laterally continuous bedding of the Aqigilik Formation, Charles Yorke River (central Borden Peninsula). Approximately 150 m of strata are depicted. NRCan photo 2019-599. All photographs by E.C. Turner.

Sinasiuvik Formation

The Sinasiuvik Formation (Fig. 18; Knight and Jackson, 1994; up to 620 m thick; type section north side of Elwin Inlet), the upper part of the abandoned Elwin Formation, gradationally overlies the Aqigilik Formation on northern Borden Peninsula. This formation is dominated by planar- and crossbedded pale quartz arenite and interbedded dark grey weathering syneresis-cracked mudstone. Knight and Jackson (1994) identify three successive transgressive members (cycles) and interpret this formation to record shallow-marine deposition, with sediment delivery from the east to northwest.

GEOCHRONOLOGY

Geochronological data constraining depositional ages of Bylot Supergroup strata are sparse. On the assumption that the basal Nauyat Formation basalt was part of the Mackenzie igneous event (Fahrig et al., 1981; Dostal et al., 1989), deposition of the Bylot Supergroup, and presumed correlative strata in the other Bylot basins, was bracketed between ca. 1267 Ma (age of Mackenzie mafic event; LeCheminant and Heaman, 1989) and 723 Ma (approximate age of Franklin mafic event dykes that crosscut the succession; Heaman et al., 1992; Pehrsson and Buchan, 1999; Denyszyn et al., 2009). A depositional age close to the age of the Mackenzie event (1267 Ma) was based on paleomagnetic evidence for a Mackenzie pole throughout deposition of the entire stratigraphic succession (Fahrig et al., 1981). The Nauyat Formation has never been directly dated, however, and it remains uncertain whether the formation is temporally and depositionally related to the Mackenzie large igneous province (LIP) or the rest of the Bylot Supergroup. It is possible that eruption of Nauyat Formation volcanic material was followed by a substantial depositional hiatus, based on the much younger ages recently obtained from overlying strata (*see* below).

Depositional ages for black shale of the Arctic Bay Formation (1092 ± 59 Ma, U-Pb-Th whole-rock black shale, Turner and Kamber, 2012; 1048 ± 12 Ma, Re-Os black shale, Gibson et al., 2018) and Victor Bay Formation (1046 ± 16 Ma; Re-Os black shale; Gibson et al., 2018) are internally consistent and indicate that deposition was considerably younger than previously thought. The lack of a direct depositional age for the Nauyat Formation and the unexpectedly young depositional age of the Arctic Bay and Victor Bay formations point to the possibility that the Nauyat Formation was not related to the Mackenzie igneous event and may have a younger depositional age (Turner et al., 2016). If the Nauyat Formation is truly as old as 1267 Ma, a substantial hiatus must be present between its deposition and that of the Arctic Bay Formation — a hiatus following deposition of either the Nauyat Formation basalt or sandstone of the overlying Adams Sound Formation.

Detrital zircon U-Pb age spectra for units in the lower part of the supergroup are consistently dominated by Archean and Paleoproterozoic cratonic sources, but Grenville-aged detrital zircon appears in strata that overlie the unconformity at the top of the Victor Bay Formation, and becomes more prominent upward, strongly suggesting that deposition of the upper part of the supergroup was coeval with incipient unroofing of the Grenville Orogen (Rainbird et al., 2012; Turner et al., 2016).

TECTONOSTRATIGRAPHIC EVOLUTION

The work of Jackson and Iannelli (1981) interpreted the Borden Basin as one of several related rifts in the Bylot basins group, and correlated the respective successions of the basins based on a layer-cake–like stratigraphic interpretation and a continental rift (aulacogen) interpretation. Based on a substantial modern stratigraphic data set (Knight and Jackson, 1994; Sherman et al., 2002; Turner, 2009, 2011; Turner and Kamber, 2012; Long and Turner, 2012; Hahn et al., 2015; Hahn and Turner, 2017) and detrital zircon geochronology (Turner et al., 2016), the tectonic history and depositional age of the basins has become clearer (Fig. 19).

Deposition of the Nauyat Formation was at least in part subaqueous (Long and Turner, 2012). Distribution and lithofacies of the Adams Sound Formation are not delimited by graben-bounding structures, but instead depict a broad, regional blanket of predominantly shallow-marine–dominated sandstone. Together, these two lowermost units depict a broad sag basin developed upon minimally extended continental crust. In contrast, distribution and lithofacies of the Arctic Bay, Fabricius Fiord, Iqqittuq, and Ikpiarjuk formations were strongly

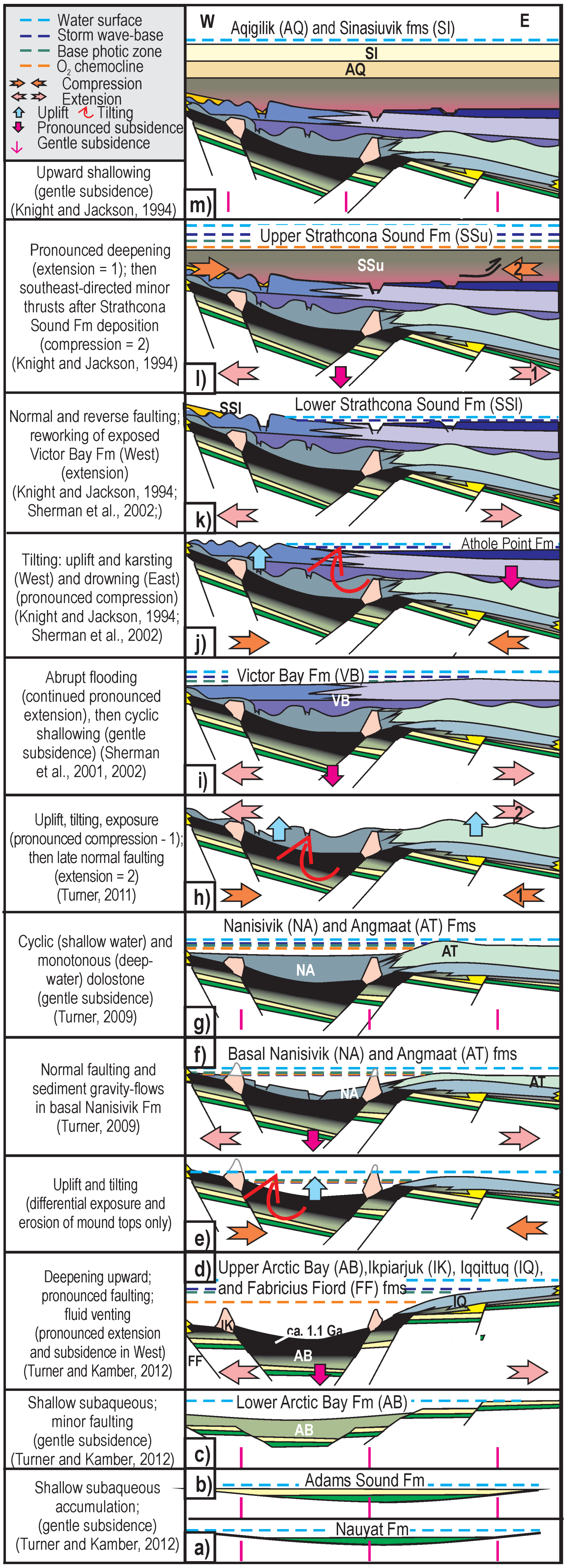

Figure 19. Tectonostratigraphic history of the Milne Inlet Graben (panels approximate west-east cross-sections; not to scale; *after* Turner et al. (2016) and previous work as indicated on left side of diagram). **a)** Nauyat Formation was deposited in a predominantly subaqueous setting in regional sag basin, possibly ca. 1270 Ma. **b)** Adams Sound Formation deposited in shallow-marine environment in a regional sag basin (timing unclear; less than 1270 Ma, more than 1100 Ma). **c)** Regional extension produced three rift-grabens of the Borden Basin; deposition of alluvial fan facies of Fabricius Fiord Formation at graben margins and sandstone cycles of the lower Arctic Bay Formation within grabens. **d)** Continued rapid subsidence in rifts produced upward fining to black shale in western Milne Inlet Graben. Ikpiarjuk Formation deep-water seep-mounds accumulated along intragraben faults surrounded by coeval black shale (ca. 1092 Ma or ca. 1048 Ma) of the upper Arctic Bay Formation and contemporaneous with Iqqittuq Formation carbonate ramp progradation in the eastern Milne Inlet Graben. **e)** Abrupt uplift and tilting exposed comparatively highstanding mound tops of Ikpiarjuk Formation, but not coeval strata of Arctic Bay Formation (deep-water shale) or Iqqittuq Formation ramp, and abruptly terminated delivery of fine clastic material. Ensuing dramatically modified, but conformably overlying seafloor strata accumulated **f)** and **g)** in an environment below the photic zone and below the storm-wave base (Nanisivik Formation; northwest), and a tectonically rimmed, low-energy, decametre-scale cyclic carbonate platform environment (Angmaat Formation; southeast). Nanisivik Formation surrounded and then buried defunct mounds of the Ikpiarjuk Formation. **h)** A second, more dramatic episode of uplift and tilting produced an unconformity surface with several hundred metres of topography. The uplift, tilting, and erosion was followed by extension that produced minor grabens and horsts that offset the unconformity surface. **i)** Extension and differential subsidence produced the carbonate ramp and deep-water basal shale of the lower Victor Bay Formation, which progressively filled the minor grabens that had locally offset the undulatory unconformity surface, followed by a prograding, low-energy carbonate ramp. **j)** A second major unconformity developed owing to a third episode of differential uplift and tilting, producing karstification in the west, but drowning (Athole Point Formation slope carbonate units) in the east. **k)** A poorly understood episode of normal and reverse faulting produced an irregular surface on which a wide range of depositional environments developed; some received detritus derived from the Grenville Orogen (lowest in lower Strathcona Sound Formation in northwest). **l)** Pronounced deepening allowed accumulation of monotonous deep-water siltstone-sandstone of the Strathcona Sound Formation, but was followed by compression and development of very localized thrust faults. **m)** Gradual shallowing and development of shallow-marine environments characterized the Aqigilik and Sinasiuvik formations.

controlled by the development of the rift geometry of the Bylot basins. The Fabricius Fiord Formation was deposited as graben-margin alluvial fans (Jackson and Iannelli, 1981). The laterally equivalent Arctic Bay Formation initially accumulated in coarsening-upward marine cycles in an overall fining-upward succession, and later transitioned to a black shale succession exhibiting widespread evidence of substantial syndepositional normal faulting on the basin floor. The upper Arctic Bay Formation black shale partially encloses deep-water carbonate seep mounds (Ikpiarjuk Formation) that accumulated in the vicinity of graben-floor faults; both Ikpiarjuk Formation and Arctic Bay Formation black shale are laterally equivalent to a prograding, northwestward-deepening shallow-water muddy carbonate ramp in the southeast (Iqqittuq Formation; Turner, 2009; Turner and Kamber, 2012; Hahn and Turner, 2017). A lacustrine setting for the Ikpiarjuk Formation based on REEY carbonate geochemistry (Hahn et al., 2015), implies that its lateral equivalents (upper Arctic Bay, Fabricius Fiord, and Iqqittuq formations) are also lacustrine, an interpretation that has been corroborated using radiogenic isotope chemostratigraphy (Gibson et al., 2019). A lacustrine interpretation for part of the Bylot Supergroup has profound implications for understanding the nature of the continental freeboard of Laurentia, which must have been minimal at least in the vicinity of the present-day Arctic Islands immediately prior to the Grenville Orogeny and assembly of Rodinia.

The presence of conspicuous rift grabens and their subbasins persisted during Arctic Bay Formation deposition and through to the beginning of uplift at the end of Victor Bay Formation deposition. Rift subsidence was interrupted twice by episodes of differential uplift and tilting, resulting in unconformities that separate: Angmaat-Nanisivik formations from the overlying Victor Bay Formation (uplift and tilting to the northeast resulted in a ubiquitous exposure surface with substantial paleotopography produced both by local horst-graben development and regional erosion into hills and valleys); and Victor Bay Formation from the overlying Strathcona Sound Formation (uplift, tilting, and karstification in the northwest; contemporaneous deepening in a southeastern marine setting of the Athole Point Formation). Each of these two exposure surfaces was followed by pronounced subsidence and resumption of sedimentation in the grabens; the repeated alternation of dramatic uplift (hundreds of metres) and tilting (compression) with rift-like subsidence (extension) suggests a tectonic setting more complex than that of an aulacogen (as inferred by Jackson and Iannelli (1981). The ensuing, gradually increasing and coarsening influx of siliciclastic sediment, starting with extraordinarily complex paleoenvironments of the predominantly deep-water Strathcona Sound Formation, and shallowing upward to deposition of shallow-marine Aqigilik and Sinasiuvik formations, together with the inception of delivery of Grenville Orogen aged zircon during deposition of the Strathcona Sound Formation, led to the suggestion that the depositional history of the basin included three distinct episodes: a regional sag basin (Nauyat and Adams Sound formations); rift subsidence (Arctic Bay, Fabricius Fiord, Iqqittuq, Angmaat, Nanisivik, and Victor Bay formations); and a tectonostratigraphically complex but overall shallowing-upward episode (Athole Point, Strathcona Sound, Aqigilik, and Sinasiuvik formations). At least part of this tectonostratigraphic evolution may have been linked to evolving far-field stresses during development of the Grenville Orogen in eastern Laurentia (Turner et al., 2016).

Knowledge of the lengthy postdepositional history of the Borden Basin is limited to intrusion of crosscutting mafic dykes of the ca. 723 Ma Franklin swarm (Heaman et al., 1992; Pehrsson and Buchan, 1999; Denyszyn et al., 2009), deposition of as much as 1800 m of Paleozoic strata (Trettin, 1969), protracted, episodic reactivation of the northwest-trending, graben-bounding and intragraben, basement-rooted faults through to Cenozoic time, with local, minor fault-related folding (Jackson and Morgan, 1978), and local deposition of Cretaceous through Cenozoic strata. The Mesoproterozoic to Cenozoic movement of various crustal fluids is documented not only in the latest Mesoproterozoic emplacement of the Nanisivik Zn orebody and geographically related base-metal showings (Hnatyshin et al., 2016), but also in various diagenetic (Hahn et al., 2018) and alteration (Sherlock et al., 2004) minerals.

PALEOBIOLOGY

Hofmann and Jackson (1991, 1994) reported a diverse assemblage of organic-walled microfossils derived from most formations in the Bylot Supergroup and representing planktonic prokaryotic and eukaryotic organisms. Kah and Knoll (1996) presented a prokaryotic benthic microbiota from chert in the Angmaat Formation. Knoll et al. (2013) reported the multicellular red alga *Bangiomorpha pubescens* from Angmaat Formation chert; the first report of this oldest known crown-group eukaryote was from putatively correlative strata of the Hunting Formation (Aston-Hunting Basin, Somerset Island; Butterfield et al., 1990; Butterfield, 2000).

Microbialite lithofacies reported from the Milne Inlet Graben include interflow stromatolites in Nauyat Formation basalt (Long and Turner, 2012), microbial laminite and domal-columnar stromatolites from the Iqqittuq Formation (Turner, 2009), deep-water seep-mound thrombolites of the Ikpiarjuk Formation (Turner, 2009; Hahn and Turner, 2017), microbial laminite from the lower halves of Angmaat Formation carbonate cycles (Turner, 2009), and microbial laminite, domal-columnar stromatolites, and stromatolite reef complexes of the Victor Bay Formation (Narbonne and James, 1996; Sherman et al., 2000, 2001, 2002). With the exception of thrombolites representing seep-mound chemotrophs reported from the Ikpiarjuk Formation (Turner, 2009; Hahn et al., 2015; Hahn and Turner, 2017), these microbial lithofacies are assumed to represent photosynthetic benthic microbial communities.

CORRELATION

The nature of any syndepositional connections among the Bylot basins remains unclear. Jackson and Iannelli (1981) attributed the Bylot basins to roughly synchronous development of repeatedly reactivated aulacogens during opening of a seaway ("Poseidon ocean") to the present-day northwest. Given new tectonostratigraphic, paleoenvironmental, and geochronological information from the Borden Basin, indicating deposition that was roughly contemporaneous with Rodinia assembly, and in view of Laurentia's central location in Rodinia, this interpretation has been revised as outlined above.

Although the Bylot basins (Borden, Aston-Hunting, Fury and Hecla, and Thule) have been correlated based on their geographic proximity and crudely similar lithostratigraphy (Fahrig et al., 1981; Jackson and Iannelli, 1981), and may have been linked, the true geographic and temporal relationships among the basins and their respective stratigraphic successions remain to be evaluated using firm criteria. Compounding the difficulty of comparing the basins is the fact that the Aston-Hunting and Fury and Hecla basins (if they are indeed separate basins) have received considerably less study than the Borden and Thule basins, and appear to contain less complete stratigraphic successions than the Borden Basin. Attempts to establish a regionally or globally correlatable chemostratigraphic scheme for the carbonate units of the Bylot Supergroup based on stable isotope geochemistry (Kah et al., 1999, 2001) have thus far met with limited success.

METALLOGENY

The past-producing Nanisivik zinc (-lead, ±silver) mine (Fig. 20, 21; 17.9 Mt at about 10% Zn+Pb; mined 1976–2002; Clayton and Thorpe, 1982; McNaughton and Smith, 1986; Arne and Kissin, 1989; Arne et al., 1991; Sutherland and Dumka, 1995) and most of the numerous, presumably related showings in the Milne Inlet Graben (Fig. 1, 22; Sangster, 1998; Scott and deKemp, 1998; Turner, 2011) are hosted by the Nanisivik Formation. Although early studies suggested that the Nanisivik deposit occupied a karstic void in the host dolostone (Geldsetzer, 1973; D.C. Ford, unpub. report, 1981; Olson, 1984; Ghazban and Ford, 1993), it later became clear that the characteristically banded ore (Fig. 21b, c) was deposited predominantly by a process of continued dissolution and precipitation along a surface between metalliferous fluid and reduced gas (Arne et al., 1991) trapped under paleo-highs in the unconformity separating Nanisivik Formation dolostone from overlying shale of the lower Victor Bay Formation (Fig. 14; Turner, 2011).

Although early fluid-inclusion work suggested an ore-forming temperature of 200°C and higher (McNaughton, 1983; McNaughton and Smith, 1986; Arne et al., 1987, 1991), which is unusually high for carbonate-hosted Zn deposits (Leach et al., 2005; Bodnar et al., 2014), more recent study yielded evidence of only low-temperature conditions of formation (Hnatyshin et al., 2016). Rhenium-osmium (Re-Os) dating of paragenetically constrained pyrite from Nanisivik and a nearby, related showing (Hawker Creek), produced an ore-forming age of 1093 ± 24 Ma (Hnatyshin et al., 2016), suggesting that ore-forming fluids were mobilized and ore precipitated during development of the contemporaneous Grenvillian Orogeny, assembly of Rodinia, and possibly even deposition of part of the upper Bylot Supergroup (Turner, 2011; Hnatyshin et al., 2016; Turner et al., 2016). This mineralization timing is compatible with previous results of both rubidium-strontium (Rb-Sr) dating of sphalerite ore (Christensen et al., 1993) and paleomagnetic dating of altered host rocks adjacent to the orebody (Symons et al., 2000; it is possible that

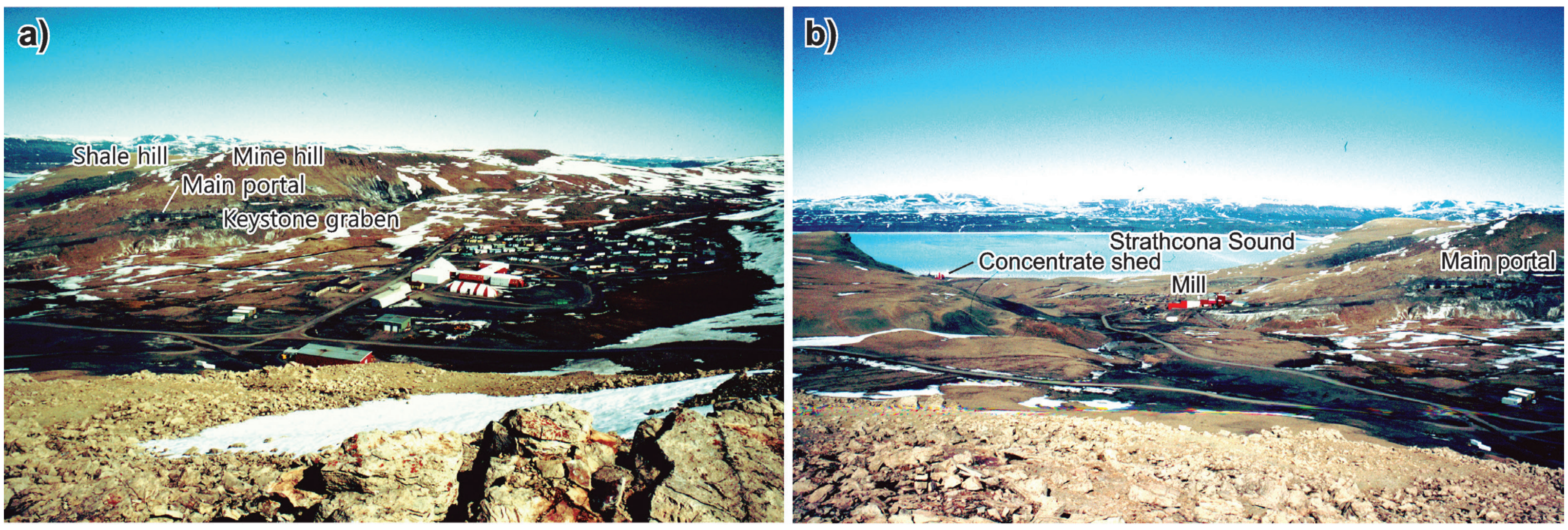

Figure 20. Nanisivik mine (1976–2002). **a)** Mine-site in 2001, one year before mine closure. Field of view is approximately 1 km wide. NRCan photo 2019-600. **b)** The road to the Nanisivik port on Strathcona Sound. Strathcona Sound (in background) is approximately 6 km wide. NRCan photo 2019-601. All photographs by E.C. Turner.

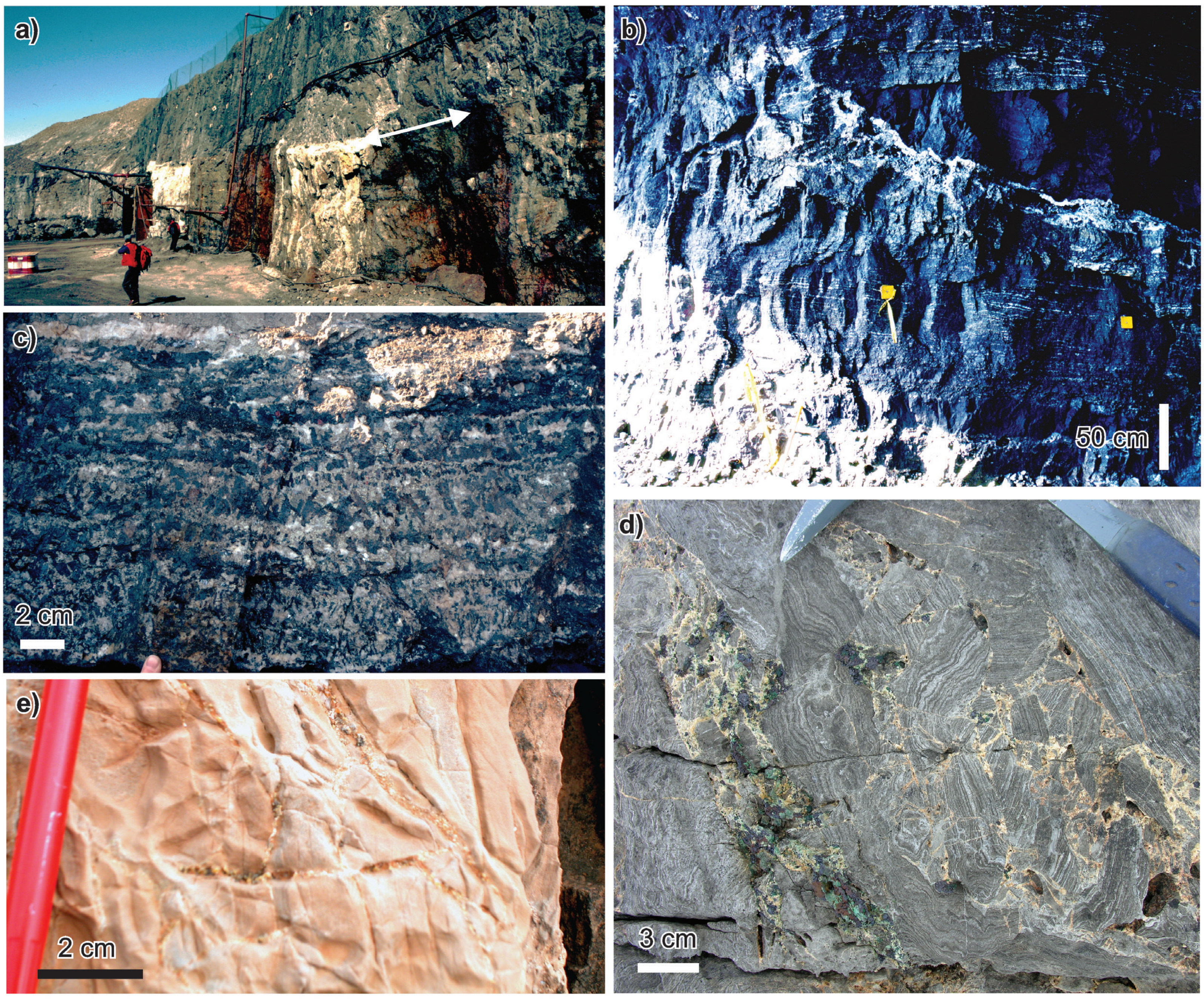

Figure 21. Characteristics of base-metal mineralization in the Milne Inlet Graben. **a)** The main portal at Nanisivik exposes the flat upper contact of the orebody (arrow); geologist is 2 m tall. NRCan photo 2019-602. **b)** Nanisivik ore is characterized by sharp contacts with host rock, and 'wings' of unaltered host rock that would be gravitationally improbable if the ore were karst-filling rather than replacive. Note dolomite spar forming at lower contact of the 'wing' at contact with characteristically banded ore (left and bottom of photo). NRCan photo 2019-603. **c)** Nanisivik ore is generally banded, like this example of sphalerite-pyrite-dolomite ore from the Oceanview pit. NRCan photo 2019-604. **d)** Showings in the Milne Inlet Graben typically consist of sulphide minerals (in this case copper-sulphide) and carbonate gangue in crackle breccia of the Nanisivik Formation. NRCan photo 2019-605. **e)** Material from an unusual showing near White Bay, in which pale sphalerite and gangue replaced the crack-fills of molar-tooth structure in the Iqqittuq Formation. NRCan photo 2019-606. All photographs by E.C. Turner.

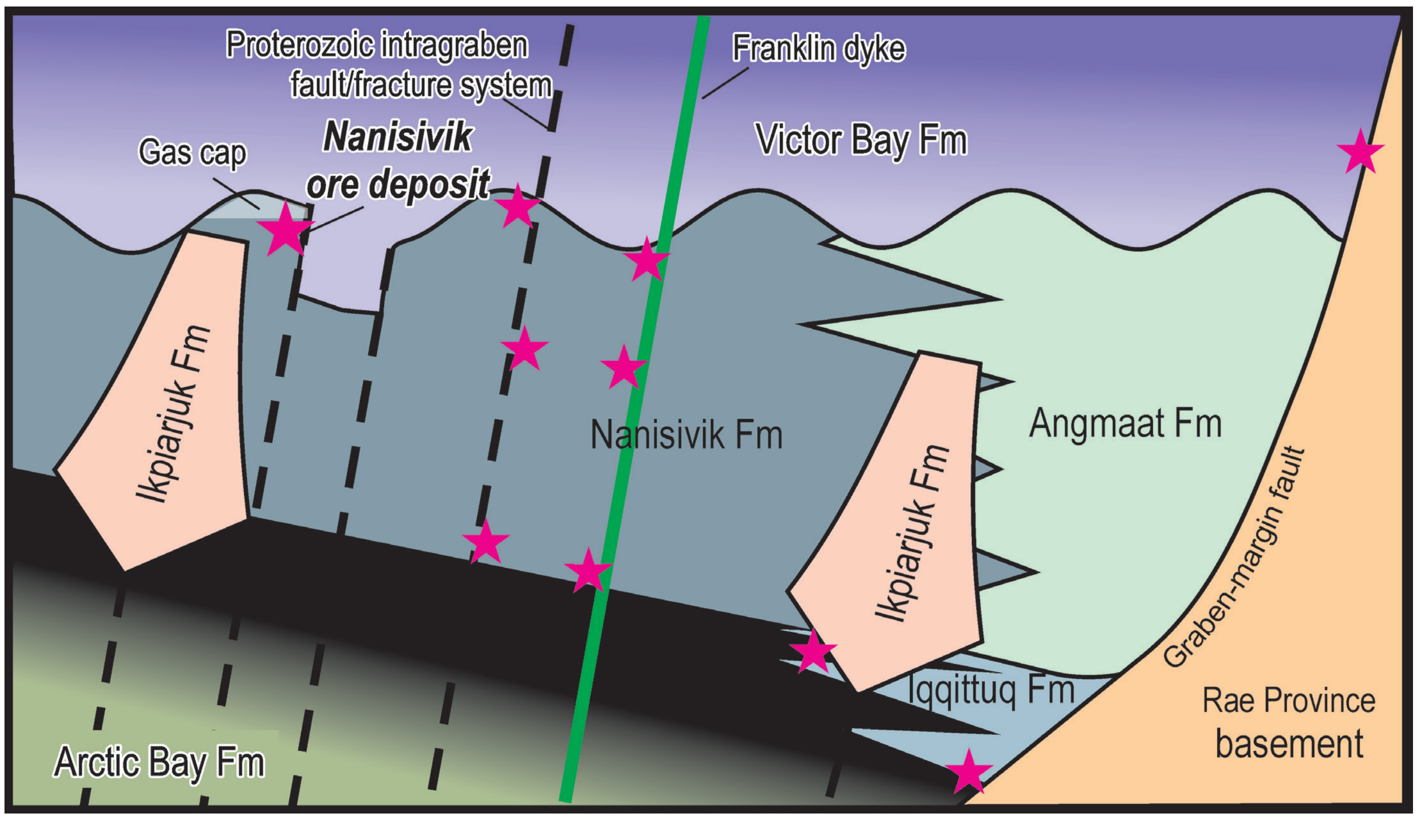

Figure 22. Stratigraphic and structural constraints on the spatial distribution of base-metal showings (stars) in the Milne Inlet Graben (*after* Turner, 2011).

this determination instead records a sedimentary depositional age). This date is also compatible with the U-Th-Pb depositional age of the Arctic Bay Formation black shale (within error; Turner and Kamber, 2012), but not with the slightly younger Re-Os depositional age determination from the Arctic Bay Formation (Gibson et al., 2018); some geochronological issues clearly remain to be resolved. The new Re-Os pyrite data set also highlighted later remobilization less than 413 Ma (Hnatyshin et al., 2016), which may reflect events similar or related to Ar-Ar geochronological data for ca. 462 Ma potassic alteration at the margin of a presumed Franklin mafic dyke that crosscuts the Nanisivik orebody (Sherlock et al., 2004). The events that caused Paleozoic metal and fluid remobilization and alteration remain unidentified, but their timing is approximately coeval with that of exposure intervals and evaporite deposition along the northern continental margin of Laurentia (Dewing et al., 2007, 2019) and may be associated with sinking and dispersal of early Paleozoic evaporitic brine.

The Nanisivik deposit is associated with a district containing numerous Zn, Pb, and rare Cu showings (Fig. 1; Sangster, 1998), most of which are in the Nanisivik Formation, and all of which have strong stratigraphic and structural constraints on their geographic and stratigraphic positions (Fig. 22; Turner, 2003, 2011).

ACKNOWLEDGMENTS

Many thanks to N. Bingham-Koslowski and R. Rainbird for critically reviewing the manuscript; all errors, omissions, and misinterpretations remain the responsibility of the author. Canada-Nunavut Geoscience Office, Polar-Continental Shelf Project, and Natural Sciences and Engineering Research Council Discovery Grants supported the author's work in the Borden Basin. The good-humoured assistance of successive, doughty companions through intermittent summers of fieldwork between 2001 and 2012 made the 2-person, fly-camp-based fieldwork possible: C Gilbert, J. Beaulieu, J. Taylor, F. Turner, R Yehia, R. Morden, and T. Chevrier.

REFERENCES

Arne, D.C. and Kissin, S.A., 1989. The significance of "diagenetic crystallization rhythmites" at the Nanisivik Pb-Zn-Ag deposit, Baffin Island, Canada; Mineralium Deposita, v. 24, p. 230–232. https://doi.org/10.1007/BF00206447

Arne, D.C., Kissin, S.A., and Curtis, L.W., 1987. A fluid inclusion study of sphalerite and dolomite from the Nanisivik lead-zinc deposit, Baffin Island, Northwest Territories, Canada; a discussion; Economic Geology and the Bulletin of the Society of Economic Geologists, v. 82, p. 1968–1971. https://doi.org/10.2113/gsecongeo.82.7.1968

Arne, D.C., Curtis, L.W., and Kissin, S.A., 1991. Internal zonation in a carbonate-hosted Zn-Pb-Ag deposit, Nanisivik, Baffin Island, Canada; Economic Geology and the Bulletin of the Society of Economic Geologists, v. 86, p. 699–717. https://doi.org/10.2113/gsecongeo.86.4.699

Blackadar, R.G., 1956. Geological reconnaissance of Admiralty Inlet, Baffin Island, Arctic archipelago, Northwest Territories; Geological Survey of Canada, Paper 55-6, 25 p. https://doi.org/10.4095/101291

Blackadar, R.G., 1970. Precambrian geology, northwestern Baffin Island, District of Franklin; Geological Survey of Canada, Bulletin 191, 89 p. https://doi.org/10.4095/100785

Bodnar, R.J., Lecumberri-Sanchez, P., Moncada, D., and Steele-MacInnis, M., 2014. Fluid inclusions in hydrothermal ore deposits; *in* Treatise on Geochemistry, Volume 13 (second edition), (ed.) H.D. Holland and K. Turekian; Elsevier, Amsterdam, The Netherlands, p. 119–142.

Butterfield, N.J., 2000. *Bangiomorpha pubescens* n.Gen., n. sp.: implications for the evolution of sex, multicellularity, and the Mesoproterozoic/Neoproterozoic radiation of eukaryotes; Paleobiology, v. 26, p. 386–404. https://doi.org/10.1666/0094-8373(2000)026%3c0386:BPNGNS%3e2.0.CO%3b2

Butterfield, N.J., Knoll, A.H., and Swett, K., 1990. A bangiophyte red alga from the Proterozoic of arctic Canada; Science, v. 250, p. 104–107. https://doi.org/10.1126/science.11538072

Christensen, J.N., Halliday, A.N., Kesler, S.E., and Sangster, D.F., 1993. Further evaluation of the Rb–Sr dating of sphalerite: the Nanisivik Precambrian MVT deposit, Baffin Island, Canada; Geological Society of America Abstracts with Programs, v. 25, p. 471.

Clayton, R.H. and Thorpe, L., 1982. Geology of the Nanisivik zinc-lead deposit; *in* Precambrian Sulphide Deposits, (ed.) R.W. Hutchinson, C.D. Spence, and J.M. Franklin; Geological Association of Canada, Special Paper 81-10, p. 739–758.

Denyszyn, S.W., Davis, D.W., and Halls, H.C., 2009. Paleomagnetism and U-Pb geochronology of the Clarence Head dikes, Arctic Canada: orthogonal emplacement of mafic dikes in a large igneous province; Canadian Journal of Earth Sciences, v. 46, p. 155–167. https://doi.org/10.1139/E09-011

Dewing, K., Turner, E.C., and Harrison, J.C., 2007. Geological history, mineral occurrences, and mineral potential of the sedimentary rocks of the Canadian Arctic Archipelago; Geological Association of Canada-Mineral Deposit Division, Special Paper 5, p. 733−753.

Dewing, K., Hadlari, T., Pearson, D.G., and Matthews, W., 2019. Early Ordovician to Early Devonian tectonic development of the northern margin of Laurentia, Canadian Arctic islands; Geological Society of America Bulletin, v. 131, p. 1075–1094. https://doi.org/10.1130/B35017.1

Dostal, J., Jackson, G.D., and Galley, A., 1989. Geochemistry of Neohelikian Nauyat plateau basalts, Borden rift basin, northwestern Baffin Island, Canada; Canadian Journal of Earth Sciences, v. 26, p. 2214–2223. https://doi.org/10.1139/e89-188

Fahrig, W.F., Christie, K.W., and Jones, D.L., 1981. Paleomagnetism of the Bylot basins: evidence for Mackenzie continental tensional tectonics; Geological Survey of Canada, Paper 81-10, p. 303–312. https://doi.org/10.4095/109368

Fustic, M., Haeri Ardakani, O., Jiang, C., Turner, E.C., Mort, A., Sanei, H., Gonzales, G., and Long, D., 2017. Preliminary petroleum potential and organic matter characterization of the Mesoproterozoic upper Arctic Bay Formation (black shale) at Shale Valley central, northern Baffin Island, Nunavut, Canada; Gussow Geoscience Conference, Lake Louise Alberta, October 8–11 (abstract).

Geldsetzer, H., 1973. The tectono-sedimentary development of an algal-dominated Helikian succession on northern Baffin Island; *in* Proceedings of the Symposium on the Geology of the Canadian Arctic, (ed.) J.D. Aitken and J.D. Glass; Geological Association of Canada–Canadian Society of Petroleum Geologists, Saskatoon, Saskatchewan, May 24–26, 1973, p. 99–126.

Ghazban, F. and Ford, D.C., 1993. Meteoric and hydrothermal karstification in dolostones of the Society Cliffs Formation, northern Baffin Island, N.W.T., Canada; International Karst Symposium, Shiraz, Iran, October 23–28, 1993; Proceedings, v. 2, p. 134–151.

Gibson, T.M., Shih, P.M., Cumming, V.M., Fischer, W.W., Crockford, P.W., Hodgskiss, M.S.W., Worndle, S., Creaser, R., Rainbird, R.H., Skulski, T.M., and Halverson, G.P., 2018. Precise age of *Bangiomorpha pubescens* dates the origin of eukaryotic photosynthesis; Geology, v. 46, p. 135–138. https://doi.org/10.1130/G39829.1

Gibson, T.M., Worndle, S., Crockford, P.W., Bui, T.H., Creaser, R.A., and Halverson, G.P., 2019. Radiogenic isotope chemostratigraphy reveals marine and nonmarine depositional environments in the late Mesoproterozoic Borden Basin, Arctic Canada; Geological Society of America Bulletin, v. 131, p. 1965–1978. https://doi.org/10.1130/B35060.1

Hahn, K.E. and Turner, E.C., 2017. Composition and history of giant lacustrine carbonate seep mounds, Mesoproterozoic Borden Basin, Arctic Canada; Precambrian Research, v. 293, p. 150–173. https://doi.org/10.1016/j.precamres.2017.03.009

Hahn, K., Turner, E.C., Babechuk, M.G., and Kamber, B.S., 2015. Deep-water seep-related carbonate mounds in a Mesoproterozoic alkaline lake, Borden Basin (Nunavut, Canada); Precambrian Research, v. 271, p. 173–197. https://doi.org/10.1016/j.precamres.2015.09.025

Hahn, K.E., Turner, E.C., Kontak, D.J., and Fayek, M., 2018. Fluid-chemical evidence for one billion years of fluid flow through Mesoproterozoic deep-water carbonate mounds (Nanisivik zinc district, Nunavut); Geochimica et Cosmochimica Acta, v. 223, p. 493–519. https://doi.org/10.1016/j.gca.2017.12.001

Heaman, L.M., LeCheminant, A.N., and Rainbird, R.H., 1992. Nature and timing of Franklin igneous events, Canada: implications for a Late Proterozoic mantle plume and the breakup of Laurentia; Earth and Planetary Science Letters, v. 109, p. 117–131. https://doi.org/10.1016/0012-821X(92)90078-A

Hnatyshin, D., Creaser, R.A., Kontak, D.J., Turner, E.C., Stern, R.A., and Morden, R., 2016. Geochronologic (ReOs), stable isotope ($\delta^{34}S$), and fluid-chemical constraints on the formation of the Mesoproterozoic-hosted Nanisivik Zn-Pb deposit, Nunavut, Canada: evidence for early diagenetic, low-temperature conditions of formation; Ore Geology Reviews, v. 79, p. 189–217. https://doi.org/10.1016/j.oregeorev.2016.05.017

Hofmann, H.J. and Jackson, G.D., 1991. Shelf-facies microfossils from the Uluksan Group (Proterozoic Bylot Supergroup), Baffin Island, Canada; Journal of Paleontology, v. 65, p. 361–382. https://doi.org/10.1017/S0022336000030353

Hofmann, H.J. and Jackson, G.D., 1994. Shale-facies microfossils from the Proterozoic Bylot Supergroup, Baffin Island, Canada; Paleontological Society, Memoir 37, 39 p.

Jackson, G.D. and Cumming, L.M., 1981. Evaporites and folding in the Neohelikian Society Cliffs Formation, northeastern Baffin Island; Geological Survey of Canada, Current Research Part C, Paper 81-1C, p. 35–44. https://doi.org/10.4095/116049

Jackson, G.D. and Davidson, A., 1978. Bylot Island map-area, District of Franklin; Geological Survey of Canada, Paper 74-2, 12 p. https://doi.org/10.4095/102501

Jackson, G.D. and Iannelli, T.R., 1981. Rift-related cyclic sedimentation in the Neohelikian Borden Basin, northern Baffin Island; Geological Survey of Canada, Paper 81-10, p. 269–302. https://doi.org/10.4095/109369

Jackson, G.D. and Morgan, W.C., 1978. Precambrian metamorphism on Baffin and Bylot islands; *in* Metamorphism in the Canadian shield, (ed.) J.A. Fraser and W.W. Heywood; Geological Survey of Canada, Paper 78-10, p. 249–267. https://doi.org/10.4095/104537

Kah, L.C. and Knoll, A.H., 1996. Microbenthic distribution in Proterozoic tidal flats: environmental and taphonomic considerations; Geology, v. 24, p. 79–82. https://doi.org/10.1130/0091-7613(1996)024%3c0079:MDOPTF%3e2.3.CO%3b2

Kah, L.C., Sherman, A.G., Narbonne, G.M., Knoll, A.H., and Kaufman, A.J., 1999. δ13C isotope stratigraphy of the Mesoproterozoic Bylot Supergroup, northern Baffin Island: implications for regional lithostratigraphic correlations; Canadian Journal of Earth Sciences, v. 36, p. 313–332. https://doi.org/10.1139/e98-100

Kah, L.C., Lyons, T.W., and Chesley, J.T., 2001. Geochemistry of a 1.2 Ga carbonate-evaporite succession, northern Baffin and Bylot islands: implications for Mesoproterozoic marine evolution; Precambrian Research, v. 111, p. 203–234. https://doi.org/10.1016/S0301-9268(01)00161-9

Knight, R.D. and Jackson, G.D., 1994. Sedimentology and stratigraphy of the Mesoproterozoic Elwin Subgroup (Aqigilik and Sinasiuvik Formations), uppermost Bylot Subgroup, Borden Rift Basin, northern Baffin Island; Geological Survey of Canada, Bulletin 455, 43 p. https://doi.org/10.4095/194068

Knoll, A.H., Wörndle, S., and Kah, L.C., 2013. Covariance of microfossil assemblages and microbialite textures across an upper Mesoproterozoic carbonate platform; Palaios, v. 28, p. 453–470. https://doi.org/10.2110/palo.2013.p13-005r

Leach, D.L., Sangster, D.F., Kelley, K.D., Large, R.R., Garven, G., Allen, C.R., Gutzmer, J., and Walters, S., 2005. Sediment-hosted lead–zinc deposits; a global perspective; Economic Geology and the Bulletin of the Society of Economic Geologists, v. 100, p. 561–607.

LeCheminant, A.N. and Heaman, L.M., 1989. Mackenzie igneous events, Canada: middle Proterozoic hotspot magmatism associated with ocean opening; Earth and Planetary Science Letters, v. 96, p. 38–48. https://doi.org/10.1016/0012-821X(89)90122-2

Lemon, R.R.H. and Blackadar, R.G., 1963. Admiralty Inlet area, Baffin Island, District of Franklin; Geological Survey of Canada, Memoir 328, 84 p. https://doi.org/10.4095/100662

Long, D.G.F. and Turner, E.C., 2012. Tectonic, sedimentary and metallogenic re-evaluation of basal strata in the Mesoproterozoic Bylot basins (NU): are unconformity-type U concentrations a realistic expectation; Precambrian Research, v. 214-215, p. 192–209. https://doi.org/10.1016/j.precamres.2011.11.005

McNaughton, K., 1983. A fluid inclusion study of the Nanisivik lead-zinc deposit, Baffin Island, NWT; M.Sc. thesis, University of Windsor, Windsor, Ontario, 95 p.

McNaughton, K. and Smith, T.E., 1986. A fluid inclusion study of sphalerite and dolomite from the Nanisivik lead–zinc deposit, Baffin Island, Northwest Territories, Canada; Economic Geology and the Bulletin of the Society of Economic Geologists, v. 81, p. 713–720. https://doi.org/10.2113/gsecongeo.81.3.713

Narbonne, G.M. and James, N.P., 1996. Mesoproterozoic deep-water reefs from Borden Peninsula, Arctic Canada; Sedimentology, v. 43, p. 827–848. https://doi.org/10.1111/j.1365-3091.1996.tb01505.x

Olson, R.A., 1984. Genesis of paleokarst and strata-bound zinc-lead sulfide deposits in a Proterozoic dolostone, northern Baffin Island, Canada; Economic Geology and the Bulletin of the Society of Economic Geologists, v. 79, p. 1059–1103. https://doi.org/10.2113/gsecongeo.79.5.1056

Pehrsson, S.J. and Buchan, K.L., 1999. Borden dykes of Baffin Island, N.W.T.: a Franklin U–Pb baddeleyite age and a paleomagnetic interpretation; Canadian Journal of Earth Sciences, v. 36, p. 65–73. https://doi.org/10.1139/e98-091

Rainbird, R., Cawood, P., and Gehrels, G.E., 2012. The Great Grenvillian sedimentation episode: record of supercontinent Rodinia's assembly; *in* Recent Advances in Tectonics of Sedimentary Basins, (ed.) C. Busby and A. Azor, Blackwell Publishing Ltd., Oxford, United Kingdom, p. 583–601.

Sangster, D.F., 1998. Mineral deposits compilation and metallogenic domains, northern Baffin Island and northern Melville Peninsula, Northwest Territories; Geological Survey of Canada, Open File 3635, scale 1:1 000 000. https://doi.org/10.4095/210026

Saumur, B.M., Skipton, D.R., St-Onge, M.R., Wodicka, N., Bros, E.R., and Weller, O.M., 2018a. Bedrock geology, Kanajuqtuuq (Paquet Bay), Nunavut, NTS 37-G north; Geological Survey of Canada, Canadian Geoscience Map 349, scale 1:100 000. https://doi.org/10.4095/306584

Saumur, B.M., Skipton, D.R., St-Onge, M.R., Wodicka, N., Bros, E.R., and Weller, O.M., 2018b. Bedrock geology, Mumiksaa–Milne Inlet, Nunavut, parts of NTS 38-B and 48-A; Geological Survey of Canada, Canadian Geoscience Map 348, scale 1:100 000. https://doi.org/10.4095/306579

Scott, D.J. and deKemp, E.A., 1998. Bedrock Geology Compilation, Northern Baffin Island and Northern Melville Peninsula; Geological Survey of Canada, Open File 3633, 3 sheets. https://doi.org/10.4095/210024

Sherlock, R.L., Lee, J.K.W., and Cousens, B.L., 2004. Geologic and geochronologic constraints on the timing of mineralisation at the Nanisivik zinc-lead Mississippi Valley-type deposit, northern Baffin Island, Nunavut, Canada; Economic Geology and the Bulletin of the Society of Economic Geologists, v. 99, p. 279–293. https://doi.org/10.2113/gsecongeo.99.2.279

Sherman, A.G., James, N.P., and Narbonne, G.M., 2000. Sedimentology of a late Mesoproterozoic muddy carbonate ramp, northern Baffin Island, Arctic Canada; *in* Carbonate Sedimentation and Diagenesis in the Evolving Precambrian World, (ed.) J.P. Grotzinger and N.P. James; Society for Sedimentary Geology, SEPM Special Publication 67, p. 275–294. https://doi.org/10.2110/pec.00.67.0275

Sherman, A.G., Narbonne, G.M., and James, N.P., 2001. Anatomy of a cyclically packaged Mesoproterozoic carbonate ramp in northern Canada; Sedimentary Geology, v. 139, p. 171–203. https://doi.org/10.1016/S0037-0738(00)00168-8

Sherman, A.G., James, N.P., and Narbonne, G.M., 2002. Evidence for reversal of basin polarity during carbonate ramp development in the Mesoproterozoic Borden Basin, Baffin Island; Canadian Journal of Earth Sciences, v. 39, p. 519–538. https://doi.org/10.1139/e01-089

Sutherland, R.A. and Dumka, D., 1995. Geology of Nanisivik mine, NWT, Canada; Society of Economic Geologists Guidebook Series 22, p. 4-12.

Symons, D.T.A., Symons, T.B., and Sangster, D.F., 2000. Paleomagnetism of the Society Cliffs dolostone and the age of the Nanisivik zinc deposits, Baffin Island, Canada; Mineralium Deposita, v. 35, p. 672–682. https://doi.org/10.1007/s001260050270

Trettin, H.P., 1969. Lower Palaeozoic sediments of northwestern Baffin Island, District of Franklin; Geological Survey of Canada, Bulletin 157, 70 p. https://doi.org/10.4095/102249

Turner, E.C., 2003. Lead-zinc showings associated with debrites shed from synsedimentary faults, Mesoproterozoic Society Cliffs Formation, northern Baffin Island, Nunavut; Geological Survey of Canada, Current Research 2003-B3, 13 p https://doi.org/10.4095/214154

Turner, E.C., 2004. Origin of basinal carbonate laminites of the Mesoproterozoic Society Cliffs Formation (Borden Basin, Nunavut), and implications for base metal mineralization; Geological Survey of Canada, Current Research 2004-B2, 12 p. https://doi.org/10.4095/215334

Turner, E.C., 2009. Mesoproterozoic carbonate systems in the Borden Basin, Nunavut; Canadian Journal of Earth Sciences, v. 46, p. 915–938. https://doi.org/10.1139/E09-062

Turner, E.C., 2011. Structural and stratigraphic controls on carbonate-hosted base-metal mineralization in the Mesoproterozoic Borden Basin (Nanisivik District), Nunavut; Economic Geology and the Bulletin of the Society of Economic Geologists, v. 106, p. 1197–1223. https://doi.org/10.2113/econgeo.106.7.1197

Turner, E.C. and Kamber, B.S., 2012. Arctic Bay Formation, Borden Basin, Nunavut (Canada): Basin evolution, black shale base-metal potential and dissolved metal systematics in the Mesoproterozoic ocean; Precambrian Research, v. 208–211, p. 1–18. https://doi.org/10.1016/j.precamres.2012.03.006

Turner, E.C., Long, D.G.F., Rainbird, R.H., Petrus, J.A., and Rayner, N.M., 2016. Late Mesoproterozoic rifting in Arctic Canada during Rodinia assembly: impactogens, trans-continental far-field stress, and zinc mineralisation; Terra Nova, v. 28, p. 188–194. https://doi.org/10.1111/ter.12207

Contents

Lower Paleozoic strata of the Labrador–Baffin Seaway (Canadian margin) and Baffin Island

N. Bingham-Koslowski[1], S. Zhang[2], and T. McCartney[3]

Bingham-Koslowski, N., Zhang, S., and McCartney, T., 2022. Lower Paleozoic strata of the Labrador–Baffin Seaway (Canadian margin) and Baffin Island; in *Geological synthesis of Baffin Island (Nunavut) and the Labrador–Baffin Seaway, (ed.) L.T. Dafoe and N. Bingham-Koslowski; Geological Survey of Canada, Bulletin 608, p. 79–106. https://doi.org/10.4095/321827*

Abstract: Lower Paleozoic strata occur offshore Labrador (Middle to Upper Ordovician), offshore Baffin Island in western Davis Strait (Upper Ordovician), as well as onshore Baffin Island (Cambrian to Silurian). Paleozoic carbonate rocks (limestone and dolostone units) dominate with occurrences of siliciclastic strata found in the offshore Labrador subsurface (in the Freydis B-87 well) and in outcrop on Baffin Island. In the Labrador–Baffin Seaway, Lower Paleozoic strata primarily exist as isolated erosional remnants, where historically, minimal effort has been made to correlate Paleozoic outliers due to their lateral discontinuity coupled with inconsistent age data. The Lower Paleozoic of the Labrador–Baffin Seaway and Baffin Island can be viewed as two subsets that do not appear to be correlatable: the southern Lower Paleozoic of the Labrador margin and the northern Lower Paleozoic of the southeastern Baffin Shelf and onshore Baffin Island.

Résumé : Des strates du Paléozoïque inférieur sont présentes au large du Labrador (Ordovicien moyen et supérieur), dans la partie occidentale du détroit de Davis au large de l'île de Baffin (Ordovicien supérieur), ainsi qu'à terre dans l'île de Baffin (du Cambrien au Silurien). Les roches carbonatées (calcaires et dolomies) constituent la lithologie dominante du Paléozoïque. Des strates silicoclastiques sont aussi présentes dans le sous-sol du fond marin au large du Labrador (dans le puits Freydis B-87) et en affleurement dans l'île de Baffin. Dans le bras de mer Labrador-Baffin, les strates du Paléozoïque inférieur se manifestent principalement sous forme de lambeaux d'érosion isolés. Par le passé, peu d'efforts ont été déployés pour établir des corrélations entre les lambeaux d'érosion paléozoïques en raison de leur discontinuité latérale et de l'incohérence des données quant à leur âge. On peut considérer les strates du Paléozoïque inférieur du bras de mer Labrador-Baffin et de l'île de Baffin comme appartenant à deux sous-ensembles non corrélables : le Paléozoïque inférieur méridional de la marge continentale du Labrador et le Paléozoïque inférieur septentrional du sud-est de la plate-forme continentale de l'île de Baffin et des secteurs émergés de l'île de Baffin.

[1]Geological Survey of Canada, 601 Booth Street, Ottawa, Ontario K1A 0E8
[2]Canada-Nunavut Geoscience Office, P.O. Box 2319, Iqaluit, Nunavut X0A 0H0
[3]Geological Survey of Canada, 1 Challenger Drive, P.O. Box 1006, Dartmouth, Nova Scotia B2Y 4A2
*Corresponding author: N. Bingham-Koslowski (email: nikole.bingham-koslowski@nrcan-nrcan.gc.ca)

INTRODUCTION

Lower Paleozoic strata are present in isolated subsurface areas of the Labrador–Baffin Seaway (Fig. 1), unconformably situated between Precambrian basement and Mesozoic or Cenozoic rocks, as well as in outcrop on Baffin Island. Offshore Ordovician carbonate and siliciclastic strata occur as erosional remnants and are encountered in seven exploration wells on the southern Labrador Shelf in the Hopedale Basin (Table 1) (Moir, 1989; Bell and Howie, 1990; Bingham-Koslowski, 2019; Bingham-Koslowski et al., 2019). Ordovician carbonate rocks are also known from drill-core samples on the southeastern Baffin Shelf (western Davis Strait; Table 2) and are inferred from seismic, magnetic, and gravity data to underlie Mesozoic and Cenozoic sediments from Frobisher Bay to Cumberland Sound (MacLean et al., 1977; Bell and Howie, 1990; Bingham-Koslowski, 2018). The Upper Ordovician marine carbonate rocks that dominate the offshore in the Labrador–Baffin Seaway were deposited on a passive margin in an epeiric sea, during a period of dynamic tectonic and biotic activity (the Taconic Orogeny and coincident closure of the Iapetus Ocean, the great Ordovician biodiversification event, and the Late Ordovician mass-extinction event). Lower Paleozoic outcrops on Baffin Island were deposited on the Arctic and Hudson platforms and are dominated by Ordovician carbonate rocks with localized occurrences of Cambrian (clastic) and Silurian (carbonate) deposits (Blackadar, 1956; Trettin 1965a, b, 1969, 1975; Zhang, 2012, 2013).

Lower Paleozoic strata along the Labrador margin are difficult to distinguish from rocks postdating rifting and basement rocks in 2-D seismic reflection profiles; however, physical samples exist in the form of ditch cuttings, side-wall cores, and conventional cores that provide age and lithological data for the rocks and aid in seismic interpretation. A handful of drill cores recovered during Geological Survey of Canada–led research cruises (Cruise 75-009, Phase V, and Cruise 77027) from the southeastern Baffin Shelf in the 1970s provide a small number of samples to ground truth the limited geophysical data and offer some insights into the Lower Paleozoic from the region (Table 2).

The geographically restricted nature of the Lower Paleozoic strata in the offshore, along with age data that was, until recently, variable and inconsistent, has prevented the division of the offshore strata into formal lithostratigraphic units (Moir, 1989). The absence of any direct Paleozoic correlations (seismic or biostratigraphic) between wells or drill cores has impeded local comparative analyses between sites. Furthermore, this has hindered the comparison of Paleozoic rocks from the Labrador–Baffin Seaway to other, potentially time-equivalent onshore-offshore deposits and prevented the incorporation of these strata into regional to global-scale paleogeographic and paleotectonic studies.

The Lower Paleozoic strata described in the following sections are divided into three regions: Labrador margin, western Davis Strait, and onshore Baffin Island. The information presented here synthesizes work conducted by Natural Resources Canada (Geo-mapping for Energy and Minerals program, Marine Conservation Targets program, and the Canada-Nunavut Geoscience Office) with supplementation from legacy studies and literature to provide a complete overview of the Lower Paleozoic from the Labrador–Baffin Seaway and from onshore Baffin Island.

LOWER PALEOZOIC STRATIGRAPHY OF THE LABRADOR MARGIN

The Labrador margin consists of two major Mesozoic–Cenozoic sedimentary basins of interest with respect to hydrocarbon exploration: the Saglek Basin to the north and the Hopedale Basin to the south (Fig. 1). The first exploration well drilled offshore Labrador was the Tenneco et al. Leif E-38 well in 1971 (Daneliuk and Bell, 1972; *see* Table 2, Bingham-Koslowski, McCartney, and Bojesen-Koefoed, this volume). Only seven of the 26 exploration wells along the margin south of Hudson Strait encountered Paleozoic strata (from north to south): Hopedale E-33, South Hopedale L-39, Tyrk P-100, Gudrid H-55, Roberval K-92, Indian Harbour M-52, and Freydis B-87 (Table 1; Fig. 2). These wells are all located within the Hopedale Basin where the Paleozoic succession unconformably overlies Precambrian crystalline basement and is unconformably overlain by Mesozoic rocks (Moir, 1989; Bell and Howie, 1990). The thickness of the Paleozoic interval underlying the Hopedale Basin ranges from 4 m thick at Tyrk P-100, to over 400 m thick in the Indian Harbour M-52 well (Canada-Newfoundland and Labrador Offshore Petroleum Board, 2007a, g). Carbonate rocks (limestone and dolostone) comprise the majority of the Paleozoic strata with siliciclastic rocks occurring only in the Freydis B-87 well (Bingham-Koslowski, 2019). The angular unconformity at the top of the Lower Paleozoic sedimentary units, as well as the presence of igneous rocks within these intervals, are interpreted to record the early stages of rifting in the Cretaceous (Bell and Howie, 1990). There is no evidence to suggest that the Paleozoic strata continue, or are preserved, northward beneath the Saglek Basin, as all wells in the Saglek Basin that extend below Mesozoic strata immediately encounter Precambrian basement and no obvious Paleozoic strata are identifiable in seismic profiles (Bell and Howie, 1990).

The Lower Paleozoic strata underlying the Hopedale Basin are geographically restricted and laterally discontinuous as determined from 2-D seismic reflection data. Lower Paleozoic strata encountered in the seven wells represent erosional remnants (McWhae et al., 1980; Miller and D'Eon, 1987) associated with Cretaceous half grabens and related structural highs (Bingham-Koslowski et al., 2019; McCartney, 2019). Seismic interpretation demonstrates that the Paleozoic in the wells is present as isolated, disconnected packets, with the possible exception of Hopedale E-33 and South Hopedale L-39, which may represent one package of Lower Paleozoic strata (Fig. 2). Until recently, the palynological data for the Paleozoic of the Labrador margin was inconsistent, providing age dates for the wells ranging from undifferentiated Paleozoic, to Ordovician, to Devonian, to Carboniferous (Moir, 1989; Bell and Howie, 1990; Williams et al., 1990); however, a biostratigraphic study based on the analysis of new palynology slides and the reassessment of archived Geological Survey of Canada (GSC) palynology slides, indicates Middle to Late Ordovician ages for the Paleozoic intervals in all seven wells (Bingham-Koslowski et al., 2019). This new age data will facilitate a better correlation of the Lower Paleozoic from the Labrador margin and potentially help to further understanding of this tectonically dynamic and biologically significant period in Earth's history — work that is currently beyond the scope of this bulletin.

With no direct correlation between wells, it is challenging to accurately address the Lower Paleozoic of the Labrador margin as one unit, particularly since the lithology of the Paleozoic varies between wells (as determined from cores (if available), ditch cuttings, and well logs) and no formal stratigraphic units for the interval have been established. As such, the following sections present a brief summary of the Paleozoic strata from each of the seven wells from the Hopedale Basin.

Hopedale E-33

The Chevron et al. Hopedale E-33 well is located approximately 64 km northeast of Hopedale, Labrador (Fig. 2) (Pandachuck and Lewis, 1978) (*see* Table 2, Bingham-Koslowski, McCartney, and Bojesen-Koefoed, this volume). Paleozoic strata occur between 1976 m and 2000 m, separated from the overlying Bjarni Formation and underlying Precambrian granite by unconformities (Table 1; Fig. 3a) (Pandachuck and Lewis 1978; Canada-Newfoundland and Labrador Offshore Petroleum Board, 2007c; Ainsworth et al., 2016). The Upper Ordovician (Sandbian; Bingham-Koslowski et al., 2019) (van Helden, 1978; Jenkins, 1984; Ainsworth et al., 2016) rocks are composed of light grey to brown limestone and dolostone units that are locally fossiliferous with ostracods, brachiopods, gastropods, and possible calcispheres identified in a sidewall core (Pandachuck and Lewis, 1978). The Upper Ordovician carbonate rocks at Hopedale E-33 are gas-bearing, and as such, a Significant Discovery Licence (SDL) has been awarded (SDL-203) (Canada-Newfoundland and Labrador Offshore Petroleum Board, 2016).

South Hopedale L-39

The Canterra et al. South Hopedale L-39 well was drilled to a total depth of 2364 m, with possible Paleozoic carbonate rocks (limestone and dolostone) encountered between 2008 m and 2221 m, unconformably overlying Precambrian granite (Table 1; Fig. 3b) (Canterra Energy Ltd., 1983; Canada-Newfoundland and Labrador Offshore Petroleum Board, 2007b; Ainsworth et al., 2016) (*see* Table 2, Bingham-Koslowski, McCartney, and Bojesen-Koefoed, this volume). Igneous

Figure 1. Regional map showing the location of exploration wells and drill cores from the Canadian margin of the Labrador–Baffin Seaway that contain Lower Paleozoic strata. Three main areas of interest include the Labrador margin (Fig. 2), the western Davis Strait region (*see* Fig. 10), and onshore Baffin Island (*see* Fig. 14). Additional projection information for all maps in this paper: Central Meridian = 60°W; Standard Parallels = 65, 75°W; Latitude of Origin = 65°N.

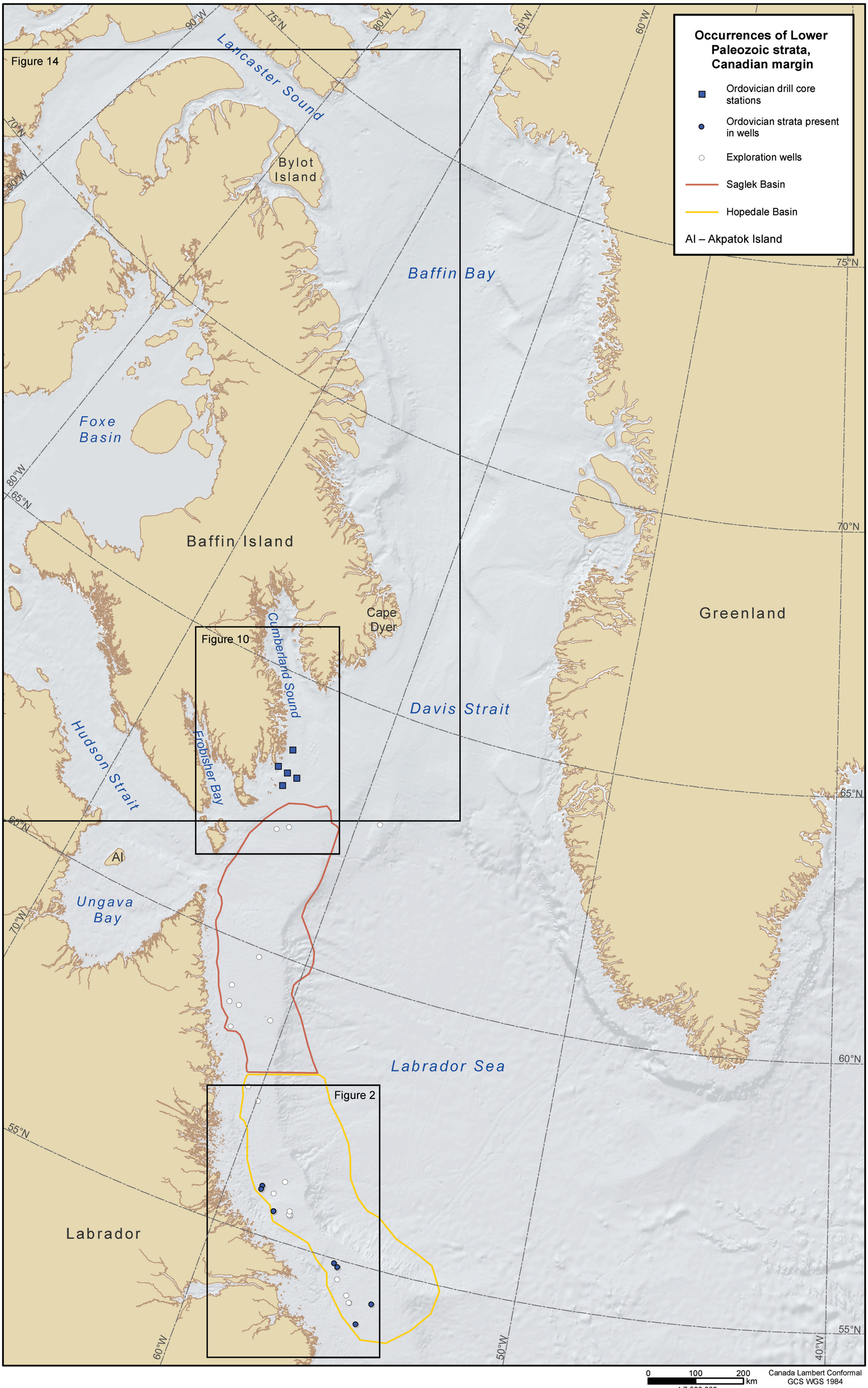
Occurrences of Lower Paleozoic strata, Canadian margin
Ordovician drill core stations
Ordovician strata present in wells
Exploration wells
Saglek Basin
Hopedale Basin
AI – Akpatok Island
Figure 14
Figure 10
Figure 2
Lancaster Sound
Bylot Island
Baffin Bay
Foxe Basin
Baffin Island
Cape Dyer
Cumberland Sound
Frobisher Bay
Hudson Strait
Davis Strait
Greenland
AI
Ungava Bay
Labrador Sea
Labrador
90°W
75°N
80°W
70°W
60°W
70°N
65°N
60°N
55°N
50°W
40°W
0
100
200
km
1:7 500 000
Canada Lambert Conformal
GCS WGS 1984

Table 1. Summary of the Lower Paleozoic strata on the Labrador margin (*see* Fig. 2 for location map).

Well name		Hopedale E-33	South Hopedale L-39	Tyrk P-100	Gudrid H-55	Roberval K-92		Indian Harbour M-52	Freydis B-87	
Location	Latitude	55°52′24.62″N	55°48′32.85″N	55°29′49.87″N	54°54′30.19″N	54°51′35.69″N		54°21′51.42″N	53°56′13.48″N	
	Longitude	58°50′48.78″W	58°50′45.01″W	58°13′47.05″W	55°52′28.47″W	55°44′32.0″W		54°23′47.81″W	54°42′35.86″W	
Total depth (m)		2069.4	2364	1739	2838	3874		3958.2	2314.1	
Paleozoic interval (m)	Top	1976	2008	1702	2663.5	3544		3531	1905.2	
	Base	2000	2221	1706	2804	3874		3958.2	2314.1	
Total Paleozoic thickness (m)		24	213	4	140.5	330		427.2	409.1	
Cored interval (m)	Top	NA	NA	NA	2676	3578	3870	3952	1934.9	2307.3
	Base				2680.9	3582.5	3874	3958.1	1941.3	2313.4

Table 2. Summary of Lower Paleozoic drill cores from the southeastern Baffin Shelf (*see* Fig. 10 for location map).

Cruise	Year	Station #	Latitude	Longitude	Recovery	Age	Age Reference
75-009, Phase V	1975	4	62°58.2′N	63°26.1′W	137 cm core	Ordovician (Caradoc)	[1]Jenkins, 1976; MacLean et al., 1977
75-009, Phase V	1975	5	63°16.2′N	63°54.6′W	126 cm core	Ordovician (Caradoc)	[2]Bolton, 1976; MacLean et al., 1977
75-009, Phase V	1975	8	63°12.8′N	63°27.2′W	Mainly gravel	Ordovician (assumed)	MacLean et al., 1977
75-009, Phase V	1975	8A	63°12.9′N	63°27.5′W	70 cm core	Ordovician (Caradoc)	[1]Jenkins, 1976; MacLean et al., 1977
75-009, Phase V	1975	8B	63°13.2′N	63°27.6′W	89 cm core	Ordovician (Caradoc)	[2]Jenkins, 1976; MacLean et al., 1977
77027	1977	026A	63°39.5′N	63°38.1′W	7 cm gravel, 83 cm core	Ordovician (assumed)	MacLean, 1978
77027	1977	028	63°11.86′N	63°00.9′W	7 cm gravel, 100 cm core	Ordovician (assumed)	MacLean, 1978

[1]W.A.M, Jenkins, GSC unpub. report 13-WAMJ-1976, 1976
[2]T.E. Bolton, GSC unpub. report 0-1-1976 TEB, 1976

units thought to be associated with Early Cretaceous rifting (Miller and D'Eon, 1987) are interbedded with the carbonate rocks from 2030 m to 2080 m with the carbonate unit below the igneous rocks (from 2080 m to 2221 m) formerly reported as undifferentiated Paleozoic (Oliver and Awai-Thorne, 1984; Moir, 1989; Ainsworth et al., 2016). The upper part of the interval has been the subject of contention, with some reports suggesting that the overlying carbonate rocks are Lower Cretaceous and that the igneous rocks are the product of extrusive flows (Oliver and Awai-Thorne, 1984; Bujak Davies Group, 1989b). Others have proposed that the entire carbonate interval is Paleozoic and that the igneous rocks represent intrusions (Moir, 1989; Ainsworth et al., 2016). Recent biostratigraphic data has confirmed that the entire sequence of carbonate rocks was deposited in a marine environment during the Late Ordovician (undifferentiated) and therefore, the igneous rocks are intrusive in nature (Bingham-Koslowski et al., 2019).

The previous published age for the Paleozoic interval at Gudrid H-55 was Carboniferous (Westphalian D to Stephanian) based on the presence and abundance of miospores (Barss, 1975; Corgnet and McWhae, 1975; Umpleby, 1979; Williams and Barss, 1979); however, recent biostratigraphic data suggest that the Carboniferous miospores are contaminants (from cavings or drilling mud) and that the presence of chitinozoans, tentatively identified as *Euconochitina* sp. and *?Fungochitina,* suggest a possible Late Ordovician age ((?) Sandbian) (Bingham-Koslowski et al., 2019). Additionally, thermal alteration indices determined from non-age-diagnostic leiospheres by Bingham-Koslowski et al. (2019), demonstrate that the strata in the Gudrid H-55 well have undergone a similar thermal history to in situ Ordovician acritarchs from the Indian Harbour M-52 and Freydis B-87 wells, further supporting a Late Ordovician age for the Paleozoic strata.

Tyrk P-100

The Total Eastcan et al. Tyrk P-100 well was drilled to a total depth of 1739 m, 4 m of which (1702 m to 1706 m) is composed of Middle to Upper Ordovician (previously undifferentiated) dolostone that unconformably overlies basement granite (Table 1; Fig. 3c) (Total Eastcan Exploration Ltd, 1979b; Oliver and Thorne, 1979; Caro et al., 1980; Canada-Newfoundland and Labrador Offshore Petroleum Board, 2007g; Bingham-Koslowski and Bojesen-Koefoed, 2019) (*see* Table 2, Bingham-Koslowski, McCartney, and Bojesen-Koefoed, this volume). Although too thin to be mapped in seismic reflection data, possible extents of the Paleozoic strata at Tyrk P-100 can be inferred from contour maps of the basement high on which Tyrk P-100 sits (Fig. 2).

Gudrid H-55

The Eastcan et al. Gudrid H-55 well was drilled to a total depth of 2838 m and penetrated Paleozoic dolostone, between 2663.5 m and 2804 m that unconformably overlies Precambrian granite (Table 1; Fig. 4) (*see* Table 2, Bingham-Koslowski, McCartney, and Bojesen-Koefoed, this volume). The dolostone units are gas-bearing, which resulted in the issuing of SDL-184 for the well (Corgnet and McWhae, 1975; Canada-Newfoundland and Labrador Offshore Petroleum Board, 2007e, 2016). A 4 m long conventional core was recovered from the Paleozoic interval between 2676 m and 2680.9 m (Fig. 4). The Paleozoic core exhibits pervasive dolomitization to the near total destruction of all macro- and microfossil content (Fig. 4b, c, d, 5a, b) (Bingham-Koslowski, 2019; Bingham-Koslowski et al., 2019). Rare shell fragments as well as possible crinoid pieces were reported in this interval (Bingham-Koslowski, 2019).

Roberval K-92

The Total Eastcan et al. Roberval K-92 well penetrated approximately 330 m of Paleozoic dolostone between 3544 m and 3874 m (total depth) (Table 1; Fig. 6) (Cadenel et al., 1978; Total Eastcan Exploration Ltd., 1979a; Steeves, 1982; Canada-Newfoundland and Labrador Offshore Petroleum Board, 2007f) (*see* Table 2, Bingham-Koslowski, McCartney, and Bojesen-Koefoed, this volume). Seven conventional cores were recovered from the well during drilling operations with two of the cores, core 6 (3578 m to 3582.5 m) and core 7 (3870 m to 3874 m), recovered from the Paleozoic interval (Fig. 6). The Paleozoic interval at Roberval K-92 has been pervasively dolomitized (Fig. 5c, d, e, f, 6b, c, d, e), similar to Gudrid H-55, resulting in very limited fossil preservation at both the macro- and microscopic scales. The dolomite in cores 6 and 7 is buff (primarily core 6) to grey (primarily core 7) and appears mottled (Fig. 6b, c, d, e) (Bingham-Koslowski, 2019). Additionally, two thin intervals (on the order of 10 cm thick) of mafic igneous rocks occur near the top of core 6, the origin of which has not yet been determined. As with Gudrid H-55, the age of the Paleozoic rocks at Roberval K-92 was previously reported as Carboniferous based on the presence of proliferous miospores (Caro and Villain, 1980; Barss, 1981; Moir, 1989; Bell and Howie, 1990; Williams et al., 1990). These miospores have since been interpreted to be contaminants and an age date of possibly Middle to Late Ordovician has been proposed based on the presence of a micro-pylomate acritarch (*?Rhopaliophora* sp.) and a chitinozoan specimen of the *Desmochitina* group (Bingham-Koslowski et al., 2019). As with Gudrid H-55, thermal alteration indices from Roberval K-92 leiospheres suggest a similar burial history with that of known in situ Ordovician acritarchs from the

Figure 2. Distribution map of Paleozoic strata along the Labrador margin based on the interpretation of 2-D seismic reflection data. Paleozoic strata are associated with rift-related structures and are found only in seven wells (Hopedale E-33, South Hopedale L-39, Tyrk P-100, Gudrid H-55, Roberval K-92, Indian Harbour M-52, and Freydis B-87) from the Hopedale Basin. There are insufficient Paleozoic strata at Tyrk P-100 (~4 m) to distinguish in the seismic data; however, the possible extent of the Paleozoic interval was approximated using a basement structure map (*modified from* Bingham-Koslowski et al., 2019).

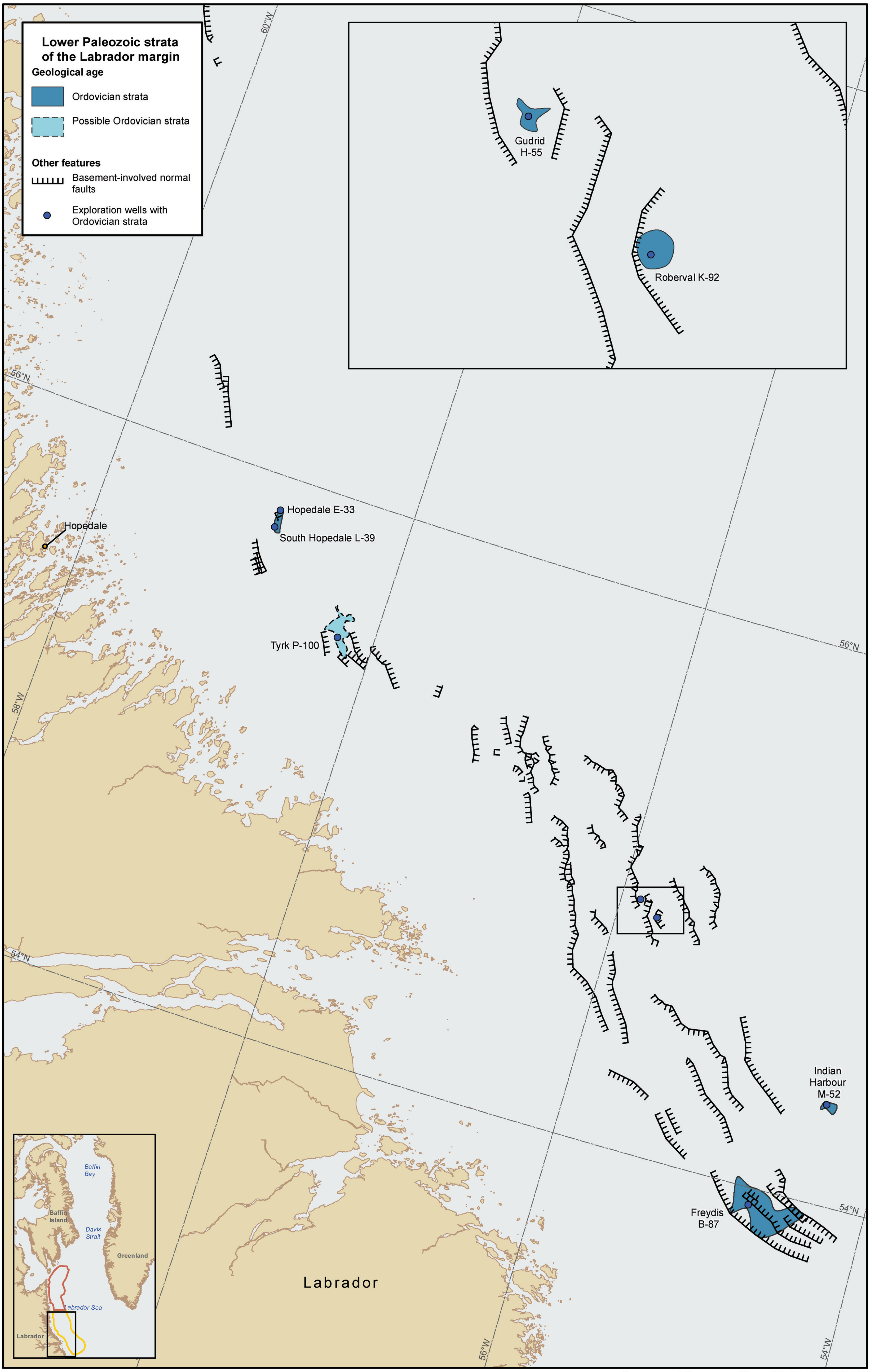
Lower Paleozoic strata of the Labrador margin
Geological age
Ordovician strata
Possible Ordovician strata
Other features
Basement-involved normal faults
Exploration wells with Ordovician strata
Gudrid H-55
Roberval K-92
Hopedale E-33
South Hopedale L-39
Hopedale
Tyrk P-100
Indian Harbour M-52
Freydis B-87
Labrador
56°N
54°N
60°W
58°W
56°W
54°W
Baffin Bay
Baffin Island
Davis Strait
Greenland
Labrador Sea
0 25 50 km
1:1 500 000
Canada Lambert Conformal
GCS WGS 1984

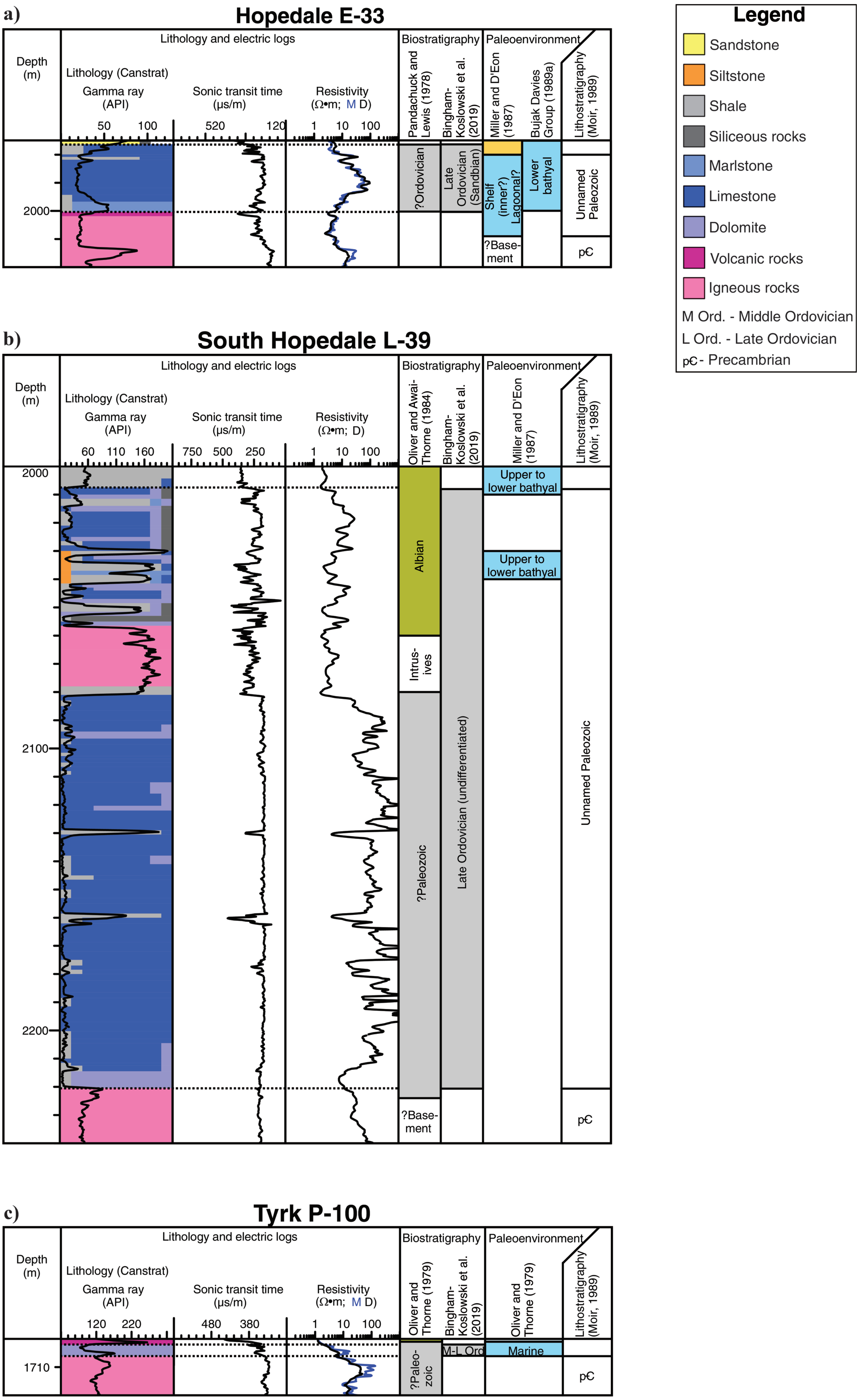

Figure 3. Well logs, biostratigraphic data, paleoenvironmental interpretations, and lithostratigraphy of the Paleozoic from **a)** Hopedale E-33, **b)** South Hopedale L-39, and **c)** Tyrk P-100. Dashed lines represent the bounding unconformities of the Paleozoic interval. Medium (M, in blue) and deep (D, in black) resistivity curves are shown if available. Lithology is based on Canstrat data (www.canstrat.com).

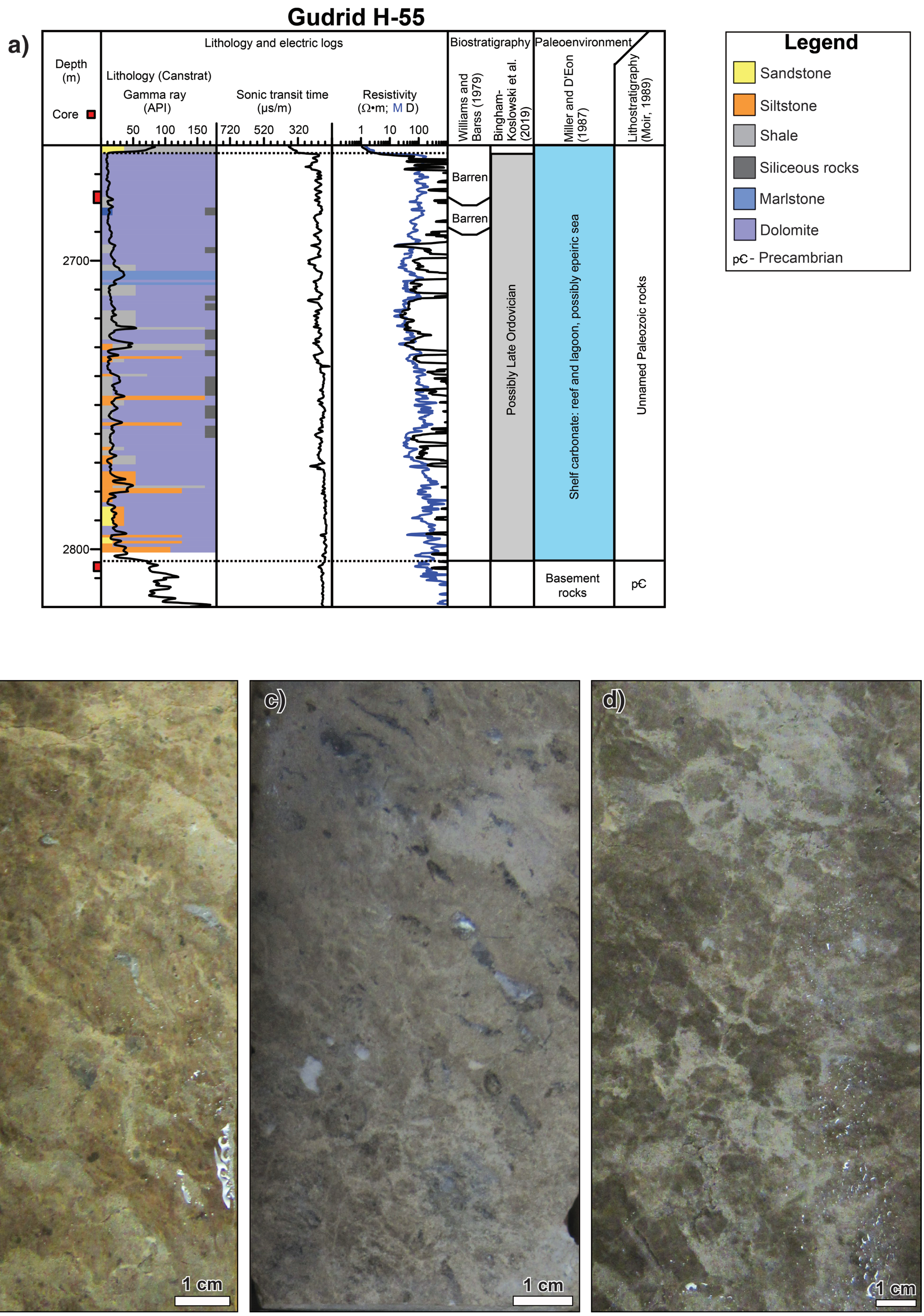

Figure 4. a) Well logs, biostratigraphic data, paleoenvironmental interpretations, lithostratigraphy, and core photographs (b, c, d) of the Paleozoic from Gudrid H-55. Dashed lines represent the bounding unconformities of the Paleozoic interval. Both medium (M, in blue) and deep (D, in black) resistivity curves are displayed. Lithology is based on Canstrat data. **b)** Mottled dolostone (top of image at 2678.85 m); NRCan photo 2019-607. **c)** Mottled dolostone with cement infilling pore spaces (top of image at 2679.41 m); NRCan photo 2019-608. **d)** Mottled dolostone (top of image at 2679.64 m); NRCan photo 2019-609. (*Modified from* Bingham-Koslowski, 2019.) All photographs by N. Bingham-Koslowski.

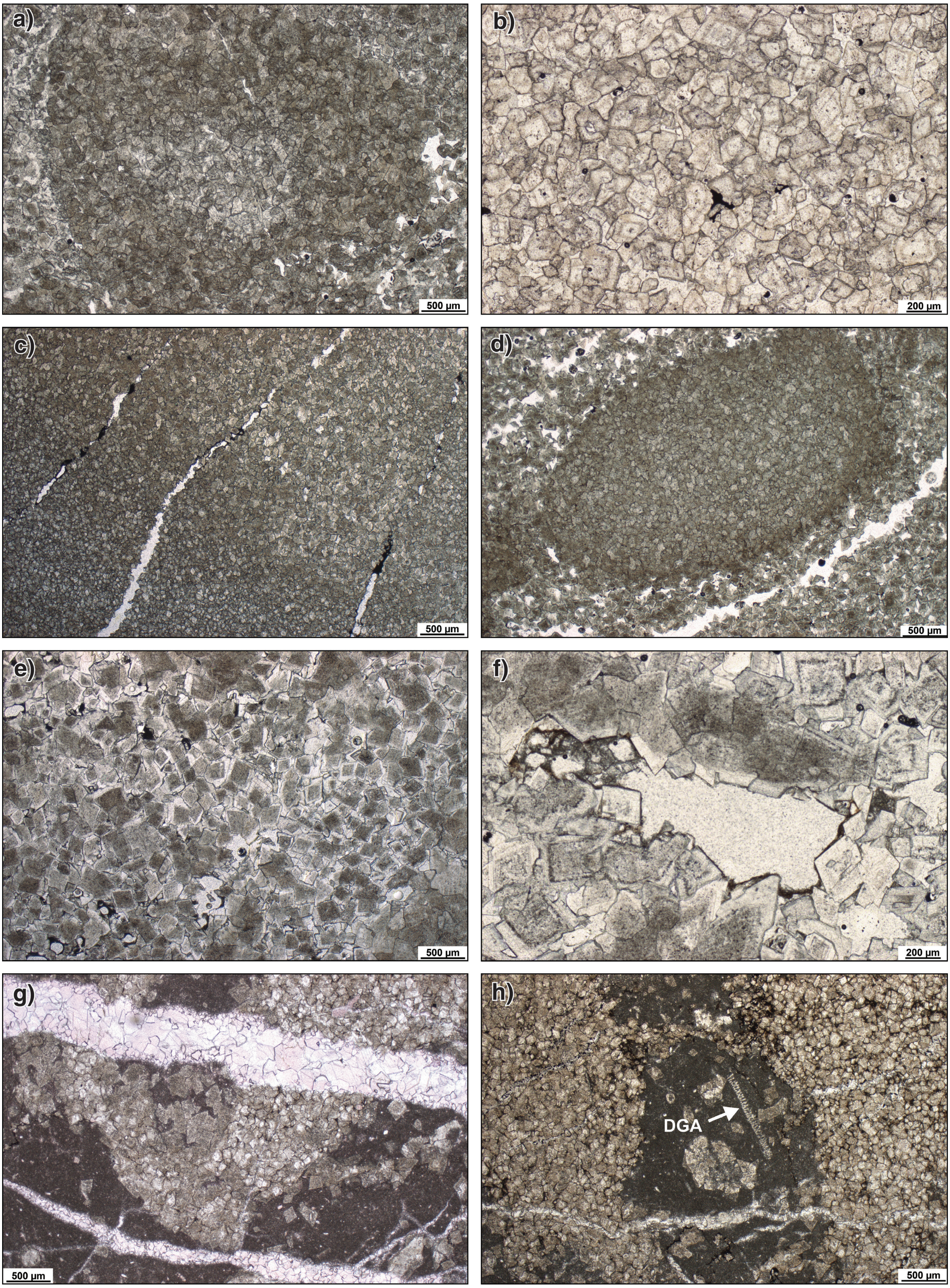

Figure 5. Thin sections from cores of the **a)**, **b)** Gudrid H-55, **c)**, **d)**, **e)**, **f)** Roberval K-92, and **g)**, **h)** Indian Harbour M-52 wells from the Labrador margin. All photomicrographs were taken in plane-polarized light (PPL). **a)** Mottled dolostone (2676.44 m, Gudrid H-55); NRCan photo 2019-610. **b)** Dolostone consisting of subhedral to euhedral dolomite exhibiting zoning (2679.43 m, Gudrid H-55); NRCan photo 2019-611. **c)** Anhedral to subhedral dolomite (3578.06 m, Roberval K-92, core 6). Note slightly mottled appearance and the presence of an unknown hydrocarbon in the fractures; NRCan photo 2019-612. **d)** A rounded patch (possible ichnofossil) of anhedral to subhedral dolomite surrounded by subhedral to euhedral dolomite (3578.78 m, Roberval K-92, core 6); NRCan photo 2019-613. **e)** Subhedral to anhedral dolomite with cloudy cores (3870 m, Roberval K-92, core 7); NRCan photo 2019-614. **f)** An unknown hydrocarbon lining a pore in subhedral to euhedral dolomite (3870.85 m, Roberval K-92, core 7); NRCan photo 2019-615. **g)** Fracture crosscutting a patch of dolomite in a fossiliferous wackestone to mudstone matrix (3952.48 m, Indian Harbour M-52); NRCan photo 2019-616. **h)** A fossiliferous wackestone with a fragment of dasycladacean green algae (DGA) surrounded by subhedral to euhedral dolomite (3955.35 m, Indian Harbour M-52); NRCan photo 2019-617 (*modified from* Bingham-Koslowski, 2019). All photographs by N. Bingham-Koslowski.

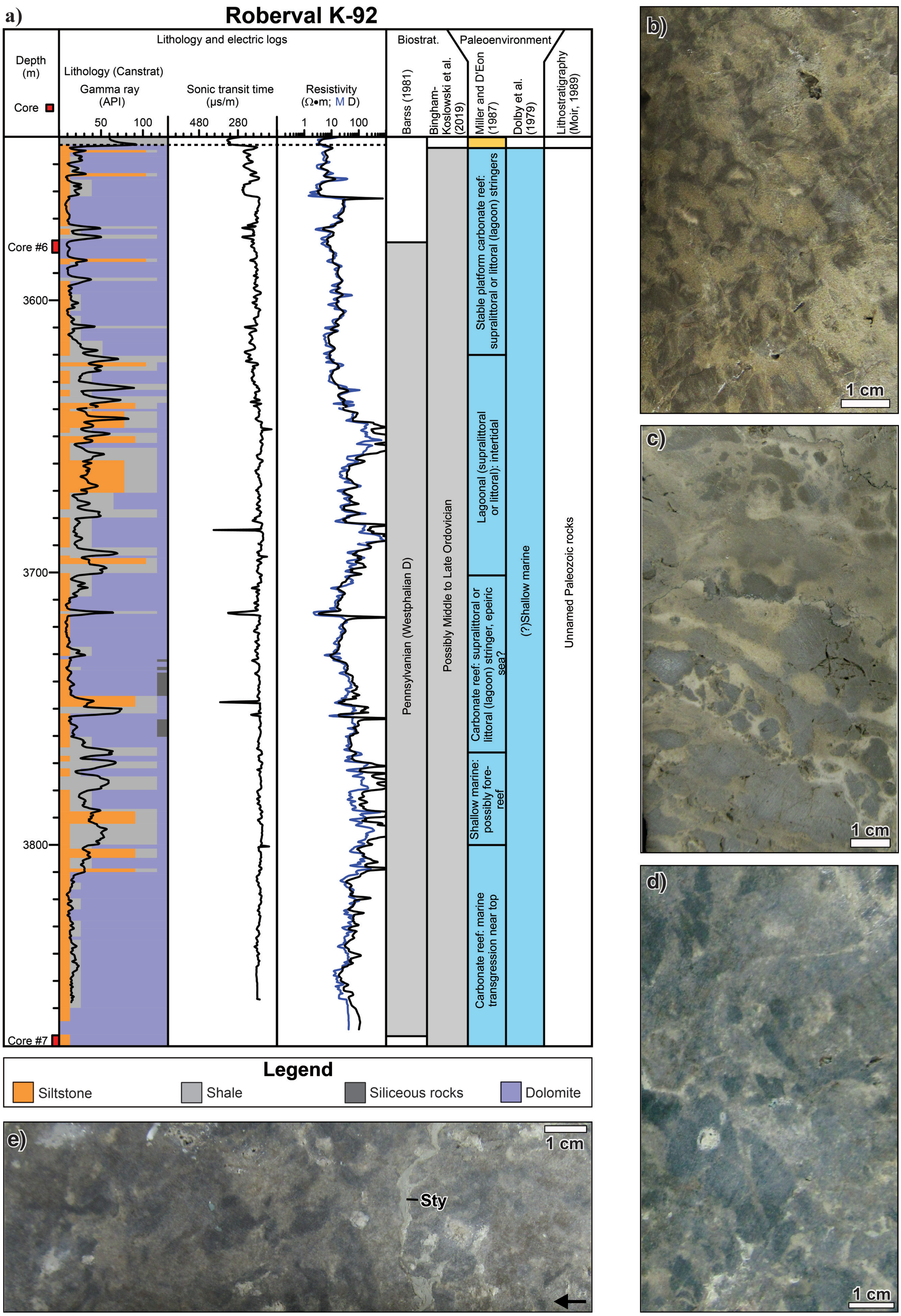

Figure 6. a) Well logs, biostratigraphic data (Biostrat.), paleoenvironmental interpretations, lithostratigraphy, and core photographs (b, c, d, e) of the Paleozoic from Roberval K-92. Dashed line represents the upper bounding unconformity (Paleozoic–Mesozoic) of the Paleozoic interval. Both medium (M, in blue) and deep (D, in black) resistivity curves are displayed. Lithology is based on Canstrat data. **b)** Mottled dolostone (core 6, top of image at 3578.53 m); NRCan photo 2019-618. **c)** Mottled and brecciated dolostone (core 6, top of image at 3579.13 m); NRCan photo 2019-619. **d)** Mottled dolostone (core 7, top of image at 3870.08 m); NRCan photo 2019-620. **e)** Mottled dolostone with alteration associated with a stylolite (Sty). Arrow indicates up direction (core 7, top of image at 3870.22 m) (*modified from* Bingham-Koslowski, 2019); NRCan photo 2019-621. All photographs by N. Bingham-Koslowski.

Indian Harbour M-52 and Freydis B-87 wells. A hydrocarbon of unknown origin is also observed within fractures and pores in thin sections from both core 6 and core 7 (Fig. 5c, e, f) (Bingham-Koslowski, 2019).

Indian Harbour M-52

The BP Columbia et al. Indian Harbour M-52 well reached a total depth of 3958.2 m and contains the thickest succession of Paleozoic strata in the Hopedale Basin, 427.2 m (3531 m to 3958.2 m) (Table 1; Fig. 7) (BP Exploration Canada Ltd., 1975; Canada-Newfoundland and Labrador Offshore Petroleum Board, 2007a) (*see* Table 2, Bingham-Koslowski, McCartney, and Bojesen-Koefoed, this volume). The Paleozoic interval is composed of (?)Middle to Upper Ordovician, light- to medium-grey to dark brown limestone and dolostone units with numerous tuffaceous beds identified from cuttings and in sidewall cores (Barnes et al., 1981; Jenkins, 1984; Miller and D'Eon, 1987; Moir, 1989; Bell and Howie, 1990). Bell and Howie (1990) divided the Paleozoic at Indian Harbour into three informal units: a lower dolomite unit (3700.1 m to 3958.2 m; grey to brown microcrystalline dolomite with limestone intervals); a middle limestone unit (3528.2 m to 3700.1 m; light grey to buff microcrystalline limestone that has been locally dolomitized, volcanic beds that may be tuffs and calcareous shale beds are also present); and an upper chert unit that straddles the Paleozoic–Mesozoic unconformity (3484.3 m to 3528.2 m; dark grey chert or quartzite). A conventional core was recovered from the Paleozoic interval (between 3952 m and 3958.1 m; Fig. 7) composed primarily of limestone with varying amounts of dolomite (Fig. 5g, h, 7b, c), including saddle dolomite (Fig. 8a, b) (Bingham-Koslowski, 2019). Fossils identified in core, sidewall cores, and thin sections include the calcimicrobe *Girvanella*, fragments of crinoids, bivalves, sponge spicules, bryozoans, dasycladacean green algae (Fig. 5h), trilobites, brachiopods, and gastropods as well as possible radiolarians and calcispheres (BP Exploration Canada Ltd., 1976; Walters, 1977; Miller and D'Eon, 1987; Bingham-Koslowski, 2019). A recent palynological study of the Paleozoic strata in the Hopedale Basin was able to refine the age of the Indian Harbour M-52 Upper Ordovician carbonate rocks, demonstrating that the top of the interval (3536.6 m to 3628 m) is Katian (the youngest Paleozoic strata observed in the Hopedale Basin) with the underlying rocks determined as Sandbian (3631.1 m to 3728.7 m), (?)Middle to Upper Ordovician (3728.7 m to 3929.9 m), and possibly Middle Ordovician at the base of the well (3929.9 m to 3957.7 m) (Bingham-Koslowski et al., 2019).

Freydis B-87

The Eastcan et al. Freydis B-87 well represents the southernmost occurrence of Paleozoic strata in the Hopedale Basin (*see* Table 2, Bingham-Koslowski, McCartney, and Bojesen-Koefoed, this volume). The well reached a total depth of 2314.1 m, 409 m of which (1905.2 m to 2314.1 m) has been identified as Paleozoic (Upper Ordovician–Sandbian) strata (Table 1; Fig. 9) (Laborde et al., 1975; Rauwerda, 1975; Plé and Ferrero, 1976; Williams, 1979; Jenkins, 1984; Moir, 1989; Bell and Howie, 1990; Williams et al., 1990; Canada-Newfoundland and Labrador Offshore Petroleum Board, 2007d; Ainsworth et al., 2016; Bingham-Koslowski et al., 2019). The presence of both siliciclastic and carbonate rocks within the Paleozoic interval has resulted in the informal subdivision of the Paleozoic into the Freydis sandstone (1905.2 m to 2238.5 m; unrelated to the Upper Cretaceous Freydis sands of the Markland sequence) and the Freydis limestone (2238.5 m to 2314.1 m) (Fig. 9) (Laborde et al., 1975; Plé and Ferrero, 1976; Bell and Howie, 1990).

The Freydis sandstone (1905.2 m to 2238.5 m) represents the only Paleozoic siliciclastic strata in the Hopedale Basin area and is composed of interbedded sandstone, siltstone, and shale units (Laborde et al., 1975; Plé and Ferrero, 1976; Miller and D'Eon, 1987; Bell and Howie, 1990; Bingham-Koslowski, 2019). Bell and Howie (1990) divided the Freydis sandstone into three units: a lower siltstone (2167.3 m to 2238.5 m; red calcareous siltstone with interbedded shale and fine-grained sandstone units), a middle limy unit (2103.0 m to 2167.3 m; interbedded light brown, argillaceous limestone and calcareous siltstone) and an upper siltstone unit (1905.2 m to 2103 m; interbedded grey to green-grey calcareous siltstone, fine-grained sandstone, and shale). Core 1 (1934.9 m to 1941.3 m) is one of two conventional cores recovered from the Freydis B-87 well and is representative of the Freydis sandstone (Fig. 8c, d, e, f, 9b, c). Bioturbation is common in the core, especially in the finer grained beds (mudstone to very fine sand) with the degree of bioturbation ranging from moderate (discrete trace fossils; Fig. 8e, 9c) to pervasive ('lam-scram') (Bingham-Koslowski, 2019). Trace fossils are observed along the length of the core with horizontal traces dominating. Centimetre-scale siltstone to fine-grained sandstone beds can be massive or can contain sedimentary structures such as planar laminations or ripple crosslaminations (Fig. 8d, 9b). An increase in carbonate content was noted in several discrete intervals. These 'carbonate' intervals are light grey and are composed of quartz sand, carbonate cement, and fossil fragments (Fig. 8c). Fossils identified in these carbonate units include shell fragments, bivalves, echinoderms, brachiopods, corals, and bryozoans (Bingham-Koslowski, 2019).

The Freydis limestone (2238.5 m to 2314.1 m) is predominantly composed of micritic, light grey to dark brown, argillaceous, fossiliferous limestone (mudstone to wackestone) with a minor amount of dolomite (Fig. 8g, h, 9d, e) (Laborde et al., 1975; Plé and Ferrero, 1976; Moir, 1989; Bell and Howie, 1990; Bingham-Koslowski, 2019). Core 2 from the Freydis B-87 well was recovered from the Freydis limestone interval (2307.3 m to 2313.4 m; Fig. 9). Macro-scale shell fossils (centimetre-scale) are visible in the core and include bivalve and gastropod specimens (Fig. 9d, e) (Bingham-Koslowski, 2019). The matrix is dominated in some samples by microbial mudstone characterized by a clotted fabric and, on occasion, the calcimicrobe *Girvanella* is present in thin sections. Fossils are common to abundant with fragments of gastropods, bivalves, crinoids, dasycladacean green algae, bryozoans (some fenestrate specimens), trilobites, brachiopods, sponge spicules, ostracods, cephalopods, and calcispheres recognized in thin section (Fig. 8g, h) (Bingham-Koslowski, 2019).

LOWER PALEOZOIC STRATIGRAPHY OF WESTERN DAVIS STRAIT

Lower Paleozoic strata are interpreted to be present offshore Baffin Island in Foxe Basin (including in the Rowley M-04 well; Lavoie et al., 2019), Hudson Strait, Ungava Bay (including in the Akpatok L-26 well; Lavoie et al., 2019), and the Davis Strait from seismic reflection, magnetic, and gravity data (MacLean and Williams, 1983; Bell and Howie, 1990) (Fig. 1). This section focuses on the Lower Paleozoic of the southeastern Baffin Shelf (in western Davis Strait) as this region falls within the study area of interest (Fig. 10). Data in this region is very limited as sampling and seismic surveys offshore have been restricted by the remote location and regulations associated with the collection of physical bedrock samples and the acquisition of subsurface geophysical data. The extent of the Paleozoic geology in the region has been mapped primarily using available low-quality seismic reflection data (both industry and Geological Survey of Canada surveys; *see* Dafoe, DesRoches, and Williams, this volume). A limited number of bedrock specimens of in situ Paleozoic rocks exist (primarily in the form of drill cores collected during Geological Survey of Canada–led research expeditions) to ground truth the geophysical interpretations. Geophysical data along with drill cores and piston cores demonstrate that the offshore subsurface geology of the southeastern Baffin Shelf is complex consisting of Precambrian to Quaternary, semiconsolidated to consolidated sedimentary (limestone and sandstone), igneous (granite and basalt), and metamorphic (gneiss) rocks (Jansa, 1976; MacLean, 1978; Bell and Howie, 1990). Paleozoic rocks were deformed prior to being covered by Mesozoic and Cenozoic successions, with several faults and folds exposed in seismic profiles and multibeam maps (MacLean et al., 1977; Bell and Howie, 1990). Bedrock is not exposed at the seafloor anywhere on the southeast Baffin Shelf, rather it is overlain by a layer of unconsolidated overburden (MacLean et al., 1977).

Ordovician strata are interpreted to underlie a significant area of the southeastern Baffin Shelf between Frobisher Bay and Cumberland Sound (Fig. 10) (*see* Dafoe, DesRoches, and Williams, this volume). The geophysical data further suggests the presence of these rocks in Frobisher Bay (also inferred from submersible observations), and at the mouth of Cumberland Sound (Grant, 1975; MacLean et al., 1982, 1986; Bell and Howie, 1990). Lower Paleozoic rocks were historically interpreted to be present between Cumberland Sound and Cape Dyer, as well as in two small structurally controlled basement depressions located to the southeast of Lady Franklin Island (MacLean, 1978). These occurrences are not shown in Figure 10 as recent mapping efforts were unable to verify the presence of Paleozoic strata (*see* Dafoe, DesRoches, and Williams, this volume). Acoustically fast, pre-Mesozoic sedimentary sequences occur locally along the eastern margin of Baffin Island between Cape Dyer and Bylot Island (Fig. 1) (MacLean et al., 1984; Bell and Howie, 1990); however, no physical specimens were recovered to verify the age and composition of these units (Bell and Howie, 1990).

The Lower Paleozoic interval on the southeastern Baffin Shelf unconformably overlies Precambrian gneiss, migmatite, and schist and is, in turn, unconformably overlain to the north and seaward (southeast) by Mesozoic to Cenozoic strata (MacLean et al., 1977; Dafoe, DesRoches, and Williams, this volume). Both the Precambrian

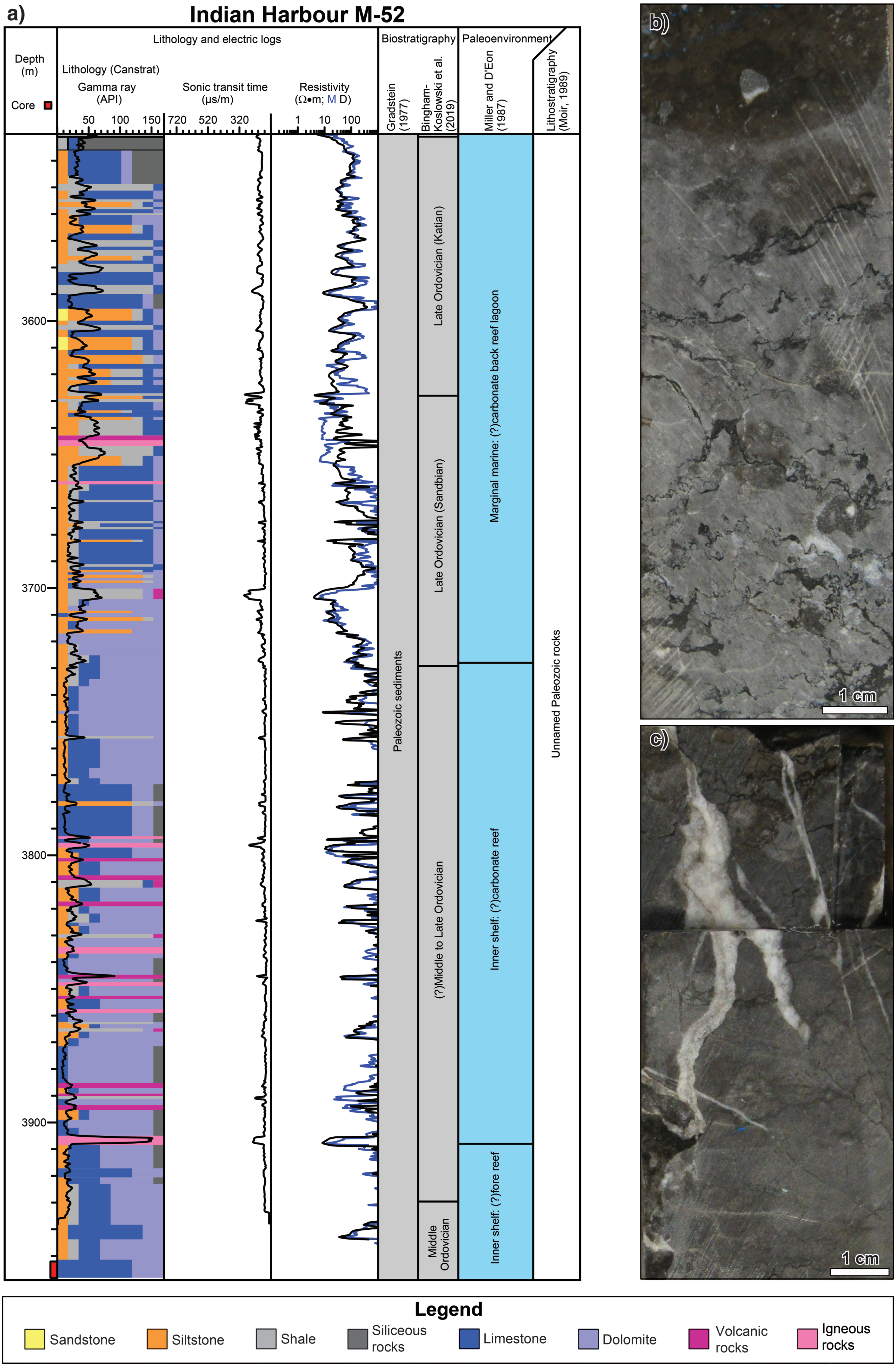

Figure 7. **a)** Well logs, biostratigraphic data, paleoenvironmental interpretations, lithostratigraphy, and core photographs (b, c) of the Paleozoic from Indian Harbour M-52. Both medium (M, in blue) and deep (D, in black) resistivity curves are displayed. Lithology is based on Canstrat data. **b)** Stylolitic limestone with dolomite (top of image at 3952.06 m); NRCan photo 2019-622. **c)** Cement-filled fracture in limestone with dolomite (top of image at 3956.46 m); NRCan photo 2019-623 (*modified from* Bingham-Koslowski, 2019). All photographs by N. Bingham-Koslowski.

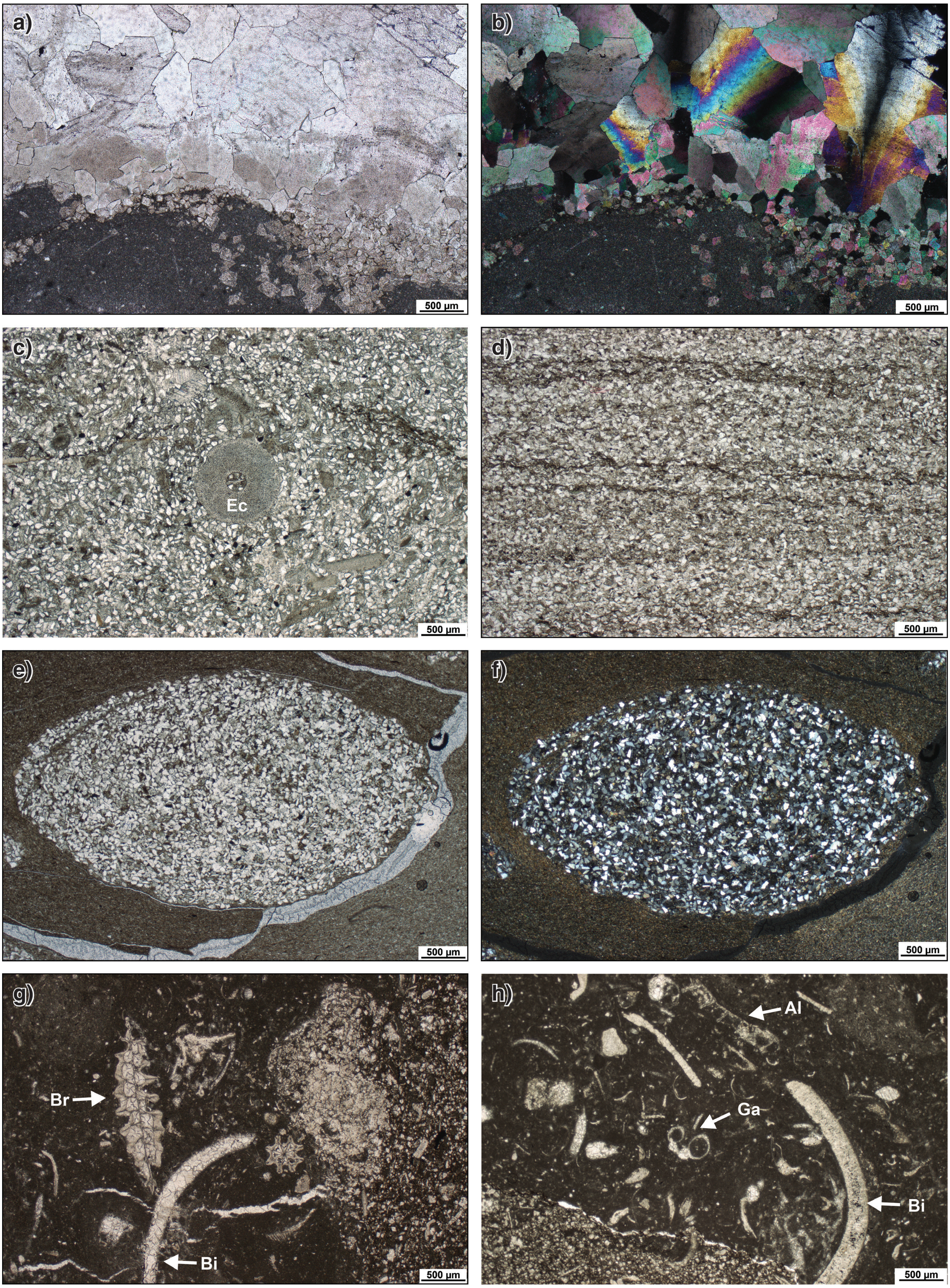

Figure 8. Thin sections from cores of the Indian Harbour M-52 (8a, b) and Freydis B-87 (8c–h) wells from the Labrador margin. Photomicrographs were either taken under plane-polarized light (PPL) or crosspolarized light (XPL). **a)** Saddle dolomite (3952.94 m, Indian Harbour M-52; PPL); NRCan photo 2019-624. **b)** Sweeping extinction of saddle dolomite (3952.94 m, Indian Harbour M-52; XPL); NRCan photo 2019-625. **c)** A fossiliferous sandstone with echinoderms (crinoid; Ec) and fossil fragments (1935.6 m, Freydis B-87, core 1; PPL); NRCan photo 2019-626. **d)** Laminated sandstone (1935.79 m, Freydis B-87, core 1; PPL); NRCan photo 2019-627. **e)** A sand-filled trace fossil in an otherwise mudstone interval (1941.15 m, Freydis B-87, core 1; PPL); NRCan photo 2019-628. **f)** Same image as in Figure 8e, but under XPL (1941.15 m, Freydis B-87, core 1); NRCan photo 2019-629. **g)** A fossiliferous wackestone with fragments of bryozoans (Br) and bivalves (Bi) in a mudstone matrix (2311.21 m, Freydis B-87, core 2; PPL); NRCan photo 2019-630. **h)** A fossiliferous wackestone with fragments of gastropods (Ga), algae (Al), and bivalves (Bi) in a mudstone matrix (2313.16 m, Freydis B-87, core 2; PPL); NRCan photo 2019-631 (*modified from* Bingham-Koslowski, 2019). All photographs by N. Bingham-Koslowski.

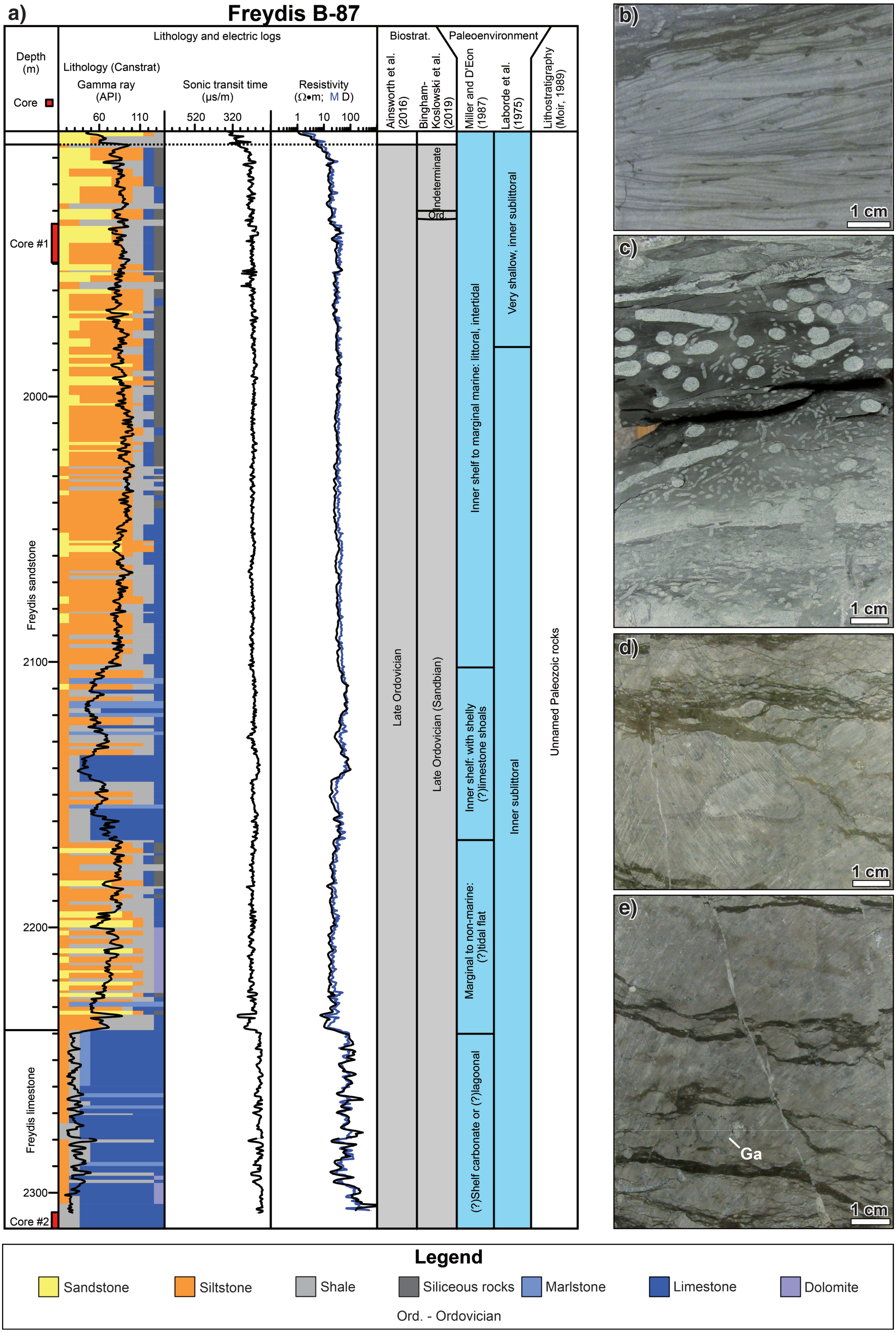

Figure 9. **a)** Well logs, biostratigraphic data (Biostrat.), paleoenvironmental interpretations, lithostratigraphy, and core photographs (b, c, d, e) of the Paleozoic from Freydis B-87. Dashed line represents the top bounding unconformity (Paleozoic–Mesozoic) of the Paleozoic interval. Both medium (M) and deep (D) resistivity curves are displayed. Lithology is based on Canstrat data. **b)** Siltstone to very fine-grained sandstone with ripple crosslaminations (core 1, top of image at 1935.82 m); NRCan photo 2019-632. **c)** Sand-filled ichnofossils in a mudstone with silt and fine-grained sand content increasing toward the base of the piece (core 1, top of image at 1940.27 m); NRCan photo 2019-633. **d)** Fossiliferous wackestone with argillaceous stringers and macroscopic shells (core 2, top of image at 2311.40 m); NRCan photo 2019-634. **e)** Fossiliferous wackestone with argillaceous stringers and a macroscopic gastropod (Ga) (core 2, top of image at 2311.47 m); NRCan photo 2019-635 (*modified from* Bingham-Koslowski, 2019). All photographs by N. Bingham-Koslowski.

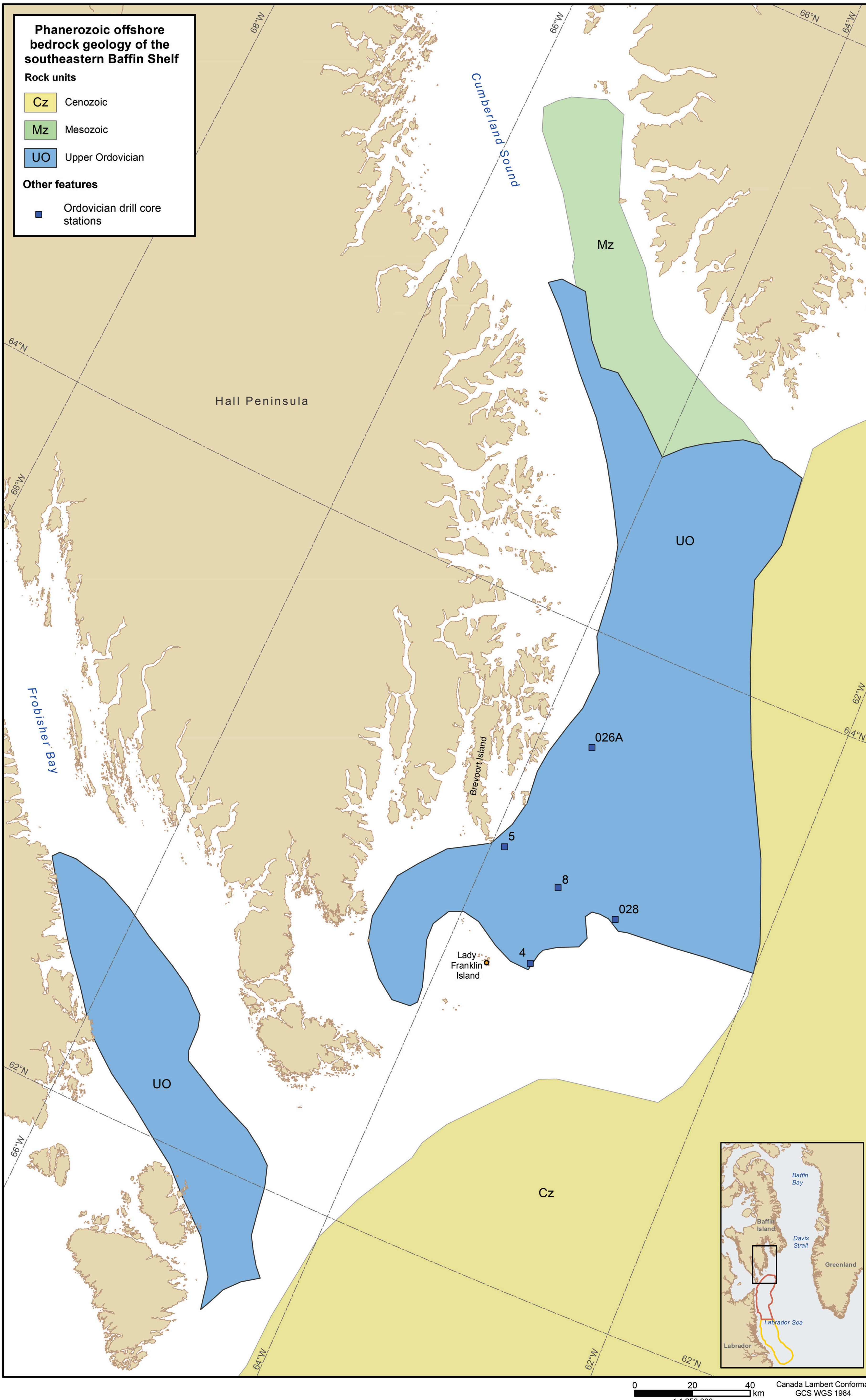
Phanerozoic offshore bedrock geology of the southeastern Baffin Shelf
Rock units
Cz Cenozoic
Mz Mesozoic
UO Upper Ordovician
Other features
Ordovician drill core stations
Cumberland Sound
Hall Peninsula
Frobisher Bay
Breyvoort Island
Lady Franklin Island
Mz
UO
UO
Cz
026A
5
8
028
4
68°W
66°W
64°W
62°W
66°N
64°N
62°N
Baffin Bay
Baffin Island
Davis Strait
Greenland
Labrador Sea
Labrador
0 20 40 km
1:1 250 000
Canada Lambert Conformal
GCS WGS 1984

and Ordovician intervals identified in geophysical data were assumed by MacLean et al. (1977) to extend seaward in the subsurface to the continent-ocean transition zone; however, the exact extent of the carbonate rocks beneath the onlapping Mesozoic–Cenozoic rocks is unknown as wells drilled on the southeastern Baffin Shelf, in western Davis Strait, terminate in Cenozoic strata (Bell and Howie, 1990). Offshore Lower Paleozoic strata have been sampled from five localities on the southeastern Baffin Shelf, resulting in the recovery of six Paleozoic limestone drill cores (Fig. 10; Table 2). These drill cores provide the only information on the age (Middle to Late Ordovician) and lithology (carbonate) of the Lower Paleozoic in the region and have been used to ground truth geophysical interpretations for the Paleozoic in western Davis Strait and adjacent areas (MacLean et al., 1977; Bingham-Koslowski, 2018).

Offshore geophysical data

The subsurface geology of offshore southeastern Baffin Island, from Hudson Strait to Cape Dyer, was largely unknown until the 1970s when Geological Survey of Canada research cruises targeted the area and collected magnetic and single-channel seismic data (Bell and Howie, 1990). Grant (1975) proposed a six geophysical unit subdivision for the subsurface of the region based on the newly acquired seismic data and magnetic profiles that grouped the geology into Precambrian, early Paleozoic, late Paleozoic to Mesozoic, and Cretaceous to Cenozoic intervals. The geophysical data suggested that the subsurface geology of the southeastern Baffin Shelf was more complicated than that of offshore Labrador (Grant, 1975). Seismic and magnetic profiles revealed folding, faulting, and the presence of diapir-like intrusions in Paleozoic to Cenozoic strata, as well as the presence of lower Cenozoic basalt flows overlying these rocks offshore of Cape Dyer (Grant, 1975). No physical bedrock samples were available north of the Labrador Shelf Bjarni H-81 well (512 km to the south) at the time to corroborate the geophysical data (MacLean and Srivastava, 1976). The single-channel seismic and magnetic data, along with Grant's observations, were used to identify areas of consolidated bedrock on the southeastern Baffin Shelf that would make suitable drill-core targets for future research cruises such as Cruise 75-009, Phase V (in 1975), and Cruise 77027 (in 1977), discussed in detail in the following sections.

Limited seismic data as well as drill cores have been collected in the region since the 1970s. The quality of the single-channel seismic data from the 1970s is considered poor by today's standards, hindering attempts to accurately map the extent of Paleozoic strata in the area, and impeding interpretations of the offshore geology. Where multichannel seismic data permitted, modifications were made to the extent of the Paleozoic along the southeastern Baffin Shelf (Fig. 10; *see* Dafoe, DesRoches, and Williams, this volume)

Collection and historical research of the offshore drill cores

Six Lower Paleozoic limestone drill cores from five localities on the southeastern Baffin Shelf were recovered in the 1970s by two Geological Survey of Canada–led research cruises: Cruise 75-009, Phase V in 1975; and Cruise 77027 in 1977 (Table 2; Fig. 10). The drill cores were collected using the Bedford Institute of Oceanography's underwater electric rock-core drill. The rock-core drill had a maximum penetration depth of 6 m below the sea floor and cut 25 mm diameter drill core (MacLean and Srivastava, 1976; MacLean, 1978).

Cruise 75-009, Phase V

Cruise 75-009, Phase V took place between September 15 and 17, 1975 aboard the *CSS Hudson* (MacLean and Srivastava, 1976). Several potential drill-core target sites were identified based on seismic reflection data prior to the cruise. Specific drill sites were then determined at sea based on shallow seismic (625 cm^3 air gun) and Huntec high-resolution deep tow system surveys (MacLean and Srivastava, 1976; MacLean et al., 1977). Areas that appeared more consolidated in seismic profiles, and therefore presented a better chance of success for coring, were preferentially targeted. Fifteen drilling attempts were made at nine locations, with six drill cores recovered from four of the locations. Four of the six drill cores (stations 4, 5, 8A, and 8B) consist of Paleozoic limestone, whereas the other two (stations 9A and 9B) are composed of gneiss (MacLean and Srivastava, 1976). The gneiss observed in the drill cores from stations 9A and 9B is thought to be representative of the Precambrian metamorphic basement; all other occurrences of metamorphic or igneous rocks in the drill cores are interpreted as erratics (MacLean et al., 1977).

Two potential subdivision schemes for the Lower Paleozoic strata based on the 1975 drill cores have been proposed. Jansa (1976) categorized the four Paleozoic drill cores from Cruise 75-009, Phase V into three lithostratigraphic units based on composition, colour, sedimentary structures, and fossil components as identified in drill-core and thin-section descriptions. Unit 1 is defined by the strata from station 4 and is described as mottled, olive to grey dolomitic limestone characterized by pebble conglomerate and breccia. Unit 2 consists of massive, pale yellow to brown skeletal wackestone that may be bioturbated and locally dolomitized as per the carbonate rocks at station 5. Unit 3 encompasses the Paleozoic strata from stations 8A and 8B and is described as being composed of dark yellow-brown, radiolarian-dominant, bituminous, micritic limestone that may exhibit minor dolomitization. MacLean and colleagues (1977), conversely divided the strata at the drill-core locations into two units based on lithological, seismic, and magnetic characteristics. Unit 1 was defined from the station 5 drill core and consists of strata with higher seismic velocities bounded by a fault to the east (between stations 5 and 8). This unit was interpreted to occur in a narrow band (up to 40 km wide) that runs along the southeast coast of Baffin Island. Unit 2 included the remaining drill cores (stations 4, 8A, and 8B) and consisted of all other Lower Paleozoic strata in the region (MacLean et al., 1977). Biostratigraphic analysis on palynomorphs and corals from the Paleozoic drill cores of Cruise 75-009, Phase V have provided a Middle to Late Ordovician age for the strata (W.A.M. Jenkins, GSC unpub. report 13-WAMJ-1976, 1976; MacLean et al., 1977).

Cruise 77027

Cruise 77027 took place aboard the *CSS Hudson* between 18 September and 13 October, 1977 (Atlantic Geoscience Centre, 1977). Drilling sites were determined based on data collected by seismic reflection (40 cubic inchair gun) and Huntec deep-tow systems. Twenty-six drilling attempts were made at 16 locations with over 7 m of drill core from six sites recovered (Atlantic Geoscience Centre, 1977; MacLean, 1978). Two of these drill cores, stations 026A and 028, are composed of Paleozoic strata (Table 2). No attempts have been made to define lithostratigraphic units in these two drill cores or to incorporate them into existing schemes (e.g. Jansa, 1976, MacLean et al., 1977). The drill cores from stations 026A and 028 are considered to be part of the same Middle to Upper Ordovician sedimentary sequence as the 1975 Paleozoic drill cores based on their proximity to the 1975 sites, as well as lithological, seismic, and magnetic similarities (MacLean, 1978). No biostratigraphic analysis has been conducted on these two drill cores to confirm their ages.

Lithological descriptions of the drill cores

Similar to the Labrador margin, no formal lithostratigraphic units have been defined for the Lower Paleozoic of the western Davis Strait region and as such, it is not possible to address the interval as one unit. The following sections summarize the lithology of each drill core collected from the southeastern Baffin Shelf.

Cruise 75-009, Phase V, station 4

Station 4 is the southernmost Paleozoic drill core, located 46 km southeast of Brevoort Island and 15 km east-northeast of Lady Franklin Island (Fig. 10) (MacLean and Srivastava, 1976). The station is underlain by westward-dipping strata (approximately 14°) that terminate against a basement high observed in seismic and magnetic data 2 km to the southeast of station 4 (MacLean et al., 1977). The drill core recovered from station 4 is 137 cm in length and composed of mottled, olive-grey to buff limestone (Fig. 11a, b, c, 12a, b) (Jansa, 1976; Bingham-Koslowski, 2018). Dolomite is present throughout the drill core, increasing toward the pervasively dolomitized base (Fig. 12b). Consequently, fossil content and mottling decrease in abundance toward the base of the drill core. Discrete trace fossils are observed in the upper 100 cm of the drill core (Fig. 11a) and fragments of trilobites, bivalves, echinoderms (crinoids), and brachiopods have also been identified in this interval (Fig. 12a). Angular to rounded, centimetre-scale intraclasts are noted throughout the upper 100 cm of the drill core, as are a pebble lag and a skeletal breccia (Fig. 11b)

Figure 10. Distribution map showing the extent of Upper Ordovician strata in western Davis Strait; the Paleozoic rock package is bounded by unconformities with the underlying Precambrian rocks and the overlying Mesozoic and Cenozoic strata. The locations of Paleozoic drill cores recovered by scientific expeditions led by the Geological Survey of Canada on the southeastern Baffin Shelf are indicated on the map. Extent of Upper Ordovician strata is from Dafoe, DesRoches, and Williams (this volume).

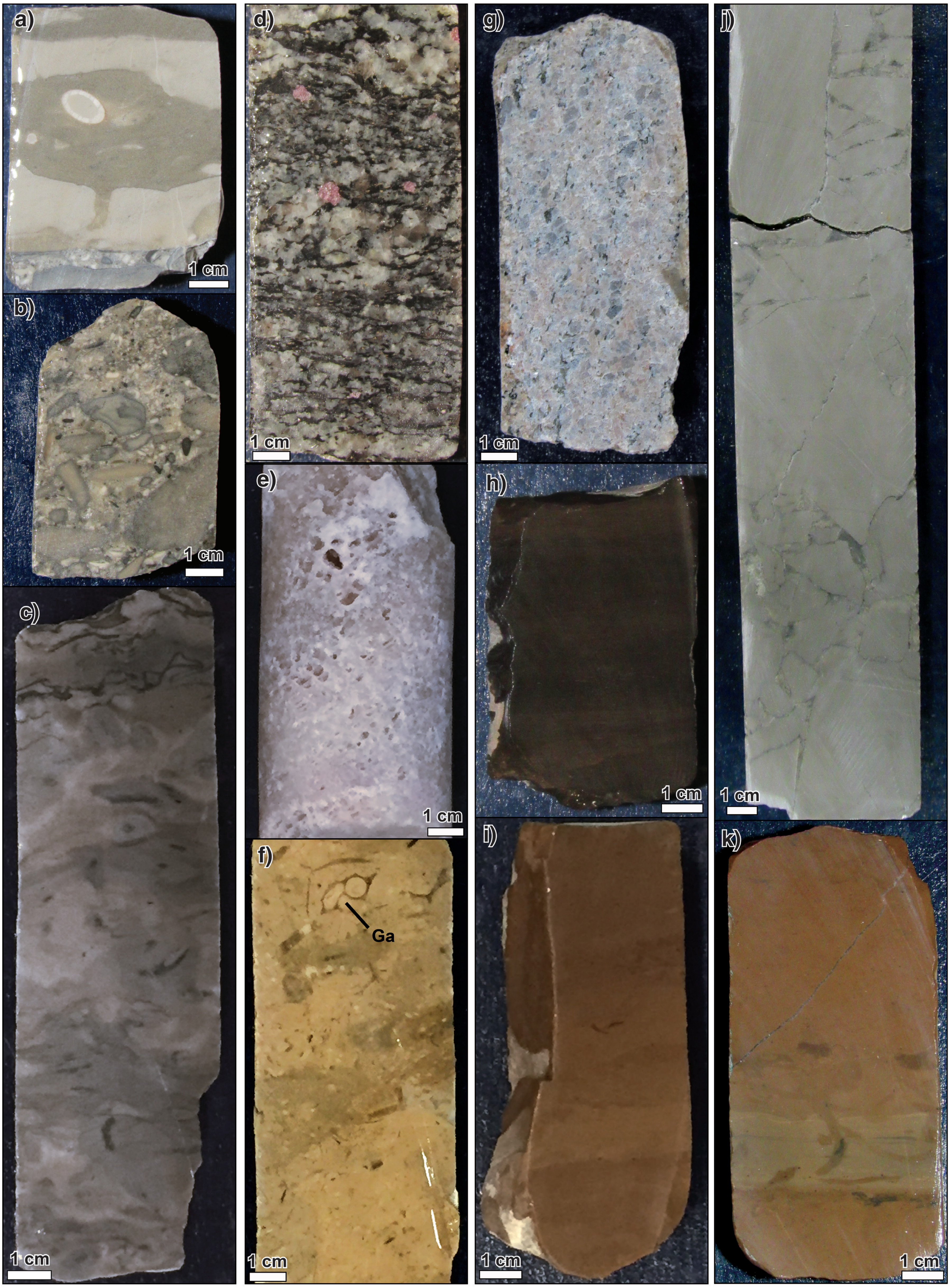

Figure 11. Drill core photographs from the southeastern Baffin Shelf. Depths are in centimetres from top of drill core. **a)** Dolomitized, fossiliferous mudstone with trace fossils and a pebble lag at the base (Cruise 75-009, Phase V, station 4, base at 30 cm); NRCan photo 2019-636. **b)** Packstone and/or breccia of angular skeletal fragments (Cruise 75-009, Phase V, station 4, base at 58 cm); NRCan photo 2019-637. **c)** Mottled fossiliferous dolostone (Cruise 75-009, Phase V, station 4, base at 121 cm); NRCan photo 2019-638. **d)** Garnet-biotite gneiss erratic in overburden (Cruise 75-009, Phase V, station 5, base at 65 cm); NRCan photo 2019-639. **e)** Colonial rugose coral (Cruise 75-009, Phase V, station 5, base at 115 cm); NRCan photo 2019-640. **f)** Fossiliferous wackestone with shell fragments and a gastropod (Ga) (Cruise 75-009, Phase V, station 5, base at 123 cm); NRCan photo 2019-641. **g)** Granite erratic in overburden (Cruise 75-009, Phase V, station 8A, base at 6.5 cm); NRCan photo 2019-642. **h)** Dark brown, organic-rich lime mudstone (Cruise 75-009, Phase V, station 8A, base at 45 cm); NRCan photo 2019-643. **i)** Mottled lime mudstone (Cruise 75-009, Phase V, station 8B, base at 38 cm); NRCan photo 2019-644. **j)** Brecciated lime mudstone (Cruise 77027, station 026A, base at 32 cm); NRCan photo 2019-645. **k)** Mottled lime mudstone with ichnofossils (Cruise 77027, station 028, base at 34 cm); NRCan photo 2019-646 (*modified from* Bingham-Koslowski, 2018). All photographs by N. Bingham-Koslowski.

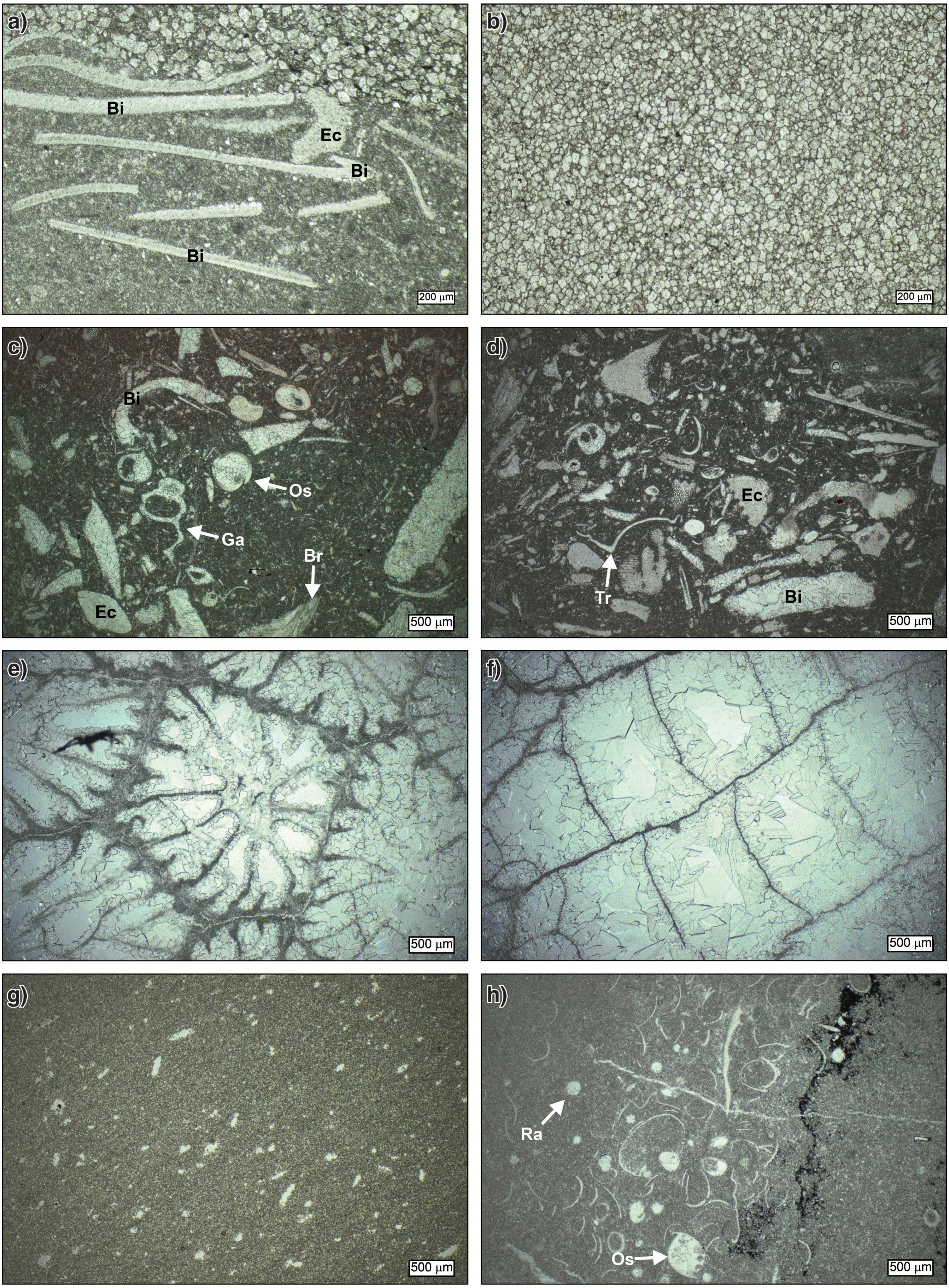

Figure 12. Thin sections from drill cores recovered from Cruise 75-009, Phase V, stations 4 (Fig. 12a, b), 5 (Fig. 12c–f), and 8 (Fig. 12g, h) from the southeastern Baffin Shelf. All photomicrographs were taken in plane-polarized light (PPL). **a)** Fragments of bivalve shells (Bi) and echinoderms (Ec) in a partially dolomitized section (station 4, piece 17, 19 inches); NRCan photo 2019-647. **b)** Pervasive dolomitization at depth in the drill core from station 4 (station 4, piece 7, 42 inches); NRCan photo 2019-648. **c)** A fossiliferous wackestone with echinoderm (Ec), bivalve (Bi), gastropod (Ga), ostracod (Os), and brachiopod (Br) fragments (station 5, piece 10, 31 inches); NRCan photo 2019-649. **d)** A fossiliferous wackestone to packstone with bivalve (Bi), trilobite (Tr), and echinoderm (Ec) fragments (station 5, piece 1, 47.5 inches); NRCan photo 2019-650. **e)** A colonial rugose coral (station 5, piece 5, 6.5 inches); NRCan photo 2019-651. **f)** A colonial rugose coral (station 5, piece 5, 6.5 inches); NRCan photo 2019-652. **g)** A finely crystalline dolomitized limestone with numerous voids that may be the result of fossil dissolution (station 8, piece 4, 13 inches); NRCan photo 2019-653. **h)** A fossiliferous layer consisting of shells, ostracods (Os), and radiolarians (Ra) (station 8, 20 inches); NRCan photo 2019-654 (*modified from* Bingham-Koslowski, 2018). All photographs by N. Bingham-Koslowski.

(Bingham-Koslowski, 2018). Organic matter content is low with a Rock Eval total organic content (TOC) value of 0.18% (MacLean et al., 1977). The lithology of the drill core has been interpreted as representing deposition in a shallow, subtidal environment above storm wave base, with the lag and breccia indicative of high-energy events (MacLean et al., 1977; Bingham-Koslowski, 2018).

Cruise 75-009, Phase V, station 5

Station 5 is located 6 km to the southeast of the southern tip of Brevoort Island and is separated from station 8 by a fault that lies 2 km east of station 5 (MacLean et al., 1977; Fig. 10). The Paleozoic rocks at station 5 have a similar magnetic profile as the strata at sites 4 and 8 (a low and overall smooth magnetic signature; MacLean et al., 1977), however, these rocks are distinctly acoustically harder, as observed in seismic profiles, with higher measured seismic velocities (MacLean et al., 1977). The drill core recovered from station 5 is 126 cm in length (Fig. 11d, e, f, 12c, d, e, f) with the top 65 cm composed of a garnet-biotite gneiss erratic in the overburden (Fig. 11d, 13g) (MacLean et al., 1977; Bingham-Koslowski, 2018). The remainder of the drill core consists of a fossiliferous wackestone to packstone with a micritic lime mud matrix that is moderately bioturbated and contains a minor amount of dolomite (Fig. 11f) (Jansa, 1976; MacLean et al., 1977; Bingham-Koslowski, 2018). Total organic carbon for the drill core was measured at 0.31% (MacLean et al., 1977). Fossil fragments identified in the drill core include echinoderms, crinoids, trilobites, brachiopods, cephalopods, corals, bryozoans, gastropods, calcispheres, sponge spicules, bivalves, dasycladacean green algae, and shell fragments (Fig. 12c, d) (Jansa, 1976; MacLean et al., 1977; Bingham-Koslowski, 2018). A colonial rugose coral, identified as the Ordovician *Favisitina sp.* by T.E. Bolton (GSC unpub. report 0-1-1976TEB, 1976), comprises approximately 5 cm of the drill core near the base (Fig. 11e, 12e, f). The presence of photosynthetic fossils coupled with a high mud content has resulted in the interpretation of a low-energy, shallow-water, open-marine depositional environment for the strata of the drill core at station 5.

Cruise 75-009, Phase V, station 8

Station 8 targeted a pronounced seismic reflector in an area where seismic reflections are observed to be gently dipping westward at an apparent dip angle of approximately 9° and have been deformed by several small faults and folds (MacLean et al., 1977). The station is positioned 24 km to the east-southeast of station 5, from which it is separated by a fault, and 27 km to the north of station 4 (Fig. 10). The first of three drilling attempts at station 8 recovered only gravel, some of which contained dolostone and fossiliferous limestone, which are interpreted as Paleozoic erratics (MacLean and Srivastava, 1976; Jansa, 1976). Fossils identified within thin sections created from the limestone gravel include shell fragments, bivalves, gastropods, ostracods, radiolarians, trilobites, and crinoids (Fig. 12g, h) (Bingham-Koslowski, 2018).

The second and third drilling attempts, stations 8A and 8B, respectively, both recovered drill cores composed of Paleozoic limestone with igneous (granite) erratics in the overburden (MacLean and Srivastava, 1976). The drill core from station 8A is 70 cm in length with 26 cm of granite overburden (Fig. 11g, 13h), and the drill core from station 8B is 89 cm long with 8 cm of granite overburden. The drill cores have similar carbonate lithologies, being composed of dark to medium brown, somewhat mottled, micritic mudstone to wackestone (Fig. 11h, i) (Jansa, 1976; MacLean et al., 1977; Bingham-Koslowski, 2018). Finely disseminated organic matter and phosphatized grains are found throughout both drill cores. Radiolarians are the most common fossil, with sponge spicules, macro-algae, shell fragments, bivalves, trilobites, and brachiopods also observed in the drill cores (Fig. 13a, b, c, d) (Jansa, 1976; Bingham-Koslowski, 2018). High-angled bedding is reported in the drill core from station 8A in the 6 cm interval below the granite overburden, suggesting that this interval may not be in situ. Discrete clusters of ichnofossils consisting of a handful of planar or vertical traces are also observed throughout station 8A drill core. Total organic carbon (TOC) measurements are the greatest at station 8 due to the abundance of disseminated organic matter in the drill cores with values of 1.37% TOC recorded at station 8A, and 0.90% TOC at station 8B (MacLean et al., 1977). The abundance of mud, pelagic fossils, and organic matter has been interpreted as being indicative of a low-energy, deep-water depositional setting with dysoxic to anoxic bottom waters (MacLean et al., 1977; Bingham-Koslowski, 2018).

Cruise 77027, station 026A

Station 026A is the northernmost station of both cruises (Fig. 10). The drill core recovered from station 026A is 83 cm in length with the top 7 cm composed of a gneiss erratic (overburden) (Bingham-Koslowski, 2018). The rest of the drill core is homogeneous, consisting of fractured and brecciated, grey lime mudstone (Fig. 11j). Radiolarians and small skeletal fragments are the only fossils observed from this drill core (Fig. 13e). The station 026A drill core is noticeably lacking in sedimentary structures and fossil content when compared to the other Paleozoic drill cores in the region (Bingham-Koslowski, 2018).

Cruise 77027, station 028

Station 028 is the easternmost station that encountered Paleozoic strata. It is located to the east of station 8 (Cruise 75-009, Phase V), and southeast of station 026A (Fig. 10). The drill core recovered from station 028 during Cruise 77027 is 100 cm in length with the top 6.5 cm composed of igneous gravel (granite and basalt) (Bingham-Koslowski, 2018). Directly below the overburden, is a short (<5 cm) section of brown to grey limestone (similar in composition to the rest of the drill core) with near-vertical bedding, suggesting that the limestone is out of place (Bingham-Koslowski, 2018). The remainder of the drill core is homogeneous, consisting of medium to buff-brown lime mudstone similar to the lithology of the drill cores from stations 8A and 8B (Fig. 11k). Vertical and horizontal trace fossils were noted throughout the limestone interval of the drill core. Fossil content identified includes radiolarian tests and sponge spicules, as well as fragments of shells, bivalves, and trilobites (Fig. 13f) (Bingham-Koslowski, 2018).

LOWER PALEOZOIC STRATIGRAPHY OF BAFFIN ISLAND

Lower Paleozoic strata are exposed on the Brodeur Peninsula (Fig. 14, area A), northwestern Baffin Island (Fig. 14, areas B and C) and on southern Baffin Island (Fig. 14, area D). They are dominated by primarily Ordovician carbonate rocks, together with local deposits of Cambrian clastic rocks on the Brodeur Peninsula and northwestern Baffin Island, as well as Silurian carbonate rocks restricted to the Brodeur Peninsula. Lower Paleozoic rocks have also been reported from the islands and peninsulas along the western margin of Baffin Island, in Foxe Basin (Trettin, 1975; Harrison et al., 2011). The summaries presented here will focus on the Lower Paleozoic of three main areas: the Brodeur Peninsula (Fig. 14, area A), northwestern Baffin Island (Fig. 14, areas B and C), and southern Baffin Island (Fig. 14, area D) where recent research has been conducted under the Geo-mapping for Energy and Minerals (GEM) Hudson Bay–Foxe Basin project (Zhang, 2012). Unlike the offshore Paleozoic strata of the Labrador margin and western Davis Strait region, the Lower Paleozoic of Baffin Island has been divided into formal lithostratigraphic units which are described in the following section.

Brodeur Peninsula (Fig. 14, area A) and northwestern Baffin Island (Fig. 14, areas B and C)

Gallery Formation

Name

The Gallery Formation was first introduced by Blackadar (1956) and named after 'The Gallery', a remarkable group of stacks, caves, arches, and near-vertical cliffs of multicoloured sandstone.

Type locality

The Gallery Formation is found on the western side of Admiralty Inlet between latitudes 72°20′N and 73°13′N (Lemon and Blackadar, 1963).

Type section

Due to the inaccessibility of the cliffs at 'The Gallery', the measured type section was established on the northeast point of Victor Bay (Fig. 14, type section 1; section 7 of Blackadar (1956) and Lemon and Blackadar (1963)), approximately at latitude 73°08′35″N, longitude 85°10′36″W, where both the bottom contact with Precambrian bedrock and the top contact with the Turner Cliffs Formation are exposed.

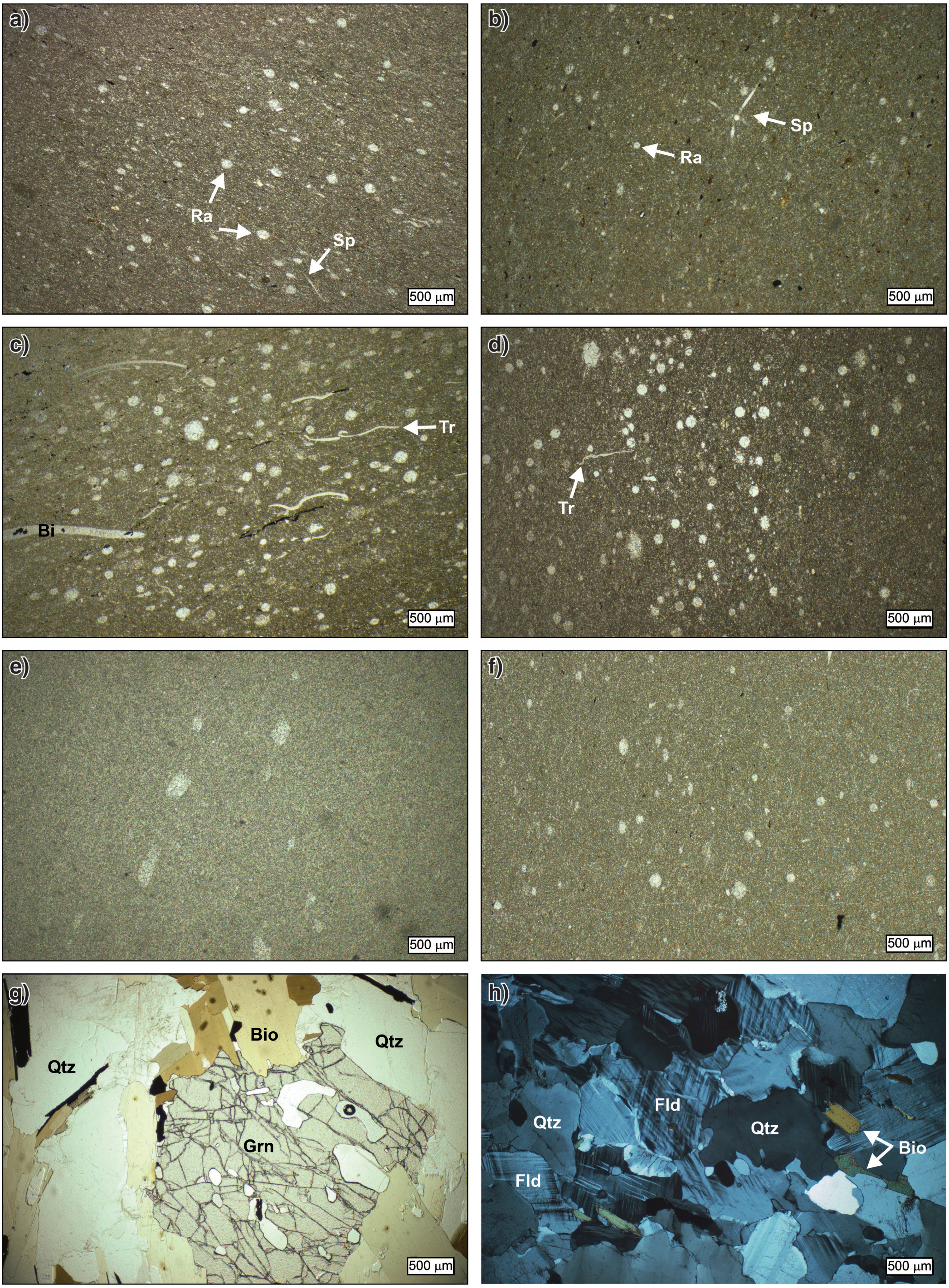

Figure 13. Thin sections from drill cores recovered from Cruise 75-009, Phase V, stations 5 (Fig. 13g), 8A (Fig. 13a, b, h), and 8B (Fig. 13c, d), as well as from Cruise 77027, stations 026A (Fig. 13e) and 028 (Fig. 13f) from the southeastern Baffin Shelf. Photomicrographs were taken in either plane-polarized light (PPL) or crosspolarized light (XPL). **a)** Radiolarians (Ra) and sponge spicules (Sp) in a lime mudstone matrix (station 8A, piece 5, 15 inches; PPL); NRCan photo 2019-655. **b)** Radiolarians (Ra) and sponge spicules (Sp) in a lime mudstone matrix (station 8A, piece 1, 27 inches; PPL); NRCan photo 2019-656. **c)** Radiolarians along with fragments of bivalves (Bi) and trilobites (Tr) in a lime mud matrix (station 8B, piece 16, 10 inches; PPL); NRCan photo 2019-657. **d)** Radiolarians and a trilobite fragment (Tr) in a lime mud matrix (station 8B, piece 6, 32 inches; PPL); NRCan photo 2019-658. **e)** Voids from possible dissolved (?)radiolarians or voids in a finely crystalline lime mud matrix (station 026A, SPL 5; PPL); NRCan photo 2019-659. **f)** Radiolarians and small fossil fragments in a lime mud matrix (station 028, SPL3; PPL); NRCan photo 2019-660. **g)** Garnet biotite gneiss erratic in overburden composed of quartz (Qtz), biotite (Bio), garnet (Grn), and opaque minerals (station 5, piece 16, 21 inches; PPL); NRCan photo 2019-661. **h)** Igneous erratic in overburden composed of quartz (Qtz), biotite (Bio), feldspar (Fld), and opaque minerals (station 8A, piece 13, 2 inches; XPL); NRCan photo 2019-662 (*modified from* Bingham-Koslowski, 2018). All photographs by N. Bingham-Koslowski.

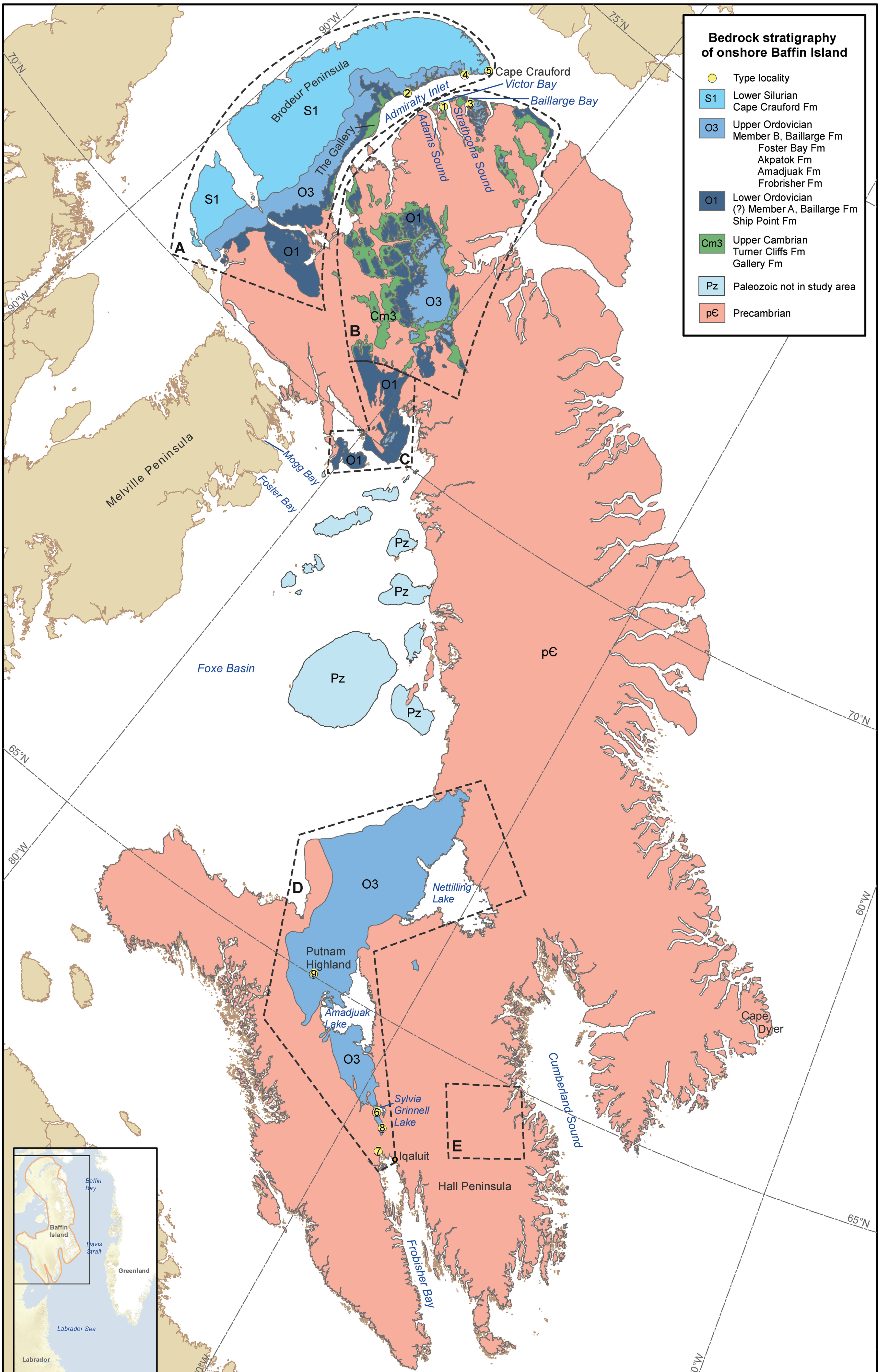

0 50 100 km
1:4 250 000
Canada Lambert Conformal
GCS WGS 1984

Lithology

At the type locality, this formation consists of about 152 m of varicoloured, medium- to coarse-grained and commonly crosslaminated quartzose sandstone. Locally, basal conglomerate, dolostone, and shale units are present (Blackadar, 1956; Lemon and Blackadar, 1963).

Distribution

The Gallery Formation outcrops on Brodeur Peninsula (Fig. 14, area A), northwestern Baffin Island (Fig. 14, area B).

Age

The Gallery Formation has been dated as late early Cambrian (Trettin, 1969, 1975), but is more likely early late Cambrian (Stewart, 1987) (Fig. 15).

Turner Cliffs Formation

Name

The Turner Cliffs Formation was first identified by Blackadar (1956) and named after the Turner Cliffs located along the western edge of Admiralty Inlet.

Type locality and type section

Turner Cliffs is due west of Adams Sound on the west coast of Admiralty Inlet (Fig. 14, type section 2; section 5 of Blackadar, 1956), approximately at latitude 72°58′44″N, longitude 86°26′49″W.

Lithology

Six members were recognized in the type section at Turner Cliffs (Lemon and Blackadar, 1963), from base to top: 1) edgewise conglomerate (18 m); 2) lower sandstone (26 m); 3) second edgewise conglomerate (12 m); 4) thin-bedded argillaceous dolostone (37 m); 5) third edgewise conglomerate (15 m) and 6) upper sandstone (27 m).

Distribution

The Turner Cliffs Formation is known from Brodeur Peninsula (Fig. 14, area A), northwestern Baffin Island (Fig. 14, area B).

Age

The age of the Turner Cliffs Formation is late Cambrian (Palmer et al., 1981; Fig. 15).

Ship Point Formation

Name

The Ship Point Formation was originally proposed by Blackadar (1956) and named after a prominent headland at the south entrance to Baillarge Bay.

Type locality and type section

The type locality for the Ship Point Formation is located on the eastern shore of Baillarge Bay, northern Baffin Island (Fig. 14, type section 3; section 8 of Blackadar, 1956), approximately at latitude 73°21′34″N, longitude 84°31′58″W.

Lithology

The Ship Point Formation was originally applied to an approximately 274 m thick succession composed of thick-bedded to massive dolostone with minor argillaceous and sandy beds that occurred between the Turner Cliffs and Baillarge formations (Blackadar, 1956; Lemon and Blackadar, 1963). It was redefined by Trettin (1975) to include the original 'upper sandstone member' (Lemon and Blackadar, 1963) of the Turner Cliffs Formation as member A of the Ship Point Formation, with the original Ship Point Formation as member B. The redefined Ship Point Formation has a total thickness of about 305 m (1000 feet) (Trettin, 1975). The formation was divided into four units by Sanford and Grant (2000) (in ascending order): unit 1, sandstone with conglomerate; unit 2, crystalline and argillaceous dolostone; unit 3, microsucrosic dolostone; and unit 4, algal and vuggy dolostone.

Distribution

Outcrops of the Ship Point Formation are known from Brodeur Peninsula (Fig. 14, area A) and northwestern Baffin Island (Fig. 14, areas B and C).

Age

Published age dates for the Ship Point Formation include late Early to early Middle Ordovician (Trettin, 1975) and Early Ordovician (Nentwich, 1987; Nentwich and Jones, 1989), but the formation is more likely late Early Ordovician (Zhang, 2013, 2018a) (Fig. 15).

Baillarge Formation

Name

The Baillarge Formation was named after Baillarge Bay on the east coast of Admiralty Inlet, northwestern Baffin Island (Lemon and Blackadar 1963), and was previously referred to as the Baillarge Bay Formation (Blackadar, 1956).

Type locality and type section

The type locality is the same as that of the Ship Point Formation on the eastern shore of Baillarge Bay, northwestern Baffin Island; the type section (Fig. 14, type section 3) is the upper part of section 8 of Blackadar (1956).

Reference section

A composite reference section was established by Trettin (1965a, b) about 25 km southwest of Cape Crauford, approximately at latitude 73°32′34.8″N, longitude 85°24′53″W (Fig. 14, type section 4).

Lithology

The Baillarge Formation consists of vague and irregularly bedded to massive limestone with a total thickness exceeding 140 m (460 feet). The formation was divided into informal members A (dolostone with some interstratified limestone) and B (fossiliferous, partly dolomitized limestone) by Trettin (1965a, b), and a disconformity was recognized between the two members (Nentwich, 1987; Nentwich and Jones, 1989).

Distribution

The Baillarge Formation occurs on Brodeur Peninsula (Fig. 14, area A) and northwestern Baffin Island (Fig. 14, area B).

Age

Published ages dates for the Baillarge Formation include latest Middle Ordovician or earliest Late Ordovician, based on the 'Arctic Ordovician' fauna (Lemon and Blackadar, 1963); late Middle Ordovician and late Middle Ordovician to middle Silurian assigned to members A and B, respectively (Trettin, 1965a, b); but the formation is more likely late Early and Late Ordovician to earliest Silurian ascribed for members A and B, respectively (Nentwich, 1987; Nentwich and Jones, 1989; Fig. 15).

Cape Crauford Formation

Name

The Cape Crauford Formation was established by Trettin (1965b) and named after Cape Crauford on the northeastern point of the Brodeur Peninsula, northwestern Baffin Island (Fig. 14).

Figure 14. Bedrock geology map of Baffin Island (*modified from* Harrison et al., 2011).

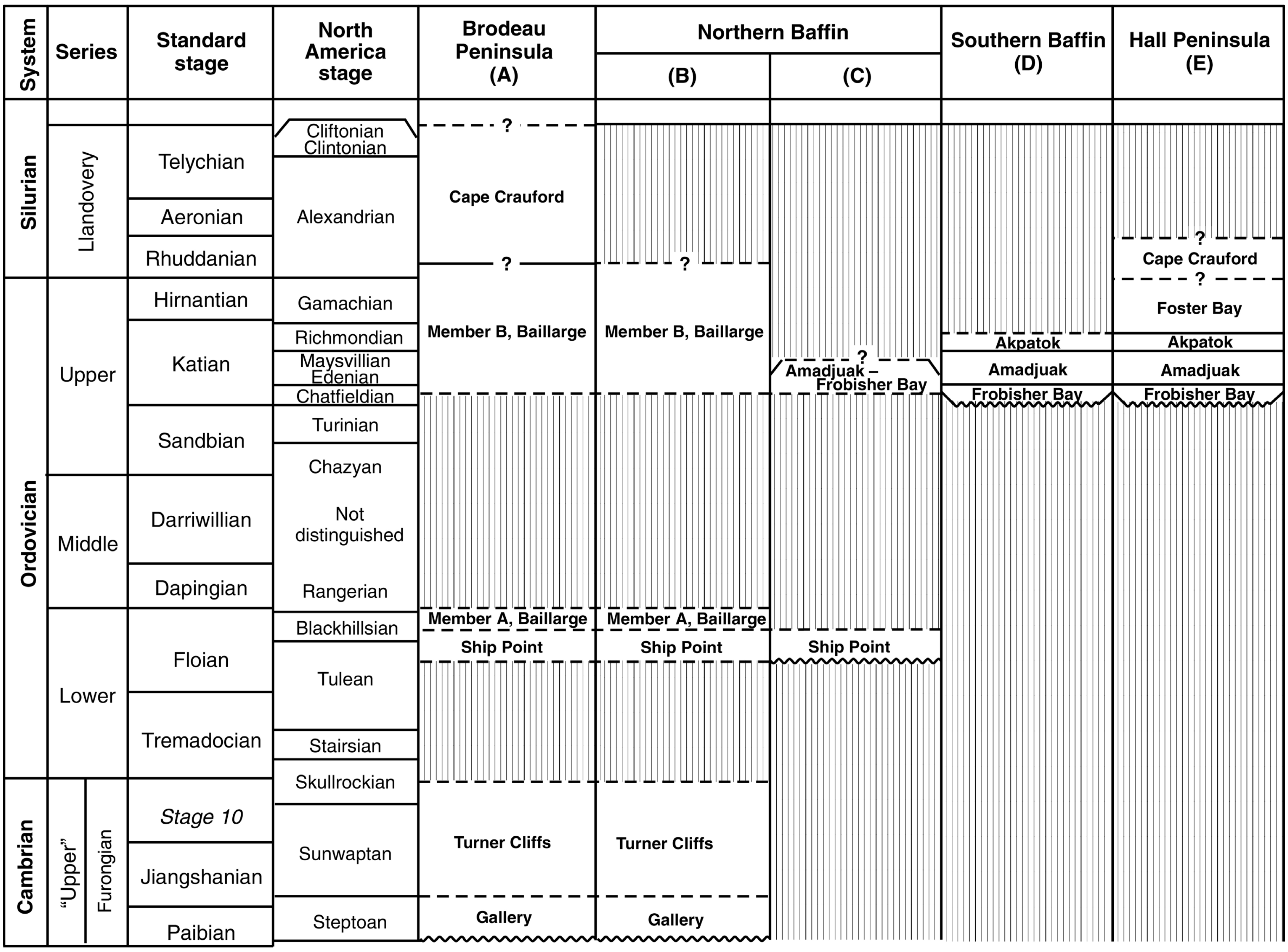

Figure 15. Paleozoic stratigraphic framework on Baffin Island. The standard and North America stages are adopted from Cohen et al. (2013) and Haq and Schutter (2008; part of Ordovician from Bergström et al., 2009), respectively. *See* Figure 14 for areas A–E.

Type locality and type section

Cape Crauford is located approximately at latitude 73°44′44.5″N, longitude 84°53′3.70″W (Fig. 14, type section 5); the type section is exposed between 2.4 km south and 3.2 km northwest of Cape Crauford.

Lithology

The formation was divided into the informal members A, B, and C by Trettin (1965b); members A and B were combined and referred to as the lower member, and member C was renamed as the upper member by Nentwich (1987) and Nentwich and Jones (1989). The lower member of the Cape Crauford Formation is dominated by carbonate solution breccia, limestone, and dolomitic limestone along with lesser amounts of calcareous dolostone and dolostone. The upper member consists of coarse-grained vuggy or mottled dolostone in its lower part and partly brecciated limestone interbedded with dolomitic limestone in its upper part.

Distribution

The Cape Crauford Formation is known from Brodeur Peninsula (Fig. 14, area A).

Age

The Cape Crauford Formation has been dated as middle Silurian (Trettin, 1965a, b) and early Silurian (Llandovery) (Nentwich, 1987; Nentwich and Jones, 1989; Fig. 15).

Southern Baffin Island (area D)

Frobisher Bay Formation

Name

The informal name 'Frobisher Bay Formation' was proposed by Sanford and Grant (1990) after the geographic name 'Frobisher Bay', an inlet near Iqaluit, the capital of Nunavut (Fig. 14). The formation name was later promoted to formal status by Sanford and Grant (2000).

Type locality and type section

The type section of the Frobisher Bay Formation is defined by sections 11 and 16 in Sanford and Grant (2000) and locality 17 in Zhang (2012). The type section starts at latitude 64°06′16.4″N, longitude 69°27′53.4″W (Fig. 14, type section 6) near the mouth of a small creek south of Sylvia Grinnell Lake and ends downstream at latitude 64°06′03.3″N, longitude 69°27′47.1″W.

Lithology

At the type section, 15 m of light brown, finely crystalline limestone in thin nodular beds unconformably rests on Precambrian metamorphic rocks. Regionally, the formation disconformably succeeds the Ship Point Formation over much of Foxe Basin. The *Goniocerus* (cephalopod) (Fig. 16a) and *Labyrinthites* (tabulate coral) (Fig. 16b) faunas are distinctive to the formation (Bolton, 1977, 2000). The diagnostic conodont species of the formation include *Ansella nevadensis, Appalachignathus delicatulus*, and *Polyplacognathus ramosus* (McCracken, 2000).

Distribution

The Frobisher Bay Formation is found on southern Baffin Island (Fig. 14, area D).

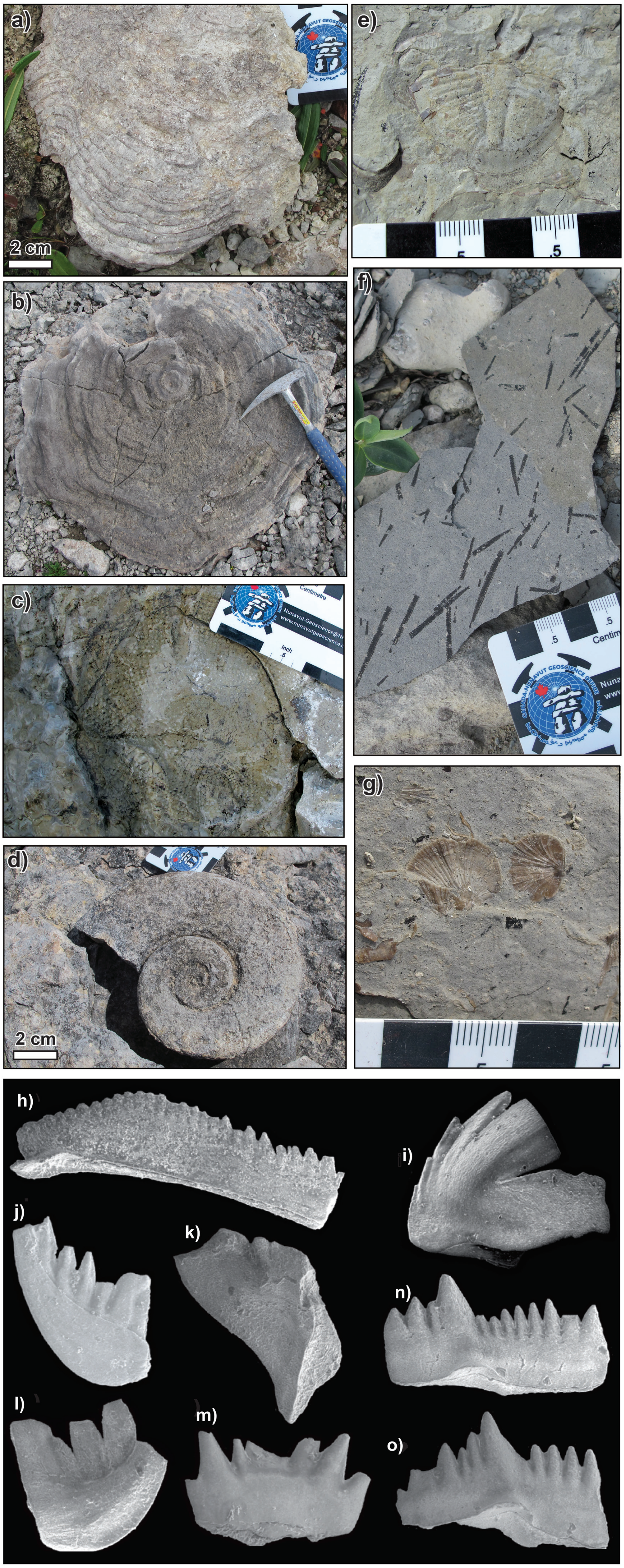

Figure 16. Distinctive fossils in the Frobisher Bay and Amadjuak formations on southern Baffin Island. **a)** Cephalopod *Gonioceras* sp.; NRCan photo 2019-663. **b)** Coral *Labyrinthites* (*Labyrinthites*) *chidlensis* Lambe; hammer head is 18.5 cm; NRCan photo 2019-664. **c)** Algae *Fisherites arcticus* (Etheridge); NRCan photo 2019-665. **d)** Gastropod *Maclurites triangularis* Teichert; NRCan photo 2019-666. **e)** Trilobite *Pseudogygites arcticus* Ludvigsen; NRCan photo 2019-667. **f)** Graptolite assemblage; NRCan photo 2019-668. **g)** Brachiopod *Paucicrura* sp.; NRCan photo 2019-669. **h)** *Appalachignathus delicatulus* Bergström, Carnes, Ethington, Votaw, and Wigley (×60) (GSC137539); NRCan photo 2019-670. **i)** *Periodon grandis* Ethington (×100) (GSC137541); NRCan photo 2019-671. **j)** *Belodina confluens* Sweet (×70) (GSC137542); NRCan photo 2019-672. **k)** *Culumbodina penna* Sweet (×55) (GSC137546); NRCan photo 2019-673. **l)** *Pseudobelodina v. vulgaris* Sweet (×100) (GSC137547); NRCan photo 2019-674. **m)** *Rhipidognathus symmetricus* Branson, Mehl, and Branson (×90) (GSC137566); NRCan photo 2019-675. **n)** *Ozarkodina elibata* Pollock, Rexroad and Nicoll (×70) (GSC137575); NRCan photo 2019-676. **o)** *Ozarkodina hassi* Pollock, Rexroad and Nicoll (×50) (GSC137577); NRCan photo 2019-677. Images 16a and 16b are from the type section of the Frobisher Bay Formation. Images 16c and 16d are from the reference section of the Amadjuak Formation. Images 16e, 16f, and 16g are from the organic-rich interval of the Amadjuak Formation at its reference section (*modified from* Zhang, 2012). Images 16h–o are of conodonts from xenoliths on Hall Peninsula (*modified from* Zhang and Pell, 2014).

Age

The Frobisher Bay Formation has been dated as late Middle Ordovician (Trentonian) (Bolton, 1977, 2000; Sanford and Grant, 2000; McCracken, 2000) and Late Ordovician (Chatfieldian) (Zhang, 2013; Fig. 15).

Amadjuak Formation

Name

The name 'Amadjuak Formation' was informally proposed by Sanford and Grant (1990) after Amadjuak Lake on southern Baffin Island (Fig. 14), and later raised to formal status by the same authors in 2000.

Type locality and type section

The type section for the Amadjuak Formation is defined as section 10 of Sanford and Grant (2000), located approximately at latitude 63°45′10.3″N, longitude 68°59′21.5″W (Fig. 14, type section 7) at Silliman's Fossil Mount, a small isolated Paleozoic outlier, 23 km due west of Iqaluit (Sanford and Grant, 2000).

Reference section

The lower part of the Amadjuak Formation is not exposed at the type section. As such, a reference section (locality 32 of Zhang (2012)) was selected between latitude 63°59′12.9″N, longitude 69°10′08.6″W and latitude 63°59′09.1″N, longitude 69°11′34.1″W (Fig. 14, type section 8), along a small creek south of Sylvia Grinnell Lake (Zhang, 2012), where the contact between the Frobisher Bay and Amadjuak formations is well exposed.

Lithology

The Amadjuak Formation is about 71 m at the type section, which comprises three units (in ascending order): unit 1, shaly limestone interbedded with black shale, which is well exposed at the reference section; unit 2, massive limestone and nodular bedded shaly limestone; and unit 3, limestone with distinct light yellowish orange discoloration. The Amadjuak Formation contains a distinctive *Fisherites* (algae) (Fig. 16c) and *Maclurites* (gastropod) (Fig. 16d) fauna (Sanford and Grant, 2000; Zhang, 2012). The conodont *Amorphognathus superbus* and other species are restricted to the formation (McCracken, 2000).

Distribution

The Amadjuak Formation is restricted to southern Baffin Island (Fig. 14, area D).

Age

Previously published ages for the Amadjuak Formation are Edenian to early Maysvillian (Late Ordovician; Sanford and Grant, 2000; McCracken 2000) and Edenian to earliest Richmondian (Late Ordovician; Zhang, 2013; Fig. 15).

Akpatok Formation

Name

The name 'Akpatok Formation' was informally proposed by Sanford and Grant (1990) after Akpatok Island located in Ungava Bay (Fig. 1). It was then raised to formal status by the same authors in 2000.

Type locality and type section

Originally there was no type section selected for the formation and as such, nearly all of the strata (>240 m) exposed on the island were included under the designation 'Akpatok Formation' (Sanford and Grant, 2000); however, an extensive field investigation and detailed biostratigraphic studies have demonstrated that only about 60 m of strata in the lower elevation of Akpatok Island belong to the formation, as the strata are nearly horizontally distributed (Zhang, 2018b).

Reference section

The Akpatok Formation was defined from a single locality on southern Baffin Island, in a creek-cut section at approximately latitude 65°01′24.1″N, longitude 72°30′35.7″W (Fig. 14, type section 9) located in the Putnam Highland area northwest of Amadjuak Lake (Sanford and Grant 2000; Zhang, 2012).

Lithology

The preserved Akpatok Formation on southern Baffin Island is about 9 m thick and consists of thin-bedded argillaceous limestone in resistant nodular beds (Sanford and Grant 2000; Zhang 2012). The conodonts *Amorphognathus ordovicicus* and *A. duftonus* are characteristic to the formation (McCracken, 2000).

Distribution

The Akpatok Formation is restricted to the Putnam Highland area northwest of Amadjuak Lake, southern Baffin Island (Fig. 14, area D).

Age

The Akpatok Formation has been dated as late Maysvillian to Richmondian (Late Ordovician; Sanford and Grant, 2000; McCracken 2000) and early Richmondian, (Late Ordovician; Zhang, 2013; Fig. 15). The Akpatok Formation represents the youngest Paleozoic strata preserved on southern Baffin Island (Zhang, 2012).

Foster Bay Formation

Name

The Foster Bay Formation was informally introduced by Sanford and Grant (1990) and named after Foster Bay on Melville Peninsula (Fig. 14). It was raised to formal status by the same authors in 2000.

Type locality and type section

The Foster Bay Formation is best exposed between Foster and Mogg bays, some 15 km west of Foster Bay, approximately latitude 69°10′02″N, longitude 82°30′35.7″W on Melville Peninsula (Fig. 14).

Lithology

The Foster Bay Formation is composed of thin- and thick-bedded dolomitic limestone and dolostone in the lower part of the formation and small reef accumulations with light to medium brown algal and stromatolitic limestone framework in the upper section of the formation (Sanford and Grant, 1990, 2000).

Distribution

The Foster Bay Formation does not exist on Baffin Island; the rubble on top of the Akpatok Formation and conodonts recovered from xenoliths on the nearby Hall Peninsula (Zhang and Pell, 2014; *see* discussion below) indicate that it was eroded off (Zhang, 2012).

Age

Foster Bay Formation ages have been previously published as late Richmondian and possibly Gamachian, Late Ordovician (Sanford and Grant, 2000; Zhang, 2013; Fig. 15).

Hall Peninsula (area E)

Hall Peninsula is located on southeastern Baffin Island (Fig. 14). Presently, this area lacks Phanerozoic sedimentary cover, except for the unconsolidated glacial deposits; however, Late Ordovician and early Silurian conodont microfossils, characterized by *Appalachignathus delicatulus, Belodina confluens-Periodon grandis, Pseudobelodina v. vulgaris-Culumbodina penna, Rhipidognathus symmetricus*, and *Ozarkodina hassi-O. elibata* faunas, have been recovered from carbonate xenoliths preserved in the Late Jurassic to Early Cretaceous kimberlites in area E (Fig. 14) (Zhang and Pell, 2013, 2014, 2016). These conodonts enable strata lost to erosion to be correlated with the Upper Ordovician Frobisher Bay, Amadjuak, Akpatok, and Foster Bay formations as well as to the lower Silurian (Zhang and Pell, 2013, 2014, 2016), with the last most likely correlated with the Cape Crauford Formation on the Brodeur Peninsula. This framework is presented in Figure 15.

Petroleum source rocks on Baffin Island

The potential for petroleum source rocks in the Paleozoic succession on Baffin Island was first reported by Macauley (1987). Recently, Zhang (2012) described one confirmed and one possible organic-rich interval in the Upper Ordovician succession based on an extensive field investigation on southern Baffin Island. Additionally, a Late Ordovician to late Silurian organic-rich xenolith was discovered by diamond exploration drilling on Hall Peninsula (Zhang et al., 2014). A summary of these findings are as follows:

- A 2 m thick black shale interval is stratigraphically located in the lower Amadjuak Formation at its reference section (Fig. 14, type section 8). A characteristic *Pseudogygites* (trilobite; Fig. 16e)-*Climacograptus* (graptolite; Fig. 16f)-*Paucicrura* (brachiopod; Fig. 16g) fauna is restricted to the interval (Zhang, 2012), which is correlated with the lower Katian (or Edenian), Upper Ordovician (Zhang and Riva, 2018). This interval contains total organic carbon (TOC) values ranging between 1.68% and 12.97% with an average of 7.8%, and yields immature Type I-II kerogen (Zhang, 2012).
- Rubble of the Foster Bay Formation was found on top of the Akpatok Formation at the reference section of the Akpatok Formation (Fig. 14, type section 9). The rubble contains TOC values ranging between 2.82% and 5.13% with an average of 4.21%, and bears immature Type II kerogen (Zhang, 2012). This is an indication that a source rock interval in the Foster Bay Formation has been eroded off Baffin Island, but may still be present in the offshore (Zhang, 2012).
- A 26 cm long black shale xenolith was recovered at 295.5 m from drill hole CHI-482–10-DD01 at latitude 64°13′22.915″N, longitude 66°18′27.612″W in kimberlite CH-31 (area E, Fig. 14) on the Hall Peninsula (Zhang et al., 2014). This xenolith yields TOC values ranging between 7.43% and 8.96% with an average of 8.04%. An age of early Silurian for the black shale xenolith was obtained by rhenium-osmium (Re-Os) isotope analysis, with uncertainty between Late Ordovician and late Silurian (Zhang et al. 2014).

Stratigraphic correlation between northwestern and southern Baffin Island

The upper Cambrian Gallery and Turner Cliffs formations, Lower Ordovician Ship Point Formation, and lower Silurian Cape Crauford Formation do not exist on southern Baffin Island. Therefore, the only issue that needs to be addressed is the stratigraphic correlation between the Baillarge Formation (Brodeur Peninsula and northwestern Baffin Island) and the Frobisher Bay, Amadjuak, Akpatok, and Foster Bay formations (southern Baffin Island).

Member A of the Baillarge Formation is dominated by dolostone (Nentwich, 1987; Nentwich and Jones, 1989), which is similar to the dolostone unit of the Ship Point Formation (Trettin, 1975); therefore, it could be part of the Ship Point Formation. The lithology of the majority of member B of the Baillarge Formation (Nentwich, 1987; Nentwich and Jones, 1989) is similar to those of the Upper Ordovician stratigraphic units on southern Baffin Island (Bolton, 1977, 2000; Sanford and Grant, 2000; McCracken, 2000; Zhang, 2012), except for the upper part of member B, which contains early Silurian *Virgiana* fauna (Nentwich and Jones, 1989). Therefore, member B of the Baillarge Formation could possibly be subdivided into the Frobisher Bay, Amadjuak, Akpatok, and Foster Bay formations and an early Silurian upper unit. Until additional data supporting a new naming scheme is available, the name and the age assignment of Baillarge Formation of Nentwich (1987) and Nentwich and Jones (1989) are tentatively employed herein (Fig. 15).

SUMMARY

Due to the sparse occurrences of Lower Paleozoic deposits offshore in the Labrador–Baffin Seaway, in conjunction with variable age data, minimal effort has been directed at correlating the Paleozoic strata in the Labrador–Baffin Seaway and onshore Baffin Island on a local (well to well) or regional basis. The Lower Paleozoic of the Labrador margin is present as isolated erosional remnants (McWhae et al., 1980; Miller and D'Eon, 1987) in seven exploration wells where it is largely confined to syn-rift structures and associated structural highs related to the opening of the Labrador Sea in the Cretaceous (Bingham-Koslowski et al., 2019), and therefore does not occur as a continuous interval that can be mapped using seismic data. Previous age data for the wells were inconsistent, with ages ranging from undifferentiated Paleozoic to Ordovician, to Devonian, to Carboniferous, further hindering local correlations (Moir, 1989; Bell and Howie, 1990; Williams et al., 1990). In light of new biostratigraphic data, which advocates a Middle to Late Ordovician age for the marine succession (Bingham-Koslowski et al., 2019), it is now possible to suggest that part of the stratigraphic succession in these wells is correlateable. Palynomorph recovery is poor to moderate from the Labrador margin due, in large part, to lithologies that hindered their preservation (primarily the abundance of dolomite), impacting the number of direct correlations that can be made. Common palynomorphs (i.e. *Asketopalla formosula* and *Polyancistrodorus columbariferus* acritarchs) were found between Hopedale E-33 (the northernmost well) and Freydis B-87 (the southernmost well) (Bingham-Koslowski et al., 2019). Some of the identifiable Late Ordovician palynomorphs (acritarchs and chitinozoans) of the Labrador margin have also been observed in Upper Ordovician strata from eastern Canada, middle North America (Ontario, Quebec, Ohio, Kentucky, Oklahoma), Sweden, Estonia, Siberia, England, as well as Scotland, suggesting that these deposits may be comparable (*see* Bingham-Koslowski et al., 2019).

The Paleozoic drill cores from the southeastern Baffin Shelf outcrop at the seafloor in an area where the subsurface has been faulted and folded preventing direct correlation between drill cores (MacLean, 1978; Bell and Howie, 1990). Despite this, the drill core successions are interpreted to be syndepositional with lithological dissimilarities attributed to lateral changes in the depositional environment (Jansa, 1976; MacLean et al., 1977). Biostratigraphical analysis has been conducted on the drill cores recovered in 1975 (stations 4, 5, 8A, and 8B), demonstrating a Middle to Late Ordovician age for the carbonate drill core strata (W.A.M. Jenkins, GSC unpub. report 13-WAMJ-1976 1976; MacLean et al., 1977). The two drill cores from 1977 (stations 026A and 028) have not been dated, but are assumed, based on location and lithology, to be time-correlative with the strata recovered from the 1975 drill cores (MacLean, 1978). The drill core from station 028 appears analogous to the drill cores recovered from stations 8A and 8B, with a similar lithology and fossil assemblage (Bingham-Koslowski, 2018). The drill core from station 026A, however, has a different appearance than the other drill cores (light grey as opposed to dark to medium brown and highly fractured) and has a more limited fossil assemblage with only possible, dissolved radiolarians observed, which are less numerous than in other drill cores. It is also the northernmost of the drill cores, and therefore these discrepancies may represent a different depositional setting or differing diagenetic histories (Bingham-Koslowski, 2018).

The lack of available bedrock samples (drill cores or dredge samples) in the offshore compared to the onshore, and the presence of formal lithostratigraphic units recognized in the Lower Paleozoic of onshore Baffin Island has complicated correlating onshore and offshore Lower Paleozoic rocks in the Baffin Island region. Jansa (1976) published tentative comparisons based on lithological and paleontological similarities of the 1975 Paleozoic drill cores to other time-equivalent onshore deposits. No detailed correlations have been made. Jansa (1976) likened the drill core from station 4 to member A of the Baillarge Formation on Baffin Island as well as to the Bad Cache Rapids Group (Hudson Platform). He compared the drill core from station 5 to late Middle and early Upper Ordovician limestone outcrops on Akpatok Island, to rocks of the Churchill River Group in Hudson Bay, to Silliman's Fossil Mount on Baffin Island, to dredge sample DW 71-030, No. 1 from Ungava Bay, to member B of the Baillarge Formation on Baffin Island, as well as to deposits along the western Greenland margin (Jansa, 1976). Jansa (1976) also equated the predominantly mudstone lithology of the drill cores from stations 8A and 8B with the Baillarge Formation on northwestern Baffin Island.

The relationship between the Ordovician strata from the Labrador margin and the southeastern Baffin Shelf is not known. The drill cores from the southeastern Baffin Shelf outcrop at the seafloor, whereas the Ordovician rocks from the Labrador Shelf are located in the subsurface, at a depth greater than 1.5 km, suggesting that the two regions have different burial histories. The Labrador margin strata have a significantly higher dolomite component that may be partly the product of a greater burial depth or representative of a different depositional and diagenetic environment. Both the drill cores from the southeastern Baffin Shelf and the carbonate conventional cores from Indian Harbour M-52 and Freydis B-87 (core 2) exhibit a similar fossil suite characteristic of the Middle to Late Ordovician (Bingham-Koslowski, 2019). Palynological assessment suggests a slightly younger age date for the drill cores from the southeastern Baffin Shelf, and their onshore analogues, with ages of Katian or younger (W.A.M. Jenkins, GSC unpub. report 13-WAMJ-1976, 1976; MacLean et al., 1977), when compared to the Labrador margin where only the top of the Indian Harbour Formation was found to be Katian, the youngest section recognized in the Lower Paleozoic of the Labrador wells (Bingham-Koslowski et al., 2019). There is no evidence to suggest that Lower Paleozoic strata exist beneath the Saglek Basin as Paleozoic rocks are not recognized in seismic data or well logs from the Saglek Basin and no physical evidence of any Lower Paleozoic rocks (including the reworking of sediments or palynomorphs) was recovered from any of the wells in this basin. The absence of Lower Paleozoic strata underlying the Saglek Basin may suggest that the Ordovician strata of the Labrador margin were deposited in a separate, possibly slightly older, depocentre and that the carbonate platform did not extend north, into what is now the Saglek Basin, to connect to the Ordovician deposits located on and around Baffin Island. The area is therefore tentatively viewed as two subregions that are not directly correlatable to one another: a southern region characterized by the Ordovician of the Labrador margin (comparable to the North America midcontinent) and a northern region defined by Lower Paleozoic strata located in Davis Strait (southeastern Baffin Shelf), on Baffin Island, in Hudson Strait, in Ungava Bay, on Akpatok Island, and along the western Greenland margin.

ACKNOWLEDGMENTS

"Lower Paleozoic strata of the Labrador–Baffin Seaway (Canadian margin) and Baffin Island" is a paper in *Geological synthesis of Baffin Island (Nunavut) and the Labrador–Baffin Seaway*, a Geo-mapping for Energy and Minerals (GEM-2) product. The summary presented here represents a collaboration between Natural Resources Canada (GEM-2 and Marine Conservation Target programs) and the Canada-Nunavut Geoscience Office. Thanks is owed to the GEM Coordination Office and GEM management for helping to facilitate the research that is summarized within. Thank you to Leith MacLeod for producing the maps, to Paul Champagne for doing the layout, to Keith Dewing and Denis Lavoie for taking time to review the content and provide feedback, and to Evelyn Inglis for scientific editing.

REFERENCES

Ainsworth, N.R., Riley, L.A., Bailey, H.W., and Gueinn, K.J., 2016. Cretaceous–Tertiary stratigraphy of the Labrador Shelf, wells: Freydis B-87, Hopedale E-33, Karlsefni A-13, North Leif I-05 & South Hopedale L-39; Riley Geoscience Ltd., Labrador Shelf Stratigraphy Study, 31 p. <https://basin.gdr.nrcan.gc.ca/wells/index_e.php> [accessed June 1, 2017]

Atlantic Geoscience Centre, 1977. Cruise Report Hudson 77-027, 27 p. <https://ed.gdr.nrcan.gc.ca/cruise_report_e.php> [accessed March 16, 2017]

Barnes, C.R., Norford, B.S., and Skevington, D., 1981. The Ordovician System in Canada: correlation chart and explanatory notes; International Union of Geological Sciences, Publication No. 8, 27 p.

Barss, M.S., 1975. Report on palynological analysis of conventional core from Eastcan et al., Gudrid H-55; Geological Survey of Canada – Atlantic, Report No. EPGS-PAL.20-75MSB, 2 p. <https://basin.gdr.nrcan.gc.ca/wells/index_e.php> [accessed November 7, 2018]

Barss, M.S., 1981. Palynological analysis of core samples from Eastcan et al. Roberval K-92; Geological Survey of Canada – Atlantic, Report No. EPGS-PAL.16-81MSB, 2 p. <https://basin.gdr.nrcan.gc.ca/wells/index_e.php> [accessed February 16, 2017]

Bell, J.S. and Howie, R.D., 1990. Paleozoic geology, Chapter 4; *in* Geology of the Continental Margin of Eastern Canada, Geology of Canada, (ed.) M.J. Keen and G.L. Williams; Geological Survey of Canada, Geology of Canada, no. 2, p. 141–165 (*also* Geological Society of America, The Geology of North America, v. I-1). https://doi.org/10.4095/132690

Bergström, S.M., Chen, X., Gutierrez-Marco, J.C., and Dronov, A., 2009. The new chronostratigraphic classification of the Ordovician System and its relations to major regional series and stages and to $\delta^{13}C$ chemostratigraphy; Lethaia, v. 42, p. 97–107. https://doi.org/10.1111/j.1502-3931.2008.00136.x

Bingham-Koslowski, N., 2018. Descriptions of drill cores and thin sections from lower Paleozoic strata, southeastern Baffin Island shelf, Nunavut; Geological Survey of Canada, Open File 8409, 80 p. https://doi.org/10.4095/308354

Bingham-Koslowski, N., 2019. Descriptions of Paleozoic cores and thin sections from the Gudrid H-55, Roberval K-92, Indian Harbour M-52, and Freydis B-87 wells, offshore Labrador (Newfoundland and Labrador); Geological Survey of Canada, Open File 8543, 142 p. https://doi.org/10.4095/313573

Bingham-Koslowski, N., Miller, M.A., McCartney, T., and Carey, J.A., 2019. Revised biostratigraphic and thermal alteration interpretations for the Paleozoic of the Hopedale Basin, offshore Labrador, Canada; Bulletin of Canadian Petroleum Geology, v. 67, no. 3, p. 185–214.

Blackadar, R.H., 1956. Geological reconnaissance of Admiralty Inlet, Baffin Island, Arctic Archipelago, Northwest Territories; Geological Survey of Canada, Paper 55-6, 25 p. https://doi.org/10.4095/101291

Bolton, T.E., 1977. Ordovician megafauna, Melville Peninsula, southeastern District of Franklin; *in* Geology of Ordovician rocks, Melville Peninsula and region, southeastern district of Franklin, (ed.) T.E. Bolton, B.V. Sanford, M.J. Copeland, C.R. Barnes, and J.K. Rigby; Geological Survey of Canada, Bulletin 269, p. 23–75. https://doi.org/10.4095/103064

Bolton, T.E., 2000. Ordovician megafauna, southern Baffin Island, Nunavut; Geological Survey of Canada, Bulletin 557, p. 39–157. https://doi.org/10.4095/211846

BP Exploration Canada Ltd., 1975. BP Columbia et al. Indian Harbour M-52; Well history-suspension report; on file at the Canada-Newfoundland and Labrador Offshore Petroleum Board, 95 p.

BP Exploration Canada Ltd., 1976. BP Columbia et al. Indian Harbour M-52; Well history-abandonment report; on file at the Canada-Newfoundland and Labrador Offshore Petroleum Board, 328 p.

Bujak Davies Group, 1989a. Biostratigraphy and maturation of 17 Labrador and Baffin shelf wells, volume 4: Hekja O-71 and Hopedale E-33; Bujak Davies Group, Report No. 86-0058, Geological Survey of Canada, Open File 1932, 70 p. https://doi.org/10.4095/130625

Bujak Davies Group, 1989b. Biostratigraphy and maturation of 17 Labrador and Baffin Shelf wells, volume 9: South Hopedale L-39 and South Labrador N-79; Geological Survey of Canada, Open File 1937, 70 p.

Cadenel, M., Plé, C., and Prim, M., 1978. Total Eastcan et al. – Roberval K-92; Well history report; on file at the Canada-Newfoundland and Labrador Offshore Petroleum Board, 72 p.

Canada-Newfoundland and Labrador Offshore Petroleum Board, 2007a. Schedule of wells Newfoundland and Labrador offshore area, BP Columbia et al. Indian Harbour M-52, 1 p. <https://www.cnlopb.ca/wp-content/uploads/wells/well50.pdf> [accessed February 16, 2017]

Canada-Newfoundland and Labrador Offshore Petroleum Board, 2007b. Schedule of wells Newfoundland and Labrador offshore area, Canterra et al. South Hopedale L-39, 1 p. <https://www.cnlopb.ca/wp-content/uploads/wells/well90.pdf> [accessed August 28, 2019]

Canada-Newfoundland and Labrador Offshore Petroleum Board, 2007c. Schedule of wells Newfoundland and Labrador offshore area, Chevron et al. Hopedale E-33, 1 p. <https://www.cnlopb.ca/wp-content/uploads/wells/well56.pdf> [accessed August 28, 2019]

Canada-Newfoundland and Labrador Offshore Petroleum Board, 2007d. Schedule of wells Newfoundland and Labrador offshore area, Eastcan et al. Freydis B-87, 1 p. <https://www.cnlopb.ca/wp-content/uploads/wells/well46.pdf> [accessed February 15, 2017]

Canada-Newfoundland and Labrador Offshore Petroleum Board, 2007e. Schedule of wells Newfoundland and Labrador offshore area, Eastcan et al. Gudrid H-55, 1 p. <https://www.cnlopb.ca/wp-content/uploads/wells/well40.pdf> [accessed February 15, 2017]

Canada-Newfoundland and Labrador Offshore Petroleum Board, 2007f. Schedule of wells Newfoundland and Labrador offshore area, Total Eastcan et al. Roberval K-92, 1 p. <https://www.cnlopb.ca/wp-content/uploads/wells/well57.pdf> [accessed February 17, 2017]

Canada-Newfoundland and Labrador Offshore Petroleum Board, 2007g. Schedule of wells Newfoundland and Labrador offshore area, Total Eastcan et al. Tyrk P-100, 1 p. <https://www.cnlopb.ca/wp-content/uploads/wells/well62.pdf> [accessed August 28, 2018]

Canada-Newfoundland and Labrador Offshore Petroleum Board, 2016. Significant Discovery Areas; 1 p. <https://www.cnlopb.ca/information/maps/> [accessed February 15, 2017]

Canterra Energy Ltd., 1983. Canterra et al. South Hopedale L-39; Well history report; on file at the Canada-Newfoundland and Labrador Offshore Petroleum Board, 102 p.

Caro, Y. and Villain, J.-M., 1980. Biostratigraphical study of the Roberval K-92 Eastcan well; Total – C.F.P. Direction Fonctionnelle Exploration, Département Laboratoires Exploration; 13 p. <https://basin.gdr.nrcan.gc.ca/wells/index_e.php> [accessed February 16, 2017]

Caro, J., Fediaevsky, A., Jourdan, A., and Villain, J.-M., 1980. Biostratigraphic study of the Tyrk P100 Eastcan well; Total – C.F.P., Direction Fonctionnelle Exploration, Département Laboratoires Exploration, 13 p. <https://basin.gdr.nrcan.gc.ca/wells/index_e.php> [accessed June 7, 2018]

Cohen, K.M., Finney, S., and Gibbard, P.L., 2013. International Chronostratigraphic Chart; International Commission on Stratigraphy, <https://stratigraphy.org/ICSchart/ChronostratChart2019-05.pdf> [accessed December 12, 2018]

Corgnet, J.L. and McWhae, J.R.H., 1975. Eastcan et al. Gudrid H-55; Well history report; on file at the Canada-Newfoundland and Labrador Offshore Petroleum Board, 45 p.

Daneliuk, B.A. and Bell, J.A., 1972. Tenneco et al. Leif E-38; Well history report; on file at the Canada-Newfoundland and Labrador Offshore Petroleum Board, 98 p.

Dolby, G., Koldijk, W.S., Oliver, E.M., Roberston, E.B., and Thorne, B.V.A., 1979. The micropaleontology, palynology, and stratigraphy of the Total Eastcan Roberval K-92 Well; Robertson Research Canada Limited, Exploration Report No. 203, 37 p. <https://basin.gdr.nrcan.gc.ca/wells/index_e.php> [accessed February 16, 2017]

Gradstein, F.M., 1977. Micropaleontology of BP Columbia et al Indian Harbour M-52, Labrador Shelf; Geological Survey of Canada – Atlantic, Report No. EPGS-PAL.37-77FMG, 4 p. <https://basin.gdr.nrcan.gc.ca/wells/index_e.php> [accessed February 16, 2017]

Grant, A.C., 1975. Geophysical results from the continental margin off southern Baffin Island; *in* Canada's Continental Margins and Offshore Petroleum Exploration, (ed.) C.J. Yorath, E.R. Parker, and D.J. Glass; Canadian Society of Petroleum Geologists, memoir 4, p. 411–431.

Haq, B.U. and Schutter, S.R., 2008. A chronology of Paleozoic sea-level changes; Science, v. 322, p. 64–68. https://doi.org/10.1126/science.1161648

Harrison, J.C., St-Onge, M.R., Petrov, O.V., Strelnikov, S.I., Lopatin, B.G., Wilson, F.H., Tella, S., Paul, D., Lynds, T., Shokalsky, S.P., Hults, C.K., Bergman, S., Jepsen, H.F., and Solli, A., 2011. Geological Map of the Arctic; Geological Survey of Canada, Map 2159A, scale 1:5 000 000. https://doi.org/10.4095/287868

Jansa, L.F., 1976. Lower Paleozoic radiolarian-bearing limestones from the Baffin Island shelf; *in* Report of Activities, Part B; Geological Survey of Canada, Paper 76-1B, p. 99–105.

Jenkins, W.A.M., 1984. Ordovician rocks in the Eastcan et al. Freydis B-87 and other wells in offshore Atlantic Canada; Canadian Journal of Earth Sciences, v. 21, p. 864–868. https://doi.org/10.1139/e84-092

Laborde, K.T., Robertson, E.B., and Sherrington, P.F., 1975. The micropalaeontology, palynology and stratigraphy of Eastcan et al. Freydis B-87 well; Robertson Research (North America) Limited, Exploration Report No. 122, 30 p. <https://basin.gdr.nrcan.gc.ca/wells/index_e.php> [accessed February 15, 2017]

Lavoie, D., Pinet, N., Zhang, S., Reyes, J., Jiang, C., Ardakani, O.H., Savard, M.M., Dhillon, R.S., Chen, Z., Dietrich, J.R., Hu, K., Craven, J.A., Roberts, B., Duchesne, M.J., Brake, V.I., Huot-Vézina, G., Galloway, J.M., McCarcken, A.D., Asselin, E., Decker, V., Beauchemin, M., Nicolas, M.P.B., Armstrong, D.K., and Hahn, K.E., 2019. Hudson Bay, Hudson Strait, Moose River, and Foxe basins: synthesis of the research activities under the Geomapping for Energy and Minerals (GEM) programs 2008-2018; Geological Survey of Canada, Open File 8507, 76 p. https://doi.org/10.4095/314653

Lemon, R.R.H. and Blackadar, R.G., 1963. Admiralty Inlet area, Baffin Island, District of Franklin; Geological Survey of Canada, Memoir 328, 84 p. https://doi.org/10.4095/108031

Macauley, G., 1987. Geochemistry of organic-rich Ordovician sediments on Akpatok and Baffin islands, Northwest Territories; Geological Survey of Canada, Open File 1502, 27 p. https://doi.org/10.4095/130275

MacLean, B., 1978. Marine geological-geophysical investigations in 1977 of the Scott Inlet and Cape Dyer-Frobisher Bay areas of the Baffin Island continental shelf; *in* Current Research, Part B; Geological Survey of Canada, Paper 78-1B, p. 13–20. https://doi.org/10.4095/103568

MacLean, B. and Srivastava, S.P., 1976. Shallow corehole drilling on the Baffin Island Shelf; *in* Report of Activities, Part A; Geological Survey of Canada, Paper 76-1A, p. 141–143. https://doi.org/10.4095/104182

MacLean, B. and Williams, G., 1983. Geological investigations of Baffin Island Shelf in 1982; *in* Current Research, Part B; Geological Survey of Canada, Paper 83-1B, p. 309–315. https://doi.org/10.4095/109337

MacLean, B., Jansa, L.F., Falconer, R.K.H., and Srivastava, S.P., 1977. Ordovician strata on the southeastern Baffin Island shelf revealed by shallow drilling; Canadian Journal of Earth Sciences, v. 14, p. 1925–1939. https://doi.org/10.1139/e77-163

MacLean, B., Srivastava, S.P., and Haworth, R.T., 1982. Bedrock structures off Cumberland Sound, Baffin Island shelf: sample and geophysical data; *in* Arctic Geology and Geophysics, (ed.) A.F. Embry and H.R. Balkwill; Canadian Society of Petroleum Geologists, Memoir 8, p. 359–365.

MacLean, B., Woodside, J.M., and Girouard, P., 1984. Geological and geophysical investigations in Jones Sound, District of Franklin; *in* Current Research, Part A; Geological Survey of Canada, Paper 84-1A, p. 359–365. https://doi.org/10.4095/119685

MacLean, B., Williams, G.L., Jennings, A., and Blakeney, C., 1986. Bedrock and surficial geology of Cumberland Sound, N.W.T.; *in* Current Research, Part B; Geological Survey of Canada, Paper 86-1B, p. 605–615. https://doi.org/10.4095/120672

McCartney, T., 2019. A qualitative comparison of continental rift structures in the sedimentary basins of the Labrador Shelf, offshore Newfoundland and Labrador, and the Malawi Rift, east Africa; Geological Survey of Canada, Open File 8634, 3 posters. https://doi.org/10.4095/315352

McCracken, A.D., 2000. Middle and Late Ordovician conodonts from the Foxe lowland of southern Baffin Island, Nunavut; *in* Geological Framework of the Ordovician System in the Southeast Arctic Platform, Nunavut, (ed.) A.D. McCracken and T.E. Bolton; Geological Survey of Canada, Bulletin 557, p. 159–216. https://doi.org/10.4095/211847

McWhae, J.R.H., Elie, R., Laughton, D.C., and Gunther, P.R., 1980. Stratigraphy and petroleum prospects of the Labrador Shelf; Bulletin of Canadian Petroleum Geology, v. 28, no. 4, p. 460–488.

Miller, P.E. and D'Eon, G.J., 1987. Labrador Shelf – Paleoenvironments (Report); Geological Survey of Canada, Open File 1722, 189 p. https://doi.org/10.4095/130598

Moir, P.N., 1989. Lithostratigraphy Labrador Sea: review and type sections; *in* East Coast Basin Atlas Series, Labrador Sea, Frontier Geoscience Program, (ed.) J.S. Bell; Geological Survey of Canada, Atlantic Geoscience Centre; p. 26–27. https://doi.org/10.4095/127166

Nentwich, F.W., 1987. Stratigraphy and sedimentology of the Ordovician and Silurian Brodeur Group, Northern Brodeur Peninsula, Baffin Island; Ph.D. thesis, University of Alberta, Edmonton, Alberta, 457 p.

Nentwich, F.W. and Jones, B., 1989. Stratigraphy and sedimentology of Ordovician and Silurian strata, Northern Brodeur Peninsula, Baffin Island; Bulletin of Canadian Petroleum Geology, v. 37, p. 428–442.

Oliver, E.M. and Awai-Thorne, B., 1984. The micropalaeontology, palynology and stratigraphy of the South Hopedale L-39, Labrador Shelf, offshore eastern Canada; Robertson Research Canada Limited, Exploration Report No. 2192, 31 p. <https://basin.gdr.nrcan.gc.ca/wells/index_e.php> [accessed June 7, 2018]

Oliver, E.M. and Thorne, B.V.A., 1979. The micropalaeontology, palynology and stratigraphy of the Total Eastcan Tyrk P-100 well; Robertson Research Canada Limited, Exploration Report No. 204A, 24 p. <https://basin.gdr.nrcan.gc.ca/wells/index_e.php> [accessed July 4, 2017]

Palmer, A.R., Cowie, J.W., and Eby, R.G., 1981. A Late Cambrian (Dresbachian, Crepicephalus Zone) fauna from the Boothia Peninsula, District of Franklin; *in* Contributions to Canadian Paleontology, (ed.) M. Kennedy; Geological Survey of Canada, Bulletin 300, p. 1–6.

Pandachuck, P.N. and Lewis, D.G., 1978. Chevron et al. Hopedale E-33; Well history report; on file at the Canada-Newfoundland and Labrador Offshore Petroleum Board, 29 p.

Plé, C. and Ferrero, J., 1976. Eastcan et al. Freydis B-87; Well history report; on file at the Canada-Newfoundland and Labrador Offshore Petroleum Board, 44 p.

Rauwerda, P.J., 1975. Biostratigraphy – Eastcan et al. Freydis B-87 well; Robertson Research (North America) Limited, 10 p. <https://basin.gdr.nrcan.gc.ca/wells/index_e.php> [accessed February 15, 2017]

Sanford, B.V. and Grant, A.C., 1990. New findings relating to the stratigraphy and structure of the Hudson Platform; *in* Current Research, Part D; Geological Survey of Canada, Paper 90-1D, p. 17–30. https://doi.org/10.4095/131335

Sanford, B.V. and Grant, A.C., 2000. Geological framework of the Ordovician system in the southeast Arctic Platform, Nunavut; *in* Geology and Paleontology of the Southeast Arctic Platform and Southern Baffin Island, Nunavut; (ed.) A.D. McCracken and T.E. Bolton; Geological Survey of Canada, Bulletin 557, p. 13–38. https://doi.org/10.4095/211845

Steeves, G.B., 1982. Total Eastcan et al. Roberval K-92; Well history report; on file at the Canada-Newfoundland and Labrador Offshore Petroleum Board, 17 p.

Stewart, W.D., 1987. Late Proterozoic to early Tertiary stratigraphy of Somerset Island and northern Boothia Peninsula, District Franklin, N.W.T; Geological Survey of Canada, Paper 83-26, 78 p. https://doi.org/10.4095/122372

Total Eastcan Exploration Ltd., 1979a. Total Eastcan et al. Roberval K-92; Well history report; on file at the Canada-Newfoundland and Labrador Offshore Petroleum Board, 272 p.

Total Eastcan Exploration Ltd., 1979b. Total Eastcan et al. Tyrk P-100; Well history report; on file at the Canada-Newfoundland and Labrador Offshore Petroleum Board, 118 p.

Trettin, H.P., 1965a. Middle Ordovician to Middle Silurian carbonate cycle, Brodeur Peninsula, Northwestern Baffin Island; Bulletin of Canadian Petroleum Geology, v. 13, p. 155–180.

Trettin, H.P., 1965b. Lower Paleozoic sediments of northwestern Baffin Island, District of Franklin; Geological Survey of Canada, Paper 64-47, 28 p. https://doi.org/10.4095/101000

Trettin, H.P., 1969. Lower Paleozoic sediments of northwestern Baffin Island; Geological Survey of Canada, Bulletin 157, 70 p. https://doi.org/10.4095/102249

Trettin, H.P., 1975. Investigations of Lower Paleozoic geology, Foxe Basin, Northeastern Melville Peninsula, and parts of northwestern and central Baffin Island; Geological Survey of Canada, Bulletin 251, 177 p. https://doi.org/10.4095/103973

Umpleby, D.C., 1979. Geology of the Labrador shelf; Geological Survey of Canada, Paper 79-13, 41 p. https://doi.org/10.4095/105927

van Helden, B.G., 1978. Chevron et al. Hopedale E-33 55°52′35″N; 58°50′25″W (East Coast Offshore); Palynology Report, 7 p. <https://basin.gdr.nrcan.gc.ca/wells/index_e.php> [accessed April 21, 2017]

Walters, R., 1977. The biostratigraphy of well Indian Harbour M-52 below 7750 ft. (BP Canada-Columbia-Chevron) Offshore Labrador, Canada; Exploration and Production Research Division, BP Research Centre, Palaeontological Branch, London Palaeontological Note EPR/LPN 3661, 15 p. <https://basin.gdr.nrcan.gc.ca/wells/index_e.php> [accessed February 16, 2017]

Williams, G.L., 1979. Eastcan et al. Freydis B-87; *in* Palynological Zonation and Correlation of Sixty-seven Wells, Eastern Canada, (ed.) M.S. Barss, J.P. Bujak, and G.L. Williams; Geological Survey of Canada, Paper 78-24, p. 89–90. https://doi.org/10.4095/104894

Williams, G.L. and Barss, M.S., 1979. Eastcan et al. Gudrid H-55; *in* Palynological Zonation and Correlation of Sixty-seven Wells, Eastern Canada, (ed.) M.S. Barss, J.P. Bujak, and G.L. Williams; Geological Survey of Canada, Paper 78–24, p. 91. https://doi.org/10.4095/104894

Williams, G.L., Ascoli, P., Barss, M.S., Bujak, J.P., Davies, E.H., Fensome, R.A., and Williamson, M.A., 1990. Biostratigraphy and related studies, Chapter 3; *in* Geology of the Continental Margin of Eastern Canada, (ed.) M.J. Keen and G.L. Williams; Geological Survey of Canada, Geology of Canada, no. 2, p. 87–137 (*also* Geological Society of America, the Geology of North America, v. I-1). https://doi.org/10.4095/132698

Zhang, S., 2012. Ordovician stratigraphy and oil shale, southern Baffin Island, Nunavut – preliminary field and post field data; Geological Survey of Canada, Open File 7199, 23 p. https://doi.org/10.4095/291521

Zhang, S., 2013. Ordovician conodont biostratigraphy and redefinition of the age of lithostratigraphic units on northeastern Melville Peninsula, Nunavut; Canadian Journal of Earth Sciences, v. 50, p. 808–825. https://doi.org/10.1139/cjes-2013-0009

Zhang, S., 2018a. Ordovician stratigraphy on the unnamed peninsula (southwestern NTS area 37F and northwestern NTS area 37C) northeast of Fury and Hecla Strait on northern Baffin Island, Nunavut; *in* Summary of Activities 2018; Canada-Nunavut Geoscience Office, p. 97–106.

Zhang, S., 2018b. Upper Ordovician conodont biostratigraphy and revised lithostratigraphy and geological map, Akpatok Island, Ungava Bay, Nunavut; Canadian Journal of Earth Sciences, v. 55, p. 52–69. https://doi.org/10.1139/cjes-2017-0145

Zhang, S. and Pell, J., 2013. Study of sedimentary rock xenoliths from kimberlites on Hall Peninsula, Baffin Island, Nunavut; *in* Summary of Activities 2012; Canada-Nunavut Geoscience Office, p. 107–112.

Zhang, S. and Pell, J., 2014. Conodonts recovered from the carbonate xenoliths in the kimberlites confirm the Paleozoic cover on the Hall Peninsula, Nunavut; Canadian Journal of Earth Sciences, v. 51, p. 142–155. https://doi.org/10.1139/cjes-2013-0171

Zhang, A. and Pell, J., 2016. Conodonts and their colour alteration index values from carbonate xenoliths in four kimberlites on Hall Peninsula, Baffin Island, Nunavut; *in* Summary of Activities 2016; Canada-Nunavut Geoscience Office, p. 1–11.

Zhang, S. and Riva, J.F., 2018. The stratigraphic position and the age of the Ordovician organic-rich intervals in the northern Hudson Bay, Hudson Strait, and Foxe basins — evidence from graptolites; Canadian Journal of Earth Sciences, v. 55, p. 897–904. https://doi.org/10.1139/cjes-2017-0266

Zhang, S., Creaser, R.A., and Pell, J., 2014. Discovery of organic-rich black shale xenolith from kimberlite on the Hall Peninsula, Nunavut and its implication for petroleum potential in Cumberland Sound; Bulletin of Canadian Petroleum Geology, v. 62, p. 125–131.

Historical development of a litho- and biostratigraphic framework for onshore Cretaceous–Paleocene deposits along western Baffin Bay

J.W. Haggart[1*], L.T. Dafoe[2], K.M. Bell[3, 4], G.L. Williams[2], E.T. Burden[5], L.D. Currie[3], R.A. Fensome[2], and A.R. Sweet[3, 6]

Haggart, J.W., Dafoe, L.T., Bell, K.M., Williams, G.L., Burden, E.T., Currie, L.D., Fensome, R.A., and Sweet, A.R., 2022. Historical development of a litho- and biostratigraphic framework for onshore Cretaceous–Paleocene deposits along western Baffin Bay; in *Geological synthesis of Baffin Island (Nunavut) and the Labrador–Baffin Seaway, (ed.) L.T. Dafoe and N. Bingham-Koslowski; Geological Survey of Canada, Bulletin 608, p. 107–135. https://doi.org/10.4095/321828*

Abstract: Cretaceous–Paleogene strata along the eastern coast of Baffin Island, on Bylot Island, and on associated islands north of Cape Dyer, have been known since the early days of exploration of Baffin Bay in the mid-nineteenth century. Studies of these strata in the 1970s–1990s established their clastic nature and revealed details of their stratigraphy, ages, and depositional settings. Onshore strata in the Cape Dyer area accumulated in close association with volcanic deposits related to late-stage rifting in the Late Cretaceous to Early Paleocene that eventually formed Baffin Bay. In contrast, deposits in more northerly areas, such as the Eclipse and North Bylot troughs on Bylot Island, exhibit similar clastic rocks, but lack conspicuous volcanic strata, and have been associated with either the Sverdrup Basin or the Baffin Bay rift. The litho- and biostratigraphy of these deposits are summarized and discussed in terms of differing and contrasting stratigraphic interpretations, age assignments, and depositional environments.

Résumé : Les strates du Crétacé-Paléogène le long de la côte est de l'île de Baffin, dans l'île Bylot et dans les îles voisines au nord du cap Dyer sont connues depuis les premiers jours de l'exploration de la baie de Baffin au milieu du XIX[e] siècle. Les études portant sur ces strates menées dans les années 1970-1990 ont établi leur nature détritique et révélé des détails sur leur stratigraphie, leur âge et leurs milieux de dépôt. Les strates en milieu terrestre dans la région du cap Dyer se sont accumulées en lien étroit avec les dépôts volcaniques associés aux phases tardives du rifting, au Crétacé tardif et Paléocène précoce, qui a abouti à la formation de la baie de Baffin. En revanche, les dépôts dans les régions plus au nord, comme ceux des cuvettes d'Eclipse et de North Bylot dans l'île Bylot, présentent des lithologies détritiques semblables, mais ne renferment pas de strates volcaniques apparentes, et ont été associés soit au bassin de Sverdrup, soit au rift de la baie de Baffin. La lithostratigraphie et la biostratigraphie de ces dépôts sont résumées et examinées sous l'angle d'interprétations stratigraphiques différentes et contrastantes, des attributions d'âge et des milieux de dépôt.

[1]Geological Survey of Canada, 1500-605 Robson Street, Vancouver, British Columbia V6B 5J3
[2]Geological Survey of Canada, 1 Challenger Drive, P.O. Box 1006, Dartmouth, Nova Scotia B2Y 4A2
[3]Geological Survey of Canada, 3303-33rd Street N.W., Calgary, Alberta T2L 2A7
[4]Present address: PetroStrat Canada Ltd., 102-902 9th Avenue S.E., Calgary, Alberta T2G 0S4
[5]Department of Earth Sciences, Memorial University of Newfoundland, P.O. Box 4200, St. John's, Newfoundland and Labrador A1C 5S7
[6]Deceased
*Corresponding author: J.W. Haggart (email: jim.haggart@nrcan-rncan.gc.ca)

INTRODUCTION

Much of the east coast of Baffin Island and adjacent Bylot Island is composed of orthogneiss, metagranite, sedimentary rock, and volcanic rock of ages ranging from Archean to Mesoproterozoic (St-Onge et al., 2009, this volume). Along this rugged, approximately 1000 km coastline, however, younger Mesozoic and Cenozoic sedimentary and volcanic strata outcrop locally, including, from south to north: limited exposures north of Cape Dyer (east-central Baffin Island); small outcrops in the vicinity of Scott Inlet (northeast Baffin Island); an extensive succession in the Eclipse Trough (northern Baffin Island at Salmon River, beneath Tasiujaq (Eclipse Sound), and on southwest Bylot Island); and exposures in the North Bylot Trough (adjacent to Maud Bight, northern Bylot Island) (Fig. 1). These limited exposures provide the only onshore analogues to the accumulations of strata of similar age that are inferred to underlie parts of the continental shelf and slope of western Baffin Bay (*see* MacLean et al., 2014; Dafoe, Dickie, and Williams, this volume), and preserve the most comprehensive stratigraphic evidence of the depositional and tectonic evolution of western Baffin Bay. Related prominent offshore basins north of Cape Dyer, from south to north, include: Scott Graben (with associated offshore oil seeps; *see* Bingham-Koslowski, McCartney, and Bojesen-Koefoed, this volume); Buchan Graben; Lady Ann Basin; and Glacier and North Water basins (the last two not shown on Fig. 1). As well, appreciable thicknesses of Cretaceous and Cenozoic strata are found within Lancaster Sound (Brent et al., 2013) and the Cenozoic Baffin Fan accumulation (Fig. 1; also *see* Fig. 1 of Dafoe, Dickie, and Williams, this volume), the latter of which may contain significant hydrocarbon reserves (Gautier et al., 2009; Harrison et al., 2011).

Most of the onshore successions adjacent to the western Baffin Bay region have been examined only cursorily, with basic stratigraphic understanding of the known local sequences. Early studies documented general localities, lithological characteristics, and broad ages, forming a framework for subsequent studies in the later part of the twentieth century; these were more detailed, but still lacked a comprehensive regional context. In the Cape Dyer area, outcrops of younger sedimentary and volcanic strata, unconformably overlying the Archean rocks that dominate the region, were first recognized by Sutherland (1853), who reported coal at 'Cape Durban' (i.e. Durban Island, now named Aggijjat; Fig. 1) during a traverse of Baffin Bay in an attempt to locate the missing Franklin Expedition. Nearby rocks at Qaqulluit (Cape Searle; Fig. 1) were subsequently described by McMillan (1910, p. 423–424), who reported several hundred metres of volcanic breccia and tuff that he dated as Tertiary; McMillan (1910, p. 458) also assigned a Tertiary date to the strata found at Aggijjat (Durban Island). Kidd (1953) subsequently described the extent of the volcanic rocks in the Qaqulluit (Cape Searle)–Cape Dyer area, noting that they form an outcrop belt 88 km long, but extend inland no more than 8 km from the shoreline, and locally are more than 900 m thick.

The first geological map showing the rocks of northern Baffin Island and adjacent Bylot Island was prepared by Haughton (1859), based on samples collected by Captain F.L. M'Clintock during several voyages of the *Fox*, also in the search for the remains of the Franklin Expedition. Haughton (1859) considered that "Silurian Limestone" formed the northern two-thirds of Bylot Island and adjacent Borden Peninsula to the west, based presumably on "specimens of brown earthy limestone" collected by M'Clintock at Haughton's locality VII, at "Possession Bay [now Bathurst Bay], south entrance into Lancaster Sound" (Haughton, 1859, p. 382) (Fig. 1). The latitude and longitude provided by Haughton (1859) for this locality plot in the area of Cape Liverpool (Fig. 1) on the north coast of Bylot Island. Paleozoic rocks are not shown on modern geological maps of this general locality, although possible outcrops of Paleozoic strata have been mapped on the north coast of Bylot Island some 100 km to the north and west (e.g. Jackson and Davidson, 1975b). McGregor (D.C. McGregor, unpub. GSC Paleontological Report Fl-21-1980-DCM, 1980) reported fossil scolecodonts (polychaete worm jaw structures) in samples collected from glacial moraine deposits just north of Bathurst Bay, leading him to suggest that possible Ordovician–Devonian rocks could be nearby. Additional samples with scolecodonts collected from west of Maud Bight also suggested the possible presence of Paleozoic strata in that area (D.C. McGregor, unpub. GSC Paleontological Report Fl-9-1972-DCM, 1972; unpub. GSC Paleontological Report Fl-7-1980-DCM, 1980), although Jackson and Davidson (1975a) questioned this interpretation on the basis of lithostratigraphy. Regardless of subsequent findings, Haughton's (1859) geological map was the first to show the presence of younger strata overlying the older "granitoid rocks" that constitute much of Bylot Island and Baffin Island's rugged eastern coast.

Relatively young sedimentary strata in the onshore northern Baffin Bay region were first recognized by Low (1906), commander and geologist on the voyage of the *Neptune* to the Baffin Bay region in 1903–1904. Low (1906) identified strata he assigned to the Tertiary on northern Baffin Island "at Pond's inlet" (i.e. present-day Pond Inlet; Fig. 1), and further reported (p. 229) that "Capt. Adams, of the whaler *Diana*, said that lignite was to be found in similar deposits near Cape Hay, on the east side of Bylot island" (actually on the island's north side; Fig. 1). This latter statement is the earliest suggestion of a stratigraphic outlier adjacent to Maud Bight, approximately 25 km east of Cape Hay. McMillan (1910, p. 458) reiterated that the sandstone and coal units of the Tasiujaq (Eclipse Sound) region should be assigned to the Tertiary. In 1910, the first recorded geological observations of the inferred Tertiary rocks on Bylot Island were made by R.S. Janes, 2nd Officer of the Dominion Government Ship (D.G.S.) *Arctic*, who noted similarities between the rocks near Salmon River with those on Bylot Island to the north, and who recognized that these strata contained fossil trees and buds, as well as coal seams (Appendix No. 6 *in* Bernier, 1911). These rocks are now known to be both Cretaceous and Pliocene (*see* Piraux, 2004; Csank et al., 2013).

It was not until the late 1960s that detailed geological mapping at 1:250 000 scale of these areas of northern Baffin Island and Bylot Island was undertaken (Jackson and Davidson, 1975a, b; Jackson et al., 1975), and broad aspects of the younger stratigraphic successions preserved in these areas became better known, including their Early Cretaceous (Albian) to early Cenozoic age. As a result of these mapping efforts, geological interest arose in the Cretaceous–Cenozoic succession preserved on Bylot Island in particular, and its comparison with successions of similar age in the Sverdrup Basin of the western Canadian Arctic. Reconnaissance mapping and stratigraphic assessments of the Cretaceous–Cenozoic strata by Miall et al. (1980) and Ioannides (1986) described the basic lithostratigraphic succession on Bylot Island and its age, determined by palynology. This interpretive framework was subsequently modified in several theses undertaken by students of Memorial University of Newfoundland in the 1980s to 1990s, which analyzed sections from the Eclipse and North Bylot troughs (Sparkes, 1989; Waterfield, 1989; Wiseman, 1991; Benham, 1991). Similarly, interest in the sedimentary and volcanic strata preserved in the Cape Dyer area, particularly their depositional and tectonic relationships with comparable strata on West Greenland (Henderson et al., 1976), led to detailed litho- and biostratigraphic investigations of these strata during the 1970s and 1980s. Burden and Langille (1990, 1991) provided details of the sedimentary succession preserved locally in the Cape Dyer area and established its Early Cretaceous to Paleocene age. Figure 2 presents a summary of stratigraphic interpretations of the onshore Cretaceous–Paleogene successions along western Baffin Bay, as established by various researchers by the end of the 1990s.

More recently, the Geological Survey of Canada's GEM (Geomapping for Energy and Minerals) program undertook detailed field studies of the Cretaceous–Paleogene outcrop succession of northeastern Baffin Island and Bylot Island between 2009 and 2018 in order to better understand the stratigraphy of the succession, its age limits, depositional environments, and provenance, and to assess how these strata may serve as an analogue for the succession preserved below the offshore continental shelf and slope of western Baffin Bay and in Lancaster Sound. Numerous samples were collected during this fieldwork, with analyses and research activities still underway (Haggart et al., 2017, 2018). Accordingly, this contribution presents a compilation of existing stratigraphic data and interpretations to provide a context for the field investigations undertaken during the GEM program. The present study provides a historical review of the assessments of the Cretaceous–Paleogene successions of Baffin and Bylot islands by geographic region, progressing from south to north, with a focus on the studies undertaken between the 1970s and 1990s.

Figure 1. Location map of northern Baffin Bay showing principal places discussed in text. Insets refer to subsequent figures in text. Onshore basin outlines *modified from* Miall et al. (1980), offshore basin outlines are *from* Keen et al. (this volume). Inset A is shown in Figure 3, inset B in Figure 6, inset C in Figure 8, inset D in Figure 9, and inset E in Figure 10. Additional projection information: Central Meridian = 60°W; Standard Parallels = 65, 75°W; Latitude of Origin = 65°N.

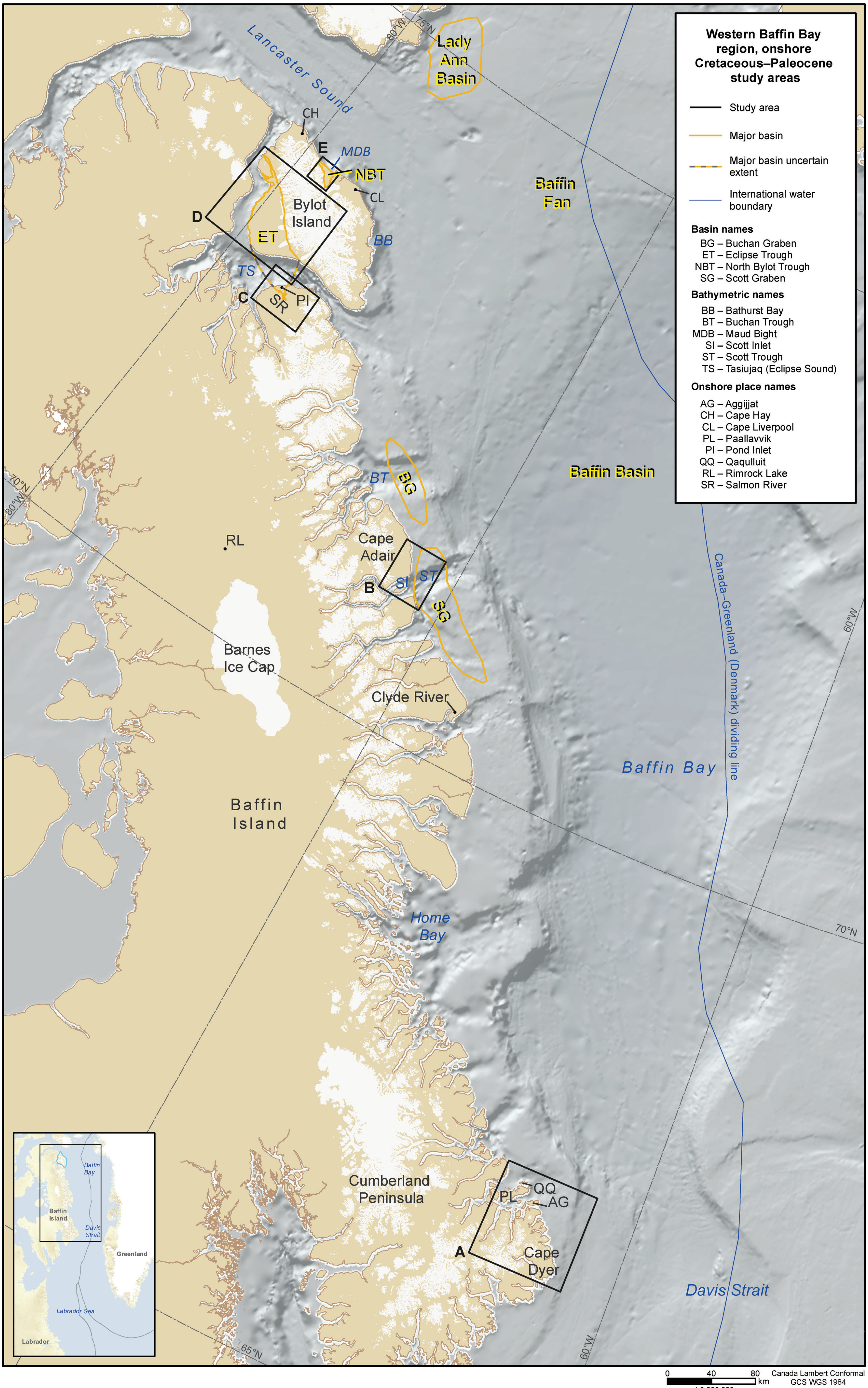
Western Baffin Bay region, onshore Cretaceous–Paleocene study areas
Study area
Major basin
Major basin uncertain extent
International water boundary
Basin names
BG – Buchan Graben
ET – Eclipse Trough
NBT – North Bylot Trough
SG – Scott Graben
Bathymetric names
BB – Bathurst Bay
BT – Buchan Trough
MDB – Maud Bight
SI – Scott Inlet
ST – Scott Trough
TS – Tasiujaq (Eclipse Sound)
Onshore place names
AG – Aggijjat
CH – Cape Hay
CL – Cape Liverpool
PL – Paallavvik
PI – Pond Inlet
QQ – Qaqulluit
RL – Rimrock Lake
SR – Salmon River
Lancaster Sound
Lady Ann Basin
Baffin Fan
Baffin Basin
Bylot Island
Cape Adair
Barnes Ice Cap
Clyde River
Baffin Island
Home Bay
Baffin Bay
Canada–Greenland (Denmark) dividing line
Cumberland Peninsula
Cape Dyer
Davis Strait
A
B
C
D
E
70°N
80°W
75°N
65°N
60°W
Greenland
Labrador Sea
Labrador
0 40 80 km
1:3 250 000
Canada Lambert Conformal
GCS WGS 1984

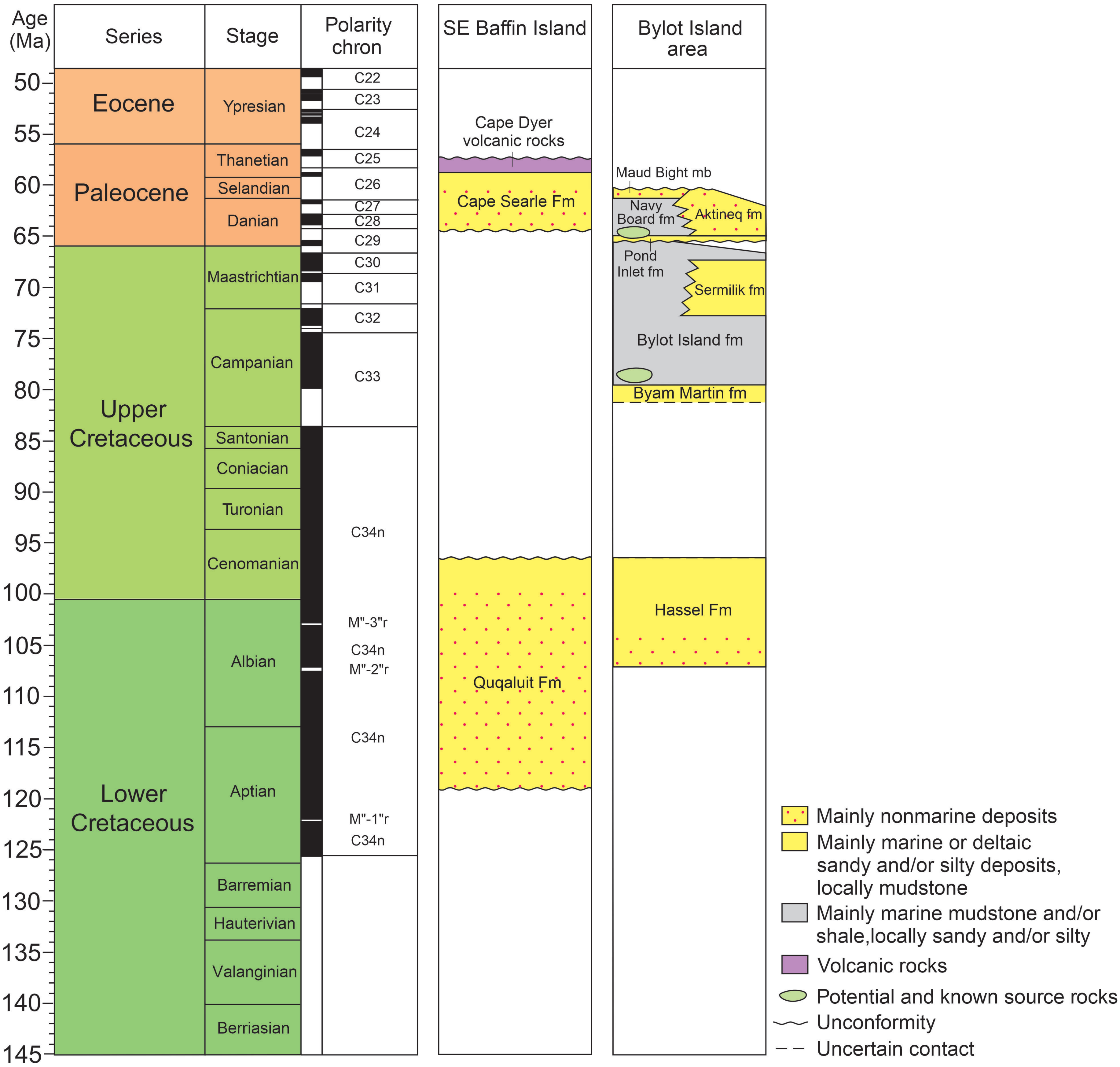

Figure 2. Summary of the onshore Cretaceous–Paleogene stratigraphic successions of the western Baffin Bay region based on research reviewed in text. Formal and informal stratigraphic names are included. Details of the stratigraphic successions of both the Cape Dyer and Bylot Island regions are presented in successive sections of this contribution. The Cape Dyer stratigraphy is *modified from* Gregersen et al. (2013) and Nøhr-Hansen et al. (2016) and based on the original work of Burden and Langille (1990, 1991). The stratigraphy of Bylot Island is *modified from* Gregersen et al. (2013) and Nøhr-Hansen et al. (2016), and includes information from the studies by McWhae et al. (1979), Miall (1986), Waterfield (1989), Harrison et al. (1999), and Haggart et al. (2011). Age limits of Bylot Island strata are based on the authors' consensus assessment of the work of various researchers (Ioannides, 1986; Sparkes, 1989; Waterfield, 1989; Wiseman, 1991; Benham, 1991). Radiometric age dates *after* Cohen et al. (2021).

CAPE DYER REGION

Details of the Cretaceous–Cenozoic sedimentary and volcanic succession preserved in the Cape Dyer area (Fig. 3, 4) were first provided by Kidd (1953). He recognized a thicker succession of basaltic flows at Padloping Island (now Paallavvik), underlain by cross-stratified agglomerate units and flat-lying grey tuff units, to which he ascribed a submarine origin. At the base of the volcanic succession on Padloping Island, and also at Durban Island (now Aggijjat), Kidd (1953) identified interstratified semiconsolidated sandstone and shale with local coal seams up to 25 cm thick; however, he was not able to confidently assess the stratigraphic relationships with the volcanic rocks. Kidd (1953) also recognized that mafic dykes penetrated at least the lower part of the volcanic pile in the area.

Lithostratigraphic succession

Clarke and Upton (1971) undertook the first detailed assessment of the sedimentary and volcanic strata preserved in the Cape Dyer to Cape Searle region (Fig. 3). They recognized units of underlying "pre-volcanic sediments" and overlying "Tertiary volcanics." The former consisted of unconsolidated white quartz sand and associated sandstone, shale, minor coal, and conglomerate, all considered terrestrial in origin. Fossil plants found within the strata were identified by W.A. Bell (*in* Clarke and Upton, 1971) as typical forms found in lower Paleocene strata of the Nuussuaq Peninsula region of West Greenland. Clarke and Upton (1971) noted that cross-stratification in the sedimentary beds suggested northeast-directed paleocurrents. They also noted that the thickness of sedimentary units across the Cape Dyer–Cape Searle region varies appreciably, with associated local variations in lithology.

Clarke and Upton (1971) provided significant detail on the stratigraphic succession and composition of the Cenozoic volcanic strata of the Cape Dyer–Cape Searle belt, recognizing both breccia facies, with giant "cross-stratification" exhibiting southwesterly dips, and flow facies, as well as numerous basaltic dykes crosscutting sedimentary strata at Cape Searle and Padloping Island (= Paallavvik). Based on a lack of inland sources for the volcanic strata, the limited geographic extent of observed dykes, and the southwesterly dip of the breccia units, Clarke and Upton (1971) posited that the volcanic rocks had a source to the northeast and were originally associated with the West Greenland basalt province (Noe-Nygaard, 1942; Clarke, 1968;

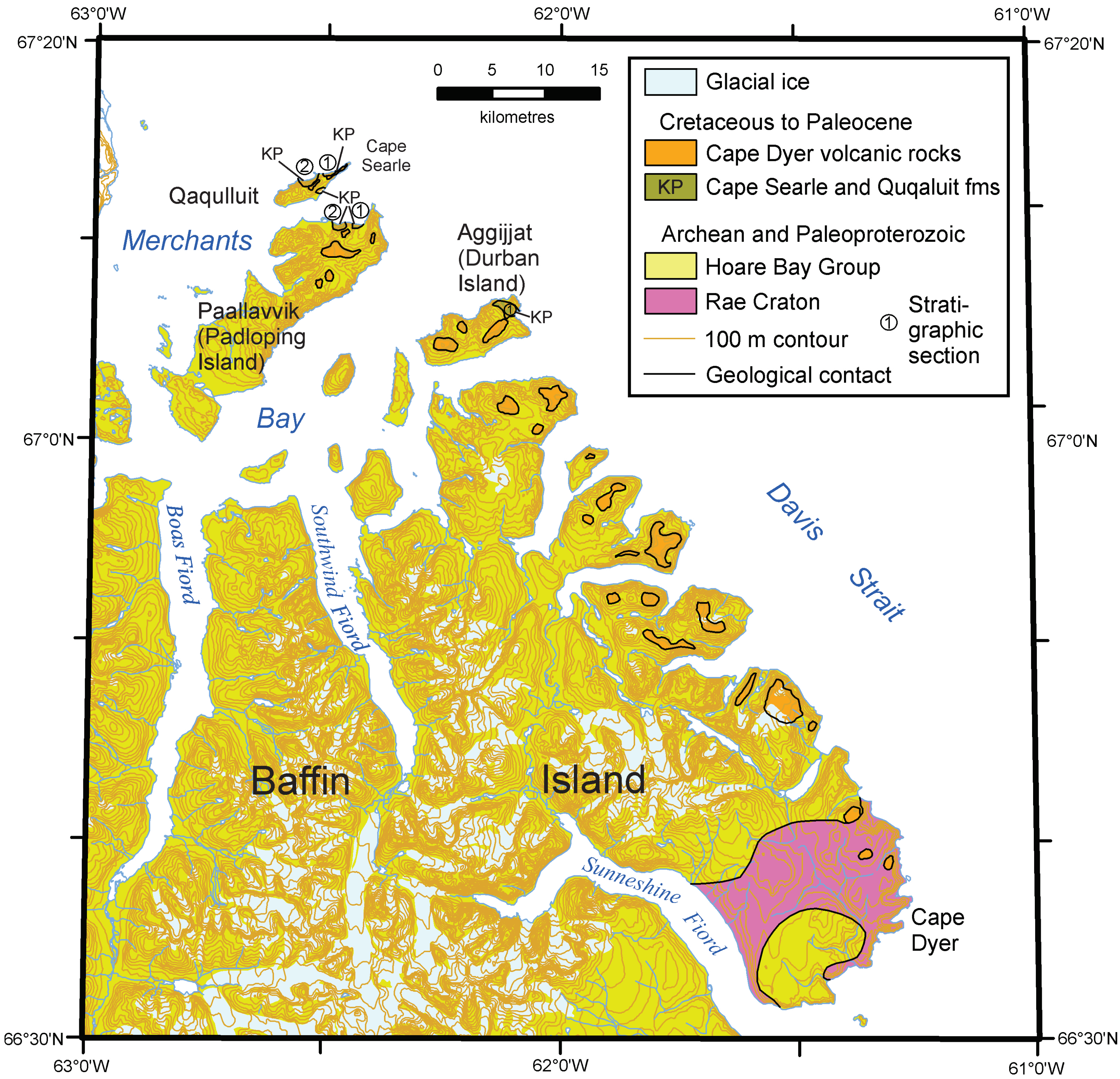

Figure 3. Generalized geological map of the Cape Dyer area, Baffin Island (inset A of Fig. 1). Based on data presented in Burden and Langille (1990), Jackson (1998), St-Onge et al. (2006), Sanborn-Barrie and Young (2013), and Sanborn-Barrie et al. (2013).

now West Greenland Basalt Group), and represented the early stages of rifting of the Baffin Bay region. MacLean et al. (1978) described basalt units sampled in rock drill cores from adjacent offshore areas and noted their similarities with the onshore exposures found on both eastern Baffin Island and West Greenland. They also observed a lack of glass in the offshore basalt samples and suggested this was evidence for eruption in a subaerial setting, in contrast with some of the onshore basalt units on both sides of Baffin Bay. Dafoe, DesRoches, and Williams (this volume) present an updated view on these volcanic rocks and link the breccia units to the ‘lava delta’ component of a volcanic margin, while Keen et al. (this volume) further describe the volcanic margins of the region in the context of plate reconstructions, showing the linkages between these rocks and those of West Greenland Basalt Group.

In several initial surveys of the stratigraphy preserved at Aggijjat (Durban Island), Paallavvik (Padloping Island), and Qaqulluit (island; also Quqaluit Island of previous workers) in the Cape Dyer area (Fig. 3), Sears (1986), Langille et al. (1986), and Langille (1987) measured and described the clastic strata preserved between small fault blocks (half-grabens) within the gneiss units (Fig. 4, 5). At Qaqulluit (island), they measured nearly 120 m of generally coarsening-upward section, including shale and sandstone beds, locally with tabular cross-stratification, shale rip-up clasts, and ironstone concretions in finer grained facies. This section rests on a highly weathered surface of granitoid basement rocks. Volcanic breccia and interbedded sandstone overlie the top of the section, presumably transitional to the overlying Cape Dyer volcanic rocks. At Paallavvik, Langille et al. (1986) and Langille (1987) constructed a composite stratigraphic section about 180 m thick, including many of the same lithologies and facies present in the Qaqulluit section. The Paallavvik section includes more abundant fine-grained lithologies, common *Metasequoia* plant fossils and permineralized logs, and local coal beds. Finally, they measured nearly 120 m of strata exposed on Aggijjat, consisting of similar lithologies to those at Qaqulluit and Paallavvik, but also including a 78 m thick interval of slumped sandstone deposits (“poorly exposed” interval shown on Fig. 5). Based on palynology, including spores, pollen, and dinoflagellate cysts (or dinocysts), Langille et al. (1986) and Langille (1987) concluded that the strata exposed on the three islands represent principally nonmarine, deltaic, and possibly shallow-shelf environments, of likely Albian–Cenomanian age, although they did not rule out the possibility of recycled Cretaceous palynomorphs within younger deposits. Sears (1986) further concluded, based on stratigraphic and facies relationships, that the exposures on the three islands represent the same deltaic complex, which likely accumulated in a rift setting; but the mid-Cretaceous age was appreciably earlier than generally accepted at the time for the onset of rifting in this part of the Labrador–Baffin Seaway.

Burden and Langille (1990) subsequently refined their interpretation of the stratigraphy present on the small islands north of Cape Dyer, proposing a formal nomenclature and updating the age of the succession (Fig. 2, 3). They assigned the basal strata resting nonconformably on the Archean–Paleoproterozoic gneissic basement rocks to the Quqaluit Formation, composed of coarse clastic deposits that accumulated in a northwest-flowing, braided-river complex in the Aptian to early Cenomanian. This formation was correlated, based on its age and lithology, with the Upernivik Næs Formation of onshore West Greenland and the Hassel Formation of the Bylot Island region and the Canadian Arctic Islands, although the sandstone units of the Quqaluit Formation are noticeably less arenaceous and more immature than those of the Hassel Formation. Building upon this interpretation of the Quqaluit Formation, Burden and Langille (1991) described a lower, Neocomian to Aptian white sandstone that was deposited in a braided-river setting, with an overlying upper Albian–Cenomanian yellow sandstone related to anastomosing or meandering river deposits. The uppermost part of this unit, however, was inferred to have

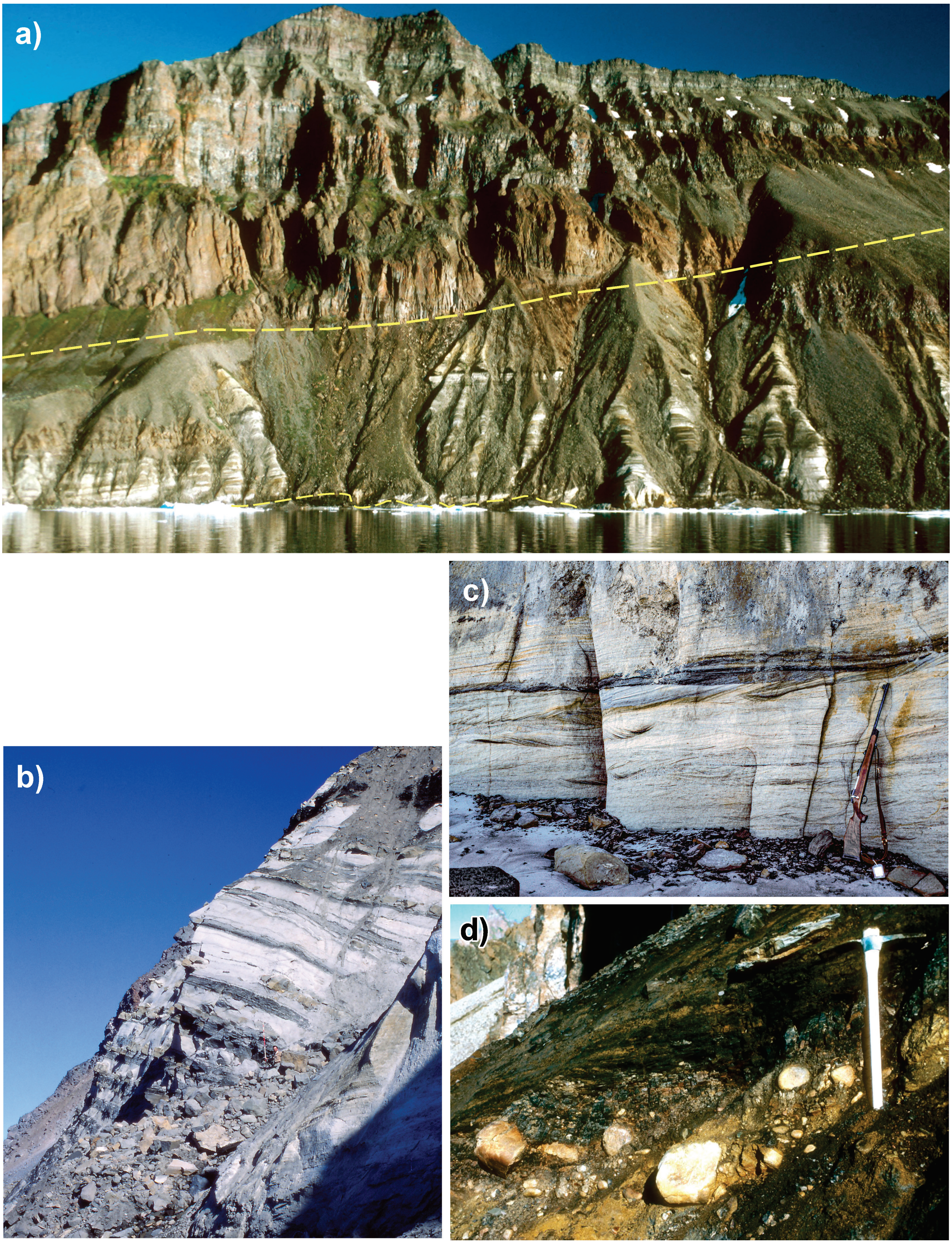

Figure 4. Photographs showing Cretaceous–Paleocene strata preserved in the Cape Dyer area of Baffin Island (inset A of Fig. 1). **a)** Quqaluit Formation type locality, Qaqulluit (island); lower yellow line just above water level shows contact of basal strata of formation unconformably overlying Archean Hoare Bay Group. Approximately 100 m of light-coloured clastic deposits make up the formation and are themselves overlain (contact shown by upper dashed yellow line) by basalt layers of the Cape Dyer volcanic rocks, comprising most of the stratigraphic section here. NRCan photo 2021-199. **b)** Massive to cross-stratified sandstone interbedded with dark mudstone with coal laminae and detritus, Quqaluit Formation, Paallavvik (Padloping Island); person with 1.5 m stick for scale. NRCan photo 2021-200. **c)** Planar- and trough-cross-stratified sandstone with pebble beds, Quqaluit Formation, Paallavvik. Rifle is 0.9 m long. NRCan photo 2021-201. **d)** Cobble- to small boulder conglomerate within carbonaceous mudstone, Cape Searle Formation, Cape Searle, Qaqulluit. Pick is 0.85 m long. NRCan photo 2021-202. *See* Figure 3 for locations. All photographs by E.T. Burden.

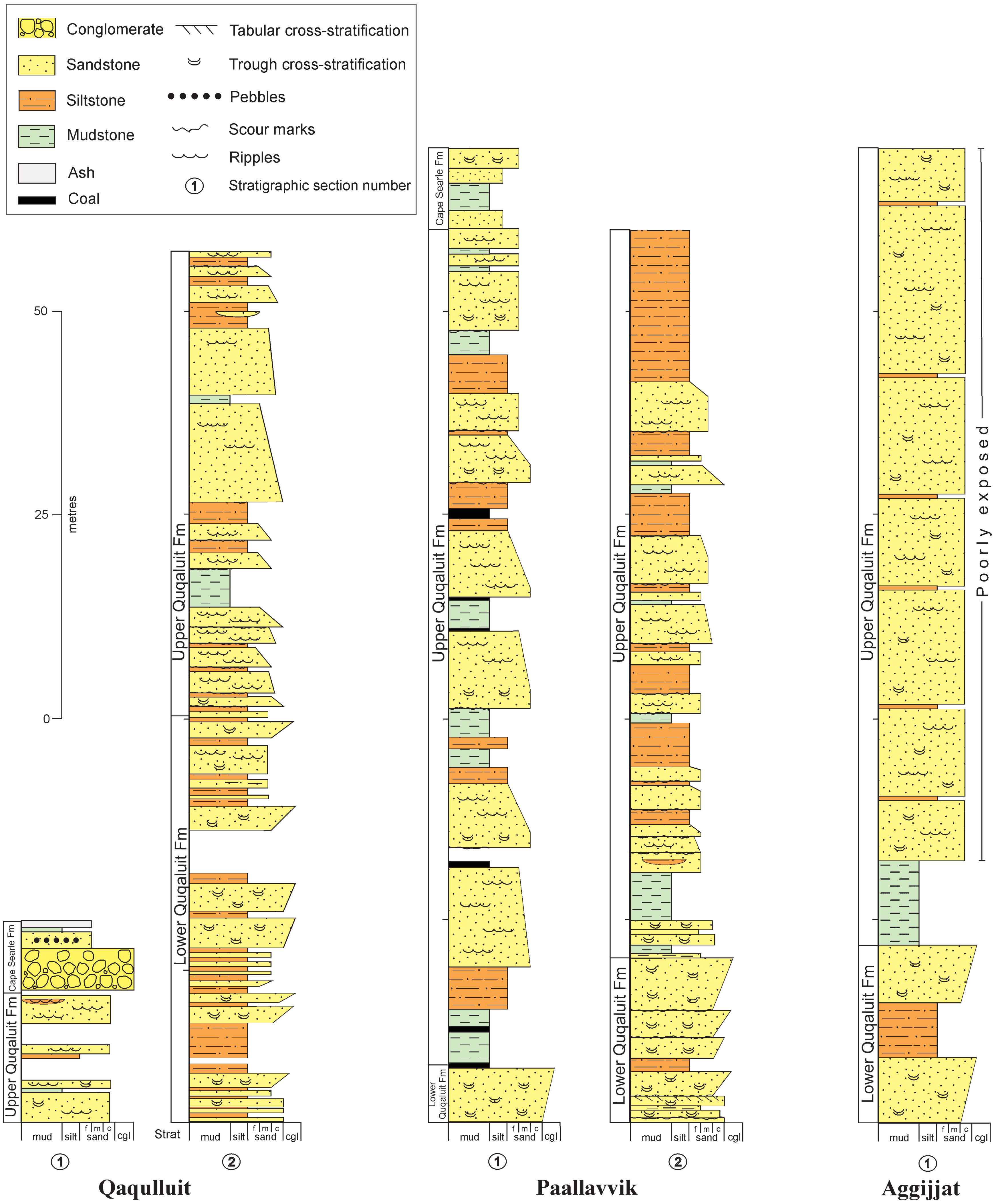

Figure 5. Summary stratigraphic sections of Cretaceous–Paleocene strata preserved in the Cape Dyer area (inset A of Fig. 1) of Baffin Island, (*modified from* Burden and Langille, 1990, 1991). Locations of measured stratigraphic sections are keyed to the map of Figure 3. c = coarse; cgl = conglomerate; f = fine; m = medium.

accumulated under brackish, marginal marine conditions, based on the presence of rare dinocysts and acritarchs. Strata overlying the Quqalurit Formation were assigned to the lower to middle Paleocene Cape Searle Formation, including sandstone, siltstone, mudstone, and conglomerate units interpreted to rest unconformably over the Quqaluit Formation, and representing rapidly deposited fluvial and debris-flow deposits interstratified with volcanic ash, all preceding the onset of late Paleocene deposition of the overlying Cape Dyer basalt units (Burden and Langille, 1990, 1991).

Biostratigraphy

Several palynological studies undertaken in the 1980s refined the age of the sedimentary rocks associated with the onshore volcanic strata of the Cape Dyer region. Holloway (1984) studied sedimentary strata on Aggijjat, Paallavvik, and at Cape Searle (Fig. 3), and recovered Cretaceous palynological assemblages from all three localities. From Aggijjat, Holloway (1984) recognized common, typically long-ranging Mesozoic forms such as *Alisporites bilateralis*, *Cedripites canadensis*, *Parvisaccites radiatus*, *Pityosporites* sp. cf. *P. constrictus*,*Podocarpidites multesimus*, and *Podocarpidites canadensis*, associated with biostratigraphically important *Densoisporites microrugulatus*, *Klukisporites foveolatus*, and *Lycopodiacidites canaliculatus*, suggesting to him a middle to late Albian age. At Paallavvik, Holloway (1984) reported the species *Appendicisporites matesovai*, *Biretisporites potoniaei*, *Cicatricosisporites annulatus*, *Cicatricosisporites australiensis* (now *Ruffordiaspora australiensis*), *Cicatricosisporites hallei*, *Cicatricosisporites auritus*, *Clavifera* sp. cf. *rudis*, *Concavissimisporites parkinii*, *Concavissimisporites* sp. cf. *C. penolaensis*, *Concavissimisporites* sp. cf. *C. punctatus*, *Densoisporites microrugulatus*, *Foveogleicheniidites confossus*, *Impardecispora apiverrucata*, *Impardecispora marylandensis*, *Klukisporites foveolatus*, *Pristinuspollenites* sp. cf. *P. microsaccus*, *Retitriletes* *marginatus*, and *Tigrisporites scurrandus*; he considered this assemblage to indicate an Albian age. Finally, he sampled the strata at Cape Searle and interpreted the assemblage of *Foveosporites canalis*, *Alisporites bilateralis*, *Alisporites grandis*, *Cicatricosisporites* sp., *Deltoidospora hallii*, and *Retitriletes* sp. as suggesting a possible age range of Berriasian to Albian (Holloway, 1984, his Table 1). The assemblages present from Aggijjat, Paallavvik, and Cape Searle, contain pollen and spores exclusively, with no marine elements, leading Holloway (1984) to conclude that the strata from all three localities have a terrestrial origin.

Burden and Langille (1991) revisited the palynology of the exposures preserved north of Cape Dyer. They identified two palynological assemblages present in the strata of the Quqaluit and Cape Searle formations, which they named the *Gemmatriletes clavatus–Cicatricosisporites potomacensis* Zone and the *Trivestibulopollenites betuloides–Pesavis parva* Zone (Table 1). According to Burden and Langille (1991), the lower part of the *Gemmatriletes clavatus–Cicatricosisporites potomacensis* Zone, from the lower part of the Quqaluit Formation, contains a low-diversity palynological assemblage of long-ranging spores and gymnosperm pollen suggesting an age of late Neocomian and Aptian. Strata in the upper part of the *Gemmatriletes clavatus–Cicatricosisporites potomacensis* Zone, in the upper part of the Quqaluit Formation, have a diverse assemblage of spores and pollen, indicating a late Albian to Cenomanian age. In the overlying Cape Searle Formation, Burden and Langille (1991) identified an appreciably younger early to middle Paleocene palynological assemblage (*Trivestibulopollenites betuloides–Pesavis parva* Zone), thus implying that a significant disconformity exists within the succession.

For the sedimentary units in the Cape Dyer region, the lithostratigraphic and biostratigraphic interpretations of Burden and Langille (1990, 1991) form a reasonable framework, with good correlation to units sampled from the nearby offshore, and their interpretation of a dominantly nonmarine setting with some shallow-marine intervals agrees with multiple other studies (*see* Dafoe, Dickie, and Williams, this volume). The overlying Cape Dyer volcanic rocks studied by Clarke and Upton (1971) can be better described as submarine breccia units and likely subaerial flows, based on more recent understanding of their formation (*see* Dafoe, DesRoches, and Williams, this volume).

In the offshore Davis Strait and northern Labrador Sea region, Fenton and Pardon (2007) undertook a comprehensive review of the litho- and biostratigraphy of strata preserved in a number of wells, both in central Davis Strait and along both margins of the seaway. This work also examined onshore exposures in the Cape Dyer area discussed above, particularly those on the islands of Qaqulluit, Paallavvik, and Aggijjat (Fig. 3). The biostratigraphic age data presented by Fenton and Pardon (2007) for these onshore successions are in reasonable agreement with those of Burden and Langille (1990, 1991), although Fenton and Pardon (2007) preferred a general Paleocene age, either early or late, for the Cape Searle Formation, and were able to constrain the age of the lower, white sandstone succession of the Quqaluit Formation as generally Aptian–Albian, in contrast to Burden and Langille (1991), who suggested a late Neocomian to Aptian age for the unit.

SCOTT INLET LOWLAND

Oil slicks were first noted off Scott Inlet and in Buchan Gulf, northeast Baffin Island, in the mid-1970s (Loncarevic and Falconer, 1977; Levy, 1978; Levy and Ehrhardt, 1981), and these observations spurred interest in associated onshore sedimentary outcrops as a possible source of the slicks. A belt of clastic deposits is preserved both on the southeastern side of Scott Inlet at Cape Come Again (informally called 'Cape Smith' by Miller et al., 1977 and 'Smith Point' by others), and also for about 25 km to the northwest of the inlet in an area referred to herein as the Scott Inlet lowland (Fig. 6).

Lithostratigraphy

Exposures of sedimentary clastic strata in the Scott Inlet lowland (Fig. 7) are associated closely with widespread Quaternary glacial features, and whether older strata are present has never been confirmed. Jackson et al. (1979) mapped poorly consolidated quartzose clastic strata in the Scott Inlet lowland region from aerial reconnaissance and assigned them a (?)Cretaceous–(?)Paleogene age, presumably based on their lithological similarity with strata of that age exposed several hundred kilometres to the northwest on Bylot Island and adjacent areas of northern Baffin Island. Jackson et al. (1979) were possibly unaware that Miller et al. (1977) had previously dated mollusk shells from 'Cape Smith' at about 45 200 BP (^{14}C and amino acid racemization dating). Subsequent compilation-scale mapping of sedimentary deposits in the Scott Inlet lowland by Scott and de Kemp (1998) assigned stream-cut exposures interpreted to sit beneath overlying Quaternary deposits to the "Cretaceous to Tertiary Eclipse Group."

Table 1. Palynological zones and important taxa for onshore Cretaceous–Paleocene strata of the Cape Dyer region, western Baffin Bay.

Early and Middle Paleocene	***Trivestibulopollenites betuloides–Pesavis parva* Zone**
	Carpinipites ancipites
	Paraalnipollenites alterniporus
	Pesavis parva
	Polyvestibulopollenites verus
	Quercoidites microhenrica
	Rhoipites crassus
	Triatriopollenites granilabratus
	Tricolpites hians
	Tricolporopollenites cingulum
	Trivestibulopollenites betuloides
	***Gemmatriletes clavatus–Cicatricosisporites potomacensis* Zone**
Late Albian to Cenomanian	Upper part of zone
	Appendicisporites matesovae
	Camarozonotriletes ambigens
	Cicatricosisporites crassiterminatus
	Foveogleicheniidites confossus
	Foveotricolpites sphaeroides
	Retitricolpites sp.
	Rousea sp. cf. *R. georgensis*
	Tappanispora sp. cf. *Tigrisporites verrucatus*
	Tricolpites sagax
Late Neocomian and Aptian	Lower part of zone
	Low diversity assemblage of spores and pollen

After Burden and Langille (1990).

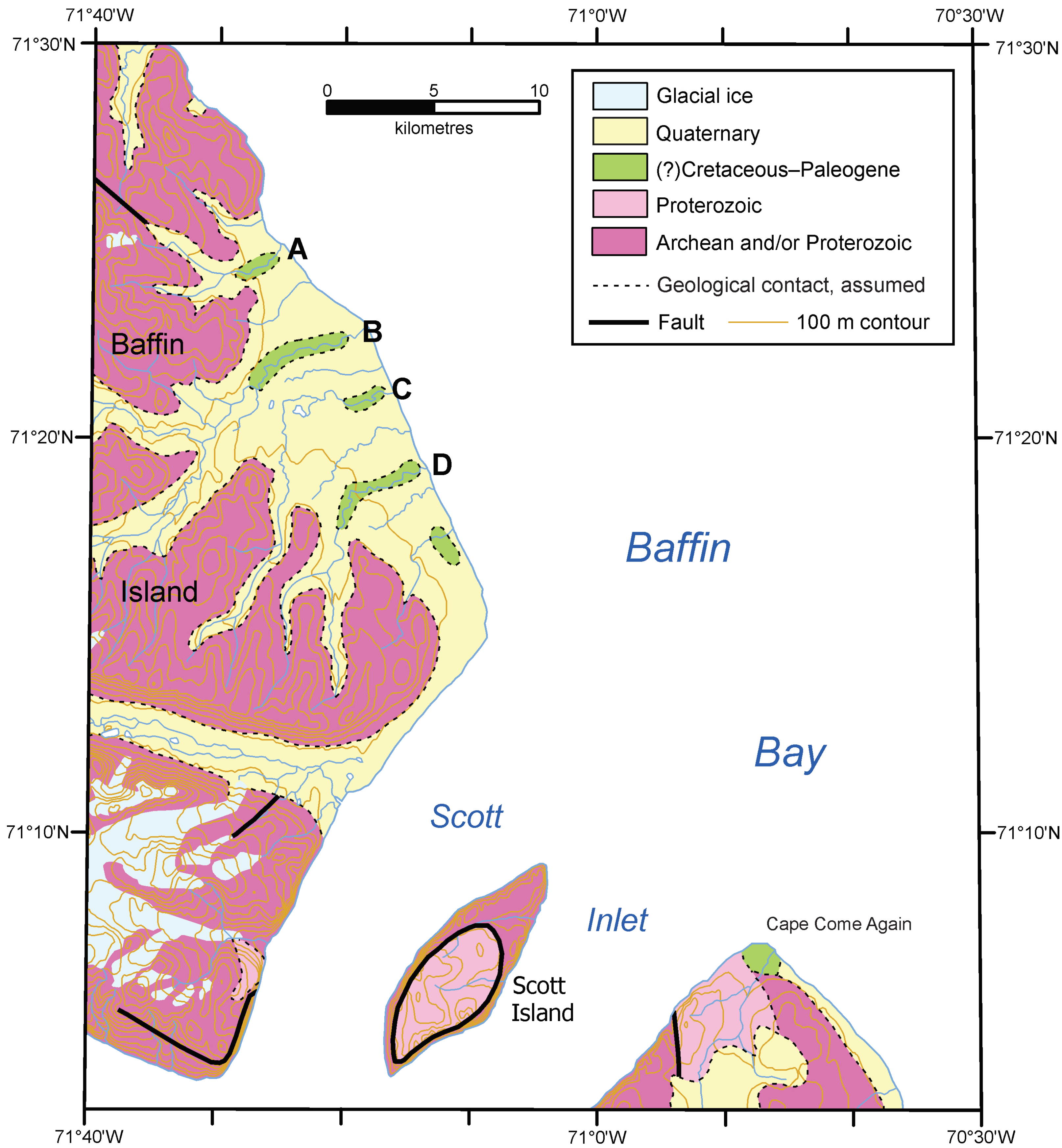

Figure 6. Generalized geological map of the Scott Inlet lowland area (inset B of Fig. 1), Baffin Island, northeast Nunavut (inset B of Fig. 1). *Modified from* Jackson et al. (1979) and Newman (1987). Letters A–D show locations of stratigraphic sections of Newman (1987).

Biostratigraphy, age, and depositional environments

Holloway (1984) examined two samples of feldspathic sand and peat units exposed along streams from the Scott Inlet lowland and identified marine dinocysts in one of them, which was assigned a late Albian–middle Cenomanian age. Burden and Holloway (1985) and Newman (1987) subsequently re-examined these samples, as well as others collected in the area, and recognized mid- to Late Cretaceous marine dinocysts, as well as a diverse assemblage of nonmarine Quaternary diatoms. They therefore suggested a Quaternary origin, but with reworked detritus derived from Cretaceous strata, possibly originating from shallow offshore sources exposed due to postglacial rebound. Based on this work, Jackson (2000) correlated the outcrop at 'Smith Point' (i.e. Cape Come Again), on the southeastern side of Scott Inlet, with the Pleistocene Clyde Foreland Formation of Feyling-Hanssen (1976), and also accepted the Quaternary interpretation of Burden and Holloway (1985) and Newman (1987) for the strata exposed northwest of Scott Inlet, suggesting these rocks may also be correlative with the Clyde Foreland Formation.

The available evidence suggests that the limited exposures of clastic strata found in the Scott Inlet lowland area, at the southeast point of the inlet and to its northwest, are of Quaternary age, but possibly sourced in part from pre-existing Cretaceous strata, and best correlated with the Clyde Foreland Formation; however, E.T. Burden, one of the present authors, has visited the area and noted that the published surveys analyzed onshore exposures restricted to within a few kilometres of the shoreline (e.g. Fig. 7a), leaving open the possibility that older strata may be present farther inland.

Rimrock Lake Inlier

Andrews et al. (1972) described a very restricted exposure of carbonate strata that they called the "Rimrock Bed" (Rimrock Lake), found at relatively high elevation (about 730 m a.s.l.) approximately 150 km west of Scott Inlet and north of the Barnes Ice Cap (*see* location in Fig. 1), and assigned it a Paleogene age based on palynomorphs. Jackson and Morgan (1978) correlated this limited exposure with Paleogene strata of the Eclipse Group preserved farther to the north; however, Refsnider et al. (2012), using uranium-series dating, subsequently demonstrated that these strata are actually late Quaternary subglacial carbonate deposits. More recent geological mapping in this area has only recognized Archean rocks with Quaternary cover (Skipton et al., 2020).

BYLOT ISLAND REGION

Structural setting

The mountainous part of Bylot Island was referred to as the "Byam Martin High" by Kerr (1980) and subdivided into the Liverpool and Central Bylot structural highs by Harrison et al. (2011). These highs

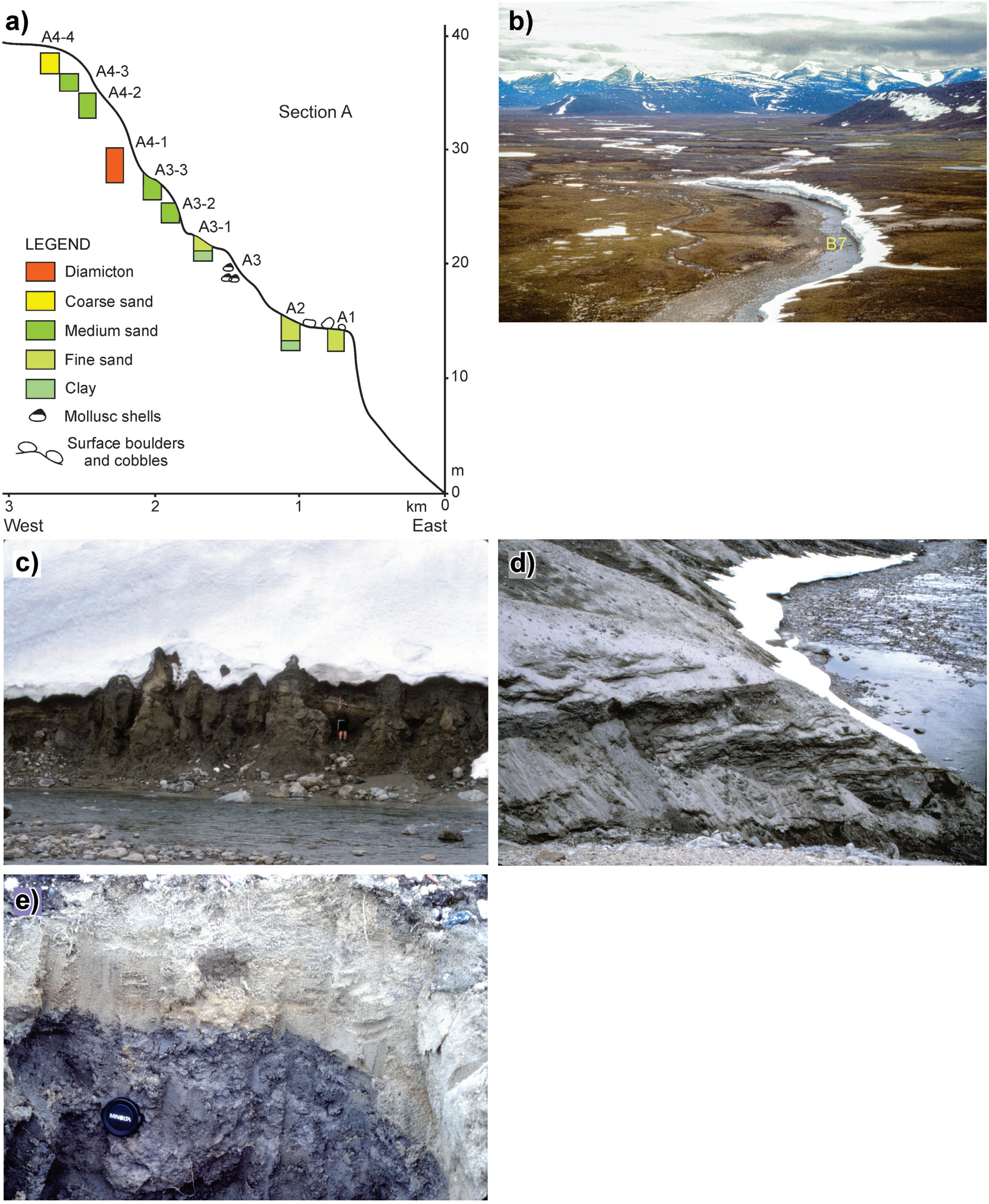

Figure 7. Stratigraphic section and photographs showing exposures of possible (?)Cretaceous–Quaternary strata in the Scott Inlet lowland area (inset B of Fig. 1), Baffin Island. *See* Figure 6 for section locations. **a)** Stratigraphic section A of Newman (1987), showing thicknesses of exposures along river bank plotted against distance from shoreline. Note general coarsening-upward trend. **b)** View of the valley of stratigraphic section B of Newman (1987), showing general terrain of the lowland. Station B7 of Newman (1987) is located beneath snowbank on north (right) side of river. Riverbank snow drifts in foreground are approximately 2.5 m tall. NRCan photo 2021-203. **c)** Station B7 of Newman (1987), showing horizontally stratified, poorly consolidated sand and mud, overlain by glacial silt and mud layers beneath snowbank. Person with stick is 1.7 m tall. NRCan photo 2021-204. **d)** Station B8 of Newman (1987), showing horizontal, cross-stratified and poorly consolidated sand and mud, locally with cobble conglomerate, overlain by buff glacial sand; bluff is approximate 15 m high from river to glacial sand. NRCan photo 2021-205. **e)** Station A3-1 of Newman (1987), showing excavated face of mud overlain by quartz-rich planar cross-stratified sand. Lens cap for scale is 6.5 cm across. NRCan photo 2021-206. All photographs by E.T. Burden.

separate exposures of Cretaceous to Paleocene strata in the Bylot Island area into two distinct regions first described by Jackson et al. (1975): Eclipse Trough (Fig. 8, 9) and North Bylot Trough (Fig. 10). Eclipse Trough is the more southerly region and is preserved on northeastern Baffin Island (Fig. 8), the southwest side of Bylot Island (Fig. 9), and possibly some areas beneath the Tasiujaq (Eclipse Sound)–Navy Board Inlet waterway. On Bylot Island, the Eclipse Trough is bounded to the east by the Aktineq Fault Zone (Jackson and Davidson, 1975b), but farther south the location of this fault is not clear (Fig. 9). Miall et al. (1980) and Jackson (2000) showed it continuing to the south-southeast under Tasiujaq and onto northern Baffin Island, whereas McWhae (1981) showed it continuing to the east-southeast beneath Tasiujaq. Vertical displacement of uplifted basement blocks along the Aktineq Fault Zone and associated fault zones is inferred to be "on the order of several thousand feet" (about 600–1200 m; Clarke, 1976).

Tasiujaq bisects the onshore exposures of the Eclipse Trough, leaving an outlier preserved along Salmon River and adjacent areas east and southwest of Pond Inlet (Fig. 8). These exposures and others nearby along the coast of Baffin Island or just inland, constitute the Salmon River region of the Eclipse Trough.

Bedding surfaces in Cretaceous to Paleocene strata in the Eclipse Trough generally dip shallowly toward the southwest and become steeper near the Aktineq Fault Zone. Along the south coast of Bylot Island near the fault zone, they become more southerly dipping. Broad, open upright folds have been mapped south of Twosnout creek (informal name) and northeast of Canada Point (Fig. 9; Jackson and Davidson, 1975b).

Farther north, the North Bylot Trough region includes Cretaceous–Paleocene strata found on the north coast of Bylot Island between the Archean to Paleoproterozoic gneiss units, which form the Liverpool and Central Bylot topographic highs (Harrison et al., 2011) (Fig. 10). The North Bylot Trough is bounded to the southwest by the Cape Hay Fault Zone, locally up to 1 km wide, and by an unnamed fault to the east that parallels a ca. 720 Ma Franklinian dyke (Jackson and Davidson, 1975b). Both of these structures have been interpreted to extend northwestward into Lancaster Sound, where they are recognized on marine seismic lines (McWhae, 1981; Harrison et al., 2006; Brent et al., 2013). Adjacent to these faults in the North Bylot Trough, Cretaceous–Paleocene strata are strongly deformed and locally steeply dipping (Benham, 1991); elsewhere in the trough, Cretaceous–Paleocene strata are gently warped and form a north-south-oriented, open anticline-syncline pair (Benham and Burden, 1990).

Lithostratigraphy and biostratigraphy of the Eclipse and North Bylot troughs

The initial interest in the Eclipse Trough sedimentary deposits stemmed from the identification of the coal deposits exposed near Pond Inlet, a stopping point for Arctic exploration vessels. These coal units, particularly well developed in the vicinity of Salmon River, were of interest as a fuel source. Indeed, Bernier (1939, p. 362) reported that "a seam of coal was found during the [1910 *Arctic*] trip and a bag taken for testing was found to be excellent for cooking purposes"; however, more specific assessments of the coals in the Salmon River area were undertaken by different workers over many years (e.g. J.D. Craig, unpub. GSC report, 1923; Mohr, 1925; B.R. MacKay, unpub. GSC report, 1925; Weeks, 1927; Research Council of Alberta, 1940; Swartzman, 1947a, b; W.L. Davison, unpub. GSC report, 1955) and concluded that the coals are of limited extent and insufficient to provide a regular power source.

Continued interest in the nature of the coal deposits and their depositional framework, as well as broader issues of hydrocarbon resource potential in the region, led to subsequent research programs of the Geological Survey of Canada (GSC) in the 1960s and 1970s, followed by an extended research program undertaken by Memorial University of Newfoundland (MUN). Each of the focused programs in the latter part of the twentieth century contributed uniquely to the lithostratigraphic understanding of the successions preserved within the Eclipse and North Bylot troughs. The most comprehensive mapping of Cretaceous–Paleogene strata was by Miall et al. (1980) for the Eclipse Trough, and by Benham (1991) for the North Bylot Trough, and their maps are shown in Figures 9 and 10, respectively. With regard to the lithostratigraphy, the MUN researchers undertook more detailed, albeit not regionally comprehensive studies; their interpretations are included in Figure 2.

Interestingly, few molluscan or other invertebrate fossil remains have been described from the Upper Cretaceous–Paleocene succession preserved on Baffin Island and adjacent Bylot Island, in contrast to the rich assemblages that have been described from coeval strata of the Nuussuaq Basin preserved onshore West Greenland (Ravn, 1918; Rosenkrantz et al., 1942; Birkelund, 1965; Kollmann and Peel, 1983). Consequently, biostratigraphic subdivision and correlation of Cretaceous–Paleocene onshore strata along the western Baffin Bay margin has relied primarily on palynology, principally dinocysts, pollen, and spores, with associated rare molluscs (e.g. Haggart et al., 2017). As noted by Miall et al. (1980), the recovery and preservation of palynoflora in these rocks is often poor, and reworking of

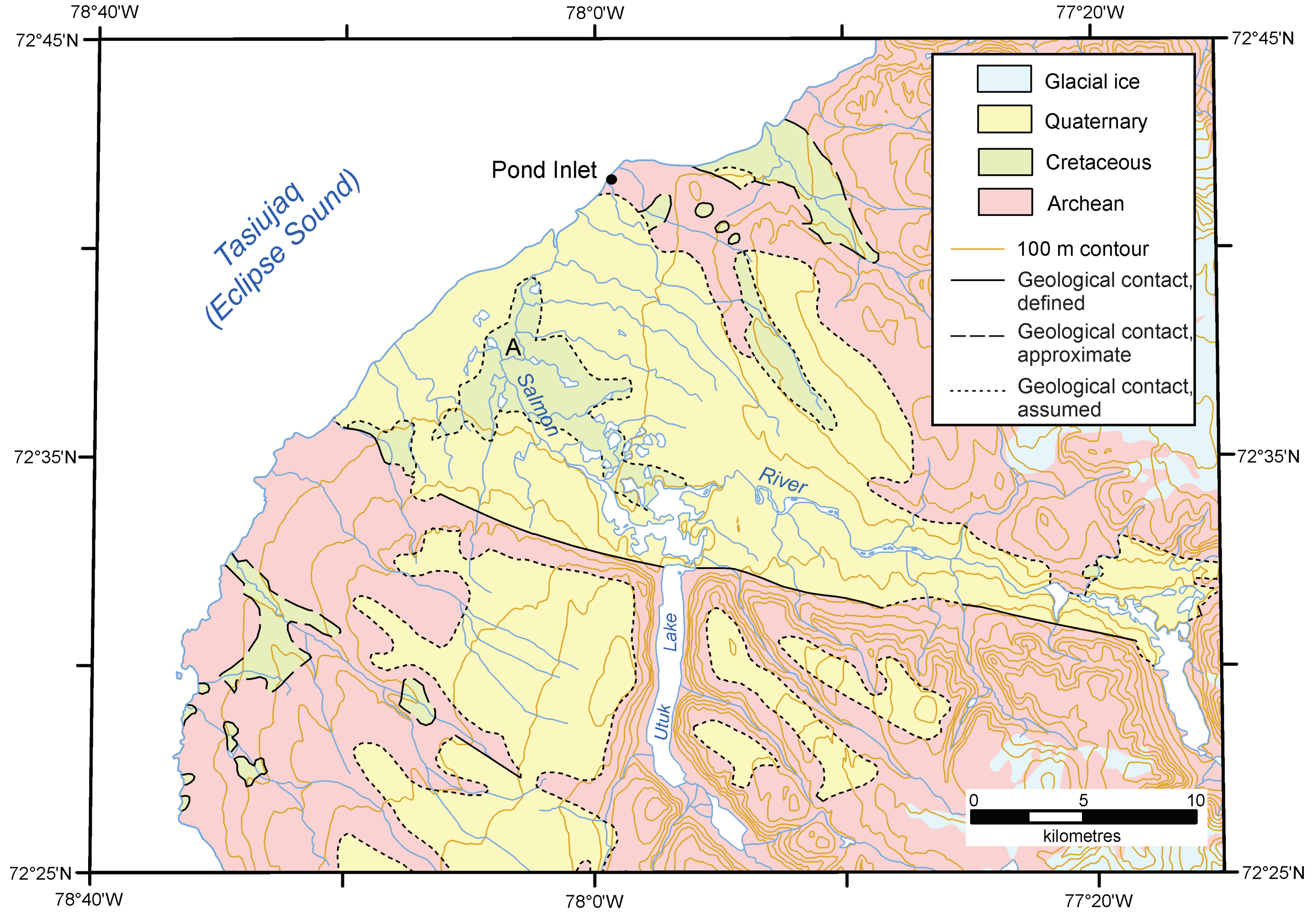

Figure 8. Generalized distribution of Cretaceous strata in the Salmon River area (inset C of Fig. 1; southern margin of the Eclipse Trough), northern Baffin Island (*after* Jackson et al. (1975) and Miall et al. (1980)). A shows location of Figure 13a.

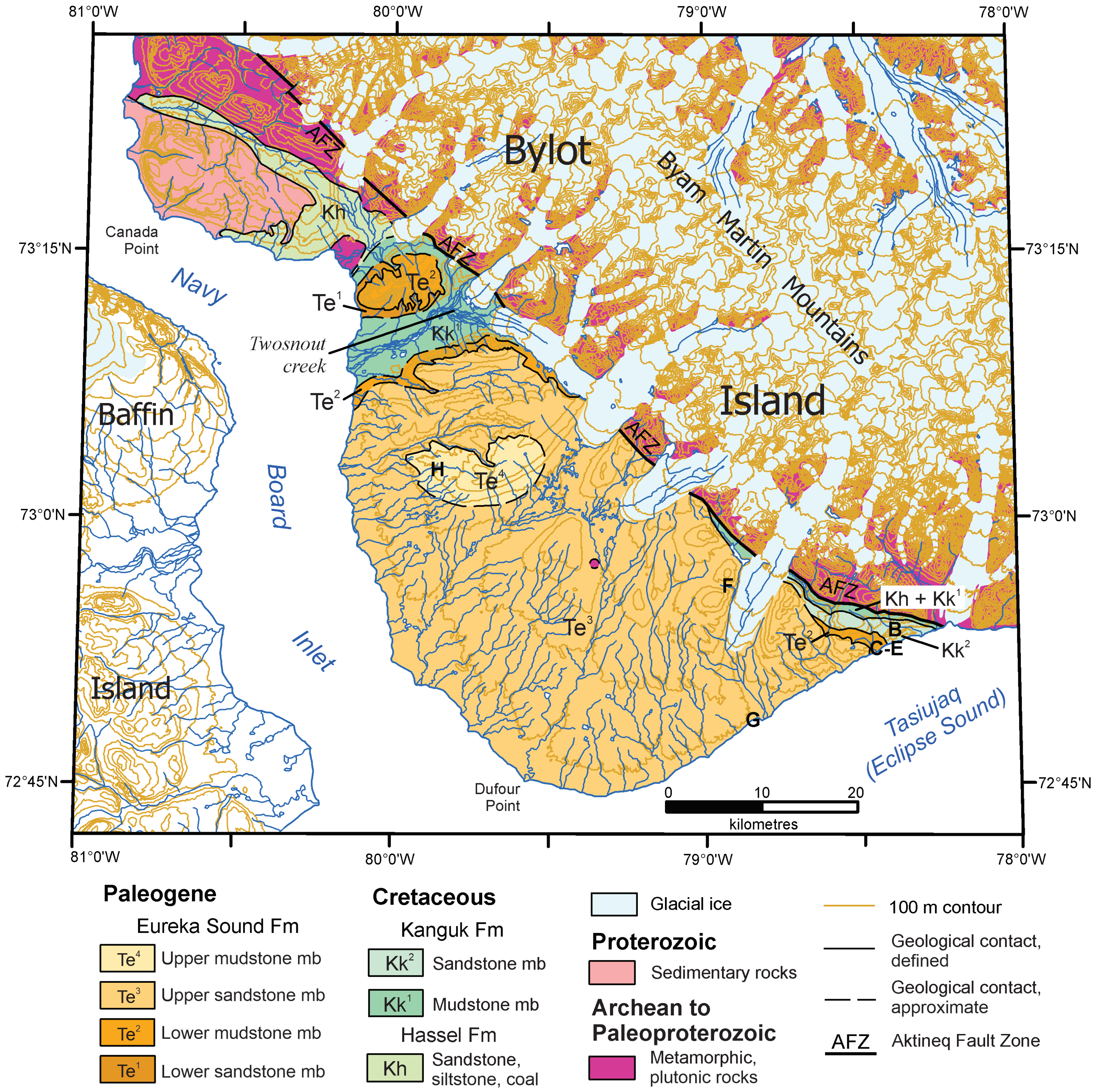

Figure 9. Generalized geological map of Cretaceous–Paleogene strata of southwestern Bylot Island (Eclipse Trough; inset D of Fig. 1), *after* Miall et al. (1980). Proterozoic and Archean geology simplified *after* Blackadar and Davison (1968), Jackson and Davidson (1975a, b), and Jackson et al. (1975). Letters B–H show locations of photographs shown in Figure 13.

palynomorphs into younger strata presents a considerable problem (Ioannides, 1986; Fenton and Pardon, 2007). Based on these palynological data, the stratigraphic succession preserved on Bylot Island provides an extended record of sedimentation beginning in the Early Cretaceous (Albian) and continuing into the Paleogene (Fig. 2).

1970s and 1980s Geological Survey of Canada research

During reconnaissance geological mapping of the northeastern Baffin Island region in the late 1960s, driven primarily by interest in mineral resource potential, Jackson and Davidson (1975a, b) and Jackson et al. (1975) briefly described the younger sedimentary succession preserved on southwestern Bylot Island and on Baffin Island in the area of Pond Inlet. They assigned these strata to the Eclipse Group, and designated the basin containing them as the Eclipse Trough (Fig. 9). These researchers recognized a variety of clastic rock types in the Eclipse Group, including mudstone, siltstone, and sandstone. Jackson and Davidson (1975a) and Jackson et al. (1975) subdivided the Cretaceous–Cenozoic section of the Eclipse Trough into four map units (Fig. 11), from oldest to youngest: unit K, consisting of quartzose sandstone; unit KT1, consisting of greywacke, mudstone, and siltstone; unit KT2, consisting of arkosic sandstone; and unit T, consisting of shale and mudstone. In the two papers, the Eclipse Group was regarded as Early Cretaceous to Eocene, based on preliminary biostratigraphic analysis of microfossils, primarily the palynological studies of W.S. Hopkins (W.S. Hopkins, unpub. GSC Paleontological Reports K-2 WSH 1969, 1969; K-6 WSH 1969, 1969; K-20-WSH-1972, 1972; T-02-WSH-1973, 1973; K-08-WSH-1977, 1977; K-01-WSH-1978, 1978; KT-23-WSH-1978, 1978; KT-25-WSH-1978, 1978). In particular, Hopkins (W.S. Hopkins, unpub. GSC Paleontological Report K-08-WSH-1977, 1977) established an Early Cretaceous age and provided a summary of the palynological age for the coal units of the Salmon River outlier of the southern Eclipse Trough.

Beginning in the 1970s, detailed regional studies of the Upper Cretaceous–Cenozoic successions of the Canadian Arctic Islands were undertaken by various parties to better understand the stratigraphic setting, regional extent, and resource potential of the rocks. As part of this effort, Miall et al. (1980) reassessed the Cretaceous–Cenozoic succession preserved in the Eclipse Trough and produced a schematic geological map and expanded stratigraphic framework for the strata (Fig. 9, 11, 12). The study focused on the south coast and Twosnout creek areas of southwest Bylot Island, but also included other localities; photographs of the strata are shown in Figure 13. Miall et al. (1980) identified a quartz-rich sandstone at the base of the succession (their map unit Kh) (Fig. 10, 11, 14), which they interpreted as resting unconformably on Precambrian rocks. They correlated this unit, which ranges from 15 to 120 m in thickness locally, with the Hassel Formation of the Sverdrup Basin to the north and west, and considered Jackson and Davidson's (1975a, b) and Jackson et al.'s (1975) unit K to be equivalent to their Hassel Formation. Palynological analysis (using pollen and spores only) of the Hassel Formation in the Eclipse Trough, particularly in the Salmon River outlier (W.S. Hopkins, unpub. GSC Paleontological Report K-08-WSH-1977, 1977), indicated an age of Albian to Cenomanian based on the presence of simple tricolpate pollen grains and spore taxa such as *Clavifera*, *Dictyophyllidites*, *Kuylisporites*, *Acanthotriletes*, *Foveosporites*, *Sestrosporites*, *Trilobosporites*, and *Appendicisporites*, and is consistent with the age of the Hassel Formation in the Sverdrup Basin (Miall et al., 1980). As described by Miall et al. (1980), the Hassel Formation consists predominantly of

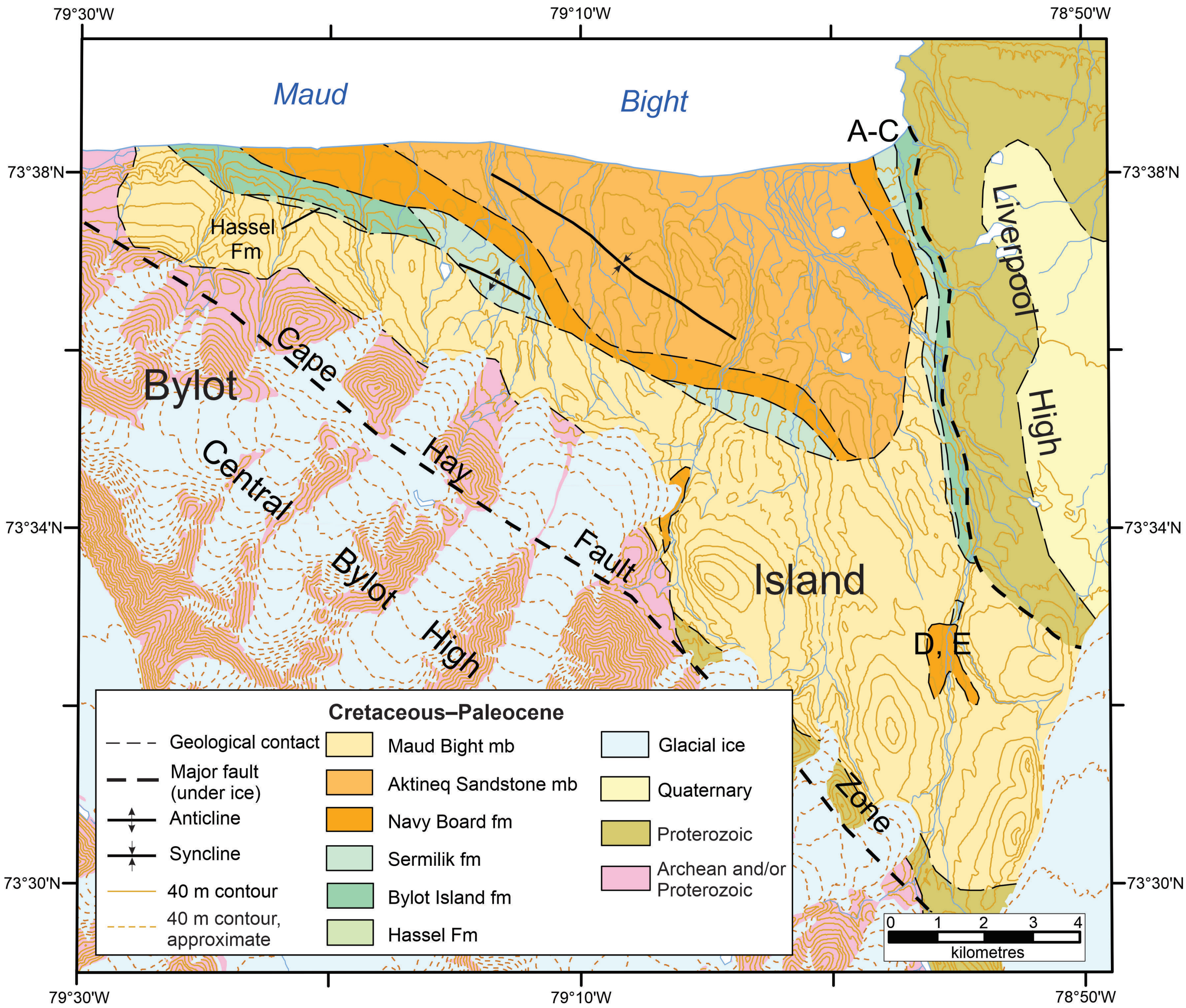

Figure 10. Generalized geological map of Maud Bight area, north Bylot Island (North Bylot Trough; inset E of Fig. 1), *modified from* Jackson and Davidson (1975a, b); Cretaceous–Paleogene geology *after* Benham and Burden (1990) and Benham (1991). Letters A–E show locations of photographs in Figure 17.

fine- to very coarse-grained quartzose sandstone, locally with pebble lenses containing clasts of quartz, metamorphic rocks, and rare sandstone ranging up to 6 cm in diameter. Coal is present locally in the formation, such as at Salmon River, as is siltstone and mudstone, and these previous authors regarded the formation as of nonmarine origin.

Miall et al. (1980) considered the Hassel Formation in the Eclipse Trough to be overlain unconformably by a widespread unit of basal mudstone (their map unit Kk^1) up to 600 m thick and an overlying and laterally interfingering sandstone (their map unit Kk^2), both of which they assigned to the Kanguk Formation (Kk). They regarded the Kanguk Formation to be the equivalent of unit KT1 of Jackson and Davidson (1975a, b) and Jackson et al. (1975). Miall et al. (1980) reported the mudstone member of the Kanguk to consist predominantly of soft grey mudstone, locally glauconitic, with fish scales and sideritic concretions. Based on the presence of silicoflagellates, radiolarians, and dinocysts, with rare foraminifera and terrestrial palynomorphs, Miall et al. (1980) dated the age of the mudstone member of the Kanguk Formation as Campanian to Maastrichtian.

In contrast to the Kk^1 mudstone unit, Miall et al. (1980) noted that the sandstone member of the Kanguk Formation is restricted to the south coast region of Bylot Island, where it overlies the mudstone member and attains a maximum thickness of 540 m. The sandstone member consists of white to light brown, medium- to coarse-grained friable sandstone, mostly massive, but with rare low-angle, planar cross-stratification. Pebble lenses and rare boulders, mostly of foliated metamorphic rocks, are noted, but also present are quartzose sandstone and intraformational mud clasts. According to Miall et al. (1980), the member contains root beds, carbonate-cemented

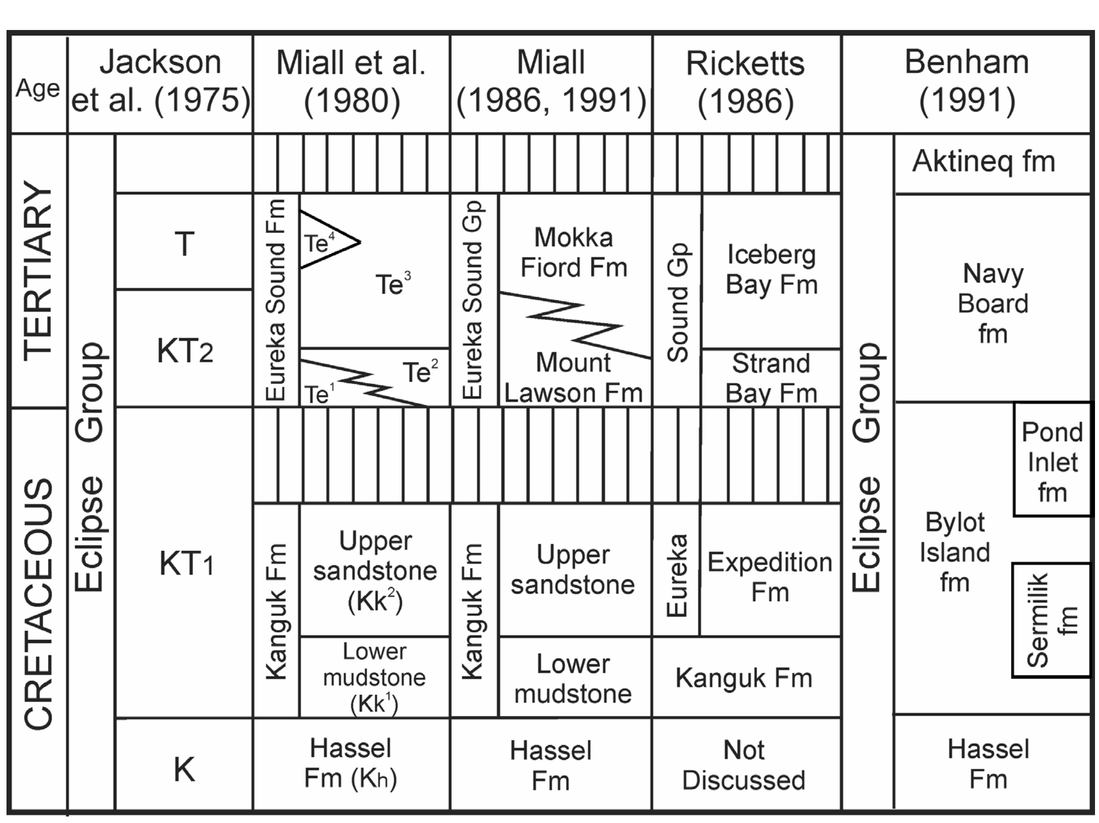

Figure 11. Summary of evolving stratigraphic framework and correlations for Cretaceous–Paleogene strata of the Eclipse Trough by Jackson et al. (1975), Miall et al. (1980), Miall (1986, 1991), Ricketts (1986), and Benham (1991). Proposals of Miall (1986) and Ricketts (1986) based on correlations with Eureka Sound Group strata of Sverdrup Basin.

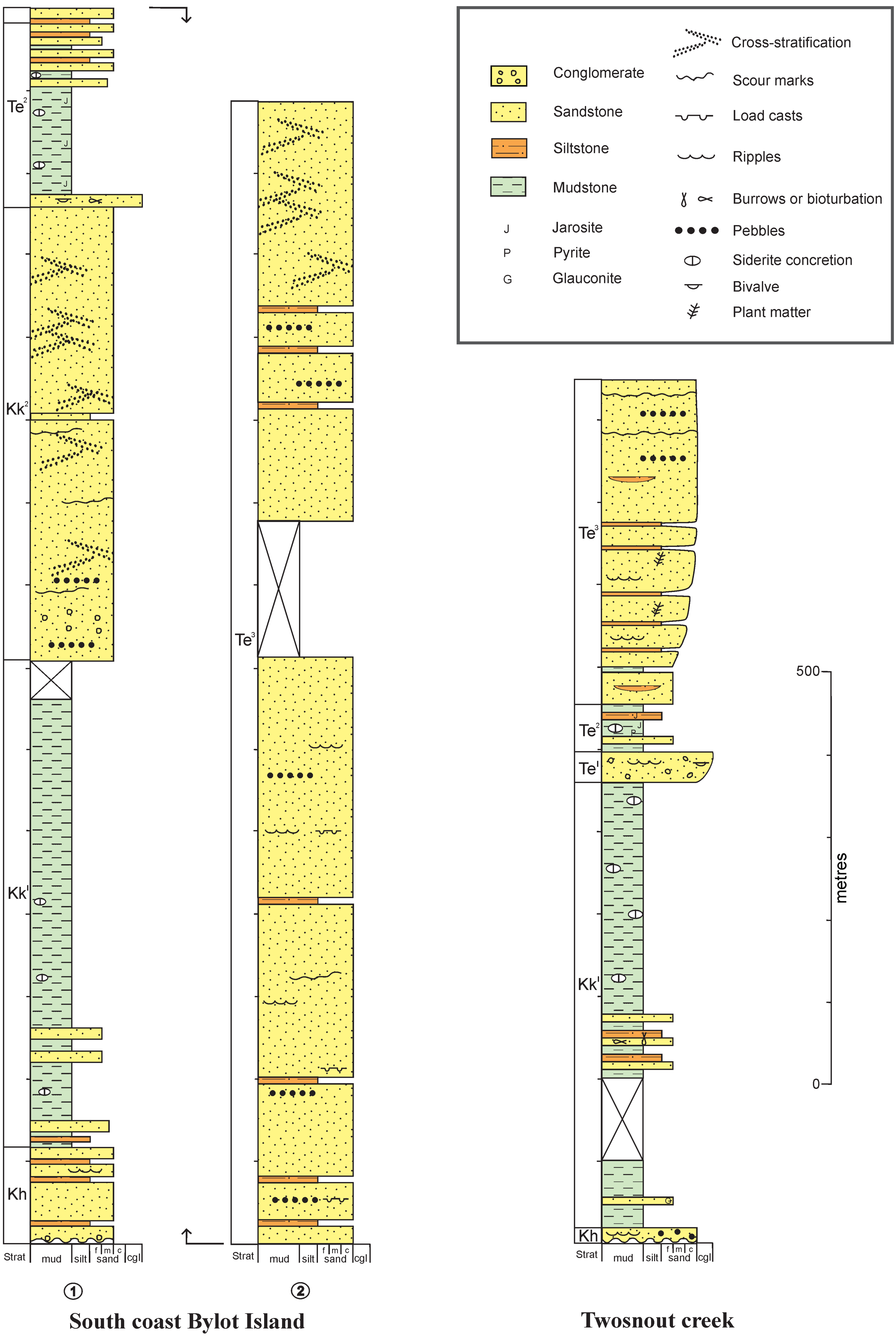

Figure 12. Schematic stratigraphic columns of Cretaceous–Paleogene strata in the Eclipse Trough, preserved along the south coast of Bylot Island and at Twosnout creek (inset D of Fig. 1), with stratigraphic nomenclature of Miall et al. (1980). *Modified from* Miall et al. (1980). c = coarse; cgl = conglomerate; f = fine; m = medium; Strat = stratigraphic unit.

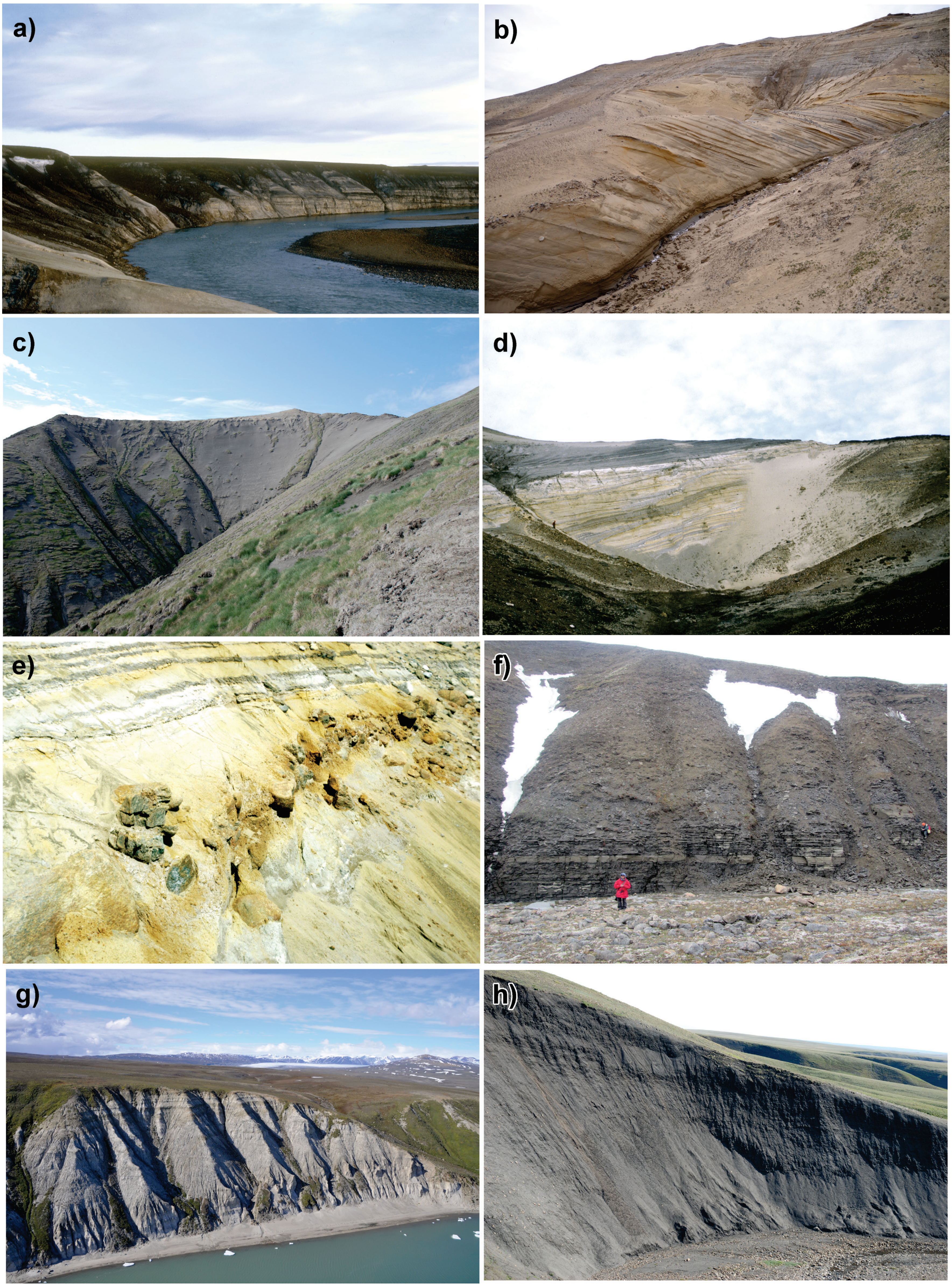

Figure 13. Photographs showing examples of Cretaceous–Paleocene strata preserved in the Eclipse Trough region of southwestern Bylot Island–northeastern Baffin Island region (insets C and D of Fig. 1). *See* Figure 7 for location of photograph 13a, Figure 9 for photographs 13b–13h. **a)** Salmon River exposures of Hassel Formation. NRCan photo 2021-207. Photograph by E.T. Burden. **b)** Low-angle planar-cross-stratified sandstone units of Sermilik formation, southwest coast Bylot Island; exposure is approximately 125 m thick. NRCan photo 2021-210. Photograph by J.W. Haggart. **c)** Mudstone units of Bylot Island formation, southwest coast Bylot Island; approximately 80 m of gently dipping strata are shown. NRCan photo 2021-211. Photograph by J.W. Haggart. **d)** Large-scale cross-stratified sandstone and siltstone of Pond Inlet formation, southwest coast Bylot Island; person for scale. NRCan photo 2021-208. Photograph by E.T. Burden. **e)** Angular boulders within sandstone of lower part of Pond Inlet formation, southwest coast of Bylot Island; foreground fractured boulder approximately 0.80 m in maximum dimension. NRCan photo 2021-209. Photograph by E.T. Burden. **f)** Interstratified sandstone and mudstone of Navy Board formation, Aktineq Glacier area of southwest Bylot Island. Person is 1.8 m tall. NRCan photo 2021-212. Photograph by J.W. Haggart. **g)** Flat-lying sandstone beds of Aktineq formation, southwest coast of Bylot Island; exposure is approximately 110 m thick. NRCan photo 2021-213. Photograph by J.W. Haggart. **h)** Flat-lying mudstone of Te^4 unit of Miall et al. (1980), southwest coast region of Bylot Island; exposure is approximately 40 m thick. NRCan photo 2021-214. Photograph by J.W. Haggart. Stratigraphic nomenclature for photographs 13b–13g *after* Sparkes (1989) and Waterfield (1989).

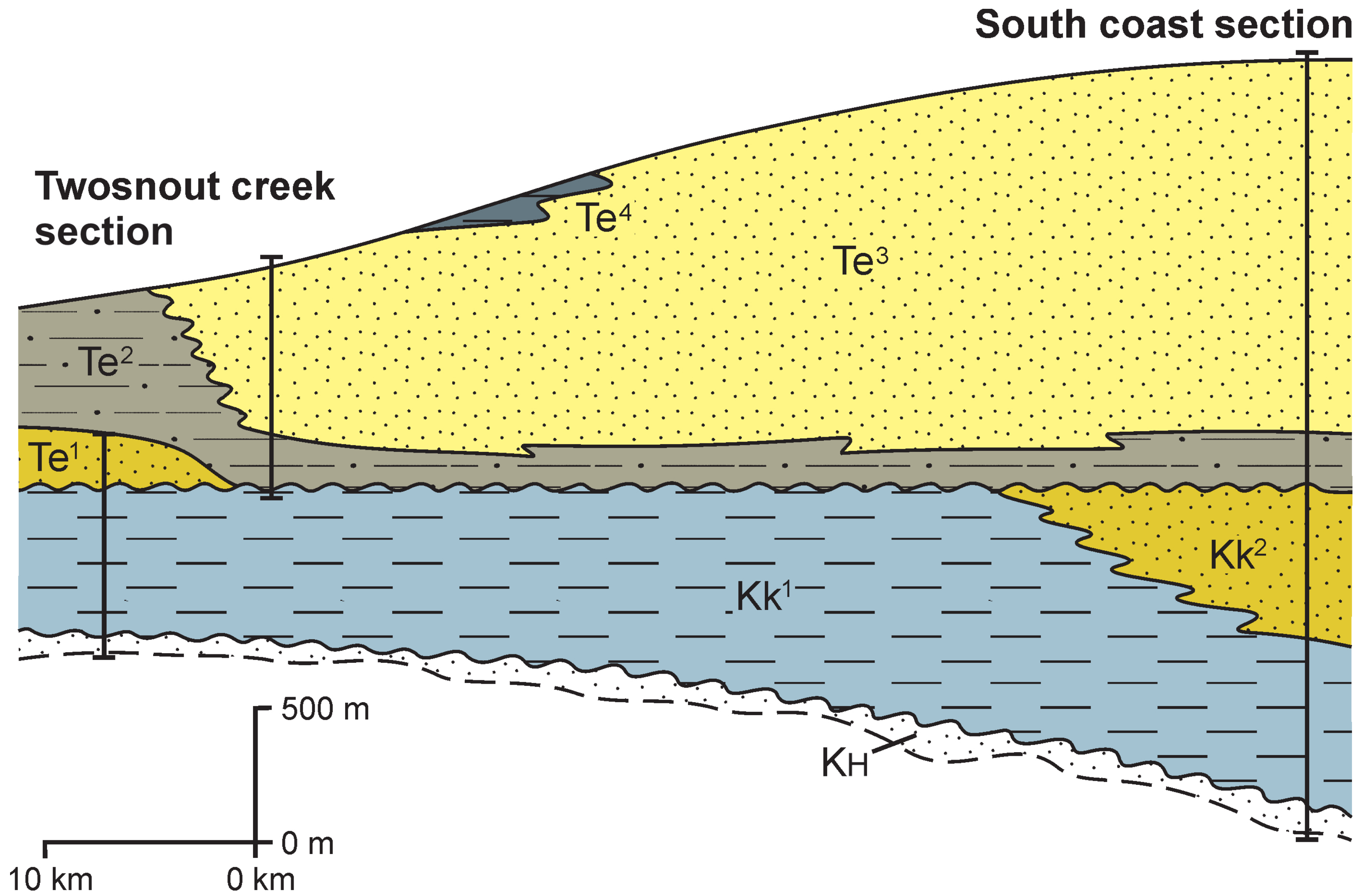

Figure 14. Schematic representation of intertonguing of Cretaceous and Paleogene coarse clastic strata preserved in southern part of the Eclipse Trough with finer grained, more offshore deposits to the northwest. *Modified from* Miall et al. (1980). Note distinct unconformities interpreted in the succession at the base of unit Kk1, spanning the Cenomanian–early Campanian, and at the base of units Te1 and Te2, spanning the latest Cretaceous–earliest Paleogene. Vertical lines correspond to schematic stratigraphic columns shown in Figure 12.

sandstone, and bivalve shell fragments that would seem to indicate a fluvial to shallow-marine, possibly deltaic setting. Miall et al. (1980) did not provide biostratigraphic data, but considered the member to be of probable Maastrichtian age based on stratigraphic relationships. They also noted the lithological similarity of their sandstone member of the Kanguk Formation with the basal Eureka Sound Formation of the Sverdrup Basin, although they considered them to be distinct units, as the sandstone and mudstone members of the Kanguk Formation in Eclipse Trough appeared to be intertonguing. Moreover, this conclusion was supported by the presence of an inferred unconformity developed on Bylot Island between the Kanguk Formation and the overlying Eureka Sound Formation (Miall et al., 1980).

Following Miall et al.'s (1980) work, Ioannides (1986) undertook a comprehensive study of diverse dinocyst assemblages from Upper Cretaceous and lower Cenozoic strata from the south coast and Twosnout creek regions of Bylot Island. In the south coast section, Ioannides recognized four intervals — I, II, III, and IV — the first three being Late Cretaceous, and IV being early Cenozoic (Table 2). In the Twosnout creek section, he outlined three similarly aged intervals, designated as Ia, IIIa, and IVa. Interval I in the south coast section was found in strata of the Kanguk Formation and was assigned a Santonian to Campanian age; it contains a rich and diverse assemblage of dinocysts, with sparse spores and pollen. Ioannides (1986) correlated the interval Ia of the Twosnout creek section with interval I of the south coast section, based on the general dinocyst similarity and several species common to both intervals. He considered interval Ia to also be of Santonian to probably early Campanian age.

Miall et al. (1980) assigned strata overlying the Kanguk Formation in the Eclipse Trough to the Eureka Sound Formation, using nomenclature characteristic at the time for Maastrichtian–Eocene strata of the Sverdrup Basin. Within the Eclipse Trough, Miall et al. (1980) recognized four local members within the Eureka Sound Formation, a lower sandstone member (Te1), a lower mudstone member (Te2), an upper sandstone member (Te3), and an upper mudstone member (Te4), in ascending stratigraphic order (Fig. 11, 14). Miall et al. (1980) could not readily assign Jackson and Davidson's (1975a, b) and Jackson et al.'s (1975) KT1, KT2, and T lithostratigraphic units directly to their members of the Eureka Sound Formation. As noted by Miall et al. (1980), their Eureka Sound Formation members are variable in thickness and not distributed everywhere across the basin, suggesting that the formation rests unconformably, possibly with angular unconformity, on the Kanguk Formation.

Miall et al.'s (1980) lower sandstone member (Te1) of the Eureka Sound Formation consists of mostly massive, white quartzose and locally glauconitic, fine- to very coarse-grained sandstone with bivalve shell fragments; 1 cm diameter pebbles of metamorphic rock fragments are present, as are shale rip-up clasts up to 50 cm long. Locally in the member, they noted horizontal grazing traces, interference ripples, contorted laminations, scour surfaces exhibiting up to 2 m of relief, and dish structures. The lower mudstone member (Te2) of Miall et al.'s (1980) Eureka Sound Formation in the Eclipse Trough consists of dark grey, silty mudstone with sideritic concretions and thin lenses of weakly calcareous-cemented, fine- to medium-grained sandstone exhibiting ripple marks, groove casts and load structures, and root and leaf impressions. The sandstone lenses tend to become thicker and more common upsection, reflecting transition into the overlying upper sandstone member of the formation. According to Miall et al. (1980), the upper sandstone member (Te3) of their Eureka Sound Formation consists of massive white to orange to brown, very fine-grained to pebbly sandstone, locally with silty and muddy interbeds; they noted silty mudstone intraclasts up to 1 m in length locally in the member, as well as liquefaction features and dish structures. Finally, Miall et al.'s (1980) youngest stratigraphic unit, the upper mudstone member (Te4), was reported to consist of dark grey, carbonaceous mudstone with rare lenses of concretionary fine-grained sandstone that conformably overlies the Te3 member.

Miall et al. (1980) considered the overall age of the Eureka Sound Formation of the Eclipse Trough as probably Paleocene, and likely extending up to the early or middle Eocene for their Te4 unit, based on pollen and spores, as well as dinocysts. These included locally abundant angiosperm pollen, such as *Momipites*, cf. *Corylus*, cf. *Carpinus*, proto-*Carya*, *Pterocarya*, *Alnus*, *Paraalnipollenites*, cf. *Myrica, (?)Extratriporopollenites, Platycarya, Platycarya*, *Chenopodium*, and the fungal spore genus *Pesavis*. Based on the above, Miall et al. (1980) suggested the presence of significant unconformities within the Cretaceous–Paleogene succession of the Eclipse Trough (Fig. 14).

Dinocyst interval II of Ioannides (1986) corresponds with the basal part of Miall et al.'s (1980) Eureka Sound Formation along the south coast of Bylot Island, but dinocysts in the interval were exclusively reworked and it was thus not assigned an age. Interval III, also within strata of the Eureka Sound Formation, was assigned a Maastrichtian age based on the first (earliest) occurrences of *Cerodinium diebelii*, *Elytrocysta druggii*, *Palaeocystodinium golzowense*, *Spinidinium uncinatum*, and *Thalassiphora pelagica*, and the absence of a number of taxa associated with interval I. Ioannides (1986) regarded interval IIIa of the Twosnout creek section as equivalent to the upper part

Table 2. Dinoflagellate cyst intervals and characteristic taxa of onshore Cretaceous–Paleocene strata of the Eclipse Trough, Bylot Island.

Possibly Early Paleocene	**Interval IV**	**Interval IVa (Twosnout creek)**	Possibly Early Paleocene
	Cordosphaeridium spp.	*Areoligera* sp.	
	Glaphyrocysta ordinata	*Cerodinium diebelii*	
	Palaeoperidinium pyrophorum	*Cerodinium speciosum*	
	Thalassiphora pelagica	*Cordosphaeridium exilimurum*	
		Cordosphaeridium inodes	
		Glaphyrocysta sp.	
		Palaeoperidinium pyrophorum	
		Thalassiphora pelagica	
Maastrichtian	**Interval III**	**Interval IIIa (Twosnout creek)**	Maastrichtian
	Cerodinium diebelii	*Cerodinium diebelii*	
	Elytrocysta druggii	*Thalassiphora pelagica*	
	Palaeocystodinium golzowense		
	Spinidinium uncinatum		
	Thalassiphora pelagica		
No age assigned	**Interval II**		
	No in situ dinoflagellate cysts		
Santonian to Campanian	**Interval I (South coast)**	**Interval Ia (Twosnout creek)**	Santonian to early Campanian
	Canningia sp. 1	*Odontochitina operculata*	
	Chatangiella ditissima	*Xenascus ceratioides*	
	Chatangiella granulifera	*Xiphophoridium alatum*	
	Chatangiella madura		
	Chatangiella verrucosa		
	Chlamydophorella? *grossa*		
	Diconodinium granulifera		
	Isabelidinium acuminatum		
	Isabelidinium cooksoniae		
	Isabelidinium microarmum		
	Laciniadinium williamsii		
	Odontochitina sp.		
	Palaeohystrichophora infusorioides		
	Spinidinium sp.		
	Trithyrodinium sp.		
	Xenascus ceratioides		
	Dinoflagellate sp. A		

After Ioannides (1986).

The columns on the right are representative of the taxa and ages in the Twosnout creek area.

of interval III of the south coast section and, hence, Maastrichtian (Table 2). He based this conclusion on the presence of *Thalassiphora pelagica* in both intervals III and IIIa and a questionable record of *Cerodinium diebelii* in one Twosnout creek sample. Interval IV contained species of *Cordosphaeridium* and *Glaphyrocysta ordinata*, *Palaeoperidinium pyrophorum*, and *Thalassiphora pelagica*, but an absence of characteristic Late Cretaceous assemblages throughout interval IV led Ioannides (1986) to conclude that the age of the interval was possibly early Paleocene.

Using outcrop sedimentology, lithofacies analysis, and paleontological content, Miall et al. (1980) proposed that the Albian–Paleocene and/or Eocene succession of the Eclipse Trough was deposited in a variety of sedimentary environments. Basal strata of the Hassel Formation were considered to represent shallow-marine intertidal or beach environments to fluvial environments — most likely, sandy low- to high-sinuosity braided settings — as evidenced by the lack of marine fossils, extensive cross-stratification, and common coal deposits. Miall et al. (1980) interpreted the overlying mudstone member of the Kanguk Formation as representing widespread marine deposition due to transgression during the Late Cretaceous. The sandstone member of the Kanguk Formation, present only along the south coast of Bylot Island and in the adjacent interior area of the island, was considered by Miall et al. (1980) to represent local deposition in a fluvial system present in the southern part of the Eclipse Trough. It conformably overlies transitional facies from the underlying mudstone member of the Kanguk Formation. Miall et al. (1980) interpreted the unconformably overlying strata of the Eureka Sound Formation to represent: local marine beach or shoreface deposits (lower sandstone member, Te^1); open-marine environments to nearshore, deltaic settings (lower mudstone member, Te^2); alluvial-plain, braided fluvial environments (upper sandstone member, Te^3); and renewed marine transgression in the Early or Middle Eocene (upper mudstone member, Te^4). Paleocurrent and facies trends within the Eclipse Trough succession suggested to Miall et al. (1980) that basin geometry was controlled by basin-margin block faulting to the east, with fluvial and deltaic facies in the southeast interfingering with marine facies to the northwest, potentially connecting with widespread marine sedimentation in the Sverdrup Basin during the Cretaceous. During the Paleocene, the trough began to infill and deposits were derived predominantly from more localized sedimentary sources and discontinuous depocentres.

1980s Memorial University of Newfoundland research

Whether the Upper Cretaceous–Cenozoic stratigraphy of the Bylot Island region could justifiably be correlated with the standard stratigraphic framework of the Sverdrup Basin was the basis for investigations by a research group at MUN. These investigations of the Eclipse and North Bylot troughs began in the mid-1980s, led by E.T. Burden, one of the present authors. (The same MUN group also undertook the detailed stratigraphic description and sampling of the

Cretaceous–Cenozoic successions exposed north of Cape Dyer and at Scott Inlet lowland discussed above.) In the Bylot Island region, they focused on the stratigraphic successions preserved along the southwest coast, in the area of the Twosnout creek in south-central Bylot Island, and in the Maud Bight area on the north coast of the island. The objectives for this research were to better understand the Cretaceous–Paleogene sedimentary successions preserved in these areas, to develop a more comprehensive biostratigraphic framework, and to establish a suitable stratigraphic nomenclature for the strata that would reflect its distinctness from the Sverdrup Basin stratigraphy and its relationship with the evolution of Baffin Bay.

The MUN research was undertaken mainly as a series of undergraduate- and Masters-level field studies and associated theses, but remains mostly unpublished. The first of these studies focused on the Eclipse Trough region and were those of Sparkes (1989), who examined the Cretaceous portion of the succession, and Waterfield (1989), who examined the overlying Paleocene succession reported by Miall et al. (1980). Wiseman (1991) further studied both the Cretaceous and Paleocene successions preserved in the Twosnout creek region. Finally, Benham (1991), with a short summary published in Benham and Burden (1990), described the Cretaceous and Cenozoic strata preserved in the fault-bounded North Bylot Trough, noting similarities and differences with the strata of Eclipse Trough. In all of these studies, detailed measurements of stratigraphic sections were undertaken and integrated with sedimentary petrography; most also involved palynostratigraphy. The resulting theses provide a wealth of litho- and biostratigraphic data, and Figure 2 summarizes the lithostratigraphic framework for the Eclipse Trough and Maud Bight proposed by the MUN research team.

Examining the Cretaceous succession preserved along the south coast of Bylot Island, Sparkes (1989) revisited the Upper Cretaceous stratigraphic framework of Miall et al. (1980), informally introducing the Byam Martin, Sermilik, and Bylot Island formations. (Informal stratigraphic nomenclature is referred to in this contribution using lowercase letters for the lithostratigraphic category, e.g. formation and member.) The first two of these units corresponded to the lower mudstone member (Kk^1) and the upper sandstone member (Kk^2), respectively, of the Kanguk Formation of Miall et al. (1980), as exposed along the south coast of Bylot Island. Sparkes (1989) did not identify any sandstone facies exposed in the Bylot Island south coast succession beneath his Byam Martin formation and assignable to the Hassel Formation of Miall et al. (1980); however, he did recognize that the Sermilik formation was a wedge of sandstone that pinched out laterally to the northwest into a deeper water marine basin containing mudstone, referring these more offshore strata to the Bylot Island formation, which overlies the Sermilik formation in the south coast succession (Fig. 15).

Sparkes (1989) dated his three Cretaceous units as mid- to late Campanian, late Campanian to early late Maastrichtian, and late Campanian to late Maastrichtian, respectively, based on the distribution of terrestrial and marine palynomorphs in the strata. Sparkes (1989) defined three informal assemblage zones based on these palynomorphs (Table 3), recognized in sections at Twosnout creek and along the Bylot Island south coast. The *Gleicheniidites* sp. cf. *G. circiniidites–Antulsporites distaverrucosus* Zone was characterized by low palynomorph diversity, but a mid- to late Campanian age was proposed based on the occurrence of Late Cretaceous palynomorph taxa *Carpinipites anciptes*, *Hazaria sheopiarii*, and *Polytriopollenites stellatus*, in combination with the age of the overlying zone. Sparkes (1989) identified the *Gleicheniidites* sp. cf. *G. circinidites–Antulsporites distaverrucosus* Zone in strata of the Byam Martin and Bylot Island formations. The *Porosipollis porosus–Aquilapollenites scabridus* (now considered *Triprojectus scabridus*) Zone was assigned a very late Campanian to mid-Maastrichtian age based on the first occurrence of several biostratigraphically important Late Cretaceous taxa such as: *Radialisporis radiatus*, *Hamulatisporis amplus*, *Wodehouseia gracile*, *Momipites wyomingensis*, *Polyvestibulopollenites trinus*, *Porosipollis porosus*, *Paleoperidinium kozlowskii*, and *Ceratiopsis diebelii* (now considered *Cerodinium*). The *Porosipollis porosus–Aquilapollenites scabridus* Zone was identified in the Sermilik and Bylot Island formations. Finally, Sparkes (1989) assigned an early late Maastrichtian age to the *Singularia aculeata–Pesavis parva* Zone, based on the first occurrence of the taxa *Pesavis parva* and *Paraalnipollenites alterniporus*. Taxa with restricted ranges characterizing the *Singularia aculeata–Pesavis parva* Zone include *Appendicisporites erdtmanii*, *Asbeckiasporites wirthi*, *Extratriporopollenites* sp. 2 of McIntyre, *Singularia aculeata*, *Manicorpus trapeziforme*, *Paralnipollenites alterniporus*, *Pesavis parva*, and *Trudopollis variabilis*. The *Singularia aculeata–Pesavis parva* Zone was identified in strata of the Sermilik and Bylot Island formations. Sparkes (1989) also included additional species that characterize these three zones, but are not restricted to them, and also noted new or unknown taxa where applicable (*see* Table 3).

Sparkes (1989) interpreted the Byam Martin formation as comprising basin-plain and turbidite deposits, succeeded upsection by deposits of braided delta and submarine facies deposits that are related to a major progradational event, represented by the Sermilik formation (Fig. 15). At the top of the Cretaceous succession, he interpreted the upper Maastrichtian Bylot Island formation as representing renewed transgression and deposition in slope, basin-plain, and distal submarine-fan environments.

Waterfield (1989) undertook a detailed stratigraphic assessment of the Paleocene succession preserved along the southwest coast of Bylot Island and correlated these rocks, as well as the underlying Cretaceous strata, with the succession seen in the Twosnout creek region to the northwest. Waterfield (1989) utilized the stratigraphic nomenclature of Sparkes (1989) for the Cretaceous strata of southwestern Bylot Island. In addition, he defined three Cenozoic units, the Pond Inlet formation, the Navy Board formation, and the Aktineq formation. The oldest Cenozoic stratigraphic unit of the south coast succession is the Pond Inlet formation, which conformably overlies the Bylot Island formation there. The Pond Inlet formation was considered to have been deposited in basin-margin settings such as fan-delta, shelf, and submarine-fan environments, and recorded marine regression in the basin. Waterfield's (1989) Pond Inlet formation, which he extended northwestward to the Twosnout creek area, where he noted that it was notably thinner and interfingered with his Navy Board formation (Fig. 16), was equivalent to Miall et al.'s (1980) Eureka Sound Formation units Te^1, Te^2, and Te^3. The Navy Board formation was considered to consist of basin-plain deposits grading upward into a deltaic sequence, all distal equivalents of the shallower water deposits of the Pond Inlet formation preserved to the southeast. Waterfield (1989) defined the Aktineq formation as a deltaic succession at the top of the Bylot Island succession, overlying both the Pond Inlet and Navy Board formations, and which prograded into the Eclipse Trough from the south as a result of relative sea-level fall.

Working principally in the section along the south coast of Bylot Island, but also examining strata in the Twosnout creek area, Waterfield (1989) described two informal assemblage biozones for uppermost Cretaceous to lower Paleocene strata of the Eclipse Trough (Table 4). The *Hamulatisporis amplus–Ulmipollenites* sp. 1 Zone was assigned a late Maastrichtian age based on the following biostratigraphically significant, but not restricted, taxa: *Carpinipites ancipites*, *Polyatripollenites stellatus*, *Polyvestibulopollenites verus*, *Pesavis parva*, *Ceratiopsis* (now *Cerodinium*) *diebelii*, and *Thalassiphora pelagica*. This zone was identified in strata of the Bylot Island formation and shares many characteristic taxa with the *Singularia aculeata–Pesavis parva* Zone of Sparkes (1989); although the *Hamulatisporis amplus–Ulmipollenites* sp. 1 Zone is found overlying strata in which the *Singularia aculeata–Pesavis parva* Zone is defined, Waterfield (1989) interpreted his zone as a continuation of Sparkes' (1989) zone. According to Waterfield (1989), the transition from the *Hamulatisporis amplus–Ulmipollenites* sp. 1 Zone to the overlying *Trivestibulopollenites betuloides–Triatripollenites* sp. 1 Zone corresponds with the boundary between the Bylot Island and Pond Inlet formations. This latter zone was assigned an early Paleocene age based on the presence of *Trivestibulopollenites betuloides*, *Sequioapollenites paleocenicus*, and *Pesavis parva*. Waterfield (1989) further subdivided this assemblage zone into subzones a and b, where subzone b is based on the increased abundance of *Carpinipites ancipites*, *Trivestibulopollenites betuloides*, and *Triatriopollenites* sp. 1, as well as the absence of dinocysts. Waterfield (1989) identified the *Trivestibulopollenites betuloides–Triatripollenites* sp. 1 Zone throughout strata of the Pond Inlet, Navy Board, and Aktineq formations, with subzone a identified locally in the Pond Inlet formation and lower Navy Board formation, and subzone b restricted to the upper Navy Board and Aktineq formations locally.

Wiseman (1991) undertook a more detailed study of the Pond Inlet formation of Waterfield (1989), as exposed in the Twosnout creek area, in order to better understand and characterize the depositional environments represented in the unit there. He documented the sedimentology, biostratigraphy, and facies associations of the formation and favoured a Maastrichtian age for the succession, in contrast with the early Paleocene age suggested by Ioannides (1986) and also by Waterfield (1989) for the exposures of the formation preserved along the southwest coast of Bylot Island. Furthermore, Wiseman (1991) used outcrop sedimentology to interpret the Pond Inlet formation in the Twosnout creek area as deposited in subaqueous fan-channel environments in a shallow-marine, presumably fan-delta, setting.

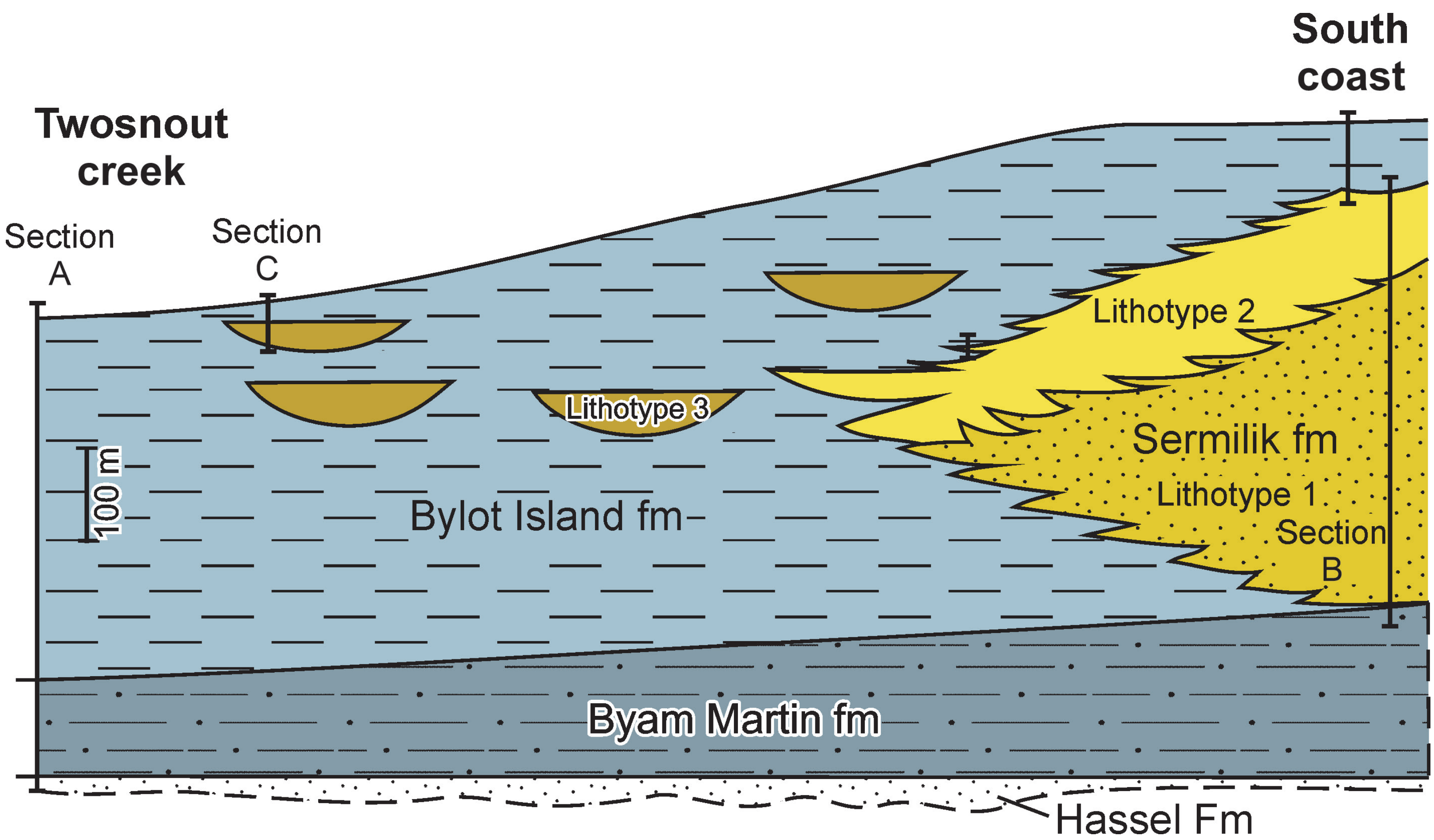

Figure 15. Interpretation of Cretaceous stratigraphy, south coast to Twosnout creek area of Bylot Island (inset D of Fig. 1), after Sparkes (1989: Fig. 4.3). Lithotypes are facies assemblages defined by Sparkes (1989); formal and informal stratigraphic units are included. Vertical bars represent stratigraphic sections presented in Sparkes (1989). Sparkes (1989) followed Waterfield (1989) in assignment of Paleogene strata overlying his Cretaceous sections; although Paleogene strata are not shown, evidence for a significant unconformity in the succession at the uppermost Cretaceous–lowermost Paleogene interval was lacking.

Table 3. Palynological zones and important taxa for onshore Cretaceous strata of the Eclipse Trough, south coast of Bylot Island and Twosnout creek area.

Early late Maastrichtian	***Singularia aculeata–Pesavis parva* Zone**
	Appendicisporites erdtmanii
	Asbeckiasporites wirthii
	Extratriporopollenites sp. 2 of McIntyre
	Mancicorpus trapeziforme
	Paraalnipollenites alterniporus
	Pesavis parva
	Singularia aculeata
	Trudopollis variabilis
Very late Campanian to mid-Maastrichtian	***Porosipollis porosus–Aquilapollenites scabridus* Zone**
	Aquilapollenites scabridus
	Caprifoliipites longus
	Ceratiopsis diebelii
	Cirratriradites teter
	Densoisporites velatus
	Hamulatisporis amplus
	Momipites wyomingensis
	Neotriangulipollis sp. 1 of Azema
	Palaeoperidinium kozlowskii
	Pityosporites alatipollenites
	Polyvestibulopollenites trinus
	Porosipollis porosus
	Radialisporis radiatus
	Rousea georgensis
	Tubifloridites lilliei
	Wodehouseia gracile
Mid- to late Campanian	***Gleicheniidites sp. cf. G. circinidites–Antulsporites distaverrucosus* Zone**
	Antulsporites distaverrucosus
	Carpinipites anciptes
	Gemmatriletes clavatus
	Gleicheniidites sp. cf. *G. circinidites*
	Hazaria sheoparii
	Ornamentifera baculata
	Polytriopollenites stellatus
After Sparkes (1989).	

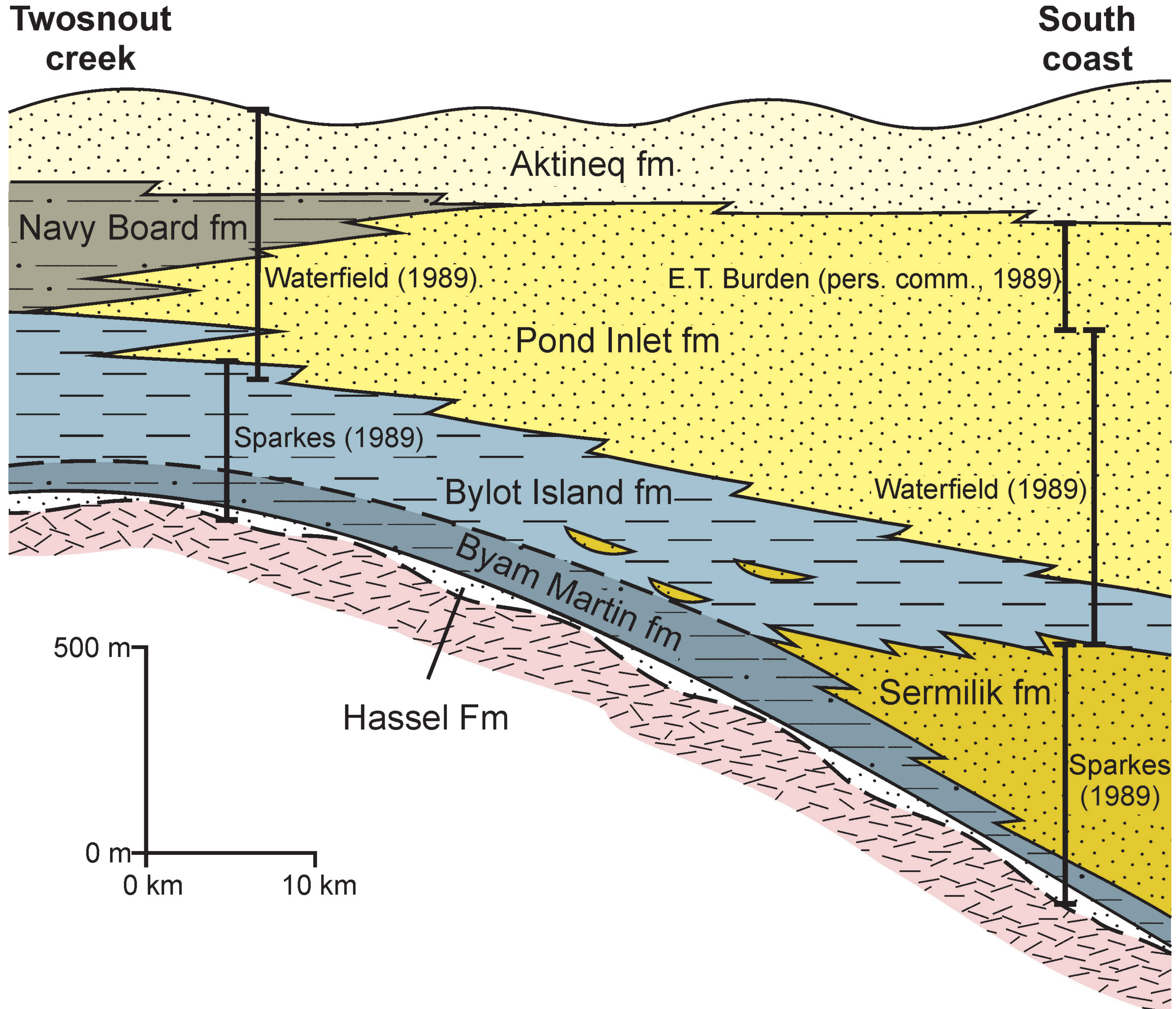

Figure 16. Schematic representation of interfingering of Cretaceous–Paleogene coarse clastic rocks within the Sermilik, Pond Inlet, and Aktineq formations preserved in the southern part of the Eclipse Trough with finer grained, more offshore deposits of the Bylot Island and Navy Board formations to the northwest in the Eclipse Trough (inset D of Fig. 1). Formal and informal stratigraphic units are included (*modified from* Waterfield, 1989). Vertical bars represent stratigraphic sections presented in Waterfield (1989).

Examining Cretaceous–Cenozoic strata in the North Bylot Trough (Fig. 10, 17), Benham (1991) and Benham and Burden (1990) recognized similarities in the stratigraphic succession to those of the Eclipse Trough, as described by Miall et al. (1980), Sparkes (1989), and Waterfield (1989); specifically, the Hassel Formation overlain by the Bylot Island, Sermilik, Navy Board, and Aktineq formations, with a newly recognized conglomerate member, the Maud Bight member, capping the succession (Fig. 2, 17). Benham (1991) did not recognize the Pond Inlet formation of the Eclipse Trough in the Maud Bight area, and suggested that a thicker Sermilik formation at Maud Bight included age-equivalent strata of the Pond Inlet formation. In addition to biostratigraphic data contributed from microfossils, Benham and Burden (1990) reported Paleocene plant macrofossils from strata in the North Bylot Trough, corroborating earlier findings of Paleocene strata in the Bylot Island area (Jackson and Davidson, 1975a; Miall et al., 1980; Waterfield, 1989).

Benham (1991) defined three biostratigraphic assemblage zones, as well as one subzone, for the North Bylot Trough strata (Table 5): 1) the *Azonia cribrata–Aquilapollenites trialatus* Zone; 2) the *Porosipollis porosus–Wodehouseia spinata* Zone; and 3) the *Paraalnipollenites alterniporus–Pesavis parva* Zone. Benham (1991) assigned the *Azonia cribrata–Aquilapollenites trialatus* Zone a late Campanian to middle Maastrichtian age, with characteristic restricted species being *Pseudoplicapollis serenus*, *Trudopollis conrector*, *Azonia cribrata*, *Wodehouseia gracile*, *Aquilapollenites reticulatus*, and *Aquilapollenites* (now *Parviprojectus*) *trialatus*. Benham (1991) also noted the presence of an interval (subzone R) within the *Azonia cribrata–Aquilapollenites trialatus* Zone characterized by a high abundance (>85%) of recycled middle to late Albian palynomorphs such as *Cicatricosisporites*, *Tappanispora*, and *Klukisporites*. The *Azonia cribrata–Aquilapollenites trialatus* Zone and subzone R are both within the Bylot Island formation.

The *Porosipollis porosus–Wodehouseia spinata* Zone of Benham (1991) was assigned a middle to late Maastrichtian age based primarily on the abundant *Porosipollis porosus* and restricted *Wodehouseia spinata* that characterize the zone, as well as *Hazaria sheoparii*. Other species restricted to the *Porosipollis porosus–Wodehouseia spinata* Zone include *Cicatricosisporites eocenicus*, *Cranwellia striata*, *Cranwellia rumseyensis*, *Triatriopollenites costatus*, *Trudopollis* ex gr. *arector*, *Beaupreaidites angulatus*, *Beaupreaidites mollis*, *Azonia jacutense*, *Wodehouseia quadrispina*, *Singularia aculeata*, and *Mancicorpus trapeziforme*. The *Porosipollis porosus–Wodehouseia spinata* Zone was identified within Sermilik formation strata of the North Bylot Trough (Benham, 1991).

Benham (1991) considered the third zone for the North Bylot Trough, the *Paraalnipollenites alterniporus–Pesavis parva* Zone, to be Early to Middle Paleocene: taxa restricted to this zone include *Striatopollis tectatus*, *Ulmoideipites krempii*, *Momipites wyomingensis*, *Caryapollenites* sp. cf. *C. inelegans*, *Complexiopollis* sp., *Aquilapollenites augustus*, *Aquilapollenites* sp. cf. *A. immiser*, *Diporicellasporites* sp. cf. *D. stacyi*, *Staphlosporonites delumbus*, *Pesavis tagluensis*, *Phragmothyrites* sp., *Callimothallus pertusus*, *Plochmopeltinites masonii*, and *Microthallites lutosus*. Benham (1991) indicated that the *Paraalnipollenites alterniporus–Pesavis parva* Zone characterizes the Navy Board and Aktineq formations of the North Bylot Trough.

Benham and Burden (1990) and Benham (1991) ascribed a threefold tectonosedimentary model for the development of the Maud Bight strata. Phase 1 of this model was represented by the arenaceous fluvial deposits of the Hassel Formation, which accumulated prior to rifting associated with Baffin Bay and Lancaster Sound and was presumably linked with deposition in the Eclipse Trough to the south. Overlying upper Campanian to middle Maastrichtian shelf mudstone units of the Bylot Island formation and middle to upper Maastrichtian quartz-rich nearshore and beach deposits of the Sermilik formation in Maud Bight reflected the initial uplift of the Byam Martin Mountains of central Bylot Island and separation from sedimentation in the Eclipse Trough. This constituted Phase 2 of the tectonic development model of Benham and Burden (1990) and Benham (1991). The final, Phase 3, episode of the tectonostratigraphic model is represented by the lower to middle Paleocene Navy Board and Aktineq formations; the former was interpreted as fluvial, braided stream, and lacustrine

Table 4. Palynological zones and important taxa for onshore Cretaceous–Paleocene strata of the Eclipse Trough, south coast of Bylot Island.

	***Trivestibulopollenites betuloides–Triatripollenites* sp. 1 Zone**
Early Paleocene	*Caryapollenites* sp. 1
	Cingutriletes clavus
	Gemmatriletes sp. 1
	Impardecispora sp. 1
	Momipites sp. 1
	Pesavis parva
	Pityosporites elongatus
	Pityosporites elongatus var. *grandis*
	Podocarpidites sp. 1
	Polyvestibulopollenites trinus
	Retriletes sp. 1
	Semioculopollis sp. 1
	Sequioapollenites paleocenicus
	Triatriopollenites sp. 1
	Tricolpites hians
	Trivestibulopollenites betuloides
	Trudopollis spp.
	***Hamulatisporis amplus–Ulmipollenites* sp. 1 Zone**
Late Maastrichtian	*Carpinipites anciptes*
	Ceratiopsis diebelii
	Ceratosporites equalis
	Cibotiumspora juncta
	Echinatisporis varispinosus
	Hamulatisporis amplus
	Intratriporopollenites sp. 1
	Pesavis parva
	Polyatripollenites stellatus
	Polyvestibulopollenites verus
	Thalassiphora pelagica
	Ulmipollenites sp. 1
	Wodehouseia sp. 1

After Waterfield (1989).

facies, whereas the latter was considered to represent meandering stream sandstone deposits and alluvial fan conglomerate units (Maud Bight member). These later units of Phase 3 represented the initiation of rifting in Baffin Bay and in the Lancaster Aulacogen (i.e. Lancaster Sound; Kerr, 1980) immediately to the north. Although Benham and Burden (1990) and Benham (1991) utilized much of the same stratigraphic nomenclature for the North Bylot Trough as initially described for the Eclipse Trough by Miall et al. (1980), Sparkes (1989), and Waterfield (1989), they did interpret the stratigraphic evolution of the successions during Phases 2 and 3 to be distinct from that of the Eclipse Trough and separated from it by the uplifted Byam Martin Mountains.

Based on his understanding of the ages and lithostratigraphic successions of Eclipse and North Bylot troughs, Benham (1991) correlated strata of these basins with other basins in the circum-Baffin Bay region (Fig. 18), including the Cape Dyer area of onshore Baffin Island, the Labrador Sea, and onshore and offshore West Greenland. One notable difference highlighted in the Benham (1991) correlation is the distinct lack of volcanic strata in the Eclipse Trough and North Bylot Trough successions compared to the significant volumes of volcanic rocks present in the Cape Dyer and West Greenland areas, adjacent to the Davis Strait transform margin. Presumably, this reflects the distant location of the former areas from active rift-related volcanism, and their location within the nonvolcanic (i.e. magma-poor) portion of the Baffin Island continental margin, now recognized as the region north of Home Bay (Skaarup et al., 2006; Dafoe, Dickie, and Williams, this volume; Keen et al., this volume).

2000s subsequent research

Fenton and Pardon's (2007) comprehensive review of the litho- and biostratigraphy of Bylot Island strata also included the south coast and Twosnout creek sections. These authors reassessed palynological samples utilized by Ioannides (1986) from both of the Bylot Island sections, but it is not clear whether they obtained any new samples from the island. They followed Miall et al. (1980) in recognizing the presence of the Hassel Formation at the base of the Bylot Island south coast succession, in contrast to Sparkes (1989), and accepted its general Albian–Cenomanian age as proposed by Miall et al. (1980). Importantly, Fenton and Pardon (2007) examining the Twosnout creek samples, recognized that the lowest sample available, from near the base of the exposed mudstone beds of the Kanguk Formation (Kk1 of Miall et al., 1980), had an age of Turonian to "(intra-) Coniacian," again older than recognized by previous workers. Younger parts of the south coast succession were assigned similar ages to those presented by Miall et al. (1980), Sparkes (1989), and Waterfield (1989), with the youngest age recognized as Danian in the lower part of the Te^3 unit of Miall et al. (1980) (equivalent to the Pond Inlet formation of Waterfield, 1989), although Fenton and Pardon (2007) acknowledged the possibility that younger Paleocene strata could be present.

DISCUSSION

Considerable work was undertaken on the Cretaceous–Paleogene stratigraphy of the onshore successions along western Baffin Bay during the 1970s to 1990s, but no comprehensive overview of the rocks was formulated and the data were never fully integrated and synthesized into a formal depositional framework for the onshore succession. As well, these studies were undertaken before the advent of modern GPS, and in some cases, studied stratigraphic sections could only be located approximately on topographic maps. For the Bylot Island region, home to the thickest, most widespread, and most stratigraphically comprehensive of the onshore successions, previous studies targeted specific, readily accessible and known localities. The result was a view of the stratigraphy limited in its scope and in the understanding of the stratigraphic relationships relative to basin geometry and sedimentation history.

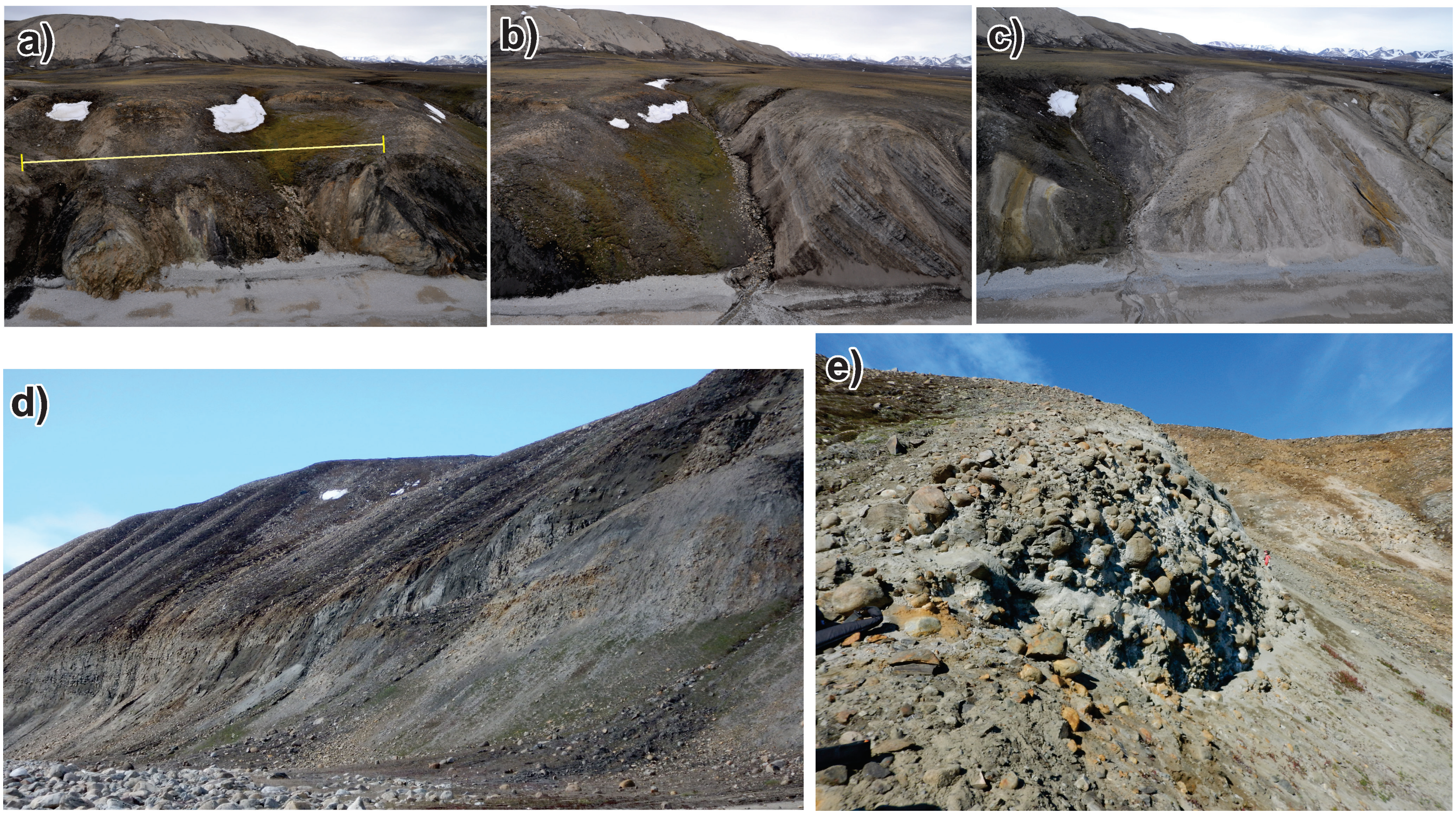

Figure 17. Photographs showing examples of Cretaceous–Paleogene strata preserved in the North Bylot Trough, north coast of Bylot Island (inset E of Fig. 1). *See* Figure 10 for photograph locations. **a), b), c)** Sequential photographs looking south-southeast, showing stratigraphy in parts of Section 3, the most complete section of strata at Maud Bight, studied by Benham (1991); rocks are deformed along faulted contact with Proterozoic strata; photographs do not fully overlap; total length of outcrop is about 0.75 km. **a)** Base of section showing strongly deformed black mudstone beds of Bylot Island formation in fault contact with Proterozoic strata; fault zone delimited by yellow line; multiple fault blocks of Proterozoic rocks are involved in the fault zone. NRCan photo 2021-215. **b)** Black mudstone in upper part of Bylot Island formation at left and covered in middle, succeeded by interstratified sandstone and mudstone transitional to overlying Sermilik formation. NRCan photo 2021-216. **c)** Buff and yellowish sandstone of Sermilik formation at left, succeeded by pale yellow sandstone of Pond Inlet formation on right. NRCan photo 2021-217 **d)** Flat-lying (?)Paleogene boulder conglomerate and interstratified sandstone of Maud Bight member of Aktineq formation of Benham (1991); total height of exposure approximately 125 m; top of hill is capped by Quaternary gravel beds and differentiating the contact of the gravel beds with the boulder conglomerate is problematic. NRCan photo 2021-218. **e)** Close-up of Maud Bight member boulder conglomerate, showing rounded nature of clasts; person for scale. NRCan photo 2021-219. All photographs by J.W. Haggart.

The initial work of Miall et al. (1980) established the broad lithological units that exist in the Eclipse Trough area of Bylot Island and their general ages. Subsequent work by the MUN research team in a series of theses (Sparkes, 1989; Waterfield, 1989; Benham and Burden, 1990; Benham, 1991; Wiseman, 1991) provided significantly more lithological and biostratigraphic detail for these units, and assigned them new nomenclature chosen to reflect their local derivation geographically distant from the successions of the High Arctic. As well, the MUN team also undertook the first investigations of the succession preserved in the North Bylot Trough, recognizing many similarities, as well as some discrepancies, compared to the Eclipse Trough succession. These results provide the best overall summary of the geology and lithostratigraphy of the Bylot Island rocks, and in the greatest detail; however, inconsistencies among these theses in ages assigned to lithological units, as well as varying interpretations of the depositional environments represented by the strata, highlight that this research needed further pursuit.

Studies in the 1970s and 1980s did not produce detailed geological maps of the Cretaceous–Paleogene succession of the onshore region due to limitations to outcrop access at the time. Thus, recognizing patterns and trends of lateral facies relationships among strata was limited, and defining the lateral and vertical extents of important stratigraphic units was not fully established. Interpretations of depositional environments of some lithostratigraphic units were often confusing and contradictory amongst the various contributions, with no clear model of changing environments and depositional patterns through time. For example, Sparkes (1989) interpreted his Byam Martin formation to consist of basin-plain and turbidite deposits that give way upsection to braided delta and submarine fan (presumed herein to be fan-delta) deposits of the progradational Sermilik formation. Unfortunately, Sparkes (1989) did not qualify the types of submarine-fan environments represented by these units — deep-marine or fan-delta settings — creating some interpretive confusion. Similarly, Waterfield (1989) assigned the Pond Inlet formation to a wide variety of depositional settings, including basin-margin fan-delta, shelf, and submarine-fan environments; he also suggested that the Navy Board formation represented basin-plain deposits grading upward into deltaic facies, a wide range of depositional settings.

Previous researchers were also influenced by regional perspectives in their correlations of the succession on Bylot Island, which is located between the Cretaceous and Cenozoic basins of the High Arctic and those of the Labrador–Baffin Seaway rift system. Miall et al. (1980) posited that the Eclipse Trough exposures represented the farthest southeastward preserved extent of the Kanguk Formation, widespread in the High Arctic, based on the lithostratigraphic and biostratigraphic similarities of the units, and was perhaps influenced by the recognition of Kanguk Formation strata on Somerset Island, approximately 450 km west of Bylot Island (Dixon et al., 1973).

Miall (1986, 1991) and Ricketts (1986) further correlated the Cenozoic succession of the Eclipse Trough with the Eureka Sound Group of the High Arctic, although each presented different lithostratigraphic schemes for the Paleogene strata of Bylot Island (Fig. 11). Miall (1986) correlated the Cenozoic lithostratigraphic units of the Eclipse Trough (i.e. Eureka Sound Formation, with members Te^1, Te^2, Te^3, and Te^4; Miall et al., 1980; Fig. 11) with the Paleocene–Eocene portion of the principally nonmarine to deltaic Paleocene–Oligocene Eureka Sound Group, exposed widely in the Sverdrup Basin to the northwest of Bylot Island (Fig. 19). The Eureka Sound Group in the Sverdrup Basin, according to Miall (1986), accumulated in at least seven distinct sedimentary basins across the Arctic, which were rarely linked regionally during their depositional histories, and the stratigraphic units within the group are markedly diachronous. For this reason, Miall (1986) based his correlations on facies assemblages, rather than strict, biostratigraphically constrained successions. Miall (1986) thus correlated units Te^1 (lower sandstone member) and Te^2 (lower mudstone member) of the Eureka Sound Formation of Miall et al. (1980), which were considered to unconformably overlie the Campanian–Maastrichtian Kanguk Formation in the Eclipse Trough, with the Paleocene to Eocene Mount Lawson Formation of the Eureka Sound Group found in more northerly parts of the Arctic. Miall et al.'s (1980) Eclipse Trough unit Te^2 (lower mudstone member) of the Eureka Sound Formation was further considered to correlate most closely with the Mount Lawson Formation, and they interpreted their unit Te^1 (the lower sandstone member of the Eureka Sound Formation) as a marine shoreline sandstone forming the basal member of the

	***Paraalnipollenites alterniporus–Pesavis parva* Zone**
Early to mid-Paleocene	*Aquilapollenites augustus*
	Aquilapollenites sp. cf. *A. immiser*
	Brachysporites cotalis
	Callimothallus pertusus
	Carpinipites ancipites
	Caryapollenites sp. cf. *C. inelegans*
	Complexiopollis sp.
	Dicellaesporites popovii
	Diporicellasporites reticulatus
	Diporicellasporites sp. cf. *D. stacyi*
	Ericaceoipollenites rallus
	Hazaria sheoparii
	Microthallites lutosus
	Momipites wyomingensis
	Monoporisporites singularis
	Paraalnipollenites alterniporus
	Pesavis parva
	Pesavis tagluensis
	Phragmothyrites sp.
	Plochmopeltinites masonii
	Polyvestibulpollenites verus
	Sequioapollenites paleocenicus
	Staphlosporonites delumbus
	Striatopollis tectatus
	Triporopollenites mullensis
	Trivestibulopollenites betuloides
	Ulmoideipites krempi
	***Porosipollis porosus–Wodehouseia spinata* Zone**
Mid- to late Maastrichtian	*Azonia jacutense*
	Beaupreaidites angulatus
	Beaupreaidites mollis
	Brachysporites cotalis
	Carpinipites ancipites
	Cicatricososporites eocenicus
	Cranwellia rumseyensis
	Cranwellia striata
	Dicellaesporites popovii
	Ericaceoipollenites rallus
	Extratriporopollenites sp. 2 of McIntyre
	Fraxinoipollenites variabilis
	Hazaria sheoparii
	Mancicorpus trapeziforme
	Paraalnipollenites alterniporus
	Pesavis parva
	Porosipollis porosus
	Sequioapollenites paleocenicus
	Singularia aculeata
	Triatriopollenites costatus
	Triporopollenites mullensis
	Trivestibulopollenites betuloides
	Trudopollis ex gr. *arector*
	Wodehouseia quadrispina
	Wodehouseia spinata
	***Azonia cribrata–Aquilapollenites trialatus* Zone**
Late Campanian to mid-Maastrichtian	*Aquilapollenites reticulatus*
	Aquilapollenites trialatus
	Azonia cribrata
	Ceratiopsis diebelli
	Densoisporites velatus
	Echinatisporis varispinosus
	Hazaria sheoparii
	Liliacidites leei
	Monoporisporites singularis
	Palaeoperidinium kozlowskii
	Porosipollis porosus
	Pseudoplicapollis serenus
	Radialisporis radiatus
	Triatriopollenites rurensis
	Trudopollis conrector
	Wodehouseia gracile

After Benham (1991).

Table 5. Palynological zones and important taxa for onshore Cretaceous–Paleocene strata of the North Bylot Trough, north coast of Bylot Island.

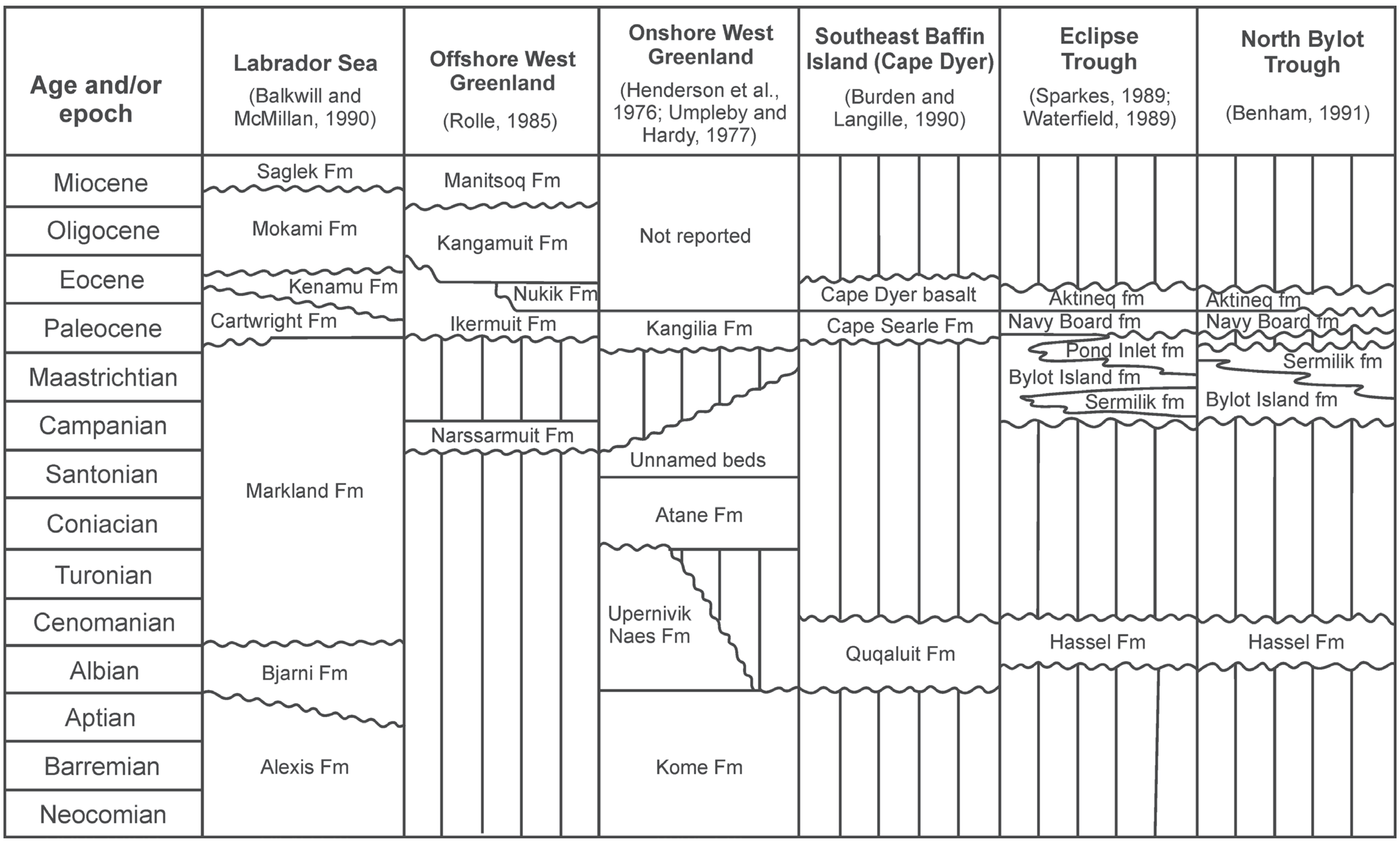

Figure 18. Correlation of Cretaceous–Cenozoic strata of the circum-Baffin Bay region, as understood ca. 1991, *after* Benham (1991).

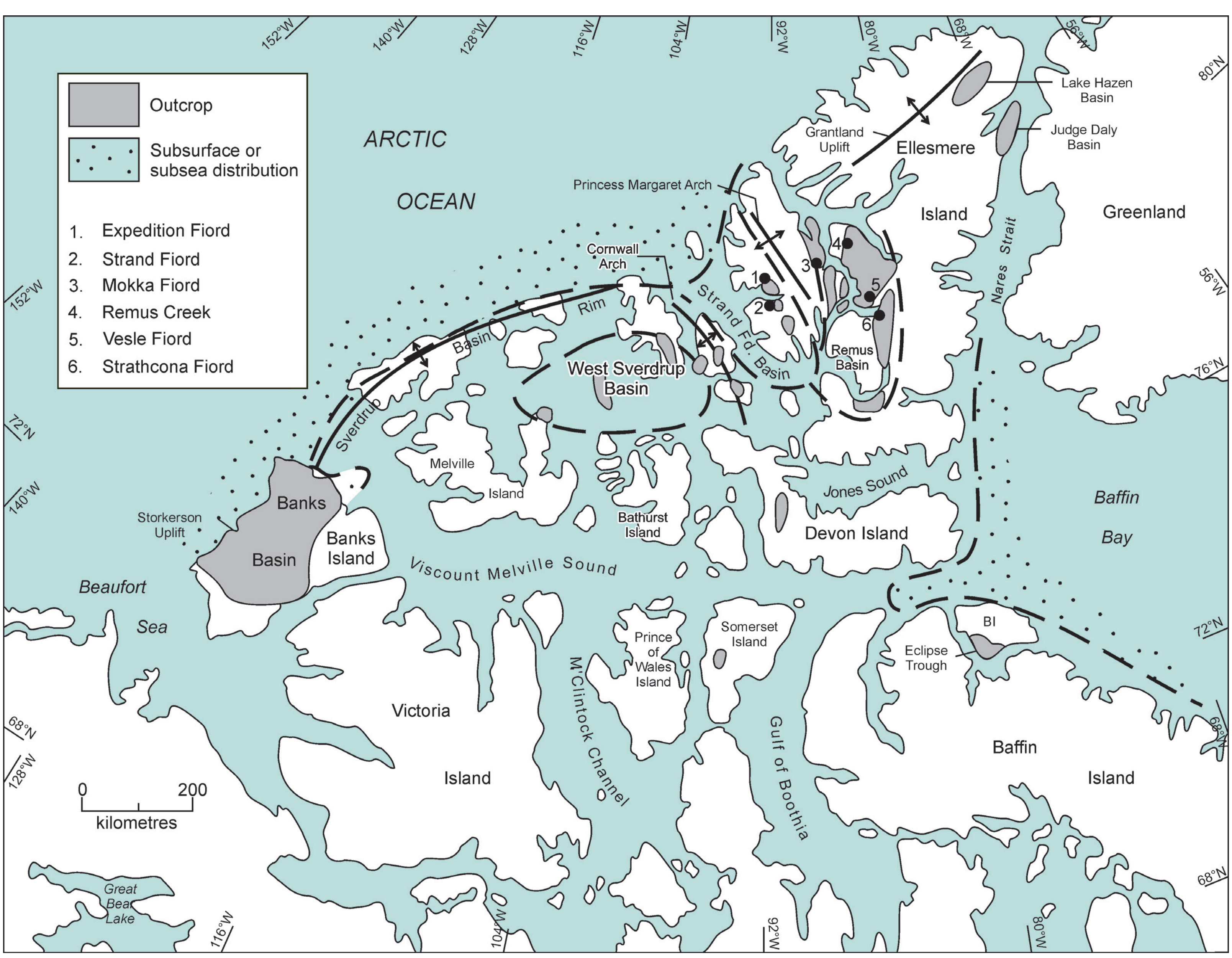

Figure 19. Map showing distribution of Eureka Sound Group depositional basins, Canadian Arctic, and also the Eclipse Trough, Bylot Island (*after* Miall, 1991). BI = Bylot Island; Fd. = Fiord.

Mount Lawson Formation. Subsequently, Miall (1986) correlated unit Te[3] (upper sandstone member) of the Eureka Sound Formation of the Eclipse Trough with the Mokka Fiord Formation of the Eureka Sound Group. Miall (1986) did not attempt to correlate the stratigraphically highest unit (Te[4], upper mudstone member) of the Miall et al. (1980) Eureka Sound Formation of the Eclipse Trough with any stratigraphic units of the Eureka Sound Group of the Sverdrup Basin.

In contrast, Ricketts (1986) suggested that some distinctive lithostratigraphic units of the Eureka Sound Group recognized in the Sverdrup Basin could also be recognized in more distant areas to the south, including the Bylot Island region (Fig. 11, 19). Ricketts (1986) thus correlated Miall et al.'s (1980) uppermost sandstone member (Kk[2]) of the Kanguk Formation on Bylot Island with his Expedition Formation of the Eclipse Sound Group within Sverdrup Basin, and Miall et al.'s (1980) overlying Te[1], Te[2], and Te[3] units of the Eclipse Trough succession with his Strand Bay and Iceberg Bay formations of the Eureka Sound Group. In subsequent publications, Ricketts (1991, 1994) did not continue to compare the Cenozoic strata of the Eclipse Trough and the Bylot Island region with Eureka Sound Group stratigraphy of the Sverdrup Basin, suggesting he may have reconsidered this hypothesis.

Neither Miall (1986) nor Ricketts (1986) took into account the large geographic distance, some 400 km, separating known exposures of the Eclipse Trough, especially the Cenozoic succession, from contemporary deposits of the Sverdrup Basin. In particular, the choice of Miall (1986, 1991) and Ricketts (1986) to apply the stratigraphic nomenclature of Eureka Sound Group rocks to the Eclipse Trough succession seemingly discounted their own statements that the subbasins containing Eureka Sound Group within the Sverdrup Basin were essentially separate depocentres throughout most of their history, with sediment supply controlled by localized tectonic highs. Given this, it might have been preferable to assign separate stratigraphic nomenclatures to each of those disjunct Paleocene–Eocene depocentres, which would have reflected their distinct lithostratigraphic and depositional characteristics. To find the same stratigraphic succession preserved in both the Eclipse Trough and Sverdrup Basin, in which sedimentation was locally controlled by different structural regimes and basement blocks, would be highly unusual. Indeed, Miall (1988) subsequently suggested that the application of stratigraphic names across such large geographic distances was perhaps inappropriate.

The MUN research team viewed the Eclipse Trough succession much differently, considering it to be an onshore extension of basins within northern Baffin Bay, and related to the tectonic evolution of that region. Thus, the group formulated a stratigraphic nomenclature for the rocks that was generally distinct from that of the schemes of Miall et al. (1980), Miall (1986, 1991), and Ricketts (1986). Unfortunately, the MUN research was never formalized in the geological literature and did not consider potential genetic linkages with the rocks of the High Arctic, other than with the Hassel Formation. Significantly, the MUN team did attempt to establish detailed biostratigraphic zonations for the Cretaceous–Paleogene strata of the troughs, but this work involved multiple biozonation schemes with limited correlation value. Application of these zonations to the rocks of Bylot Island resulted in different ages for some lithostratigraphic units: for example, Wiseman (1991) assigned a Maastrichtian age to the Pond Inlet formation in the Twosnout creek area, whereas both Ioannides (1986) and Waterfield (1989), also using palynology, assigned these strata to the Early Paleocene.

Despite these limitations, studies in the 1970s and 1980s established a number of significant contributions regarding the Eclipse and North Bylot troughs and correlative strata of onshore Baffin Island. They also helped to define research opportunities and objectives of the Geological Survey of Canada's Geomapping for Energy and Minerals (GEM) Program. These can be summarized as follows.

- The broad overall patterns of Cretaceous–Paleogene sedimentation preserved in the onshore sedimentary successions adjacent to western Baffin Bay were identified (Jackson and Davidson, 1975a; Jackson et al., 1975), and details of their depositional environments were subsequently established (Miall et al., 1980; Sparkes, 1989, Waterfield, 1989, Benham, 1991). These studies provide an analogue for the nature and depositional environments of the sedimentary successions preserved in the offshore shelf and slope areas of western Baffin Bay; a relationship later demonstrated by Dafoe et al. (2019b).
- The similarity of the Cretaceous stratigraphic succession of the Eclipse Trough to that of the Sverdrup Basin of the High Arctic was noted by Miall et al. (1980), and both Miall (1986, 1991) and Ricketts (1986) attempted correlation of the Cenozoic strata of the Eclipse Trough with the Eureka Sound Group of the High Arctic; however, these researchers minimized the potential influence of the evolving tectonism related to the Labrador–Baffin Seaway rift system in the deposition of the Eclipse Trough succession.
- Studies in the 1970s to 1990s led to the recognition that the Cretaceous–Paleogene succession of the Eclipse and North Bylot troughs, as well as of the Cape Dyer area, included a complexity of strata with laterally interfingering facies relationships, changing depositional environments, and internal discontinuities; this contrasts with the 'layer-cake' view of the stratigraphy that existed earlier. Subsequent detailed assessment of paleoenvironments, including trace-fossil analysis, has revealed: Lower Cretaceous fluvial, lake-margin, and shoreface strata; Upper Cretaceous outer shelf (or more distal) to foreshore deposits; and Paleocene deltaic, shoreface, foreshore, and estuarine settings (Dafoe and Haggart, 2018; Dafoe et al., 2019a).
- Cretaceous–Paleogene sedimentation in the Bylot Island region was recognized to have taken place in two distinct depocentres — the Eclipse and North Bylot troughs (Jackson and Davidson, 1975a, b; Miall et al., 1980). These depocentres shared a similar history during the Cretaceous, but diverged somewhat during the Paleogene, due to evolving tectonic activity related to rifting and evolution of Baffin Bay (Benham and Burden, 1990; Benham, 1991). Studies by Haggart et al. (2018) have further confirmed that similar units can be identified in both troughs, with lateral facies changes also being a significant factor in lithostratigraphic relationships within each trough.
- The MUN research group established that the Eclipse Trough succession is stratigraphically much more complete than had been considered previously (Miall et al., 1980; Miall, 1986; Ricketts, 1986), with biostratigraphic evidence indicating more or less continuous deposition from the late Campanian and through the late Maastrichtian to Paleocene (Sparkes, 1989; Waterfield, 1989; Benham, 1991). Although preliminary, recent GEM work has suggested that the Eclipse Trough may contain an even more complete stratigraphic succession, possibly from the Albian–Cenomanian through to the Selandian, with settings from nonmarine to open ocean (Haggart et al., 2017, 2018), in rough agreement with the limited analyses of Fenton and Pardon (2007).
- In addition to establishing a biostratigraphic zonal sequence for the North Bylot Trough strata, Benham (1991) also undertook a comprehensive taxonomic review of floral taxa found there, and included new and unknown taxa in the definition of his floral zones. These comprehensive descriptions and identifications provide a significant resource to help refine and improve understanding of the stratigraphic ranges for many of these biostratigraphically significant taxa. For example, more recent understanding of the biostratigraphic range of *Parviprojectus trialatus* (formerly *Aquilapollenites trialatus*) suggests that Benham's *Azonia cribrata–Aquilapollenites trialatus* Zone is more likely to be Campanian rather than late Campanian to middle Maastrichtian (Braman and Sweet, 2012). Subsequent preliminary study by Haggart et al. (2018) has further revealed additional new palynomorphs, as well as recognizing known floral taxa comparable to established palynoevents in the region (e.g. Nøhr-Hansen et al., 2016).
- Sedimentation and volcanism in the Cape Dyer area was linked to rift-related development and tectonism of Baffin Bay and with the magmatic province of West Greenland (Burden and Langille, 1990).
- The importance of palynostratigraphic control to elucidate details of basin stratigraphy, changing depositional environments, and ages of stratigraphic units was recognized (Ioannides, 1986; Sparkes, 1989; Waterfield, 1989; Wiseman, 1991), as was the significant challenge of differentiating relatively flat-lying, poorly indurated Paleogene coarse clastic strata from adjacent Quaternary deposits (Burden and Holloway, 1985; Newman, 1987).

In the late 2000s, the Geological Survey of Canada initiated the Geo-mapping for Energy and Minerals (GEM) program, with a project targeting the onshore Cretaceous–Paleogene sedimentary successions along western Baffin Bay. The objective of this project was to re-examine this stratigraphy in the context of geological mapping, and to interpret the ages of the onshore strata and their paleoenvironments, the sequence stratigraphic history of the onshore basins, their sedimentary provenance, and their uplift histories. Research is ongoing and results are still forthcoming, but reviews of field programs and preliminary assessments of new geological understandings have been presented in a series of abstracts and contributions (Haggart et al., 2011, 2017, 2018; Galloway et al., 2012; Brent et al., 2013; Dafoe and Haggart, 2018; Dafoe et al., 2019a, b; Currie et al., 2020). These are beyond the scope of this review.

SUMMARY

A number of researchers examined the onshore Cretaceous–Paleogene deposits of the eastern Baffin Island region during the 1970s to 1990s, and attempted to formulate stratigraphic frameworks that described these strata and their depositional setting. The age control for these studies was based exclusively on palynology (pollen and spores and dinocysts) since molluscs, foraminifera, and radiolarians were conspicuously absent from the strata, or limited in abundance. It was recognized that stratigraphic successions in all areas studied consist almost exclusively of clastic deposits: sandstone, siltstone, mudstone, and conglomerate. The geographically and stratigraphically restricted Cretaceous–Paleogene deposits of the Cape Dyer region (Burden and Langille, 1990, 1991) are associated with volcanic strata of Paleogene age, and interpreted to reflect the onset of seafloor spreading in southern Baffin Bay (Keen et al., this volume). In contrast, the much thicker and complete successions of the Eclipse Trough and North Bylot Trough regions lack any association with volcanic strata. For this reason, as well as the notable similarity of the Cretaceous lithostratigraphic succession of the Eclipse Trough with that of the Sverdrup Basin of the High Arctic, the stratigraphic framework established by Miall et al. (1980) for the Eclipse Trough succession, and subsequently followed by Miall (1986, 1991) and Ricketts (1986), utilized nomenclature from the Sverdrup Basin to describe the succession. Researchers from Memorial University of Newfoundland (Sparkes, 1989; Waterfield, 1989; Benham and Burden, 1990; Benham, 1991; Wiseman, 1991) took a different approach to the study of the Eclipse Trough and North Bylot Trough successions, considering them to have developed in response to tectonic activity associated with rifting of the Baffin Bay region. The result was a stratigraphic interpretation that diverged significantly from that of the earlier researchers, while describing the same lithostratigraphic units. In terms of understanding the overall onshore Cretaceous–Paleogene history of the northwest Baffin Bay region, little clarity has been established regarding the tectonic events that have controlled that depositional history.

This review of the existing literature on the onshore Cretaceous–Paleogene successions of the western Baffin Bay region by researchers during the 1970s to 1990s reveals differing interpretations of stratigraphic successions, incomplete and outdated biostratigraphic assessments, and conflicting models of ages and depositional environments for these strata. To address these issues, the Geological Survey of Canada's GEM program, undertaken during the period 2009 to 2020, included field studies targeting the onshore strata of Bylot Island and associated areas; the new data resultant from these studies will provide clarity regarding the stratigraphic architecture of the onshore successions of the western Baffin Bay region, utilizing a biochronological framework that is based on modern taxonomic thinking and comprehensive biostratigraphic occurrence data. Future biostratigraphic work on Bylot Island in particular should focus on developing an event stratigraphy integrating terrestrial and marine fossils to resolve ages and propose correlations, both locally and regionally. Such future study will hopefully make it possible to better understand the evolving paleoenvironmental and depositional history of the onshore Cretaceous–Paleocene strata, and elucidate the finer details of their stratigraphic correlation. A modern stratigraphic framework for the strata will also allow their sequence-stratigraphic history to be established, enhancing correlations with associated offshore successions. As well, such a framework will provide the necessary stratigraphic context for studies of sediment petrography and provenance to establish the basin geometries and depositional histories, and to assess basement thermal and uplift history.

ACKNOWLEDGMENTS

The authors thank the community of Pond Inlet and its Hamlet Council, the Mittimatalik Hunters and Trappers Organization (MHTO), and the Qikiqtani Inuit Association (QIA), for permission to undertake fieldwork in the northern Baffin Island and Bylot Island region, and also acknowledge Parks Canada (Sirmilik National Park) staff members Carey Elverum and Maryse Mahey for help in navigating permitting issues. The authors also gratefully acknowledge the logistics and organizational support of Polar Continental Shelf Program (PCSP). Carol Wagner, Alexina Morrison-Boileau, Hillary Taylor, all of GSC Vancouver; Glenn Woodsworth in Vancouver; and Leith MacLeod of GSC Atlantic, provided help with figure compilation. Warren Wulff, Librarian at GSC-Vancouver, provided invaluable support in locating older literature. Finally, Chris Jauer and Gordon Oakey are thanked for thoughtful reviews of the manuscript.

REFERENCES

Andrews, J.T., Guennel, G.K., Wray, J.L., and Ives, J.D., 1972. An early Tertiary outcrop in north-central Baffin Island, Northwest Territories, Canada: environment and significance; Canadian Journal of Earth Sciences, v. 9, no. 3, p. 233–238. https://doi.org/10.1139/e72-019

Balkwill, H.R. and McMillan, N.J., 1990. Mesozoic-Cenozoic geology of the Labrador Shelf; Chapter 7 *in* Geology of the Continental Margin of Eastern Canada, (ed.) M.J. Keen and G.L. Williams; Geological Survey of Canada, Geology of Canada, no. 2, p. 295–324 (*also* Geological Society of America, The Geology of North America, v. I-1, p. 295–324). https://doi.org/10.4095/132708

Benham, P.H., 1991. Stratigraphy and palynology of Cretaceous and Tertiary rocks, North Bylot Trough, Bylot Island, Northwest Territories, Canada; M.Sc. thesis, Memorial University of Newfoundland, St. John's, Newfoundland and Labrador, 360 p.

Benham, P.H. and Burden, E.T., 1990. Stratigraphy of Cretaceous–Tertiary rocks of North Bylot Trough, Bylot Island, N.W.T.; *in* Current Research, Part D; Geological Survey of Canada, Paper 90-1D, p. 179–185. https://doi.org/10.4095/131353

Bernier, J.E., 1911. Report on the Dominion Government Expedition to the northern waters and Arctic Archipelago of the D.G.S. "Arctic" in 1910, under command of J.E. Bernier, Officer in Charge and Fishery Officer; Government Printing Bureau, Ottawa, Ontario, 161 p.

Bernier, J.E., 1939. Master Mariner and Arctic Explorer: a Narrative of Sixty Years at Sea from the Logs and Yarns of Captain J.E. Bernier; Le Droit, Ottawa, Ontario, 409 p.

Birkelund, T., 1965. Ammonites from the Upper Cretaceous of West Greenland; Meddelelser om Grønland, v. 179, no. 7, 192 p.

Blackadar, R.G. and Davison, W.L., 1968. Geology, Navy Board Inlet, District of Franklin; Geological Survey of Canada, Map 1236A, scale 1:250 000. https://doi.org/10.4095/107498

Braman, D.R. and Sweet, A.R., 2012. Biostratigraphically useful Late Cretaceous-Paleocene terrestrial palynomorphs from the Canadian Western Interior Sedimentary Basin; Palynology, v. 36, Supplement 1, p. 8–35. https://doi.org/10.1080/01916122.2011.642127

Brent, T.A., Chen, Z., Currie, L.D., and Osadetz, K., 2013. Assessment of the conventional petroleum resource potential of Mesozoic and younger structural plays within the proposed National Marine Conservation Area, Lancaster Sound, Nunavut; Geological Survey of Canada, Open File 6954, 44 p. https://doi.org/10.4095/289615

Burden, E. and Holloway, D., 1985. Palynology and age of the Scott Inlet inliers of Baffin Island (Northwest Territories); Canadian Journal of Earth Sciences, v. 22, p. 1542–1545. https://doi.org/10.1139/e85-160

Burden, E.T. and Langille, A.B., 1990. Stratigraphy and sedimentology of Cretaceous and Paleocene strata in half-grabens on the southeast coast of Baffin Island, Northwest Territories; Bulletin of Canadian Petroleum Geology, v. 38, no. 2, p. 185–196.

Burden, E.T. and Langille, A.B., 1991. Palynology of Cretaceous and Tertiary strata, northeast Baffin Island, Northwest Territories, Canada: implications for the history of rifting in Baffin Bay; Palynology, v. 15, p. 91–114. https://doi.org/10.1080/01916122.1991.9989392

Clarke, D.B., 1968. The basalts of Svartenhuk Peninsula, progress report; Grønlands Geologiske Undersøgelse, Rapport, v. 15, p. 15–17.

Clarke, B.S., 1976. Tertiary and Mesozoic stratigraphy of Bylot Island, N.W.T.; report prepared for Norlands Petroleum Limited; on file with the Canada Energy Regulator, Calgary, Alberta, National Energy Board Report 511-1-12-21, 81 p.

Clarke, D.B. and Upton, B.G.J., 1971. Tertiary basalts of Baffin Island: field relations and tectonic setting; Canadian Journal of Earth Sciences, v. 8, p. 248–258. https://doi.org/10.1139/e71-025

Cohen, K.M., Finney, S.C., Gibbard, P.L., and Fan, J.-X., 2013. The ICS International Chronostratigraphic Chart; Episodes, v. 36, p. 199–204 (version updated 2021). <http://www.stratigraphy.org/ICSchart/ChronostratChart2021-05.pdf>

Csank, A.Z., Fortier, D., and Leavitt, S.W., 2013. Annually resolved temperature reconstructions from a late Pliocene–early Pleistocene polar forest on Bylot Island, Canada; Palaeogeography, Palaeoclimatology, Palaeoecology, v. 369, p. 313–322. https://doi.org/10.1016/j.palaeo.2012.10.040

Currie, L.D., Brent, T.A., and Turner, E.C., 2020. Offshore bedrock geology of Eclipse Sound and Pond Inlet: connecting the structure and stratigraphy of Bylot and northern Baffin islands; Canadian Journal of Earth Sciences, v. 57, no. 10, p. 1254–1267. https://doi.org/10.1139/cjes-2019-0159

Dafoe, L.T. and Haggart, J., 2018. Ichnology and sedimentology of Cretaceous and Paleogene strata on Bylot Island, Nunavut: development of a rift-basin succession in Baffin Bay; Atlantic Geoscience Society, 44th Colloquium and Annual General Meeting, Program and Abstracts, p. 19–20.

Dafoe, L.T., Haggart, J.W., Williams, G.L., and Stimson, M., 2019a. Ichnology and paleoenvironmental interpretations of the Cretaceous–Paleocene rift succession of northeast Baffin Island region, Nunavut, Canada; American Association of Petroleum Geologists (AAPG), Annual Convention and Exhibition, p. 1–2 (abstract).

Dafoe, L.T., Haggart, J.W., and Williams, G.L., 2019b. Onshore-offshore comparisons of the Cretaceous and Paleogene strata from Bylot Island and the western Baffin Bay margin, Nunavut; Atlantic Geoscience Society, 45th Colloquium and Annual General Meeting, Fredericton, New Brunswick, February 8–9, 2019, Program and Abstracts, p. 24–25.

Dixon, J., Hopkins, W.S., Jr., and Dixon, O.A., 1973. Upper Cretaceous marine strata on Somerset Island, N.W.T; Canadian Journal of Earth Sciences, v. 10, p. 1337–1339. https://doi.org/10.1139/e73-118

Fenton, J.P.G. and Pardon, A.M., 2007. Sequence stratigraphic correlation of Cretaceous–Palaeogene strata, Labrador Sea and Davis Strait. Biostratigraphic and sequence stratigraphic correlation of 33 wells. Volume 1: text, figures and appendices. Report No. 6851/Ib, Project No. Ib/GF556; report prepared for Fugro Robertson Limited, Llandudno, United Kingdom, on file at Canada–Newfoundland and Labrador Offshore Petroleum Board, St. John's, Newfoundland and Labador, 193 p.

Feyling-Hanssen, R.W., 1976. The stratigraphy of the Quaternary Clyde Foreland Formation, Baffin Island, illustrated by the distribution of benthic foraminifera; Boreas, v. 5, p. 77–94. https://doi.org/10.1111/j.1502-3885.1976.tb00333.x

Galloway, J.M., Sweet, A.R., Pugh, A., Schröder-Adams, C.J., Swindles, G.T., Haggart, J.W., and Embry, A.F., 2012. Correlating middle Cretaceous palynological records from the Canadian High Arctic based on a section from the Sverdrup basin and samples from the Eclipse Trough; Palynology, v. 36, no. 2, p. 277–302. https://doi.org/10.1080/01916122.2012.670411

Gautier, D.L., Bird, K.J., Charpentier, R.R., Grantz, A., Houseknecht, D.W., Klett, T.R., Moore, T.E., Pitman, J.K., Schenk, C.J., Schuenemeyer, C.J., Sørensen, K., Tennyson, M.E., Valin, Z.C., and Wandrey, C.J., 2009. Assessment of undiscovered oil and gas in the Arctic; Science, v. 324, p. 1175–1179. https://doi.org/10.1126/science.1169467

Gregersen, U., Hopper, J.R., and Knutz, P.C., 2013. Basin seismic stratigraphy and aspects of prospectivity in the NE Baffin Bay, northwest Greenland; Marine and Petroleum Geology, v. 46, p. 1–18. https://doi.org/10.1016/j.marpetgeo.2013.05.013

Haggart, J.W., Sweet, A.R., Williams, G.L., Currie, L., McNicoll, V., Burden, E.T., Benham, P.H., and Galloway, J., 2011. Paleoenvironments and correlation of Cretaceous-Paleogene strata, Bylot Island, Nunavut; AAPG Meeting - the Polar Petroleum Potential Conference & Exhibition, Halifax, Nova Scotia, AAPG Search and Discovery Article, 1 p. (abstract).

Haggart, J.W., Burden, E.T., Clark, K., Currie, L.D., Dafoe, L.T., Enoogoo, J., Herrle, J.O., Schröder-Adams, C.J., Sweet, A.R., Williams, G.L., and Fensome, R.A., 2017. Report of activities 2017, GEM-2 Baffin Project: Onshore Cretaceous-Paleogene Stratigraphic Studies, Northern Baffin Bay Region; Geological Survey of Canada, Open File 8324, 10 p. https://doi.org/10.4095/306084

Haggart, J.W., Dafoe, L.T., Tremblay, T., Burden, E.T., Williams, G.L., Fensome, R.A., Currie, L.D., Enoogoo, J., Clark, K., Herrle, J.O., and Schröder-Adams, C.J., 2018. Onshore Cretaceous-Paleogene Stratigraphic Studies, Nunavut: GEM-2 Baffin Project, Report of Activities 2018; Geological Survey of Canada, Open File 8475, 9 p. https://doi.org/10.4095/311303

Harrison, J.C., Mayr, U., McNeil, D.H., Sweet, A.R., McIntyre, D.J., Eberle, J.J., Harington, C.R., Chalmers, J.A., Dam, G., and Nøhr-Hansen, H., 1999. Correlation of Cenozoic sequences of the Canadian Arctic region and Greenland; implications for the tectonic history of northern North America; Bulletin of Canadian Petroleum Geology, v. 47, p. 223–254.

Harrison, J.C., Brent, T.A., and Oakey, G.N., 2006. Bedrock geology of the Nares Strait region of Arctic Canada and Greenland with explanatory text and GIS content; Geological Survey of Canada, Open File 5278, 61 p. https://doi.org/10.4095/222524

Harrison, J.C., Brent, T.A., and Oakey, G.N., 2011. Baffin Fan and its inverted rift system of Arctic eastern Canada: stratigraphy, tectonics and petroleum resource potential; *in* Arctic Petroleum Geology, (ed.) A. Spencer, A. Embry, D. Gautier, A. Stoupakova, and K. Sørensen; Geological Society of London, Memoir 35, p. 595–626. https://doi.org/10.1144/M35.40

Haughton, S., 1859. Geological account of the Arctic Archipelago, drawn up principally from the specimens collected by Captain F.L. M'Clintock, R.N., from 1849-1859; App. IV *in* The voyage of the 'Fox' in the Arctic seas. A narrative of the discovery of the fate of Sir John Franklin and his companions, by F.L. M'Clintock; John Murray, London, United Kingdom, p. 372–399.

Henderson, G., Rosenkrantz, A., and Schiener, E.J., 1976. Cretaceous–Tertiary sedimentary rocks of West Greenland; *in* Geology of Greenland, (ed.) A. Escher and W.S. Watt; Geological Survey of Greenland, Copenhagen, Denmark, p. 340–362.

Holloway, D.C., 1984. Palynomorph biostratigraphy of coastal sediments from eastern Baffin Island; B.Sc. thesis, Memorial University of Newfoundland, St. John's, Newfoundland and Labrador, 52 p.

Ioannides, N.S., 1986. Dinoflagellate cysts from Upper Cretaceous-lower Tertiary sections, Bylot and Devon islands, Arctic Archipelago; Geological Survey of Canada, Bulletin 371, 99 p. https://doi.org/10.4095/123641

Jackson, G.D., 1998. Geology, Okoa Bay-Padloping Island area, District of Franklin, Northwest Territories; Geological Survey of Canada, Open File 3532, scale 1:250 000. https://doi.org/10.4095/209911

Jackson, G.D., 2000. Geology of the Clyde-Cockburn Land map area, north-central Baffin Island, Nunavut; Geological Survey of Canada, Memoir 440, 303 p. https://doi.org/10.4095/211268

Jackson, G.D. and Davidson, A., 1975a. Bylot Island map-area, District of Franklin; Geological Survey of Canada, Paper 74-29, 12 p. https://doi.org/10.4095/102501

Jackson, G.D. and Davidson, A., 1975b. Geology, Bylot Island, District of Franklin; Geological Survey of Canada, Map 1397A, scale 1:250 000. https://doi.org/10.4095/109007

Jackson, G.D. and Morgan, W.C., 1978. Geology, Conn Lake, District of Franklin; Geological Survey of Canada, Map 1458A, scale 1:250 000. https://doi.org/10.4095/109162

Jackson, G.D., Davidson, A., and Morgan, W.C., 1975. Geology of the Pond Inlet map-area, Baffin Island, District of Franklin (38A, 38B, part of 48A); Geological Survey of Canada, Paper 74-25, 33 p. https://doi.org/10.4095/102498

Jackson, G.D., Morgan, W.C., and Davidson, A., 1979. Geology, Buchan Gulf-Scott Inlet, District of Franklin; Geological Survey of Canada, Map 1449A, scale 1:250 000. https://doi.org/10.4095/109159

Kerr, J.W., 1980. Structural framework of Lancaster Aulacogen, Arctic Canada; Geological Survey of Canada, Bulletin 319, 24 p. https://doi.org/10.4095/102164

Kidd, D.J., 1953. Geology; *in* Baffin Island Expedition, 1953: a preliminary field report, by P.D. Baird and other members of the expedition; Arctic, v. 6, p. 240–243.

Kollmann, H.A. and Peel, J.S., 1983. Paleocene gastropods from Nûgssuaq, West Greenland; Grønlands Geologiske Undersøgelse, Bulletin 146, 115 p.

Langille, A.B., 1987. Sedimentology and palynology of Cretaceous and Tertiary strata, southeast Baffin Island, Northwest Territories, Canada; B.Sc. thesis, Memorial University of Newfoundland, St. John's, Newfoundland and Labrador, 163 p.

Langille, A.B., Burden, E.T., Sears, W.B., and Holloway, D.C., 1986. Geological investigation of Cretaceous? strata beneath Cape Dyer Basalts (Paleocene?), Baffin Island, District of Franklin; *in* Current Research, Part A; Geological Survey of Canada, Paper 86-1A, p. 483–488. https://doi.org/10.4095/120412

Levy, E.M., 1978. Visual and chemical evidence for a natural seep at Scott Inlet, Baffin Island, District of Franklin; *in* Current Research, Part B; Geological Survey of Canada, Paper 78-1B, p. 21–26. https://doi.org/10.4095/103569

Levy, E.M. and Ehrhardt, M., 1981. Natural seepage of petroleum at Buchan Gulf, Baffin Island; Marine Chemistry, v. 10, p. 355–364. https://doi.org/10.1016/0304-4203(81)90014-1

Loncarevic, B.D. and Falconer, R.K., 1977. An oil slick occurrence off Baffin Island; Geological Survey of Canada, Paper 77-1A, p. 523–524. https://doi.org/10.4095/102743

Low, A.P., 1906. Cruise of the *Neptune* - report on the Dominion Government Expedition to Hudson Bay and the Arctic Islands on board the D.G.S. *Neptune*, 1903-1904; Government Printing Bureau, Ottawa, 355 p., 1 map, scale 1:3 168 000. https://doi.org/10.4095/216126

MacLean, B., Falconer, R.K.H., and Clarke, D.B., 1978. Tertiary basalts of western Davis Strait: bedrock core samples and geophysical data; Canadian Journal of Earth Sciences, v. 15, no. 5, p. 773–780. https://doi.org/10.1139/e78-083

MacLean, B., Williams, G., and Zhang, S., 2014. New insights into the stratigraphy and petroleum potential of the Baffin shelf's Cretaceous rocks; Bulletin of Canadian Petroleum Geology, v. 62, no. 4, p. 289–310. https://doi.org/10.2113/gscpgbull.62.4.289

McMillan, J.G., 1910. Report of J.G. McMillan, geologist of the '*Arctic*' Expedition, 1908-1909; *in* Report on the Dominion of Canada Government Expedition to the Arctic Islands and Hudson Strait on board the D.G.S. '*Arctic*', (ed.) J.E. Bernier; Government Printing Bureau, Ottawa, Ontario, p. 382–491.

McWhae, J.R.H., 1981. Structure and spreading history of the northwestern Atlantic region from the Scotian Shelf to Baffin Bay; *in* Geology of the North Atlantic Borderlands, (ed.) J.W. Kerr and A.J. Fegusson; Canadian Society of Petroleum Geologists, Memoir 7, p. 299–332.

McWhae, J.R.H., Gunther, P.R., and Shade, B., 1979. Canadian Arctic Islands geological field operation (Lancaster Sound segment); Indian and Northern Affairs Department, Canada, Canadian Oil and Gas Lands Administration report, 319 p.

Miall, A.D., 1986. The Eureka Sound Group (Upper Cretaceous - Oligocene), Canadian Arctic Islands; Bulletin of Canadian Petroleum Geology, v. 34, no. 2, p. 240–270.

Miall, A.D., 1988. The Eureka Sound Group: alternative interpretations of the stratigraphy and paleogeographic evolution - Discussion; *in* Current Research, Part D; Geological Survey of Canada, Paper 88-1D, p. 143–147. https://doi.org/10.4095/122672

Miall, A.D., 1991. Late Cretaceous and Tertiary basin development and sedimentation, Arctic Islands; Chapter 15 *in* Geology of the Innuitian Orogen and Arctic Platform of Canada and Greenland, (ed.) H.P. Trettin; Geological Survey of Canada, Geology of Canada no. 3, p. 437–458 (*also* Geological Society of America, The Geology of North America, v. E, p. 437–458). https://doi.org/10.4095/133997

Miall, A.D., Balkwill, H.R., and Hopkins, W.W., 1980. Cretaceous and Tertiary sediments of Eclipse Trough, Bylot Island area, Arctic Canada, and their regional setting; Geological Survey of Canada, Paper 79-23, 20 p. https://doi.org/10.4095/102162

Miller, G.H., Andrews, J.T., and Short, S.K., 1977. The last interglacial–glacial cycle, Clyde foreland, Baffin Island, N.W.T.: stratigraphy, biostratigraphy, and chronology; Canadian Journal of Earth Sciences, v. 14, p. 2824–2857. https://doi.org/10.1139/e77-249

Mohr, C.B., 1925. Report of analysis; Canada Department of Mines, Laboratory of Fuel Testing Station, Report No. 778, Canada Department of Mines, Ottawa, Ontario, 1 p.

Newman, L.A., 1987. Quaternary stratigraphy of the Scott Lowland, Baffin Island, Northwest Territories; B.Sc. thesis, Memorial University of Newfoundland, St. John's, Newfoundland and Labrador, 53 p.

Noe-Nygaard, A., 1942. On the geology and petrography of the West Greenland basalt province. Part III. The plateaubasalts of Svartenhuk Peninsula; Meddelelser om Grønland, v. 137, no. 3, 78 p.

Nøhr-Hansen, H., Williams, G.L., and Fensome, R.A., 2016. Biostratigraphic correlation of the western and eastern margins of the Labrador-Baffin Seaway and implications for the regional geology; Geological Survey of Denmark and Greenland, Bulletin 37, 74 p.

Piraux, O., 2004. Contexte paléogéographique de la forêt fossile de l'Île Bylot, Arctique canadien; M.Sc. thesis, Université Laval, Québec, Quebec, 124 p.

Ravn, J.P.J., 1918. De marine Kridtaflejringer I Vest-Grønland og deres fauna; Meddelelser om Grønland, v. 56, no. 9, p. 309–380.

Refsnider, K.A., Miller, G.H., Hillaire-Marcel, C., Fogel, M.L., Ghaleb, B., and Bowden, R., 2012. Subglacial carbonates constrain basal conditions and oxygen isotopic composition of the Laurentide Ice Sheet over Arctic Canada; Geology, v. 40, no. 2, p. 135–138. https://doi.org/10.1130/G32335.1

Research Council of Alberta, 1940. Sample of coal from Pond Inlet, Baffin Island, sent by J.A. Watson, Hudson's Bay Co.; Research Council of Alberta, report, 1 p.

Ricketts, B.D., 1986. New formations in the Eureka Sound Group, Canadian Arctic Islands; *in* Current Research, Part B; Geological Survey of Canada, Paper 86-1B, p. 363–374. https://doi.org/10.4095/120661

Ricketts, B.D., 1991. Delta evolution in the Eureka Sound Group, western Axel Heiberg Island: the transition from wave-dominated to fluvial-dominated deltas; Geological Survey of Canada, Bulletin 402, 72 p. https://doi.org/10.4095/132169

Ricketts, B.D., 1994. Basin analysis, Eureka Sound Group, Axel Heiberg and Ellesmere islands, Canadian Arctic Archipelago; Geological Survey of Canada, Memoir 439, 126 p. https://doi.org/10.4095/194814

Rosenkrantz, A., Noe-Nygaard, A., Gry, H., Munck, S., and Laursen, D., 1942. A geological reconnaissance of the southern part of the Svartenhuk Peninsula West Greenland; Meddelelser om Grønland, v. 135, no. 3, p. 1–72.

Sanborn-Barrie, M. and Young, M., 2013. Geology, Durban Harbour, Baffin Island, Nunavut; Geological Survey of Canada, Canadian Geoscience Map 38 (preliminary edition), scale 1:100 000. https://doi.org/10.4095/292015

Sanborn-Barrie, M., Young, M., Keim, R., and Hamilton, B., 2013. Geology, Sunneshine Fiord, Baffin Island, Nunavut; Geological Survey of Canada, Canadian Geoscience Map 6 (preliminary edition), scale 1:100 000. https://doi.org/10.4095/288931

Scott, D.J. and de Kemp, E.A., 1998. Bedrock geology compilation, northern Baffin Island and northern Melville Peninsula, Northwest Territories; Geological Survey of Canada, Open File 3633, scale 1:500 000. https://doi.org/10.4095/210024

Sears, W.B., 1986. An investigation of sedimentary outliers on Quqaluit, Padloping and Durban islands, Baffin Island; B.Sc. thesis, Memorial University of Newfoundland, St. John's, Newfoundland and Labrador, 77 p.

Skaarup, N., Jackson, H.R., and Oakey, G., 2006. Margin segmentation of Baffin Bay/Davis Strait, eastern Canada based on seismic reflection and potential field data; Marine and Petroleum Geology, v. 23, no. 1, p. 127–144. https://doi.org/10.1016/j.marpetgeo.2005.06.002

Skipton, D.R., Saumur, B.M., St-Onge, M.R., Bros, E.R., Acosta-Gongora, P., Kelly, C.J., O'Brien, M.E., Weller, O.M., and Johnston, S.T., 2020. Bedrock geology, Barnes Ice Cap northwest, Baffin Island, Nunavut, NTS 37-E west; Geological Survey of Canada, Canadian Geoscience Map 402, scale 1:100 000. https://doi.org/10.4095/314657

Sparkes, K.E., 1989. Stratigraphy and terrestrial palynology of Late Cretaceous Eclipse Group strata, Bylot Island, Northwest Territories, Canada; B.Sc. thesis, Memorial University of Newfoundland, St. John's, Newfoundland and Labrador, 195 p.

St-Onge, M.R., Jackson, G.D., and Henderson, I., 2006. Geology, Baffin Island (south of 70°N and east of 80°W), Nunavut; Geological Survey of Canada, Open File 4931, scale 1:500 000. https://doi.org/10.4095/222520

St-Onge, M.R., Van Gool, J.A.M., Garde, A.A., and Scott, D.J., 2009. Correlation of Archaean and Palaeoproterozoic units between northeastern Canada and western Greenland: constraining the pre-collisional upper plate accretionary history of the Trans-Hudson orogen; Geological Society of London, Special Publications, v. 318, p. 193–235. https://doi.org/10.1144/SP318.7

Sutherland, P.C., 1853. On the geological and glacial phænomena of the coasts of Davis' Strait and Baffin's Bay; Quarterly Journal of the Geological Society of London, v. 9, p. 296–312. https://doi.org/10.1144/GSL.JGS.1853.009.01-02.45

Swartzman, E., 1947a. Report on a study of the physical and chemical characteristics of coal occurring at Pond Inlet, Baffin Island, Northwest Territories; Canada Bureau of Mines, Fuel Research Laboratories, Report No. 58, 26 p.

Swartzman, E., 1947b. Concluding report on the briquetting amenability of coal from Pond Inlet, Salmon River, Baffin Island, conducted for the Administration of the Northwest Territories; Canada Bureau of Mines, Fuel Research Laboratories, Report No. 64, 17 p.

Waterfield, J.J., 1989. Stratigraphy, sedimentology and palynology of Cretaceous and Tertiary strata, southwest Bylot Island, Northwest Territories, Canada; M.Sc. thesis, Memorial University of Newfoundland, St. John's, Newfoundland and Labrador, 260 p.

Weeks, L.J., 1927. The geology of parts of eastern Arctic Canada; Geological Survey of Canada, Summary Report, 1925 Part C, p. 136C–141C. https://doi.org/10.4095/103442

Wiseman, T.R., 1991. Sedimentology of the Maastrichtian, Pond Inlet formation (channelized turbidite system), Bylot Island, Northwest Territories, Canada; B.Sc. thesis, Memorial University of Newfoundland, St. John's, Newfoundland and Labrador, 133 p.

Contents

Stratigraphy of the Labrador margin: a synthesis and new perspectives

L.T. Dafoe[1*], K. Dickie[1], G.L. Williams[1], and T. McCartney[1]

Dafoe, L.T., Dickie, K., Williams, G.L., and McCartney, T., 2022. Stratigraphy of the Labrador margin: a synthesis and new perspectives; in *Geological synthesis of Baffin Island (Nunavut) and the Labrador–Baffin Seaway, (ed.) L.T. Dafoe and N. Bingham-Koslowski; Geological Survey of Canada, Bulletin 608, p. 137–180. https://doi.org/10.4095/321829*

Abstract: The Labrador Sea formed during rifting between North America and Greenland beginning in the Early Cretaceous, with subsequent seafloor spreading from the Maastrichtian (chron C31) to Early Paleocene (chron C27n) that ended by chron C13 (earliest Oligocene). Early Cretaceous rifting resulted in accumulation of Alexis Formation basalt units and Bjarni Formation nonmarine and marginal marine clastic rocks. In the Late Cretaceous, extension focused further offshore as sag basin conditions formed across the shelf, with a basinwide transgression of Markland Formation shale and localized Freydis Member sandstone development. A Middle Paleocene to Early Eocene regression formed Gudrid Formation shoreline sandstone units, with correlative Cartwright Formation marine shale units. This was followed by an Early Eocene transgression of the Kenamu Formation and Middle Eocene Leif Member shoreline development. During the Late Eocene through Pleistocene, transgression took place once again at the base of the Mokami Formation, with subsequent development of the partly correlative shallow-marine sandstone units of the Saglek Formation.

Résumé : La mer du Labrador s'est formée à la faveur du rifting entre l'Amérique du Nord et le Groenland, à partir du Crétacé précoce, et de l'expansion subséquente des fonds marins qui s'est amorcée entre le Maastrichtien (chrone C31) et le Paléocène précoce (chrone C27n), pour prendre fin au chrone C13 (Oligocène initial). Le rifting du Crétacé précoce a entraîné l'accumulation des unités de basalte de la Formation d'Alexis et des roches clastiques non marines et margino-marines de la Formation de Bjarni. Au Crétacé tardif, l'extension était concentrée plus loin au large alors que des conditions de bassin d'affaissement s'établissaient sur la plate-forme continentale et que se déposaient, à la faveur d'une transgression s'étendant à l'ensemble du bassin, le shale de la Formation de Markland et, de manière plus localisée, le grès du Membre de Freydis. Une régression du Paléocène moyen à l'Éocène précoce a entraîné le dépôt des grès littoraux de la Formation de Gudrid et des shales marins corrélatifs de la Formation de Cartwright. Une transgression subséquente s'est traduite par le dépôt de la Formation de Kenamu à l'Éocène précoce et des unités littorales du Membre de Leif à l'Éocène moyen. Au cours de l'Éocène tardif et du Pléistocène, une transgression s'est de nouveau déroulée, se manifestant initialement par le dépôt de la Formation de Mokami et, par la suite, par celui des grès de milieu marin peu profond, en partie corrélatifs, de la Formation de Saglek.

[1]Geological Survey of Canada, 1 Challenger Drive, P.O. Box 1006, Dartmouth, Nova Scotia B2Y 4A2
*Corresponding author: L.T. Dafoe (email: Lynn.Dafoe@nrcan-rncan.gc.ca)

INTRODUCTION

The continental margin of Labrador borders the western edge of the Labrador Sea, is about 1000 km in length, and includes the offshore region between approximately latitude 54–61°N and longitude 45–65°W, forming the southwestern portion of the Labrador–Baffin Seaway (Fig. 1). This continental margin evolved as a result of rifting during the Early Cretaceous as Greenland began separating from the paleo-North American Plate (Roest and Srivastava, 1989). Rifting along the Labrador margin was initially focused under the present-day shelf and slope creating large, northwest-southeast oriented half-grabens and grabens that infilled with syn-rift sediments (Bell, 1989). Extension continued into the Late Cretaceous, but was concentrated farther offshore (Dickie et al., 2011). The onset of seafloor spreading started at chron C31 in the Maastrichtian along the central Labrador margin (Keen et al., 2018a) and by chron C27n (Danian) along the northern part of the margin (Keen et al., 2018b). The direction of seafloor spreading changed between chron C25n and C24n (Thanetian) to be more east-west, resulting in a change in orientation of the spreading centre and fracture zones, as well as substantial strike-slip motion to the north in Davis Strait. Spreading ended by chron C13 near the Eocene–Oligocene boundary (Oakey and Chalmers, 2012).

This tectonic history shaped the development of the Labrador margin, and following early exploration efforts in the region, the margin was studied from a structural, stratigraphic, and petroleum systems perspective (e.g. McMillan, 1973, 1980; Srivastava et al., 1981; Balkwill, 1987; Bell, 1989; Balkwill and McMillan, 1990; Bell and Campbell, 1990; Dickie et al., 2011). The region was subdivided into the Hopedale and Saglek basins, substantial depocentres located to the south and north, respectively (Fig. 1). The Okak Arch, a prominent basement high, separates these basins (Fig. 2; McMillan, 1980; Balkwill, 1987). The Hopedale Basin extends south of the Okak Arch to the Cartwright Arch (McMillan, 1980), a basement feature likely underlain by Proterozoic rocks of the Grenville Province (Fig. 2; Funck et al., 2001). The margin along the seaward edge of the Hopedale Basin is considered to be magma-poor and is underlain by a zone of serpentinized and possibly exhumed continental mantle (Fig. 2; Keen et al., 2018a). The Saglek Basin extends northward from the Okak Arch to the Lady Franklin Arch, offshore southeast Baffin Island (Balkwill, 1987). The central and northern portions of this basin lie near the Ungava Fault Zone, an area of regional transform, strike-slip motion (Fig. 2; Oakey and Chalmers, 2012). The Labrador Sea Basin includes the central Labrador Sea region, which is underlain by oceanic crust (Balkwill and McMillan, 1990). A regional sediment thickness map is presented in Keen et al. (this volume), showing the two major depocentres of the Hopedale and Saglek basins. Other basins have been mapped along the Labrador margin, but these have not been formally described (*see* https://www.cnlopb.ca/information/maps).

Major volcanism occurred in the region in the Paleocene and Eocene, beginning around chron C27n, at the onset of region-wide seafloor spreading and is thought to be linked to the arrival of a mantle plume in Davis Strait at about 61 Ma (Storey et al., 1998, 2007; Larsen et al., 2009). Much of the volcanism is focused along the magma-rich extensional margin segment north of the Snorri Fracture Zone (Fig. 2). Here, Keen et al. (2012) defined elements of a typical volcanic margin, including seaward-dipping reflectors, lava delta escarpments, and inner flows (cf. Planke et al., 2000). Keen et al. (2018b) interpreted this magma-rich margin to have developed following magma-poor conditions in which a transition zone of possible serpentinized mantle developed seaward of extended continental crust (*see also* Keen et al., this volume). Evidence of later magmatism is also recorded in volcanic rocks within overlying Eocene strata (Keen et al., 2018b, their Fig. 2). Although the focus of magmatic activity is along the northern Labrador margin, thin volcanic intervals extend south into the Hopedale Basin, where they overlie parts of the magma-poor margin (Chian et al., 1995; Keen et al., 2012, 2018a, this volume).

The stratigraphic succession encountered in wells along the present-day Labrador Shelf includes a Lower Cretaceous syn-rift fill, an Upper Cretaceous sag-basin or late rift unit (Dickie et al., 2011), and a subsequent post-rift succession from the late Maastrichtian to late Eocene which is then covered by postdrift deposition (Keen et al., 2018a). Industry exploration took place in the 1970s and early 1980s, with 26 wells drilled during that time, and subsequent interest has resulted in further seismic data collection along the margin. Umpleby (1979) was the first to develop a stratigraphic framework for the Labrador margin based on some of the early wells drilled on the Labrador Shelf, which included four formations and associated members. This work was subsequently revised in McWhae et al. (1980) into the eight formations still recognized today: Alexis, Bjarni (Snorri Member), Markland (Freydis Member), Cartwright, Gudrid, Kenamu (Brown Mudstone and Leif members), Mokami, and Saglek (Fig. 3).

In studying the Eastern Canadian margin, McWhae (1981) defined five regional unconformities tied to the stratigraphy of offshore Labrador. An initial chronostratigraphic chart for the Labrador margin was then developed by Balkwill (1987) and included rift, drift, and post-drift megasequences. Following this, Moir (1989) presented a revised lithostratigraphic assessment of the Labrador margin wells, and discussed the validity of the lithostratigraphic nomenclature, which was further refined by Balkwill and McMillan (1990) based on the available well and seismic data at that time. Since these earlier studies, additional work has been conducted on the lithostratigraphy and seismic stratigraphy of the region (e.g. Jauer et al., 2009; Wielens and Williams, 2009; Dickie et al., 2011; Jauer et al., 2014). An updated tectonostratigraphic chart was presented by Dickie et al. (2011) using modern seismic data and revised biostratigraphic control. The petroleum potential of the region has also been refined (Jauer et al., 2014; Carey et al., 2020; Bingham-Koslowski, McCartney, and Bojesen-Koefoed, this volume). Biostratigraphic assessments have provided vital age constraints, as well as paleoenvironmental determinations and key studies have included assessment of palynomorphs (Williams and Bujak, 1977; Barss et al., 1979; Bujak Davies Group, 1989a; Fenton and Pardon, 2007; Ainsworth et al., 2014, 2016; Fensome, 2015; Nøhr-Hansen et al., 2016; Dafoe and Williams, 2020a, b) and foraminifera (Gradstein and Williams, 1976; Gradstein and Srivastava, 1980; Bujak Davies Group, 1989a; Ainsworth et al., 2014, 2016), with limited control from nannofossils (J.A. Crux, and G. Gard, unpub. rept., 2004).

This paper summarizes previous studies relating to the stratigraphy of the Labrador margin, and also presents new results based on analyses and integration of existing interpretations with new regional seismic mapping. Specifically, the present study illustrates and describes new interpretations relating to revisions of the lithostratigraphy, key seismic profiles, and distribution maps of three main intervals: Cretaceous, lower Cenozoic, and upper Cenozoic.

DATA AND METHODS

The study region encompasses the offshore Labrador margin including the Hopedale Basin and the southern portion of the Saglek Basin, south of Hudson Strait (Fig. 1), as well as the central Labrador Sea, with interpretations extending offshore to the Greenland (Denmark) 200 nautical mile (nm) territorial boundary (data shown in maps are contained in the GIS data included with this volume). Overall, the southern portion of the Saglek Basin shows a fairly continuous genetic relationship with the Hopedale Basin. This is in contrast to the northern portion of the Saglek Basin, a transform margin that has been subjected to extensive Paleocene volcanism and is filled with siliciclastic rocks that are indicative of shallower depositional setting in the Davis Strait (Miller and D'Eon, 1987; Dafoe, DesRoches, and Williams, this volume).

Well data

This region includes 20 industry exploration wells drilled between 1971 and 1983 in the Hopedale Basin and six wells in the southern portion of the Saglek Basin (Fig. 1; Table 1). Data sets collected from these wells and released from confidentiality can be obtained from the Canada–Newfoundland and Labrador Offshore Petroleum Board (www.cnlopb.ca). General information about these wells is also on the BASIN Database (http://basin.gdr.nrcan.gc.ca). Lithological logs are primarily sourced from Canstrat (http://canstrat.com). Existing well data used in the present study include well history reports, biostratigraphic reports, well logs (note that sonic velocity is the inverse of sonic transit time shown in the well plots), lithological summaries, and lithostratigraphic compilations. Determination of the biostratigraphy

→

Figure 1. The Labrador margin and central Labrador Sea study region showing bathymetry (General Bathymetric Chart of the Oceans, 2014), as well as the location of released multichannel seismic data (select unreleased data are also shown) and industry exploration wells. Basin outlines are from Keen et al. (this volume). L1 and L2 indicate the seismic reflection lines 1 and 2 shown in Figure 9. Additional projection information: Central Meridian = 60°W; Standard Parallels = 65, 75°W; Latitude of Origin = 65°N.

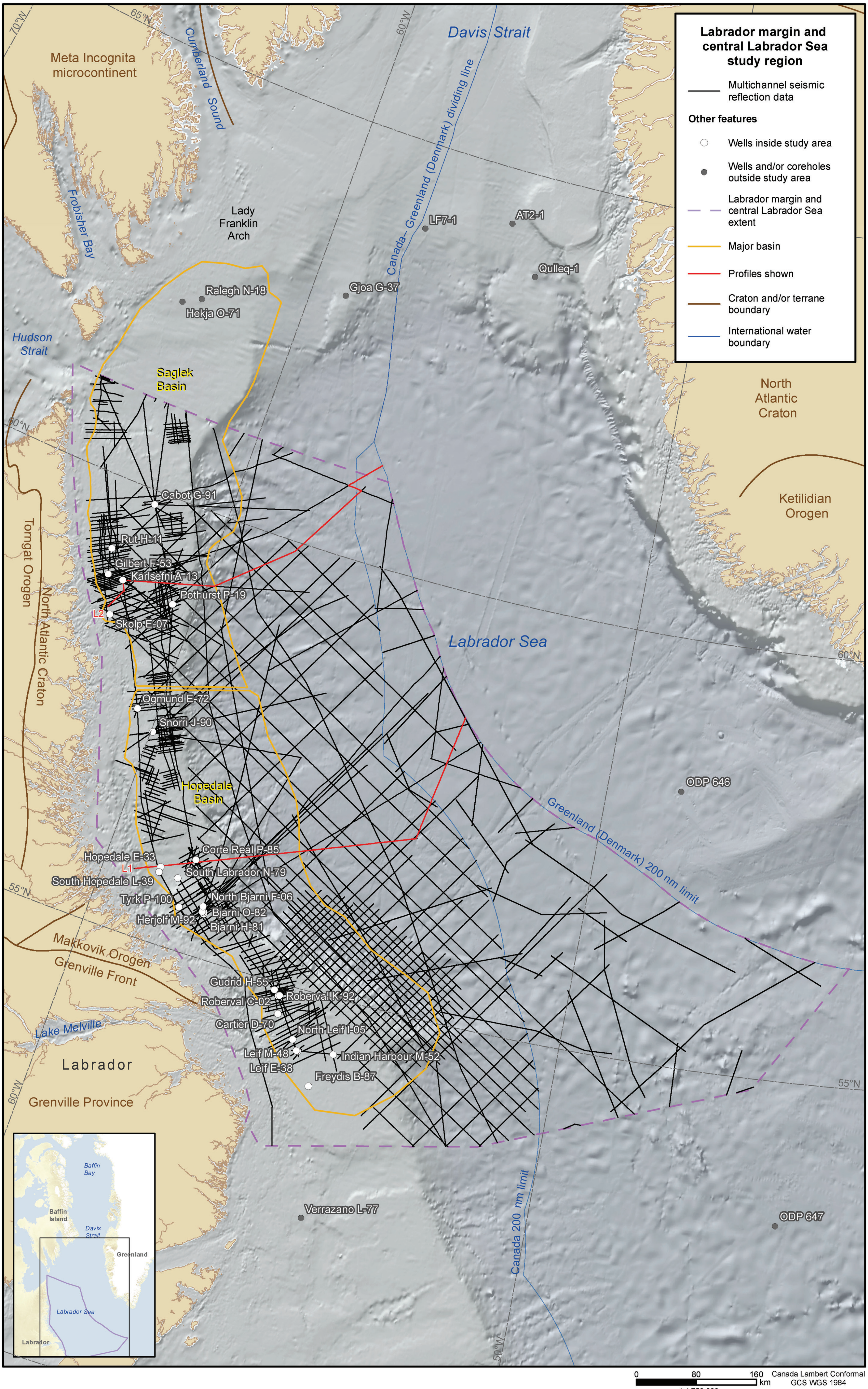
Labrador margin and central Labrador Sea study region
Multichannel seismic reflection data
Other features
Wells inside study area
Wells and/or coreholes outside study area
Labrador margin and central Labrador Sea extent
Major basin
Profiles shown
Craton and/or terrane boundary
International water boundary
70°W
65°N
60°W
Davis Strait
Meta Incognita microcontinent
Cumberland Sound
Canada- Greenland (Denmark) dividing line
Frobisher Bay
Lady Franklin Arch
LF7-1
AT2-1
Qulleq-1
Ralegh N-18
Hekja O-71
Gjoa G-37
Hudson Strait
Saglek Basin
North Atlantic Craton
60°N
Ketilidian Orogen
Cabot G-91
Rut H-11
Gilbert F-53
Karlsefni A-13
Pothurst P-19
L2
Skolp E-07
Torngat Orogen
North Atlantic Craton
Labrador Sea
60°N
Ogmund E-72
Snorri J-90
Hopedale Basin
ODP 646
Greenland (Denmark) 200 nm limit
Hopedale E-33
Corte Real P-85
L1
South Labrador N-79
South Hopedale L-39
Tyrk P-100
North Bjarni F-06
Bjarni O-82
Herjolf M-92
Bjarni H-81
55°N
Makkovik Orogen
Grenville Front
Gudrid H-55
Roberval C-02
Roberval K-92
Cartier D-70
North Leif I-05
Lake Melville
Leif M-48
Indian Harbour M-52
Leif E-38
Labrador
Freydis B-87
Grenville Province
60°W
55°N
Verrazano L-77
ODP 647
Canada 200 nm limit
50°W
Baffin Bay
Baffin Island
Davis Strait
Greenland
Labrador Sea
Labrador
0
80
160
km
1:4 750 000
Canada Lambert Conformal
GCS WGS 1984

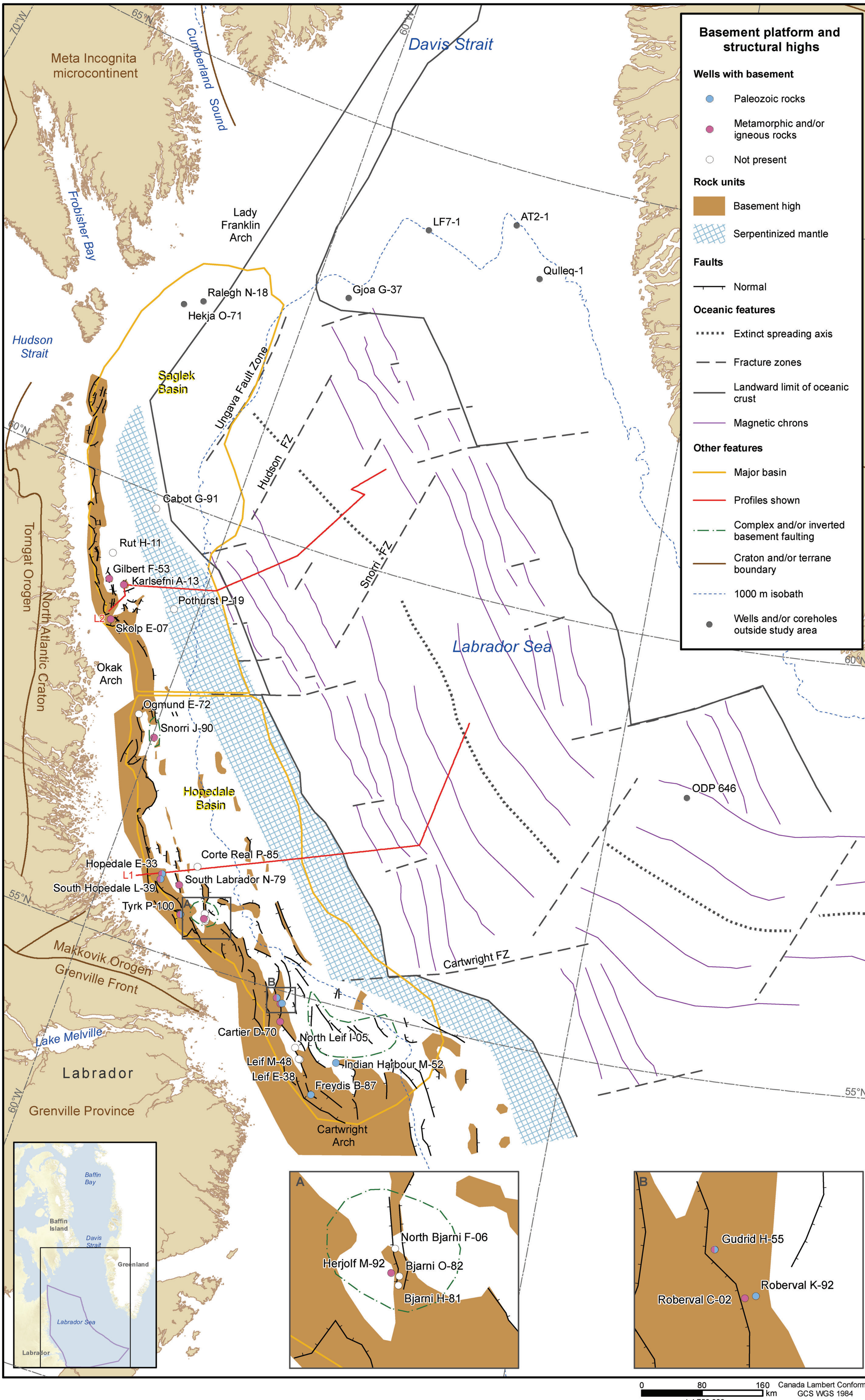
Basement platform and structural highs
Wells with basement
Paleozoic rocks
Metamorphic and/or igneous rocks
Not present
Rock units
Basement high
Serpentinized mantle
Faults
Normal
Oceanic features
Extinct spreading axis
Fracture zones
Landward limit of oceanic crust
Magnetic chrons
Other features
Major basin
Profiles shown
Complex and/or inverted basement faulting
Craton and/or terrane boundary
1000 m isobath
Wells and/or coreholes outside study area
Davis Strait
Labrador Sea
Hudson Strait
Frobisher Bay
Cumberland Sound
Meta Incognita microcontinent
Lady Franklin Arch
Ralegh N-18
Hekja O-71
LF7-1
AT2-1
Qulleq-1
Gjoa G-37
Saglek Basin
Ungava Fault Zone
Hudson FZ
Snorri FZ
Cabot G-91
Rut H-11
Gilbert F-53
Karlsefni A-13
Pothurst P-19
Skolp E-07
L2
Torngat Orogen
North Atlantic Craton
Okak Arch
Ogmund E-72
Snorri J-90
Hopedale Basin
Corte Real P-85
Hopedale E-33
L1
South Labrador N-79
South Hopedale L-39
Tyrk P-100
ODP 646
Makkovik Orogen
Grenville Front
Cartwright FZ
Cartier D-70
North Leif I-05
Leif M-48
Leif E-38
Indian Harbour M-52
Freydis B-87
Cartwright Arch
Lake Melville
Labrador
Grenville Province
65°N
60°N
55°N
70°W
60°W
Baffin Bay
Baffin Island
Davis Strait
Greenland
Labrador Sea
Labrador
A
North Bjarni F-06
Herjolf M-92
Bjarni O-82
Bjarni H-81
B
Gudrid H-55
Roberval K-92
Roberval C-02
0
80
160
km
1:4 750 000
Canada Lambert Conformal
GCS WGS 1984

Figure 2. Distribution map of the pre-rift basement platform and major basement highs in brown. The location of relevant basement rock samples encountered in wells (Precambrian and Paleozoic) is shown. Faults are described further in Keen et al. (this volume). The zone of serpentinized mantle is from Keen et al. (2018a, b, this volume), and basin outlines are from Keen et al. (this volume). L1 and L2 indicate the seismic reflection lines 1 and 2 shown in Figure 9. A well that shows the interval "not present" may not have drilled deep enough to intersect the interval, is cased through that interval, lacks related strata deposited at that location, or associated strata were later removed through erosion. Additional projection information: Central Meridian = 60°W; Standard Parallels = 65, 75°W; Latitude of Origin = 65°N. FZ = Fracture zone.

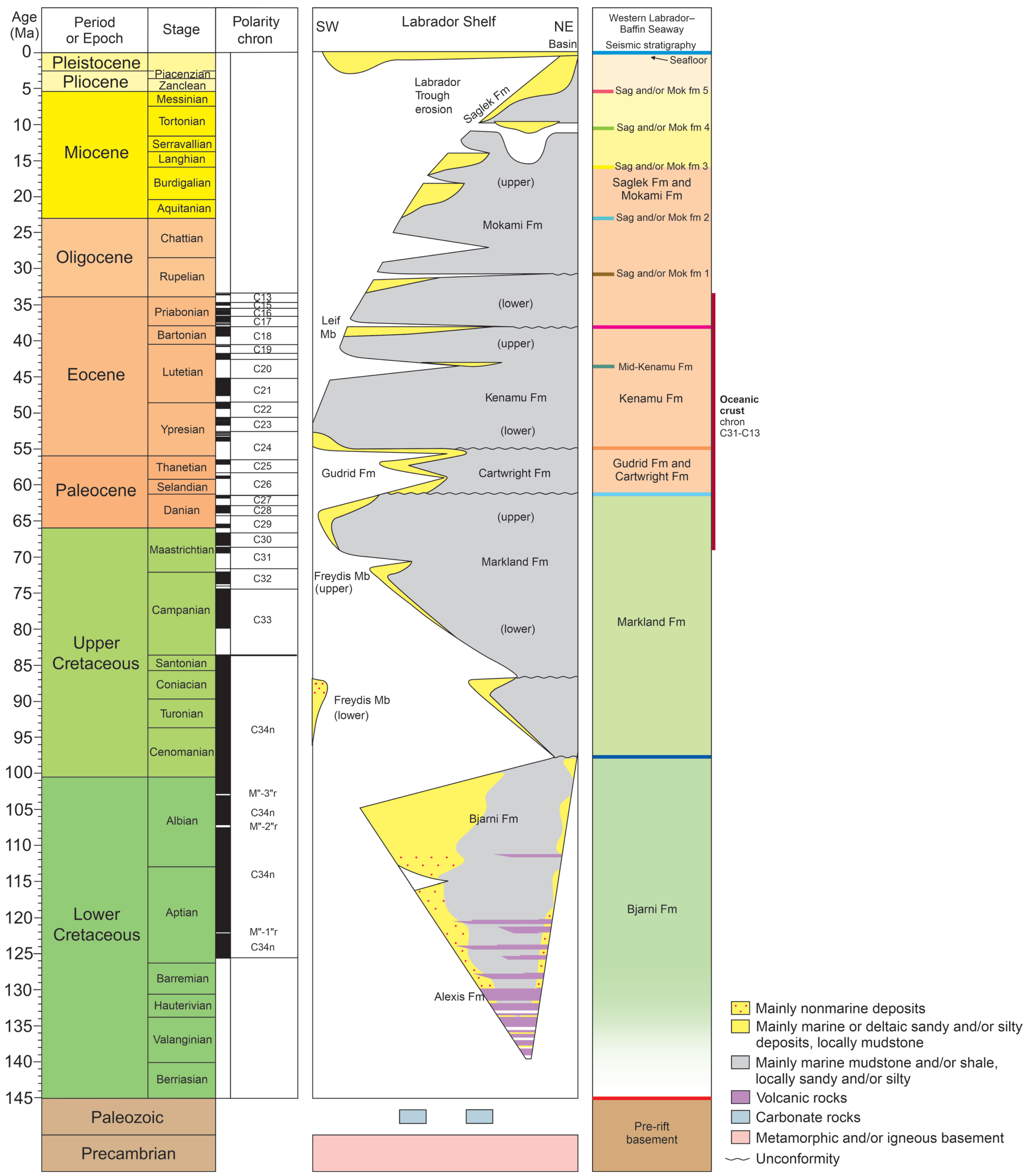

Figure 3. Lithostratigraphic column for the Labrador Shelf modified from Dickie et al. (2011) and Nøhr-Hansen et al. (2016) against the timescale and magnetostratigraphy of Gradstein et al. (2012). The western Labrador–Baffin Seaway seismic stratigraphy is based on the Labrador margin and coloured horizons correspond to those shown in Figure 9. Mok = Mokami, Sag = Saglek.

Table 1. Listing of wells drilled on the Labrador margin with locations in decimal degrees.

Well	Basin	Latitude (°N) (NAD83)	Longitude (°W) (NAD83)	Water depth (m)	Spud date	Operator	Total depth (TD, m)
Bjarni H-81	Hopedale Basin	55.508	57.701	139.0	8/29/1973	Eastcan et al.	2515.2
Bjarni O-82	Hopedale Basin	55.530	57.709	144.0	7/30/1979	Total Eastcan et al.	2650.0
Cabot G-91	Saglek Basin	59.840	61.733	179.8	7/31/1976	Eastcan et al.	289.9
Cartier D-70	Hopedale Basin	54.651	55.674	310.0	9/27/1975	Eastcan et al.	1926.9
Corte Real P-85	Hopedale Basin	56.080	58.202	438.0	10/2/1981	Petro Canada et al.	4551.0
Freydis B-87	Hopedale Basin	53.937	54.710	178.6	7/2/1975	Eastcan et al.	2314.0
Gilbert F-53	Saglek Basin	58.874	62.139	183.0	10/9/1979	Total Eastcan et al.	3608.0
Gudrid H-55	Hopedale Basin	54.908	55.875	299.3	7/14/1974	Eastcan et al.	2839.0
Herjolf M-92	Hopedale Basin	55.532	57.747	139.0	8/28/1976	Eastcan et al.	4086.1
Hopedale E-33	Hopedale Basin	55.874	58.847	549.9	8/9/1978	Chevron et al.	2072.2
Indian Harbour M-52	Hopedale Basin	54.364	54.397	197.8	8/21/1975	BP-Columbia et al.	3958.1
Karlsefni A-13	Saglek Basin	58.871	61.777	174.7	8/10/1975	Eastcan et al.	4148.9
Leif E-38	Hopedale Basin	54.292	55.097	167.6	8/13/1971	Tenneco et al.	1084.2
Leif M-48	Hopedale Basin	54.296	55.121	165.2	8/1/1973	Eastcan et al.	1879.1
North Bjarni F-06	Hopedale Basin	55.592	57.763	150.0	9/28/1980	Petro Canada et al.	2813.0
North Leif I-05	Hopedale Basin	54.411	55.252	144.0	9/14/1980	Petro Canada et al.	3513.0
Ogmund E-72	Hopedale Basin	57.525	60.443	156.2	8/16/1980	Petro Canada et al.	3094.0
Pothurst P-19	Saglek Basin	58.815	60.525	193.0	7/11/1982	Petro Canada et al.	3992.0
Roberval C-02	Hopedale Basin	54.852	55.767	276.0	7/7/1980	Petro Canada et al.	2823.2
Roberval K-92	Hopedale Basin	54.860	55.742	268.5	10/2/1978	Total Eastcan et al.	3874.0
Rut H-11	Saglek Basin	59.171	62.279	124.0	7/14/1981	Petro Canada et al.	4474.0
Skolp E-07	Saglek Basin	58.440	61.768	166.5	7/22/1978	Total Eastcan et al.	2992.0
Snorri J-90	Hopedale Basin	57.329	59.961	140.8	7/28/1975	Eastcan et al.	3209.8
South Hopedale L-39	Hopedale Basin	55.809	58.846	580.0	7/13/1983	Canterra et al.	2364.0
South Labrador N-79	Hopedale Basin	55.813	58.441	449.9	8/3/1980	Chevron et al.	3571.5
Tyrk P-100	Hopedale Basin	55.497	58.230	117.0	7/18/1979	Total Eastcan et al.	1739.0

and paleoenvironments was derived primarily from palynomorphs, but both dinoflagellate cysts (dinocysts) and foraminifera provide good age constraints for Upper Cretaceous and Cenozoic rocks. The authors discuss the biostratigraphy, mainly from a palynological perspective, which includes miospores (spores and pollen) and dinocysts. Whereas most of these analyses have been conducted on cuttings, those of conventional cores have enhanced age control (e.g. Dafoe and Williams, 2020a). Since the compilation of this paper, a revised assessment of the paleoenvironments and lithostratigraphy of the Labrador Shelf wells has been published in Dafoe (2021) and readers are referred to that work for an updated understanding of the wells.

Seismic reflection data

A map showing the location of released and some proprietary, 2-D seismic reflection data, can be found in Figure 1. Data used in the interpretation along the Labrador margin includes a total of over 128 000 line-kilometres. A data set, collected since 2000, constitutes 60% of the total. These modern seismic lines used in this study's interpretation form a regional grid with spacing generally ranging from 10 km to 30 km, with a recording depth of 9 s to 15 s two-way traveltime. These data were acquired using long streamers (generally 8 km or more) and processed using modern demultiple removal algorithms (e.g. "radon") and pre-stack time migration. One survey included pre-stack depth migration. The main companies and/or institutions (contractors) who acquired these data sets include: the Geological Survey of Denmark and Greenland (www.eng.geus.dk/), the Geological Survey of Canada (https://basin.gdr.nrcan.gc.ca/index_e.php), ION Geophysical (www.iongeo.com/), and TGS-NOPEC Geophysical Company ASA (TGS; www.tgs.com).

Other seismic lines interpreted on the Labrador margin are from older, vintage data sets (1972–1992). These were acquired using shorter streamers and with only 6 to 8 s two-way traveltime of data. These lines were processed with older demultiple algorithms and had post-stack rather than pre-stack migration. These data sets were used where modern seismic data coverage was reduced to 30 km spacing or more, primarily north of latitude 58°N. More information regarding seismic surveys on the Labrador margin can be obtained from the regulator, Canada–Newfoundland and Labrador Offshore Petroleum Board at www.cnlopb.ca.

STRATIGRAPHIC FRAMEWORK

Stratigraphic nomenclature

The lithostratigraphy of the Labrador margin has been revised several times, and the general validity of these changes is discussed here. In 1983, the first North American Stratigraphic Code was established by the North American Commission on Stratigraphic Nomenclature. Prior to that, the Committee on Stratigraphic Nomenclature (1933) and the American Commission on Stratigraphic Nomenclature (1961, 1970) published codes, but these were not necessarily applied by Canadian geologists at the time. An International Stratigraphic Guide was, however, developed in 1976 (Hedberg, 1976). Present standards for North American stratigraphy are found within the 2005 North American Stratigraphic Code (North American Commission on Stratigraphic Nomenclature, 2005).

The lithostratigraphy of the Labrador margin was first developed by Umpleby (1979) and modified by McWhae et al. (1980) prior to establishment of the North American Stratigraphic Code. Some further recommended changes to the lithostratigraphy by Balkwill (1987), as well as Balkwill and McMillan (1990) followed the establishment of the 1983 code. The development of the lithostratigraphy of the Labrador margin by the above authors has not always abided by either the International or the North American standards. For example, according to Article 22c of the North American Stratigraphic Code (North American Commission on Stratigraphic Nomenclature, 2005), a type section "can never be changed". It is unclear from the International Stratigraphic Guide, which was in place at the time of McWhae et al.'s (1980) work, whether a type section could be changed to a new locality. Despite this ambiguity, the revised type sections of McWhae et al. (1980) have been accepted. In addition to this, McWhae et al. (1980) 'split' some formations into different units, but retained the original formation name — a practice that is not permitted by the 2005 code, but is not clearly defined in the 1976 Guide; however, under Article 19 in the 2005 North American Stratigraphic Code, revisions of type and reference section boundaries are permitted if the change "will make a unit more natural and useful" (p. 1565, North American Commission on Stratigraphic Nomenclature, 2005). Balkwill (1987) and Balkwill and McMillan (1990) primarily introduced informal members that fall outside stratigraphic codes since they were not formally established or described.

Despite these questions regarding the validity of the lithostratigraphic revisions, the work of Umpleby (1979) and McWhae et al. (1980) formed a sound lithostratigraphic framework. A listing of type and reference sections, established primarily by these authors is found in Table 2, and lithostratigraphic assignments for the wells generally follows that of Moir (1989), which built upon the initial framework and expanded it to wells drilled after 1980. Moir (1989) presented some refinements to the lithostratigraphic picks in several wells, with some changes affecting type and reference sections that are considered revisions in the present study, but were not clearly presented as such in the original work. The present authors use a published lithostratigraphic column (Fig. 3) modified from Dickie et al. (2011) and Nøhr-Hansen et al. (2016).

Lithostratigraphic overview

In this study, the previous work conducted along the Labrador margin is described, but with new interpretation from: the integration of existing studies; revised assessments of the wells; and new, regional seismic mapping. Whereas the Cenozoic succession of the Labrador margin is relatively complete, much of the Eocene to Middle Miocene is missing along the West Greenland margin (Gregersen et al., 2013, 2018, 2019, this volume). To show regional correlations for the entire Labrador–Baffin Seaway, Dafoe, Williams et al. (this volume) divide the Cenozoic at the level of the D1 horizon from the West Greenland margin (Gregersen et al., 2013, 2018, 2019, this volume), which is Middle Miocene. Here, the present authors follow this subdivision along the equivalent Saglek and/or Mokami formation 3 (SM3) horizon that divides the Saglek and Mokami formations (Fig. 3). Accordingly, the stratigraphy is discussed below in terms of the formations within four broad intervals: Lower Cretaceous, Upper Cretaceous, Paleocene–Eocene, and Oligocene–Pleistocene, but the present study illustrates and discusses the distribution of the Cretaceous as a whole and the Cenozoic is divided into lower and upper intervals at the Middle Miocene level.

The basin successions sit atop pre-rift basement which generally includes: crystalline rocks (e.g. Bell, 1989; Wasteneys et al., 1996), Paleozoic successions (e.g. Balkwill, 1987; Bingham-Koslowski, Zhang, and McCartney, this volume), a continent-ocean transition zone, and oceanic crust (Fig. 2). The Lower Cretaceous interval includes local accumulations of the alkali basalt units of the Alexis Formation that are possibly as old as Valanginian (Fig. 3; Umpleby, 1979; Bell, 1989; Dickie et al., 2011), as well as the nonmarine to shallow marine sandstone and shale units of the Lower Cretaceous Bjarni Formation that comprise the initial graben fill (McWhae et al., 1980; Bell, 1989; Balkwill and McMillan, 1990; Dickie et al., 2011). Overlying these strata are shelfal and deeper marine Cenomanian to Middle Paleocene Markland Formation shale units and lesser Freydis Member sandstone units (McWhae et al., 1980; Bell, 1989; Balkwill and McMillan, 1990; Dafoe and Williams, 2020b).

Overlying the Markland Formation, the Paleocene–Eocene interval includes the Cartwright and Gudrid formations, subsequently overlain by the Kenamu Formation. The Cartwright Formation is a middle Paleocene to Lower Eocene claystone representing shelf and deeper water deposition, with the correlative Gudrid Formation comprising nearshore, shallow-marine sandstone units (Umpleby, 1979; McWhae et al., 1980; Balkwill and McMillan, 1990; Dafoe and Williams, 2020a). Above this, the Kenamu Formation blankets the margin with a Lower to Middle Eocene shale, siltstone, and fine-grained sandstone succession, indicative of shelf and slope deposition, with shallow-marine Leif Member sandstone units at the top (McWhae et al., 1980; Balkwill and McMillan, 1990). Above this is the Upper Eocene to Oligocene shelfal claystone units of the Mokami Formation and the partly coeval, Oligocene to Middle Miocene, Saglek Formation shoreline sandstone and conglomerate units (Umpleby, 1979; McWhae et al., 1980). The Cenozoic strata are subdivided at the Middle Miocene level within the Mokami and Saglek formations, forming the lower and upper Cenozoic intervals.

PRE-RIFT BASEMENT

Onshore-offshore correlations

The nature of basement rock underlying the Labrador margin changes along strike (Bell, 1989). The onshore Labrador terrane (Fig. 2) is primarily composed of the Archean North Atlantic Craton, which is composed of the Saglek Block in the north and the Hopedale Block to the south with intervening Mesoproterozoic plutonic suites (St-Onge et al., 2009). Accordingly, the North Atlantic Craton rocks primarily comprise orthogneiss rocks, greenstone belts, and granitoid intrusions (St-Onge et al., 2009) that have been extended into the offshore based on basement rocks encountered in wells (Table 3; Bell, 1989; Wasteneys et al., 1996). South of the North Atlantic Craton and north of the inlet into Lake Melville, the Makkovik Orogen widens eastward and is also extrapolated into the offshore (Fig. 2; Table 3; Wasteneys et al., 1996; Hall et al., 2002). This orogen formed during Paleoproterozoic continental convergence involving the accretion of arc and back-arc units, as well as a possible small Archean terrane (St-Onge et al., 2009). The southern boundary of this unit is the Grenville Front, marking the northern edge of the Grenville Province and the limit of the widespread Meso- to Neoproterozoic Grenvillian Orogeny (Gower, 1996). Near the coastline, the Grenville Province primarily includes orthogneiss units and granitoid plutons of the Groswater Bay Terrane and, to a lesser extent, the Hawke River Terrane that includes granodiorite-diorite, gneiss, and granitic plutons (Gower, 1996). Basement rocks encountered in wells offshore encompass: gneiss, granite, granodiorite, monzonite, and syenite (Fig. 4–7; Table 3; Corgnet and McWhae, 1975; Chevron Standard Ltd., 1980; Wasteneys et al., 1996), with their offshore correlations from Wasteneys et al. (1996) summarized in Table 3.

Locally, Paleozoic basement rocks are sampled in some wells in the Hopedale Basin (Fig. 2, 5, 8; Table 3). These strata are primarily composed of carbonate rocks with lesser siliciclastic rocks (Corgnet and McWhae, 1975; BP Exploration Canada Ltd., 1976; Plé and Ferrero, 1976; Cadenel et al., 1978; Pandachuck and Lewis, 1978; Total Eastcan Exploration Ltd., 1979; Canterra Energy Ltd., 1983; Bell, 1989; Bingham-Koslowski, 2019; Bingham-Koslowski et al., 2019). The age of these rocks is not always well constrained due to diagenetic alteration (Bingham-Koslowski, 2019) and were initially interpreted as: generalized Paleozoic (Robertson Research Ltd., 1979, 1984; Moir, 1989), Carboniferous and/or Pennsylvanian (Corgnet and McWhae, 1975; Williams and Barss, 1979; Williams et al., 1990), and Ordovician (Williams, 1979c; Williams, 1981; Ainsworth et al., 2016); however, the age of the rocks has been generally constrained to the Middle to Late Ordovician based on new sampling and palynological analyses by Bingham-Koslowski et al. (2019). The distribution of these Ordovician rocks is shown in Bingham-Koslowski et al. (2019) and Bingham-Koslowski, Zhang, and McCartney (this volume). On seismic reflection data, it is challenging to differentiate carbonate rocks from Alexis Formation basalt, as both are typically characterized by high-amplitude seismic signatures (Dickie et al., 2011). Additionally, sedimentary layering is not always evident in Paleozoic strata, so it is difficult to separate these rocks from Precambrian basement. Faulting in pre-rift basement rocks has been shown in Bell (1989) and McCartney (2019).

Distribution and seismic character

A basement platform (defined as less than 3500 m depth to basement; *see also* Keen et al., this volume) follows the coastline of the Labrador margin (Fig. 2) and is wider in the south than in the north with promontories formed by the Okak and Cartwright arches. Outboard of the platform are basement ridges found at greater depths, which form prominent features onto which sedimentary strata onlap. Across this margin, basement terranes include undeformed continental crust near the coastline (Funck and Louden, 1999; Funck et al., 2001), faulted and thinned continental crust, hyperextended continental crust, serpentinized and/or exhumed continental mantle, and finally, oceanic crust underlying the deep-water Labrador Sea (Fig. 2, 9; Chian et al., 1995; Keen et al., 2018a, b). Fault trends are generally oriented southeast-northwest (*see* Keen et al., this volume) with small areas of complex and inverted basement structures (Fig. 2) that generally correspond to offsets in the margin (Dickie et al., 2011). The region of faulted and thinned continental crust along the Hopedale Basin margin is distributed across a wider region than along the Saglek Basin margin where the platform is narrower and drops more steeply into the depocentre.

Table 2. Listing of lithostratigraphic type and reference sections for the Labrador margin

Formation	Reference	Reference no.	Section	Well	Base (m)	Top (m)	Base (ft)	Top (ft)	Thickness (m)	Comment
Alexis Formation	Umpleby (1979)	1	Type	Bjarni H-81	2515	2255	8252	7400	260	
Alexis Formation	McWhae et al. (1980)	2	Reference	Herjolf M-92	4048	3751	13282	12306	297	Umpleby's (1979) original base of the Bjarni Formation type section was at 3767 m, which was refined by McWhae et al. (1980) to 3751 m, bringing the top of the Alexis Formation up to 3751 m.
Bjarni Formation	Umpleby (1979), modified by McWhae et al. (1980)	2	Type	Herjolf M-92	3751	2614	12306	8576	1137	Umpleby's (1979) original base of the type section was at 3767 m, which was refined by McWhae et al. (1980) to 3751 m.
Bjarni Formation	McWhae et al. (1980)	2	Reference	Bjarni H-81	2255	2150	7400	7050	105	
Bjarni Formation (Snorri Member)	Umpleby (1979), modified by McWhae et al. (1980)	2	Type	Snorri J-90	3150	3024	10332	9919	126	The original designation by Umpleby (1979) was 3061 to 3027 m, which was modified by McWhae et al. (1980) to 3150 to 3024 m. Moir (1989) further modified the boundaries to 3048 to 3027 m, but those of McWhae et al. (1980) agree with prominent well-log changes.
Cartwright Formation	McWhae et al. (1980)	2	Type	Bjarni H-81	1975	1820	6480	5972	155	Umpleby's (1979) original Cartwright Formation type section was from 2650 to 2393 m in the Gudrid H-55 well, but that section became Markland Formation under the McWhae et al. (1980) designation and redefinition of the Cartwright Formation.
Cartwright Formation	McWhae et al. (1980)	2	Reference	Herjolf M-92	2211	1963	7254	6441	248	
Cartwright Formation	McWhae et al. (1980)	2	Reference	Leif M-48	1780	1695	5840	5561	85	McWhae et al. (1980) considered the overlying interval from 1695 to 1666 m to be an upper tongue of the Gudrid Formation.
Gudrid Formation	Umpleby (1979), modified by McWhae et al. (1980)	2	Type	Gudrid H-55	2393	2179	7850	7150	214	Umpleby (1979) established the Gudrid Sand Member, but this unit was brought to formation status by McWhae et al. (1980).
Gudrid Formation	McWhae et al. (1980)	2	Reference	Cartier D-70	1857	1795	6091	5890	62	Lower Gudrid tongue of McWhae et al. (1980).
Gudrid Formation	McWhae et al. (1980)	2	Reference	Cartier D-70	1763	1713	5785	5620	50	Upper Gudrid tongue of McWhae et al. (1980).
Kenamu Formation	McWhae et al. (1980)	2	Type	Leif M-48	1666	1222	5465	4010	444	
Kenamu Formation	McWhae et al. (1980)	2	Reference	Cartier D-70	1713	1275	5620	4183	438	
Kenamu Formation	McWhae et al. (1980)	2	Reference	Karlsefni A-13	3036	2191	9960	7188	845	McWhae et al. (1980) also suggested 2043 m as an alternative top, however, this top is inconsistent with the change in log character typical of the top Kenamu Formation (*see* text).
Kenamu Formation (Brown Mudstone Member)	McWhae et al. (1980)	2	Type	Leif M-48	1666	1381	5465	4530	285	Umpleby's (1979) original Saglek Formation and associated Brown Mudstone Member were defined from the Freydis B-87 well (1321–1131 m for the member), but both type sections were abandoned by McWhae et al. (1980).
Kenamu Formation (Leif Member)	Umpleby (1979), modified by McWhae et al. (1980)	2	Type	Karlsefni A-13	2394	2191	7854	7188	203	Umpleby's (1979) original Leif Sand Member for the Saglek Formation was redesignated as part of the Kenamu Formation as the Leif Member by McWhae et al. (1980).
Kenamu Formation (Leif Member)	McWhae et al. (1980)	2	Reference	Leif M-48	1298	1257	4260	4124	41	This interval was the "Leif Sandstone" of McWhae and Michel (1975).

Table 2. (cont.) Listing of lithostratigraphic type and reference sections for the Labrador margin

Formation	Reference	Reference no.	Section	Well	Base (m)	Top (m)	Base (ft)	Top (ft)	Thickness (m)	Comment
Markland Formation	McWhae et al. (1980)	2	Type	Bjarni H-81	2150	1975	7050	6480	175	
Markland Formation	McWhae et al. (1980), modified by Moir (1989)	3	Reference	Freydis B-87	1788	1492	5866	4896	296	McWhae et al. (1980) included the strata underlying the Freydis Member as part of the Markland Formation down to 1875 m; however, biostratigraphic constraints place this interval in the Early Cretaceous and consistent with the Bjarni Formation and Snorri Member, in part. Thus, Moir (1989) modified the lower boundary of the Markland Formation in this well to 1788 m, consistent with the base of the Freydis Member.
Markland Formation	McWhae et al. (1980)	2	Reference	Gudrid H-55	2663	2393	8738	7850	270	
Markland Formation	McWhae et al. (1980)	2	Reference	Herjolf M-92	2614	2211	8576	7254	403	
Markland Formation (Freydis Member)	Umpleby (1979), modified by McWhae et al. (1980) and later by Moir (1989)	3	Type	Freydis B-87	1788	1730	5866	5676	58	Umpleby's (1979) designation was for the Freydis Sand Member of the Cartwright Formation from 1789 to 1734 m. McWhae et al. (1980) modified this to 1875 to 1731 m, but included strata with an age consistent with the Bjarni Formation. Moir (1989) brought the upper boundary up by 1 m and retained a lower boundary 1 m shallower than Umpleby's (1979) original depth (1788–1730 m).
Markland Formation (Freydis Member)	McWhae et al. (1980), modified by Moir (1989), and subsequently modified by Dafoe and Williams (2020b)	5	Reference	Skolp E-07	2460	2022	8069	4446	438	McWhae et al. (1980) defined three intervals of Freydis Member sandstone units within the Markland Formation between 2427 and 1355 m, but did not specify the intervals further: total thickness of sandstone units was 647 m. Balkwill and McMillan (1990) suggested a revised base of 1782 m; however, Moir (1989) placed the base at 2472 m. Moir (1987) divided the Freydis into "tongue 1" from 1707 to 1355 m and "tongue 2" from 2472 to 2008 m. This was further refined by Dafoe and Williams (2020b) to include two Freydis Member intervals from 2460 to 2022 m and 1707 to 1243 m.
					1707	1243	5599	4446	464	
Mokami Formation	McWhae et al. (1980)	2	Type	Snorri J-90	1715	997	5625	3270	718	The Mokami Formation defined by McWhae et al. (1980) was originally part of Umpleby's (1979) Saglek Formation.
Mokami Formation	McWhae et al. (1980)	2	Reference	Bjarni H-81	1334	725	4375	2377	609	Equivalent to the "Upper Lutites" of McWhae and Michel (1975), but their lower log pick was uncertain ((?)1334 m).
Saglek Formation	McWhae et al. (1980)	2	Type	Snorri J-90	997	267	3270	876	730	Umpleby's (1979) original type section from the Freydis B-87 well (1131–1027 m) was abandoned by McWhae et al. (1980) when they redefined the formation. McWhae et al. (1980) reported an uncertain top ((?)267 m).
Saglek Formation	McWhae et al. (1980)	2	Reference	Bjarni H-81	725	222	2377	728	503	Equivalent to the "Upper Coarse Arkosic Sands" of McWhae and Michel (1975). McWhae et al. (1980) reported an uncertain top ((?)222 m).

The reference number is tied to the source noted in the well plots. For reference numbers, *see* 'Sections and lithostratigraphy' in Figure 4b.

Table 3. Summary of basement rock types and ages sampled in offshore Labrador wells.

Well	Basement rock type	Rock type source	Interval (m; Moir, 1989[1]; CNLOPB, 2007[2])	K-Ar[1] and U-Pb[2] isotope age (Ma); or representative biostratigraphic age	Age date source	Onshore correlation (Wasteneys et al., 1996)
Cartier D-70	Granodiorite	Wasteneys et al. (1996)	1927–1910[1]	1332 ± 45[1]; 1800[2]	Ferrero and Plé (1976)[1]; Wasteneys et al. (1996)[2]	Makkovik Orogen
Gilbert F-53	Amphibolite gneiss	Wasteneys et al. (1996)	3608–3550[1]	1917 ± 64[1]; 3742 ± 12[2]	Petro-Canada Exploration Inc. (1980a)[1]; Wasteneys et al. (1996)[2]	North Atlantic Craton (Nain Province)
Gudrid H-55	Granite	Corgnet and McWhae (1975)	2838–2804[1]	1710 ± 57[1]	Corgnet and McWhae (1975)[1]	
Herjolf M-92	Granodiorite-quartz monzonite	Wasteneys et al. (1996)	4086–4048[1]	1427 ± 51[1]; 1801.4 ± 5[2]	Ferrero and Plé (1977a)[1]; Wasteneys et al. (1996)[2]	Makkovik Orogen
Hopedale E-33	Anorthosite	Wasteneys et al. (1996)	2069.4–2000[2]	1269 ± 4[2]	Wasteneys et al. (1996)[2]	North Atlantic Craton (Nain Province)
Karlsefni A-13	Garnet-biotite quartzo-feldspathic gneiss	Wasteneys et al. (1996)	4149–4129[1]	1537 ± 55[1]; 2680[2]	Ferrero and Plé (1977b)[1]; Wasteneys et al. (1996)[2]	North Atlantic Craton (Nain Province)
Roberval C-02	Foliated quartz monzonite-granodiorite	Wasteneys et al. (1996)	2823–2803[1]	1189 ± 40[1]; 1813 ± 4[2]	Petro-Canada Exploration Inc. (1980b)[1]; Wasteneys et al. (1996)[2]	Makkovik Orogen
Skolp E-07	Migmatitic quartz diorite gneiss	Wasteneys et al. (1996)	2992–2967[1]	1016 ± 35[1]; 997 ± 39[1]; 3213 +21/-3.6[2]	Prim et al. (1978)[1]; Wasteneys et al. (1996)[2]	North Atlantic Craton (Nain Province)
Snorri J-90	Granodioritic gneiss	Wasteneys et al. (1996)	3210–3148[1]	1066 ± 41[1]; 3171[2]	McWhae et al. (1975)[1]; Wasteneys et al. (1996)[2]	North Atlantic Craton (Nain Province)
South Hopedale L-39	Foliated granite-granitic gneiss	Wasteneys et al. (1996)	2364–2220[2]	1895 ± 8[2]	Wasteneys et al. (1996)[2]	Makkovik Orogen
South Labrador N-79	Syenite	Chevron Standard Ltd. (1980)	3571–3548[1]	None		
Tyrk P-100	Alkali-feldspar granite-granitic gneiss	Wasteneys et al. (1996)	1739–1706[1]	1864.4 ± 3.1[2] and 1839.1 ± 4.7[2] (likely ages of migmitization only)	Wasteneys et al. (1996)[2]	Makkovik Orogen
Freydis B-87	Limestone	Plé and Ferrero (1976)	2314–1905[1]	Ordovician (Caradocian)[1]; Late Ordovician[2]; Late Ordovician (Sandbian)[3]	Williams (1979c)[1]; Ainsworth et al. (2016)[2]; Bingham-Koslowski et al. (2019)[3]	
Gudrid H-55	Dolostone	Corgnet and McWhae (1975)	2804–2663[1]	Carboniferous[1]; Pennsylvanian[2]; possibly Late Ordovician[3]	Corgnet and McWhae (1975)[1]; Williams and Barss, 1979)[2]; Bingham-Koslowski et al. (2019)[3]	
Hopedale E-33	Limestone	Pandachuck and Lewis (1978)	2000–1976[2]	Ordovician (Tremadocian)[1]; Late Ordovician (Sandbian)[2]	Williams (1981)[1]; Bingham-Koslowski et al. (2019)[2]	
Indian Harbour M-52	Limestone	BP Exploration Canada Ltd. (1976)	3959–3528[1]	Paleozoic[1]; Middle (?)Ordovician to Late Ordovician (Katian and Sandbian)[2]	Moir (1989)[1]; Bingham-Koslowski et al. (2019)[2]	
RobervalK-92	Dolostone	Cadenel et al. (1978)	3874–3544[1]	Pennsylvanian[1]; possibly Middle to Late Ordovician[2]	Williams et al. (1990)[1]; Bingham-Koslowski et al. (2019)[2]	
South Hopedale L-39	Limestone	Canterra Energy Ltd. (1983)	2220–2008[1]	(?)Paleozoic[1]; Late Ordovician (undifferentiated)[2]	Robertson Research Ltd. (1984)[1]; Bingham-Koslowski et al. (2019)[2]	
Tyrk P-100	Dolostone	Total Eastcan Exploration Ltd. (1979)	1706–1702[1]	(?)Paleozoic[1]; Middle to Late Ordovician (undifferentiated)[2]	Robertson Research Ltd. (1979)[1]; Bingham-Koslowski et al. (2019)[2]	

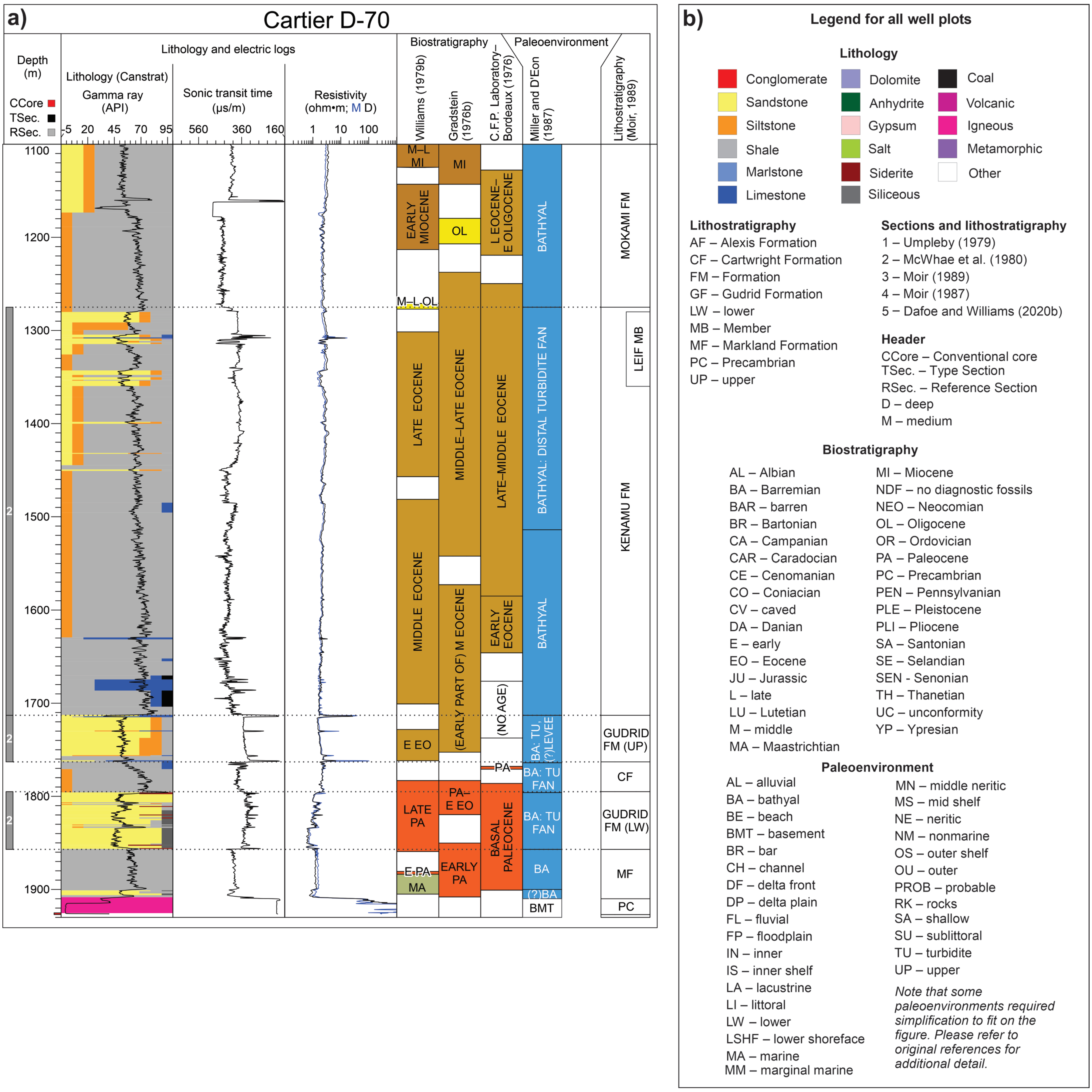

Figure 4. a) The Cartier D-70 well, showing fundamental wireline logs, lithology (Canstrat), conventional core locations, key biostratigraphic studies, paleoenvironmental interpretations, and lithostratigraphy. Reference sections for the Gudrid and Kenamu formations are shown. **b)** Common legend for abbreviations in figures 5 to 8, 11 to 14, and 16 to 18. Note that all the abbreviations may not appear on each of these figures.

Along the outer margin, the transition zone, thought to be serpentinized mantle, generally shows a lack of faulting and a more transparent internal seismic character (Fig. 2, 9; Keen et al., 2018a, b). This zone is bounded to the east by the landward limit of oceanic crust (LLOC) defined by Keen et al. (this volume; Fig. 2, 9). The landward limit of oceanic crust is marked by the U-graben along the central Labrador margin (line 1, Fig. 9a; Keen et al., 2018a), but is complicated by the development of a magma-rich margin to the north where volcanic rocks are interpreted to overlie older strata and the basement transition zone (line 2, Fig. 9b; Keen et al., 2018b). The oldest oceanic crust is of chron C31 age along the central Labrador margin (Keen et al., 2018a), but may be as young as chron C27n to the north; the youngest oceanic crust is of chron C13 and is found at the extinct seafloor spreading axis (Fig. 2, 9; Oakey and Chalmers, 2012; Keen et al., 2018b).

LOWER CRETACEOUS INTERVAL

Alexis Formation

Lithostratigraphy

The earliest dated syn-rift rocks that accumulated beneath the Labrador Shelf are the Alexis Formation alkali basalt flows (Table 4; Fig. 3). These are found along the southern part of the Labrador margin (Fig. 10), overlying the probable offshore extensions of the Makkovik Orogen and possibly the Grenville Province (Bell, 1989; Wasteneys et al., 1996), although the offshore extension of the Grenville Front may actually lie southwest of the wells that sampled the Alexis Formation (Funck et al., 2001). The type section of the Alexis Formation is found in the Bjarni H-81 well from 2515 to 2255 m (Fig. 11; Umpleby, 1979). Here, it consists of about 260 m of red- and green-weathered basalt units alternating with amygdaloidal basalt units with evidence of secondary hydrothermal alteration (Umpleby, 1979; Dafoe and Williams, 2020a). Potassium-argon (K-Ar) isotope dating on core samples at two depths yielded ages of 142 ± 7 Ma and 125 ± 6 Ma (Table 4; recalculated from Corgnet and McWhae, 1973a). The reference section for the Alexis Formation established by McWhae et al. (1980) is from the Herjolf M-92 well from 4048 to 3767 m (Fig. 6). In this well, the rocks comprise variably weathered, red, brown, green, or grey basalt and other volcanic rocks (Ferrero, and Plé, 1977a; Dafoe and Williams, 2020a). A K-Ar age of 123 ± 5 Ma for the basalt units was recorded from core 3 of this well (Table 4; recalculated from Ferrero and Plé, 1977a). Five other wells on the Labrador Shelf encountered rocks assigned to the Alexis Formation (Table 4; Fig. 10, 12).

There is a significant spread in ages from samples of the Alexis Formation within the same well (e.g. Bjarni H-81) and, in some cases, from the same conventional core interval (e.g. Roberval K-92 and Leif M-48; Table 4). Whereas Cretaceous volcanism could have occurred over a long period of time, there are two caveats to the above ages:

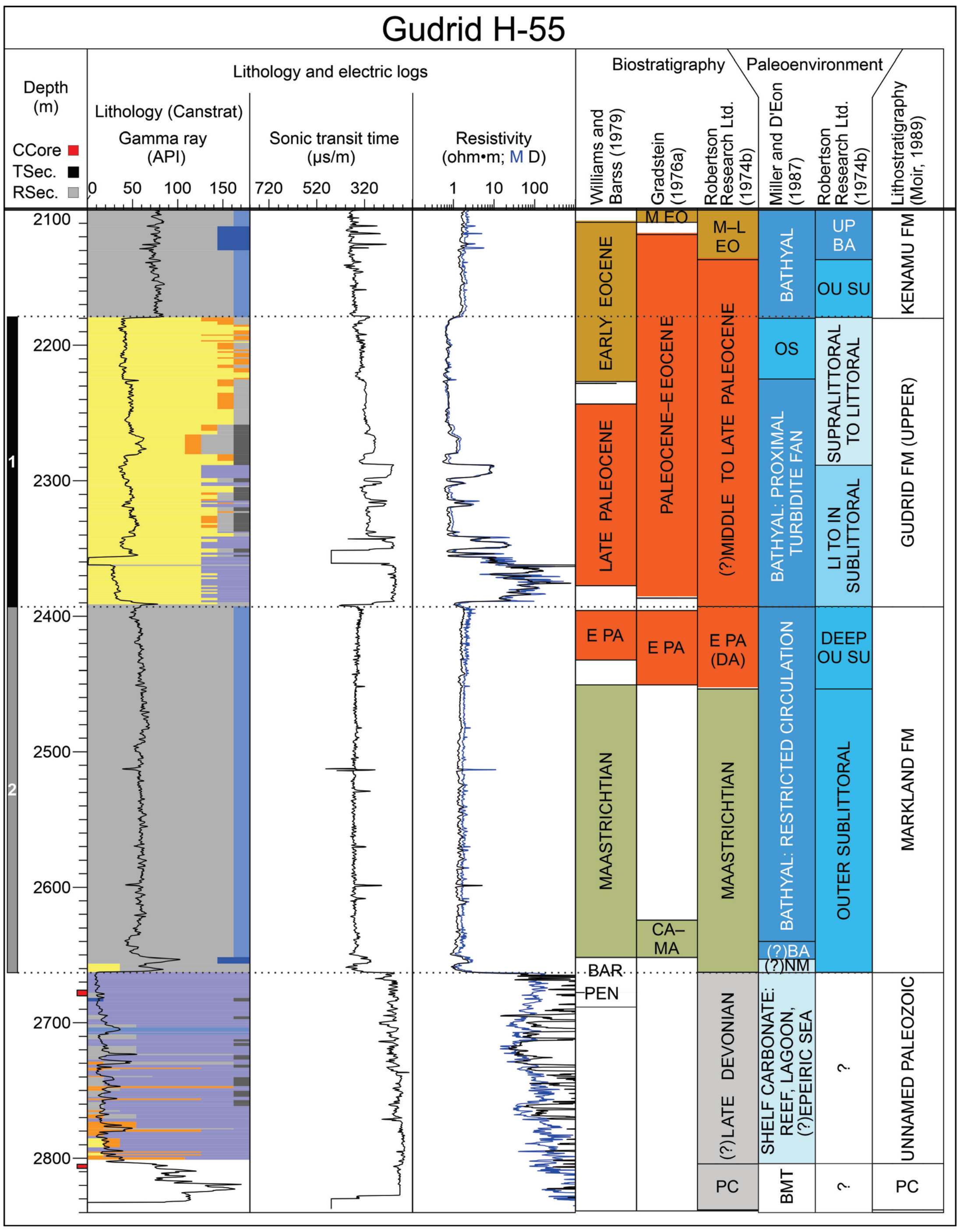

Figure 5. The Gudrid H-55 well, showing fundamental wireline logs, lithology (Canstrat), conventional core locations, key biostratigraphic studies, paleoenvironmental interpretations, and lithostratigraphy. The type section for the Gudrid Formation and a reference section for the Markland Formation are shown. *See* Figure 4b for legend.

1) weathering and/or alteration is likely to have influenced resultant age dates, as many of the rocks are described as weathered in nature (Table 4); and 2) K-Ar whole-rock age dating is known to have minimal accuracy (Lee, 2014). No new age dating has been conducted on these rocks with more modern techniques (e.g. Ar-Ar isotopes). Whereas the range in reported ages is quite extensive (142–92 Ma), many are within the Barremian to early Aptian (Table 4), which is relatively consistent with, or even slightly older than, the oldest age of the Bjarni Formation (*see* 'Bjarni Formation' section); however, there are two instances where the ages are questionable. Firstly, Umpleby (1979) suggested that the age and tuffaceous character of the interval at Indian Harbour M-52 may indicate that it is unrelated to the Alexis Formation; although, other descriptions suggest some basaltic composition (BP Exploration Canada Ltd., 1976) and alteration or weathering could be a factor. Secondly, in Roberval K-92 (Table 4) the Cenomanian sample is overlain by well established, Lower Cretaceous (Albian–Aptian) Bjarni Formation sandstone units (Ainsworth et al., 2014; Nøhr-Hansen et al., 2016; Williams, 2017b). Umpleby (1979) also noted that the 142 ± 7 Ma (recalculated) age at Bjarni H-81 was from altered rock and was probably too old. In the 1976 time scale of van Hinte (1976b; Kent and Gradstein, 1986), this age fell within the Jurassic Period. Thus, Umpleby (1979) proposed an earliest age of Berriasian–Valanginian for the Alexis Formation, which according to the van Hinte (1976a) time scale, was approximately 120 to 135 Ma, now considered middle Valanginian to early Aptian on the Gradstein et al. (2012) time scale.

As Labrador Shelf wells have only sampled some of the Alexis Formation (Fig. 10), older or younger Alexis Formation rocks may exist elsewhere along the margin. Accordingly, Dickie et al. (2011) placed the oldest syn-rift Alexis Formation rocks at the base of the Valanginian, and the present authors concur with their assessment. The youngest age of these basalt units is more difficult to constrain, but could be as young as Albian (as at Leif M-48; Table 4) or even early Late Cretaceous. Dafoe and Williams (2020a) noted volcanic rocks in core 1 of Bjarni O-82 (within the Bjarni Formation) that appear to be middle Albian–Cenomanian, but these are interbedded basalt and tuff that differ from the typical Alexis Formation basalt. Younger volcanic rocks are also seen on the West Greenland margin, as discussed below.

Related regional rocks

In southwest Greenland, Late Triassic to Late Jurassic dyke swarms are interpreted to be related to early extension (Larsen et al., 2009; Secher et al., 2009). An extensive coast-parallel, alkali basalt dyke swarm in southwest Greenland, dated at 144 to 133 Ma (Valanginian–Hauterivian) is linked with significant regional stretching and was likely associated with lava flows that were later eroded (Larsen et al., 2009). Gregersen et al. (2018) confirmed volcanic rocks and interbedded upper Cenomanian to lower Turonian claystone units in the AT2-1 well on the central West Greenland margin (Fig. 10), whereas Larsen et al. (2009) reported localized onshore sills and dykes along southern West Greenland dated at 115 Ma and 106 Ma.

Onshore Labrador, Tappe et al. (2007) published Early Cretaceous ages for a nephelinite suite in the Ford's Bight region of coastal Labrador (Fig. 10); however, Peace et al. (2016) analyzed samples from the same study area and found no strong evidence for an Early Cretaceous dyke swarm in the Makkovik Orogen. Instead, Peace et al. (2016) associated the Early Cretaceous igneous rocks in the Ford's Bight area with the diatreme described by Wilton et al. (2002). Provisional biostratigraphy from a breccia closely associated with the diatreme suggests it erupted through Jurassic and Lower Cretaceous sedimentary rocks (King and McMillan, 1975).

Distribution and seismic reflection character

Carey et al. (2020) used synthetic seismograms to model the seismic reflection character of the Alexis Formation volcanic rocks at the seven well locations described above and correlated the formation to seismic reflection data. Seismic character at these well locations is generally higher amplitude than overlying reflections, but varies depending on seismic data vintage, making interpretation of the top of the Alexis Formation away from the wells difficult. Accordingly, the mapped distribution shown in Figure 10 likely represents only the minimum extent of the Alexis Formation basalt units. The largest accumulation is mapped in the Bjarni well area, with flows extending to the Tyrk P-100 well. To the south of this, the Alexis Formation can only be confidently mapped adjacent to the wells, except for one small occurrence near the Roberval wells (Fig. 10). The base of the formation can be difficult to differentiate from underlying crystalline basement, so the thickness of the basalt units beyond the well control

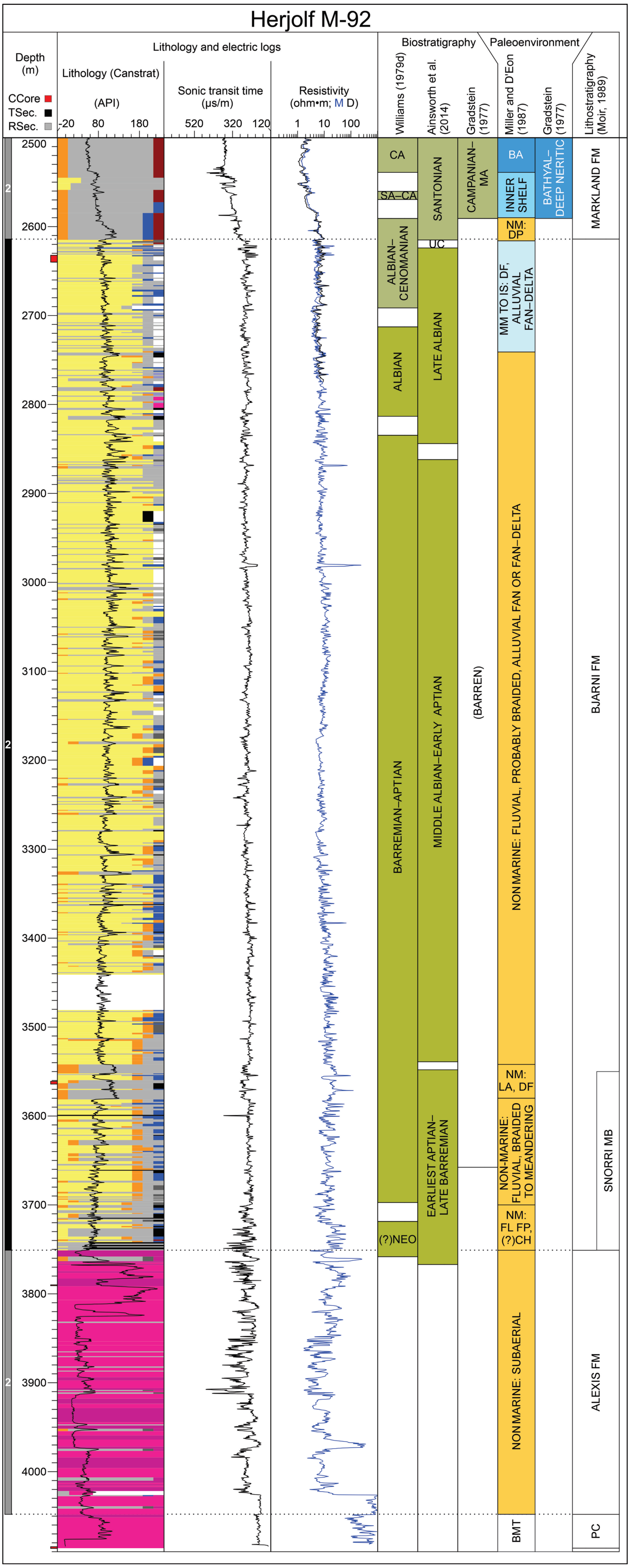

Figure 6. The Herjolf M-92 well, showing fundamental wireline logs, lithology (Canstrat), conventional core locations, key biostratigraphic studies, paleoenvironmental interpretations, and lithostratigraphy. The type section for the Bjarni Formation and a reference section for the Alexis Formation are indicated (the full reference section for the Markland Formation is shown in Fig. 14). *See* Figure 4b for legend.

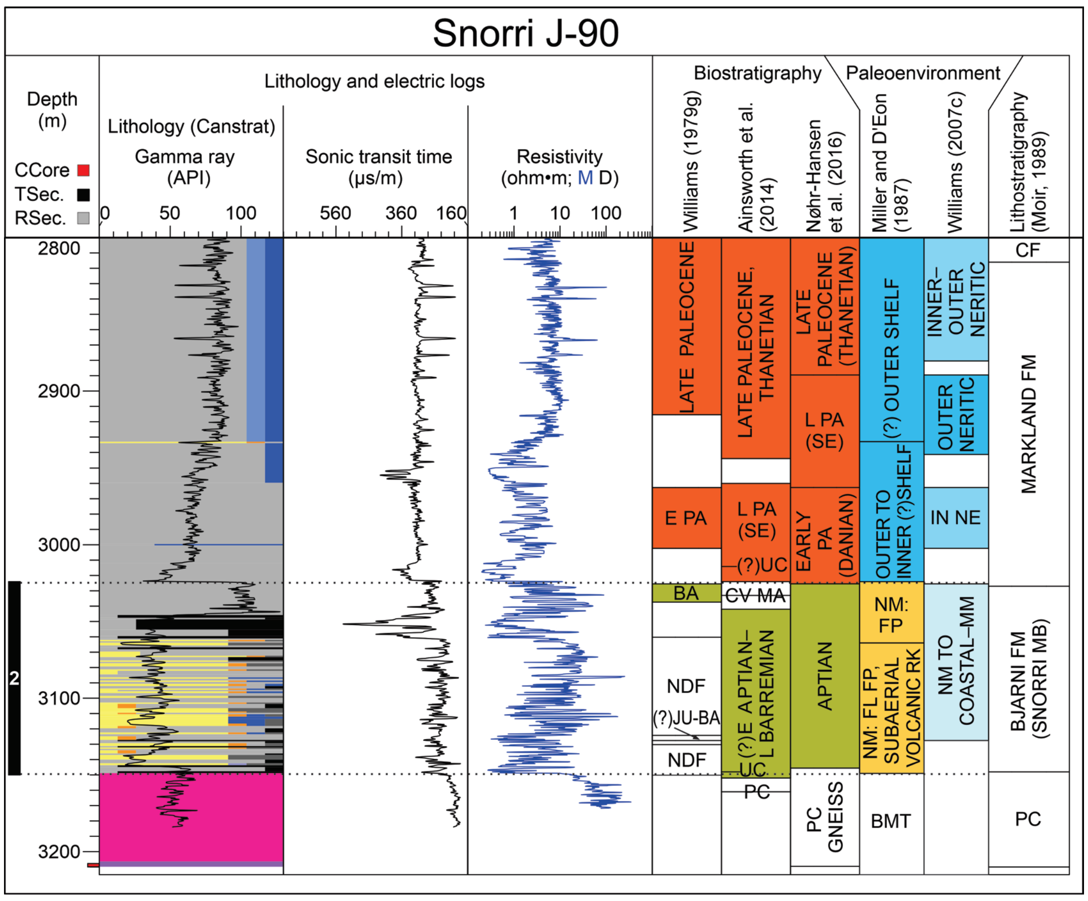

Figure 7. The Snorri J-90 well, showing fundamental wireline logs, lithology (Canstrat), conventional core locations, key biostratigraphic studies, paleoenvironmental interpretations, and lithostratigraphy. The type section for the Snorri Member of the Bjarni Formation is shown. *See* Figure 4b for legend.

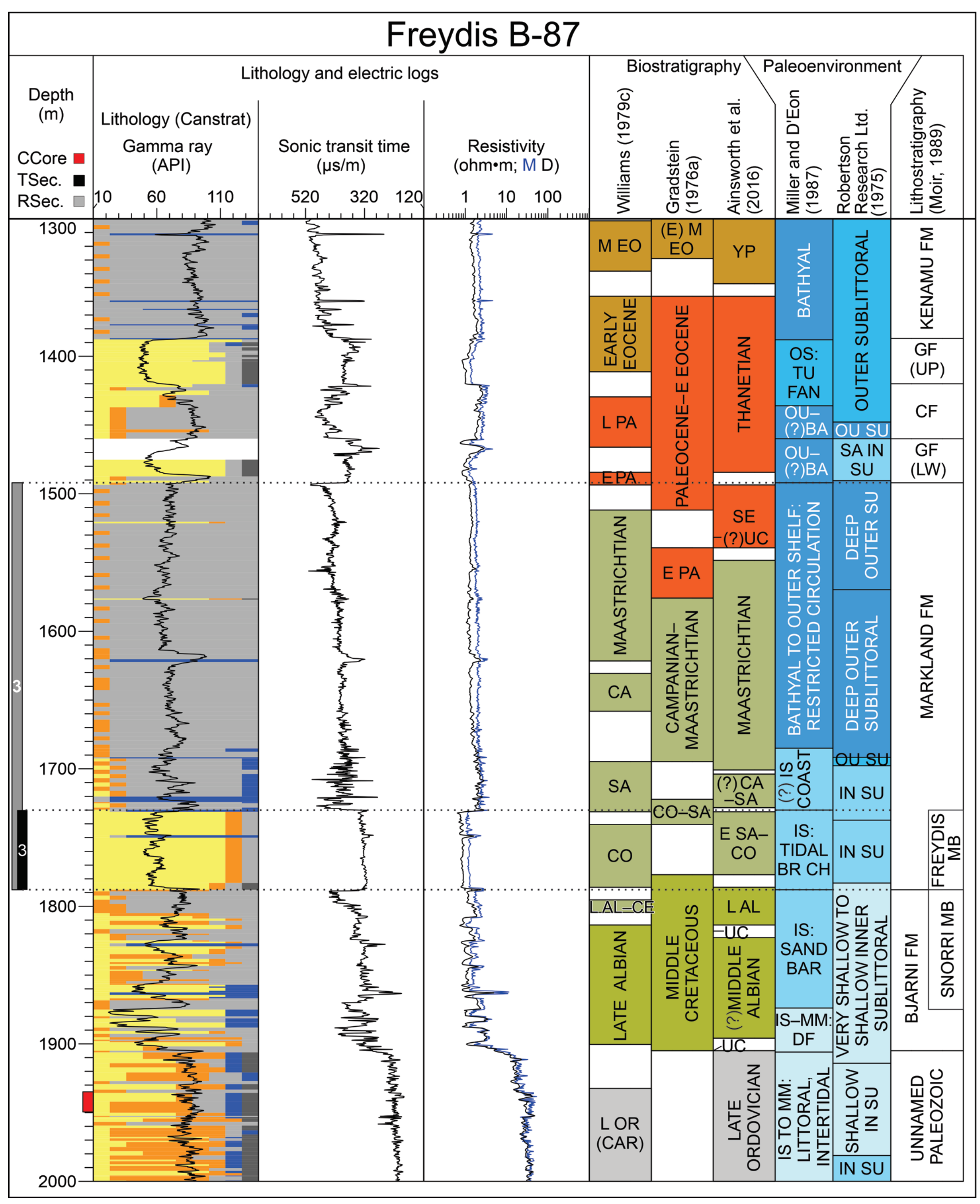

Figure 8. The Freydis B-87 well, showing fundamental wireline logs, lithology (Canstrat), conventional core locations, key biostratigraphic studies, paleoenvironmental interpretations, and lithostratigraphy. The type section for the Freydis Member of the Markland Formation and a reference section for the Markland Formation are indicated. *See* Figure 4b for legend.

Figure 9. Seismic lines oriented southwest to northeast that illustrate stratigraphic relationships for the Labrador margin and western Labrador Sea (*see* Fig. 1 for location). **a)** Line 1 through the Hopedale Basin crossing the Hopedale E-33 (projected 1 km) and Corte Real P-85 (projected 3 km) wells and extending out to the extinct seafloor spreading axis at the Greenland (Denmark) 200 nm territorial boundary. This margin is magma-poor. Seismic data courtesy of NRCan. **b)** Line 2 through the Saglek Basin and across the magma-rich margin where basement transitions from rifted, thinned continental crust through a transitional zone and then onto the basalt units of the volcanic margin. Seismic data courtesy (DC) of TGS[1], ION Geophyscial[2], and the Federal Institute for Geosciences and Natural Resources (Hannover; lines BGR/77-5 and BGR/77-12)[3]. A legend of the horizons is shown and associated coloured intervals indicate the key units and their relationship to the distribution maps shown in other figures. IF = inner flows, SDR = seaward-dipping reflectors.

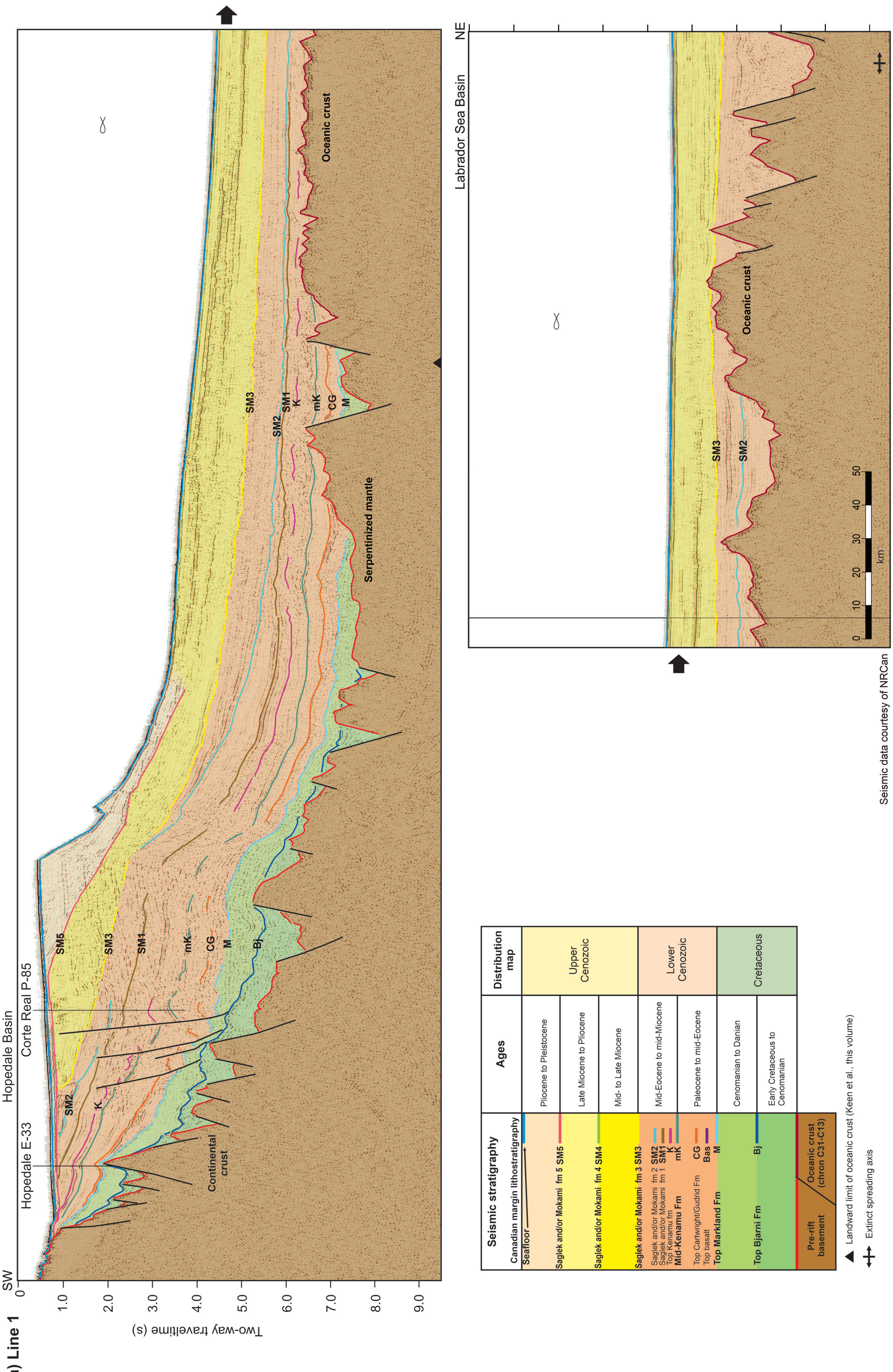
a) Line 1
SW
NE
Hopedale Basin
Hopedale E-33
Corte Real P-85
Labrador Sea Basin
Two-way traveltime (s)
0
1.0
2.0
3.0
4.0
5.0
6.0
7.0
8.0
9.0
SM5
SM3
SM2
SM1
K
mK
CG
M
Bj
Continental crust
Serpentinized mantle
Oceanic crust
0
10
20
30
40
50
km
Seismic data courtesy of NRCan
Seismic stratigraphy
Canadian margin lithostratigraphy
Ages
Distribution map
Seafloor
Saglek and/or Mokami fm 5 SM5
Pliocene to Pleistocene
Upper Cenozoic
Saglek and/or Mokami fm 4 SM4
Late Miocene to Pliocene
Mid- to Late Miocene
Saglek and/or Mokami fm 3 SM3
Saglek and/or Mokami fm 2 SM2
Saglek and/or Mokami fm 1 SM1
Top Kenamu fm K
Mid-Kenamu Fm mK
Mid-Eocene to mid-Miocene
Lower Cenozoic
Top Cartwright/Gudrid Fm CG
Top basalt Bas
Top Markland Fm M
Paleocene to mid-Eocene
Cenomanian to Danian
Cretaceous
Top Bjarni Fm Bj
Early Cretaceous to Cenomanian
Pre-rift basement
Oceanic crust (chron C31-C13)
Landward limit of oceanic crust (Keen et al., this volume)
Extinct spreading axis

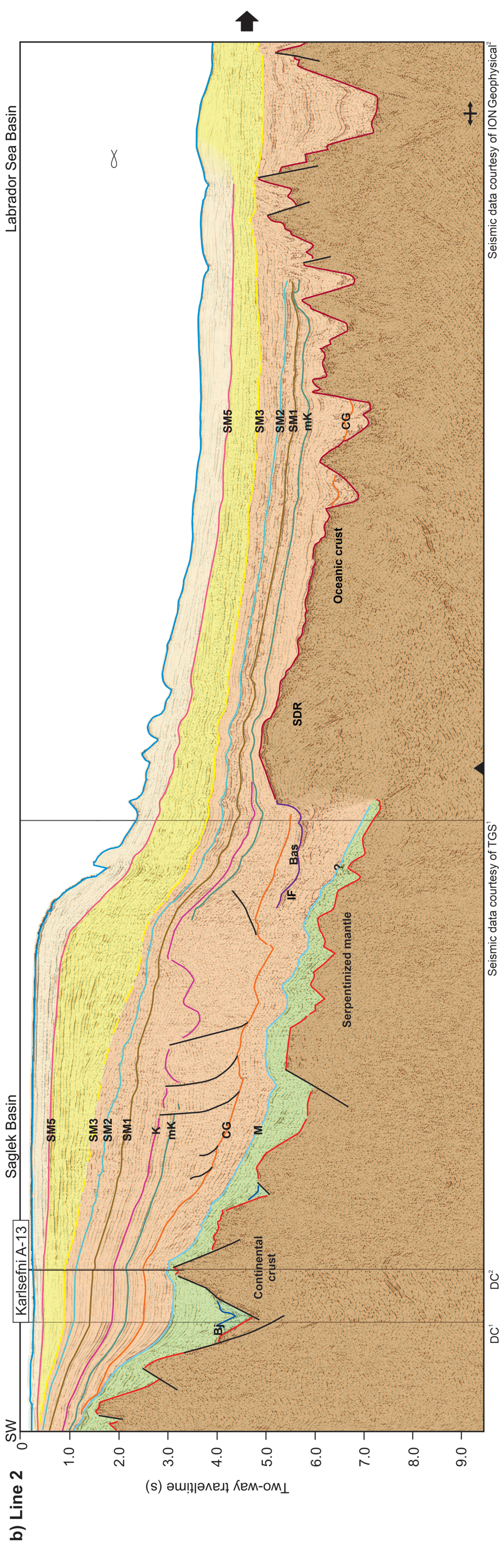

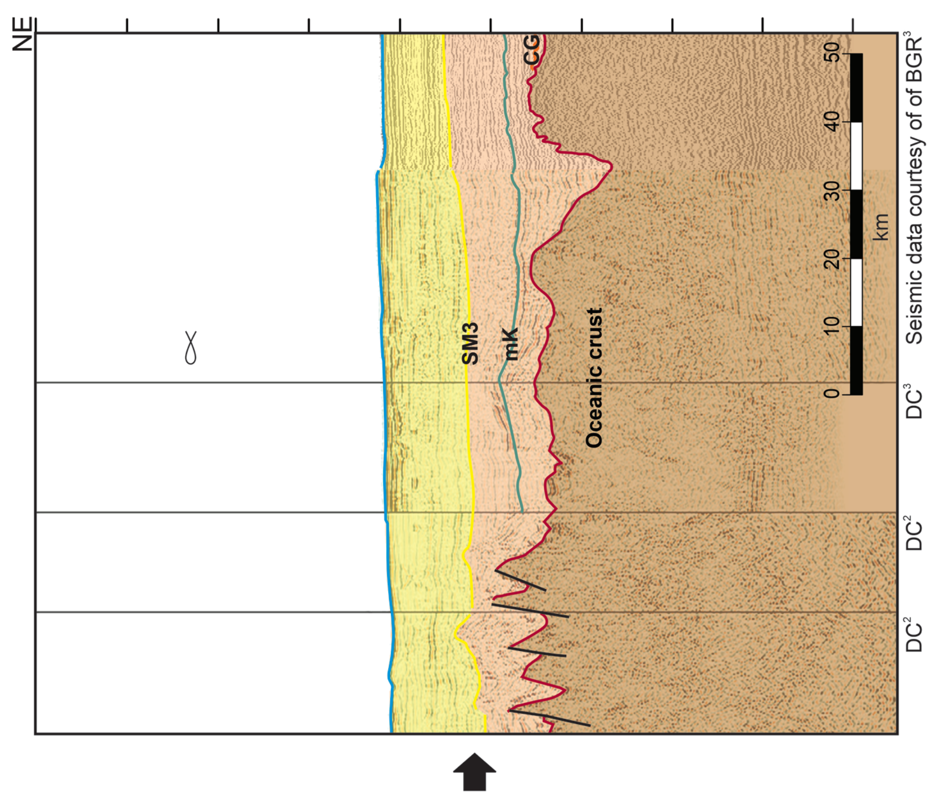

Figure 9. (cont.)

Table 4. Summary of age dates and lithologies of Alexis Formation intervals in offshore Labrador wells.

Well	Alexis Formation interval (m)	K-Ar isotope age date	Recalculated K-Ar isotope age date	Age date sample source	General lithology
Bjarni H-81	2514.6–2255.5[1]	122 ± 6 Ma[2]	125 ± 6 Ma	Core 2 (2274 m; 7460 ft.)	Weathered and altered basalt[10]
		139 ± 7 Ma[2]	142 ± 7 Ma	Core 3 (2512 m; 8241.5 ft.)	
Herjolf M-92	4048.5–3751[1]	121 ± 5 Ma[3]	123 ± 5 Ma	Core 3 (no specific depth given)	Weathered and altered basalt[10]
Tyrk P-100	1702–1523[1]	None	None	None	Basalt, tuff, and hornfels[4]
Roberval K-92	3544–3188[1]	98.1 ± 4.6 Ma[5]	100 ± 5 Ma	Core 4 (3417.60 m)	Basalt[5]
		122 ± 7 Ma[5]	125 ± 7 Ma	Core 4 (3422.90 m)	
		124 ± 5 Ma[5]	127 ± 5 Ma	Core 4 (3414.45 m)	
		129 ± 6 Ma[6]	132 ± 6 Ma	Core 3 (no specific depth given)	
Leif M-48	1879.1–1839[1]	104 ± 5 Ma[10]	106 ± 5 Ma	Core 1 (unknown depth)	Altered basalt[10]
		131 ± 6 Ma[7]	134 ± 6 Ma	Core 1 (1879 m; 6167 ft.)	
North Leif I-05	3444–3394[1]	None	None	None	Weathered basalt[8]
Indian Harbour M-52	3484–3250[1]	90.1 ± 3.8 Ma[9]	92 ± 4 Ma	Cuttings (3490–3510 m; 11 450–11 515 ft.)	Weathered and altered lapilli tuff[10]

[1](Canada-Newfoundland and Labrador Offshore Petroleum Board, 2007)
[2](Corgnet and McWhae, 1973a)
[3](Ferrero and Plé, 1977a)
[4](Cadenel et al., 1978)
[5](Total Eastcan Exploration Ltd., 1979)
[6](Krueger Enterprises, Inc., 1979)
[7](Corgnet and McWhae, 1973b)
[8](Petro Canada Exploration Inc., 1981)
[9](BP Exploration Canada Ltd., 1976)
[10](Umpleby, 1979)

The original K-Ar isotope age dates were recalculated using the *ArAR* software from Mercer and Hodges (2016).
The decay constants used in the original studies were from Aldrich and Wetherill (1958), with the K isotopic abundance values from Nier (1950) used in the recalculation, but the ^{40}K value was adjusted to 0.0122 as reported in the original studies. The 104 Ma age from Leif M-48 was reported by Umpleby (1979) and the original report could not be located, but the values were assumed to be the same as the other reports.
The decay constants and K isotopic abundance values from Steiger and Jager (1977) were used in the recalculation.

cannot be accurately estimated. In addition, attempts at correlating magnetic anomaly maps with the location of the Alexis Formation basalt units have not produced conclusive results, probably due to the limited thickness of the basalt (*see* Table 4).

Bjarni Formation

Lithostratigraphy

In the Hopedale and Saglek basins, the Bjarni Formation overlies the Alexis Formation or the unconformity with Precambrian basement or pre-rift Paleozoic rocks (the "Labrador Unconformity" of McWhae (1981)); however, similar Early Cretaceous ages for the Bjarni and Alexis formations suggests that these units could also be interbedded, especially at depths within grabens or half-grabens that have not been sampled (Fig. 3). McWhae and Michel (1975) introduced the term "Bjarni sandstone" for a unit intersected in Bjarni H-81 from 2257 to 2150 m (Fig. 11). This name was formalized by Umpleby (1979) as the Bjarni Formation with the type section designated in Herjolf M-92 from 3767 to 2614 m, an interval primarily composed of coarse-grained, arkosic sandstone units with silty shale and thin coal seams initially thought to be Barremian to early Cenomanian (Fig. 6). McWhae et al. (1980) suggested an alternative base at 3751 m in this well (thus reducing the type section to 1137 m thick), which forms a more consistent log pick for the top of the underlying Alexis Formation basalt units (Fig. 6). The original section described by McWhae and Michel (1975) from 2255 to 2150 m (105 m thick) in Bjarni H-81 was described as a reference section by McWhae et al. (1980; Fig. 11). In general, the Bjarni Formation includes coarse-grained arkosic sandstone, fine-grained sandstone, conglomerate, carbonaceous shale, and thin coal seams (Umpleby, 1979; McWhae et al., 1980). The Bjarni Formation sandstone units in the Hopedale Basin often possess a high radioactivity (Umpleby, 1979) expressed as an anomalously high gamma-ray log signature due to the abundance of feldspar grains.

To delineate the shale-dominated portions of the Bjarni Formation, Umpleby (1979) further defined the Snorri Member for the interval 3061 to 3027 m in Snorri J-90 (Fig. 7). This interval was described as a radioactive grey to dark brown-maroon, silty shale with abundant plant remains and thin coal seams, as well as an underlying unit characterized by coal seams up to 2 m thick and interbedded with dark grey, silty shale and medium-grained sandstone. This unit was also identified by Umpleby (1979) from the lowermost 217 m of Herjolf M-92, again comprised of shale with coal (Fig. 6). McWhae et al. (1980) indicated that the Snorri Member could not be recognized regionally. These authors modified Umpleby's type section for the Snorri Member such that the coaly unit was at the top of the Bjarni Formation and the interval extended from 3150 to 3024 m in Snorri J-90 (126 m thick; Fig. 7). Moir (1989) further refined this unit from 3048 to 3027 m; however, McWhae et al.'s (1980) boundaries are better suited to significant well-log changes, resulting in the slight discrepancy seen in Figure 7 between the type section and lithostratigraphic assignment of

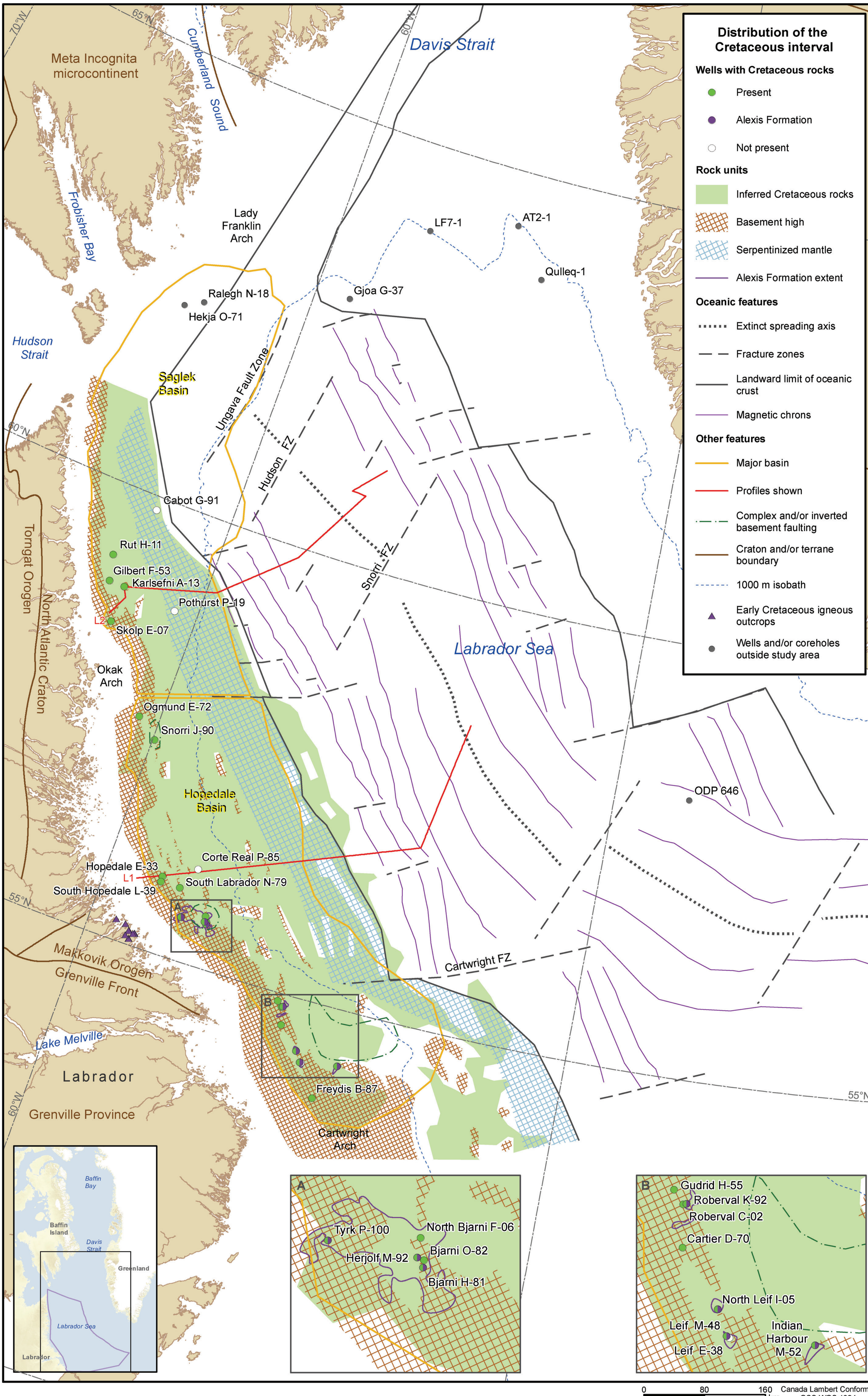
Distribution of the Cretaceous interval
Wells with Cretaceous rocks
Present
Alexis Formation
Not present
Rock units
Inferred Cretaceous rocks
Basement high
Serpentinized mantle
Alexis Formation extent
Oceanic features
Extinct spreading axis
Fracture zones
Landward limit of oceanic crust
Magnetic chrons
Other features
Major basin
Profiles shown
Complex and/or inverted basement faulting
Craton and/or terrane boundary
1000 m isobath
Early Cretaceous igneous outcrops
Wells and/or coreholes outside study area
Davis Strait
Meta Incognita microcontinent
Cumberland Sound
Frobisher Bay
Hudson Strait
Lady Franklin Arch
Ralegh N-18
Hekja O-71
Gjoa G-37
LF7-1
AT2-1
Qulleq-1
Saglek Basin
Ungava Fault Zone
Hudson FZ
Snorri FZ
Cabot G-91
Rut H-11
Gilbert F-53
Karlsefni A-13
Pothurst P-19
Skolp E-07
L2
Torngat Orogen
North Atlantic Craton
Okak Arch
Labrador Sea
Ogmund E-72
Snorri J-90
Hopedale Basin
ODP 646
Corte Real P-85
Hopedale E-33
L1
South Labrador N-79
South Hopedale L-39
Makkovik Orogen
Grenville Front
Cartwright FZ
Lake Melville
Labrador
Grenville Province
Freydis B-87
Cartwright Arch
55°N
60°N
65°N
70°W
60°W
Baffin Bay
Baffin Island
Davis Strait
Greenland
Labrador Sea
Labrador
A
Tyrk P-100
North Bjarni F-06
Herjolf M-92
Bjarni O-82
Bjarni H-81
B
Gudrid H-55
Roberval K-92
Roberval C-02
Cartier D-70
North Leif I-05
Leif M-48
Leif E-38
Indian Harbour M-52
0
80
160
km
1:4 750 000
Canada Lambert Conformal
GCS WGS 1984

Figure 10. Distribution map of the Cretaceous interval for the Labrador margin showing the extent of the Alexis Formation basalts and the sedimentary succession. Onshore locations of Cretaceous igneous rocks from Tappe et al. (2007) and Peace et al. (2016) are also shown. The inner edge of the serpentinized mantle (Keen et al., 2018a, b; this volume) forms the basinward extent of the Bjarni Formation. Basin outlines are from Keen et al. (this volume). L1 and L2 indicate the seismic reflection lines 1 and 2 shown in Figure 9. A well that shows the interval "not present" may not have drilled deep enough to intersect the interval, is cased through that interval, lacks related strata deposited at that location, or associated strata were later removed through erosion. Additional projection information: Central Meridian = 60°W; Standard Parallels = 65, 75°W; Latitude of Origin = 65°N.

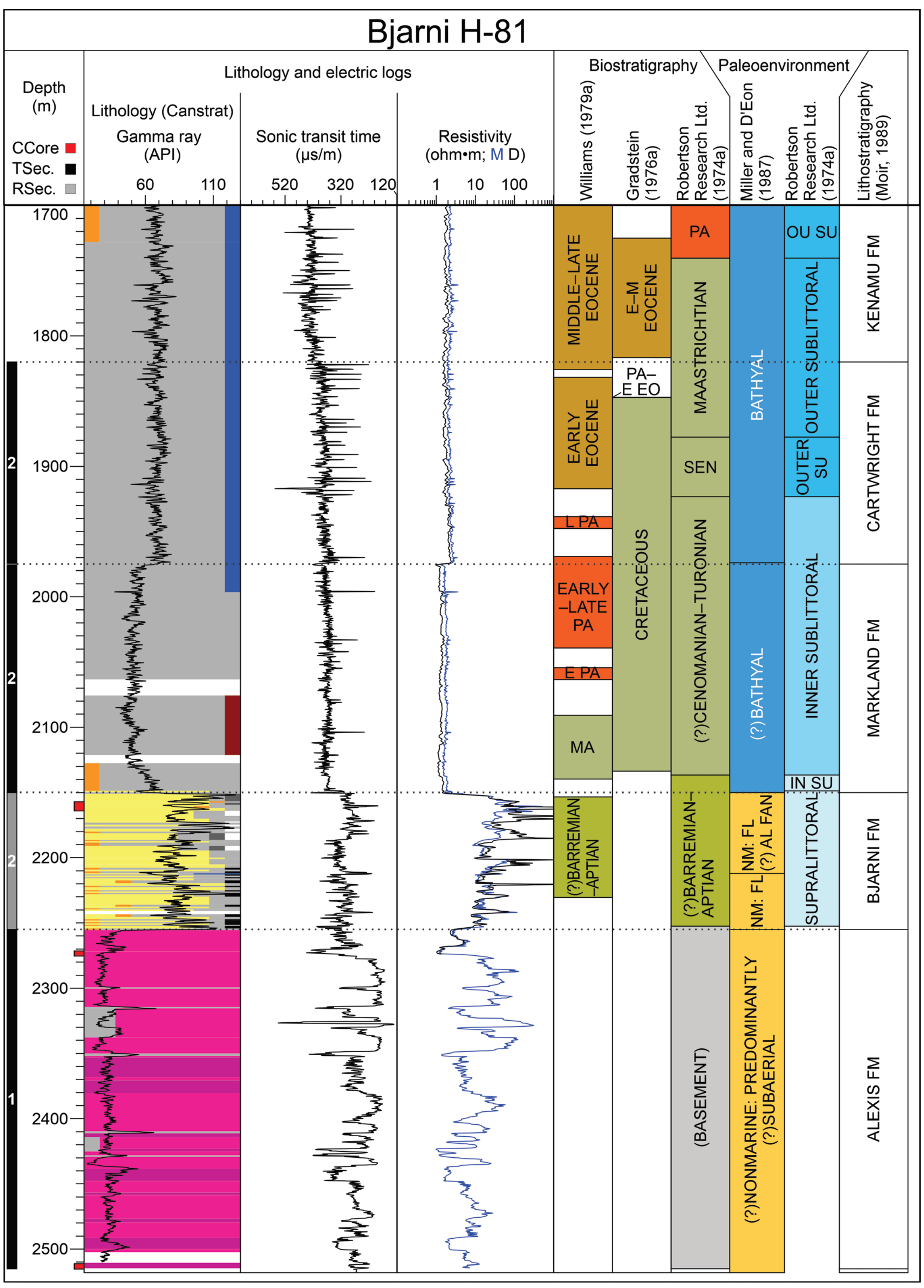

Figure 11. The Bjarni H-81 well, showing fundamental wireline logs, lithology (Canstrat), conventional core locations, key biostratigraphic studies, paleoenvironmental interpretations, and lithostratigraphy. Type sections for the Alexis, Markland, and Cartwright Formations and a reference section for the Bjarni Formation are shown. *See* Figure 4b for legend.

Moir (1989). In addition to Snorri J-90 and Herjolf M-92, Moir (1989) defined a Snorri Member in Freydis B-87 (Fig. 8), Hopedale E-33, North Leif I-05, Ogmund E-72, Roberval K-92, Skolp E-07 (Fig. 13), South Hopedale L-39, South Labrador N-79, and Tyrk P-100; however, many of these intervals are relatively sandstone-prone, suggesting that there is gradation between the shale-dominated Snorri Member and sandstone-dominated Bjarni Formation.

Several authors (Umpleby, 1979; Bell, 1989; Balkwill and McMillan, 1990; Dickie et al., 2011) have identified the Bjarni Formation as a syn-rift graben fill occupying structural lows in northwest-oriented grabens and half-grabens formed during extension. The contacts of the Bjarni Formation are generally distinctive in both well and seismic data. The base of the formation is distinguished from the underlying, higher velocity Precambrian basement rocks, Ordovician carbonate rocks, or Alexis Formation basalt units in seismic data, and there is an abrupt lithological change that is also seen in well logs. At the top of the Bjarni Formation is a discontinuity, termed the "Avalon Unconformity" (McWhae et al., 1980), with the deeper marine Markland Formation that appears to mark a transition from early-rift to late-rift stages along the Labrador margin (Dickie et al., 2011).

McWhae et al. (1980) recognized the presence of local unconformities within the Bjarni Formation and suggested that it could be subdivided. Balkwill (1987) delineated a lower nonmarine interval confined to half-grabens and an upper, partly marine succession that onlaps and can overstep graben confines. The lower "member" was described as containing feldspathic, lithic, coaly, partly conglomeratic, fine- to very coarse-grained quartzose arenite, with nonmarine fossils. Conversely, the upper "member" is sandy, clayey, carbonaceous siltstone and shale with nonmarine and shallow-marine fossil occurrences. Balkwill and McMillan (1990) expanded further on these informal members and considered the lower member to be absent north of latitude 58°N (in the southern part of the Saglek Basin). The boundary between these informal lower and upper members may lie within the middle to late Albian (Balkwill and McMillan, 1990); however, refinements to biostratigraphic ages (e.g. Nøhr-Hansen et al., 2016) in combination with paleoenvironmental determinations (e.g. Miller and D'Eon, 1987) suggest revision to some of these lower and upper divisions, such as the one proposed for North Leif I-05. In this well, the nonmarine section based on Miller and D'Eon (1987) is thin and ends in the early Albian of Dafoe and Williams (2020b). Furthermore, Dickie et al. (2011) indicated that even on modern

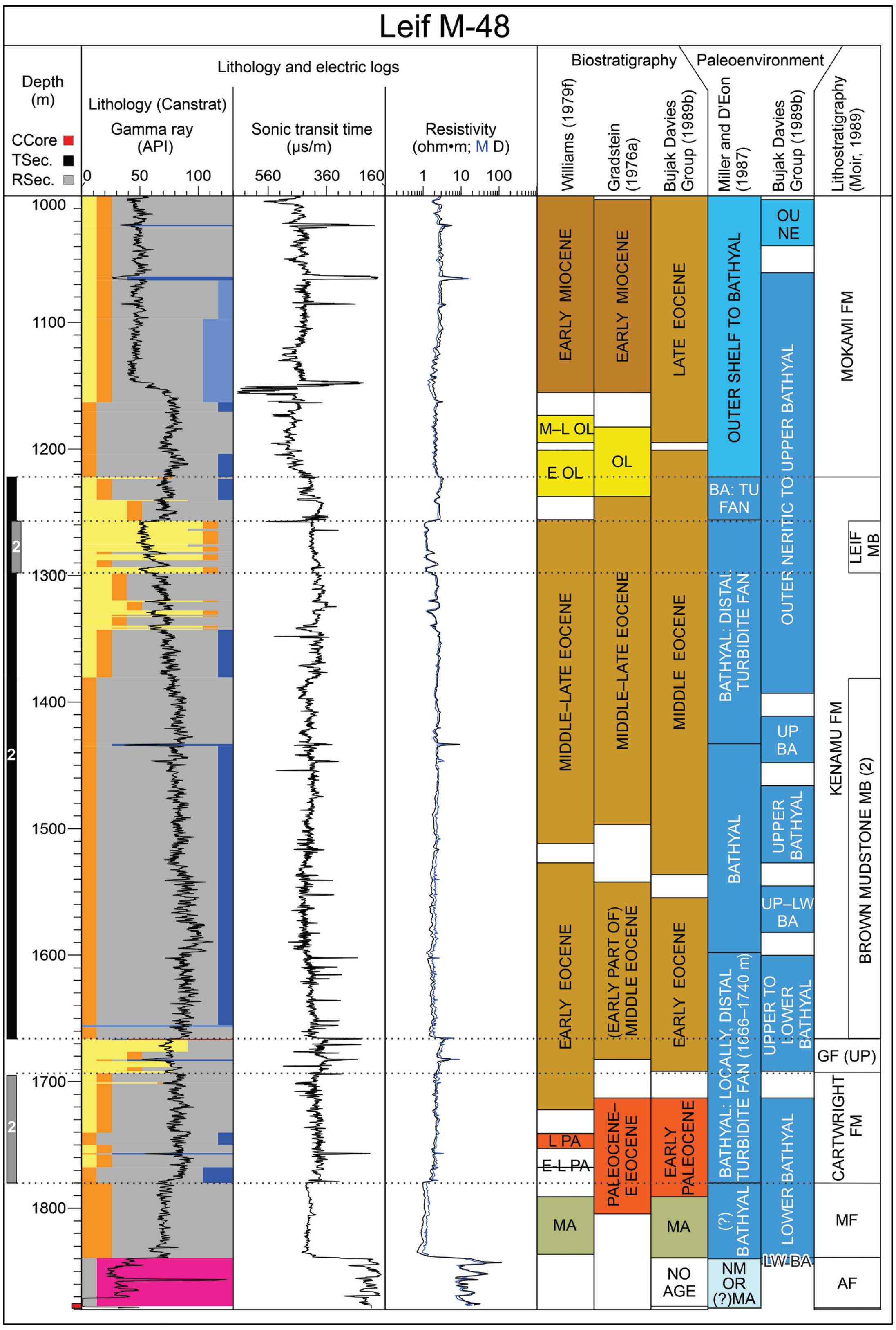

Figure 12. The Leif M-48 well, showing fundamental wireline logs, lithology (Canstrat), conventional core locations, key biostratigraphic studies, paleoenvironmental interpretations, and lithostratigraphy. The type sections for the Kenamu Formation and Brown Mudstone Member of that formation and reference sections for the Cartwright Formation and Leif Member of the Kenamu Formation are indicated. *See* Figure 4b for legend.

seismic data, the Bjarni Formation syn-rift fill has little distinguishing character to permit mapping of lithologically controlled facies within the grabens. They suggested that sandstone units likely flank basement highs and finer grained shale units occupy distal or central graben areas, but proximity to a source area could also influence this interplay. Thrane (2014) found that the Bjarni Formation in the Saglek Basin wells was sourced from the Archean Hopedale Block, with Proterozoic rocks from the Grenville Province and Makkovik Orogen being the dominant sediment source in the Hopedale Basin; however, the high feldspar content, and thus immature nature of the Bjarni Formation sandstone units suggests that they were primarily derived from the erosion of relatively nearby basement highs (Balkwill and McMillan, 1990). Dafoe and Williams (2020a) also noted that there were clasts within the Bjarni Formation that directly resemble the crystalline basement rocks sampled deeper within the same wells.

Biostratigraphy

Ages for the Bjarni Formation have been determined almost exclusively from miospores: dinocysts are rare (Nøhr-Hansen et al., 2016). Based on palynological analysis, Williams (1979d) dated the type section of the Bjarni Formation in Herjolf M-92 as Barremian–Aptian to Albian–Cenomanian (Fig. 6). Ainsworth et al. (2014) considered the age to range from late Barremian–earliest Aptian to late Albian. According to these authors, the Bjarni Formation was unconformably overlain by Santonian to Campanian sediments of the Markland Formation. Comparing the two sets of ages suggests that the Bjarni Formation in the type section must be predominantly Aptian–Albian. The age of the Bjarni Formation in the reference section of Bjarni H-81 is less conclusive: (?)Barremian–Albian (Robertson Research Ltd., 1974a) or (?)Barremian–Aptian (Fig. 11; Williams, 1979a). Balkwill and McMillan (1990) suggested that the Bjarni Formation could be as old as Neocomian or even Jurassic since the lowermost Bjarni Formation sediments are not drilled within the deepest parts of grabens.

The type section for the Snorri Member of the Bjarni Formation in Snorri J-90 was initially interpreted as Barremian in its uppermost few metres with a questionable (?)Jurassic–Barremian age near its base (Williams, 1979g; Fig. 7). Ainsworth et al. (2014) later dated all of the Snorri Member in the Snorri J-90 well as late Barremian–(?)early Aptian; however, later work by Nøhr-Hansen et al. (2016) placed the entire member in the Aptian. Furthermore, Nøhr-Hansen et al. (2016) in their palynological analysis of 19 wells from the Labrador–Baffin Seaway, including ten from the Labrador Shelf, did not recognize any Barremian intervals; however, they did confirm the existence of Aptian Bjarni Formation in the following wells: Bjarni O-82, Roberval K-92, Snorri J-90, and South Labrador N-79, all of which are in the Hopedale Basin. In contrast, Dafoe and Williams (2020a) considered core 2 (3563.8 m) in Herjolf M-92 and core 1 in Bjarni H-81 (2157.0 m) as Barremian–Aptian. According to Nøhr-Hansen et al. (2016), Albian sediments occur in Bjarni O-82, North Leif E-05, and Ogmund E-72 in the Hopedale Basin and Skolp E-07 in the Saglek Basin, but are missing from several others, indicating a major unconformity.

Whether the Bjarni Formation extends into the Cenomanian has long been debated as many biostratigraphic studies reported Albian–Cenomanian ages in the uppermost part of the Bjarni Formation (Table 5; Fig. 6, 8). Based on analyses of conventional core intervals located near the top of the formation, several intervals previously interpreted to range from Albian–Cenomanian to Turonian–Coniacian (Bjarni O-82, Herjolf M-92, North Bjarni F-06, Roberval K-92, and Tyrk P-100; Table 5; Fig. 6) are now considered to be from the Albian (Dafoe and Williams, 2020a). In addition to these results, palynological and micropaleontological analyses of sections in some of the same wells and also in Freydis B-87 (Fig. 8), Ogmund E-72, Skolp E-07 (Fig. 13), and South Labrador N-79 (Table 5; Ainsworth et al.,

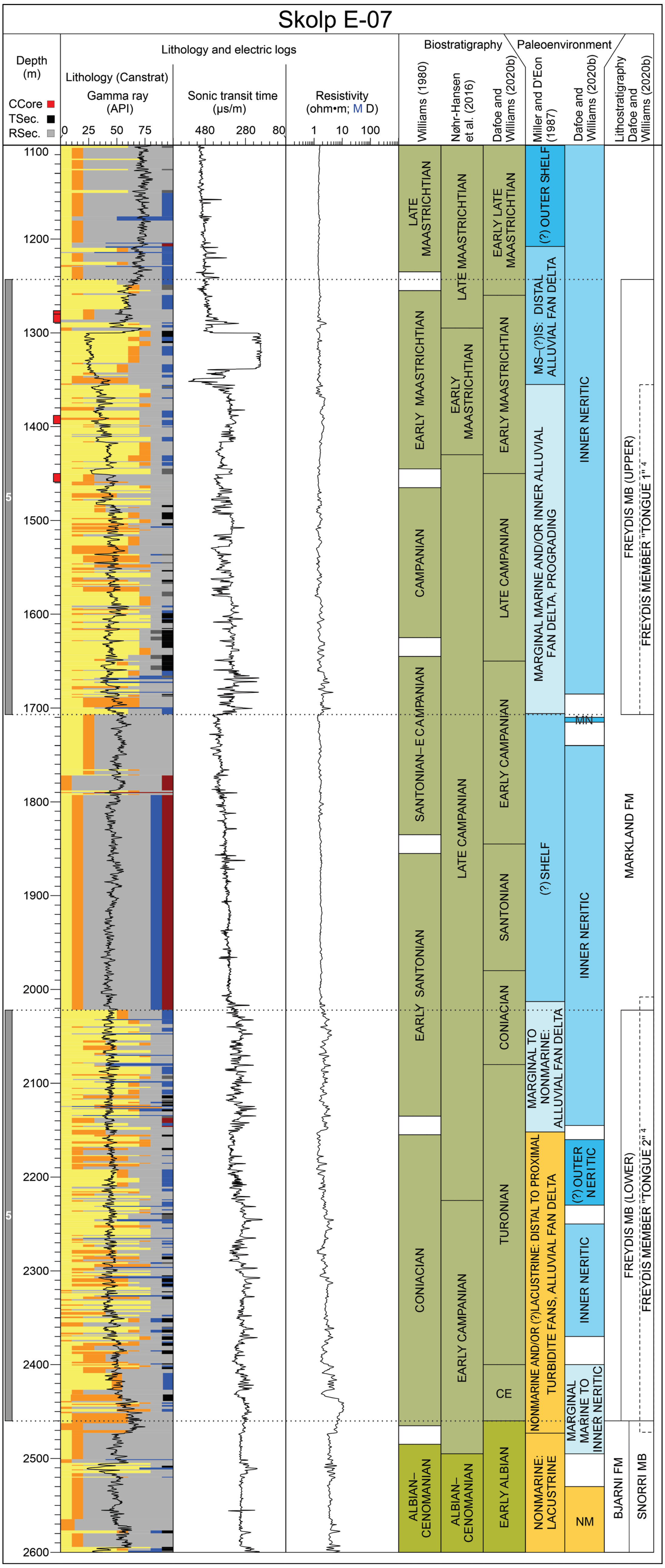

Figure 13. The Skolp E-07 well, showing fundamental wireline logs, lithology (Canstrat),conventional core locations, key biostratigra-phic studies, paleoenvironmental interpretations, and lithostratigraphy (in this figure the lithostratigraphy is from Dafoe and Williams, 2020b). The reference sections for the Freydis Member of the Markland Formation are shown, with Freydis Member tongues from Moir (1987). *See* Figure 4b for legend.

Table 5. Summary of contentious ages reported for the uppermost Bjarni Formation and consensus age based on relevant studies.

Well	Top of Bjarni Formation (Moir, 1989)	Interval	Age of upper Bjarni Formation	Age reference	Justification for refined age	Refined age for uppermost Bjarni Formation
Bjarni O-82	2285 m	2305–2295 m	Turonian–Coniacian	Williams (2007d)		Middle–late Albian
		2330–2295 m	Turonian–Coniacian	Nøhr-Hansen et al. (2016)		
		2295–2265 m	Campanian	Nøhr-Hansen et al. (2016)	Interval spans a significant log change and likely extends into the uppermost Bjarni Formation due to cavings.	
		2304–2293.3 m	Middle–late Albian	Dafoe and Williams (2020a)	Based on core 2 within the same interval of the well as the previous ages described above, and near the top of the Bjarni Formation.	
		2291–2293 m	Middle Albian–Cenomanian	Dafoe and Williams (2020a)	This age range for core 1 is based on a single pollen species.	
Freydis B-87	1788 m	1804.4–1795.3 m	Late Albian–Cenomanian	Williams (1979c)		Late Albian
		1813.6–1786.1 m	Late Albian	Ainsworth et al. (2016)	Based on modern palynology and micropaleontology analyses.	
Herjolf M-92	2614 m	2691.4–2590.8 m	Albian–Cenomanian	Williams (1979d)		Albian, possibly late
		2844–2624 m	Late Albian	Ainsworth et al. (2014)	Based on modern palynology and micropaleontology analyses.	
		2639.9–2632.28 m	Albian	Dafoe and Williams (2020a)	Based on core 1 within the same interval as the other two studies listed above, and near the top of the Bjarni Formation.	
North Bjarni F-06	2423 m	2490–2420 m	Turonian–Coniacian	Bujak Davies Group (1989b)		Early–late Albian
		2590–2430 m	Late Albian	Ainsworth et al. (2014)	Based on modern palynology and micropaleontology analyses.	
		2458–2452 m	Early Albian or older	Dafoe and Williams (2020a)	Based on core 1 within the same interval of the well as the previous studies listed above, and close to the top of the Bjarni Formation.	
North Leif I-05	2820 m	2830–2810 m	Early–middle Albian	Bujak Davies Group (1989c)		Cenomanian–Turonian (Markland Formation)
		2805–2730 m	Late Albian–early Cenomanian	Ainsworth et al. (2016)		
		3120–2790 m	Late Albian	Nøhr-Hansen et al. (2016)		
		2820–2720 m	Cenomanian–Turonian	Dafoe and Williams (2020b)	The shale interval from 2821 to 2723 m that was considered Markland Formation (Moir, 1989) is now only within the Upper Cretaceous section.	
Ogmund E-72	1712 m	1755–1685 m	Late Albian–Cenomanian	Bujak Davies Group (1989c)		Late Aptian–late Albian
		2530–1730 m	Late Aptian–late Albian	Ainsworth et al. (2014)	Based on modern palynology and micropaleontology analyses.	
		1920–1785 m	(?)Cenomanian	Nøhr-Hansen et al. (2016)	Questionable results.	
		1785–1590 m	Late Campanian	Nøhr-Hansen et al. (2016)	Interval spans a significant well-log change and likely extends the Late Cretaceous into the underlying Bjarni Formation due to cavings.	
Roberval K-92	3080 m	3130–3090 m	Late Albian–early Cenomanian	Bujak Davies Group (1989d)		Aptian–early Albian
		3190–3090 m	Late–(?)middle Albian	Ainsworth et al. (2014)		
		3160–3090 m	Aptian	Nøhr-Hansen et al. (2016)		
		3090–3070 m	Santonian	Nøhr-Hansen et al. (2016)	Interval spans a significant well-log change and likely extends the Late Cretaceous into the underlying Bjarni Formation due to cavings.	
		3220–3090 m	Aptian	Williams (2017b)		
		3112.5–3095 m	Early Albian or older	Dafoe and Williams (2020a)	Based on core 2 within the same interval of the well as the previous studies listed above, and near the top of the Bjarni Formation.	

Table 5. (cont.) Summary of contentious ages reported for the uppermost Bjarni Formation and consensus age based on relevant studies.

Well	Top of Bjarni Formation (Moir, 1989)	Interval	Age of upper Bjarni Formation	Age reference	Justification for refined age	Refined age for uppermost Bjarni Formation
Skolp E-07	2472 m	2855–2485 m	Albian–Cenomanian	Williams (1980)		Early Albian
		2985–2495 m	Albian–Cenomanian	Nøhr-Hansen et al. (2016)		
		2915–2460 m	Early Albian	Dafoe and Williams (2020b)	Palynology samples were analyzed every 15 m between 2415 to 2610 m to improve resolution of biostratigraphic ages. Lacking prominent well log changes, the top Bjarni Formation was redesignated at 2460 m.	
South Hopedale L-39	1920 m	2070–1970 m	Early–middle Albian	Bujak Davies Group (1989e)		Middle Albian
		1950–1940 m	Middle Albian	Bujak Davies Group (1989e)	The top of the Bjarni Formation correlates to a subtle well-log change that corresponds with the base of Bujak Davies Group's (1989e) Late Cretaceous (Santonian) interval.	
		2060–1915 m	Albian	Oliver and Awai-Thorne (1984)		
		2010–1990 m	Middle–late Albian	Ainsworth et al. (2016)		
		1980–1950 m	Cenomanian	Ainsworth et al. (2016)	Whereas Ainsworth et al. (2016) suggested a possible unconformity at 1975 m within the Cenomanian, this depth does not correlate with previous results that suggest an Early Cretaceous age.	
		1940–1910 m	Early–middle Turonian	Ainsworth et al. (2016)	All other Turonian ages for the Bjarni Formation have been refuted by analyses of conventional core intervals. Accordingly, the Bjarni Formation does not likely extend into the Turonian.	
South Labrador N-79	3496 m	3571.5–3515 m	Barremian–early Aptian	Bujak Davies Group (1989e)		Aptian, possibly early
		3548–3510 m	Barremian–early Aptian	Williams (2007b)		
		3548–3510 m	Aptian	Nøhr-Hansen et al. (2016)	Their revised assessment of palynomorph age ranges suggest Aptian rather than Barremian to Aptian.	
		3510–3440 m	Coniacian	Nøhr-Hansen et al. (2016)	Interval spans a significant well-log change and likely extends the Late Cretaceous into the underlying Bjarni Formation due to cavings.	
Tyrk P-100	1195 m	1245–1185 m	Late Albian–Cenomanian	Oliver and Thorne (1979)		Middle–late Albian
		1530–1160 m	Early–middle Albian	Bujak Davies Group (1989f)	This interval extends above Moir's (1989) Bjarni Formation top and the significant well-log change at 1182 m.	
		1190–1185 m	Middle–late and late Albian	Dafoe and Williams (2020a)	Based on core 1 located above the top of Moir's (1989) Bjarni Formation, bringing the top of the formation to 1182 m at a significant well-log change about 3 m above core 1.	

2014, 2016; Nøhr-Hansen et al., 2016; Dafoe and Williams, 2020b) have provided new results that indicate an Aptian to Albian age for the top of the Bjarni Formation. In several instances, prominent well-log changes indicate the position of the top Bjarni Formation unconformity with the overlying Upper Cretaceous section, but cavings have likely resulted in misinterpretation of Late Cretaceous ages into the Bjarni Formation as defined by Moir (1989). This is likely the case in the results of Nøhr-Hansen et al. (2016) in Bjarni O-82, Ogmund E-72, Roberval K-92, and South Labrador N-79. In the South Hopedale L-39 well, a Cenomanian result from Ainsworth et al. (2016) disagrees with previous Albian ages for the interval from about 1980 to 1920 m (Table 5; Oliver and Awai-Thorne, 1984; Bujak Davies Group, 1989e). A Turonian age for the Bjarni Formation has been otherwise refuted in other wells based on analyses of conventional core intervals (Dafoe and Williams, 2020a). Also in South Hopedale L-39, the Cenomanian section of Ainsworth et al. (2016) does not appear to correlate with a log change that would indicate the top of the Bjarni Formation. In this case, pre-existing Albian ages appear to be more consistent with regional results. Finally, an interval previously considered to be partly Albian–Cenomanian in North Leif I-05 (Bujak Davies Group, 1989c; Ainsworth et al., 2014; Nøhr-Hansen et al., 2016) is now considered Cenomanian–Turonian and remains a part of the Markland Formation based on the study by Dafoe and Williams (2020b). Based on the above, the age of the Bjarni Formation is likely late Barremian to late Albian, but older sedimentary rocks may be present at depths within structures underlying the Labrador Shelf, possibly interbedded with Alexis Formation basalt units (Fig. 3).

Paleoenvironments

In the original description, Umpleby (1979) described the Bjarni Formation as delta-plain sandstone units deposited during mild tectonism, with shale and coal of the Snorri Member possibly reflecting low topographic relief. McWhae et al. (1980) expanded this to include channels and coal swamps in addition to deltaic deposits. Paleoenvironments during the Early Cretaceous were initially considered to be predominantly nonmarine on the Labrador margin (Gradstein and Williams, 1976). This conclusion was based on the recognition, at the time, of only miospores in the palynological assemblages and the absence of foraminifera; however, from the occasional occurrences of the dinocyst genera *Nyktericysta* and *Vesperopsis* on both margins of the Labrador–Baffin Seaway, Nøhr-Hansen in Sønderholm et al. (2003) and Nøhr-Hansen et al. (2016) concluded that there were occasional marginal-marine episodes. This is supported by the presence of rare specimens of other dinocyst species, as well as *Nyktericysta* and *Vesperopsis*, as in the Aptian of South Labrador N-79 (Nøhr-Hansen et al., 2016) and the Albian of North Leif I-05 (Dafoe and Williams, 2020b) and Ogmund E-72 (Dafoe and Williams, 2020a), all in the Hopedale Basin. Thus, the dinocyst data indicate that the paleoenvironment fluctuated between nonmarine and shallow marine, possibly lagoonal in the Aptian–Albian.

In a detailed lithological study, Miller and D'Eon (1987) described the pre-Albian Bjarni Formation strata as alluvial fan, fluvial, lacustrine, and alluvial fan-delta deposits with some coal and floodplain accumulations where subsidence was less rapid. Similarly, Balkwill and McMillan (1990) considered the conglomerate units in the lower Bjarni Formation to represent alluvial fans and scree-slope deposits, with riverine sandstone units including both braided and meandering morphologies. Miller and D'Eon (1987) only noted rare marine influence prior to the Albian, which included brackish conditions, tidal influence, and local deltaic activity (e.g. North Leif I-05). Further, Miller and D'Eon (1987) interpreted Albian strata to denote shallow-marine incursions. They reported indications of strong tidal currents such as shale drapes, rhythmic bedding, shale clasts, and shell fragment horizons within deltaic deposits. Additionally, they postulated that a northward increase in tidal range might be expected if there was a long narrow rift valley along the Labrador margin. Based on dip-direction data, Miller and D'Eon (1987) suggested that most sediment during this time was derived from onshore Labrador sources, but some appears to have also come from the West Greenland margin.

In a study of conventional core intervals, Dafoe and Williams (2020a) integrated sedimentological, ichnological, and palynological data to determine paleoenvironments for 14 Bjarni Formation core intervals from ten wells on the Labrador margin. These cores are generally Albian (ten intervals) and were recovered from near the top of the formation, and were interpreted as reflecting shallow-marine deposition in river-influenced, river-dominated, and wave-influenced deltaic settings, as well as two occurrences of restricted marine settings and an in situ nearshore volcanic accumulation (Dafoe and Williams, 2020b). The remaining Bjarni Formation core intervals were determined to be Barremian–Aptian or Aptian and deposited in fluvial or restricted marine bay settings (Dafoe and Williams, 2020b). One interval of river-influenced deltaic deposits was noted from core 1 of Bjarni H-81; however, the older, Barremian–Aptian age is inconsistent with core intervals from the nearby wells intersecting similar strata of Albian age. Overall, the results of Dafoe and Williams (2020b) and previous authors suggest nonmarine and lesser restricted marine deposition in the Barremian–Aptian and predominantly shallow-marine deposition during the Albian.

Previous offshore mapping

Cretaceous sedimentary rocks underlie much of the Labrador margin (Fig. 10). Earlier studies within the region discovered thick sedimentary basins underlying the Labrador Sea (Srivastava, 1986; Fader et al., 1989; Bell, 1989; Balkwill and McMillan, 1990; Oakey and Chalmers, 2012) and showed various distributions of these strata landward of oceanic crust; however, their data sets were relatively sparse compared to the 2-D multichannel seismic coverage of the present day (*see* Fig. 1). The earliest syn-rift strata were deposited during the rifting between Greenland and North American (Oakey and Chalmers, 2012). In the Early Cretaceous, basement rocks were extended and thinned, resulting in the formation of grabens and half-grabens infilled with syn-rift strata of the Bjarni Formation, along with volcanic rocks of the Alexis Formation (Dickie et al., 2011).

Seismic reflection character

On seismic reflection data, the Bjarni Formation forms a moderate to weakly layered interval capped by high-amplitude reflections. It is overlain by lower velocity, seismically transparent, shale units of the Markland Formation (line 1; Fig. 9a). The infill of grabens and half-grabens is characterized by growth of strata against faults, and these depressions can be filled to locally overfilled (line 1; Fig. 9a) or underfilled (line 2; Fig. 9b). The top of the Bjarni Formation forms a distinctive unconformity that correlates with the relatively high-amplitude reflection seen on seismic data. This was recognized by Dickie et al. (2011) as their horizon 2, and in the present study is labelled as the top of the Bjarni Formation (Bj horizon; Fig. 9). The regional distribution of Cretaceous sedimentary rocks as a whole is described below in conjunction with the overlying Markland Formation (*see* 'Distribution of the Cretaceous interval' section).

UPPER CRETACEOUS INTERVAL

Markland Formation

Lithostratigraphy

McWhae et al. (1980) introduced the Markland Formation for a unit comprising green to dark grey shale, silty shale, rare siltstone, and sandstone, with thin, brown, dolomitic limestone beds: the proposed age was given as Late Cretaceous to Danian (Fig. 3). Balkwill and McMillan (1990) further described the shale as siderite-bearing, partly micaceous, and commonly fissile, locally with trace glauconitic sandstone. This interval was originally included in the Cartwright Formation by Umpleby (1979), but the presence of a distinctive base and top to the shale succession above the Bjarni Formation convinced McWhae et al. (1980) to propose a new formation name. The type section for the Markland Formation is in the Bjarni H-81 well from 2150 to 1975 m (175 m thick), the "indurated silty shales" of McWhae and Michel (1975) from the same well (Fig. 11). In addition to the type section, McWhae et al. (1980) proposed reference sections including 2614 to 2211 m in Herjolf M-92 (403 m thick; Fig. 14) and 2663 to 2393 m in Gudrid H-55 (270 m thick; Fig. 5). They also proposed a reference section in Freydis B-87 from 1875 to 1492 m (383 m including Freydis Member sandstone units from 1875–1731 m); however, biostratigraphic data in this latter well indicate that the lower part of McWhae et al.'s (1980) interval is Early Cretaceous and in part correlates with the Bjarni Formation (Snorri Member). Accordingly, Moir (1989) modified the lower boundary of this reference section to 1788 m at the base of the Freydis Member, thus making the Markland Formation 296 m thick in Freydis B-87 (Fig. 8). Balkwill and McMillan (1990) reported the thickest Markland Formation succession from the Gilbert F-53 well (about 753 m), including Freydis member sandstone units, but the Markland Formation in Skolp E-07 is about 1117 m (Fig. 13; Moir, 1989). In terms of sediment sources, Thrane (2014) suggested that the Markland Formation was derived from the Hopedale Block, Saglek Block, and Makkovik Orogen.

Due to its distinctive lithology, the base of the fine-grained Markland Formation is well defined where it overlies the Bjarni Formation, Alexis Formation, or pre-rift basement rocks. The transition from underlying rocks may also display a decrease in resistivity log signature at this lower contact. Above the Markland Formation, contact with the overlying sandstone-bearing Gudrid Formation and fine-grained Cartwright Formation, is unconformable to disconformable, respectively (McWhae et al., 1980). This upper contact is marked by a decrease in sonic velocity and a general increase in the resistivity log (Balkwill and McMillan, 1990). This is especially pronounced where the Gudrid Formation overlies it, but can also be seen at the contact with the Cartwright Formation shale units.

McWhae et al. (1980) assigned the nearshore, sandstone-bearing facies within the Markland Formation to the Freydis Member. The name was originally used by Total Eastcan for an Upper Cretaceous sandstone in the Freydis B-87 well and formally proposed as the Freydis Sand Member by Umpleby (1979) for his original Cartwright Formation. Umpleby (1979) designated the type section as the interval 1789 to 1734 m (55 m thick) in the Freydis B-87 well, which McWhae et al. (1980) revised to 1875 to 1731 m (144 m thick) to include Upper Cretaceous heterolithic shale and sandstone units found below the original type section (Fig. 8); however, Williams (1979c) considered most of the interval below 1795 m as Cenomanian and older, consistent with the Bjarni Formation (although now considered to be late Albian and older; Table 5). Moir (1989) and Balkwill and McMillan (1990) thus restricted the Freydis Member type section to the interval 1788 to 1730 m or 1728 m, respectively, based on lithology, well logs, seismic character, and biostratigraphy; however, 1730 m is more consistent with the log change in the well, resulting in a thickness of 58 m (Fig. 8). McWhae et al. (1980) also proposed a reference section for the Freydis Member from 2427 to 1355 m in the Skolp E-07 well (Fig. 13). These authors noted there were three sandstone intervals, which were not specified other than an indication of a total sand thickness of 647 m. Balkwill and McMillan (1990) suggested a much shallower revised base of 1782 m; but Moir (1989) placed the base of the Freydis Member even deeper in Skolp E-07 at 2472 m. In his earlier work, Moir (1987) divided the Freydis Member into a lower 'tongue 2' from 2472 to 2008 m and an upper 'tongue 1' from 1707 to 1355 m (Fig. 13). Dafoe and Williams' (2020b) assessment of the Bjarni Formation (Table 5) places the top of the formation at 2460 m, which marks a shallower base for the Markland Formation and lower Freydis Member. Furthermore, the present authors agree with the Freydis Member assignments of these same authors from 2460 to 2022 m and 1707 to 1243 m.

The Freydis Member consists of light grey, fine- to coarse-grained, quartzose sandstone and poorly sorted arkosic sandstone with an argillaceous matrix (McWhae et al., 1980). Siltstone and shale units are less common and accessory minerals include pyrite, siderite, and glauconite. McWhae et al. (1980) recognized that one or several sandstone units could be present within the Markland Formation such that the base of the Freydis Member is the bottom of the lowest sandstone unit in the Markland Formation shale and the top is the first sandstone interval of significant thickness (i.e. tens of metres). Balkwill and McMillan (1990) considered that the Freydis Member could be up to 1200 m thick based on their mapping offshore Cape Chidley, but the thickest individual succession was reported as 464 m in Skolp E-07 (Table 2; Dafoe and Williams, 2020b). Dickie et al. (2011) described a transition between the Bjarni and Markland formations, a Cenomanian–Coniacian unit deposited during marine transgression within deeper graben structures forming the section seen between their 2 and 2′ unconformities. Sandstone units deposited within this interval were informally referred to as the 'lower' Freydis Member, and upper Campanian sandstone units as the 'upper' Freydis Member. Here the present authors consider this transitional unit to be part of the Markland Formation (e.g. North Leif I-05; Dafoe and Williams, 2020b) and retain Moir's (1987) and Dickie et al.'s (2011) informal 'lower' and 'upper' Freydis Member units.

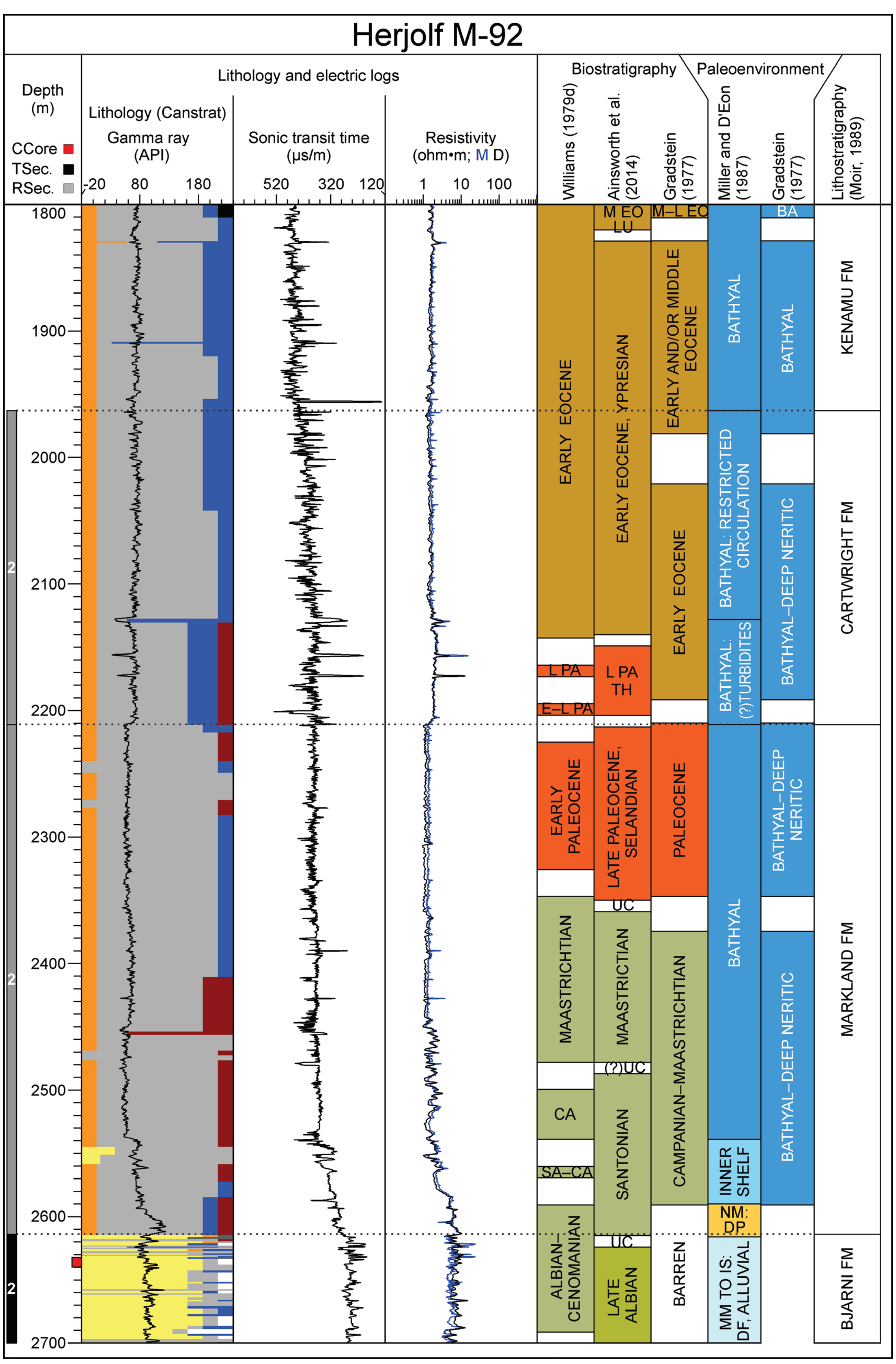

Figure 14. The Herjolf M-92 well, showing fundamental wireline logs, lithology (Canstrat), conventional core locations, key biostratigraphic studies, paleoenvironmental interpretations, and lithostratigraphy. Reference sections for the Markland and Cartwright formations are indicated, and the full type section for the Bjarni Formation is shown in Figure 6. *See* Figure 4b for legend.

Biostratigraphy

McWhae et al. (1980) initially considered the Markland Formation as Cenomanian–Turonian to Early Paleocene. In the type section, the Barremian–Aptian interval of Robertson Research Ltd. (1974a) extends into the lowermost Markland Formation in Bjarni H-81, but the log change at 2150 m forms a clear base to the formation (Fig. 11). Reworking during Markland Formation transgression may explain the anomalously older ages reported at the base of the Markland Formation. Ages for the overlying strata are also conflicting. Robertson Research Ltd. (1974a) considered it to be (?)Cenomanian–Turonian, but Williams (1979a) cited an age of Maastrichtian to Early–Late Paleocene. The latter age determination is not dissimilar to that of Gradstein et al. (1994), who considered the section to be Paleocene overlain by Eocene sediments, but earlier work by Gradstein (1976a) suggested a Cretaceous age (Fig. 11).

It was previously shown that the top of the Bjarni Formation in Herjolf M-92 is Albian (possibly late; Table 5; *see* 'Bjarni Formation' section). Accordingly, Cenomanian strata may be present at the base of the Markland Formation reference section based on Williams (1979d), but this would result in a significant unconformity or condensed section within shelfal to bathyal shale units with the overlying Santonian–Campanian strata (Fig. 14; Gradstein, 1977; Miller and D'Eon, 1987). More likely, the section is Santonian through Early Paleocene or Selandian (Williams, 1979d; Ainsworth et al., 2014). Ainsworth et al. (2014) further noted missing Campanian and Danian intervals, but these unconformities or condensed sections were not previously recognized (e.g. Dickie et al., 2011) and may be a result of uncertainties within the data sets.

McWhae et al. (1980) also specified the interval 2663 to 2393 m in Gudrid H-55 as a reference section for the Markland Formation (Fig. 5). This section is much younger compared to the shale units preserved in other wells, but has a relatively consistent Maastrichtian to Early Paleocene (Danian) age based on multiple biostratigraphic studies (Fig. 5; Robertson Research Ltd., 1974b; Gradstein, 1976a; Williams and Barss, 1979). Based on various biostratigraphic studies, strata with a relatively consistent Coniacian through Early Paleocene (possibly extending into the Middle Paleocene or Selandian) age occur in the final reference section of the Markland Formation in Freydis B-87 (Fig. 8; Gradstein, 1976a; Williams, 1979c; Ainsworth et al., 2016). Here, the Freydis Member is Coniacian to possibly early Santonian (Williams, 1979c; Ainsworth et al., 2016) and is thus consistent with the 'lower' Freydis Member. Younger Markland Formation strata were confirmed from Roberval K-92 as likely early Campanian from conventional core (Dafoe and Williams, 2020a).

In general, Balkwill and McMillan (1990) reported a condensed, discontinuous, and sometimes absent Cenomanian–Santonian succession (especially Cenomanian–Turonian) on the Labrador Shelf, perhaps reflecting biostratigraphic control. The discrepancy in the age of the basal beds of the Markland Formation is explained by the diachronous nature of the base of the formation due to transgressive onlap against basement highs during overall sag-basin deposition (cf. Dickie et al., 2011); however, wells that are drilled within structures, such as Skolp E-07, intersect a more complete Upper Cretaceous section and record older ages seen near the base of grabens or half-grabens. The Markland Formation in Skolp E-07 extends from 2472 to 1355 m (2460 m, based on this study; Fig. 13). Late Cretaceous ages vary for this unit placing the oldest rocks in the Coniacian (Williams, 1980), early Campanian (Nøhr-Hansen et al., 2016), or Cenomanian (Dafoe and Williams, 2020b). The study by Dafoe and Williams (2020b) involved denser sampling over the Bjarni to Markland formation boundary in order to resolve the ages therein. These authors still found thick Campanian and Maastrichtian strata, as well as relatively thick Cenomanian and Turonian rocks. Parts of the Markland Formation in this well form reference sections for the Freydis Member, which is Cenomanian to Coniacian (lower member) and Campanian to early Maastrichtian (upper member) based on Dafoe and Williams (2020b). Core intervals from this well also showed Maastrichtian (cores 1–3) and late Campanian ages (core 5; Dafoe and Williams, 2020a). Also from the 'upper' Freydis Member, upper Campanian sandstone units are present in cores 1 and 2 of Gilbert F-53 (Dafoe and Williams, 2020a).

In addition to results from the Skolp E-07 well, Dafoe and Williams (2020b) confirmed a Cenomanian–Turonian section between major log breaks in North Leif I-05, with the Albian Bjarni Formation below and Campanian section above. These log breaks tie to unconformities noted in seismic reflection data by Dickie et al. (2011; their 2 and 2′ unconformities). A similar set of unconformities (top Bjarni Formation and near the base of the Markland Formation) is noted from South Labrador N-79 (Williams, 2007b; Nøhr-Hansen et al., 2016), but the section is further abbreviated in this well making the stratigraphic relationships less clear. Parts of the Cenomanian to Santonian section are missing in a number of wells, suggesting a regionally extensive regression that may explain the unconformity within the Markland Formation, as illustrated in Figure 3.

One significant difference between the results of Ainsworth et al. (2014, 2016) and other studies (e.g. Williams (1979a–g, 2007a–e, 2017a, b), and Nøhr-Hansen et al. (2016)) is that the former do not recognize the occurrence of Danian strata on the Labrador margin. Whereas they recognized both early and late Danian based on several dinocyst events, Nøhr-Hansen et al. (2016) noted that the Danian seems to be missing or incomplete in the wells they studied, with the exception of South Labrador N-79. Although McWhae et al. (1980) restricted their reference sections to the Hopedale Basin, the thickest shale succession of the Markland Formation is in Gilbert F-53 in the Saglek Basin, where it extends from 3550 to 2459 m (Moir, 1989). For this interval, Williams (2007e) and Nøhr-Hansen et al. (2016) were in very close agreement on an early Campanian through early Selandian age with an extensive Danian section. A Danian section within the Markland Formation is thus recognized in Bjarni O-82, Gilbert F-53, Gudrid H-55, Karlsefni A-13, North Leif I-05, Roberval C-02, Roberval K-92, Skolp E-07, Snorri J-90, and South Labrador N-79 (Robertson Research Ltd. 1974b; Williams, 2007b, c, d, e; Nøhr-Hansen et al., 2016; Williams, 2017b; Dafoe and Williams, 2020b). In addition, the Markland Formation appears to extend into the Selandian based on Ainsworth et al. (2014, 2016) in Freydis B-87, Herjolf M-92, Karlsefni A-13, North Bjarni F-06, Roberval K-92, and South Hopedale L-39. Whereas definition of stages within the Paleocene varies between Ainsworth et al. (2014, 2016) and other authors, Selandian sediments in the Markland Formation have also been noted by others in Snorri J-90 and Karlsefni A-13, as well as in Bjarni O-82, Gilbert F-53, North Leif I-05, and South Labrador N-79 (Williams, 2007b, d, e; Nøhr-Hansen et al., 2016; Dafoe and Williams, 2020b). Collating the above results, the age of the Markland Formation appears to range from the Cenomanian to within the early part of the Selandian.

Paleoenvironments

In the original description of the Markland Formation, McWhae (1980) proposed a neritic to upper bathyal setting, with the Freydis Member representing nearshore deltaic sandstone units. In contrast, Balkwill and McMillan (1990) considered the Markland Formation to be marginal marine to middle shelf based on dinocysts and foraminifera. From detailed lithological studies, Miller and D'Eon (1987) suggested that the Turonian through Santonian was deposited under tidal-influenced deltaic activity, open-marine conditions, and estuaries, as well as lacustrine settings in the southern part of the Saglek Basin. During the same time frame, Nøhr-Hansen et al. (2016) considered the paleoenvironments in the Labrador–Baffin Seaway to be predominantly inner neritic based on palynomorphs. Presumably, several rivers were discharging sediments and nutrients into the seaway, thus providing ideal conditions for dinoflagellate reproduction; however, the low diversity of miospores suggests that the hinterland had a sparse vegetation cover or the coarse nature of the sedimentary influx destroyed miospores during transportation (Nøhr-Hansen et al., 2016).

Above the Santonian, Miller and D'Eon (1987) interpreted Campanian deposits as outer shelf to bathyal in the Hopedale Basin and marginal marine (deltaic, estuarine, bays and/or lagoons, and inner shelf successions) in the southern part of the Saglek Basin. Subsequent Maastrichtian and Lower Paleocene shale units were interpreted as deep neritic to bathyal, reflecting reduced oxygenation, typical of slope-equivalent settings during maximum marine onlap (Miller and D'Eon, 1987). It should be noted that a shelf-slope break was not established until deposition of the Kenamu Formation in the Eocene (Dickie et al., 2011) and prior to that reference to the 'slope' suggests equivalent water depths, greater than about 200 m. Similarly, Nøhr-Hansen et al. (2016) identified more open-ocean, presumably deeper water conditions in the Campanian–Maastrichtian, as shown in Gilbert F-53 in the Saglek Basin and Bjarni O-82 and South Labrador N-79 in the Hopedale Basin. Within outer shelf to open-ocean deposits in Gilbert F-53, they further identified the dinocyst taxa *Impagidinium* and sometimes abundant *Palaeoperidinium pyrophorum*; the former was considered an open-ocean indicator by Dale (1996). Species of *Palaeoperidinium*, where abundant, are generally taken to be indicative of inner neritic to coastal settings (Eshet et al., 1994: Brinkhuis et al., 1998); however, Nøhr-Hansen et al. (2016) reasoned that it could also be abundant in areas of upwelling, such as at shelf edges. During this later part of the Cretaceous, bathyal (open ocean) settings were also proposed for several wells, including Leif M-48 and Herjolf M-92 (Fig. 11, 14; Gradstein, 1977; Bujak Davies Group, 1989b), but proximal wells show shallower, shelfal settings overall such as in Skolp E-07 and Snorri J-90 (Fig. 7, 13; Williams, 2007b; Dafoe and Williams, 2020b); however, Dafoe and Williams (2020a) also confirmed outer shelf deposition in core 5 of Skolp E-07 and slope-equivalent, open-ocean deposition in the early Campanian in core 1 of Roberval K-92, within shale units near the base of the Markland Formation in that well.

Using microfossils and seismic morphology, Balkwill and McMillan (1990) indicated that the Freydis Member sandstone units that were confined to grabens represented syntectonic deltaic and shoreface deposits influenced by rivers, tides, and waves. The thinner, sigmoidal wedges of the Freydis Member were likely wave-dominated deltas that contributed sand to distal fans seen within the shale package (Balkwill and McMillan, 1990). In their study of conventional core intervals, Dafoe and Williams (2020a) analyzed seven cores of the Markland Formation (mostly from the Freydis Member) from Gilbert F-53 and Skolp E-07. The depositional paleoenvironments include upper Campanian through Maastrichtian river-influenced, deltaic, and lagoonal settings and alternating shoreface to outer-shelf deposition, with deltaic and shoreface sandstone units clearly representing the Freydis Member. In general, the Markland Formation shale units appear to represent shelfal conditions during the early Late Cretaceous, but deeper marine, open ocean to bathyal in the Campanian–Maastrichtian. The Freydis Member is, however, interpreted as shallow marine, mostly deltaic and shoreface settings with confirmed riverine influence, although tides and waves may also have been locally significant factors during deposition.

Previous offshore mapping

By the Late Cretaceous, the focus of rifting shifted further offshore (Dickie et al., 2011) where the crust became hyperextended and continental mantle was serpentinized and potentially exhumed (Keen et al., 2018a, b). During this time, sediments of the Markland Formation infilled the subsiding sag basin (Dickie et al., 2011), forming a wedge of shale units that thins basinward (Fig. 9; Balkwill, 1987). Bell (1989) presented maps of the Markland Formation distribution, net sandstone content and paleogeography along the shelf. As noted previously, the Markland Formation onlaps major basement highs and the basement platform, resulting in the diachronous nature of the oldest deposits intersected in Labrador Shelf wells. Accordingly, Balkwill (1987) considered the Santonian–Danian upper Markland Formation strata to be the primary marine shale unit along the margin that oversteps grabens to overlie the Bjarni Formation, Alexis Formation basalt units, or basement rock. Balkwill and McMillan (1990) considered the thin lower Markland Formation to have limited distribution due to depositional starvation.

McWhae et al. (1980) noted that the Freydis Member is only present in proximal wells and Balkwill (1987) described the Freydis Member as partly fault-bounded, narrow wedges of sandstone found in some proximal locations around the basement hinges of both the Hopedale and Saglek basins (e.g. Skolp E-07 and Freydis B-87). He also described Freydis Member sandstone units forming hinge-parallel, sigmoidal wedges with basinward-dipping internal reflectors. The distribution of these rocks is unclear, as they can resemble the syntectonic Bjarni Formation (Balkwill and McMillan, 1990) and the overlying Gudrid Formation. Dickie et al. (2011) further defined informal 'lower' and 'upper' Freydis Member sandstone units, whereas Bell (1989) mapped the net sandstone content, indicating Freydis Member development. In later studies, Dafoe et al. (2017a, 2018) suggested that the younger, upper Freydis Member shoreline clinoforms step landward of the lower sandstone unit, indicating progressive transgression during Markland Formation deposition.

Seismic reflection character

The Bjarni Formation is overlain by the relatively low-velocity, seismically transparent shale units of the Markland Formation capped by the M horizon (line 1; Fig. 9a; Dickie et al., 2011). These shale units onlap and downlap the underlying Bjarni Formation and pre-rift basement rocks forming a seaward-thickening wedge that thins in distal regions where it eventually downlaps onto oceanic crust (Fig. 9). Significant thicknesses are seen in the Saglek Basin (line 2; Fig. 9b) as compared to the Hopedale Basin (line 1; Fig. 9a). In some proximal locations (e.g. Freydis B-87 and Skolp E-07), the Markland Formation develops into a shallow-marine, deltaic sandstone succession of the Freydis Member with poorly to well developed clinoforms. In these locations, the interface between the Bjarni and Markland formations is more difficult to delineate due to limited velocity contrast between the two sandstone units. Farther offshore where strata are more deeply buried and seismic data quality deteriorates, this interface may also be poorly imaged.

The top of the Markland Formation is often marked by a clear trough on the seismic data, which develops as a result of the decrease in velocity with respect to the overlying formations. Where sandstone units of the Gudrid Formation cover the Markland Formation, the velocity contrast is most pronounced and the trough is strongest. Since the top Markland reflection forms a regional marker, it is used in the present study as a proxy for mapping the top of the Cretaceous interval, although it is slightly younger, ranging into the early part of the Selandian.

Distribution of the Cretaceous interval

Cretaceous sedimentary strata including the Bjarni and Markland formations have been intersected by a number of wells in the Hopedale and Saglek basins and their distribution is mapped (Fig. 10) by ties to the seismic grid. The landward limit of these rocks onlaps the shallowing basement platform (line 1; Fig. 9a, 12). Locally, where deep grabens have developed, Cretaceous strata may extend farther landward than the seismic data coverage (e.g. line 2; Fig. 9b). The seaward edge of Cretaceous sedimentary rocks onlaps and downlaps onto oceanic crust near the Early Paleocene chron C27n (Srivastava and Roest, 1999). Similarly, since the serpentinized and possibly exhumed mantle formed in the Late Cretaceous (Keen et al., 2018a, b, this volume), the distribution of Lower Cretaceous strata must be landward of this zone (Fig. 9, 10). Along the magma-rich margin of the southern part of the Saglek Basin (Keen et al., 2012, 2018b, this volume), Upper Cretaceous strata overlying a transitional zone and/or serpentinized mantle region became deeply buried under volcanic flows associated with the formation of this margin (line 2; Fig. 9b; *see* 'Paleocene–Eocene volcanic rocks' section). In the Saglek Basin, Lower Cretaceous strata of the Bjarni Formation appear to be thin (e.g. Skolp E-07; line 2; Fig. 9b) or absent, although the basin contains thicker Upper Cretaceous and younger sedimentary rocks than seen in the Hopedale Basin (line 1; Fig. 9a).

Along the southern Labrador margin, a region of inverted basement and Lower Cretaceous strata has been mapped (Fig. 10). Upper Cretaceous sedimentary rocks onlap this high. This feature developed in approximately the mid-Cretaceous along a complex, basement fault zone that coincides with an offset in the margin around the Cartwright Arch (Dickie et al., 2011). A similar margin offset coincides with a complex, likely inverted fault zone around the Bjarni wells in the central Hopedale Basin. Here, however, Upper Cretaceous shale units overstep this complex, providing a seal for the gas discoveries in that area. The offset in the margin here coincides with a Proterozoic basement shear zone extending seaward from the onshore, Makkovik Orogen (Hall et al., 2002). Perhaps these mid-Cretaceous structures signal the onset of late-stage rifting as it began to focus farther offshore into the hyperextended domain (Keen et al., 2018a).

In the Late Eocene, faulting and deformation of Upper Cretaceous and younger sedimentary rocks occurred over regions of the outer shelf (lines 1 and 2; Fig. 9) where large-scale faults (Balkwill and McMillan, 1990) detached as deep as the interface between the Bjarni and Markland formations.

PALEOCENE–EOCENE INTERVAL

Paleocene–Eocene volcanic rocks

Igneous rocks and previous offshore mapping

Oceanic crust underlies the central Labrador Sea and primarily comprises Paleocene–Eocene basalt flows (Keen et al., 2012, 2018b). Keen et al. (2012) followed the volcanostratigraphy of Planke et al. (2000) and identified the elements of a typical magma-rich margin including seaward-dipping reflectors, lava delta escarpments, and inner flows on the northern Labrador margin. Similarly, Chalmers (1997) interpreted a magma-rich region on the conjugate, West Greenland margin. Unlike the Western Davis Strait region (*see* Dafoe, DesRoches, and Williams, this volume) these volcanic rocks have not been drilled along the Labrador margin; however, a Paleocene (59 Ma, K-Ar whole-rock determination) diabase sill was intersected in Rut H-11 (Petro-Canada Inc., 1983) and was later confirmed in seismic data to be part of a Paleocene to Eocene sill complex (Keen et al., 2018b). These dark greyish-green rocks (Petro-Canada Inc., 1983) include mainly pyroxene and plagioclase, consistent with a laccolith-type intrusion (Shaw et al., 1984).

Distribution and seismic character

In Figure 15, the distribution of Paleocene–Eocene volcanic rocks is shown for the study region. The magma-rich northern margin (Keen et al., 2012) includes a large region of seaward-dipping reflectors that is more extensive than shown previously due to newly acquired seismic data in that region (*see* Keen et al., this volume). The interpreted volcanic margin has been provisionally extended northward, although the volcano-stratigraphic elements of Planke et al. (2000) are less distinct here (*see* Keen et al., this volume). Inboard of the magma-rich margin is a package of volcanic rocks interpreted as inner flows (Keen et al., 2012, 2018b). On seismic data, it generally forms a moderate to highly reflective unit up to 0.5 s two-way traveltime thick, which likely covers Cretaceous strata (line 2; Fig. 9b). Landward of the magma-rich escarpment, are landward flows and possible sills. These cover a large region and also extend onto the southern Labrador margin (Fig. 15). The occurrences appear as patches of bright reflections that align with sedimentary reflections at the top of the Markland Formation or within the overlying Cartwright Formation (Keen et al., 2018a). They occur along the more distal parts of the Saglek and Hopedale basins and resemble some of the sills mapped within the Newfoundland Basin (Shillington et al., 2006). An example of this can be seen on line 1 (Fig. 9b), at 6 s two-way traveltime and about 50 km landward of the landward limit of oceanic crust.

The Paleocene volcanic sill intersected by Rut H-11 (Petro-Canada Inc., 1983), appears to be part of an intrusive sill complex, which formed along the edge of the basement platform in the Saglek Basin (Fig. 15; Keen et al., 2018b). Formation of this complex may have been initiated at the same time as the onset of seafloor spreading, but sills continued to form in sedimentary rocks as young as the Middle–Late Eocene (Kenamu Formation; Keen et al., 2018b).

Cartwright and Gudrid formations

Lithostratigraphy

Total Eastcan proposed the name Cartwright for a Paleocene to Lower Eocene shale (*see* McWhae et al., 1980). Following proposal of this name, Umpleby (1979) established the Cartwright Formation, but expanded it to include both Upper Cretaceous and Paleocene mudstone and shale units (Fig. 3), with a type section in Gudrid H-55 from 2650 to 2393 m (Fig. 5). The age of the formation was then restricted by McWhae et al. (1980) to the Middle Paleocene to Early Eocene. These authors described the formation as brown-grey claystone, silty claystone, and siltstone, with thin partings of fine-grained, buff sandstone and thin brown carbonate beds, in addition to traces of glauconite, pyrite, and mica. The base of the formation is marked by a decrease in density and increase in resistivity log signatures, as well as a change in coloration from the grey Markland Formation shale units. McWhae et al. (1980) further noted a log change showing a subtle velocity decrease and lesser resistivity decrease into the overlying brown claystone units of the Kenamu Formation (e.g. Fig. 11, 14, 16), termed the 'Brown Mudstone Member' by Umpleby (1979) who also recognized this boundary.

The Cartwright Formation type section assigned by McWhae et al. (1980) is in the Bjarni H-81 well from 1975 to 1820 m (155 m thick; Fig. 11). A reference section was established in Leif M-48 from 1780 to 1695 m (85 m thick; Fig. 12), with an upper Gudrid Formation tongue overlying this interval from 1695 to 1666 m. McWhae et al. (1980) also established a reference section in Herjolf M-92 from 2211 to 1963 m (248 m thick; Fig. 14). In a subsequent study, Balkwill and McMillan (1990) divided the Cartwright Formation into informal lower and upper members with the base of the upper member defining the early Late Paleocene (these members align with their middle and upper Gudrid members, *see* discussion below).

The Gudrid Sand Member was chosen by Umpleby (1979) as a sandstone succession from 2393 to 2179 m (214 m thick) in Gudrid H-55 (Fig. 3, 5). Whereas Eastcan had identified a 'Cartier Sand' in their well history reports, Umpleby (1979) indicated that the sand was best developed in Gudrid H-55 and named the unit after this well. Subsequently, McWhae et al. (1980) determined that the Middle Paleocene to Lower Eocene sandstone was coeval to the redefined Cartwright Formation and raised the status of the Gudrid to formation level. They further described reference sections in Cartier D-70 from 1857 to 1795 m (62 m thick, lower tongue) and from 1763 to 1713 m (50 m thick, upper tongue, Fig. 4). The formation consists of quartzose and feldspathic sandstone, often poorly sorted, with argillaceous and dolomitic cement, as well as glauconite and trace coal fragments (Umpleby, 1979; McWhae et al., 1980). Umpleby (1979) suggested that the sandstone units of the Gudrid Formation were transported to their present location by the ancestral Churchill River, as he recognized that other wells, such as in the Bjarni and Leif areas do not have extensive sandstone units of this age. Thrane (2014) indicated that the Gudrid Formation sandstone units were sourced from the Saglek Block, Hopedale Block, Makkovik Orogen, and Grenville Province, similar to the provenance for the Markland and Bjarni formations.

Two sandstone intervals, recognized in Cartier D-70, are separated by a tongue of the Cartwright Formation shale (Umpleby, 1979; McWhae et al., 1980) and were informally named the lower and upper Gudrid tongues by McWhae et al. (1980). Balkwill and McMillan (1990) downgraded the Gudrid Formation to member status and described a lower member (Markland Formation equivalent) and middle and upper Gudrid members (Cartwright Formation equivalents). They considered the lower Gudrid member as a coastal sandstone facies of probable Danian age, and the middle (Middle to Late Paleocene) and upper (Late Paleocene–Early Eocene) Gudrid members to also represent coastal sandstone units. Balkwill and McMillan (1990) identified the lower Gudrid member in the Ogmund E-72, Roberval K-92, Cartier D-70, and Gilbert F-53 wells; however, existing and newly revised biostratigraphic ages (e.g. Nøhr-Hansen et al., 2016) do not place these sandstone units in the Danian, but rather in the Selandian or younger, consistent with McWhae et al.'s (1980) lower Gudrid Formation tongue. In addition, one of the key problems with Balkwill and McMillan's (1990) interpretation is that their middle Gudrid member has not been drilled in the Hopedale Basin, but was defined from the Hekja O-71 well farther to the north (*see* Dafoe, DesRoches, and Williams, this volume). The sandstone units in this well are now considered late Thanetian (Nøhr-Hansen et al., 2016; Dafoe and Williams, 2020a) or basal Ypresian (Williams, 2007a), which is consistent with the upper Gudrid Formation tongue of McWhae et al. (1980) and the upper Gudrid member of Balkwill and McMillan (1990).

Wherease some have adopted the revisions to the stratigraphy by Balkwill and McMillan (1990; e.g. Jauer et al., 2014; Thrane, 2014; Nøhr-Hansen et al., 2016), following the work of McWhae et al. (1980), Dickie et al. (2011) retained the Gudrid Formation status, but only mentioned that several sandstone lobes were present. Early on, the Gudrid Formation was recognized as having two sandstone intervals (McWhae et al., 1980; Miller and D'Eon, 1987; Moir, 1989). Successive results from Dafoe et al. (2017a, b, 2018) have confirmed that the Gudrid Formation sandstone units are Selandian to earliest Ypresian and represent two distinct progradational lobes related to regressive events. Based on the above discussion, there appears to be only two Gudrid Formation sandstone lobes, and the third Danian lobe of Balkwill and McMillan (1990) is absent. Accordingly, the original definition of the Gudrid Formation is consistent with the results of Dafoe et al. (2017a, b, 2018) and subdivision of the sandstone units into the informal 'lower' and 'upper' Gudrid Formation (as in Moir, 1989) fits the current understanding of the lithostratigraphic interval. Using this definition of the Gudrid Formation, the top is sharply bounded above by Umpleby's (1979) 'Brown Mudstone Member' of the Kenamu Formation, which is of lower velocity, and the boundary is based on both sonic logs and a lithological change (McWhae et al., 1980). The base of the Gudrid Formation is also lithologically distinct from the Markland Formation shale units, marked by an increase in velocity and decrease in gamma-ray log signature.

Biostratigraphy

According to some authors, the type section of the Cartwright Formation in Bjarni H-81 includes Upper Cretaceous strata (Fig. 11; Gradstein, 1976a; Robertson Research Ltd., 1974a); however, the mostly Late Paleocene to Early Eocene age determined by Williams (1979a) most closely agrees with the regional lithostratigraphic framework. The reference section in Leif M-48 was also generally found to be Early Paleocene to Early Eocene (Fig. 12; Gradstein, 1976a; Williams, 1979g; Bujak Davies Group, 1989b). In Herjolf M-92, the Cartwright Formation appears to include a thick Lower Eocene section, but again typically ranges from Early–Late Paleocene or Thanetian to Early Eocene or Ypresian (Fig. 14; Williams, 1979d; Ainsworth et al., 2014). In addition to these sections, less abbreviated successions

Figure 15. Distribution map of Paleocene to mid-Miocene (lower Cenozoic) interval for the Labrador margin with the location of the basement platform and highs, wells, and the distribution of volcanic features. Seaward-dipping reflectors are modified from Keen et al. (2012), and the magma-poor and magma-rich margins are described in Keen et al. (this volume). Basin outlines are from Keen et al. (this volume). L1 and L2 indicate the seismic reflection lines 1 and 2 shown in Figure 9. A well that shows the interval "not present" may not have drilled deep enough to intersect the interval, is cased through that interval, lacks related strata deposited at that location, or associated strata were later removed through erosion. Additional projection information: Central Meridian = 60°W; Standard Parallels = 65, 75°W; Latitude of Origin = 65°N.

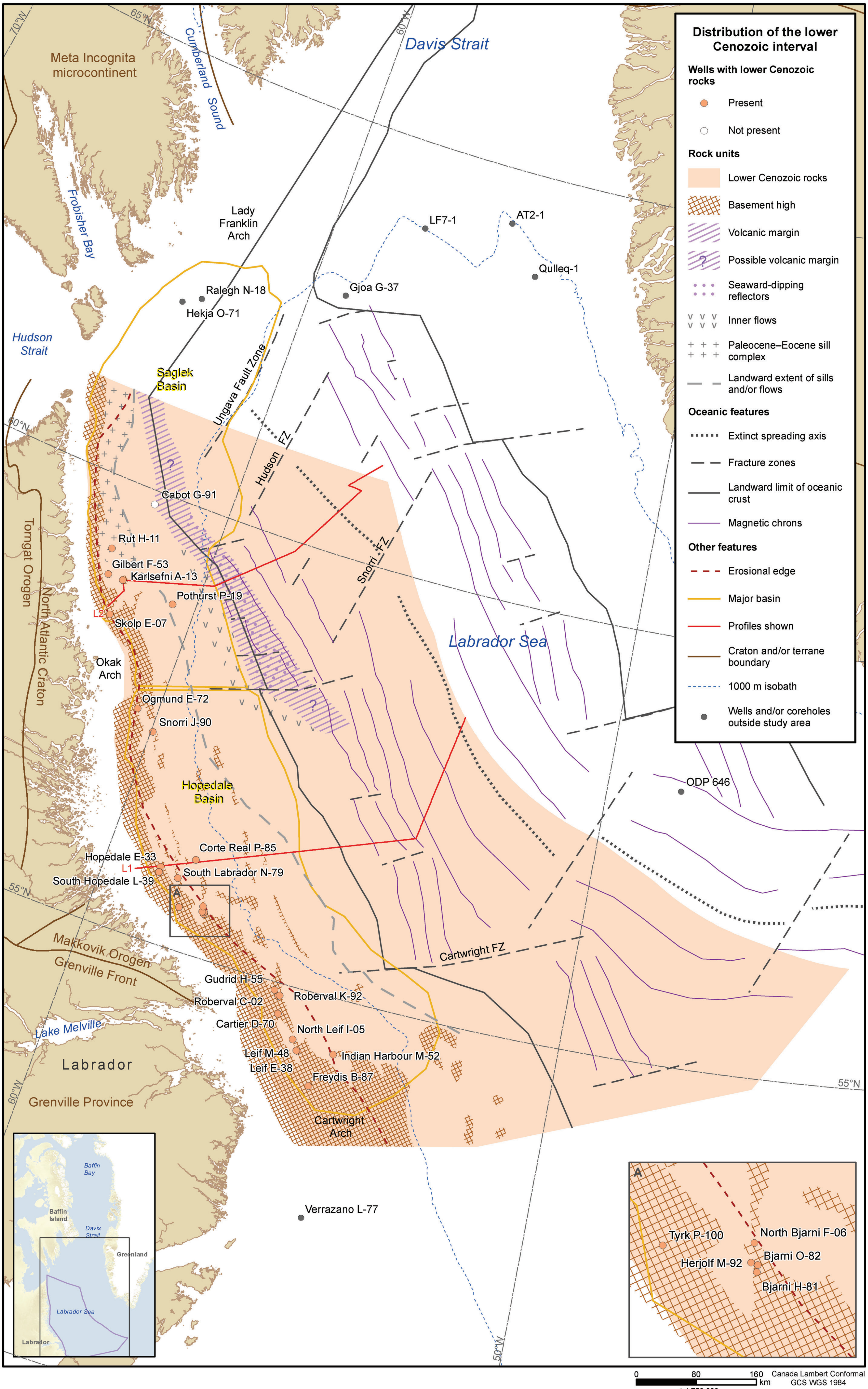
Distribution of the lower Cenozoic interval
Wells with lower Cenozoic rocks
Present
Not present
Rock units
Lower Cenozoic rocks
Basement high
Volcanic margin
Possible volcanic margin
Seaward-dipping reflectors
Inner flows
Paleocene–Eocene sill complex
Landward extent of sills and/or flows
Oceanic features
Extinct spreading axis
Fracture zones
Landward limit of oceanic crust
Magnetic chrons
Other features
Erosional edge
Major basin
Profiles shown
Craton and/or terrane boundary
1000 m isobath
Wells and/or coreholes outside study area
Meta Incognita microcontinent
Cumberland Sound
Davis Strait
Frobisher Bay
Hudson Strait
Lady Franklin Arch
Ralegh N-18
Hekja O-71
Gjoa G-37
LF7-1
AT2-1
Qulleq-1
Saglek Basin
Ungava Fault Zone
Hudson FZ
Snorri FZ
Cabot G-91
Rut H-11
Gilbert F-53
Karlsefni A-13
Pothurst P-19
L2
Skolp E-07
Okak Arch
Torngat Orogen
North Atlantic Craton
Ogmund E-72
Snorri J-90
Hopedale Basin
Labrador Sea
ODP 646
Corte Real P-85
Hopedale E-33
L1
South Labrador N-79
South Hopedale L-39
A
Makkovik Orogen
Grenville Front
Cartwright FZ
Gudrid H-55
Roberval C-02
Roberval K-92
Cartier D-70
North Leif I-05
Leif M-48
Leif E-38
Indian Harbour M-52
Freydis B-87
Cartwright Arch
Lake Melville
Labrador
Grenville Province
Verrazano L-77
70°W
65°N
60°W
60°N
55°N
50°W
Baffin Bay
Baffin Island
Davis Strait
Greenland
Labrador Sea
Labrador
Tyrk P-100
North Bjarni F-06
Bjarni O-82
Herjolf M-92
Bjarni H-81
0 80 160 km
1:4 750 000
Canada Lambert Conformal
GCS WGS 1984

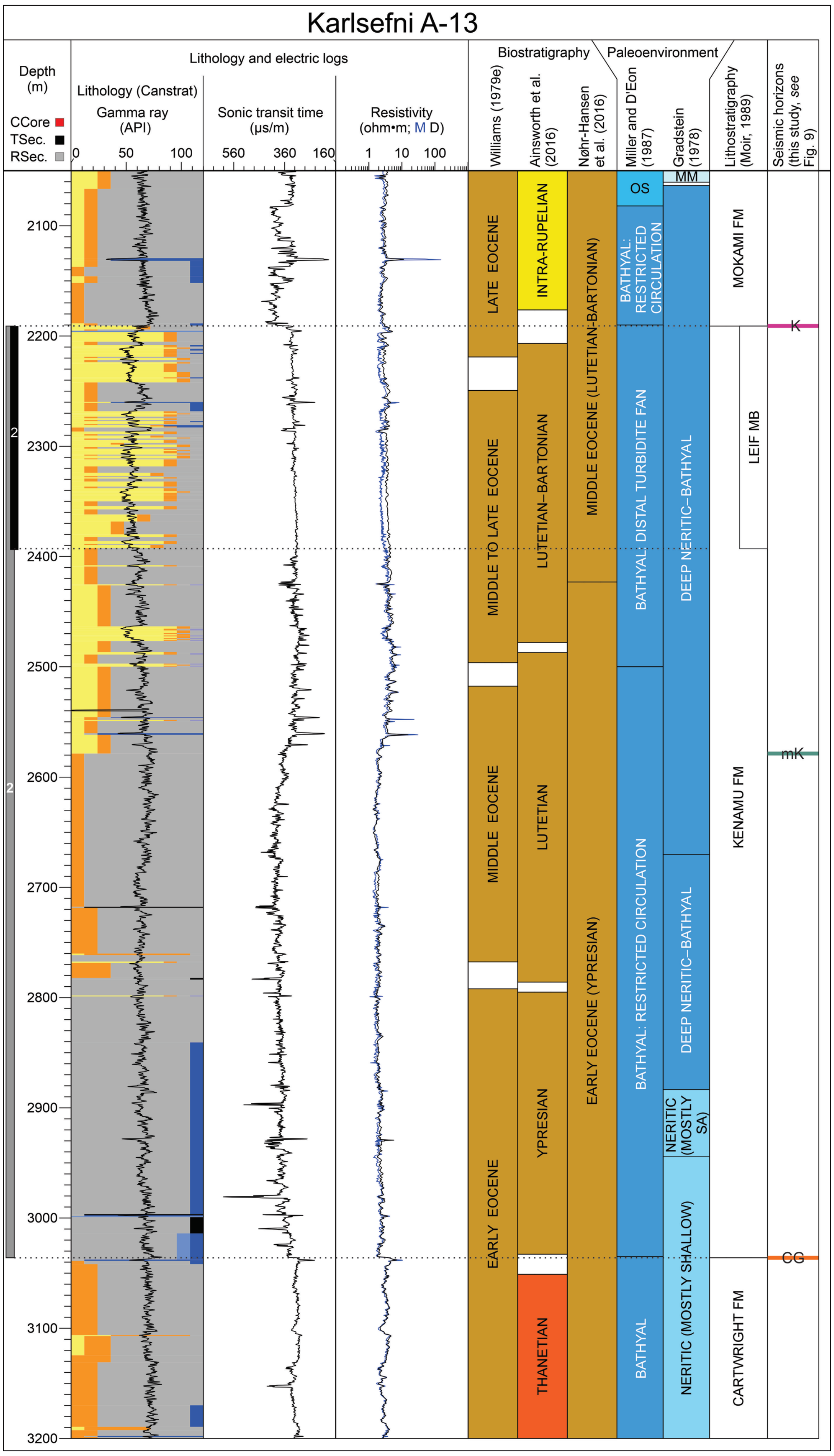

Figure 16. The Karlsefni A-13 well, showing fundamental wireline logs, lithology (Canstrat), key biostratigraphic studies, paleoenvironmental interpretations, and lithostratigraphy. The type section for the Leif Member of the Kenamu Formation and a reference section for the Kenamu Formation are indicated. *See* Figure 4b for legend. K = top Kenamu Fm, mK = mid-Kenamu Fm, CG = top Cartwright and/or Gudrid Fm.

of the Cartwright Formation occur in Gilbert F-53, Karlsefni A-13 (Fig. 16), Snorri J-90, and South Labrador N-97. In these wells, Nøhr-Hansen et al. (2016) recognized the shale units of the Cartwright Formation as Thanetian to early Ypresian in all of the wells, but also noted a late Selandian interval in Gilbert F-53. Perhaps the most convincing age constraints come from the study of conventional cores by Dafoe and Williams (2020a). In the thick Cartwright Formation succession of the Karlsefni A-13 well, core 1 (nearly 300 m below the top of the formation) was dated as Selandian to Thanetian, but falls on the Thanetian–Ypresian boundary of Nøhr-Hansen et al. (2016). Accordingly, the age of the Cartwright Formation would appear to include the late Selandian based on both core analyses from Karlsefni A-13 (Dafoe and Williams, 2020b) and Nøhr-Hansen et al.'s (2016) study of the Gilbert F-53 well, and ranges into the early Ypresian.

For the Gudrid Formation in the type section of Gudrid H-55 (Fig. 5), Williams (1979g) reported a Late Paleocene to Early Eocene age similar to that of Gradstein (1976a), but slightly younger than the (?)Middle to Late Paleocene assignment of Robertson Research Ltd. (1974b). The Gudrid Formation in Cartier D-70 was constrained to the Late Paleocene for the lower unit and Early Eocene for the upper unit by Williams (1979b), but other biostratigraphic studies have significant intervals without any age assignment and are less conclusive (Fig. 4). In addition to the type and reference sections, supporting evidence for the age of the Gudrid Formation was found in the Roberval C-02 well by Williams (2017b), who dated it as Thanetian–early Ypresian (Williams, 2017b). Nearby, in the Roberval K-92 well, the correlative Gudrid Formation sandstone was also found to be Thanetian to early Ypresian. Dafoe and Williams (2020a) interpreted core 1 of Ogmund E-72 as basal Ypresian and core 1 of Snorri J-90 as late Thanetian to earliest Ypresian, both characterizing the Gudrid Formation. The Gudrid Formation thus appears to be Thanetian–basal Ypresian in age, but may have Selandian equivalents to the Cartwright Formation that have not been sampled.

Paleoenvironments

McWhae et al. (1980) suggested that the claystone units of the Cartwright Formation were deposited in outer shelf, or more likely, slope-equivalent water depths (bathyal). Thin sandstone units within the claystone units were further interpreted as turbidite sequences, but the evidence for this is not conclusive. This interpretation is consistent with that of Miller and D'Eon (1987) based on their lithological study; however, assessment of core 1 from Karlsefni A-13 by Dafoe and Williams (2020a) indicate that the sandy mudstone units of the Cartwright Formation in that well are consistent with wave-influenced prodelta deposition during the Selandian–Thanetian. This indicates a much shallower setting for the Cartwright Formation than previously proposed, but is consistent with the relatively proximal, landward position of that particular well.

In contrast to the Cartwright Formation, there has been significant controversy over the depositional settings of the Gudrid Formation. Umpleby (1979) indicated that the Gudrid Formation had a continental affinity due to the presence of lignite beds, poor degree of sorting, immature nature of the sediment, and lack of marine fossils; however, he also suggested shallow subtidal deposition based on an examination of core 1 from Snorri J-90, which contains burrowed, laminated, and graded strata. In the same core interval, Dafoe and Williams (2020a) considered the bioturbated sandstone to be an upper Thanetian to lowest Ypresian storm-dominated, delta-front deposit. In seismic data, Balkwill (1987) recognized the sigmoidal, seaward-tapering morphologies of the Gudrid Formation sandstone units and also suggested that they were deltas with downdip mounds reflecting turbidite fans. This was expanded upon in Balkwill and McMillan (1990), where they considered the sigmoidal wedges of the lower Gudrid Formation as deltaic clinoforms that typically grade into outer neritic shale units, and the upper Gudrid Formation as shallow-marine shoreface or deltaic sandstone units with interdeltaic shale units and downslope (undrilled) turbidite fans. A shoreline setting for the Gudrid Formation was further confirmed by Dafoe et al. (2018) from their integrated well and seismic study.

Alternatively, McWhae et al. (1980) suggested that the Gudrid Formation represented turbidite deposits, deep-sea fan, and channel deposits that accumulated in an outer shelf to slope and rise setting. Their assessment of the same core 1 from Snorri J-90 suggested bouma-cycle, sand-shale alternations, reflecting distal turbidite deposits (McWhae et al., 1980). Miller and D'Eon (1987) agreed that the Gudrid Formation sandstone units were coarse-grained turbidite and grain-flow deposits (e.g. Fig. 5), except at Snorri J-90 and Ogmund E-72, where they indicated that shallow-marine bar sandstone units and lower shoreface settings were present. Foraminiferal studies generally agree with the distal paleoenvironments. Gradstein and Srivastava (1980) recorded foraminiferal assemblages dominated by often large, agglutinated taxa in lower Paleogene sediments from the Labrador Shelf wells. Such assemblages are indicative of bathyal conditions. Gradstein (1975) interpreted the paleoenvironment for the Gudrid Formation in the type section (Gudrid H-55) as deep water, presumably equating with a slope or bathyal setting. Conversely, Robertson Research Ltd. (1974b) interpreted the same section as sublittoral to supralittoral, but their interpretation for this part of the well was based on lithology (Fig. 5).

One distinctive aspect of the dinocyst assemblages in the Paleogene of the Labrador Shelf is the sometimes common to abundant occurrence of the *Areoligera gippingensis* complex (Nøhr-Hansen et al., 2016). Members of this complex are abundant in the Danian–Selandian of South Labrador N-79, in the Maastrichtian to Thanetian of Gilbert F-53, and in the Thanetian of Karlsefni A-13. Paleoenvironmental interpretations based on abundances of this species yield conflicting interpretations. Heilmann-Clausen (1994) regarded *Areoligera gippingensis* to be concentrated in offshore paleoenvironments, recording abundant specimens of the species in the latest Selandian–early Thanetian of the *Alisocysta margarita* zone, in Denmark. Since the areoligeraceans are gonyaulacaceans, logic dictates that they are most likely to be autotrophic and would be more abundant farther offshore, but this may not be the case, since Powell et al. (1996), in a study of the Thanetian type section of southern England, noted intervals where *Areoligera gippingensis* was abundant. According to Powell et al. (1996), these events denoted restricted, high-energy, marginal marine settings, characteristic of transgressive regimes. Thus, the areoligeracean abundances seem to support either an open-marine or a shallow-water setting in a high-energy domain. The present authors agree with the high abundances as representative of a restricted, high-energy, marginal marine setting for wells offshore Labrador.

There is less contention about the Cartwright Formation, which appears to have been deposited in prodeltaic to outer shelf or possibly slope-equivalent water depths. The Gudrid Formation, however, has competing distal-marine and shallow-marine interpretations. Based on the existing body of work on the Gudrid Formation, a shallow-marine deltaic or shoreface interpretation fits with most lithological and core observations, but also with interpretation of seismic morphologies (*see* below). To explain the discrepancy in paleoenvironments noted for the interval sampled by core 1 of Snorri J-90, Dafoe and Williams (2020b) suggested that cavings from overlying deep-water shale cuttings may have masked the signature of the thin Gudrid Formation sandstone units in that well. This may be the case with other wells on the Labrador Shelf.

Previous offshore mapping

The work of Bell (1989) provided isopach, net sandstone, and paleogeographic maps of the Cartwright and/or Gudrid formations along the shelf. The lower and upper Gudrid Formation intervals were interpreted as asymmetric, wedge-shaped bodies with internal sigmoidal reflections (Balkwill and McMillan, 1990). Dickie et al. (2011) described the seismic character of some of the sandstone units of the Gudrid Formation as shingled and indicative of forced regression. Like the underlying Upper Cretaceous section, large-scale, downslope Cenozoic faulting above a detachment surface also affected the Cartwright Formation (Balkwill and McMillan, 1990).

Seismic reflection character

On seismic data, the Cartwright and Gudrid Formation interval, demarcated at the top by the CG horizon, forms a relatively thin wedge of strata that onlaps landward against the underlying Markland Formation and eventually thins basinward, onlapping against oceanic crust (Fig. 9). The Cartwright Formation is generally characterized by a relatively low-amplitude internal character consistent with a shale-dominated interval and a higher amplitude upper boundary. The Gudrid Formation, where present, consists of a package of high-amplitude, prograding clinoform reflections with a distinct, shingled seismic facies near the base, and combined with the paleoenvironment determined through well samples is suggestive of shoreline sandstone accumulation.

Kenamu Formation

Lithostratigraphy

In the initial study of the stratigraphy, Umpleby (1979) named the Saglek Formation for the strata lying above the Cartwright Formation, and included in it the Brown Mudstone and Leif members. On the basis of lithological change and the presence of unconformities, McWhae et al. (1980) modified the initial framework to define the Kenamu Formation as the shale and mudstone interval lying above the Cartwright Formation (Fig. 3). They revised the Saglek Formation to include strata lying above the Kenamu and overlying Mokami formations, but abandoned the original type sections for both the Saglek Formation and Leif Member. Balkwill and McMillan (1990) indicated that abandonment of Umpleby's (1979) original type sections for the Saglek Formation from the Karlsefni A-13 well (1131–1027 m) and the Leif Member from the same well (2394–2191 m) was not permitted according to the North American Commission on Stratigraphic Nomenclature (1983); however, Balkwill and McMillan (1990; and later, others, including this study) have continued to recognize the Kenamu, Mokami, and Saglek formations as defined by McWhae et al. (1980).

The Kenamu Formation was described by McWhae et al. (1980) as brown-grey, silty shale, shale, siltstone, and fine-grained sandstone that is locally calcareous and glauconitic with a slightly calcareous, silty, brown mudstone comprising a lower interval. These authors considered the age of the formation to be Early to Late Eocene and possibly earliest Oligocene. The type section of the unit was established in Leif M-48 from 1666 to 1222 m (444 m thick; Fig. 12). McWhae et al. (1980) further defined reference sections in Cartier D-70 from 1713 to 1275 m (438 m thick; Fig. 4) and in Karlsefni A-13 from 3036 to 2191 m (845 m thick; Fig. 16). They suggested that the top of the reference section in Karlsefni A-13 could be raised to 2043 m; however, this pick is inconsistent with the change in log character typical for the top Kenamu Formation. McWhae et al. (1980) defined the log character of the basal brown mudstone and shale units of the Kenamu Formation as having slightly lower velocity and sometimes lower resistivity than the underlying Cartwright Formation shale units (e.g. Fig. 10, 14, 16). The top of the Kenamu Formation, however, forms a distinct log signature that shows a resistivity and sonic velocity decrease (McWhae et al., 1980) and a gamma-ray log increase into the shale units of the overlying Mokami Formation.

As noted above, Umpleby (1979) designated the type section of the Brown Mudstone Member as 1321 to 1131 m in Freydis B-87. McWhae et al. (1980) suggested a new type section in Leif M-48 from 1666 to 1381 m (285 m thick; Fig. 12), but only described it as a more shale-dominated section. The member was originally described as a generally massive, brown-grey to dark grey mudstone with interbeds of micritic and finely crystalline limestone throughout (Umpleby, 1979). Whereas some wells do show a striking change from the brown-grey Cartwright Formation shale units into the brown mudstone of the Kenamu Formation, this is not regionally consistent, and many of the mudstone and claystone units from the Cenozoic section are brown.

The "Leif Sandstone" was an informal name for a thin sandstone unit found in Leif M-48 from 1298 to 1257 m (41 m thick; McWhae and Michel, 1975). This unit was initially thought to be Late Eocene in age and was elevated to member status by Umpleby (1979) as the Leif Sand Member (of the Saglek Formation) with the type section in the Karlsefni A-13 well from 2394 to 2191 m (203 m thick; Fig. 16). McWhae et al. (1980) retained the Leif Member within their Kenamu Formation and identified the reference section as that designated by McWhae and Michel (1975) in Leif M-48 (Fig. 12). Lithologically, the unit is fine-grained, quartzose, white to light grey-brown sandstone, often glauconitic, with varying proportions of interbedded siltstone and mudstone (Umpleby, 1979; McWhae et al., 1980). Umpleby (1979) described the upper boundary as sharp and defined by a prominent log change. The sandstone units sometimes form up to three stacked, coarsening-upward units (Balkwill and McMillan, 1990; Dafoe and Williams, 2020b). In terms of source area, Leif Member sandstone units may have been derived from outlets near Hudson Strait and Hamilton Inlet and basement terranes comprising the Okak Arch (Balkwill, 1987).

Three informal members within the Kenamu Formation have been described by Balkwill (1987) and Balkwill and McMillan (1990): 1) a "lower Kenamu" comprising fining-upward, slightly silty, grey shale with Early Eocene marine fossils; 2) a "middle Kenamu" that coarsens upward into siltstone and fine-grained sandstone in proximal settings and is again marine, but Early to Middle Eocene; and 3) an "upper Kenamu" consisting of coarsening-upward siltstone to shoreface and coastal sandstone units of the Leif Member. Dafoe et al. (2017a) also identified a lower Ypresian shoreline clinothem near the basement hinge in the lowermost Kenamu Formation that likely forms part of the "lower Kenamu." Higher in the section, Dickie et al. (2011) interpreted a Lutetian lowstand with possible sandstone accumulation seaward of the shelf edge followed by transgression and highstand accumulation of the upper Kenamu Formation (Fig. 3). Dafoe et al. (2016), however, described a Lutetian hiatus linked to a flooding event within overall shelf deposits, which is more consistent with the shelfal paleoenvironments recorded in the shale units. This Lutetian break in section may correspond to the top of Balkwill and McMillan's (1990) "middle Kenamu" interval.

Biostratigraphy

The age of the Kenamu Formation, according to McWhae et al. (1980) was Early to Late Eocene, but Gradstein and Srivastava (1980) and Barss et al. (1979) extended the age into the earliest Oligocene. In the type section at Leif M-48 (Fig. 11), Williams (1979f) and Gradstein et al. (1994) found the Kenamu to extend into the Early Oligocene, and considered it as old as the Early or early Middle Eocene, respectively. This differs slightly from that of Bujak Davies Group (1989b), who considered it to range from the Early to Middle Eocene only. At Cartier D-70, the reference section was generally found to be Early to Late Eocene (Fig. 4; Gradstein, 1976b; CFP Laboratory–Bordeaux, 1976; Williams, 1979b). The thick Kenamu Formation reference section at Karlsefni A-13 (Fig. 16) was suggested to be Early to Late Eocene (Williams, 1979e) or Ypresian to Lutetian–Bartonian (Ainsworth et al., 2016; Nøhr-Hansen et al., 2016).

In a study of the Roberval C-02 and K-92 wells, Williams (2017b) determined the age of the Kenamu Formation to be Ypresian–Bartonian, with thick Priabonian sediments lying above the formation in both wells. Dafoe and Williams (2020b) also considered the Kenamu Formation in North Leif I-05 to be Ypresian–Bartonian. In both studies, the youngest age of the Kenamu Formation (and Leif Member, which sits at the top) was latest Bartonian. Accordingly, Dafoe et al. (2017a) considered the top of the Kenamu Formation to be in the middle to late Bartonian. The general consensus seems to be that the formation is predominantly Ypresian–late Bartonian. In some wells, the Lutetian section of the Kenamu Formation is attenuated. An example is in Roberval C-02 where its thickness is only 30 m (Williams, 2017b). In other wells, such as North Leif I-05, upper Lutetian sediments appear to be absent (Dafoe and Williams, 2020b). This suggests that there is a hiatus within the Lutetian on the Labrador Shelf, as was recognized by Dickie et al. (2011) and Dafoe et al. (2016).

Umpleby (1979) gave the age of the Brown Mudstone Member, as determined from foraminifera and palynomorphs, as Middle Eocene. The revised type section in Leif M-48 (Fig. 12) was studied by Williams (1979f) and Gradstein (1976a) and they found the age to be Early or early Middle Eocene to within the Middle–Late Eocene; however, Bujak Davies Group (1989b) suggested that the interval encompassing the Brown Mudstone Member was restricted to the Early to Middle Eocene. These findings indicate that the Brown Mudstone Member is Early to Late Eocene, but most likely Early to Middle Eocene since it occurs at the base of the Kenamu Formation and the top of the formation is constrained in the Bartonian.

According to Umpleby (1979), the foraminifera and palynomorphs indicated a Late Eocene age for the Leif Member. McWhae et al. (1980) later considered the member to be Late Eocene to possibly earliest Oligocene. In the type section in Leif M-48, Williams (1979f) and Gradstein (1976a) determined the member to be Middle–Late Eocene (Fig. 4); however, Bujak Davies Group (1989b) found it to be Middle Eocene only. In Karlsefni A-13, both Ainsworth et al. (2016) and Nøhr-Hansen et al. (2016) dated the interval that includes the Leif Member reference section as Lutetian–Bartonian, and Williams (1979e) placed it in the Middle to Late Eocene. Most subsequent authors (e.g. Dickie et al., 2011) have considered the unit to be Middle to Late Eocene; however, Williams (2017b) in a study of the Roberval C-02 and K-92 wells determined that the age of the Leif Member was late Bartonian in Roberval C-02. Similarly, in North Leif I-05 where the sandstone is well developed, the member falls within the Bartonian (Dafoe and Williams, 2020b). Accordingly, Dafoe et al. (2017a) refined the timing of the Leif Member regression as Bartonian with the end of deposition in the middle to late Bartonian.

Paleoenvironments

McWhae et al. (1980) considered the Kenamu Formation to have been deposited in a marine shelf and slope (bathyal water depths) setting with a shallowing-upward trend. Miller and D'Eon (1987) also suggested bathyal turbidite deposition with the possibility of deltas on the shelf. Based on foraminifera and palynomorphs, Balkwill and McMillan (1990) indicated that their informal lower and middle members formed in outer neritic to bathyal water depths. Similarly, Umpleby (1979) indicated that his Brown Mudstone Member was entirely marine and that the lithology could indicate turbidite deposition under water depths as much as 500 m since there was no evidence of a former shelf. Slightly shallower settings were interpreted for the Kenamu Formation in Roberval C-02 by Doeven and McIntyre (1980): deep to shallow neritic, but Williams (2017b) considered these strata to represent primarily open-ocean to shelfal deposits. Ainsworth et al. (2014) also interpreted the Kenamu Formation in the nearby Roberval K-92 as being deposited in a bathyal environment. Based on seismic interpretation, Dickie et al. (2011) and Dafoe et al. (2018) noted development of a shelf-edge break and distal fan deposits within the Kenamu Formation.

A shelfal to slope and/or bathyal setting is generally agreed upon for the Kenamu Formation claystone units, but the paleoenvironment of the Leif Member has been more contentious. In his discussion of the member, Umpleby (1979) noted that older, deeper water foraminifera might have been reworked into shallow-marine sediments, but contamination from cavings sourced from overlying deep-water shale units is more likely. As Umpleby (1979) observed, a shallow-marine setting is substantiated by the presence of coal in the Leif Member in Herjolf M-92. Similarly, in their study of sidewall cores from Leif M-48, McWhae et al. (1980) found no evidence of thin, rhythmic bedding typical of turbidite deposits, so they suggested neritic (possibly tidal) deposition for the Leif Member. Gradstein and Srivastava (1980) also interpreted the Leif Member as a neritic, possibly tidal, deposit. Dafoe et al. (2017a, 2018) further utilized seismic morphologies to interpret the member as a thin, low-angle shoreline clinothem that formed at the end of Kenamu Formation deposition. Miller and D'Eon (1987) suggested that the seismic data imply a shallow gradient in which tides and storm waves may have affected deposition of the sandstone units.

Other studies tend to suggest deeper water depositional conditions for the Leif Member. Miller and D'Eon (1987) interpreted the sandstone units as turbiditic in nature rather than deltaic, at least for the Hopedale Basin, but deltaic in the Saglek Basin. In a sample from 1690 m in Roberval C-02 from the Leif Member sandstone units, Williams (2017b) recorded *Impagidinium*, generally an indicator of open-ocean waters. This paleoenvironmental setting could, however, be explained by cavings from the overlying transgressive shale units since the sandstone interval is very thin in this well. Dafoe and Williams (2020b) determined the prevalent paleoenvironments in North Leif I-05 for the Kenamu Formation as outer shelf to open ocean, with a marked shallowing above 1930 to 1920 m to inner neritic conditions, but they did not specifically address the interval containing the Leif Member. Utilizing micropaleontological data, Balkwill and McMillan (1990) found that foraminifera suggested a deep-marine setting for their upper member, but that palynomorphs indicated a shallow-marine to coastal setting, which they thought was probably more accurate. Obviously, conditions of deposition for these units varied considerably across the Labrador margin, likely in relation to proximity to the sediment source and paleoshoreline; however, multiple lines of evidence (palynology, lithology, and seismic morphology) indicate that the Leif Member was deposited under shallow-marine, likely deltaic conditions.

Previous offshore mapping

Bell (1989) presented maps of the Kenamu Formation distribution, net sandstone content, and paleogeography along the shelf based on existing data at the time. This unit onlaps the underlying Cartwright and Gudrid formations as it was deposited during a major transgression of the margin (Dickie et al., 2011). Within the Kenamu Formation, Dickie et al. (2011) interpreted a Lutetian lowstand, but this condensed interval was later suggested to be linked to transgressive flooding of the margin due to the distal marine paleoenvironments encountered in the wells (Dafoe et al., 2016). Further upsection, the upper Kenamu Formation exhibits coarsening-upward cycles reflecting highstand progradation. These strata form shallowly dipping, prograding reflections within the upper part of the Kenamu Formation locally grading into the Leif Member sandstone units (Dickie et al., 2011). At the top of the Kenamu Formation, McWhae et al. (1980) noted onlap in seismic reflection data and Dickie et al. (2011) further described this boundary as transgressive in nature. Balkwill (1987), Balkwill and McMillan (1990), and Dickie et al. (2011) all commented on the recognizable character of the top of the Kenamu Formation in that it forms a widespread, strong seismic reflection along the inner shelf where sonic logs show a distinct decrease in velocity. This is probably due to coastal sandstone development truncated during subsequent transgression. Cenozoic faulting also affected the Kenamu Formation (Balkwill, 1987; Balkwill and McMillan, 1990). This slope instability was suggested to approximately correlate with the end of Kenamu Formation deposition as a result of a Late Eocene bolide impact at Mistastin Lake (Dickie et al., 2011).

Seismic reflection character

The Kenamu Formation forms a basinward thickening wedge of strata that is generally characterized by flat-lying, parallel reflections and is capped by the top Kenamu Formation horizon (K; Fig. 9). The base of the formation primarily onlaps landward against the Cartwright and Gudrid formations, but in highly proximal positions, the wedge onlaps Markland Formation and pre-rift basement rocks (Fig. 9). This onlap relationship is consistent with a widespread transgression at the base of the Kenamu Formation. A mid-Kenamu Formation marker (mK), of approximate Lutetian age, forms a moderate amplitude reflector within otherwise low-amplitude or transparent strata. Higher amplitude reflections are seen near the top of the Kenamu Formation where sandstone units become more prevalent within the shale units and especially in relation to development of the Leif Member (line 1; Fig. 9a). Development of shallower paleoenvironments and associated sandstone units at the top of the Kenamu Formation results in a relatively distinct K horizon, at least within the present-day shelf. As shown in Figure 9, the Kenamu Formation is involved in large-scale Cenozoic faulting of the margin that is seen in both the Hopedale and Saglek basins. Whereas some faults extend into younger strata (line 1; Fig. 9a), elsewhere faulting appears to terminate at about the top of the Kenamu Formation (line 2; Fig. 9b). Eventually the wedge of sediments thins basinward to onlap against the ridge of oceanic crust surrounding the spreading centre (Fig. 9).

OLIGOCENE–PLEISTOCENE INTERVAL

Mokami and Saglek formations

Lithostratigraphy

The Saglek Formation was established by Umpleby (1979) with the type section in the Freydis B-87 well from 1131 to 1027 m (104 m thick). He described two members within the formation, the Brown Mudstone Member at the base, the Leif Sand Member within the middle of the formation, and then an overlying sequence of silty and sandy mudstone units. This original designation did not account for the thick sandstone units seen in the upper Cenozoic section in many of the Labrador Shelf wells. Accordingly, McWhae et al. (1980) proposed the Kenamu Formation in place of the lower beds of Umpleby's (1979) Saglek Formation, which was then overlain by their newly established Mokami Formation (similar to the informal "Lutite Sequence" of McWhae and Michel (1975)), and thus restricted the original Saglek Formation (Fig. 3).

McWhae et al. (1980) described the Mokami Formation as generally brown claystone and soft shale with thinner beds of siltstone, sandstone, and calcareous sandstone and limestone, with accessory components including glauconite, pyrite, and molluscan shell debris. In particular, these authors indicated that the percentage of silt and sand increased upward within the unit. The type section was defined in Snorri J-90 from 1715 to 997 m (718 m thick; Fig. 17). McWhae et al. (1980) further established a reference section in Bjarni H-81 from 1334 to 725 m (609 m thick; Fig. 18), which was the interval denoted as the "Upper Lutites" by McWhae and Michel (1975). At the time, the Mokami Formation was considered Early Oligocene to Middle Miocene, but possibly as old as latest Eocene (McWhae et al., 1980; Balkwill and McMillan, 1990). The base of the Mokami Formation is defined where claystone units succeed silty and sandy shale units of the Kenamu Formation corresponding to resistivity and sonic velocity log decreases (McWhae et al., 1980), with a generalized gamma-ray log increase as compared to the underlying Kenamu Formation. The top of the claystone units was interpreted as the "Beaufort Unconformity", where it is overlain by the sandstone and conglomerate of the Saglek Formation (McWhae et al., 1980).

McWhae et al. (1980) restricted Umpleby's (1979) Saglek Formation to very porous, white, brown to grey, unconsolidated, feldspathic and cherty sandstone that is poorly sorted, fine- to coarse-grained, and locally conglomeratic. The unit contains abundant pelecypod fragments, lignite, and glauconite with lesser siltstone and claystone interbeds. These sandstone units were termed the "Upper Coarse Arkosic Sands" in Bjarni H-81 and Leif M-48 by McWhae and Michel (1975). The revised type section of the Saglek Formation was designated by McWhae et al. (1980) from 997 m to possibly 267 m (730 m thick) in Snorri J-90, with an uncertain upper boundary (Fig. 17). These authors further defined a reference section in Bjarni H-81 from 725 m to possibly 222 m (503 m thick), with the upper boundary again being uncertain (Fig. 18). McWhae et al. (1980) defined the base of the Saglek Formation as the lithological change from the brown claystone units of the Mokami Formation into the sandstone units of the Saglek Formation. The top of the Saglek Formation was interpreted as an erosional unconformity with the overlying Quaternary sediments, but is difficult to pick due to well casings (McWhae and Michel, 1975; McWhae et al., 1980). The immature nature of the conglomeratic sandstone units suggests a nearby terrain source of high relief composed of plutonic and metamorphic rocks in addition to reworked palynomorphs that indicate erosion of sedimentary rocks of Carboniferous, Jurassic, Cretaceous, and Cenozoic ages (Balkwill, 1987; Balkwill and McMillan, 1990). Due to such reworking, McWhae et al. (1980) could not be more definitive regarding an initial age assessment of the Saglek Formation sandstone units than to bracket them as Middle–Late Miocene to Pliocene; however, they did note that they were thicker in the Saglek Basin (locally over 1000 m) as compared to the Hopedale Basin.

Balkwill (1987) recognized that the contact between the Mokami and Saglek formations is diachronous and gradational with an unconformity developed landward where the contact is more abrupt, as seen in some wells (Fig. 17, 18; Balkwill and McMillan, 1990). These authors further interpreted subunits within the Mokami and Saglek formations: lower Mokami, upper Mokami, lower Saglek (coeval to the upper Mokami), and upper Saglek informal members. The Mokami Formation was divided into the informal units based on what was described as a prominent unconformity separating the two stratigraphic intervals (presumably this equates to the Saglek and/or Mokami formation horizon 2 (SM2) in Fig. 9, but it was not clearly illustrated in the original study). These units were retained by Dickie et al. (2011; Fig. 3). Balkwill and McMillan (1990) further described the lower Mokami member as a coarsening-upward, shale-dominated interval of Late Eocene to Oligocene age. They defined an unconformity within this member, which likely equates to the prominent Rupelian horizon identified by Dickie et al. (2011) on the outer shelf and is shown here as the Saglek and/or Mokami formation horizon 1 (SM1) in Figure 9 (but which is not interpreted as an unconformity in this study based on the work by Dafoe et al. (2017a, b)). The upper Mokami member is the distal mudstone equivalent of the lower Saglek Formation member (*see* below), and was interpreted as Late Oligocene to Middle or Late Miocene (Balkwill and McMillan, 1990). In their study, Dafoe et al. (2017a) indicated that the Mokami Formation displayed both progradation and aggradation with minor, intervening retrogradational intervals. These minor transgressive events may account for some of the surfaces previously described as unconformities within shelfal deposits of the lower member of the Mokami Formation (Balkwill, 1987; Balkwill and McMillan, 1990; Dickie et al., 2011). Both the lower and upper Mokami members appear to become sandier northward into Saglek Basin (Balkwill and McMillan, 1990).

The Saglek Formation was divided into informal lower and upper members representing two progradational wedges found in both the Hopedale and Saglek basins (Balkwill, 1987; Balkwill and McMillan, 1990). The lower Saglek was initially proposed as an Upper Oligocene to Upper Miocene prograding wedge, and the upper Saglek as Late Miocene to Pliocene. Balkwill and McMillan (1990) interpreted a Late Miocene unconformity separating the lower and upper Saglek Formation, and Balkwill (1987) indicated that this unconformity includes localized wide, deep channels with several hundred metres of relief, especially in the Hudson Strait and central and southern

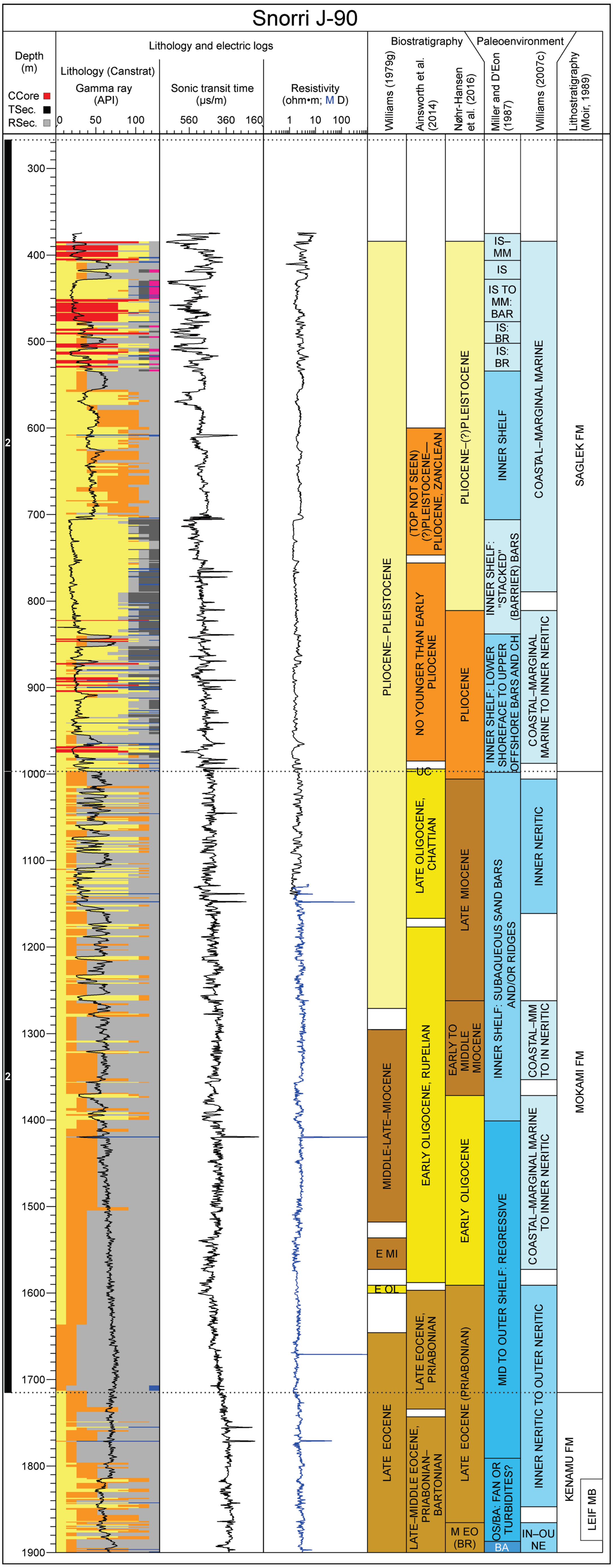

Figure 17. The Snorri J-90 well, showing fundamental wireline logs, lithology (Canstrat), key biostratigraphic studies, paleoenvironmental interpretations, and lithostratigraphy. The type sections for the Mokami and Saglek formations are indicated. *See* Figure 4b for legend.

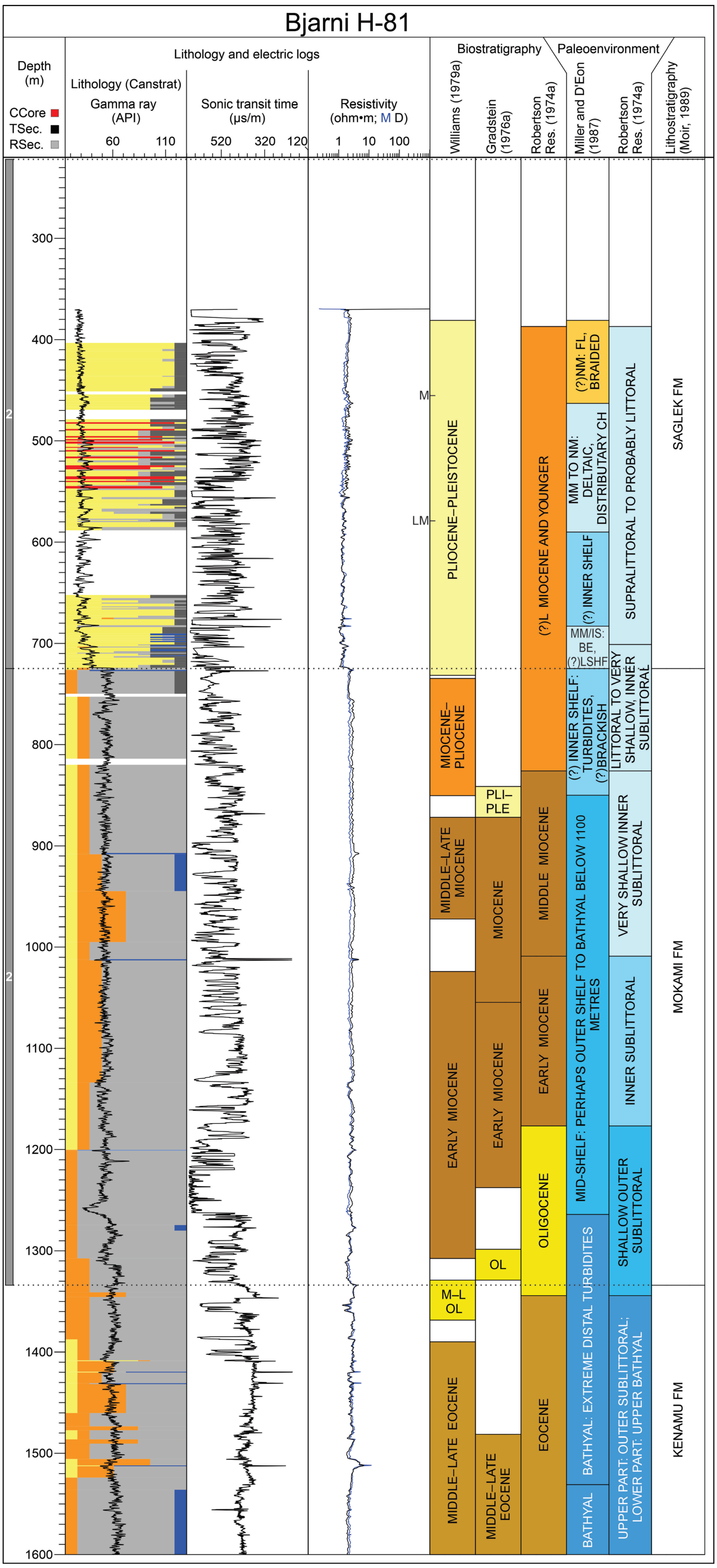

Figure 18. The Bjarni H-81 well, showing fundamental wireline logs, lithology (Canstrat), key biostratigraphic studies, paleoenvironmental interpretations, and lithostratigraphy. Reference sections for the Mokami and Saglek formations are also shown. Revised picks from this study for the top of the Lower Miocene (LM) and Miocene (M) are shown. *See* Figure 4b for legend. Robertson Res. = Robertson Research Ltd., MM/IS = marginal marine and/or inner shelf.

portions of the Hopedale Basin. Subsequently, Dickie et al. (2011) noted four intervals of Saglek Formation sandstone units: two lower clinothems (their Saglek Formation 'a' and 'b' units), a successive channellized unit (their unit 'c'), and the present-day, shelf-building clinothem (their unit 'd'). It is not entirely clear, but the base of the upper Saglek member of Balkwill (1987) and Balkwill and McMillan (1990) is probably equivalent to the uppermost channellized and clinothem units of Dickie et al. (2011), having a similar Late Miocene age and seismic morphology. Dickie et al. (2011) proposed a possible Pliocene–Pleistocene age for the uppermost shelf-building clinothem, which was corroborated by Dafoe et al. (2018). Accordingly, the lower Saglek Formation interval, is equivalent to the lowermost two clinothems of Dickie et al. (2011) with tops in the Early and Middle Miocene, older than originally thought. These units of the Saglek Formation were later described as shelf-edge deltas with related fan deposits, and their regressive, erosional bases were found to be late Rupelian and Middle Miocene (Dafoe et al., 2017a, b, 2018).

Biostratigraphy

Balkwill and McMillan (1990) gave an age of Late Eocene to Middle to Late Miocene for the Mokami Formation; however, they highlighted some of the difficulties associated with assigning ages to the Neogene rocks in the Labrador Sea. These difficulties include missing section, the coarseness of the clastic rocks (detrimental to palynomorph preservation), sparseness of assemblages, preservation, cavings, and reworking. According to Ainsworth et al. (2014), the age of the Mokami Formation at the type section (Snorri J-90) is Priabonian to Chattian (Fig. 17). Nøhr-Hansen et al. (2016) came up with a somewhat different interpretation assigning an age of Priabonian to earliest Pliocene, but not recognizing any Chattian. Williams (1979g) also found the type section to range from the Late Eocene to the Pliocene–Pleistocene, but similarly did not record any Chattian. It is difficult to reconcile these age differences other than to observe that other authors, including Gradstein et al. (1994) and Williams (2007c), have observed an attenuated Oligocene section in other wells. The age range of the Mokami Formation in the Bjarni H-81 reference section is equally varied (Fig. 18). Gradstein (1976a) recognized Oligocene through Pliocene–Pleistocene, as did Williams (1979a); however, Robertson Research Ltd. (1974a) also found Oligocene at the base, but broadly interpreted (?)Upper Miocene and younger strata at the top of the formation.

In a study of Roberval C-02 and Roberval K-92 by Williams (2017b), the Mokami Formation was assigned to the Bartonian (latest) to Rupelian or within the Chattian and interpreted as being deposited in a shallowing-upward shelfal environment. Similarly, the thick section in North Leif I-05 was also found to be Bartonian (latest) to Rupelian (Dafoe and Williams, 2020b). Dafoe et al. (2017a) found that the transgressive event marking the base of the Mokami Formation is middle to late Bartonian. From the above data, the present authors' conclusion is that the Mokami Formation is primarily late Middle Eocene (late Bartonian) to Oligocene (possibly near the end of the Rupelian) within the wells as confirmed by Dafoe et al. (2017a). Younger Mokami Formation shale units are seen in distal wells on the Labrador Shelf such as in Corte Real P-85 and Indian Harbour M-52, and seismic interpretation of more shale-prone intervals suggests a basinward younging of Mokami Formation strata that are equivalent to the Saglek Formation sandstone units encountered in the wells.

McWhae et al. (1980) redesignated the type section of the Saglek Formation in Snorri J-90 and considered the age of the formation to be Middle–Late Miocene to Pliocene, but with a high degree of reworking in the assemblages. Like the Mokami Formation, difficulties in determining precise ages result from the diachronous nature of the formation, poor quality and sparseness of the assemblages, extensive reworking, coarse-grained nature of the lithologies, absence of conventional and sidewall cores, and casings in upper portions of the wells. In the type section at Snorri J-90, Williams (1979g), Ainsworth et al. (2014), and Nøhr-Hansen et al. (2016) generally found the Saglek Formation to be Pliocene to Pleistocene (Fig. 17); however, it could extend into the latest part of the Chattian based on Ainsworth et al. (2014), although they identified an unconformity within the uppermost Chattian, in addition to a missing Miocene section. In the Bjarni H-81 reference section, Robertson Research Ltd. (1974a) gave a (?) Late Miocene and younger age for the interval now included in the Saglek Formation (Fig. 18). In the same well, Williams (1979a) considered the Saglek Formation to be Pliocene–Pleistocene; however, the present authors' re-evaluation of the listing of palynomorphs identified by Williams (1979a) seems to indicate that the Lower Miocene extends up to 579 m and the top of the Miocene is at 455 m.

Outside of the type and reference sections, Williams (2017b) dated the Saglek Formation in Roberval K-92 as Chattian and in Roberval C-02 as Chattian and Aquitanian–Burdigalian, the top being based on the highest occurrence of *Osmundacidites wellmannii*, which was considered to equate with the top of the Burdigalian by Nøhr-Hansen et al. (2016); however, Williams (1986), recorded *Osmundacidites wellmannii* from the Middle to Late Miocene. Since Williams (2017b) based the range on the topmost sample in Roberval C-02, presumably it does not define the youngest age of the formation. In other analyses, the formation is defined as Rupelian to Early Miocene in North Leif I-05 (with the Chattian missing) and Rupelian to Serravallian in Skolp E-07 (but with absent Langhian section; Dafoe and Williams, 2020b). Relying more heavily on these studies, the age of the Saglek Formation would generally appear to be as old as Rupelian and extend into the Middle Miocene; however, as noted on seismic data (*see* below), the Saglek Formation likely extends into the Pliocene–Pleistocene, forming the final major shelf-building clinothem along the margin (Dickie et al., 2011). Younger ages reported in some wells may be due to cavings and poor recovery from the sandstone intervals.

Paleoenvironments

In their original definition of the Mokami Formation, McWhae et al. (1980) indicated an overall neritic depositional setting. Miller and D'Eon (1987) postulated that the formation represented mostly quiet, open-marine deposition, but they also described sandbars and deltas in proximal regions of the Hopedale Basin. To the north, the same authors interpreted nonmarine fluvial and lacustrine sediments. Similarly, Balkwill and McMillan (1990) found the lower Mokami Formation to be deep neritic in the Late Eocene with subsequent inner neritic settings in the Hopedale Basin, but shallowing to nonmarine or marginal marine conditions in the Saglek Basin. A useful parameter for determining paleoenvironments is the relative percentage of miospores to dinocysts. In the type section for the Mokami Formation in Snorri J-90, Williams (2007c) used this technique to determine that the paleoenvironmental setting varies from outer neritic in the lower part to marginal marine and inner neritic in the middle and inner neritic in the upper part (Fig. 17). Similar settings were reported from the reference section (Fig. 18; Miller and D'Eon, 1987; Robertson Research Ltd., 1974a). Accordingly, the Mokami Formation appears to include shelfal to marginal marine settings, possibly including some nonmarine intervals.

McWhae et al. (1980) considered the Saglek Formation to have been deposited in a strandplain or paralic setting, as indicated by lignite beds and pyritic wood fragments; however, pelecypod fragments, glauconite, benthic foraminifera, and dinocysts suggest a shallow-marine setting such as that proposed by Balkwill (1987) and Balkwill and McMillan (1990): coalescing deltas with steep, seaward-facing slopes. Miller and D'Eon (1987) also proposed deltaic progradation in both the Hopedale and Saglek basins, with a brackish embayment and barrier-bar system developed in the southern part of the Saglek Basin. The Saglek Formation in the type section in Snorri J-90 was deposited in marginal marine and/or coastal to inner neritic settings (Williams, 2007c), and again similar settings are found in the reference section of Bjarni H-81 (Fig. 18; Miller and D'Eon, 1987; Robertson Research Ltd., 1974a). Marginal marine to inner neritic conditions beginning in the Rupelian may be related to: the cessation of seafloor spreading at chron C13 or the development of the Antarctic Ice Sheet and onset of global (eustatic) sea-level fall (Nøhr-Hansen et al., 2016). The Saglek Formation therefore represents deltaic to inner-shelf deposition.

Previous offshore mapping

Some of the early mapping of the Mokami and Saglek formations was undertaken by Balkwill (1987), Bell (1989), and Balkwill and McMillan (1990). They considered the Mokami Formation to be thickest in the central parts of the Saglek and Hopedale basins, but to extend across the shelf and thin both landward and basinward by onlap and downlap relationships. Balkwill (1987) suggested that the upper Mokami Formation downlaps on the lower Mokami basinward. Later work by Dickie et al. (2011) described a Rupelian-aged seismic horizon within the Mokami Formation that is especially prominent in the outer-shelf region, but steps upsection in a landward direction above a slightly expanded shelf interval. In regard to the Saglek Formation, Balkwill and McMillan (1990) recognized oblique and sigmoidal reflectors interpreted as clinoforms forming two progradational wedges in both Hopedale and Saglek basins. They further reported maximum thicknesses of the lower part of the Saglek Formation on the shelf with landward thinning due to erosional truncation at the seafloor. The upper Saglek Formation is, however, thickest below the shelf edge (Balkwill and McMillan, 1990). Dickie et al. (2011) also commented on the series of prograding sandy clinothems as well as a channelled unit found locally along the margin (Fig. 3). Building on this previous work, Dafoe et al. (2017a, b) described the Saglek Formation as forming shelf-edge deltas with related fan deposits overlain by an uppermost progradational Pleistocene wedge. Balkwill (1987) further commented that the Mokami Formation might also be involved in Cenozoic faulting.

Seismic reflection character

The Mokami and Saglek formations are mapped as a regional package of sediments sitting above the Kenamu Formation and forming the present-day shelf (Fig. 9). The package is divided by the Saglek and/or Mokami formation horizons 1 to 5 that correlate to unconformities at the base of clinothems or minor transgressive flooding events and are tied to the lithostratigraphic column of Dickie et al. (2011; SM1 through SM5; Fig. 3, 9). In general, the Saglek and Mokami formations form a thick regressive sequence contributing a significant thickness of sediment in both the Hopedale (line 1; Fig. 9a) and Saglek (line 2; Fig. 9b) basins. This wedge thins landward and can be truncated at the seafloor by erosion related to extensive glacial trough development on the Labrador Shelf (Fig. 1, 9a).

Mokami Formation shale units at the base of the informal lower Mokami member are generally conformable and overstep the Kenamu Formation showing local landward onlap. The Saglek and/or Mokami formation 1 (SM1) horizon (horizon 6 of Dickie et al., 2011) forms a prominent seismic reflection within Oligocene strata, especially in the outer shelf. Above this, continued deposition of Mokami Formation shale units took place until SM2, which forms the base of the oldest Saglek Formation clinothem that is well developed in the Hopedale Basin (line 1; Fig. 9a), but poorly defined in the Saglek Basin (line 2; Fig. 9b). The overlying SM3 horizon forms the base of another sandstone clinothem succession in Hopedale Basin (Fig. 3), and although sandstone units are present in the Saglek Basin, clinoforms are not observed (line 2; Fig. 9b). Accordingly, the presence of Saglek Formation sandstone units is known from well intersections, but the extent of these is uncertain in the Saglek Basin due to the lack of clear clinoform morphologies. The clinothems in the Hopedale Basin grade basinward into the Mokami Formation shale units. The intervening SM4 horizon is not regionally mappable along the Labrador margin and is thus not shown on Figure 9; however, overlying SM5 forms a prominent horizon at the base of the final present-day, coarse-grained shelf-building clinothem. This unit can include thin (line 1; Fig. 9a) to more prominent (line 2; Fig. 9b) topsets deposited in the Pliocene–Pleistocene. The entire Saglek and/or Mokami formation wedge of sediments thins basinward with onlap or downlap against oceanic crust (and locally the Kenamu Formation) with the SM3 to seafloor interval retaining significant thicknesses in the Labrador Sea Basin (Fig. 9). Locally, the entire sedimentary wedge may also be involved in the large-scale Cenozoic faulting noted in previous studies (Fig. 9; Balkwill, 1987; Balkwill and McMillan, 1990; Deptuck et al., 2007; Dickie et al., 2011).

LOWER AND UPPER CENOZOIC INTERVAL DISTRIBUTION MAPS

The Cenozoic section along the Labrador margin comprises a thick sequence of strata that includes the Cartwright, Gudrid, Kenamu, Mokami, and Saglek formations, which is divided in this study at the level of the SM3 horizon within the Saglek and Mokami formations. In landward settings, this horizon forms the base of the second Saglek Formation clinothem (Fig. 3, 9). The distribution maps for both the early and late Cenozoic intervals are thus described below.

Distribution of the lower Cenozoic interval

Lower Cenozoic sedimentary rocks cover much of the western part of the Labrador Sea (Fig. 15). The interval spans about 47 Ma and includes several formations: Cartwright, Gudrid, Kenamu, and lower parts of both the Mokami and Saglek formations. This package is thickest within the depocentres of the Hopedale and Saglek basins accounting for much of the sediment deposited there (*see* Keen et al., this volume; their Fig. 8) and over oceanic crust where it thickens into deep fracture zones and the extinct spreading axis (Fig. 9). Within the southeast quadrant of the map (Fig. 15), the entire sedimentary cover becomes very thin over oceanic crust, so only remnants of lower Cenozoic strata may be present in that area. In addition to sedimentary rocks, the lower Cenozoic package contains igneous intrusive and extrusive rocks, primarily of Middle–Late Paleocene age, which form high-amplitude reflections on the seismic data. These rocks are concentrated along the northern Labrador margin. Two wells in the northern Saglek Basin, Hekja O-71 and Ralegh N-18, intersected a thick volcanic sequence interbedded with Selandian and Thanetian clastic rocks (*see* Dafoe, DesRoches, and Williams, this volume).

The 'near-base' of the lower Cenozoic sequence is approximated by the top of the Markland Formation (within the Selandian), a regional, moderately strong reflection on seismic data. It forms a peak in proximal areas where there may be deltaic successions of the Freydis Member. More distally, these grade into shale units and the reflection changes into a fairly strong trough, where the Markland Formation seismic velocities are less than the overlying Gudrid Formation sandstone units.

The seismic horizon SM3, of Middle Miocene age delineates the top of this lower Cenozoic interval and lies within the Mokami and/or Saglek formations. The seismic expression of SM3 is weak and discontinuous, except for where it correlates with the base of the second clinothem. At its proximal edge, SM3 is truncated by an angular unconformity with the overlying glacial till (Fig. 9). The location of this truncation is mapped as the erosional edge on Figure 15. Landward of this line, successively older strata are truncated at the seafloor up to the westernmost edge of lower Cenozoic distribution where the interval onlaps the shallowing basement platform and is overlain by glacial till. Erosion of the top of this package is most pronounced along the western edge of the Hopedale Basin (line 1; Fig. 9a) and off the mouth of Hudson Strait where glacial activity was concentrated (Andrews et al., 2001).

Distribution of the upper Cenozoic interval

Upper Cenozoic sedimentary rocks cover most of the western Labrador Sea, forming a regressive, layered sedimentary wedge which prograded and thickens rapidly seaward of the erosional edge (red dashed line on Fig. 19). The package includes the upper parts of the Mokami and Saglek formations (Fig. 3, 9). As a result of significant clinothem development in the Pliocene–Pleistocene, the upper Cenozoic is thickest at the present-day shelf edge (Fig. 9). Off the shelf, in deep water, the upper Cenozoic sequence contains numerous mass-transport complexes with their characteristic, chaotic seismic facies (lines 1 and 2, beyond the base of the slope; Fig. 9). Sedimentary cover becomes very thin over the oceanic basement in the southeast portion of the study region (Fig. 19), and only remnants of upper Cenozoic sediments may be present in that region.

On the shelf, the base of the upper Cenozoic strata contains an interval of channelling and mass transport (Dickie et al., 2011) that is most evident in the regions of the Labrador Trough (line 1, at Corte Real P-85; Fig. 9a). Similar features are also imaged below the outer shelf in the Saglek Basin (line 2; Fig. 9b) where they are more deeply buried. A contourite-drift system developed in the mid-Pliocene, signalling an intensification of bottom-water currents, and was followed by Pleistocene, high-angle prograding clinoforms that built the steep, modern-day shelf edge (Myers and Piper, 1988). Inboard of the main sedimentary wedge shown in Figure 19 (i.e. landward of the erosional edge), only a relatively thin layer of flat-lying, upper Quaternary till remains of the upper Cenozoic section. It lies upon a high-angle unconformity that cuts into the dipping beds in the underlying section (line 1; Fig. 9a). The till is thickest off the mouth of Hudson Strait as described by Andrews et al. (2001).

CONCLUSIONS

This study brings together existing knowledge with new mappingto provide further insights into the lithostratigraphy, age, paleoenvironments, seismic character, and distribution of major sedimentary packages and volca-nic rocks along the Labrador margin and extending into the centralLabrador Sea region. The lithostratigraphic designations of the Labrador margin were initially formulated by

Figure 19. Distribution map of the Middle Miocene to Pleistocene (upper Cenozoic) interval along the Labrador margin with the location of the basement platform and highs, in addition to wells. Basin outlines are from Keen et al. (this volume). L1 and L2 indicate the seismic reflection lines 1 and 2 shown in Figure 9. A well that shows the interval "not present" may not have drilled deep enough to intersect the interval, is cased through that interval, lacks related strata deposited at that location, or associated strata were later removed through erosion. Additional projection information: Central Meridian = 60°W; Standard Parallels = 65, 75°W; Latitude of Origin = 65°N.

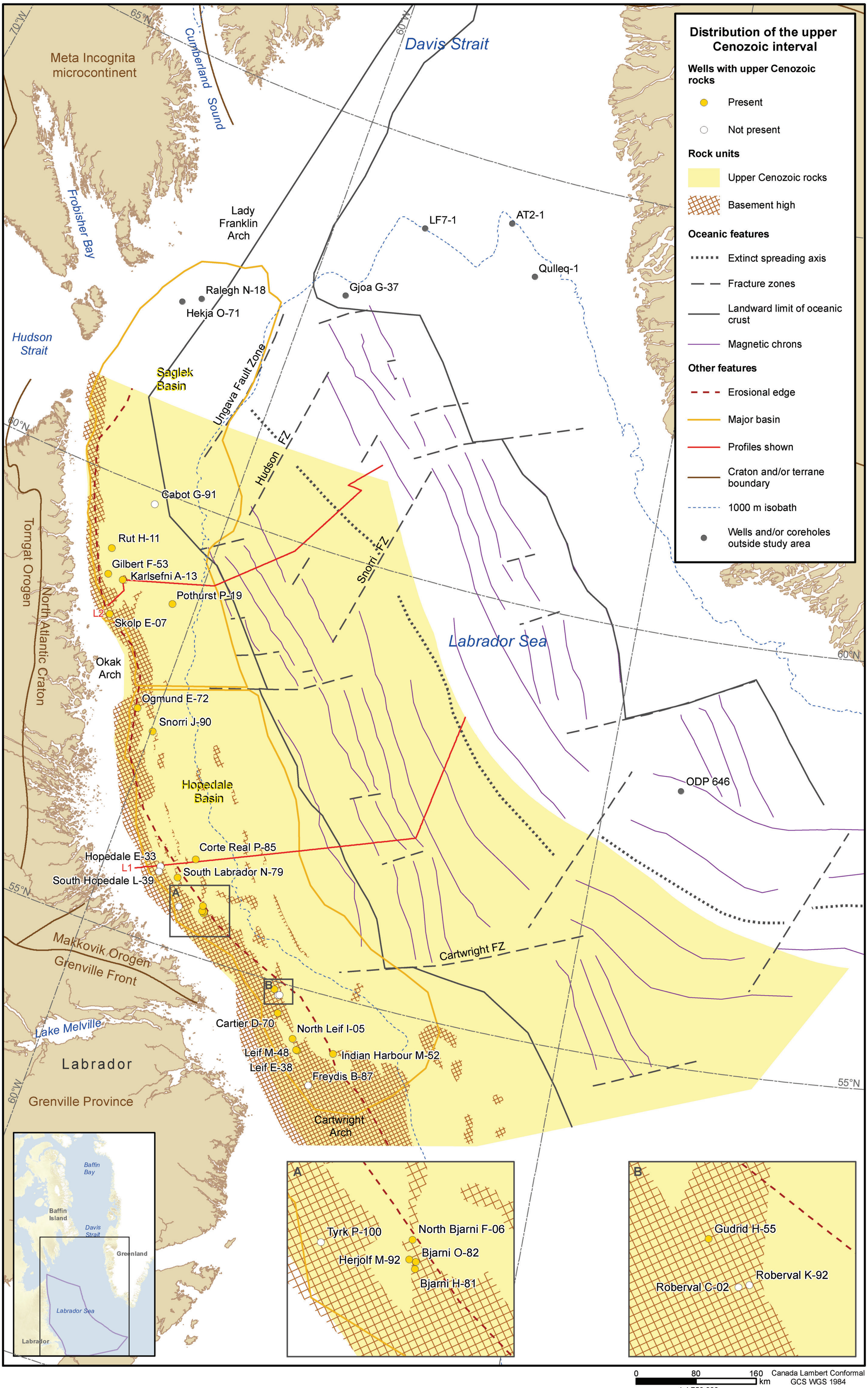
Distribution of the upper Cenozoic interval
Wells with upper Cenozoic rocks
Present
Not present
Rock units
Upper Cenozoic rocks
Basement high
Oceanic features
Extinct spreading axis
Fracture zones
Landward limit of oceanic crust
Magnetic chrons
Other features
Erosional edge
Major basin
Profiles shown
Craton and/or terrane boundary
1000 m isobath
Wells and/or coreholes outside study area
Davis Strait
Cumberland Sound
Meta Incognita microcontinent
Frobisher Bay
Hudson Strait
Lady Franklin Arch
Ralegh N-18
Hekja O-71
Gjoa G-37
LF7-1
AT2-1
Qulleq-1
Saglek Basin
Ungava Fault Zone
Hudson FZ
Snorri FZ
Cabot G-91
Rut H-11
Gilbert F-53
Karlsefni A-13
Pothurst P-19
Skolp E-07
L2
Torngat Orogen
North Atlantic Craton
Okak Arch
Labrador Sea
Ogmund E-72
Snorri J-90
Hopedale Basin
ODP 646
Corte Real P-85
Hopedale E-33
L1
South Labrador N-79
South Hopedale L-39
Makkovik Orogen
Grenville Front
Cartwright FZ
Cartier D-70
North Leif I-05
Leif M-48
Leif E-38
Indian Harbour M-52
Freydis B-87
Cartwright Arch
Lake Melville
Labrador
Grenville Province
Baffin Bay
Baffin Island
Davis Strait
Greenland
Labrador Sea
Labrador
A
Tyrk P-100
North Bjarni F-06
Herjolf M-92
Bjarni O-82
Bjarni H-81
B
Gudrid H-55
Roberval K-92
Roberval C-02
65°N
70°W
60°N
55°N
60°W
0
80
160
km
1:4 750 000
Canada Lambert Conformal
GCS WGS 1984

Umpleby (1979), and modified by McWhae et al. (1980). As a result, changes such as the proposal of new type sections and subdivision of formations, while retaining the original names, took place prior to the development of the first North American Stratigraphic Code in 1983, but there were no clear guidelines regarding these types of changes at the time. Accordingly, the present authors accept the eight proposed formations and their formal members: Alexis, Bjarni (Snorri Member), Markland (Freydis Member), Gudrid, Cartwright, Kenamu (Brown Mudstone and Leif members), Mokami, and Saglek. Subsequent changes to this framework relate mostly to the naming of informal members later undertaken by Balkwill (1987) and Balkwill and McMillan (1990), some of which aid in understanding the depositional history of the units. There are likely similarities in regional unconformities and units along the eastern Canadian margin, but the current study does not support all of the ages and nature of the surfaces as proposed by McWhae (1981).

The stratigraphic succession sits atop pre-rift basement that includes offshore extensions of the Archean gneiss and anorthosite units of the North Atlantic Craton and granodiorite and granitic gneiss units of the Proterozoic Makkovik Orogen. Basement rocks of the Grenville Province underlie the southernmost part of the margin. In Hopedale Basin, Ordovician carbonate and siliciclastic rocks are locally sampled in wells as a pre-rift platform succession, but these are poorly constrained in seismic data. A map of the pre-rift basement platform and significant basement ridges is shown, as well as southeast-northwest–oriented faults. Seaward of the platform, the continental crust becomes hyperextended. Further outboard is a zone of partially serpentinized and possibly exhumed continental mantle with oceanic crust underlying the Labrador Sea Basin. These diverse basement zones form the underlying structure influencing the stratigraphic succession along the margin.

The Alexis Formation is composed of basalt with varied ages based on the K-Ar whole-rock isotopic analyses, which were conducted on samples that were often reported as weathered or altered. The present study suggests that the age is likely constrained to the Valanginian to Albian, but could be younger. This agrees with regional occurrences of igneous rocks related to the onset of extension and with the notion that older Alexis Formation basalt units may be present at depth within undrilled portions of deep basement structures. The minimum extent of the Alexis Formation with the largest flows found in the Bjarni well area are shown in the present study. These rocks are likely locally interbedded with Bjarni Formation sandstone, shale, conglomerate, and coal units. These sedimentary rocks include the fine-grained, coal-bearing Snorri Member recognized in several wells. Based on new biostratigraphic results compiled in this study, the Bjarni Formation is no longer considered to range into the Cenomanian and/or Turonian, and is defined here as late Barremian to late Albian, but older rocks may be present at depth in grabens and half-grabens. The depositional setting for this unit in the Barremian–Aptian includes nonmarine (fluvial, alluvial, and lacustrine) and restricted marine settings, but within the Albian, it becomes shallow marine with deltaic deposition predominating. The Bjarni Formation shows characteristic growth of strata into faults, is weakly to moderately layered and infills deeper basement structures. A major unconformity marks the top of the Bjarni Formation and likely represents the transition from early to late rift stages (McWhae et al., 1980; McWhae, 1981; Dickie et al., 2011) that the present authors now consider to be at the Albian–Cenomanian boundary (Dafoe and Williams, 2020b).

Overlying the Bjarni Formation is the Markland, which consists of grey shale units, with sandstone units of the Freydis Member. The base of the formation is diachronous across the region due to transgressive onlap against the top of Bjarni Formation–filled grabens and major basement structures, which accounts for the limited extent of lower Upper Cretaceous section. The formation is Cenomanian to early Selandian with two Freydis Member units of Cenomanian–Coniacian and Campanian–Maastrichtian age. The depositional setting of the Markland Formation began as shelfal and became deeper marine, open ocean and/or bathyal by the Campanian–Maastrichtian. Deltaic or shoreface sandstone units of the Freydis Member were deposited in proximal settings and show a predominance of riverine influence. The transgressive nature of the Markland Formation is evident in its seismic character as it onlaps the underlying Bjarni Formation and pre-rift basement rocks. It is commonly a transparent interval on seismic data, as is characteristic of a shale-prone lithology. Within the Markland Formation an unconformity is noted in a few wells and locally in seismic data (the 2′ horizon of Dickie et al., 2011). This may represent a regression, but related sandy proximal facies have not been sampled. Cretaceous rocks of the Bjarni and Markland formations (Barremian to early Selandian) onlap and/or downlap onto the basement platform and oceanic crust. The distribution of Lower Cretaceous strata is restricted to regions landward of the zone of serpentinized mantle (chron C31), whereas Upper Cretaceous rocks can also be found landward of chron C27n. The Bjarni Formation is thick in Hopedale Basin and thinner in the southern portion of the Saglek Basin, whereas the Markland Formation is thicker in the Saglek Basin.

The lower Cenozoic interval includes Paleocene–Eocene volcanic rocks that form part of the magma-rich margin segment offshore of northern Labrador and are presumed to be of chron C27n age, but are not intersected in the wells. The present study illustrates the related, regional extent of landward flows and/or sills of about the same age and the distribution of a sill complex intersected in the Rut H-11 well in Saglek Basin. At about the same time, the Cartwright Formation and coeval Gudrid Formation were accumulating as brown-grey shale and quartzose sandstone units, respectively. The present authors follow the lithostratigraphic designations of McWhae et al. (1980) and recognize informal lower and upper Gudrid Formation intervals. In the wells, the upper Selandian to lower Ypresian Cartwright Formation represents prodeltaic, outer-shelf and slope-equivalent settings. The Gudrid Formation is Thanetian to early Ypresian, but Selandian rocks equivalent to those of the Cartwright Formation may exist, and the sandstone units are interpreted as deltaic or shoreface deposits, consistent with the lithology and clinoform morphologies seen in seismic data. Cavings from overlying, deeper marine Kenamu Formation rocks may explain the deeper water signal recorded by some microfossil studies of the Gudrid Formation. The base of the Gudrid Formation forms a significant unconformity above the Markland Formation, but the Cartwright Formation is conformable at its base.

The brown-grey shale, claystone, and siltstone units comprising the Kenamu Formation, are Ypresian to late Bartonian. At the base of the formation, the Brown Mudstone Member is likely Early–Middle Eocene, whereas the Leif Member is middle–late Bartonian. Sandstone units of the Leif Member reflect shallow-marine, deltaic settings based on results from palynology, lithology, and seismic morphology. The Kenamu Formation was deposited in shelfal to slope and/or bathyal water depths, with a general shallowing-upward trend following the widespread transgression that demarcates the base of the formation. An intervening Lutetian hiatus likely indicates a period of marine flooding at about the mid-Kenamu.

Brown claystone and siltstone units comprise the Mokami Formation, and the partially coeval Saglek Formation is composed of sandstone and conglomerate units. The base of the Mokami Formation forms a marine transgression above Leif Member shoreline sandstone units. Subsequent minor transgressive and regressive events divide the Mokami and Saglek formations into informal members as proposed by Balkwill and McMillan (1990), with well defined unconformities at the base of Saglek Formation deltaic clinothems. In the wells, the Mokami Formation is Bartonian to Rupelian (Early Oligocene), but younger claystone units likely exist basinward as correlative intervals of the Saglek Formation sandstone units. The Saglek Formation is Rupelian to Middle Miocene in age within the Labrador Shelf wells, but likely as young as the Pliocene–Pleistocene where it forms the uppermost, shelf-building clinothem. Unlike underlying units, the Mokami Formation was deposited in shelfal to marginal marine and possibly nonmarine settings, whereas the Saglek Formation reflects increased upward shallowing with an inner shelf to deltaic depositional environment. The present study subdivides the entire Saglek and/or Mokami formation section by five seismic horizons, four of which are relatively regional in extent, with SM3 separating the lower from the upper Cenozoic section. The lower Cenozoic interval, which includes the Cartwright, Gudrid, Kenamu, and lower parts of the Mokami and Saglek formations, onlaps the basement platform and thins basinward against oceanic crust. The upper Cenozoic section, comprising upper Saglek Formation and distal Mokami Formation–equivalents includes two major clinothems on the shelf and related mass-transport complexes along the slope and in the deep central Labrador Sea Basin. Upper Quaternary tills locally extend landward where both Cenozoic intervals are truncated at the seafloor due to glacial trough development.

Overall, the lithostratigraphy of the Labrador margin remains a sound framework. The present study integrates older data sets with new age constraints and modern seismic data sets and relates their distribution to current crustal studies. This serves to illuminate both the stratigraphic and tectonic history of the thick sedimentary basins deposited offshore Labrador.

ACKNOWLEDGMENTS

The authors would like to acknowledge support of this work through the Baffin Island and the Labrador–Baffin Seaway Geological Synthesis activity under the Geo-mapping for Energy and Minerals program (GEM-2). The authors thank TGS, ION Geophysical and the Federal Institute for Geosciences and Natural Resources (Hannover) for permission to show seismic data. Thanks to J. Ineson and C. Campbell for their detailed and constructive reviews. The authors are grateful to L. MacLeod for her design and compilation of the maps, to S. Hynes for some of the GIS compilation and processing, and to P. Champagne for his dedicated work on the seismic figures.

REFERENCES

Ainsworth, N.R., Riley, L.A., Bailey, H.W., and Gueinn, K.J., 2014. Cretaceous–Tertiary stratigraphy of the Labrador Shelf; Riley Geoscience Ltd.; on file with the Canada–Newfoundland and Labrador Offshore Petroleum Board, St. John's, Newfoundland and Labrador, 56 p.

Ainsworth, N.R., Riley, L.A., Bailey, H.W., and Gueinn, K.J., 2016. Cretaceous–Tertiary stratigraphy of the Labrador Shelf; Riley Geoscience Ltd.; on file with the Canada–Newfoundland and Labrador Offshore Petroleum Board, St. John's, Newfoundland and Labrador, 31 p.

Aldrich, L.T. and Wetherill, G.W., 1958. Geochronology by radioactive decay; Annual Review of Nuclear Science, v. 8, no. 1, p. 257–298.

American Commission on Stratigraphic Nomenclature, 1961. Code of stratigraphic nomenclature; American Association of Petroleum Geologists Bulletin, v. 45, no. 5, p. 645–665.

American Commission on Stratigraphic Nomenclature, 1970. Code of stratigraphic nomenclature; American Association of Petroleum Geologists; 45 p. (second edition).

Andrews, J.T., Jennings, A.E., and MacLean, B., 2001. Late Quaternary stratigraphy of Hatton and Resolution basins, east of Hudson Strait; *in* Marine Geology of Hudson Strait and Ungava Bay, Eastern Arctic Canada: Late Quaternary Sediments, Depositional Environments, and Late Glacial-deglacial History Derived from Marine and Terrestrial Studies, (ed.) B. MacLean; Geological Survey of Canada, Bulletin 566, p. 57–64. https://doi.org/10.4095/212208

Balkwill, H.R., 1987. Labrador basin: structural and stratigraphic style; *in* Sedimentary Basins and Basin-Forming Mechanisms, (ed.) C. Beaumont and A.J. Tankard; Canadian Society of Petroleum Geologists, Memoir, v. 12, p. 17–43.

Balkwill, H.R. and McMillan, N.J., 1990. Mesozoic-Cenozoic geology of the Labrador Shelf, Chapter 7 (part 1); *in* Geology of the Continental Margin of Eastern Canada, Volume 2, (ed.) M.J. Keen and G.L. Williams; Geological Survey of Canada, Geology of Canada, p. 295–324 (*also* Geological Society of America, The Geology of North America, v. I-1). https://doi.org/10.4095/132708

Barss, M.S., Bujak, J.P., and Williams, G.L., 1979. Palynological zonation and correlation of sixty-seven wells, eastern Canada; Geological Survey of Canada, Paper 78-24, 118 p. https://doi.org/10.4095/104894

Bell, J.S., 1989. Labrador Sea; Geological Survey of Canada, East Coast Basin Atlas Series, 135 p. https://doi.org/10.4095/127152

Bell, J.S. and Campbell, G.R., 1990. Petroleum Resources; Chapter 12 *in* Geology of the Continental Margin of Eastern Canada, (ed.) M.J. Keen and G.L. Williams; Geological Survey of Canada, Geology of Canada, no. 2, p. 677–720 (*also* Geological Society of America, The Geology of North America, v. I-1, p. 677–720). https://doi.org/10.4095/132720

Bingham-Koslowski, N., 2019. Descriptions of Paleozoic cores and thin sections from the Gudrid H-55, Roberval K-92, Indian Harbour M-52, and Freydis B-87 wells, offshore Labrador (Newfoundland and Labrador); Geological Survey of Canada, Open File 8543, 142 p. https://doi.org/10.4095/313573

Bingham-Koslowski, N., Miller, M.A., McCartney, T., and Carey, J.S., 2019. Revised biostratigraphic and thermal alteration interpretations for the Paleozoic of the Hopedale Basin, offshore Labrador, Canada; Bulletin of Canadian Petroleum Geology, v. 67, p. 185–214.

BP Exploration Canada Ltd., 1976. Well history-abandonment report BP Columbia et al Indian Harbour M-52; on file with the Canada–Newfoundland and Labrador Offshore Petroleum Board, St. John's, Newfoundland and Labrador, 323 p.

Brinkhuis, H., Bujak, J.P., Smit, J., Versteegh, G.J.M., and Visscher, H., 1998. Dinoflagellate-based sea surface temperature reconstructions across the Cretaceous–Tertiary boundary; Palaeogeography, Palaeoclimatology, Palaeoecology, v. 141, p. 67–83. https://doi.org/10.1016/S0031-0182(98)00004-2

Bujak Davies Group, 1989a. Biostratigraphy and Maturation of 17 Labrador and Baffin Shelf wells, Volume 1: Scope, methodology, format and recommendations; Geological Survey of Canada, Open File 1929, 92 p. https://doi.org/10.4095/130622

Bujak Davies Group, 1989b. Biostratigraphy and Maturation of 17 Labrador and Baffin Shelf wells, Volume 5: Leif M-48 and North Bjarni F-06; Geological Survey of Canada, Open File 1933, 63 p. https://doi.org/10.4095/130626

Bujak Davies Group, 1989c. Biostratigraphy and Maturation of 17 Labrador and Baffin Shelf wells, Volume 6: North Leif I-05 and Ogmund E-72; Geological Survey of Canada, Open File 1934, 91 p. https://doi.org/10.4095/130627

Bujak Davies Group, 1989d. Biostratigraphy and Maturation of 17 Labrador and Baffin Shelf wells, Volume 8: Roberval K-92 and Rut H-11; Geological Survey of Canada, Open File 1936, 90 p. https://doi.org/10.4095/130629

Bujak Davies Group, 1989e. Biostratigraphy and Maturation of 17 Labrador and Baffin Shelf wells, Volume 9: South Hopedale L-39 and South Labrador N-79; Geological Survey of Canada, Open File 1937, 88 p. https://doi.org/10.4095/130630

Bujak Davies Group, 1989f. Biostratigraphy and Maturation of 17 Labrador and Baffin Shelf wells, Volume 10: Tyrk P-100; Geological Survey of Canada, Open File 1938, 35 p. https://doi.org/10.4095/130631

Cadenel, M., Plé, C., and Prim, M., 1978. Well history report Total Eastcan et al Roberval K-92; on file with the Canada–Newfoundland and Labrador Offshore Petroleum Board, St. John's, Newfoundland and Labrador, 72 p.

Canada–Newfoundland and Labrador Offshore Petroleum Board, 2007. Canada–Newfoundland and Labrador Offshore Petroleum Board Schedule of Wells: St. John's, Newfoundland: <http://www.cnlopb.ca/wells/> [accessed November 5, 2018].

Canterra Energy Ltd., 1983. Final well report Canterra et al South Hopedale L-39; on file with the Canada–Newfoundland and Labrador Offshore Petroleum Board, St. John's, Newfoundland and Labrador, 96 p.

Carey, J.S., McCartney, T., Hanna, M.C., Lister, C.J., and Kung, L.E., 2020. Quantitative petroleum resource assessment of the Labrador margin; Geological Survey of Canada, Open File 8535 (ed. rev), 104 p. https://doi.org/10.4095/326017

CFP Laboratory – Bordeaux, 1976. Micropaleontology; *in* Well History Report Eastcan et al. Cartier D-70; on file with the Canada–Newfoundland and Labrador Offshore Petroleum Board, St. John's, Newfoundland and Labrador, 22 p.

Chalmers, J.A., 1997. The continental margin off southern Greenland: along-strike transition from an amagmatic to a volcanic margin; Journal of the Geological Society, v. 154, p. 571–576. https://doi.org/10.1144/gsjgs.154.3.0571

Chevron Standard Ltd., 1980. Chevron et al South Labrador N-79, South Labrador, East Coast Offshore, Canada, Final Well Report; on file with the Canada–Newfoundland and Labrador Offshore Petroleum Board, St. John's, Newfoundland and Labrador, 65 p.

Chian, D.P., Louden, K.E., and Reid, I., 1995. Crustal structure of the Labrador Sea conjugate margin and implications for the formation of nonvolcanic continental margins; Journal of Geophysical Research, v. 100, p. 24239–24253. https://doi.org/10.1029/95JB02162

Committee on Stratigraphic Nomenclature, 1933. Classification and nomenclature of rock units; Geological Society of America Bulletin, v. 44, no. 2, p. 423–459, (*also* American Association of Petroleum Geologists Bulletin, v. 17, no. 7, p. 843– 868.

Corgnet, J.L. and McWhae, J.R.H., 1973a. Well history report Eastcan et al Bjarni H-81; on file with the Canada–Newfoundland and Labrador Offshore Petroleum Board, St. John's, Newfoundland and Labrador, 45 p.

Corgnet, J.L. and McWhae, J.R.H., 1973b. Well history report Eastcan et al Leif M-48; on file with the Canada–Newfoundland and Labrador Offshore Petroleum Board, St. John's, Newfoundland and Labrador, 57 p.

Corgnet, J.L. and McWhae, J.R.H., 1975. Well history report Eastcan et al Gudrid H-55; on file with the Canada–Newfoundland and Labrador Offshore Petroleum Board, St. John's, Newfoundland and Labrador, 42 p.

Dafoe, L.T., 2021. Paleoenvironmental analyses and revised lithostratigraphic assignments for 28 wells of the Hopedale and Saglek basins, offshore eastern Canada; Geological Survey of Canada, Open File 8810, 1 .zip file. https://doi.org/10.4095/328477

Dafoe, L.T. and Williams, G.L., 2020a. Lithological, sedimentological, ichnological, and palynological analysis of 37 conventional core intervals from 15 wells, offshore Labrador (Newfoundland and Labrador) and southeast Baffin Island (Nunavut); Geological Survey of Canada, Bulletin 613, 146 p. https://doi.org/10.4095/315362

Dafoe, L.T. and Williams, G.L., 2020b. Palynological analysis of the two Labrador Shelf wells, Petro-Canada et al. North Leif I-05 and Total Eastcan et al. Skolp E-07, offshore eastern Canada: new age, paleoenvironmental and lithostratigraphic interpretations; Geological Survey of Canada, Open File 8670, 1 .zip file. https://doi.org/10.4095/321502

Dafoe, L.T., Dickie, K., Williams, G.L., Jauer, C.D., Li., Q., Dehler, S., Potter, D.P., Hynes, S., Patton, E., Bates, J., Haggart, J.W., and Clark, K., 2016. Report of activities for the Stratigraphic and Tectonic Framework for the Baffin Bay Petroleum Systems (2016); Geological Survey of Canada, Open File 8144, 10 p. https://doi.org/10.4095/299240

Dafoe, L.T., Dickie, K., Williams, G.L., and Keen, C.E., 2017a. A late rift to post-rift shoreline clinoform and shelf-edge model for the offshore Labrador margin, Canada; 5th Atlantic Conjugate Margins Conference, Porto de Galinhas, Brazil, August 22–25, 2017, 1 p. (abstract).

Dafoe, L.T., Dickie, K., Williams, G.L., and Keen, C.E., 2017b. Regional Cenozoic stratigraphic correlations on the passive margin of the North Atlantic: comparison between Orphan Basin and the Labrador Margin; *in* Atlantic Geoscience Society 43rd Colloquium and Annual Meeting, Fredericton, New Brunswick, 10–11 February 2017, Program and Abstracts, p. 24–25.

Dafoe, L.T., Dickie, K., and Williams, G.L., 2018. A clinoform trajectory model for Late Cretaceous and Cenozoic sedimentation on the Labrador-Baffin Island Margins; 6th Conjugate Margins Conference, Halfax, Nova Scotia, August 19–23, 2018, Program and Abstracts, p. 74.

Dale, B., 1996. Dinoflagellate cyst ecology: modelling and geological applications; *in* Palynology: Principles and Applications 3, (ed.) J. Jansonius and D.C. McGregor; American Association of Stratigraphic Palynologists Foundation, Dallas, Texas, p. 1249–1275.

Deptuck, M.E., Mosher, D.C., Campbell, D.C., Hughes-Clarke, J.E., and Noseworthy, D., 2007. Along slope variations in mass failures and relationships to major Plio-Pleistocene morphological elements, SW Labrador Sea; *in* Submarine Mass Movements and their Consequences, (ed.) V. Lykousis, D. Sakellariou, and J. Locat; Springer, Dordrecht, The Netherlands, p. 37–45. https://doi.org/10.1007/978-1-4020-6512-5_5

Dickie, K., Keen, C.E., Williams, G.L., and Dehler, S.A., 2011. Tectonostratigraphic evolution of the Labrador Margin, Atlantic Canada; Marine and Petroleum Geology, v. 28, p. 1663–1675. https://doi.org/10.1016/j.marpetgeo.2011.05.009

Doeven, P.H. and McIntyre, D.J., 1980. Biostratigraphy of the Petro-Canada et al. Roberval C-02 well; Petro-Canada Geological Research and Services Biostratigraphy Group, Project B/S 74; on file with the Canada–Newfoundland and Labrador Offshore Petroleum Board, St. John's, Newfoundland and Labrador, 16 p.

Eshet, Y., Almogi-Labin, A., and Bein, A., 1994. Dinoflagellate cysts, paleoproductivity and upwelling systems: a Late Cretaceous example from Israel; Marine Micropaleontology, v. 23, p. 231–240. https://doi.org/10.1016/0377-8398(94)90014-0

Fader, G.B., Cameron, G.D.M., and Best, M.A. (comp.), 1989. Geology of the Continental Margin of Eastern Canada; Geological Survey of Canada, Map 1705A, scale 1:5 000 000.

Fensome, R.A., 2015. Palynological analysis of two Labrador Shelf wells: Petro Canada et al. Rut H-11 and Eastcan et al. Karlsefni A-13; Geological Survey of Canada, Open File 7738, 21 p. https://doi.org/10.4095/295616

Fenton, J.P.G., and Pardon, A.M., 2007. Sequence stratigraphic correlation of Cretaceous–Palaeogene strata, Labrador Sea and Davis Strait. Biostratigraphic and sequence stratigraphic correlation of 33 wells. Volume 1: text, figures and appendices. Report No. 6851/Ib, Project No. Ib/GF556; report prepared for Fugro Robertson Limited, Llandudno, United Kingdom, on file at Canada–Newfoundland and Labrador Offshore Petroleum Board, 177 p.

Ferrero, J. and Plé, C., 1976. Well history report Eastcan et al Cartier D-70; on file with the Canada–Newfoundland and Labrador Offshore Petroleum Board, St. John's, Newfoundland and Labrador, 44 p.

Ferrero, J. and Plé, C., 1977a. Well history report Eastcan et al Herjolf M-92; on file with the Canada–Newfoundland and Labrador Offshore Petroleum Board, St. John's, Newfoundland and Labrador, 86 p.

Ferrero, J. and Plé, C., 1977b. Well history report Eastcan et al Karlsefni A-13; on file with the Canada–Newfoundland and Labrador Offshore Petroleum Board, St. John's, Newfoundland and Labrador, 55 p.

Funck, T. and Louden, K.E., 1999. Wide-angle seismic transect across the Torngat Orogen, northern Labrador: evidence for a Proterozoic crustal root; Journal of Geophysical Research, v. 104, no. B4, p. 7463–7480. https://doi.org/10.1029/1999JB900010

Funck, T., Louden, K.E., and Reid, I.D., 2001. Crustal structure of the Grenville Province in southeastern Labrador from refraction seismic data: evidence for a high-velocity lower crustal wedge; Canadian Journal of Earth Sciences, v. 38, p. 1463–1478. https://doi.org/10.1139/e01-026

General Bathymetric Chart of the Oceans, 2014. GEBCO 2014 Grid; International Hydrographic Organization and the Intergovernmental Oceanographic Commission (of UNESCO). <www.gebco.net> [accessed May 7, 2015]

Gower, C.F., 1996. The evolution of the Grenville Province in eastern Labrador, Canada; *in* Precambrian Crustal Evolution in the North Atlantic Region, (ed.) T.S. Brewer; Geological Society, London, Special Publication 112, p. 197–218. https://doi.org/10.1144/GSL.SP.1996.112.01.11

Gradstein, F.M., 1975. Preliminary biostratigraphic (foraminifers) analysis of Eastcan et al. Gudrid H-55, Labrador Shelf; Geological Survey of Canada–Atlantic, Report No. EPGS-PAL.17-75FMG, 3 p. <https://basin.gdr.nrcan.gc.ca/wells/index_e.php> [accessed March 2, 2018]

Gradstein, F.M., 1976a. Labrador Shelf foraminiferal stratigraphy I; Geological Survey of Canada–Atlantic, Report No. EPGS-PAL.5-76FMG, 20 p. <https://basin.gdr.nrcan.gc.ca/wells/index_e.php> [accessed March 2, 2018]

Gradstein, F.M., 1976b. Labrador Shelf foraminiferal stratigraphy I - supplement; Eastcan Cartier D-79; Geological Survey of Canada–Atlantic, Report No. EPGS-PAL.13-76FMG, 3 p. <https://basin.gdr.nrcan.gc.ca/wells/index_e.php> [accessed March 2, 2018]

Gradstein, F.M., 1977. Labrador Shelf foraminiferal stratigraphy, Eastcan et al. Herjolf M-92; Geological Survey of Canada–Atlantic, Report No. EPGS-PAL.36-77FMG, 3 p. <https://basin.gdr.nrcan.gc.ca/wells/index_e.php> [accessed March 2, 2018]

Gradstein, F.M., 1978. Labrador Shelf foraminiferal stratigraphy I – supplement; Eastcan et al. Karlsefni H-13, Labrador Shelf; Geological Survey of Canada–Atlantic, Report No. EPGS-PAL.12-78FMG, 2 p. <https://basin.gdr.nrcan.gc.ca/wells/index_e.php> [accessed March 2, 2018]

Gradstein, F.M. and Srivastava, S.P., 1980. Aspects of Cenozoic stratigraphy and paleoceanography of the Labrador Sea and Baffin Bay; Palaeogeography, Palaeoclimatology, Palaeoecology, v. 30, p. 261–295. https://doi.org/10.1016/0031-0182(80)90061-9

Gradstein, F.M. and Williams, G.L., 1976. Biostratigraphy of the Labrador Shelf, Part 1; Geological Survey of Canada, Open File 349, 39 p. https://doi.org/10.4095/100443

Gradstein, F.M., Kaminski, M.A., Berggren, W.A., Kristiansen, I.L., and D'Ioro, M.A., 1994. Cenozoic biostratigraphy of the North Sea and Labrador Shelf; Micropaleontology, v. 40, Supplement, 152 p. https://doi.org/10.2307/1485906

Gradstein, F.M., Ogg, J.G., Schmitz, M., and Ogg, G., 2012. The Geologic Time Scale 2012; Elsevier B.V., Oxford, United Kingdom, 1144 p.

Gregersen, U., Hopper, J.R., and Knutz, P., 2013. Basin seismic stratigraphy and aspects of prospectivity in the NE Baffin Bay, Northwest Greenland; Marine and Petroleum Geology, v. 46, p. 1–18. https://doi.org/10.1016/j.marpetgeo.2013.05.013

Gregersen, U., Andersen, M.S., Nøhr-Hansen, H., Sheldon, E., Kokfelt, T.F., Olivarius, M., Knudsen, C., Jakobsen, K.G., and Adolfssen, J.S., 2018. New subsurface mapping offshore southern West Greenland using geophysical and geological data; Geological Survey of Denmark and Greenland Bulletin, v. 41, p. 57–62. https://doi.org/10.34194/geusb.v41.4342

Gregersen, U., Knutz, P.C., Nøhr-Hansen, H., Sheldon, E., and Hopper, J.R., 2019. Tectonostratigraphy and evolution of the West Greenland continental margin; Bulletin of the Geological Society of Denmark, v. 67, p. 1–21.

Hall, J., Louden, K.E., Funck, T., and Deemer, S., 2002. Geophysical characteristics of the continental crust along the Lithoprobe Eastern Canadian Shield Onshore–Offshore Transect (ECSOOT): a review; Canadian Journal of Earth Sciences, v. 39, no. 5, p. 569–587. https://doi.org/10.1139/e02-005

Hedberg, H.D. (ed.), 1976. International Stratigraphic Guide; John Wiley and Sons, Wiley-Interscience Publications, New York, New York, 200 p.

Heilmann-Clausen, C., 1994. Review of Paleocene dinoflagellates from the North Sea region; GFF, v. 116; Geological Society of Sweden, Stockholm, p. 51–53. https://doi.org/10.1080/11035899409546149

Jauer, C., Wielens, H., and Williams, G., 2009. Hydrocarbon prospectivity of Davis Strait and Labrador Shelf: seismic setting and stratigraphy for Gjoa G-37, Hekja O-71, Rut H-11, Gilbert F-53, Karlsefni A-13, and Skolp E-07; Geological Survey of Canada, Open File 5910, 6 sheets. https://doi.org/10.4095/247336

Jauer, C.D., Oakey, G.N., Williams, G., and Wielens, J.B.W.H., 2014. Saglek Basin in the Labrador Sea, east coast Canada; stratigraphy, structure and petroleum systems; Bulletin of Canadian Petroleum Geology; v. 62, special issue, p. 232–260. https://doi.org/10.2113/gscpgbull.62.4.232

Keen, C.E., Dickie, K., and Dehler, S., 2012. The volcanic margins of the northern Labrador Sea: Insights to the rifting process; Tectonics, v. 31, cit. no. TC1011, 13 p. https://doi.org/10.1029/2011TC002985

Keen, C.E., Dickie, K., and Dafoe, L.T., 2018a. Structural characteristics of the ocean-continent transition along the rifted continental margin, offshore central Labrador; Marine and Petroleum Geology, v. 89, p. 443–463. https://doi.org/10.1016/j.marpetgeo.2017.10.012

Keen, C.E., Dickie, K., and Dafoe, L.T., 2018b. Structural evolution of the rifted margin off northern Labrador: The role of hyperextension and magmatism; Tectonics, v. 37, p. 1955–1972. https://doi.org/10.1029/2017TC004924

Kent, D.V. and Gradstein, F.M., 1985. A Cretaceous and Jurassic geochronology; Geological Society of America Bulletin, v. 96, p. 1419–1427. https://doi.org/10.1130/0016-7606(1985)96%3c1419:ACAJG%3e2.0.CO%3b2

King, A.F. and McMillan, N.J., 1975. A Mid-Mesozoic breccia from the coast of Labrador; Canadian Journal of Earth Sciences, v. 12, no. 1, p. 44–51. https://doi.org/10.1139/e75-005

Krueger Enterprises, Inc., 1979. Potassium-Argon age determination report of analytical work (Roberval K-92); on file with the Canada–Newfoundland and Labrador Offshore Petroleum Board, St. John's, Newfoundland and Labrador, 7 p.

Larsen, L.M., Heaman, L.M., Creaser, R.A., Duncan, R.A., Frei, R., and Hutchinson, M., 2009. Tectonomagmatic events during stretching and basin formation in the Labrador Sea and the Davis Strait: evidence from age and composition of Mesozoic to Palaeogene dyke swarms in West Greenland; Journal of the Geological Society, v. 166, p. 999–1012. https://doi.org/10.1144/0016-76492009-038

Lee, J.K.W., 2014. Ar-Ar and K-Ar dating; *in* Encyclopedia of Scientific Dating Methods, (ed.) W.J. Rink and J. Thompson; Springer, Dordrecht, Netherlands, 978 p. https://doi.org/10.1007/978-94-007-6304-3

McCartney, T., 2019. A qualitative comparison of continental rift structures in the sedimentary basins of the Labrador Shelf, offshore Newfoundland and Labrador, and the Malawi Rift, East Africa; Geological Survey of Canada, Open File 8634, 3 posters. https://doi.org/10.4095/315352

McMillan, N.J., 1973. Shelves of Labrador Sea and Baffin Bay; *in* Future Petroleum Provinces of Canada, (ed.) R.G. McCrossan; Canadian Society of Petroleum Geology, Memoir, v. 1, p. 473–515.

McMillan, N.J., 1980. Geology of the Labrador Sea and its Petroleum Potential; *in* Proceeding—World Petroleum Congress, International, v. 10, Wiley, Chichester, United Kingdom, p. 165–175.

McWhae, J.R.H., 1981. Structure and spreading history of the northwestern Atlantic region from the Scotian Shelf to Baffin Bay; *in* Geology of the North Atlantic Borderlands, (ed.) J.W. Kerr, A.J. Fergusson, and L.C. Machan; Canadian Society of Petroleum Geologists, Memoir 7, p. 299–332.

McWhae, J.R.H. and Michel, W.F.E., 1975. Stratigraphy of Bjarni H-81 and Leif E-48, Labrador Shelf; Bulletin of Canadian Petroleum Geology, v. 23, p. 361–382.

McWhae, J.R.H., Ferrero, J., and Plé, C., 1975. Well history report Eastcan et al Snorri J-90; on file with the Canada–Newfoundland and Labrador Offshore Petroleum Board, St. John's, Newfoundland and Labrador, 67 p.

McWhae, J.R.H., Elie, R., Laughton, K.C., and Gunther, P.R., 1980. Stratigraphy and petroleum prospects of the Labrador Shelf; Bulletin of Canadian Petroleum Geology, v. 28, p. 460–488.

Mercer, C.M. and Hodges, K.V., 2016. *ArAR* — A software tool to promote the robust comparison of K–Ar and $^{40}Ar/^{39}Ar$ dates published using different decay, isotopic, and monitor-age parameters; Chemical Geology, v. 440, p. 148–163. http://doi.org/10.1016/j.chemgeo.2016.06.020

Miller, P.E. and D'Eon, G.J., 1987. Labrador Shelf – Paleoenvironments; Geological Survey of Canada, Open File 1722, 186 p. https://doi.org/10.4095/130598

Moir, P.N., 1987. Stratigraphic picks, Total-Eastcan *et al.* Skolp E-07; Geological Survey of Canada – Atlantic, Report No. EPGS-STRAT.27-87PNM, 2 p. <https://basin.gdr.nrcan.gc.ca/wells/index_e.php> [accessed March 2, 2018]

Moir, P.N., 1989. Lithostratigraphy 1: Review and type sections; *in* East Coast Basin Atlas Series, Labrador Sea, (co-ord.) J.S. Bell; Geological Survey of Canada, p. 26. https://doi.org/10.4095/127166

Myers, R.A. and Piper, D.J.W., 1988. Seismic stratigraphy of late Cenozoic sediments in the northern Labrador Sea: a history of bottom circulation and glaciation; Canadian Journal of Earth Sciences, v. 25, p. 2059–2074. https://doi.org/10.1139/e88-191

Nier, A.O., 1950. A redetermination of the relative abundances of the isotopes of carbon, nitrogen, oxygen, argon, and potassium; Physical Review, v. 77, no. 6, p. 789–793.

Nøhr-Hansen, H., Williams, G.L., and Fensome, R.A., 2016. Biostratigraphic correlation of the western and eastern margins of the Labrador–Baffin Seaway and implications for the regional geology; Geological Survey of Denmark and Greenland Bulletin, v. 37, 74 p.

North American Commission on Stratigraphic Nomenclature, 1983. North American Stratigraphic Code; American Association of Petroleum Geologists Bulletin, v. 67, no. 5, p. 841–875.

North American Commission on Stratigraphic Nomenclature, 2005. North American Stratigraphic Code; American Association of Petroleum Geologists Bulletin, v. 89, p. 1547–1591. https://doi.org/10.1306/07050504129

Oakey, G.N. and Chalmers, J.A., 2012. A new model for the Paleogene motion of Greenland relative to North America: plate reconstructions of the Davis Strait and Nares Strait regions between Canada and Greenland; Journal of Geophysical Research, v. 117, cit. no. B10401. https://doi.org/10.1029/2011JB008942

Oliver, E.M. and Awai-Thorne, B., 1984. The micropalaeontology, palynology and stratigraphy of the South Hopedale L-39 well, Labrador Shelf, offshore Eastern Canada; Robertson Research Canada Limited, on file with the Canada–Newfoundland and Labrador Offshore Petroleum Board, St. John's, Newfoundland and Labrador, 29 p.

Oliver, E.M. and Thorne, B.V.A., 1979. The micropalaeontology, palynology and stratigraphy of the Total Eastcan Tyrk P-100 well; Robertson Research Canada Limited, on file at the Canada–Newfoundland and Labrador Offshore Petroleum Board, St. John's, Newfoundland and Labrador, 20 p.

Pandachuck, P.N. and Lewis, D.G., 1978. Well history report Chevron et al Hopedale E-33; on file with the Canada–Newfoundland and Labrador Offshore Petroleum Board, St. John's, Newfoundland and Labrador, 29 p.

Peace, A.L., McCaffrey, K.J.W., Imber, J., Phethean, J., Nowell, G., Gerdes, K., and Dempsey, E., 2016. An evaluation of Mesozoic rift-related magmatism on the margins of the Labrador Sea: implications for rifting and passive margin asymmetry; Geosphere, v. 12, no. 6, p. 1701–1724. https://doi.org/10.1130/GES01341.1

Petro-Canada Exploration Inc., 1980a. Well history report Petro-Canada et al Gilbert F-53; on file with the Canada–Newfoundland and Labrador Offshore Petroleum Board, St. John's, Newfoundland and Labrador, 176 p.

Petro-Canada Exploration Inc., 1980b. Well history report Petro-Canada et al Roberval C-02; on file with the Canada–Newfoundland and Labrador Offshore Petroleum Board, St. John's, Newfoundland and Labrador, 151 p.

Petro Canada Exploration Inc., 1981. Well history report Petro-Canada et al North Leif I-05; on file with the Canada–Newfoundland and Labrador Offshore Petroleum Board, St. John's, Newfoundland and Labrador, 222 p.

Petro-Canada Inc., 1983. Well history report Petro-Canada et al Rut H-11; on file with the Canada–Newfoundland and Labrador Offshore Petroleum Board, St. John's, Newfoundland and Labrador, 79 p.

Planke, S., Symonds, P.A., Alvestad, E., and Skogseid, J., 2000. Seismic volcanostratigraphy of large volume basaltic extrusive complexes on rifted margins; Journal of Geophysical Research, v. 105, p. 19335–19351. https://doi.org/10.1029/1999JB900005

Plé, C. and Ferrero, J., 1976. Well history report Eastcan et al Freydis B-87; on file with the Canada–Newfoundland and Labrador Offshore Petroleum Board, St. John's, Newfoundland and Labrador, 42 p.

Powell, A.J., Brinkhuis, H., and Bujak, J.P., 1996. Upper Paleocene–lower Eocene dinoflagellate cyst sequence biostratigraphy of southeast England; *in* Correlation of the early Paleogene in Northwest Europe, (ed.) R.W.O.B. Knox, R.M. Corfield, and R.E. Dunay; Geological Society Special Publications, London, v. 101, p. 145–183. https://doi.org/10.1144/GSL.SP.1996.101.01.10

Prim, M., Cadenel, M., Ameller, J.H., and Plé, C., 1978. Well history report Total Eastcan et al Skolp E-07; on file with the Canada–Newfoundland and Labrador Offshore Petroleum Board, St. John's, Newfoundland and Labrador, 154 p.

Robertson Research Ltd., 1974a. The micropaleontology, palynology and stratigraphy of the Eastcan et al. Bjarni H-81 well; Robertson Research Exploration Report No. 58, on file with the Canada–Newfoundland and Labrador Offshore Petroleum Board, St. John's, Newfoundland and Labrador, 19 p.

Robertson Research Ltd., 1974b. The micropaleontology, palynology and stratigraphy of the Eastcan et al. Gudrid H-55 well; Robertson Research Exploration Report No. 92, on file with the Canada–Newfoundland and Labrador Offshore Petroleum Board, St. John's, Newfoundland and Labrador, 23 p.

Robertson Research Ltd., 1975. The micropaleontology, palynology and stratigraphy of Eastcan et al. Freydis B-87 well; Robertson Research Exploration Report No. 122, on file with the Canada–Newfoundland and Labrador Offshore Petroleum Board, St. John's, Newfoundland and Labrador, 27 p.

Robertson Research Ltd., 1979. The micropalaeontology, palynology and stratigraphy of the Total Eastcan Tyrk P-100 well; on file with the Canada–Newfoundland and Labrador Offshore Petroleum Board, St. John's, Newfoundland and Labrador, 20 p.

Robertson Research Ltd., 1984. The micropalaeontology, palynology and stratigraphy of the South Hopedale L-39 well, Labrador Shelf, offshore Eastern Canada; on file with the Canada–Newfoundland and Labrador Offshore Petroleum Board, St. John's, Newfoundland and Labrador, 29 p.

Roest, W.R. and Srivastava, S.P., 1989. Sea-floor spreading in the Labrador Sea: a new reconstruction; Geology, v. 17, p. 1000–1003. https://doi.org/10.1130/0091-7613(1989)017%3c1000:SFSITL%3e2.3.CO%3b2

Secher, K., Heaman, L.M., Nielsen, T.F.D., Jensen, S.M., Schjøth, F., and Creaser, R.A., 2009. Timing of kimberlite, carbonatite, and ultramafic lamprophyre emplacement in the alkaline province located 64°–67° N in southern West Greenland; Lithos, v. 112, p. 400–406. https://doi.org/10.1016/j.lithos.2009.04.035

Shaw, D., Rodrigue, G., and Meloche, D., 1984. Petrology of Petro-Canada et al. Rut H-11, Labrador Shelf. Proprietary report for Frontier Exploration, Newfoundland-Labrador District, on file with the Canada–Newfoundland and Labrador Offshore Petroleum Board, St. John's, Newfoundland and Labrador, 23 p.

Shillington, D.J., Holbrook, W.S., Van Avendonk, H.J.A., Tucholke, B.E., Hopper, J.R., Louden, K.E., Larsen, H.C., and Nunes, G.T., 2006. Evidence for asymmetric nonvolcanic rifting and slow incipient oceanic accretion from seismic reflection data on the Newfoundland margin; Journal of Geophysical Research, v. 111, cit. no. B09402. https://doi.org/10.1029/2005JB003981

Sønderholm, M., Nøhr-Hansen, H., Bojesen-Koefoed, J.A., Dalhoff, F., and Rasmussen, J.A., 2003. Regional correlation of Mesozoic-Paleogene sequences across the Greenland–Canada boundary; Danmarks og Grønlands Geologisske Undersøgelse, Rapport 2003/25, 175 p.

Srivastava, S.P., 1986. Depth to basement in the Labrador Sea; *in* Geological maps and Geological sections of the Labrador Sea; Geological Survey of Canada, Paper 85-16, Figure 6. https://doi.org/10.4095/120602

Srivastava, S.P. and Roest, W.R., 1999. Extent of oceanic crust in the Labrador Sea; Marine and Petroleum Geology, v. 16, p. 65–84. https://doi.org/10.1016/S0264-8172(98)00041-5

Srivastava, S.P., Falconer, R.K.H., and MacLean, B., 1981. Labrador Sea, Davis Strait, Baffin Bay: geology and geophysics – a review; *in* Geology of the North Atlantic Borderlands, (ed.) J.W. Kerr, A.J. Fergusson, and L.C. Machan; Canadian Society of Petroleum Geologists, Memoir, v. 7, p. 333–398.

Steiger, R.H. and Jäger, E., 1977. Subcommission on geochronology: convention on the use of decay constants in geo- and cosmochronology; Earth and Planetary Science Letters, v. 36, p. 359–362.

St-Onge, M.R., Van Gool, J.A.M., Garde, A.A., and Scott, D.J., 2009. Correlation of Archean and Paleoproterozoic units between northeastern Canada and western Greenland: cnstraining the pre-collisional upper plate accretionary history of the trans-Hudson orogen; *in* Earth Accretionary Systems in Space and Time, (ed.) P.A. Cawood and A. Kroner; Geological Society, London, Special Publication 318, p. 193–235. https://doi.org/10.1144/SP318.7

Storey, M., Duncan, R.A., Pedersen, A.K., Larsen, L.M., and Larsen, H.C., 1998. Ar-40/Ar-39 geochronology of the west Greenland tertiary volcanic province; Earth and Planetary Science Letters, v. 160, p. 569–586. https://doi.org/10.1016/S0012-821X(98)00112-5

Storey, M., Duncan, R.A., and Tegner, C., 2007. Timing and duration of volcanism in the North Atlantic Igneous Province: implications for geodynamics and links to the Iceland hotspot; Chemical Geology, v. 241, no. 3–4, p. 264–281 https://doi.org/10.1016/j.chemgeo.2007.01.016

Tappe, S., Foley, S.F., Stracke, A., Romer, R.L., Kjarsgaard, B.A., Heaman, L.M., and Joyce, N., 2007. Craton reactivation on the Labrador Sea margins: $^{40}Ar/^{39}Ar$ age and Sr-Nd-Hf-Pb isotope constraints from alkaline and carbonatite intrusives; Earth and Planetary Science Letters, v. 256, no. 3–4, p. 433–454. https://doi.org/10.1016/j.epsl.2007.01.036

Thrane, K., 2014. Provenance study of Paleocene and Cretaceous clastic sedimentary rocks from the Davis Strait and the Labrador Sea, based on U-Pb dating of detrital zircons; Bulletin of Canadian Petroleum Geology, v. 62, p. 330–396. https://doi.org/10.2113/gscpgbull.62.4.330

Total Eastcan Exploration Ltd., 1979. Well history report Total Eastcan et al Tyrk P-100; on file with the Canada–Newfoundland and Labrador Offshore Petroleum Board, St. John's, Newfoundland and Labrador, 118 p.

Umpleby, D.C., 1979. Geology of the Labrador shelf; Geological Survey of Canada, Paper 79-13, 40 p. https://doi.org/10.4095/105927

Van Hinte, J.E., 1976a. A Cretaceous time scale; American Association of Petroleum Geologists Bulletin, v. 60, no. 4, p. 498–516.

Van Hinte, J.E., 1976b. A Jurassic time scale; American Association of Petroleum Geologists Bulletin, v. 60, no. 4, p. 489–497.

Wasteneys, H.A., Wardle, R.J., and Krogh, T.E., 1996. Extrapolation of tectonic boundaries across the Labrador shelf: U–Pb geochronology of well samples; Canadian Journal of Earth Sciences, v. 33, no. 9, p. 1308–1324. https://doi.org/10.1139/e96-099

Wielens, H.J.B.W. and Williams, G.L., 2009. Stratigraphic cross section Gjoa-Snorri, Saglek – Hopedale Basin, in the Labrador Sea on the east coast of Canada, from North to South; Geological Survey of Canada, Open File 5903, 1 sheet. https://doi.org/10.4095/247636

Williams, G.L., 1979a. Eastcan et al. Bjarni H-81; *in* Palynological zonation and correlation of sixty-seven wells, eastern Canada, M.S. Barss, J.P. Bujak, and G.L. Williams; Geological Survey of Canada, Paper 78-24, p. 86–88. https://doi.org/10.4095/104894

Williams, G.L., 1979b. Eastcan et al. Cartier D-70; *in* Palynological zonation and correlation of sixty-seven wells, eastern Canada, M.S. Barss, J.P. Bujak, and G.L. Williams; Geological Survey of Canada, Paper 78-24, p. 88–89. https://doi.org/10.4095/104894

Williams, G.L., 1979c. Eastcan et al. Freydis B-87; *in* Palynological zonation and correlation of sixty-seven wells, eastern Canada, M.S. Barss, J.P. Bujak, and G.L. Williams; Geological Survey of Canada, Paper 78-24, p. 89–90. https://doi.org/10.4095/104894

Williams, G.L., 1979d. Eastcan et al. Herjolf M-92; *in* Palynological zonation and correlation of sixty-seven wells, eastern Canada, M.S. Barss, J.P. Bujak, and G.L. Williams; Geological Survey of Canada, Paper 78-24, p. 92–93. https://doi.org/10.4095/104894

Williams, G.L., 1979e. Eastcan et al. Karlsefni A-13; *in* Palynological zonation and correlation of sixty-seven wells, eastern Canada, M.S. Barss, J.P. Bujak, and G.L. Williams; Geological Survey of Canada, Paper 78-24, p. 94–95. https://doi.org/10.4095/104894

Williams, G.L., 1979f. Eastcan et al. Leif M-48; *in* Palynological zonation and correlation of sixty-seven wells, eastern Canada, M.S. Barss, J.P. Bujak, and G.L. Williams; Geological Survey of Canada, Paper 78-24, p. 96–97. https://doi.org/10.4095/104894

Williams, G.L., 1979g. Eastcan et al. Snorri J-90; *in* Palynological zonation and correlation of sixty-seven wells, eastern Canada, M.S. Barss, J.P. Bujak, and G.L. Williams; Geological Survey of Canada, Paper 78-24, p. 97–98. https://doi.org/10.4095/104894

Williams, G.L., 1980. Palynological analysis of Eastcan et al. Skolp E-07, Labrador Shelf; Geological Survey of Canada–Atlantic, Report No. EPGS-PAL.6-80GLW, 3 p. <https://basin.gdr.nrcan.gc.ca/wells/index_e.php> [accessed March 2, 2018]

Williams, G.L., 1981. Palynological Analysis of Chevron et al. Hopedale E-33, Labrador Shelf; Geological Survey of Canada, Report No. EPGS-PAL. 26-81GLW, 9 p. <https://basin.gdr.nrcan.gc.ca/wells/index_e.php> [accessed March 2, 2018]

Williams, V.E., 1986. Palynological study of the continental shelf sediments of the Labrador Sea;. Ph.D. thesis, University of British Columbia, Vancouver, British Columbia, 210 p.

Williams, G.L., 2007a. Palynological analysis of Aquitaine et al. Hekja O-71, Saglek Basin, Davis Strait, offshore eastern Canada; Geological Survey of Canada, Open File 5448, 19 p. https://doi.org/10.4095/224259

Williams, G.L., 2007b. Palynological analysis of Chevron et al. South Labrador N-79, Hopedale Basin, Labrador Shelf, offshore eastern Canada; Geological Survey of Canada, Open File 5446, 27 p. https://doi.org/10.4095/224257

Williams, G.L., 2007c. Palynological analysis of Eastcan et al. Snorri J-90, Hopedale Basin, Labrador Shelf, offshore eastern Canada; Geological Survey of Canada, Open File 5447, 23 p. https://doi.org/10.4095/224258

Williams, G.L., 2007d. Palynological analysis of Total Eastcan et al. Bjarni O-82, Hopedale Basin, Labrador Shelf, Offshore Eastern Canada; Geological Survey of Canada, Open File 5439, 22 p. https://doi.org/10.4095/224256

Williams, G.L., 2007e. Palynological analysis of Total Eastcan et al. Gilbert F-53, Saglek Basin, Labrador Shelf, offshore eastern Canada; Geological Survey of Canada, Open File 5450, 24 p. https://doi.org/10.4095/224261

Williams, G.L., 2017a. Palynological analyses of the two Labrador Shelf wells, Petro-Canada et al. Corte Real P-85 and Petro-Canada et al. Pothurst P-19, offshore Newfoundland and Labrador; Geological Survey of Canada, Open File 8182, 50 p. https://doi.org/10.4095/299653

Williams, G.L., 2017b. Palynological Analysis of the two Labrador Shelf Wells, Petro-Canada et al. Roberval C-02 and Total Eastcan et al. Roberval K-92, offshore Newfoundland and Labrador; Geological Survey of Canada, Open File 8183, 63 p. https://doi.org/10.4095/299645

Williams, G.L. and Barss, M.S., 1979. Eastcan et al. Gudrid H-55; *in* Palynological zonation and correlation of sixty-seven wells, eastern Canada, M.S. Barss, J.P. Bujak, and G.L. Williams; Geological Survey of Canada, Paper 78-24, p. 91. https://doi.org/10.4095/104894

Williams, G.L. and Bujak, J.P., 1977. Cenozoic palynostratigraphy of offshore eastern Canada; American Association of Stratigraphic Palynologists, Contributions Series 5A, p. 14–47.

Williams, G.L., Ascoli, P., Barss, M.S., Bujak, J.P., Davies, E.H., Fensome, R.A., and Williamson, M.A., 1990. Biostratigraphy and related studies, Chapter 3; *in* Geology of the Continental Margin of Eastern Canada, (ed.) M.J. Keen and G.L. Williams; Geological Survey of Canada, Geology of Canada, no. 2, p. 87–137 (*also* Geological Society of America, The Geology of North America, v. I-1).

Wilton, D.H.C., Taylor, R.C., Sylvester, P.J., and Penney, G.T., 2002. A review of kimberlitic and Ultramafic lamprophyre intrusives from northern Labrador; Current Research Newfoundland Department of Mines and Energy, Geological Survey, Report 02-1, p. 343–352.

Contents

A structural and stratigraphic framework for the western Davis Strait region

L.T. Dafoe[1*], K.J. DesRoches[1], and G.L. Williams[1]

Dafoe, L.T., DesRoches, K.J., and Williams, G.L., 2022. A structural and stratigraphic framework for the western Davis Strait region; in *Geological synthesis of Baffin Island (Nunavut) and the Labrador–Baffin Seaway, (ed.) L.T. Dafoe and N. Bingham-Koslowski; Geological Survey of Canada, Bulletin 608, p. 181–218. https://doi.org/10.4095/321831*

Abstract: Western Davis Strait lies within the Labrador–Baffin Seaway rift system, which began forming in the Early Cretaceous as Greenland separated from North America. At chron C27n (Danian), regional seafloor spreading began, as well as significant magmatism. The opening direction changed from southeast–northwest to more north–south in the Thanetian–Ypresian between chrons C25n and C24n, resulting in significant strike-slip motion through the Davis Strait region until seafloor spreading ended at chron C13, near the Eocene–Oligocene boundary. This tectonism has influenced the stratigraphy preserved in basins within western Davis Strait, including confirmed Cretaceous successions in the Lady Franklin Basin and Cumberland Sound; however, regional overprinting of Paleocene–Eocene volcanic rocks obscures pre-rift basement and possible older strata over much of the region. Three industry wells and several seabed samples of bedrock help constrain the stratigraphic distribution of Cretaceous and Cenozoic strata based on the lithostratigraphy of the well sampled Labrador margin.

Résumé : La partie occidentale du détroit de Davis se situe dans le système de rift du bras de mer Labrador-Baffin, dont la formation s’est amorcée au Crétacé précoce par la séparation du Groenland de l’Amérique du Nord. Au chrone C27n (Danien), a débuté l’expansion régionale des fonds marins ainsi qu’un important magmatisme. Au cours du Thanétien-Yprésien, entre le chrone C25n et le chrone C24n, l’orientation de l’ouverture, initialement sud-est–nord-ouest, s’est rapprochée d’un axe nord-sud, ce qui a provoqué un important mouvement de coulissage dans la région du détroit de Davis jusqu’à la fin de l’expansion des fonds marins au chrone C13, près de la limite Éocène-Oligocène. Cette activité tectonique a eu une influence sur la stratigraphie conservée dans les bassins de la partie occidentale du détroit de Davis, y compris des successions confirmées du Crétacé dans la baie Lady Franklin et la baie Cumberland. Toutefois, dans la majeure partie de la région, la superposition de roches volcaniques du Paléocène-Éocène masque le socle qui existait avant la formation du rift, et peut-être aussi des strates plus anciennes. Trois puits de l’industrie et plusieurs échantillons du fond marin contribuent à encadrer la répartition stratigraphique des strates du Crétacé et du Cénozoïque en se fondant sur la lithostratigraphie de la marge du Labrador pour laquelle on dispose de nombreux échantillons.

[1]Geological Survey of Canada, 1 Challenger Drive, P.O. Box 1006, Dartmouth, Nova Scotia B2Y 4A2
*Corresponding author: L.T. Dafoe (email: lynn.dafoe@nrcan-rncan.gc.ca)

INTRODUCTION

Within the central portion of the Labrador–Baffin Seaway, the western Davis Strait study region comprises the offshore area from about latitude 61°N to 67°N and longitude 57°W to 65°W and west of the international boundary between the waters of Canada and Greenland (Fig. 1). It is within the bounds of the Davis Strait that includes a topographic sill with shallow water depths (<700 m) lying between the Labrador Sea to the south and Baffin Bay to the north. Much of the region also constitutes the southeast Baffin Shelf.

Some of the early interpretations of the geology and evolution of the region were proposed by McMillan (1973), Beh (1975), Grant (1975), and Srivastava et al. (1981, 1982). Like the Labrador margin, this region formed during rifting and extension between the Greenland and paleo-North America plates, which began in the Early Cretaceous (Roest and Srivastava, 1989). Unlike the Labrador margin, however, less is known about the extent of Cretaceous rifting because of limited sampling, extensive Paleogene basalt flows that mask the underlying structure and stratigraphy, and generally low-resolution seismic data. Seafloor spreading likely took place at the same time as that of the northern Labrador margin, by chron C27n (Keen et al., 2018b); although, earlier spreading occurred along the central Labrador margin beginning at chron C31 during the Maastrichtian (Keen et al., 2018a). As a result of this tectonism, a magma-rich margin formed offshore Cape Dyer (Skaarup et al., 2006), but the western Davis Strait region appears to be dominated by magma-rich conditions (Keen et al., this volume). A major tectonic event that influenced the western Davis Strait region was the change in direction of seafloor spreading between chrons C25n and C24n, which resulted in significant translational motion, including transpression that would have impacted existing Cretaceous and Paleocene structures and sedimentary successions (Chalmers and Pulvertaft, 2001; Oakey and Chalmers, 2012). Seafloor spreading ended by chron C13 (Oakey and Chalmers, 2012) in the earliest Oligocene (Rupelian).

Kerr (1967) first postulated the presence of a transform fault through the Davis Strait, and proposed the term Ungava Transform Fault, a term adopted by Le Pichon et al. (1971). McWhae (1981) described compression along the Ungava Transform Fault, which was later referred to as a zone of faulting and deformation (Rice and Shade, 1982; Balkwill, 1987), now known as the Ungava Fault Zone (Chalmers and Pulvertaft, 2001). Srivastava et al. (1982) confirmed the presence of a related structural high oriented northeast–southwest through the Davis Strait in accordance with a free-air gravity anomaly high and seismic reflection and refraction data. They further concluded that much of the high, in particular the western side, comprised continental crust that was likely separated from the North American Plate and translated northeastward during the change in plate motion and related strike-slip faulting. These authors thus defined the Davis Strait High. Folding, faulting, and diapir-like structures in the area were also identified along the southeast Baffin Shelf (Grant, 1975; MacLean et al., 1982).

Major volcanism in the Labrador–Baffin Seaway began around the time of seafloor spreading (chron C27n; Danian), especially in the Davis Strait region and has been linked to the arrival of a mantle plume at approximately 61 Ma (Storey et al., 1998, 2007; Larsen et al., 2009). Accordingly, volcanic rocks form a significant component of the western Davis Strait region. Onshore at Cape Dyer, Baffin Island, basalt units occur within a narrow outcrop band along the coastline (Clarke and Upton, 1971). Related offshore basaltic cover was first recognized by Grant (1975), but single-channel seismic data could only image volcanic rocks near the seafloor. Based on magnetic anomaly patterns and the ridges they observed, MacLean et al. (1982) suggested that basalt units could be present in the subsurface over much of the southeast Baffin Shelf. Extensive volcanic rocks were later mapped by Skaarup et al. (2006) as both basalt units near the seafloor and, more commonly, basalt units at depth masking underlying strata and pre-rift basement. Across the international boundary in the Lady Franklin Basin, Sørensen (2006) mapped flood basalt units in two regions around both the Hecla and Maniitsoq volcanic eruption centres (or volcanic highs) and another centre near the Gjoa G-37 well, the Gjoa Eruption Centre (or Gjoa High; Fig. 1; Sørensen, 2006).

These volcanic and basement structures form the framework for sedimentary depocentres in the study area. The Saglek Basin, originally defined by Umpleby (1979), extends from the northern offshore Labrador margin to the southeast Baffin Shelf. To the south, it is bounded by the Okak Arch, a prominent basement high (McMillan, 1980). Balkwill (1987) defined the Lady Franklin Arch (previously called the Lady Franklin High by Wade et al. (1977)) as a boundary separating the northeastern segment of the Saglek Basin from rocks of the Cumberland Basin found farther north (Fig. 1). The southern and northern segments of the Saglek Basin, separated by the Hudson Strait, strike northwest and northeast, respectively. Jauer and Budkewitsch (2010) and Jauer et al. (2014) extended the Saglek Basin northward of the Lady Franklin Arch, but this differs from the previously established basin boundaries. Here, Balkwill (1987) defined the Cumberland Basin, a depocentre oriented southwest–northeast and bounded to the northwest by Cumberland Peninsula and to the southwest by Hall Peninsula and the Lady Franklin Arch (Fig. 1). The Davis Strait High separates the Cumberland Basin from the Lady Franklin Basin to the southeast (Chalmers and Pulvertaft, 2001). To the west of the Cumberland Basin, Cumberland Sound contains a graben with significant sedimentary successions (Hood and Bower, 1975).

Sørensen (2006) mapped the Lady Franklin Basin, offshore southern West Greenland, which primarily sits on the West Greenland margin, but extends into the western Davis Strait region (Fig. 1). The basin fill consists of a thick succession of Cretaceous and Cenozoic strata and is one of the deepest basins offshore south-central West Greenland (Sørensen, 2006), with over 4 km of strata throughout much of the basin (Keen et al., this volume). East of Cape Dyer, Gregersen and Bidstrup (2008) described the North Ungava Basin (named by Christiansen et al., 2002), which lies upon a remnant ocean basin (Oakey and Chalmers, 2012) and thus has a relatively young (Cenozoic) fill. Keen et al. (this volume), present a regional sediment thickness map that illustrates the generally thin nature of strata in the region aside from the northern part of the Saglek Basin, and parts of Lady Franklin and Cumberland basins.

Industry exploration in the western Davis Strait area took place in the 1970s and early 1980s (Fig. 1). Two wells, Hekja O-71 and Ralegh N-18, were drilled in the northern Saglek Basin, the former including a significant gas discovery. A third well, Gjoa G-37, was drilled farther northeast, but south of the Lady Franklin Basin. With only these three wells drilled in the northern part of the Saglek Basin, the lithostratigraphic framework from the Labrador margin to the south has been applied to the wells with general success (Balkwill, 1987; Moir, 1987a, b, c; Balkwill and McMillan, 1990; Jauer et al., 2014; Nøhr-Hansen et al., 2016; Dafoe, 2021). The formations defined from the Labrador margin (Fig. 2; Umpleby, 1979; McWhae et al., 1980; Bell, 1989; Moir, 1989; Balkwill and McMillan, 1990; Jauer et al., 2009; Wielens and Williams, 2009; Dickie et al., 2011; Dafoe, 2021; Dafoe, Dickie, Williams, and McCartney, this volume) that are encountered in these wells include the Markland, Cartwright, Gudrid, Kenamu (Leif Member), Mokami, and Saglek. Along the West Greenland margin, Rolle (1985) and Gregersen et al. (2018) studied offshore wells in Davis Strait (*see* Gregersen et al., this volume), with some local similarities to the stratigraphy of the Labrador margin. In addition to the wells in the region, sampling of bedrock near the seabed was conducted in western Davis Strait and resulted in the identification of Precambrian, Paleozoic, Cretaceous, and Cenozoic rocks (Srivastava, 1974; Jansa, 1976; MacLean, 1977, 1978, 1980; MacLean and Falconer, 1977, 1979; MacLean et al., 1977, 1978, 1982, 1986, 2014; MacLean and Srivastava, 1981; MacLean and Williams, 1983; Bingham-Koslowski, 2018; Dafoe and Williams, 2020a).

McWhae (1981) linked regional units by mapping six unconformities from the Scotian Shelf to the eastern Baffin Island margin using well and geophysical control including: Lower Jurassic, Lower Cretaceous, mid-Cretaceous, Lower Paleocene, mid-Tertiary ((?)Lower Oligocene), and Middle to Upper Miocene surfaces. Age constraints in western Davis Strait are derived from microfossil studies such as palynology (e.g. Nøhr-Hansen et al., 2016) and radiometric ages from crystalline and igneous rocks (e.g. Williamson et al., 2000). Paleoenvironmental changes over time have also been described by Bujak Davies Group (1989c), Miller

Figure 1. a) Western Davis Strait study area showing bathymetry (General Bathymetric Chart of the Oceans, 2014), as well as the location of multichannel seismic data, profiles shown in this study (red lines), industry exploration wells, and GSC bedrock samples (seabed drill cores and relevant piston cores). Cruise samples are shown and labelled on the applicable stratigraphic distribution maps. Basin outlines are from Keen et al. (this volume). The Maniitsoq and Hecla highs are from Sørensen (2006) and the revised Gjoa High and unnamed high are from this study. Additional projection information: Central Meridian: 60°W; Standard Parallels: 65, 75°W; Latitude of Origin: 65°N.

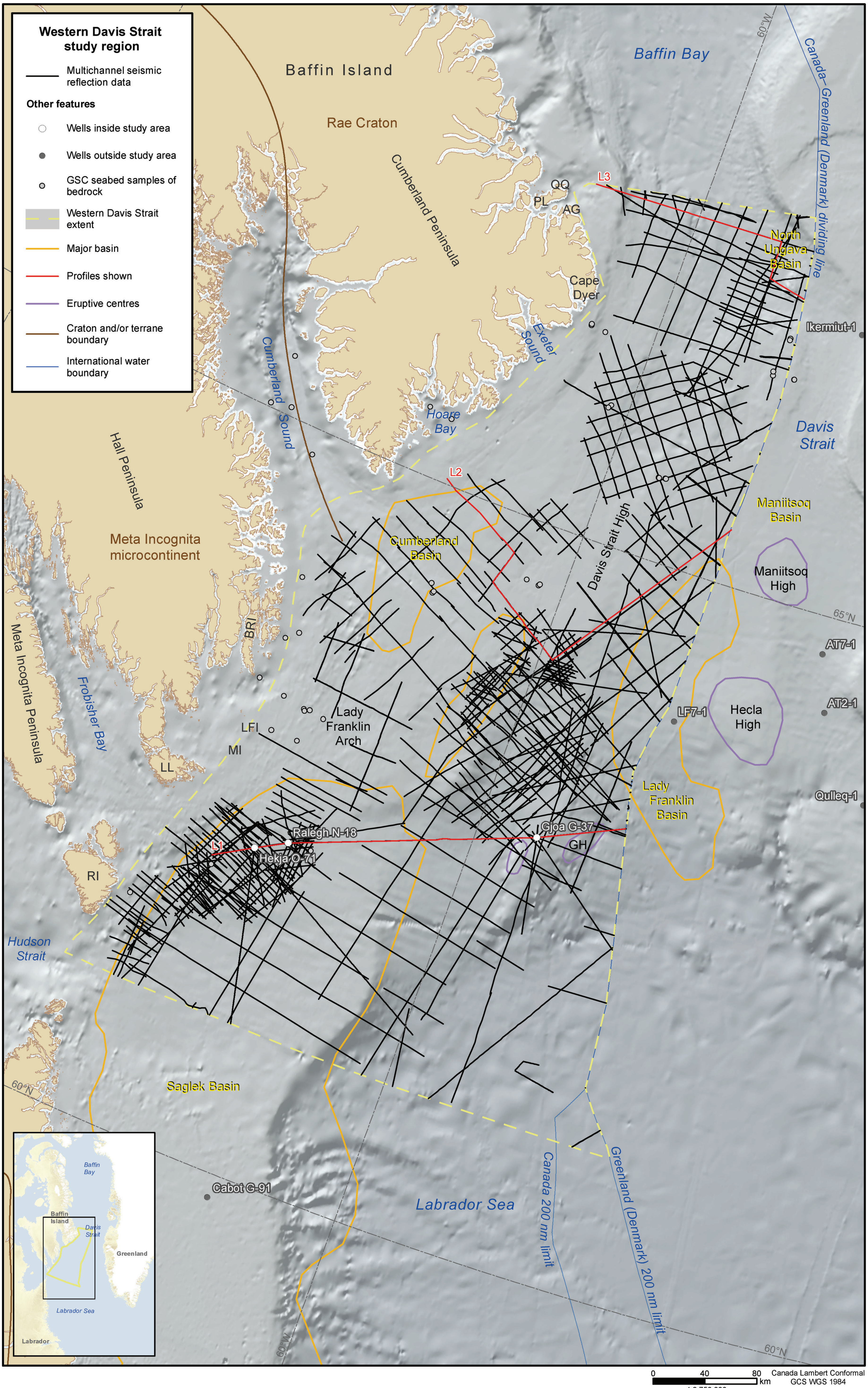
Western Davis Strait study region
Multichannel seismic reflection data
Other features
Wells inside study area
Wells outside study area
GSC seabed samples of bedrock
Western Davis Strait extent
Major basin
Profiles shown
Eruptive centres
Craton and/or terrane boundary
International water boundary
Baffin Island
Rae Craton
Cumberland Peninsula
Baffin Bay
Canada–Greenland (Denmark) dividing line
L3
QQ
PL
AG
North Ungava Basin
Cape Dyer
Exeter Sound
Ikermiut-1
Cumberland Sound
Hoare Bay
Davis Strait
Hall Peninsula
L2
Maniitsoq Basin
Cumberland Basin
Davis Strait High
Meta Incognita microcontinent
Maniitsoq High
65°N
60°W
BRI
AT7-1
Meta Incognita Peninsula
Frobisher Bay
Lady Franklin Arch
LF7-1
Hecla High
AT2-1
LFI
MI
LL
Lady Franklin Basin
Qulleq-1
Ralegh N-18
Gjoa G-37
L1
Hekja O-71
GH
RI
Hudson Strait
60°N
Saglek Basin
Cabot G-91
Labrador Sea
Canada 200 nm limit
Greenland (Denmark) 200 nm limit
Baffin Bay
Baffin Island
Davis Strait
Greenland
Labrador Sea
Labrador
0
40
80
km
1:2 750 000
Canada Lambert Conformal
GCS WGS 1984

Basin names
CB – Cumberland Basin
LFB – Lady Franklin Basin
MNB – Maniitsoq Basin
NUB – North Ungava Basin
SGB – Saglek Basin
Bathymetric names
CS – Cumberland Sound
ES – Exeter Sound
FB – Frobisher Bay
HB – Hoare Bay
HS – Hudson Strait
Geological structures
DSH – Davis Strait High
GH – Gjoa High
HH – Hecla High
LFA – Lady Franklin Arch
MH – Maniitsoq High
UFZ – Ungava Fault Zone
Onshore place names
AG – Aggijjat
BRI – Brevoort Island
CD – Cape Dyer
CP – Cumberland Peninsula
HP – Hall Peninsula
LFI – Lady Franklin Island
LL – Loks Land
MI – Monumental Island
MIP – Meta Incognita Peninsula
PL – Paallavvik
QQ – Qaqulluit
RI – Resolution Island

Figure 1. b) Abbreviations of key place names for Figures 1a, 3, 5, 7, and 10.

and D'Eon (1987), Williams (2007a, b), Nøhr-Hansen et al. (2016), and Dafoe (2021), and show that depositional settings are typically shallower and lithologies often sandier than the Labrador margin (Miller and D'Eon, 1987). The thick Cenozoic section in the southern part of the study region can also be linked to development of the Bell River System, which likely drained through Hudson Strait into the northernmost Saglek Basin (McMillan, 1973; Duk-Rodkin and Hughes, 1994).

The petroleum potential of the region has mostly focused on the northern part of the Saglek Basin where a significant gas discovery was found in Hekja O-71 (Bell and Campbell, 1990; Wielens and Jauer, 2009; Jauer et al., 2014; Bingham-Koslowski, McCartney, and Bojesen-Koefoed, this volume). Other indicators of a viable petroleum system include hydrothermal vents interpreted from seismic data (Jauer, 2009), potential sea-surface slicks (Budkewitsch et al., 2013), and identification of potential fairways near the exploration wells (Jauer et al., 2014). Whereas the Lower Cretaceous shale units in Cumberland Sound proved to be immature (MacLean et al., 2014), it is possible that extensive volcanism in the region may have locally contributed to enhanced maturation of Mesozoic or Cenozoic shale units (Jauer et al., 2019).

The present study integrates existing knowledge of the stratigraphic succession including well and sample data and previous mapping efforts with new insights and regional seismic mapping. The focus is on understanding the nature and distribution of the syn- and post-rift sedimentary infill and underlying pre-rift basement. Results are shown and described as they relate to revised lithostratigraphic assignments in the wells, seismic interpretation, and distribution maps of three main intervals: Cretaceous, lower Cenozoic, and upper Cenozoic.

DATA AND METHODS

This paper describes previous work conducted in the western Davis Strait region, but new results are also presented based on: analyses and integration of existing interpretations; revised assessments of the wells; and new, regional seismic mapping (data shown in maps are included in the GIS data included with this volume). The stratigraphy is divided into three intervals: Cretaceous, lower Cenozoic, and upper Cenozoic. Like the Labrador margin (*see* Dafoe, Dickie, Williams, and McCartney, this volume), the Cenozoic succession is relatively complete as compared to that of the West Greenland margin where much of the Eocene to Middle Miocene is missing (Gregersen et al., 2013, 2018, 2019, this volume). In order to show regional correlations of the three stratigraphic intervals for the entire Labrador–Baffin Seaway, Dafoe, Williams et al. (this volume) divide the Cenozoic using the D1 horizon of Middle Miocene age from the West Greenland margin (Gregersen et al., 2013, 2018, 2019, this volume). This subdivision is followed here at the level of the Saglek and/or Mokami formation 3 (SM3) horizon within the Saglek and Mokami formations. This horizon forms a regional marker in the western Davis Strait area and is used in this paper to discuss the lower and upper portions of the Saglek and Mokami formations separately. In the very southeast of the study region, interpretations are extended offshore to the Danish 200 nautical mile (nm) territorial boundary (Fig. 1).

Well and sample data

Industry exploration wells were drilled between 1979 and 1982 in the northern part of the Saglek Basin (Hekja O-71 and Ralegh N-18) and farther east (Gjoa G-37; Fig. 1; Table 1). Data sets collected from these wells and released from confidentiality can be obtained from the National Energy Board (http://www.neb-one.gc.ca) and related well samples are curated at the Canada–Nova Scotia Offshore Energy Board (https://www.cnsopb.ns.ca). General information about the wells can also be found on the BASIN database (https://basin.gdr.nrcan.gc.ca), and lithological logs are primarily sourced from Canstrat (https://canstrat.com). Existing well data used in this study include: well history reports, biostratigraphic reports, well logs, lithological summaries, and lithostratigraphic compilations. Lithostratigraphic assignments for the wells follow that of Moir (1987a, b, c), with refinements from this study as noted in the text and in Table 2. Since the compilation of this paper, a revised assessment of the paleoenvironments and lithostratigraphy of the Labrador Shelf wells has been published in Dafoe (2021) and readers are referred to that work for an updated understanding of the wells.

Bedrock samples were collected from the region during Geological Survey of Canada (GSC) cruises from 1974 to 1985 (Fig. 1). A list of the cruises and related samples, which include seabed drill cores and bedrock fragments encountered in surficial piston cores is found in Table 3. Information regarding these cruises and the samples can be found on the Expedition Database (https://ed.gdr.nrcan.gc.ca), and location and technical information for the samples in Table 3 are sourced from this database. Samples are labelled according to cruise number and original sample station number (e.g. a sample collected at station number 109 during cruise 80028 is shown as 80028-109). Bedrock corehole samples are 2.54 cm in diameter and generally a few centimetres to a few tens of centimetres in length and often sampled overburden material during the bedrock coring process, but the overburden is not accounted for in the length of bedrock reported for each station (*see* MacLean et al., 2014). A general assessment of the material took place during the initial collection to determine if bedrock was recovered (cf. MacLean et al., 2014; Dafoe and Williams, 2020a). Detailed analyses and summaries of previous findings of the sedimentary samples from coreholes and piston cores are presented in MacLean et al. (2014) and Dafoe and Williams (2020a), and basalt drill-core samples are also described in Dafoe and Williams (2020a).

The wells and seabed samples of bedrock have been studied using standard paleontological and sedimentological techniques including palynological analyses, where appropriate. The biostratigraphy of wells and samples in the region is mostly described from a palynological perspective, including miospores (spores and pollen) and dinoflagellate cysts (dinocysts). As the sections in the wells, as well as the bedrock samples, are generally considered marine, ages for the Mesozoic and Cenozoic strata are based on dinocysts, which provide more precise age and paleoenvironmental determinations in those strata, rather than pollen and spores (*see* Nøhr-Hansen et al., 2016); however, well samples are predominantly cuttings, so only youngest or last occurrences (LO) can be used for most age determinations. Analyses from conventional cores and corehole samples of bedrock provide enhanced age control from in situ material, so first occurrences (FO) can also be studied (e.g. MacLean et al., 2014; Dafoe and Williams, 2020a, b).

Seismic data

The publicly released, 2-D multichannel seismic reflection data used in the western Davis Strait includes approximately 75 000 line kilometres (Fig. 1). Most of these data were collected in the 1970s and early 1980s by Imperial Oil, Bundesanstalt für Geowissenschaften und Rohstoffe (BGR), Aquitaine, Compagnie Générale de Géophysique (CGG), Petro-Canada, Eureka Exploration, Canterra Energy, Gulf Canada, Esso Resources, and Shell Canada (*see* the BASIN database for further details). The lines are mainly regional, varying in penetration from 5 s to 7 s two-way traveltime (twt). Only critical lines and surveys were migrated, generally using a single velocity, finite difference migration to improve interpretation (Dafoe et al., 2016a, b). Much of the data suffers from relatively limited frequency content due to conversion to digital data from analogue plots. The remainder of the multichannel seismic data used in this study forms a more

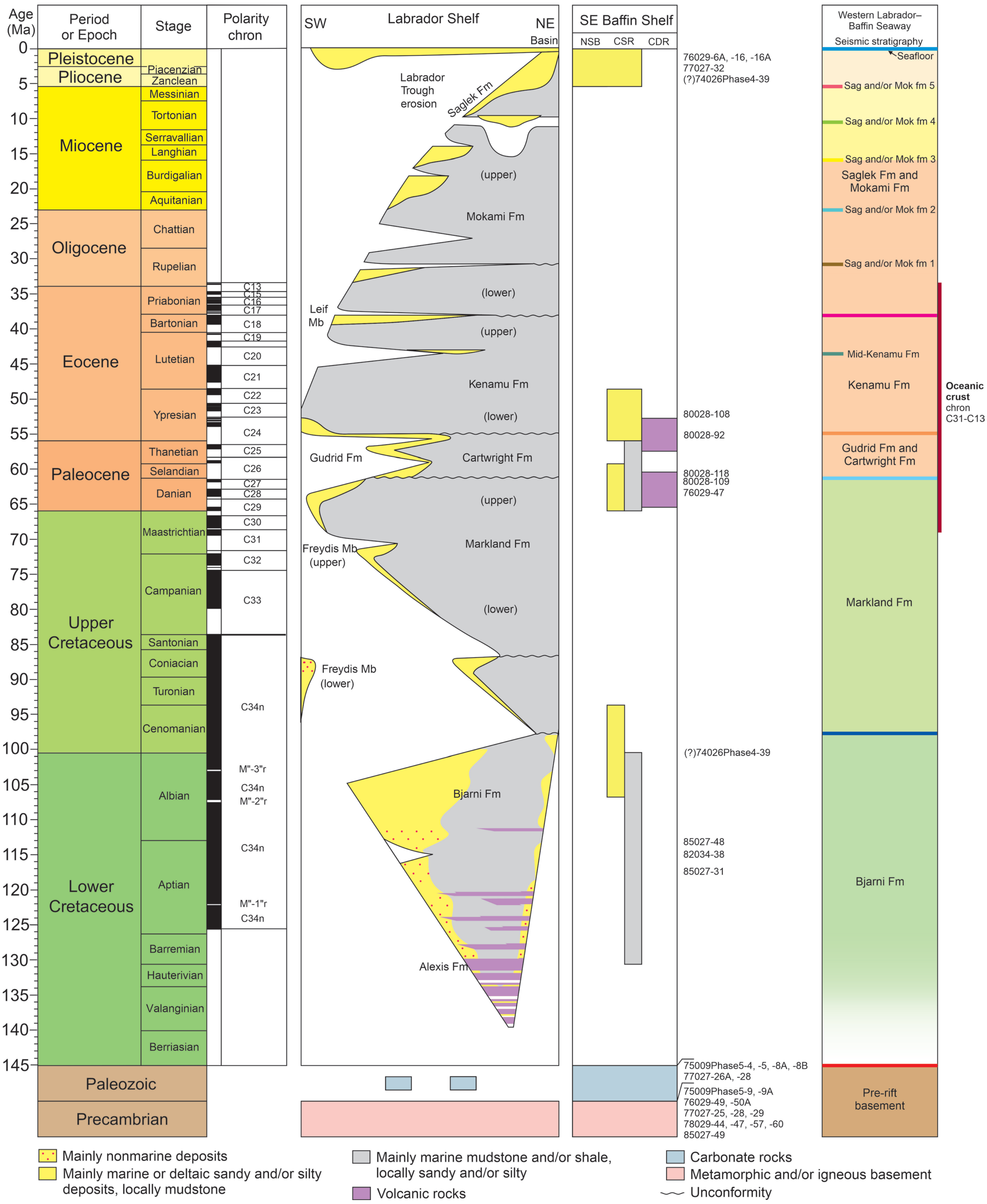

Figure 2. Lithostratigraphic column for the Labrador Shelf modified from Dickie et al. (2011) and Nøhr-Hansen et al. (2016) against the time scale and magnetostratigraphy of Gradstein et al. (2012). This column is applicable to the stratigraphy identified in exploration wells in the northern Saglek Basin. The southeast (SE) Baffin Shelf column includes the northernmost Saglek Basin (NSB), Cumberland Sound region (CSR), and Cape Dyer region (CDR). This column is based on seabed samples of bedrock with lithologies and the most recent age assessments corresponding to references in Table 3. Related station numbers are listed to the right of the column, approximately centred next to the relevant unit shown in the column. The western Labrador–Baffin Seaway seismic stratigraphy is based on the Labrador margin and coloured horizons correspond to those shown in Figure 4. Mok = Mokami, Sag = Saglek.

Table 1. List of industry exploration wells in the western Davis Strait region.

Well	Basin	Latitude (°N) (NAD83)	Longitude (°W) (NAD83)	Water depth (m)	Spud date	Operator	Total depth (TD; m)
Gjoa G-37	Saglek Basin	62.941	59.107	1000.0	7/12/1979	Esso-H.B.	3998.0
Hekja O-71	Saglek Basin	62.181	62.978	350.8	7/17/1979	Aquitaine et al.	4566.0
Ralegh N-18	Saglek Basin	62.299	62.548	339.0	8/1/1982	Canterra et al.	3858.0

Table 2. Formation tops for the western Davis Strait exploration wells.

Gjoa G-37				Hekja O-71				Ralegh N-18		
Moir (1987c)				Moir (1987a)				Moir (1987a)		
Formation	Base (m)	Top (m)		Formation	Base (m)	Top (m)		Formation	Base (m)	Top (m)
(?) Saglek Fm	1455	1026		Saglek Fm	1730	363		Saglek Fm	1515	600
Mokami Fm	1646	1455		Mokami Fm	2175	1730		Mokami Fm	1720	1515
Leif Mb	1728	1650		Leif Mb	2428	2175		Leif Mb	2241	1720
Kenamu Fm	2013	1646		Kenamu Fm	3104	2175		Kenamu Fm	3331	1720
Cartwright Fm	2701	2013		Gudrid tongue	3364	3212		Gudrid tongue	3515	3485
"(Unnamed basalts)"	3794	2701		Cartwright Fm	3545	3104		Cartwright Fm	3833	3331
Markland Fm	3998	3794		"(Unnamed basalts)"	4566	3545		(L Cretaceous basalt)	3858	3833
This study				This study				This study		
Formation	Base (m)	Top (m)		Formation	Base (m)	Top (m)		Formation	Base (m)	Top (m)
Mokami Fm	1588	1455		Saglek Fm	1415	417		Saglek Fm	1515	692
Leif Mb	1728	1588		Leif Mb	1575	1415		Mokami Fm	1720	1515
Kenamu Fm	2013	1588		Kenamu Fm	3212	1415		Leif Mb	2241	1720
Cartwright Fm	2701	2013		Gudrid Fm	3364	3212		Kenamu Fm	3485	1720
Unnamed basalt	3145	2701		Cartwright Fm	3545	3364		Gudrid Fm	3515	3485
Unnamed basalts and Markland Fm	3794	3145		Unnamed basalt	4566	3545		Cartwright Fm	3833	3485
Markland Fm	3998	3794						Unnamed basalt	3858	3833

Data from Moir (1987a, b, c) and this study

L = Late

modern data set consisting of about 5000 line kilometres of high-quality, multichannel data collected by TGS-NOPEC Geophysical Company ASA (TGS) from 2000 to 2002. These lines were shot using a 6 km long streamer and recorded 8 s (twt) of data. More information on these surveys can be found at https://www.tgs.com. In addition, select single-channel seismic surveys were studied near the mouth of Cumberland Sound as described in the text, and more information on these surveys can be found on the Expedition Database. Unless otherwise noted, reference to 'seismic data' includes only the multichannel surveys shown in Figure 1.

PRE-RIFT BASEMENT

In this study, pre-rift basement underlies strata associated with Mesozoic–Cenozoic rifting and is considered to consist of Precambrian rocks that may be locally overlain by Paleozoic sedimentary strata. In seismic interpretation, the pre-rift basement can only be mapped where it occurs at shallower depths or where there is minimal Paleocene–Eocene volcanic cover. Accordingly, much of the acoustic basement in the region includes these volcanic rocks (*see* 'Paleocene–Eocene volcanic rocks' section) and forms the strongest reflection below the seafloor (Skaarup et al., 2006). In this section, however, the focus is on the pre-rift basement (Fig. 3).

Onshore geology

Onshore southeast Baffin Island, Precambrian gneissic rocks are present at the tips of both Hall and Meta Incognita peninsulas, as well as supracrustal rocks of the Lake Harbour Group that form Resolution Island near the mouth of Hudson Strait (Fig. 1; St-Onge et al., 2009). The exposures on Lady Franklin and Monumental islands, offshore Hall Peninsula, are also composed of Precambrian granitic gneiss (Grant, 1975). To the north, Cumberland Peninsula includes Precambrian gneiss units and the Paleoproterozoic Hoare Bay Group of the Rae Craton (St-Onge et al., 2009). The heads of both Cumberland Sound and Frobisher Bay are characterized by the Cumberland Batholith, a continental margin arc formed during subduction following accretion of the Meta Incognita microcontinent to the Rae Craton in the Paleoproterozoic (Fig. 3; St-Onge et al., 2009). The only known onshore occurrence of Paleozoic rocks in this area is Silliman's Fossil Mountain at the head of Frobisher Bay (Miller et al., 1954); however, sedimentary xenoliths within kimberlites from Hall Peninsula provide evidence of Upper Ordovician and Lower Silurian rocks that must have been present on Hall Peninsula at one time, including carbonate rocks and black shale (Fig. 3; Zhang and Pell, 2014; Zhang et al., 2014).

Previous offshore mapping and sampling

In the offshore, pre-rift basement composed of both Precambrian and lower Paleozoic rocks has been mapped and forms a framework for basin development in the region (Fig. 3). Some of the earliest seismic mapping was conducted by Grant (1975). He found Precambrian rocks to have an irregular seabed surface and incoherent seismic character with substantial magnetic anomaly signatures. In contrast, Paleozoic successions were defined by a smooth to blocky surface profile with some seismic penetration showing stratification and a nonmagnetic signature.

The understanding of basement rock types in the western Davis Strait region was significantly enhanced by seabed corehole sampling (Fig. 3, Table 3) with correlation to single-channel seismic surveys completed by the GSC during marine cruises in the 1970s and early 1980s. Offshore Hall Peninsula and just south of the mouth of Cumberland Sound, biotite gneiss cores were recovered from 75009PHASE5 stations 9 and 9A (MacLean and Srivastava, 1976; Jansa 1976; MacLean et al., 1977). Based on station 9A, the gneiss samples are Precambrian (1604 ± 40 Ma and 1611 ± 39 Ma; K-Ar age) similar to those of the nearby Monumental and Lady Franklin islands and southern Baffin Island (Jansa, 1976; MacLean et al., 1977). In the vicinity of these samples, MacLean and Falconer (1977) also described Precambrian drill core 76029-49 comprising quartz-biotite gneiss. Similarly, just south of these localities, a core of garnet-biotite gneiss, recovered east of Monumental Island at 77027-29, resulted in the interpretation of a more extensive platform of Precambrian rocks exposed near the seafloor than previously thought (MacLean, 1978). These samples are part of a Precambrian basement high trending northeast from Loks Land and including the Monumental and Lady Franklin islands.

Bedrock samples have not been recovered from outer Frobisher Bay; however, Grant (1975) mapped a major fault that skirts the southwestern coastline extending northeast of Resolution Island (Fig. 3). The bay is underlain by Precambrian rocks along its northeastern edge with presumed Paleozoic (likely Ordovician) rocks abutting the major normal fault and roughly corresponding to a Bouguer gravity low and associated half-graben (Grant, 1975; MacLean and Falconer, 1979; Jauer et al., 2014; *see* Fig. 5, Keen et al., this volume). The presence of Precambrian basement also extends east of Resolution Island where it was sampled by drill core 76029-50A, composed of light grey, garnetiferous gneiss (MacLean and Falconer, 1977). This gneiss resembles that of the Meta Incognita Peninsula and indicates a Precambrian age, and not the basaltic affinity proposed by Skaarup et al. (2006), for the shallow basement in this region. East of Frobisher Bay, the western edge of the northernmost Saglek Basin is well defined by a Bouguer gravity high where there is contrast between crystalline basement near the seafloor and thick sediments to the west (Jauer et al., 2014; *see* Fig. 5, Keen et al., this volume). Here, the continental margin is defined by a few large normal faults subsequently onlapped by basalt units (Balkwill, 1987).

Grant (1975) mapped Paleozoic rocks within Cumberland Sound, and Hood and Bower (1975) expanded this to include possible Cretaceous sedimentary rocks: shallow drill cores and single-channel seismic interpretation later confirmed that both successions are present (Fig. 3; *see* 'Cretaceous interval' section; MacLean and Williams, 1983; MacLean et al., 1986). Upper Ordovician (Caradoc age) rocks were sampled offshore Hall Peninsula and just south of the mouth of Cumberland Sound, where six limestone drill cores (Fig. 3; Table 3) were collected

Table 3. List of GSC bedrock samples collected during marine cruises including seabed drill cores and bedrock fragments recovered from surficial piston cores.

Expedition	Year	Original station no.	General location	Latitude (°N)	Longitude (°W)	Sample type	Length of bedrock core (cm)	Water depth (m)	Rock type	Description	Age	Paleoenvironment or geological setting	Other analyses
75009PHASE5	1975	9	Cumberland Sound region	63.19	63.10	Rock drill	66	176	Metamorphic (gneiss)	Biotite gneiss (Jansa, 1976; MacLean et al., 1977)			
75009PHASE5	1975	9A	Cumberland Sound region	63.18	63.08	Rock drill	158	176	Metamorphic (gneiss)	Biotite gneiss (Jansa, 1976; MacLean et al., 1977)	1604 ± 40 Ma and 1611 ± 39 Ma (K-Ar age; MacLean et al., 1977)		
76029	1976	49	Cumberland Sound region	63.18	62.77	Rock drill	104	218	Metamorphic (gneiss)	Quartz-biotite-feldspar gneiss (MacLean and Falconer, 1977)			Compressional wave velocity: 5.0–6.1 km/s (average 5.5 km/s; from four samples from stations 49 and 50A; MacLean and Falconer, 1977)
76029	1976	50A	Northern Saglek Basin	61.56	64.38	Rock drill	172	194	Metamorphic (gneiss)	Light grey, garnetiferous gneiss (MacLean and Falconer, 1977)			Compressional wave velocity: 5.0–6.1 km/s (average 5.5 km/s; from four samples from stations 49 and 50A; MacLean and Falconer, 1977)
77027	1977	25	Cumberland Sound region	64.02	63.93	Rock drill	370	197	Metamorphic (gneiss)	Biotite gneiss (MacLean, 1978)			
77027	1977	29	Cumberland Sound region	62.97	63.01	Rock drill	108	182	Metamorphic (gneiss)	Garnet-biotite gneiss (MacLean, 1978)			
78029	1978	44	Cape Dyer region	66.39	61.11	Rock drill	76	164	Metamorphic	Metamorphic rock (MacLean and Falconer, 1979)			
78029	1978	47	Cape Dyer region	66.40	61.11	Rock drill	72	166.4	Metamorphic	Metamorphic rock (MacLean and Falconer, 1979)			
78029	1978	57	Cape Dyer region	65.45	63.12	Rock drill	232	195.7	Metamorphic	Metamorphic rock (MacLean and Falconer, 1979)			
78029	1978	60	Cape Dyer region	65.43	62.72	Rock drill	144	124.4	Metamorphic	Metamorphic rock (MacLean and Falconer, 1979)			
85027	1985	49	Cumberland Sound region	65.03	65.55	Rock drill	37	220	Metamorphic (gneiss)	Hornblende-pyroxene gneiss (MacLean et al., 1986)			
75009PHASE5	1975	4	Cumberland Sound region	62.97	63.43	Rock drill	137	157	Limestone	Mottled, olive-grey, dolomitic limestone with bioturbation, peloids, flat-pebble breccia, and skeletal breccia (Jansa, 1976; MacLean et al., 1977; Bingham-Koslowski, 2018)	Ordovician (MacLean et al., 1977)	Intertidal to shallow subtidal with storm deposits (Jansa, 1976; MacLean et al., 1977); shallow water (Bingham-Koslowski, 2018)	TOC: 0.61% (Zhang, 2013)
75009PHASE5	1975	5	Cumberland Sound region	63.27	63.91	Rock drill	54	358	Limestone	Massive, yellow-brown, skeletal wackestone to packstone, bioturbated with minor dolomite and diverse fossil types (Jansa, 1976; MacLean et al., 1977; Bingham-Koslowski, 2018)	Ordovician (Caradoc; MacLean et al., 1977)	Open-marine, low-energy, deeper intralittoral setting (Jansa, 1976; MacLean et al., 1977); photic zone (Bingham-Koslowski, 2018)	TOC: 0.38% (Zhang, 2013)

See references in text; *modified from* Dafoe and Williams (2020a).
Samples are organized by rock types separated by bold black lines (and then by expedition number and original station number) in the following order: metamorphic basement rock, limestone basement rock, basalt rock units, and sedimentary rock units.
Total organic carbon (TOC) and vitrinite reflectance (Ro) values are shown, with some averaged from multiple samples (Zhang, 2013).
Velocity measurements include those from eight samples from stations 76029-21 and 76029-47 and also four from 76029-49 and 76029-50A that are also reported together (MacLean and Falconer, 1977).

Table 3. (cont.) List of GSC bedrock samples collected during marine cruises including seabed drill cores and bedrock fragments recovered from surficial piston cores.

Expedition	Year	Original station no.	General location	Latitude (°N)	Longitude (°W)	Sample type	Length of bedrock core (cm)	Water depth (m)	Rock type	Description	Age	Paleoenvironment or geological setting	Other analyses
75009PHASE5	1975	8A	Cumberland Sound region	63.22	63.46	Rock drill	45	165	Limestone	Yellow-brown, radiolaria-bearing, bituminous, micritic limestone with pervasive dolomitization and some fossil fragments and bioturbation (Jansa, 1976; Bingham-Koslowski, 2018)	Ordovician (Caradoc; MacLean et al., 1977)	Low-energy setting with poor oxygenation such as the outer shelf to epibathyal (Jansa, 1976; MacLean et al., 1977); deeper water (Bingham-Koslowski, 2018)	TOC: 2.685% (Zhang, 2013)
75009PHASE5	1975	8B	Cumberland Sound region	63.22	63.46	Rock drill	83	165	Limestone	Yellow-brown, radiolaria-bearing, bituminous, micritic limestone with pervasive dolomitization and some fossil fragments and mottling (Jansa, 1976; Bingham-Koslowski, 2018)	Ordovician (Caradoc; MacLean et al., 1977)	Low-energy setting with poor oxygenation such as the outer shelf to epibathyal (Jansa, 1976; MacLean et al., 1977); deeper water (Bingham-Koslowski, 2018)	TOC: 0.915% (Zhang, 2013)
77027	1977	26A	Cumberland Sound region	63.66	63.63	Rock drill	83	373	Limestone	Grey limestone with fine-grained calcite crystals, stylolites and some radiolarians (MacLean, 1978; Bingham-Koslowski, 2018)	Possibly middle–late Ordovician based on similarities to previously cored material (MacLean, 1978)	Deeper water (Bingham-Koslowski, 2018)	TOC: 0.1% (Zhang, 2013)
77027	1977	28	Cumberland Sound region	63.198	63.014	Rock drill	100	179	Limestone	Dark brown, micritic limestone with radiolaria casts and finely disseminated organic material, bioturbation, and fossil fragments (MacLean, 1978; Bingham-Koslowski, 2018)	Possibly middle–late Ordovician based on similarities to previously cored material (MacLean, 1978)	Deeper water (Bingham-Koslowski, 2018)	
76029	1976	21	Offshore Cape Dyer	65.92	60.31	Rock drill	13	408	Amygdaloidal basalt	Reddish-brown, highly amygdaloidal to aphanitic basalt, with vesicles infilled with zeolite minerals, and some oxidation, but not overly weathered (MacLean and Falconer, 1977; MacLean et al., 1978; Dafoe and Williams, 2020a)		Possibly from near the top of the flow (MacLean et al., 1978); near the top of a basalt flow (Dafoe and Williams, 2020a)	
76029	1976	22	Offshore Cape Dyer	65.90	60.34	Rock drill	37	404	Aphanitic to amygdaloidal basalt	Dark grey, aphanitic to amygdaloidal basalt, with small zeolite mineral–filled vesicles (MacLean and Falconer, 1977; Dafoe and Williams, 2020a)		From a flow (MacLean et al., 1978); from at depth within a basalt flow (Dafoe and Williams, 2020a)	Compressional wave velocity: 5.2–6.0 km/s (average 5.6 km/s; from eight samples from stations 22 and 47; MacLean and Falconer, 1977); 5.3 km/s (MacLean et al., 1978)

See references in text; *modified from* Dafoe and Williams (2020a).
Samples are organized by rock types separated by bold black lines (and then by expedition number and original station number) in the following order: metamorphic basement rock, limestone basement rock, basalt rock units, and sedimentary rock units.
Total organic carbon (TOC) and vitrinite reflectance (Ro) values are shown, with some averaged from multiple samples (Zhang, 2013).
Velocity measurements include those from eight samples from stations 76029-21 and 76029-47 and also four from 76029-49 and 76029-50A that are also reported together (MacLean and Falconer, 1977).

Table 3. (cont.) List of GSC bedrock samples collected during marine cruises including seabed drill cores and bedrock fragments recovered from surficial piston cores.

Expedition	Year	Original station no.	General location	Latitude (°N)	Longitude (°W)	Sample type	Length of bedrock core (cm)	Water depth (m)	Rock type	Description	Age	Paleoenvironment or geological setting	Other analyses
76029	1976	47	Offshore Cape Dyer	66.38	60.84	Rock drill	37	391	Aphanitic and vesicular basalt	Dark grey, aphanitic to vesicular basalt, with large vesicles, small black phenocrysts, and a coarser grained and less altered texture as compared to 76029-21 and -22 (MacLean and Falconer, 1977; MacLean et al., 1978; Dafoe and Williams, 2020a)	Late Cretaceous to early Tertiary (report to MacLean and Falconer (1977) on whole rock basalt using K-Ar age); 62.9 ± 2.5 Ma (Danian; Ar-Ar age on whole rock basalt; Williamson et al., 2000).	From near the top of a basalt flow (Dafoe and Williams, 2020a)	Compressional wave velocity: 5.2–6.0 km/s (average 5.6 km/s; MacLean and Falconer, 1977) and 5.4 km/s (MacLean et al., 1978)
77027	1977	21	Offshore Cumberland Peninsula	65.57	59.04	Rock drill	12	452	Aphanitic basalt	Grey, aphanitic basalt, possibly bedrock (MacLean, 1977; Dafoe and Williams, 2020a)		From at depth within a basalt flow (Dafoe and Williams, 2020a)	
77027	1977	21B	Offshore Cumberland Peninsula	65.57	59.03	Rock drill	12.5	457	Aphanitic and porphyritic basalt	Dark grey, aphanitic to porphyritic basalt, with small black to brown phenocrysts (MacLean, 1978; Dafoe and Williams, 2020a)		From at depth within a basalt flow (Dafoe and Williams, 2020a)	
80028	1980	88	Central Davis Strait	66.48	57.86	Rock drill	43	555	Aphanitic basalt	Grey, aphanitic and locally amygdaloidal to porphyritic basalt, with small black phenocrysts and white zeolite mineral infills in larger vesicles (MacLean, 1980; Dafoe and Williams, 2020a)		From at depth within a basalt flow (Dafoe and Williams, 2020a)	
80028	1980	89	Central Davis Strait	66.48	57.86	Rock drill	27	560	Aphanitic and amygdaloidal basalt	Aphanitic to amygdaloidal, dark grey basalt, with white mineral infills in vesicles (MacLean, 1980; Dafoe and Williams, 2020a)		From near the top of a basalt flow (Dafoe and Williams, 2020a)	
80028	1980	91	Central Davis Strait	66.76	57.77	Rock drill	7.50	660	Amygdaloidal to vesicular basalt	Dark grey, amygdaloidal to vesicular basalt with possible stilbite mineral infills in vesicles (MacLean, 1980; Dafoe and Williams, 2020a)		From near the top of a basalt flow (Dafoe and Williams, 2020a)	
80028	1980	92	Central Davis Strait	66.75	57.77	Rock drill	16	648	Aphanitic to brecciated basalt	Dark grey, aphanitic to brecciated basalt, with rimmed clasts, basaltic fragments, and red mineral crystals (MacLean, 1980; Williamson et al., 2000; Dafoe and Williams, 2020a)	55.1 ± 2.3 Ma (Ypresian; Ar-Ar age on whole-rock basalt; Williamson et al., 2000)	Possible subaqueous setting (Dafoe and Williams, 2020a)	

See references in text; *modified from* Dafoe and Williams (2020a).
Samples are organized by rock types separated by bold black lines (and then by expedition number and original station number) in the following order: metamorphic basement rock, limestone basement rock, basalt rock units, and sedimentary rock units.
Total organic carbon (TOC) and vitrinite reflectance (Ro) values are shown, with some averaged from multiple samples (Zhang, 2013).
Velocity measurements include those from eight samples from stations 76029-21 and 76029-47 and also four from 76029-49 and 76029-50A that are also reported together (MacLean and Falconer, 1977).

Table 3. (cont.) List of GSC bedrock samples collected during marine cruises including seabed drill cores and bedrock fragments recovered from surficial piston cores.

Expedition	Year	Original station no.	General location	Latitude (°N)	Longitude (°W)	Sample type	Length of bedrock core (cm)	Water depth (m)	Rock type	Description	Age	Paleoenvironment or geological setting	Other analyses
80028	1980	93	Central Davis Strait	66.50	57.49	Rock drill	21	530	Aphanitic basalt	Aphanitic basalt (MacLean, 1980; Dafoe and Williams, 2020a)		Possibly from at depth within a basalt flow (Dafoe and Williams, 2020a)	
80028	1980	94	Central Davis Strait	66.50	57.49	Rock drill	17	530	Aphanitic to vesicular basalt	Dark grey, aphanitic basalt, with rare amygdales (MacLean, 1980; Dafoe and Williams, 2020a)		From near the top of a basalt flow (Dafoe and Williams, 2020a)	
80028	1980	98	Offshore Cumberland Peninsula	65.56	59.15	Rock drill	5	452	Aphanitic basalt	Rubbly, green to black, aphanitic basalt, possibly forming bedrock core (MacLean, 1980; Dafoe and Williams, 2020a)		From at depth within a basalt flow (Dafoe and Williams, 2020a)	
80028	1980	99	Offshore Cumberland Peninsula	65.56	59.15	Rock drill	17	455	Aphanitic basalt	Aphanitic, dark grey basalt with no evidence of weathering (MacLean, 1980; Dafoe and Williams, 2020a)		From at depth within a basalt flow (Dafoe and Williams, 2020a)	
80028	1980	100	Offshore Cumberland Peninsula	65.56	59.14	Rock drill	16	455	Aphanitic basalt	Medium grey, aphanitic basalt that is plagioclase-rich (MacLean, 1980; Dafoe and Williams, 2020a)		From at depth within a basalt flow (Dafoe and Williams, 2020a)	
80028	1980	106	Cumberland Sound region	64.58	60.40	Rock drill	18	367	Aphanitic basalt	Medium grey, aphanitic basalt, with some white minerals infilling fractures (MacLean, 1980; MacLean et al., 1982; Dafoe and Williams, 2020a)		From at depth within a basalt flow (Dafoe and Williams, 2020a)	
80028	1980	107	Cumberland Sound region	64.59	60.39	Rock drill	13	367	Amygdaloidal basalt	Dark grey, amygdaloidal basalt, with white to pink zeolite mineral infills and some calcite (MacLean, 1980; MacLean et al., 1982; Dafoe and Williams, 2020a)		From at depth within a basalt flow (Dafoe and Williams, 2020a)	
82034	1982	21	Central Davis Strait	66.51	57.88	Rock drill	14	569	Aphanitic basalt	Dark grey, aphanitic basalt bedrock, with rare amygdales (MacLean and Williams, 1983; Dafoe and Williams, 2020a)		From at depth within a basalt flow (Dafoe and Williams, 2020a)	
74026PHASE4	1974	39	Cumberland Sound region	64.27	61.94	Rock drill	18	287	Sandstone	Well consolidated sandstone (Srivastava, 1974; MacLean et al., 2014)	Late Albian–Cenomanian (Williams, pers. comm., *in* MacLean et al., 1977; unpublished data by Williams, reported *in* MacLean et al., 2014)		

See references in text; *modified from* Dafoe and Williams (2020a).
Samples are organized by rock types separated by bold black lines (and then by expedition number and original station number) in the following order: metamorphic basement rock, limestone basement rock, basalt rock units, and sedimentary rock units.
Total organic carbon (TOC) and vitrinite reflectance (Ro) values are shown, with some averaged from multiple samples (Zhang, 2013).
Velocity measurements include those from eight samples from stations 76029-21 and 76029-47 and also four from 76029-49 and 76029-50A that are also reported together (MacLean and Falconer, 1977).

Table 3. (cont.) List of GSC bedrock samples collected during marine cruises including seabed drill cores and bedrock fragments recovered from surficial piston cores.

Expedition	Year	Original station no.	General location	Latitude (°N)	Longitude (°W)	Sample type	Length of bedrock core (cm)	Water depth (m)	Rock type	Description	Age	Paleoenvironment or geological setting	Other analyses
76029	1976	6A	Northern Saglek Basin	62.31	62.19	Rock drill	53	385	Siltstone	Light brown-grey, semiconsolidated, poorly sorted, sandy siltstone, with calcareous mudstone, forams, and plant fragments, as well as massive bedding and very coarse sand grains and small pebbles (MacLean and Falconer, 1977; Dafoe and Williams, 2020a)	Pliocene to Recent with reworked Cretaceous and Paleozoic palynomorphs (F.M. Gradstein and G.L. Williams, pers. comm. *in* MacLean and Falconer, 1977)	Brackish, shallow marine (F.M. Gradstein, pers. comm. *in* MacLean and Falconer, 1977); distal marine, possibly shelfal with ice-rafting (Dafoe and Williams, 2020a)	
76029	1976	16	Cumberland Sound region	64.33	62.04	Rock drill	44	283	Siltstone	Medium brown-grey, semiconsolidated, poorly sorted, sandy siltstone, with calcareous mudstone, forams, massive bedding, and very coarse sand, granules, and small pebbles (MacLean and Falconer, 1977; Dafoe and Williams, 2020a)	Pliocene to Recent with reworked Aptian–Cenomanian, Senonian–Early Paleocene and Eocene palynomorphs (F.M. Gradstein and G.L. Williams, pers. comm. *in* MacLean and Falconer, 1977)	Shallow, open shelf (F.M. Gradstein, pers. comm. *in* MacLean and Falconer, 1977); distal marine, possibly shelfal with ice-rafting (Dafoe and Williams, 2020a)	
76029	1976	16A	Cumberland Sound region	64.33	62.01	Rock drill	33	285	Siltstone	Medium brown-grey, semiconsolidated, poorly sorted, sandy siltstone, with calcareous mudstone, forams, and subangular to subrounded pebbles and granules (MacLean and Falconer, 1977; Dafoe and Williams, 2020a)	Pliocene to Recent with reworked Aptian–Cenomanian, Senonian–Early Paleocene and Eocene palynomorphs (F.M. Gradstein and G.L. Williams, pers. comm. *in* MacLean and Falconer, 1977)	Shallow, open shelf (F.M. Gradstein, pers. comm. *in* MacLean and Falconer, 1977); distal marine, possibly shelfal with ice-rafting (Dafoe and Williams, 2020a)	
77027	1977	27	Cumberland Sound region	63.59	63.79	Rock drill	15	219	Siltstone	Fine-grained, sandy, light grey-buff siltstone that is semiconsolidated, with pebbles and granules throughout, and rare shell fragments (MacLean, 1978; Dafoe and Williams, 2020)	Likely similar to 76029-16 and -16A (Dafoe and Williams, 2020a)	Distal marine, possibly shelfal with ice-rafting (Dafoe and Williams, 2020a)	
77027	1977	32	Northern Saglek Basin	61.96	63.47	Piston core (cutter)	162	475	Sandstone	Semiconsolidated sandstone with scattered granules and pebbles, as well as forams (MacLean, 1978; Dafoe and Williams, 2020a)	Pliocene–Quaternary (F.M. Gradstein pers. comm., *in* MacLean, 1978)	Open marine (Gradstein, pers. comm. *in* MacLean, 1978); marine (Dafoe and Williams, 2020a)	
80028	1980	108	Cumberland Sound region	64.59	60.61	Rock drill	18	375	Sandstone	Moderately consolidated, muddy, dark-brown, very fine-grained sandstone, with loading structures, planar laminations, deformation and/or mottling, and marine trace fossils (MacLean, 1980; MacLean et al., 1982; Dafoe and Williams, 2020a)	Early Eocene (G.L. Williams, pers. comm. *in* MacLean et al., 1982)	Marine, based on the presence of dinocysts (G.L. Williams, pers. comm. *in* MacLean et al., 1982); distal inner shelf (Dafoe and Williams, 2020a)	TOC: 1.84% (Zhang, 2013)

See references in text; *modified from* Dafoe and Williams (2020a).
Samples are organized by rock types separated by bold black lines (and then by expedition number and original station number) in the following order: metamorphic basement rock, limestone basement rock, basalt rock units, and sedimentary rock units.
Total organic carbon (TOC) and vitrinite reflectance (Ro) values are shown, with some averaged from multiple samples (Zhang, 2013).
Velocity measurements include those from eight samples from stations 76029-21 and 76029-47 and also four from 76029-49 and 76029-50A that are also reported together (MacLean and Falconer, 1977).

Table 3. (cont.) List of GSC bedrock samples collected during marine cruises including seabed drill cores and bedrock fragments recovered from surficial piston cores.

Expedition	Year	Original station no.	General location	Latitude (°N)	Longitude (°W)	Sample type	Length of bedrock core (cm)	Water depth (m)	Rock type	Description	Age	Paleoenvironment or geological setting	Other analyses
80028	1980	109	Cumberland Sound region	64.59	60.61	Rock drill	29	375	Sandstone	Medium brown, silty, very fine-grained sandstone with organic detritus, coarse sand grains, local bioturbation (marine trace fossils), and extensive convoluted bedding (MacLean, 1980; MacLean et al., 1982; Dafoe and Williams, 2020a)	Early Eocene (G.L. Williams, pers. comm. *in* MacLean et al., 1982); Danian–Selandian with reworked Lower Cretaceous spores and Upper Cretaceous dinocysts (MacLean et al., 2014)	Inner neritic (MacLean et al., 2014); delta front (Dafoe and Williams, 2020a)	TOC: 1.38% (Zhang, 2013)
80028	1980	118	Cumberland Sound region	64.28	61.93	Rock drill	65	296	Mudstone	Grey to brown, silty mudstone that is poorly lithified, mottled, with an apparent chaotic appearance, a strong, petroliferous odour in which bubbles emanated from the core upon recovery, very fine-grained sandstone laminae, convoluted bedding, and microfaults (MacLean, 1980; MacLean and Srivastava, 1981; MacLean et al., 1982; Dafoe and Williams, 2020a)	Late Paleocene to Early Eocene (G.L. Williams, pers. comm. *in* MacLean et al., 1982); Paleocene (G.L. Williams, unpub. data in MacLean et al., 2014)	Prodelta (Dafoe and Williams, 2020a)	
82034	1982	38	Cumberland Sound region	64.82	64.58	Rock drill	6	724	Mudstone	Dark grey, semiconsolidated mudstone to dark-grey to black shale, with terrestrially sourced organic matter and micaceous minerals (MacLean and Williams, 1983; MacLean et al., 2014; Dafoe and Williams, 2020a)	Aptian–Cenomanian (MacLean and Williams, 1983); Early Cretaceous, but could be reworked (MacLean et al., 2014)	Quiet-water setting (Dafoe and Williams, 2020a)	TOC: 6.44%; Ro: 0.5% (Zhang, 2013)
85027	1985	31	Cumberland Sound region	65.39	65.51	Piston core	Bedrock fragments in sediment	896	Shale	Friable dark grey shale, mudstone and siltstone with coal fragments (MacLean et al., 1986, 2014; Dafoe and Williams, 2020a)	Age similar to 85027-48 (MacLean et al., 1986); Early Cretaceous possibly Barremian–Albian with possible Aptian to middle Albian age (MacLean et al., 2014)	Nonmarine, possible proximity to a shoreline or marginal marine (MacLean et al., 1986, 2014); quiet-water setting, possibly floodplain or lagoonal (Dafoe and Williams, 2020a)	
85027	1985	48	Cumberland Sound region	65.06	65.21	Rock drill	9	890	Mudstone	Dark grey, semiconsolidated mudstone to dark-grey to black shale (MacLean et al., 1986, 2014; Dafoe and Williams, 2020a)	Barremian–Aptian (MacLean et al., 1986); Aptian–Albian (MacLean et al., 2014)	Nonmarine, possible proximity to a shoreline (MacLean et al., 2014); quiet-water setting, possibly floodplain or lagoonal (Dafoe and Williams, 2020a)	TOC: 5.24%; Ro: 0.42% (Zhang, 2013)

See references in text; *modified from* Dafoe and Williams (2020a).
Samples are organized by rock types separated by bold black lines (and then by expedition number and original station number) in the following order: metamorphic basement rock, limestone basement rock, basalt rock units, and sedimentary rock units.
Total organic carbon (TOC) and vitrinite reflectance (Ro) values are shown, with some averaged from multiple samples (Zhang, 2013).
Velocity measurements include those from eight samples from stations 76029-21 and 76029-47 and also four from 76029-49 and 76029-50A that are also reported together (MacLean and Falconer, 1977).

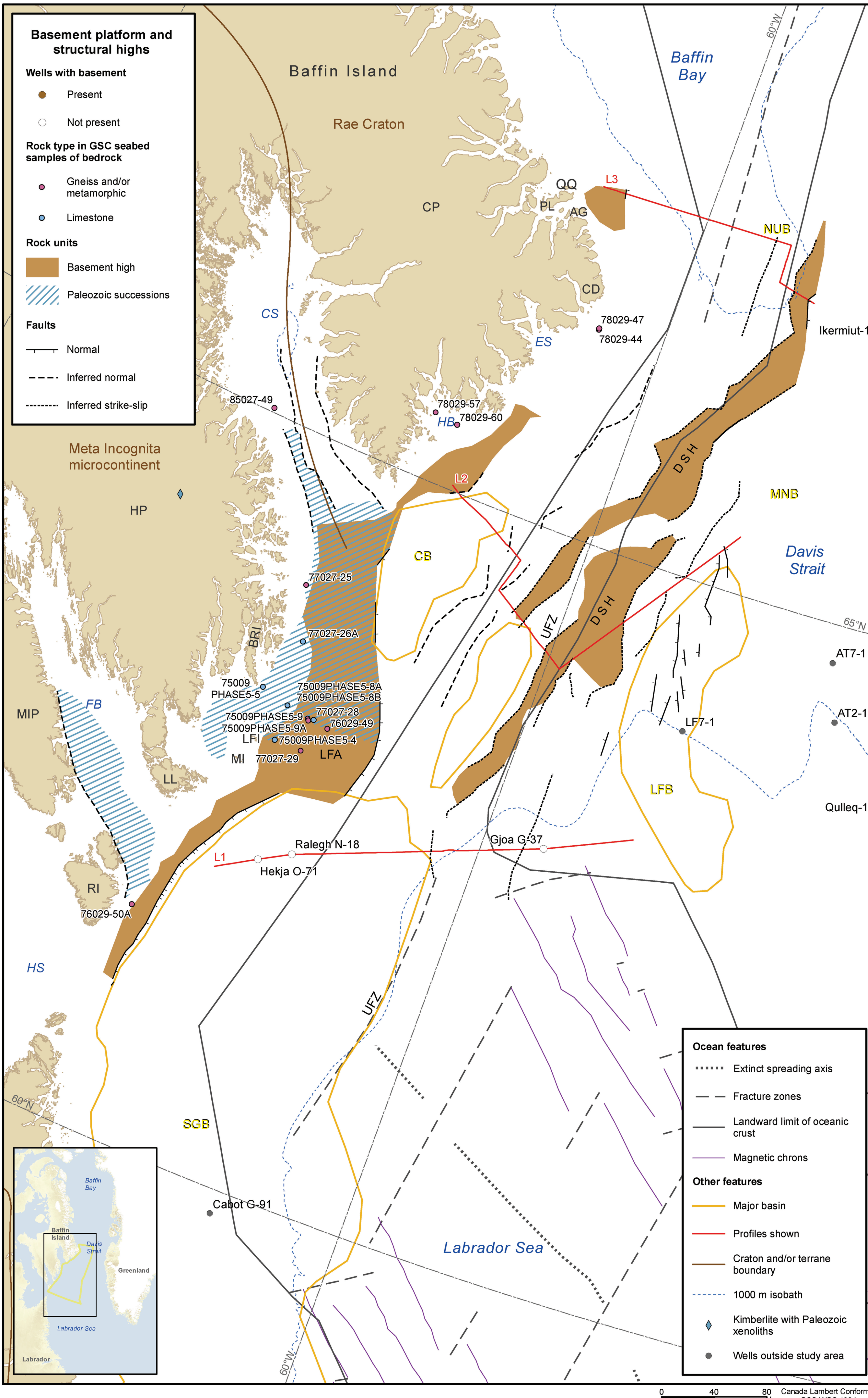
Basement platform and structural highs
Wells with basement
Present
Not present
Rock type in GSC seabed samples of bedrock
Gneiss and/or metamorphic
Limestone
Rock units
Basement high
Paleozoic successions
Faults
Normal
Inferred normal
Inferred strike-slip
Baffin Island
Rae Craton
Baffin Bay
QQ
L3
PL
AG
CP
NUB
CD
CS
78029-47
78029-44
ES
Ikermiut-1
85027-49
78029-57
HB
78029-60
Meta Incognita microcontinent
DSH
L2
MNB
HP
CB
Davis Strait
77027-25
65°N
UFZ
DSH
BRI
77027-26A
AT7-1
75009 PHASE5-5
75009PHASE5-8A
75009PHASE5-8B
MIP
FB
75009PHASE5-9
77027-28
AT2-1
75009PHASE5-9A
76029-49
LF7-1
LFI
75009PHASE5-4
MI
77027-29
LFA
LL
LFB
Qulleq-1
Ralegh N-18
Gjoa G-37
L1
Hekja O-71
RI
76029-50A
HS
UFZ
60°N
SGB
Cabot G-91
Labrador Sea
60°W
Baffin Bay
Baffin Island
Davis Strait
Greenland
Labrador Sea
Labrador
Ocean features
Extinct spreading axis
Fracture zones
Landward limit of oceanic crust
Magnetic chrons
Other features
Major basin
Profiles shown
Craton and/or terrane boundary
1000 m isobath
Kimberlite with Paleozoic xenoliths
Wells outside study area
0
40
80
km
1:2 750 000
Canada Lambert Conformal
GCS WGS 1984

Figure 3. Distribution map of the pre-rift basement platform and major basement highs in brown. The distribution of lower Paleozoic successions along this platform (in blue pattern) is *modified from* Grant (1975), MacLean (1978), and MacLean et al. (1977, 1982, 1986), where multichannel seismic data provide improved resolution of the subsurface (*see* text). The locations of relevant drill core samples (Precambrian and Paleozoic) are shown. Faults are described further in Keen et al. (this volume). Basin outlines are from Keen et al. (this volume). The kimberlite location with Paleozoic xenoliths is from Zhang et al. (2014). Faults in Frobisher Bay and Cumberland Sound are *modified from* MacLean and Falconer (1979) and MacLean et al. (1986), respectively. Major Precambrian boundaries are *modified from* St-Onge et al. (2009) in this figure and subsequent maps. *See* Figure 1b for abbreviated names. Additional projection information: Central Meridian: 60°W; Standard Parallels: 65, 75°W; Latitude of Origin: 65°N.

during marine cruises 75009PHASE5 (stations 4, 5, 8A, and 8B; Jansa, 1976; MacLean and Srivastava, 1976; MacLean et al., 1977) and 77027 (stations 26A and 28; MacLean, 1978). These limestone units are olive-grey to yellow brown or brown, micritic to fossil-bearing with varying degrees of dolomitization (Jansa, 1976, MacLean, 1978; Bingham-Koslowski, 2018; *see also* Bingham-Koslowski, Zhang, and McCartney, this volume). MacLean et al. (1977) determined an age of Late Ordovician (Caradoc) for some of the drill cores based on the presence of chitinozoa, scolecodonts, and corals, and measured a high velocity for these rocks (5.1–6.5 km/s). In single-channel seismic data, the strata appear folded and faulted and are dipping at 9° to 24° in various orientations (MacLean et al., 1977).

MacLean and Falconer (1979) considered the Ordovician rocks near Brevoort Island to be in fault contact with Precambrian basement, but the fault is not seen in seismic data likely due to poor seismic coverage near the shoreline. This boundary is constrained, however, by the recovery of biotite gneiss at 77027-25 from the southwestern end of Cumberland Sound (Fig. 3; MacLean, 1978). MacLean et al. (1977) further suggested an embayment of Ordovician rocks west of Lady Franklin and Monumental islands based on single-channel seismic data (Fig. 3). Two small structural depressions thought to contain Ordovician rocks south of 75009PHASE5-4 were based on seismic and magnetic interpretations (MacLean, 1978), and may suggest that Paleozoic rocks were once more extensive across the region, but are now preserved as erosional remnants. This interpretation is consistent with the presence of Paleozoic rocks found onshore as xenoliths within kimberlites (Zhang and Pell, 2014; Zhang et al., 2014). Within Cumberland Sound, MacLean et al. (1986) refined the geology based on sampling and single-channel seismic surveys and found that the inner portion of the sound is underlain by Precambrian rocks. Here, the seabed morphology is highly irregular, and the rocks comprise hornblende-pyroxene gneiss (85027-49; MacLean et al., 1986). Based on seismic character, the outer part of the sound is underlain by Ordovician carbonate rocks forming a 10 to 15 km wide band that extends about 70 km northwestward into the sound. The Ordovician carbonate rocks, which are in fault contact with Cretaceous rocks (*see* 'Cretaceous interval' section; MacLean et al., 1986, 2014), are unconformably overlain by younger strata to the east and north (MacLean et al., 1977).

Grant (1975) mapped Paleozoic rocks farther northward along the coast offshore Cumberland Peninsula. Although there are no samples of Paleozoic rocks collected from the Hoare Bay area, MacLean and Falconer (1979) collected metamorphic rocks at 78029-57 and -60 (Fig. 3; Table 3). These samples correlate with a smooth magnetic anomaly signature (*see* Fig. 6, Keen et al., this volume) and step-like faulting in Precambrian basement (MacLean and Falconer, 1979). Subsequently, using single-channel seismic data, MacLean et al. (1982) mapped a narrow zone of Paleozoic strata lying about 10 to 25 km outboard of Precambrian rocks exposed near the seafloor along the southern edge of Cumberland Peninsula. Carbonate float samples collected from Exeter Sound (Kranck, 1966) support this interpretation; however, this narrow zone does not correspond well with the negative free-air or Bouguer gravity anomalies (*see* Fig. 4, 5, Keen et al., this volume) previously suggested to mark areas with thick Paleozoic strata both here and seaward of the mouth of Cumberland Sound (MacLean et al., 1982; Skaarup et al., 2006; Jauer et al., 2014, 2019). Outboard of Cumberland Sound, there is some overlap of the known distribution of Paleozoic strata with the gravity anomalies, but the correlation is not definitive.

Farther north off Exeter Sound and south of Cape Dyer, metamorphic rocks were collected at 78029-44 and -47 (Fig. 3; Table 3) allowing for delineation of a boundary between Precambrian basement to the west (MacLean and Falconer, 1979) and basalt units to the east (*see* 'Paleocene–Eocene volcanic rocks' section). These authors further noted a change in the magnetic anomaly signature, which is highly positive to the east where the basalt units lie, compared to the more negative anomalies at 78029-44 and -47 (*see* Fig. 6, Keen et al., this volume). MacLean et al. (1982) further suggested that a continuation of the gravity low below the basalt units near Cape Dyer could indicate thin basalt flows overlying older sedimentary rocks, but this has not been confirmed. Farther east on the Davis Strait High, dredge sampling revealed a significant portion of marine carbonate rocks of a possible inverted Paleozoic (Upper Ordovician) platform succession, as well as sandstone, and Precambrian crystalline and igneous rocks (Dalhoff et al., 2006). Refraction studies in the region indicate that the Davis Strait High represents thick Precambrian basement (Suckro et al., 2013). Archean crystalline basement and Upper Ordovician–Lower Silurian carbonate rocks were also interpreted from the south-central West Greenland margin (Dalhoff et al., 2006). Basement rock was also sampled by the LF7-1 well in the Lady Franklin Basin just east of the international boundary and comprises metamorphic rocks consistent with pre-rift basement (Gregersen et al., 2018).

Distribution and seismic reflection character

Unlike the rifted margins of Baffin Bay to the north and the Labrador Sea to the south, pre-rift basement in the western Davis Strait is rugged, and locally shallow (Fig. 3, 4). Both Precambrian and Paleozoic rocks form the basement platform along the western edge of the study region and are in fault contact with younger sedimentary strata to the east (Fig. 3). Offshore Meta Incognita Peninsula and southern Hall Peninsula, Precambrian basement is abruptly faulted, forming a narrow basement platform that likely extends landward of the seismic data. To the north of this, the Lady Franklin Arch forms a major basement platform. Based on the previous sampling and mapping described above, this feature includes Precambrian basement rocks, as well as Paleozoic successions that can be seen as locally folded and faulted where seismic data quality is fair. Farther north, the basement platform swings toward the mouth of Cumberland Sound where Paleozoic rock stretches across the mouth of the sound. Northward of the mouth of Cumberland Sound, the seismic data generally do not extend far enough landward to capture the basin-bounding fault (Fig. 1, 3). Here, the edge of the basement platform is modified from the mapping of MacLean et al. (1982), where the present study shows a much narrower zone near the southern tip of Cumberland Peninsula where the Cumberland Basin is widest (Fig. 3).

Figure 4. Seismic lines crossing the western Davis Strait region (*see* Fig. 1 for profile locations). **a)** Line 1 through the southern portion of the western Davis Strait region intersecting all three of the exploration wells in the northern part of the Saglek Basin and near the Gjoa High. Pre-rift basement is locally seen in seismic data, but is primarily defined by refraction seismic from Funck et al. (2007). Seismic data courtesy of TGS. **b)** Line 2 extends through the central portion of the western Davis Strait region. Rugged basement includes pre-rift basement, basalt units, and oceanic crust (*see* Keen et al., this volume). In the Cumberland Basin area, lower seismic resolution and a lack of samples does not permit detailed mapping. Equivalent horizons to the Labrador margin are shown in the Canadian portion of the Lady Franklin Basin. Seismic data courtesy of TGS, Suncor, and Canada Cities Services. **c)** Line 3 is a seismic profile through the northern portion of the western Davis Strait region. The margin is abruptly faulted with extensive basalt cover forming prominent SDR. Cretaceous stratigraphic units are just visible at the eastern end of the line. Seismic data courtesy of TGS. The GSC marine sample locations are shown and listed in the sample legend. A legend of the horizons is shown and associated coloured intervals indicate the key units and their relationship to the distribution maps shown in other figures. Cret = Cretaceous; DF[1] = seismic data from Suncor[1]; DSH = Davis Strait High; Eq = equivalent horizons to the Labrador margin stratigraphy; proj. = projected; SDR = seaward-dipping reflectors.

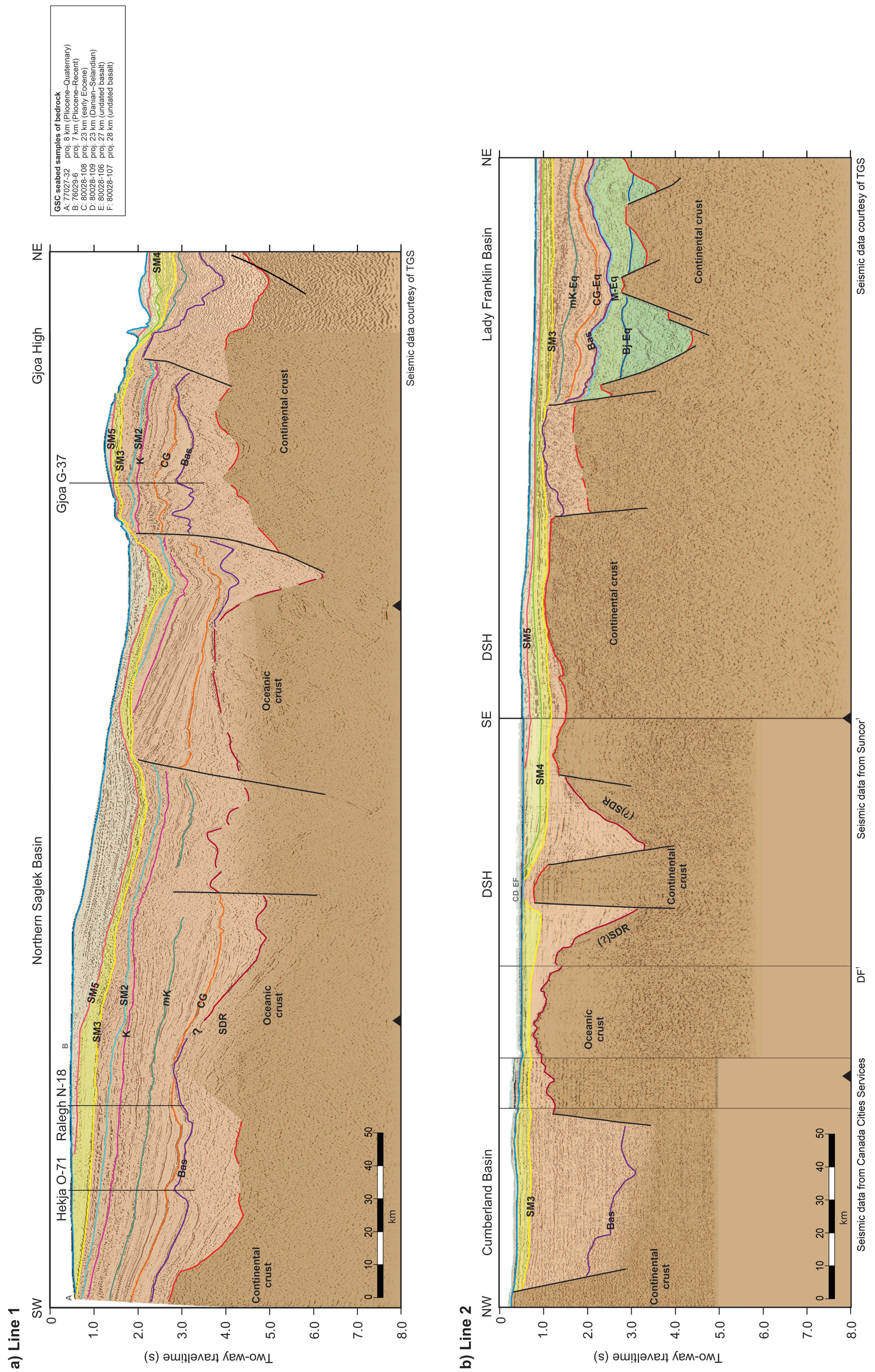
a) Line 1
SW
NE
Two-way traveltime (s)
Hekja O-71
Ralegh N-18
Northern Saglek Basin
Gjoa G-37
Gjoa High
GSC seabed samples of bedrock
A: 77027-32 proj. 8 km (Pliocene–Quaternary)
B: 76029-6 proj. 7 km (Pliocene–Recent)
C: 80028-108 proj. 23 km (early Eocene)
D: 80028-109 proj. 23 km (Danian–Selandian)
E: 80028-106 proj. 27 km (undated basalt)
F: 80028-107 proj. 28 km (undated basalt)
SM5
SM4
SM3
SM2
K
mK
CG
Bas
SDR
Oceanic crust
Continental crust
km
Seismic data courtesy of TGS
b) Line 2
NW
Cumberland Basin
DSH
SE
DSH
Lady Franklin Basin
NE
Two-way traveltime (s)
SM3
SM4
SM5
Bas
(?)SDR
mK-Eq
CG-Eq
M-Eq
Bj-Eq
Oceanic crust
Continental crust
km
Seismic data from Canada Cities Services
DF
Seismic data from Suncor
Seismic data courtesy of TGS

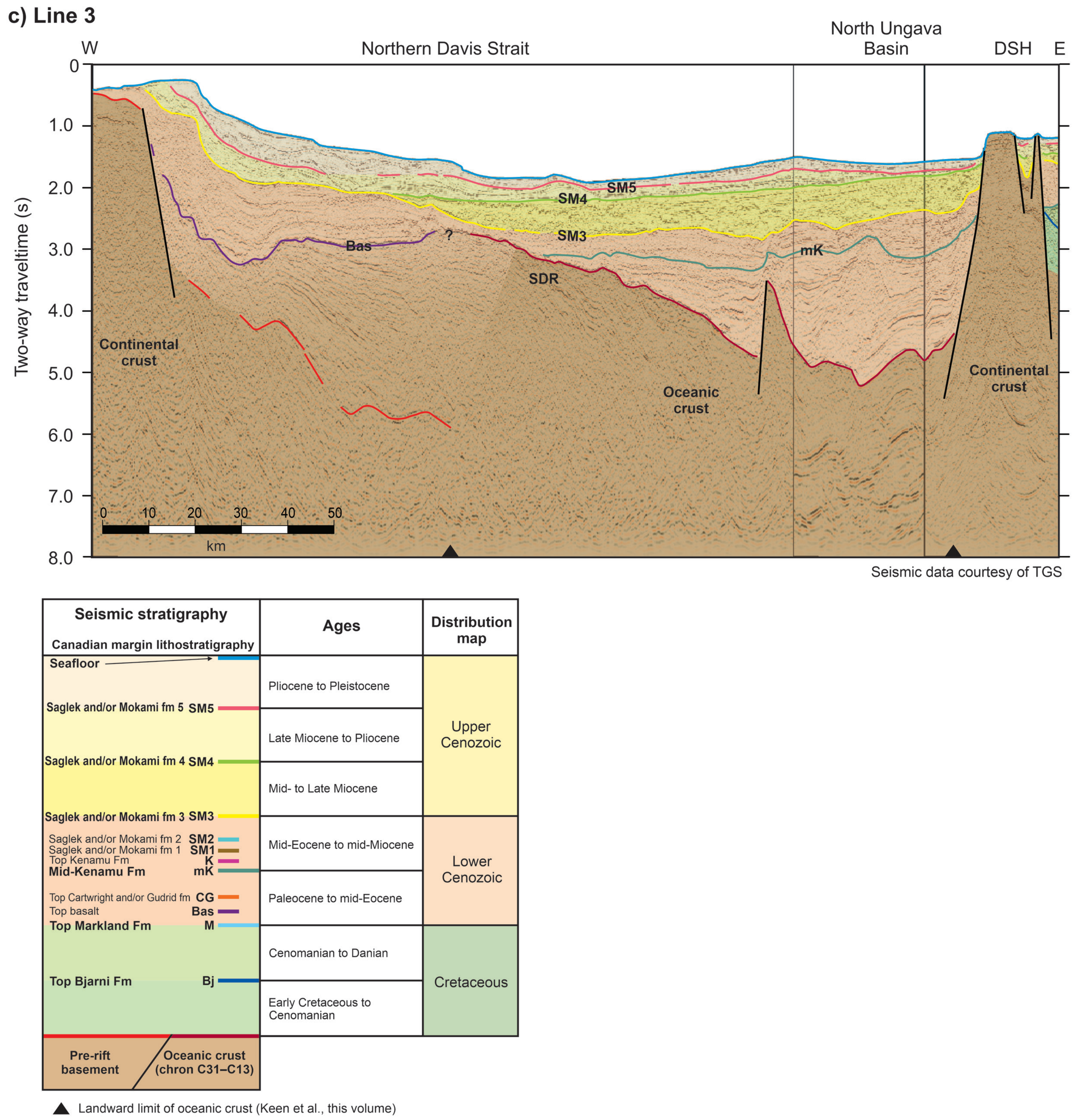

Figure 4. (cont.) Seismic lines crossing the western Davis Strait region (*see* Fig. 1 for profile locations).

The extent of Paleozoic rocks at the seafloor where they form part of the basement platform is shown in Figure 3 and is based on this study's seismic interpretation that modifies the original mapping by Grant (1975), MacLean (1978), and MacLean et al. (1977, 1982, 1986), along the northeastern and northern boundaries. Minor refinements are shown to the northeastern edge which is marked by significant downfaulting into the Cumberland Basin. MacLean et al. (1982) mapped Paleozoic strata offshore Cumberland Peninsula; however, the single-channel seismic data (from GSC cruises 80028 and 80035: data not shown) do not conclusively reveal the presence of stratified rocks forming basement. This, in addition to the narrowing of the platform at the southeastern tip of Cumberland Peninsula suggests that basement here reflects only Precambrian rocks exposed at the seafloor, consistent with nearby corehole samples in Hoare Bay. This interpretation differs from that of Jauer et al. (2019) where they defined Paleozoic basins both south and north of the Cumberland Sound region. Their southern basin overlaps part of the region containing Paleozoic drill core samples and the region shown in Figure 3, but extends northeast of the basement platform into the well established (?)Mesozoic–Cenozoic Cumberland Basin.

The eastern side of the study region is marked by a prominent, fault-bounded, northeast-trending basement ridge system approximately 560 km long, the Davis Strait High (Fig. 3). This ridge system is interpreted in the present study as cored by pre-rift, likely Precambrian and possibly Paleozoic rocks (cf. Suckro et al., 2013). Unlike previous studies, two ridges are shown separated by faults and a narrow, but relatively deep trough (1–1.5 s two-way traveltime; Fig. 4b). Between the Davis Strait High and the volcanic ridge that bounds the eastern side of Cumberland Basin (*see* 'Paleocene–Eocene volcanic rocks' section), a narrow depocentre is seen that deepens southward into a small, unnamed basin (Fig. 4b). The northern segment of the Davis Strait High narrows to the south (Fig. 4b) and widens to the north (Fig. 4c) where there is a bend in the trend of the high (Fig. 3). The southern Davis Strait High segment is exceptionally wide at its northern end and shows a step-like, faulted eastern edge where basalt flows have flooded over a downfaulted block (Fig. 4b; *see* 'Paleocene–Eocene volcanic rocks' section). The structure then narrows and subsides to the south (Fig. 3, 4a). The Davis Strait High is bounded by inferred, nearly vertical, strike-slip faults forming a major part of the Ungava Fault Zone. Pre-rift basement is also seen at depth below the Lady Franklin Basin where normal faults form grabens and half-grabens (Fig. 4b), but elsewhere pre-rift basement is typically obscured by volcanic cover (*see* 'Paleocene–Eocene volcanic rocks' section). At the northern edge of the study region, the continental margin is again steeply faulted adjacent to the narrow basement platform, but possible pre-rift basement is interpreted below thick volcanic cover (Fig. 4c).

CRETACEOUS INTERVAL

Lithostratigraphy, biostratigraphy, and paleoenvironments

Following discovery of the Lower Cretaceous Bjarni Formation within the Hopedale Basin and southern part of the Saglek Basin, offshore Labrador, the potential for equivalent rocks farther north was investigated. The first report of Cretaceous rocks was from seaward of the mouth of Cumberland Sound, where a sandstone drill core was recovered (Fig. 5; Table 3; 74026PHASE4-39; Srivastava, 1974) and dated late Albian–Cenomanian (MacLean et al., 1977; MacLean et al., 2014). MacLean et al. (2014) suggested that further sampling was needed to confirm the presence of Lower Cretaceous rocks in this region, but 74026PHASE4-39 is no longer available for further assessment (Dafoe and Williams, 2020a). Pliocene–Pleistocene rocks (stations 76029-16 and 16A; *see* 'Middle Miocene–Pleistocene interval' section) located only 8 km away from this station contain reworked palynomorphs including Cretaceous forms, which suggests that 74026PHASE4-39 could be significantly younger, containing reworked taxa.

Several seabed samples of bedrock were later recovered from within Cumberland Sound (Fig. 5; Table 3). Sample 82034-38 comprises semiconsolidated mudstone rich in organic matter from a terrestrial source (MacLean and Williams, 1983; Dafoe and Williams, 2020a). The core was initially assessed as Aptian to Cenomanian (MacLean and Williams, 1983), but later only confirmed as Early Cretaceous, possibly not extending into the late Albian (MacLean et al., 2014). Further drilling of shallow coreholes in 1985 in Cumberland Sound recovered additional Cretaceous samples. Sample 85027-48 is semiconsolidated mudstone to shale, lithologically similar to 82034-38 (MacLean et al., 1986; Dafoe and Williams, 2020a). MacLean et al. (1986) determined an initial Barremian–Aptian age; however, a later study revised the age to Aptian–Albian based on the presence of the spore *Costatoperforosporites foveolatus*, with a possible Aptian to middle Albian age suggested by the absence of late Albian *Rugubivesiculites* and tricolpate pollen (MacLean et al., 2014). To the northwest of this sample, the piston core cutter from 85027-31 recovered black, friable shale, siltstone, and mudstone fragments with an age similar to that of 85027-48, although a Barremian age could not be excluded (MacLean et al., 1986, 2014; Dafoe and Williams, 2020a). The initial assessment suggested that both of the 1985 samples are nonmarine to marginal marine in origin. Although MacLean et al. (2014) found them to reflect a nonmarine setting, the presence of rare acritarchs (organic-walled microfossils of unknown origin) could indicate proximity to a paleoshoreline or could be the result of reworking. Accordingly, Dafoe and Williams (2020a) postulated quiet-water settings consistent with either floodplain or lagoonal deposition. These samples confirm that Cretaceous rifting took place within Cumberland Sound.

North of Cape Dyer at the edge of the study area, the Quqaluit Formation is found onshore Paallavvik, Qaqulluit, and Aggijjat islands (Fig. 5). This formation was defined by Burden and Langille (1990) as sandstone and lesser siltstone and coal beds with a characteristic change from lower, white sandstone to overlying yellow sandstone. Burden and Langille (1991) found the lower sandstone units to be Neocomian and Aptian, but the overlying yellow sandstone units were younger, late Albian to Cenomanian. The white sandstone units reflect braided river successions, overlain by the anastomosing or meandering river deposits of the yellow sandstone units (Burden and Langille, 1990). The uppermost part of the succession was found to contain rare and poorly preserved dinocysts and acritarchs suggesting brackish, marginal marine conditions (Burden and Langille, 1991).

The limited information regarding Cretaceous strata in the western Davis Strait region is insufficient to allow for the erection of formal units, and the lithostratigraphic nomenclature from the Labrador margin is utilized in this study for the Mesozoic–Cenozoic succession, as was done previously (*see* 'Introduction' section). The Markland Formation is primarily Late Cretaceous, but is known to extend into the Danian (McWhae et al., 1980; Dickie et al., 2011) and even into the early Selandian (Dafoe, Dickie, Williams, and McCartney, this volume). Williams (2007b) and Nøhr-Hansen et al. (2016) identified Danian silty shale beds interbedded with basalt at the base of the Gjoa G-37 well (Fig. 6), but basal Danian strata were not intersected. Nøhr-Hansen et al. (2002) proposed a fivefold subdivision of the Paleocene, with the second oldest being the *Palaeocystodinium bulliforme* (P2) Zone that is present at the base of the Gjoa G-37 well. These are the oldest Paleocene rocks identified in the region, and were assigned to the Markland Formation, extending up to 3794 m (Table 2; Moir, 1987b). In Gjoa G-37, the Selandian of Williams (2007b) was restricted to 3560 to 3400 m by Nøhr-Hansen et al. (2016), resulting in a much thicker Thanetian interval (Fig. 6). This difference results from Nøhr-Hansen et al. (2016) extending the LO of *Alisocysta margarita* into the Thanetian, whereas Williams (2007b) considered its LO to approximately equate with the Selandian–Thanetian boundary. The present study follows Williams (2007b), which is consistent with the 59.5 and 59.2 Ma (late Selandian) ages from Williamson et al. (2000) for the core 1 basalt interval just below 2900 m and within Williams's (2007b) Selandian interval.

Accordingly, shale units interbedded between the basalt units up to 3145 m are considered here to be Markland Formation, with the youngest being early Selandian. Since the Markland Formation is mostly Late Cretaceous in age, the shale units in Gjoa G-37 (as defined above) are included in the present study on the Cretaceous distribution map (Fig. 5). The shale units are lithologically similar to those of the Markland Formation from the Hopedale Basin and southern segment of the Saglek Basin: grey to grey-brown, fissile and silty, but generally lack macrofossil material. The interval spanning the Markland Formation in Gjoa G-37 was interpreted as possible nonmarine deposits ((?)lacustrine), deepening to inner to outer shelf and bathyal near the top (Miller and D'Eon, 1987). Alternatively, Williams (2007b) indicated an inner to outer neritic setting based on the presence of dinocysts, with relative deepening upward. The Markland Formation on the Labrador margin is strictly marine in nature, so a shelfal setting is consistent, but shallower than bathyal depths recorded in some Labrador Shelf wells (*see* Dafoe, Dickie, Williams, and McCartney, this volume). The two other industry wells in the region did not intersect Markland Formation rocks.

Whereas Lower Cretaceous sandstone beds may be present in Cumberland Basin based on 74026PHASE4-39, Aptian to middle Albian (and possibly Barremian) mudstone beds are confirmed in Cumberland Sound. These mudstone units reflect nonmarine to possibly nearshore settings; although, thick shale and mudstone units within the Bjarni Formation of the Labrador margin are not common, the samples from Cumberland Sound generally resemble some intervals of the Bjarni Formation. Dafoe and Williams (2020b) described grey to grey-brown, primarily shale-dominated Bjarni Formation cores from the Herjolf M-92, Hopedale E-33, North Leif I-05, and Tyrk P-100 wells, as generally containing rare marine trace fossils, with dinocysts either lacking or sparse. The authors interpreted these core intervals as reflecting restricted bay or distal delta-front to prodeltaic settings in which either brackish and/or dysoxic conditions may have hampered dinoflagellate populations. Similar shallow-marine deposition may have taken place in Cumberland Sound during the Early Cretaceous and these rocks could be considered Bjarni Formation equivalents, but more specifically part of the shale-dominated Snorri Member. The onshore Quqaluit Formation may represent a more proximal fluvial sandstone succession in the Aptian, but was deposited in marginal marine settings in the late Albian–Cenomanian, similar to the Bjarni Formation, offshore Labrador. Lithologically, the Danian–lower Selandian Markland Formation rocks in Gjoa G-37 appear generally consistent with those of the Labrador margin, apart from being interbedded with basalt units and deposited in slightly shallower settings.

Previous offshore mapping

Cretaceous rocks (Fig. 5) in Cumberland Sound are inferred to be in fault contact with Precambrian rocks along the northeastern edge of the sound, with the innermost northwestern part poorly constrained by single-channel seismic studies (Fig. 3, 5; MacLean and Williams, 1983; MacLean et al., 1986). Cretaceous strata are also in fault contact with Paleozoic strata along the southwestern margin of Cumberland Sound (Fig. 3) and have been deformed by folding, faulting, and erosional denudation (MacLean et al., 1986). Outside Cumberland Sound, seismic mapping near 74026PHASE4-39 (e.g. Skaarup et al., 2006) suggests that it is unlikely that Cretaceous rocks lie close to the seabed in that region.

Regionally in western Davis Strait, the presence of Cretaceous rocks is speculative. Based on samples present in Baffin Bay, MacLean et al. (2014) indicated that there was likely a marine connection through Davis Strait during at least part of the Cretaceous, suggesting that equivalent strata may be present. Grant (1975) delineated an approximately 100 to 150 km wide zone of Cretaceous to Cenozoic strata seaward of the Precambrian and Paleozoic rocks exposed near the seafloor. Others have suggested that the southeast Baffin Shelf is mainly covered by Cenozoic rocks with only localized Mesozoic strata (MacLean, 1978). Balkwill (1987) recognized that within the northern part of the Saglek Basin and the Cumberland Basin, equivalent rocks of the Bjarni Formation could be intercalated with, and buried below Paleocene–Eocene volcanic flows (*see* 'Paleocene–Eocene volcanic rocks' section), but they could not be resolved in the seismic data. Miller and D'Eon (1987) postulated that if Cretaceous strata were present in the region, they would be nonmarine, but the area may also have been preferentially exposed at that time resulting in erosion rather than deposition. Balkwill and McMillan (1990) identified a "mid-Cretaceous marker" with underlying parallel-layered reflectors possibly equivalent to the Bjarni Formation, but they did not describe the distribution of the marker.

With regard to the Upper Cretaceous section, Balkwill and McMillan (1990) indicated that intercalation of the Markland Formation shale beds with the Paleocene basalt units in the northernmost Saglek Basin and probably along the southeast Baffin Shelf made seismic mapping difficult. They further suggested that the Freydis Member of the Markland Formation could not be traced north of Hudson Strait due to abrupt thinning. Subsequent studies were also not able to delineate the distribution of Cretaceous rocks (Jauer et al., 2014). If Bjarni- or Freydis-like sandstone beds are present, Jauer et al. (2014) predicted that they would be located under the volcanic rocks along the northwestern Saglek Basin margin.

Whereas mapping of Cretaceous deposits remains enigmatic over much of the western Davis Strait region, the Lady Franklin Basin has a well established Cretaceous section that extends into the east-central portion of the study area (Fig. 5). Offshore southwest Greenland, Sørensen (2006) divided the Cretaceous succession into two units separated by an unconformity of presumed mid-Cretaceous age. He interpreted the lower unit as Lower Cretaceous interbedded sandstone and mudstone units based on the development of a fan-like, progradational geometry seen in seismic data. Subsequently, Gregersen et al. (2018) mapped upper Albian to Cenomanian conglomerate, claystone, and thin sandstone units using the LF7-1, AT7-1, and AT2-1 wells (their mega-unit G; *see also* Gregersen et al., this volume). An unconformity within the Lower Cretaceous was further noted in the Maniitsoq Basin by Sørensen (2006), but it could not be seen in the Lady Franklin Basin. Sørensen (2006) also interpreted an Upper Cretaceous mudstone succession with laterally equivalent Fylla sandstone units up to 200 m thick in the northern Lady Franklin Basin: lowstand deposits of possible Santonian age. Further upsection, the Kangeq sequence is thought to be a deep-water mudstone with a possible Campanian unconformity in the central and northern Lady Franklin Basin (Sørensen, 2006). Similar sandstone and conglomerate units overlain by thick claystone beds of Late Cretaceous to Paleocene age were mapped by Gregersen et al. (2018; their mega-unit F; *see also* Gregersen et al., this volume). The Lower Cretaceous stratigraphy resembles that of the Bjarni Formation, whereas the thick Upper Cretaceous mudstone units can be equated with the Markland Formation, with Fylla sandstone beds possibly equivalent to the Freydis Member.

Distribution and seismic reflection character

This study's results further confirm that regional mapping of Cretaceous rocks in the western Davis Strait region is not generally possible (Fig. 5). The poor penetration of seismic systems through thick basaltic flows do not allow for clear imaging of presumed underlying, Cretaceous rocks. Localized areas show potential for the presence of Cretaceous strata, but these are poorly imaged and not mappable. In Gjoa G-37, it is possible that the Danian shale beds are underlain by Upper Cretaceous Markland Formation deposits, but this relationship is not clear on seismic data (Fig. 4a). The present study predicts that Cretaceous rocks would be most likely in Cumberland Basin inboard of major structuring and the landward limit of oceanic crust (*see* Keen et al., this volume). Whereas 74026PHASE4-39 has been identified as Cretaceous from this basin, the present interpretation in Figure 4b shows a nearby cross-section through the basin where Paleocene–Eocene basalt units are interpreted at depth. Although there is upturning of beds in this region possibly due to diapirism (MacLean and Falconer, 1979; MacLean et al., 1982), these would not be significant enough to bring Cretaceous rocks to the seafloor: they would otherwise be found only at depth below the basalt flows. This region is near the Cumberland Sound graben in which a slightly modified distribution of Cretaceous rocks is shown in Figure 5 based on MacLean et al. (1986), but also following the trend of the Bouguer gravity low in that region to redefine the northwestern boundary (*see* Fig. 5, Keen et al., this volume).

Cretaceous rocks within the Lady Franklin Basin on the West Greenland margin could be mapped with a high degree of confidence into the Canadian portion of this basin, as well as the northwestward continuation of the smaller Maniitsoq Basin (Fig. 5); however, since there are no samples of these rocks, they are considered to be 'inferred' Cretaceous. The Lady Franklin and Maniitsoq basins are underlain by faulted and rotated basement blocks with faults generally trending to the northwest, forming half-grabens and grabens (Fig. 3, 4b). The lower part of the Cretaceous section (top Bjarni-Formation equivalent; BJ-Eq) shows stratal growth against normal faults, indicating active extension during deposition. This succession is overlain by a more subdued package of low-amplitude reflections consistent with a thick shale succession and possibly with the Upper Cretaceous claystone units seen to the east by Sørensen (2006) and Gregersen et al. (2018). This unit locally includes high-amplitude seismic reflections, presumably representing the Fylla sandstone units (northeast end of Fig. 4b), but the unit overall can be equated with the Markland Formation. Rift structures are generally filled with Lower Cretaceous sediments, but compressional deformation is evident at the top Markland Formation–equivalent (Mk-Eq) horizon and basin inversion is also likely in the Lower Cretaceous section. Seismic data show 1 to 2.5 s two-way traveltime of Cretaceous rocks, but these are locally overlain and intruded by igneous flows and sills throughout the basin, similar to the West Greenland margin (Sørensen, 2006; Gregersen et al., 2018). The western margin of the Lady Franklin Basin is demarcated by an inferred strike-slip fault that abruptly juxtaposes the Cretaceous rift basin against Precambrian basement overlain by basalt flows (Fig. 3, 4b). Volcanic flows typically extend eastward from the high and partially obscure seismic coherency under the westernmost edge of the basin.

PALEOCENE–MIDDLE MIOCENE INTERVAL

Paleocene–Eocene volcanic rocks

Lithology, biostratigraphy, age, and paleoenvironments

Unlike the Early Cretaceous alkali Alexis Formation basalt units along the Labrador margin, the basaltic rocks in the western Davis Strait region are younger and compositionally different: tholeiites with MORB affinities (Williamson et al., 2000). These tholeiites are linked to the low-pressure, water-rich volatiles from ocean-spreading (Balkwill and McMillan, 1990) and are found in exploration wells in the northernmost Saglek Basin and in bedrock corehole samples (Fig. 7). These rocks are related to Paleocene volcanic rocks onshore Cape Dyer, Baffin Island (Clarke and Upton, 1971) and also to those onshore and offshore central West Greenland (Clarke and Pedersen, 1976; Johnson et al., 1982; Larsen and Dalhoff, 2006; Nelson et al., 2015; Larsen et al., 2016).

Onshore basaltic rocks

Onshore Baffin Island, Clarke and Upton (1971) described Late Paleocene basalt units (58 ± 2 Ma; K-Ar age) located in an outcrop belt from Cape Dyer to Qaqulluit (island; 90 km to the northwest), and restricted to 10 km from the coastline (Fig. 7). The basalt units encompass flat-lying, subaerial volcanic rocks lying on either Precambrian basement or thin intervals of terrestrial sedimentary rocks that lie upon basement. Locally, Clarke and Upton (1971) subdivided the basalt unit into a lower subaqueous, volcanic breccia and an upper subaerial flow unit. The flows thin rapidly inland and consist of olivine-rich basalt. The most complete section was noted from Cape Searle at the tip of Qaqulluit (island) where 150 m of subaqueous breccia beginning at sea level are overlain by 300 m of subaerial flows. Clarke and Upton (1971) described the breccia (both orange and black) as containing hyaloclastic basalt fragments and large blocks. The subaqueous nature of these rocks was confirmed by the presence of stratification, type and degree of alteration, inclusion of significant amounts of basaltic glass, and high water content. Large-scale crossbedding in the breccia is consistent with the 'lava delta' component of volcanic (magma-rich) margins (cf. Planke et al., 2000). According to Clarke and Upton (1971), the breccia could have been erupted in water depths of up to 70 m with a source located to the northeast, but uplift has raised these outcrops 150 to 500 m above paleosea-level. Overlying flows are olivine-rich and weathered grey locally with average thicknesses of 3.5 m per flow. Individual flows are characterized by a basal chilled interval, a massive interval, an upper vesicular zone with vesicles that may be filled by zeolites, and the uppermost part of the flow that can contain glass, pahoehoe structures, and a red alteration suggesting oxidation (Clarke and Upton, 1971). Both the thinning of flows and increase in oxidation of flow tops upward suggests that volcanism waned over time. Clarke and Upton (1971) also noted basaltic dykes that paralleled the coastline and were compositionally the same as the flows.

Figure 5. Distribution map of the Cretaceous interval for the western Davis Strait region. The distribution within Cumberland Sound is modified from MacLean et al. (1986) with an inner boundary near 85027-31. A small, previously mapped outlier of Cretaceous to the northwest could not be confirmed with the given data set. The Markland Formation identified in Gjoa G-37 is Danian to early Selandian and thus represents the uppermost part of this study's 'Cretaceous' interval. Basin outlines are from Keen et al. (this volume). Cretaceous onshore outcrop locations of the Quqaluit Formation are from Burden and Langille (1990, 1991) and Jackson (1998). *See* Figure 1b for abbreviated names. Additional projection information: Central Meridian: 60°W; Standard Parallels: 65, 75°W; Latitude of Origin: 65°N.

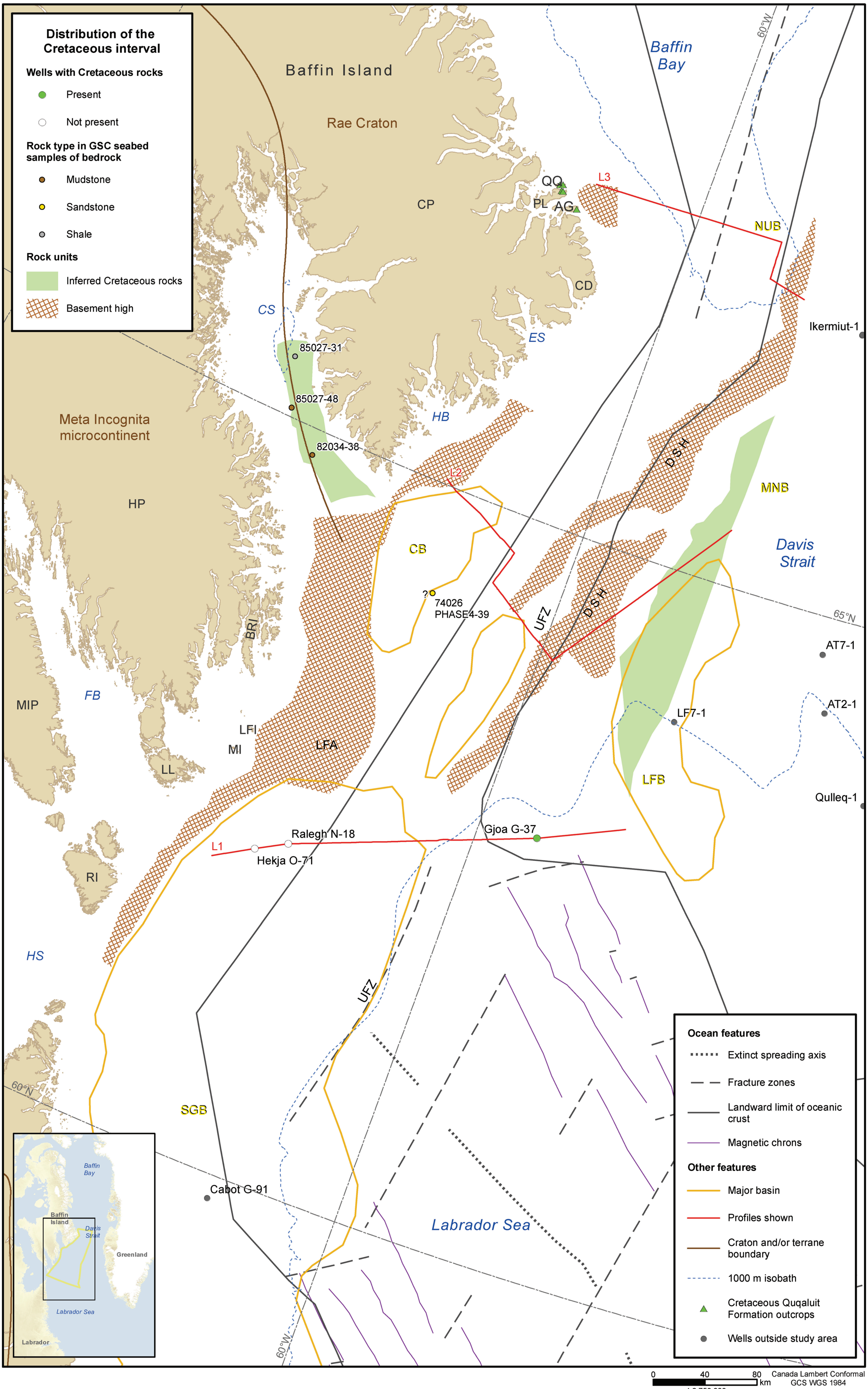
Distribution of the Cretaceous interval
Wells with Cretaceous rocks
Present
Not present
Rock type in GSC seabed samples of bedrock
Mudstone
Sandstone
Shale
Rock units
Inferred Cretaceous rocks
Basement high
Baffin Island
Rae Craton
Baffin Bay
Meta Incognita microcontinent
Davis Strait
Labrador Sea
QO
PL
AG
CP
CD
CS
ES
HB
HP
BRI
FB
MIP
LFI
MI
LL
LFA
RI
HS
SGB
CB
UFZ
DSH
MNB
NUB
LFB
L1
L2
L3
85027-31
85027-48
82034-38
74026 PHASE4-39
Ikermiut-1
AT7-1
AT2-1
LF7-1
Qulleq-1
Ralegh N-18
Hekja O-71
Gjoa G-37
Cabot G-91
60°W
65°N
60°N
Ocean features
Extinct spreading axis
Fracture zones
Landward limit of oceanic crust
Magnetic chrons
Other features
Major basin
Profiles shown
Craton and/or terrane boundary
1000 m isobath
Cretaceous Quqaluit Formation outcrops
Wells outside study area
Greenland
Labrador
0 40 80 km
1:2 750 000
Canada Lambert Conformal
GCS WGS 1984

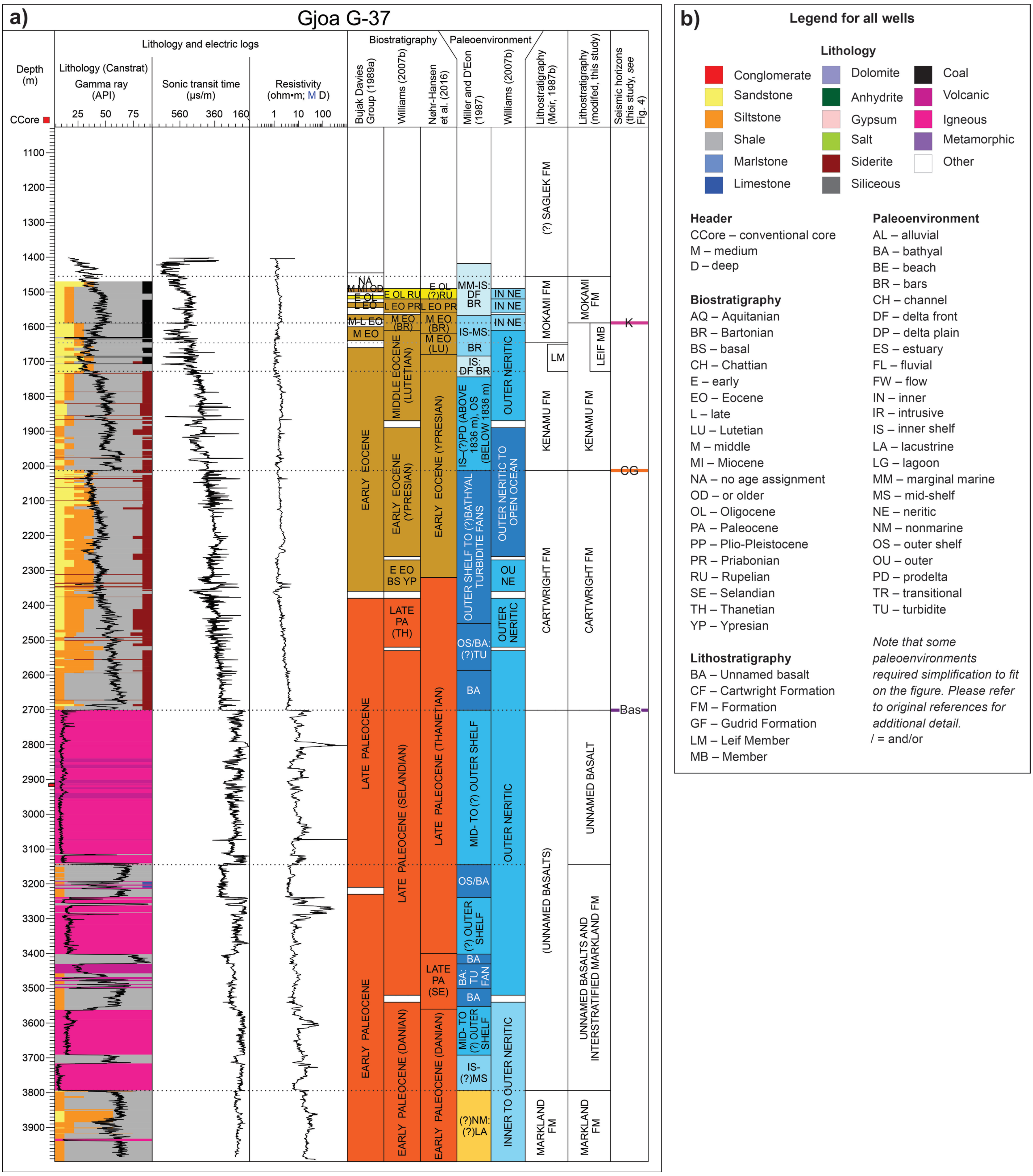

Figure 6. The Gjoa G-37 well showing fundamental wireline logs, lithology (Canstrat), conventional core locations, key biostratigraphic studies, paleoenvironmental interpretations, and lithostratigraphy. A revised set of lithostratigraphic picks for this study is also shown and listed in Table 2. Seismic ties from Figure 4 are also shown. *See* Figure 1b for abbreviated names. **b)** A legend for the well plots shown in the present study.

Figure 7. Distribution map of Paleocene to Middle Miocene (lower Cenozoic) interval for the western Davis Strait region with the location of the basement platform and highs, relevant seabed samples from GSC marine cruises, and the distribution of volcanic features. Seaward dipping reflectors are modified from Skaarup et al. (2006), Keen et al. (2012), and Suckro et al. (2013). Volcanic margins are described in Keen et al. (this volume) and the margin east of Cape Dyer is modified from Skaarup et al. (2006). Basin outlines are from Keen et al. (this volume). Lower Cenozoic onshore outcrop locations of the Cape Searle Formation are from Burden and Langille (1990, 1991) and Jackson (1998), with basalt outcrop locations from Clarke and Upton (1971). *See* Figure 1b for abbreviated names. Additional projection information: Central Meridian: 60°W; Standard Parallels: 65, 75°W; Latitude of Origin: 65°N.

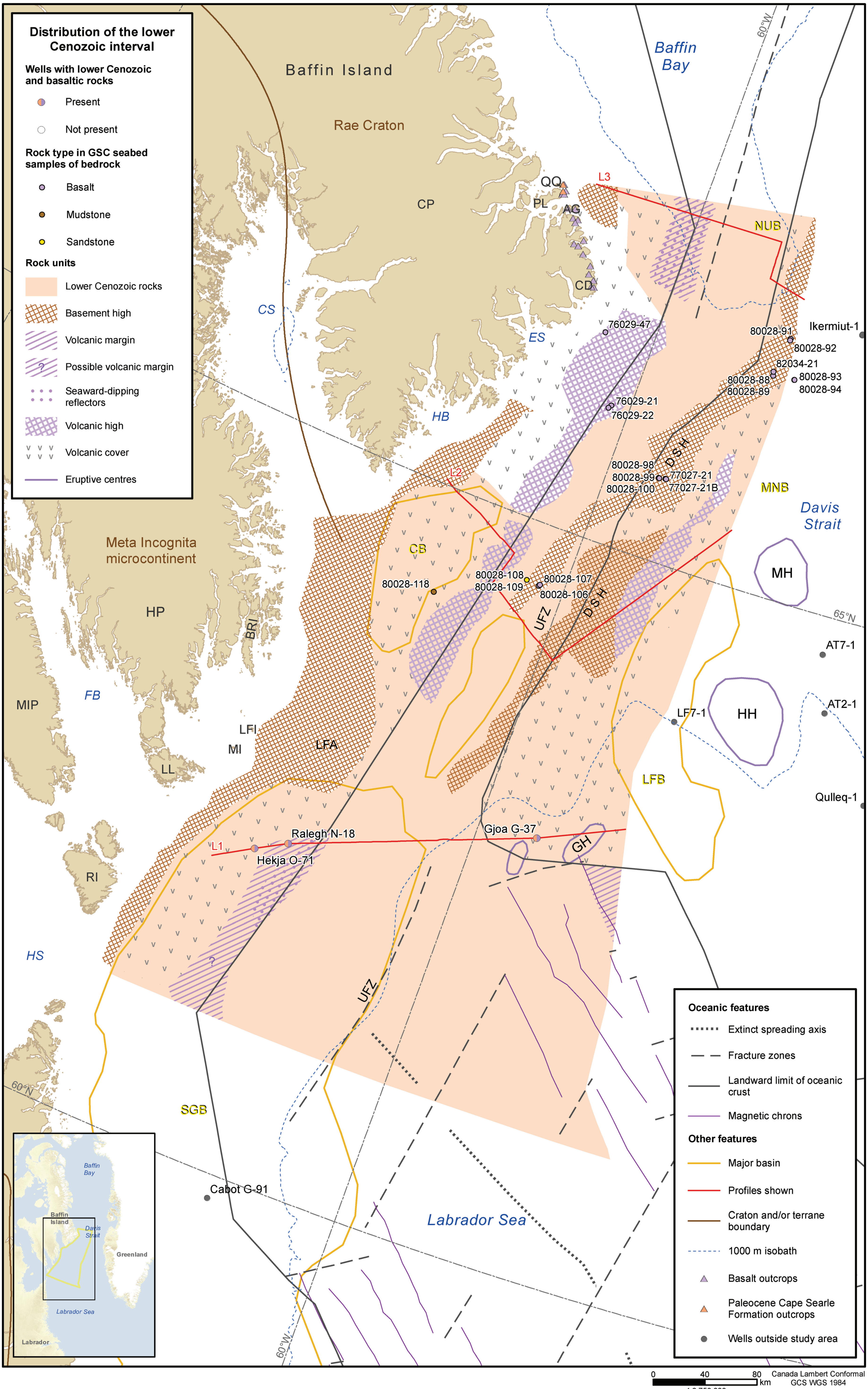
Distribution of the lower Cenozoic interval
Wells with lower Cenozoic and basaltic rocks
Present
Not present
Rock type in GSC seabed samples of bedrock
Basalt
Mudstone
Sandstone
Rock units
Lower Cenozoic rocks
Basement high
Volcanic margin
Possible volcanic margin
Seaward-dipping reflectors
Volcanic high
Volcanic cover
Eruptive centres
Baffin Island
Rae Craton
Baffin Bay
Meta Incognita microcontinent
Davis Strait
Labrador Sea
CP
HP
MIP
FB
CS
ES
HB
QQ
PL
AG
CD
L1
L2
L3
NUB
MNB
CB
LFB
SGB
MH
HH
GH
UFZ
DSH
BRI
LFI
MI
LFA
LL
RI
HS
76029-47
76029-21
76029-22
80028-91
80028-92
82034-21
80028-88
80028-89
80028-93
80028-94
80028-98
80028-99
80028-100
77027-21
77027-21B
80028-108
80028-109
80028-107
80028-106
80028-118
Ikermiut-1
AT7-1
AT2-1
LF7-1
Qulleq-1
Ralegh N-18
Hekja O-71
Gjoa G-37
Cabot G-91
60°W
65°N
60°N
Oceanic features
Extinct spreading axis
Fracture zones
Landward limit of oceanic crust
Magnetic chrons
Other features
Major basin
Profiles shown
Craton and/or terrane boundary
1000 m isobath
Basalt outcrops
Paleocene Cape Searle Formation outcrops
Wells outside study area
Baffin Bay
Baffin Island
Davis Strait
Greenland
Labrador Sea
Labrador
0 40 80 km
1:2 750 000
Canada Lambert Conformal
GCS WGS 1984

Industry wells

All three of the wells on the western side of the Davis Strait intersect basalt intervals at or near their base (Fig. 4a, 7). Klose et al. (1982) described the stratigraphy and structure at the Hekja O-71 and Gjoa G-37 wells. They found the lowermost 1000 m in Hekja O-71 included volcanic rocks with interbedded chalky clays, which they considered to be Early Cretaceous to Danian (Fig. 8). In Gjoa G-37, Klose et al. (1982) recorded 1300 m of interbedded Paleocene marine shale and volcanic rocks (Fig. 6). Below 3825 m in the Ralegh N-18 well, dark greenish-grey basalt with rare shale showing evidence of weathering is present (Fig. 9; Canterra Energy Ltd., 1982). Core samples from Hekja O-71 and Gjoa G-37 allow more detailed interpretations. Williamson and Villeneuve (2002) described a sample from core 3 (4352–4355 m) of Hekja O-71 as a greyish-green, flow-top breccia above a medium- to coarse-grained diabase-type interval (possibly a sill). Dafoe and Williams (2020b) found a similar succession of mostly brecciated basalt with lesser aphanitic basalt. They noted rimmed clasts in the breccia and suggested that this reflected rapid quenching and a subaqueous, hyaloclastic origin within a lava delta. In the same well, the overlying core 2 (3556–3555 m) is located near the top of the basalt and includes varicoloured, rubbly to indurated material with an apparent brecciated fabric consistent with shallow-marine to intermittent subaerial exposure and alteration (Dafoe and Williams, 2020b). Samples from a single core between 2920.5 m and 2912 m in Gjoa G-37 were described as subaerial basalt flows based on transitions from massive flows to vesicular to amygdaloidal flow tops with rubbly intervals, possibly reflecting some degree of weathering (Williamson and Villeneuve, 2002; Dafoe and Williams, 2020b).

The Cape Dyer onshore breccia units are similar to those sampled and described from Hekja O-71, interpreted to be part of a subaqueous lava delta succession (Williamson and Villeneuve, 2002; Keen et al., 2012; Dafoe and Williams, 2020b). Previous interpretation by Miller and D'Eon (1987) for the upper part of the basalt unit in Hekja O-71 included a marginal marine, subaerial to subaqueous setting and Williams (2007a) found the interval to represent inner neritic conditions based on palynomorphs (Fig. 8). Core 2 of this well appears to reflect weathered basalt within a siliceous or rhyolitic matrix, indicating a shallower setting at least at the top of the volcanic interval, which could reflect exposed lava delta topsets (Dafoe and Williams, 2020b). The onshore basalt flows at Cape Dyer also resemble core material from the Gjoa G-37 well, interpreted as subaerial basalt flows based on the aphanitic to amygdaloidal texture suggesting flow and flow-top accumulations (Williamson and Villeneuve, 2002; Dafoe and Williams, 2020b); however, this is inconsistent with reported paleoenvironments of middle to outer shelf for this part of the well, and the entire shale and basalt section was interpreted as inner shelf to bathyal (Fig. 6; Miller and D'Eon, 1987; Williams, 2007b). Shale deposition may, however, reflect marine conditions that alternated with shallow-marine or subaerial basalt outpourings, but bathyal to subaerial paleoenvironmental fluctuations are not likely. This discrepancy could also be the result of a limited representation of the basalt unit by the conventional core sample or palynomorph contamination by cavings from overlying deepwater strata.

From the well history reports, Klose et al. (1982) noted two ages for the Hekja O-71 basalt flows: 119 Ma from Krueger Laboratories and 105 Ma from the Aquitaine Company of Canada. Similarly, a K-Ar age of 83 ± 2 Ma was reported for the thin interval of basalt at the base of the Ralegh N-18 well (Canterra Energy Ltd., 1982). Despite these initial K-Ar ages, it was known early on that these rocks were not related to the Cretaceous Alexis Formation (Balkwill, 1987), and that the incorrect ages could be due to alteration of the basalt units (MacLean et al., 1990). Later Ar-Ar analyses resulted in ages of 59.5 ± 1.0 Ma and 59.2 ± 1.8 Ma for two samples from Gjoa G-37, consistent with a mid-Paleocene eruption event (Williamson et al., 2000); however, the sample from Hekja O-71 produced an age of 48.7 ± 1.3 Ma (Williamson et al., 2000), but exhibited significant heterogeneity in argon isotopes, suggesting an unreliable age, potentially due to excess argon.

Palynological evidence places the basalt units within the Gjoa G-37, Ralegh N-18, and Hekja O-71 wells as old as late Danian, but primarily Selandian to earliest Thanetian (Fig. 6, 8, 9; Williams, 2007a, b; Nøhr-Hansen et al., 2016). Palynomorphs are generally not preserved within basaltic lava flows, so cavings could account for some of the reported ages; however, the interbedding of shale and basalt in Gjoa G-37 (Fig. 6) permits a more robust palynological interpretation as the sedimentary intervals would provide material in which palynomorphs were preserved. In this well, the present study follows Williams (2007b) in which the basalt flows are late Danian–late Selandian. In Hekja O-71, the Selandian extends from 4566 to 3940 m according to Williams (2007a); however, occasional recovery of dinocysts including *Palaeoperidinium pyrophorum* which has its LO at 3640 m, indicates that the P4 Zone of Nøhr-Hansen *in* Sønderholm et al. (2003), which equates with the Selandian–Thanetian boundary, extends to this depth (Nøhr-Hansen et al., 2016). The age of the basalt units was further refined by analyses of core 2 between 3556 and 3555 m (Dafoe and Williams, 2020b). The bottom sample (3555.97 m) contained diatoms, one specimen of the conifer *Pinuspollenites*, and a questionable specimen of the dinocyst *Palaeocystodinium bulliforme*. If the latter is truly a specimen of *P. bulliforme* it would be indicative of the Selandian (Nøhr-Hansen et al., 2016), extending it even further up the well. The Thanetian is characterized by the P5 and P6 zones of Nøhr-Hansen *in* Sønderholm et al. (2003), which occur in Hekja O-71, Ralegh N-18, and Gjoa G-37. In the first two wells, the basalt flows just extend into the lowest part of this stage (Nøhr-Hansen et al., 2016), but in Gjoa G-37 they are older according to Williams (2007b).

Bedrock corehole samples

In addition to Paleocene basalt units sampled in exploration wells, corehole samples of basalt bedrock were recovered on several GSC marine cruises (Fig. 2, 7; Table 3). Three basalt drill cores were recovered from southeast of Cape Dyer (76029-21, -22, and -47). Samples 21 and 22 comprise reddish-brown to dark-grey, aphanitic to amygdaloidal basalt with zeolite minerals infilling vesicles, whereas the core from station 47 is dark-grey, coarser grained, aphanitic to vesicular basalt, with some black phenocrysts (MacLean and Falconer, 1977; MacLean et al., 1978; Dafoe and Williams, 2020a). Dafoe and Williams (2020a) interpreted these rocks to be from near the top of a basalt flow, or at depth within a flow in the case of station 22. The magnetic and petrological characteristics resemble those of the onshore basalt flows, but there is a lack of glass, which suggests subaerial emplacement (MacLean et al., 1978) like that of the onshore flows. Although these rocks are highly altered, Williamson et al. (2000) determined an age for 76029-47 of 62.9 ± 2.5 Ma (Danian) based on Ar-Ar age dating techniques, which is consistent with initiation of Paleocene volcanism in the region (cf. Storey et al., 1998, 2007; Larsen et al., 2009).

Farther southeast of Cape Dyer on the Davis Strait High, drill core 77027-21B recovered (Fig. 7) aphanitic, dark-grey basalt, with small phenocrysts, but the in situ nature of the sample was unclear (MacLean, 1978; Dafoe and Williams, 2020a). A nearby drill core, 77027-21, is also thought to be possible basalt bedrock (MacLean, 1977), with an aphanitic texture and grey colour (Dafoe and Williams, 2020a). Both samples were interpreted to have formed at depth within basalt flows (Dafoe and Williams, 2020a). Near these samples, MacLean (1980) recovered additional basalt samples from cruise 80028 at stations 98, 99, and 100, but it was less certain if they all represented in situ basalt bedrock. The samples are described as aphanitic, dark grey to green basalt that formed at depth within basalt flows (Dafoe and Williams, 2020a), and all lie on a wide basement high forming the northern part of the Davis Strait High (Fig. 7). Near the southern end of the same basement ridge and east of the mouth of Cumberland Sound, MacLean (1980) and MacLean et al. (1982) reported basalt from 80028-106 and 80028-107. These were further described as medium- to dark-grey, aphanitic or amygdaloidal basalt with zeolite or calcite infills in vesicles and some fracture fills, and which resulted from crystallization at depth within basalt flows (Dafoe and Williams, 2020a). Directly east of Cape Dyer, basalt thought to be in place was recovered during cruise 80028 at stations 88, 89, 91, 92, 93, and 94 (MacLean, 1980). These basalt units are dark grey, aphanitic, amygdaloidal, vesicular, and brecciated in nature with local phenocrysts and zeolite mineral infills in vesicles, as well as rimmed and fragmented clasts in 80028-92 (Dafoe and Williams, 2020a). Dafoe and Williams (2020a) suggested that these samples formed at depth from within a flow where they are dominated by a more aphanitic texture, but from a flow top where they are more amygdaloidal or vesicular, with station 80028-92 possibly having formed in a subaqueous setting. Near 80028-88 and 80028-89, sample 82034-21 also recovered dark grey, aphanitic basalt bedrock with rare amygdales suggesting crystallization at depth within a flow (MacLean and Williams, 1983; Dafoe and Williams, 2020a). These drill cores were obtained from (or just off) the Davis Strait High basement structure that forms a continuous ridge sampled by some of the other basalt drill cores described above. Sample 80028-92 produced an Ar-Ar age date of 55.1 ± 2.3 Ma (Williamson et al., 2000) consistent with an earliest Eocene (Ypresian) extrusion. Refraction studies have confirmed that the Davis Strait High is cored by Precambrian basement rock with

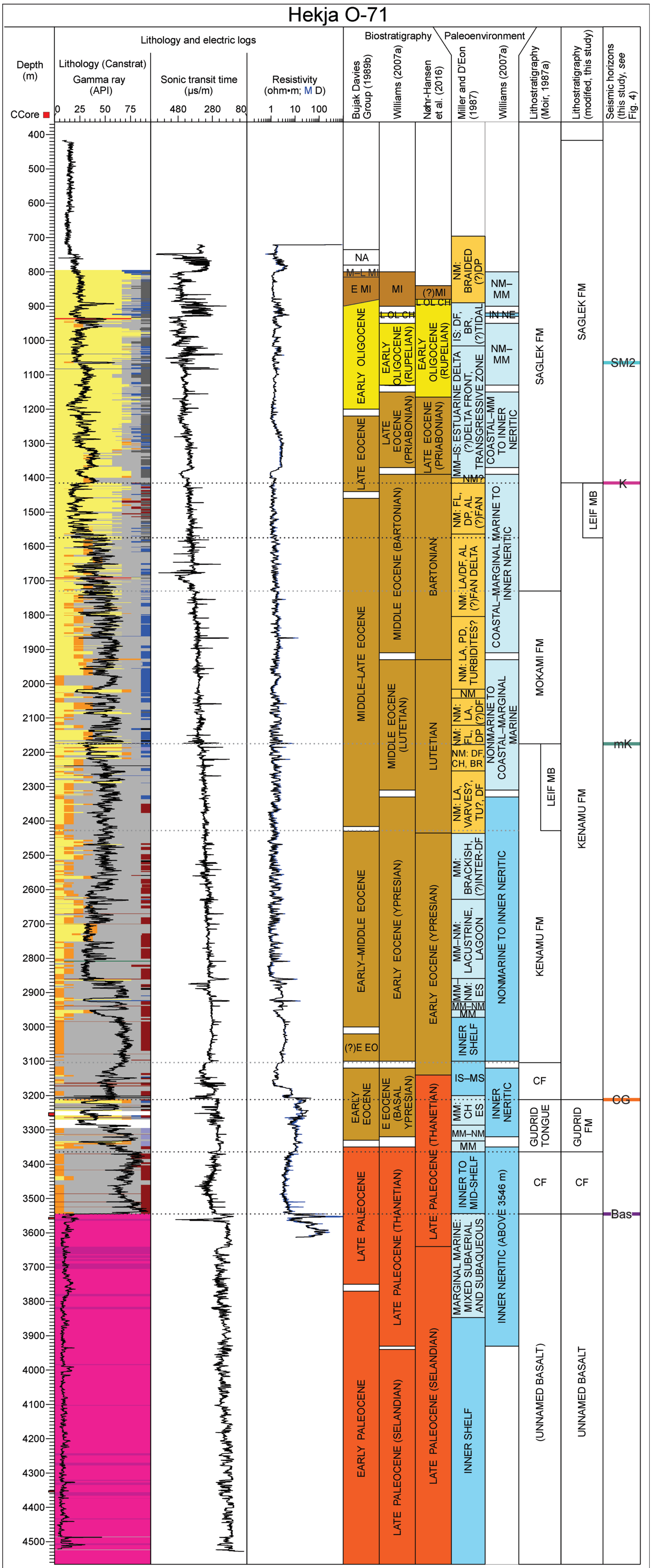

Figure 8. The Hekja O-71 well showing fundamental wireline logs, lithology (Canstrat), conventional core locations, key biostratigraphic studies, paleoenvironmental interpretations, and lithostratigraphy. A revised set of lithostratigraphic picks for this study is also shown and listed in Table 2. Seismic ties from Figure 4 are also shown. *See* legend in Figure 6b.

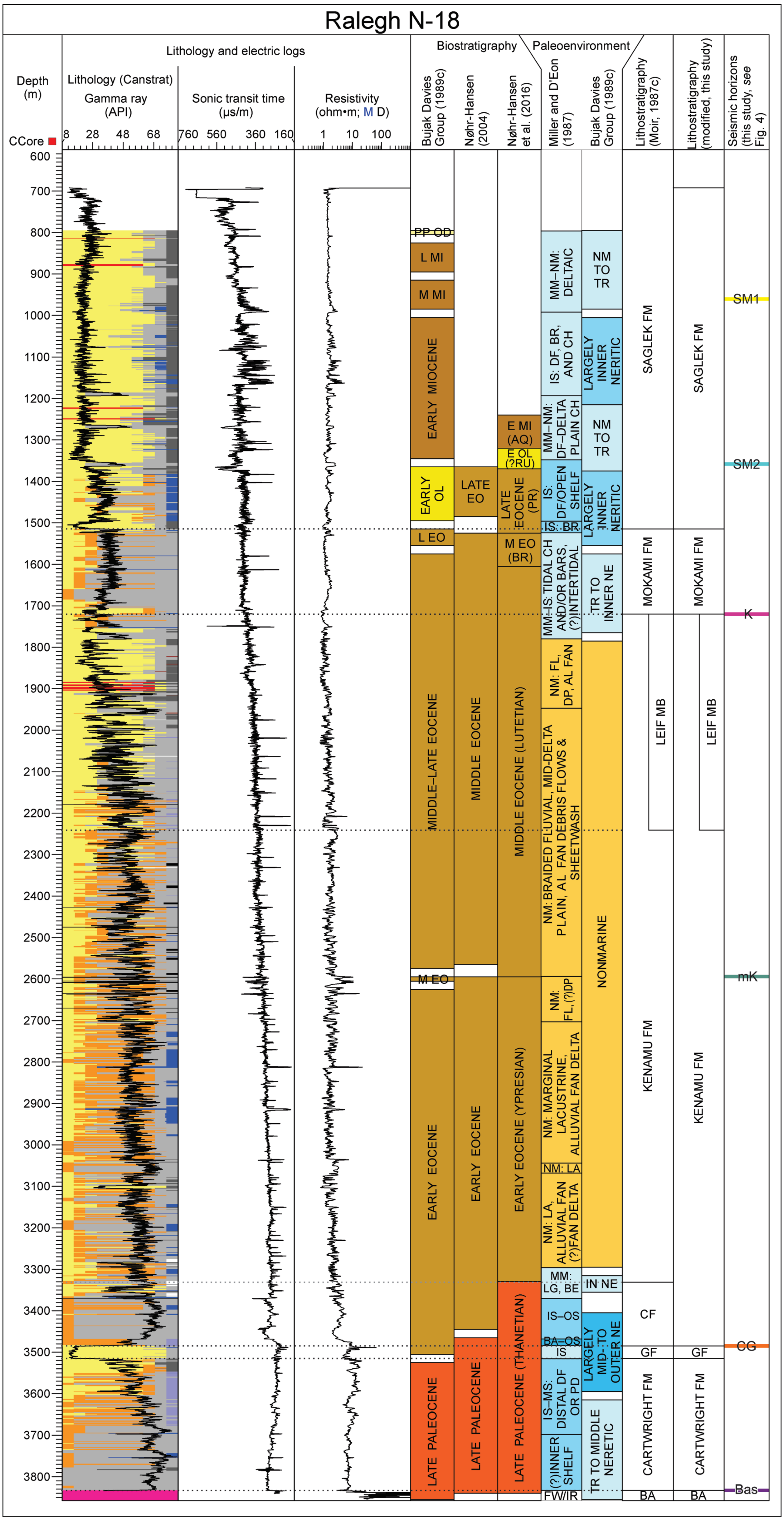

Figure 9. The Ralegh N-18 well showing fundamental wireline logs, lithology (Canstrat), key biostratigraphic studies, paleoenvironmental interpretations, and lithostratigraphy. A revised set of lithostratigraphic picks for this study is also shown and listed in Table 2. Seismic ties from Figure 4 are also shown. *See* legend in Figure 6b.

only a thin basalt cover (Suckro et al., 2013), which is presumably the source of the material recovered from the coreholes. Overall, late Danian–earliest Thanetian, subaqueous lava deltas and subaerial flows are found along the western margin of the study region and in Gjoa G-37. Basalt flows on the Davis Strait High and located further east appear to be slightly younger, earliest Eocene.

Previous offshore mapping

In the western Davis Strait region, there has been an ongoing effort to map the volcanic rocks. Igneous rocks tend to have a magnetic signature, but the basalt units in the study region correspond to both positive and negative anomalies and are far more extensive than those onshore (Hood and Bower, 1975). Grant (1975) mapped some of the basalt flows outcropping near seafloor, noting their proximity to onshore rocks near Cape Dyer. Others have mapped volcanic ridges in the western Davis Strait region based on single-channel seismic data and correlations to the seabed corehole samples described above (MacLean and Falconer, 1977, 1979; MacLean et al., 1978, 1982). Further mapping of these volcanic rocks was conducted by Skaarup et al. (2006) using multichannel seismic data. They mapped basalt units present near the seafloor and at depth that masked basement due to their high-amplitude character that obscures deeper signals. Based on a refraction profile offshore Cumberland Peninsula, Suckro et al. (2013) suggested that basalt flows likely cover much of the continental crust in the region.

The extent of volcanic rocks northeast and southeast offshore Cape Dyer was mapped by Grant (1975) and later refined by MacLean et al. (1978). These basaltic rocks have short-wavelength and high-amplitude magnetic anomalies (up to 2000 nT; MacLean et al., 1978) due to their presence near the seafloor (*see* Fig. 6, Keen et al., this volume). In addition to this mapping, several basaltic ridges were described in the region. East and southeast of Cape Dyer, a basalt high was interpreted to be in fault contact to the northwest with sedimentary strata (part of the northern Davis Strait High in Fig. 7; Grant, 1975; MacLean et al., 1978, 1982; Skaarup et al., 2006). This structure was shown along trend with a second basalt high to the south based on drill core samples (80028-106 and 80028-107; MacLean et al., 1982; Skaarup et al., 2006). A third basalt outcropping near the seabed was also reported south-southeast of Cape Dyer (Grant, 1975; MacLean et al., 1978, 1982), which was later mapped as a continuation of the Cape Dyer basalt high (Skaarup et al., 2006). A fourth structure east of the mouth of Cumberland Sound was described by MacLean and Falconer (1979) as a diapiric feature, possibly associated with basaltic rocks lying on trend to the north. MacLean et al. (1982) interpreted the structure, based on seismic and potential field data, as basalt cored, with a steep western flank, a flat to undulating top, and a moderately sloped eastern edge. They proposed a continuation of the structure southward in the subsurface based on magnetic signatures, a relationship that was confirmed by Balkwill (1987). Near the international boundary with Danish West Greenland territory, MacLean et al. (1982) identified a fifth high (their ‘ridge 4’), which they also interpreted as volcanic in origin. These features form parts of those shown in Figure 7 and are further described below in relation to this study (*see* ‘Distribution and seismic reflection character’ section).

Within the basaltic highs, Grant (1975) observed to the east near Cape Dyer closely spaced reflections dipping 8 to 10° thought to delineate flows possibly interbedded with sediments. Dipping reflectors were also noted by MacLean and Falconer (1977) on single-channel seismic data trending from Cape Dyer toward 76029-22 and even farther seaward, suggesting that these rocks postdate those described onshore (Clarke and Upton, 1971). MacLean et al. (1978) found these dipping reflections to possess apparent dips ranging from 7 to 20° to the east or southeast. Also near 76029-21 and 76029-22, Suckro et al. (2013) noted dipping reflections within volcanic rocks on multichannel seismic data. These layered volcanic rocks are seaward-dipping reflectors (cf. Planke et al., 2000) extending both northeast and southeast of the Cape Dyer onshore volcanic rocks (Fig. 7; Skaarup et al., 2006). Keen et al. (2012) mapped additional seaward-dipping reflectors outboard of the Hekja O-71 and Ralegh N-18 wells (Fig. 7). Related to the seaward-dipping reflectors, a series of at least two lava deltas (cf. Planke et al., 2000) can be seen in the northern Saglek Basin in seismic data (Keen et al., 2012), with the landward occurrence being drilled at Hekja O-71. These features were first noted by Balkwill (1987) who described them as landward-facing, high-angle reflections composed of subaqueously formed, brecciated and fractured, microcrystalline, olivine basalt flows and vitric tuff beds that onlap faulted basement. Balkwill and McMillan (1990) further commented on their similarity to the giant clinoforms seen in the onshore Cape Dyer basalt units. The presence of seaward-dipping reflectors and lava deltas indicates the development of oceanic crust as part of a magma-rich (volcanic) margin (cf. Planke et al., 2000), which was suggested for the region east of Cape Dyer by Skaarup et al. (2006; Fig. 7). Based on seismic mapping, Keen et al. (this volume) further define possible volcanic margins extending northwest of Cape Dyer and within northernmost Saglek Basin (Fig. 7).

The Gjoa G-37 well contains basalt flows intercalated with marine shale units of the Markland Formation (*see* ‘Cretaceous interval’ section; Moir, 1987b; Jauer and Budkewitsch, 2010; Dafoe, 2021), and is located near an intrusive igneous plug (MacLean et al., 1982; Balkwill, 1987; Balkwill and McMillan, 1990; Sørensen, 2006). On seismic data, this igneous structure is flat topped with moderate to steep flanks and a structureless interior. Sørensen (2006) named and described the Gjoa Eruption Centre (or Gjoa High) as an elevated basalt edifice 32 km east of the Gjoa G-37 well, about 12.5 km wide and 1.5 km above the surrounding top basalt horizon (Fig. 4a, 7).

In the Lady Franklin Basin, sills and dykes commonly intrude the Cretaceous section (Sørensen, 2006). Gregersen et al. (2018) noted the presence of bowl or V-shaped, strong reflections near their G1 horizon (top Early to middle Cretaceous) interpreted as sills with a large complex located in the Lady Franklin Basin. Nearby, volcanic rocks have also been dated as late Cenomanian to early Turonian (Gregersen et al., 2018) in LF7-1, but a thin interval of Paleocene basalt flows was also mapped there (Gregersen et al., 2018). Accordingly, sills and dykes in the western Lady Franklin Basin may be Paleocene–Eocene, but could also be older.

Distribution and seismic reflection character

The present study shows two elements of the basalt units in the region: the distribution of the volcanic cover where it impedes imaging of underlying strata and pre-rift basement, and the location of volcanic highs (Fig. 7). Where seismic data coverage exists, a thick cover of basalt appears to be present throughout much of the region and is mapped as the top of basalt (Bas; Fig. 4). The exceptions to a thick basalt cover are over pre-rift basement highs (Fig. 4b), along steep margins of basement highs where volcanic rocks onlap against basement (Fig. 4c), and over the Lady Franklin Basin (Fig. 4b). Inboard volcanic cover from about Exeter Sound to Qaqulluit Island and including the onshore basalt units described by Clarke and Upton (1971) lies outside the seismic data coverage, but is modified from earlier mapping by Grant (1975), MacLean et al. (1978, 1982). In the seismic data set, oceanic basalt flows resemble volcanic cover lying above continental crust and sedimentary strata. Along seismic refraction lines (e.g. Funck et al., 2007; Suckro et al., 2013), however, these relationships are clearer (*see* Keen et al., this volume). The landward limit of oceanic crust (black triangles) is shown in Figure 4 for the conjugate margins and the present study tentatively assigns oceanic crust between them, except where continental fragments are present (Fig. 4b, 7). Oceanic crust is also well established in the southeast corner of the study region, based on interpretation of magnetic data, which shows it primarily lies outboard of chron C25n (Late Paleocene; Roest and Srivastava, 1989; Keen et al., this volume).

The western edge of the study region is characterized by a basalt cover that tapers out against the steep basin-bounding fault of the basement platform (Fig. 3, 7), a relationship mapped with a moderate to high confidence level. Elsewhere, the confidence level of mapping acoustic basement (i.e. volcanic cover) can be low where data resolution is poor and the seismic-stratigraphic relationships are less clear (e.g. western end of Fig. 4b). In the Lady Franklin Basin, pre-rift basement can be mapped with a reasonable degree of confidence as the volcanic cover is thin (Fig. 4b). Here, basalt units are thick adjacent to the southern segment of the Davis Strait High, but thin rapidly, generally forming a discontinuous flow lying above Cretaceous strata. Northeast of Cape Dyer, basalt units extend into the offshore. The North Ungava Basin (Christiansen et al., 2002) appears to be floored by oceanic basalt flows (Fig. 4c; Oakey and Chalmers, 2012; Keen et al., this volume), indicating that overlying strata must be Late Paleocene or younger; however, syn-rift strata are locally present northwest of Cape Dyer both onshore and just offshore Paallavvik (island) (*see* Dafoe, Dickie, and Williams, this volume). The northeastern part of the Cumberland Basin may also extend below the basalt cover that occurs east and south of Cape Dyer.

In addition to the basalt cover, thick igneous rocks form prominent ridges in the study area. The present study builds upon the mapping efforts (*see* ‘Previous offshore mapping’ section above) of Grant (1975), MacLean et al. (1978, 1982), MacLean and Falconer, (1979), and Skaarup et al. (2006) to interpret an extension of the basaltic high southeast of Cape Dyer southward to near the Lady Franklin Arch (Fig. 4b, 7). This ridge is relatively continuous and forms the eastern boundary of the Cumberland Basin, resulting in a more restricted basin compared to that initially described by Balkwill (1987). The basaltic high shows moderate to steep margins on both sides, but it is on this ridge that seaward-dipping reflectors have been noted along its eastern edge (e.g. Suckro et al., 2013; Fig. 7). Additional dipping reflectors are noted farther south on Figure 4b on either side of the northern arm of the Davis Strait High and could also be seaward-dipping reflectors.

Farther east, additional basaltic ridges were initially interpreted (MacLean et al., 1982; Skaarup et al., 2006), but what is now known as the Davis Strait High was found to be cored by pre-rift, likely Precambrian basement based on refraction studies (Suckro et al., 2013). Accordingly, the Davis Strait High is mapped in the present study as two pre-rift basement highs surrounded by inferred strike-slip faults (Fig. 3, 4; *see* 'Pre-rift basement' section; *see also* Keen et al., this volume). The east-central portion of the Davis Strait High steps down due to faulting, but has a thick basalt cover that forms a prominent igneous ridge (cf. Suckro et al., 2013). This ridge extends to the south where it abuts more elevated pre-rift basement rocks of the southern segment of the Davis Strait High (Fig. 4b). Basalt recovered from coreholes atop the Davis Strait High indicate the presence of a thin basalt cover as previously suggested by Suckro et al. (2013), but this is not generally seismically resolvable above the strong pre-rift basement reflector.

The remaining igneous features are found near Gjoa G-37 and include the Gjoa High (Sørensen, 2006). Another volcanic high is mapped to the southwest of Gjoa G-37 and is comparable in size to the Gjoa eruptive centre, but it has not been previously identified or named. Based on the age of basalt units found regionally (Clarke and Upton, 1971; Williamson et al., 2000; Nøhr-Hansen et al., 2016), it is possible the Middle–Late Paleocene units are restricted to the band of volcanic rocks found on and offshore Cape Dyer and the corresponding ridge extending southward. Accordingly, latest Paleocene–Early Eocene basalt units may be limited to the central parts of Davis Strait, including flows overlying the Davis Strait High, which is consistent with the 55.1 ± 2.3 Ma age for 80028-92 west of the Ikermiut-1 well (Williamson et al., 2000; Dafoe and Williams, 2020a).

Cartwright and Gudrid formations

Lithostratigraphy

Lying above the basalt units in the western Davis Strait wells is the Cartwright Formation (Fig. 2), originally defined by Umpleby (1979) and initially considered late Coniacian to Early Paleocene; however, McWhae et al. (1980) restricted the formation to the Paleocene and Early Eocene (*see* Dafoe, Dickie, Williams, and McCartney, this volume). The Cartwright Formation is a shale- or claystone-dominated interval, in contrast to the sandstone-dominated, correlative Gudrid Formation (Umpleby, 1979). Lower and upper informal members comprise two intervals of the Gudrid Formation (Umpleby, 1979; McWhae et al., 1980; Moir, 1989; *see* Dafoe, Dickie, Williams, and McCartney, this volume).

In Hekja O-71 and Ralegh N-18, Moir (1987a, c) placed the Cartwright Formation both below and above thin intervals of Gudrid Formation sandstone units (Fig. 8, 9). Balkwill and McMillan (1990) subsequently divided the Cartwright Formation in the northernmost Saglek Basin and southeast Baffin Shelf into lower and upper members, separated by the Gudrid Formation, based on seismic and well log markers; however, the shale succession lying above the Gudrid Formation represents transgressive flooding, which is consistent with the nature of the basal Kenamu Formation (Dafoe et al., 2017; Dafoe, 2021; *see* Dafoe, Dickie, Williams, and McCartney, this volume). Accordingly, the shale units lying above the Gudrid Formation in both wells are reassigned in the present study to the Kenamu Formation (Fig. 8, 9). This restricts the Cartwright Formation in the three wells to the shale and claystone units lying above the Paleocene basalt flows, forming a generally coarsening-upward interval into the thin Gudrid Formation sandstone, where present. The grey to brown shale or claystone of the Cartwright Formation is more siltstone-dominated upward with local sandstone intervals, as well as rare limestone and/or marlstone beds (Fig. 6, 8, 9). The shale and claystone units also contain rare plant remains, rare siderite, trace coal, and minor glauconite; they may be barren of macrofossils or contain scattered shell and other fossil fragments.

The Gudrid Formation is present in only Hekja O-71 and Ralegh N-18 (Fig. 8, 9). Originally, the sandstone units in Hekja O-71 were considered part of Balkwill and McMillan's (1990) informal 'middle Gudrid member'; however, revised biostratigraphic ages confirm that these sandstone units encompass part of the upper Thanetian to Ypresian upper Gudrid Formation (Fig. 8; Williams, 2007a; Nøhr-Hansen et al., 2016; Dafoe and Williams, 2020b; Dafoe, 2021), making Balkwill and McMillan's 'middle Gudrid member' inconsistent with the stratigraphic framework presented herein (*see* Dafoe, Dickie, Williams, and McCartney, this volume). The lower sandstone of the Gudrid Formation, offshore Labrador, is Selandian to Thanetian (*see* Dafoe, Dickie, Williams, and McCartney, this volume). In the present study region, this timeframe is dominated by subaqueous basalt flows and deeper water, Cartwright Formation shale beds, suggesting that clastic sediment supply was overwhelmed by volcanic rocks or the depositional setting was sufficiently distal to preclude sandstone accumulation at the well localities.

In Hekja O-71, the Gudrid Formation sandstone units span the interval 3364 to 3212 m (Fig. 8; Moir, 1987a) and are interbedded with shale and siltstone beds. Klose et al. (1982) referred to these as the informal "Hekja sand". These rocks were described as light grey-brown, fine- to coarse-grained, subangular, poorly sorted, slightly pyritic and slightly glauconitic, micaceous, partly arkosic, partly lithic, coaly quartz sandstone units with calcite and kaolinite cements (Balkwill and McMillan, 1990; MacLean et al., 1990). The presence of coal beds is revealed by low sonic-log velocities (elevated transit times). Dafoe and Williams (2020b) described the sandstone from core 1 of this part of the well as coarse grained and buff-beige, with massive to crossbedded intervals, lesser herringbone cross-stratification, and small pebbles. A similar, but more well developed sandstone is encountered in Ralegh N-18 where there is a more gradual coarsening-upward interval from shale, to silty shale, to sandy shale, followed by the clean sandstone units of the Gudrid Formation from 3515 to 3485 m (Fig. 9; Moir, 1987c). These sandstone beds are medium- to coarse-grained, arkosic with abundant feldspar and kaolinite (a product of feldspar degradation), as well as glauconite and shell fragments (Balkwill and McMillan, 1990). Moir (1987b) did not recognize a Gudrid Formation interval in Gjoa G-37, where only slightly sandy shale beds are evident (Fig. 6).

In addition to the samples from the wells, scattered seabed corehole samples provide additional constraints on the distribution of the Cartwright and Gudrid formations (Fig. 2, 7; Table 3). East of the mouth of Cumberland Sound on the edge of the northern Davis Strait High, cores were recovered from 80028-108 and 80028-109 (MacLean, 1980). Dafoe and Williams (2020a) described station 80028-108 as muddy, very fine-grained sandstone with loading structures, planar lamination, and deformation, and with marine trace fossils. Similarly, station 80028-109 includes silty, brown, very fine-grained sandstone beds with organic detritus, convoluted bedding, and rare marine trace fossils (Dafoe and Williams, 2020a). These were assigned to the Early Eocene by MacLean et al. (1982) based on the dinocyst assemblages, but MacLean et al. (2014) refined the age of 80028-109 as Danian–Selandian, with reworked Early Cretaceous spores and Late Cretaceous dinocysts. Due to their proximity and similar lithology, 80028-108 is likely of the same age. The Early Paleocene age and grain size suggest a quiet-water setting thought to be delta front for station 80028-109 and distal inner shelf for station 80028-108 (Dafoe and Williams, 2020a), consistent with proximal facies of the Cartwright Formation also seen offshore Labrador in the Karlsefni A-13 well (Dafoe and Williams, 2020b); although, correlation with the uppermost Markland Formation is also possible.

Southeast of the mouth of Cumberland Sound, MacLean (1980) reported on a sedimentary core from 80028-118. This sample was later described as a grey to brown, poorly lithified, silty mudstone with a mottled, chaotic appearance and a petroliferous odour (gas bubbles emanated vigorously from the core following recovery), with very fine-grained sandstone laminae, convoluted bedding, and microfaults (MacLean and Srivastava, 1981; Dafoe and Williams, 2020a). A Late Paleocene to Early Eocene age was reported based on palynological analysis (MacLean et al., 1982), but modified to Paleocene by MacLean et al. (2014). The age and lithology are generally consistent with that of the Cartwright Formation, and Dafoe and Williams (2020a) indicated a prodelta paleoenvironment. MacLean and Srivastava (1981) suggested that the gas emanating from the core could account for the acoustic opacity seen in single-channel seismic data nearby. The sample lies near station 74026PHASE4-39, which recovered a core that was assigned a late Albian–Cenomanian age (Fig. 5; MacLean et al., 1977, 2014) and also near 76029-16 and 76029-16A of Pliocene to Recent age (*see* 'Middle Miocene–Pleistocene' section; MacLean and Falconer, 1977). It is unlikely that such a range of ages are exposed at the seafloor in such close proximity; however, MacLean and Falconer (1979) reported upturned beds against the western flank of a diapiric high in this region, which could account for some spread in age. Data quality in this region is poor, probably due to the masking of reflections by gas, but MacLean et al. (1982) also reported refraction velocities of 2 to 3 km/s consistent with 2 km of sedimentary rock underlain by 3.89 km/s material, which could reflect underlying older sedimentary strata.

Onshore in the southeast Baffin Island area, Paleocene sedimentary rocks locally occur beneath volcanic rocks (Clarke and Upton, 1971) and form the Cape Searle Formation (Fig. 7; Burden and Langille, 1990). These rocks consist of sandstone, siltstone, mudstone, clast- and matrix-supported conglomerate, and thin beds of basaltic volcanic ash that sit atop the Quqaluit Formation (Burden and Langille, 1990). The age of the Cape Searle Formation is Early to Middle Paleocene (Burden and Langille, 1991).

In terms of sediment provenance, onshore at Aggijjat (island), 35 m of coal and black shale beds are overlain by reddish arkose units bearing tourmaline, which can be linked to erosion of granite on the island and to a small graben-like structure at its northeastern end (Clarke and Upton, 1971). In the offshore, the textural and mineralogical immaturity of the sandstone in Ralegh N-18 also reflects sourcing from nearby Precambrian rock exposures (Balkwill and McMillan, 1990). Thrane (2014) studied the provenance of Paleocene rocks in this well and found Mesoarchean–Neoarchean, Proterozoic, Grenvillian, Nain plutonic suite, and Appalachian Orogen source material based on zircon populations. The presence of Grenvillian material in Ralegh N-18, could indicate increased erosion of the mountainous region at that time and a concordant, more widespread distribution of the detritus (Thrane, 2014). Other local sources are also likely in the offshore. Dafoe and Williams (2020b) suggested that anomalous red and green minerals in core 1 of Hekja O-71 from the Gudrid Formation were consistent with weathered volcanic rocks observed in the underlying core 2, indicating that there was some exposure and erosion of volcanic rocks in the region also supplying sediment, at least locally.

Biostratigraphy

The generalized age of both the Cartwright and Gudrid formations are reassessed in Dafoe, Dickie, Williams, and McCartney (this volume) and found to be late Selandian–Ypresian and Thanetian–Ypresian, respectively; although, they further suggested that Selandian Gudrid Formation may be present, but not preserved in the wells. In Gjoa G-37, Williams (2007b) considered the Cartwright Formation to be late Selandian–Ypresian (Fig. 6). In the same well, Nøhr-Hansen et al. (2016) found the interval to be late Thanetian to Ypresian, and Bujak Davies Group (1989a) more generally considered it Late Paleocene to Early Eocene. Despite some variation in the subdivision of the Paleocene, the Early Eocene (Ypresian) section of the Cartwright Formation is relatively consistent between the different studies (Fig. 6), but the Selandian age for the base of the Cartwright Formation is preferred in the present study.

Restricting the Cartwright Formation to the shale interval below the Gudrid Formation in Hekja O-71 results in an exclusively Late Paleocene age for the Cartwright Formation strata (Fig. 8). Based on palynological analyses, Bujak Davies Group (1989b) considered this interval as Late Paleocene; however, the oldest foraminifera they identified were Eocene. Williams (2007a) subdivided the Paleocene in this well into the Selandian and Thanetian with the Cartwright Formation being within the later part of the Thanetian. Nøhr-Hansen et al. (2016) also found the Cartwright Formation to be Thanetian, but they extended the Paleocene upward in the well resulting in the Cartwright Formation interval (3545–3364 m) being within the early part of the Thanetian. The overlying Gudrid Formation in Hekja O-71 was first considered Early Eocene (Bujak Davies Group, 1989b) and later refined to basal Ypresian (Williams, 2007a), but then considered to be in the later part of the Thanetian (Fig. 8; Nøhr-Hansen et al., 2016).

Similarly, restricting the Cartwright Formation to the shale units below the Gudrid Formation in Ralegh N-18 results in a Late Paleocene age (Fig. 9) for this interval. The biostratigraphy of the Ralegh N-18 well was first analyzed in depth by Bujak Davies Group (1989c), who found the oldest foraminifera to be Eocene, but the oldest dinocysts to be Late Paleocene. They recognized two zones in the Paleocene, the older *Alisocysta circumtabulata* Zone and the younger *Cerodinium speciosum* Zone, both of which they considered to be Late Paleocene. Nøhr-Hansen (2004) included the interval 3840 to 3465 m in the Late Paleocene, with strata assignable to the *Areoligera gippingensis* Biozone extending from 3840 to 3605 m and strata assignable to the *Apectodiniun augustum* Biozone extending from 3565 to 3465 m. Nøhr-Hansen et al. (2016) plotted the LO of *Alisocysta circumtabulata* at 3835.9 m just above total depth, which is considered in the present study to suggest that Selandian rocks are present; however, much of the formation is considered Thanetian. As in Hekja O-71, the Gudrid Formation is Early Eocene (Bujak Davies Group, 1989c) or Late Paleocene (Thanetian; Nøhr-Hansen, 2004; Nøhr-Hansen et al., 2016).

In Gjoa G-37, the absence of the P3 Zone (Nøhr-Hansen *in* Sønderholm et al., 2003) suggests that there is a hiatus with strata assignable to the P2 Zone directly overlain by strata of the P4 Zone at the boundary between the Danian and Selandian (Nøhr-Hansen *in* Sønderholm et al., 2003). This hiatus may equate with the "Bylot Unconformity" of McWhae (1981), but Nøhr-Hansen et al. (2016) discounted this correlation, arguing that the occurrence of Danian strata made it a more complicated story. This missing section could reflect a minor hiatus related to basalt emplacement or cavings from overlying strata could account for the reported ages. Also in Gjoa G-37, there is a hiatus between the Thanetian and Ypresian according to Nøhr-Hansen *in* Sønderholm et al. (2003). Mechanisms in which these breaks in sedimentation formed are unclear, but considering the distal marine paleoenvironments spanning both breaks, they could be related to condensed sections.

Overall, the Cartwright Formation appears to be primarily late Selandian–Thanetian, but ranges into the Ypresian where the Gudrid Formation sandstone units are not developed (Gjoa G-37). The limited nature of this formation may be related to the outpouring of basalt flows and a lack of accommodation space for sediment accumulation. The corehole samples, however, extend the distribution of the Cartwright Formation onto the southeast Baffin Shelf. In terms of the Gudrid Formation sandstone units, both the Hekja O-71 and Ralegh N-18 wells indicate a late Thanetian to basal Ypresian age, consistent with the upper Gudrid Formation from the Labrador margin (Dafoe, Dickie, Williams, and McCartney, this volume).

Paleoenvironments

Depositional environments for the Cartwright Formation from proximal to distal include inner to middle shelf in Hekja O-71 (Fig. 8; Miller and D'Eon, 1987; Williams, 2007a), transitional to outer neritic with possible delta-front or prodeltaic successions in Ralegh N-18 (Fig. 9; Bujak Davies Group, 1989c; Miller and D'Eon, 1987), and outer neritic to open-ocean and/or bathyal settings with possible turbidite fans in Gjoa G-37 (Fig. 6; Miller and D'Eon, 1987; Williams, 2007b). Similarly, in 80028-109, MacLean et al. (2014) reported an inner neritic depositional setting, and Dafoe and Williams (2020a) refined this to a delta-front setting. Accordingly, a shelfal setting in proximal regions and more distal shelf or bathyal settings further basinward is consistent with the Cartwright Formation from the Labrador margin (Dafoe, Dickie, Williams, and McCartney, this volume).

The Gudrid Formation was deposited in shallower depositional settings than the Cartwright Formation. In Hekja O-71, the interbedded sandstone and shale units were interpreted as nonmarine to mostly marginal marine (estuarine channel; Miller and D'Eon, 1987), lower delta plain (Balkwill and McMillan, 1990), inner neritic (Fig. 8; Williams, 2007a), and delta front (Jauer and Budkewitsch, 2010). Based on the sedimentary structures and lithology of core 1 from this well, Dafoe and Williams (2020b) suggested a tidal channel setting. The thin interval of sandstone in Ralegh N-18 has been interpreted as a more distal, inner shelf (Miller and D'Eon, 1987) to middle to outer neritic deposit (Fig. 9; Bujak Davies Group, 1989c). These seemingly distal settings could be a result of coarse sample spacing of cuttings and cavings with the thin sandstone interval being poorly resolved between the under- and overlying shale units. Conversely, Balkwill and McMillan (1990) interpreted these sandstone beds as shallow-marine, shoreface deposits. The coarsening-upward nature of the sandstone units and blocky gamma-ray signature are consistent with a shoreface setting, as opposed to a shelf succession. Similarly, the onshore, approximately coeval, Lower–Middle Paleocene Cape Searle Formation locally occurring beneath volcanic rocks, was interpreted to reflect intermittent marine settings based on the presence of degraded and/or reworked dinocysts (Burden and Langille, 1990). These rocks appear to be more proximal than those found in the offshore wells, but could be consistent with Gudrid Formation sandstone units and proximal equivalents of Cartwright Formation shale units. In summary, the Gudrid Formation represents shallow-marine shoreface, tidal channel, and lagoonal settings.

Previous offshore mapping

Based on seismic mapping, the Cartwright Formation has been postulated to attain maximum thickness in the central part of the Saglek Basin, offshore Hudson Strait (Balkwill and McMillan, 1990); however, this may include the shale sitting atop the Gudrid Formation, which is now considered part of the overlying Kenamu Formation

(Fig. 5, 6). Northward along the southeast Baffin Shelf, Balkwill and McMillan (1990) suggested that the Cartwright Formation is indistinct seismically where shale units of the Kenamu Formation overlie it; however, the top of the Gudrid Formation in Hekja O-71 forms a distinct seismic marker (Balkwill and McMillan, 1990). Jauer (2009) mapped the top of the Gudrid Formation in the Hekja O-71 and Ralegh N-18 area and proposed additional nearby structural traps possibly related to hydrocarbon venting at the seafloor. Jauer and Budkewitsch (2010) further expanded on this work to describe the Ralegh N-18 well within a structural low, and Jauer et al. (2014) mapped a Gudrid Formation sandstone fairway that extends about 100 km south of Hekja O-71.

In the Lady Franklin Basin, Sørensen (2006) identified a unit of mostly Paleocene age overlain by an unconformity close to the top of the Paleocene. Although it is difficult to correlate, Sørensen's (2006) intra-Lower Eocene unit may also be partly correlative to the Cartwright and/or Gudrid formations. He defined the upper of the two Lower Eocene units as strongly progradational sandstone and claystone units that could be similar to the Gudrid Formation; although, some of this succession could also be related to the Kenamu Formation.

Distribution and seismic reflection character

Based on the seismic data and lack of sampling, the top Cartwright and/or Gudrid formation horizon (CG) is only mappable in the northernmost Saglek Basin where the wells provide control and seismic resolution is fair to good (Fig. 4a). The horizon caps a thin series of high-amplitude reflections underlain by a lower amplitude package consistent with a thin, sandstone-dominated upper Gudrid Formation underlain by Cartwright Formation shale. Near the Hekja O-71 well, the horizon is characterized by discontinuous dish-shaped features possibly related to small channels and consistent with the tidal channel interpretation for the Gudrid Formation sandstone beds proposed by Dafoe and Williams (2020b). Northwest of Hekja O-71, at the basin margin, a high-amplitude wedge comprising generally low-angle, downlapping and prograding reflections locally occurs above the top basalt horizon (not shown) possibly reflecting a lower Gudrid Formation shoreline sandstone. Basinward, structural complexity does not permit extensive regional mapping of the Cartwright and/or Gudrid formation horizon except near Gjoa G-37. Here, there is minor postdepositional folding and faulting affecting a basal wedge of strata that thins to the east and is marked by high-amplitude reflections that may equate with possible turbidite fan accumulations as interpreted by Miller and D'Eon (1987). This wedge thickens westward, but the upper part of the Cartwright Formation thickens to the east and appears to be less affected by deformation (Fig. 4a).

Kenamu Formation

Lithostratigraphy

As defined by McWhae et al. (1980), the Kenamu Formation is a shale- and siltstone-dominated interval with lesser fine-grained sandstone that was initially thought to be Early to Late Eocene and possibly earliest Oligocene (Fig. 2; *see* Dafoe, Dickie, Williams, and McCartney, this volume). The Leif Member of the Formation is a sandstone-dominated interval, which was defined by Umpleby (1979) as a fine-grained, quartz-rich sandstone with varying siltstone and mudstone. Balkwill (1987) and Balkwill and McMillan (1990) subdivided the Kenamu Formation into three informal members: a lower, fining-upward silty shale; a middle, coarsening-upward interval from shale to siltstone and fine-grained sandstone; and an upper member that coarsens into siltstone and sandstone beds of the Leif Member.

The log signature of the Kenamu Formation is characterized by a decrease in velocity and resistivity logs from the underlying Cartwright and Gudrid formations. The top is also distinctive, with a further decrease in resistivity and sonic velocity (McWhae et al., 1980). Balkwill and McMillan (1990) noted that the trends seen in their Kenamu Formation informal members in the Hopedale and southernmost Saglek basins are not apparent in the northern part of the Saglek Basin, possibly due to the more proximal depositional settings there. If the base of the Kenamu Formation is modified to mark the transgression above the Gudrid Formation sandstone beds (3212 m in Hekja O-71 and 3484 m in Ralegh N-18; *see* 'Cartwright and Gudrid formations' section), the log signatures then show an increase in gamma ray, decrease in sonic velocity, and decrease in resistivity consistent with that of the Labrador margin (Fig. 8, 9). The base of the formation is not well defined by the same set of logs in Gjoa G-37. Here, there is a sharp increase in gamma ray and subtle decrease in sonic velocity, but no notable change in the resistivity, possibly due to similar shale units present both below and above the lithostratigraphic boundary (Fig. 6). By revising the base of the Kenamu Formation, a clear, fining-upward interval can be seen at the base of the formation in both Hekja O-71 (to about 3050 m) and Ralegh N-18 (to about 3400 m), although the relationship is less clear in Gjoa G-37.

The top of the Kenamu Formation is considered to be in the late Bartonian with the Leif Member constrained to the Bartonian (Fig. 2; Dickie et al., 2011; Dafoe, 2021; Dafoe, Dickie, Williams, and McCartney, this volume); however, in Hekja O-71, biostratigraphic ages (Williams, 2007a; Nøhr-Hansen et al., 2016) are inconsistent with the lithostratigraphic assignment of the Leif Member by Moir (1987a). Moir (1987a) placed the top of the Leif Member in what is now considered the middle Lutetian (Fig. 8; Williams, 2007a; Nøhr-Hansen et al., 2016). Instead, the top of the Kenamu Formation can be placed at 1415 m at a small shale break in the sandstone succession, consistent with a marine transgression (albeit brief compared to the Labrador margin; *see* Dafoe, Dickie, Williams, and McCartney, this volume) above the top of the Kenamu Formation and of late Bartonian age. The Leif Member could then be revised to extend from 1575 to 1415 m forming a sandstone-dominated interval at the top of the Kenamu Formation in Hekja O-71. Above this unit, log signatures show a slight decrease in sonic velocity and overall increase in gamma-ray values, but resistivity appears to increase rather than decrease. In comparison, the log signatures at the top of Moir's (1987a) Kenamu Formation do not correspond to the general trends recorded from the Labrador margin. The changes to the lithostratigraphic assignment in the present study can also be related to the coarsening-upward members defined by Balkwill and McMillan (1990). In Hekja O-71, Moir's (1987a) Leif Member marks the top of a generally coarsening-upward interval, which is likely equivalent to the informal middle member, but this relationship cannot be seen in the other two wells. The uppermost coarsening-upward member then corresponds to our revised picks for the Leif Member in Hekja O-71 and Moir's (1987c) Leif Member in Ralegh N-18 (Fig. 9); however, the Leif Member in these wells generally has a more ragged gamma-ray signature than seen to the south, offshore Labrador.

In Ralegh N-18, the Leif Member as picked by Moir (1987c) again appears to have its top in the late Lutetian (Nøhr-Hansen et al., 2016); however, in this well, the Lutetian section is anomalously thick compared to the condensed intervals seen on the Labrador margin (Dafoe, Dickie, Williams, and McCartney, this volume). Conversely, Bujak Davies Group (1989c) interpreted the same interval as Middle–Late Eocene and Nøhr-Hansen (2004) assigned a Middle Eocene (Lutetian–Bartonian) age. The present study favours these latter ages and the original designation of the Leif Member by Moir (1987c). In Goja G-37, Moir (1987b) considered the Leif Member to be present at 1728 to 1650 m and then capped by a very thin interval of the Kenamu Formation up to 1646 m. It is unclear why the Leif Member was not extended to 1588 m to the top of the sandier, coal-bearing unit, but this study does so here (Fig. 6). The presence of coal detritus, glauconite, and shell fragments in this interval suggests a relatively shallow-marine, possibly deltaic setting consistent with Leif Member deposition elsewhere, although the interval is not as sandstone dominated as typical Leif Member sandstone beds from the Labrador margin (Dafoe, 2021; Dafoe, Dickie, Williams, and McCartney, this volume).

In the northern portion of the Saglek Basin, the Kenamu Formation is sandier and siltier than along the Labrador margin. In the former region, the succession includes grey to brown shale and claystone units that become siltier and sandier upward, including discrete sandstone beds, which locally possess a heterolithic character and produce a corresponding ragged gamma-ray log signature. The formation is notably glauconitic at its base in Hekja O-71 and Ralegh N-18 (as defined above), consistent with transgressive flooding. Rare fossil fragments (foraminifera, shells, ostracods) occur, but are more prevalent within the shale- and claystone-dominated intervals. Carbonaceous plant remains and rare coal and coarse sand grains are also present. The Leif Member becomes coarser grained and cleaner upward into medium- to coarse-grained, clear to brown, sandstone beds with pebbles and poor sorting. As with the Kenamu Formation in the northern part of the Saglek Basin, a ragged gamma-ray signature is typical and illustrates the heterolithic, but sandstone-dominated nature of these strata. The formation contains scattered carbonaceous plant remains and rare glauconite and shell fragments. In terms of source areas, Balkwill and McMillan (1990) suggested that Cumberland Sound and Hudson Strait might have been major outlets allowing for thick accumulations of Kenamu Formation deposits.

Biostratigraphy

The Kenamu Formation along the Labrador margin is Ypresian–late Bartonian with Leif Member development in the middle–late Bartonian (Dafoe, 2021; Dafoe, Dickie, Williams, and McCartney, this volume). Thick Eocene deposits are present in Hekja O-71 and the Kenamu Formation, based on the present study (*see* 'Lithostratigraphy' section), conforms well with the above biostratigraphic age range (Fig. 8). Bujak Davies Group (1989b) considered the revised Kenamu Formation interval in this well to be Early–Late Eocene and Williams (2007a) found it to be Ypresian to late Bartonian, results that were essentially verified by Nøhr-Hansen et al. (2016). The revised Leif Member is middle–late Bartonian (Williams, 2007a; Nøhr-Hansen et al., 2016).

In the nearby Ralegh N-18 well, the Eocene section is again thick and interpretations are relatively consistent between different studies (Fig. 9). The placement of the base of the Kenamu Formation in this well, according to the present study, is late Thanetian (Nøhr-Hansen, 2004; Nøhr-Hansen et al., 2016) to Early Eocene (Bujak Davies Group, 1989c). Uncharacteristically, the Kenamu Formation ranges up into the Lutetian of Nøhr-Hansen et al. (2016), but as discussed above, the Middle–Late Eocene ages of Bujak Davies Group (1989a) and Nøhr-Hansen (2004) are preferred here. Accordingly, the Leif Member is likely Middle Eocene (Bujak Davies Group, 1989a; Nøhr-Hansen, 2004). In Gjoa G-37 the Kenamu Formation is Early–Middle Eocene (Bujak Davies Group, 1989a) or Ypresian to Bartonian (Williams, 2007b; Nøhr-Hansen et al., 2016).

There is a hiatus between the Lutetian and Bartonian in Gjoa G-37 and Ralegh N-18 and possibly in Hekja O-71 and in a number of wells on the Labrador Shelf (Nøhr-Hansen et al., 2016). It seems to equate with the "Mid-Eocene Unconformity" of Dalhoff et al. (2003) and the E1 horizon of Gregersen et al. (2018). Generally, the hiatus results in an attenuated Lutetian section, but in Ralegh N-18 it appears to primarily affect the Bartonian based on Nøhr-Hansen et al. (2016). In general, however, the Middle–Upper Eocene section is condensed in both Gjoa G-37 and Ralegh N-18. The age of the Kenamu Formation and Leif Member match well with that of the Labrador margin, following revisions to the base and top of the units. The Kenamu Formation is Ypresian (possibly late Thanetian) to Bartonian and the Leif Member is restricted to the Bartonian.

Key palynoevents characterize the Eocene of the Kenamu Formation. Abundances of the genus *Apectodinium*, which has a restricted age of Thanetian–Ypresian mark the Paleocene–Eocene Thermal Maximum and warm-water conditions during the earliest Eocene (Bujak and Brinkhuis, 1998; Crouch et al., 2001; Nøhr-Hansen et al., 2016). Dinocyst assemblages attain their maximum diversity in the Ypresian, with several species having their LOs at the top of this stage (Nøhr-Hansen et al., 2016). One of these is *Piladinium columna*, which occurs throughout equivalent strata on the Labrador Shelf and in Gjoa G-37. A key event marking the top of the Ypresian in Hekja O-71 is the acme of *Azolla*, a fresh-water fern, in addition to three acmes of *Azolla* spp. in Gjoa G-37 and one in Ralegh N-18 marking another period of warm-water conditions (Nøhr-Hansen et al., 2016). Above this, the Lutetian contains several dinocyst species with attenuated ranges (Nøhr-Hansen et al., 2016). *Eatonicysta ursulae* has its LO just above the base of the Lutetian, close to the top of the nannofossil NP14a Zone (Bujak, 1994). This is the logic for placing the base of the Lutetian at 1680 m in Gjoa G-37 (Nøhr-Hansen et al., 2016). In Hekja O-71, the LO of *Hystrichosphaeridum tubiferum* indicates an age of early Lutetian, and the occurrence of *Alterbidinium*? *bicellulum* as in Gjoa G-37 denotes the top of the stage (Nøhr-Hansen et al., 2016). In younger strata, taxa that have their LO at the top of the Bartonian include the pollen *Extratriporopollenites*.

Paleoenvironments

In the three wells (Fig. 4b, 6, 8, 9), the Kenamu Formation (as delineated above) reflects bathyal, open ocean, outer neritic, or inner neritic settings at its base (Miller and D'Eon, 1987; Bujak Davies Group, 1989c; Williams, 2007a, b; Dafoe, 2021). The deposits then shallow upward into outer shelf, inner shelf, marginal marine (estuarine, lagoonal, delta front, bar), and nonmarine (lacustrine, alluvial fan delta, fluvial, delta plain) settings based on lithological and biostratigraphic studies (Miller and D'Eon, 1987; Bujak Davies Group, 1989c; Williams, 2007a, b; Dafoe, 2021). These environments are generally much shallower than seen to the south in either the Hopedale Basin or southern portion of the Saglek Basin; however, the general shallowing-upward trend is consistent (Dafoe, Dickie, Williams, and McCartney, this volume).

The presence of dinocysts within the Kenamu Formation as described above suggests that marine conditions were maintained. Palynomorph assemblages in Gjoa G-37 indicate predominantly outer shelf settings with open-ocean episodes presumably denoting deeper water conditions (Williams, 2007b). This is in contrast to Hekja O-71 and Ralegh N-18, where marginal marine to inner-neritic paleoenvironments prevailed, with occasional episodes of nonmarine deposition (Williams, 2007a). Confirmation of nonmarine to nearshore deposition in Ralegh N-18 is derived from the common occurrence of the freshwater alga *Pediastrum* (Nøhr-Hansen, 2004) and common *Taurodinium granulatum,* a lacustrine to brackish-water dinocyst. *Taurodinium granulatum* is also common in Hekja O-71 and *Pediastrum* occurs sporadically (Nøhr-Hansen et al., 2016). An acme of the alga *Paralecaniella indentata* in Ralegh N-18 at the Paleocene–Eocene boundary (Nøhr-Hansen, 2004) further suggests shallow-marine settings. *Paralecaniella* is abundant in marginal marine paleoenvironments, but can be present in inner-neritic settings, presumably in the vicinity of deltas or river estuaries, where there is an influx of fresh water (Elsik, 1977). Other authors, including Lebedeva (2010), have proposed that *Paralecaniella* preferred coastal, high-energy, marine settings. Accordingly, the palynological evidence suggests that Hekja O-71 and Ralegh N-18 were close to the shoreline during Kenamu Formation deposition, but were in an area dominated by shallow-marine rather than nonmarine conditions.

As noted above, *Azolla* is common in some Ypresian samples, especially in Gjoa G-37 and Ralegh N-18, but also occurs in Hekja O-71 (Nøhr-Hansen et al., 2016). This small, moss-like, freshwater to brackish-water fern is notable for its nitrogen-fixing properties (van Kempen et al., 2012) and may be an ideal source of hydrocarbons. Brinkhuis et al. (2006) suggested that the high concentrations of *Azolla* in some of the wells of this region denoted overspill of fresh water from the Arctic, which they considered periodically entered the Labrador–Baffin Seaway; however, Nøhr-Hansen et al. (2016) considered that any Arctic-sourced freshwater would have flowed along the eastern margin of the Greenland plate, based on paleogeographic maps of Monger et al. (2014) and Fensome et al. (2014). Since *Azolla* is not found in any of the West Greenland wells, another possibility is that *Azolla* was transported by rivers draining the Canadian landmass.

The Leif Member (Fig. 5, 6) primarily reflects deposition in shallower water environments including outer neritic, middle to inner shelf (delta front and bar), but more characteristically marginal marine to nonmarine settings (lacustrine, delta front, tidal channel, alluvial fan delta, fluvial, and delta plain) based on lithological and biostratigraphic studies in the wells (Miller and D'Eon, 1987; Bujak Davies Group, 1989c; Williams, 2007a, b; Dafoe, 2021). Along the Labrador margin, the Leif Member is a shallow-marine deposit, reflecting deltaic or shoreface settings (Umpleby, 1979; McWhae et al., 1980; Dafoe, 2021; Dafoe, Dickie, Williams, and McCartney, this volume). Considering the overall shallower depositional settings in the northern part of the Saglek Basin, it is possible that much of the Leif Member in northernmost Saglek Basin could reflect both deltaic and nonmarine (fluvial) deposition. As described above, the Leif Member in Gjoa G-37 is more consistent with a shallow-marine, deltaic deposit than shelfal as previously postulated by Miller and D'Eon (1987) and Williams (2007b).

Previous offshore mapping

The top of the Kenamu Formation is one of the most regionally recognizable seismic reflectors in the Saglek and Hopedale basins, traceable over 1200 km (Balkwill and McMillan, 1990). This is because the horizon reflects the top of a coarsening-upward unit that is truncated in the present-day inner and middle shelf by an overlying transgressive shale. Based on their mapping, Balkwill and McMillan (1990) reported that the Kenamu Formation is likely to attain its maximum thickness in the central part of the Saglek Basin east of Hudson Strait. Farther northward, upper Kenamu Formation rocks are locally tilted and eroded at the margins of some fault blocks and volcanic highs or lie near the present-day seafloor (Balkwill, 1987). Whereas the unit is well developed seismically on the Labrador Shelf, Balkwill (1987) indicated that it is less discernible along the southeast Baffin Shelf.

Just east of the international boundary in the Lady Franklin Basin, Sørensen (2006) mapped a top Paleogene horizon, but also showed that much of the Eocene and Oligocene were represented by a hiatus and cannot be easily correlated with the Kenamu Formation. Similarly, Gregersen et al. (2018) mapped their mega-unit D, mostly Eocene, that they described as primarily composed of mass flows such as slumps and basin fans. This would represent a more distal setting than observed in industry wells in western Davis Strait.

Distribution and seismic reflection character

The top of the Kenamu Formation (K) is not a distinct seismic surface as it is to the south along the Labrador margin (Fig. 4a). This is in part due to the sandy nature of both the Leif Member and overlying Mokami and Saglek formations, resulting in a poor lithological contrast and lack of impedance contrast (Fig. 4a, 8, 9); however, seismic interpretation provides good correlation between Hekja O-71 and Ralegh N-18 at the top Kenamu horizon (K; Fig. 4a). Using these wells, the K horizon can be regionally extended in the northernmost Saglek Basin area where data are of fair quality (Fig. 4a). The Leif Member sandstone does not appear to be as seismically perceptible as it is to the south (*see* Dafoe, Dickie, Williams, and McCartney, this volume). An intervening mid-Kenamu horizon (mK) is Lutetian based on correlation to the Hekja O-71 and Ralegh N-18 wells (Fig. 8, 9). The horizon is of moderate amplitude, but notably separates underlying flat-lying, parallel reflections in the lower Kenamu Formation from the overlying more seismically chaotic interval characterizing the upper Kenamu Formation. This may reflect a more mudstone-dominated lower succession from the sandier upper interval that likely includes deltaic deposits with distributary channels. The mK horizon also corresponds to the top of the Leif Member of Moir (1987a) in Hekja O-71 and a coaly interval in Ralegh N-18, both suggesting an upward shallowing from the basal Kenamu Formation.

Lower Mokami and Saglek formations

Lithostratigraphy

Both the Mokami and Saglek formations are intersected in the three exploration wells, but much of the section represents the lower portions of these formations (pre-Middle Miocene; Fig. 6, 8, 9). McWhae et al. (1980) established the Mokami Formation as a brown claystone and soft shale with lesser siltstone, sandstone, and calcareous sandstone and limestone. The Saglek Formation was erected by Umpleby (1979), but later restricted by McWhae et al. (1980) to white, brown, and grey, unconsolidated, feldspathic and cherty sandstone that is poorly sorted, fine- to coarse-grained, and locally contains conglomerate (*see* Dafoe, Dickie, Williams, and McCartney, this volume).

With this study's proposed lithostratigraphic modifications to the Kenamu Formation and Leif Member in Hekja O-71 (*see* 'Kenamu Formation' section), only a sandstone-dominated Saglek Formation remains at the top of the well (Fig. 8). The base of the Saglek Formation is now considered to be at 1415 m and the top is placed at 417 m at the top of the gamma-ray log that shows low values consistent with sandstone. There is, however, a thin interval of Mokami Formation shale in Ralegh N-18 and at the top of Gjoa G-37 (Fig. 6, 9; Moir, 1987b, c). In these two wells, the Mokami Formation consists of grey to brown, silty to sandy claystone with common fossil fragments (pelecypods and gastropods). There are also rare sandstone and limestone beds, as well as local glauconite, coal fragments, and carbonaceous plant remains. Conversely, the Saglek Formation is sandstone dominated and found in the upper part of Hekja O-71 and Ralegh N-18. The top of the Saglek Formation in Ralegh N-18 is again restricted to the top of the gamma-ray log where low values imply the presence of sandstone. Whereas Moir (1987b) indicated a possible Saglek Formation interval at 1455–1026 m in Gjoa G-37, the log evidence is inconclusive. Where present in the wells, the Saglek Formation sandstone units are brown, grey to clear, mostly coarse-grained, but poorly sorted and include very coarse grains and pebbles with thin conglomerate beds. Locally, claystone interbeds are also present. Fossil fragments (pelecypods, indeterminate shell fragments, gastropods, and scaphopods) are rare to common and minor glauconite and rare wood and coal fragments also occur near the top of the succession. Overall, the gamma-ray log shows multiple coarsening-upward intervals, especially in Hekja O-71, but a general sandier-upward trend persists.

Biostratigraphy

In Hekja O-71, the upper section of the well is essentially part of the lower Saglek Formation with possible younger Miocene strata preserved at the top (Fig. 8). This interval was assigned to the Late Eocene to Middle–Late Miocene by Bujak Davies Group (1989b), and later studies generally agree, but with more uncertainty, that the uppermost section is Miocene, or questionably Miocene (Fig. 8; Williams, 2007a; Nøhr-Hansen et al., 2016). Notably, the Saglek Formation is older than seen on the Labrador margin (Rupelian; Dafoe, Dickie, Williams, and McCartney, this volume) with its base in the latest Bartonian (Williams, 2007a; Nøhr-Hansen et al., 2016). The more proximal depositional settings in this part of the basin likely account for older sandstone accumulations, as the source was likely near the well locality. One of the most reliable markers for the top of the Priabonian is the dinocyst *Lentinia serrata*, which has its LO just within the Rupelian, but is used as a top Priabonian marker in the Labrador–Baffin Seaway (e.g. at 1165 m in Hekja O-7; Nøhr-Hansen et al., 2016). An attenuated Upper Oligocene (Chattian) section was reported by Bujak Davies Group (1989b) and Williams (2007a), with a single sample at 895–880 m dated as Chattian by Nøhr-Hansen et al. (2016).

Nearby in Ralegh N-18, the thin claystone interval of the Mokami Formation is Middle to Late Eocene (Bujak Davies Group, 1989c; Nøhr-Hansen et al., 2016). As discussed above, much of the interval is likely Bartonian, which is consistent with the base of the Mokami Formation offshore Labrador (Dafoe, Dickie, Williams, and McCartney, this volume); however, the unit only ranges into the Priabonian instead of the Rupelian, which is again likely a function of proximity to clastic sources. The age of the overlying Saglek Formation is poorly constrained likely due to the coarse-grained nature of the strata and possible reworking. Bujak Davies Group (1989b) considered the lower Saglek Formation to be Early Oligocene (based on assignment to their *Areosphaeridium arcuatum* Zone) to Middle Miocene, with Upper Oligocene rocks being absent. Nøhr-Hansen (2004) and Nøhr-Hansen et al. (2016) placed the base in the Late Eocene (Priabonian). Above this, Nøhr-Hansen et al. (2016) also recorded questionable Lower Oligocene (Rupelian), missing Upper Oligocene section, and a Lower Miocene (Aquitanian) interval; however, based on species of the dinocyst *Chiropteridium* recorded from 1260 m, this uppermost interval could well be Chattian.

In the more distal Gjoa G-37 well, the Mokami Formation claystone was initially considered to be Middle Eocene–Early Oligocene and Middle Miocene or older by Bujak Davies Group (1989a), who suggested there was a Late Oligocene to possibly Early Miocene hiatus. Williams (2007b) and Nøhr-Hansen et al. (2016) found the interval to include Bartonian through Priabonian strata overlain by a Lower Oligocene (Rupelian) interval. Aside from the Middle Miocene age of Bujak Davies Group (1989a), the Bartonian–Rupelian age is consistent with the Labrador margin as described by Dafoe, Dickie, Williams, and McCartney (this volume).

In general, the Mokami Formation of western Davis Strait is Middle Eocene (likely Bartonian) to Rupelian, and the Saglek Formation sandstone units are older, ranging from latest Bartonian to Middle Miocene with attenuated Chattian. Hiatuses are difficult to detect in the younger Paleogene and Neogene sections, because the coarse-grained nature of the sediments destroys most palynomorphs through pulverizing action; however, the hiatus within the Oligocene can also extend into the Miocene (Nøhr-Hansen et al., 2016), and may correspond to the regional unconformity, termed the "Baffin Bay Unconformity" by McWhae (1981). The Oligocene unconformity broadly correlates with the cessation of seafloor spreading in the earliest Oligocene in the northern Labrador Sea and Davis Strait; however, Nøhr-Hansen et al. (2016) considered the development of the Antarctic circum-polar current between 33 and 30 Ma, which marked the onset of Antarctic glaciation, triggering a worldwide drop in sea level as an alternative explanation for the unconformity. This explanation is more consistent with truncation at the base of a thick prograding sandstone succession as seen in seismic data (Fig. 4a; *see* 'Distribution and seismic reflection character' section below).

Paleoenvironments

The Mokami Formation in Ralegh N-18 (Fig. 9) was deposited in marginal marine to outer shelf and/or neritic environments including tidal channel and/or bars and intertidal settings (Miller and D'Eon, 1987; Bujak Davies Group, 1989c; Dafoe, 2021). At the more distal Gjoa G-37 well, the setting is remarkably similar: marginal marine to inner shelf and/or neritic, including delta front and inner to middle shelf bars (Miller and D'Eon, 1987; Williams, 2007b; Dafoe, 2021). In general, Balkwill and McMillan (1990) found that there was a shallowing in their lower Mokami member to nonmarine or marginal marine conditions along the southeast Baffin Shelf and in Saglek Basin during the Oligocene, indicating that shelves were emergent during that time. Whereas shallow-water settings are seen in the Mokami Formation of the Labrador margin, water depths also range into outer shelf to bathyal and/or slope (*see* Dafoe, Dickie, Williams, and McCartney, this volume). Accordingly, the transgression associated with the base of the Mokami Formation in Hopedale Basin (Dafoe, Dickie, Williams, and McCartney, this volume) is much less distinctive in the western Davis Strait region.

The lower part of the Saglek Formation reflects even shallower water conditions and ranges from inner neritic to marginal marine and nonmarine settings. This included coastal to marginal marine and even inner neritic and/or shelf settings (estuarine, delta plain, delta front, shoreface, transgressive, bar, tidal; Miller and D'Eon, 1987; Williams, 2007a; Dafoe, 2021) in the Hekja O-71 well (Fig. 10). Moving offshore to Ralegh N-18 (Fig. 9), the formation is nonmarine, transitional and/or marginal marine, to inner shelf and/or neritic, including delta front, shoreface, tidal channel, delta plain, channel, bar, and more open shelf conditions (Miller and D'Eon, 1987; Bujak Davies Group, 1989c; Dafoe, 2021). Despite these interpretations, the palynomorphs (Williams, 2007a, b), presence of marine macrofossil fragments, and clinoform morphologies seen in seismic data (*see* 'Distribution and seismic reflection character' section) are suggestive of shallow-marine to inner-shelf deposition. Offshore West Greenland, however, dinocysts in the Middle Miocene of Qulleq-1 situated far to the east (Fig. 7) include specimens of the genus *Impagidinium* (Nøhr-Hansen et al., 2016), which usually indicates an open-marine environment and implies that deeper water conditions prevailed along that side of the Labrador–Baffin Seaway.

Distribution and seismic reflection character

Within the lower part of the Mokami and Saglek formations, two horizons are seismically mappable in the vicinity of the wells and separate progradational units (Fig. 4a). At the base of the package, the top Kenamu Formation horizon (K) is overlain by a subtly prograding interval that equates to sandstone development in Hekja O-71 and Ralegh N-18 as part of the Saglek Formation. Clinoforms are long and low-angle and show downlap onto the K horizon. These clinoforms are capped by the Saglek and/or Mokami formation 2 horizon (SM2) that forms the base of a second, overlying progradational clinoform succession also correlated with sandstone units in the two wells. Here, the wells appear to intersect topsets with clinoform foresets found northeast of Ralegh N-18 (Fig. 4a). This clinoform unit has prograded basinward of the underlying unit, but still lies inboard of the present-day shelf break. The Saglek and/or Mokami formation horizon 3 (SM3) caps the top of this prograding clinoform succession and the top of the lower Cenozoic interval.

Distribution of the lower Cenozoic interval

The distribution of the package of rocks encompassing the Cartwright, Gudrid, Kenamu, and lower portions of the Saglek and Mokami formations is shown in Figure 7. This succession forms a Paleocene (late Selandian) to Middle Miocene package of strata. The top of this, a horizon in the middle of the Saglek and Mokami formations, is the SM3 horizon. This surface is tied to the Ralegh N-18 well that extends up into Miocene section within Saglek Formation sandstone units (Fig. 9). The horizon is seismically distinctive as the base of a major, low-angle, prograding clinoform succession (Fig. 4a). In the well, there is no definitive evidence for erosion at the base of the clinoform, but some truncation is likely farther basinward where underlying topsets intersect SM3. The SM3 horizon can be approximately equated with D1, a mid-Miocene unconformity on the West Greenland margin, where well control indicates a significant missing section (Fig. 4a; Gregersen et al., 2018). Outside of well control in the northern part of the Saglek Basin, correlation with published lines from the Greenland margin (e.g. Sørensen, 2006; Gregersen and Bidstrup, 2008; Gregersen et al., 2018) allows for mapping of SM3 across the present study region (Fig. 4b, 7). The distinct clinoform morphology lying above the horizon is not observed regionally, presumably due to a lack of sediment supply (e.g. northwest side of Fig. 4b). Despite this, horizon SM3 can be mapped regionally where it becomes more conformable locally, drapes major structures, or is found within mass-transport deposits (Fig. 4). Generally, horizons lying between the Paleocene basalt flows (Bas) and horizon SM3 could not be correlated outside of the northernmost Saglek Basin due to the structural complexity and low resolution and sparse distribution of seismic data there (Fig. 4b, c).

The lower Cenozoic succession (Fig. 7) shows pinch-out against the basement platform along the western side of the region. In addition, horizon SM3 onlaps against the northern segment of the Davis Strait High, but extends over the southern segment (Fig. 4b, c). The lower Cenozoic package also breaches the volcanic high outside Cumberland Sound, the volcanic high along the southern segment of the Davis Strait High, and the volcanic eruption centres near Gjoa G-37, but onlaps against the remaining volcanic highs (Fig. 4b, 7). North of Hoare Bay, the mapped extent of the lower Cenozoic package is limited by onlap against the basalt high and by the landward extent of seismic data. North of Cape Dyer, shallow basement near the edge of seismic data coverage is again onlapped and partially covered by lower Cenozoic strata (Fig. 4c, 7).

MIDDLE MIOCENE–PLEISTOCENE INTERVAL

Upper Mokami and Saglek formations

Lithostratigraphy and biostratigraphy

There are limited Middle Miocene to Pleistocene, upper Mokami and Saglek Formation rocks preserved in the three exploration wells. In Hekja O-71, a thin Middle to Upper or uncertain Miocene section (Fig. 8; Bujak Davies Group, 1989b; Williams, 2007a; Nøhr-Hansen et al., 2016) and the overlying, sandy succession based on gamma-ray log character likely forms part of the upper Saglek Formation. Along the Labrador margin, Dafoe, Dickie, Williams, and McCartney (this volume) indicated that the Saglek Formation was only found to be as young as Middle Miocene in the wells, but that it likely extends to the Pliocene–Pleistocene based on a substantial clinoform forming the present day shelf as seen in seismic data. In Ralegh N-18, the Middle Miocene to Pliocene–Pleistocene interval of Bujak Davies Group (1989c) is consistent with the latter part of the Saglek Formation with their Late Miocene based on assignment to their *Operculodinium centrocarpum* Zone.

In addition to the industry wells, bedrock corehole samples further confirm the distribution of the upper Saglek Formation (Fig. 2, 10; Table 2). Drill cores from off the mouth of Cumberland Sound and offshore Hall Peninsula were recovered during cruise 76029 (stations 6A, 16, and 16A; MacLean and Falconer, 1977). The cores comprise poorly sorted, semiconsolidated, brown-grey, sandy siltstone with calcareous mud, and contain foraminifera, massive bedding, plant fragments, and coarse sand to small pebbles throughout (MacLean and Falconer, 1977; Dafoe and Williams, 2020a). These cores were studied for foraminifera and palynomorphs and found to be Pliocene to Recent, but contained reworked Paleozoic, Aptian–Cenomanian, Senonian–Early Paleocene, and Eocene palynomorphs (MacLean and Falconer, 1977). The samples from stations 16 and 16A are only 8 km from the upper Albian–Cenomanian sandstone core 74026PHASE4-39 (Fig. 10; Srivastava, 1974; MacLean and Falconer, 1977), and considering the prevalence of reworking in these younger samples, it is possible that 74026PHASE4-39 reflects similar strata. At the mouth of Frobisher Bay, MacLean (1978) and Dafoe and Williams (2020a) reported the recovery of a small sample of semiconsolidated sandstone with granules and small pebbles in the cutting head of a piston corer at station 77027-32 located southwest of 76029-6A. Foraminifera from this sample provided a similar Pliocene–Quaternary age (MacLean, 1978) and were regarded as glacial in origin. At the southwestern end of Cumberland Sound, station 77027-27 sampled semiconsolidated, grey-buff, sandy siltstone, with granules and pebbles, but an analysis of the age was not undertaken (MacLean, 1978; Dafoe and Williams, 2020a); however, based on the lithology and location, this material is probably of similar age and origin as the other four samples from the region (Dafoe and Williams, 2020a). Overall, these samples reflect upper Saglek Formation rocks and are consistent with a lithology expected for the uppermost shelf-building clinoform unit described by Dickie et al. (2011; their unit 'd'; Fig. 2), which is Pliocene–Pleistocene (Dafoe et al., 2018) and seen locally in seismic data in the western Davis Strait (*see* 'Distribution and seismic reflection character' section).

Balkwill and McMillan (1990) found that the upper Mokami Formation member became sandier northward in Saglek Basin and along the southeast Baffin Shelf, where it is designated as the Saglek Formation. Thus, moving northward along the margin, the Mokami and Saglek formations are diachronous. Due to the coarse-grained nature of these deposits, the main river systems, which followed Hudson Strait, Frobisher Bay and Cumberland Sound, were probably short, high-gradient rivers compared to those of offshore Labrador (Balkwill and McMillan, 1990).

Paleoenvironments

The upper part of the Saglek Formation in Hekja O-71 reflects shallow-water conditions including nonmarine to marginal marine settings (Miller and D'Eon, 1987; Williams, 2007a; Dafoe, 2021; Fig. 8). In Ralegh N-18, the formation is nonmarine to transitional and/or marginal marine including deltaic and shoreface deposition (Miller and D'Eon, 1987; Bujak Davies Group, 1989c; Dafoe, 2021). Despite these interpretations, the palynomorphs (Williams, 2007a, b) and the presence of marine macrofossil fragments are both suggestive of shallow-marine to shelfal deposition rather than nonmarine. The coarsening-upward and slightly ragged gamma-ray log character are consistent with deltaic deposition and the clinoforms seen in seismic data (*see* 'Distribution and seismic reflection character' section).

In regard to the upper Saglek Formation preserved in drill cores, the microfossil assemblage for 76029-6A is consistent with a brackish, shallow-marine setting, but 76029-16 and -16A are more consistent with a shallow, open-shelf environment with ice-rafting (MacLean and Falconer, 1977). Glacial ice was likely an important source of sediment and a relatively shallow shelf setting is consistent with the presence of plant detritus (MacLean and Falconer, 1977; Dafoe and Williams, 2020a). Likewise, 77027-32 contains foraminifera, indicating deposition under open-marine conditions (MacLean, 1978). During the Pliocene–Pleistocene, it is possible that water depths had increased as a result of subsidence, resulting in an overall deepening trend in the later part of the upper Cenozoic section. In Qulleq-1, specimens of the genus *Impagidinium* extend into the Late Miocene and Early Pliocene (Nøhr-Hansen et al., 2016), indicating continued open-marine paleoenvironments along the West Greenland margin.

Previous offshore mapping

As the Mokami and Saglek formations have not previously been subdivided at this study's SM3 level, previous interpretations of the formations as a whole are described here. The Mokami Formation downlaps onto the Kenamu Formation on the southeast Baffin Shelf, but it onlaps farther south in the central part of the Saglek Basin (Balkwill and McMillan, 1990). In general, the sandy nature of the post-Eocene succession in northern Saglek Basin and on the southeast Baffin Shelf results in a limited shale succession that could be equated with the Mokami Formation, but it may be more extensive distally or farther from sedimentary sources or sample locations.

MacLean et al. (1990) suggested that the Saglek Formation covers much of the southeast Baffin Shelf, but is thicker where it fills structural lows (Balkwill and McMillan, 1990). The lower part of the Saglek Formation is widely distributed here as the proximal equivalent of the upper Mokami Formation to the south, offshore Labrador (Balkwill and McMillan, 1990), which explains the age discrepancies noted in the wells in this study. Balkwill (1987) described the Saglek Formation as locally lacking the large clinoforms seen to the south; however, east and south of Hekja O-71 and Ralegh N-18, Skaarup et al. (2006) identified an uppermost prograding sedimentary wedge gently dipping basinward that is thickest at the present-day shelf edge and correlates with a free-air gravity anomaly high (*see* Fig. 5, Keen et al., this volume). Strata sampled at 76029–6A may be part of the same prograding package seen in single-channel seismic data (MacLean and Falconer, 1977). In addition to localized clinoform successions, channelling has been noted east of Hudson Strait forming shore-parallel channels 40 to 50 km wide and filled with up to 2 km of sediment (Balkwill and McMillan, 1990; Jauer et al., 2014). Other parts of the Saglek Formation are involved in localized structuring such as near 76029-16 and 76029-16A that flank a volcanic high. In the Hudson Strait area, Cumberland Sound, and Frobisher Bay, thick Pleistocene deposits lie unconformably at the top of the upper Cenozoic interval (Balkwill and McMillan, 1990).

According to Sørensen (2006), in the Lady Franklin Basin, the Neogene is up to about 600 m thick, but is described as transgressive, with about 35 Ma of missing section between it and the underlying Paleogene sediments. Sørensen (2006) further defined a possible Late Miocene unconformity and uppermost Pliocene–Pleistocene contourites, prograding sequences, and slumps. Gregersen et al. (2018) in the same basin, mapped their mega-units 'D' through 'B' of mostly Miocene to Pliocene age with unit 'A' being Pliocene–Pleistocene. These seismic-stratigraphic units were described as mass flows, drifts, slides, and other mass-mobilization features, but south and southwest shelf progradation took place and was probably linked to glaciation.

Distribution and seismic reflection character

As described above, the upper parts of the Saglek and Mokami formations lying above horizon SM3 are defined by a large, low-angle progradational package (Fig. 4a). Clinoforms prograde, but are relatively low amplitude likely due to minimal impedance contrast within a thick sandstone succession, evident at Ralegh N-18 and farther basinward. Also mentioned previously, the base of this unit is equated with the D1 horizon of Gregersen et al. (2018) along the south-central West Greenland margin (Fig. 4b). Similar to the lower Cenozoic interval, the seismic-stratigraphic framework from the West Greenland margin provides control for regional mapping along the Canadian margin and outside the northern part of the Saglek Basin. Clinoforms lying above horizon SM3 are only weakly developed elsewhere (Fig. 4c) and locally correlate to slump or mass-transport deposits basinward of the present-day shelf edge (Fig. 4a, c). An intervening Saglek and/or Mokami formation 4 (SM4) horizon, equated to the C1 horizon of the West Greenland margin (Gregersen et al., 2018), can be locally mapped and may signify a change in the depositional regime to enhanced contourite and submarine processes above (Fig. 4c). In addition, the B1 horizon of Gregersen et al. (2018) can be correlated over much of the region as the Saglek and/or Mokami formation 5 (SM5) horizon (Fig. 4) and appears to represent a slight change in progradational character. Above this horizon, clinoforms are progradational with little preservation of topsets (Fig. 4a) and form the present-day shelf edge (Fig. 4), with associated contourite and mass-transport deposits locally seen along the slope (Fig. 4c).

Distribution of the upper Cenozoic interval

Figure 10 shows the distribution of sedimentary strata younger than the SM3 horizon: this figure is largely similar to the lower Cenozoic distribution map, but includes only the upper Saglek and Mokami formations of Middle Miocene to Pleistocene age (Fig. 7). Along the basement platform on the western edge of the study region, this interval is either truncated at the seafloor or onlaps the platform, but extends out to the eastern edge of the study region along the international boundary. Most notably, the upper Cenozoic interval is truncated at the seafloor several tens of kilometres east of the basement platform near Resolution Island; however, thick Quaternary (Holocene) sediments are present across this region (Praeg et al., 1986; Andrews et al., 2001) and lie unconformably over both the lower and upper Cenozoic intervals. Locally upper Cenozoic strata may even drape the basement platform (e.g. the Lady Franklin Arch). More extensive Pleistocene cover could also account for the sandstone core 77027-27 east of Brevoort Island, but this area is beyond the seismic data coverage. In other parts of the study region, the entire unit can be quite thin where it drapes major structures (Fig. 4). The interval overlies the southern segment of the Davis Strait High (Fig. 4b), but generally onlaps the northern portion of the high (Fig. 4c). The upper Cenozoic strata cover most of the basaltic highs, albeit as a relatively thin cover over shallow portions of the highs (Fig. 4b), except for the one south of Cape Dyer, which lies near the seafloor.

CONCLUSIONS

The western Davis Strait region lies between the Labrador Sea to the south, Baffin Bay to the north, and west of the International Boundary with Greenland. During rifting between the paleo-North American and Greenland plates and corresponding opening of the Labrador–Baffin Seaway, the western Davis Strait region experienced Cretaceous through Early Paleocene extension, followed by seafloor spreading beginning at chron C27n. Subsequently, deformation associated with the change in plate motions (between chrons C25n and C24n) took place, resulting in extensive translational motion in the Davis Strait, until seafloor spreading ended in the Late Eocene (chron C13). This tectonic history affected basement structure in the region and the related accommodation space available for sediment accumulation. A shallow basement platform is mapped along the western edge of the region and comprises offshore extensions of Precambrian crystalline rocks, and an overlying pre-rift Paleozoic succession sitting within and outside the mouth of Cumberland Sound, both of which are constrained by corehole samples and seismic interpretation. The distribution of Paleozoic rocks is modified from previous studies with an absence of Paleozoic rocks north of the southeastern tip of Cumberland Peninsula. Precambrian rocks also are interpreted to form the core of two ridges that comprise the Davis Strait High (but that likely have some basaltic cover), as well as the Lady Franklin Arch, which separates the northernmost Saglek Basin from Cumberland Basin to the north.

Crustal extension during the Cretaceous is indicated by a graben structure in Cumberland Sound that contains Lower Cretaceous bedrock samples, with fine-grained lithologies, possibly equivalent to the Snorri Member of the Bjarni Formation, reflecting restricted marine settings. Basinward, a postulated Cretaceous sample from

Figure 10. Distribution map of the Middle Miocene to Pleistocene (upper Cenozoic) interval along the western Davis Strait region with the location of the basement platform and highs and relevant seabed samples from GSC marine cruises. Basin outlines are from Keen et al. (this volume). *See* Figure 1b for abbreviated names. Additional projection information: Central Meridian: 60°W; Standard Parallels: 65, 75°W; Latitude of Origin: 65°N.

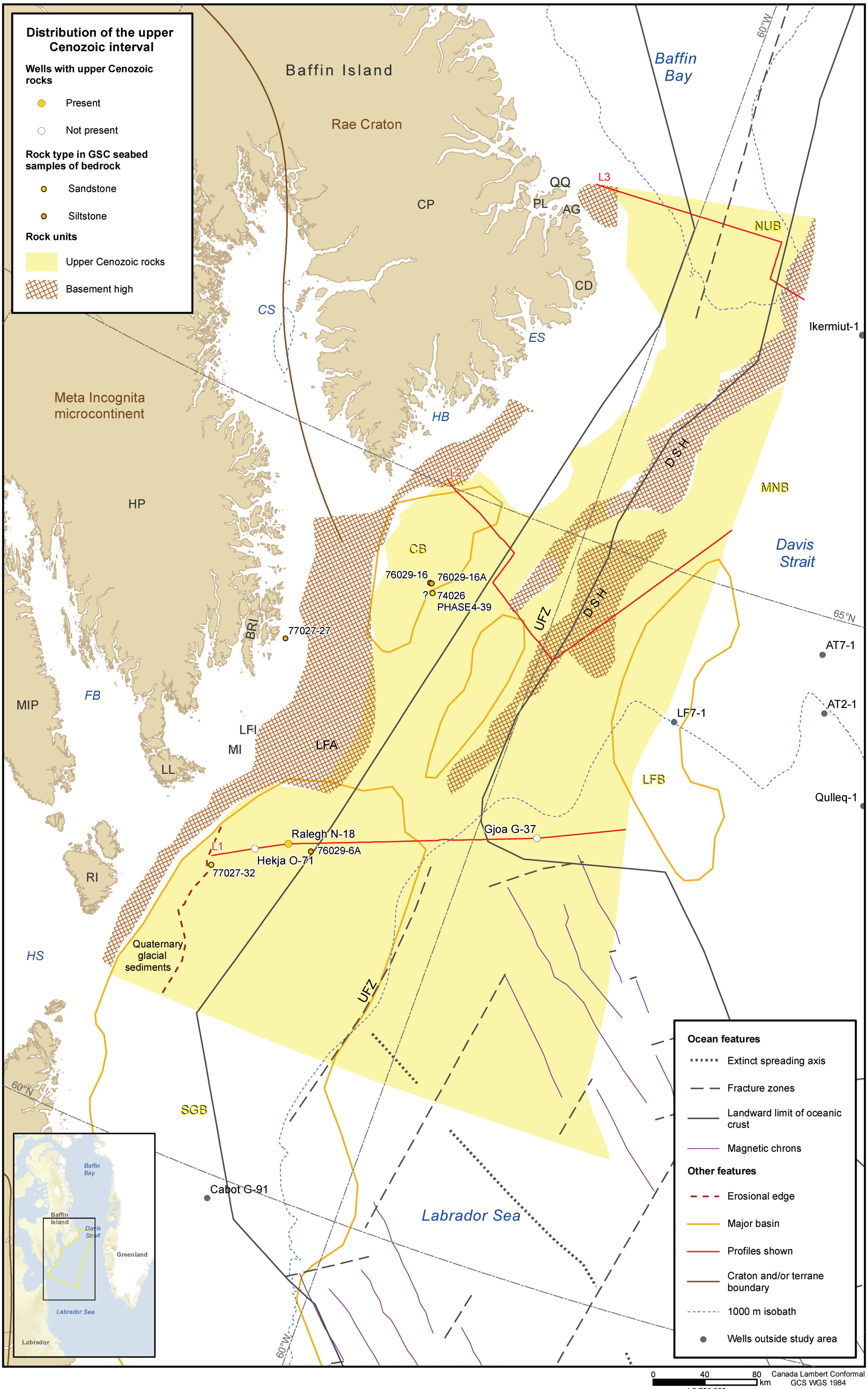
Distribution of the upper Cenozoic interval
Wells with upper Cenozoic rocks
Present
Not present
Rock type in GSC seabed samples of bedrock
Sandstone
Siltstone
Rock units
Upper Cenozoic rocks
Basement high
Baffin Island
Rae Craton
Baffin Bay
60°W
QQ
L3
PL
AG
CP
NUB
CD
CS
ES
Ikermiut-1
Meta Incognita microcontinent
HB
DSH
L2
MNB
HP
CB
Davis Strait
76029-16
76029-16A
?
74026
PHASE4-39
DSH
UFZ
65°N
BRI
77027-27
AT7-1
FB
MIP
LF7-1
AT2-1
LFI
MI
LFA
LL
LFB
Qulleq-1
Ralegh N-18
Gjoa G-37
L1
Hekja O-71
76029-6A
77027-32
RI
HS
Quaternary glacial sediments
UFZ
60°N
SGB
Ocean features
Extinct spreading axis
Fracture zones
Landward limit of oceanic crust
Magnetic chrons
Other features
Erosional edge
Major basin
Profiles shown
Craton and/or terrane boundary
1000 m isobath
Wells outside study area
Cabot G-91
Labrador Sea
Baffin Bay
Baffin Island
Davis Strait
Greenland
Labrador Sea
Labrador
60°W
0
40
80
km
1:2 750 000
Canada Lambert Conformal
GCS WGS 1984

Cumberland Basin is suggested to be significantly younger with reworked Cretaceous palynomorphs similar to nearby corehole samples. A thick succession of Lower to Upper Cretaceous rocks is also inferred from within the Canadian portions of the Lady Franklin and Maniitsoq basins, and is confirmed in the LF7-1 well on the south-central West Greenland margin. Here, growth of strata into normal faults signifies deposition during active extension similar to strata from the Bjarni Formation, and the overlying seismically transparent unit resembles the shale units of the Markland Formation. Cretaceous rocks may also be locally present below the regionally extensive volcanic cover inboard of the landward limit of oceanic crust, especially in the Cumberland Basin and northern part of the Saglek Basin, but this has not been confirmed. The Markland Formation, of Late Cretaceous to early Selandian age is, however, represented by Paleocene shale intervals at the base of Gjoa G-37, some of which are interstratified with basalt flows.

As a result of a mantle plume arriving in the region in the Paleocene, volcanic rocks cover much of the western Davis Strait region as a package of high-amplitude, discontinuous reflectors that generally mask the underlying stratigraphy and structure except for the thin cover in the Lady Franklin Basin. In the three wells and along the western margin of the study region, these rocks can be as old as Danian, but appear to be mostly Selandian to Thanetian based on both palynological and radiometric age dates. East of the landward limit of oceanic crust, however, basal Ypresian basalt flows occur over the Davis Strait High, supporting a diachronous eruption age. Sills and dykes in the Lady Franklin Basin may be of similar age, but could also be older based on Cretaceous volcanic rocks drilled nearby on the West Greenland margin. The present study shows the extent of both volcanic cover and highs. Basalt forms a large ridge bordering the eastern side of Cumberland Basin, which may be related to volcanic margin development similar to that seen to the north offshore Cape Dyer and to the south at Hekja O-71. The Gjoa High is refined and a nearby unnamed volcanic high is mapped to the southwest. Another ridge of basalt lies on downfaulted basement along the eastern edge of the Davis Strait High.

The volcanic features, basement structures, and faulting make stratigraphic correlations throughout the region difficult, due to limited sampling and the inability to extend correlations over large basement and volcanic highs; however, lithostratigraphic units have been extrapolated northward from the Labrador margin into the three exploration wells and show similar characteristics in lithology and log character, but are generally coarser grained and represent shallower water settings compared to the south. Seabed bedrock drill cores provide further information on the lithology, paleoenvironments, and age of stratigraphic intervals. The Cenozoic includes the Cartwright, Gudrid, Kenamu, and lower Mokami and Saglek formations, comprising the lower Cenozoic interval, and the upper portions of the Mokami and Saglek formations, comprising the upper Cenozoic interval.

Shale and/or claystone dominate the Cartwright Formation, whereas the Gudrid Formation is composed of sandstone. The Cartwright Formation shale beds are herein restricted to those lying below the Gudrid Formation in the wells, but three drill cores in the central part of the study region extend the distribution of these rocks. These shale units are Selandian–Thanetian, but extend into the Ypresian where the Gudrid Formation is absent. Only the upper Gudrid Formation is sampled in the northern part of the Saglek Basin and is late Thanetian–Ypresian. The shale units reflect shelfal paleoenvironments (possibly even bathyal) and the sandstone units represent marginal marine tidal channel and shoreface settings. In seismic data, the top Cartwright and/or Gudrid formation is a high-amplitude, distinct, and mappable horizon in the vicinity of the wells and may show local tidal-channel development.

The overlying Kenamu Formation is sandier and siltier than seen along the Labrador margin, but is still dominated by grey-brown shale or claystone. The present study extends the Kenamu Formation deeper in the Hekja O-71 and Ralegh N-18 wells such that the log signature and transgressive character match with that seen along the Labrador margin. The top of the Kenamu Formation and Leif Member are reinterpreted in Hekja O-71 and Gjoa G-37 to better match the lithology, biostratigraphy, and seismic constraints. The overall changes to lithostratigraphic assignments agree more closely with the informal members of Balkwill and McMillan (1990) and with a Ypresian to Bartonian (Early–Middle Eocene) age for the Kenamu Formation. The shale units reflect shelfal to bathyal and marginal marine deposition and the sandstone beds of the Leif Member are consistent with fluviodeltaic to marginal marine settings. Unlike the Labrador margin, the top Kenamu Formation is not seismically distinct due to a lack of impedance contrast between the Leif Member or Kenamu Formation shale units and the overlying sandstone or sandy claystone of the Mokami and Saglek formations.

Finally, the Mokami Formation is grey-brown, silty to sandy claystone, reflecting nonmarine to shelfal conditions. Conversely, the Saglek Formation is a poorly sorted, locally conglomeratic sandstone, representing nonmarine to shallow-marine settings: this formation includes prograding, sandy clinoforms and channellized intervals seen locally in the region. The lithostratigraphic assignments in the wells for both formations are modified in the present study. The Markland Formation ranges from the Bartonian to Rupelian, consistent with the Labrador margin, but the lower part of the Saglek Formation is older than the rocks seen on the Labrador margin (latest Bartonian), likely due to a proximity to the sediment source and the overall shallow depositional settings. The Mokami Formation transgression is less distinctive than on the Labrador margin with shallow-marine to shelfal settings, whereas the Saglek Formation reflects inner shelf to shallow-marine conditions characterized by two prograding clinothems capped by the SM3 horizon. Cumulatively, the lower Cenozoic interval is regionally distributed except over some crystalline basement and volcanic highs. Limited post-Middle Miocene Saglek Formation is preserved in the wells, but at least five coreholes are attributed to the uppermost Pliocene–Quaternary interval. In this younger section of the Saglek Formation, depositional environments are shelfal to shallow marine, with a possible deepening trend related to subsidence following glaciation. A large prograding clinothem with intervening seismic horizons is locally observed. The upper Cenozoic interval is again distributed over much of the region, but onlaps some basement and volcanic highs, and, in places, is only attributed to late Quaternary (Holocene) cover.

A combination of the exploration wells, coreholes, previous mapping efforts, and the lithostratigraphy of the Labrador margin and seismic stratigraphic framework from the West Greenland margin allows for regional mapping and interpretation in the western Davis Strait region. This is the first study to provide detailed mapping and interpretation of the stratigraphic succession and structural complexity of the region.

ACKNOWLEDGMENTS

The authors would like to acknowledge support of this work through the Baffin Island and the Labrador–Baffin Seaway Geological Synthesis activity under the Geo-mapping for Energy and Minerals program (GEM-2). Thanks to Canada Cities Services, Suncor, and TGS for allowing the authors to show the seismic data. The authors wish to acknowledge the constructive reviews of Jon Ineson and Brian MacLean. A special thanks to Leith MacLeod for design and compilation of the maps. The authors thank Dawn Kellett for her helpful discussions and interpretation of some of the K-Ar and Ar-Ar age dating results. Tom Brent, Chris Jauer, and Paul Lake kindly provided some of the legacy seismic data compilation and processing of the regional data. Thanks to Ulrik Gregersen for providing interpretation at the northeastern end of seismic line 1 and the authors are indebted to Sheila Hynes for some of the GIS compilation and processing. A special thanks to Paul Champagne for his dedicated work on the seismic line figures.

REFERENCES

Andrews, J.T., Jennings, A.E., and MacLean, B., 2001. Late Quaternary stratigraphy of Hatton and Resolution basins, east of Hudson Strait; *in* Marine Geology of Hudson Strait and Ungava Bay, Eastern Arctic Canada: Late Quaternary Sediments, Depositional Environments, and Late Glacial-Deglacial History Derived from Marine and Terrestrial Studies, (ed.) B. MacLean; Geological Survey of Canada, Bulletin 566, p. 57–64. https://doi.org/10.4095/212208

Balkwill, H.R., 1987. Labrador basin: structural and stratigraphic style; *in* Sedimentary Basins and Basin-Forming Mechanisms, (ed.) C. Beaumont and A.J. Tankard; Canadian Society of Petroleum Geologists, Memoir, v. 12. p. 17–43.

Balkwill, H.R. and McMillan, N.J., 1990. Mesozoic-Cenozoic geology of the Labrador Shelf; *in* Chapter 7 of Geology of the Continental Margin of Eastern Canada, (ed.) M.J. Keen and G.L. Williams; Geological Survey of Canada, Geology of Canada, no. 2, p. 295–324 (*also* Geological Society of America, The Geology of North America, v. I-1). https://doi.org/10.4095/132708

Beh, R.L., 1975. Evolution and geology of western Baffin Bay and Davis Strait, Canada; *in* Canada's Continental Margins and Offshore Petroleum Exploration, (ed.) D.J. Yorath and E.R. Parker; Canadian Society of Petroleum Geologists, Memoir 4, p. 453–476.

Bell, J.S., 1989. Labrador Sea; Geological Survey of Canada, East Coast Basin Atlas Series, 135 p. https://doi.org/10.4095/127152

Bell, J.S. and Campbell, G.R., 1990. Petroleum Resources, Chapter 12; *in* Geology of the Continental Margin of Eastern Canada, Volume 2, (ed.) M.J. Keen and G.L. Williams; Geological Survey of Canada, Geology of Canada, p. 677–720 (*also* Geological Society of America, The Geology of North America, v. I-1). https://doi.org/10.4095/132720

Bingham-Koslowski, N., 2018. Descriptions of drill cores and thin sections from lower Paleozoic strata, southeastern Baffin Island shelf, Nunavut; Geological Survey of Canada, Open File 8409, 78 p. https://doi.org/10.4095/308354

Brinkhuis, H., Schouten, S., Collinson, M.E., Sluijs, A., Sinninghe-Damste, J.S., Dickens, G.R., Huber, M., Cronin, T.M., Onodera, J., Takahashi, K., Bujak, J.P., Stein, R., van der Burgh, J., Eldrett, J.S., Harding, I.C., Lotter, A.F., Sangiorgi, F., van Konijnenburg-van Cittert, H., de Leeuw, J.W.,…and the Expedition 302 Scientists, 2006. Episodic fresh surface waters in the early Eocene Arctic Ocean; Nature, v. 441, no. 7093, p. 606–609. https://doi.org/10.1038/nature04692

Budkewitsch, P., Pavlic, G., Oakey, G., Jauer, C., and Decker, V., 2013. Reconnaissance mapping of suspect oil seep occurrences in Baffin Bay and Davis Strait using satellite radar: preliminary results; Geological Survey of Canada, Open File 7068, 1 .zip file. https://doi.org/10.4095/292280

Bujak, J.P., 1994. New dinocyst taxa from the Eocene of the North Sea; Journal of Micropalaeontology, v. 13, p. 119–131. https://doi.org/10.1144/jm.13.2.119

Bujak, J.P. and Brinkhuis, H., 1998. Global warming and dinocyst changes across the Paleocene/Eocene epoch boundary; *in* Late Paleocene–early Eocene climatic and biotic events in the marine and terrestrial records, (ed.) M.-P. Aubry, S.G. Lucas, and W.A. Berggren; Columbia University Press, New York, New York, p. 277–295.

Bujak Davies Group, 1989a. Biostratigraphy and Maturation of 17 Labrador and Baffin Shelf wells, Volume 3: Gilbert F-53 and Gjoa G-37; Geological Survey of Canada, Open File 1931, 65 p. https://doi.org/10.4095/130624

Bujak Davies Group, 1989b. Biostratigraphy and maturation of 17 Labrador and Baffin shelf wells, Volume 4: Hekja O-71 & Hopedale E-3; Geological Survey of Canada, Open File 1932, 54 p. https://doi.org/10.4095/130625

Bujak Davies Group, 1989c. Biostratigraphy and maturation of 17 Labrador and Baffin shelf wells, Volume 7: Pothurst P-19 and Ralegh C-02; Geological Survey of Canada, Open File 1935, 54 p. https://doi.org/10.4095/130628

Burden, E.T. and Langille, A.B., 1990. Stratigraphy and sedimentology of Cretaceous and Paleocene strata in half-grabens on the southeast coast of Baffin Island, Northwest Territories; Bulletin of Canadian Petroleum Geology, v. 38, p. 185–196.

Burden, E.T. and Langille, A.B., 1991. Palynology of Cretaceous and Tertiary strata, northeast Baffin Island, Northwest Territories, Canada: implications for the history of rifting in Baffin Bay; Palynology, v. 15, p. 91–114. https://doi.org/10.1080/01916122.1991.9989392

Canterra Energy Ltd., 1982. Well History Report Canterra et al Ralegh N-18; on file with the Canada–Newfoundland and Labrador Offshore Petroleum Board (C-NLOPB), 146 p.

Chalmers, J.A. and Pulvertaft, T.C.R., 2001. Development of the continental margins of the Labrador Sea: a review; *in* Non-volcanic Rifling of Continental Margins: a Comparison of Evidence from Land and Sea, (ed.) R.C.L. Wilson, R.B. Whitmarsh, B. Taylor, and N. Froitzhelm; Geological Society, London, Special Publications, v. 187, p. 77–105. https://doi.org/10.1144/GSL.SP.2001.187.01.05

Christiansen, F.G., Olsen, J.C., Planke, S., Amundsen, H.E.F., Bojensen-Koefoed, J.A., Dalhoff, F., Myklebust, R., Nøhr-Hansen, H., and Sønderholm, M., 2002. West Greenland basin development — new evidence of old sediments; American Association of Petroleum Geologists Hedberg Conference, abstract 90022, 3 p.

Clarke, D.B. and Pedersen, A.K., 1976. Tertiary volcanic province of West Greenland; *in* Geology of Greenland, (ed.) A. Esher and W.S. Watt; Geological Survey of Greenland, Copenhagen, Denmark, p. 364–385.

Clarke, D.B. and Upton, B.G.J., 1971. Tertiary basalts of Baffin Island: field relations and tectonic setting; Canadian Journal of Earth Sciences, v. 8, p. 248–258. https://doi.org/10.1139/e71-025

Crouch, E.M., Heilmann-Clausen, C., Brinkhuis, H., Morgans, H.E.G., Rogers, K.M., Egger, H., and Schmitz, B., 2001. Global dinoflagellate event associated with the late Paleocene thermal maximum; Geology, v. 29, no. 4, p. 315–318. https://doi.org/10.1130/0091-7613(2001)029%3c0315:GDEAWT%3e2.0.CO%3b2

Dafoe, L.T., 2021. Paleoenvironmental analyses and revised lithostratigraphic assignments for 28 wells of the Hopedale and Saglek basins, offshore eastern Canada; Geological Survey of Canada, Open File 8810, 209 p. https://doi.org/10.4095/328477

Dafoe, L.T. and Williams, G.L., 2020a. A reassessment of Mesozoic–Cenozoic seabed samples of bedrock from the western Davis Strait and eastern Baffin Island margin, offshore Nunavut: new insights into their lithology, age, and paleoenvironment of deposition; Geological Survey of Canada, Open File 8702, 41 p. https://doi.org/10.4095/321758

Dafoe, L.T. and Williams, G.L., 2020b. Lithological, sedimentological, ichnological, and palynological analysis of 37 conventional core intervals from 15 wells, offshore Labrador (Newfoundland and Labrador) and southeast Baffin Island (Nunavut); Geological Survey of Canada, Bulletin 613, 146 p. https://doi.org/10.4095/315362

Dafoe, L.T., Dickie, K., Williams, G.L., Jauer, C.D., Hynes, S., Brent, T.A., Li, Q., Oakey, G.N., Potter, D.P., Haggart, J.W., Smyth, H.R., Currie, L.D., Sweet, A.R., DesRoches, K., and Szlavko, B., 2016a. Report of activities for the stratigraphic and tectonic framework for the Baffin Bay Petroleum Systems: GEM 2 Baffin Project; Geological Survey of Canada, Open File 7960, 10 p. https://doi.org/10.4095/297248

Dafoe, L.T., Dickie, K., Williams, G.L., Jauer, C.D., Li, Q., Dehler, S., Potter, D.P., Hynes, S., Patton, E., Bates, J., Haggart, J.W., and Clark, K., 2016b. Report of activities for the Stratigraphic and Tectonic Framework for the Baffin Bay Petroleum Systems (2016); Geological Survey of Canada, Open File 8144, 10 p. https://doi.org/10.4095/299240

Dafoe, L.T., Dickie, K., Williams, G.L., and Keen, C.E., 2017. A late rift to post-rift shoreline clinoform and shelf-edge model for the offshore Labrador margin, Canada; 5th Atlantic Conjugate Margins Conference, August 22th–25th, 2017, Pernambuco, Brazil, 1 p. (abstract).

Dafoe, L.T., Dickie, K., and Williams, G.L., 2018. A clinoform trajectory model for Late Cretaceous and Cenozoic sedimentation on the Labrador-Baffin Island margins; *in* Program and Abstracts, 2018 Conjugate Margins Conference; Halifax, Nova Scotia, August 19–22, 2018, p. 74.

Dalhoff, F., Chalmers, J.A., Gregersen, U., Nøhr-Hansen, H., Rasmussen, J.A., and Sheldon, E., 2003. Mapping and facies analysis of Paleocene–mid-Eocene seismic sequences, offshore southern West Greenland; Marine and Petroleum Geology, v. 20, p. 935–986. https://doi.org/10.1016/j.marpetgeo.2003.09.004

Dalhoff, F., Larsen, L.M., Ineson, J.R., Stouge, S., Bojesen-Koefoed, J.A., Lassen, S., Kuijpers, A., Rasmussen, J.A., and Nøhr-Hansen, H., 2006. Continental crust in the Davis Strait: new evidence from seabed sampling; Geological Survey of Denmark and Greenland Bulletin, v. 10, p. 33–36. https://doi.org/10.34194/geusb.v10.4901

Dickie, K., Keen, C.E., Williams, G.L., and Dehler, S.A., 2011. Tectonostratigraphic evolution of the Labrador Margin, Atlantic Canada; Marine and Petroleum Geology, v. 28, p. 1663–1675. https://doi.org/10.1016/j.marpetgeo.2011.05.009

Duk-Rodkin, A. and Hughes, O.L., 1994. Tertiary-Quaternary drainage of the pre-glacial Mackenzie Basin; Quaternary Geology, v. 22–23, p. 221–241. https://doi.org/10.1016/1040-6182(94)90015-9

Elsik, W.C., 1977. Contributions of stratigraphic palynology (with emphasis on North America), Cenozoic palynology; American Association of Stratigraphic Palynologists, Contribution Series 5a, 169 p.

Fensome, R.A., Blakey, R., Clague, J., Harrison, C., Monger, J., Storer, J., Williams, G., Dehler, S., Duk-Rodkin, A., Eberth, D., Hickson, C., Leckie, D., MacRae, A., Mathewes, R., Nassichuk, W., Price, R., Rybczynski, N., Wielens, H., Williamson, M.-C., Yorath, C., 2014. Final approach: Canada 65.5 million years ago; Chapter 10 *in* Four Billion Years and Counting: Canada's Geological Heritage, (ed.) R.A. Fensome, G.L. Williams, A. Achab, J. Clague, D. Corrigan, J. Monger, and G. Nowlan; Canadian Federation of Earth Sciences and Nimbus Publishing, Halifax, Nova Scotia, p. 192–215.

Funck, T., Jackson, H.R., Louden, K.E., and Klingelhöfer, F., 2007. Seismic study of the transform-rifted margin in Davis Strait between Baffin Island (Canada) and Greenland: What happens when a plume meets a transform; Journal of Geophysical Research, v. 112, no. B4, cit. no. B04402. https://doi.org/10.1029/2006JB004308

General Bathymetric Chart of the Oceans (GEBCO), 2014. GEBCO 2014 Grid; International Hydrographic Organization and the Intergovernmental Oceanographic Commission (of UNESCO). www.gebco.net [accessed May 19, 2015]

Gradstein, F.M., Ogg, J.G., Schmitz, M., and Ogg, G., 2012. The Geologic Time Scale 2012; Elsevier B.V., Oxford, United Kingdom, 1144 p.

Grant, A.C., 1975. Geophysical results from the continental margin off southern Baffin Island; *in* Canada's Continental Margins and Offshore Petroleum Exploration, (ed.) D.J. Yorath and E.R. Parker; Canadian Society of Petroleum Geologists, Memoir 4, p. 411–431.

Gregersen, U. and Bidstrup, T., 2008. Structures and hydrocarbon prospectivity in the northern Davis Strait area, offshore West Greenland; Petroleum Geoscience, v. 14, p. 151–166. https://doi.org/10.1144/1354-079308-752

Gregersen, U., Hopper, J.R., Knutz, P., 2013. Basin seismic stratigraphy and aspects of prospectivity in the NE Baffin Bay, northwest Greenland; Marine and Petroleum Geology, v. 46, p. 1–18.

Gregersen, U., Andersen, M.S., Nøhr-Hansen, H., Sheldon, E., Kokfelt, T.F., Olivarius, M., Knudsen, C., Jakobsen, K.G., and Adolfssen, J.S., 2018. New subsurface mapping offshore southern West Greenland using geophysical and geological data; Geological Survey of Denmark and Greenland Bulletin, v. 41, p. 57–62. https://doi.org/10.34194/geusb.v41.4342

Gregersen, U., Knutz, P.C., Nøhr-Hansen, H., Sheldon, E., and Hopper, J.R., 2019. Tectonostratigraphy and evolution of the West Greenland continental margin; Bulletin of the Geological Society of Denmark, v. 67, p. 1–21. <https://2dgf.dk/publikationer/bulletin/bulletin-volume-67-2019/>

Hood, P. and Bower, M., 1975. Aeromagnetic reconnaissance of Davis Strait and adjacent areas; *in* Canada's Continental Margins and Offshore Petroleum Exploration, (ed.) D.J. Yorath and E.R. Parker; Canadian Society of Petroleum Geologists, Memoir 4, p. 433–451.

Jackson, G.D., 1998. Geology, Okoa Bay-Padloping Island area, District of Franklin, Northwest Territories; Geological Survey of Canada, Open File 3532, scale 1:250 000. https://doi.org/10.4095/209911

Jansa, L.F., 1976. Lower Paleozoic radiolarian-bearing limestones from the Baffin Island shelf; *in* Report of Activities, Part B; Geological Survey of Canada, Paper 76-1B, p. 99–105. https://doi.org/10.4095/104085

Jauer, C.D., 2009. Hekja O-71, a major stranded gas discovery offshore Baffin Island with seismic examples of probable gas vents; Geological Survey of Canada, Open File 6432, 1 sheet. https://doi.org/10.4095/248252

Jauer, C.D. and Budkewitsch, P., 2010. Old marine seismic and new satellite radar data: petroleum exploration of northwest Labrador Sea, Canada; Marine and Petroleum Geology, v. 27, p. 1379–1394. https://doi.org/10.1016/j.marpetgeo.2010.03.003

Jauer, C., Wielens, H., and Williams, G., 2009. Hydrocarbon prospectivity of Davis Strait and Labrador Shelf: seismic setting and stratigraphy for Gjoa G-37, Hekja O-71, Rut H-11, Gilbert F-53, Karlsefni A-13, and Skolp E-07; Geological Survey of Canada, Open File 5910, 6 sheets. https://doi.org/10.4095/247336

Jauer, C.D., Oakey, G.N., Williams, G., and Wielens, J.B.W.H., 2014. Saglek Basin in the Labrador Sea, east coast Canada; stratigraphy, structure and petroleum systems; Bulletin of Canadian Petroleum Geology, v. 62, issue 4, p. 232–260. https://doi.org/10.2113/gscpgbull.62.4.232

Jauer, C.D., Oakey, G.N., and Li, Q., 2019. Western Davis Strait, a volcanic transform margin with petroliferous features; Marine and Petroleum Geology, v. 107, p. 59–80. https://doi.org/10.1016/j.marpetgeo.2019.05.004

Johnson, G.L., Srivastava, S.P., Campsie, J., and Rasmussen, M., 1982. Volcanic rocks in the Labrador Sea and environs and their relation to the evolution of the Labrador Sea; *in* Current Research, Part B; Geological Survey of Canada, Paper 82-1B, p. 7–20. https://doi.org/10.4095/124903

Keen, C.E., Dickie, K., and Dehler, S.A., 2012. The volcanic margins of the northern Labrador Sea: insights to the rifting process; Tectonics, v. 31, no. 1, cit. no. TC1011. https://doi.org/10.1029/2011TC002985

Keen, C.E., Dickie, K., and Dafoe, L.T., 2018a. Structural characteristics of the ocean-continent transition along the rifted continental margin, offshore central Labrador; Marine and Petroleum Geology, v. 89, no. 2, p. 443–463. https://doi.org/10.1016/j.marpetgeo.2017.10.012

Keen, C.E., Dickie, K., and Dafoe, L.T., 2018b. Structural evolution of the rifted margin off northern Labrador: the role of hyper-extension and magmatism; Tectonics, v. 37, p. 1955–1972. https://doi.org/10.1029/2017TC004924

Kerr, J.W., 1967. A submerged continental remnant beneath the Labrador Sea; Earth and Planetary Science Letters, v. 2, p. 283–289. https://doi.org/10.1016/0012-821X(67)90143-4

Klose, G.W., Malterre, E., McMillan, N.J., and Zinkan, C.G., 1982. Petroleum exploration offshore southern Baffin Island, northern Labrador Sea, Canada; *in* Arctic Geology and Geophysics, (ed.) A.F. Embry and H.R. Balkwill; Canadian Society of Petroleum Geologists, Memoir 8, Proceedings of the Third International Symposium on Arctic Geology, Calgary, Alberta, p. 233–244.

Kranck, K., 1966. Sediments of Exeter Bay, Baffin Island, District of Franklin; Geological Survey of Canada, Paper 66-8, 60 p. https://doi.org/10.4095/100941

Larsen, L.M. and Dalhoff, F., 2006. Composition, age, and geological and geotectonic significance of igneous rocks dredged from the northern Labrador Sea and the Davis Strait; Danmarks og Grønlands Geologiske Undersøgelse, Rapport, 2006/43, 67 p.

Larsen, L.M., Heaman, L.M., Creaser, R.A., Duncan, R.A., Frei, R., and Hutchison, M., 2009. Tectonomagmatic events during stretching and basin formation in the Labrador Sea and the Davis Strait: evidence from age and composition of Mesozoic to Palaeogene dyke swarms in West Greenland; Journal of the Geological Society, v. 166, p. 999–1012. https://doi.org/10.1144/0016-76492009-038

Larsen, L.M., Pedersen, A.K., Tegner, C., Duncan, R.A., Hald, N., and Larsen, J.G., 2016. Age of Tertiary volcanic rocks on the West Greenland continental margin: volcanic evolution and event correlation to other parts of the North Atlantic Igneous Province; Geological Magazine, v. 153, no. 3, p. 487–511. https://doi.org/10.1017/S0016756815000515

Le Pichon, X., Hyndman, R.D., and Pautot, G., 1971. Geophysical study of the opening of the Labrador Sea; Journal of Geophysical Research, v. 76, p. 4724–4743. https://doi.org/10.1029/JB076i020p04724

Lebedeva, N.K., 2010. Palynofacies in Upper Cretaceous sediments of Northern Siberia; Stratigrafiya Geologicheskaya Korrelyastiya, v. 18, no. 5, p. 70–87 (Original in Russian. English version: v. 18, p. 532–549).

MacLean, B., 1977. Hudson 77-027; Geological Survey of Canada, 27 p. <https://ed.gdr.nrcan.gc.ca/cruise_report_e.php> [accessed April 18, 2019]

MacLean, B., 1978. Marine geological-geophysical investigations in 1977 of the Scott Inlet and Cape Dyer-Frobisher Bay areas of the Baffin Island continental shelf; *in* Current Research, Part B; Geological Survey of Canada, Paper 78-1B, p. 13–20. https://doi.org/10.4095/103568

MacLean, B., 1980. Cruise report C.S.S. Hudson 80-028; Geological Survey of Canada, 31 p. <https://ed.gdr.nrcan.gc.ca/cruise_report_e.php> [accessed April 7, 2019]

MacLean, B. and Falconer, R.K.H., 1977. Baffin Island shelf — shallow corehole drilling, 1976; *in* Report of Activities, Part B; Geological Survey of Canada, Paper 77-1B, p. 125–127. https://doi.org/10.4095/102768

MacLean, B. and Falconer, R.K.H., 1979. Geological/geophysical studies in Baffin Bay and Scott Inlet – Buchan Gulf and Cape Dyer-Cumberland Sound areas of the Baffin Island Shelf; *in* Current Research, Part B; Geological Survey of Canada, Paper 79-1B, p. 231–244. https://doi.org/10.4095/105432

MacLean, B. and Srivastava, S.P., 1976. Shallow corehole drilling on the Baffin Island shelf; *in* Report of Activities, Part A; Geological Survey of Canada, Paper 76-1A, p. 141–143. https://doi.org/10.4095/104182

MacLean, B. and Srivastava, S.P., 1981. Petroliferous core from a diapir east of Cumberland Sound, Baffin Island; *in* Current Research, Part A; Geological Survey of Canada, Paper 81-1A, p. 399–400. https://doi.org/10.4095/109551

MacLean, B. and Williams, G.L., 1983. Geological investigations of Baffin Island shelf in 1982; *in* Current Research, Part B; Geological Survey of Canada, Paper 83-1B, p. 309–315. https://doi.org/10.4095/109337

MacLean, B., Jansa, L.F., Falconer, R.K.H., and Srivastava, S.P., 1977. Ordovician strata on the southeastern Baffin Island shelf revealed by shallow drilling; Canadian Journal of Earth Sciences, v. 14, p. 1925–1939. https://doi.org/10.1139/e77-163

MacLean, B., Falconer, R.K.H., and Clarke, D.B., 1978. Tertiary basalts of western Davis Strait: bedrock core samples and geophysical data; Canadian Journal of Earth Sciences, v. 15, p. 773–780. https://doi.org/10.1139/e78-083

MacLean, B., Srivastava, S.P., and Haworth, R.T., 1982. Bedrock structures off Cumberland Sound, Baffin Island shelf: core sample and geophysical data; *in* Arctic Geology and Geophysics, (ed.) A.F. Embry and H.R. Balkwill; Canadian Society of Petroleum Geologists, Memoir 8, Proceedings of the Third International Symposium on Arctic Geology, p. 279–295.

MacLean, B., Jennings, A., and Blakeney, C., 1986. Bedrock and surficial geology of Cumberland Sound, N.W.T.; *in* Current Research, Part B; Geological Survey of Canada, Paper 86-1B, p. 605–615. https://doi.org/10.4095/120672

MacLean, B., Williams, G.L., and Srivastava, S.P., 1990. Geology of Baffin Bay and Davis Strait; *in* Chapter 7 of Geology of the Continental Margin of Eastern Canada, (ed.) M.J. Keen and G.L. Williams; Geological Survey of Canada, Geology of Canada, no. 2, p. 325–348 (*also* Geological Society of America, The Geology of North America, v. I-1, p. 325–348). https://doi.org/10.4095/132710

MacLean, B., Williams, G., and Zhang, S., 2014. New insights into the stratigraphy and petroleum potential of the Baffin shelf's Cretaceous rocks; Bulletin of Canadian Petroleum Geology, v. 62, p. 289–310. https://doi.org/10.2113/gscpgbull.62.4.289

McMillan, N.J., 1973. Shelves of Labrador Sea and Baffin Bay; *in* Future Petroleum Provinces of Canada, (ed.) R.G. McCrossan; Canadian Society of Petroleum Geology, Memoir, v. 1, p. 473–515.

McMillan, N.J., 1980. Geology of the Labrador Sea and its Petroleum Potential; *in* World Petroleum Congress International, Proceedings, v. 10; Wiley, Chichester, United Kingdom, p. 165–175.

McWhae, J.R.H., 1981. Structure and spreading history of the northwestern Atlantic region from the Scotian Shelf to Baffin Bay; *in* Geology of the North Atlantic Borderlands, (ed.) J.W. Kerr, A.J. Fergusson, and L.C. Machan; Canadian Society of Petroleum Geologists, Memoir 7, p. 299–332.

McWhae, J.R.H., Elie, R., Laughton, K.C., and Gunther, P.R., 1980. Stratigraphy and petroleum prospects of the Labrador Shelf; Bulletin of Canadian Petroleum Geology, v. 28, p. 460–488.

Miller, P.E. and D'Eon, G.J., 1987. Labrador Shelf — Paleoenvironments; Geological Survey of Canada, Open File 1722, 186 p. https://doi.org/10.4095/130598

Miller, A.K., Youngquist, W., and Collinson, C., 1954. Ordovician cephalopod fauna of Baffin Island; Geological Society of America, Memoir 62, 166 p.

Moir, P.N., 1987a. Stratigraphic picks, Aquitaine et al. Hekja O-71; Geological Survey of Canada – Atlantic, Report No. EPGS-STRAT.33-87PNM, 1 p. <https://basin.gdr.nrcan.gc.ca/wells/index_e.php> [accessed January 3, 2019]

Moir, P.N., 1987b. Stratigraphic picks, Esso H.B. Gjoa G-37; Geological Survey of Canada – Atlantic, Report No. EPGS-STRAT.34-87PNM, 2 p. <https://basin.gdr.nrcan.gc.ca/wells/index_e.php> [accessed January 3, 2019]

Moir, P.N., 1987c. Stratigraphic picks, Canterra et al. Ralegh N-18; Geological Survey of Canada – Atlantic, Report No. EPGS-STRAT.32-87PNM, 2 p. <https://basin.gdr.nrcan.gc.ca/wells/index_e.php> [accessed January 3, 2019]

Moir, P.N., 1989. Lithostratigraphy 1: Review and type sections; *in* East Coast Basin Atlas Series, Labrador Sea, (co-ord.) J.S. Bell; Geological Survey of Canada, p. 26–27. https://doi.org/10.4095/127166

Monger, J., Blakey, R., Eberth, D., Harrison, C. Colpron, M., Cordey, F., Dehler, S., Evenchick, C., Fensome, R., MacRae, A., Nelson, J., Nowlan, G., Olsen, P., Poulton, T., Price, R., Sweet, A., Therrien, F., Wielens, H., Williams, G., Yorath, C., Zelenitsky, D., and Zonneveld, J.P., 2014. Pangea breaks up and mountains rise: Canada 251 to 65.5 million years ago; Chapter 9 *in* Four Billion Years and Counting: Canada's Geological Heritage, (ed.) R.A. Fensome, G.L. Williams, A. Achab, J. Clague, D. Corrigan, J. Monger, and G. Nowlan; Canadian Federation of Earth Sciences and Nimbus Publishing, Halifax, Nova Scotia, p. 160–188.

Nelson, C.E., Jerram, D.A., Clayburn, J.A.P., Halton, A.M., and Roberge, J., 2015. Eocene volcanism in offshore southern Baffin Bay; Marine and Petroleum Geology, v. 67, p. 678–691. https://doi.org/10.1016/j.marpetgeo.2015.06.002

Nøhr-Hansen, H., 2004. Dinoflagellate cyst stratigraphy of the Ralegh N-18 well, Saglek Basin, Davis Strait, offshore eastern Canada; Geological Survey of Denmark and Greenland, Report 2004/34, 67 p.

Nøhr-Hansen, H., Sheldon, E., and Dam, G., 2002. A new biostratigraphic scheme for the Paleocene onshore West Greenland and its implications for the timing of the pre-volcanic evolution; *in* The North Atlantic Igneous Province: Stratigraphy, Tectonic, Volcanic and Magmatic Processes, (ed.) D.W. Jolley and B.R. Bell; Geological Society of London, Special Publications, v. 197, p. 111–156. https://doi.org/10.1144/GSL.SP.2002.197.01.06

Nøhr-Hansen, H., Williams, G.L., and Fensome, R.A., 2016. Biostratigraphic correlation of the western and eastern margins of the Labrador–Baffin Seaway and implications for the regional geology; Geological Survey of Denmark and Greenland Bulletin, v. 37, 74 p.

Oakey, G.N. and Chalmers, J.A., 2012. A new model for the Paleogene motion of Greenland relative to North America: Plate reconstructions of the Davis Strait and Nares Strait regions between Canada and Greenland; Journal of Geophysical Research, v. 117, cit. no. B10401. https://doi.org/10.1029/2011JB008942

Planke, S., Symonds, P.A., Alvestad, E., and Skogseid, J., 2000. Seismic volcanostratigraphy of large volume basaltic extrusive complexes on rifted margins; Journal of Geophysical Research, v. 105, p. 19335–19351. https://doi.org/10.1029/1999JB900005

Praeg, D.B., MacLean, B., Hardy, I.A., and Mudie, P.J., 1986. Quaternary geology of the southeast Baffin Island continental shelf; Geological Survey of Canada, Paper 85-14, 38 p. https://doi.org/10.4095/120617

Rice, P.D. and Shade, B.D., 1982. Reflection seismic interpretation and seafloor spreading history of Baffin Bay; *in* Arctic Geology and Geophysics, (ed.) A.F. Embry and H.R. Balkwill; Canadian Society of Petroleum Geologists, Memoir 8, Proceedings of the Third International Symposium on Arctic Geology, p. 245–265.

Roest, W.R. and Srivastava, S.P., 1989. Sea-floor spreading in the Labrador Sea: a new reconstruction; Geology, v. 17, no. 11, p. 1000–1003. https://doi.org/10.1130/0091-7613(1989)017%3c1000:SFSITL%3e2.3.CO%3b2

Rolle, F., 1985. Late Cretaceous – Tertiary sediments offshore central West Greenland: lithostratigraphy, sedimentary evolution, and petroleum potential; Canadian Journal of Earth Sciences, v. 22, p. 1001–1019. https://doi.org/10.1139/e85-105

Skaarup, N., Jackson, H.R., and Oakey, G., 2006. Margin segmentation of Baffin Bay/Davis Strait, eastern Canada based on seismic reflection and potential field data; Marine and Petroleum Geology, v. 23, p. 127–144. https://doi.org/10.1016/j.marpetgeo.2005.06.002

Sønderholm, M., Nøhr-Hansen, H., Bojesen-Koefoed, J.A., Dalhoff, F., and Rasmussen, J.A., 2003. Regional correlation of Mesozoic–Palaeogene sequences across the Greenland–Canada boundary; Danmarks og Grønlands Geologiske Undersøgelse, Rapport 2003/25, 175 p.

Sørensen, A.B., 2006. Stratigraphy, structure and petroleum potential of the Lady Franklin and Maniitsoq Basins, offshore southern West Greenland; Petroleum Geoscience, v. 12, p. 221–234. https://doi.org/10.1144/1354-079305-692

Srivastava, S.P., 1974. Cruise report Hudson 74–026, Phase IV; Geological Survey of Canada, 26 p. <https://ed.gdr.nrcan.gc.ca/cruise_report_e.php> [accessed March 18, 2019]

Srivastava, S.P., Falconer, K.H., and MacLean, B., 1981. Labrador Sea, Davis Strait, Baffin Bay: Geology and geophysics — a review; *in* Geology of the North Atlantic Borderlands, (ed.) J.W. Kerr, A.J. Fergusson, and L.C. Machan; Canadian Society of Petroleum Geologists, Memoir, v. 7, p. 333–398.

Srivastava, S.P., MacLean, B., Macnab, R.F., and Jackson, H.R., 1982. Davis Strait: structure and evolution as obtained from a systematic geophysical survey; *in* Arctic Geology and Geophysics, (ed.) A.F. Embry and H.R. Balkwill; Canadian Society of Petroleum Geologists, Memoir 8, Proceedings of the Third International Symposium on Arctic Geology, p. 267–278.

St-Onge, M.R., Van Gool, J.A., Garde, A.A., and Scott, D.J., 2009. Correlation of Archaean and Palaeoproterozoic units between northeastern Canada and western Greenland: constraining the pre-collisional upper plate accretionary history of the Trans-Hudson orogeny; Geological Society of London, Special Publications, v. 318, p. 193–235. https://doi.org/10.1144/SP318.7

Storey, M., Duncan, R.A., Pedersen, A.K., Larsen, L.M., and Larsen, H.C., 1998. Ar-40/Ar-39 geochronology of the west Greenland tertiary volcanic province; Earth and Planetary Science Letters, v. 160, p. 569–586. https://doi.org/10.1016/S0012-821X(98)00112-5

Storey, M., Duncan, R.A., and Tegner, C., 2007. Timing and duration of volcanism in the North Atlantic Igneous Province: Implications for geodynamics and links to the Iceland hotspot; Chemical Geology, v. 241, no. 3-4, p. 264–281. https://doi.org/10.1016/j.chemgeo.2007.01.016

Suckro, S.K., Gohl, K., Funck, T., Heyde, I., Schreckenberger, B., Gerlings, J., and Damm, V., 2013. The Davis Strait crust — a transform margin between two oceanic basins; Geophysical Journal International, v. 193, no. 1, p. 78–97. https://doi.org/10.1093/gji/ggs126

Thrane, K., 2014. Provenance study of Paleocene and Cretaceous clastic sedimentary rocks from the Davis Strait and the Labrador Sea, based on U-Pb dating of detrital zircons; Bulletin of Canadian Petroleum Geology, v. 62, p. 330–396. https://doi.org/10.2113/gscpgbull.62.4.330

Umpleby, D.C., 1979. Geology of the Labrador shelf; Geological Survey of Canada, Paper 79-13, 40 p. https://doi.org/10.4095/105927

van Kempen, M.M.L., Smolders, A.J.P., Lamers, L.P.M., and Roelofs, J.G.M., 2012. Micro-halocline enabled nutrient recycling may explain extreme *Azolla* event in the Eocene Arctic Ocean; PLoS One, v. 7, no. 11, p. e50159. https://doi.org/10.1371/journal.pone.0050159

Wade, J.A., Grant, A.C., Sanford, B.V., and Barss, M.S., 1977. Basement structures, eastern Canada and adjacent areas; Geological Survey of Canada, Map 1400A, scale 1:200 000. https://doi.org/10.4095/109057

Wielens, H.J.B.W. and Jauer, C.D., 2009. Saglek Basin: at least one petroleum system in an ultra-frontier basin with great potential; Canadian Society of Petroleum Geologists–Canadian Society of Exploration Geophysicists–Canadian Well Logging Society Convention: Frontiers and Innovation, p. 53–56 (abstract).

Wielens, H.J.B.W. and Williams, G.L., 2009. Stratigraphic cross section Gjoa-Snorri, Saglek–Hopedale Basin, in the Labrador Sea on the east coast of Canada, from North to South; Geological Survey of Canada, Open File 5903, 1 sheet. https://doi.org/10.4095/247636

Williams, G.L., 2007a. Palynological analysis of Aquitaine et al. Hekja O-71, Saglek Basin, Davis Strait, offshore eastern Canada; Geological Survey of Canada, Open File 5448, 19 p. https://doi.org/10.4095/224259

Williams, G.L., 2007b. Palynological analysis of Esso-H.B. Gjoa G-37, Saglek Basin, Davis Strait, offshore eastern Canada; Geological Survey of Canada, Open File 5449, 19 p. https://doi.org/10.4095/224260

Williamson, M.-C. and Villeneuve, M.E., 2002. Age of basaltic rocks recovered from drilling in the Davis Strait, Eastern Canada; on file with the Canada–Nova Scotia Offshore Energy Board, Halifax, Nova Scotia, 7 p.

Williamson, M.-C., Villeneuve, M., Jackson, R., and MacLean, B., 2000. Argon Geochronology of basaltic rocks recovered from drilling on the Baffin Island shelf and in the Davis Strait, Eastern Canada; American Geophysical Union, v. 81, p. 1361 (abstract).

Zhang, S., 2013. Rock Eval[6] and vitrinite reflectance data from Baffin Island Shelf and Hudson Strait; Geological Survey of Canada, Open File 7341, 32 p. https://doi.org/10.4095/292376

Zhang, S. and Pell, J., 2014. Conodonts recovered from the carbonate xenoliths in the kimberlites confirm the Paleozoic cover on the Hall Peninsula, Nunavut; Canadian Journal of Earth Sciences, v. 51, p. 142–155. https://doi.org/10.1139/cjes-2013-0171

Zhang, S., Creaser, R.A., and Pell, J., 2014. Discovery of organic-rich black shale xenolith from kimberlite on the Hall Peninsula, Nunavut and its implication for petroleum potential in Cumberland Sound; Bulletin of Canadian Petroleum Geology, v. 62, p. 125–131.

Stratigraphy of western Baffin Bay: a review of existing knowledge and some new insights

L.T. Dafoe[1*], K. Dickie[1], and G.L. Williams[1]

Dafoe, L.T., Dickie, K., and Williams, G.L., 2022. Stratigraphy of western Baffin Bay: a review of existing knowledge and some new insights; in *Geological synthesis of Baffin Island (Nunavut) and the Labrador–Baffin Seaway, (ed.) L.T. Dafoe and N. Bingham-Koslowski; Geological Survey of Canada, Bulletin 608, p. 219–246. https://doi.org./10.4095/321846*

Abstract: Sedimentary basins within the Labrador–Baffin Seaway are the product of rifting between Greenland and the paleo-North American Plate. Rifting started in the Early Cretaceous, with seafloor spreading initiated in the Paleocene and ending near the Eocene–Oligocene boundary. A change in the spreading direction in the latest Paleocene resulted in transform offsets in the Davis Strait and along fracture zones in Baffin Bay, with deformation in northern Baffin Bay during the Eurekan Orogeny. Since the stratigraphy of western Baffin Bay is poorly constrained, analogues are used from the well studied Labrador and West Greenland margins and exposures on nearby Bylot Island. The generally northwest-trending basement structures are infilled with Cretaceous strata, which are overlain by a seaward-thickening wedge of post-rift Paleocene to Middle Miocene sedimentary rocks. Finally, a thick Middle Miocene and younger interval blankets the deep water and oceanic crust, with clinoforms locally developed on the shelf.

Résumé : Les bassins sédimentaires du bras de mer Labrador-Baffin découlent d'un rifting entre le Groenland et la paléoplaque nord-américaine. Cette distension a débuté au Crétacé précoce, alors que l'expansion des fonds marins s'est amorcée au Paléocène pour se terminer près de la limite Éocène-Oligocène. Un changement dans la direction de l'expansion au Paléocène terminal a entraîné des décalages par failles transformantes dans le détroit de Davis et le long de zones de fracture dans la baie de Baffin, et une déformation a touché la partie nord de la baie de Baffin pendant l'orogenèse eurékienne. Puisque la stratigraphie de la partie occidentale de la baie de Baffin est mal circonscrite, nous utilisons des analogues fournis par les marges bien étudiées du Labrador et de l'ouest du Groenland ainsi que par des affleurements de l'île Bylot située à proximité. Les structures du socle, généralement de direction nord-ouest, sont remplies de strates du Crétacé, lesquelles sont surmontées d'un prisme de roches sédimentaires s'épaississant vers le large composé de roches post-rift du Paléocène au Miocène moyen. Pour finir, une succession du Miocène moyen et de temps plus récents forme une épaisse couverture en eau profonde s'étendant à la croûte océanique. Sur la plate-forme continentale, des clinoformes y sont localement développées.

[1]Geological Survey of Canada, 1 Challenger Drive, P.O. Box 1006, Dartmouth, Nova Scotia B2Y 4A2
*Corresponding author: L.T. Dafoe (email: Lynn.Dafoe@nrcan-rncan.gc.ca)

INTRODUCTION

Baffin Bay forms the northern extension of the Labrador–Baffin Seaway rift system and includes a deep central basin and asymmetric shelf platforms, which are narrower on the western side of the bay (Fig. 1). The western Baffin Bay study region spans from about longitude 58 to 80°W and latitude 67 to 77°N, with water depths ranging from a few hundred metres on the Baffin Shelf and slope to over 2000 m in central Baffin Bay. On the Baffin Shelf, a series of shallow banks and transverse troughs are submarine extensions of the fjords of Baffin Island, relics of the Laurentide Ice Sheet (Fig. 1; MacLean et al., 1990).

The basins comprising the Labrador–Baffin Seaway began forming during Early Cretaceous rifting between Greenland and the paleo-North American Plate (Roest and Srivastava, 1989). Although the delineation of magnetic chrons in Baffin Bay is poor, there is general acceptance of the onset of seafloor spreading offshore central Labrador by chron C31 (Maastrichtian; Keen et al., 2018a) and then offshore northern Labrador and in Baffin Bay by chron C27n (Early Paleocene; Oakey and Chalmers, 2012; Keen et al., 2018b). This initial phase of seafloor spreading was interrupted by a change in the direction of plate motions between chrons C25n and C24n (approximately the Paleocene–Eocene boundary), which resulted in sinistral strike-slip motion along the Ungava Fault Zone through the Davis Strait and along major fracture zones in Baffin Bay (Chalmers and Pulvertaft, 2001; Oakey and Chalmers, 2012). Major volcanic outpouring began in the Selandian, roughly coincident with the onset of seafloor spreading, and is thought to reflect the arrival of a mantle plume in the region of Davis Strait, around 61 Ma (Storey et al., 1998, 2007; Larsen et al., 2009). Seafloor spreading ended by chron C13 in the Late Eocene (Oakey and Chalmers, 2012). As a result of this complex rift history, Baffin Bay is ringed by magma-rich margins in the south, and magma-poor margins in the north (Reid and Jackson, 1997; Skaarup et al., 2006; Funck et al., 2012; Keen et al., this volume).

Onshore eastern Baffin Island, Archean orthogneiss units of the Rae Craton extend from Home Bay to Bylot Island with Mesoproterozoic cover along northern Baffin Island and locally on Bylot Island (Jackson and Iannelli, 1981; St-Onge et al., 2009, this volume; Turner, this volume). From Home Bay southward to Cape Dyer, the Rae Craton is overlain by a Paleoproterozoic continental-margin sequence and the Cumberland batholith (St-Onge et al., 2009). Offshore along western Baffin Bay, the lack of exploration wells and detailed sampling (MacLean et al., 1990) has presented challenges to understanding the subsurface geology, resulting in reliance on geophysical data, including reflection and refraction seismic and potential field data. Some of the early work on the geology and evolution of the region was summarized by McMillan (1973), and further analyses were undertaken by Beh (1975) and Hood and Bower (1975). Later, Srivastava et al. (1981) provided a summary of the tectonic evolution of the Labrador–Baffin Seaway based on available data at that time. Rice and Shade (1982) conducted some of the early work on multichannel seismic data interpretation, including analyses of the structure and stratigraphy in northern Baffin Bay. Later studies focused on more detailed mapping, defining the structural trend in pre-rift basement from Home Bay to Devon Island as northwest-oriented grabens and basement ridges running parallel to the coast (Jackson et al., 1992). North of Devon Island, offshore grabens trend in a more northerly direction, whereas the Lancaster Sound and Jones Sound grabens trend westerly (MacLean et al., 1990; Jackson et al., 1992; Harrison et al., 2011a). Jackson et al. (1992) identified structural features in this northern part of Baffin Bay consistent with strike-slip motion in the region and Harrison et al. (2011a) presented evidence of compressional deformation. This folding, faulting, and tectonic inversion is a result of the Eurekan Orogeny that affected the Canadian Arctic Islands beginning in the Paleocene and ending by the late Eocene (Jackson et al., 1992; Harrison et al., 2011a; Oakey and Chalmers, 2012; Gion et al., 2017). Farther offshore in Baffin Bay, controversy over the nature of the crust continued for several decades, but it is now generally accepted as oceanic within the centre of the bay and possibly partly under Lancaster Sound as seafloor spreading propagated westward in the Eocene (e.g. Oakey and Chalmers, 2012).

Major basins along western Baffin Bay have been delineated primarily by seismic reflection and refraction studies. Keen et al. (this volume) present a new regional compilation of sediment thickness calculated in depth for the Labrador–Baffin Seaway, which highlights major basins in the region. The southernmost of these includes Scott and Buchan grabens (Fig. 1), filled by syn- and postrift sediments (Jackson et al., 1992) likely 4 to 6 km thick in aggregate (Jackson et al., 1977; Keen et al., this volume). Farther north, Keen and Barrett (1973) identified sedimentary accumulations in Lancaster Sound using seismic reflection and refraction and potential-field data. Related depocentres on Bylot Island include the North Bylot Trough, interpreted to extend offshore into Lancaster Sound (Harrison et al., 2011a; Brent et al., 2013), and Eclipse Trough primarily located on southeast Bylot Island (Fig. 1; Jackson et al., 1975). Philpots Ridge, a basement high, separates Lancaster Sound from basins to the north (Fig. 1; Harrison et al., 2011a). Here, sedimentary basins were identified in Jones Sound and Smith Sound in the early 1970s using geophysical data (Keen and Barrett, 1972, 1973). Jackson et al. (1992) refined this early work using seismic reflection data and mapped four sedimentary basins in northernmost Baffin Bay: Lady Ann, Glacier, Carey, and North Water (Fig. 1). The Lady Ann Basin was thought to comprise two half-grabens (Reid and Jackson, 1997), whereas Jones Sound was interpreted to contain lower Paleozoic or younger folded and faulted sedimentary strata, based on acoustic and magnetic data (MacLean et al., 1984). Glacier Basin is a half-graben trending northerly offshore Ellesmere Island (Jackson et al., 1992; Harrison et al., 2011a, Keen et al., this volume), and farther northward, into Smith Sound, sedimentary basins were likely affected by strike-slip motion (Reid and Jackson, 1997), part of a larger strike-slip system through Nares Strait (von Gosen et al., 2019). Finally, in central Baffin Bay is the deep-water Baffin Basin (MacLean et al., 1990).

Although there are no deep exploration wells in the study area, Lower Cretaceous to Paleocene sedimentary rocks have been mapped on nearby Bylot Island and northeast Baffin Island within the Eclipse and North Bylot troughs (Fig. 1; Jackson et al., 1975; Clarke, 1976; Miall et al., 1980; Ioannides, 1986; Haggart et al., this volume). On Bylot Island, Lower Cretaceous rocks are in fault contact with Mesoproterozoic sedimentary or crystalline basement rocks (Brent et al., 2013). Strata described by Miall et al. (1980) and Ioannides (1986) were equated with formations found to the northwest on the Canadian Arctic Islands, but were later informally renamed by Sparkes (1989), Waterfield (1989), Wiseman (1991), and Benham (1991). In the Paallavvik (island) area off of east-central Baffin Island, Burden and Langille (1990, 1991) also identified Lower Cretaceous and lower Middle Paleocene rocks underlying Late Paleocene basalt units (Clarke and Upton, 1971) and sitting unconformably above pre-rift basement.

The West Greenland margin along northeastern Baffin Bay is characterized by the widest and deepest basins in Baffin Bay, which contain Lower Cretaceous and younger rocks (Gregersen et al., 2019, this volume). Onshore central West Greenland, the Nuussuaq Basin has been studied extensively (e.g. Pedersen and Pulvertaft, 1992; Nøhr-Hansen et al., 2002; Dam et al., 1998), as have exploration wells offshore southern West Greenland (Rolle, 1985) and central West Greenland (Gregersen et al., 2019). Whittaker et al. (1997) confirmed the presence of large structures and sedimentary basins in the Melville Bay area, including the Melville Bay Graben with more than 13 km of sedimentary infill (*see* Gregersen et al., this volume; *see* Keen et al., this volume). Using an extensive modern seismic data set, Gregersen et al. (2013) identified eight seismic-stratigraphic units, A through H, and their bounding horizons A1 to H1, in regional mapping of the West Greenland margin (Gregersen et al., 2016, 2019, this volume). Knutz et al. (2015) extended this framework to the Lower Miocene to Pleistocene ODP Site 645 in western Baffin Bay using age constraints from that corehole (Fig. 1).

Because of the lack of well data, early stratigraphic studies along western Baffin Bay were mainly based on correlations with the Labrador Shelf (McMillan, 1973; McWhae, 1981). Along the Labrador margin, eight formations were defined by Umpleby (1979) and McWhae et al. (1980) and further described in Balkwill and McMillan (1990), Dickie et al. (2011), and Dafoe, Dickie, Williams, and McCartney (this volume; Fig. 2). Primarily using geophysical

Figure 1. a) The western Baffin Bay study area showing bathymetry for the region (General Bathymetric Chart of the Oceans, 2014), as well as the location of multichannel seismic data, seismic profiles shown in Figure 4, ODP Site 645, GSC cruise samples containing bedrock material (seabed drill cores, dredges, and bedrock fragments from within a piston core), and key place names. Cruise samples are shown and labelled in detail on the applicable distribution maps. Basin outlines are from Keen et al. (this volume). Additional projection information is as follows: Central Meridian = 60°W; Standard Parallels = 65, 75°W; Latitude of Origin = 65°N.

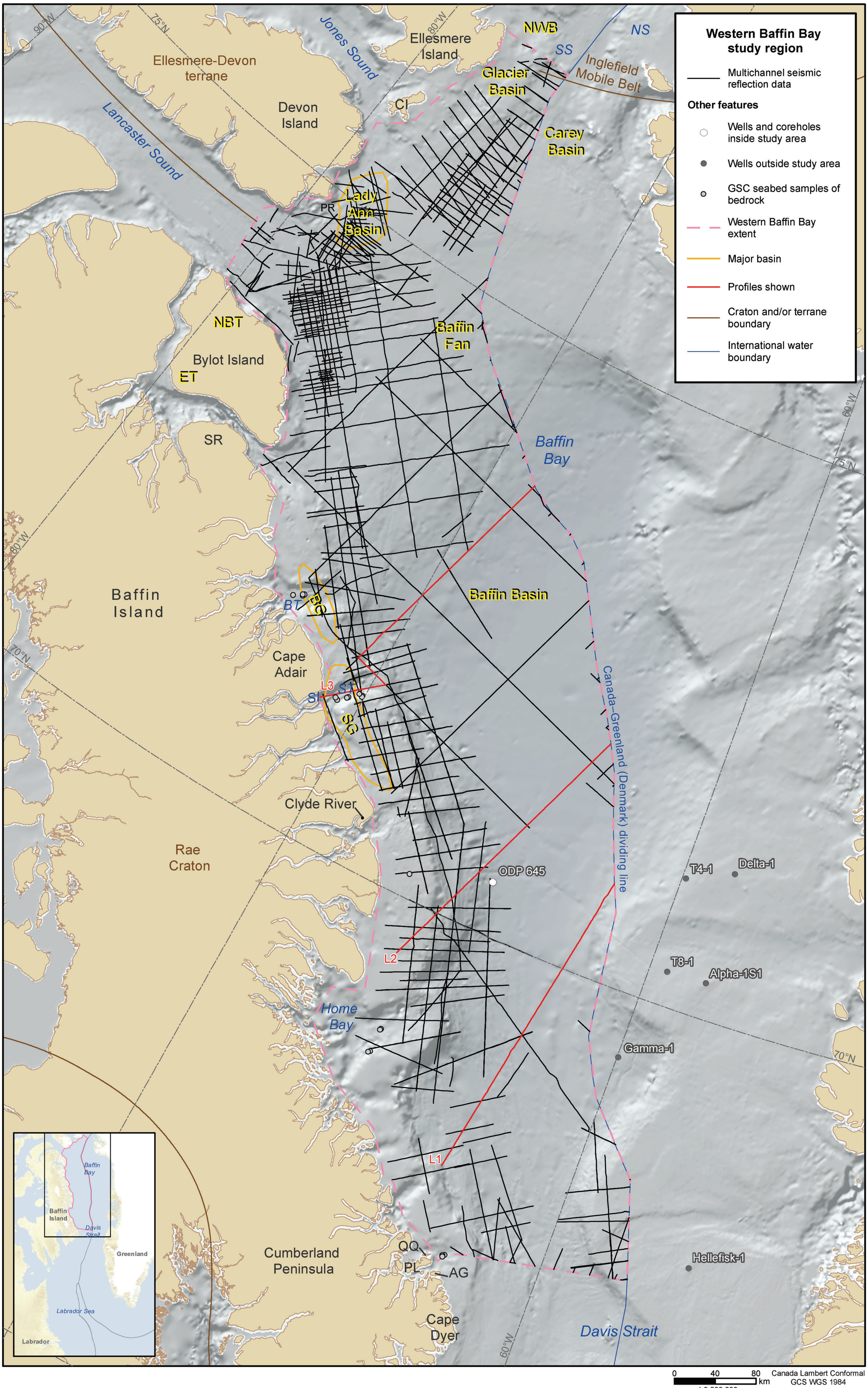
Western Baffin Bay study region
Multichannel seismic reflection data
Other features
Wells and coreholes inside study area
Wells outside study area
GSC seabed samples of bedrock
Western Baffin Bay extent
Major basin
Profiles shown
Craton and/or terrane boundary
International water boundary
Ellesmere-Devon terrane
Devon Island
Ellesmere Island
Jones Sound
Lancaster Sound
NWB
NS
SS
Inglefield Mobile Belt
Glacier Basin
Carey Basin
CI
Lady Ann Basin
PR
NBT
Bylot Island
ET
SR
Baffin Fan
Baffin Bay
Baffin Basin
Baffin Island
BT
BC
Cape Adair
L3
SI
ST
SG
Clyde River
Rae Craton
ODP 645
L2
Home Bay
L1
Canada–Greenland (Denmark) dividing line
T4-1
Delta-1
T8-1
Alpha-1S1
Gamma-1
Hellefisk-1
Cumberland Peninsula
QQ
PL
AG
Cape Dyer
Davis Strait
90°W
80°W
75°N
70°N
60°W
Baffin Bay
Baffin Island
Davis Strait
Greenland
Labrador Sea
Labrador
0
40
80
km
1:3 500 000
Canada Lambert Conformal
GCS WGS 1984

Basin names

BG – Buchan Graben
CYB – Carey Basin
ET – Eclipse Trough
GB – Glacier Basin
LAB – Lady Ann Basin
NBT – North Bylot Trough
NWB – North Water Basin
SG – Scott Graben

Bathymetric names

BT – Buchan Trough
NS – Nares Strait
SI – Scott Inlet
SS – Smith Sound
ST – Scott Trough

Geological structures

BFZ – Bower Fracture Zone
FZ – Fracture zone
PR – Philpots Ridge

Onshore place names

AG – Aggijjat
CI – Coburg Island
PL – Paallavvik
QQ – Qaqulluit
SR – Salmon River

Figure 1. b) Abbreviation list for figures 1a, 3, 5, 6, and 8. Note that all the legend items may not appear on each of the maps.

control, Rice and Shade (1982) focused on northwestern Baffin Bay and identified unconformities that they equated with the regional unconformities recognized by McWhae (1981). In addition to these studies, several marine cruises by the Geological Survey of Canada resulted in the collection of seabed samples of basement, Cretaceous, and Cenozoic rocks along the Baffin Shelf (Fig. 1; MacLean, 1978, 1980, 1985; MacLean and Falconer, 1979; Levy and MacLean, 1981; MacLean et al., 1981, 2014; MacLean and Williams, 1983; Dafoe and Williams, 2020a), providing additional stratigraphic constraints.

On the continental slope offshore of the Home Bay region, is the only deep subsurface sampling in western Baffin Bay—the ODP Site 645 coreholes. (Fig. 1; Srivastava et al., 1987). These coreholes intersected three main lithological units within the Neogene section (Srivastava et al., 1987), reaching total depth in Lower Miocene strata (Dafoe and Williams, 2020c), and providing key age constraints for the younger section. Harrison et al. (2011a) utilized the stratigraphic framework established for Site 645 and divided the sedimentary sequence of northern Baffin Bay into several seismic depositional units, constraining the age of the Baffin Fan, a presumed Eocene to Pleistocene wedge of strata off the mouth of Lancaster Sound that was sourced from continental-scale rivers and ice streams feeding through Lancaster Sound, Jones Sound, and Nares Strait. Brent et al. (2013) subsequently modified this work for the Lancaster Sound area, identifying early rift, rift, early spreading, late spreading, postspreading, and subpolar glacial and polar glacial units.

The petroleum potential of the region has been implied by the discovery of oil seeps found within the Scott and Buchan grabens (Loncarevic and Falconer, 1977; Levy and Ehrhardt, 1981; MacLean et al., 1981), possibly from a mid-Cretaceous source rock (Fowler et al., 2005) similar in age to the onshore oil seeps on Disko Island, West Greenland (Bojesen-Koefoed et al., 2007). Studies summarizing the petroleum potential of the region include those by Bell and Campbell (1990), Harrison et al. (2011a), Brent et al. (2013), Atkinson et al. (2017), and Bingham-Koslowski, McCartney, and Bojesen-Koefoed (this volume).

In this contribution, existing knowledge of the stratigraphic succession of western Baffin Bay is integrated, including a review of earlier sampling and mapping efforts, with new regional seismic mapping and interpretations. The stratigraphy is discussed in relation to the lithostratigraphic framework of the Labrador margin and the distribution of three major stratigraphic intervals: Cretaceous, lower Cenozoic, and upper Cenozoic. The focus is on understanding the nature of the basement and the distribution and nature of the sedimentary basin infill.

DATA AND METHODS

This paper describes previous studies addressing the stratigraphy of western Baffin Bay, but the authors further present new results based on analysis and integration of existing interpretations, revised assessments of the samples in the region, and new regional seismic mapping (data shown in maps are included in the GIS data included with this volume). As an analogue for the western Baffin Bay region, the stratigraphy of the Labrador margin is used as it forms a relatively complete and well studied stratigraphic section in the Cretaceous and Cenozoic (Fig. 2). This is in contrast to the Cenozoic succession of the West Greenland margin, which contains significant stratigraphic breaks from the Eocene to Middle Miocene as seen in many wells (Gregersen et al., 2013, 2018, 2019, this volume). In order to present regional correlations for the entire Labrador–Baffin Seaway for three main stratigraphic intervals (Cretaceous, lower Cenozoic, and upper Cenozoic), Dafoe, Williams et al. (this volume) divide the Cenozoic using the D1 horizon from the West Greenland margin, which is Middle Miocene (Gregersen et al., 2013, 2018, 2019, this volume). This subdivision is followed in this study by using the equivalent Saglek and/or Mokami formation 3 horizon (SM3) to subdivide the Cenozoic at about the Middle Miocene level for western Baffin Bay. In addition, the present authors show the western Baffin Bay portions of the seismic interpretations from Dafoe, Williams et al. (this volume), for which much of line 2 and the Baffin Basin portion of line 3 are derived from the work of P. Knutz at the Geological Survey of Denmark and Greenland and tie to the profiles from the West Greenland margin as shown in Gregersen et al. (this volume; their Fig. 40, 41).

Well and sample data

The present study area includes one ODP site (Leg 105, Site 645), drilled in 1985 on the slope of the eastern Baffin Island margin, east of the hamlet of Clyde River (Fig. 1). Data sets and reports for this well can be obtained from the International Ocean Discovery Program website (http://iodp.tamu.edu), including well logs (e.g. gamma ray, sonic velocity, and resistivity). Additional well data used in this paper are derived from the ODP Site 645 report (Srivastava et al., 1987), which outlined lithological summaries, lithological unit designations, biostratigraphy, and paleoenvironments. Additional biostratigraphic studies for this well include independent palynological analyses (Head et al., 1989; de Vernal and Mudie, 1989; Fenton and Pardon, 2007; Dafoe and Williams, 2020c) and foraminiferal analyses (Kaminski et al., 1989; Fenton and Pardon, 2007). An integrated paleoenvironmental assessment of Site 645 was also discussed in more detail in Dafoe and Williams (2020c).

Bedrock samples were collected from the Baffin Shelf during GSC marine cruises from 1977 to 1985 (Fig. 1). A list of the cruises and related samples, which include shallow drill cores, dredge samples, and bedrock fragments recovered from a surficial piston core, is found in Table 1. Information regarding these cruises and the samples can be found on the Expedition Database (http://ed.gdr.nrcan.gc.ca), and technical data in Table 1 were derived from this database. Samples are named based on the cruise number and original sample station number (e.g. cruise 80028 and station 7 is labelled as 80028-7). Bedrock drill cores are 2.54 cm in diameter, generally a few centimetres to a few tens of centimetres in length (as a result of limitations encountered during drilling), and can include overburden material also collected during the drilling process (but these materials are not accounted for in the length of bedrock collected). A general assessment of the drill core material took place during its initial collection to determine if bedrock (as opposed to overburden) was in fact recovered (*see* MacLean et al., 2014; *see also* Dafoe and Williams, 2020a). A compilation and detailed analyses of the sedimentary bedrock samples is presented in Dafoe and Williams (2020a), including sedimentological and ichnological observations and related paleoenvironmental interpretations of the bedrock samples, as well as some new palynological age determinations, building upon the initial studies (*see* Table 1 for references) and that of MacLean et al. (2014). Bedrock samples and Site 645 are schematically shown in Figure 2 based on the most recent age constraints and lithological descriptions.

Seismic data

The seismic data set used in interpretation along the western Baffin Bay study region consists of over 32 000 line-kilometres of seismic data (Fig. 1), with the bulk of this being vintage data sets acquired between 1968 and 1982. A loose grid of modern seismic data, with over 2700 line-kilometres and a spacing of about 300 km, was acquired by TGS-NOPEC Geophysical Company ASA (TGS; https://www.tgs.com) in western Baffin Bay in 2008. These data have recording depths of over 9 s two-way traveltime and were acquired using long streamers (generally 8 km or more) and then processed with modern demultiple removal algorithms (e.g. "radon") and prestack time migration. Vintage data sets were acquired using shorter streamers and with 5 to 7 s two-way traveltime of data. These were processed with older demultiple algorithms and had poststack

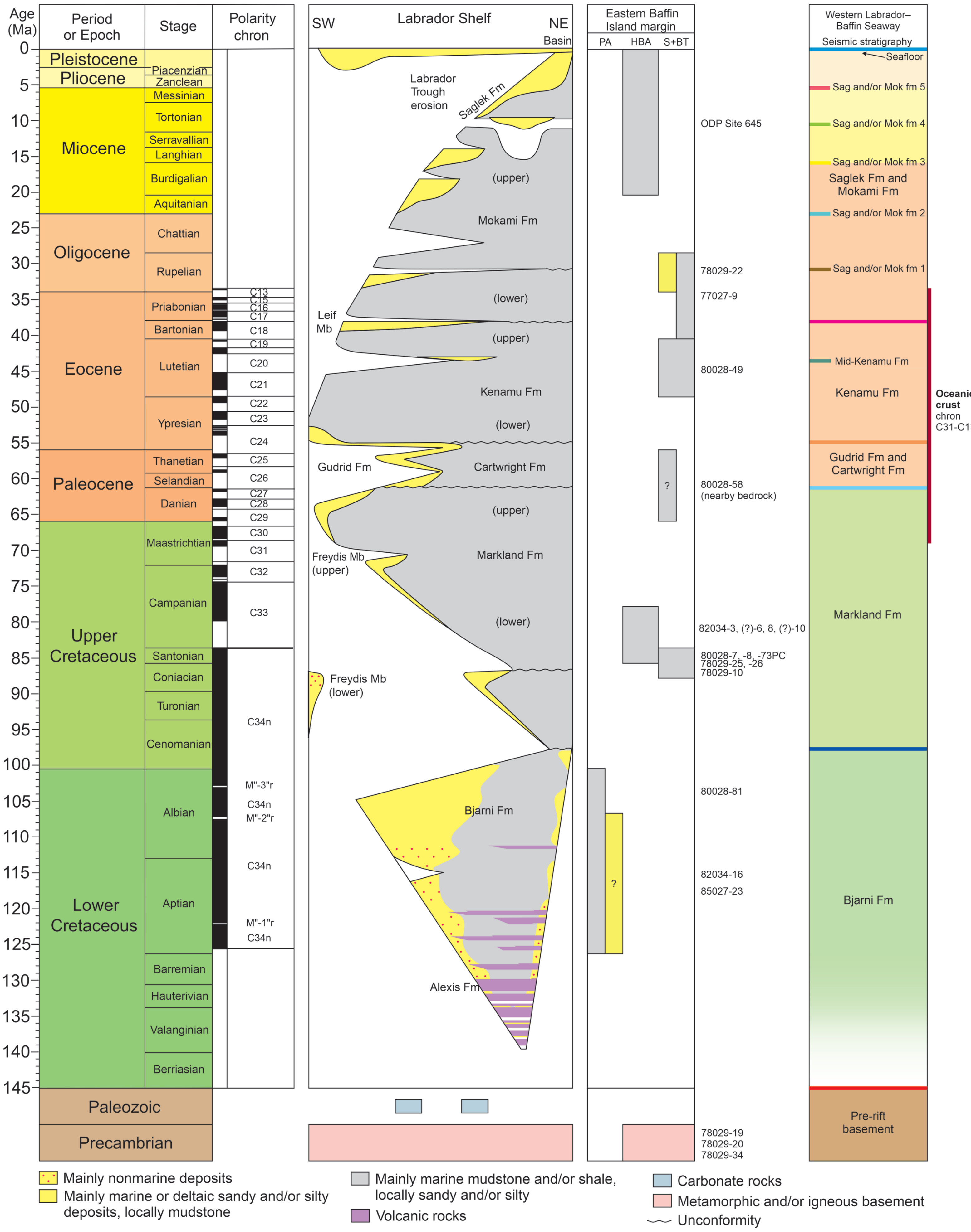

Figure 2. Lithostratigraphic column showing intervals sampled by the ODP Site 645 corehole and GSC seabed samples (*see* Table 1) for the Paallavvik (island) area (PA), Home Bay area (HBA), and Scott and Buchan Troughs (S+BT) plotted against the geological time scale and magnetostratigraphy of Gradstein et al. (2012). This column is based on bedrock samples summarized in Table 1. Related sample designations are listed to the right of the column approximately centred to the relevant unit in the column. The Labrador margin stratigraphy (*see* Dafoe, Dickie, Williams, and McCartney, this volume) and western Labrador–Baffin Seaway seismic stratigraphy (based on the Labrador margin) are also shown. For the seismic stratigraphy, the tops of formations are defined by coloured horizons and some intervening horizons are further defined in the Kenamu and Saglek and/or Mokami formations. Mok = Mokami, Sag = Saglek.

migration rather than prestack migration. Over half of the vintage lines had not been migrated following their acquisition, so poststack migrations were conducted on key surveys (Dafoe et al., 2016a, b). A map showing the available released data can be found in Figure 1.

BASEMENT

Onshore geology

The Rae Craton (Fig. 3), which is composed primarily of Archean orthogneiss units, underlies Baffin Island from Home Bay northward to Bylot Island (St-Onge et al., 2009, this volume). Small outcrops of the Archean Mary River Group metavolcanic rocks (St-Onge et al., 2009) and the Mesoproterozoic Borden Basin strata (Jackson et al., 1975) also lie on and near Bylot Island. The Borden Basin occupies the northern part of Baffin Island and extends locally onto northern Bylot Island and is characterized by sedimentary and volcanic rocks associated with aulacogen formation during the amalgamation of Laurentia (Jackson and Iannelli, 1981; Turner, 2009; Hahn and Turner, 2013; Turner, this volume). South of Home Bay, the Rae Craton is overlain by the Paleoproterozoic Piling and/or Hoare Bay groups, forming a continental-margin sequence (St-Onge et al., 2009). These rocks are further overprinted by the Cumberland batholith, a continental-margin arc formed during subduction following accretion of the Meta Incognita microcontinent to the Rae Craton (St-Onge et al., 2009). Along western Baffin Island, Paleozoic (Cambrian to Silurian) strata overlie Archean and Proterozoic rocks (Scott and de Kemp, 1998; Bingham-Koslowski, Zhang, and McCartney, this volume). These carbonate rocks comprise much of Devon and Ellesmere islands, overlying the older Archean to Proterozoic gneiss units and metasedimentary rocks

Table 1. List of Geological Survey of Canada bedrock samples collected during marine cruises.

Expedition	Year	Original station no.	General location	Latitude (°N)	Longitude (°W)	Sample type	Length of bedrock core (cm)	Water depth (m)	Rock type	Description	Age	Paleoenvironment	Other analyses (Zhang, 2013)
78029	1978	19	Scott Trough	71.40	70.05	Rock drill	61	267	Metamorphic	Metamorphic rock (MacLean and Falconer, 1979; MacLean et al., 1981)			
78029	1978	20	Scott Trough	71.39	70.06	Rock drill	73	267	Metamorphic	Metamorphic rock (MacLean and Falconer, 1979; MacLean et al., 1981)			
78029	1978	34	Home Bay area	70.21	66.71	Rock drill	95	118.9	Metamorphic	Metamorphic rock (MacLean and Falconer, 1979)			
77027	1977	9	Scott Trough	71.33	70.37	Dredge	n.a.	567	Mudstone	Calcareous concretion (boulder size), mainly fine-grained calcite with silt- to sand-sized quartz grains and other detrital material including fossil fragments (MacLean, 1978); concretion could be derived from a shale interval based on diagenesis (L. Jansa, pers. comm. *in* MacLean, 1978); calcareous mudstone concretion with organic fragments, silt-sized quartz grains, and possible siderite (Dafoe and Williams, 2020a)	Late Eocene (G.L. Williams, pers. comm. *in* MacLean (1978); late Eocene–early Oligocene (MacLean and Williams, 1983)	Neritic (MacLean, 1978); likely marine (Dafoe and Williams, 2020a)	
78029	1978	10	Buchan Trough	71.89	72.92	Rock drill	19	310	Mudstone	Dark grey, calcareous siltstone and organic-rich silty mudstone with glauconite and siderite (MacLean and Falconer, 1979; MacLean et al., 2014); dark grey, silty mudstone characterized by a *Zoophycos* Ichnofacies trace-fossil suite (Dafoe and Williams, 2020a)	Late Cretaceous (G.L. Williams, pers. comm. *in* MacLean and Falconer, 1979); Campanian (MacLean et al., 1981); late Coniacian (MacLean et al., 2014)	Probably neritic (MacLean and Falconer, 1979; MacLean et al., 1981); outer shelf (Dafoe and Williams, 2020a)	TOC: 0.89%
78029	1978	22	Scott Trough	71.32	70.40	Dredge	n.a.	550–640	Sandstone	Dark grey, calcareous sandstone concretion with plant remains (MacLean and Falconer, 1979; MacLean et al., 1981); muddy sandstone to sandy mudstone with faint laminations and possible glauconite (Dafoe and Williams, 2020a)	Late Eocene to early Oligocene (MacLean et al., 1981); no older than Rupelian (Dafoe and Williams, 2020a)	Shallow, nearshore setting (MacLean et al., 1981); distal inner shelf to proximal outer shelfal (Dafoe and Williams, 2020a)	
78029	1978	25	Buchan Trough	71.91	72.90	Rock drill	18	298	Mudstone	Dark grey, calcareous siltstone and organic-rich silty mudstone with glauconite and siderite (MacLean and Falconer, 1979; MacLean et al., 2014); silty mudstone with sandstone laminae, load structures and bioturbation consistent with a distal *Cruziana* Ichnofacies (Dafoe and Williams, 2020a)	Late *Cretaceous* (G.L. Williams, pers. comm. *in* MacLean and Falconer, 1979); Campanian (MacLean et al., 1981); late Coniacian–Santonian (MacLean et al., 2014)	Probably neritic (MacLean and Falconer, 1979; MacLean et al., 1981); proximal outer shelf (Dafoe and Williams, 2020a)	TOC: 0.51%
78029	1978	26	Buchan Trough	71.90	72.94	Rock drill	71	539.5	Siltstone	Dark grey, calcareous siltstone and organic-rich silty mudstone with glauconite and siderite (MacLean and Falconer, 1979; MacLean et al., 2014); muddy siltstone with planar and wavy laminations, sandy lenses, organic detritus, mudstone laminae, and a trace-fossil suite consistent with a stressed expression of the distal *Cruziana* Ichnofacies (Dafoe and Williams, 2020a)	Late *Cretaceous* (G.L. Williams, pers. comm. *in* MacLean and Falconer, 1979); Campanian (MacLean et al., 1981); late Coniacian–Santonian (MacLean et al., 2014)	Probably neritic (MacLean and Falconer, 1979; MacLean et al., 1981); distal prodelta (Dafoe and Williams, 2020a)	TOC: 0.63%

Modified from Dafoe and Williams (2020a)Samples include seabed drill cores, dredge samples, and bedrock fragments from within a piston core.
Samples are organized by rock types separated by a bold black line (and then by expedition number and original station number) in the following order: metamorphic rock and sedimentary rock units.
Total organic carbon (TOC) and vitrinite reflectance (Ro) values are from Zhang (2013), and some were averaged from multiple samples.

Table 1. (cont.) List of Geological Survey of Canada bedrock samples collected during marine cruises.

Expedition	Year	Original station no.	General location	Latitude (°N)	Longitude (°W)	Sample type	Length of bedrock core (cm)	Water depth (m)	Rock type	Description	Age	Paleoenvironment	Other analyses (Zhang, 2013)
80028	1980	7	Buchan Trough	71.85	73.16	Rock drill	44	562	Mudstone	Mudstone-siltstone (MacLean, 1980); dark grey, calcareous siltstone and organic-rich silty mudstone with glauconite and siderite (MacLean et al., 2014); dark grey, silty mudstone, with wavy and planar lamination, soft-sediment deformation, and a trace-fossil suite characteristic of a stressed expression of the *Zoophycos* Ichnofacies (Dafoe and Williams, 2020a)	Late Coniacian–early Santonian (MacLean et al., 2014)	Prodelta (Dafoe and Williams, 2020a)	TOC: 1.71%
80028	1980	8	Buchan Trough	71.85	73.16	Rock drill	4	585	Mudstone	Mudstone-siltstone (MacLean, 1980) revised to dark grey, calcareous siltstone and organic-rich silty mudstone with glauconite and siderite (MacLean et al., 2014); dark grey sandy mudstone with planar and wavy laminations, soft-sediment deformation and a stressed expression the distal *Cruziana* Ichnofacies (Dafoe and Williams, 2020a)	Late Coniacian–early Santonian (MacLean et al., 2014)	Prodelta (Dafoe and Williams, 2020a)	TOC: 1.66%
80028	1980	49	Scott Trough	71.26	70.61	Rock drill	9	650	Mudstone	(?)Gravel (MacLean, 1980); dark brown mudstone fragments with a possible reddish stain (Dafoe and Williams, 2020a)	Lutetian (Dafoe and Williams, 2020a)	Inner neritic (Dafoe and Williams, 2020a)	
80028	1980	58	Scott Trough	71.27	70.68	Rock drill	10	743	Mudstone	Limestone, thought to be from the Cretaceous or Tertiary sequence (Levy and MacLean, 1981; MacLean et al., 1981; Harrison et al., 2011a); dark grey-brown, carbonate-cemented mudstone with cone-in-cone structures and stylolites (Dafoe and Williams, 2020a)			TOC: 0.85%
80028	1980	73	Scott Trough	71.40	70.15	Piston core	n.a.	432	Shale	Numerous black shale fragments from the lower part of the piston core (MacLean et al., 1981; MacLean et al., 2014); fissile shale fragments with a yellow, sulphurous coating and angular shape suggesting minimal transport distances (Dafoe and Williams, 2020a)	Campanian (MacLean et al., 1981); late Coniacian–early Santonian, probably late Coniacian (MacLean et al., 2014)	Rich assemblage of dinocysts indicates a marine setting (MacLean et al., 2014); quiet-water, shelfal setting (Dafoe and Williams, 2020a)	TOC: 1.61%; Ro: 0.59%
80028	1980	81	Paallavvik (island) area	67.27	62.15	Rock drill	6	265	Siltstone	Mudstone-siltstone (MacLean, 1980) revised to dark grey silty mudstone (MacLean et al., 2014); muddy siltstone with faint laminations, rare mottling, organic detritus and scattered granules and pebbles (Dafoe and Williams, 2020a)	Late Albian (MacLean et al., 2014)	Nonmarine (MacLean et al., 2014); quiet-water setting, possibly floodplain (Dafoe and Williams, 2020a)	TOC: 2.64%

Modified from Dafoe and Williams (2020a)Samples include seabed drill cores, dredge samples, and bedrock fragments from within a piston core.
Samples are organized by rock types separated by a bold black line (and then by expedition number and original station number) in the following order: metamorphic rock and sedimentary rock units.
Total organic carbon (TOC) and vitrinite reflectance (Ro) values are from Zhang (2013), and some were averaged from multiple samples.

Table 1. (cont.) List of Geological Survey of Canada bedrock samples collected during marine cruises.

Expedition	Year	Original station no.	General location	Latitude (°N)	Longitude (°W)	Sample type	Length of bedrock core (cm)	Water depth (m)	Rock type	Description	Age	Paleoenvironment	Other analyses (Zhang, 2013)
82034	1982	3	Home Bay	68.87	65.66	Rock drill	19	659	Siltstone	Semiconsolidated dark grey mudstone, siltstone, and sandstone (MacLean and Williams, 1983; MacLean et al., 2014); dark grey mudstone with mica minerals (Dafoe and Williams, 2020a)	Campanian (MacLean and Williams, 1983); late Santonian–early Campanian (MacLean et al., 2014)	Mid-shelf (MacLean et al., 2014); quiet-water setting (Dafoe and Williams, 2020a)	TOC: 2.58%
82034	1982	6	Home Bay	68.86	65.67	Rock drill	1	530	Siltstone	Small amount of bedrock (MacLean and Williams, 1983) described as semiconsolidated dark grey mudstone, siltstone, and sandstone (MacLean et al., 2014); siltstone (Dafoe and Williams, 2020a)			
82034	1982	8	Home Bay	68.65	65.67	Rock drill	15	?	Mudstone	Semiconsolidated mudstone, organic-rich with a petroliferous odor (MacLean and Williams, 1983); dark grey, friable mudstone (Dafoe and Williams, 2020a)	Late Cretaceous (MacLean and Williams, 1983); Santonian (MacLean et al., 2014)	Presence of dinocysts suggests marine (MacLean and Williams, 1983; MacLean et al., 2014); quiet-water setting, likely shelfal (Dafoe and Williams, 2020a)	TOC: 3.74%
82034	1982	10	Home Bay	68.64	65.70	Rock drill	17	460	Sandstone	Semiconsolidated dark grey mudstone, siltstone, and sandstone (MacLean and Williams, 1983; MacLean et al., 2014); grey, muddy sandstone with planar lamination, organic detritus, and mudstone laminae (Dafoe and Williams, 2020a)	Late Cretaceous (MacLean and Williams, 1983)	Presence of dinocysts suggests a marine setting (MacLean and Williams, 1983); deltaic (Dafoe and Williams, 2020a)	TOC: 5.73%; Ro: 0.5%
82034	1982	16	Paallavvik (island) area	67.26	62.19	Rock drill	6	368	Mudstone	Semiconsolidated, fine-grained clastic sediment with coal fragments (MacLean and Williams, 1983; MacLean et al., 2014); mudstone with sandstone laminae (Dafoe and Williams, 2020a)	Albian (MacLean and Williams, 1983); Aptian to middle Albian (MacLean et al., 2014)	Nonmarine, but possible proximity to a shoreline (MacLean and Williams, 1983; MacLean et al., 2014); quiet-water setting, possibly floodplain or lagoonal (Dafoe and Williams, 2020a)	
85027	1985	23	Paallavvik (island) area	67.25	62.18	Rock drill	117	?	Sandstone	Well consolidated calcareous sandstone (MacLean, 1985; MacLean et al., 2014); silty grey sandstone with tabular crossbedding, planar lamination, massive bedding, wave ripple cross-stratification, mudstone rip-up clasts, and organic detritus (Dafoe and Williams, 2020a)	Unknown age, but may be related to the white sandstone of Aptian–early Albian age on Qaqulluit (island; MacLean et al., 2014)	Fluvial or shallow marine (Dafoe and Williams, 2020a)	TOC: 7.84%; Ro: 0.44%

Modified from Dafoe and Williams (2020a)Samples include seabed drill cores, dredge samples, and bedrock fragments from within a piston core.
Samples are organized by rock types separated by a bold black line (and then by expedition number and original station number) in the following order: metamorphic rock and sedimentary rock units.
Total organic carbon (TOC) and vitrinite reflectance (Ro) values are from Zhang (2013), and some were averaged from multiple samples.

that outcrop along the northern edge of Baffin Bay (including some exposures of the Proterozoic Thule Basin) and form the Ellesmere-Devon terrane (Fig. 3; St-Onge et al., 2009; Harrison et al., 2011b).

Previous offshore mapping and sampling

The offshore pre-rift basement under western Baffin Bay forms a key component in mapping and understanding the distribution of stratigraphic units within grabens and half-grabens. In their study, Jackson et al. (1992) found a northwest-oriented structural trend from Home Bay to Devon Island that included grabens and basement ridges running parallel to the coast (Fig. 3). Along this part of the margin, most basins are half-grabens, such as the Scott Graben (Jackson et al., 1992), and the continental basement is typically downfaulted abruptly, consisting of rotated and eroded blocks with a locally thin sedimentary cover (Rice and Shade, 1982; Jackson et al., 1992). Farther offshore, the top of oceanic basement forms a more rugose surface (Jackson et al., 1992). North of Bylot Island, offshore Devon and Ellesmere islands, the structural trend changes to north-northeast, and small basins are developed locally (Fig. 3; Jackson et al., 1992). The continental basement underlying western Baffin Bay is likely composed of Archean and Paleoproterozoic granitoid rocks, gneissic rocks, metasedimentary strata, and other supracrustal rocks (MacLean et al., 1990; Harrison et al., 2011a). Localized sampling has shown that Rae Craton metamorphic rocks underlie parts of the offshore (Table 1; Fig. 2, 3). Southeast of Clyde River, near ODP Site 645, drill core 78029-34 sampled metamorphic bedrock (MacLean and Falconer, 1979). Farther north, outboard of Scott Inlet, MacLean and Falconer (1979) identified linear basement ridges, along which drill cores of metamorphic rock were recovered (78029-19 and 78029-20; inset A, Fig. 3; MacLean and Falconer, 1979; MacLean et al., 1981). Offshore Buchan Trough, MacLean et al. (1981) proposed that Precambrian basement rocks likely underlie the Cretaceous strata sampled from the seafloor. Offshore Bylot Island, the basement could include both Precambrian and prerift sedimentary rocks (Rice and Shade, 1982).

Based on elevated interval velocities (5–6.2 km/s) and intermediate refraction velocities in northern Baffin Bay, Harrison et al. (2011a) suggested the possibility that both Mesoproterozoic prerift and lower Paleozoic (Cambrian–Silurian) rocks could be present above crystalline basement. Proterozoic metasediments are now known from coreholes in the Melville Bay region, which have been correlated with deep reflections there (Nøhr-Hansen et al., 2018; Gregersen et al., this volume). Mesoproterozoic Borden Basin and Thule Basin equivalents have been interpreted beneath Lancaster Sound (Kerr, 1980; Atkinson et al., 2017) and south of Coburg Island (Harrison et al., 2011a), based on reflection seismic interpretation, as well as beneath Lady Ann Basin (Harrison et al., 2011a), the Carey Basin area (Reid and Jackson, 1997), and south of North Water Basin (Funck et al., 2006), based on refraction velocities. Outcrops of Paleozoic strata are widespread along western Baffin Island (Scott and de Kemp, 1998; Bingham-Koslowski, Zhang, and McCartney, this volume) and along the southeast Baffin Shelf (MacLean and Srivastava, 1976; Jansa, 1976; MacLean et al., 1977; MacLean, 1978; Bingham-Koslowski, Zhang, and McCartney, this volume; Dafoe, DesRoches, and Williams, this volume). Whereas Paleozoic rocks have not been sampled in Baffin Bay, reworked Carboniferous palynomorphs have been reported from West Greenland wells (MacLean et al., 1990). Successions considered to be Paleozoic have been interpreted beneath Lancaster Sound (Kerr, 1980; Harrison et al., 2011a; Brent et al., 2013; Atkinson et al., 2017), Jones Sound (Keen and Barrett, 1973; MacLean et al., 1984), offshore northeastern Baffin Island (Rice and Shade, 1982), and as far south as the Home Bay region (Keen et al., 1974; Fader et al., 1989), based primarily on the presence of deep, layered reflections on seismic reflection data.

Distribution and seismic reflection character

In this study, a map of the basement platform (defined as less than 3500 m depth; *see* Keen et al., this volume) and basement highs is presented, with ties to known samples, as well as corresponding fault trends (Fig. 3). Key seismic lines illustrate the basement character (Fig. 4). As described in previous studies and Keen et al. (this volume), normal faults generally trend northwest from Cape Dyer to the Bylot Island area (Fig. 3). This trend changes to a more northerly orientation in northwestern Baffin Bay, where structures are more complex. In general, basement is shallow below the Baffin Shelf except for large half-grabens or grabens in the Home Bay region and at Scott and Buchan grabens. The typical basement platform is shown in Figure 4b where it lies at about 2 s two-way traveltime depth, before shallowing further at a major basement ridge and then downfaulting steeply eastward into the Baffin Basin. Scott Graben forms one of the deepest rift-grabens along this margin and is filled by up to 3.5 s two-way traveltime of sedimentary strata (Fig. 4c). It is a half-graben bounded to the southwest by a major fault and to the northeast by a basement ridge sampled by 78029-19 and 78029-20. Additional smaller grabens can be seen northeast of the basement ridge. Beneath the slope on Figure 4a and 4c the continental crust appears to dip beneath a volcanic layer (Keen et al., this volume). Northward, across the mouth of Lancaster Sound (Fig. 3), is a complex basement ridge structure with several smaller ridges farther offshore. Farther north, the Lady Ann Basin forms a basement low offshore Devon Island, and the basement platform widens to the northeast. Additional basins in northern Baffin Bay are difficult to define with the available seismic data set.

Seaward of the present-day Baffin Shelf, the basement generally drops steeply, as a result of crustal thinning and subsidence. The nature of the transition between continental and oceanic crust is not completely clear and is discussed further in Keen et al. (this volume), and the present authors show the location of their landward limit of oceanic crust on the maps and seismic profiles of this study (Fig. 3, 4). In the south (Fig. 4a), this transition is interpreted as a possible volcanic margin and is marked by a basement ridge with high-amplitude reflections ((?)inner flows) lying inboard (Fig. 4a; *see* 'Paleocene-Eocene volcanic rocks' section; Keen et al., this volume). Seaward of this is a slightly rugose oceanic basement followed by a deep extinct spreading axis (Fig. 4a). The continental-ocean transition appears to be more abrupt off Home Bay (Fig. 4b), where a basement high drops steeply down to oceanic basement (Fig. 4b). Farther offshore, the seismic line crosses the large 64°W fracture zone, seen as a topographic low in the basement. Seaward of Scott Graben (Fig. 4c), smooth continental basement (possibly masked by volcanic flows) becomes more rugose, suggestive of oceanic basement, near the base of the present-day slope. Basinward, the extinct spreading axis also forms a distinct structural low.

STRATIGRAPHIC OVERVIEW

This study interprets the Cretaceous and Cenozoic stratigraphic sections underlying western Baffin Bay based on seismic reflection data tied to the bedrock samples collected by the GSC, as well as to ODP Site 645 for the Neogene section. In addition, the stratigraphy is interpreted in relation to analogues including: the Cretaceous and Cenozoic stratigraphy of the Labrador margin, where there is a well established lithostratigraphy and biostratigraphy (*see* Dafoe, Dickie, Williams, and McCartney, this volume); the nearby onshore Lower Cretaceous through Paleocene succession of Bylot Island and east-central Baffin Island (*see* Haggart et al., this volume); and the conjugate West Greenland margin (*see* Gregersen et al., this volume). In particular, the present authors describe the stratigraphy in light of the lithostratigraphic framework of the Labrador margin, inferring intervals that relate to this stratigraphy. For each stratigraphic interval, the available samples, previous offshore mapping, and their seismic character are described based on the present study. Three main intervals are interpreted and their distribution mapped: Cretaceous, lower Cenozoic, and upper Cenozoic.

CRETACEOUS INTERVAL

Stratigraphic analogues

The only physical evidence for the presence of offshore Cretaceous rocks in the study region is from seabed samples of bedrock (Table 1; Fig. 5). Accordingly, this study uses these known data points, but also relies on the seismic-stratigraphic character

Figure 3. Distribution of the basement platform of western Baffin Bay at 3500 m and isolated basement highs (*after* Keen et al., this volume), as well as the location of relevant GSC seabed samples of basement rock (*see* Table 1 for more details). Faults, basin outlines, and the landward limit of oceanic crust are from Keen et al. (this volume). Fracture zones and the location of the extinct seafloor spreading axis are from Oakey and Chalmers (2012). The ODP Site 645 corehole did not penetrate deep enough to intersect basement. Additional projection information is as follows: Central Meridian = 60°W; Standard Parallels = 65, 75°W; Latitude of Origin = 65°N. FZ = Fracture zone. For abbreviations *see* Figure 1b.

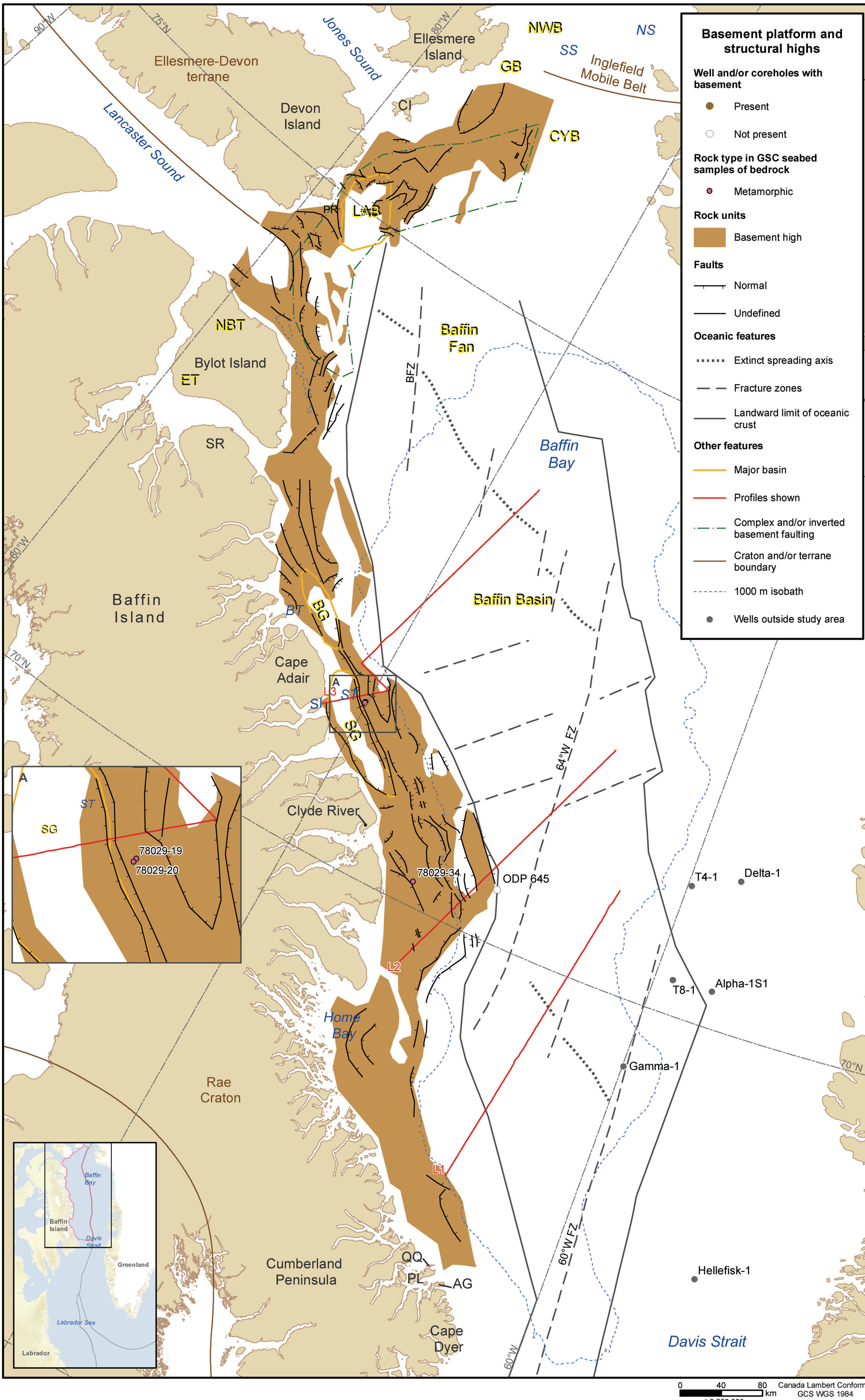

Basement platform and structural highs
Well and/or coreholes with basement
Present
Not present
Rock type in GSC seabed samples of bedrock
Metamorphic
Rock units
Basement high
Faults
Normal
Undefined
Oceanic features
Extinct spreading axis
Fracture zones
Landward limit of oceanic crust
Other features
Major basin
Profiles shown
Complex and/or inverted basement faulting
Craton and/or terrane boundary
1000 m isobath
Wells outside study area
Ellesmere-Devon terrane
Ellesmere Island
Devon Island
Jones Sound
Lancaster Sound
NWB
NS
SS
GB
Inglefield Mobile Belt
CI
CYB
PR
LAB
NBT
Bylot Island
ET
SR
Baffin Fan
BFZ
Baffin Bay
Baffin Basin
Baffin Island
BT
BG
Cape Adair
A
L3
ST
SI
SG
64°W FZ
Clyde River
78029-19
78029-20
78029-34
ODP 645
T4-1
Delta-1
T8-1
Alpha-1S1
L2
Home Bay
Gamma-1
Rae Craton
L1
Cumberland Peninsula
QQ
PL
AG
Cape Dyer
60°W FZ
Hellefisk-1
Davis Strait
Baffin Bay
Baffin Island
Davis Strait
Greenland
Labrador Sea
Labrador
90°W
80°W
75°N
70°N
60°W
0
40
80
km
1:3 500 000
Canada Lambert Conformal
GCS WGS 1984

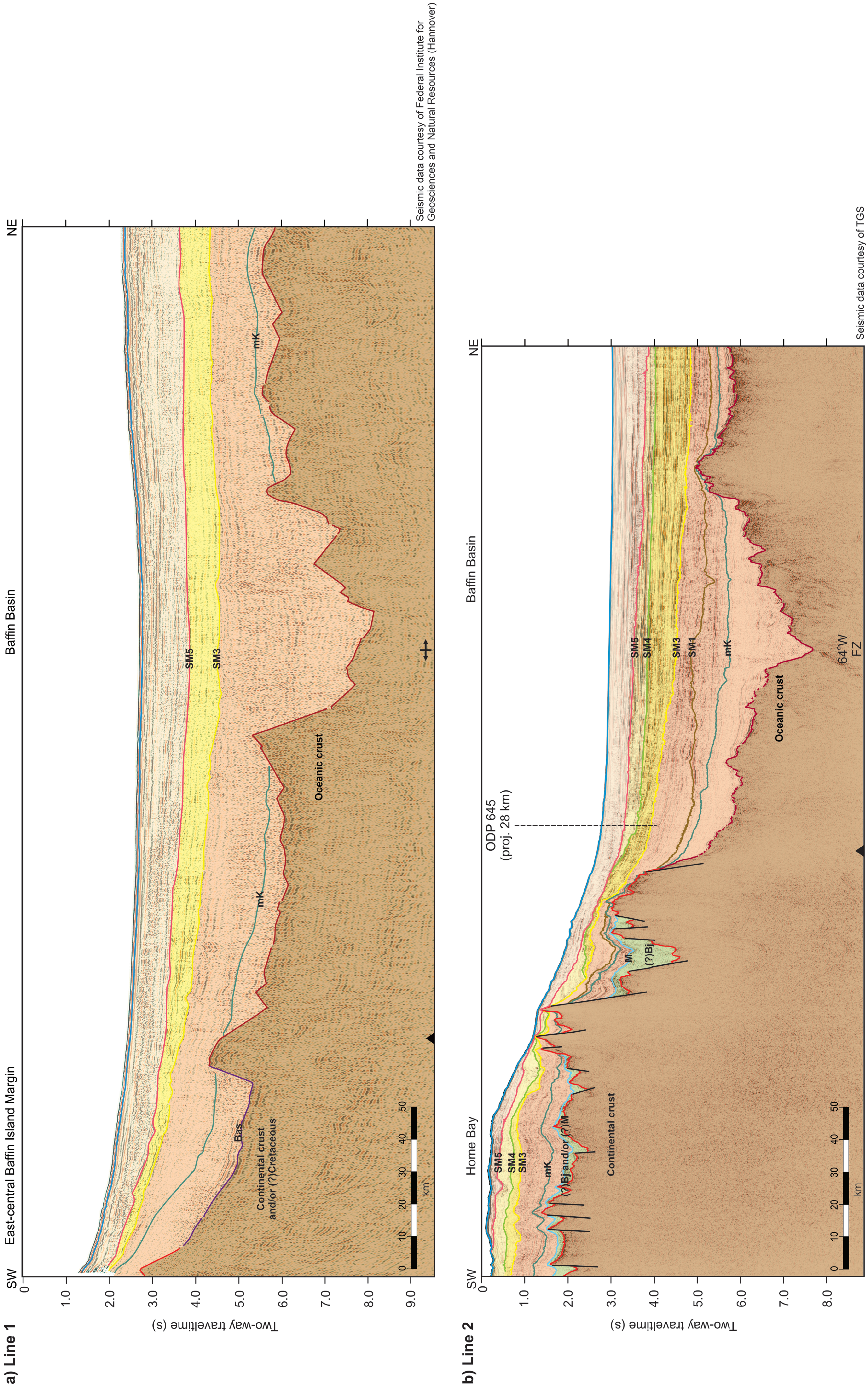
a) Line 1
SW
NE
East-central Baffin Island Margin
Baffin Basin
Two-way traveltime (s)
0
1.0
2.0
3.0
4.0
5.0
6.0
7.0
8.0
9.0
SM5
SM3
mK
Bas.
Continental crust and/or (?)Cretaceous
Oceanic crust
0
10
20
30
40
50
km
Seismic data courtesy of Federal Institute for Geosciences and Natural Resources (Hannover)
b) Line 2
SW
NE
Home Bay
Baffin Basin
ODP 645 (proj. 28 km)
Two-way traveltime (s)
SM5
SM4
SM3
SM1
mK
(?)Bj and/or (?)M
(?)Bj
M
Continental crust
Oceanic crust
64°W FZ
km
Seismic data courtesy of TGS

Figure 4. Seismic lines crossing the Baffin Island margin, with the line locations shown in Figure 1. **a)** Line 1 outboard of the southern portion of the east-central Baffin Island margin north of Cape Dyer. This line does not capture the present-day shelf, but only shows the slope and deep Baffin Basin. Seismic data courtesy of the Federal Institute for Geosciences and Natural Resources (Hannover; line BGR08-304). **b)** Line 2 crossing the Home Bay region showing a shallow basement platform with overlying Upper Cretaceous and Cenozoic strata. The ODP Site 645 corehole location is projected 28 km to the northwest onto this line and was shifted downward to match most seismic horizons that correspond to those at the corehole location (*see* Fig. 7). Seismic data courtesy of TGS. proj. = projection, FZ = Fracture zone.

and knowledge of the tectonic evolution of the region from other margins of the seaway to map the Cretaceous interval along western Baffin Bay. On the Labrador margin, Cretaceous strata include the Early Cretaceous Alexis (alkaline basalt) and Lower Cretaceous Bjarni (sandstone, conglomerate, shale, and coal) formations, and the Upper Cretaceous to Selandian Markland Formation shale and its Freydis Member sandstone units (Fig. 2; Umpleby, 1979; McWhae et al., 1980; Dafoe, 2021; Dafoe, Dickie, Williams, and McCartney, this volume). These units have been sampled in numerous wells along the Labrador margin and are mapped regionally in seismic data (Bell, 1989; Balkwill and McMillan, 1990; Dickie et al., 2011; Dafoe, Dickie, Williams, and McCartney, this volume). The Bjarni Formation typically shows growth into fault planes since it was deposited during the early rift phase (Dickie et al., 2011), and is late Barremian to late Albian (Dafoe, Dickie, Williams, and McCartney, this volume). In contrast, the Upper Cretaceous Markland Formation (Cenomanian to early Selandian) may overstep the grabens to drape the underlying structure. It is a relatively seismically transparent unit since it is a thick, shale-prone interval (Balkwill and McMillan, 1990; Dickie et al., 2011; Dafoe, Dickie, Williams, and McCartney, this volume).

Cretaceous rocks are also present onshore Bylot Island and northern Baffin Island within the Eclipse and North Bylot troughs (Fig. 5; Jackson et al., 1975; Clarke, 1976; Miall et al., 1980; Ioannides, 1986; Haggart et al., this volume). In Eclipse Trough, Miall et al. (1980) subdivided the Cretaceous strata into two formations, the Lower Cretaceous, fluvial-dominated Hassel Formation, and the Upper Cretaceous, marine mudstone-dominated Kanguk Formation. On southwest Bylot Island, the Kanguk Formation was later subdivided into informal units, the Upper Cretaceous shale-dominated Bylot Island and Byam Martin formations, and the sandstone-dominated Sermilik formation (Sparkes, 1989; Waterfield, 1989; Benham, 1991; Benham and Burden, 1990; Wiseman, 1991; Haggart et al., this volume). In the Salmon River area, Jackson et al. (1975) mapped several Cretaceous localities also shown in Haggart et al. (this volume), but here only the best described outcrops are shown in Figure 5. With the exception of portions of the Hassel Formation, much of this succession reflects marine settings with shallow-marine deposition taking place in the Early Cretaceous and more distal marine conditions developing in the Late Cretaceous (Dafoe and Haggart, 2018; Dafoe et al., 2019). Possible Cretaceous rocks have also been postulated in the onshore Clyde River area (Jackson et al., 1979; *see* Haggart et al., this volume).

Along the conjugate West Greenland margin, the Lower Cretaceous to Cenomanian stratigraphic package (unit G of Gregersen et al., 2013, 2019, this volume) shows growth along extensional faults during the early rift phase. Lower Cretaceous rocks of this interval were recovered from shallow coreholes just off of Kap York in northeastern Baffin Bay, including sandstone, mudstone, and thin coal units deposited in nonmarine to shallow-marine settings (floodplain, swamp, lake, prodelta, shoreface, and bay) during the early rift phase (Nøhr-Hansen et al., 2018). These coreholes also contain Upper Cretaceous marine mudstone units with lesser sandstone units formed under anoxic to dysoxic conditions in outer shelf, prodelta, and distal delta-front settings (Nøhr-Hansen et al., 2018); part of the overlying Upper Cretaceous unit F, which includes marine mudstone, sandstone, and local conglomerate units is also sampled in industry wells (Gregersen et al., 2019, this volume).

Lower Cretaceous Bjarni Formation equivalent

Onshore in the east-central Baffin Island area, on Aggijjat, Paallavvik, and Qaqulluit (islands; Fig. 5), Burden and Langille (1990) defined two new formations lying above weathered Precambrian gneiss and below the Cape Dyer basalt units. The older unit, the Quqaluit Formation, was primarily deposited during the Early Cretaceous as braided and meandering river deposits. This formation, which ranges from a few centimetres to more than 122 m thick, is variably bedded, pebbly to fine-grained, crossbedded, white to yellow, subarkose and quartz arenite, with lesser wacke, siltstone, and coal beds (Burden and Langille, 1990). The lower, white, braided river sandstone units were replaced upward by yellow, anastomosed or meandering river deposits. Burden and Langille (1991) noted that there was a distinct lithological break between the white, and overlying yellow sandstone units of the Quqaluit Formation, as well as a dramatic increase in palynomorph diversity in the yellow sandstone units. The change in colour and depositional setting were equated with differences in age of the Quqaluit Formation: the white sandstone units were considered to be late Neocomian and Aptian, whereas the yellow sandstone units are late Albian and Cenomanian, possibly indicating an unconformity between the two rocks types. Later, Fenton and Pardon (2007) suggested an Aptian–late Albian age for the lower white sandstone units and a late Albian age for the overlying yellow sandstone units, possibly indicating little missing section. Very rare and poorly preserved dinoflagellate cysts (dinocysts) and acritarchs (organic-walled microfossils of unknown origin) are found in shale and siltstone units at the top of the Quqaluit Formation on Paallavvik (island), indicating the establishment of brackish, marginal marine conditions (Burden and Langille, 1990).

About 13 km offshore of Paallavvik (island), the bedrock sample 80028-81 contains a muddy siltstone interval of late Albian age and nonmarine affinity, possibly deposited in a floodplain setting (Fig. 5; Table 1; MacLean, 1980; MacLean et al., 2014; Dafoe and Williams, 2020a). Nearby drill core 82034-16 sampled mudstone with sandstone laminae, coal fragments, and a miospore assemblage that indicates an Albian age (MacLean and Williams, 1983; Dafoe and Williams, 2020a). Burden and Langille (1990) suggested that this sample was probably equivalent to onshore Quqaluit Formation rocks. MacLean et al. (2014) reanalyzed the sample, concluding that it was Aptian–Albian and deposited in a nonmarine setting, but possibly close to a paleoshoreline due to the presence of acritarchs, and Dafoe and Williams (2020a) indicated that a floodplain or lagoonal depositional setting was plausible. During 1985, drill core 85027-23 was collected in the same region (Fig. 5; MacLean, 1985) and consists of silty sandstone, with crossbedding, planar lamination, and mudstone rip-up clasts (Dafoe and Williams, 2020a). No age could be determined for this sample due to its coarse-grained nature, but it bears similarity to the Neocomian to Aptian white sandstone units of the Quqaluit Formation found onshore (MacLean et al., 2014). The fluvial to shallow-marine setting proposed by Dafoe and Williams (2020a) also mirrors that of this nearby onshore succession. Juxtaposition of such different lithologies between the closely spaced 1985 and earlier samples could indicate a lateral or stratigraphic heterogeneity, common in fluvial settings, or that sample 85027-23 reflects a slightly different age, possibly older strata due to its association with the older, white Quqaluit Formation sandstone units. Overall, these samples compare well with the Bjarni Formation sandstone and its Snorri Member mudstone units in age and lithology (Fig. 2). The depositional settings tend toward a more nonmarine signature, typical for the lower Bjarni Formation, but less common in the middle to late Albian when deltaic and shallow-marine settings prevailed (Dafoe and Williams, 2020d; Dafoe, 2021; Dafoe, Dickie, Williams, and McCartney, this volume).

Upper Cretaceous Markland Formation equivalent

Bedrock drill cores were recovered in the Home Bay area at stations 82034-3, 82034-6, 82034-8, and 82034-10, from two localities about 24 km apart and consist of semiconsolidated mudstone, siltstone, and lesser sandstone units, with some planar laminae and organic detritus (Fig. 5; Table 1; MacLean and Williams, 1983; Dafoe and Williams, 2020a). The samples were found to be Campanian (82034-3) or more generally, Late Cretaceous (82034-8 and 82034-10), based on dinocyst assemblages (MacLean and Williams, 1983). Sample 82034-8 had a petroliferous odour, indicating an organic-rich, potential source rock. Stations 82034-5 and 82034-6 are thought to have intersected short intervals of material similar to those at 82034-3 (only 82034-6 is shown on Fig. 5; MacLean and Williams, 1983), but the in situ nature of these samples is suspect since little material was recovered. MacLean et al. (2014) later studied some of these samples and found 82034-3 to be late Santonian–early Campanian and deposited in a

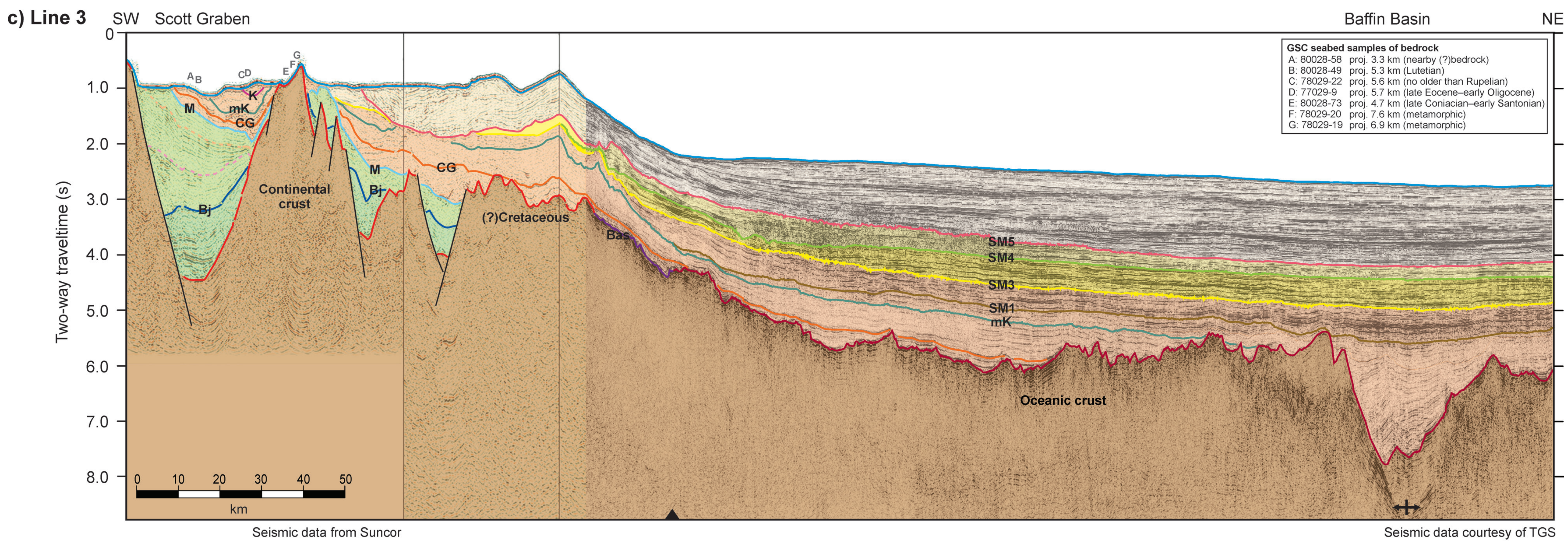

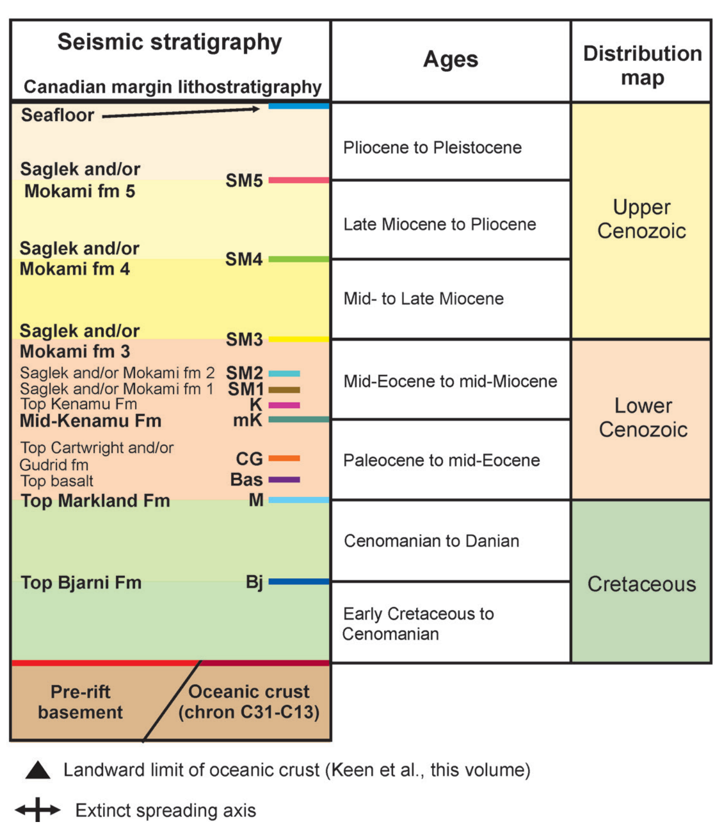

Figure 4. (cont.) Seismic lines crossing the Baffin Island margin, with the line locations shown in Figure 1. **c)** Line 3 through the Scott Graben showing the bounding basement ridge and a small outer half-graben and graben transitioning to a smoother continental basement possibly overlain by volcanic rocks (Bas) and then oceanic crust in deeper water. Infill in grabens and half-grabens is primarily Cretaceous. Seismic data courtesy of Suncor and TGS. proj. = projection.

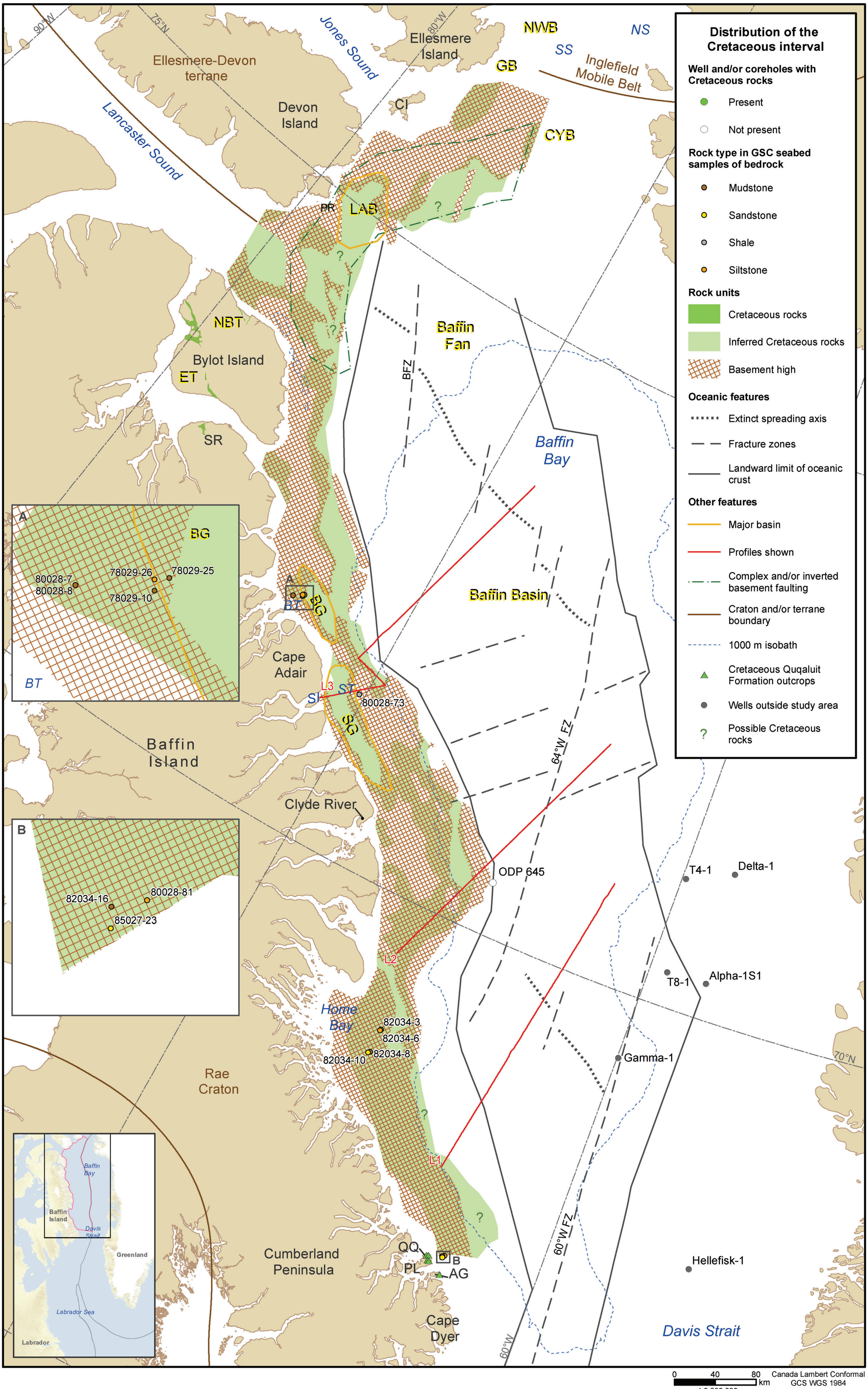
Distribution of the Cretaceous interval
Well and/or coreholes with Cretaceous rocks
Present
Not present
Rock type in GSC seabed samples of bedrock
Mudstone
Sandstone
Shale
Siltstone
Rock units
Cretaceous rocks
Inferred Cretaceous rocks
Basement high
Oceanic features
Extinct spreading axis
Fracture zones
Landward limit of oceanic crust
Other features
Major basin
Profiles shown
Complex and/or inverted basement faulting
Craton and/or terrane boundary
1000 m isobath
Cretaceous Quqaluit Formation outcrops
Wells outside study area
Possible Cretaceous rocks
Ellesmere-Devon terrane
Jones Sound
Ellesmere Island
NWB
NS
SS
GB
Inglefield Mobile Belt
Devon Island
CI
CYB
Lancaster Sound
PR
LAB
NBT
Bylot Island
ET
SR
Baffin Fan
BFZ
Baffin Bay
Baffin Basin
BG
BT
Cape Adair
L3
ST
SI
80028-73
SG
Baffin Island
Clyde River
ODP 645
64°W FZ
T4-1
Delta-1
L2
T8-1
Alpha-1S1
Home Bay
82034-3
82034-6
82034-8
82034-10
Gamma-1
Rae Craton
L1
Cumberland Peninsula
QQ
PL
AG
B
Cape Dyer
60°W FZ
Hellefisk-1
Davis Strait
70°N
75°N
80°W
90°W
60°W
A
80028-7
80028-8
78029-26
78029-25
78029-10
82034-16
80028-81
85027-23
Baffin Bay
Baffin Island
Davis Strait
Greenland
Labrador Sea
Labrador
0 40 80 km
1:3 500 000
Canada Lambert Conformal
GCS WGS 1984

mid-shelf setting, and 82034-8 to be Santonian. Dafoe and Williams (2020a) further postulated a shelfal setting for station 82034-8 and deltaic for station 82034-10.

In Scott Trough, Cretaceous samples include rock fragments from a piston core and possibly from a drill core (Fig. 5; Table 1). Black shale fragments in piston core 80028-73 from the outer part of Scott Trough were assigned a Campanian age by MacLean et al. (1981) and were later reanalyzed and found to be consistent with the late Coniacian to early Santonian, but are probably late Coniacian (MacLean et al., 2014). The fragments increase in abundance and size toward the base of the core and their friable and angular nature suggests a nearby source (Dafoe and Williams, 2020a), possibly strata exposed at the seafloor subcropping at a relatively steep angle adjacent to the nearby basement high (Fig. 4c). The shale has a rich dinocyst assemblage, indicating marine deposition, likely on the shelf (MacLean et al., 2014; Dafoe and Williams, 2020a). During the same cruise, a short drill core of calcareous mudstone with cone-in-cone structures (sample 80028-58; Dafoe and Williams, 2020a) was recovered from the floor of Scott Trough and interpreted as part of the Cretaceous or Cenozoic sequence (Levy and MacLean, 1981; Table 1). Dafoe and Williams (2020a), however, suggested that the core interval may not be from in situ material since it does not fill the full width of the core barrel. Furthermore, the presence of cone-in-cone structures suggests a possible affinity with similar lithofacies noted in Paleocene rocks on Bylot Island (Dafoe et al., 2019); therefore, sample 80028-58 may represent Paleocene strata possibly sourced from nearby bedrock exposures (*see* Fig. 6; Dafoe and Williams, 2020a).

North of Scott Inlet, along the floor of Buchan Trough, GSC cruise 78029 collected three sedimentary bedrock drill cores (stations 10, 25, and 26) consisting of dark grey siltstone to silty mudstone units with abundant glauconite, interpreted as Late Cretaceous and of a neritic origin (Fig. 5; Table 1; MacLean and Falconer, 1979; MacLean et al., 1981). Dafoe and Williams (2020a) refined the observations to include the presence of local sandstone laminae, load structures, organic detritus, and trace fossils consistent with the distal *Cruziana* and *Zoophycos* ichnofacies, indicating deposition in outer shelf and prodelta settings. During a subsequent cruise, 80028-7 and 80028-8 recovered silty and sandy mudstone samples with wavy and planar lamination, soft-sediment deformation, and stressed expressions of the *Zoophycos* and distal *Cruziana* ichnofacies representing prodelta settings (Fig. 5; Table 1; MacLean, 1980; Dafoe and Williams, 2020a). MacLean et al. (2014) found the samples from Buchan Trough to be late Coniacian to early Santonian (80028-7), Santonian, but possibly late Coniacian (78029-26 and 78029-25), and late Coniacian (78029-10).

The Upper Cretaceous bedrock samples from the Baffin Shelf are dominated by upper Coniacian–lower Campanian mudstone units, consistent with the Markland Formation of the Labrador margin (Fig. 2). The samples indicate prodelta, shelf, and outer shelf deposition, slightly more proximal than settings interpreted for the Markland Formation, offshore Labrador (*see* Dafoe, Dickie, Williams, and McCartney, this volume). Furthermore, prodeltaic settings indicate fluvial influx and plausible Freydis Member–equivalent shoreline sandstone units may be present in the region.

Based on these offshore samples and nearby onshore occurrences, the age of the oldest synrift strata, Bjarni Formation equivalent, that may exist along the western Baffin Bay is constrained by: the onshore Bylot Island Hassel Formation of Albian–Cenomanian age (Miall et al., 1980); the onshore Quqaluit Formation of late Neocomian to Aptian and late Albian and Cenomanian age (Burden and Langille, 1990, 1991); and offshore samples near Paallavvik (island) of confirmed Aptian–Albian age (Fig. 5; Table 1; MacLean, 1980; MacLean and Williams, 1983; MacLean et al., 2014). The presence of Upper Cretaceous sedimentary strata, predominantly mudstone units, across the Baffin Shelf is established by shallow drill core and seabed samples (Fig. 5; Table 1), and reflects a widespread Markland Formation equivalent in the study region.

Previous offshore mapping

By analogy with adjacent rifted margins, Rice and Shade (1982) interpreted Cretaceous deposits within rift structures of northern Baffin Bay, whereas others mapped more generalized, thick Cretaceous–Cenozoic sedimentary successions in Baffin Bay (e.g. Grant, 1988; Fader et al., 1989; Jackson et al., 1992). Harrison et al. (2011a) identified synrift strata that indicate accumulation during active, listric normal faulting in half-grabens (i.e. growth-faulting), and Oakey and Chalmers (2012) mapped the distribution of Cretaceous and younger sedimentary strata along the margin. Cumulatively, these authors recognized synrift Lower and Upper Cretaceous strata in Lancaster Sound, and northward into Smith Sound, with thick successions in Scott Graben, Lancaster Central Graben, Lady Ann Basin, Glacier Basin, Jones Sound Basin, and Carey Basin.

In the Paallavvik (island) and Home Bay areas, MacLean et al. (2014), using single-channel seismic data, interpreted folded and faulted Cretaceous strata. Farther north, MacLean and Falconer (1979) inferred the presence of acoustically hard, presumably Cretaceous, sedimentary rocks below the Scott Trough region, and older strata below the Upper Cretaceous rocks sampled from Buchan Trough. Subsequently, MacLean et al. (1981), using seismic reflection data and bedrock samples, postulated Lower Cretaceous sedimentary rocks within both Scott and Buchan grabens, but reasoned that a thicker succession was present in the former, based on potential fields and seismic data. In Scott Graben, Harrison et al. (2011a) also interpreted a Lower Cretaceous unit and growth along faults within overlying Upper Cretaceous to Danian synrift rocks up to 2 s two-way traveltime thick. They further suggested that the Upper Cretaceous interval may include two discrete stratigraphic units, but its thickness varies. Northward, outboard of Cape Adair, MacLean et al. (1981) interpreted thick Cretaceous strata separated from Buchan Graben by a narrow basement ridge. Harrison et al. (2011a) suggested that higher than predicted seismic interval velocities (3.9–4.1 km/s) in Lancaster Sound indicate that the Lower Cretaceous is better cemented or of different composition than the onshore Cretaceous strata typically found on the Arctic Islands, or might contain some component of igneous rocks.

Distribution and seismic reflection character

Mapping of Cretaceous sedimentary strata in western Baffin Bay involves a high degree of uncertainty compared to the Labrador margin. The seaward extent of Cretaceous strata (which may also include Lower–Middle Paleocene strata as it does along the Labrador margin; Dafoe, Dickie, Williams, and McCartney, this volume) is demarcated by the extent of Markland Formation–equivalent rocks (horizon M) and likely approaches the landward limit of oceanic crust defined by Keen et al. (this volume; Fig. 4, 5), which is thought to be of a similar, Middle Paleocene age (Oakey and Chalmers, 2012). Cretaceous strata are interpreted to have accumulated during active faulting, based primarily on growth of strata into fault surfaces (Fig. 4). Along the southern part of the study region, Cretaceous strata may be buried under Paleogene volcanic rocks associated with the magma-rich margin segment (Fig. 4a, 5; *see* 'Paleocene–Middle Miocene interval' section below; Skaarup et al., 2006; Keen et al., this volume). In the Home Bay area, Cretaceous rocks sit on the relatively shallow basement platform, but can also be found in small grabens and half-grabens that are poorly imaged on seismic data (Fig. 4b, 5). The thickness of Cretaceous strata in this area varies, however, and is generally quite thin.

From offshore Clyde River to Bylot Island, Cretaceous sedimentary strata are generally restricted to grabens between large basement ridges (Fig. 4c). The Scott and Buchan grabens are the largest, forming half-grabens with the thickest Cretaceous rocks exhibiting growth strata against the bounding faults. These features mirror the structural setting within the Melville Bay Graben and Kivioq Basin on the West Greenland conjugate margin (Whittaker et al., 1997; Gregersen et al., 2019, this volume; Dafoe, Williams et al., this volume). Along northwestern Baffin Bay, Cretaceous strata are inferred, deeply buried under the Baffin Fan, but are concentrated in structural lows in that region.

Figure 5. Distribution of Cretaceous rocks along western Baffin Bay with the location of the basement platform and highs, as well as relevant seabed samples from GSC marine cruises. Basin outlines and the landward limit of oceanic crust are from Keen et al. (this volume). Distribution on Bylot Island is from Jackson et al. (1975; near Salmon River, Baffin Island), Miall (1980; in Eclipse Trough), and Benham (1991; in North Bylot Trough), but these earlier works did not have the resolution to subdivide the Paleocene (uppermost Markland Formation equivalent) in detail, so only the Cretaceous is shown. Localities on east-central Baffin Island are from Burden and Langille (1990, 1991) and Jackson (1998). Fracture zones and the location of the extinct seafloor spreading axis are from Oakey and Chalmers (2012). Additional projection information is as follows: Central Meridian = 60°W; Standard Parallels = 65, 75°W; Latitude of Origin = 65°N. FZ = Fracture zone. For abbreviations *see* Figure 1b.

Complex deformation during the Eurekan Orogeny in northern Baffin Bay has led to uncertainty in mapping the distribution of Cretaceous strata there. Near the mouth of Lancaster Sound where sedimentary successions are thinner, however, Cretaceous strata appear to be inverted over a large basement block (e.g. Harrison et al., 2011a).

Cretaceous strata in Scott Graben can be subdivided based on: the occurrence of probable upper Coniacian rocks in sample 80028-73 (MacLean et al., 2014) from along the eastern edge of the basin (but slightly offline of line 3; Fig. 4c); a similar landward proximal half-graben in Saglek Basin sampled by the Skolp E-07 well (Dafoe and Williams, 2020b; Dafoe, Dickie, Williams, and McCartney, this volume); and the stratigraphy in grabens along the northern West Greenland margin (Gregersen et al., 2019, this volume). The present authors interpret a Lower Cretaceous section at the base of Scott Graben forming a Bjarni Formation equivalent (Fig. 4c). This interval shows clear growth into the western bounding fault and includes moderate- to high-amplitude reflectors capped by horizon Bj. The Lower Cretaceous section is overlain by a thicker Upper Cretaceous Markland Formation equivalent denoted at the top by horizon M (Fig. 4c). This interval is comprised of two packages of low-amplitude seismic reflections, each transitioning upward into intervals with high-amplitude reflections (demarcated by dashed horizons in Fig. 4c). These intervals are then capped by a third, low-amplitude seismic unit below horizon M. Reflections are generally subparallel and there appears to be growth into the fault surface, although it is unclear if this is synrift. As in the region near the Skolp E-07 well of offshore Labrador, the present authors interpret two Freydis Member–equivalent sandstone intervals at the top of each of the lower two packages, an interpretation that suggests progradation into the basin during two main episodes in the Late Cretaceous (Fig. 2; *see* Dafoe, Dickie, Williams, and McCartney, this volume). The thick nature of Upper Cretaceous rocks as compared to the Lower Cretaceous section is also seen along the West Greenland margin (Gregersen et al., 2019, this volume). In contrast, however, the basement platform was higher along western Baffin Bay during the Late Cretaceous, such that Markland Formation–equivalent strata drape basement locally and are more restricted to basement lows (Fig. 4). This is seen outboard of Scott Graben within the smaller graben and half-graben structures that are generally filled by Upper Cretaceous strata and a thin Lower Cretaceous interval that again shows well developed growth into faults (Fig. 4c). Cretaceous strata could be present further offshore on this seismic profile, but their presence is unclear from the data, possibly due to thin Paleogene volcanic cover indicated by the top basalt horizon (Bas).

The interpretation of the Scott Graben in this study differs from that of Harrison et al. (2011a). Structurally, they illustrate a graben with compressional features (i.e. basin inversion), whereas the results here indicate a half-graben and little evidence of inversion this far south along the Baffin Shelf. Within the graben, Harrison et al. (2011a) interpreted a thick succession of lower (Neocomian to Albian) and upper (Cenomanian to Danian) synrift fill, but these strata terminate at greater depths against the bounding fault. Accordingly, the upper part of the present authors' Markland Formation–equivalent unit is interpreted in Harrison et al. (2011a) as Upper Paleocene rocks. Rationale for this discrepancy includes the present study's correlation to 80028-73, correctly located within the graben in this study (but projected 4.7 km), as well as use of the analogue models described above. Additionally, new age constraints from 80028-49 (Lutetian; Dafoe and Williams, 2020a) indicate that Paleocene strata may be much thinner than suggested by Harrison et al. (2011a), similar to the Labrador margin (*see* Dafoe, Dickie, Williams, and McCartney, this volume).

PALEOCENE–MIDDLE MIOCENE INTERVAL

Paleocene–Eocene volcanic rocks

During the Paleocene and Early Eocene, volcanism affected southern Baffin Bay, Davis Strait, and the northern Labrador Sea. Skaarup et al. (2006) mapped a magma-rich (volcanic) margin offshore of Cape Dyer, and this feature has been extended farther north by Keen et al. (this volume), as shown on Figure 6. The volcanic margin is associated with the arrival of a hotspot in Davis Strait at the onset of seafloor spreading in the Early Paleocene (Oakey and Chalmers, 2012). The southern end of this feature in Davis Strait (*see* Fig. 4c in Dafoe, DesRoches, and Williams, this volume) forms a large plateau with thick inner flows and landward-dipping lava deltas, as well as prominent seaward-dipping reflections, features that Planke et al. (2000) used to define a volcanic margin. North of this, in southwestern Baffin Bay, the margin can only be defined by a structural high near the onset of oceanic crust (Fig. 4a). High-amplitude reflections on seismic data (Bas on Fig. 4a) may represent inner flows, but well defined seaward-dipping reflections have not been imaged here and the structural highs are not as large as the volcanic escarpments mapped along the northern Labrador margin (Keen et al., 2012; *see* Fig. 9b in Dafoe, Dickie, Williams, and McCartney, this volume).

Related Paleocene volcanic rocks found onshore at Cape Dyer (Fig. 6) are flat-lying basalt flows with a lava delta succession (Clarke and Upton, 1971). These are described in greater detail in Dafoe, DesRoches, and Williams (this volume). On the West Greenland margin, in the Delta-1 well, Nelson et al. (2015) reported lava flows of a subaerial nature and Early Eocene age coinciding with a later phase of volcanism in the region; however, Eocene volcanism was probably more extensive along the West Greenland margin than the Canadian margin (Nelson et al., 2015), especially as the hotspot tracked eastward over time (Keen et al., this volume). Accordingly, the magma-rich margin north of Cape Dyer is likely Paleocene. A bedrock basalt sample from the seafloor south of Cape Dyer was found to be Danian, but younger Eocene basalt units may be present along this margin as indicated by an early Ypresian sample from central Davis Strait (Dafoe and Williams, 2020a; Dafoe, DesRoches, and Williams, this volume). Farther north along the eastern Baffin Island margin, another smaller region of volcanic cover was mapped outboard of Cape Adair (Fig. 6). This relatively smooth, high-amplitude basement signature, basinward of faulted continental crust (Fig. 4c) is interpreted in this study to indicate a localized region of volcanism potentially linked with Paleocene fracture zones identified there by Oakey and Chalmers (2012; Fig. 6).

Cartwright Formation equivalent

Along the Labrador margin, the Cartwright Formation is a shale- or claystone-dominated interval that was restricted to the Middle Paleocene to Early Eocene (Umpleby, 1979; McWhae et al., 1980; Dafoe, Dickie, Williams, and McCartney, this volume). The laterally equivalent Gudrid Formation is a sandstone-dominated succession of the same age and composed of two informal members, forming wedge-shaped, progradational shoreline packages on seismic data (Fig. 2; Umpleby, 1979; McWhae et al., 1980; Balkwill and McMillan, 1990; Dickie et al., 2011; Dafoe, Dickie, Williams, and McCartney, this volume). Dafoe, Dickie, Williams, and McCartney (this volume) constrain the age of the Cartwright Formation to the late Selandian to early Ypresian.

Onshore east-central Baffin Island, Burden and Langille (1990) interpreted the Cape Searle Formation as fluvial, debris-flow, and volcanic ash deposits from centimetres to 10 m thick which include subarkosic sandstone, siltstone, mudstone, clast- and matrix-supported boulder conglomerate, and thin beds of basaltic volcanic ash. The formation is also found on Paallavvik and Qaqulluit (islands) and lies unconformably over the Cretaceous Quqaluit Formation, with the boundary defined by a clast-supported boulder conglomerate (Burden and Langille, 1990). Burden and Langille (1991) dated the Cape Searle Formation as Early to Middle Paleocene, corresponding approximately to the uppermost Markland Formation and lowermost Gudrid Formation and/or Cartwright Formation equivalents. Similarly, Fenton and Pardon (2007) determined a Paleocene age, but indicated that either Early or Late Paleocene was possible. Degraded and/or reworked and unidentifiable dinocysts indicate at least partly marine conditions during deposition, and overlying basalt units are in conformable contact with the sedimentary strata (Burden and

Figure 6. Distribution map of lower Cenozoic (Paleocene–Middle Miocene) rocks along western Baffin Bay with the location of the basement platform and highs, relevant seabed samples from GSC marine cruises, and the distribution of volcanic rocks. Distribution onshore Bylot Island includes all Paleogene rocks as they are based on older maps that did not separate the Paleocene into stages (Jackson et al., 1975; Miall et al., 1980; Benham, 1991). On northeast Baffin Island, additional outcrops are shown in Haggart et al. (this volume), and only the most well documented outcrops are shown here. Localities on southeastern Baffin Island are from Burden and Langille (1990, 1991) and Jackson (1998). Basin outlines and the landward limit of oceanic crust are from Keen et al. (this volume). Fracture zones and the location of the extinct seafloor spreading axis are from Oakey and Chalmers (2012). Additional projection information is as follows: Central Meridian = 60°W; Standard Parallels = 65, 75°W; Latitude of Origin = 65°N. FZ = Fracture zone. For abbreviations *see* Figure 1b.

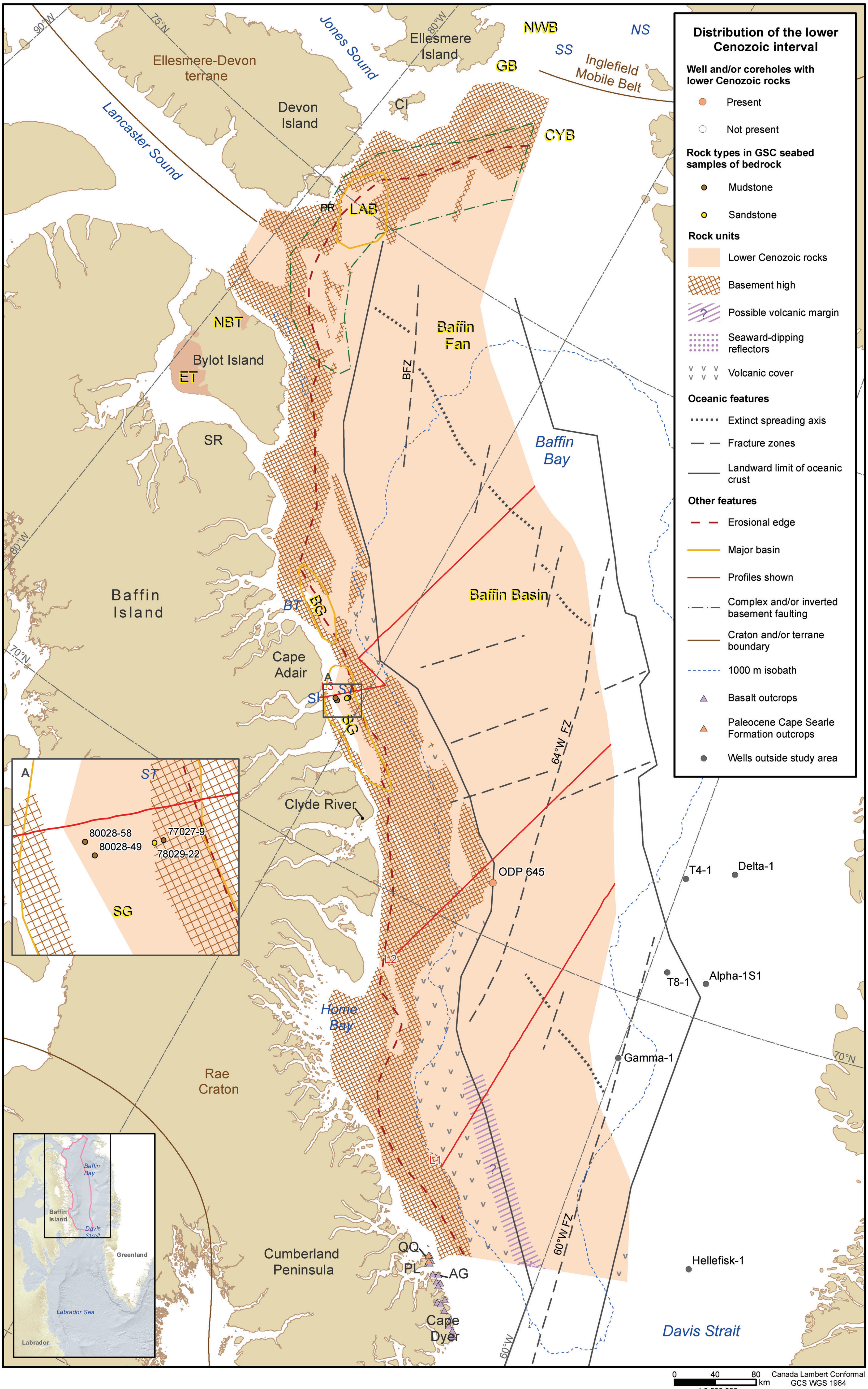
Distribution of the lower Cenozoic interval
Well and/or coreholes with lower Cenozoic rocks
Present
Not present
Rock types in GSC seabed samples of bedrock
Mudstone
Sandstone
Rock units
Lower Cenozoic rocks
Basement high
Possible volcanic margin
Seaward-dipping reflectors
Volcanic cover
Oceanic features
Extinct spreading axis
Fracture zones
Landward limit of oceanic crust
Other features
Erosional edge
Major basin
Profiles shown
Complex and/or inverted basement faulting
Craton and/or terrane boundary
1000 m isobath
Basalt outcrops
Paleocene Cape Searle Formation outcrops
Wells outside study area
Ellesmere-Devon terrane
Devon Island
Ellesmere Island
Jones Sound
Lancaster Sound
NWB
GB
NS
SS
Inglefield Mobile Belt
CI
CYB
PR
LAB
NBT
Bylot Island
ET
SR
Baffin Fan
BFZ
Baffin Bay
Baffin Basin
Baffin Island
BT
BG
Cape Adair
A
L3
ST
SI
SG
Clyde River
ODP 645
64°W FZ
T4-1
Delta-1
T8-1
Alpha-1S1
Gamma-1
L2
Home Bay
Rae Craton
L1
Cumberland Peninsula
QQ
PL
AG
Cape Dyer
60°W FZ
Hellefisk-1
Davis Strait
80028-58
80028-49
77027-9
78029-22
Baffin Bay
Baffin Island
Davis Strait
Greenland
Labrador Sea
Labrador
90°W
75°N
80°W
60°W
70°N
0
40
80
km
1:3 500 000
Canada Lambert Conformal
GCS WGS 1984

Langille, 1990). These same authors suggested that the Cape Searle Formation represents both pre-eruption and intereruption facies. Accordingly, these rocks may be proximal equivalents of the Gudrid and/or Cartwright formations.

Although there are no samples of Cartwright or Gudrid formation equivalents from western Baffin Bay, a calcareous mudstone collected from Scott Trough (80028-58) may be Paleocene based on similarities to rocks of this age from onshore Bylot Island (Dafoe et al., 2019), as described above (Fig. 2, 6). Due to diagenetic factors, little can be interpreted about the depositional setting of this rock, but the lithology and presumed age are consistent with a Cartwright Formation equivalent. Nonmarine limestone of purported early Cenozoic age was also reported from onshore Baffin Island north of the Barnes Ice Cap at an elevation of 730 m (Andrews et al., 1972); however, based on uranium-series dating, these strata have been reinterpreted as Quaternary, subglacially precipitated carbonate crusts formed on bedrock and till clasts (Refsnider et al., 2012).

Seismic reflection character

The Cartwright Formation is discontinuous in the region and difficult to map without constraints from drilling; however, a thin interval along the seismic profile through the Scott Graben is interpreted in this study and demarcated at the top by the Cartwright and/or Gudrid formation horizon (CG; Fig. 4c), and based on sample 80028-58 (although this sample is projected 3.3 km). The interval displays a low to moderate amplitude, locally chaotic seismic character, similar to that seen along the Labrador margin (Dafoe, Dickie, Williams, and McCartney, this volume). In Scott Graben, the Cartwright Formation equivalent appears to be a thin, relatively transparent seismic unit, that is probably composed of shale units since the clinoforms and the distinct, high-amplitude reflections typical of the Gudrid Formation in the offshore Labrador region, are not observed. Seaward of Scott Graben, the unit onlaps the large basement ridge and then downlaps basinward onto continental basement, finally pinching out against oceanic crust, presumably of about chron C25n (late Paleocene) age. Again, the present interpretation differs slightly from that of Harrison et al. (2011a), based on new understanding of the seabed samples: this study presents a much thinner upper Paleocene section in both Scott Graben and also basinward, than was reported previously.

Kenamu Formation equivalent

The Kenamu Formation is a Lower to Upper Eocene shale and mudstone succession on the Labrador margin, overlying the Cartwright and/or Gudrid formations (McWhae et al., 1980; Balkwill and McMillan, 1990). Whereas the Leif Member is a formal, sandstone-dominated unit at or near the top of the Kenamu Formation, Balkwill and McMillan (1990) also proposed informal units within the formation, including a "lower," fining-upward unit, then a "middle," coarsening-upward succession, and capped by the coarsening-upward interval containing the Leif Member. Based on revised biostratigraphic constraints, it appears that the Kenamu Formation is Ypresian to late Bartonian (Dafoe, Dickie, Williams, and McCartney, this volume).

The only Lower to Middle Eocene sample from the eastern Baffin Island margin is drill core 80028-49 from Scott Trough, which consists of fragments reported as "gravel?" by MacLean (1980). These fragments were re-examined by Dafoe and Williams (2020a) and found to be dark brown mudstone of Middle Eocene (Lutetian) age that were deposited in an inner neritic setting (Fig. 6). Lithologically, this sample compares to the Kenamu Formation, but the inner neritic setting is shallower than seen in wells on the Labrador margin during the Lutetian, when strata were typically deposited in outer shelf to deeper water conditions, consistent with minor marine flooding (Dafoe et al., 2016a; Dafoe, 2021; Dafoe, Dickie, Williams, and McCartney, this volume). This discrepancy is likely a function of the proximity of the Scott Graben to the basin margin.

Previous offshore mapping

In general, MacLean et al. (1990) described the Cenozoic strata of western Baffin Bay as flat lying to gently eastward dipping, with some evidence of folding and faulting. Others have noted, however, that faulting and deformation, including localized inversion, do not extend above the mid-Cenozoic (Rice and Shade, 1982), or chron C13 time (Harrison et al., 2011a). This would be near the top Kenamu Formation equivalent, but erosion within the troughs crossing the shelf may have locally removed some of these strata. Harrison et al. (2011a) identified upper Paleocene to Eocene strata truncated at the seafloor along Scott Trough, which would be approximately Kenamu Formation–equivalent strata. In the same general region, MacLean (1978) noted a unit of relatively flat-lying strata of possible Eocene or older age based on dredge samples in that area.

Elsewhere in northern Baffin Bay, Harrison et al. (2011a) interpreted two Eocene units in Carey Basin and three in Lady Ann Basin, based on seismic interpretation, with prograding clinoforms found in the latter (possibly Leif Member equivalents). In Jones Sound, Harrison et al. (2011a) identified prograding strata in a presumed Thanetian–Eocene package that they divided into three sequences, and indicated that compressive deformational structures were present in the basin. Based on their mapping, Harrison et al. (2011a) postulated that sedimentation was focused within major grabens receiving locally derived sediments during the Paleocene–Eocene when Baffin Bay would have been narrower, and when Lancaster Sound and Nares Strait may have been important sources of sediment (Harrison et al., 2011a).

On the conjugate West Greenland Margin, seismic-stratigraphic unit E is Paleocene to Eocene (Lutetian) and overlies a major unconformity (the F1 horizon) near the top of the Cretaceous (Gregersen et al., 2013, 2019, this volume). Along northern West Greenland, unit E is thick and includes submarine-fan and mass-flow deposits, possibly with local sandstone units (Gregersen et al., 2019, this volume) that could be equivalent to the Cartwright and lower Kenamu formations.

Seismic reflection character

In Scott Graben, the presence of Paleogene samples provides some constraints over the distribution of Kenamu Formation–equivalent rocks there. This study shows two horizons in the graben (Fig. 4c), a mid-Kenamu Formation–equivalent marker (mK) and a local top Kenamu Formation–equivalent horizon (K), based on the available seabed samples of bedrock and seismic morphology. Along the Labrador margin, the mK horizon is Lutetian (Dafoe, Dickie, Williams, and McCartney, this volume), and the equivalent level in Scott Graben is constrained by the Lutetian sample 80028-49. The mK marker in Scott Graben caps a higher amplitude, downlapping infill sequence with some poorly organized internal reflectivity, possibly indicating sourcing from the nearby basement highs. The marker may correspond to the top of the informal "middle Kenamu member" (*see* Dafoe, Dickie, Williams, and McCartney, this volume). In Scott Graben, the K horizon is also constrained by sampling of overlying Rupelian (or younger) strata in sample 78029-22. Unfortunately, the K horizon and upper Kenamu Formation–equivalent interval cannot be mapped beyond Scott Graben without further control.

The mK marker forms a key horizon on the conjugate West Greenland margin (E1; Gregersen et al., 2013, 2019, this volume), with which the present authors link this study's interpretation. Outboard of the Scott Graben, the mK marker was mapped as the top of a seaward-thickening wedge that eventually thins basinward to onlap oceanic basement in the middle of Baffin Basin (Fig. 4c). The horizon also caps the top of a generally 0.5 s two-way traveltime unit in the Home Bay region, where it onlaps against the higher basement ridges. Also in this region, the mK horizon tops an interval containing slump-deformed deposits below the present-day slope, and again drapes over oceanic basement in Baffin Basin (Fig. 4b). The mK marker has also been interpreted farther south off the east-central Baffin Island margin, but the internal character is poorly defined (Fig. 4a).

This study's interpretation of the Scott Graben region differs somewhat from that of Harrison et al. (2011a), as it considers the Kenamu Formation equivalent (primarily an Eocene interval) to be thicker, and the underlying Paleocene interval to be thinner, based on seabed samples of bedrock, not considered by these previous authors. East of the graben, the present authors also interpret thicker Eocene strata based on correlations to more recent mapping and profiles on the West Greenland margin (Dafoe, Williams et al., this volume). The Kenamu Formation–equivalent rocks are inferred to onlap oceanic crust of similar age as shown in Figures 4a and 4c.

Lower–upper Mokami Formation and lower Saglek Formation equivalents

The Mokami Formation overlies the Kenamu Formation along the Labrador margin and was defined as a claystone-dominated succession (McWhae et al., 1980); it was subsequently subdivided informally into lower and upper members (Balkwill and McMillan, 1990). The Saglek Formation is partly correlative with the Mokami Formation, but is a sandstone-dominated interval (Umpleby, 1979; McWhae et al., 1980; Balkwill and McMillan, 1990). Dafoe, Dickie, Williams, and McCartney (this volume) suggest that the Mokami Formation is as old as Bartonian to Oligocene in certain wells, but probably extends into the Pliocene basinward of the well locations.

In addition, they postulate that the Saglek Formation is Rupelian to Middle Miocene based on the wells, but extends into the Pliocene–Pleistocene from seismic interpretation. Parts of both the lower and upper Mokami Formation and only part of the lower Saglek Formation can be attributed to the lower Cenozoic interval (Fig. 2).

Along the eastern Baffin Island margin, three sampled intervals can be considered as part of the Mokami Formation equivalent (Fig. 2). The first sample was dredged from the wall of Scott Trough during cruise 77027, between 658 and 475 m water depth at station 9 and consists of a boulder-sized, dark grey, calcareous mudstone concretion with fine-grained calcite cement and silt- to sand-sized quartz grains (Line 3; Fig. 4c, 6; MacLean, 1978; Dafoe and Williams, 2020a). A few fossil fragments and sponge spicules were found in the concretion and the presence of ferroan sparry calcite replacing skeletal grains is thought to indicate that it formed within a shale interval (MacLean, 1978). The age of this sample was initially determined as Late Eocene (MacLean, 1978), but reworked Senonian palynomorphs were subsequently identified in it and the age revised to Late Eocene–Early Oligocene (MacLean and Williams, 1983). The lithology and presence of dinocysts in the concretion is consistent with deposition in a neritic setting (MacLean, 1978; Dafoe and Williams, 2020a). Also, along the wall of Scott Trough, a dredge sample was collected between 640 to 550 m water depth at station 78029-22 (Fig. 6; Table 1). This sample is a dark grey, calcareous muddy sandstone concretion with plant remains, glauconite, and faint laminations (MacLean and Falconer, 1979; MacLean et al., 1981; Dafoe and Williams, 2020a). The age was initially determined to be Late Eocene–Early Oligocene (MacLean et al., 1981), but was revised to no older than Rupelian (Dafoe and Williams, 2020a). Furthermore, Dafoe and Williams (2020a) postulated a distal inner shelf to proximal outer shelf setting based on the palynomorphs, deeper than the nearshore setting proposed by MacLean et al. (1981).

Finally, in the Home Bay area, the ODP Site 645 (Fig. 7) intersected about 230 m of Lower to Middle Miocene strata (Burdigalian–early Serravallian; Dafoe and Williams, 2020c) at the base of the corehole, which has been previously considered as part of unit D from the West Greenland margin (Knutz et al., 2015) and thus part of the lower Cenozoic interval of this study. This muddy sandstone to sandy mudstone (described in more detail in the 'ODP Site 645' section below) was interpreted to reflect outer neritic to open-ocean depositional settings by Srivastava et al. (1987), but redescribed as inner shelf to prodeltaic deposits by Dafoe and Williams (2020c). All three samples described above are lithologically consistent with the Mokami Formation, with the Upper Eocene–Lower Oligocene dredge samples closely resembling the lithology and paleoenvironment of the Mokami Formation from Labrador Shelf wells. The Burdigalian–lower Serravallian section in Site 645 is, however, younger than Mokami Formation rocks encountered in Labrador Shelf wells, but Mokami Formation rocks of this age were postulated by Dafoe, Dickie, Williams, and McCartney (this volume) to be present farther offshore Labrador. A shelfal to prodeltaic setting is also consistent with the Mokami Formation, offshore Labrador (Dafoe and Williams, 2020b; Dafoe, 2021; Dafoe, Dickie, Williams, and McCartney, this volume).

Previous offshore mapping

Based on their seismic mapping, Harrison et al. (2011a) inferred that Oligocene and Miocene strata are missing from inshore grabens along western Baffin Bay, but suggested widespread distribution and modest thicknesses of these strata on the slope and basin floor, as well as within the Baffin Fan, along the northern edge of Baffin Bay, and eastward toward Carey Basin. During the Oligocene–Miocene, grabens along the shelf may have been overfilled or exposed and eroded, supplying delta systems farther seaward (Harrison et al., 2011a). During this time, delta progradation outboard of Lancaster Sound, Carey Basin (sourced from Nares Strait), and seaward of Jones Sound and Lady Ann Basin was also noted by Harrison et al. (2011a).

Lower part of the Baffin Fan

Rice and Shade (1982) recognized a thick sedimentary section over 6 s two-way traveltime thick in the "Bylot Basin" of northern Baffin Bay. This postrift section forms the present-day shelf (Jackson et al., 1992) and was later named the Baffin Fan by Harrison et al. (2011a). This feature comprises a thick Oligocene to present-day sedimentary wedge that was deposited off the mouth of Lancaster Sound, Jones Sound, and Smith Sound. The fan presumably began forming in the earliest Selandian, with substantial thickening from the Oligocene onward, prograding seaward in northern Baffin Bay to cover oceanic crust with thick sedimentary accumulations. This wedge of sediments buried basement structures and Cretaceous through Danian synrift strata, and was overprinted by the deformation associated with the Eurekan Orogeny (Harrison et al., 2011a). The oldest units of the Baffin Fan (approximately Thanetian–Eocene) contain parallel internal reflections and offlapping clinoforms downdip, with the bases of these sometimes characterized by incised channels (Harrison et al., 2011a). Overlying this is an inferred Oligocene to Middle Miocene unit that correlates to Harrison's seismic unit 3 in Site 645 (Fig. 7) where they noted the formation of clinoforms outboard of Lancaster Sound.

Distribution and seismic reflection character

The top of the lower Cenozoic interval (Paleocene–Middle Miocene) as interpreted in this study is marked by the Saglek and/or Mokami formation–equivalent horizon 3 (SM3), which ties with a well established marker on the West Greenland margin of about Middle Miocene age (their D1 horizon; Gregersen et al., 2013, 2019, this volume; Dafoe, Williams et al., this volume). Sandstone dredge sample 78029-22 from Scott Trough indicates the presence of Oligocene rocks within Scott Graben, although the top of the interval has been removed within the glacial trough (Fig. 4c). Outboard of Scott Graben, the SM3 horizon subdivides the Saglek and Mokami formations, and may be locally truncated by a younger regressive event (Fig. 4c). The interval below SM3 and above horizon mK thickens seaward over Baffin Basin (Fig. 4c). An intervening horizon, the Saglek and/or Mokami formation–equivalent horizon 1 (SM1), onlaps or merges with the underlying mK horizon and is equivalent to the D2 horizon from the West Greenland margin (Gregersen et al., 2019, this volume; Dafoe, Williams et al., this volume), but cannot be mapped farther inboard. Below SM1, a thick package of presumed Upper Eocene–Lower Oligocene strata that fills the extinct seafloor spreading axis (Fig. 4a, 4c), likely corresponds to the final, slow phase of seafloor spreading. Southward, in the Home Bay region (Fig. 4b) the lower Saglek and/or Mokami formation equivalent, between mK and SM3, is about 0.5 s two-way traveltime thick on the shelf, thinning below the slope and then thickening into the deeper Baffin Basin where the stratigraphy has been disrupted by channelling and mass-transport complexes. Farther south (Fig. 4a), the mK to SM3 interval again shows thickening into Baffin Basin, where it drapes structures. In comparison to the work of Harrison et al. (2011a), this study shows Oligocene to Middle Miocene strata deeper in the section seaward of Scott Graben, particularly below the shelf break. The present authors' rationale for this discrepancy is similar to that of the underlying Kenamu Formation.

Distribution of Paleocene–Middle Miocene (lower Cenozoic) interval

The Middle Miocene seismic horizon SM3 bounds the top of the lower Cenozoic interval and its base is the top Markland Formation equivalent, horizon M. On seismic reflection sections, these boundaries are highly variable in amplitude, and internal layering is commonly less distinct than in the Cretaceous section beneath it or in the upper Cenozoic section overlying it. These lower Cenozoic sedimentary rocks cover most of western Baffin Bay, forming a seaward-thickening wedge (Fig. 4, 6). As this sedimentary wedge approaches land, it has become truncated in some regions, especially the deep troughs, creating an angular unconformity with the overlying glacial till or seafloor (Fig. 4c). The seaward edge of this truncation is shown as an erosional edge on Figure 6. Elsewhere, the lower Cenozoic unit generally onlaps the shallowing basement platform near the coastline, and extends into the mouth of Lancaster Sound and west of the map area in that region. The lower Cenozoic package is thickest seaward of the erosional edge, within the Baffin Fan (Harrison et al., 2011a) and on oceanic crust within deep fracture zones and the extinct seafloor spreading axis (Lines 1–3; Fig. 4). This package does not overstep some of the larger basement highs (e.g. Line 3; Fig. 4c, 6). In addition, the Eurekan Orogeny during the Eocene resulted in a zone of complex faulting, folding, and structural inversion in northern Baffin Bay, which affected much of the lower Cenozoic interval (Fig. 6).

MIDDLE MIOCENE–PLEISTOCENE INTERVAL

Upper Mokami Formation and lower–upper Saglek Formation equivalents

The ODP Site 645 provides key Neogene constraints in Baffin Bay (Fig. 8) as it contains the only samples of this age from western Baffin Bay (Fig. 2) and, for this reason, is summarized in detail below. Located east of Home Bay, this corehole was drilled into the lower slope and reached total depth in Lower Miocene rocks. Most

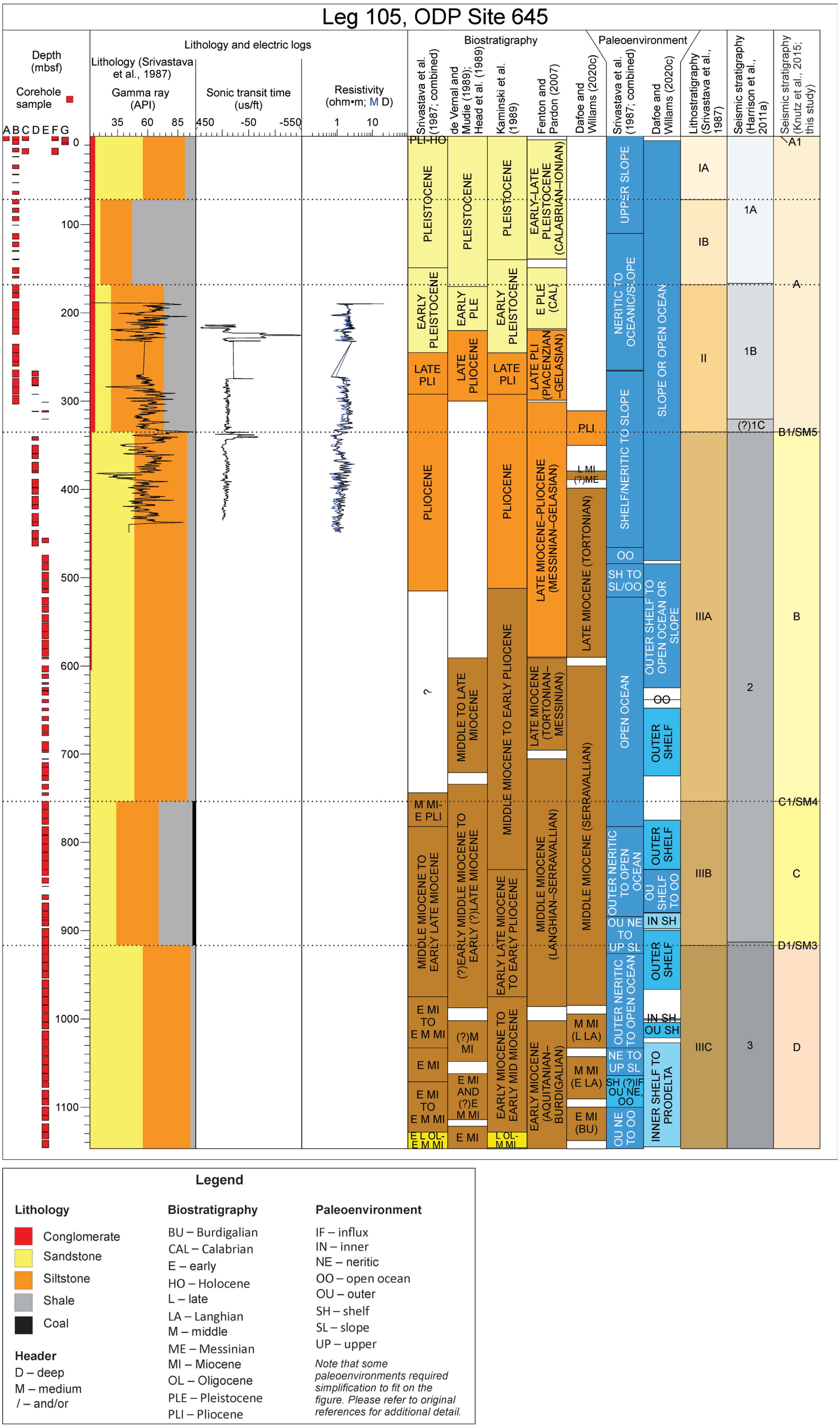

Figure 7. Leg 105, ODP Site 645 profile. The lithologies are generalized from Srivastava et al. 1987 (their Fig. 9, Table 2, and descriptions in the related text). The ages from Srivastava et al. (1987) are from their Figure 26 showing a combined age using foraminifera, nannofossils, diatoms, dinocysts, and radiolarians (although more generalized ages are presented in their summary). Ages from Kaminski et al. (1989) are estimated from their Figure 3 and the associated core depths. SF = seafloor, SM = Saglek and/or Mokami formation, mbsf = metres below seafloor

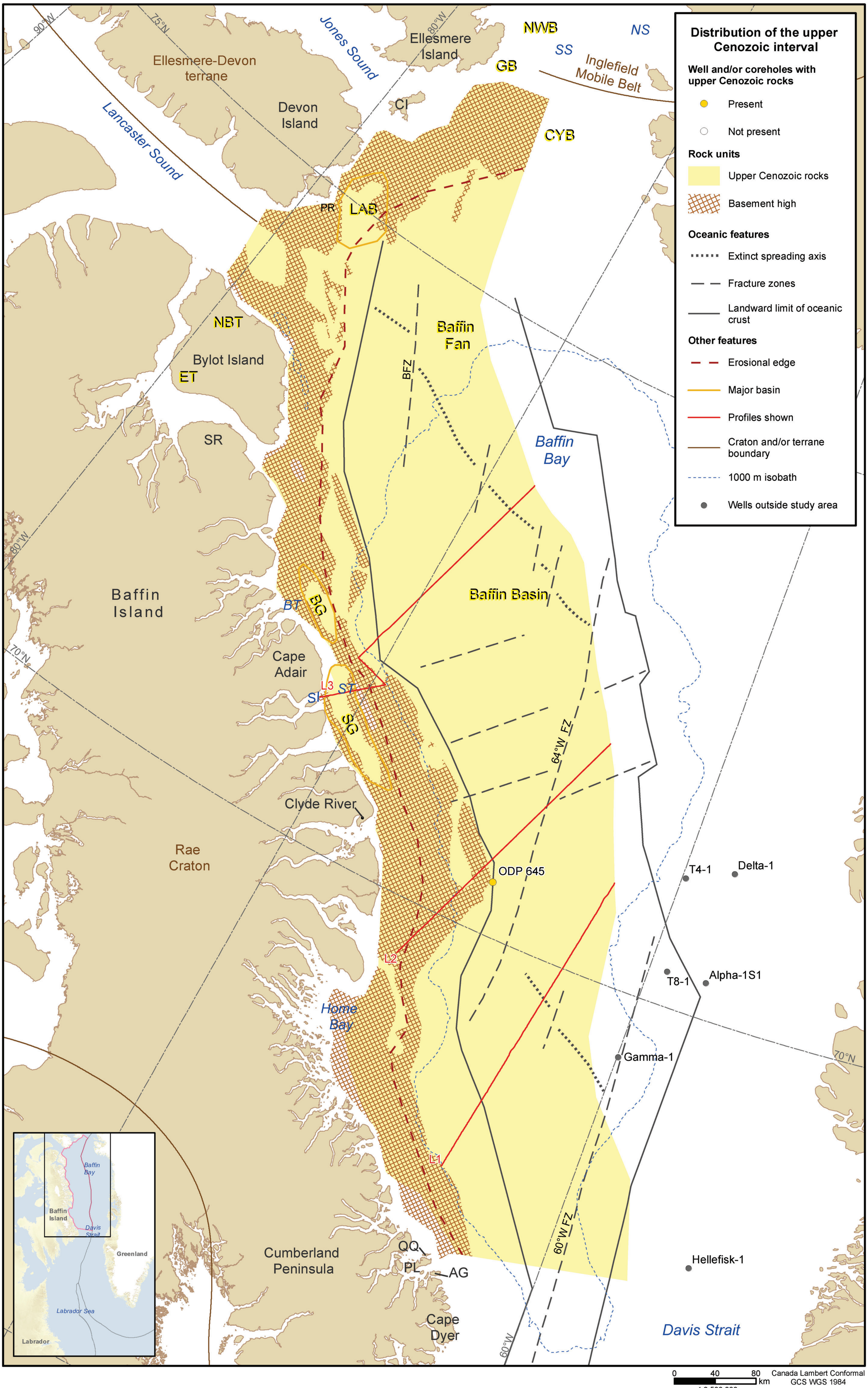
Distribution of the upper Cenozoic interval
Well and/or coreholes with upper Cenozoic rocks
Present
Not present
Rock units
Upper Cenozoic rocks
Basement high
Oceanic features
Extinct spreading axis
Fracture zones
Landward limit of oceanic crust
Other features
Erosional edge
Major basin
Profiles shown
Craton and/or terrane boundary
1000 m isobath
Wells outside study area
Ellesmere-Devon terrane
Devon Island
Ellesmere Island
Jones Sound
Lancaster Sound
NWB
NS
SS
GB
Inglefield Mobile Belt
CI
CYB
PR
LAB
NBT
Bylot Island
ET
SR
Baffin Fan
BFZ
Baffin Bay
Baffin Basin
Baffin Island
BT
BG
Cape Adair
L3
SI
ST
SG
64°W FZ
Clyde River
Rae Craton
ODP 645
T4-1
Delta-1
L2
T8-1
Alpha-1S1
Home Bay
Gamma-1
L1
60°W FZ
Cumberland Peninsula
QQ
PL
AG
Hellefisk-1
Cape Dyer
Davis Strait
90°W
75°N
80°W
70°N
60°W
Greenland
Labrador Sea
Labrador
0
40
80
km
1:3 500 000
Canada Lambert Conformal
GCS WGS 1984

Figure 8. Distribution map of the upper Cenozoic (Middle Miocene–Pleistocene) rocks along the eastern Baffin Island margin with the location of the basement platform and highs and the ODP Site 645, which intersected this interval. Basin outlines and the landward limit of oceanic crust are from Keen et al. (this volume). Fracture zones and the location of the extinct seafloor spreading axis are from Oakey and Chalmers (2012). Additional projection information is as follows: Central Meridian = 60°W; Standard Parallels = 65, 75°W; Latitude of Origin = 65°N. FZ = Fracture zone. For abbreviations *see* Figure 1b.

of the core, however, lies within the upper Cenozoic interval (Middle Miocene–Pleistocene; Dafoe and Williams, 2020c) and is equivalent to the upper Mokami and lower to upper Saglek Formation of the Labrador margin.

ODP Site 645

During ODP Leg 105 in 1985, Site 645 was drilled in about 2020 m water depth along the continental slope offshore eastern Baffin Island, with seven corehole sites, A through G, for a total depth of 1147.1 mbsf (metres below seafloor; Fig. 1, 7; Srivastava et al., 1987). The succession cored was divided into three main units and associated subunits (Fig. 7, right), as described by Srivastava et al. (1987). The basal portion of Site 645 equates with the lower Cenozoic interval, but is discussed here in relation to the original lithological units proposed by Srivastava et al. (1987; Fig. 7).

Lithological units

The basal unit III is subdivided into three subunits (Fig. 7; Srivastava et al., 1987). The lowermost, subunit IIIC (1147.1–916.8 mbsf) consists of muddy, fine- to medium-grained sandstone and silty mudstone with some glauconitic sandstone. This subunit is moderately to abundantly bioturbated (trace fossil suites throughout the corehole are documented in Dafoe and Williams (2020c)) in the coarser grained intervals, with more stratified, fine-grained interbeds and soft-sediment deformation also present. Above this, subunit IIIB (916.8–753.4 mbsf) is olive-grey, muddy sandstone to dark grey, silty mudstone with interbedded medium grey, calcareous, silty claystone units with some local laminations. The maximum grain size is very fine- to fine-grained sand and moderate to abundant bioturbation is common. Small gastropods and carbonaceous plant fragments are also present locally. The upper subunit, IIIA (753.4–335 mbsf) is a poorly sorted, olive-grey, muddy sandstone and silty mudstone with small dispersed pebbles consisting mostly of shale, minor friable sandstone, carbonate, and granitic fragments. The degree of bioturbation varies and rare primary sedimentary structures are present locally (Srivastava et al., 1987).

Higher in the corehole, unit II (335–168.1 mbsf; Fig. 7) includes predominantly grey, silty mud, clayey silt, and silty clay, all with dropstones up to cobble size. Facies alternations occur at the decimetre to 2 m scale with both bioturbated and faintly laminated beds represented. There was poor core sample recovery in the lowermost 30 m of unit II, necessitating definition of the base of the unit from well logs. Detrital carbonate content is about 5% on average, dropstone compositions include granite, gneiss, and carbonate (limestone and/or dolostone), and quartz and feldspar are abundant and may indicate a mature source.

Unit I was subdivided into two subunits by Srivastava et al. (1987; Fig. 7). The unit characteristically includes detrital carbonate grains of cobble to clay size, but mostly silt- and clay-sized carbonate sediment in subunit IB (note that detrital carbonate is accounted for under the clay, silt, sand, and pebble- and/or cobble-sized material in the lithology column; Fig. 7). Subunit IB (168.1–71.6 mbsf) comprises interbedded grey, detrital carbonate, silty clay to dark olive-grey, silty mud, with dropstones up to cobble size: minor bioturbation is also present, but primary structures are rare. Carbonate content ranges from less than 10% to more than 50%, averaging 30–40%. The uppermost subunit IA (71.6–0 mbsf) consists of interbedded light tan to grey, gravel-bearing detrital carbonate sand and silty mud with scattered dropstones ranging up to cobble size. Beds are cyclic in nature, over tens of centimetres, up to 2 m thick, with minor bioturbation and a 20% mean detrital carbonate content.

Biostratigraphy

The biostratigraphy of Site 645 has been addressed in a number of studies, with results from some of these shown in Figure 7. Based on a combination of microfossil evidence, a preliminary biostratigraphic assessment of Site 645 was conducted by Srivastava et al. (1987) who identified lower Upper Oligocene to lower Middle Miocene through Pleistocene–Holocene strata in the corehole. Subsequent biostratigraphic studies of the corehole focused on particular microfossil groups. The palynological study of hole 645E by Head et al. (1989) provided a stratigraphic subdivision based on five dinocyst zones of Early Miocene to Middle–Late Miocene age (Fig. 7). De Vernal and Mudie (1989) assessed hole 645B and interpreted Upper Pliocene, lowermost Pleistocene, and Pleistocene intervals. Benthic agglutinated and benthic calcareous foraminifera were used by Kaminski et al. (1989) to reassess the ages in Site 645, where they recognized a thin interval of upper Oligocene to Middle Miocene strata at the bottom of the section to Pleistocene at the top (Fig. 7).

As is apparent from these results, there is considerable overlap in the biostratigraphic interpretations of Site 645, but these studies show variability in age determinations, poorly constrained intervals, and did not assign stages, except for the work of Fenton and Pardon (2007), wherein stages were generally grouped together. Accordingly, Dafoe and Williams (2020c) reassessed holes 645E and 645D to refine the ages of the pre-Pliocene section using event stratigraphy rather than zonations. This new work yielded an overall age range of Early Miocene (Burdigalian) to Pliocene (Fig. 7). In the study by Dafoe and Williams (2020c), the Lower to Middle Miocene (Burdigalian to Serravallian) includes lithological subunits IIIC, IIIB, and the bottom of IIIA, but is dominated by Serravallian strata. The Serravallian is then capped by a Tortonian unit further succeeded by a possible thin Messinian section, potentially indicating a condensed section. Finally, a Pliocene section was noted by Dafoe and Williams (2020c) at the top of the studied samples, where the Upper Miocene and lowest Pliocene covers the remaining portion of lithological subunit IIIA, and deposition of the base of unit II beginning in the Pliocene. Comparable ages were reported by Fenton and Pardon (2007), but the breakdown to individual stages in this study provides an enhanced understanding of depositional patterns through time. Using the work of de Vernal and Mudie (1989), the remainder of unit II is Late Pliocene–Early Pleistocene, and unit I appears to be restricted to the Pleistocene.

Paleoenvironment, paleoclimate, and depositional processes

Based on the biostratigraphic analyses, including foraminifera, diatoms, nannofossils, and palynomorphs, Srivastava et al. (1987) interpreted paleoenvironments of deposition for Site 645 (Fig. 7). Their assessment shows outer shelf to slope or open-ocean conditions for much of the corehole, with a thin interval representing shelfal influx near the base. Similarly, Fenton and Pardon (2007) found upper to lower bathyal settings for the entire corehole. These settings roughly agree with the interpretation of Head et al. (1989), who identified marine palynomorphs indicating cool-water, but neritic conditions for hole 645E. Head et al. (1989) also interpreted an initially temperate climate up until the Middle to early Late Miocene, which subsequently deteriorated. Enhanced terrigenous influx and the disappearance of some dinocysts in the Middle to Late Miocene could also be related to changes in oceanography or climate. In hole 645B, de Vernal and Mudie (1989) interpreted a possible neritic influx based on dinocysts, but the upper Lower Pleistocene to Holocene is lacking palynoflora, possibly due to cold climatic conditions. In the Upper Pliocene and lowermost Pleistocene section, de Vernal and Mudie (1989) noted that the pollen and spores are indicative of open, coniferous, boreal forest to forest tundra in neighbouring onshore areas. This contrasts with the upper Lower Pleistocene to Holocene interval that generally has few palynomorphs, although productive horizons are found intermittently.

Using an integrated approach of studying both lithofacies and palynomorphs, Dafoe and Williams (2020c) were able to refine the paleoenvironmental interpretations for much of the corehole (Fig. 7). They utilized both relative abundances of gonyaulacalean and peridinialean dinocysts, as well as relative abundances of herbaceous, woody, and amorphous material. In their facies analyses, they combined sedimentological and ichnological findings from photographed intervals. Results from these two analyses were integrated, and interpreted paleoenvironments illustrate paleoenvironmental fluctuations that had not been previously documented. In particular, they found intervals representing inner shelf to prodeltaic settings at and near the base of the corehole in subunits IIIC and IIIB, with outer shelf to open-ocean conditions fluctuating during deposition of much of subunit IIIB and the base of subunit IIIA. Finally, Dafoe and Williams

(2020c) found the onset of fully open-ocean or slope conditions at the top of the corehole for the upper part of subunit IIIA, as well as in units II and I (Fig. 7).

Srivastava et al. (1987) interpreted depositional processes for each of the lithological units of Site 645, based on their biostratigraphy and lithological characteristics. These authors noted that subunit IIIC is intensely bioturbated and reflects good oxygenation and strong bottom currents. Storm reworking may also have resulted in movement of sediment during deposition of subunit IIIC (Srivastava et al., 1987; Dafoe and Williams, 2020c). In contrast, subunit IIIB is finer grained and consistent with bottom current deposition and possible turbidity currents (Srivastava et al., 1987). Turbidity currents may have transported shale clasts during deposition of subunit IIIA, but ice-rafting is more plausible (Srivastava et al., 1987; Dafoe and Williams, 2020c). The probable source of this material was Mesozoic or Paleogene mudstone and shale units exposed on the shelf, as documented by GSC samples of bedrock. Hiscott et al. (1989) also interpreted possible bottom-current and gravity-flow deposits in subunit IIIA. The sand at the base of unit II may be related to turbidity current transport from a littoral or shelf setting, and bottom currents may also have played a role in overall deposition (Srivastava et al., 1987). Finally, ice-rafting was the dominant depositional process inferred for unit I, as evidenced by a distinct lack of primary sedimentary structures, although downslope processes, such as turbidity currents, may also have been important (Srivastava et al., 1987; Hiscott et al., 1989). The large proportion of detrital carbonate seen in lithological unit I was inferred by Srivastava et al. (1987) to reflect sourcing from Paleozoic bedrock north of Baffin Bay, and the decrease in detrital carbonate content at the boundary between units I and II may indicate a change in source area for the dropstones.

In terms of glaciation, Srivastava et al. (1987) found the first abundance of dropstones and coarse-grained strata at 340 mbsf (near the base of unit II) or possibly even at 465 mbsf, but further noted isolated pebbles and granules as deep as 605 mbsf, showing good agreement with the 600 mbsf determined by Thiébault et al. (1989; within the lower half of subunit IIIA). Based on this and other evidence, the onset of continental glaciation has been proposed to start at 8 Ma (Srivastava et al., 1987), 9 Ma (Thiébault et al., 1989), and 9.5 to 7.4 Ma (Head et al., 1989). Using more precise timing with stages, Dafoe and Williams (2020c) showed that the 600 mbsf depth equated with the latest Serravallian, or about 11.63 Ma according to the time scale of Gradstein et al. (2012).

Correlation to the Labrador margin

The lithological units of Site 645 are dominated by muddy sandstone, and silty mudstone and mudstone consistent with a Mokami Formation–equivalent unit. The strata are younger, however, than those drilled on the Labrador margin, but consistent with distal equivalents of the Saglek Formation predicted for the Labrador Shelf (Dafoe, Dickie, Williams, and McCartney, this volume). The depositional settings at the base of the corehole are typical of the Mokami Formation, but deeper shelf and slope conditions in the middle and upper part of the corehole are more distal that those encountered on the Labrador Shelf, which were drilled in more proximal locations. As distal marine Mokami Formation strata have not been sampled from the Labrador margin, Site 645 represents an important record of Neogene stratigraphy in the deeper basin from part of the Labrador–Baffin Seaway.

Previous offshore mapping

The original seismic stratigraphy of Srivastava et al. (1987) divided the strata of Site 645 into four main seismic units. Their basal seismic unit 4 included strata below Site 645. This was overlain by their seismic unit 3, which included their lithological subunit IIIC and some underlying strata, and then by seismic unit 2, corresponding to their lithological subunits IIIA and IIIB. Srivastava et al.'s (1987) uppermost seismic unit 1 approximately correlates with lithological units I and II (although the base is 50 m below the base of lithological unit II). These units were modified slightly by Harrison et al. (2011a) in their regional interpretation of northern Baffin Bay and are shown in Figure 7. In their study of the Neogene succession, Knutz et al. (2015) equated their D1 horizon with the top of subunit IIIC (forming the top of their unit D) and the top of subunit IIIB with their C1 horizon (bracketing the top of a thin unit C; Fig. 7). Furthermore, lithological subunit IIIA was equated to their seismic unit B, with the top being their B1 horizon, and Knutz et al.'s (2015) seismic unit A corresponds to units I and II (the top marked by A1).

Age and lithological constraints from Site 645 provide some insight into the regional distribution and seismic character of the Neogene deposits, which are probably present across much of Baffin Bay (MacLean et al., 1990). The base of the uppermost Upper Miocene to Middle Pliocene unit of the Baffin Fan correlates to the base of Harrison et al.'s, (2011a) seismic unit 2 in Site 645, an interval thought to contain two distinct sedimentary wedges. Also in this interval, clinoforms and large, possibly nested, channellized features ranging from 5 to 25 km wide and up to nearly 0.9 s two-way traveltime deep were identified outboard of Lancaster Sound (Rice and Shade, 1982; Harrison et al., 2011a).

Contourites dominate the Neogene succession on the conjugate West Greenland margin, forming the seismic stratigraphic units C through A found there (Knutz et al., 2015; Gregersen et al., 2019, this volume). Studying the upper stratigraphic section, Knutz et al. (2015) related contourite accumulations to the high-latitude Pliocene warming event and associated geostrophic currents along eastern Baffin Bay. They found that current-induced sedimentation increased in the Middle Miocene and ended by the Late Pliocene with the onset of global cooling. Prograding clinoforms related to trough-mouth fan development and early glacial advances also dominated the uppermost unit A deposition (Knutz et al., 2015).

Seismic reflection character

The base of the Upper Cenozoic section in this study is the Middle Miocene horizon SM3, with the top being the seafloor. Constraints for mapping the SM3 and overlying horizons, Saglek and/or Mokami formation–equivalent 4 and 5 (SM4 and SM5) are from correlation with the West Greenland margin where an extensive seismic stratigraphy is well established (Gregersen et al., 2013, 2018, 2019; Knutz et al., 2015). The present authors relate the SM4 and SM5 horizons to the C1 and B1 horizons, respectively (Fig. 7). In Site 645, this study follows the correlations of major horizons from Knutz et al. (2015), equating SM3 with D1, SM4 with C1, and SM5 with B1 (Fig. 7).

Overall, the upper Cenozoic unit forms a thick succession that can be over 2 s two-way traveltime thick within the deep-water northern regions of Baffin Basin (Fig. 4c). The horizons SM4 and SM5, of about Late Miocene and Pliocene age, respectively, can be interpreted across much of the study region. The SM4 horizon is conformable to channellized locally, with underlying mass-transport deposits or slumped intervals (Fig. 4b, c). This horizon caps a thin unit on the present-day shelf that likely reflects shelfal deposition (Fig. 4b, c), but thickens seaward into Baffin Basin (Fig. 4b, c). The overlying SM5 horizon is channellized locally and shows truncation of underlying strata, especially where there are large mass-transport complexes (Fig. 4c). This horizon caps a unit containing some channellized deposits on the present-day shelf (Fig. 4b) and related slump deposits at the shelf edge and along the slope (Fig. 4b, c), as well as areas that accumulated very little sediment over large basement highs (Fig. 4b). The interval is thickest at the base of the slope where mass-transport deposits are present and then thins basinward. An interval overlying SM5 preserves topsets and small clinoforms near the present-day shelf edge (Fig. 4b), as well as thick slumped successions (Fig. 4c). These correlate downslope with mass-transport deposits and deep-water successions that thicken basinward (Fig. 4).

Distribution of Middle Miocene–Pleistocene (upper Cenozoic) interval

The upper Cenozoic interval includes the upper Saglek and/or Mokami formation equivalents from the Middle Miocene to Pleistocene, from the SM3 horizon to the seafloor. These strata cover most of western Baffin Bay, forming a progradational sedimentary wedge that thickens rapidly seaward of the erosional edge shown in Figure 8. The erosional edge of the sedimentary wedge can be seen in Figure 4 where SM3 is truncated at the seafloor. Inboard of the thick sedimentary wedge and the erosional edge, thin or patchy Upper Quaternary till appears to cover much of the seafloor (e.g. Li et al., 2011), onlapping the basement platform and often extending beyond the seismic data coverage (Fig. 8). The presence and thickness of the tills is difficult to determine, as the seismic reflection around the seafloor is often obscured by multiples (ringing). Where these Quaternary sediments are thicker, they are relatively flat-lying above a high-angle unconformity with the underlying sedimentary rocks (e.g. landward side of Scott Graben; Fig. 4c). Local elevated basement platform rocks are onlapped by upper Cenozoic rocks and may be free of Quaternary cover.

The Middle Miocene to Pleistocene sequence of the Baffin Basin becomes thickest in the deep water, and numerous mass-transport complexes are found at the base of the slope (e.g. Line 2; near the projected ODP Site 645 location; Fig. 4b). The lower Cenozoic unit also thickens northward into the Baffin Fan (Harrison et al., 2011a). Knutz et al. (2015) described the lower part of the upper Cenozoic section as a contourite-drift system, which developed from the increased intensity of deep-ocean circulation in Baffin Bay, whereas the upper section is characterized by high-angle clinoforms that mark the onset of the northern hemisphere glaciation. The latter built seaward to form the present-day, high-angle shelf edge, which is better developed on the eastern side of Baffin Bay (*see* Dafoe, Williams et al., this volume).

SUMMARY

The western Baffin Bay study region lies at the northern end of the Labrador–Baffin Seaway rift system. Extension in the bay began in the Early Cretaceous, resulting in rifting of the paleo-North American plate and the separation of Greenland. This was followed by seafloor spreading in the Paleocene, a change in spreading direction near the Paleocene–Eocene boundary, and the termination of seafloor spreading near the Eocene–Oligocene boundary. Subsidence of the margins has resulted in thick strata covering oceanic crust in central Baffin Basin. The prerift basement comprises predominately Archean Rae Craton orthogneiss units, which are sampled locally in the offshore; however, Paleoproterozoic metasedimentary and volcanic rocks and Paleozoic sedimentary strata likely underlie parts of the offshore, especially in the Lancaster Sound region where such rocks are seen nearby onshore.

Although the synrift succession is poorly constrained, the presence of both Lower and Upper Cretaceous rocks is known from seabed sampling of bedrock along the margin and nearby onshore outcrops. Lower Cretaceous, synrift (Bjarni Formation equivalent) strata were found in seabed samples from east-central Baffin Island and are tied to nearby onshore outcrops of similar character and age. The Aptian–Albian strata sampled are lithologically similar to those of the Bjarni Formation on the Labrador margin, including the Snorri Member, but tend toward more nonmarine deposition, possibly due to the proximal location of these samples in Baffin Bay. Thick Upper Cretaceous strata blanket the Lower Cretaceous and are exposed near the seabed, as indicated by samples from Home Bay, Scott Graben, and Buchan Graben. These upper Coniacian–lower Campanian mudstone units are consistent with the Markland Formation of the Labrador margin and reflect similar shelfal settings, albeit slightly shallower marine environments than those in the Labrador Shelf wells. This study interprets a generally thin Lower Cretaceous section of growth-fault origin in Scott Graben, and possibly elsewhere along the Baffin Shelf. The Upper Cretaceous section is consistent with seismic analogues from the Labrador and West Greenland margins: similar to strata encountered in the Skolp E-07 well and Melville Bay Graben. On seismic sections covering western Baffin Bay, growth faulting of Upper Cretaceous rocks is less certain, and much of the succession appears to drape underlying basement and Lower Cretaceous strata; although, the distribution of Cretaceous strata indicates that the Cretaceous section is mainly confined to basement lows. The Scott Graben is subdivided to show the Bjarni Formation and Markland Formation equivalents, with two possible Freydis Member–equivalent intervals.

Plausible Paleocene volcanic rocks present along the southern portion of western Baffin Bay likely represent a volcanic margin as they locally include prominent seaward-dipping reflectors and inner flows. Volcanic rocks are also mapped north of the volcanic margin segment, offshore Cape Adair, possibly associated with a fracture zone in that region. The correlative Cartwright Formation equivalent may have been sampled in a single drill core in Scott Trough, and similarly, the overlying Kenamu Formation equivalent is known from dredge and seabed drill core samples of bedrock from Scott Trough. As was the case with Cretaceous samples, the Kenamu Formation–equivalent rocks reflect shallower depositional settings than those of the Labrador Shelf wells, which again is likely related to the proximity of the graben to the basin margin. Samples of the Mokami Formation equivalents from Scott Trough and Site 645 are lithologically consistent with that of the Labrador margin, with similar or younger (as in Site 645) ages. Again, depositional settings are generally shallower than the equivalent strata of offshore Labrador. The Cartwright, Kenamu, and parts of the Saglek and Mokami formation equivalents form the lower part of the Baffin Fan, a thick accumulation of sediments in northern Baffin Bay. These rocks are further mapped in Scott Graben based on sample constraints and seismic character, with offshore intervals tending to thicken basinward. Overall, the lower Cenozoic interval generally thickens into the Baffin Basin, especially over the extinct spreading axis and fracture zones, and is thin or has been removed within glacial troughs on the Baffin Shelf.

The Neogene section is well constrained by Site 645, which broadly equates to the upper part of the Baffin Fan. Strata of Site 645 are divided into three main lithological units of Early Miocene to Pleistocene age, forming stratigraphic equivalents to the upper Mokami Formation, but representing more distal marine strata not encountered on the Labrador margin. The section can be subdivided by two seismic horizons: SM4 and SM5 that equate to seismic markers C1 and B1 from the West Greenland margin and the tops of lithological subunits IIIB and IIIA, respectively. The upper Cenozoic interval thickens northward in Baffin Bay and also basinward into Baffin Basin. In landward proximal regions, the unit can be mostly composed of Quaternary cover. On the present-day shelf, prograding clinoforms are evident and have aided in building out the present-day shelf over time.

Building on the previous work in the region, the authors relate the stratigraphy of western Baffin Bay to the well sampled Labrador margin, the seismic-stratigraphic framework from the West Greenland margin, and onshore rift-related outcrops. Based on integration of recent studies with new seismic interpretation and regional mapping, this study provides a more comprehensive synthesis and some new insights into the geology of western Baffin Bay.

ACKNOWLEDGMENTS

The authors would like to acknowledge support of this work through the Baffin Island and the Labrador–Baffin Seaway Geological Synthesis activity under the Geo-mapping for Energy and Minerals program (GEM-2). The authors thank the Federal Institute for Geosciences and Natural Resources (Hannover), Suncor, and TGS-NOPEC Geophysical Company ASA for allowing the authors to show proprietary and released seismic data. Thanks to P. Knutz and U. Gregersen for providing interpretations for much of seismic line 2 and the Baffin Basin portion of line 3. The authors acknowledge the comprehensive and helpful reviews by J. Haggart and J. Ineson. A special thanks to L. MacLeod for design and compilation of the maps, and to P. Champagne for his work drafting the seismic figures. Thanks to T. Brent, K. DesRoches, and P. Lake for some of the legacy seismic data compilation and processing in the region, and thanks to S. Hynes for some of the GIS compilation and processing.

REFERENCES

Andrews, J.T., Guennel, G.K., Wray, J.L., and Ives, J.D., 1972. An early Tertiary outcrop in north-central Baffin Island, Northwest Territories, Canada: environment and significance; Canadian Journal of Earth Sciences, v. 9, p. 233–238. https://doi.org/10.1139/e72-019

Atkinson, E.A., Fustic, M., Hanna, M.C., and Lister, C.J., 2017. Qualitative assessment of petroleum potential in Lancaster Sound region, Nunavut; Geological Survey of Canada, Open File 8297, 18 p. https://doi.org/10.4095/305321

Balkwill, H.R. and McMillan, N.J., 1990. Mesozoic-Cenozoic geology of the Labrador Shelf; Chapter 7 (part 1) *in* Geology of the Continental Margin of Eastern Canada, (ed.) M.J. Keen and G.L. Williams; Geological Survey of Canada, Geology of Canada, no. 2, p. 295–324 (*also* Geological Society of America, The Geology of North America, v. I-1). https://doi.org/10.4095/132708

Beh, R.L., 1975. Evolution and geology of western Baffin Bay and Davis Strait, Canada; *in* Canada's Continental Margins and Offshore Petroleum Exploration, (ed.) D.J. Yorath and E.R. Parker; Canadian Society of Petroleum Geologists, Memoir 4, p. 453–476.

Bell, J.S., 1989. Labrador Sea; Geological Survey of Canada, East Coast Basin Atlas Series, 135 p. https://doi.org/10.4095/127152

Bell, J.S. and Campbell, G.R., 1990. Petroleum Resources; Chapter 12 *in* Geology of the Continental Margin of Eastern Canada, (ed.) M.J. Keen and G.L. Williams; Geological Survey of Canada, Geology of Canada, no. 2, p. 295–324 (*also* Geological Society of America, The Geology of North America, v. I-1). https://doi.org/10.4095/132720

Benham, P.H., 1991. Stratigraphy and palynology of Cretaceous and Tertiary rocks, North Bylot Trough, Bylot Island, Northwest Territories, Canada; M.Sc. thesis, Memorial University of Newfoundland, St. John's, Newfoundland and Labrador, 361 p.

Benham, P.H. and Burden, E.T., 1990. Stratigraphy of Cretaceous–Tertiary rocks of North Bylot Trough, Bylot Island, N.W.T.; *in* Current Research, Part D; Geological Survey of Canada, Paper 90-1D, p. 179–185. https://doi.org/10.4095/131353

Bojesen-Koefoed, J.A., Bidstrup, T., Christiansen, F.G., Dalhoff, F., Gregersen, U., Nytoft, H.P., Nøhr-Hansen, H., Pedersen, A.K., and Sønderholm, M., 2007. Petroleum seepages at Asuk, Disko, West Greenland – implications for regional petroleum exploration; Journal of Petroleum Geology, v. 30, p. 219–236. https://doi.org/10.1111/j.1747-5457.2007.00219.x

Brent, T.A., Chen, Z., Currie, L.D., and Osadetz, K., 2013. Assessment of the conventional petroleum resource potential of Mesozoic and younger structural plays within the proposed National Marine Conservation Area, Lancaster Sound, Nunavut; Geological Survey of Canada, Open File 6954, 44 p. https://doi.org/10.4095/289615

Burden, E.T. and Langille, A.B., 1990. Stratigraphy and sedimentology of Cretaceous and Paleocene strata in half-grabens on the southeast coast of Baffin Island, Northwest Territories; Bulletin of Canadian Petroleum Geology, v. 38, p. 185–196.

Burden, E.T. and Langille, A.B., 1991. Palynology of Cretaceous and Tertiary strata, northeast Baffin Island, Northwest Territories, Canada: implications for the history of rifting in Baffin Bay; Palynology, v. 15, p. 91–114. https://doi.org/10.1080/01916122.1991.9989392

Chalmers, J.A. and Pulvertaft, T.C.R., 2001. Development of the continental margins of the Labrador Sea: a review; Geological Society, London, Special Publications, v. 187, no. 1, p. 77–105. https://doi.org//10.1144/GSL.SP.2001.187.01.05

Clarke, B.W., 1976. Tertiary and Mesozoic stratigraphy of Bylot Island, N.W.T.; report prepared for Norlands Petroleum Limited; on file with the Canada Energy Regulator, Calgary, Alberta, National Energy Board Report 511-1-12-21, 81 p.

Clarke, D.B. and Upton, B.G.J., 1971. Tertiary basalts of Baffin Island; field relations and tectonic setting; Canadian Journal of Earth Sciences, v. 8, p. 248–258. https://doi.org/10.1139/e71-025

Dafoe, L.T., 2021. Paleoenvironmental analyses and revised lithostratigraphic assignments for 28 wells of the Hopedale and Saglek basins, offshore eastern Canada; Geological Survey of Canada, Open File 8810, 209 p. https://doi.org/10.4095/328477

Dafoe, L.T. and Haggart, J., 2018. Ichnology and sedimentology of Cretaceous and Paleogene strata on Bylot Island, Nunavut: development of a rift-basin succession in Baffin Bay; Atlantic Geoscience Society, 44th Colloquium, February 2–3, 2018, Truro, Nova Scotia, p. 19–20 (abstract).

Dafoe, L.T. and Williams, G.L., 2020a. A reassessment of Mesozoic–Cenozoic seabed samples of bedrock from the western Davis Strait and eastern Baffin Island margin, offshore eastern Canada: new insights into their lithology, age, and paleoenvironment of deposition; Geological Survey of Canada, Open File 8702, 41 p. https://doi.org/10.4095/321758

Dafoe, L.T. and Williams, G.L., 2020b. Palynological analysis of the two Labrador Shelf wells, Petro-Canada et al. North Leif I-05 and Total Eastcan et al. Skolp E-07, offshore eastern Canada: new age, paleoenvironmental and lithostratigraphic interpretations; Geological Survey of Canada, Open File 8670, 103 p., 10 sheets. https://doi.org/10.4095/321502

Dafoe, L.T. and Williams, G.L., 2020c. Palynostratigraphic and integrated paleoenvironmental assessment of the ODP Site 645 corehole in Baffin Bay, offshore eastern Canada; Geological Survey of Canada, Open File 8701, 61 p., 4 sheets. https://doi.org/10.4095/321736

Dafoe, L.T. and Williams, G.L., 2020d. Lithological, sedimentological, ichnological, and palynological analysis of 37 conventional core intervals from 15 Wells, offshore Labrador, Canada; Geological Survey of Canada, Bulletin 613, 146 p. https://doi.org/10.4095/315362

Dafoe, L.T., Dickie, K., Williams, G.L., Jauer, C.D., Hynes, S., Brent, T.A., Li, Q., Oakey, G.N., Potter, D.P., Haggart, J.W., Smyth, H.R., Currie, L.D., Sweet, A.R., DesRoches, K., and Szlavko, B., 2016a. Report of activities for the Stratigraphic and Tectonic Framework for the Baffin Bay Petroleum Systems: GEM 2 Baffin Project; Geological Survey of Canada, Open File 7960, 10 p. https://doi.org//10.4095/297248

Dafoe, L.T., Dickie, K., Williams, G.L., Jauer, C.D., Li, Q., Dehler, S., Potter, D.P., Hynes, S., Patton, E., Bates, J., Haggart, J.W., and Clark, K., 2016b. Report of activities for the stratigraphic and tectonic framework for the Baffin Bay Petroleum Systems (2016), GEM-2 Baffin Project; Geological Survey of Canada, Open File 8144, 10 p. https://doi.org//10.4095/299240

Dafoe, L.T., Haggart, J.W., and Williams, G.L., 2019. Onshore-offshore comparisons of the Cretaceous and Paleogene strata from Bylot Island and the western Baffin Bay margin, Nunavut; 45th Atlantic Geoscience Society Colloquium; Fredericton, New Brunswick, February 8–9, p. 24 (abstract).

Dam, G., Larsen, M., and Sørensen, J.C., 1998. Sedimentary response to mantle plumes: implications from Palaeocene onshore successions, West and East Greenland; Geology, v. 26, p. 207–210. https://doi.org/10.1130/0091-7613(1998)026%3c0207:SRTMPI%3e2.3.CO%3b2

de Vernal, A. and Mudie, P.J., 1989. Late Pliocene to Holocene palynostratigraphy at ODP Site 645, Baffin Bay; *in* Proceedings of the Ocean Drilling Program, Scientific Results, v. 105, (ed.) S.P. Srivastava, M.A. Arthur, B. Clement, A. Aksu, J. Baldauf, G. Bohrmann, W. Busch, T. Cederberg, M. Cremer, K. Dadey, A. de Vernal, J. Firth, F. Hall, M. Head, R. Hiscott, R. Jarrard, M. Kaminski, D. Lazarus, A.-L. Monjanel, . . . H. Zimmerman, p. 387–399. https://doi.org/10.2973/odp.proc.sr.105.133.1989

Dickie, K., Keen, C.E., Williams, G.L., and Dehler, S.A., 2011. Tectonostratigraphic evolution of the Labrador margin, Atlantic Canada; Marine and Petroleum Geology, v. 28, p. 1663–1675. https://doi.org/10.1016/j.marpetgeo.2011.05.009

Fader, G.B., Cameron, G.D.M., and Best, M.A. (comp.), 1989. Geology of the Continental Margin of Eastern Canada; Geological Survey of Canada, Map 1705A, scale 1:5 000 000. https://doi.org/10.4095/127347

Fenton, J.P.G., and Pardon, A.M., 2007. Sequence stratigraphic correlation of Cretaceous–Palaeogene strata, Labrador Sea and Davis Strait. Biostratigraphic and sequence stratigraphic correlation of 33 wells. Volume 1: text, figures and appendices. Report No. 6851/Ib, Project No. Ib/GF556; report prepared for Fugro Robertson Limited, Llandudno, United Kingdom, on file at Canada–Newfoundland and Labrador Offshore Petroleum Board, St. John's, Newfoundland and Labrador, 177 p.

Fowler, M., Stasiuk, L., and Avery, M., 2005. Potential petroleum systems in the Labrador and Baffin Shelf areas, offshore north eastern Canada; *in* Organic Geochemistry: Challenges for the 21st Century, (ed.) F.J. González-Vila, J.A. González-Pérez, and G. Almendros; 22nd International Meeting on Organic Geochemistry, Seville, Spain, September 12–16, 2005, v. 1, p. 463–464 (abstract). https://digital.csic.es/bitstream/10261/3957/1/BOOK%20OF%20ABSTRACTS%20PORTADA%20VOL%201.pdf

Funck, T., Jackson, H.R., Dehler, S.A., and Reid, I.D., 2006. A refraction seismic transect from Greenland to Ellesmere Island, Canada: the crustal structure in southern Nares Strait; Polarforschung, v. 74, no. 1-3, p. 97–112. https://doi.org//10013/epic.29927.d001

Funck, T., Gohl, K., Damm, V., and Heyde, I., 2012. Tectonic evolution of southern Baffin Bay and Davis Strait: results from a seismic refraction transect between Canada and Greenland; Journal of Geophysical Research, v. 117, no. B4, cit. no. B04107. https://doi.org/10.1029/2011JB009110

General Bathymetric Chart of the Oceans, 2014. GEBCO 2014 Grid; International Hydrographic Organization and the Intergovernmental Oceanographic Commission (of UNESCO). <www.gebco.net> [accessed May 19, 2015]

Gion, A.M., Williams, S.E., and Muller, R.D., 2017. A reconstruction of the Eurekan Orogeny incorporating deformation constraints; Tectonics, v. 36, issue 2, p. 304–320. https://doi.org/10.1002/2015TC004094

Gradstein, F.M., Ogg, J.G., Schmitz, M., and Ogg, G. (ed.), 2012. The Geologic Time Scale 2012; Elsevier B.V., Oxford, United Kingdom, 1176 p. https://doi.org/10.1016/C2011-1-08249-8

Grant, A.C., 1988. Depth to basement of the continental margin of eastern Canada; Map 1707A *in* Geology of the Continental Margin of Eastern Canada, (ed.) M.J. Keen and G.L. Williams; scale 1:5 000 000 (*also* Geological Society of America, The Geology of North America, v. I-2). https://doi.org/10.4095/125185

Gregersen, U., Hopper, J.R., and Knutz, P., 2013. Basin seismic stratigraphy and aspects of prospectivity in the NE Baffin Bay, Northwest Greenland; Marine and Petroleum Geology, v. 46, p. 1–18. https://doi.org/10.1016/j.marpetgeo.2013.05.013

Gregersen, U., Knutz, P.C., and Hopper, J.R., 2016. New geophysical and geological mapping of the eastern Baffin Bay region, offshore West Greenland; Geological Survey of Denmark and Greenland Bulletin, v. 35, p. 83–86.

Gregersen, U., Andersen, M.S., Nøhr-Hansen, H., Sheldon, E., Kokfelt, T.F., Olivarius, M., Knudsen, C., Jakobsen, K.G., and Adolfssen, J.S., 2018. New subsurface mapping offshore southern West Greenland using geophysical and geological data; Geological Survey of Denmark and Greenland Bulletin, v. 41, p. 57–62. https://doi.org/10.34194/geusb.v41.4342

Gregersen, U., Knutz, P.C., Nøhr-Hansen, H., Sheldon, E., and Hopper, J.R., 2019. Tectonostratigraphy and evolution of the West Greenland continental margin; Bulletin of the Geological Society of Denmark, v. 67, p. 1–21.

Hahn, K. and Turner, E.C., 2013. Mesoproterozoic deep-water carbonate mound lithofacies, Borden Basin, Nunavut; Geological Survey of Canada, Current Research 2013-11, 14 p. https://doi.org/10.4095/292439

Harrison, J.C., Brent, T.A., and Oakey, G.N., 2011a. Baffin Fan and its inverted rift system of Arctic eastern Canada: stratigraphy, tectonics and petroleum resource potential; *in* Arctic Petroleum Geology, (ed.) A.M. Spencer, A.F. Embry, D.L. Gautier, A.V. Stoupakova, and K. Sørensen; Geological Society, London, Memoirs, v. 35, p. 595–626. https://doi.org/10.1144/M35.40

Harrison, J.C., St-Onge, M.R., Petrov, O.V., Strelnikov, S.I., Lopatin, B.G., Wilson, F.H., Tella, S., Paul, D., Lynds, T., Shokalsky, S.P., Hults, C.K., Bergman, S., Jepsen, H.F., and Solli, A., 2011b. Geological map of the Arctic; Geological Survey of Canada, Map 2159A, scale 1:5 000 000. https://doi.org/10.4095/287868

Head, M.J., Norris, G., and Mudie, P.J., 1989. Palynology and dinocyst stratigraphy of the Miocene in ODP Leg 105, Hole 645E, Baffin Bay; *in* Proceedings ODP, Scientific Results, v. 105, (ed.) S.P. Srivastava, M.A. Arthur, B. Clement, A. Aksu, J. Baldauf, G. Bohrmann, W. Busch, T. Cederberg, M. Cremer, K. Dadey, A. de Vernal, J. Firth, F. Hall, M. Head, R. Hiscott, R. Jarrard, M. Kaminski, D. Lazarus, A.-L. Monjanel, . . . H. Zimmerman; Ocean Drilling Program, College Station, Texas, p. 467–514. https://doi.org/10.2973/odp.proc.sr.105.137.1989

Hiscott, R.N., Cremer, M., and Aksu, A.E., 1989. Evidence from sedimentary structures for processes of sediment transport and deposition during post-Miocene time at Sites 645, 646, and 647, Baffin Bay and the Labrador Sea; *in* Proceedings of the Ocean Drilling Program, Scientific Results, v. 105, (ed.) S.P. Srivastava, M.A. Arthur, B. Clement, A. Aksu, J. Baldauf, G. Bohrmann, W. Busch, T. Cederberg, M. Cremer, K. Dadey, A. de Vernal, J. Firth, F. Hall, M. Head, R. Hiscott, R. Jarrard, M. Kaminski, D. Lazarus, A.-L. Monjanel, . . . H. Zimmerman; Ocean Drilling Program, College Station, Texas, p. 53–63. https://doi.org/10.2973/odp.proc.sr.105.119.1989

Hood, P. and Bower, M., 1975. Aeromagnetic reconnaissance of Davis Strait and adjacent areas; *in* Canada's Continental Margins and offshore petroleum exploration, (ed.) D.J. Yorath and E.R. Parker; Canadian Society of Petroleum Geologists, Memoir 4, p. 433–451.

Ioannides, N.S., 1986. Dinoflagellate cysts from Upper Cretaceous-Lower Tertiary sections, Bylot and Devon islands, Arctic Archipelago; Geological Survey of Canada, Bulletin 371, 99 p. https://doi.org/10.4095/123641

Jackson, G.D., 1998. Geology, Okoa Bay-Padloping Island area, District of Franklin, Northwest Territories; Geological Survey of Canada, Open File 3532, 1 sheet, scale 1:250 000. https://doi.org/10.4095/209911

Jackson, G.D. and Iannelli, T.R., 1981. Rift-related cyclic sedimentation in the Neohelikian Borden Basin, northern Baffin Island; *in* Proterozoic Basins of Canada, (ed.) F.H.A. Campbell; Geological Survey of Canada, Paper 81-10, p. 269–302. https://doi.org/10.4095/109369

Jackson, G.D., Davidson, A., and Morgan, W.C., 1975. Geology of the Pond Inlet map-area, Baffin Island, District of Franklin (38A, 38B, part of 48A); Geological Survey of Canada, Paper 74-25, 33 p. https://doi.org/10.4095/102498

Jackson, H.R., Keen, C.E., and Barrett, D.L., 1977. Geophysical studies on the eastern continental margin of Baffin Bay and in Lancaster Sound; Canadian Journal of Earth Sciences, v. 14, no. 9, p. 1991–2001. https://doi.org/10.1139/e77-170

Jackson, G.D., Morgan, W.C., and Davidson, A., 1979. Geology, Buchan Gulf-Scott Inlet, District of Franklin; Geological Survey of Canada, Map 1449A, scale 1:250 000. https://doi.org/10.4095/109159

Jackson, H.R., Dickie, K., and Marillier, F., 1992. A seismic reflection study of northern Baffin Bay: implication for tectonic evolution; Canadian Journal of Earth Sciences, v. 29, p. 2353–2369. https://doi.org/10.1139/e92-184

Jansa, L.F., 1976. Lower Paleozoic radiolarian-bearing limestones from the Baffin Island shelf; *in* Report of Activities, Part B; Geological Survey of Canada, Paper 76-1B, p. 99–105. https://doi.org/10.4095/104085

Kaminski, M.A., Gradstein, F.M., Scott, D.B., and Mackinnon, K.D., 1989. Neogene benthic foraminifer biostratigraphy and deep-water history of Sites 645, 646, and 647, Baffin Bay and Labrador Sea; *in* Proceedings of the Ocean Drilling Program, Scientific Results, v. 105, (ed.) S.P. Srivastava, M.A. Arthur, B. Clement, A. Aksu, J. Baldauf, G. Bohrmann, W. Busch, T. Cederberg, M. Cremer, K. Dadey, A. de Vernal, J. Firth, F. Hall, M. Head, R. Hiscott, R. Jarrard, M. Kaminski, D. Lazarus, A.-L. Monjanel, . . . H. Zimmerman; Ocean Drilling Program, College Station, Texas, p. 731–756.

Keen, C.E. and Barrett, D.L., 1972. Seismic refraction studies in Baffin Bay: an example of a developing ocean basin; Geophysical Journal of the Royal Astronomical Society, v. 30, no. 3, p. 253–271. https://doi.org/10.1111/j.1365-246X.1972.tb05812.x

Keen, C.E. and Barrett, D.L., 1973. Structural characteristics of some sedimentary basins in northern Baffin Bay; Canadian Journal of Earth Sciences, v. 10, p. 1267–1278. https://doi.org/10.1139/e73-112

Keen, C.E., Keen, M.J., Ross, D.I., and Lack, M., 1974. Baffin Bay; small ocean basin formed by seafloor spreading; The American Association of Petroleum Geologists Bulletin, v. 58, p. 1089–1108.

Keen, C.E., Dickie, K., and Dehler, S.A., 2012. The volcanic margins of the northern Labrador Sea: insights to the rifting process; Tectonics, v. 31, no. 9, cit. no. TC1011. https://doi.org/10.1029/2011TC002985.

Keen, C.E., Dickie, K., and Dafoe, L.T., 2018a. Structural characteristics of the ocean-continent transition along the rifted continental margin, offshore central Labrador; Marine and Petroleum Geology, v. 89, no. 2. p. 443–463. https://doi.org/10.1016/j.marpetgeo.2017.10.012

Keen, C.E., Dickie, K., and Dafoe, L.T., 2018b. Structural evolution of the rifted margin off northern Labrador: the role of hyper-extension and magmatism; Tectonics, v. 37, issue 7, p. 1955–1972. https://doi.org/10.1029/2017TC004924

Kerr, J.W.M., 1980. Structural framework of Lancaster Aulacogen, Arctic Canada; Geological Survey of Canada, Bulletin 319, 24 p. https://doi.org/10.4095/102164

Knutz, P.C., Hopper, J.R., Gregersen, U., Nielsen, T., and Japsen, P., 2015. A contourite drift system on the Baffin Bay–West Greenland margin linking Pliocene Arctic warming to poleward ocean circulation; Geology, v. 43, p. 907–910. https://doi.org/10.1130/G36927.1

Larsen, L.M., Heaman, L.M., Creaser, R.A., Duncan, R.A., Frei, R., and Hutchison, M., 2009. Tectonomagmatic events during stretching and basin formation in the Labrador Sea and the Davis Strait: evidence from age and composition of Mesozoic to Palaeogene dyke swarms in West Greenland; Journal of the Geological Society, v. 166, p. 999–1012. https://doi.org/10.1144/0016-76492009-038

Levy, E.M. and Ehrhardt, M., 1981. Natural seepage of petroleum at Buchan Gulf, Baffin Island; Marine Chemistry, v. 10, p. 355–364. https://doi.org/10.1016/0304-4203(81)90014-1

Levy, E.M. and MacLean, B., 1981. Natural hydrocarbon seepage at Scott Inlet and Buchan Gulf, Baffin Island Shelf: 1980 update; *in* Current Research, Part A; Geological Survey of Canada, Paper 81-1A, p. 401–403. https://doi.org/10.4095/109550

Li, G., Piper, D.J.W., and Campbell, D.C., 2011. The Quaternary Lancaster Sound trough-mouth fan, NW Baffin Bay; Journal of Quaternary Science, v. 26, p. 511–522. https://doi.org/10.1002/jqs.1479

Loncarevic, B.D. and Falconer, R.K., 1977. An oil slick occurrence off Baffin Island; *in* Report of Activities, Part A; Geological Survey of Canada, Paper 77-1A, p. 523–524. https://doi.org/10.4095/102743

MacLean, B., 1978. Marine geological-geophysical investigations in 1977 of the Scott Inlet and Cape Dyer-Frobisher Bay areas of the Baffin Island continental shelf; *in* Current Research, Part B; Geological Survey of Canada, Paper 78-1B, p. 13–20. https://doi.org/10.4095/103568

MacLean, B., 1980. Cruise report C.S.S. Hudson 80-028; Geological Survey of Canada, Cruise Report, Expedition Database, 31 p. <https://ed.gdr.nrcan.gc.ca/cruise_report_e.php> [accessed January 1, 2016]

MacLean, B., 1985. Preliminary report of cruise activities – CSS Hudson 85-027. Geological Survey of Canada, Cruise Report, Expedition Database, 54 p. <https://ed.gdr.nrcan.gc.ca/cruise_report_e.php> [accessed September 2, 2015]

MacLean, B. and Falconer, R.K.H., 1979. Geological-geophysical studies in Baffin Bay and Scott Inlet–Buchan Gulf and Cape Dyer–Cumberland Sound areas of the Baffin Island Shelf; *in* Current Research, Part B; Geological Survey of Canada, Paper 79-1B, p. 231–244. https://doi.org/10.4095/105432

MacLean, B. and Srivastava, S.P., 1976. Shallow corehole drilling on the Baffin Island shelf; *in* Report of Activities, Part A; Geological Survey of Canada, Paper 76-1A, p. 141–143. https://doi.org/10.4095/104182

MacLean, B. and Williams, G.L., 1983. Geological investigations of Baffin Island shelf in 1982; *in* Current Research, Part B; Geological Survey of Canada, Paper 83-1B, p. 309–315. https://doi.org/10.4095/109337

MacLean, B., Jansa, L.F., Falconer, R.K.H., and Srivastava, S.P., 1977. Ordovician strata on the southeastern Baffin Island shelf revealed by shallow drilling; Canadian Journal of Earth Sciences, v. 14, p. 1925–1939. https://doi.org/10.1139/e77-163

MacLean, B., Falconer, R.K.H., and Levy, E.M., 1981. Geological, geophysical and chemical evidence for natural seepage of petroleum off the northeast coast of Baffin Island; Bulletin of Canadian Petroleum Geology, v. 29, p. 75–95.

MacLean, B., Woodside, J.M., and Girouard, P., 1984. Geological and geophysical investigations in Jones Sound, District of Franklin; *in* Current Research, Part A; Geological Survey of Canada, Paper 84-1A, p. 359–365. https://doi.org/10.4095/119685

MacLean, B., Williams, G.L., and Srivastava, S.P., 1990. Geology of Baffin Bay and Davis Strait; Chapter 7 (part 2) *in* Geology of the Continental Margin of Eastern Canada, (ed.) M.J. Keen and G.L. Williams; Geological Survey of Canada, Geology of Canada, no. 2, p. 325–348 (*also* Geological Society of America, The Geology of North America, v. I-1). https://doi.org/10.4095/132710

MacLean, B., Williams, G., and Zhang, S., 2014. New insights into the stratigraphy and petroleum potential of the Baffin Shelf's Cretaceous rocks; Bulletin of Canadian Petroleum Geology; Baffin Bay Special Issue, v. 62, no. 4, p. 289–310.

McMillan, N.J., 1973. Shelves of Labrador Sea and Baffin Bay, Canada; *in* Future Petroleum Provinces of Canada, (ed.) R.G. McCrossan; Canadian Society of Petroleum Geologists, Memoir 1, p. 473–515.

McWhae, J.R.H., 1981. Structure and spreading history of the northwestern Atlantic region from the Scotian Shelf to Baffin Bay; *in* Geology of the North Atlantic Borderlands, (ed.) J.W. Kerr, A.J. Fergusson, and L.C. Machan; Canadian Society of Petroleum Geologists, Memoir 7, p. 299–332.

McWhae, J.R.H., Elie, R., Laughton, K.C., and Gunther, P.R., 1980. Stratigraphy and petroleum prospects of the Labrador Shelf; Bulletin of Canadian Petroleum Geology, v. 28, p. 460–488.

Miall, A.D., Balkwill, H.R., and Hopkins, W.S., Jr., 1980. Cretaceous and Tertiary sediments of Eclipse Trough, Bylot Island area, Arctic Canada, and their regional setting; Geological Survey of Canada, Paper 79-23, 20 p. https://doi.org/10.4095/102162

Nelson, C.E., Jerram, D.A., Clayburn, J.A.P., Halton, A.M., and Roberge, J., 2015. Eocene volcanism in offshore southern Baffin Bay; Marine and Petroleum Geology, v. 67, p. 678–691. https://doi.org/10.1016/j.marpetgeo.2015.06.002

Nøhr-Hansen, H., Sheldon, E., and Dam, G., 2002. A new biostratigraphic scheme for the Paleocene onshore West Greenland and its implications for the timing of the pre-volcanic evolution; *in* The North Atlantic Igneous Province: Stratigraphy, Tectonic, Volcanic and Magmatic Processes, (ed.) D.W. Jolley and B.R. Bell; Geological Society, London, Special Publications, v. 197, p. 111–156. https://doi.org/10.1144/GSL.SP.2002.197.01.06

Nøhr-Hansen, H., Pedersen, G.K., Knutz, P., Bojesen-Koefoed, J., Sliwinska, K.K., and Hovikoski, J., 2018. Potential Cretaceous source-rocks from the north-east Baffin Bay, West Greenland; Global Analogues of the Atlantic Margin, American Association of Petroleum Geologists, Europe Regional Conference, May 2–3, 2018, Lisbon, Portugal, article 90325, 2 p.

Oakey, G.N. and Chalmers, J.A., 2012. A new model for the Paleogene motion of Greenland relative to North America: plate reconstructions of the Davis Strait and Nares Strait regions between Canada and Greenland; Journal of Geophysical Research, v. 117, issue B10, cit. no. B10401. https://doi.org/10.1029/2011JB008942

Pedersen, G.K. and Pulvertaft, T.C.R., 1992. The nonmarine Cretaceous of the West Greenland Basin, onshore West Greenland; Cretaceous Research, v. 13, p. 263–272. https://doi.org/10.1016/0195-6671(92)90002-8

Planke, S., Symonds, P.A., Alvestad, E., and Skogseid, J., 2000. Seismic volcanostratigraphy of large volume basaltic extrusive complexes on rifted margins; Journal of Geophysical Research, v. 105, p. 19335–19351. https://doi.org/10.1029/1999JB900005

Refsnider, K.A., Miller, G.H., Hillaire-Marcel, C., Fogel, M.L., Ghaleb, B., and Bowden, R., 2012. Subglacial carbonates constrain basal conditions and oxygen isotopic composition of the Laurentide Ice Sheet over Arctic Canada; Geology, v. 40, no. 2, p. 135–138. https://doi.org/10.1130/G32335.1

Reid, I. and Jackson, H.R., 1997. Crustal structure of northern Baffin Bay: seismic refraction results and tectonic implications; Journal of Geophysical Research, v. 102, no. B1, p. 523–542. https://doi.org/10.1029/96JB02656

Rice, P.D. and Shade, B.D., 1982. Reflection seismic interpretation and seafloor spreading history of Baffin Bay; *in* Arctic Geology and Geophysics, (ed.) A.F. Embry and H.R. Balkwill; Canadian Society of Petroleum Geology, Memoir 8, Proceedings of the Third International Symposium on Arctic Geology, p. 245–265.

Roest, W.R. and Srivastava, S.P., 1989. Sea-floor spreading in the Labrador Sea: a new reconstruction; Geology, v. 17, no. 11, p. 1000–1003. https://doi.org/10.1130/0091-7613(1989)017%3c1000:SFSITL%3e2.3.CO%3b2

Rolle, F., 1985. Late Cretaceous – Tertiary sediments offshore central West Greenland: lithostratigraphy, sedimentary evolution, and petroleum potential; Canadian Journal of Earth Sciences, v. 22, p. 1001–1019. https://doi.org/10.1139/e85-105

Scott, D.J. and de Kemp, E.A., 1998. Bedrock geology compilation, northern Baffin Island and northern Melville Peninsula, Northwest Territories; Geological Survey of Canada, Open File 3633, 3 sheets. https://doi.org/10.4095/210024

Skaarup, N., Jackson, H.R., and Oakey, G., 2006. Margin segmentation of Baffin Bay/Davis Strait, eastern Canada based on seismic reflection and potential field data; Marine and Petroleum Geology, v. 23, p. 127–144. https://doi.org/10.1016/j.marpetgeo.2005.06.002

Sparkes, K.E., 1989. Stratigraphy and terrestrial palynology of Late Cretaceous Eclipse Group Strata, Bylot Island, Northwest Territories, Canada; M.Sc. thesis, Memorial University of Newfoundland, St. John's, Newfoundland and Labrador, 195 p.

Srivastava, S.P., Falconer, K.H., and MacLean, B., 1981. Labrador Sea, Davis Strait, Baffin Bay: Geology and geophysics – a review; *in* Geology of the North Atlantic Borderlands, (ed.) J.W. Kerr, A.J. Fergusson, and L.C. Machan; Canadian Society of Petroleum Geologists, Memoir 7, p. 333–398.

Srivastava, S.P., Arthur, M.A. Clement, B. Aksu, A., Baldauf, J., Bohrmann, G., Busch, W., Cederberg, T., Cremer, M., Dadey, K., de Vernal, A., Firth, J., Hall, F., Head, M., Hiscott, R., Jarrard, R., Kaminski, M., Lazarus, D., Monjanel, . . . Zimmerman, H., 1987. Site 645; *in* Proceedings of the Ocean Drilling Program, v. 105, part A, Initial Reports, p. 61–418. https://doi.org/10.2973/odp.proc.ir.105.104.1987

St-Onge, M.R., Van Gool, J.A., Garde, A.A., and Scott, D.J., 2009. Correlation of Archaean and Palaeoproterozoic units between northeastern Canada and western Greenland: constraining the pre-collisional upper plate accretionary history of the Trans-Hudson orogen; Geological Society of London, Special Publications, v. 318, p. 193–235. https://doi.org/10.1144/SP318.7

Storey, M., Duncan, R.A., Pedersen, A.K., Larsen, L.M., and Larsen, H.C., 1998. $^{40}Ar/^{39}Ar$ geochronology of the west Greenland tertiary volcanic province; Earth and Planetary Science Letters, v. 160, p. 569–586. https://doi.org/10.1016/S0012-821X(98)00112-5

Storey, M., Duncan, R.A., and Tegner, C., 2007. Timing and duration of volcanism in the North Atlantic Igneous Province: implications for geodynamics and links to the Iceland hotspot; Chemical Geology, v. 241, no. 3-4, p. 264–281. https://doi.org/10.1016/j.chemgeo.2007.01.016

Thiébault, F., Cremer, M., Debrabant, P., Foulon, J., Nielson, O.B., and Zimmerman, H., 1989. Analysis of sedimentary facies, clay mineralogy, and geochemistry of the Neogene-Quaternary sediments in ODP Site 645, Baffin Bay; *in* Proceedings of the Ocean Drilling Program, Scientific Results, v. 105, (ed.) S.P. Srivastava, M.A. Arthur, B. Clement, A. Aksu, J. Baldauf, G. Bohrmann, W. Busch, T. Cederberg, M. Cremer, K. Dadey, A. de Vernal, J. Firth, F. Hall, M. Head, R. Hiscott, R. Jarrard, M. Kaminski, D. Lazarus, A.-L. Monjanel, . . . H. Zimmerman; Ocean Drilling Program, College Station, Texas, p. 83–90. https://doi.org/10.2973/odp.proc.sr.105.111.1989

Turner, E.C., 2009. Mesoproterozoic carbonate systems in the Borden Basin, Nunavut; Canadian Journal of Earth Sciences, v. 46, p. 915–938. https://doi.org/10.1139/E09-062

Umpleby, D.C., 1979. Geology of the Labrador shelf; Geological Survey of Canada, Paper 79-13, 40 p. https://doi.org/10.4095/105927

Von Gosen, W., Piepjohn, K., Gilotti, J.A., McClelland, W.C., and Reinhardt, L., 2019. Structural evidence for sinistral displacement on the Wegener Fault in southern Nares Strait, Arctic Canada; *in* Circum-Arctic Structural Events: Tectonic Evolution of the Arctic Margins and Trans-Arctic Links with Adjacent Orogens, (ed.) K. Piepjohn, J.V. Strauss, L. Reinhardt, and W.C. McClelland; The Geological Society of America, Special Paper no. 541. https://doi.org/10.1130/2018.2541(18)

Waterfield, J.J., 1989. Stratigraphy, sedimentology and palynology of Cretaceous and Tertiary strata, southwest Bylot Island, Northwest Territories, Canada; M.Sc. thesis, Memorial University of Newfoundland, St. John's, Newfoundland and Labrador, 260 p.

Whittaker, R.C., Hamann, N.E., and Pulvertaft, T.C.R., 1997. A new frontier offshore northwest Greenland: structure, basin development, and petroleum potential of the Melville Bay Area; American Association of Petroleum Geologists, AAPG Bulletin, v. 81, p. 978–998.

Wiseman, T.R., 1991. Sedimentology of the Maastrichtian, Pond Inlet formation (channelized turbidite system), Bylot Island, Northwest Territories, Canada; B.Sc. thesis, Memorial University of Newfoundland, St. John's, Newfoundland and Labrador, 133 p.

Zhang, S., 2013. Rock Eval[6] and vitrinite reflectance data from Baffin Island Shelf and Hudson Strait; Geological Survey of Canada, Open File 7341, 32 p. https://doi.org/10.4095/292376

Stratigraphy of the West Greenland margin

U. Gregersen[1*], P.C. Knutz[1], G.K. Pedersen[1], H. Nøhr-Hansen[1], J.R. Ineson[1], L.M. Larsen[1], J.R. Hopper[1], J.A. Bojesen-Koefoed[1], G. Dam[1], T. Funck[1], and J. Hovikoski[1]

Gregersen, U., Knutz, P.C., Pedersen, G.K., Nøhr-Hansen, H., Ineson, J.R., Larsen, L.M., Hopper, J.R., Bojesen-Koefoed, J.A., Dam, G., Funck, T., and Hovikoski, J., 2022. Stratigraphy of the West Greenland margin; in *Geological synthesis of Baffin Island (Nunavut) and the Labrador–Baffin Seaway, (ed.) L.T. Dafoe and N. Bingham-Koslowski; Geological Survey of Canada, Bulletin 608, p. 247–309. https://doi.org/10.4095/321849*

Abstract: The stratigraphy and the geological evolution of the West Greenland margin from the Labrador Sea to Baffin Bay in both the onshore and offshore areas are described. The primary data sets include seismic reflection surveys, wells, and outcrops. In addition, seabed samples, seismic refraction and magnetic data, onshore and offshore maps, and stratigraphic compilations were used. The basins of the West Greenland continental margin are described in three regions from the south to the north: southern West Greenland basins, central West Greenland basins, and northern West Greenland basins. Each region includes a description of the stratigraphy and evolution from the Archean to the Quaternary, divided into six phases: pre-rift and early extension, early rift, subsidence and rifting, late rift, drift, and post-drift. Finally, the regions are correlated and described in a tectonostratigraphic context together with analogues from the Canadian conjugate margin.

Résumé : Nous décrivons la stratigraphie et l'évolution géologique de la marge de l'ouest du Groenland, de la mer du Labrador jusqu'à la baie de Baffin, tant en milieu côtier qu'extracôtier. Les principaux jeux de données se rapportent à des levés de sismique-réflexion, à des puits et à des affleurements. De plus, nous avons utilisé des échantillons du fond marin, des données de sismique-réfraction et des données magnétiques, des cartes des milieux côtier et exracôtier ainsi que des compilations stratigraphiques. Les bassins de la marge continentale de l'ouest du Groenland sont décrits suivant trois régions, qui sont du sud au nord : les bassins de l'ouest du Groenland Sud, les bassins de l'ouest du Groenland Central et les bassins de l'ouest du Groenland Nord. Pour chaque région, nous fournissons une description de la stratigraphie et de l'évolution échelonnée de l'Archéen jusqu'au Quaternaire en adoptant une division en six phases : pré-rift et distension précoce; rift précoce; subsidence et rifting; rift tardif; dérive; et post-dérive. Enfin, les régions sont corrélées et décrites suivant une approche tectonostratigraphique en intégrant des analogues de la marge conjuguée du Canada.

[1]Geological Survey of Denmark and Greenland, Oester Voldgade 10, 1350 Copenhagen K, Denmark
*Corresponding author: U. Gregersen (email: ug@geus.dk)

Contents

INTRODUCTION

This is a summary of the stratigraphy and the geological evolution of the West Greenland margin and covers onshore and offshore areas within the Greenland sector between approximately latitudes 58°N and 76°N (Fig. 1, 2). The description is divided into an introductory part and three sections providing a summary of the geology in each of the subregions: southern West Greenland, central West Greenland, and northern West Greenland. Finally, a summary of the tectonostratigraphic evolution of the West Greenland margin with correlation to the Canadian margin is presented. Cretaceous and Paleogene successions are described in the most detail reflecting the level of knowledge especially from outcrops along central West Greenland, as they are key successions for understanding the evolution of the margin as a whole.

The West Greenland margin is subdivided based on characteristic elements in the geological evolution and for ease of describing the geology of such a vast area. The boundaries between the three regions are placed along the boundaries of major basins or structures in the offshore and are projected eastward into the onshore areas. The boundary between the southern and central West Greenland margin is the northern boundary of the Sisimiut Basin–Ikermiut Fault Zone projected eastward to the coast at latitude 68°N (Fig. 2). The boundary between the central and northern West Greenland margin is the Upernavik Escarpment–southern boundary of the Upernavik Basin projected eastward to the coast at latitude 73°15′N (Fig. 2). The Greenland sector boundary with Canada including the 200 Nautical Mile (NM) sector limit south of Greenland (Fig. 2) is the western and southern limit of the description and mapping of the West Greenland margin in this paper. This is a national sector boundary and not a geological boundary. For an overview with introduction to all regions described in papers of this volume, please *see* Bingham-Koslowski, Dafoe et al. (this volume).

Previous work

The geological knowledge from the onshore areas of West Greenland rests on more than a century of mapping and studies by numerous expeditions and field trips (e.g. Henriksen et al., 2009). Since the 1970s, the acquisition of seismic data and drilling of exploration wells (*see* e.g. Christiansen, 2011) has promoted ongoing studies of the region and resulted in considerable knowledge of the margin in the offshore.

Some of the key references, which are particularly relevant here, cover a range of topics, e.g. Dawes (1997), Dam et al. (1998a, b, c, 2009), Japsen et al. (2006), Henriksen et al. (2009), Pedersen and Nøhr-Hansen (2014), Sørensen et al. (2017), and Pedersen et al. (2017, 2018). Studies regarding geological and/or geophysical offshore mapping, stratigraphy, and basin evolution include: Rolle (1985), Chalmers et al. (1993, 1995, 1999), Whittaker et al. (1997), Chalmers and Pulvertaft (2001), Christiansen et al. (2001), Skaarup (2001, 2002), Dalhoff et al. (2003, 2006), Larsen and Dalhoff (2006, 2007), Sørensen (2006), Stouge et al. (2007), Døssing (2011), Nielsen et al. (2011), Schenk (2011), Knutsen et al. (2012), Gregersen et al. (2013, 2016, 2018, 2019, U. Gregersen, P.C. Knutz, J.R. Hopper, and H. Nøhr-Hansen, work in progress, 2021), Alsulami et al. (2015), Knutz et al. (2015, 2019, P.C. Knutz, C. Harrison, T. Brent, U. Gregersen, J.R. Hopper, and H. Nøhr-Hansen, work in progress, 2021) and Hofmann et al. (2016, 2018).

Key biostratigraphic studies include: Nøhr-Hansen (2003), Piasecki (2003), Nøhr-Hansen et al. (2016, 2018, 2021), and Sheldon et al. (2018).

Volcanic rocks and their stratigraphy, evolution, and dating were discussed in detail in Clarke and Pedersen (1976), Larsen (1977), Hald and Larsen (1987), Storey et al. (1998), Larsen et al. (1999, 2009, 2016), Larsen and Pulvertaft (2000), Larsen and Pedersen (2009), Nelson et al. (2015), and Pedersen et al. (2017, 2018).

Bojesen-Koefoed et al. (1999, 2004), Bojesen-Koefoed (2011), and Hjuler et al. (2017) have dealt with petroleum systems and source rocks of the region.

Finally, crustal structure and plate reconstructions include studies by: Chian and Louden (1994), Jackson and Reid (1994), Reid and Jackson (1997), Funck et al. (2006, 2007, 2012), Gerlings et al. (2009), Damm (2010), Oakey and Chalmers (2012), Suckro et al. (2012), Hosseinpour et al. (2013), and Altenbernd et al. (2014, 2015, 2016).

Data and methods

The geological and geophysical data used here include released company data and published work, but with a few exceptions specified in each case. Data are from geological and geophysical investigations including geological sampling, drilling, and other fieldwork and operations as described and referenced below. The coverage of seismic and well data is shown in Figure 1. For further information on the seismic data *see* GEUS website (www.geus.dk) and Keen et al. (this volume).

The margin offshore West Greenland is divided into seismic stratigraphic mega-units, and the tectonostratigraphy follows that of Gregersen et al. (2019), which describes the geological history of the region (Fig. 3). The seismic stratigraphy is divided into successions based on the particular architecture and stratal relationships of seismic reflectors (e.g. Payton, 1977), as it is applied to the chronostratigraphy and geology from well ties. Seismic stratigraphic units are further associated with significant tectonic events during the tectonostratigraphic phases (Fig. 3). The mega-units, from the shallowest to the deepest, are labelled as A to H, and are divided by unconformities or correlative conformities at their top from A1 (top of A: seabed) to Hx (top of the acoustic basement). In places where a deep, pre-Cretaceous basin (mainly Ordovician and/or Proterozoic successions) is interpreted, a subunit in the top of mega-unit H is included between horizon H1 and Hx (Fig. 3). The seismic and geological characteristics and well ties associated with the mega-units, their bounding surfaces, and tectonostratigraphy are described below in relation to each of the three subregions of the West Greenland margin.

Regional geology

The West Greenland margin is mainly underlain by continental crust, but to the west it is based by a crustal transition zone and then oceanic crust (Fig. 2). The margin includes a number of sedimentary basins and structures developed since the Proterozoic, but most are Cretaceous to Cenozoic, with these younger successions being related to the opening of the Labrador-Baffin Seaway (Fig. 3) (Gregersen, 2014; Gregersen et al., 2019).

Basement

Prior to rifting between Greenland and North America, the craton underwent a number of orogenic phases during the Archean to Paleoproterozoic, forming mostly east-west oriented sutures and belts (St-Onge et al., 2009). Onshore, the basement in most of West Greenland comprises Archean to Proterozoic crystalline rocks and subordinate Proterozoic metasedimentary and sedimentary rocks (Fig. 2; Henriksen et al., 2009). Following formation of the craton, extension began in the Cretaceous (Roest and Srivastava, 1989) and eventually led to formation of the Labrador–Baffin Seaway. The resulting nature of the underlying crust along the West Greenland margin, including continental crust, crustal transition zones, and oceanic crust in the Labrador Sea, Davis Strait, and Baffin Bay, is described in many studies mostly involving refraction data and in some cases reconstructions (Chian and Louden, 1994; Chalmers and Pulvertaft, 2001; Skaarup, 2001, 2002; Dalhoff et al., 2006; Funck et al., 2007, 2012; Gerlings et al., 2009; Oakey and Chalmers, 2012; Suckro et al., 2012; Hosseinpour et al., 2013; Altenbernd et al., 2014, 2015, 2016). The tectonic evolution of the region is discussed further in Keen et al. (this volume).

Pre-Cretaceous

Some of the oldest known metasedimentary and sedimentary rocks from onshore West Greenland are rocks of the Paleoproterozoic Karrat Group and the Meso- to Neoproterozoic Thule Supergroup (Fig. 3) (*see* 'Central West Greenland basins' and 'Northern West Greenland basins' sections). The Karrat Group (supracrustal rocks) consist of a several kilometre thick metamorphosed sedimentary rock body, including marble, pelite, and quartzite (Henriksen et al., 2009), that has not been sampled offshore.

Figure 1. a) Map of the West Greenland margin described here with the position of wells and released seismic reflection lines (2008 and older). More information on the data is available from the Geological Survey of Denmark and Greenland (https://eng.geus.dk/) and from the Greenland National Petroleum Data Repository (https://greenpetrodata.gl/public/landing/osolanding.html?r=s3/). See Figure 1b for definition of abbreviations.

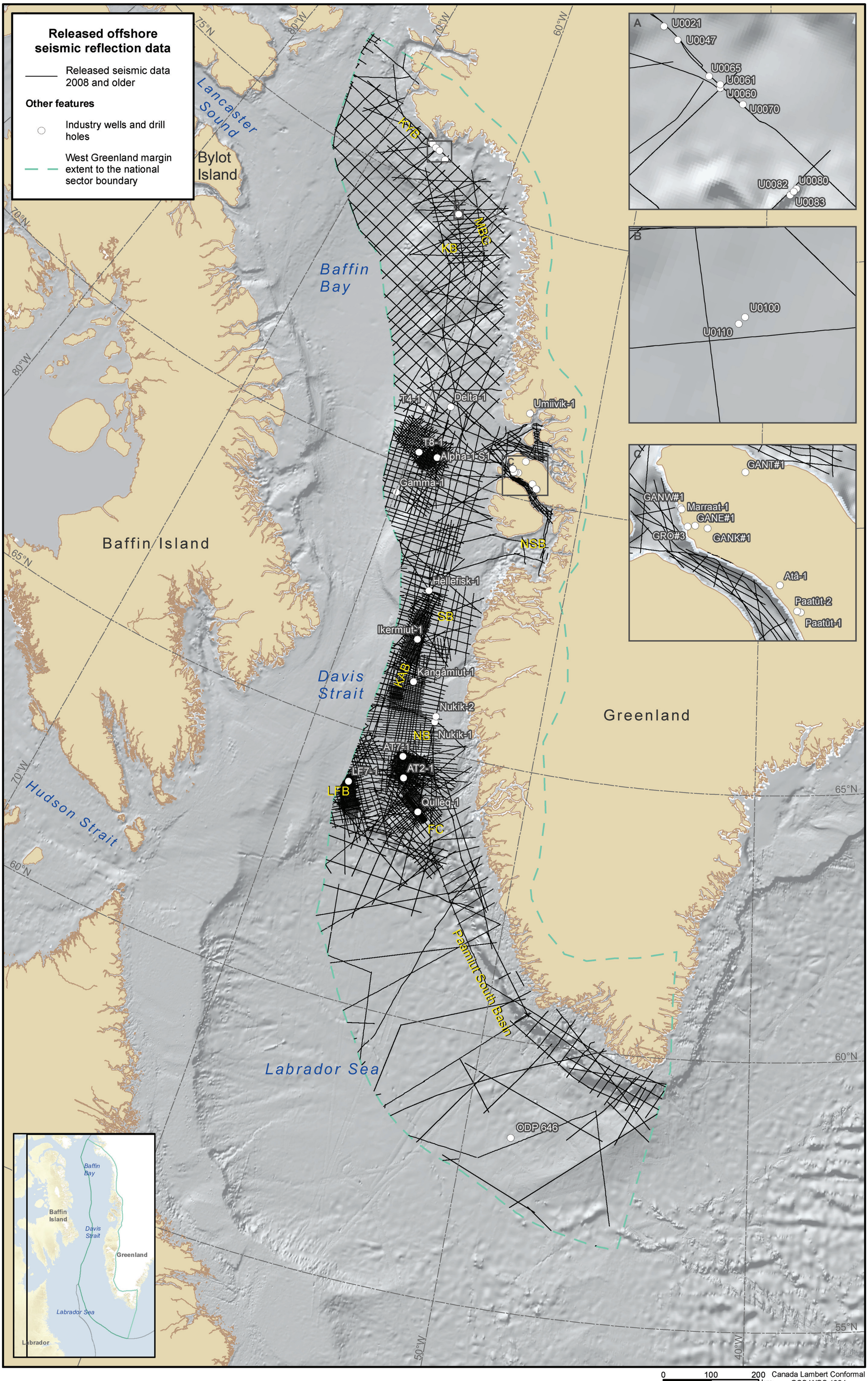
Released offshore seismic reflection data
Released seismic data 2008 and older
Other features
Industry wells and drill holes
West Greenland margin extent to the national sector boundary
Lancaster Sound
Bylot Island
Baffin Bay
Baffin Island
Davis Strait
Hudson Strait
Labrador Sea
Greenland
KYB
NBG
KB
NSB
SB
KAB
NB
LFB
FC
Paamiut South Basin
T4-1
Delta-1
Umiivik-1
T8-1
Alpha-1 S1
Gamma-1
Hellefisk-1
Ikermiut-1
Kangamiut-1
Nukik-2
Nukik-1
AT7-1
AT2-1
LF7-1
Qulleq-1
ODP 646
U0021
U0047
U0065
U0061
U0060
U0070
U0082
U0080
U0083
U0100
U0110
GANT#1
GANW#1
Marraat-1
GANE#1
GRO#3
GANK#1
Atâ-1
Paatût-2
Paatût-1
Labrador
75°N
70°N
65°N
60°N
55°N
80°W
70°W
60°W
50°W
40°W
0 100 200 km
1:7 500 000
Canada Lambert Conformal
GCS WGS 1984

Common legend for abbreviations

Basin names:

FC – Fylla Structural Complex
KAB – Kangâmiut Basin
KB – Kivioq Basin
KYB – Kap York Basin
LFB – Lady Franklin Basin
MBG – Melville Bay Graben
NB – Nuuk Basin
NSB – Nuussuaq Basin
SB – Sisimiut Basin

Geologic structure names:

BFZ – Bower Fracture Zone
CFZ – Cartwright Fracture Zone
FZ – Fracture zone
HFZ – Hudson Fracture Zone
HH – Hecla High
MH – Maniitsoq High
SFZ – Snorri Fracture Zone
UFZ – Ungava Fault Zone

Figure 1. b) Common legend for abbreviations used in Figures 1a, 4, 5, and 6. Note that all the abbreviations may not appear in each of these figures.

The Thule Basin (Fig. 2) comprises Proterozoic sandstone, mudstone, and carbonate and volcanic rocks of the Thule Supergroup (ca. 1270–650 Ma) (Dawes, 1997). Other studies have suggested that kilometres thick successions of the Thule Supergroup also occur in the offshore (Reid and Jackson, 1997; Funck et al., 2006; Gregersen et al., 2013). In 2012, shallow wells recovered such rocks in northeast Baffin Bay (G. Acton, G. Claypool, I. Delusina, G. Dunbar, H. Evans, P. Ferretti, G. Guerin, L. Holloway, S. Ishman, P.C. Knutz, L. Krissek, D. Kulhanek, T.L. Insua, J. Lauren, D. Maloney, D. Naafs, H. Nøhr-Hansen, M. Olney, C. Richter, M. Storms, S. Woodard, and J. Wright, unpub. report, 2012; Nøhr-Hansen et al., 2018, 2021). These rocks were deposited in terrestrial to shallow-marine environments in an intracontinental or continental margin setting (Dawes, 1997). Farther north, lower Paleozoic siliciclastic and carbonate rocks are found onshore north Greenland in the Franklinian Basin, which in the southern part is dominated by shelf to slope deposits and in the northern part by deeper water deposits (Higgins et al., 1991).

Ordovician carbonate rocks are sampled from the seabed in the Davis Strait region and farther east at an onshore location ("Fossilik") (Stouge et al., 2007; Bojesen-Koefoed, 2011). In addition, occurrences of Ordovician sedimentary rocks are known along Eastern Canada (Bingham-Koslowski, McCartney et al., this volume) and north Greenland (Higgins et al., 1991) and indicate widespread basin development during the Ordovician. Reworked Upper Paleozoic and Jurassic palynomorphs from the Qulleq-1 well offshore southern West Greenland (Piasecki, 2003) further indicate pre-Cretaceous deposition, but the present distribution of Paleozoic to Jurassic rocks is unknown.

Late Triassic to Late Jurassic (223–150 Ma) ultramafic, alkaline dykes mark initial Mesozoic extension in southern West Greenland, which was followed by Late Jurassic to Early Cretaceous extensional phases (150 Ma and 140–133 Ma; Larsen et al., 2009). Fission track data suggests that this long-lasting extensional regime was interrupted by two phases of continental uplift in southern West Greenland (ca. 215 ± 5 Ma and ca. 155 ± 5 Ma; Japsen et al., 2006).

Cretaceous to Paleocene

Two regional rift phases separated by periods of tectonic quiescence and subsidence occurred along much of the West Greenland continental margin (Fig. 3). Firstly, Early to mid-Cretaceous rifting (the early rift phase) was followed by thermal basin subsidence during most of the Late Cretaceous with local tectonic episodes. Subsequently, Late Cretaceous–early Paleocene rifting (the late rift phase) took place, intervened by uplift episodes (Whittaker et al., 1997; Chalmers and Pulvertaft, 2001; Dam et al., 2000, 2009; Gregersen et al., 2013, 2018).

Cretaceous to Cenozoic sedimentary siliciclastic successions are known from wells drilled offshore 1976–1977, 2000, and during 2010–2012 and such rocks are also known onshore central West Greenland (*see* detailed descriptions below; Fig. 3, 4, 5, 6).

Lower to mid-Cretaceous successions include continental to marginal marine deposits, grading into Upper Cretaceous marine deposits along much of the West Greenland margin (Fig. 3) (Rolle, 1985; Christiansen et al., 2001; Dam et al., 2009; G. Acton, G. Claypool, I. Delusina, G. Dunbar, H. Evans, P. Ferretti, G. Guerin, L. Holloway, S. Ishman, P.C. Knutz, L. Krissek, D. Kulhanek, T.L. Insua, J. Lauren, D. Maloney, D. Naafs, H. Nøhr-Hansen, M. Olney, C. Richter, M. Storms, S. Woodard, and J. Wright, unpub. report, 2012; Gregersen et al., 2019). The Nuussuaq Basin in central West Greenland contains extensive outcrops of Lower Cretaceous to Paleocene rocks including continental, fluviodeltaic, and marine siliciclastic sediments that constitute the Nuussuaq Group (Fig. 3) (Dam et al., 2009; *see* 'Central West Greenland Basins' section).

Along the northern part of the margin, a consortium of eight companies led by Shell in 2012 drilled shallow coreholes (eleven sites) in northeast Baffin Bay (Fig. 1, 3) and recovered mostly Cretaceous sedimentary rocks (G. Acton, G. Claypool, I. Delusina, G. Dunbar, H. Evans, P. Ferretti, G. Guerin, L. Holloway, S. Ishman, P.C. Knutz, L. Krissek, D. Kulhanek, T.L. Insua, J. Lauren, D. Maloney, D. Naafs, H. Nøhr-Hansen, M. Olney, C. Richter, M. Storms, S. Woodard, and J. Wright, unpub. report, 2012; Nøhr-Hansen et al., 2018, 2021). Farther south, eight exploration wells (drilled 2010–2011) recovered mainly Cretaceous and Cenozoic sedimentary rocks. Two of these wells (Alpha-1 and Delta-1) also recovered Paleogene lava flows (Nelson et al., 2015; Sheldon et al., 2018; Gregersen et al., 2019). The offshore well stratigraphy displays significant hiatuses within the Campanian to Early Paleocene interval (Nøhr-Hansen et al., 2016), likely related to local uplift events with erosion or nondeposition (Fig. 3, *see* below Fig. 12; Gregersen et al., 2018, 2019). The offshore record gaps are partly concomitant with strata discontinuities observed in the Nuussuuaq Basin related to uplift during rifting (Dam et al., 1998a, 2009; Chalmers and Pulvertaft, 2001; *see* Fig. 3)

Paleogene volcanism

The main phase of volcanism on the West Greenland margin commenced in the Danian (at ca. 64 Ma), with additional major volcanic successions developed during the Paleogene (Fig. 2, 3; Larsen et al., 2016). The volcanism in West Greenland is best described from the Nuussuaq Basin (the West Greenland Basalt Group; Clarke and Pedersen, 1976; Larsen et al., 2016; Pedersen et al., 2017, 2018; *see* 'Central West Greenland Basins' section). During the Paleocene and Eocene, flood basalts and other volcanic rocks developed across large parts of the central West Greenland continental margin (Skaarup, 2001; Nelson et al., 2015; Larsen et al., 2016). The onset of volcanism on the West Greenland continental margin is likely connected with the initiation of seafloor spreading (Oakey and Chalmers, 2012; Larsen et al., 2016). Oceanic crust was formed during seafloor spreading in the central parts of the Labrador Sea and Baffin Bay during the Paleocene–Eocene (drift phase), in an initially west-northwest to east-southeast direction (chrons C27n–C25n) and later mainly north-south (chrons C25n–C13n; Oakey and Chalmers, 2012). Seafloor spreading may have started as early as the Maastrichtian in the Labrador Sea (Keen et al., 2018), but was regionally taking place by the Paleocene (Oakey and Chalmers, 2012). These regional drift phase movements caused compression and/or transpression and formation of structural highs, basins, and faults, mostly in the central and northern parts of the West Greenland margin, and some of the structures were reactivated along pre-existing rift structures (Chalmers et al., 1993; Oakey and Chalmers, 2012; Gregersen et al., 2013).

Post-Eocene

The mid- to late Cenozoic development of the West Greenland continental margin was influenced by uplift episodes in central and southern West Greenland during parts of the Oligocene and Miocene–Pliocene (Chalmers, 2000; Japsen et al., 2006; Sørensen, 2006; Knutsen et al., 2012). Cenozoic uplift also occurred in the Melville Bay area (Whittaker et al., 1997; Gregersen et al., 2013). Uplift resulted in extensive erosion of highland and provided sediment sources for deposition in the offshore (Chalmers, 2000; Knutsen et al., 2012; Knutz et al., 2015; P.C. Knutz, C. Harrison, T. Brent, U. Gregersen, J.R. Hopper, and H. Nøhr-Hansen, work in progress, 2021).

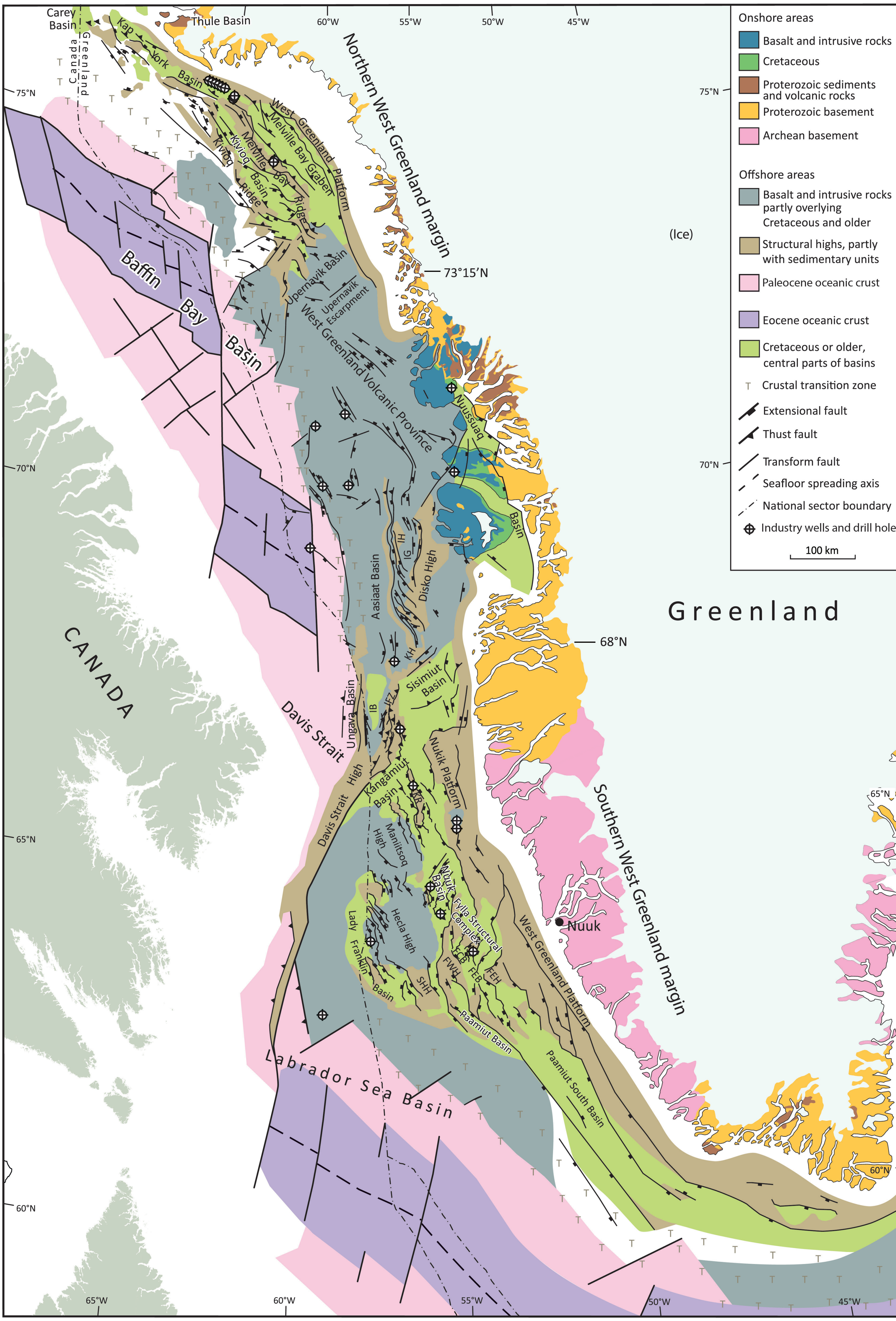

Figure 2. Tectonostratigraphic element map of the West Greenland margin. The map shows the main structural elements and faults, main portions of Cretaceous or older basins, and the extent of Paleogene volcanic cover. The onshore geology is from Henriksen et al. (2009) and the Canadian portion of the oceanic crust is from Oakey and Chalmers (2012). The figure also shows the southern, central, and northern subdivision of the West Greenland margin. Elements of this map are used in the compilation maps of Dafoe, Williams, et al. (this volume) and Keen et al. (this volume). *After* Gregersen et al. (2019).

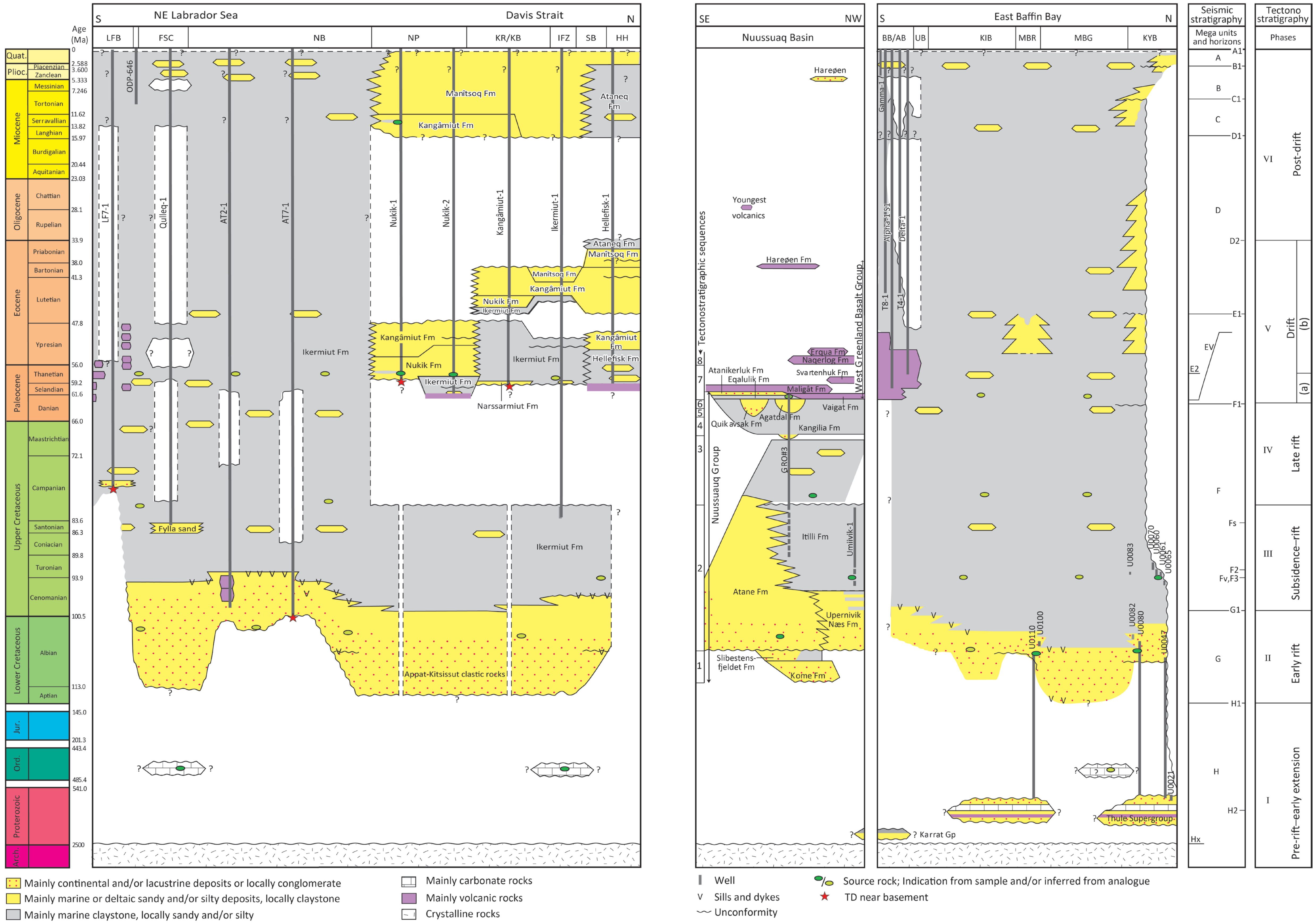
Age (Ma)
Quat.
Plioc.
Piacenzian
Zanclean
Messinian
Tortonian
Serravallian
Langhian
Burdigalian
Aquitanian
Miocene
Chattian
Rupelian
Oligocene
Priabonian
Bartonian
Lutetian
Ypresian
Eocene
Thanetian
Selandian
Danian
Paleocene
Maastrichtian
Campanian
Santonian
Coniacian
Turonian
Cenomanian
Upper Cretaceous
Albian
Aptian
Lower Cretaceous
Jur.
Ord.
Proterozoic
Arch.
0
2.588
3.600
5.333
7.246
11.62
13.82
15.97
20.44
23.03
28.1
33.9
38.0
41.3
47.8
56.0
59.2
61.6
66.0
72.1
83.6
86.3
89.8
93.9
100.5
113.0
145.0
201.3
443.4
485.4
541.0
2500
S
NE Labrador Sea
Davis Strait
N
LFB
FSC
NB
NP
KR/KB
IFZ
SB
HH
ODP-646
LF7-1
Qulleq-1
AT2-1
AT7-1
Nukik-1
Nukik-2
Kangâmiut-1
Ikermiut-1
Hellefisk-1
Manitsoq Fm
Kangâmiut Fm
Ataneq Fm
Manitsoq Fm
Nukik Fm
Ikermiut Fm
Kangâmiut Fm
Hellefisk Fm
Ikermiut Fm
Narssarmiut Fm
Fylla sand
Appat-Kitsissut clastic rocks
SE
NW
Nuussuaq Basin
Hareøen
Youngest volcanics
Hareøen Fm
Tectonostratigraphic sequences
West Greenland Basalt Group
Erqua Fm
Nagerlog Fm
Svartenhuk Fm
Atanikerluk Fm
Eqalulik Fm
Maligât Fm
Vaigat Fm
Agatdal Fm
Quikavsak Fm
Kangilia Fm
Nuussuaq Group
GRO#3
Itilli Fm
Umiivik-1
Atane Fm
Upernivik Næs Fm
Slibestens-fjeldet Fm
Kome Fm
S
East Baffin Bay
N
BB/AB
UB
KIB
MBR
MBG
KYB
Gamma-1
Alpha-1 S1
Delta-1
T8-1
T4-1
U0083
U0070
U0061
U0065
U0082
U0080
U0047
U0110
U0100
U0021
Thule Supergroup
? Karrat Gp
Seismic stratigraphy
Mega units and horizons
A
A1
B1
B
C1
C
D1
D
D2
E1
EV
E2
F1
F
Fs
F2
Fv,F3
G1
G
H1
H
H2
Hx
Tectono stratigraphy
Phases
VI
Post-drift
V
Drift
(b)
(a)
IV
Late rift
III
Subsidence–rift
II
Early rift
I
Pre-rift–early extension
Mainly continental and/or lacustrine deposits or locally conglomerate
Mainly marine or deltaic sandy and/or silty deposits, locally claystone
Mainly marine claystone, locally sandy and/or silty
Mainly carbonate rocks
Mainly volcanic rocks
Crystalline rocks
Well
Sills and dykes
Unconformity
Source rock; Indication from sample and/or inferred from analogue
TD near basement

Figure 3. Stratigraphic summary scheme of West Greenland basins from Archean to present with well positions in the three described regions (*see* text), from south (left) to north (right). The dominant lithology is shown by colours with its main lithostratigraphy. The seismic stratigraphy with mega-units and the tectonostratigraphy divided into phases are shown to the right. *See also* Figure 3 of Gregersen et al. (2019) for more information on this scheme. Abbreviations: LFB = Lady Franklin Basin; FSC = Fylla Structural Complex; NB = Nuuk Basin; NP = Nukik Platform; KR = Kangâmiut Ridge; KB = Kangâmiut Basin; IFZ = Ikermiut Fault Zone; SB = Sisimiut Basin; HH = Hellefisk High; BB = Baffin Bay Basin; AB = Aasiaat Basin; UB = Upernavik Basin; KIB = Kivioq Basin; MBR = Melville Bay Ridge; MBG = Melville Bay Graben; KYB = Kivioq Basin. *Modified from* Gregersen et al. (2019).

During parts of the late Cenozoic, marine contourite drifts and fans were deposited along the southern and northern West Greenland margins (Nielsen et al., 2011). The Pliocene–Pleistocene on the West Greenland margin was dominated by glaciations and glacially induced shelf progradation toward the west and southwest with trough mouth fans, truncation, and incision of major troughs (Knutz et al., 2015, 2019; Hofmann et al., 2016; Slabon et al., 2016).

SOUTHERN WEST GREENLAND BASINS

U. Gregersen, H. Nøhr-Hansen, P.C. Knutz, L.M. Larsen, and J.R. Ineson

The southern West Greenland margin includes the region south of latitude 68°N and from the Sisimiut Basin–Ikermiut Fault Zone (IFZ) and southward (Fig. 7). This margin includes a number of sedimentary basins and structures preserved in both the offshore and onshore.

Pre-Cretaceous

Onshore successions

Archean–Proterozoic

The southern West Greenland onshore mainly consists of Archean (3200–2600 Ma, locally more than 3800 Ma) and Paleoproterozoic (2000–1750 Ma) crystalline basement rocks (Fig. 8) dominated by orthogneiss units with enclaves of granitoid and supracrustal rocks (Henriksen et al., 2009). The principle rock units of West Greenland can be correlated to onshore Eastern Canada, supporting the interpretation that the Precambrian basement of the conjugate margins formed an integral part of the Laurentian shield before the opening of the Labrador–Baffin Seaway (Henriksen et al., 2009; St-Onge et al., 2009). Basement along the central part of the southern West Greenland and parts of eastern Labrador belongs to the same North Atlantic craton composed of Archean crystalline rocks, whereas orogenic belts occur to the north and south (Henriksen et al., 2009; St-Onge et al., 2009). The northern part of south West Greenland was formed during the Nagssugtoqidian Orogeny and comprises Archean rocks, whereas the southernmost part of Greenland was formed during the Ketilidian Orogeny and consists of juvenile Paleoproterozoic gneiss units and granitoid rocks (Henriksen et al., 2009). The crystalline basement is cut by intrusions of different ages, mainly Paleoproterozoic and Mesozoic dykes (Henriksen et al., 2009; Larsen et al., 2009).

The oldest supracrustal rocks include Archean amphibolite and metamorphic rocks of sedimentary origin, including schist, metagreywacke, metacarbonate and/or marble and banded iron-formation of the Isua supracrustal sequence (Nutman et al., 1984; Rosing et al., 1996; Henriksen et al., 2009). Among the best preserved supracrustal sedimentary rocks in the Ketilidian area is an approximately 1200 m thick succession of shale and greywacke with subordinate quartzite, conglomerate, and carbonate rocks of probable Paleoproterozoic age (Vallen Group; Fig. 8), and a thick Mesoproterozoic succession (Eriksfjord Formation) that includes about 1800 m of fluvial and eolian sandstone and conglomerate (Clemmensen, 1988) and volcanic rocks (about 1600 m thick) within an east-northeast–trending continental rift associated with major intrusive complexes (Gardar Province) at approximately latitude 61°N (Henriksen et al., 2009).

Ordovician

The preserved onshore record of Phanerozoic sedimentary rocks along southwest Greenland is very restricted, but an extensive cover probably existed prior to Cenozoic uplift and erosion (Japsen et al., 2006). The oldest preserved Phanerozoic rocks known are Ordovician. Ordovician limestone occurs north of Nuuk at Fossilik (Fig. 9, 10) as blocks in a volcanic ‘fall-back’ breccia within basement gneiss (Secher et al., 2009). Oil stains in the carbonate are indicative of generation from an anoxic source rock (Bojesen-Koefoed, 2011). The limestone clasts yield three discrete conodont assemblages indicative of the late Early–early Middle Ordovician, middle Ordovician, and Late Ordovician ages (Stouge and Peel, 1979; Smith and Bjerreskov, 1994; Fig. 9). Comparable assemblages are reported from offshore dredge samples in the Davis Strait (*see* below; Fig. 9, 10).

Triassic-Jurassic

During the Late Triassic to Late Jurassic (223–150 Ma), ultramafic-alkaline magmas intruded the basement between latitudes 61°24′N and 65°24′N, forming forming small dykes and central intrusions (Larsen et al., 2009; Fig. 11). The magmas were generated in small volumes at great depths, probably at the asthenosphere–lithosphere boundary or in the deep part of the lithosphere. The melting is interpreted to have resulted from incipient lithospheric stretching leading to localized pressure release; at around 150 Ma, a change of melt composition suggests increased extension and thinning of the lithosphere (Larsen et al., 2009). The Fossilik Ordovician carbonate rocks discussed above occur as blocks within a Middle Jurassic diatreme (164.2 ± 1.8 Ma, Secher et al., 2009), emplaced during early rifting. In Labrador, an ultramafic lamprophyric breccia diatreme at Ford’s Bight near Aillik Bay has yielded Early Jurassic to Early Cretaceous microfossils (King and McMillan, 1975). Alkaline dykes in the same area are also Early Cretaceous (Tappe et al., 2007).

Offshore successions

The offshore area southwest and south of Greenland includes large structures and basins, and the margin is drilled by several wells (Fig. 3, 7, 12, 13, 14, 15, 16).

Archean

Archean crystalline basement rocks were recovered from the Nukik Platform (Nukik-1 well; Rolle, 1985). Crystalline basement rocks are also known from the Nuuk Basin, where granite, granodiorite, and tonalite were recovered (AT7-1 well), and from the Lady Franklin Basin (LF7-1 well), where gneiss was drilled (Fig. 3; Capricorn Greenland Exploration (Cairn Energy PLC), unpub. report, 2011; Gregersen et al., 2018). The U-Pb dating of zircon crystals from some of the samples of the AT7-1 well yielded ages of about 3190–2730 Ma, making the rocks comparable in composition and age to the crystalline basement onshore West Greenland (Gregersen et al., 2018). In addition, seabed sampling on the side of the submarine Fylla Canyon west of the Fylla Structural Complex (Fig. 3) recovered Archean gneiss samples (2740 ± 150 Ma) of probable local origin, which are also comparable with the gneiss unit from onshore West Greenland (Dalhoff et al., 2006).

Figure 4. Map showing the extent of Cretaceous successions and wells with Cretaceous rocks along the West Greenland continental margin. The map also shows the confidence level of Cretaceous rocks being present. “Present” indicates a high confidence of Cretaceous successions documented in at least one well or shallow borehole, which ties to seismic correlation within a basin. “Inferred” indicates that Cretaceous rocks are likely to be present, but not confirmed by a well or shallow borehole. White indicates the likely absence of Cretaceous rocks or not drilled. Deeper portions of Cretaceous basins are shown in Figure 2. The map is based on recent work by Gregersen et al. (2018, 2019) and this study. *See* Figure 1b for definition of abbreviations.

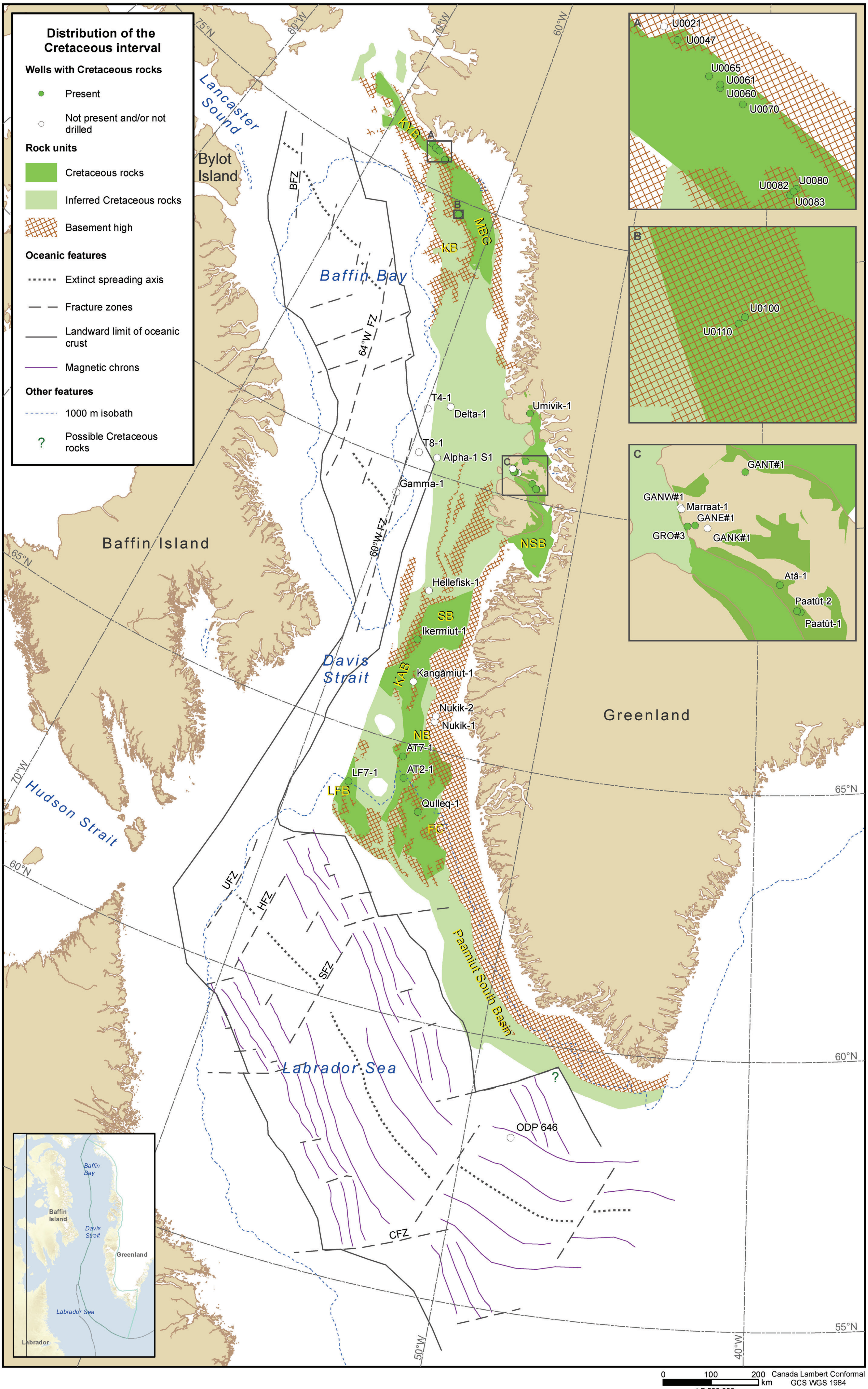
Distribution of the Cretaceous interval
Wells with Cretaceous rocks
Present
Not present and/or not drilled
Rock units
Cretaceous rocks
Inferred Cretaceous rocks
Basement high
Oceanic features
Extinct spreading axis
Fracture zones
Landward limit of oceanic crust
Magnetic chrons
Other features
1000 m isobath
Possible Cretaceous rocks
Lancaster Sound
Bylot Island
Baffin Bay
Baffin Island
Davis Strait
Hudson Strait
Labrador Sea
Greenland
BFZ
64°W FZ
60°W FZ
UFZ
HFZ
SFZ
CFZ
KYB
MBC
KB
NSB
SB
KAB
NB
LFB
FC
Paamiut South Basin
T4-1
Delta-1
T8-1
Alpha-1 S1
Gamma-1
Umivik-1
Hellefisk-1
Ikermiut-1
Kangâmiut-1
Nukik-2
Nukik-1
AT7-1
AT2-1
LF7-1
Qulleq-1
ODP 646
A
U0021
U0047
U0065
U0061
U0060
U0070
U0082
U0080
U0083
B
U0100
U0110
C
GANT#1
GANW#1
Marraat-1
GANE#1
GRO#3
GANK#1
Atâ-1
Paatût-2
Paatût-1
75°N
80°W
70°W
60°W
65°N
60°N
55°N
50°W
40°W
Baffin Bay
Baffin Island
Davis Strait
Greenland
Labrador Sea
Labrador
0 100 200 km
1:7 500 000
Canada Lambert Conformal
GCS WGS 1984

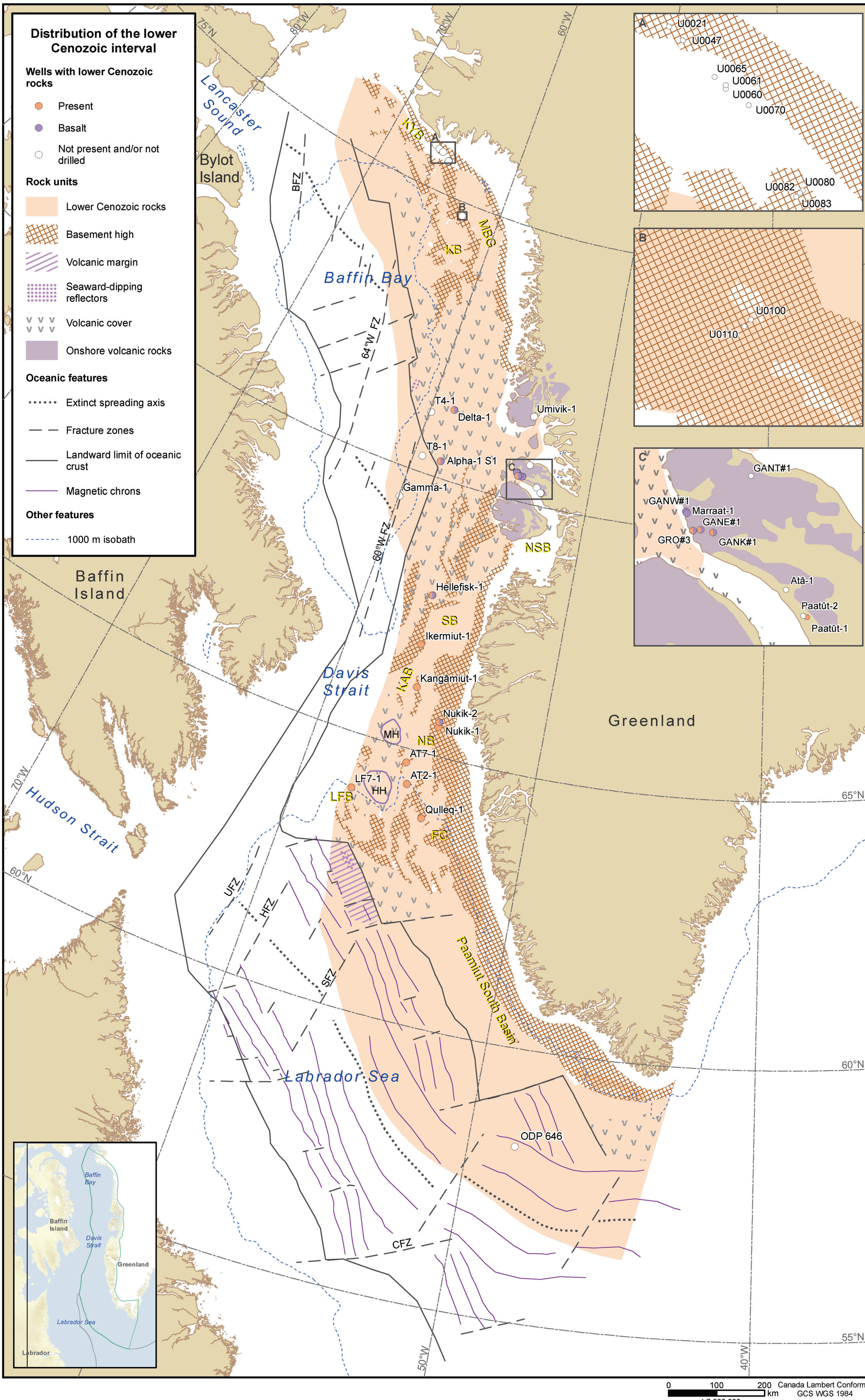

Distribution of the lower Cenozoic interval
Wells with lower Cenozoic rocks
Present
Basalt
Not present and/or not drilled
Rock units
Lower Cenozoic rocks
Basement high
Volcanic margin
Seaward-dipping reflectors
Volcanic cover
Onshore volcanic rocks
Oceanic features
Extinct spreading axis
Fracture zones
Landward limit of oceanic crust
Magnetic chrons
Other features
1000 m isobath
Lancaster Sound
Bylot Island
Baffin Bay
Baffin Island
Davis Strait
Hudson Strait
Labrador Sea
Greenland
Paamiut South Basin
BFZ
64°W FZ
60°W FZ
UFZ
HFZ
SFZ
CFZ
KTB
KB
MBC
NSB
SB
KAB
MH
NB
HH
LFB
FC
T4-1
Delta-1
Umivik-1
T8-1
Alpha-1 S1
Gamma-1
Hellefisk-1
Ikermiut-1
Kangâmiut-1
Nukik-2
Nukik-1
AT7-1
AT2-1
LF7-1
Qulleq-1
ODP 646
U0021
U0047
U0065
U0061
U0060
U0070
U0082
U0080
U0083
U0100
U0110
GANT#1
GANW#1
Marraat-1
GANE#1
GRO#3
GANK#1
Atâ-1
Paatût-2
Paatût-1
75°N
65°N
60°N
55°N
80°W
70°W
60°W
50°W
40°W
0
100
200
km
1:7 500 000
Canada Lambert Conformal
GCS WGS 1984

Figure 5. Map showing the extent of lower Cenozoic successions and wells with lower Cenozoic rocks along the West Greenland continental margin. The map also shows the confidence level of lower Cenozoic rocks being present. "Present" indicates a high confidence of lower Cenozoic successions documented in at least one well or shallow borehole, which ties to seismic correlation within a basin. White indicates the likely absence of lower Cenozoic successions or not drilled. The outline of interpreted areas with volcanic rocks and structural highs from Figure 2 are also shown. The map is based on recent work by Gregersen et al. (2018, 2019) and this study. *See* Figure 1b for definition of abbreviations.

Ordovician

Seabed sampling has revealed examples of Paleozoic strata within the acoustic basement on the Davis Strait High and in the Fylla Canyon (Fig. 3, 7, 10). Dredge samples from the Davis Strait High include Ordovician carbonate rocks that show consistent facies types and stratigraphic ages (Fig. 9, 10), suggesting they are representative of bedrock and correlate with Ordovician records from onshore (Fossilik: Fig. 10; Dalhoff et al., 2006), and with Ordovician carbonate rocks from Canada (Stouge et al., 2007). Ordovician carbonate rocks are known from the Foxe Basin and Ungava Bay–Hudson Strait areas (Bell, 1989; Sanford and Grant, 2000). Ordovician samples were analyzed and documented oil-stained carbonate rocks from the Davis Strait High and a potential source rock from the Fylla Canyon with a Hydrocarbon Index of 400–500 (Fig. 10; Bojesen-Koefoed, 2011).

The eastern Davis Strait High probably consists of continental crust at the boundary of a transform fault zone — the Ungava Fault Zone — as indicated by seismic refraction data (Funck et al., 2012). Seabed samples of tholeiitic basalt flows showing evidence of crustal contamination indicate the presence of continental crust in the Davis Strait High (Dalhoff et al., 2006). Accordingly, the high may be a complex mélange of thrusted continental basement, Paleozoic sediments, Mesozoic sediments, Paleogene basalt flows, and perhaps slivers of oceanic crust from earlier seafloor spreading (Oakey and Chalmers, 2012). Complex structuring may explain the shallow occurrence of Ordovician carbonate rocks sampled by dredging. Similar Paleozoic rocks may be preserved in deeper adjacent basins (as an upper part of mega-unit H) such as at the base of the Sisimiut Basin (Fig. 13; Gregersen et al., 2019).

Jurassic

Evidence of Jurassic strata is very limited in this region. Reworked Middle–Upper Jurassic and Lower Cretaceous palynomorphs were recovered from a gravity core in the seabed on the east flank of the Fylla Canyon (Fig. 7, 16; Dalhoff et al., 2006). Additionally, reworked Upper Paleozoic and Jurassic palynomorphs have also been reported from the Miocene succession in the Qulleq-1 well (Piasecki, 2003).

Seismic stratigraphy

The continental margin offshore southwest Greenland from the seabed to the acoustic basement has been divided into seismic stratigraphic mega-units A–H, mainly based on seismic reflection sections and well data (Gregersen et al., 2018, 2019; Fig. 3). The deepest and oldest mega-unit H is the acoustic basement and is interpreted where the section appears to be acoustically transparent or where there is a loss of seismic resolution, as would be expected for igneous, metasedimentary, or other massive rocks (Fig. 14, 15). Within the acoustic basement, interpretation is hampered or impossible, often due to multiples or other coherent noise. In a few areas (from Kap York Basin to northern Melville Bay Graben and from Sisimiut Basin to Davis Strait High) it has been possible to interpret pre-Cretaceous basins as an upper part of mega-unit H (*see* above) (Fig. 3; Gregersen et al., 2019).

The deep basement along southwest Greenland consists of continental crust along most of the margin, flanked by a transitional zone and oceanic crust more centrally in the Labrador Sea (Fig. 7, 17; Oakey and Chalmers, 2012). A number of seismic refraction studies have also discussed and located the oceanic crust, transition zone, and continental crust (Chian and Louden, 1994; Funck et al., 2007; Gerlings et al., 2009). Additional detail discussing the crustal domains can be found in Keen et al. (this volume).

Based on onshore occurrences and offshore samples the acoustic basement (below horizon Hx) is probably crystalline crust, but upper parts may locally also include pre-Cretaceous metasedimentary rocks or other dense sedimentary rocks, such as the Karrat Group or Paleozoic carbonate rocks (*see* above; Fig. 3, 9, 10, 13).

Cretaceous

Onshore successions

Cretaceous igneous intrusive rocks are known from onshore south West Greenland. Between 140 Ma and 133 Ma (Berriasian to Valanginian), the more than 400 km long south West Greenland dyke swarm (Fig. 11) was emplaced into a coast-parallel, steeply seaward-dipping fracture system, indicating a pronounced stress field and a significant regional stretching and rifting event (Watt, 1969; Larsen et al., 1999, 2009). The basaltic compositions indicate relatively large degrees of melting of asthenospheric mantle. The up to 40 m thick dykes must have fed a succession of lava flows that have been eroded away. The coast-parallel fracture system hosting the dykes mimics the system of parallel faults on the shelf adjacent to the dyke swarm, suggesting that these faults were also initiated around 140 Ma. It is possible that intrusive or extrusive igneous rocks of this age also occur in the offshore areas. The dykes indicate regional rifting in the early part of the Early Cretaceous (Larsen et al., 2009), and are equivalent in age and composition to the volcanic rocks of the Alexis Formation on the conjugate Labrador margin (Williamson et al., 1994).

A camptonite ('wet' alkali basalt) sill in South Greenland was emplaced at 115 Ma, and a 16 km long, coast-parallel phonolite dyke at Frederikshåb Isblink was emplaced at 106 Ma (Larsen et al., 2009) in the later part of the early rift phase.

Offshore successions

Cretaceous sedimentary and igneous successions are known from wells in structures and basins offshore south West Greenland and are included in the seismic mega-units F and G (Fig. 3). The distribution outline of Cretaceous successions offshore West Greenland based on mainly wells and seismic interpretation is shown in Figure 4. The Cretaceous successions are locally some kilometres thick offshore south West Greenland, but are highly variable. The thicknesses of Cretaceous and older successions in deep parts of sedimentary basins are most places in southern West Greenland approximately 2–4 km thick (U. Gregersen, P.C. Knutz, J.R. Hopper, and H. Nøhr-Hansen, work in progress, 2021). The thickest Cretaceous and older successions in sedimentary basins of the West Greenland margin are located in the Nuussuaq Basin and the Melville Bay Graben (*see* 'Central West Greenland Basins' and 'Northern West Greenland Basins' sections below). The thickest Upper Cretaceous succession drilled along the southern West Greenland margin occurs in the AT2-1 well (1702 m) and includes both sedimentary and volcanic rocks; a 1520 m thick sedimentary succession was encountered in the LF7-1 well, and a 1075 m thick sedimentary succession in the Qulleq-1 well (Fig. 12; Christiansen et al., 2001; Capricorn Greenland Exploration (Cairn Energy PLC), unpub. report, 2011; Nøhr-Hansen et al., 2016). The oldest Cretaceous rocks recovered from offshore southern West Greenland are igneous. Basalt dredged from a seamount in the Labrador Sea at latitude 62°50.5′N and dated at 119 Ma (Aptian) may represent an intrusion or lava flow from the offshore or nearby coastal zone (Larsen and Dalhoff, 2006).

Figure 6. Map showing the extent of upper Cenozoic successions and wells with upper Cenozoic rocks along the West Greenland continental margin. The map also shows the confidence level of upper Cenozoic rocks being present. "Present" indicates a high confidence of upper Cenozoic successions documented in at least one well or shallow borehole, which ties to seismic correlation within a basin. The outline of structural highs from Figure 2 are also shown. The map is based on recent work by Gregersen et al. (2018, 2019) and this study. *See* Figure 1b for definition of abbreviations.

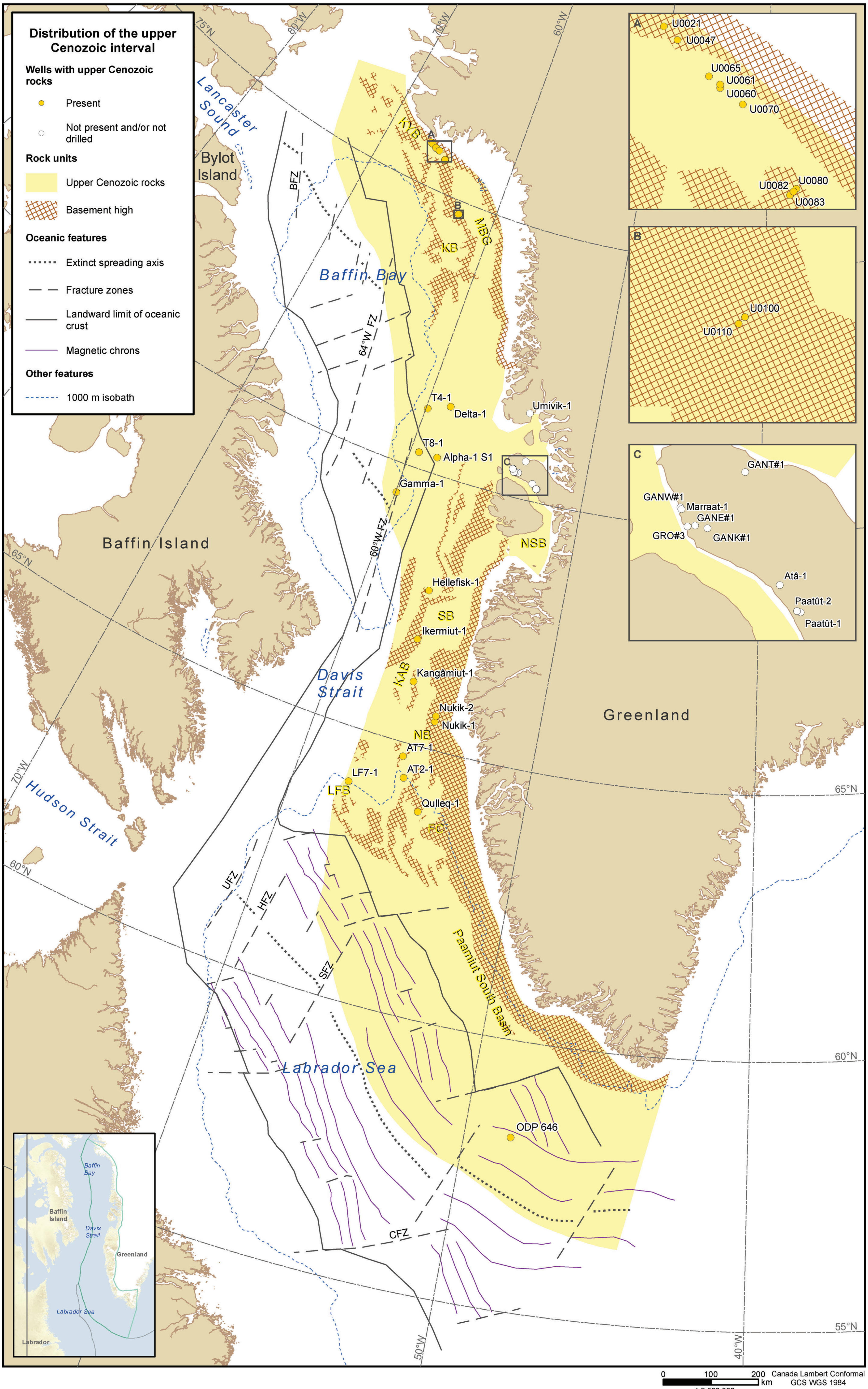
Distribution of the upper Cenozoic interval
Wells with upper Cenozoic rocks
Present
Not present and/or not drilled
Rock units
Upper Cenozoic rocks
Basement high
Oceanic features
Extinct spreading axis
Fracture zones
Landward limit of oceanic crust
Magnetic chrons
Other features
1000 m isobath
Lancaster Sound
Bylot Island
Baffin Bay
Baffin Island
Davis Strait
Hudson Strait
Labrador Sea
Greenland
Paamiut South Basin
BFZ
64°W FZ
60°W FZ
UFZ
HFZ
SFZ
CFZ
KYB
KB
MBG
NSB
SB
KAB
NB
LFB
FC
T4-1
Delta-1
Umivik-1
T8-1
Alpha-1 S1
Gamma-1
Hellefisk-1
Ikermiut-1
Kangâmiut-1
Nukik-2
Nukik-1
AT7-1
AT2-1
LF7-1
Qulleq-1
ODP 646
A
U0021
U0047
U0065
U0061
U0060
U0070
U0082
U0080
U0083
B
U0100
U0110
C
GANT#1
GANW#1
Marraat-1
GANE#1
GRO#3
GANK#1
Atâ-1
Paatût-2
Paatût-1
75°N
80°W
70°W
60°W
65°N
60°N
55°N
50°W
40°W
Baffin Bay
Baffin Island
Davis Strait
Greenland
Labrador Sea
Labrador
0
100
200
km
1:7 500 000
Canada Lambert Conformal
GCS WGS 1984

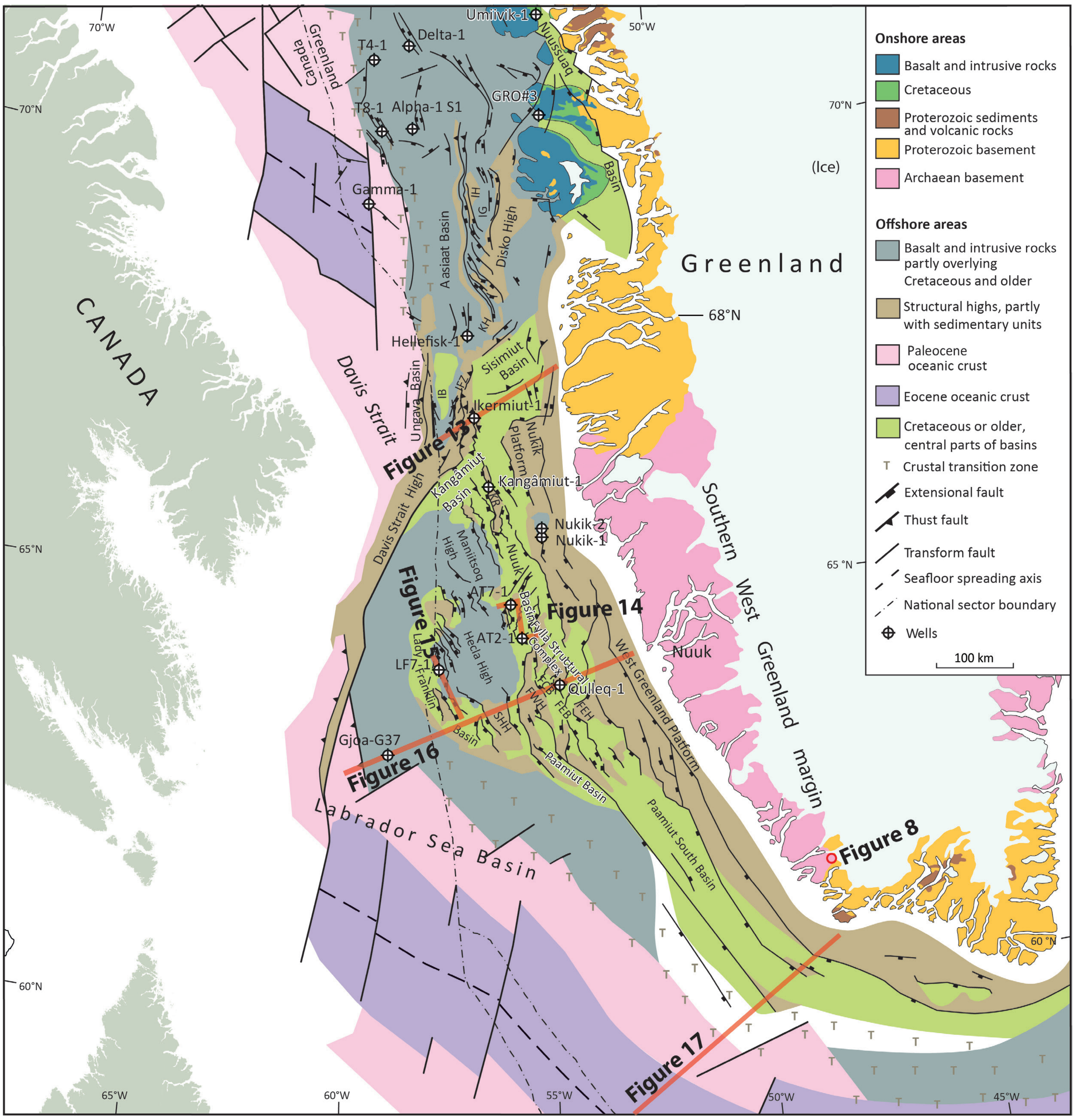

Figure 7. Tectonostratigraphic elements map of southern West Greenland. The location of Figure 8 is shown by a red circle, and geological sections in Figures 13–17 are shown by red lines. From the southern part of Figure 2.

Figure 8. Photograph showing the basal part of the Ketilidian supracrustal succession in southern West Greenland (central Grænseland), looking north and modified from Henriksen et al. (2009). The grey Archean basement gneiss units in the upper left of the image are overlain by Paleoproterozic metasedimentary rocks of the Vallen Group dipping 25° to the right. The unconformity is indicated by the dashed red line; the red-brown staining of the uppermost Archean represents the weathered regolith beneath the unconformity. The location of the photograph is shown in Figure 7. Photograph by A.A. Garde, 1997.

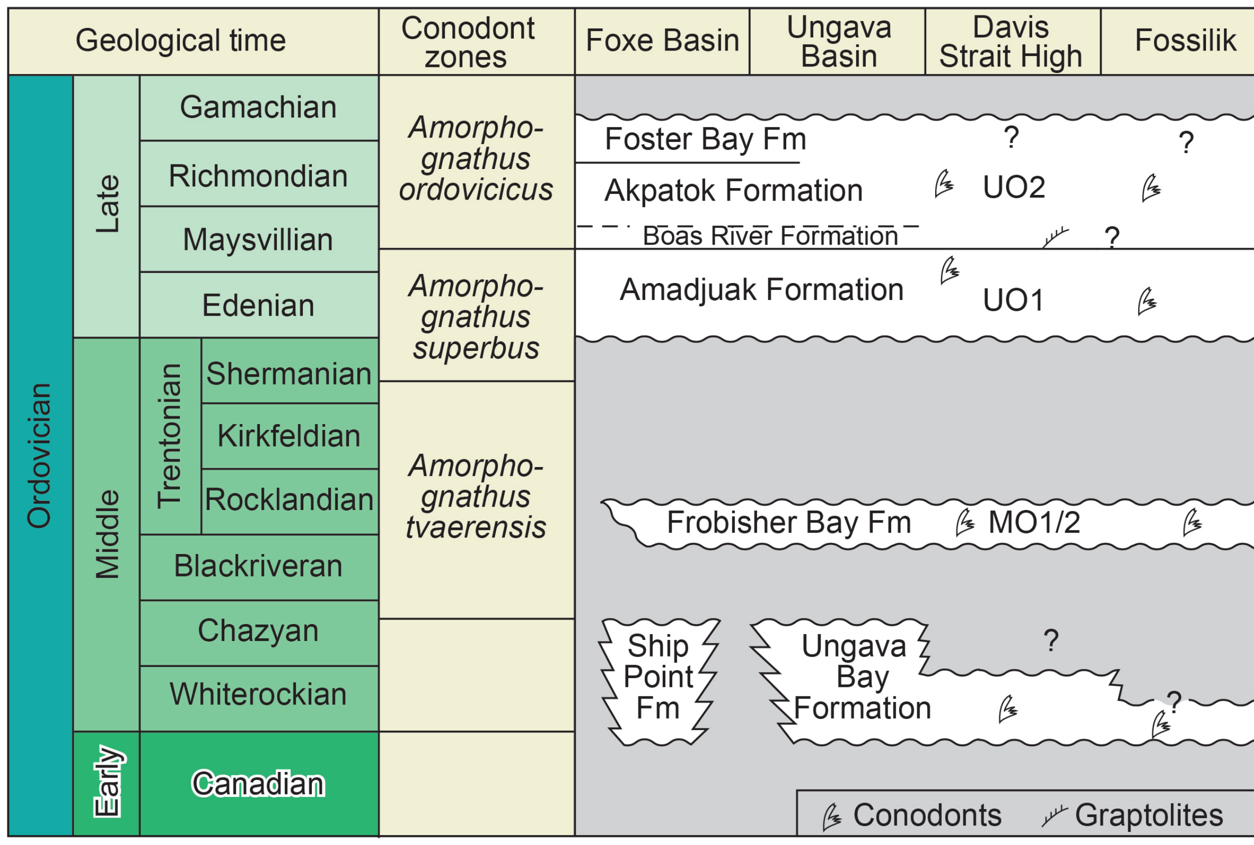

Figure 9. Stratigraphic correlation scheme of Ordovician strata from the West Greenland margin (Davis Strait High and Fossilik) and Eastern Canada (Foxe Basin, Ungava Basin) from Stouge et al. (2007). MO1/2 = Middle Ordovician conodont assemblages 1 and 2 of Stouge et al. (2007); UO1, UO2 = Upper Ordovician conodont assemblages 1, and 2 of Stouge et al. (2007).

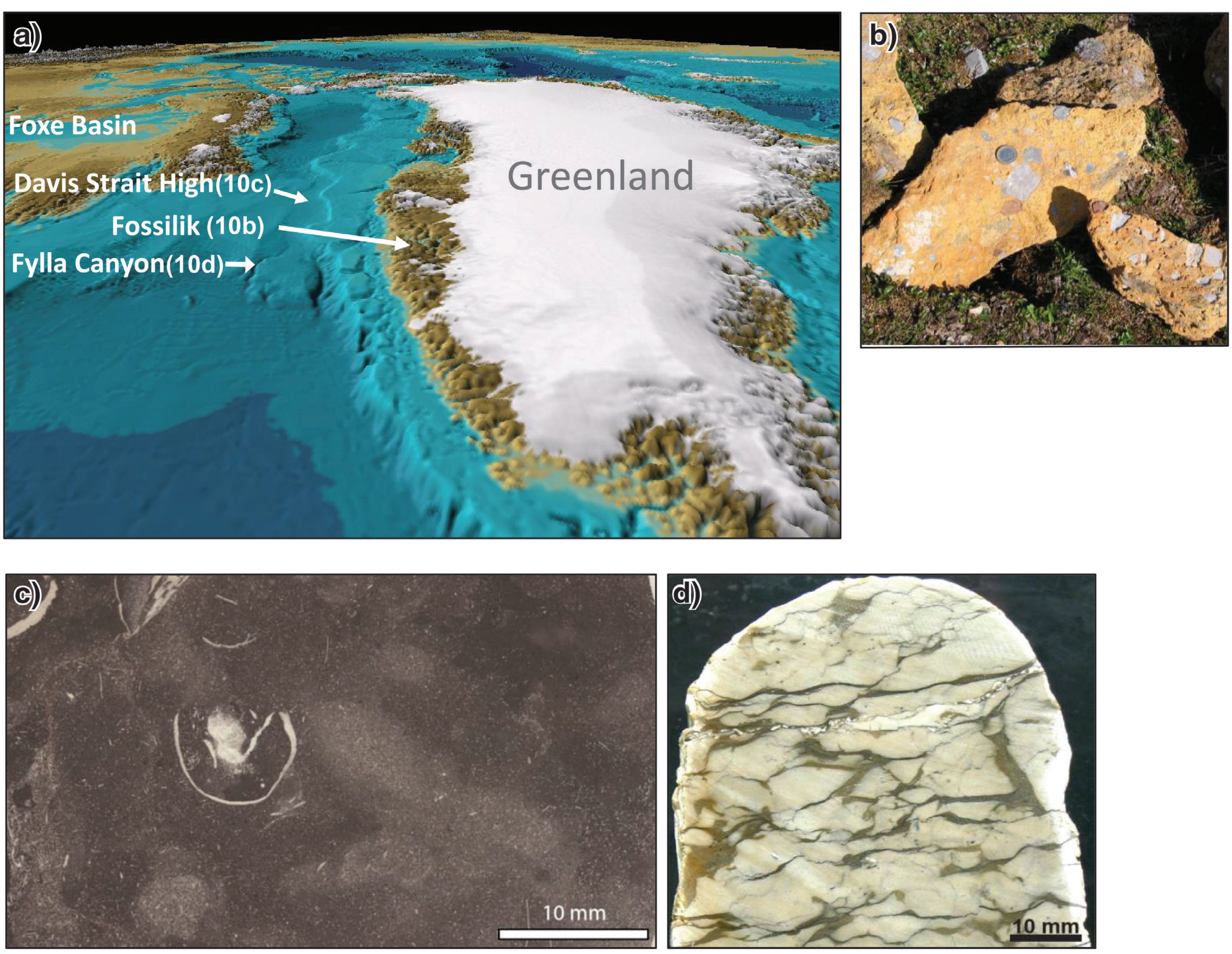

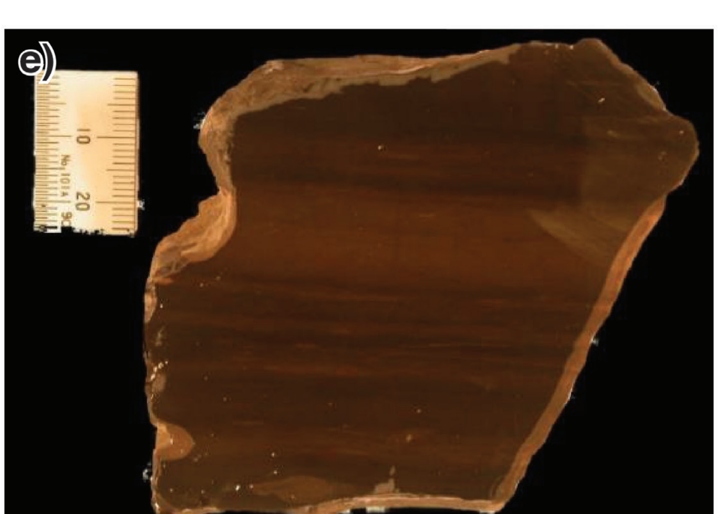

Figure 10. Ordovician carbonate rocks from the southern West Greenland margin. **a)** Location of samples illustrated in Figures 10b–d (Bojesen-Koefoed, 2011). **b)** Fossilik breccia: angular blocks of grey Ordovician limestone within a brown (dolomitic) tuff matrix; one euro coin (1.6 cm diameter) for scale. Photograph by K. Secher, 2004. **c), d)** Ordovician dredge samples from the Davis Strait High are dominated by lime mudstone and skeletal wackestone. Polished slab (d) shows the nodular, burrow-mottled character and dark argillaceous solution seams. Photograph by J. Boserup, 2006. Thin section (c) illustrates a burrow-mottled skeletal wackestone fabric with coarser skeletal brachiopod fragments (Stouge et al., 2007). **e)** Ordovician seabed sample from the Fylla Canyon on the west flank of the Fylla Structural Complex (Fig. 16). It shows dark, laminated carbonate with a high organic content, representing a good oil-prone source rock; scale is in millimetres (Bojesen-Koefoed, 2011).

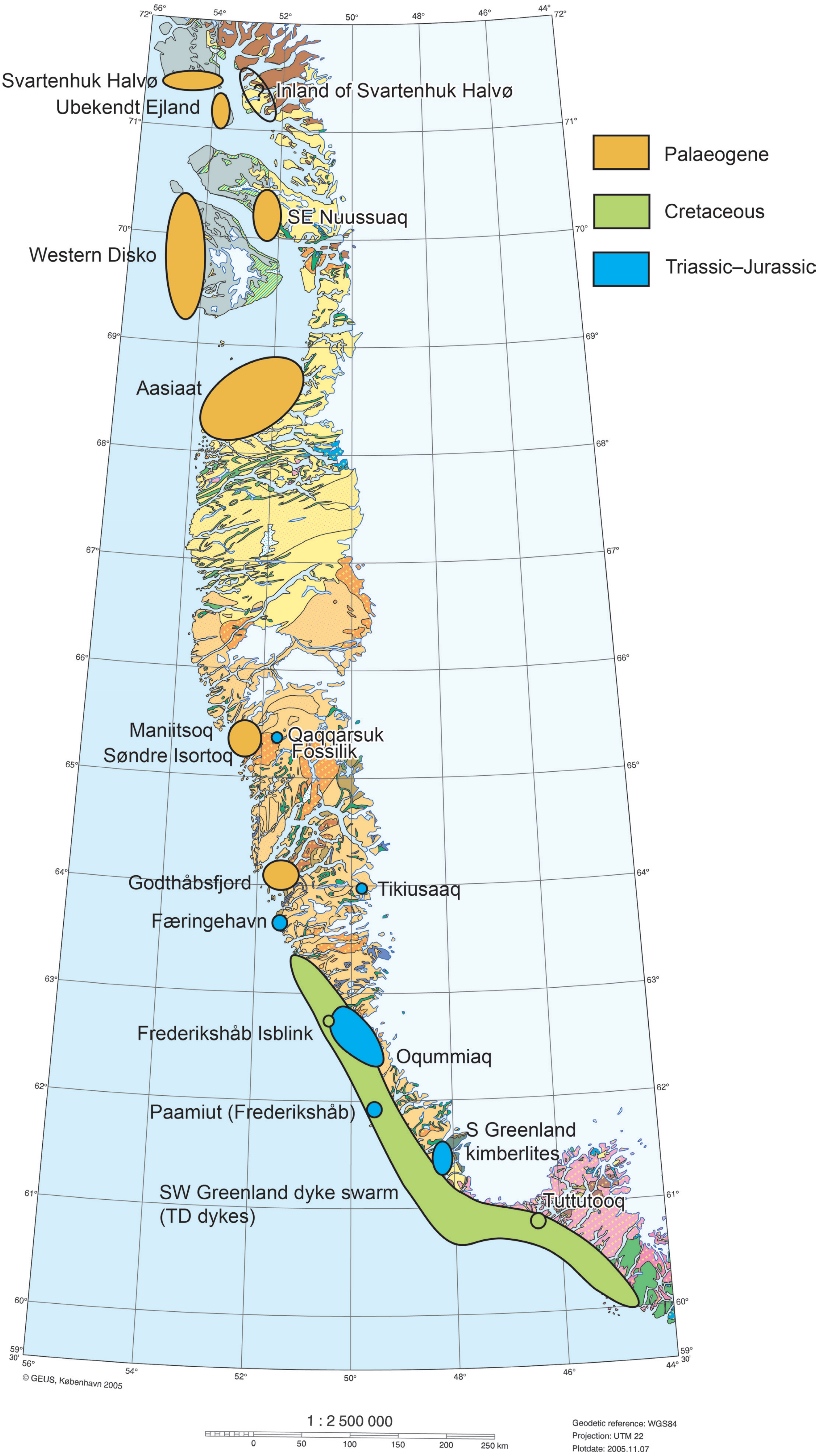

Figure 11. Map showing the extent and ages of dykes along the West Greenland margin (latitude 60°–72°N) (Larsen, 2006).

Lithostratigraphy

The Appat-Kitsissut clastic unit

The Appat-Kitsissut clastic unit is a thick Early- to mid-Cretaceous succession (Gregersen et al., 2018, 2019) and is dominated by conglomerate and sandstone that is drilled in the lower part of the AT7-1 well above crystalline basement in the Nuuk Basin (Capricorn Greenland Exploration (Cairn Energy PLC), unpub. report, 2011; Gregersen et al., 2018; Fig. 3, 14).

The lower part of the clastic unit is about 200 m thick and includes a succession of (?)upper Albian–(?)Cenomanian conglomerate with weathered basement fragments, sandstone, and thin claystone. It ties to mega-unit G below horizon G1 (at 2782 m) (Fig. 3, 14; Gregersen et al., 2018). Upper part of the clastic rocks is a less than 100 m thick sandstone-dominated succession with thin claystone and correlates with the lower part of mega-unit F and is (?)Cenomanian–(?)Turonian (Fig. 3).

The Fylla sandstone unit

A thick upper Santonian sandstone dominated succession (323 m thick) is known from the lower part of the Qulleq-1 well in the Fylla Structural Complex (Fig. 3, 12 and 16) (Christiansen et al., 2001; Nøhr-Hansen et al., 2016). This Fylla sandstone unit was mapped by Sørensen (2006) on large parts of the south West Greenland margin. Upper Santonian sandstone units have not been recovered from the more recent wells (Fig. 3). A study of the zircon provenance of Cretaceous and Paleogene sandstone units in the Nuussuaq Basin and in the Hellefisk-1 and Qulleq-1 wells (Scherstén and Sønderholm, 2007) concluded that the sediment was derived primarily from the West Greenland Archean crystalline basement. Two discrete Proterozoic zircon populations were recorded in the Fylla sandstone of the Qulleq-1 well, however, indicating episodic sediment supply probably from Labrador and/or East Greenland.

Ikermiut Formation

Upper Cretaceous to Paleogene claystone-dominated marine successions are widely represented in the region (Fig. 3) and belong to the Ikermiut Formation defined in the Ikermiut-1 well (Rolle, 1985). It is the oldest formally defined formation offshore West Greenland. The age of the Ikermiut Formation is Late Cretaceous (early Campanian) to middle Eocene (Nøhr-Hansen et al., 2016) and is at least 2085 m thick (drilled to TD) in the type well Ikermiut-1 (Fig. 12), where it correlates with seismic mega-units F and E, but it probably thickens into depocentres such as the Sisimiut Basin (Fig. 13). It is composed of carbonaceous marine mudstone units, which are dark and generally organic-rich in the lower (Cretaceous) parts of the formation. Thus, it shows an upward decrease in organic content and increase in thin, fine-grained sandstone and siltstone units. Thin hyaloclastic beds and volcanic fragments also occur locally in the Paleocene (Nukik-2 well). The formation is similar to the Itilli Formation of the Nuussuaq Basin (Dam et al., 2009) and could be as old (*see* 'Central West Greenland Basins' section). The formation is also similar to the Markland and Cartwright formations on the Labrador Shelf (Umpleby, 1979; McWhae et al., 1980; Rolle, 1985).

Claystone-dominated successions have also been drilled in structures of the Lady Franklin Basin (LF7-1 well: Campanian–Maastrichtian; Gregersen et al., 2018), the Nuuk Basin (AT2-1 well: Turonian–Campanian; AT7-1 well: Cenomanian–Turonian to Coniacian; Gregersen et al., 2018), the Fylla Structural Complex (Qulleq-1 well: Lower Campanian; Christiansen et al., 2001; Nøhr-Hansen et al., 2016), and in the Ikermiut Fault Zone in the Ikermiut Basin (Ikermiut-1 well: Lower Campanian; Rolle, 1985; Nøhr-Hansen et al., 2016) (Fig. 12).

The youngest known Cretaceous sedimentary rocks offshore are Maastrichtian marine mudstone units encountered in the LF7-1 well, with a bathyal microfossil fauna of agglutinating foraminifera (Sheldon et al., 2018). The LF7-1 well seems to record a thick upper Campanian, lower- and upper Maastrichtian and Danian mudstone succession (Fig. 15; Gregersen et al., 2018) that probably all belongs to the Ikermiut Formation (Fig. 3).

In addition to the wells, seabed samples recovered by GEUS in 2004–2006 and analyzed biostratigraphically (palynology and micropaleontology) demonstrate Upper Cretaceous sediments over some of the basins and structures offshore south West Greenland, including the Davis Strait High and seamounts west of Nuuk (Dalhoff et al., 2006, F. Dalhoff, J.A. Bojesen-Koefoed, L.M. Larsen, J.R. Ineson, S. Stouge, H. Nøhr-Hansen, E. Sheldon, and F.G. Christiansen, Geological Survey of Denmark and Greenland, unpub. report, 2008). These seabed samples are probably mostly transported (i.e. ice rafted); although some may have been derived from local seafloor exposures at highs and canyons. Such places include the Davis Strait High, that were thrusted and/or uplifted in the Paleogene, and uplifted and/or rifted flanks of structural highs, such as at the Fylla Canyon at the western Fylla Structural Complex (Fig. 10, 13, 16).

Seismic stratigraphy

Mega-units G and F are of Early to mid-Cretaceous and Late Cretaceous to early Paleocene age, respectively, and occur across large areas of the West Greenland continental margin, except for over eroded structural highs and volcanic centres (Fig. 3, 4, 7). The thickness of the Lower Cretaceous (mega-unit G) is uncertain, but probably reaches a kilometre or more in the deepest basins such as the Kangâmiut and Sisimiut basins (Fig. 13). The Upper Cretaceous to Paleocene mega-unit F includes strata up to approximately 2–3 km thick in the depocentres of the Lady Franklin Basin (Fig. 15) and in basins mainly in eastern and southern parts of the Fylla Structural Complex (Fig. 16), whereas thicknesses are generally less in the Nuuk Basin (Fig. 14).

Large rift structures with local wedge-shaped units illustrating growth along extensional faults developed during the Early to mid-Cretaceous within mega-unit G (Fig. 13, 14, 15, 16, 17). This mega-unit ties with the Appat-Kitsissut clastic unit in the lower part of the AT7-1 well in the Nuuk Basin (Fig. 3, 14; Gregersen et al., 2018).

The AT2-1 well intersected a structure below seismic horizon Fv in the lowermost part of mega-unit F with a volcanic-dominated succession (Fig. 14; Gregersen et al., 2018). This approximately 1.2 km thick succession of the Atammik Volcano comprises volcaniclastic conglomerate and alkaline volcanic rocks of 98–93 Ma age from radiometric (U-Pb) zircon age dating (Knudsen et al., 2020).

Strong, bowl- or V-shaped seismic reflections occur mostly in the upper parts of mega-unit G, but also in the lowermost parts of mega-unit F (in mid-Cretaceous strata) and are mapped in connection with the eastern and southern part of the volcanic Maniitsoq and Hecla highs and the Nuuk and Lady Franklin basins between about latitude 63°N–66°N (Fig. 14; Gregersen et al., 2018). These features crosscut the generally more concordant seismic reflections reflecting the sedimentary infill. They are interpreted as volcanic intrusions (mainly sills) forming part of a larger intrusion complex — the Atammik sill complex — in the Nuuk and Lady Franklin basins. The sills probably formed below thick sedimentary successions during major regional Paleogene volcanism, which also formed the volcanic successions on the Maniitsoq, Hecla, and Gjoa highs, and which is documented in the Hellefisk-1, Nukik-2, and Gjoa-G37 wells (*see* below).

The lower part of mega-unit F shows local large variations in thickness, seismic reflectivity, continuity, and amplitude, whereas the upper part of the unit is typically more uniform. The lower part of mega-unit F is correlated with the AT7-1 well, where it is dominated by sandstone, conglomerate, and subordinate claystone of (?)Cenomanian–(?)Turonian age (Gregersen et al., 2018). This succession is overlain by a thicker Cenomanian–Turonian to Coniacian claystone-dominated interval (Fig. 3; Gregersen et al., 2018). Most of mega-unit F is characterized by successions with conformable, continuous reflections, which correlate to mudstone-dominated intervals such as in the LF7-1 and Qulleq-1 wells (Fig. 12, 15, 16). Mounded reflections, within the upper part of the unit, are interpreted as mass-transport complexes including submarine fans and turbidite units, whereas trough-like features may represent incised canyons or major channels (e.g. Fig. 14, 15: southeast of the Hecla High).

Early Cenozoic

Onshore successions

No sedimentary rocks of early Cenozoic age are known from onshore areas of southern West Greenland. Samples of Cenozoic igneous rocks have been obtained from dykes in south West Greenland (Fig. 11): a coast-parallel basalt dyke at latitude 66°27′N has an age of 64.0 ± 1.3 Ma (Larsen et al., 2009).

Offshore successions

Paleogene sedimentary and igneous successions are known from wells west of Greenland and are included in mega-unit E and the lower part of mega-unit D (Fig. 3). The distribution of lower Cenozoic successions offshore West Greenland based on mainly wells and seismic interpretation outlined here is shown in Figure 5.

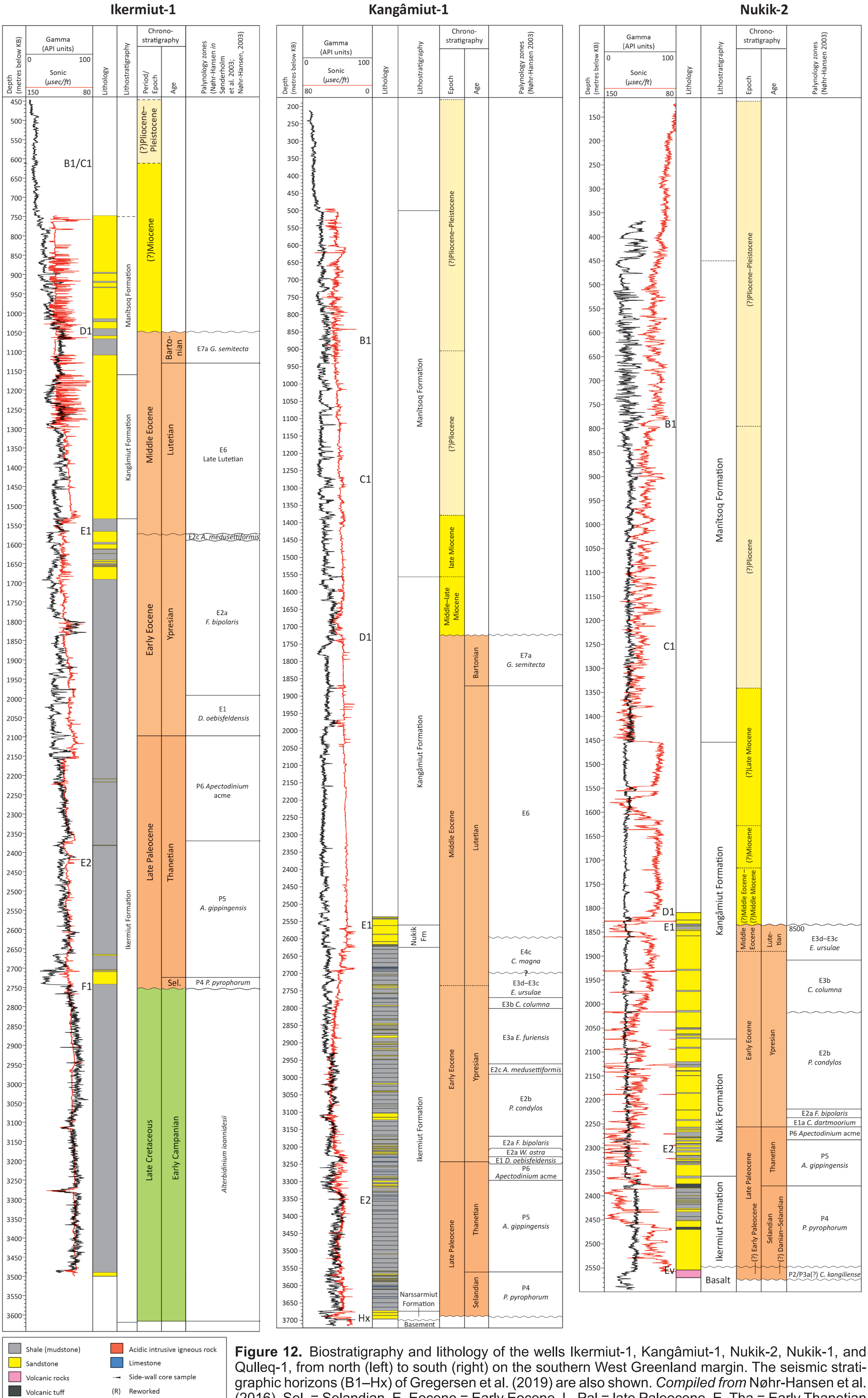

Figure 12. Biostratigraphy and lithology of the wells Ikermiut-1, Kangâmiut-1, Nukik-2, Nukik-1, and Qulleq-1, from north (left) to south (right) on the southern West Greenland margin. The seismic stratigraphic horizons (B1–Hx) of Gregersen et al. (2019) are also shown. *Compiled from* Nøhr-Hansen et al. (2016). Sel. = Selandian, E. Eocene = Early Eocene, L. Pal = late Paleocene, E. Tha = Early Thanetian

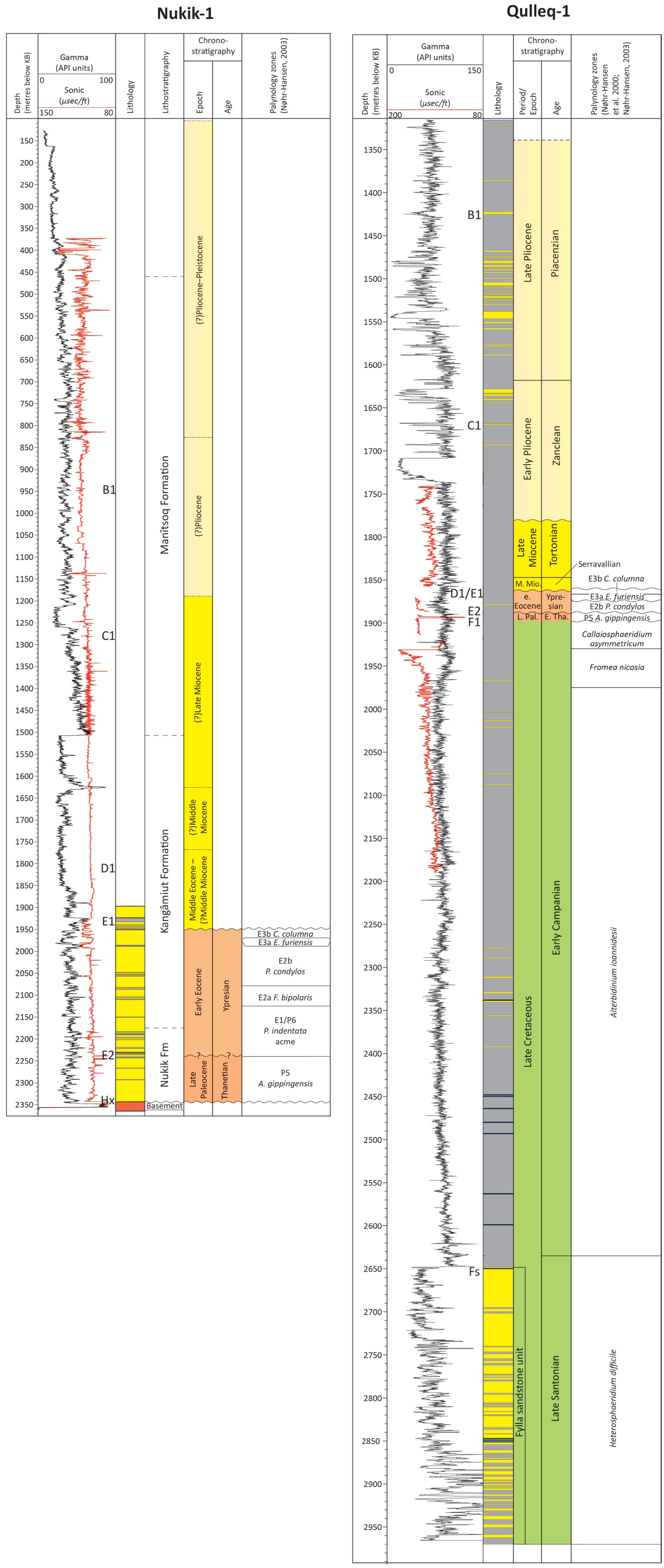

Figure 12. (cont.)

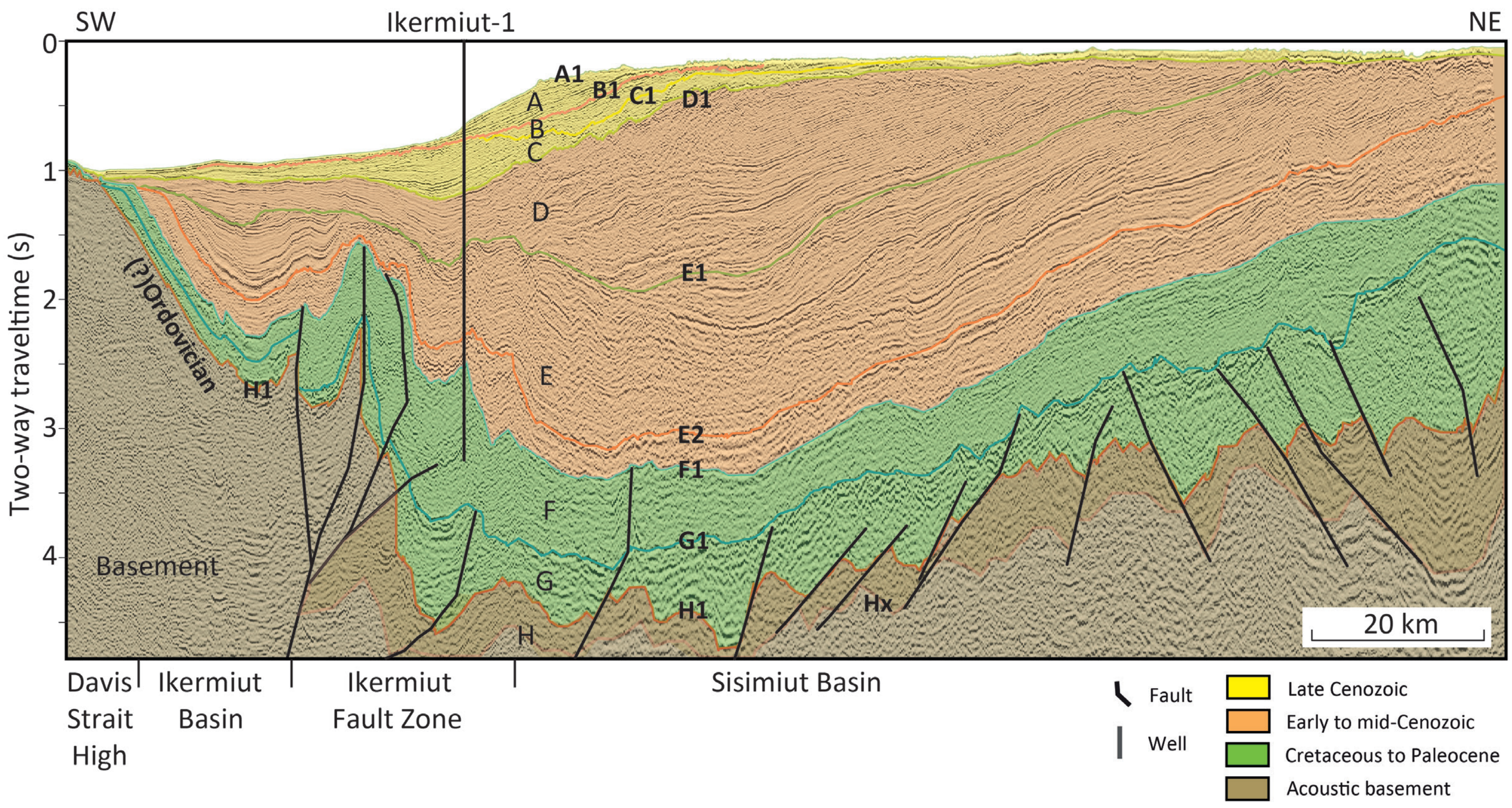

Figure 13. A northeast-southwest geosection through the Davis Strait area intersecting the Ikermiut-1 well. Deep pre-Cretaceous successions below horizon H1, probably including Ordovician rocks, unconformably overlain by Early- to mid-Cretaceous strata of mega-unit G. Upper Cretaceous and Cenozoic marine sedimentary successions are drilled by the Ikermiut-1 well (mega-units A–F). Cretaceous and older sections form parts of structural ridges due to compression and/or transpression in the early Cenozoic. Late Cenozoic successions (units A–D) show minor shelf progradation toward the southwest. The location of the section is shown in Figure 7. Gregersen et al. (2019); the shown reprocessed seismic line (GGU1990-06RE) is courtesy of Spectrum Geo Ltd.

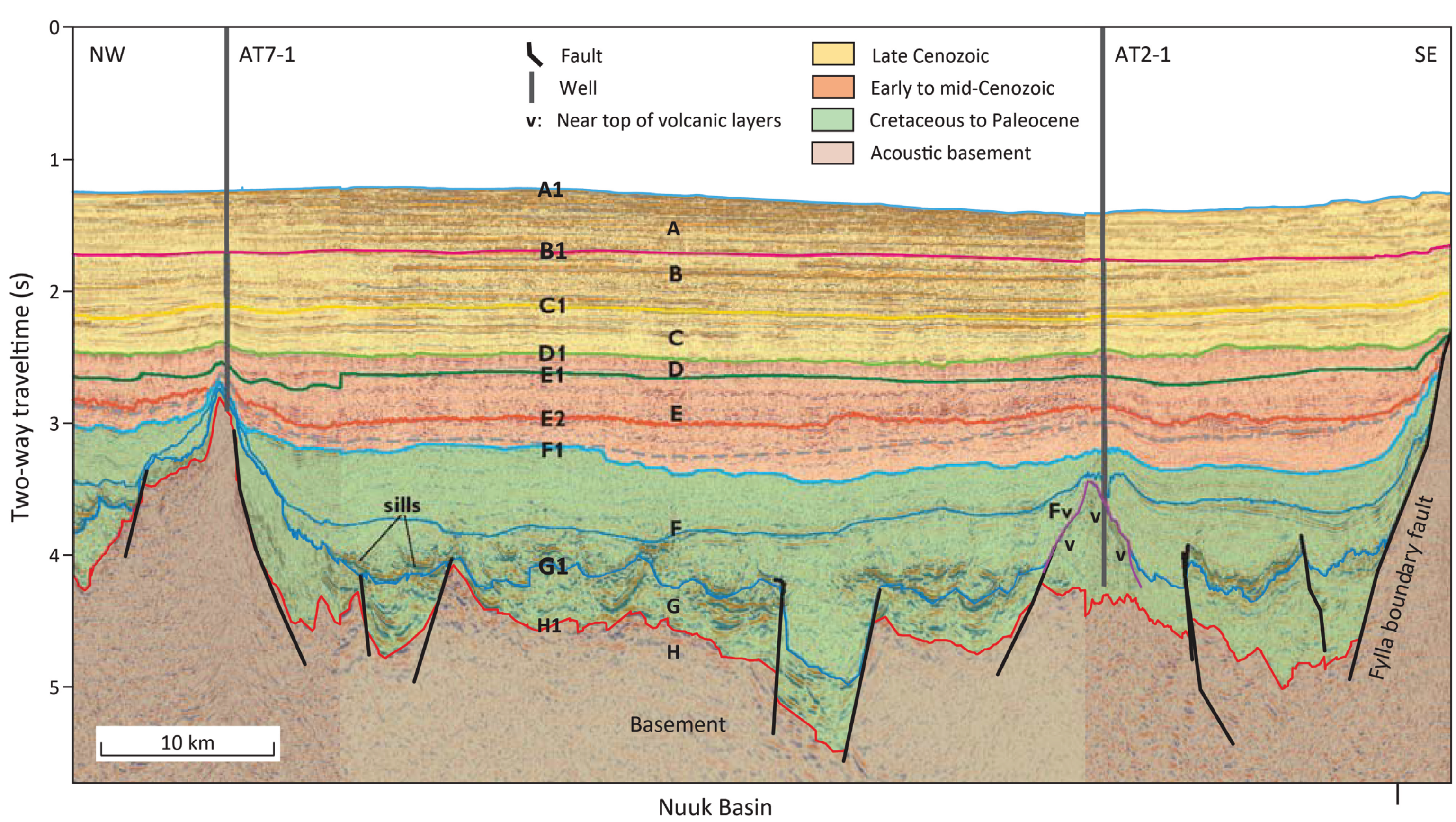

Figure 14. Composite northwest-southeast section across the Nuuk Basin showing large structures and the AT2-1 and AT7-1 wells. The succession from the seabed to the basement is divided using seismic stratigraphic horizons A1–H1 into seismic mega-units A–H; tentative ages (maximum timespans) of the major successions are shown in colour. The deeper parts of the section are dominated by a Cretaceous sedimentary succession in rifted basins, and by a local volcanic succession and sills. The location of the section is shown in Figure 7 (Gregersen et al., 2018). Seismic data courtesy of TGS.

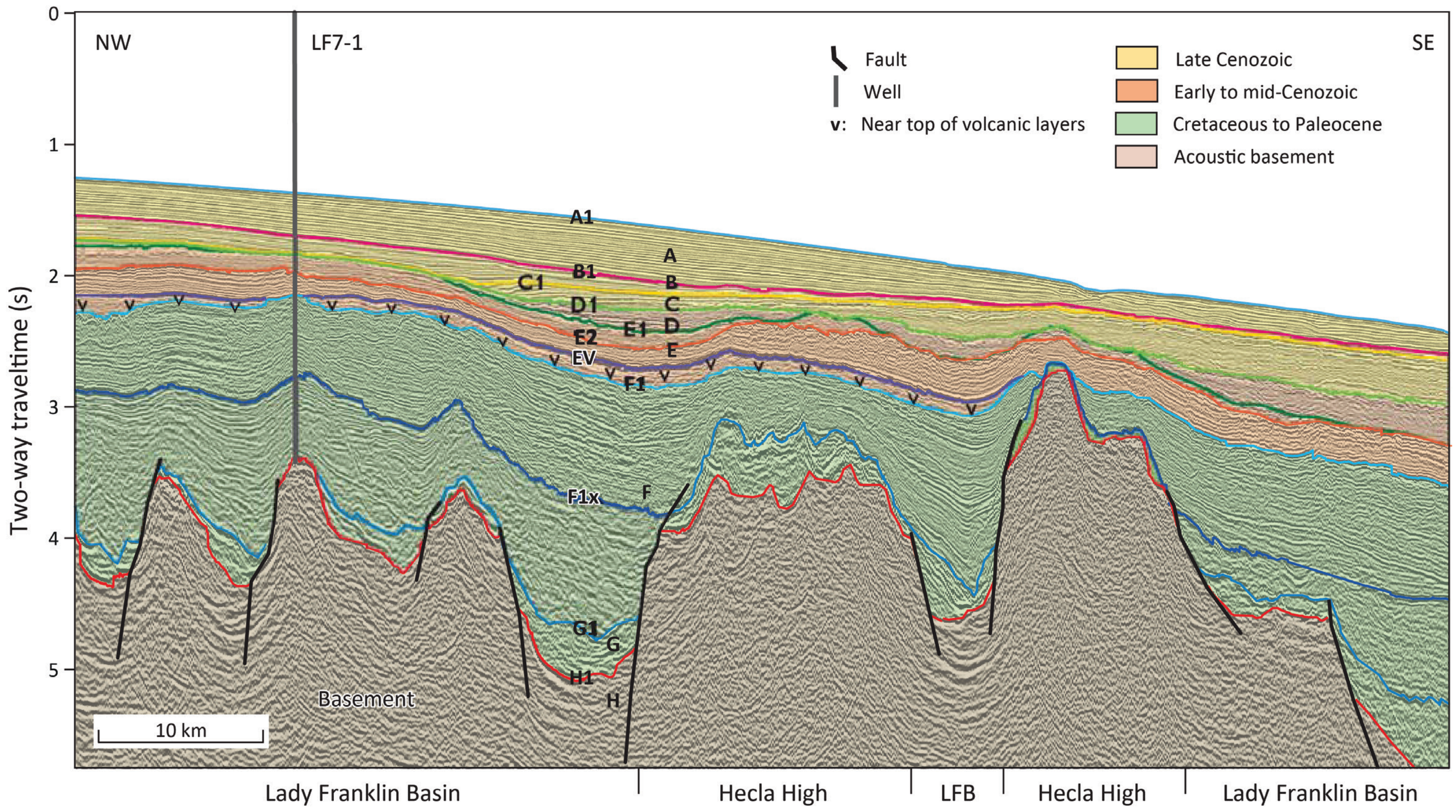

Figure 15. A composite northwest-southeast section across the Lady Franklin Basin (LFB), intersecting the LF7-1 well. It is dominated by Cretaceous successions (units F and G) and includes rifted structures with fault blocks. A thin Paleogene volcanic succession overlies the Cretaceous–Paleocene sedimentary succession (unit F). A Miocene–Pliocene contourite succession (within mega-units B and C) occurs southeast of the LF7-1 well. *See* Figure 14 for legend. The location of the section is shown in Figure 7 (Gregersen et al., 2018). Seismic data courtesy of TGS.

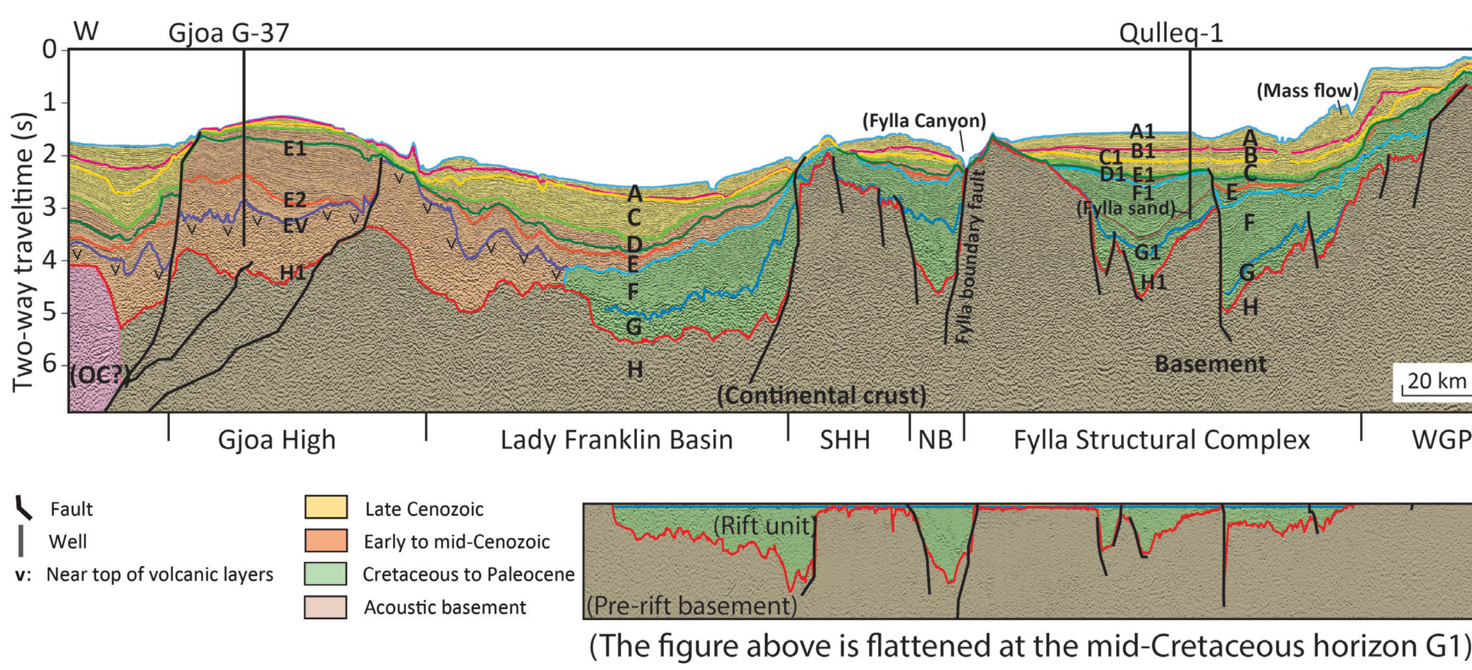

Figure 16. An east-west geosection, intersecting the Qulleq-1 and Gjoa G-37 wells. The section shows large Cretaceous basins drilled in the Qulleq-1 well and rifted fault blocks mostly along the Greenland margin. Thick Paleogene sedimentary and volcanic successions were drilled on the Gjoa High (Gregersen et al., 2019). The lowermost figure shows Lower to mid-Cretaceous rifted basins, reconstructed (flattened) at horizon G1. *See* Figure 14 for legend. The location of the section is shown in Figure 7. SHH = South Hecla High; NB = Nuuk Basin; WGP = West Greenland Platform. Seismic data courtesy of TGS.

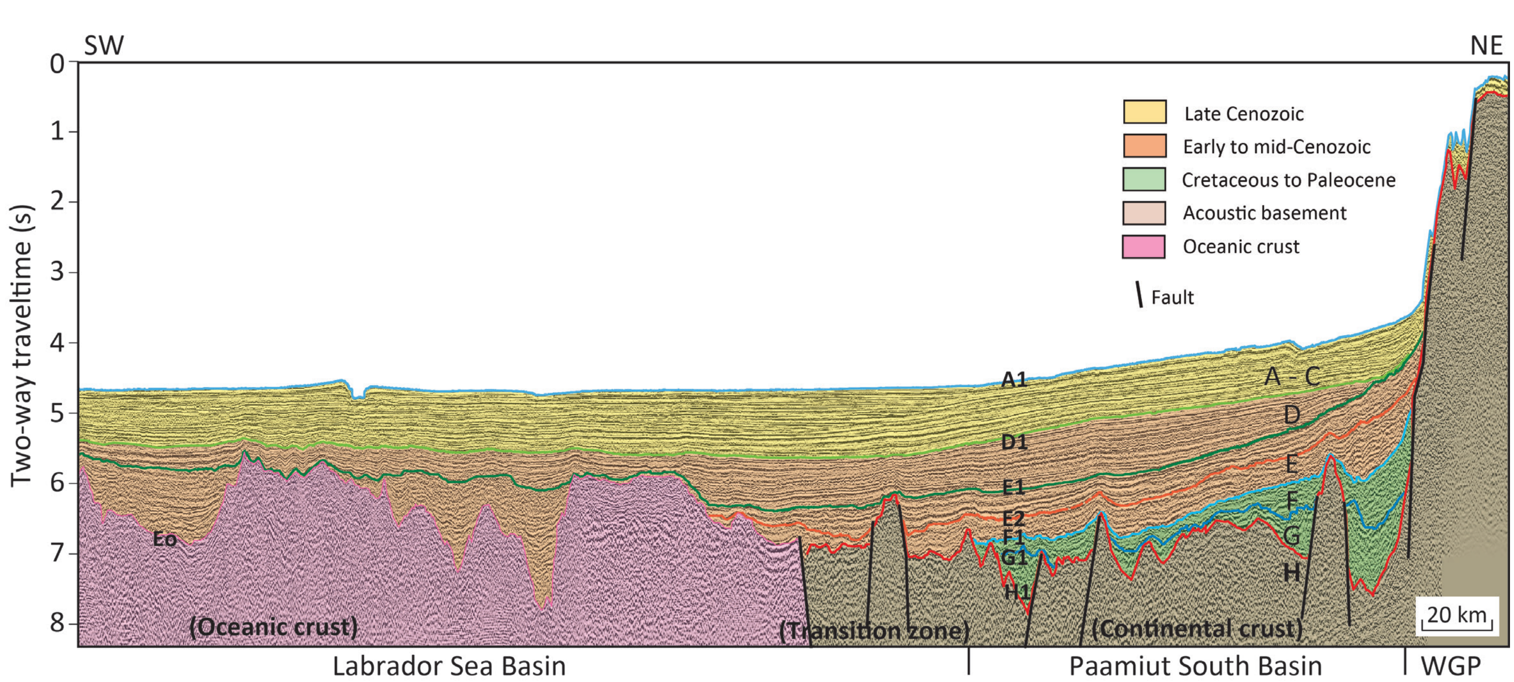

Figure 17. A southwest-northeast geosection from the Labrador Sea Basin to Greenland. Early- to mid-Cretaceous rift basins (unit G) overlain by Upper Cretaceous to Paleocene (unit F) and Cenozoic successions are interpreted to dominate the Greenland margin. A crustal transition zone and oceanic crust are interpreted in the Labrador Sea Basin. *See* Figure 13 for legend. The location of the section is shown in Figure 7. Seismic line is reprocessed by GEUS from seismic data acquired by BGR.

Lithostratigraphy

Formations in the oldest wells Hellefisk-1, Ikermiut-1, Kangâmiut-1, Nukik-1, and Nukik-2 (Fig. 3, 12) were formally defined and described by Rolle (1985), with recent biostratigraphy by Nøhr-Hansen et al. (2016) as summarized below.

Ikermiut Formation

The Ikermiut formation is mudstone dominated with some sandstone, and is of Late Cretaceous to Paleogene age (Fig. 12) (Rolle, 1985; *see* further description above).

Narssarmiut Formation

The Narssarmiut Formation is of probable Selandian age (Nøhr-Hansen et al., 2016) and is 26 m thick in the type section (Kangâmiut-1; Fig. 12). It consists of pebbly, kaolinitic arkosic sandstone and carbonaceous shale units (Rolle, 1985).

Hellefisk Formation

The Hellefisk Formation is of late Paleocene to early Eocene age (Nøhr-Hansen et al., 2016) and is 617 m thick in the type section (Hellefisk-1), located on the central West Greenland margin (Rolle, 1985; Fig. 1, 2, 3). It is dominated by silty, glauconitic mudstone with interbedded, poorly sorted sandstone and a 75 m thick interval of quartz arenite sandstone. It was deposited in a mainly delta plain and nearshore to shallow marine, high-energy environment.

Nukik Formation

The Nukik Formation is of late Paleocene to middle Eocene age (Nøhr-Hansen et al., 2016) and is 286 m thick in the type section (Nukik-2; Fig. 12). It typically consists of coarsening-upward successions of thin-bedded, unconsolidated, and poorly sorted sandstone and mudstone, locally containing glauconite and lignite debris. A turbidite origin has been suggested for some parts of the formation, indicating a relatively deep-marine setting (Rolle, 1985).

Kangâmiut Formation

The Kangâmiut Formation is of Eocene to possibly Miocene age (Nøhr-Hansen et al., 2016). It is 1005 m thick in the type well of Kangâmiut-1 and about 620 m thick in both the Nukik-1 and Nukik-2 wells (Fig. 12); it correlates with most of seismic mega-unit D, which thickens into the Sisimiut Basin (Fig. 13). It is dominated by unconsolidated, well sorted marine sand, interbedded with mudstone, and is mostly mineralogically mature, but some sand intervals contain glauconite and dolomite, in addition to lignite, pyrite, and shell fragments. It is interpreted to represent a shallow-marine shelf deposit, including prograding deltaic facies (Rolle, 1985).

Manîtsoq Formation

The Manîtsoq Formation is mainly late Cenozoic, but may locally be as old as middle Eocene (e.g. Ikermiut-1 well; Nøhr-Hansen et al., 2016; Fig. 12). It is 1055 m thick in Kangâmiut-1, the type section, with nearly the same thickness in the Nukik-1 and Nukik-2 wells (Fig. 12). It thins toward the north as documented by the Ikermiut-1 well (Fig. 12), but is probably variable both in thickness and age across the margin. It is an upward-coarsening unit dominated by unconsolidated, argillaceous arkosic sandstone. Glauconite and interbedded silty and sandy mudstone are observed in the lower levels of the formation, whereas shell debris is evident higher in the formation. It is interpreted to represent marine, shallow shelf deposits, including progradational fan-delta lobes and marine sand bodies (Rolle, 1985).

Ataneq Formation

The Ataneq Formation is tentatively considered to be late Eocene to late Miocene in age (Nøhr-Hansen et al., 2016) and is only known from the Hellefisk-1 well where it is 331 m thick. It is mostly composed of interbedded fine-grained sandstone, siltstone, and silty mudstone in fining-upward cycles, with localized coarse-grained sandstone and carbonaceous mudstone beds, glauconite, shell, and lignite fragments. It is considered to record delta-plain to shallow-marine deposits (Rolle, 1985).

Paleogene volcanism

Paleogene volcanic rocks are interpreted to be present over large areas of the southern West Greenland margin, including the Nukik High, Davis Strait High, Maniitsoq High, Hecla High, and forming the oceanic crust farther west (Fig. 7). Dredging on the northern Davis Strait High around latitude 66°30′N produced several vesicular lava blocks of picrite interpreted to be of local origin, indicating that parts of the high reached above sea level (Larsen and Dalhoff, 2006). The rocks have chemical compositions closely akin to the picrite units on Baffin Island and in the Nuussuaq Basin. A basalt sample was dated at 63.35 ± 0.74 Ma (Larsen and Dalhoff, 2006). This volcanism may have been sourced by the developing 'leaky transform' Ungava Fault Zone with its associated thick igneous crust on the western side of the Davis Strait High (Funck et al., 2012; Larsen and Williamson, 2020).

The central parts of the Hecla High are considered to represent a volcanic centre (Sørensen, 2006). The $^{40}Ar/^{39}Ar$ dating of samples obtained by dredging south of the high (south of latitude 63°30′N) revealed Paleogene igneous rocks (Larsen and Dalhoff, 2006, 2007). The oldest sample is a rhyolite with a Paleocene age of 59.3 ± 0.4 Ma, and nine basalt samples gave Eocene ages of 56.5 Ma to 48.4 Ma. Larsen and Dalhoff (2006, 2007) discussed the possible origins of the rocks and concluded that a source in the Hecla High volcanic centre is the most likely, and a local ice cap on the Hecla High could have dispersed lava material into the surrounding area.

On the Nukik Platform, the Nukik-2 well comprises in its lowest part a thick interval of dolerite units of assumed Paleocene age, and a few volcaniclastic horizons and thin dolerite units occur in the overlying late Paleocene sediments (Rolle, 1985; Hald and Larsen, 1987; Nøhr-Hansen, 2003; Nøhr-Hansen et al., 2016).

Seabed sampling of prominent seamount structures south of 63°N (south of the Lady Franklin Basin) produced samples of basalt that yielded mostly early Eocene ages and are probably of continental character (similar to basalt flows from the Hecla High), and a few local basanite units, indicating a relatively thick lithosphere (Larsen and Dalhoff, 2006).

On the Canadian margin, basaltic volcanic rocks encountered in the Gjoa G-37, Hekja O-71, and Ralegh N-18 wells are all situated within or beneath Paleocene sediments (Nøhr-Hansen, 2003; Nøhr-Hansen et al., 2016; Larsen and Williamson, 2020).

Seismic stratigraphy

The lower Cenozoic seismic stratigraphy is correlated to wells: the uppermost part of mega-unit F equates to Upper Cretaceous to Danian successions, mega-unit E correlates with mid-Paleocene to mid-Eocene successions, and mega-unit D is equivalent to upper Eocene to mid-Miocene successions (Fig. 3). The uppermost part of the seismic stratigraphic mega-unit F correlates with Danian successions, as shown at the LF7-1 well (Fig. 3, 15; Gregersen et al., 2018), and a thin Danian interval may also be present in the AT2-1 well near the boundary between mega-units E and F (Sheldon et al., 2018). Horizon F1 marks a prominent unconformity over many structures with indications of truncation and incision with local thinning of the underlying mega-unit F (Fig. 14, 15, 16, 17). This erosional character of F1 reflects the development of hiatuses with variable timespans from the Late Cretaceous to Paleocene (Fig. 3). The hiatuses span parts of the late Campanian to Paleocene in the AT2-1 and parts of Coniacian to Paleocene in the AT7-1 well (Fig. 3) (Gregersen et al., 2018; Sheldon et al., 2018). Major hiatuses were also noted in the Qulleq-1 (early Campanian to early Thanetian) and Ikermiut-1 (early Campanian to Selandian) wells (Christiansen et al., 2001; Nøhr-Hansen et al., 2016; Fig. 12). Missing Upper Cretaceous to Danian sections in the wells shown in Figure 3 probably indicate erosion associated with tectonic events, such as inversion and/or uplift. In some of the drilled structures (e.g. at Qulleq-1 well), truncated strata at horizon F1, reconstructions of seismic profiles and basin modelling indicate that approximately 0.5 km to 1 km of Upper Cretaceous to lower Paleocene successions (upper parts of unit F) were probably removed over some structures (U. Gregersen, P.C. Knutz, J.R. Hopper, and H. Nøhr-Hansen, work in progress, 2021).

Seismic mega-unit E includes widespread Paleogene volcanic successions (Fig. 2, 3; Gregersen et al., 2018, 2019). The top of the volcanic successions is interpreted to occur at the Ev horizon (Fig. 15, 16) with ties to the Hellefisk-1, Nukik-2, and Gjoa-G37 wells, and to the Alpha-1 S1 and Delta-1 wells in the central West Greenland margin (Gregersen et al., 2019). Oceanic crust is interpreted below the Eo horizon (Fig. 17). Seismic interpretation of the volcanic successions mostly includes seismic units that show a downward loss of reflectivity and resolution, such that the base of the volcanic rocks is not imaged. In parts of the margin, the volcanic cover below horizon Ev thins sufficiently to resolve underlying strata such as at the southwest Hecla High to Lady Franklin Basin area (Fig. 15). Interpretation of the volcanic succession is supported by well ties and additional published data (e.g. refraction models and seabed sampling; *see* above).

The seismic mega-unit E also includes the sedimentary Ikermiut, Narssarmiut, Hellefisk, Nukik, and Kangâmiut formations (Fig. 3). The mega-unit shows significant lateral variation in thickness in the region and is thickest in the Kangâmiut and Sisimiut basins (>1500 m) and thins over basement structures (Fig. 13). The unit has probably been eroded over some highs, as indicated by truncation of underlying reflections, evidence of incision and hiatuses (e.g. in the Fylla Structural Complex; Fig. 16). Alternatively, the thinning may also represent limited deposition over pre-existing highs, as suggested by onlap of upper parts of mega-unit E, including horizon E2 (latest Paleocene–early Eocene), onto previously formed basement structures or older oceanic crust (Fig. 17). The mega-unit shows large variation in seismic facies and geometries with continuous to chaotic reflections, and local internal progradational reflections and mounded features (Fig. 14, 17).

Seismic horizon E2 is correlated with upper Paleocene (Thanetian) successions (Nøhr-Hansen et al., 2016) in most of the south West Greenland wells (Fig. 3; Gregersen et al., 2018). It correlates with the unconformity between upper Paleocene (lower Thanetian) and lower Eocene (Ypresian) successions in the Qulleq-1 well (Fig. 12) (Christiansen et al., 2001). The horizon E2 also correlates to upper Paleocene successions in the AT2-1 and AT7-1 wells (Fig. 14), and is approximately equivalent to the sequence boundary 3000 of Dalhoff et al. (2003). The horizon E2 onlaps horizon Ev (top of volcanic rocks) locally on elevated highs, such as on the Hecla High and the Maniitsoq High.

Seismic horizon E1 correlates to the mid-Eocene unconformity of Dalhoff et al. (2003) and ties in most of the south West Greenland wells with a mid-Eocene unconformity and/or hiatus separating Eocene from Miocene successions (Nukik-1, Nukik-2, and Qulleq-1) or occur within middle Eocene (Lutetian) successions (e.g. Ikermiut-1, Kangâmiut-1; Nøhr-Hansen et al., 2016) (Fig. 3, 12).

Mega-unit D is mid-Eocene to mid-Miocene and includes the Ikermiut, Nukik, Kangâmiut, Manîtsoq, and Ataneq formations (Fig. 3). This mega-unit shows significant lateral variations in thickness, being thickest in the Kangâmiut and Sisimiut basins (>1000 m) and thinning over basement structures. The unit onlaps or downlaps onto the underlying unit E toward highs and local deformed ridges (Fig. 13, 15, 16, 17). The seismic character includes continuous, moderate to locally strong reflections with local progradation from marginal and elevated areas into basins (e.g. from the Davis Strait High into the Kangâmiut Basin (north-south) or east-west across the Sisimiut Basin; Fig. 13). In basinal areas (e.g. Kangâmiut Basin), the unit is locally intersected by many small, near-vertical, near-parallel faults that may form polygonal fault arrays in more clay-rich deposits. Seismic geometries in mega-units E and D include slope wedges and mounded features at the foot of structural highs; such features are suggestive of sediment transport processes producing slump bodies and basin-floor fans, for example (Fig. 13, 16).

Mega-unit D is absent in the LF7-1 and Qulleq-1 wells (Fig. 3, 15, 16), probably due to erosion. Toward the margins of structures (e.g. Davis Strait High) local truncation and canyons occur in the upper parts of the unit. As Oligocene successions are not present in the older wells (Nøhr-Hansen et al., 2016; Fig. 12), this may indicate increased erosion during the late Paleogene or early Neogene. Causes for this apparent regional hiatus are uncertain, but may include uplift with erosion, nondeposition, or other factors; however, an Oligocene succession is present in the Nuuk Basin (AT2-1 and AT7-1; Capricorn Greenland Exploration (Cairn Energy PLC), unpub. report, 2011) and its presence cannot be ruled out elsewhere in the region.

Late Cenozoic

Onshore successions

No Miocene and Pliocene sedimentary rocks are known from the onshore of southern West Greenland; however, Quaternary successions, including glaciogenic deposits, are present. See 'Central West Greenland Basins' section for further details on Quaternary sediments.

Offshore successions

Neogene to Quaternary sedimentary successions are known from exploration wells in basins west of Greenland (Fig. 3; Nøhr-Hansen et al., 2016) and from shallow drilling in ODP and DSDP wells (e.g. Head et al., 1989; Kaminski et al., 1989; Piasecki, 2003). The late Cenozoic seismic stratigraphy is correlated to wells and includes the uppermost part of mega-unit D (Miocene; *see* above), mega-unit C and B (Miocene–Pliocene), and mega-unit A (Pliocene–Quaternary; Fig. 3, 13, 14, 15, 16, 17). The upper Miocene to Quaternary sedimentary successions are generally poorly constrained from exploration wells with few samples and fossils (Nøhr-Hansen et al., 2016). Parts of the Neogene succession in the vicinity of Qulleq-1 were deposited in an open, deep-marine shelf (Piasecki, 2003). A diverse middle to late Miocene (Serravallian to Tortonian) dinoflagellate flora with abundant cysts found in the Qulleq-1 well is probably related to the warmest climate and deepest water during the Neogene, whereas a progressively cooler climate during the Pliocene caused serious depletion of the dinoflagellate fauna (Piasecki, 2003). South of Greenland, shallow coring (ODP site 646; Fig. 3) documented a Miocene to recent fine-grained succession composed of silt and clay, with scattered coarse grains up to cobble size in the upper late Pliocene to Quaternary (Cremer, 1989). Quaternary sediments sampled from the seabed include hemipelagic fine-grained deposits alternating with layers rich in ice-rafted debris (Dalhoff et al., 2006). The distribution of upper Cenozoic successions offshore West Greenland based on mainly wells and seismic interpretation outlined here is shown in Figure 6.

Seismic stratigraphy

In the central parts of the margin, seismic sections show mostly continuous reflections in mega-units A–D (Fig. 14); however, this interval locally shows large mounded subunits with downlap, convergent reflections or back-stepping crests that are interpreted as contourite complexes (Fig. 15: left parts of mega-units B–C). Such features in mega-units A–D form part of the middle Miocene to recent Davis Strait Drift Complex and were mapped by Nielsen et al. (2011) in the Davis Strait and northeast Labrador Sea (latitude 63–66°N). In addition, erosional features, mass-flow deposits, faults at seabed, channels and canyons, diapiric features, bottom simulating reflections, and ploughmarks have been mapped along the southern West Greenland margin (Christiansen et al., 2002).

Farther south, another large sedimentary complex, the Eirik Drift, was formed by ocean currents and is of Miocene to recent age and drilled by ODP site 646 (Srivastava et al., 1987; Müller-Michaelis et al., 2013), and the drilled section corresponds to the mega-units A–C in this study (Gregersen et al., 2019). These kilometre-thick drift complexes record a complex history of ocean current activity related to climate variations.

Mega-unit C is late Miocene and includes successions of the Kangâmiut, Manîtsoq, and Ataneq formations (Fig. 3). The mega-unit shows significant lateral variation in thickness and is thickest in the Sisimiut and Lady Franklin basins and farther south in the east Labrador Sea (Fig. 15). The unit typically onlaps or downlaps the underlying mega-unit D toward highs or local deformed basement ridges (Fig. 15). Mega-unit B is of latest Miocene–Pliocene age and mega-unit A is of latest Pliocene–Pleistocene age, and they include successions of the Manîtsoq and Ataneq formations (Fig. 3). The mega-units show significant lateral variations in thickness (500–1000 m). Mega-unit B is thickest in north-south depocentres both along the Nukik Platform and farther west in the Kangâmiut and Nuuk basins. Mega-unit A is thickest in north-south elongated basins along the outer part of the Nukik Platform and farther south where possible large trough-mouth fans prograde toward the west (Fig. 16). Large channellized canyons are formed in the seabed (Fig. 16). Some of them are probably the result of submarine currents flowing from north to south, such as the Northwest Atlantic Mid-Ocean Channel, the growth pattern of which is interpreted from seismic data (Klaucke et al., 1998). The northeasternmost branches of a channellized canyon system that may be related to this current originate at the south West Greenland margin with one canyon west of the South Hecla High and the Fylla Canyon west of the Fylla Structural Complex (Fig. 16). They merge to form one submarine canyon farther south in the Labrador Sea (Fig. 17). Large contourite drifts, slides, and other forms of mass-mobilization developed during the Miocene to Pleistocene (Nielsen et al., 2011) within mega-units A–C. In addition, west- and southwest-directed shelf progradation occurred (Fig. 16), probably related to glaciations.

CENTRAL WEST GREENLAND BASINS

G.K. Pedersen, H. Nøhr-Hansen, G. Dam, L.M. Larsen, U. Gregersen, P.C. Knutz, J.R. Hopper, and J.A. Bojesen-Koefoed

The central West Greenland margin is located between latitudes 68°N and 73°15′N onshore, and offshore from the Hellefisk-1 or northern boundary of the Sisimiut Basin and to the Upernavik

Escarpment (Fig. 18a). The central West Greenland margin includes the Nuussuaq Basin, which contains excellent outcrops of the Cretaceous ((?)Aptian and/or Albian–Maastrichtian) to Paleocene prevolcanic siliciclastic sedimentary rocks of the Nuussuaq Group (Dam et al., 2009). These are overlain by volcanic rocks, with thin interbasaltic sedimentary units, of the West Greenland Basalt Group (Fig. 18b) (Clarke and Pedersen, 1976; Larsen and Pulvertaft, 2000; Dam et al., 2009; Larsen et al., 2016; Pedersen et al., 2017, 2018). The onshore parts of the Nuussuaq Basin are covered by geological maps and by five photogrammetrical cross-sections (Pedersen et al., 2006b; Garde and Marker, 2010). An east-west schematic tectonic cross-section through Nuussuaq and into the offshore areas has been published by Green et al. (2013). The rocks of the West Greenland Basalt Group cover large areas offshore and limit the seismic interpretation of prevolcanic units. The geology offshore central West Greenland is known from six exploration wells, Hellefisk-1, Alpha-1/S1, Delta-1, Gamma-1, T4-1, and T8-1 (Fig. 18a).

Outcrops of the Nuussuaq Basin have attracted geological expeditions since 1806. Early studies reflect the academic interests of paleobotanists and geologists examining the exploitation of coal beds. Later, the marine invertebrate faunas of Upper Cretaceous and Danian units were studied in detail. Sedimentological studies accompanied the interest in hydrocarbon exploration, and recently the Nuussuaq Basin has gained additional importance as an analogue for the basins offshore West Greenland (*see* historical overview in Dam et al. (2009)).

Pre-Cretaceous

Onshore successions

The pre-Cretaceous rocks of the Greenland craton are exposed east of the boundary fault of the Nuussuaq Basin (Fig. 18a, b). They comprise Archean and Proterozoic rocks and form part of the Nagssugtoqidian orogenic belt to the south and the Rinkian fold belt to the north (Henriksen et al., 2009). Much of the central West Greenland geology is shown in Garde and Marker (2010). Within the Nuussuaq Basin, the Precambrian is overlain by Lower Cretaceous sandstone units and Paleocene volcanic rocks.

Archean

The Greenland craton east of the Nuussuaq Basin consists mainly of late Archean (ca. 2800 Ma) orthogneiss units intercalated with units of strongly deformed Archean supracrustal rocks (Henriksen et al., 2009). The latter comprise both metavolcanic and metasedimentary rocks (Garde and Steenfelt, 1999). The principal rock units of West Greenland may be correlated to onshore areas of Eastern Canada and indicate that these Precambrian basement rocks formed an integral part of the Laurentian shield before opening of the Labrador Sea–Baffin Bay (Henriksen et al., 2009; St-Onge et al., 2009). The lithologies south of Disko Bugt are part of the Nagssugtoqidian Orogen, which includes deformed Archean rocks (Henriksen et al., 2009). These are also referred to as the Aasiaat domain, which correlates to the Meta Incognita Microcontinent in eastern Canada (St-Onge et al., 2009). The Kangâmiut dyke swarm (ca. 2040 Ma) is well preserved in the Archean craton, but was deformed and metamorphosed within the Nagssugtoqidian Orogen belt (Henriksen et al., 2009). The boundary between the Nagssugtoqidian and Rinkian fold belts is probably located within a high-strain belt in Disko Bugt (Conelly and Thrane, 2005). The Rinkian fold belt correlates to the Rae Craton of Eastern Canada (Henriksen et al., 2009; St-Onge et al., 2009).

Proterozoic

Proterozoic supracrustal rocks, mostly of pelitic and semipelitic metasedimentary origin, are prominent in the central part of the Nagssugtoqidian Orogeny. The rocks, which include marble, calc-silicate rocks, and locally graphitic pelite units were originally deposited 2000–1920 Ma ago. They are cut by sheets of 1910 Ma quartz diorite (Henriksen et al., 2009). North of Nuussuaq, Archean gneiss units are overlain by and interfolded with the thick, sedimentary Paleoproterozoic Karrat Group (Henriksen et al., 2009).

Karrat Group

The Paleoproterozoic Karrat Group consists of siliciclastic-carbonate-volcanic rocks that were deposited unconformably on Archean crystalline basement rocks (Fig. 3). The group is exposed from about latitude 71°N to about latitude 75°N, and is intruded by the Prøven

a)

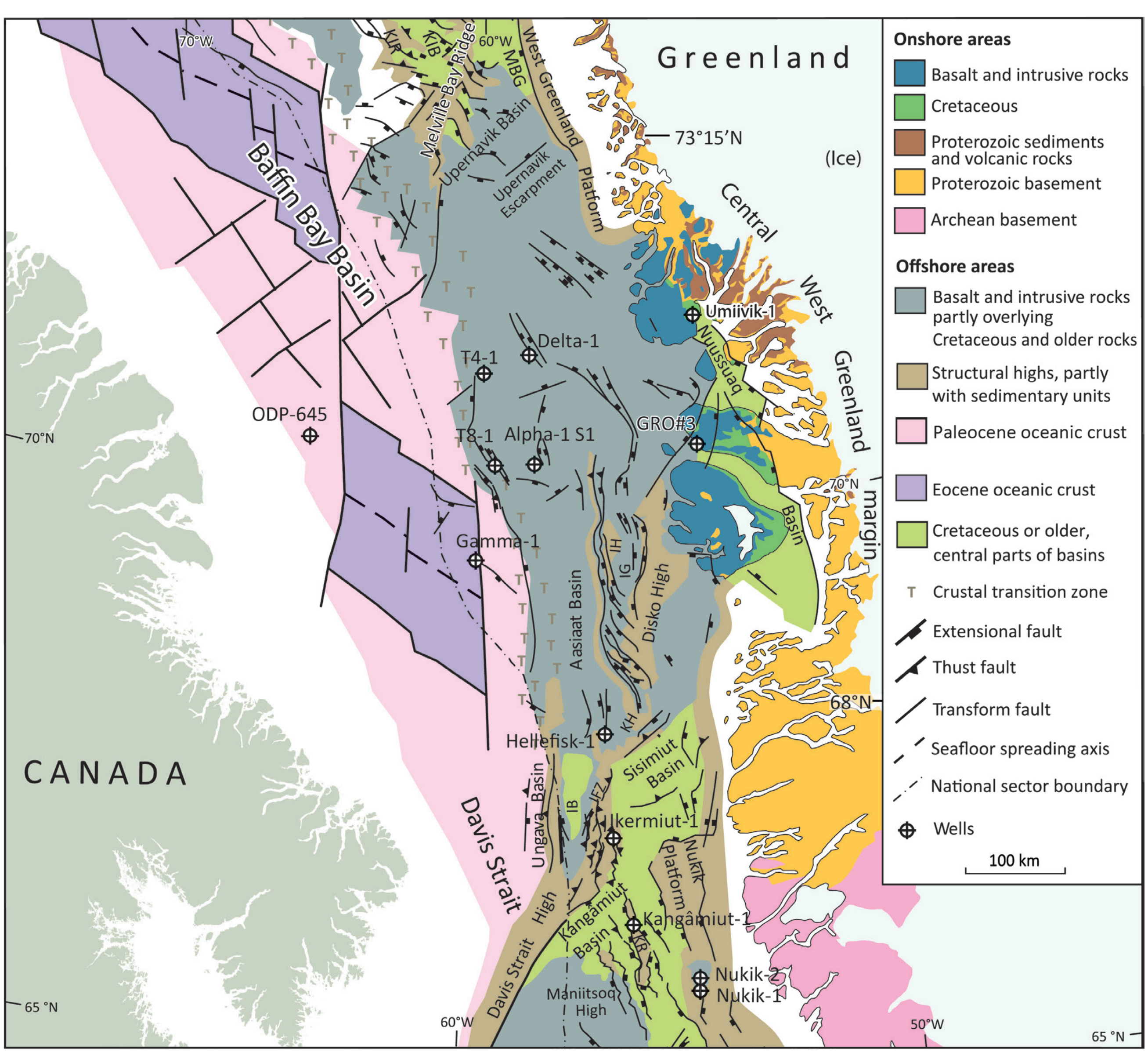

Figure 18. Maps of the central West Greenland margin. **a)** Geological map showing the full extent of the central West Greenland margin between the Sisimiut Basin combined with latitude 68°N eastward, and to the north at the Upernavik Escarpment combined with latitude 73°15′N eastward. The map shows the extent of Cretaceous successions (green and/or dark green) except where covered by Paleogene volcanic successions (grey and/or dark grey). Major faults and exploration and/or deep wells are also shown (from the central part of Fig. 2).

b)

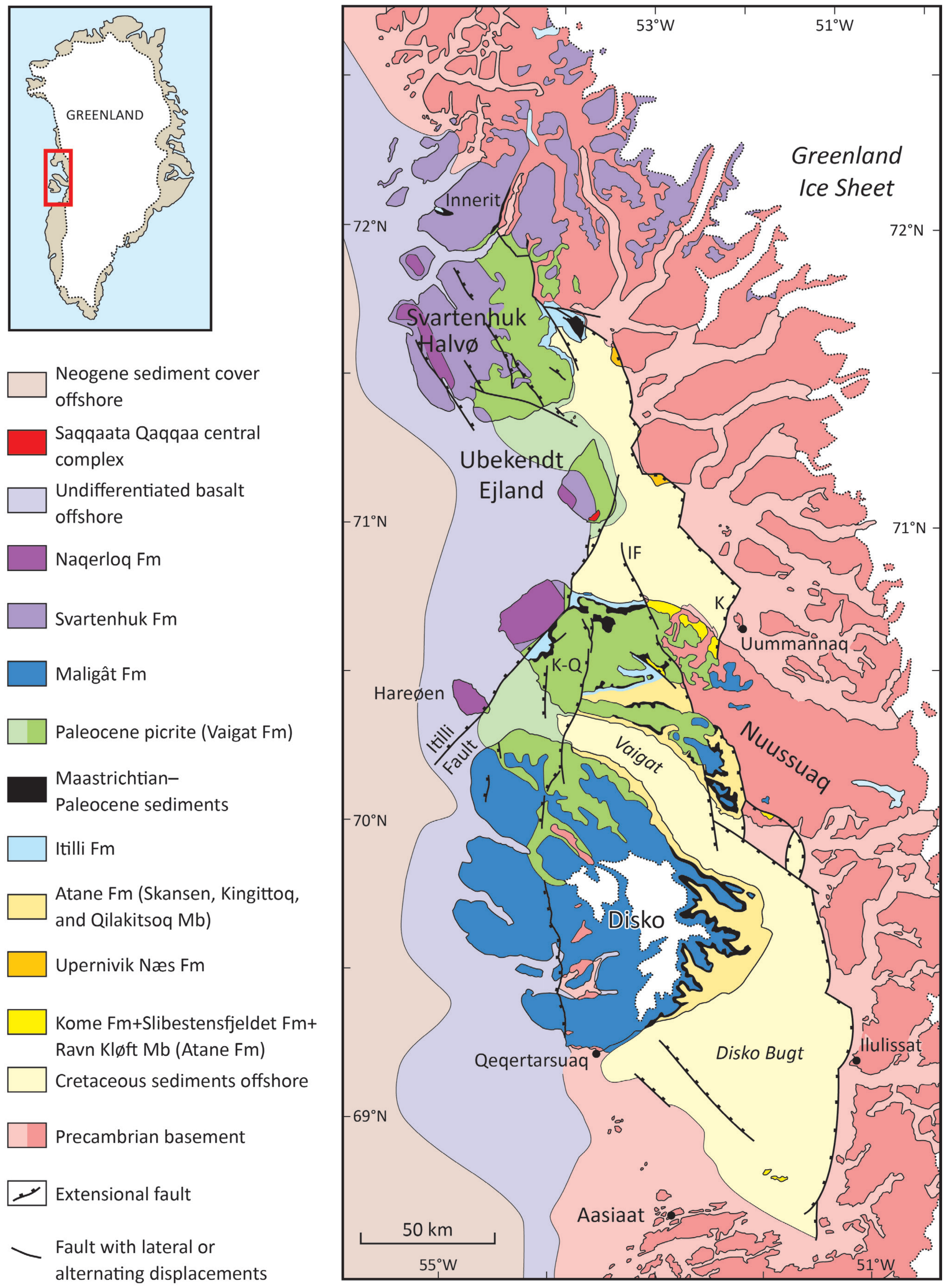

Figure 18 (cont.) b) Geological map of the Nuussuaq Basin with sedimentary formations of the Nuussuaq Group and volcanic formations of the West Greenland Basalt Group (Pedersen et al., 2017).

Igneous Complex (Henriksen et al., 2009). Conelly et al. (2006) suggested that the sedimentary and volcanic rocks of the Karrat Group were deposited on the passive margin of the Rae Craton. The rocks probably correlate with Proterozoic sedimentary successions in the Foxe Fold Belt in northeastern Canada (Henriksen et al., 2009, and references herein). The Nuussuaq Basin boundary fault crosses the islands of Qeqertarsuaq and Upernivik Ø, and separates the Karrat Group (the Qeqertarssuaq Formation) to the east from the Cretaceous Upernivik Næs Formation to the west (Escher and Pulvertaft, 1976; Fig. 18a, b). The group was originally divided into three formations (Henderson and Pulvertaft, 1967, 1987; Henriksen et al., 2009). Ongoing geological mapping shows marked lateral variations in lithology within the Karrat Group, suggesting that the group can be divided into two units, separated by an unconformity. The lower Karrat Group consists of the Qeqertarssuaq Formation, whereas the Kangilleq, Mârmorilik, Qaarsukassak, and Nûkavsak formations constitute the upper Karrat Group (Rosa et al., 2017, 2018). North of Upernavik, the group consists of undifferentiated paragneisses. Due to the complex structural geology it is difficult to estimate the thicknesses of the formations (Rosa et al., 2018).

The Qeqertarssuaq Formation is metamorphosed in amphibolite facies and includes quartzite, mica schist, and garnet amphibolite units, which are folded with Archean rocks. It is mainly exposed at the island of Qeqertarsuaq and at Kangilleq Fjord and is overlain by the Kangilleq Formation at most localities and locally by the Nûkavsak Formation (Rosa et al., 2017).

The Qaarsukassak Formation is about 20 m thick in the type section where it comprises a basal conglomerate overlain by quartzite and metacarbonate rocks with Pb-Zn mineralization. The formation overlies Archean basement with incised paleovalleys discussed by Guarnieri et al. (2016). Locally, the Qaarsukassak Formation is erosively truncated by the Nûkavsak Formation, which comprises interbedded pelite and semipelite (greywacke units), interpreted as a turbidite succession.

The Nûkavsak Formation overlies the Qaarsukassak Formation or rests directly on the basement. It locally fills the incised valleys in the Archean basement (Guarnieri et al., 2016).

The Mârmorilik Formation is dominated by calcitic marble, which overlies a thin basal quartzite. Lead-zinc mineralization in the marble was exploited at the Black Angel mine from 1973 to 1990 (Thomassen, 1991). The Mârmorilik Formation is not observed to be in contact with other formations of the Karrat Group north of Maarmorilik.

Finally, the Kangilleq Formation includes metavolcanic rocks in greenschist facies that are found throughout the southern Karrat region. Primary structures are locally preserved and show that the Kangilleq Formation includes pillow lavas, hyaloclastite breccia units, and subaerial lava flows. The lower boundary of the formation (toward the Qeqertarssuaq Formation) is a regional unconformity. The upper boundary of the Kangilleq Formation is locally transitional where volcanic rocks are interbedded with the overlying metaturbidites of the Nûkavsak Formation (Rosa et al., 2018).

c)

Figure 18 (cont.) c) Map with geographic names of localities, onshore wells and boreholes mentioned in the 'Central West Greenland basins' section.

Anap Nunâ Group

The Anap Nunâ Group is exposed at latitude 70°N, just west of the Greenland Ice Sheet. It consists of a lower unit of marble and orthoquartzite overlain by shallow-water siltstone and sandstone units. Well preserved sedimentary structures demonstrate that the degree of deformation and metamorphism is low (Garde and Steenfelt, 1999). The group is correlated with the Karrat Group north of latitude 71°N.

Prøven Igneous Complex

The Paleoproterozoic Prøven Igneous Complex at latitude 72°10′N–73°10′N consists mainly of charnockitic rocks that intrude Archean gneiss and metasedimentary rocks of the Karrat Group. Isotope data indicate that the igneous complex formed by anataxis of Archean gneiss and Paleoproterozoic sedimentary rocks at depth. Melting is suggested to have been induced by upwelling of hot asthenospheric mantle following a continental collision in the Disko Bugt area (Thrane et al., 2005; Henriksen et al., 2009). Zircon crystals from the complex form a distinct marker in provenance studies (Scherstén and Sønderholm, 2007).

Ordovician

The Ordovician record is restricted to chertified pebbles in the Atane Formation in the Nuussuaq Basin (Dam et al., 2009). A few of these pebbles yield Ordovician gastropods (Pedersen and Peel, 1985; Peel, 2019). An outcrop of Ordovician carbonate rocks is found at Fossilik north of Nuuk; *see* 'Southern West Greenland Basins' section.

Triassic and Jurassic

Pre-Cretaceous igneous rocks in central West Greenland are restricted to a small ultramafic-alkaline dyke in the Uummannaq region, dated to 186 Ma (Larsen et al., 2009). On the conjugate margin, the Chidliak kimberlite province on central Baffin Island has been dated at a slightly younger age of 157–139 Ma (Heaman et al., 2015). Dam et al. (2020) discussed the importance of canyons eroded into the Precambrian basement rocks in central West Greenland, and suggested that the canyons may have formed during the Triassic and Jurassic.

Offshore successions

Geophysical gravity modelling (Skaarup, 2001, 2002), seismic refraction work (Funck et al., 2012), and plate reconstructions (Oakey and Chalmers, 2012) suggest that most of the central West Greenland margin is underlain by a basement of crystalline continental crust. Thus, the continental margin offshore central West Greenland is likely floored by Archean to Proterozoic crystalline basement rocks (Fig. 3) similar to onshore outcrops and offshore samples from the West Greenland margin.

It is possible, however, that large parts of the margin also include pre-Cenozoic sedimentary basins (*see* below). Interpretation of sub-volcanic sedimentary successions from geophysical data offshore central West Greenland is very uncertain, but such successions may be indicated from gravity modelling (*see* below: 'Offshore successions' in 'Cretaceous'). Apart from ice-rafted debris, no pre-Cretaceous igneous rocks have been recovered offshore central West Greenland (F. Dalhoff and L.M. Larsen, unpub. report, 2007).

Cretaceous

Onshore successions

The Nuussuaq Basin contains the only exposures of Cretaceous to Paleogene sediments along the West Greenland margin (Chalmers and Pulvertaft, 2001, Dam et al., 2009; Fig. 18b). It is interpreted as a rift basin that formed along the edge of the Greenland craton with a north-striking boundary fault that can be traced from southeast of Disko to Svartenhuk Halvø (Fig. 18b; Rosenkrantz and Pulvertaft, 1969; Chalmers et al., 1999). In detail, the fault system is made up of northwest-southeast to north-northeast–south-southwest oriented fault segments with basinward dips of 47°–73° and downthrows of 2 km (Chalmers et al., 1999). Prominent faults within the basin include the Kuugannguaq-Qunnilik (K–Q) Fault and the Itilli Fault (Fig. 18b; Chalmers et al., 1999). The basin continues offshore below lower Cenozoic volcanic rocks of the West Greenland Basalt Group (described below). The western margin of the Nuussuaq Basin is poorly known and is tentatively placed near the present west coasts of Disko and Nuussuaq (Chalmers et al. 1999; Knutsen et al., 2012). The basin was probably connected to the West Greenland Cretaceous seaway along the northwest and southwest Greenland continental margin (*see* below 'Offshore successions' in 'Cretaceous"section).

The Nuussuaq Basin includes a thick succession of siliciclastic sedimentary rocks of Cretaceous and early Cenozoic age ((?)Aptian and/or Albian to Paleocene) belonging to the Nuussuaq Group (Dam et al., 2009; Fig. 19, 20, 21, 22, 23). Gravity modelling suggests thicknesses up to 10 km (Chalmers et al. 1999). Paleocene sediments include synvolcanic deposits, which are overlain by a thick series of volcanic rocks, most of which erupted during the Paleocene (Larsen et al., 2016; Pedersen et al., 2017, 2018). Calcareous invertebrate fossils (ammonites, bivalves, and echinoderms) are known from the Cretaceous Atane and Itilli formations and from the Paleocene Kangilia and Agatdalen formations (Dam et al., 2009). Palynological studies provide age constraints for most of the formations (Nøhr-Hansen, 1996, 2003; Nøhr-Hansen et al., 2002, 2016; Fensome et al., 2016). In several formations the palynomorph assemblages are of low diversity and low relative abundance. Together with a relatively high sedimentation rate, this results in each succession being characterized by one or only a few palynoevents (Pedersen and Nøhr-Hansen, 2014). Figure 24 provides an overview of the paleontology and biostratigraphy of the Cretaceous formations.

Plate tectonic reconstructions indicate the presence of a narrow seaway in the Baffin Bay, the Davis Strait, and the Labrador Sea prior to seafloor spreading in the Paleocene (Oakey and Chalmers, 2012; Hosseinpour et al., 2013). The positions of the Cretaceous shorelines are poorly known due to uplift and erosion (Green et al., 2013). Sedimentary facies and paleogeographic reconstructions predict terrestrial to marginally marine environments in the Lower Cretaceous and marine environments in the Upper Cretaceous.

Marine fossils are absent from the Early Cretaceous of the Nuussuaq Basin, as they are also absent from the Aptian to early Cenomanian Quqalulit Formation at Cape Dyer, Baffin Island (Burden and Langille, 1990, 1991); however, the ammonite fauna from the Nuussuaq Basin indicates a marine connection to the Western Interior Seaway during most of the Late Cretaceous (Birkelund, 1965). In addition, Birkelund (1965) suggested that a marine connection to European faunas existed in the Campanian–Maastrichtian. Geochemical analyses of oil stains from migrating hydrocarbons in the Nuussuaq Basin and potential source rocks also suggest that a Mesozoic seaway may have existed between Greenland and Canada (Bojesen-Koefoed et al., 2004). The regional correlation of Mesozoic–Paleogene sequences across the Greenland–Canada boundary was discussed by Sønderholm et al. (2003). Combination of regional seismic stratigraphy and sedimentary successions has led to a division of the Cretaceous succession into three tectonostratigraphic phases: early rift, subsidence, and late rift (Dam et al., 2009), which are described further in the next section (Fig. 3).

Outcrops of Cretaceous sediments of the Nuussuaq Group are exposed in coastal cliffs and in stream sections from Grønne Ejland (a small island south of Disko: Fig. 18c) to the northern part of the Svartenhuk Halvø (Fig. 18b). The sediments are all siliciclastic and represent fluvial, lacustrine, deltaic, and marine shoreface environments, as well as marine deep-water environments (Dam et al., 2009). The largest and most continuous outcrops are on Nuussuaq.

<u>*Cretaceous tectonostratigraphic phases and lithostratigraphy of the Nuussuaq Group*</u>

The nonmarine, estuarine, and deltaic (?)Aptian and/or Albian to lower Cenomanian deposits constitute the regional early rift phase, corresponding to the tectonostratigraphic sequence TSS 1 (Dam et al., 2009) of the Nuussuaq Basin (Fig. 3). These deposits include the Kome and the Slibestensfjeldet formations, the lower part of the Atane Formation (the Ravn Kløft Member, the Skansen Member, and the Kingittoq Member), and the Upernivik Næs Formation (Dam et al., 2009; Fig. 3, 19). Dinoflagellate cysts (dinocysts) and invertebrate macrofossils indicate that fully marine conditions are rare in these units, which suggests that the eastern part of the Baffin Bay at this time was dominated by brackish to freshwater environments. Deltaic deposits of the Atane Formation formed at the mouth of a large river that may have drained a large part of the interior of Greenland (Olsen, 1993; Dam et al., 2020).

<u>*Kome Formation*</u>. This formation comprises fluvial sandstone units and coal-bearing floodplain deposits with strong lateral facies variations in the strata. The Kome Formation overlies Precambrian basement, which is locally strongly weathered, but, in some areas, shows only slight kaolinization (Pulvertaft, 1979; Midtgaard, 1996b; Dam et al., 2009) (Fig. 20). The Kome Formation is exposed in a 30 km coastal section between Kuuk and Ikorfat (Fig. 18b, c). The oldest sediments occur to the southeast (Kuuk, Majorallattorfik). In the Kuuk area, the outcrops of the Kome Formation are bounded to the east by the main boundary fault system (Pulvertaft, 1979). The proximity to the fault is not reflected in the sedimentary facies, which suggests that the Kome Formation originally covered areas east of Kuuk. The boundary fault was active during TSS 1 and may have been re-activated later.

The Kome Formation contains macrofossil plants, dominantly ferns and cycads, which constitute the Early Cretaceous Kome Flora (Nordenskiöld, 1871; Steenstrup, 1883a, b; Heer, 1883a, b; Boyd, 1998). The absence of dicotyledons (Late Cretaceous angiosperms) indicates an Early Cretaceous age. The very sparse content of age-diagnostic markers in the Kome Formation still leaves open the question of whether it is of late Aptian, early Albian, or middle Albian age (Pedersen and Nøhr-Hansen, 2014; Fig. 24).

<u>*Slibestensfjeldet Formation*</u>. The fluvial Kome Formation is overlain by the Slibestensfjeldet Formation, which includes fine-grained sandstone with wave-generated sedimentary bedforms in the east and grey, silty mudstone in the west (Fig. 21). The upper part of the formation is coarsening upward (Dam et al., 2009), and the formation overlies a drowning surface that is exposed along a 13 km long coastal section between Slibestensfjeldet and Ikorfat (Fig. 18c).

Wave ripples and hummocky- or swaley cross-stratification indicate a wave- and storm-dominated shoreface environment (Midtgaard, 1996a). The presence of freshwater and brackish water dinocysts indicate that a large lake or a brackish water embayment was situated in the Nuussuaq Basin in the middle to early late Albian (Pedersen and Nøhr-Hansen, 2014).

<u>*Lower part of the Atane Formation*</u>. The Cretaceous succession on Disko and in southern and central Nuussuaq belongs to the Atane Formation (Fig. 19). The formation is up to 800 m thick in individual outcrops, but seismic data indicate that it is at least 3 km thick. The siliciclastic deposits show a cyclic depositional pattern, and the formation is interpreted as deltaic. The Atane Formation represents an aggradational depositional system (Fig. 22; Dam et al., 2009) with local transgressions or regressions. Delta plain mudstone units with coal beds and fluvial sandstone units are prominent to the southeast and paleocurrent directions are to the southwest, west, and northwest (Johannessen and Nielsen, 1982; Pedersen and Pulvertaft, 1992; Olsen, 1993). The source area was probably located east of the

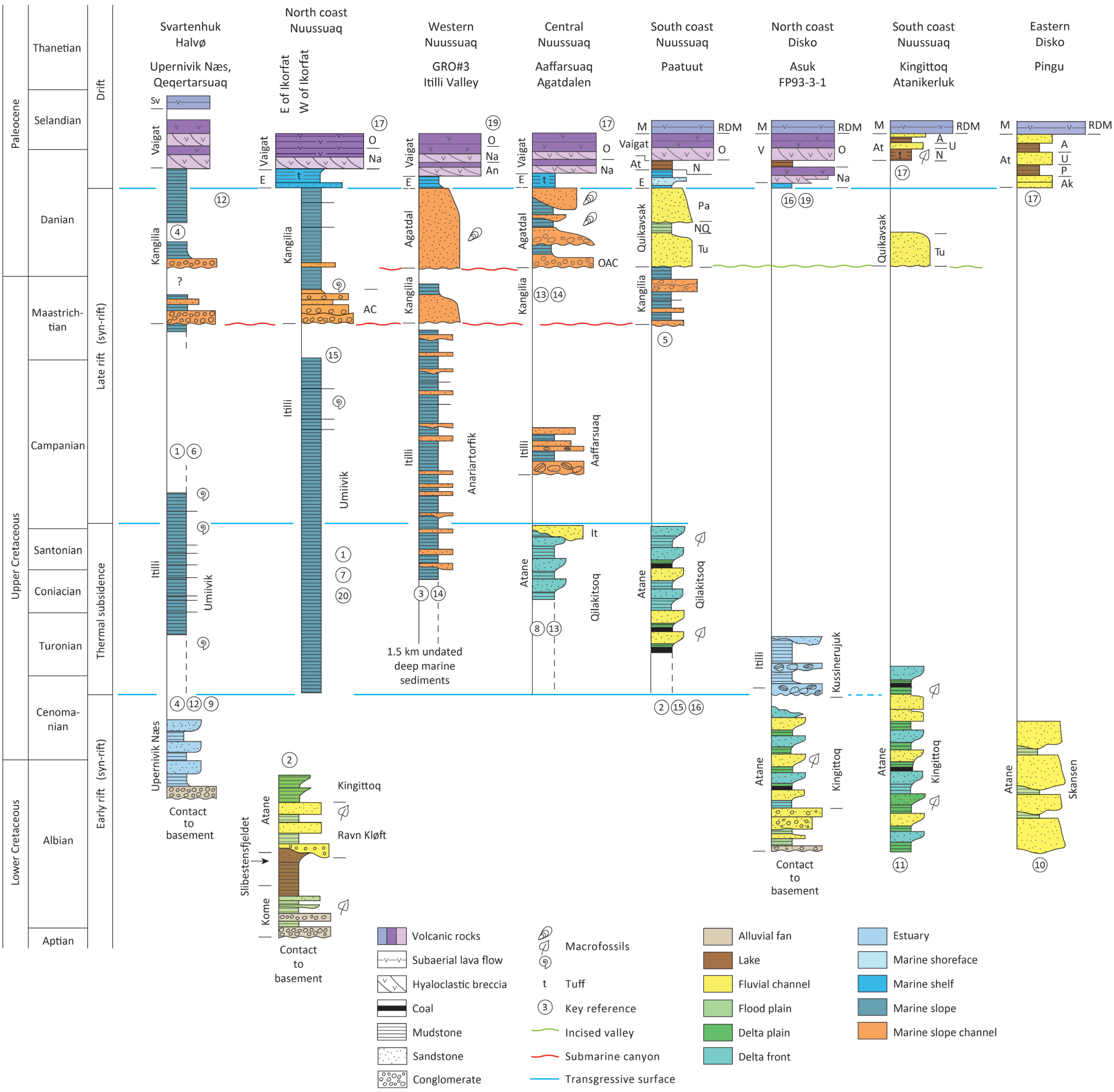

Figure 19. Lithostratigraphy, the Nuussuaq Group. Schematic sedimentological logs, which each illustrate areas larger than a single outcrop. The main tectonostratigraphic units of Figure 3 are shown (*modified from* Dam et al., 2009). Place names are located in Figure 18c. Only the older volcanic formations (Vaigat, Maligât, and Svartenhuk formations) are indicated. Names of the formations are shown to the left of the columns, the members to the right. The vertical axis of the diagram indicates time, *see* text for information on thicknesses of the successions. Abbreviations: A = Assoq Member (Atanikerluk Formation), Ak = Akunneq Member (Atanikerluk Formation), An = Anaanaa Member, At = Atanikerluk Formation, AC = Annertuneq Conglomerate Member (Kangilia Formation), E = Eqalulik Formation, It = Itivnera bed (Atane Formation), M = Maligât Formation, N = Naujât Member (Atanikerluk Formation), Na = Naujánguit Member (Vaigat Formation), NQ = Nuuk Qiterleq Member (Quikavsak Formation), O = Ordlingassoq Member (Vaigat Formation), OAC = Oyster–Ammonite Conglomerate Bed (Kangilia Formation), P = Pingu Member (Atanikerluk Formation), Pa = Paatuutkløften Member (Quikavsak Formation), RDM = Rinks Dal Member (Maligât Formation), Sv = Svartenhuk Formation, Tu = Tupaasat Member (Quikavsak Formation), U = Umiusat Member (Atanikerluk Formation), V = Vaigat Formation. Key references by numbers in circles: 1 = Birkelund (1965), 2 = Boyd (1998), 3 = Christiansen et al. (1999), 4 = Christiansen et al. (2000), 5 = Dam and Nøhr-Hansen (2001), 6 = Dam et al. (1998b), 7 = Dam et al. (1998c), 8 = Dam et al. (2000), 9 = Koch (1964), 10 = Koppelhus and Pedersen (1993), 11 = Lanstorp (1999), 12 = Larsen and Pulvertaft (2000), 13 = Nøhr-Hansen (1996), 14 = Nøhr-Hansen et al. (2002), 15 = Olsen and Pedersen (1991), 16 = Pedersen et al. (2017, 2018), 17 = Pedersen et al. (2006b), 18 = Piasecki et al. (1992), 19 = Storey et al. (1998), 20 = Pedersen and Nøhr-Hansen (2014).

Figure 20. The early rift succession at Ikorfat, north coast of Nuussuaq represented by the Precambrian basement overlain by the Kome and Slibestensfjeldet formations and the Ravn Kløft and Kingittoq (Ki) members of the Atane Formation. The Itilli Formation represents the thermal subsidence phase, and the Eqalulik (E) and the Vaigat formations represent the drift phase. For location *see* Figure 18c; for scale, the base of the Vaigat Formation is at around 900 m a.s.l. (Dam et al., 2009). Photograph by M. Sønderholm, 2008.

boundary fault, below the modern ice cap. The lower boundary of the Atane Formation is only exposed in northern Nuussuaq at the base of the Ravn Kløft Member. The upper boundary is exposed in central Nuussuaq where an angular, erosional unconformity separates the Qilakitsoq Member (Atane Formation) from the overlying Aaffarsuaq Member (Itilli Formation; Dam et al., 2000).

The Atane Formation is divided into four members: the Skansen Member (fluvial), the Ravn Kløft Member (estuarine), the Kingittoq Member (deltaic with rare marine dinocysts in its upper part), and the Qilakitsoq Member (deltaic, with some marine dinocysts, and occasional marine invertebrates; Dam et. al., 2009). The Skansen, Ravn Kløft, and Kingittoq members constitute the lower part of the Atane Formation, which was deposited during the late-middle Albian to early Cenomanian (Fig. 24).

The Skansen Member is characterized by white to yellow, very friable sandstone with a sheet geometry (Dam et al., 2009). These are intercalated with heterolithic sandstone and mudstone rich in plant debris and include thin coal beds. The 20–30 m thick intervals reflect a cyclic depositional pattern, with the sandstone interpreted as braided river deposits. The channel lags contain pebbles of chert and silicified Ordovician limestone (Pedersen and Peel, 1985; Peel, 2019). Carbonaceous mudstone, sandstone, and coal beds are interpreted as lake or swamp deposits within a floodplain or upper delta-plain environment (Fig. 19, 24) (Dam et al., 2009).

The Ravn Kløft Member of the Atane Formation is tripartite. The lower boundary is an erosional surface that truncates the Slibestensfjeldet Formation. This boundary is well exposed in gullies east of Ikorfat (Fig. 19, 20), and it is overlain by 30–60 m of conglomeratic to coarse-grained fluvial sandstone. The palynological assemblage of this unit is dominated by miospores with common charcoal. In the middle part of the member, mudstone and sandstone form coarsening-upward units interpreted as thick deltaic successions. The upper part of the member contains amalgamated, multistorey, fluvial sandstone sheets (Midtgaard, 1996b; Dam et al., 2009). The Ravn Kløft Member is thickest near its type section in the gorge named J.P.J. Ravn Kløft (*see* Fig. 22, 51 *in* Dam et al., 2009). The Ravn Kløft Member is conformably overlain by delta-plain deposits of the Kingittoq Member (Midtgaard, 1996b; Dam et al., 2009). A late Albian age is suggested for the Ravn Kløft Member (Fig. 24) (Pedersen and Nøhr-Hansen, 2014).

The Kingittoq Member of the Atane Formation, is known from outcrops along the north coast of Disko, the south coast of Nuussuaq (between Atanikerluk and Kingittoq), and the north coast of Nuussuaq from Ikorfat to Talerua (Fig. 18b, c). The member includes sandstone deposited in distributary channels, delta-plain deposits with thin coal beds, and delta-front deposits with wave-generated sedimentary structures characteristic of marine delta-front deposits, although no dinocysts indicate fully marine conditions (Bojesen-Koefoed, et al. 2001; Pedersen et al., 2006c; Dam et al., 2009; Jensen and Pedersen, 2010). A few dinocysts, however, indicate transition to marginal marine conditions in the upper part of the Kingittoq Member (Pedersen and Nøhr-Hansen, 2014). Marginal marine conditions are also indicated by bivalves found at Kingittoq (Ravn, 1918). In southern Nuussuaq, the age of the Kingittoq Member ranges from middle-late Albian at Tartunaq to early Cenomanian at Qallunnguaq (Lanstorp, 1999; Fig. 19, 24).

Upernivik Næs Formation. This formation is known from Upernivik Ø, Qeqertarsuaq, and Itsaku (southeast Svartenhuk Halvø). The formation is about 1600 m thick at Upernivik Næs where it is dominated by sandstone (Fig. 19). This contains plant macrofossils and a poor palynological assemblage (Dam et al., 2009). Terrestrial to near-shore depositional environments characterize the formation. Coarse-grained sandstone units with pebble lags were deposited in braided fluvial channels. Fine-grained sandstone units, locally with mud-draped foresets and heterolithic crosslaminated sandstone units are interpreted as estuarine deposits. Sandstone beds interbedded with heterolithic mudstone and mudstone units rich in comminuted plant debris are interpreted as coastal plain deposits. Coarsening-upward successions of mudstone to sandstone represent deltaic deposits (Midtgaard, 1996b; Dam et al., 2009). The age of the formation ranges from middle or late Albian to middle Cenomanian (Fig. 24).

Subsidence phase

The transition from the early rift phase to the subsidence phase is marked by a major marine flooding surface in the middle to late Cenomanian (Dam et al., 2009, Pedersen and Nøhr-Hansen, 2014; Fig. 19). The subsidence phase (middle Cenomanian to earliest Campanian) includes the deltaic Qilakitsoq Member (the upper part of the Atane Formation) in southern Nuussuaq, and the deep-water marine deposits of the Itilli Formation, which is known from outcrops and boreholes in northern and western Nuussuaq and at Svartenhuk Halvø (Fig. 18a, b, c, 19). The regional tectonostratigraphic subsidence phase corresponds to the tectonostratigraphic sequence TSS 2 (Dam et al., 2009) of the Nuussuaq Basin (Fig. 3).

Upper part of the Atane Formation. The Qilakitsoq Member constitutes the upper part of the Atane Formation. Excellent exposures of the member are found along the south coast of Nuussuaq

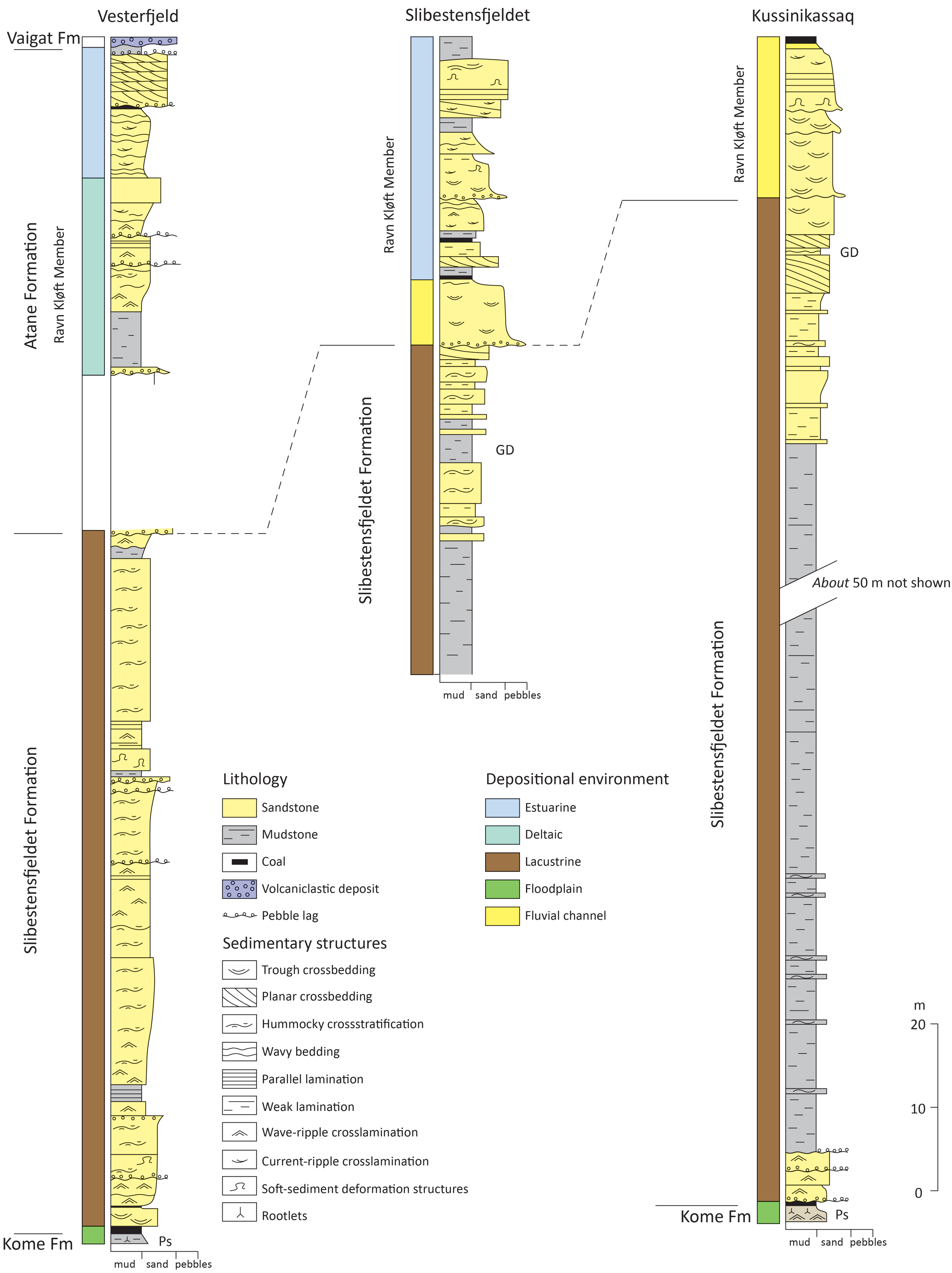

Figure 21. The Slibestensfjeldet Formation: the sedimentological logs illustrate the lateral facies variation from sandstone with wave-generated structures in the east (left) to silt-streaked mudstone to the west (right) in a lacustrine to brackish-water environment. The logs were measured at the north coast of Nuussuaq by Midtgaard (1996b) between Majorallatarfik and Kussinikassaq (Fig. 18c). GD = Gilbert Delta, Ps = Paleosol (Dam et al., 2009).

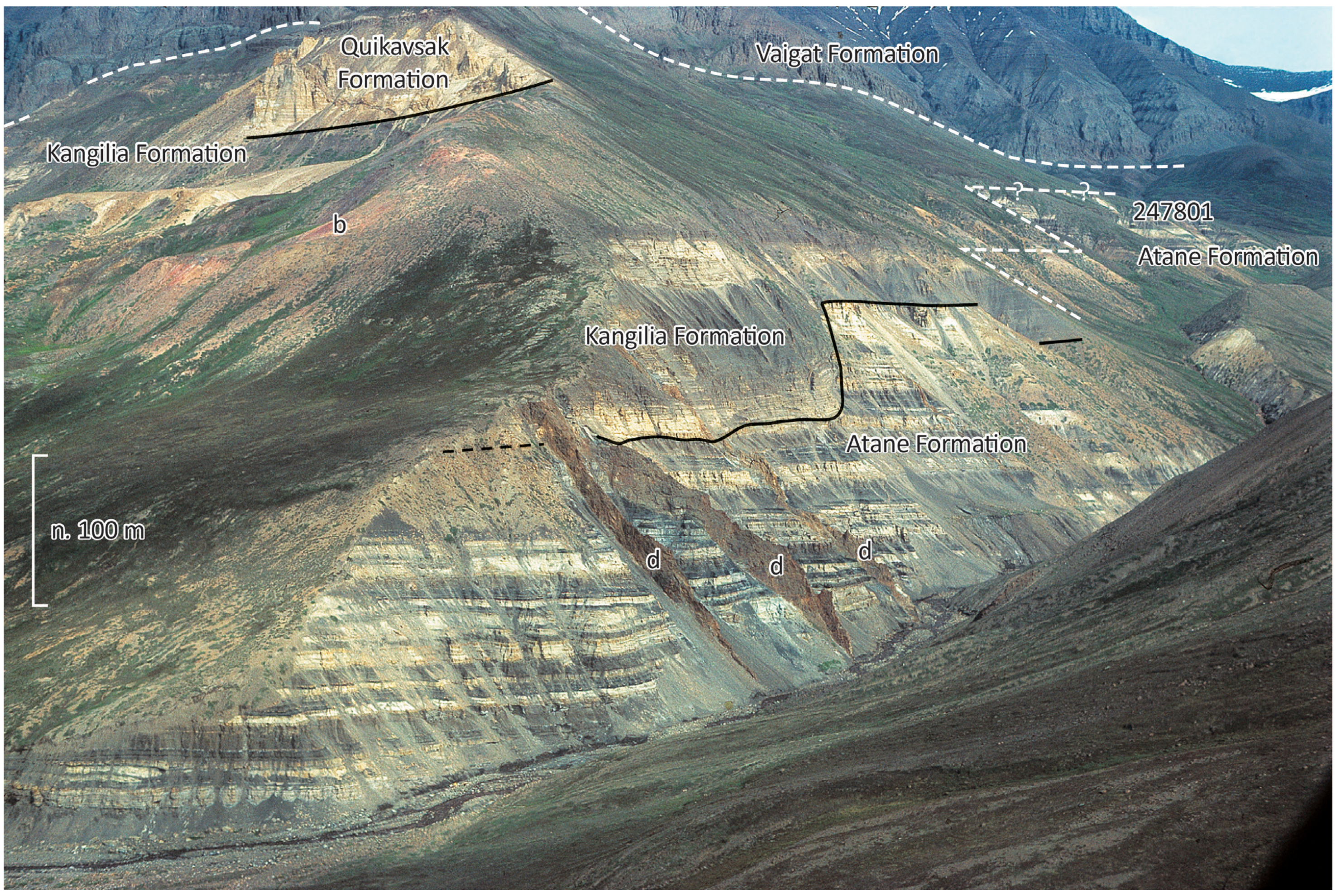

Figure 22. The deltaic Atane Formation has an aggradational stacking pattern. Type section of the formation at Ataata Kuua, south coast of Nuussuaq (Fig. 18c). The upper part of the Atane Formation represents the thermal subsidence phase. The formation is truncated by a submarine erosional surface, which is overlain by the Danian Kangilia Formation (Dam and Nøhr-Hansen, 2001). Sandstone units of the Paatuutkløften Member (Quikavsak Formation) fill an incised valley in the Kangilia Formation. The Kangilia and Quikavsak formations both represent the late rift phase. The following drift phase is represented by the sedimentary Eqalulik Formation (not seen in photograph) and the volcanic Vaigat Formation (Naujánguit Member). A schematic sedimentological log is included in Figure 19. 247801 = position of borehole Atâ-1 (Fig. 1), b = burnt shale (red colour), d = dyke. (Dam et al., 2009). Photograph by G.K. Pedersen, 1988.

from Paatuut to Nuuk Killeq, and in central Nuussuaq on the northern slope of the Aaffarsuaq valley (Fig. 18c). It is dominated by delta-front deposits with a sparse marine palynoflora. Bioturbated shoreface sandstone beds, which formed during high-frequency transgressions of the delta plain, are relatively prominent (Pedersen and Bromley, 2006; Dam et al., 2009). Delta-plain deposits are subordinate (Fig. 22). The base of a multistorey fluvial complex at Qallunnguaq and Kingittoq (Jensen and Pedersen, 2010) forms the lower boundary of the Qilakitsoq Member (Pedersen and Nøhr-Hansen, 2014). A regional marine transgression in the middle and late Cenomanian is indicated by the occurrence of marine dinocysts above the channel complex (Pedersen and Nøhr-Hansen, 2014). The age of the Qilakitsoq Member ranges from late Cenomanian to late Santonian or earliest Campanian (Fig. 19, 24). The Qilakitsoq Member represents shallow-water deposition during the tectonostratigraphic subsidence phase (Fig. 3). This aggradational pattern indicates a high sedimentation rate for the delta deposits.

Itilli Formation. This formation includes all the Upper Cretaceous deep-water marine deposits of the Nuussuaq Basin and is subdivided into the Kussinerujuk, Umiivik, Anariartorfik, and Aaffarsuaq members (Dam et al., 2009; Fig. 19). The formation is known from outcrops in northern, central, and western Nuussuaq and at Svartenhuk Halvø, as well as from a number of boreholes, notably Umiivik-1 borehole and the deep GRO#3 well (Fig. 18a 19; Dam and Sønderholm, 1994; Dam et al., 1998b, 2009). Deposition occurred mainly from high- and low-density turbidity currents (Fig. 23).

The base of the Itilli Formation is interpreted as a regional marine transgression in the middle- to late Cenomanian (and possibly early Turonian), known also from the Kanguk Formation on Ellesmere Island, Nunavut, Canada (Núñez-Betelu et al., 1994). In the Nuussuaq Basin, this transgression is recorded within the Ikorfat Fault Zone, and in northern Disko at the base of the Kussinerujuk Member (Pedersen and Nøhr-Hansen, 2014). The lower successions in Umiivik-1 and GRO#3 are not dated since the dinocysts are altered beyond recognition due to high diagenetic temperatures (Dam et al., 2009, Fig. 19).

The Kussinerujuk Member includes mudstone, heterolithic sandstone, and intraformational conglomerate dominated by mudclasts. The lower boundary of the member is an erosional surface, which truncates the Kingittoq Member of the Atane Formation in northern Disko (Pulvertaft and Chalmers, 1990; Dam et al., 2009; Fig. 19). A low-diversity assemblage of marine dinocysts suggests an early late Cenomanian age (Fig. 24). A 90 m thick section with an oil-seep at Asuk (northern Disko) is dated as late Albian–late Cenomanian (Bojesen-Koefoed et al., 2007). The above evidence indicates that a late Cenomanian drowning of an incised valley led to deposition of the Kussinerujuk Member in northern Disko (Pedersen and Nøhr-Hansen, 2014).

The Umiivik-1 borehole was drilled to 1200 m depth to investigate the presence of oil-prone source rocks in mid-Cretaceous strata of the region with near-complete core recovery. The core is dominated by mudstone that is interpreted as having been deposited from low-velocity, low-density turbidity currents. Several dolerite intrusions, with a cumulative thickness of 240 m, have severely altered the marine mudstone units and limit the possibilities for both detailed organic geochemical and palynological studies in the deeper part of the borehole (Dam et al., 1998a). These strata belong to the Umiivik Member of the Itilli Formation (Dam et al., 2009).

At Svartenhuk Halvø a small outcrop on the northern side of the valley Usuit Kuussuat shows that the mudstone units of the Umiivik Member are overlain by the volcanic Kakilisaat and Nerutusoq members of the Vaigat Formation (Larsen and Pulvertaft, 2000). These informal members are not discussed.

Exposures of the Umiivik Member at Svartenhuk Halvø and Itsaku include ammonites, which indicate a late Turonian to early Campanian age for the member (Birkelund, 1965). The Umiivik Member at Svartenhuk Halvø includes six dinocyst intervals representing the Coniacian to upper Santonian (Nøhr-Hansen, 1996). The oldest datable sample, recovered at 658 m depth in the Umiivik-1 borehole, is post-middle Turonian (Pedersen and Nøhr-Hansen, 2014; Fig. 24). In northern Nuussuaq, Campanian (to (?)Maastrichtian) mudstone units of the Umiivik Member are exposed at Kangilia and Annertuneq, and were sampled in the GANT#1 borehole (Fig. 18c). This part of the Umiivik Member was deposited during the late rift tectonostratigraphic phase. In the GANT#1 well, the mudstone units are interbedded with 10–25 m thick intervals of conglomeratic sandstone units deposited from high-density sediment gravity flows (Fig. 23).

The Anariartorfik Member is known from western Nuussuaq, from outcrops in the Itilli and Tunorsuaq valleys. It was cored in the FP94-9-01 borehole, but was not cored in the deeper GRO#3 well (Fig. 18a, c; Dam et al., 2009). The member includes mudstone beds up to 15 m thick, thinly interbedded sandstone and mudstone several tens of metres thick, chaotic beds up to 30 m thick, and

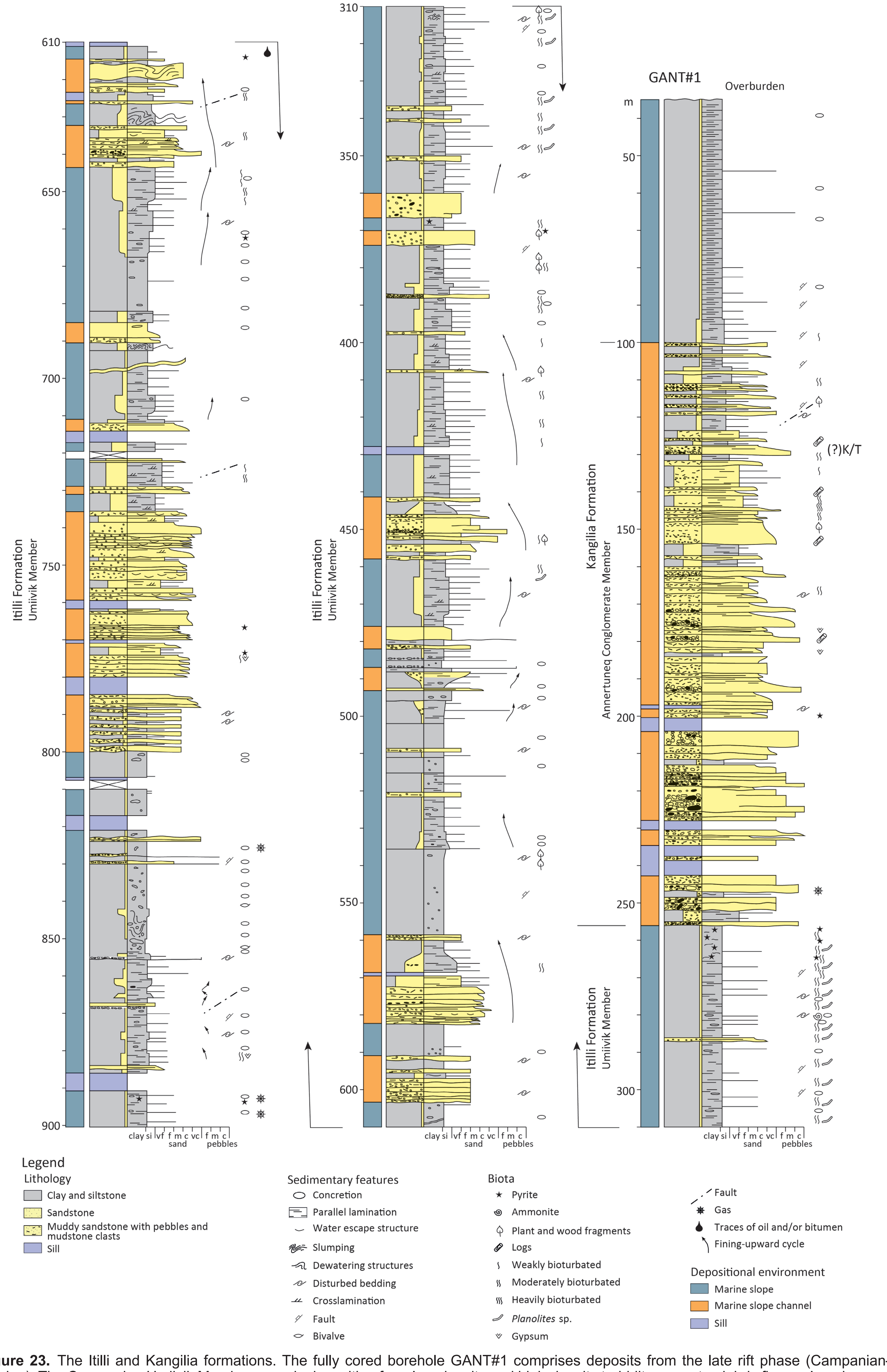

Figure 23. The Itilli and Kangilia formations. The fully cored borehole GANT#1 comprises deposits from the late rift phase (Campanian–Danian). The Campanian Umiivik Member records deposition from low-density and high-density turbidity currents, debris flows, slumping, and fall-out from suspension. The Upper Maastrichtian Kangilia Formation comprises the Annertuneq Conglomerate Member, which was deposited from debris flows and high-density turbidity currents. The member reaches its maximum thickness of 140 m in GANT#1. The overlying part of the Kangilia Formation is dominated by mudstone units deposited from low-density turbidity currents. The Cretaceous–Tertiary boundary is located at approximately 130 m. For location of borehole *see* Figure 18c (Dam et al., 2009).

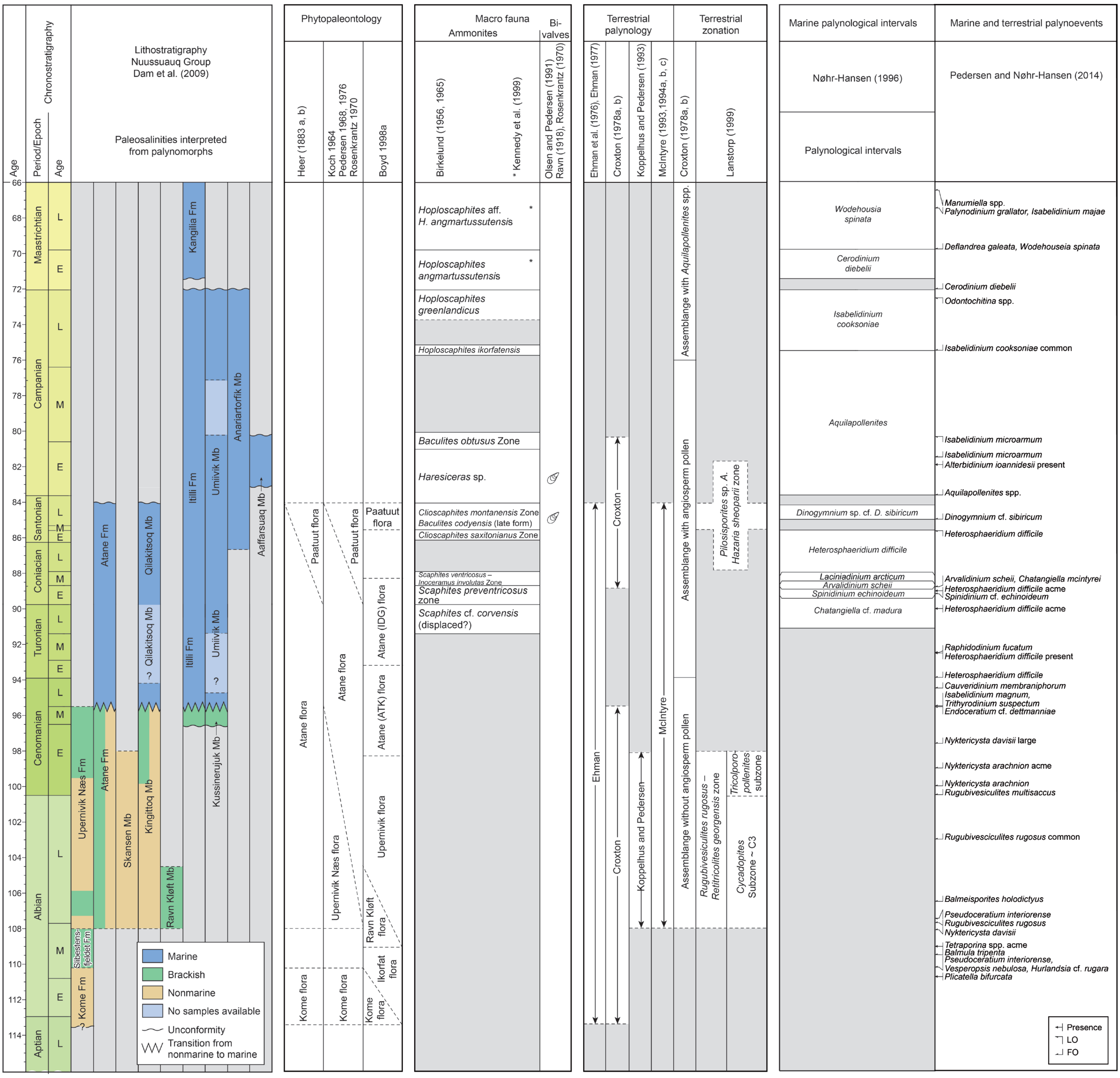

Figure 24. Biostratigraphy of the Cretaceous deposits of the Nuussuaq Group onshore. The zonations are based on phytopaleontology, ammonites, terrestrial palynology, and marine palynological intervals based on marine dinoflagellate cysts (dinocysts). FO = First occurrence, LO = Last occurrence. Includes data from publications listed in the top of the diagram.

coarse- to very coarse-grained sandstone units up to 50 m thick (Dam and Sønderholm, 1994; Dam et al., 2009). Macrofossils are rare, but palynomorphs are abundant in the middle and upper parts of the GRO#3 well.

The Anariartorfik Member was deposited in a fault-controlled slope environment. Most of the sandstone units were deposited from high-density turbidity currents. The mudstone units and the interbedded sandstone and mudstone units were deposited from traction currents or waning low-density currents in unconfined interchannel slope environments (Dam and Sønderholm, 1994). Palynomorphs in the GRO#3 well at depths of 1520–960 m indicate a (?)Coniacian–(?)early Maastrichtian age for the Anariartorfik Member (Nøhr-Hansen, 1997). Palynomorphs are not preserved in the lower parts of the Anariartorfik Member, but it is thought that the lower parts were deposited during the middle and/or late Cenomanian to (?)Coniacian (Dam et al., 2009). The lower part of the Anariartorfik Member is within the tectonostratigraphic subsidence phase, whereas the upper (Campanian–Maastrichtian) part of the member is within the late rift phase.

Late rift phase

The late rift phase occurred during the Late Cretaceous (Campanian–Maastrichtian) and earliest Cenozoic (Danian) and corresponds to the tectonostratigraphic sequences TSS 3 to TSS 6 (Dam et al., 2009) of the Nuussuaq Basin (Fig. 3). The phase included significant faulting that formed an angular unconformity between the Qilakitsoq Member (Atane Formation) and the Aaffarsuaq Member (Itilli Formation) in the Aaffarsuaq valley, central Nuussuaq (Dam et al., 2000). Gregersen et al. (2018, 2019) identified the unconformity between the late rift phase and drift phase (horizon F1) in offshore seismic sections north and south of the areas covered by volcanic rocks. The late rift phase includes the Kangilia, Agatdal, and Quikavsak formations. The Kangilia Formation is of upper Maastrichtian and Danian age and the Cretaceous–Tertiary boundary is located in the lower part of the formation (Nøhr-Hansen and Dam, 1997). The Kangilia Formation, as well as the Danian Agatdal and Quikavsak formations, are described below.

Aaffarsuaq Member. This member of the Itilli Formation is known from outcrops in central Nuussuaq (the Aaffarsuaq valley) and includes lower Campanian deep-water marine mudstone and sandstone units. The lower boundary of the Aaffarsuaq Member is an erosional unconformity toward the Qilakitsoq Member (Atane Formation). Outcrops show an angular unconformity between northward-dipping strata of the Atane Formation and horizontal strata of the Itilli Formation (Dam et al., 2000). The Qilakitsoq Member is of upper Santonian and locally lowermost Campanian age. The Aaffarsuaq Member is early Campanian or younger. The biostratigraphic data thus place a line of events within a narrow time interval. Deposition of nearly horizontal deltaic deposits continued until the earliest Campanian. The strata were faulted, and eroded during a transgression. The resulting angular unconformity is overlain by nearly horizontal, deep-water marine deposits of early Campanian age (Dam et al., 2000, 2009; Pedersen and Nøhr-Hansen, 2014).

Cretaceous paleontology and biostratigraphy

Paleontological studies of the Nuussuaq Basin have been carried out since 1883 when O. Heer first described the fossil macroflora of West Greenland. Later contributions to the paleontology of the Nuussuaq Basin took place during the 18 "Nuussuaq Expeditions" between 1938 and 1968, of which 16 were led by Rosenkrantz (1970). Since 1968, the former Geological Survey of Greenland (GGU), now the Geological Survey of Denmark and Greenland (GEUS), has carried out numerous hydrocarbon and coal-related studies. A detailed historical review of the geological studies of the Nuussuaq Basin is given in Dam et al. (2009). Paleontological studies of the Cretaceous in the Nuussuaq Basin are illustrated in Figure 24.

Phytopaleontology. Heer (1883a, b) described Steenstrup's collection of several hundred plant fossils from the Nuussuaq Basin and divided the Cretaceous (late Aptian to late Santonian) flora into the Kome, Atane, and Paatuut floras (Fig. 24). The plant fossils, which Heer referred to as the Kome flora, were collected from the Kome and Slibestensfjeldet formations. The samples containing the Atane flora were collected at several localities, representing the Skansen, Kingittoq, and Qilakitsoq members. The Paatuut flora is derived from the Qilakitsoq Member.

Heer (1883b) described plant fossils from Upernivik Næs as part of the lower Atane flora, whereas Koch (1964) recognized a separate flora (Upernivik Næs flora). Recently, this has been named the Upernivik flora (Boyd, 1998). Pedersen (1968, 1976) revised the genera in the Kome flora. The contemporaneous, or slightly older, flora in the Ikorfat area forms the separate Ikorfat flora (Boyd, 1998). This latter work also established the distinct Ravn Kløft flora, which is broadly contemporaneous with the Upernivik Næs flora of Rosenkrantz (1970). Boyd (1998) suggested a lower Atane (ATK) flora described from plant beds at Atanikerluk (Fig. 18c) and an upper Atane (IDG) flora described from plant beds between Pingu and Qullissat (Fig. 18c). The Paatuut flora was interpreted by Boyd (1990, 1992, 1993, 1994).

Macrofauna. Birkelund (1956, 1965) established a Late Cretaceous (late Turonian to late Maastrichtian) ammonite biostratigraphy. The oldest ammonite recorded is a fragment of *Scaphites* cf. *corvensis* from the Umiivik Member (Itilli Formation) at Svartenhuk Halvø. This species indicates a latest Turonian age, but was not collected in situ (Birkelund, 1965, p. 158). The ammonites *Scaphites preventricosus svartenhukensis* (Birkelund), *Clioscaphites* sp. aff. *saxitonianus* (McLearn) and *Haresiceras* spp. from the Umiivik Member have been described from several localities on Svartenhuk Halvø, indicating a Coniacian to early Campanian age for the upper part of the Umiivik Member (Birkelund, 1965; Fig. 19, 24).

The ammonites *Scaphites* cf. *Svartenhukensis*, *Scaphites ventricosus, Clioscaphites* sp. aff. *Saxitonianus*, and *Baculites codyensis* from the Qilakitsoq Member of the Atane Formation indicate an early and/or middle Coniacian to late Santonian age. The ammonites *Baculites obtusus* found at Scaphitesnæsen in Turritellakløft (Agatdal, Central Nuussuaq) indicate a latest early Campanian to earliest middle Campanian age for the Aaffarsuaq Member of the Itilli Formation. Late Campanian ammonites (e.g. *Scaphites (Hoploscaphites) ikorfatensis* and *S. (H.) greenlandicus*) occur at several localities along the north coast of Nuussuaq in the Umiivik Member of the Itilli Formation.

The Maastrichtian of Nuussuaq, central West Greenland, has yielded two successive ammonite faunas. They were revised by Kennedy et al. (1999) on the basis of new stratigraphical and dinocyst data. The older early Maastrichtian assemblage, with *Hoploscaphites angmartussutensis* belongs to the *Cerodinium diebelii* palynofloral interval of Nøhr-Hansen (1996) and occurs in reworked concretions in the 'Danian Oyster-ammonite Conglomerate Bed' of the Kangilia Formation in Agatdalen. A younger monospecific assemblage with *H.* aff. *H. angmartussutensis* occurs within 10 m of the Cretaceous–Cenozoic boundary in the lower part of the Kangilia Formation at northern Nuussuaq and belongs to the *Wodehouseia spinata* palynofloral interval of Nøhr-Hansen (1996). None of the ammonites collected are accompanied by mudstone that contains the dinocysts markers for the uppermost Maastrichtian.

A sparse fauna of marine bivalves, including *Sphenoceramus patootensis, Sphenoceramus pinniformis*, and *Oxytoma tenuicostata,* and echinoids is known from the Qilakitsoq Member of the Atane Formation at southern and central Nuussuaq (Ravn, 1918; Olsen and Pedersen, 1991). Rosenkrantz (1970) reported large bivalve shells of the early Campanian inoceramid *Sphenoceramus* from the Aaffarsuaq Member (Itilli Formation).

Terrestrial palynology and zonation. The terrestrial palynology of the Albian to Santonian succession was examined by Ehman and others (D.A. Ehman, D.E. Dodero, and J.C. Wise, unpub. GEUS Report File 17592, 1976), Ehman (D.A. Ehman, unpub GEUS Report File 17594, 1977), and McIntyre (D.J. McIntyre, unpub. Department of Natural Resources Canada Paleontological report 2-DJM-1993, 1993; D.J. McIntyre, unpub. Department of Natural Resources Canada Paleontological reports 3-DJM-1994, 6-DJM-1994, and 13-DJM-1994, 1994). Koppelhus and Pedersen (1993) described the spore and pollen flora from the upper Albian to Cenomanian Skansen Member of the Atane Formation. Croxton (1976; C.A. Croxton, unpub. GEUS Report File 16961, 1978; C.A. Croxton, unpub. GEUS Report File 28069, 1978) considered the terrestrial palynology of the entire Cretaceous sedimentary succession of the region and tentatively dated and divided the succession into three parts based on the pollen content: an Albian to late Cenomanian assemblage without angiosperm pollen, a Turonian to middle Campanian assemblage with angiosperm pollen, and a late Campanian to late Maastrichtian assemblage with *Aquilapollenites* spp.

Lanstorp (1999) described the terrestrial palynomorphs from three sections through the Atane Formation on the south coast of Nuussuaq (Tartunaq, Atanikerluk, and Paatuut West) and divided the spore and pollen assemblages into two biozones, of which one has two subzones (Fig. 24): the *Rugubivesiculites rugosus–Retitricolpites georgensis* Assemblage-Zone, *Cycadopites* Subzone of middle–late Albian age, the *Rugubivesiculites rugosus–Retitricolpites georgensis* Assemblage-Zone, *Tricolporopollenites* Subzone of early Cenomanian age, and the *Pilosisporites* sp. A–*Hazaria sheopiarii* Assemblage-Zone of late Santonian–early Campanian age. The common occurrences of the acritarch *Limbicysta*, together with dinocysts belonging to the genus *Nyktericysta*, indicate that upper Albian nearshore marine environments were probably brackish. These acritarch and dinocyst species are also common in the Sverdrup Basin, Canadian Arctic Islands (MacRae et al., 1996; Pedersen and Nøhr-Hansen, 2014).

Marine palynological zonation and marine palynological events. Nøhr-Hansen (1996) divided the (?)upper Turonian to upper Maastrichtian succession into 10 intervals based on Upper Cretaceous dinocyst biostratigraphy. The lower six intervals are based on samples from shallow cores near Umiivik and are within the Umiivik Member of the Itilli Formation. These are dated (?)late Turonian to (?)early Campanian. The *Aquilapollenites* interval is of early to middle Campanian age and is within the Aaffarsuaq Member (Itilli Formation) at central Nuussuaq. The *Isabelidinium cooksoniae* interval is of upper Campanian age and is within the Umiivik Member (Itilli Formation). These were sampled from shallow cores and outcrops west of Ikorfat, north coast of Nuussuaq. They are also found within the Anariatorfik Member (Itilli Formation) in the GRO#3 borehole southwestern Nuussuaq. The two youngest Maastrichtian intervals within the Kangilia Formation are recorded along the north coast of Nuussuaq west of Ikorfat (Nøhr-Hansen and Dam, 1997). Pedersen and Nøhr-Hansen (2014) improved and expanded the Cretaceous biostratigraphy from the Nuussuaq Basin, with more than 40 marine and terrestrial palynological events recorded from the Albian to Maastrichtian succession (Fig. 24).

Offshore successions

No Cretaceous successions have been drilled offshore central West Greenland, where the deepest explorations wells (Alpha-1 S1, Delta-1, and Hellefisk-1) terminated in Paleogene volcanic rocks (Fig. 3); however, based on geophysical modelling and the general setting, it is likely that Paleocene volcanic rocks (Fig. 25a) overlie older sedimentary rocks. Seabed samples offshore central West Greenland include Cretaceous and Paleocene rocks (*see* below).

A low-velocity zone below the Hellefisk-1 well (Funck et al., 2012; Fig. 25b) as well as gravity modelling and seismic interpretation (Skaarup, 2001, 2002; Fig. 25c) indicate a sedimentary interval between Paleogene basalt successions and underlying basement. In addition, comparison between the Upper Cretaceous oils and possible source rocks in the Nuussuaq Basin and Ellesmere Island and areas farther south offshore Canada indicate a Cretaceous seaway between Canada and Greenland (Bojesen-Koefoed et al., 2004). Major Cretaceous sedimentary basins have been mapped and documented from wells in northeastern Baffin Bay and south of about

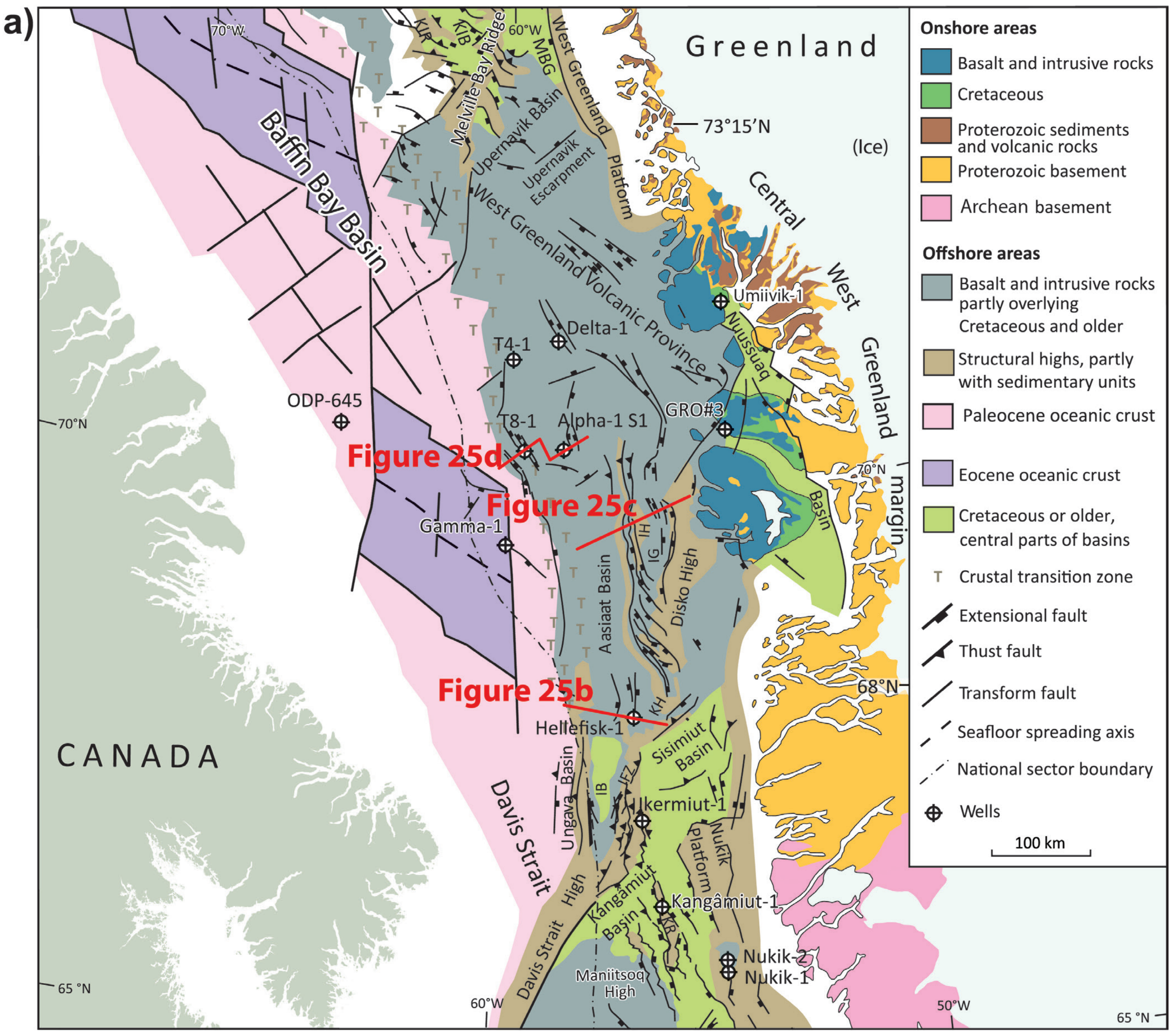

Figure 25. a) Geological map of the central West Greenland margin with main structures and basins (same as Fig. 18a). Wells and seismic sections in Figures 25b–d are shown.

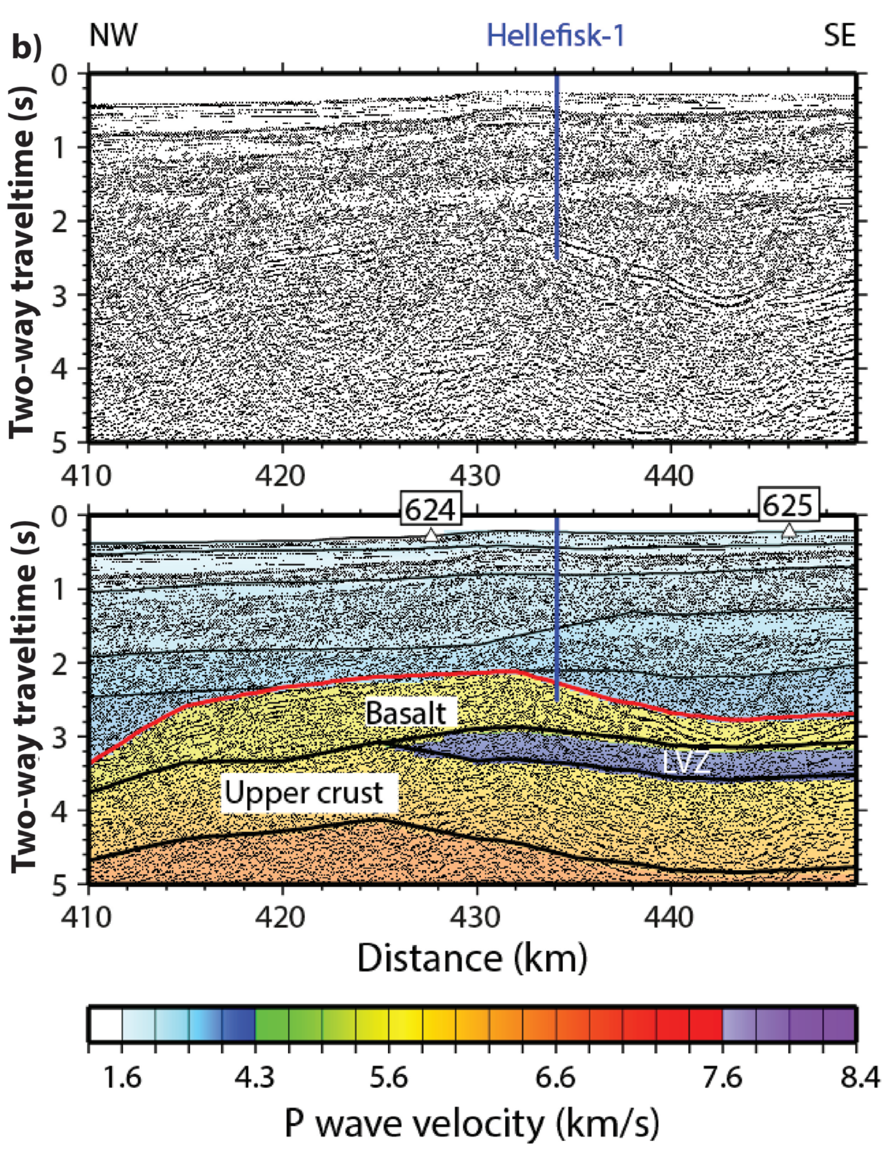

Figure 25 (cont.) b) Seismic section northwest-southeast at the Hellefisk-1 well shown with no interpretation (upper profile) and with P-wave velocities (km/s) from a refraction model (lower profile). 'LVZ' is a low velocity zone below basalt (Funck et al., 2012).

latitude 68°N (Gregersen et al., 2013, 2018, 2019), and from the Nuussuaq Basin, where Cretaceous to Danian sedimentary rocks are partly covered by volcanic successions (Chalmers et al., 1999; Dam et al., 2009).

Prevolcanic sedimentary basins are thus inferred to extend from the Nuussuaq Basin to the Ilulissat Graben and Aasiaat Basin and connect to other basins to the north and to the south in the West Greenland margin as illustrated in Figures 3 and 4.

Offshore Cretaceous paleontology and biostratigraphy

Seabed sampling (dredge and gravity core) was carried out in 2006 in the region from the Nuussuaq Basin to the western Aasiaat Basin (F. Dalhoff and L.M. Larsen, unpub. report, 2007). Many of the samples probably represent ice-rafted debris, but some may be clasts eroded from marine subcrops. The dredge samples include Precambrian basement rocks (mostly) and basaltic rocks (about 3–30%) with minor sedimentary rocks (less than 5%; F. Dalhoff and L.M. Larsen, unpub. report, 2007). Some of the sedimentary rocks contain Cretaceous–Paleocene palynomorphs (F. Dalhoff, J.A. Bojesen-Koefoed, L.M. Larsen, J.R. Ineson, S. Stouge, H. Nøhr-Hansen, E. Sheldon, and F.G. Christiansen, Geological Survey of Denmark and Greenland, unpub. report, 2008), further evidence for the likelihood of Cretaceous strata in parts of offshore central West Greenland.

Early Cenozoic

Onshore successions

The late rift and drift phases occurred during the latest Cretaceous and early Cenozoic along central West Greenland (Fig. 3). Intense volcanic activity dominated the area, both onshore and offshore, during the Paleocene and Eocene (Larsen et al., 2016). The upper part of the Nuussuaq Group is overlain by the West Greenland Basalt Group, which consists of more than 5 km of well exposed volcanic rocks in the Nuussuaq Basin (Fig. 20, 22; *see also* Fig. 31) (Clarke and Pedersen, 1976; Larsen, 1977; Larsen and Pulvertaft, 2000; Pedersen et al., 2006b, 2017, 2018).

Latest Cretaceous and early Cenozoic tectonostratigraphic phases and lithostratigraphy of the Nuussuaq Group

The late rift phase

This tectonostratigraphic phase took place from the Campanian–Danian to the earliest Selandian and includes the tectonostratigraphic sequences TSS 3 to TSS 6 of Dam et al. (2009). The Cretaceous–Cenozoic boundary has been identified in the lower part of the Kangilia Formation between TSS 4 and TSS 5 (Nøhr-Hansen and Dam, 1997; Dam et al., 1998c, 2009).

The (?)upper Maastrichtian Kangilia Formation truncates the Umiivik Member in outcrops at Kangilia and Annertuneq and in the GANT#1 borehole (Fig. 18c). In the GRO#3 well, the contact between the Anariartorfik Member and the Kangilia Formation is also interpreted as erosional (Dam et al., 2009). Subsequently, the

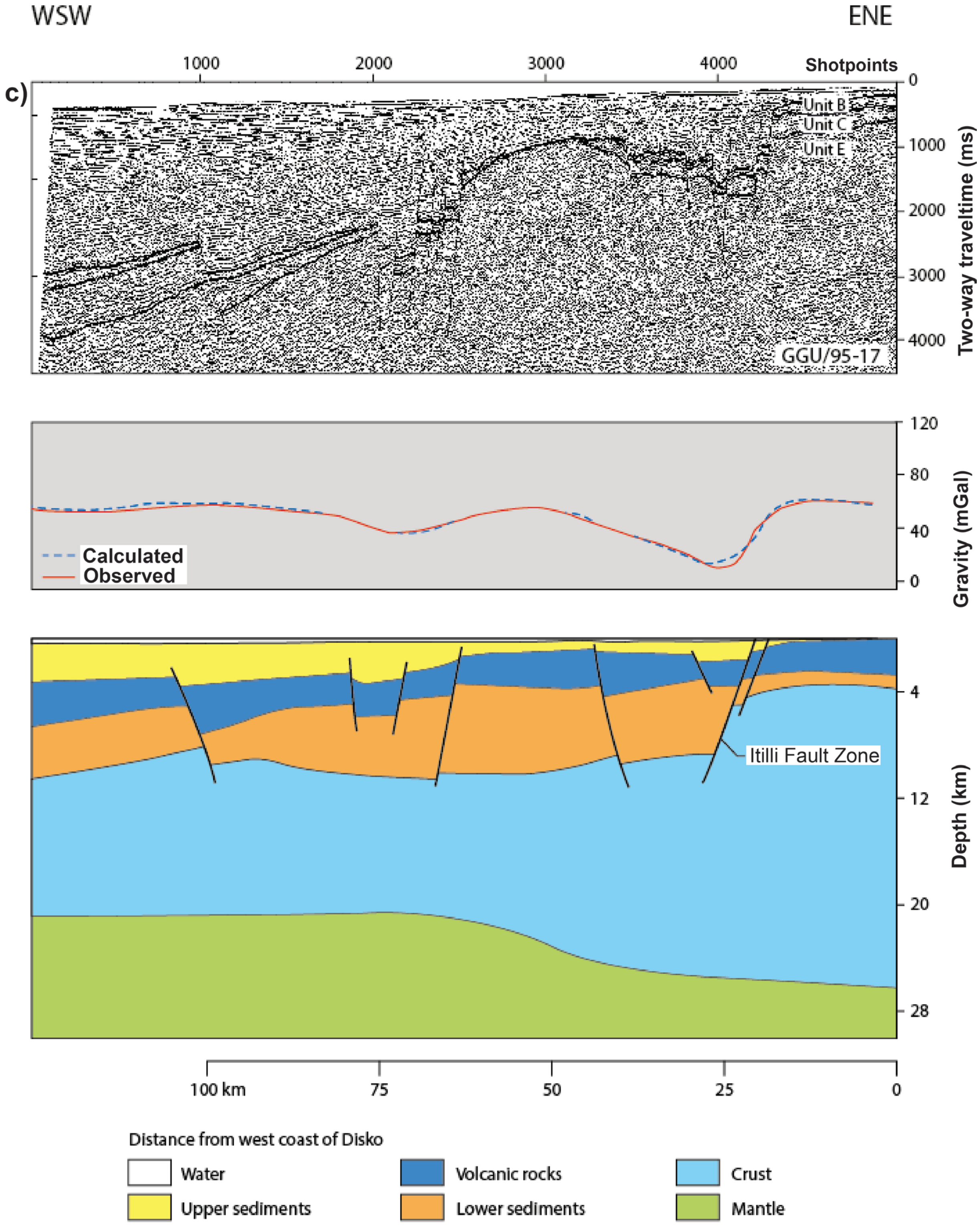

Figure 25 (cont.) c) Seismic section west-southwest–east-northeast with interpreted horizons of the Paleogene volcanic succession divided into seismic stratigraphic units. In addition, the figure shows Bouger gravity data and model and a geological model along the same section (Skaarup, 2002).

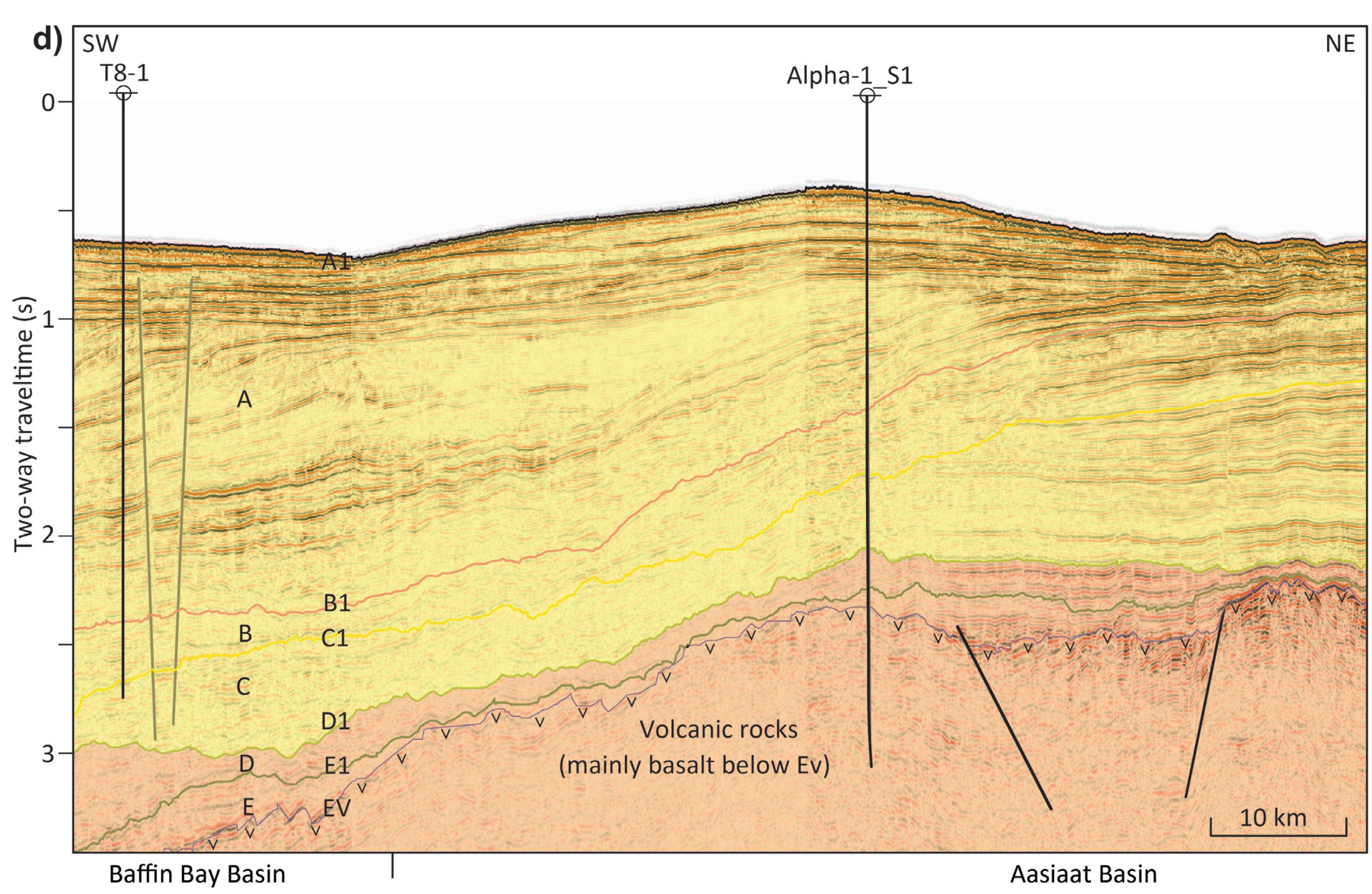

Figure 25 (cont.) d) Seismic section northeast-southwest through the T8-1 and Alpha-1 S1 wells, showing the approximately 2 km thick volcanic succession overlain by Eocene mudstone of mega-unit E (Gregersen et al., 2019). Seismic data courtesy of Capricorn Greenland Exploration (Cairn Energy PLC).

marine Agatdal and the fluvial Quikavsak formations were deposited in incised valley systems. The inferred rapid changes in relative sea level are interpreted to have been related to the arrival of a mantle plume causing uplift and erosion prior to eruption of the West Greenland Basalt Group (Dam and Nøhr-Hansen, 2001).

Kangilia Formation. In the late Maastrichtian, marine-incised valleys with considerable relief define the lower boundary of the Kangilia Formation (Fig. 23) (Dam et al., 2009). In northern Nuussuaq, valleys are eroded into the Itilli Formation and the valley floors are overlain by the Annertuneq Conglomerate Member, which is up to 140 m thick, and deposited from channellized, high-density turbidity currents. In southern Nuussuaq, at Ataata Kuua, a submarine valley eroded into the Atane Formation is interpreted as a sequence boundary associated with uplift and formation of a hiatus in the eastern part of the Nuussuaq Basin (Dam et al., 1998a, 2009; Dam and Nøhr-Hansen, 2001; Fig. 22). The Cretaceous–Cenozoic boundary has been identified above the Annertuneq Conglomerate Member (Fig. 23; Nøhr-Hansen and Dam, 1997). The Kangilia Formation is characterized by dark mudstone with thin sandstone beds deposited from low-density turbidity currents. In northern Nuussuaq, the formation is up to 440 m thick and is of late Maastrichtian to Danian age (Dam et al., 2009).

Quikavsak Formation. The Danian Quikavsak Formation fills two valley systems incised into the Atane and the Kangilia formations in southern Nuussuaq. The formation is divided into three members, the Tupaasat, Nuuk Qiterleq, and Paatuutkløften members (Fig. 26). The Tupaasat Member is dominated by coarse-grained fluvial sandstone and overlies a marked erosional surface. The Nuuk Qiterleq Member consists of sandstone and mudstone with numerous in situ and drifted remains of trees. The lower boundary of the Paatuutkløften Member is an erosion surface and truncates the two older members. It consists of medium- to coarse-grained, fluvial to estuarine sandstone in an overall fining- and thinning-upward succession (Fig. 19, 22, 26; Dam and Sønderholm, 1998; Dam and Nøhr-Hansen, 2001; Dam, 2002).

The incised valley systems formed during two tectonic phases of uplift. The first created the erosional boundary between the deep-water turbiditic mudstone of the Kangilia Formation and the fluvial sandstone of the Tupaasat Member. The second phase formed the erosional lower boundary of the Paatuutkløften Member. This member is overlain by deep-water marine mudstone of the Eqalulik Formation, indicating a phase of rapid subsidence in the late Danian (Dam et al., 2009).

Agatdal Formation. This formation is known from central and western Nuussuaq, the Agatdal area, and the GRO#3 well. The formation includes marine mudstone with several thick, lenticular conglomerate and sandstone units (Fig. 27). The sandstone intervals of the Agatdal Formation are rich in marine invertebrate fossils (Rosenkrantz, 1970; *see also* Dam et al., 2009). The macrofossils indicate a relatively shallow, marine depositional environment (Petersen and Vedelsby, 2000). In contrast, the sedimentary mudstone and intercalated conglomerate are interpreted as deposited from high- and low-density turbidity currents in submarine channels in a slope environment. The fossils are thus redeposited (Dam et al., 2009).

Most fossil groups indicate a late Danian age for the formation, possibly during nannoplankton zones NP3–lower NP4. In the GRO#3 well, dinocysts and nannofossils indicate an age not younger than NP4 (late Danian or early Selandian; Nøhr-Hansen et al., 2002; *see* below Fig. 28). The age of the Agatdal Formation suggests that it is coeval with the incised valley systems of the Quikavsak Formation in southern Nuussuaq and with most of the upper part of the Kangilia Formation in northern Nuussuaq (Nøhr-Hansen et al., 2002).

Drift phase

This phase is recorded by the middle Paleocene–Eocene succession and includes the tectonostratigraphic sequences TSS 7 and TSS 8 of the Nuussuaq Basin (Dam et al., 2009; Fig. 3). The drift phase includes the marine Eqalulik Formation and the nonmarine Atanikerluk Formation (Fig. 19). Some relatively thin, intravolcanic

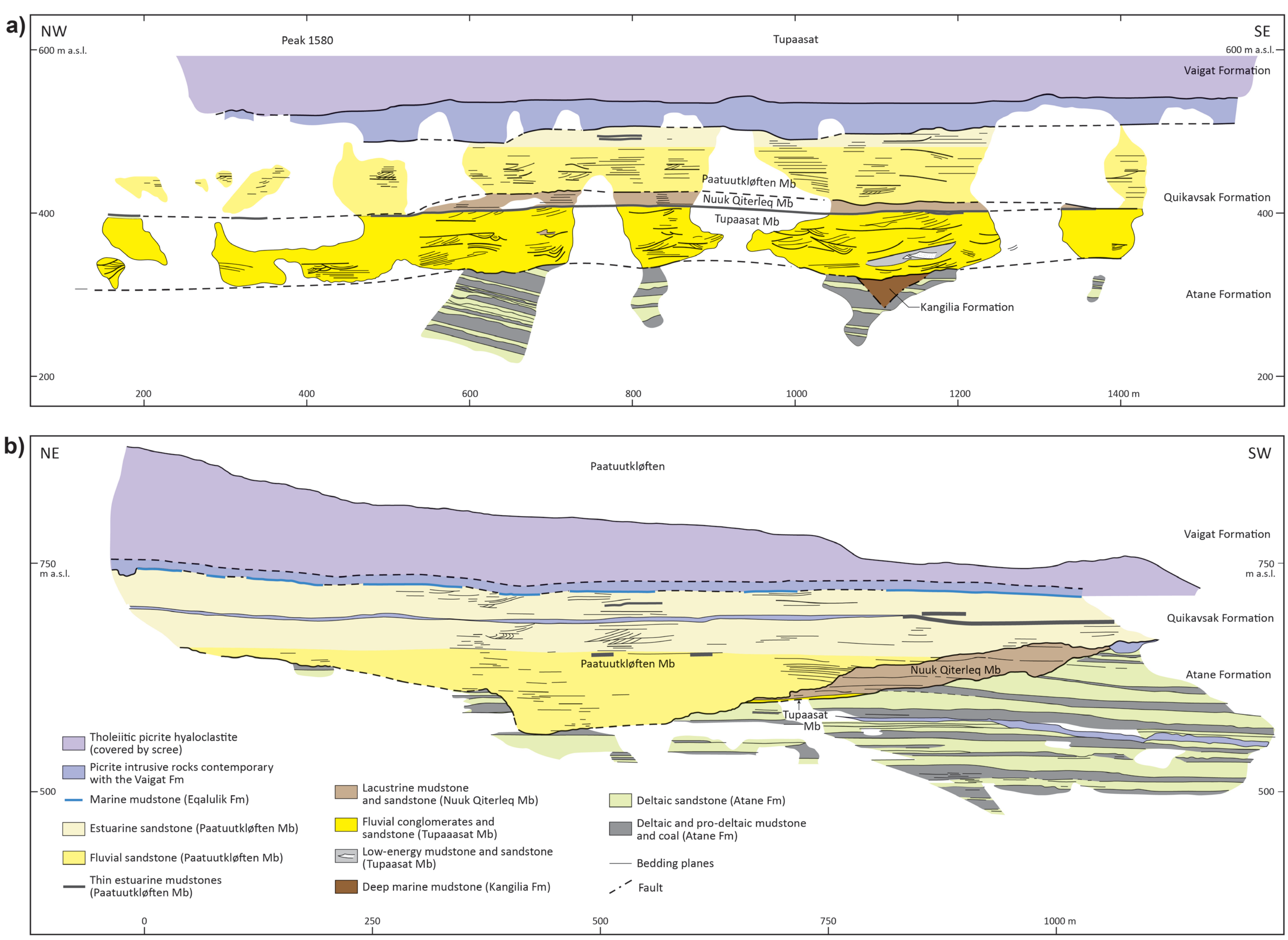

Figure 26. The Quikavsak Formation comprises the fill of two incised valleys that formed during the late rift phase. The upper diagram shows a section parallel to the valley, the lower diagram is a cross-section. The fluvial sandstone units of the Tupaasat Member filled the oldest valley and were deposited during catastrophic flows (Dam, 2002). The overlying Nuuk Qiterleq Member represents fluviolacustrine deposits. Both of these members were truncated by the second phase of incision, which was followed by deposition of fluvial and estuarine sandstone units (the Paatuutkløften Member). Outcrops at the south coast of Nuussuaq, between Paatuut and Nuuk Qiterleq (Fig. 18c). Horizontal and vertical distances in metres (Dam et al., 2009). Dashed lines are inferred lithostratigraphic boundaries.

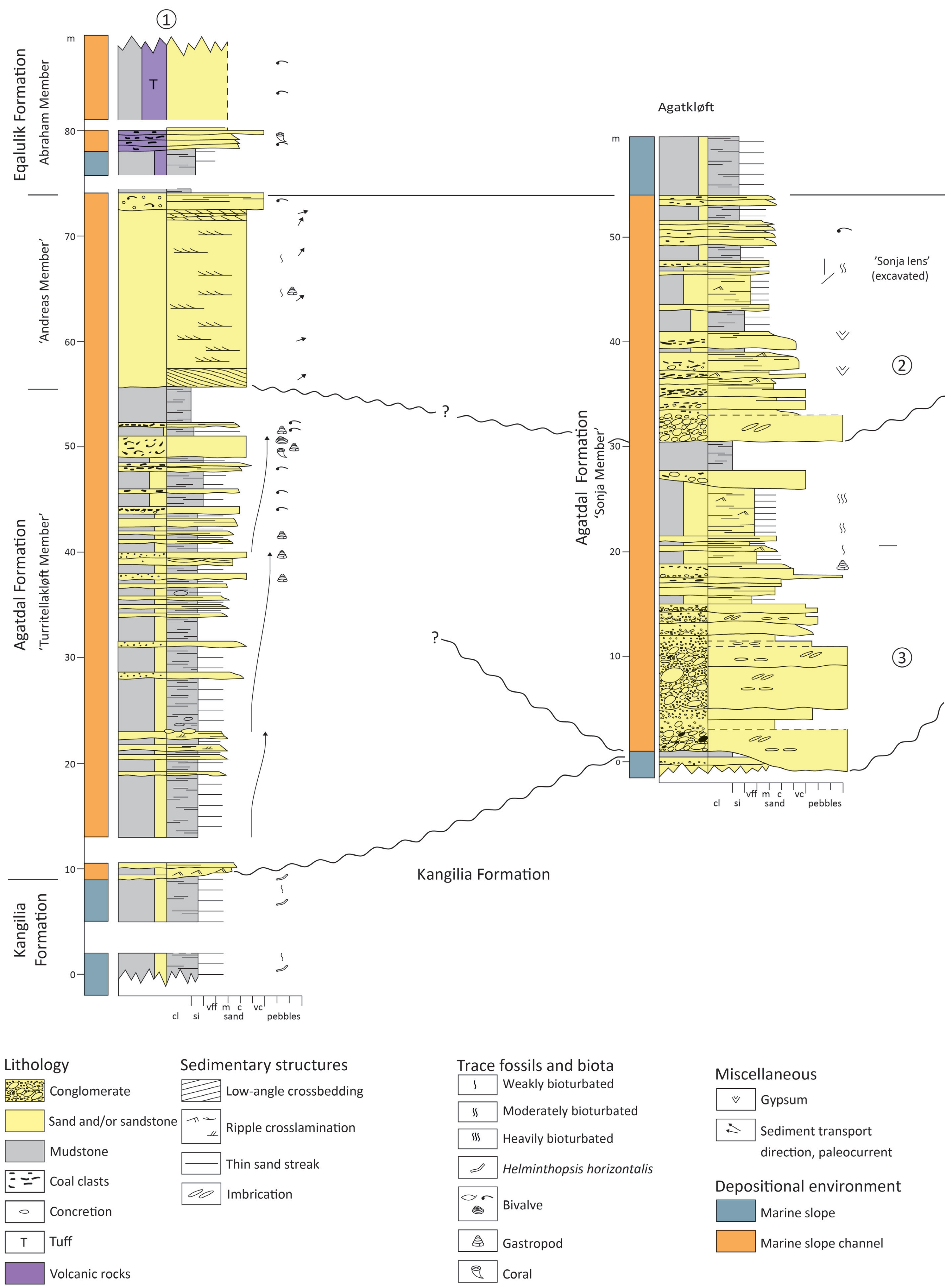

Figure 27. Schematical logs of the Agatdal Formation, Agatdalen in central Nuussuaq. The mudstone and conglomerate units were deposited in a submarine canyon. Note the erosional surfaces, and the vertical and lateral changes in lithology. The formation has yielded a rich assemblage of invertebrate fossils. Shallow-marine macrofossils are preserved in deep-water mudstone. Long arrows indicate upward-coarsening successions. For location *see* Figure 18c (Dam et al., 2009).

sedimentary units, overlain by the Svartenhuk Formation, are briefly described below in the section on the lower Cenozoic volcanic succession (*see* below Fig. 30).

Eqalulik Formation. The formation includes mudstone, tuff beds, and volcaniclastic sandstone, but sedimentary structures are rarely recognized due to poor exposures and scree. The type section is defined in the GANE#1 well, where the formation is 100 m thick (Dam et al., 2009: their Fig. 119, 121). The macrofossils and the dinocysts indicate a marine depositional environment. Water depths up to 700 m have been estimated from the height of the foresets in the overlying hyaloclastite breccia units illustrated by Figures 85 and 87 in Pedersen et al. (2017).

The tuff layers in the Eqalulik Formation may be correlated with the volcanic Anaanaa and Naujánguit members of the Vaigat Formation (Fig. 19, 28, 29). The Eqalulik Formation is visibly diachronous, reflecting the progressive eastward progradation of the hyaloclastite fans of the Vaigat Formation (Pedersen et al., 2006a, b; Dam et al., 2009); however, the biostratigraphic resolution is rarely good enough to resolve this diachronism. The Anaanaa Member is normally magnetized and correlates to magnetic polarity Chron C27n, 62.5–60.2 Ma (Storey et al., 1998; Riisager and Abrahamsen, 1999; Larsen et al., 2016). A latest Danian–early Selandian age (upper NP4 zone) was determined for the lowermost part of the Eqalulik Formation (Nøhr-Hansen et al., 2002; Fig. 28). Dinocysts from sedimentary rocks associated with the Naujánguit Member correlate to NP5–NP6 zones (Piasecki et al., 1992).

The Eqalulik Formation includes the Abraham Member, which is restricted to central Nuussuaq (Dam et al., 2009). The member is 10–20 m thick and consists of black fossiliferous mudstone and grey sandy mudstone with fossiliferous reworked volcaniclastic sandstone and tuff units derived from the Ilugissoq graphite andesite volcano (Pedersen and Larsen, 2006; Pedersen et al., 2017, p. 109–120).

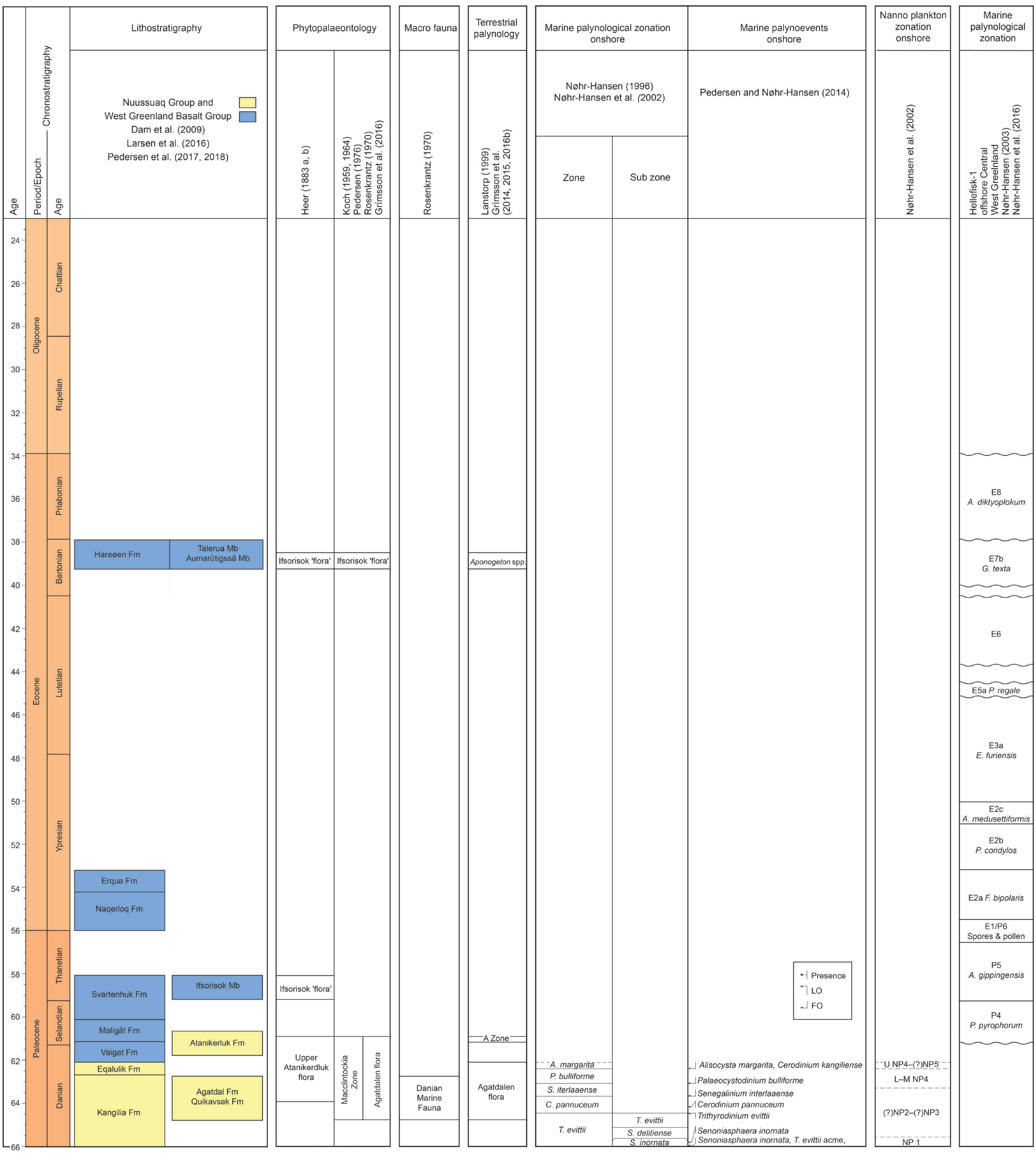

Figure 28. Biostratigraphy of the early Cenozoic deposits onshore and offshore central West Greenland. The zonation of the onshore deposits is based on phytopaleontology, macrofauna, marine and terrestrial palynology, and the marine nannoplankton zonation. Offshore deposits of the Hellefisk-1 well are divided into marine palynological zones. FO = First occurrence; LO = Last occurrence. Includes data from publications listed in the top of the diagram.

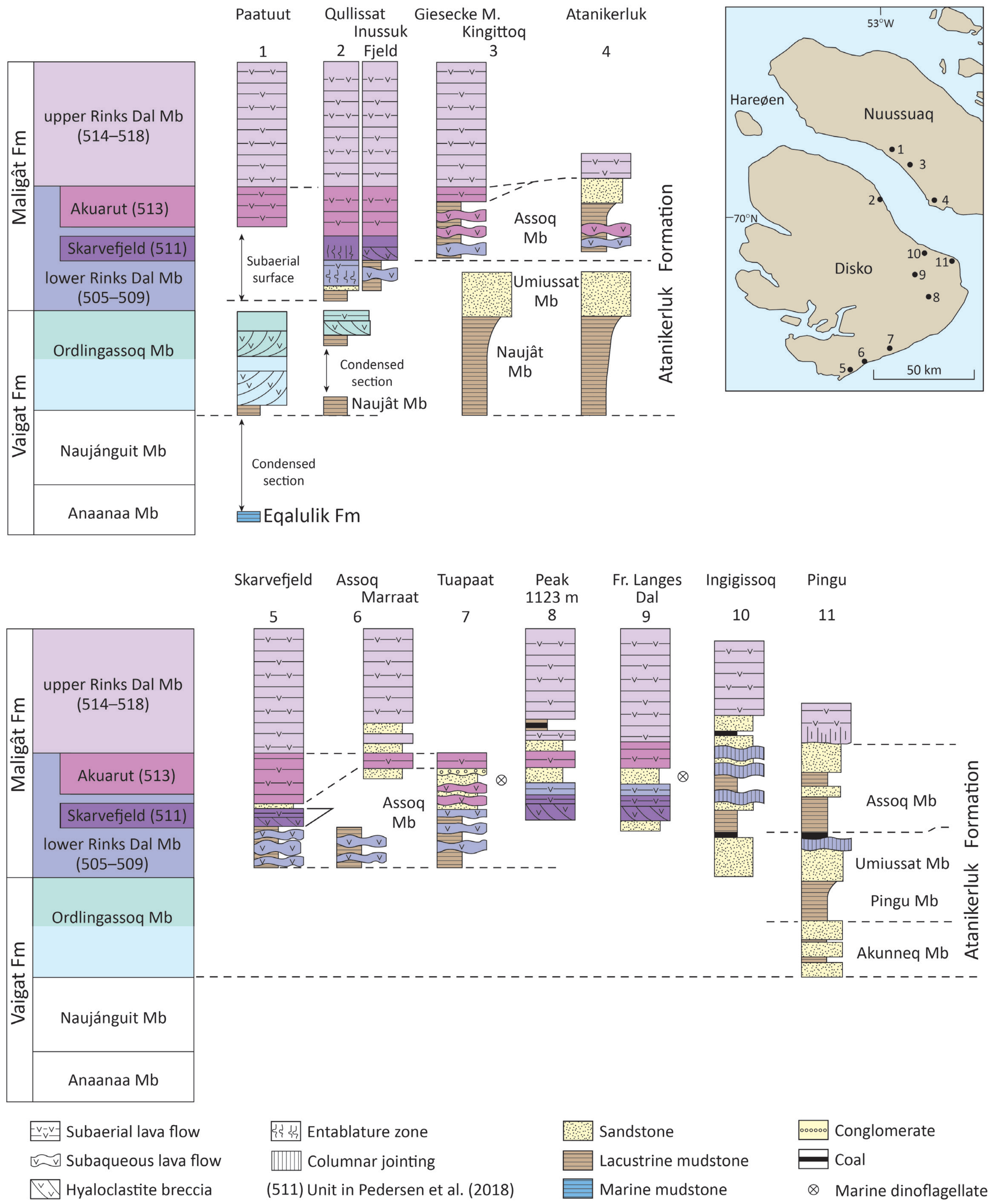

Figure 29. The Atanikerluk Formation comprises nonmarine synvolcanic deposits accumulated in lacustrine and fluvial environments. Two coarsening-upward successions are correlated with the volcanic lithostratigraphy. Location of the schematic logs are shown on the inset map. The numbers 505–518 are lithological unit codes, *see* Pedersen et al. (2018). Giesecke M. = Giesecke Monument, Fr. Langes Dal = Frederik Langes Dal. Dam et al. (2009).

Atanikerluk Formation. This formation, present in eastern Nuussuaq and at Disko, is up to 500 m thick and comprises nonmarine, early synvolcanic black shaly mudstone, grey mudstone interbedded with thin layers of sandstone or tuff, heterolithic sandstone, and fine-grained friable sandstone. The lacustrine and fluvial Atanikerluk Formation is subdivided into five members, of which the Akunneq Member is known only from northeast Disko (Fig. 28; Pedersen et al., 1998; Dam et al., 2009). Two coarsening-upward sedimentary successions are recognized. The lower succession includes the Naujât or Pingu members and is overlain by the Umiussat Member. The upper succession consists of the Assoq Member. The Atanikerluk Formation correlates with the volcanic Ordlingassoq Member (Vaigat Formation) and with the Rinks Dal Member (Maligât Formation) and thus is younger than the Eqalulik Formation (Fig. 19, 28, 29). Both the Ordlingassoq and the Rinks Dal members have been Ar-Ar dated to 60–61 Ma within Chron C26r (Storey et al., 1998; Riisager and Abrahamsen, 1999; Larsen et al., 2016; Pedersen et al., 2017, 2018). The lower part of the Atanikerluk Formation has yielded macrofossil plants (Koch, 1959, 1963), spores, and pollen, including mid-Paleocene species (Hjortkjær, 1991). Local occurrences of marine dinocysts in the Assoq Member in southern Disko suggest occasional marine inundations (Piasecki et al., 1992; Dam et al., 2009).

Early Cenozoic paleontology and biostratigraphy of the Nuussuaq Basin

Phytopaleontology. Heer (1883a, b) distinguished two Tertiary floras from the Nuussuaq Basin, the 'Upper Atanikerluk A' and the 'Upper Atanikerluk B' flora (Fig. 28). After thorough fieldwork these floras were located by B.E. Koch (1959). The 'Upper Atanikerdluk A' flora represents the middle part of the Quikavsak Formation (the Nuuk Qiterleq Member), and the 'Upper Atanikerluk B' flora occurs in the basal part of the overlying Atanikerluk Formation (the Naujât Member). A Paleocene age was suggested for both floras, as the same species were found in the marine Agatdal Formation that has yielded 27 species (Koch, 1959, 1963). Both floras were referred to the Paleocene Macclintockia Zone (Koch, 1959) spanning the middle Danian to early Selandian interval.

Grímsson et al. (2016b) revised the stratigraphy for the Paleocene Agatdalen flora and stated that many of the fossils originated in the late Danian (64–62 Ma) Agatdal Formation, the remainder belonging to either the Agatdal Formation or the overlying Eqalulik Formation.

Heer (1883a, b) also described a limited flora from western Nuussuaq (Ifsorisoq) and Hareøen (Aumarûtigssâ). Koch (1963) questioned whether the different outcrops represent the same or different stratigraphic levels of intravolcanic sediments. At Ifsorisoq, the flora is preserved in tuff layers of the intravolcanic Ifsorisoq Member (Fig. 30). It correlates with the upper part of the volcanic Svartenhuk Formation, which is (?)Thanetian (Larsen et al. 2016). At Hareøen, the middle Eocene Aumarûtigssâ Member forms the lower part of the Hareøen Formation (Grímsson et al., 2015; Larsen et al., 2016).

Terrestrial palynology and zonation. The pollen of the Danian (lower Paleocene) Agatdalen flora has been studied by Grímsson et al. (2016b) and the spores and pollen of the Selandian Atanikerluk Formation have been studied by Croxton (1976; C.A. Croxton, unpub. GEUS Report File 16961, 1978, C.A. Croxton, unpub. GEUS Report File 28069, 1978), Hjortkjær (1991), Larsen et al. (1992), Lanstorp (1999) and D.J. McIntyre (pers. comm., 2009). Lanstorp (1999) suggested an A Zone age based on the presence of the genus *Alnipollenites* for the Naujât Member (lower part of the Atanikerluk Formation). The Fagaceae pollen and the *Aponogeton* pollen assemblages were described by Grímsson et al. (2014, 2015, 2016a) from the Eocene Aumarûtigssâ Member at Hareøen (Fig. 28).

Macrofauna and microfauna. The Agatdal Formation is the most fossiliferous of the marine units in West Greenland, with more than 500 described macrofossil species. The mudstone of the former Turritellakløft Member and the sandstone and conglomerate of the former Sonja Member are generally poor in marine fossils, but locally contain a very rich marine fauna, known mainly from the 'Sonja lens'. This lenticular unit was originally 7 m wide and 0.7 m thick and was completely excavated by Rosenkrantz and his co-workers. It yielded a fauna dominated by bivalves and gastropods, but also includes scleractinian corals, octocorals, asteroids, crinoids, echinoids, serpulids, brachiopods, bryozoans, scaphopods, crustaceans, fish, foraminifera, coccoliths, and palynomorphs (Bendix-Almgreen, 1969; Hansen, 1970, 1980; Rosenkrantz, 1970; Szczechura, 1971; Floris, 1972; Perch-Nielsen, 1973; Henderson et al., 1976; Kollmann and Peel, 1983; Collins and Wienberg Rasmussen, 1992; Petersen and Vedelsby, 2000, Rasmussen et al., 2003) (Fig. 27). This suite of fossils are Danian as noted in Figure 19.

Marine palynological zonation and marine palynological events. The dinocyst assemblages of the Kangilia and Agatdal formations were described by Hansen (1980), and dinocysts from the intrabasaltic sediments of the Danian to Selandian Vaigat and Maligât formations were described by Piasecki et al. (1992). Nøhr-Hansen et al. (2002) and Pedersen and Nøhr-Hansen (2014) have established a dinocyst zonation and event stratigraphy for the Danian Kangilia and Eqalulik formations on Nuussuaq. Five dinocyst zones and three subzones were described and correlated with stratigraphically important nannofossils of the nannoplankton zones NP1 to upper NP4 and/or (?)NP5 (Fig. 28).

Petroleum occurrences in the Nuussuaq Basin

Petroleum seepages and stains are widespread in the Nuussuaq Basin (Bojesen-Koefoed et al., 1999). Between the north coast of Disko and the south coast of Svartenhuk Halvø, five different oil types have been documented (the Marraat, the Niaqornaarsuk, the Eqalulik, the Kuugannguaq, and the Itilli oil types) (Christiansen et al., 1996; Bojesen-Koefoed et al., 1999, 2004, 2007; Pedersen et al., 2006c; Bojesen-Koefoed, 2011). Volcanic rocks host the majority of the petroleum occurrences. A series of stratigraphic boreholes from the Melville Bay show the presence of middle Albian and Cenomanian–Turonian source rocks and are discussed in the 'Northern West Greenland basins' section. The petroleum occurrences from West Greenland to Canada are summarized in Bingham-Koslowski, McCartney et al. (this volume).

Paleocene–Eocene volcanism: West Greenland Basalt Group

The Nuussuaq Basin offers excellent exposures of Paleogene volcanic rocks (Fig. 30, 31, 32). These serve as important analogues for the Cenozoic volcanic succession in the offshore (Fig. 18a, b). The Paleocene succession includes a lower formation of picritic hyaloclastite and subaerial lavas (the Vaigat Formation) and two overlying formations of basalt, mainly subaerial lavas (the Maligât and Svartenhuk formations) (Pedersen et al., 2017, 2018) (Fig. 31). The Eocene succession includes three basalt formations, one found regionally (the Naqerloq Formation) and two local formations (the Erqua and Hareøen formations) (Fig. 30). The volcanic development of the Nuussuaq Basin is described below, with comparisons to contemporaneous development elsewhere in Baffin Bay and the Labrador Sea.

Vaigat Formation (Late Danian to Selandian, 62–61 Ma). The Vaigat Formation is globally exceptional because it consists of up to several kilometres of picrites. The volcanic rocks overlie and interdigitate with sediments of the Nuussuaq Basin. They form a north-south elongated volcanic dome extending from Disko to Svartenhuk Halvø, with a maximum stratigraphic thickness in excess of 5 km on Ubekendt Ejland and tapering to the south, east, and north (Fig. 18b). Its southern, eastern, and northern delimitations are depositional, and here the volcanic lithologies are bounded by mudstone and sandstone of the Atanikerluk Formation. To the west, it is interpreted to continue onto the shelf. The Vaigat Formation was deposited during three major volcanic episodes, corresponding to the Anaanaa, Naujánguit, and Ordlingassoq members. The oldest part of the Anaanaa Member is known from drill cores and from a small area in western Nuussuaq. From there, the eruption sites moved gradually eastward, filling the basin with hyaloclastite and subaerial lava flows (Fig. 31; Pedersen et al., 1993, 2017; Larsen and Pedersen, 2009). Whereas the Anaanaa Member and the lower part of the Naujánguit Member are normally magnetized, the major (middle and upper) part of the Vaigat Formation is reversely magnetized. The reversely magnetized rocks are 61.1 ± 2.0 Ma to 61.5 ± 1.0 Ma from Ar-Ar dating (Storey et al., 1998), placing them within magnetic polarity Chron C26r (62.2–59.2 Ma). Thus, the Anaanaa Member is assumed to correlate to Chron C27n (62.5–62.2 Ma) (Riisager and Abrahamsen, 1999; Fig. 30, 32).

Similar picritic volcanic rocks are found at Cape Dyer on Baffin Island (Clarke and Upton, 1971) and are also normally magnetized (Deutsch et al., 1971). Thus they most likely correlate to the Anaanaa Member (Pedersen et al., 2002). Areas with volcanic rocks also extend seaward from Cape Dyer (MacLean et al., 1978; Skaarup et al., 2006). Rocks sampled from drilling near Cape Dyer are described by MacLean et al. (1978) as vesicular, apparently subaerial, olivine-phyric (?picritic). Samples from farther south are described as plagioclase-phyric (?basaltic).

A plate reconstruction at magnetic polarity Chron C27n (62.5–62.2 Ma) shows Cape Dyer and northern Disko situated only 180 km apart (Skaarup et al., 2006; Oakey and Chalmers, 2012), less than the 260 km north-south extent of the onshore exposure of the Vaigat Formation. It is likely that picritic volcanism extended over the whole basinal area between the two margins. Eruption sites would have been local, but the volcanic products, consisting mainly of marine hyaloclastite, could have merged into a coherent deposit. As described in the 'Southern West Greenland basins' section, picrite units of Danian age were also erupted on or along the Davis Strait High about 300 km south of Disko.

Maligât Formation (Selandian, 61–60 Ma). The demise of the Vaigat Formation must have involved the establishment of deep crustal magma chambers where the picritic parent magmas stalled, precipitated olivine, and formed magmas with a basaltic composition that make up the Maligât Formation (Larsen and Pedersen, 2009), which overlies the Vaigat Formation. The Maligât Formation extends over Disko and Nuussuaq east of the Itilli Fault, but not farther north (Fig. 18b; Larsen et al., 2016; Pedersen et al., 2018). It is dated at 61.3 ± 0.8 Ma to 60.2 ± 1.0 Ma (Storey et al., 1998), is reversely magnetized, and erupted within Chron C26r (62.2–59.2 Ma; Riisager and Abrahamsen, 1999). The formation is centred on Disko just south of the dome of the Vaigat Formation and is up to 2000 m thick. It includes the largest number of individual lava flows in western Disko (Pedersen et al., 2003, 2005, 2018). The Maligât Formation is therefore considered to continue westward onto the shelf as part of the large lava plateau observed offshore.

A basalt sill intruding Cretaceous sediments in the southeastern part of Disko Bugt has an age of 60.81 ± 0.88 Ma (Larsen et al., 2009) and is also part of this activity.

In the northern part of the Nuussuaq Basin on northern Svartenhuk Halvø and farther north, this period was presumably a time of volcanic quiescence and erosion, leading to deposition of quartzofeldspathic sediments and reworked volcaniclastic material (Fig. 30).

Svartenhuk Formation (Late Selandian to Thanetian, 60–58 Ma). The Svartenhuk Formation was mapped on Svartenhuk Halvø by Larsen and Grocott (1991) and described by Larsen and Pulvertaft (2000). Larsen and Larsen (2010) noted that the formation consists of two geochemically contrasting parts, a lower succession of low-potassium basalt and an upper succession of geochemically enriched basalt. Larsen et al. (2016) found that the lower part was of late Paleocene age, whereas the upper part was Eocene. They therefore

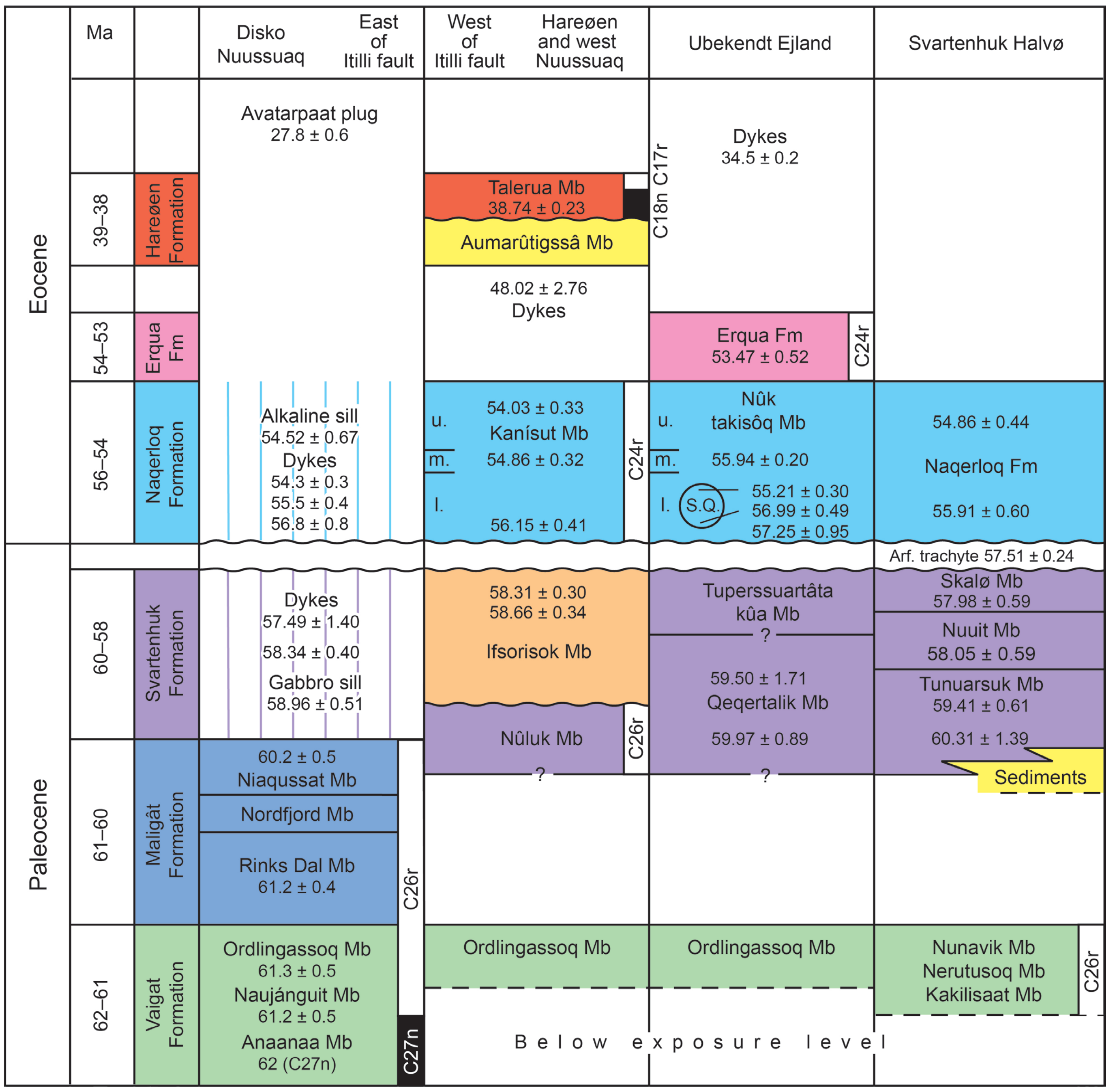

Figure 30. Stratigraphic scheme of the West Greenland Basalt Group in the Nuussuaq Basin. For location of place names *see* Figure 18c. Abbreviations: S.Q. = Sarqâta qáqâ central complex, Arf. trachyte = Arfertuarsuk trachyte flow, l. = Lower, m. = Middle, u. = Upper. Paleomagnetic chrons (C27n to C17r) are indicated. Vertical scale indicates ages, not thicknesses (Larsen et al., 2016).

Figure 31. Hyaloclastite units and subaerial lava flows. Sandstone, mudstone, and thin coal beds (the Upper Cretaceous Qilakitsoq Mb of the Atane Formation) are overlain by volcanic rocks of the West Greenland Basalt Group (Vaigat Formation). The lower, dark part of the volcanic succession (Naujánguit Mb) consists of foreset-bedded hyaloclastite breccia units (Hy) produced by quenching during entry of subaerial lava flows into the sea, with basin fill prograding from left to right in the picture (west to east). The height of the foresets, up to 730 m, indicates the paleo-water depths. The upper, light grey part of the volcanic succession (Ordlingassoq Mb) consists of subaerial picrite lava flows (La). Nuuk Qiterleq, south coast of the Nuussuaq peninsula (Fig. 18c); height of mountain peak 1400 m. Photograph by A.K. Pedersen, 1988.

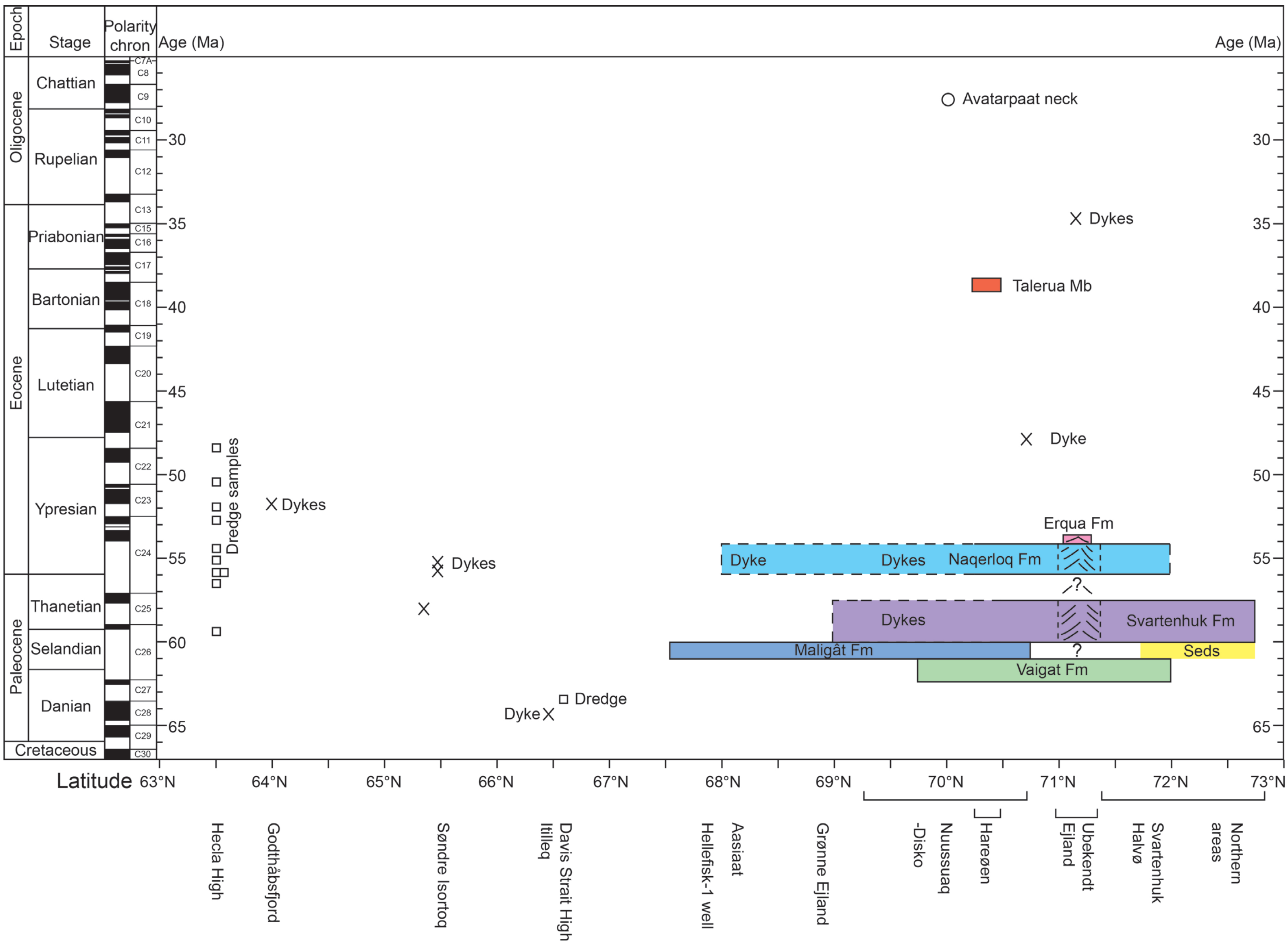

Figure 32. Extent and ages of Tertiary igneous rocks along the West Greenland margin at latitude 63°N to 73°N. Stages and magnetic polarity chrons after the Geological Time Scale 2012 from the International Commission on Stratigraphy (https://www.iugs.org/ics). Refer to Figure 30 for formation and age colour code; the line pattern for Ukekendt Ejland suggests a central volcano. Note that dykes belonging to a volcanic formation may occur outside the current areal extent of the lava succession (Larsen et al., 2016) Seds = Sediments

redefined the Svartenhuk Formation to include only the Paleocene part and defined a new formation, the Naqerloq Formation, for the Eocene interval. This usage is followed here (Fig. 30, 32).

The basalt units of the Svartenhuk Formation extend from Ubekendt Ejland to Svartenhuk Halvø and eastward and northward to latitude 72°45′N. Within the Nuussuaq Basin, the formation overlies the Vaigat Formation and interdigitates with Paleocene sediments. In the northwestern part, it rests on Precambrian gneiss east of the eastern boundary fault. The formation is dated at 60.31 ± 1.39 Ma to 57.98 ± 0.59 Ma (Larsen et al., 2016). Thus, there does not seem to be much age difference, if any, between the latest Maligât Formation and the oldest Svartenhuk Formation and they may be essentially contemporaneous, but originated in different volcanic systems. The younger parts of the formation have ages of 58 Ma and are definitely younger than the Maligât Formation. The Svartenhuk Formation is up to 2000 m thick and there is no indication of thinning toward the coast. Thus, it is likely that the formation continues into the offshore lava plateau.

The Svartenhuk and Maligât formations are distinguishable from each other by small differences in their trace-element chemistry. Widespread dykes on Disko and Nuussuaq have chemical compositions similar to lava flows of the Svartenhuk Formation, and two dated dykes on Disko and a gabbro sill in Disko Bugt have ages around 59–58 Ma. With both ages and chemical compositions identical to those of the Svartenhuk Formation, this strongly suggests that lava units of the Svartenhuk Formation were present on Disko and Nuussuaq, but have been removed by erosion (Fig. 30, 32; Larsen et al., 2016).

The volcanic succession on Ubekendt Ejland evolved independently. The upper Paleocene basalt succession there is compositionally variable and does not correspond to any of the neighbouring successions to the north and south. This suggests that a local central volcanic complex had developed on Ubekendt Ejland at this time.

On Nuussuaq west of the Itilli Fault, there is an undated basalt succession (the Nûluk Member) believed to be around 60 Ma; it is overlain by the Ifsorisok Member, a 200 m thick basaltic mass-flow deposit overlain by 30 m of sediments with tuff layers dated to 58.7 Ma and 58.3 ± 0.3 Ma (Larsen et al., 2016). The mass-flow deposit indicates considerable tectonic movements and related erosion between 60 Ma and 58.7 Ma, when basalt flows of the Svartenhuk Formation were deposited in other areas of the Nuussuaq Basin.

Between the Paleocene (Thanetian) and the Eocene (Ypresian), there was a period of near-quiescence between 58 Ma and 56 Ma (Fig. 30). Where exposures allow observations, the Paleocene volcanic succession is unconformably overlain by the Eocene succession, suggesting tectonic movements during the intervening period; however, the horizon is often poorly exposed and is not well studied. The period encompasses Chron C25n (57.7–57.1 Ma).

Naqerloq Formation dykes, sills, and central intrusion (earliest Ypresian, 56–54 Ma). In contrast to the Paleocene low-potassium magmas, early Eocene volcanism produced geochemically enriched magmas with significantly higher contents of incompatible elements including potassium (Hald, 1976; Larsen, 1977; Larsen and Larsen, 2010). In the Nuussuaq Basin, these basalt flows and some more evolved rocks are referred to as the Naqerloq Formation, dated at 57.2 ± 1.0 Ma to 54.0 ± 0.3 Ma (Larsen et al., 2016). The formation is reversely magnetized (Riisager et al., 1999, 2003) and was erupted during the long magnetic polarity Chron C24r (57.1–54.0 Ma; Fig. 32).

Enriched basalt and subordinate acid tuff units of the Naqerloq Formation form thick lava piles in western Nuussuaq and Hareøen (Kanísut Member), western Ubekendt Ejland (Nûk takisôq Member), and western Svartenhuk Halvø. The formation is preserved in the westernmost coastal areas where it appears as west-dipping faulted blocks and most likely continues in the offshore areas.

Basaltic dykes of a similar enriched composition and a similar early Eocene age occur throughout Disko and Nuussuaq and are considerably more widespread than the present outcrops of the Naqerloq Formation lava succession, which are erosional remnants. The magmas also intruded as thick sills and sheets along the eastern boundary fault toward the gneissic highlands in eastern Nuussuaq. Thus, there is substantial evidence that the Naqerloq Formation originally extended well beyond its present limits and into the southern and eastern part of the Nuussuaq Basin (Fig. 32).

The Naqerloq Formation on Ubekendt Ejland is much more variable than in the areas to the north and south. It contains more acidic rocks and tuffs and some alkaline lavas, suggesting that a central volcanic complex with an underlying magma chamber was well developed at this time (Fig. 32). The Sarqâta qáqâ central intrusive complex, emplaced near the base of the basalt succession on southern Ubekendt Ejland, may represent a high-level intrusion into the volcanic edifice 4–5 km below the surface.

Erqua Formation (Early Ypresian, 54–53 Ma). The Erqua Formation is the youngest lava formation on Ubekendt Ejland. It is reversely magnetized and its age of 53.47 ± 0.52 Ma places it very close to the end of magnetic polarity Chron C24r (54.0 Ma; Fig. 32). Its occurrence in a small area in westernmost Ubekendt Ejland is structurally controlled, and whether it was originally more widespread or was locally formed cannot be determined. In the former case, the formation may still be present in the offshore.

Late dykes in the westernmost onshore areas. A few dykes that cut the highest parts of the volcanic succession in western Nuussuaq and western Svartenhuk Halvø have compositions that are less enriched than those of the Naqerloq Formation. One such dyke in westernmost Nuussuaq has an age of 48.0 ± 2.7 Ma and may be related to a part of the offshore volcanic succession that is younger than the Naqerloq Formation. The magnetic properties of these dykes are unknown.

Hareøen Formation (Mid-Eocene (Bartonian), 39–38 Ma). On Hareøen, the 38.7 ± 0.2 Ma lava flows of the Talerua Member of the Hareøen Formation overlie the lava flows of the Kanísut Member, in places with a poorly exposed sedimentary horizon (Aumarûtigssâ Member) in between (Hald, 1976). Whereas the Kanísut Member is faulted and tilted 10° to 20°, the Talerua Member is subhorizontal, attesting to tectonism in the foregoing period. The lava flows in the lower part of Talerua Member are normally magnetized, whereas those in the upper part are reversely magnetized, and the succession correlates to magnetic polarity Chrons C18n.1n and C17r (Fig. 30, 32; Schmidt et al., 2005). The seaward extent of the member is unconstrained.

Offshore successions

Early Cenozoic sedimentary and igneous successions of the drift phase are known from wells drilled on structural highs and within basins west of Greenland (Fig. 3). Seismic ties to six exploration wells (Alpha-1 S1, Delta-1, Gamma-1, Hellefisk-1, T4-1, and T8-1; Fig. 1, 3) constrain the ages of mega-unit E, a Paleocene to mid-Eocene volcanic and sedimentary succession, and mega-unit D, comprising late Eocene to mid-Miocene sediments, principally of marine origin (Fig. 3).

Volcanic successions

The volcanic succession west of the Nuussuaq Basin of mega-unit E is divided into five different seismic stratigraphic subunits labelled A (youngest) to E (oldest) with a total thickness ranging from 2 km to more than 5.2 km (Skaarup, 2002) (Fig. 25c). The Alpha-1 S1 well terminates in a thick succession of Paleogene volcanic rocks (Fig. 25d; Gregersen et al., 2019). The Hellefisk-1 well south of Disko penetrates 694 m of Paleocene basaltic subaerial lava flows (Rolle, 1985; Hald and Larsen, 1987; Larsen and Williamson, 2020).

The lowermost parts of the Alpha-1 S1 and Delta-1 wells drilled into approximately kilometre thick (2073 m and 1136 m, respectively) basaltic lavas of probable Paleocene–Eocene ages (Capricorn Greenland Exploration (Cairn Energy PLC), unpub. report, 2011) (Fig. 3). Radiometric dating ($^{40}Ar/^{39}Ar$) indicates an early Eocene age for the main part of the volcanic succession in the Delta-1 well (Nelson et al., 2015).

Both wells are located at the outer boundary (about longitude 58°30′W) of the volcanic units A–E mapped by Skaarup (2001, 2002) and the mapped succession tentatively correlates to the wells; however, it is not clear from present seismic correlation exactly which of the units were drilled, but as units B and C are the most westward and most extensive units they may have been drilled, which is in accordance with the considerations and geochemistry below.

Selandian, 61–60 Ma: offshore volcanism contemporaneous with the Maligât Formation

The offshore lava plateau extends south to the areas around latitude 67°30′N where a basalt succession more than 700 m thick was formed at the same time as the Maligât Formation. The succession was drilled in the Hellefisk-1 well and dated at 60.63 ± 0.87 Ma (Fig. 32). The Maligât Formation and its southern equivalents may be included in the southern parts of seismic units B and C of Skaarup (2001, 2002).

Late Selandian to Thanetian, 60–58 Ma: offshore volcanism correlated with the Svartenhuk Formation

Offshore, seismic units B and C mapped by Skaarup (2001, 2002), are possible equivalent to the Svartenhuk Formation. Basalt flows geochemically similar to the Svartenhuk Formation were drilled in 2010 and 2011 in two exploration wells, the Alpha-1 S1 well west of northern Disko and the Delta-1 well west of Ubekendt Ejland. In the Alpha-1 S1 well, 2073 m of volcanic rocks were drilled and the well terminated in basalt at 4801 m measured depth below rotary table (Fig. 25d). The succession includes basalt and an unusually large proportion of silicic rocks interpreted to be due to crustal contamination (B. Bell, unpub. report for Capricorn Greenland Exploration (Cairn Energy PLC), 2011). In the Delta-1 well, the volcanic succession drilled is basaltic and 1136 m of volcanic rock were drilled. The well terminated at 2977 m measured depth below rotary table within the succession. The lowest 170 m are geochemically similar to the Svartenhuk Formation, whereas the overlying basalt units are dated as Eocene and are similar to the Naqerloq Formation onshore (D.A. Jerram, unpub. report for Capricorn Greenland Exploration (Cairn Energy PLC), project PO-32413, 2012; Nelson et al., 2015).

Earliest Ypresian, 56–54 Ma: offshore volcanism correlated with the Naqerloq Formation

Offshore, the Delta-1 well penetrated 960 m of enriched basalt flows similar to the Naqerloq Formation and dated to the early Eocene around 55 Ma (D.A. Jerram, unpub. report for Capricorn Greenland Exploration (Cairn Energy PLC), project PO-32413, 2012; Nelson et al., 2015).

Latest Ypresian around 48 Ma: offshore volcanism correlated with the dykes in the westernmost onshore areas

The youngest offshore seismic unit of Skaarup (2001, 2002), unit A, is normally magnetized and not represented onshore. Skaarup (2001, 2002) suggested it may be of Chron C24n in age; however, it may also include younger rocks unknown in the onshore areas. As shown in Figure 32 there is plenty of ‘room’ for additional volcanic units offshore. They could belong to any normal magnetic polarity chron from C24n (54.0–52.6 Ma) and younger.

Mid-Eocene (Bartonian), 39–38 Ma: offshore volcanism correlated with the Hareøen Formation

Earth’s polarity field was primarily normally magnetized during the period 40–36 Ma (C18n to C16n), and as the aeromagnetic pattern offshore shows large areas with normally magnetized igneous rocks (Rasmussen, 2002), it is possible that igneous activity in this period was concentrated on the shelf away from the onshore areas where igneous activity had essentially ceased.

Offshore lower Cenozoic sedimentary rocks and structures

Postvolcanic Eocene sediments (uppermost part of mega-unit E) have only been encountered as a thin mudstone interval (less than 50 m) in Alpha-1 S1 that drapes over an intensely faulted top volcanic horizon (Ev) (Fig. 25d). During the late Eocene to early middle Miocene, thick sedimentary packages infilled the inverted rift basins offshore West Greenland (Rolle, 1985; Nøhr-Hansen, 2003). This development from a late drift phase to passive margin development corresponds to seismic mega-unit D (*see* Fig. 41, below). The Eocene–Oligocene Kangâmiut Formation (e.g. drilled in Hellefisk-1 and Kangâmiut-1 wells) represents the lower part of mega-unit D, and is characterized by high-energy shelf and delta-front deposits alternating with lagoonal deposits interpreted as transgressive-regressive cycles (Rolle, 1985). A thin unit of marine mudstone of likely early Miocene age, was drilled in the Alpha-1 and Delta-1 wells; in seismic sections, this unit appears as a condensed section of mega-unit D draping over the volcanic highs (Fig. 25d). In the Baffin Bay basin, mega-unit D is developed as a sedimentary package displaying relatively continuous reflections that onlap the top of unit E (P.C. Knutz, C. Harrison, T. Brent, U. Gregersen, J.R. Hopper, and H. Nøhr-Hansen, work in progress, 2021).

In seismic profiles, volcanic deposits are characterized by disrupted reflections with downward loss of resolution, contrasting with the more continuous reflectivity of overlying sedimentary strata. The top of the volcanic succession (horizon Ev) is generally marked by strong amplitude reflections (Fig. 25b, c, d). The volcanic succession and overlying draping reflections (above horizon Ev) are cut by north- and northwest-trending extensional faults, forming narrow graben-like structures and pull-apart basins. Examples include the Ilulissat Graben and minor grabens east and north of the Alpha-1 S1 well (Fig. 25a, c, d). These extensional features are probably related to regional northward drift of Greenland and associated strike-slip tectonic events (Gregersen and Bidstrup, 2008). In other parts, the Paleocene–Eocene drift phase resulted in basin inversion and compression along structural highs, exemplified by the Ikermiut Fault Zone (Gregersen and Bidstrup, 2008) and the Melville Bay Ridge (Gregersen et al., 2013). The Tunoqqu surface at the top of the volcanic Naujánguit Member (in central Nuussuaq) probably formed into a structural anticline as a result of late Paleocene inversion and may include possible exploration targets (Hopper et al., 2016; Sørensen et al., 2017).

Early Cenozoic palynology in offshore areas

Marine palynological zonation

In 1977, Arco Greenland Incorporated drilled the exploration well Hellefisk-1. The total depth was 3201 m and (?)Paleocene basalt units were encountered (Rolle, 1985; Nøhr-Hansen, 2003). In palynological studies based on 45 cutting samples and 53 side wall cores, Nøhr-Hansen (2003) and Nøhr-Hansen et al. (2016) recognized 11 palynological zones spanning the Selandian to Priabonian. The upper 700 m of the well was tentatively dated as (?)late Eocene to Pleistocene based on a sparse palynological assemblage. No Oligocene palynomorphs were recognized.

Late Cenozoic

Onshore successions

Neogene

Neogene onshore deposits are unknown in West Greenland (Henriksen et al., 2009). This agrees well with the uplift model of Green et al. (2013). These authors identified two major planation surfaces, which formed at sea level in the Miocene (11 Ma) and Pliocene (5 Ma). The Miocene peneplain is presently at altitudes of 750 m to 2000 m onshore in Nuussuaq and at depth up to 1500 m offshore, west of Nuussuaq (Green et al., 2013).

Quaternary

During most of the Pleistocene, Greenland was completely, or almost completely, covered by ice. Surficial glacial deposits are widespread on the present ice-free land areas and on the adjacent shelf. The ice sheet experienced waxing and waning through multiple glacial-interglacial cycles. The present ice cover consists of the Greenland Ice Sheet, local ice caps and glaciers (Henriksen et al., 2009). The Greenland Ice Sheet covers an area of 1 716 000 km^2 (Citterio and Ahlstrøm, 2013) and has a volume of 2.99 x 10^6 km^3 (Morlighem et al., 2017). The Jakobshavn Isbræ is the largest marine-terminating glacier in West Greenland. A series of deep ice-cores from the Greenland Ice Sheet has provided a wealth of paleoclimatic data for the Eemian, Weichselian, and Holocene. The ice cores from the Greenland Ice Core Project (GRIP) and the North Greenland Ice Core Project (NGRIP) are Global Boundary Stratotype Section and Point sites (GSSP) for lower boundaries of the Holocene Series and/or Epoch, as well as the Greenlandian and the Northgrippian stages of the Holocene (e.g. Dansgaard et al., 1993; Greenland Ice-core Project (GRIP) Members, 1993; Meese et al., 1997; Johnsen et al., 2001; Dahl-Jensen et al., 2002; NEEM community members, 2013; Raisbeck et al., 2007; Rasmussen et al., 2008; Steffensen et al., 2008; Svensson et al., 2008; Walker et al., 2008, 2012, 2018).

Repeated phases of erosion have left little evidence of the extent of the ice sheet during much of the Pleistocene (Funder et al., 2004; Strunk et al., 2017). Sedimentary deposits older than the Last Glacial Maximum (LGM) are generally only preserved locally (Símonarsson, 1981; Funder et al., 2004). Interglacial deposits have been reported from a number of sites in central West Greenland. Four middle Pleistocene to Eemian marine events have been described from the Nuussuaq Basin (Bennike et al., 1994). The Disko Bugt was deglaciated rapidly in the early Holocene (10.5–10 ka BP.; Funder and Hansen, 1996; Rasch, 2000; Weidick and Bennike, 2007; Wangner et al., 2018). The Quaternary to modern sediments include moraines and rock glaciers; undifferentiated landslipped masses; talus and solifluction deposits; alluvial fan-, braided river-, and fluvial plain deposits; peat; and raised marine deposits.

Offshore successions

The upper Cenozoic development of the West Greenland margin is represented by a thick sedimentary succession that is subdivided into mega-units A, B, and C based on the regional seismic stratigraphy (Fig. 25d; Knutz et al., 2015, P.C. Knutz, C. Harrison, T. Brent, U. Gregersen, J.R. Hopper, and H. Nøhr-Hansen, work in progress, 2021; Gregersen et al., 2018, 2019). The shelf margin package of mega-unit C forms an aggradational to progradational sediment prism that is strongly eroded toward the basin margin (Fig. 25d). The regional signature of margin erosion and slope instability suggests that the margin was tectonically adjusted during the latest Miocene and/or early Pliocene, possibly associated with a continental uplift episode (onset 11–10 Ma) in the Disko-Nuussuaq region (Japsen et al., 2006).

Seismic stratigraphic correlation to Delta-1 and ODP site 645 indicates a late Miocene age for mega-unit C (Knutz et al., 2015, 2019). This age is supported by correlation to wells south of central West Greenland, e.g. Manîtsoq and Ataneq formations (Rolle, 1985; Nøhr-Hansen et al., 2016).

Mega-unit B is characterized by mounded deposits, featuring upslope climbing sediment waves that onlap or overstep the erosional flank of the upper Miocene sediment package (mega-unit C) (Knutz et al., 2015). These contourite depositional patterns suggest that sedimentation was driven by a system of northward boundary currents along the West Greenland margin. Seismic stratigraphic ties to wells and boreholes indicate a general Pliocene age for mega-unit B, but the exact bounding ages are uncertain (Knutz et al., 2015, 2019).

Mega-unit A is characterized by major progradation of the shelf margin and deposition of trough-mouth fans assigned to glacial outlets (or paleo-icestreams) that extended from the West Greenland fjord system (Hofmann et al., 2016). Based on the age information from preglacial sediments (mega-unit B), the onset of glacial progradation associated with large-scale shelf glaciation probably occurred during the late Pliocene–early Pleistocene (Hofmann et al., 2016; Knutz et al., 2019). Thus, mega-unit A is mainly Pleistocene.

NORTHERN WEST GREENLAND BASINS

P.C. Knutz, J.R. Ineson, H. Nøhr-Hansen, U. Gregersen, G.K. Pedersen, J. Hovikoski, J.R. Hopper, and J.A. Bojesen-Koefoed

The northern West Greenland continental margin includes a number of sedimentary basins and structural regions from the Upernavik Escarpment at about latitude 73°N to the Thule Basin extending north of latitude 76°N (Fig. 2, 3, 33). The geology and stratigraphy of the region are shown in Figures 33–42, below and are described from the oldest to the youngest successions in onshore and offshore areas.

Pre-Cretaceous

Onshore successions

Archean–Proterozoic

The oldest rocks known from northern West Greenland are Mesoarchean gneiss units with enclaves of supracrustal rocks (Henriksen et al., 2009). The gneiss units are a part of the Archean Rae Craton, which also constitutes a major part of the conjugate northern Baffin Island and Bylot Island (St-Onge et al., 2009), which were once part of a single craton. Archean intrusions occur in some places, and are more prevalent toward the north, such as in coastal areas at Kap York (Henriksen et al., 2009).

Some of the oldest supracrustal rocks of sedimentary origin known in West Greenland belong to the Paleoproterozoic Karrat Group (ca. 2000–1870 Ma) and occur mostly in the central parts of West Greenland (Henriksen et al., 2009) and up to about latitude 75°N. The succession consists of kilometre thick metamorphosed sedimentary rocks, including marble, pelite, and quartzite, deposited in a shelf to rift setting (*see* 'Central West Greenland basins' section for further description). It may also occur farther west as part of the acoustic basement below the present seabed, but has not been sampled.

Thule Supergroup

Meso- to Neoproterozoic sedimentary rocks belonging to the Thule Supergroup of the intracratonic Thule Basin outcrop in northern West Greenland between approximately latitudes 76°N and 79°N (Fig. 33, 34, 35) (Dawes, 1997). These rocks unconformably overlie crystalline basement and were deposited in continental to shallow-marine environments in a rifted continental margin or intracratonic setting (Dawes, 1997). The northern flank of the Thule Basin is overstepped

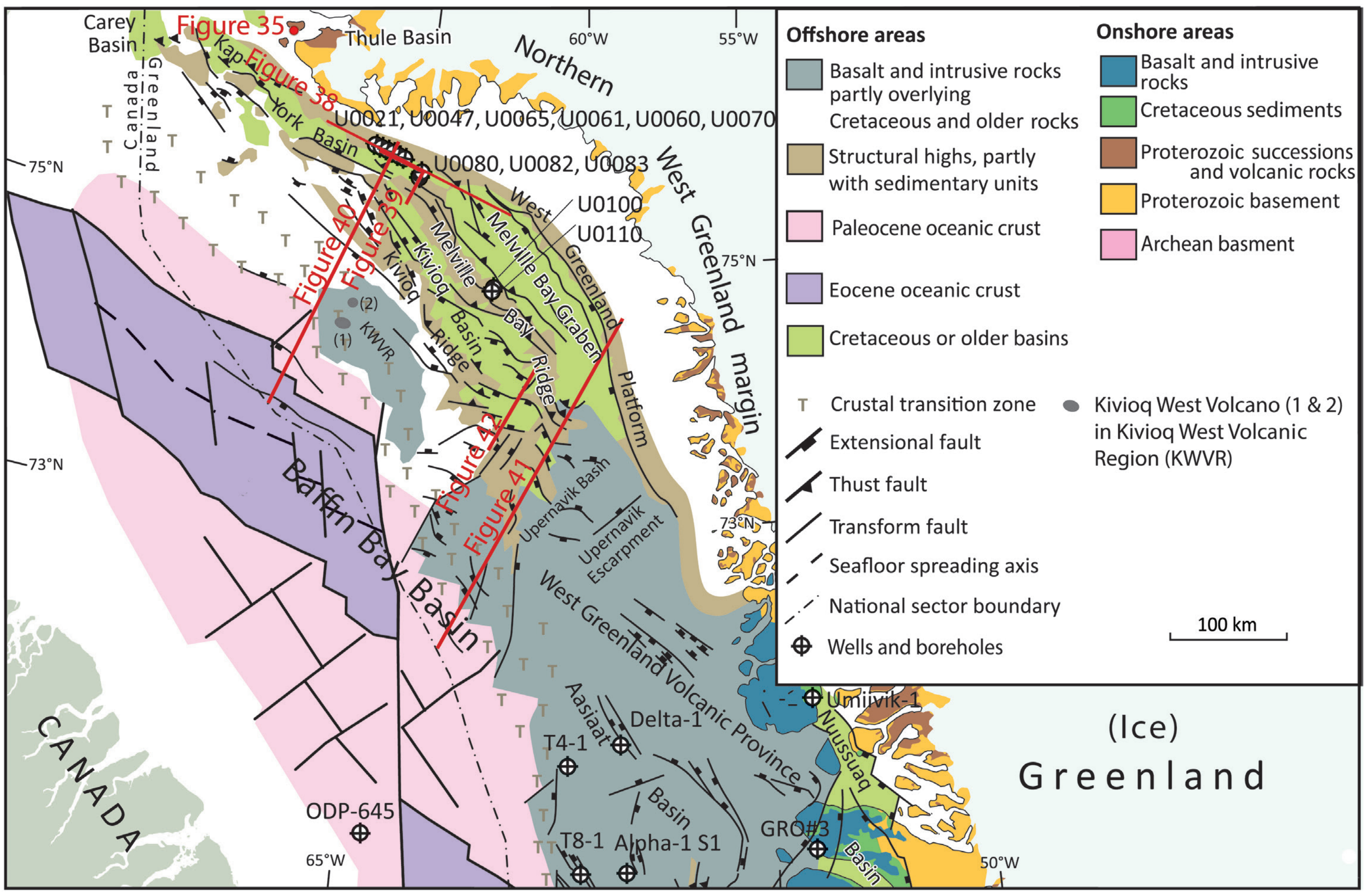

Figure 33. Tectonic elements map for the northern West Greenland margin. From the northern part of Figure 2. The distribution of sedimentary basins with Proterozoic and Cretaceous rocks and areas with volcanic rocks in the northwest Greenland–Baffin Bay region are shown. Position of the photograph in Figure 35 and positions of wells and boreholes and seismic transects in Figures 38–42 are shown.

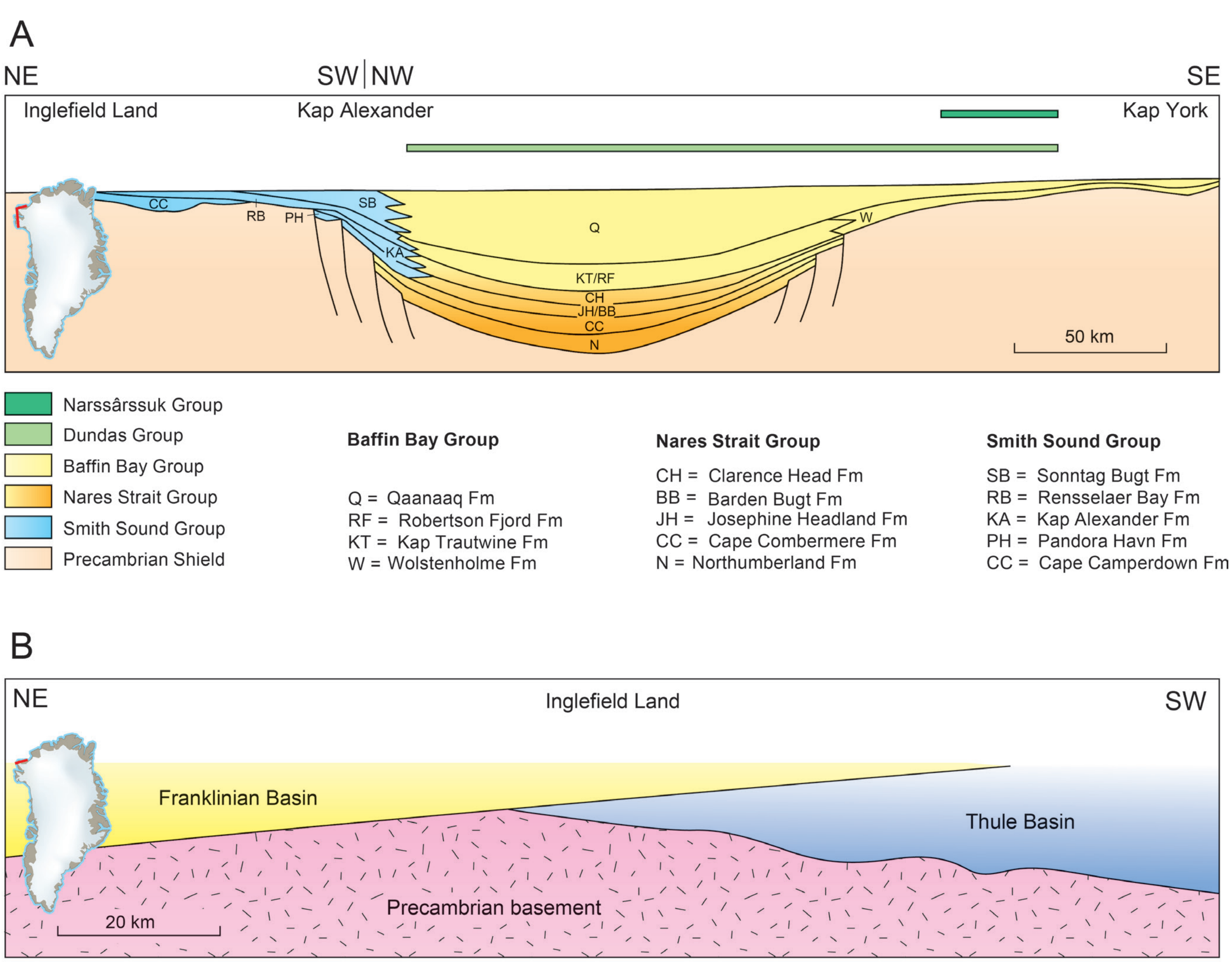

Figure 34. Stratigraphic relationships of the Thule Basin, North-West Greenland. **a)** Schematic cross-section of Thule Basin showing spatial relationships of the five groups of the Thule Supergroup (Dawes, 1997), as *modified from* Henriksen et al. (2009). **b)** Stratigraphic sketch depicting the relationships between the Thule Basin and the Franklinian Basin, unconformably overlying crystalline basement, in a southwest-northeast transect in Inglefield Land. Locations of the cross-sections are shown with red lines in the small index maps.

by Lower Paleozoic strata of the Franklinian Basin (Fig. 34). The Thule Supergroup (ca. 1270–650 Ma) is at least 6 km thick and includes continental to shallow-water sandstone, mudstone, and carbonate and volcanic rocks; it is divided into 36 lithostratigraphic units: 5 groups, 15 formations, and 16 members (Dawes, 1997).

The lower Thule Supergroup comprises three groups: the Smith Sound, Nares Strait, and Baffin Bay groups. The Smith Sound Group is only recognized in the northern, marginal reaches of the basin and is stratigraphically equivalent to the more basin-axial Nares Strait and Baffin Bay groups (Dawes, 1997; Fig. 34). The upper Thule Supergroup, the Dundas, and Narssârssuk groups, are restricted to the central and southern Thule Basin, the latter group being confined to a northwest-trending graben system that extends southward to the shores of Melville Bay (Fig. 35).

Dawes (1997) provided detailed descriptions of the Thule Basin stratigraphy. The Smith Sound Group (up to 700 m thick) comprises sandstone and shale with subordinate stromatolitic carbonate rocks, representing nonmarine (fluvial and lacustrine) and shallow-marine environments. The Nares Strait Group, up to 1200 m thick, is dominated by sandstone and basaltic volcanic rocks with subordinate shale- and carbonate-dominated intervals; the volcanic rocks include flows, sills, and volcaniclastic deposits. Sedimentary facies are indicative of alluvial plain, coastal, and marine-shelf environments. The conformably overlying Baffin Bay Group is the most widespread unit of the Thule Basin reaching a maximum thickness of up to 1300 m. Sandstone and quartz-pebble conglomerate dominate, with subordinate mudstone intervals; the group is largely nonmarine and of fluvial-lacustrine origin, but probable marine, finer grained sediments occur in the upper levels of the group. The Dundas Group (2–3 km

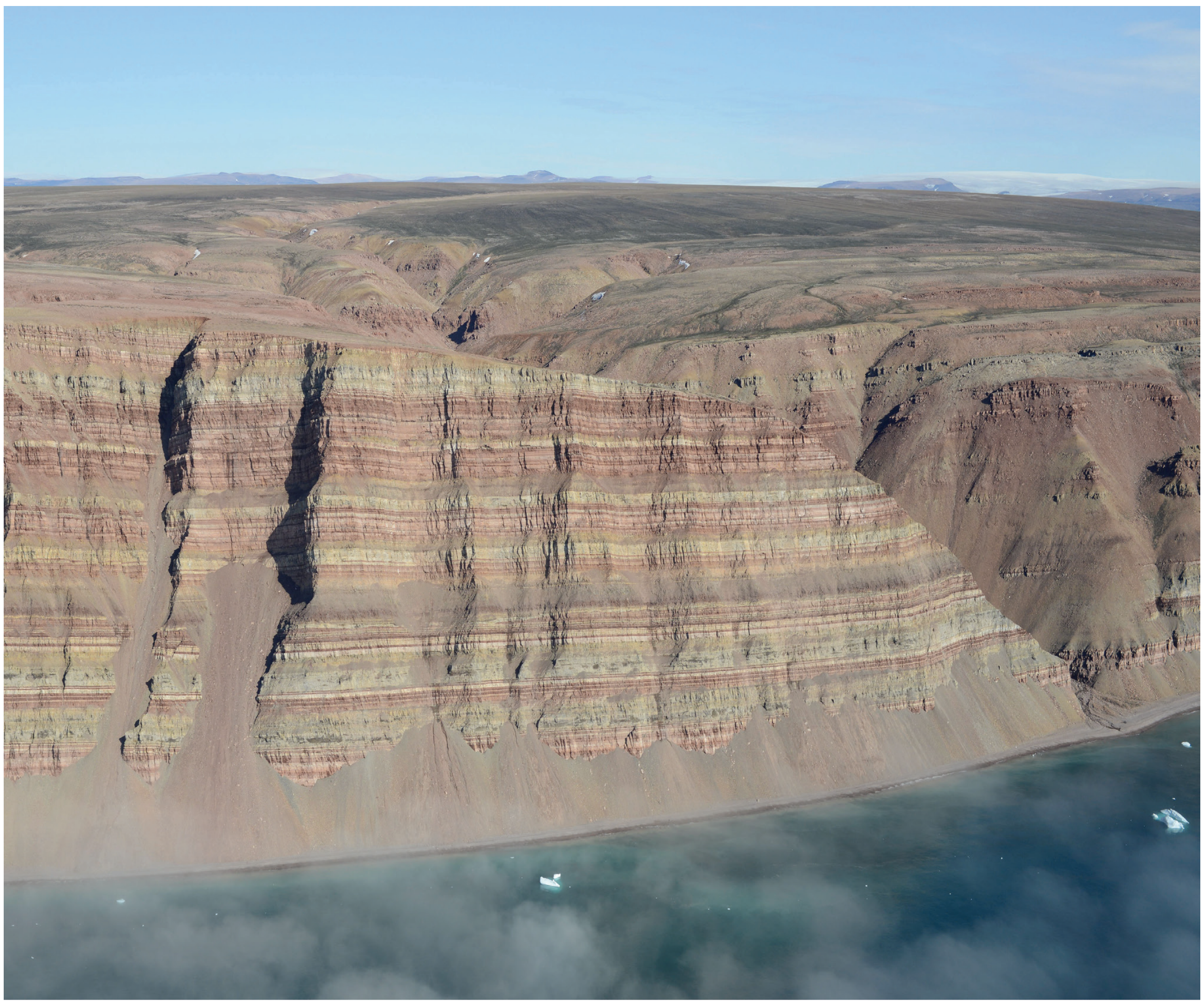

Figure 35. Cyclic alternation of siliciclastic rocks (largely redbeds) and pale carbonate rocks of the Narssârssuk Group in southern Saunders Ø; the height of the cliffs is about 300 m. Photograph by C. Knudsen, 2012. Location of the photograph is shown in Figure 33.

thick) conformably overlies the Baffin Bay Group and comprises sandstone, siltstone, and shale with subordinate carbonate and evaporite deposits; a range of probable marine environments is indicated from deltaic to offshore. The youngest group in the Thule Basin, the Narssârssuk Group (1.5–2.5 km thick), comprises a cyclic carbonate-siliciclastic redbed succession with local evaporite (Fig. 35), and represents deposition in a low-energy, hypersaline, peritidal environment, perhaps analogous to a modern coastal sabkha.

The Thule Supergroup outcrops widely in the northern Baffin Bay to Nares Strait region and parts of the lower Thule Supergroup as defined from Greenland are recognized on Ellesmere Island (Dawes, 1997). Recent offshore drilling of cored shallow boreholes in northeast Baffin Bay (Fig. 33) proved the presence of Proterozoic rocks tentatively placed within the Upper Thule Supergroup (G. Acton, G. Claypool, I. Delusina, G. Dunbar, H. Evans, P. Ferretti, G. Guerin, L. Holloway, S. Ishman, P.C. Knutz, L. Krissek, D. Kulhanek, T.L. Insua, J. Lauren, D. Maloney, D. Naafs, H. Nøhr-Hansen, M. Olney, C. Richter, M. Storms, S. Woodard, and J. Wright, unpub. report, 2012). Interpretation of offshore geophysical data supports the occurrence of the supergroup between Greenland and Canada in the offshore (*see* below).

Paleozoic

There are no known occurrences of outcropping Paleozoic sedimentary rocks in northern West Greenland, but there are farther north. The onshore geology of north Greenland and Ellesmere Island is overwhelmingly dominated by the mainly Lower Paleozoic Franklinian Basin (Higgins et al., 1991). This broadly east-trending basin, representing the northern continental margin of Laurentia, was initiated in the late Neoproterozoic, accumulated up to 8 km of mainly marine-shelf and deep-water carbonate and siliciclastic rocks and was deformed in the Ellesmerian Orogeny in the Devonian–Carboniferous (Higgins et al., 1991; Trettin et al., 1991). Although strictly north of the study area on the West Greenland margin, Cambrian Franklinian strata outcrop on Inglefield Land immediately to the north where they overstep onto the northern flank of the Thule Basin (Fig. 34b).

Offshore successions

Proterozoic

Stratigraphic sections of inferred Proterozoic age were cored in the U0021 (48 m thick), U0047 (32 m), U0080 (8 m), and U0110 (9 m) shallow corings in the Melville Bay region (G. Acton, G. Claypool, I. Delusina, G. Dunbar, H. Evans, P. Ferretti, G. Guerin, L. Holloway, S. Ishman, P.C. Knutz, L. Krissek, D. Kulhanek, T.L. Insua, J. Lauren, D. Maloney, D. Naafs, H. Nøhr-Hansen, M. Olney, C. Richter, M. Storms, S. Woodard, and J. Wright, unpub. report, 2012; Nøhr-Hansen et al., 2021; Fig. 1, 3, 33, *see* 36–39). The thicker core sections show a striking cyclicity, units up to 5 m thick dominated by fine-grained siliciclastic rocks that are typically dark red-brown alternating with pale, cream or mid-grey carbonate rocks forming units 0.5 m to 3 m in thickness (*see* Fig. 37). The siliciclastic rocks are typified by red (hematitic) dolomitic sandy mudstone and very fine-grained sandstone; textural and colour mottling is attributed primarily to haloturbation — fabric disruption due to early evaporite dissolution in an ephemeral fluvial-lacustrine setting (Rieke et al., 2003; Catto et al., 2018). The carbonate units are of two main types. The first is mud-cracked microbial laminite, locally with evaporite pseudomorphs, stromatolites, and flat-pebble conglomerate units that record deposition on intertidal and supratidal low-energy carbonate mud flats. The second includes carbonate grainstone and packstone, locally preserving ooidal fabrics, which record deposition on shallow subtidal nearshore carbonate sand shoals. Cyclic alternation of the carbonate and siliciclastic associations probably reflects episodic flooding and subsequent tidal flat and alluvial progradation. Given the lithological similarities (Fig. 35, 36, 37), the structural trends, and the geographic proximity, the cored sections are considered to correlate with the Narssârssuk Group of the upper Thule Supergroup, which was described in Dawes (1997).

Paleozoic

Paleozoic strata correlative with the shelf facies of the Franklinian Basin may be present locally in northern Baffin Bay based on seismic data (*see* below), but were absent in the boreholes of northeast Baffin Bay.

Seismic stratigraphy

Seismic data from the northwest Greenland margin indicate the presence of thick, pre-rift sedimentary basins below Mesozoic formations. These ancient stratal packages form the upper part of seismic mega-unit H that is delimited at its top by a widespread unconformity (horizon H1) (Gregersen et al., 2019). In the Melville Bay area of northeast Baffin Bay, at least three pre-Cretaceous subunits can be distinguished below H1 (*see* Fig. 38). The successions are separated by horizons H2 and Hx (from the shallowest to the deepest, respectively) in the Kap York Basin, the northern Melville Bay Graben and the northern Kivioq Basin (Fig. 3, 33, *see* 38; Gregersen et al., 2019). The position of the acoustic basement (below horizon Hx) is comparable to the position of the continental crust basement of seismic refraction studies (Altenbernd et al., 2015). Seismic refraction data from northern Baffin Bay–southern Nares Strait indicate a continuous layer, up to about 2–4 km thick with seismic velocities between 4.5–5 km/s which may represent the Thule Supergroup overlying continental crust (Reid and Jackson, 1997; Funck et al., 2006). In addition, seismic reflection data suggest the presence of such sedimentary basins in the southern Nares Strait (Neben et al., 2006).

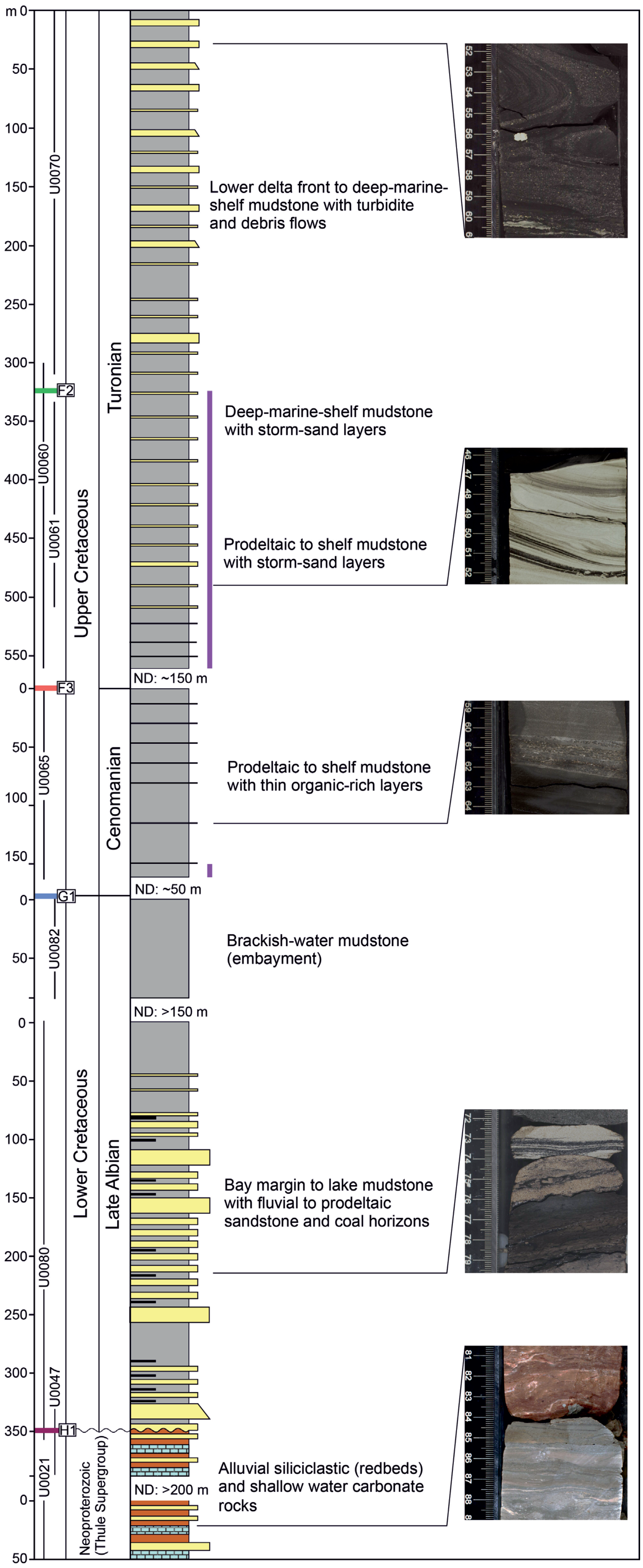

Figure 36. Composite stratigraphy and sedimentary summary log of the northeast Baffin Bay cores recovered from the Kap York Basin during expedition 344S in 2012 (*see* G. Acton, G. Claypool, I. Delusina, G. Dunbar, H. Evans, P. Ferretti, G. Guerin, L. Holloway, S. Ishman, P.C. Knutz, L. Krissek, D. Kulhanek, T.L. Insua, J. Lauren, D. Maloney, D. Naafs, H. Nøhr-Hansen, M. Olney, C. Richter, M. Storms, S. Woodard, and J. Wright, unpub. report, 2012; Nøhr-Hansen et al., 2021. Seismic horizons F2, F3, G1, and H1 (coloured horizontal bars) and stratigraphic coverage of core sites (represented by vertical black lines with well numbers) are indicated in the left-hand column (*see also* Fig. 3, 39). Gross depositional environment and core photo examples are shown to the right. Source rock intervals, defined by consistent HI greater than 200 are marked by vertical bars (purple). ND = section not drilled. Figure by P.C. Knutz based on work by GEUS. Photographs from the expedition 344S.

In the Kap York Basin, Proterozoic sediments of the Thule Supergroup form the upper part of mega-unit H (below horizon H1; *see* Fig. 38), as verified by shallow coring (Fig. 37). The pre-Cretaceous succession is kilometres thick and characterized by stacked packages. Some of these reflection patterns may correspond to the large-scale cycles of interbedded sandstone and carbonate rocks observed for the Narssârssuk Group in coastal profiles in the Thule Fjord (Fig. 35) (Dawes, 1997). Based on the shallow coring information from northeast Baffin Bay (*see* above) and interpretation of seismic data (Fig. 38), it is possible that parts of the Thule Supergroup succession form a regional element of mega-unit H that possibly becomes thinner and wedges out farther south in the east Baffin Bay area.

Paleozoic deposits are not known with certainty. Over some of the structural highs, thin packages displaying strong reflections are locally observed as part of mega-unit H. A possible interpretation of these features is that they represent local remnants of Paleozoic limestone deposits resting on Thule Supergroup formations.

Cretaceous

Offshore successions

Cretaceous rocks are not known from onshore northern West Greenland; however, Cretaceous sediments have been cored at several sites in northeast Baffin Bay (G. Acton, G. Claypool, I. Delusina, G. Dunbar, H. Evans, P. Ferretti, G. Guerin, L. Holloway, S. Ishman, P.C. Knutz, L. Krissek, D. Kulhanek, T.L. Insua, J. Lauren, D. Maloney, D. Naafs, H. Nøhr-Hansen, M. Olney, C. Richter, M. Storms, S. Woodard, and J. Wright, unpub. report, 2012; Fig. 3, 36, 37, 38, 39, 40). A succession of dipping strata beneath a thin Quaternary cover was drilled in the Kap York Basin, complemented by two sites farther south on the western fringe of the the Melville Bay Ridge, within successions that can be correlated into the Melville Bay Graben (Fig. 2, 3).

Lower Cretaceous sediments of likely Albian age were recovered at sites U0047, U0080, U0082, U0100, and U0110 (Fig. 3, 36) (G. Acton, G. Claypool, I. Delusina, G. Dunbar, H. Evans, P. Ferretti, G. Guerin, L. Holloway, S. Ishman, P.C. Knutz, L. Krissek, D. Kulhanek, T.L. Insua, J. Lauren, D. Maloney, D. Naafs, H. Nøhr-Hansen, M. Olney, C. Richter, M. Storms, S. Woodard, and J. Wright, unpub. report, 2012; Nøhr-Hansen et al., 2021). The main lithologies were homogenous to heterolithic mudstone and fine-grained, often bioturbated, sandstone with rare, thin coal beds and coarser grained sand (Fig. 36). Inferred sedimentary environments include swamp-floodplain, lake, prodelta, shoreface, and deep bay, which, in combination with palynological results and seismic configuration, suggest accumulation in a large nonmarine to brackish embayment formed during initial rifting. Wireline log data from site U0080 suggest that numerous quartz-rich sandstone intervals, up to 15 m thick, may have been drilled, but not recovered due to poor consolidation (Fig. 36). Given this interpretation, the accumulated net sand thickness is almost 100 m with an average porosity of 25%.

An Upper Cretaceous succession of black, marine mudstone with varying amounts of discrete sandstone layers was recovered from sites U0060, U0061, U0065, U0070, and U0083 in the Kap York Basin (Fig. 3, 36) (Nøhr-Hansen et al., 2021). The sediments are dated as late Cenomanian to middle Turonian, spanning a time interval from approximately 95 Ma to 92 Ma; the Cenomanian–Turonian transition is not recorded in a core, however biostratigraphic analyses indicate that it may occur somewhere between the upper part of core U0065 and the lower part of core U0060 (Fig. 36) (Nøhr-Hansen et al., 2021). The Cenomanian–Turonian boundary corresponds approximately to a regional seismic reflector at horizon F3 (Fig. 36, 38, 39). Depositional environments range from anoxic outer shelf and prodelta fringe to oxygen-restricted lower delta front (Nøhr-Hansen et al., 2021). The organic richness and petroleum potential of the Cenomanian–Turonian succession is variable, reflecting changes in depositional environment through time, but the most promising source rock interval is the Turonian anoxic shelf facies encountered in sites U0060 and U0061 (Nøhr-Hansen et al., 2021). Such settings could be present within the regional southward extent of the Cenomanian–Turonian seismic unit, forming depocentres of more than 1000 m thickness in the Melville Bay Graben (*see* below).

Despite the overall marine setting, the basin was influenced by abundant supply of organic-rich sediments from nearby terrestrial sources, presumably located to the north and west of the coring sites (Nøhr-Hansen et al., 2021). The presence of mass flows and occasional volcaniclastic horizons in the Turonian interval (sites U0060–U0070) corresponds with marked increases in sedimentary thicknesses within locally developed half-graben

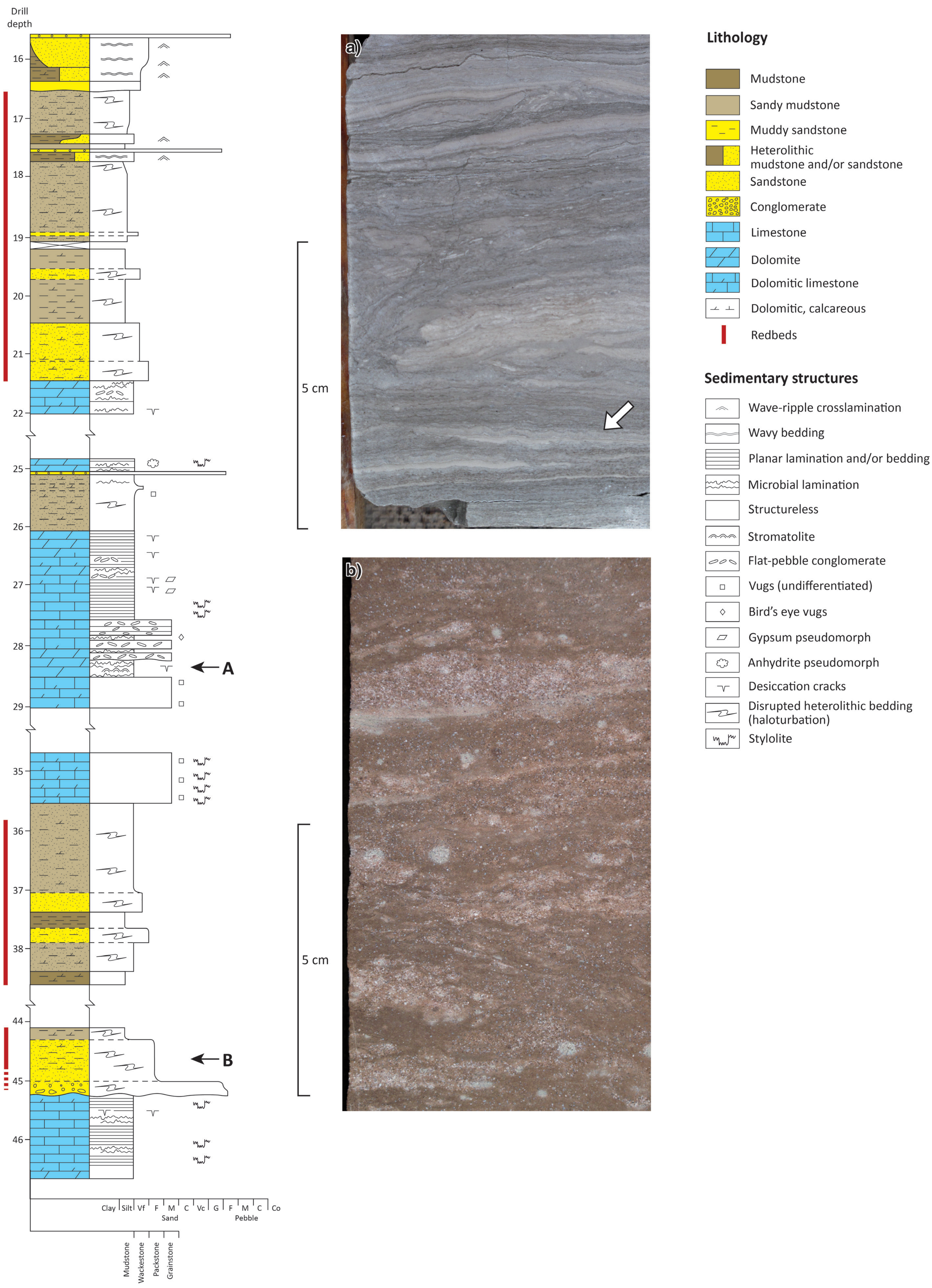

Figure 37. Sedimentological log of part of the cored Proterozoic succession in the U0021 borehole in the Kap York Basin (*see* Fig. 33 for location), illustrating the alternation of microbialite-dominated carbonate and mud-rich siliciclastic redbeds (location of facies photographs indicated on log). **a)** Microbially laminated dolomite. Note the tufted, irregular nature of the lamination (arrow), local disruption of the lamination probably due to desiccation, and lenses of flat-pebble conglomerate (top right). Core 7R3 (28.15–28.25 m). **b)** Mottled, weakly heterolithic sandy-silty mudstone. Note the discontinuous laminae, lenses, and patches of very fine- to fine-grained sand enveloped by the darker dolomitic mudstone component. The common disrupted fabric in this facies (haloturbation) is attributed to evaporite growth and dissolution. Core 9R1 (44.65–44.75 m). Figure and photographs by J.R. Ineson.

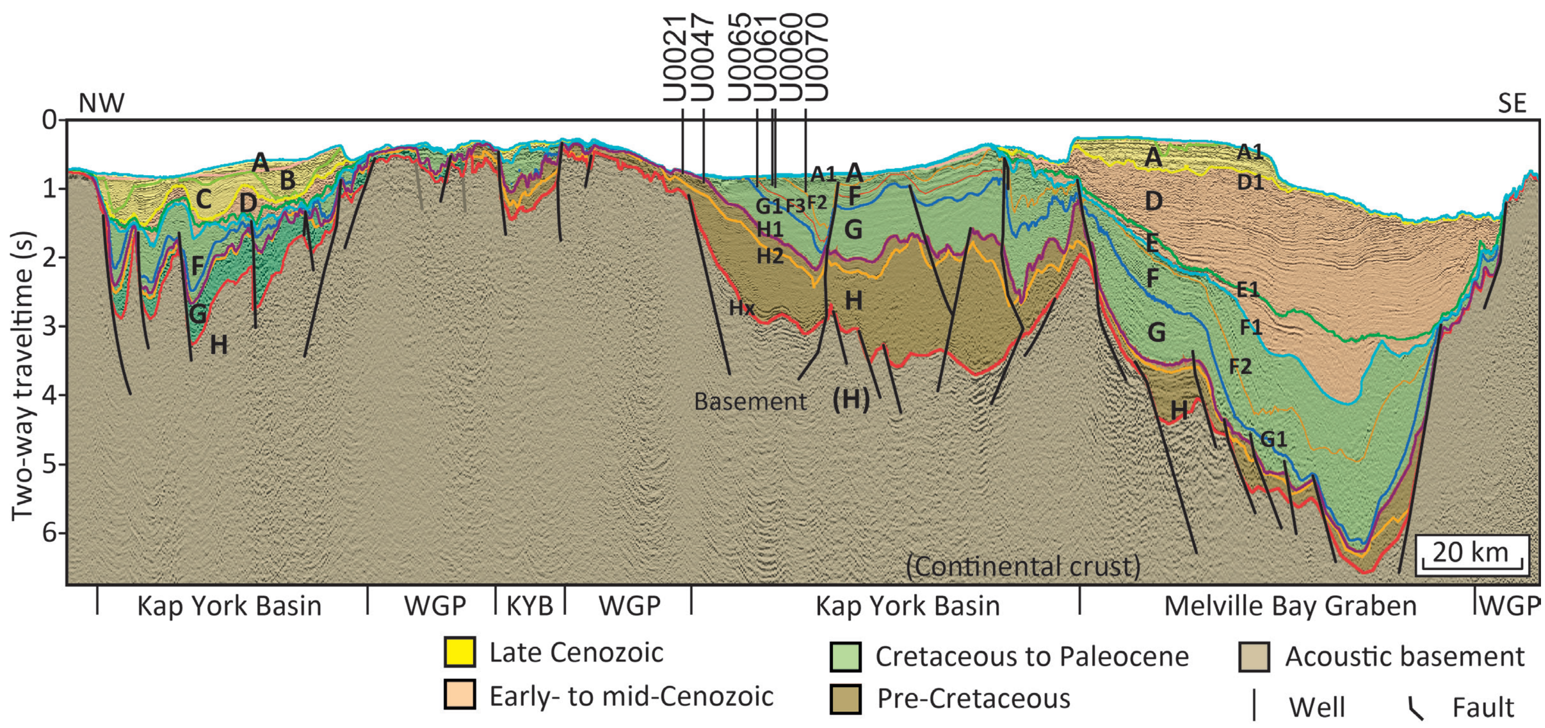

Figure 38. Seismic section across the Kap York Basin (KYB), West Greenland Platform (WGP), and Melville Bay Graben with seismic stratigraphy, ages of mega-units and shallow core sites indicated. Location of the section is shown in Figure 33 (Gregersen et al., 2019). Seismic data courtesy of TGS.

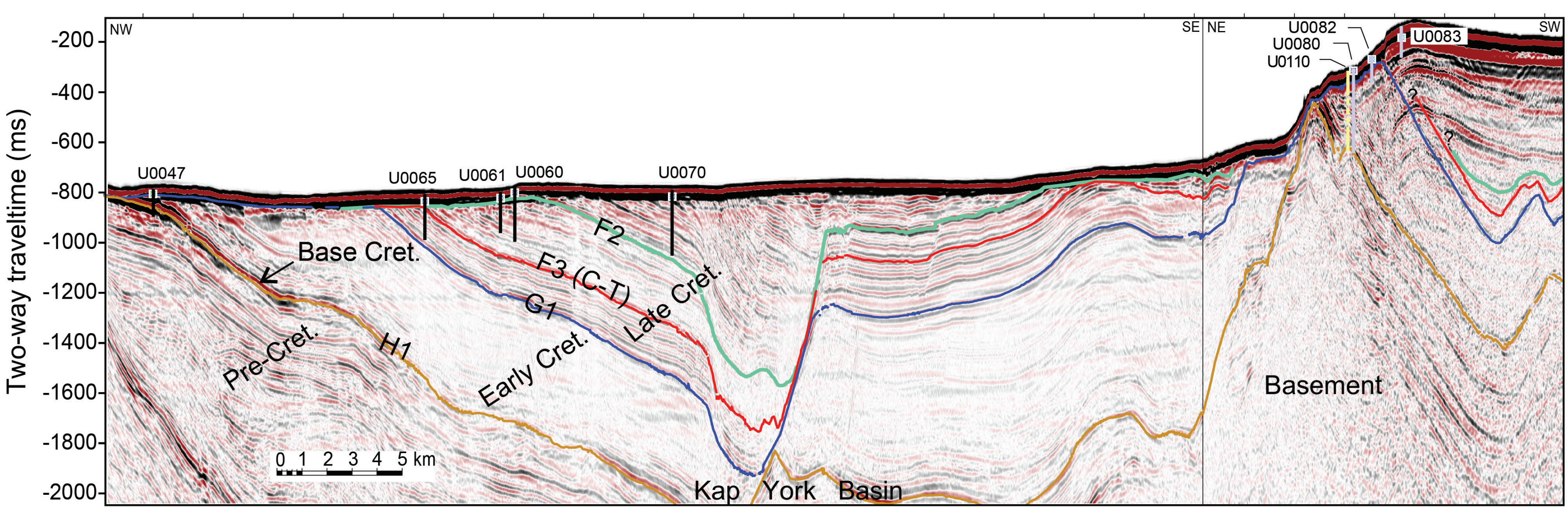

Figure 39. Seismic section across the Kap York Basin with seismic stratigraphy and shallow core sites indicated. Location of the section is shown in Figure 33 (Nøhr-Hansen et al., 2021). Cret. = Cretaceous. C-T = Near the Cenomanian–Turonian transition. Seismic data courtesy of TGS.

structures (Fig. 39). Basin development of the Melville Bay Graben with wedge-formed units of mega-unit F may also reflect intensified rifting and/or extension that continues throughout the Upper Cretaceous (Gregersen et al., 2013, 2019).

Seismic stratigraphy

Cretaceous rift basins offshore northwest Greenland are formed over a prominent unconformity (horizon H1) that apparently represents a hiatus of more than ca. 500 Ma (Proterozoic to Early Cretaceous; Fig. 3, 36, 39) and less than 400 Ma if Ordovician rocks are present. On the regional seismic data, the base Cretaceous horizon often lacks an angular character (Fig. 39); in other words, it is apparently conformable with underlying pre-rift strata, masking the major time gap it represents; however, onlap of unit G against horizon H1 toward Kivioq Ridge and Melville Bay Ridge has been observed (Gregersen et al., 2019).

The Lower Cretaceous succession corresponds to mega-unit G defined in the regional seismic data (Gregersen et al., 2013, 2016). Correlation of the seismic interpretation to the stratigraphic corehole sites described above, suggests that the Lower Cretaceous interval is more than 2000 m thick in the northern Melville Bay Graben, Kap York Basin, and Kivioq Basin (Fig. 40). These thick clastic wedges are generally characterized by a poorly defined, and locally transparent, seismic reflection character, but with more coherent parallel reflections seen along the base of mega-unit G. The enhanced seismic reflectivity corresponds to the sampled Albian succession containing coarse-grained intervals with interspersed coaly horizons (sites U0047, U0080, and U0110). This points to widespread deposition of deltaic and shoreface sand in the northeast Baffin Bay region, presumably bordering a large marine embayment that formed during the early rift phase.

Mega-unit F is attributed to the Upper Cretaceous succession (Gregersen et al., 2013; Fig. 3). The stratigraphy from core sites U0060, U0061, U0065, U0070, and U0083 indicate a Cenomanian–Turonian age (G. Acton, G. Claypool, I. Delusina, G. Dunbar, H. Evans, P. Ferretti, G. Guerin, L. Holloway, S. Ishman, P.C. Knutz, L. Krissek, D. Kulhanek, T.L. Insua, J. Lauren, D. Maloney, D. Naafs, H. Nøhr-Hansen, M. Olney, C. Richter, M. Storms, S. Woodard, and J. Wright, unpub. report, 2012; Nøhr-Hansen et al., 2021) for the lower part of mega-unit F (Fig. 3, 36, 39). The relatively conformable successions of mega-unit F within the Kap York Basin are characterized by continuous, parallel seismic reflections (Fig. 39) that in the coreholes corresponds to organic-rich mudstone with carbonate-enriched intervals, and with storm-sand and turbidite layers (Fig. 36). The successions are subdivided by horizons F2 and F3, respectively of Turonian and Cenomanian age (Fig. 36). Due to its strong seismic character, parts of these successions (near horizon F2) can be traced into the neighbouring Melville Bay Graben and northern Kivioq Basin (Fig. 40, 41).

During the Late Cretaceous, the depocentres shifted southward and eastward resulting in a more than 3500 m thick sedimentary succession in the central parts of Melville Bay Graben. The seismic observations and results from the core analyses point to a major change in depositional environment and notably the establishment of fully marine conditions between the Aptian and mid-late Cenomanian (Fig. 36; Nøhr-Hansen et al., 2021). This environmental change corresponds to the development of clastic depocentres and half-graben features along the structural highs, associated with a late rift stage (Fig. 40, 41; Whittaker et al., 1997; Gregersen et al., 2013). It is possible that a southward trend in sediment transport may have continued into the northern Melville Bay Graben, although clastic input was likely influenced by local sources along the basin margins, in response to ongoing tectonic subsidence along extensional boundary

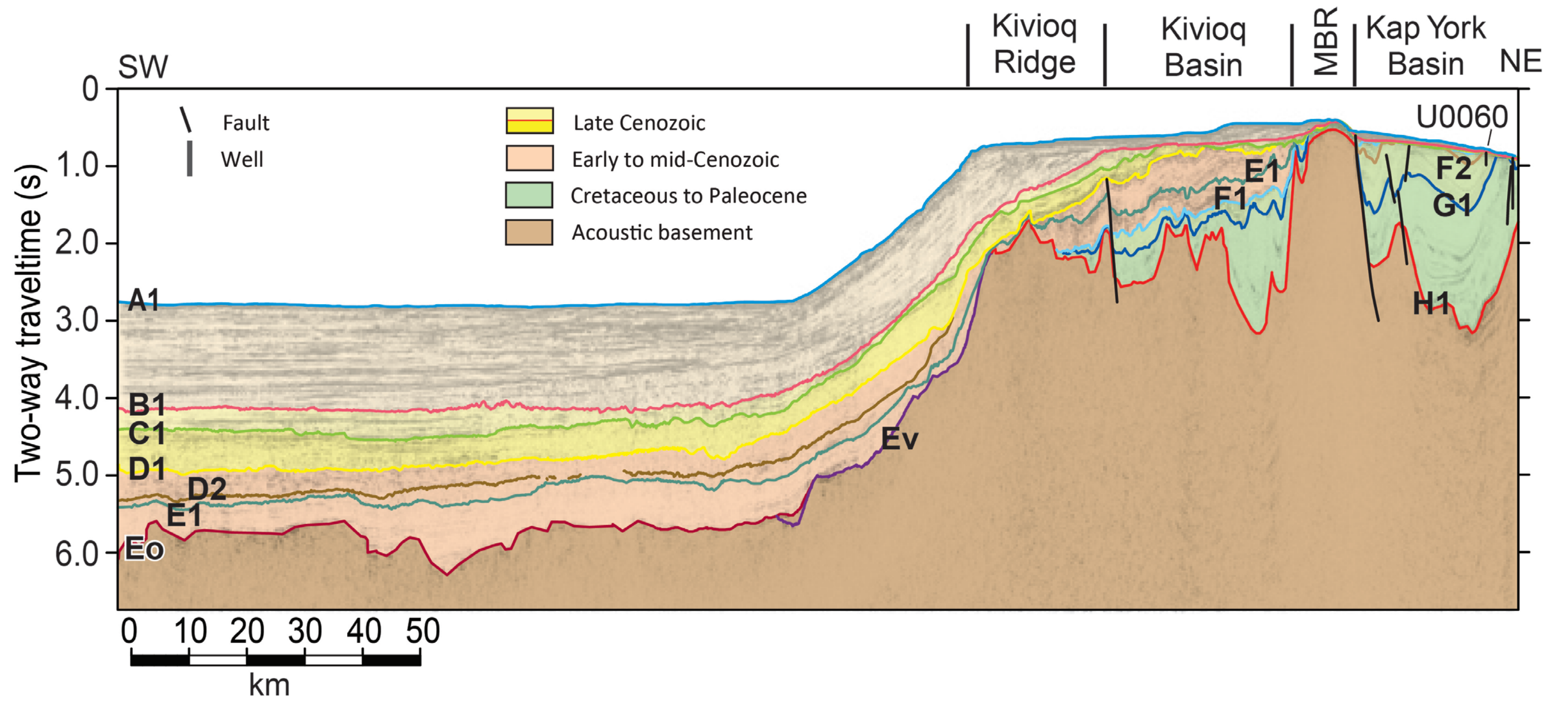

Figure 40. Detail from regional seismic cross-section, showing the configuration of sedimentary basins and structural elements from northeast Baffin Bay, intersecting the Kap York Basin. Position of the shallow core U0060 is shown. *See* Figure 3 for tectonostratigraphic division. Location of the section is shown in Figure 33. Seismic data courtesy of TGS.

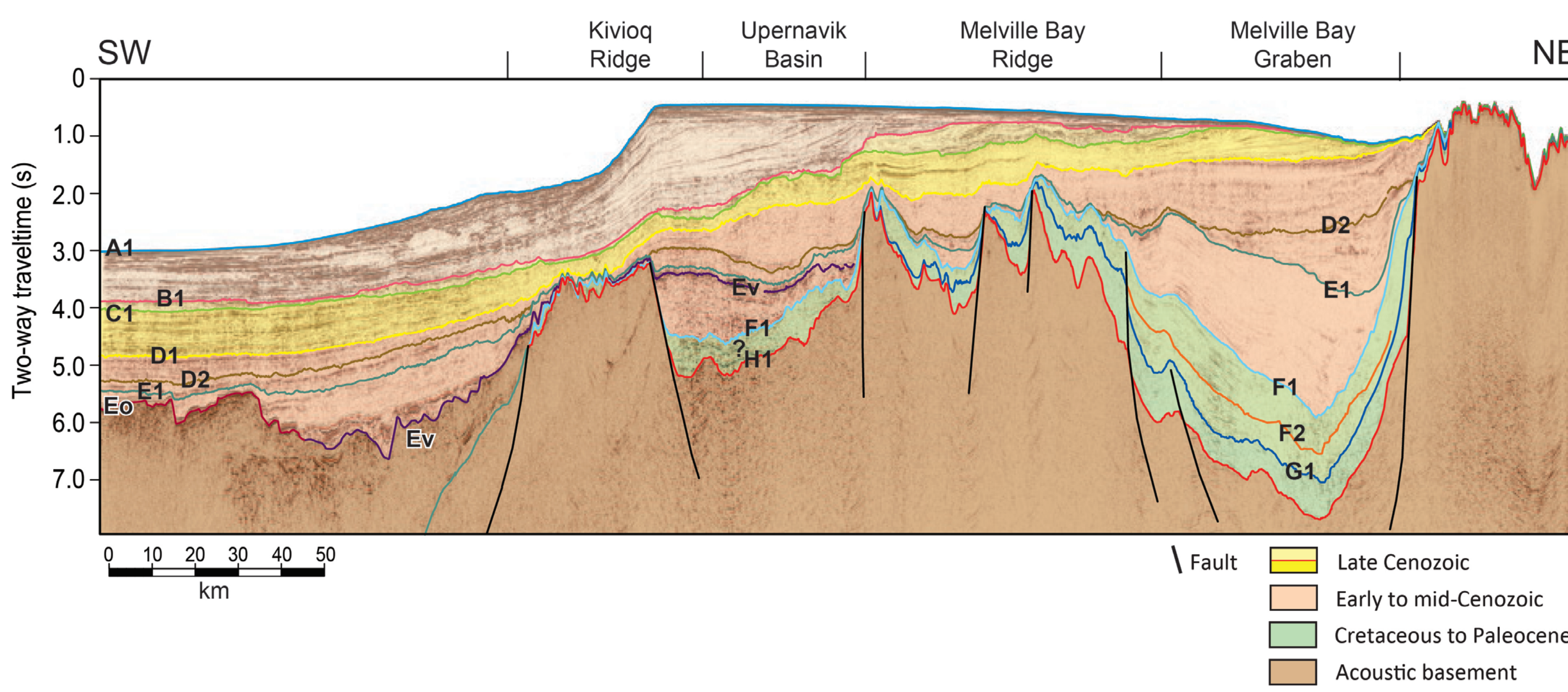

Figure 41. Detail from regional seismic cross-section showing the basin-tectonic configuration from Baffin Bay across the northeast Baffin Bay, intersecting the southern Melville Bay Graben. *See* text and Figure 3 for explanation of tectonostratigraphic division. Location of the section is shown in Figure 33 (P.C. Knutz, C. Harrison, T. Brent, U. Gregersen, J.R. Hopper, and H. Nøhr-Hansen, work in progress, 2021). Seismic data courtesy of TGS.

faults. During the latest Cretaceous–early Paleogene the central highs: Melville Bay Ridge and the Kivioq Ridge, developed into a more prominent features with added structural complexity (Fig. 40, 41). The post-Turonian, Late Cretaceous section remains undrilled in eastern Baffin Bay, but assuming a contiguous north-south development of the rift basins, it is likely that the thick basin infill of mega-unit F corresponds to the mostly mud-prone successions encountered in the Ikermiut-1 well and basins farther south (Chalmers et al., 1993; Gregersen and Skaarup, 2007).

Early Cenozoic

Onshore successions

No sedimentary Paleogene rocks are known from present onshore areas of northern West Greenland.

Offshore successions

Early Cenozoic deposits are also not known from wells offshore northern West Greenland; however, reworked dinocyst assemblages identified in cored and dredged Quaternary deposits suggests that Paleocene–Oligocene sedimentary deposits are present in the region (Nøhr-Hansen et al., 2021). The distribution of lower Cenozoic successions offshore West Greenland based on mainly wells and seismic interpretation is shown in Figure 5.

Seismic stratigraphy

Seismic mega-unit E is generally attributed to the early Cenozoic interval (Gregersen et al., 2013). Biostratigraphy from the lowermost part of Alpha-1 S1 that principally drilled a volcanic succession is uncertain, but may suggest a late Paleocene–Eocene age (Fig. 25d). Due to the lack of firm age control, the chronostratigraphy of mega-unit E mainly relies on correlation to wells drilled off central and southern West Greenland (e.g. Hellefisk-1, Ikermiut-1; Fig. 3). The formation of mega-unit E is considered to be time-equivalent to sedimentary formations on Ellesmere Island (Miall, 1986; Ricketts and Stephenson, 1994), but the lack of borehole information prevents further comparison between these rocks.

In the Melville Bay Graben area, the horizon F1 below mega-unit E is seen as an unconformity marked by onlap against inverted sections of mega-unit F toward the basin flanks (Fig. 41; Gregersen et al., 2013). The age of this transition is not known from nearby samples, but comparison to seismic interpretation and to wells farther south suggest a Danian age (Fig. 3). This associates horizon F1 with the termination of late rifting and onset or early development of active seafloor spreading in central Baffin Bay (Oakey and Chalmers, 2012; Gregersen et al., 2019).

Deposition of mega-unit E reflects a change in the syntectonic setting, marked by reactivated faults and strike-slip movements along the structural highs, causing inversion of the older rift sediments (Gregersen et al., 2013, 2019). The pronounced structural development of the ridges, juxtaposed to thick basin-infilling strata, is associated with a northward drift, and counterclockwise rotation of Greenland during opening of Labrador Sea and Baffin Bay (Gregersen et al., 2013; P.C. Knutz, C. Harrison, T. Brent, U. Gregersen, J.R. Hopper, and H. Nøhr-Hansen, work in progress, 2021).

In the southernmost part of the area, toward the Upernavik Escarpment, mega-unit E is apparently influenced by late Paleocene–early Eocene volcanism, presumably related to the development of the West Greenland Volcanic Province (Fig. 33; *see* 'Central West Greenland basins' section). A substantial succession of early Cenozoic sediments is interpreted above horizon F1, with thicknesses up to 2500 m formed locally in the southern Melville Bay Graben and Upernavik Basin (Fig. 41). The top of mega-unit E (horizon E1) is represented by a disconformity, inferred to be mid-Eocene (approximately near base Lutetian; Fig. 3).

Above this horizon, subunit D2 (below horizon D2: Fig. 41) indicates a change in depositional style marked by deposition of basin-floor fans with sediment transport predominantly oriented along the axis of the basin (P.C. Knutz, C. Harrison, T. Brent, U. Gregersen, J.R. Hopper, and H. Nøhr-Hansen, work in progress, 2021). The sedimentary geometries associated with fan deposition, seen in Kivioq Basin, Melville Bay Graben, and Baffin Bay Basin are probably controlled by sediment sources toward north, such as the Nares Strait region (Knutz et al., 2012). These may have become active as a consequence of a Greenland–North America Plate collision during the final phase of continental drift, resulting in the Eurekan Orogeny on Ellesmere Island. Plate reconstructions and geochronological data suggests that the compression in the high Arctic ended after geomagnetic Chron 13 (early Oligocene; Tegner et al., 2011; Oakey and Chalmers, 2012), possibly as late as early Miocene (Riediger et al., 1984).

Late Cenozoic

Onshore successions

Neogene deposits are not known from onshore locations in northern West Greenland. Quaternary sediments resting on Greenland bedrock are known from outcrop field studies in many parts of northwest Greenland although the chronology remains sparse and the records fragmented (Funder et al., 2004).

Offshore successions

A series of Neogene sediments, mainly upper Miocene to Pliocene strata, have been drilled by wells (Alpha-1 S1, Delta-1, and T8-1) immediately south of the region (Fig. 3; *see* 'Central West Greenland basins' section). The information gained is limited by the nature of the cuttings samples from these wells. Quaternary sediments of marine, glacial-marine, and subglacial character are known from shallow cores and stratigraphic coreholes (e.g. Knutz et al., 2019). The distribution of upper Cenozoic successions offshore West Greenland based on mainly wells and seismic interpretation is shown in Figure 6.

Seismic stratigraphy

The early-middle Miocene is represented by the upper part of mega-unit D based on ties to ODP site 645, western Baffin Bay (Knutz et al., 2015). Mega-unit D forms a thick package of relatively continuous, parallel strata that thins updip along the ridge flanks by onlap onto horizon E1 (Fig. 41, 42). The Paleogene–Neogene boundary may correspond to horizon D2 in the lower part of mega-unit D, but there is no stratigraphic age control for this section. In the north, such as in Kap York Basin, the unit is largely absent or truncated east of the Melville Bay Ridge (Fig. 40), whereas in the southern part of the area, a thin interval of mega-unit D covers structural highs (Fig. 41). The sedimentary strata are intersected by steep, closely spaced faults, considered to be formed by porewater expulsion during burial. The unit is mainly attributed to marine hemipelagic sedimentation occasionally influenced by gravity-flow deposits that are near seismic resolution.

The upper Miocene and Pliocene successions are represented by mega-units C and B, respectively (Knutz et al., 2015). Mega-unit C is comprised of sedimentary prisms with internal seismic geometries ranging from parallel reflections to broad, mounded features. A late Miocene (approximately Tortonian) age for this unit is inferred from biostratigraphic records derived from the Alpha-1 well (Knutz et al., 2019). The sedimentary prisms probably formed as a combination of shelf build-out and transport by along-shelf ocean currents that have redistributed sediments emanating from fluvial sources along the West Greenland margin.

Mega-Unit B is mainly associated with deposition of wave-form contourites deposited by persistent ocean currents in an upper slope setting (Knutz et al., 2015). The succession is particular prominent over erosional scarps that truncate the underlying mega-unit (C) along the middle section of the continental margin (Fig. 42). Westward of the mid-shelf position, mega-units C and B are strongly modified by slope redeposition that is manifest by large mass-transport deposits that extend into the deep basin of Baffin Bay.

Mega-unit A is constructed by prograding glaciogenic wedges (Fig. 41) and deposition by ice streams that likely began in the late Pliocene (Knutz et al., 2019). Enhanced thicknesses of this unit (up to several kilometres) were generated by the Melville Bay and Upernavik trough-mouth fans that shape the present-day north West Greenland margin toward Baffin Bay (Newton et al., 2017; Knutz et al., 2019). Areas between the glacial troughs that rise toward shallow seabed banks, are characterized by flat-lying aggradational packages or asymmetric, mounded features interpreted as grounding zone wedges (Dowdeswell and Fugelli, 2012). Pleistocene sediments are sparse on the shelf margin due to high-energy conditions and iceberg erosion, but may attain metre-scale thicknesses in the deep basins and fjord systems (Andresen et al., 2014).

TECTONOSTRATIGRAPHIC SUMMARY OF THE WEST GREENLAND MARGIN

U. Gregersen, J.R. Hopper, G. Dam, and P.C. Knutz

Introduction

The West Greenland continental margin is an extensive area consisting of many basins and structures (Fig. 2) with a complex geological history (Fig. 3). The development of the sedimentary basins along the West Greenland margin is closely associated with a number of tectonic events that enable the evolution to be divided into distinct tectonostratigraphic phases (Gregersen et al., 2019). From oldest to youngest, the main phases are: pre-rift and early extension (pre-Cretaceous), early rift (Early to mid-Cretaceous), subsidence and rifting (mid-Cretaceous to early Campanian), late rift (Campanian to early Paleocene), drift (Paleocene to Eocene), and post-drift (post-Eocene). In a recent compilation, the regional tectonic development has been separated into two tectonic-sedimentary elements (TSE): The West Greenland rifted composite TSE encompassing the rifting phases and the Baffin Bay TSE representing the syn-drift and post-drift phases (U. Gregersen, P.C. Knutz, J.R. Hopper, and H. Nøhr-Hansen, work in progress, 2021; P.C. Knutz, C. Harrison, T. Brent, U. Gregersen, J.R. Hopper, and H. Nøhr-Hansen, work in progress, 2021).

The definition of each phase is based on the interpretation of large structures and regional unconformities, major changes in structural development, major changes in paleodrainage systems, and where possible, correlation to adjacent regions. Each phase includes at least one significant tectonic event, including significant faulting, uplift or subsidence, rifting pulses, and volcanism (including oceanic crust formation). Each tectonostratigraphic phase affects large parts of the margin, but not necessarily all of it. In addition, the phases are not necessarily synchronous along the entire margin, but might affect one segment of the margin early on and later along strike in another segment. The basis for this tectonostratigraphic summary section is the more comprehensive descriptions in the previous sections: southern-, central-, and northern West Greenland basins, and Dam et al. (2009) and Gregersen et al. (2019).

Pre-rift and early extension (Archean to earliest Cretaceous)

Although the pre-Cretaceous history likely involves many distinct tectonostratigraphic phases, the limited exposure of these rocks both onshore and offshore prevents detailed subdivision of pre-Cretaceous development into clear sequences and is considered here as a single phase. Archean–Proterozoic rocks dominate the onshore areas and have been found offshore in wells. Very limited Paleozoic and pre-Cretaceous Mesozoic rocks are known in the region, but are found locally, especially as onshore intrusions and dykes. Thus, much of their associated tectonic history is speculative. Combined with the lack of stratigraphic sequences over major time intervals, a robust tectonostratigraphic framework cannot be established with confidence. The following discussion is subdivided into three key time intervals important for the tectonostratigraphic development: Precambrian, Ordovician, and Triassic–earliest Cretaceous (incipient rifting).

Precambrian

The West Greenland to Eastern Canadian craton experienced a number of orogenic phases during Archean to Paleoproterozoic times and are subdivided by suture zones and mobile belts (St-Onge et al., 2009). The oldest metasedimentary and sedimentary rocks include the Vallen Group and the Karrat Group and are Paleoproterozoic (2000–1850 Ma; Henriksen et al., 2009; *see* 'Central West Greenland basins' section)

The Meso- to Neoproterozoic Thule Supergroup (1270−650 Ma) is an up to 6 km thick mostly unmetamorphosed succession of continental to shallow-water sandstone, mudstone, carbonate, and volcanic rocks overlaying crystalline rocks in the Thule Basin (Dawes, 1997; *see* 'Northern West Greenland basins' section). The supergroup is mainly exposed in northwest Greenland, but parts of the supergroup are also exposed locally on Ellesmere Island, northeastern Canada (Dawes, 1997).

The Thule Basin is characterized by fault-bounded blocks and intrusive and extrusive igneous rocks are common, indicating that evolution of the supergroup was controlled by extension and basin sagging in a divergent plate regime (Dawes, 1997). The Thule Supergroup was divided into formal lithostratigraphic groups and formations by Dawes (1997), who also outlined an overall tectonic development: some groups were likely controlled by a main stage of basin expansion and block faulting (e.g. the Baffin Bay Group) followed by accelerated basin subsidence, extensional faulting and sagging (the Dundas Group). A large number of dykes and sills on the West Greenland coast, not only in the Thule Supergroup (Dawes, 1997), but also farther south reflect many tectonic events through the Archean and the Proterozoic (Henriksen et al., 2009). Interpretation of seismic refraction and reflection data in the northern Baffin Bay supports the presence of a several kilometre thick unit of consolidated sedimentary rocks, which is likely the offshore equivalent of the Thule Supergroup. On seismic reflection data, the top of this unit can be tied to shallow cores in the Kap York Basin, within which Thule Supergroup rocks were recovered (*see* 'Northern West Greenland basins' section).

Ordovician

The only Paleozoic rocks found in West Greenland are a few Ordovician carbonate and shale seabed samples from the Davis Strait High and in the Fylla Canyon and from a few onshore localities in Greenland (Fig. 10). The general depositional environment was a shallow, carbonate shelf platform with restricted siliciclastic input in a tectonically stable margin setting (Stouge et al., 2007). Onshore, Ordovician pebble clasts are found within Cretaceous sediments in the Nuussuaq Basin (Dam et al., 2009; Peel, 2019) and samples of Ordovician are found at Fossilik (north of Nuuk; Fig. 10b). Samples from the Davis Strait High and Fossilik showed oil stains and a sample from the Fylla Canyon is consistent with an oil-prone source rock (Bojesen-Koefoed, 2011). The cumulative evidence suggests that a broad carbonate platform once existed over much of the West Greenland margin that was probably uplifted by later tectonic events and partly eroded away. The Ordovician may be regarded as a once widespread pre-rift unit, which probably was connected to the Ordovician successions along Eastern Canada (Foxe Basin and Hudson Bay) and north Greenland (Franklinian Basin; Higgins et al., 1991).

Triassic–Early Cretaceous incipient rifting

Along the proto-Northeast Atlantic east of Greenland, multiple phases of rifting occurred from the late Paleozoic and throughout the Mesozoic. In Baffin Bay and the Labrador Sea, indications of similar events are not clear since rocks of this age are scarce, but intracontinental extension cannot be ruled out. A few samples within wells include reworked Jurassic palynomorphs from southwest Greenland indicate pre-Cretaceous sedimentary successions (Piasecki, 2003). Thus, there is the possibility that some of the extensional basins in

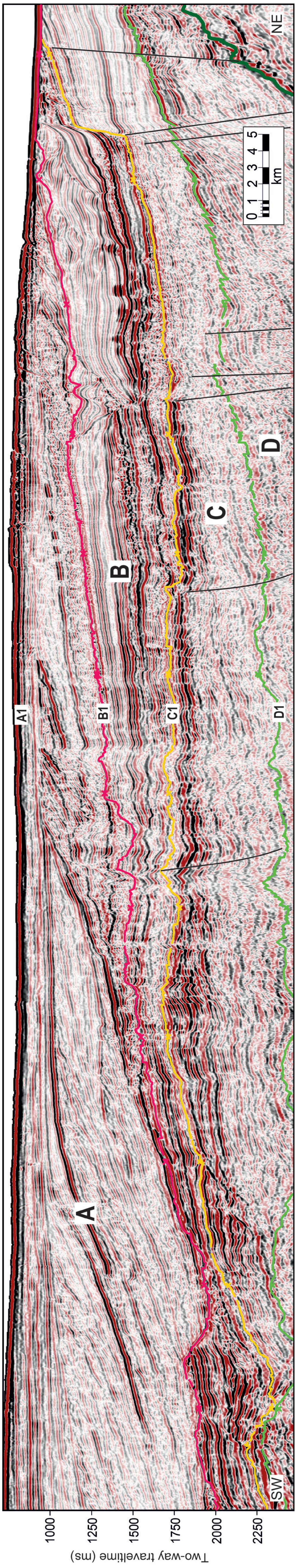

Figure 42. Seismic section showing wavy contourite deposits of likely Pliocene age (mega-unit B), formed over a prominent erosional scar incising the late Miocene sediment package (mega-unit C). The contourite drift deposits are covered by prograding units representing the early stages of glaciogenic trough-mouth fan build-out (mega-unit A) (Knutz et al., 2019). Mega-unit D forms a thick basin-infilling sequence that is densely faulted and deformed, presumably as a result of compaction and dewatering. Location of the section is shown in Figure 33 (Knutz et al., 2015). Seismic data courtesy of TGS.

the region are floored by Jurassic to earliest Cretaceous sedimentary rocks. In addition, extensional events beginning at this time would have thinned the lithosphere, an effect that basin subsidence and thermal models of the region should consider.

The recent documentation of Triassic and Jurassic rift-related dykes onshore along southern West Greenland (Fig. 11) supports the notion of intracontinental extension taking place farther to the north (Larsen et al., 2009). Late Triassic to late Jurassic (223–150 Ma) ultramafic, alkaline dykes may mark initial Mesozoic stretching in West Greenland, which was followed by late Jurassic to Early Cretaceous extensional phases (150 Ma and 140–133 Ma; Larsen et al., 2009). In addition, the onset of two exhumation and/or cooling phases (215 ± 5 Ma and 155 ± 5 Ma) in southern West Greenland could be in response to extension (Japsen et al., 2009).

Recently, the tectonostratigraphy of the West Greenland margin is described to constitute a rifted composite tectonosedimentary element (CTSE), divided into a pre-Cretaceous tectonosedimentary element and a Cretaceous tectonosedimentary element, with the tectonosedimentary elements being composed of mega-units (U. Gregersen, P.C. Knutz, J.R. Hopper, and H. Nøhr-Hansen, work in progress, 2021). The pre-Cretaceous tectonosedimentary element was formed during the pre-rift and early extension phase (upper part of mega-unit H), whereas the Cretaceous tectonosedimentary element (including mega-units F and G) was formed during the Cretaceous tectonic phases described below.

Early rift phase (Early- to mid-Cretaceous)

The early rift phase began during Early Cretaceous time and established the basic architecture of many basins along the West Greenland margin (Fig. 2, 3) and formed the first Mesozoic basins that can be mapped. Stretching and extensional tectonism during the late Early- to mid-Cretaceous was accommodated by large rotated fault blocks that controlled basin development in the Labrador Sea and Baffin Bay along both the West Greenland and Canadian continental margins (Whittaker et al., 1997; Chalmers and Pulvertaft, 2001).

Deeply buried, rifted basins with extensional faulting occur along most parts of the south West Greenland margin (Gregersen et al., 2018, 2019). The early rift phase resulted in north-northwest- to northwest striking deep-seated faults and major structures along most parts of both the southern and northern West Greenland margins (Fig. 2; Chalmers et al., 1993). Along north West Greenland, some of the largest structures were reactivated in the late rift and drift phases to form the main ridges there (Whittaker et al., 1997; Gregersen et al., 2013).

The oldest known Cretaceous tectonostratigraphic units on the West Greenland margin are middle-late Albian in the Nuussuaq Basin synrift deposits of the fluviodeltaic Kome Formation and Slibestensfjeldet Formation comprising Tectonostratigraphic sequence 1 (TSS-1) of Dam et al. (2009) (Fig. 3). In offshore areas, equivalent successions likely occur and are known farther northwest and southwest along the margin. Correlation of subvolcanic rocks with Cretaceous successions immediately west of the Nuussuaq Basin into offshore areas cannot be carried out with confidence since these units have not been penetrated by any offshore wells and the imaging below basalt is difficult; however, it is likely that Cretaceous or older basins are present below the Paleogene volcanic succession (Fig. 3, 4; Gregersen et al., 2019). A large Mesozoic seaway probably connected basins between Canada and Greenland from the Atlantic Ocean to the Cretaceous Western Interior Seaway in North America and into the Arctic Ocean (Bojesen-Koefoed et al., 2004).

Rifted basin successions of Early Cretaceous or older rocks are interpreted on the regional seismic data along eastern Baffin Bay (mega-unit G; Fig. 3) and are separated from Upper Cretaceous successions by a mid-Cretaceous unconformity in many places (Whittaker et al., 1997; Gregersen et al., 2013). Recent work by Nøhr-Hansen et al. (2018) from shallow wells in the Kap York Basin and on the Melville Bay Ridge, shows that Lower Cretaceous heterolithic successions with nonmarine to brackish sandstone, mudstone, and coal beds were deposited during a rifting event. These deposits rest unconformably on Proterozoic strata, which may be the equivalent of the Thule Supergroup (Fig. 36, 37, 38, 39). Albian deposits drilled in northeast Baffin Bay are similar to upper Lower Cretaceous deposits in the Nuussuaq Basin (Fig. 19, 20, 21) that may mark the final part of the early rift phase. On seismic sections, they tie with mega-unit G in northeast Baffin Bay (Fig. 3, 38, 39; Gregersen et al., 2019).

Along the south West Greenland margin, seismic mega-unit G (Fig. 3, 13) or equivalent units (e.g. the Kitsissut and Appat sequences of Chalmers et al., 1993) occur in many places, but were only recently drilled and dated (Fig. 3; Gregersen et al., 2018). In the Nuuk Basin, Albian to Cenomanian sedimentary successions that include thick conglomerate, thin sandstone, and mudstone in the AT7-1 well, correlate to mega-unit G (Fig. 3, 14; Gregersen et al., 2018). Other basins and structures, including the Lady Franklin (Fig. 15), Fylla Structural Complex (Fig. 16), Kangâmiut Basin, and Sisimiut Basin (Fig. 13), show similar units with rotated fault blocks in the deeper parts of the basins (Chalmers and Pulvertaft, 2001; Sørensen, 2006; Døssing, 2011; Gregersen et al., 2019).

Volcanism occurred in the region at this time as well, with a large coast parallel, phonolitic dyke of Albian age (106.1 ± 1.5 Ma) in southern West Greenland (Larsen et al., 2009). In addition, kilometre thick Cenomanian–Turonian volcanic rocks are documented (Knudsen et al., 2020) from the Nuuk Basin in a volcanic structure from the AT2-1 well (Fig. 14; Gregersen et al., 2018). The volcanism is related to rifting, either as a late part of the regional early rift phase or as a separate later pulse.

The earliest rift-related successions along the conjugate Canadian margin are slightly older than in southern West Greenland. Along the Labrador margin, coast parallel grabens and half grabens within the Saglek and Hopedale basins include the Bjarni Formation, which is likely Barremian to Cenomanian (Dickie et al., 2011; Dafoe, Williams et al., this volume). Successions below the Bjarni Formation include Lower Cretaceous volcanic rocks and locally interbedded sediments of the Alexis Formation, which are associated with the earliest stages of rifting (Balkwill and McMillan, 1990; Dickie et al., 2011).

Farther north in the west Baffin Bay region, Early Cretaceous rifted basins are also known from the Lancaster Sound and Baffin Shelf, and Barremian to Cenomanian successions were included in an early synrift phase (Harrison et al., 2011). Onshore Baffin, Bylot, and Devon islands, the continental to marginal marine Albian to Cenomanian Hassel Formation was also deposited during rifting (Harrison et al., 2011) and may be equivalent to parts of the Atane Formation of the Nuussuaq Basin.

Subsidence and rifting phase (mid-Cretaceous to early Campanian)

The Late Cretaceous is marked by regional subsidence and increasingly marine conditions. Thick mudstone-dominated successions were deposited across much of the West Greenland continental margin, including Cenomanian–Turonian and thick Campanian mudstone and/or shale of the Ikermiut and Itilli formations (Fig. 3, 12; Rolle, 1985; Christiansen et al., 2001; Nøhr-Hansen et al., 2016, 2018). A marine drowning took place in the Nuussuaq Basin and a large marine delta — the Atane delta — was established there (Pedersen and Pulvertaft, 1992; Dam et al., 2009; Pedersen and Nøhr-Hansen, 2014). These Upper Cretaceous mudstone units may be key for understanding the petroleum potential of the region. They likely include good seals, and given the right composition could be important source rocks.

Five oil types have been identified from seeps in the Nuussuaq Basin that are likely generated from Cretaceous to Paleocene source rocks (Bojesen-Koefoed et al., 1999) and oils thought to be generated from Cenomanian–Turonian (Itilli oil type) and Paleocene (Marraat oil type) source rocks are particularly of regional importance (Bojesen-Koefoed, 2011). Possible source rocks that may be related to the Itilli oil have also been identified from northeast Baffin Bay (Nøhr-Hansen et al., 2018, 2021), and farther north, where equivalent and excellent source rocks are known from the Kanguk Formation of Axel Heiberg Island (Núñez-Betelu et al., 1994). Thus, a Cenomanian–Turonian source rock succession is thought to be widespread along the conjugate Greenland and Canadian margins (Bojesen-Koefoed, 2011).

In northeast Baffin Bay, seismic successions with concordant reflections also indicate low-energy and gradual deposition of mudstone at the level interpreted as mid-Cretaceous (Whittaker et al., 1997). In the Kap York Basin, a thick succession with Upper Cretaceous black, organic-rich marine mudstone was sampled in several wells (Fig. 36) (Nøhr-Hansen et al., 2018, 2021). Well ties to seismic data show that these rocks occur within the lower part of mega-unit F, near horizon F3 (Fig. 3, 38, 39; Gregersen et al., 2019).

An issue with clearly delineating this phase of the development is that, in many places, subsidence includes some local rifting. Thus, it can be difficult to distinguish between this phase and the preceding and subsequent major rift phases. In the Melville Bay Graben, wedges of basin fill indicate renewed rifting (Whittaker et al., 1997), but it is uncertain exactly when this late rifting started; however, in the Nuussuaq Basin, it is evident that the late rift phase was initiated in the Early Campanian (Dam et al., 2000). Such wedges are also observed along the south West Greenland continental margin and form along faults within mega-unit F (Fig. 14, 16; Gregersen et al., 2018, 2019). In addition, the timing of local and renewed rifting probably differs from basin to basin along strike (Gregersen et al., 2013), further complicating the ability to distinguish between the rift phases and thermal subsidence phases.

Late rift phase (early Campanian to early Paleocene)

During the Campanian and through to the early Paleocene, a renewed phase of significant rifting affected most of the margin, especially in the Labrador Sea region, Nuussuaq Basin, and parts of eastern Baffin Bay (Whittaker et al., 1997; Dam et al., 2000, 2009; Chalmers and Pulvertaft, 2001; Gregersen et al., 2013).

In the southern region in the Labrador Sea, this phase is marked by north- to northeast-striking deep-seated faults and structures that crosscut the northwest trends of the early rift phase (Fig. 2; Chalmers et al., 1993; Gregersen et al., 2019). This rifting and associated rift-shoulder uplift formed some of the largest structures in south West Greenland, such as the Fylla Structural Complex (FSC; Fig. 2). The fault blocks of the Fylla Structural Complex appear as large tilted structures with eroded crests and in Qulleq-1 a hiatus occurs from the early Campanian to late Paleocene (Fig. 3, 12) at horizon F1 (Fig. 16) (Christiansen et al., 2001; Nøhr-Hansen et al., 2016). In addition, Campanian to Paleocene successions are absent in the Ikermiut-1, AT2-1, and AT7-1 wells at the F1 horizon (Fig. 3, 13, 14) (Nøhr-Hansen et al., 2016; Gregersen et al., 2018). It is likely that large parts of these strata were eroded as the structural highs developed in response to the late rifting.

In the Nuussuaq Basin, the late rift phase was initiated in the early Campanian and ceased by the Danian (Dam et al., 2000, 2009). It includes two Upper Cretaceous and two Paleocene tectonostratigraphic sequences (TSS 3 to TSS 4 and TSS 5 to TSS 6, respectively: Fig. 3), with a number of tectonic rifting events in the early Campanian and late Maastrichtian–Danian, including block faulting and uplift (Dam et al., 2000, 2009). In addition, volcanism of central West Greenland initiated during the Danian (Larsen et al., 2016).

The late rift phase was associated with regional uplift and canyon and/or valley incision related to the arrival of the Mantle Plume (Dam et al., 1998a; Dam, 2002). These valleys and canyons were probably major sediment input points, feeding mass-flows and/or fans in the offshore. The 'TSS' division of the Nuussuaq Basin and some of the regional hiatuses and unconformities are shown in Figure 3.

In the large volcanic rock–covered area offshore central West Greenland (Fig. 2), prevolcanic successions have not been drilled, but subvolcanic basins ((?)Danian–Cretaceous or older) are likely present. This may be supported by a 'low-velocity zone' below the volcanic rocks at Hellefisk-1 well from a refraction seismic study (Fig. 25b; Funck et al., 2012) and a zone with 'lower sediments' from a gravity modelling study (Fig. 25c; Skaarup, 2001, 2002). Farther north, along the northern West Greenland margin, the Upper Cretaceous includes thick mudstone-dominated successions deposited in large basins with periodically active boundary faults. This tectonism formed large wedge-shaped units of mega-unit F within half grabens that are especially well developed in the Melville Bay Graben and the Kivioq Basin and indicate active rifting during their deposition (Whittaker et al., 1997; Gregersen et al., 2013, 2019).

Along the Canadian margin of Baffin Bay, Cretaceous rift basins are interpreted in the Lancaster Sound and along the Baffin Shelf and the successions are divided into major units: an Early Cretaceous to Cenomanian early rift unit, and a rift unit with two sequences from late Cenomanian (ca. 95 Ma) to the top of Danian (Harrison et al., 2011). One good example of a rift basin is Scott Graben, known to contain seeps of Upper Cretaceous oil (MacLean et al., 1981; Harrison et al., 2011). The top of the late rift successions is marked by unconformities associated with the onset of seafloor spreading at Cape Dyer (Burden and Langille, 1991) and in Eclipse Trough (Miall et al., 1980).

Drift phase (Paleocene to Eocene)

By the early Paleocene, regional volcanism initiated along central West Greenland. Lithospheric breakup, oceanic crust formation, and the onset of a post-rift drift phase initiated during magnetic polarity Chron C27n (Chalmers and Laursen, 1995; Chalmers and Pulvertaft, 2001; Oakey and Chalmers, 2012; Larsen et al., 2016). A recent study by Keen et al. (2018) suggested that oceanic crust formation may have started as early as Chron C31 (latest Cretaceous) in the Labrador Sea.

In the Nuussuaq Basin, the boundary between the late rift phase (syn-rift TSS 6) and the overlying sedimentary and volcanic successions of the drift phase (TSS 7) is mid- to late Danian (Dam et al., 2009; Fig. 3). In the offshore, the age of this boundary is more difficult to constrain, but it is generally unconformable (horizon F1) toward structural highs and likely formed during the latest Cretaceous to Paleocene (Fig. 3, 16, 41; Gregersen et al., 2019).

Paleogene volcanism initiated during the early part of the drift phase with picritic hyaloclastites and lava flows of the Vaigat Formation extending from central West Greenland across the Davis Strait to Cape Dyer on Baffin Island (Larsen and Pedersen, 2009; Larsen et al., 2016). The lithostratigraphy, geology, and geochemistry of the volcanic rocks of the Vaigat Formation and the Maligât Formation and associated intrusions on Disko and Nuussuaq (Nuussuaq Basin) are documented in comphrehensive publications by Pedersen et al. (2017, 2018). The volcanic rocks overlying Paleocene to Cretaceous sedimentary rocks in the Nuussuaq Basin are well known from outcrops and/or field mapping and onshore wells (Dam et al., 2009; Pedersen et al., 2017).

During the Paleocene and Eocene, flood basalt, picrite, and other volcanic rocks formed over large areas of central West Greenland, Davis Strait, and southern Baffin Bay (Skaarup, 2001; Larsen et al., 2016; Larsen and Williamson, 2020). Paleogene volcanic rocks were drilled west of Greenland in Alpha-1 S1, Delta-1, Hellefisk-1, and Nukik-2 (Fig. 3, 25b, d) (Rolle, 1985; Hald and Larsen, 1987; Nelson et al., 2015; Nøhr-Hansen et al., 2016; Gregersen et al., 2019).

Seafloor spreading separated Greenland from Canada in a west-northwest–east-southeast direction, most pronounced from magnetic anomaly chrons C27n–C25n, and a reorientation of the spreading direction toward north-south occurred at chron C25n followed by the cessation of seafloor spreading by chron C13 (Oakey and Chalmers, 2012). These regional plate motions resulted in compression and transpression, including inversion of basins and faults in the central and northern parts of the West Greenland margin (e.g. Chalmers et al., 1993; Oakey and Chalmers, 2012; Gregersen et al., 2013).

A major complication for understanding the Paleocene–Eocene regional tectonics is the opening of the Northeast Atlantic east of Greenland at about 56 Ma (chron C24). With spreading occurring both to the southeast and southwest of the Greenland Plate, the net motion of Greenland was due north during this time, causing major compression in northern Greenland and Ellesmere Island during the Eurekan Orogeny (Trettin, 1991; Arne et al., 1998). This represented a major change in motion of the Greenland Plate, resulting in complex structures that overprinted many of the Cretaceous basins, including major inversion structures that increase in intensity toward the north (Whittaker et al., 1997; Gregersen et al., 2013).

The onset of the drift phase in the Paleocene–Eocene thus represents an important, but complex time of basin and structural development of the region. Key events that mark this period include:

- The development of the largest structural highs along the northern West Greenland margin, the Melville Bay and Kivioq ridges (Fig. 2). These show erosional truncation of the Upper Cretaceous successions (Fig. 41) suggesting that the ridges were emergent and may have been important sediment sources for the Eocene and later basins in the region (Whittaker et al., 1997; Gregersen et al., 2013; P.C. Knutz, C. Harrison, T. Brent, U. Gregersen, J.R. Hopper, and H. Nøhr-Hansen, work in progress, 2021).
- The development of a large inversion structure within the Nuussuaq Basin during the very latest Paleocene (Sørensen et al., 2017). This is documented by mapping of the Tunoqqu surface, a key marker horizon in the lower Selandian basalt succession that formed as a horizontal surface, but is now gently folded. Overlying Eocene volcanic successions are undeformed (Sørensen et al., 2017).
- Compression and transpression along parts of the Davis Strait High and the Ikermiut Fault Zone, causing thrust faults and flower structures, associated inversion of local ridges, and the formation of small pull-apart basins at the flanks of structures during the late Paleocene to early Eocene (Fig. 2, 13; Chalmers and Pulvertaft, 2001; Gregersen and Bidstrup, 2008).
- The local development of north-trending pull-apart basins formed on the central West Greenland margin by sinistral transpression due to the northward motion of the Greenland Plate relative to the North American Plate. These include the Ilulissat Graben as well as a number of minor grabens (Fig. 2; Gregersen and Bidstrup, 2008). The top of the volcanic successions has been faulted by this transpression. Recent dating of flood basalt samples, drilled in the Delta-1 well west of the Nuussuaq Basin (Fig. 2, 3) yielded radiometric ages in the early Eocene (Nelson et al., 2015).

- Presence of upper Eocene–(?) lower Oligocene fan deposits infilling the deep basins in central and northeast Baffin Bay which may be associated with the final phase of Eurekan compression (Knutz et al., 2012; P.C. Knutz, C. Harrison, T. Brent, U. Gregersen, J.R. Hopper, and H. Nøhr-Hansen, work in progress, 2021).

The cumulative evidence suggests that changes in spreading direction between Greenland and North America, coupled with the near simultaneous opening of the northeast Atlantic Ocean, had a significant impact on the structural and stratigraphic development of the West Greenland margin. The drift phase was thus far from passive, especially during the latest Paleocene–earliest Eocene and late Eocene–early Oligocene.

Post-drift phase (post-Eocene)

The post-Eocene marks the time when seafloor spreading between West Greenland and Eastern Canada ceased. By the early Oligocene (C13, ca. 35 Ma) the spreading systems in the Labrador Sea and Baffin Bay ended in favour of Northeast Atlantic seafloor spreading that eventually resulted in opening of Fram Strait (Engen et al., 2008). The northward motion of Greenland required to accommodate Labrador Sea extension was impeded by the plates to the north, resulting in the final Eurekan compressional phase (Tegner et al., 2011), though details of the Arctic plate boundaries remain uncertain.

Parts of uppermost Eocene, Oligocene, and lower Miocene successions of mega-unit D are mostly absent in wells from the southern West Greenland margin and southern Baffin Bay (Fig. 3; Nøhr-Hansen et al., 2016) and may indicate erosion or nondeposition over structural highs. It cannot be ruled out that major parts of the margin were exposed during these times, but this remains to be firmly established.

A latest Eocene to Oligocene period with onset of uplift has been described for the Nuussuaq Basin (Japsen et al., 2006). The late Cenozoic in central West Greenland was apparently influenced by up to 2 km of uplift during the mid- to late Cenozoic with discrete uplift phases taking place from about 36–30 Ma, 11–10 Ma, and 7–2 Ma (Japsen et al., 2006). Marine Paleocene sediments of the Nuussuaq Basin are presently located more than 1 km above sea level on Nuussuaq, supporting significant post-Paleocene uplift episodes (Japsen et al., 2006; Bonow et al., 2014). As a result of uplift, large areas were eroded and provided sediment supply into the offshore (Chalmers, 2000), although the upper Cenozoic strata is highly variable in thickness (Knutsen et al., 2012). Uplift and inversion of structures in the offshore basin are very important for understanding the development of the petroleum systems and reservoirs. Erosion and potential removal of significant overburden affects the pressures and fluid migration pathways, as well as the thermal structure of the basins. Thus, uplift is a complication that must be considered.

In the Miocene to Pleistocene successions (mega-units A–D) fewer large faults and other indications of tectonism are found, although some faulting occurred in the shallow section, mainly near boundary faults or as minor extensional fault systems (Gregersen et al., 2013). Despite the lack of borehole information, the late Oligocene–early Miocene was possibly a phase of relative tectonic quiescence judging from the seismic signature of mud-prone infilling strata that is typical for the upper part of mega-unit D (Knutz et al., 2015). By middle Miocene, the depositional signatures indicate a more energetic environment with development of a major aggradational prism along the northwest West Greenland margin (mega-unit C; Fig. 41). The upper Miocene sediment geometries are attributed to shelf progradation and along-slope transport by nearshore marine currents (Knutz et al., 2015). A regional, submarine unconformity related to slope instability and mass transport into Baffin Bay marks the top of mega-unit C. This late Miocene event of widespread shelf margin erosion points to a regional tectonic adjustment, possibly related to uplift of central West Greenland (Japsen et al., 2006) although the nature of the unconformity remains to be tested by offshore drilling. Marine sedimentation continued in the Pliocene with focused deposition of contourite units on the upper slope in Baffin Bay (mega-unit B) (Knutz et al., 2015) and offshore south West Greenland, known as the Davis Strait Drift Complex (Nielsen et al., 2011) and the Eirik Drift (e.g. Srivastava et al., 1987), which correlate to the successions of mega-units A–C (Fig. 3, 17; Gregersen et al., 2019).

Major sediment progradation linked to shelf-edge advances of the Greenland Ice Sheet into Baffin Bay (mega-unit A: Fig. 41) likely began during the late Pliocene (Hofmann et al., 2016; Knutz et al., 2019); however, the development of a glacial climate regime in the adjacent land areas around Baffin Bay may have occurred earlier, possibly in the early Pliocene (Korstgård and Nielsen, 1989) or late Miocene, commensurate with glaciation in southeast Greenland (St John and Krissek, 2002). Along the eastern Davis Strait, large submarine slides have been linked with early Pliocene glaciation on the southern West Greenland margin (Nielsen and Kuijpers, 2013). The glaciogenic succession of mega-unit A (Fig. 41) includes large trough-mouth fans that form prominent features, especially along the West Greenland margin and in the northern parts of Baffin Bay (Newton et al., 2017; Hofmann et al., 2018). In the Melville Bay region and the Nuussuaq Basin, the sediment dispersal related to early Pleistocene ice-sheet advances was apparently influenced by local tectonic structures (Hofmann et al., 2016; Knutz et al., 2019). Moreover, incision by ice streams and the transfer of glacially eroded sediments to the shelf margins may have induced passive tectonic activity and fault reactivation, although the sediment-isostatic effects remains to be quantified.

ACKNOWLEDGMENTS

The constructive comments from the reviewers are appreciated. Spectrum Geo Ltd. (Fig. 13), TGS-NOPEC Geophysical Company ASA (Fig. 14–16, 38–42), and Cairn Energy PLC (Capricorn Greenland Exploration) (Fig. 25d) are acknowledged for the display of the seismic data. Drafting work of nearly all figures by Jette Halskov, and on Figure 4–6 by Leith MacLeod is much appreciated.

REFERENCES

Alsulami, S., Paton, D.A., and Cornwell, D.G., 2015. Tectonic variation and structural evolution of the West Greenland continental margin; American Association of Petroleum Geologists, AAPG Bulletin, v. 99, p. 1689–1711. https://doi.org/10.1306/03021514023

Altenbernd, T., Jokat, W., Heyde, I., and Damm, V., 2014. A crustal model for northern Melville Bay, Baffin Bay; Journal of Geophysical Research, JGR Solid Earth, v. 119, p. 8610–8632. https://doi.org/10.1002/2014JB011559

Altenbernd, T., Jokat, W., Heyde, I., and Damm, V., 2015. Geophysical evidence for the extent of crustal types and the type of margin along a profile in the northeastern Baffin Bay; Journal of Geophysical Research, JGR Solid Earth, v. 120, p. 7337–7360. https://doi.org/10.1002/2015JB012307

Altenbernd, T., Jokat, W., Heyde, I., and Damm, V., 2016. Insights into the crustal structure of the transition between Nares Strait and Baffin Bay; Tectonophysics, v. 691, p. 31–47. https://doi.org/10.1016/j.tecto.2016.04.001

Andresen, C.S., Kjeldsen, K.K., Harden, B., Nørgaard-Pedersen, N., and Kjær, K.H., 2014. Outlet Glacier dynamics and bathymetry at Upernavik Isstrøm and Upernavik Isfjord, North-West Greenland; Geological Survey of Denmark and Greenland Bulletin, v. 31, p. 79–82. https://doi.org/10.34194/geusb.v31.4668

Arne, D.C., Zentilli, M., Grist, A.M., and Collins, M., 1998. Constraints on the timing of thrusting during the Eurekan orogeny, Canadian Arctic Archipelago: an integrated approach to thermal history analysis; Canadian Journal of Earth Sciences, v. 35, p. 30–38. https://doi.org/10.1139/e97-088

Balkwill, H.R. and McMillan, N.J., 1990. Mesozoic–Cenozoic geology of the Labrador shelf. Chapter 7 (Part 1); *in* Geology of the Continental Margin of Eastern Canada, volume 2., (ed.) M.J. Keen and G.L. Williams; Geological Survey of Canada, Geology of Canada, p. 295–324 (*also* Geological Society of America, The Geology of North America, v. I-1). https://doi.org/10.4095/132710

Bell, J.S. (co-ord.), 1989. East Coast Basin Atlas Series: Labrador Sea; Atlantic Geoscience Centre, Geological Survey of Canada, Bedford Institute of Oceanography, Dartmouth, Nova Scotia, 112 p. https://doi.org/10.4095/127152

Bendix-Almgreen, S.E., 1969. Notes on the Upper Cretaceous and Lower Tertiary fish faunas of northern West Greenland; Meddelelser fra Dansk Geologisk Forening, v. 19, p. 204–217.

Bennike, O., Hansen, K.B., Penney, D.N., Knudsen, K.L., and Rasmussen, K.L., 1994. Quaternary marine stratigraphy and geochronology in Central West Greenland; Boreas, v. 23, no. 2, p. 194–215. https://doi.org/10.1111/j.1502-3885.1994.tb00599.x

Birkelund, T., 1956. Upper Cretaceous belemnites from West Greenland; Bulletin Grønlands Geologiske Undersøgelse, v. 13, 28 p. (*also* Meddelelser om Grønland, v. 137, p. 9.)

Birkelund, T., 1965. Ammonites from the Upper Cretaceous of West Greenland; Meddr Grønland, v. 179, no. 7, 192 p.

Bojesen-Koefoed, J.A., 2011. West Greenland petroleum systems. An overview of source rocks and oil seepages and their implications for offshore petroleum exploration; Geological Survey of Denmark and Greenland, Danmarks og Grønlands Geologiske Undersøgelse Rapport 2011/42, 49 p.

Bojesen-Koefoed, J.A., Christiansen, F.G., Nytoft, H.P., and Pedersen, A.K., 1999. Oil seepage onshore West Greenland: evidence of multiple source rocks and oil mixing; *in* Petroleum Geology of Northwest Europe; Proceedings of the 5th Conference, (ed.) A.J. Fleet and S.A.R. Boldy; Geological Society, London, p. 305–314. https://doi.org/10.1144/0050305

Bojesen-Koefoed, J.A., Dam, G., Nytoft, H.P., Pedersen, G.K., and Petersen, H.I., 2001. Drowning of a nearshore peat-forming environment, Atane Formation (Cretaceous) at Asuk, West Greenland: sedimentology, organic petrography and geochemistry; Organic Geochemistry, v. 32, p. 967–980. https://doi.org/10.1016/S0146-6380(01)00072-9

Bojesen-Koefoed, J.A., Nytoft, H.P., and Christiansen, F.G., 2004. Age of oils in West Greenland: was there a Mesozoic seaway between Greenland and Canada; Geological Survey of Denmark and Greenland Bulletin, v. 4, p. 49–52. https://doi.org/10.34194/geusb.v4.4783

Bojesen-Koefoed, J.A., Bidstrup, T., Christiansen, F.G., Dalhoff, F., Gregersen, U., Nytoft, H.P., Nøhr-Hansen, H., Pedersen, A.K., and Sønderholm, M., 2007. Petroleum seepages at Asuk, Disko, West Greenland: implications for regional petroleum exploration; Journal of Petroleum Geology, v. 30, p. 219–236. https://doi.org/10.1111/j.1747-5457.2007.00219.x

Bonow, J.M., Japsen, P., and Nielsen, T.F.D., 2014. High-level landscapes along the margin of southern East Greenland—A record of tectonic uplift and incision after breakup in the NE Atlantic; Global and Planetary Change, v. 116, p. 10–29. https://doi.org/10.1016/j.gloplacha.2014.01.010

Boyd, A., 1990. A preliminary report on the lithostratigraphy and biostratigraphy of the Late Cretaceous Pautût flora from West Greenland; *in* Symposium Proceedings, Paleofloristic and Paleoclimatic Changes in the Cretaceous and Tertiary, Prague, August 28–September 1, 1989, p. 91–98.

Boyd, A., 1992. Revision of the Late Cretaceous Pautût Flora from West Greenland: Gymnospermopsida (Cycadales, Cycadeoidales, Caytoniales, Ginkgoales, Coniferales); Palaeontographica. Abteilung B, Paläophytologie, v. 225, p. 105–172.

Boyd, A., 1993. Paleodepositional setting of the Late Cretaceous Pautût Flora from West Greenland as determined by sedimentological and plant taphonomical data; Palaeogeography, Palaeoclimatology, Palaeoecology, v. 103, p. 251–280. https://doi.org/10.1016/0031-0182(93)90145-9

Boyd, A., 1994. Some limitations in using leaf physiognomic data as a precise method for determining paleoclimates with an example from the Late Cretaceous Pautût Flora of West Greenland; Palaeogeography, Palaeoclimatology, Palaeoecology, v. 112, p. 261–278. https://doi.org/10.1016/0031-0182(94)90076-0

Boyd, A., 1998. Macroleaf biostratigraphy of the Early Cretaceous beds in West Greenland; Zentralblatt für Geologie und Paläontologie, v. 1, p. 1455–1468.

Burden, E.T. and Langille, A.B., 1990. Stratigraphy and sedimentology of Cretaceous and Paleocene strata in half-grabens on the southeast coast of Baffin Island, Northwest Territories; Bulletin of Canadian Petroleum Geology, v. 38, p. 185–196.

Burden, E.T. and Langille, A.B., 1991. Palynology of Cretaceous and Tertiary strata, northeast Baffin Island, Northwest Territories, Canada: implications for the history of rifting in Baffin Bay; Palynology, v. 15, p. 91–114. https://doi.org/10.1080/01916122.1991.9989392

Catto, R., Taggart, S., and Poole, G., 2018. Petroleum geology of the Cygnus gas field, UK North Sea: from discovery to development; *in* Petroleum geology of NW Europe: 50 years of Learning – Proceedings of the 8th Petroleum Geology Conference, (ed.) M. Bowman and B. Levell; Geological Society, London, p. 307–318.

Chalmers, J.A., 2000. Offshore evidence for Neogene uplift in central West Greenland; Global and Planetary Change, v. 24, p. 311–318. https://doi.org/10.1016/S0921-8181(00)00015-1

Chalmers, J.A. and Laursen, K.H., 1995. Labrador Sea: the extent of continental and oceanic crust and the timing of the onset of seafloor spreading; Marine and Petroleum Geology, v. 12, p. 205–217. https://doi.org/10.1016/0264-8172(95)92840-S

Chalmers, J.A. and Pulvertaft, T.C.R., 2001. Development of the continental margins of the Labrador Sea – a review; *in* Non-Volcanic Rifting of Continental Margins: A Comparison of Evidence from Land and Sea, (ed.) R.C.L. Wilson, R.B. Whitmarsh, B. Taylor, and N. Froitzheim; Geological Society, London, Special Publications, v. 187, p. 77–105. https://doi.org/10.1144/GSL.SP.2001.187.01.05

Chalmers, J.A., Pulvertaft, T.C.R., Christiansen, F.G., Larsen, H.C., Laursen, K.H., and Ottesen, T.G., 1993. The southern West Greenland continental margin: rifting history, basin development, and petroleum potential; *in* Petroleum Geology of NW Europe: Proceedings of the 4th Conference, (ed.) J.R. Parker; Geological Society, London, p. 915–931. https://doi.org/10.1144/0040915

Chalmers, J.A., Dahl-Jensen, T., Bate, K.J., and Whittaker, R.C., 1995. Geology and petroleum prospectivity of the region offshore southern West Greenland - a summary. The Geological Survey of Denmark and Greenland, Copenhagen, Denmark; GGU Report, v. 165, p. 13–21.

Chalmers, J.A., Pulvertaft, T.C.R., Marcussen, C., and Pedersen, A.K., 1999. New insight into the structure of the Nuussuaq Basin, central West Greenland; Marine and Petroleum Geology, v. 16, p. 197–224. https://doi.org/10.1016/S0264-8172(98)00077-4

Chian, D. and Louden, K.E., 1994. The continent-ocean crustal transition across the southwest Greenland margin; Journal of Geophysical Research, v. 99, p. 9117–9135. https://doi.org/10.1029/93JB03404

Christiansen, F.G., 2011. Greenland petroleum exploration: history, breakthroughs in understanding and future challenges; *in* Arctic Petroleum Geology, (ed.) A.M. Spencer, A.F. Embry, D.L. Gautier, A.V. Stoupakova, and K. Sørensen; Geological Society, London, Memoirs, v. 35, p. 647–661. https://doi.org/10.1144/M35.42

Christiansen, F.G., Bojesen-Koefoed, J.A., Dam, G., Nytoft, H.-P., Larsen, L.M., Pedersen, A.K., and Pulvertaft, T.C.R., 1996. The Marraat oil discovery on Nuussuaq, West Greenland: evidence for a latest Cretaceous–earliest Tertiary oil prone source rock in the Labrador Sea–Melville Bay region; Bulletin of Canadian Petroleum Geology, v. 44, p. 39–54.

Christiansen, F.G., Boesen, A., Bojesen-Koefoed, J.A., Chalmers, J.A., Dalhoff, F., Dam, G., Hjortkjær, B.F., Kristensen, L., Larsen, L.M., Marcussen, C., Mathiesen, A., Nøhr-Hansen, H., Pedersen, A.K., Pedersen, G.K., Pulvertaft, T.C.R., Skaarup, N., and Sønderholm, M., 1999. Petroleum geological activities in West Greenland in 1998; Geology of Greenland Survey Bulletin, v. 183, p. 46–56. https://doi.org/10.34194/ggub.v183.5204

Christiansen, F.G., Dalhoff, F., Bojesen-Koefoed, J.A., Chalmers, J.A., Dam, G., Marcussen, C., Nøhr-Hansen, H., Nielsen, T., Pedersen, A.K., Riisager, P., and Sønderholm, M., 2000. Petroleum geological activities in West Greenland in 1999; Geology of Greenland Survey Bulletin, v. 186, p. 88–96.

Christiansen, F.G., Bojesen-Koefoed, J.A., Chalmers, J.A., Dalhoff, F., Mathiesen, A., Sønderholm, M., Dam, G., Gregersen, U., Marcussen, C., Nøhr-Hansen, H., Piasecki, S., Preuss, T., Pulvertaft, C.R., Rasmussen, J.A., and Sheldon, E., 2001. Petroleum geological activities in West Greenland in 2000; Bulletin - Grønlands Geologiske Undersøgelse, v. 189, p. 24–33. https://doi.org/10.34194/ggub.v189.5150

Christiansen, F.G., Bojesen-Koefoed, J.A., Chalmers, J.A., Dalhoff, F., Marcussen, C., Nielsen, T., Nøhr-Hansen, H., and Sønderholm, M., 2002. Petroleum geological activities in West Greenland in 2001; Bulletin - Grønlands Geologiske Undersøgelse, v. 191, p. 84–89. https://doi.org/10.34194/ggub.v191.5133

Citterio, M. and Ahlstrøm, A.P., 2013. Brief communication "The aerophotogrammetric map of Greenland ice masses"; The Cryosphere, v. 7, p. 445–449. https://doi.org/10.5194/tc-7-445-2013

Clarke, D.B. and Pedersen, A.K., 1976. Tertiary volcanic province of West Greenland; *in* Geology of Greenland, (ed.) A. Escher and W.S. Watt; Geological Survey of Greenland, Copenhagen, p. 365–385.

Clarke, D.B. and Upton, B.G.J., 1971. Tertiary basalts of Baffin Island: field relations and tectonic setting; Canadian Journal of Earth Sciences, v. 8, p. 248–258. https://doi.org/10.1139/e71-025

Clemmensen, L.B., 1988. Aeolian morphology preserved by lava cover, the Precambrian Mussartut Member, Eriksfjord Formation, South Greenland; Bulletin of the Geological Society of Denmark, v. 37, p. 105–116.

Collins, J.S.H. and Wienberg Rasmussen, H., 1992. Upper Cretaceous–lower Tertiary decapod crustaceans from West Greenland; Bulletin - Grønlands Geologiske Undersøgelse, v. 162, p. 1–46.

Connelly, J.N. and Thrane, K., 2005. Rapid determination of Pb isotopes to define Precambrian allochthonous domains: an example from West Greenland; Geology, v. 33, p. 953–956. https://doi.org/10.1130/G21720.1

Connelly, J.N., Thrane, K., Krawiec, A.W., and Garde, A.A., 2006. Linking the Palaeoproterozoic Nassugtoqidian and Rinkian orogens through the Disko Bugt region of West Greenland; Journal of the Geological Society, v. 163, p. 319–335. https://doi.org/10.1144/0016-764904-115

Cremer, M., 1989. Texture and microstructure of Neogene-Quaternary sediments, ODP sites 645 and 646, Baffin Bay and Labrador Sea; *in* Scientific Results. Ocean Drilling Program, (ed.) S.P. Srivastava, M.A. Arthur, B. Clement, A. Aksu, J. Baldauf, G. Bohrmann, W. Busch, T. Cederberg, M. Cremer, K. Dadey, A. De Vernal, J. Firth, F. Hall, M. Head, R. Hiscott, R. Jarrard, M. Kaminski, D. Lazarus, A.-L. Monjanel, O.B. Nielsen, R. Stein, F. Thiebault, J. Zachos, and H. Zimmerman; College Station, Texas, v. 105, p. 7–20. https://doi.org/10.2973/odp.proc.sr.105.1989

Croxton, C.A., 1976. Sampling of measured sections for palynological and other investigations between 69°and 72°N, central West Greenland; Rapport Grønlands Geologiske Undersøgelse, v. 80, p. 36–39.

Dahl-Jensen, D., Gundestrup, N.S., Miller, H., Watanabe, O., Johnsen, S.J., Steffensen, J.P., Clausen, H.B., Svensson, A., and Larsen, L.B., 2002. The NorthGrip deep drilling programme; Annals of Glaciology, v. 35, p. 1–4. https://doi.org/10.3189/172756402781817275

Dalhoff, F., Chalmers, J.A., Gregersen, U., Nøhr-Hansen, H., Rasmussen, J.A., and Sheldon, E., 2003. Mapping and facies analysis of Paleocene–Mid-Eocene seismic sequences, offshore southern West Greenland; Marine and Petroleum Geology, v. 20, p. 935–986. https://doi.org/10.1016/j.marpetgeo.2003.09.004

Dalhoff, F., Larsen, L.M., Ineson, J.R., Stouge, S., Bojesen-Koefoed, J.A., Lassen, S., Kuijpers, A., Rasmussen, J.A., and Nøhr-Hansen, H., 2006. Continental crust in the Davis Strait: new evidence from seabed sampling; Geological Survey of Denmark and Greenland Bulletin, v. 10, p. 33–36. https://doi.org/10.34194/geusb.v10.4901

Dam, G., 2002. Sedimentology of magmatically and structurally controlled outburst valleys along rifted volcanicmargins: examples from the Nuussuaq Basin, West Greenland; Sedimentology, v. 49, p. 505–532. https://doi.org/10.1046/j.1365-3091.2002.00457.x

Dam, G. and Nøhr-Hansen, H., 2001. Mantle-plumes and sequence stratigraphy; Late Maastrichtian-Early Paleocene of West Greenland; Bulletin of the Geological Society of Denmark, v. 48, p. 189–207.

Dam, G. and Sønderholm, M., 1994. Lowstand slope channels of the Itilli succession (Maastrichtian-Lower Paleocene), Nuussuaq, West Greenland; Sedimentary Geology, v. 94, p. 49–71. https://doi.org/10.1016/0037-0738(94)90146-5

Dam, G. and Sønderholm, M., 1998. Sedimentological evolution of a fault–controlled Early Paleocene incised valley system, Nuussuaq Basin, West Greenland; *in* Relative Role of Eustasy, Climate, and Tectonism in Continental Rocks, (ed.) K.W. Shanley and P.B. McCabe; Society for Sedimentary Geology, Special Publication, v. 59, p. 109–121. https://doi.org/10.2110/pec.98.59.0109

Dam, G., Larsen, M., and Sønderholm, M., 1998a. Sedimentary response to mantle plumes; implications from Paleocene onshore successions, West and East Greenland; Geology, v. 26, p. 207–210. https://doi.org/10.1130/0091-7613(1998)026%3c0207:SRTMPI%3e2.3.CO%3b2

Dam, G., Nøhr-Hansen, H., Christiansen, F.G., Bojesen-Koefoed, J.A., and Laier, T., 1998b. The oldest marine Cretaceous sediments in west Greenland (Umiivik-1 borehole) — record of the Cenomanian–Turonian Anoxic Event; Geology of Greenland Survey Bulletin, v. 180, p. 128–137. https://doi.org/10.34194/ggub.v180.5096

Dam, G., Nøhr-Hansen, H., and Kennedy, W.J., 1998c. The northernmost marine Cretaceous–Tertiary boundary section: Nuussuaq, West Greenland; Geology of Greenland Survey Bulletin, v. 180, p. 138–144. https://doi.org/10.34194/ggub.v180.5097

Dam, G., Nøhr-Hansen, H., Pedersen, G.K., and Sønderholm, M., 2000. Sedimentary and structural evidence of a new early Campanian rift phase in the Nuussuaq Basin, West Greenland; Cretaceous Research, v. 21, p. 127–154. https://doi.org/10.1006/cres.2000.0202

Dam, G., Pedersen, G.K., Sønderholm, M., Midtgaard, H., Larsen, L.M., Nøhr-Hansen, H., and Pedersen, A.K., 2009. Lithostratigraphy of the Cretaceous-Paleocene Nuussuaq Group, Nuussuaq Basin, West Greenland; Geological Survey of Denmark and Greenland Bulletin, v. 19, 171 p. https://doi.org/10.34194/geusb.v19.4886

Dam, G., Sønderholm, M., and Sørensen, E.V., 2020. Inherited basement canyons: impact on sediment distribution in the North Atlantic; Terra Nova, v. 32, issue 4, p. 272–280. https://doi.org/10.1111/ter.12459

Damm, V., 2010. The Expedition of the Research Vessel “Polarstern” to the Arctic in 2010 (ARK-XXV/3); Berichte zur Polar- und Meeresforschung (Reports on Polar and Marine Research), Volume 621; Alfred Wegener Institute for Polar and Marine Research, Bremerhaven, 234 p. https://doi.org/10.2312/BzPM_0621_2010

Dansgaard, W., Johnsen, S.J., Clausen, H.B., Dahl-Jensen, D., Gundestrup, N.S., Hammer, C.U., Hvidberg, C.S., Steffensen, J.P., Sveinbjörnsdottir, A.E., Jouzel, J., and Bond, G., 1993. Evidence for general instability of past climate from a 250-kyr ice-core record; Nature, v. 364, p. 218–220. https://doi.org/10.1038/364218a0

Dawes, P.R., 1997. The Proterozoic Thule Supergroup, Greenland and Canada: history, lithostratigraphy and development; Bulletin Grønlands Geologiske Undersøgelse, v. 174, 150 p. https://doi.org/10.34194/ggub.v174.5025

Deutsch, E.R., Kristjansson, L.G., and May, B.T., 1971. Remanent magnetism of lower Tertiary lavas on Baffin Island; Canadian Journal of Earth Sciences, v. 8, p. 1542–1552. https://doi.org/10.1139/e71-143

Dickie, K., Keen, C.E., Williams, G.L., and Dehler, S.A., 2011. Tectonostratigraphic evolution of the Labrador margin, Atlantic Canada; Marine and Petroleum Geology, v. 28, p. 1663–1675. https://doi.org/10.1016/j.marpetgeo.2011.05.009

Døssing, A., 2011. Fylla Bank: structure and evolution of a normal-to-shear rifted margin in the northern Labrador Sea; Geophysical Journal International, v. 187, p. 655–676. https://doi.org/10.1111/j.1365-246X.2011.05184.x

Dowdeswell, J.A. and Fugelli, E.M.G., 2012. The seismic architecture and geometry of grounding-zone wedges formed at the marine margins of past ice sheets; Geological Society of America Bulletin, v. 124, p. 1750–1761. https://doi.org/10.1130/B30628.1

Engen, O., Faleide, J.I., and Dyreng, T.K., 2008. Opening of the Fram Strait gateway: A review of plate tectonic constraints; Tectonophysics, v. 450, p. 51–69. https://doi.org/10.1016/j.tecto.2008.01.002

Escher, A. and Pulvertaft, T.C.R., 1976. Rinkian mobile belt of West Greenland; *in* Geology of Greenland, (ed.) A. Escher and W.S. Watt; The Geological Survey of Greenland, Copenhagen, p. 104–119.

Fensome, R.A., Nøhr-Hansen, H., and Wiliams, G.L., 2016. Cretaceous and Cenozoic dinoflagellate cysts and other palynomorphs from the western and eastern margins of the Labrador–Baffin Seaway; Geological Survey of Denmark and Greenland Bulletin, v. 36, 143 p. https://doi.org/10.34194/geusb.v36.4397

Floris, S., 1972. Scleractinian corals from the Upper Cretaceous and Lower Tertiary of Nûgssuaq, West Greenland; Bulletin Grønlands Geologiske Undersøgelse, v. 100, 132 p.

Funck, T., Jackson, H.R., Dehler, S.A., and Reid, I.D., 2006. A refraction seismic transect from Greenland to Ellesmere Island, Canada: the crustal structure in southern Nares Strait; Polarforschung, v. 74, p. 97–112. https://doi.org/10.2312/polarforschung.74.1-3.97

Funck, T., Jackson, H.R., Louden, K.E., and Klingelhöfer, F., 2007. Seismic study of the transform-rifted margin in Davis Strait between Baffin Island (Canada) and Greenland: what happens when a plume meets a transform; Journal of Geophysical Research, v. 112, 22 p. https://doi.org/10.1029/2006JB004308

Funck, T., Gohl, K., Damm, V., and Heyde, I., 2012. Tectonic evolution of southern Baffin Bay and Davis Strait: results from a seismic refraction transect between Canada and Greenland; Journal of Geophysical Research, v. 117, 24 p. https://doi.org/10.1029/2011JB009110

Funder, S. and Hansen, L., 1996. The Greenland ice sheet – a model for its culmination and decay during and after the last glacial maximum; Bulletin of the Geological Society of Denmark, v. 42, p. 137–152.

Funder, S., Jennings, A., and Kelly, M., 2004. Middle and late Quaternary glacial limits in Greenland; Developments in Quaternary Sciences, v. 2, pt. B, p. 425–430. https://doi.org/10.1016/S1571-0866(04)80210-0

Garde, A.A. and Marker, M., 2010. Geological map of Greenland, Kangerlussuaq/Søndre Strømfjord – Nuussuaq, sheet 3; Geological Survey of Denmark and Greenland, Copenhagen, scale: 1:500 000 (second edition)

Garde, A.A. and Steenfelt, A., 1999. Precambrian geology of Nuussuaq and the area north-east of Disko Bugt, West Greenland *in* Precambrian Geology of the Disko Bugt Region, West Greenland, (ed.) F. Kalsbeek; Geology of Greenland Survey Bulletin, v. 181, p. 6–40 (Appendix A).

Gerlings, J., Funck, T., Jackson, H.R., Louden, K.E., and Klingelhöfer, F., 2009. Seismic evidence for plume-derived volcanism during formation of the continental margin in southern Davis Strait and northern Labrador Sea; Geophysical Journal International, v. 176, p. 980–994. https://doi.org/10.1111/j.1365-246X.2008.04021.x

Green, P.F., Lidmar-Bergström, K., Japsen, P., Bonow, J.M., and Chalmers, J.A., 2013. Stratigraphic landscape analysis, thermochronology and the episodic development of elevated, passive continental margins; Geological Survey of Denmark and Greenland Bulletin, v. 30, 150 p. https://doi.org/10.34194/geusb.v30.4673

Greenland Ice-core Project (GRIP) Members, 1993. Climate instability during the last interglacial period recorded in the GRIP ice core; Nature, v. 364, p. 203–207. https://doi.org/10.1038/364203a0

Gregersen, U., 2014. The West Greenland Continental margin; *in* Tectonostratigraphic Atlas of the North-East Atlantic region, (ed.) J.R. Hopper, T. Funck, M. Stoker, U. Árting, G. Peron-Pinvidic, H. Doornenbal, and C. Gaina; Geological Survey of Denmark and Greenland, Copenhagen, p. 321–325.

Gregersen, U. and Bidstrup, T., 2008. Structures and hydrocarbon prospectivity in the northern Davis Strait area, offshore West Greenland; Petroleum Geoscience, v. 14, p. 151–166. https://doi.org/10.1144/1354-079308-752

Gregersen, U. and Skaarup, N., 2007. A mid-Cretaceous prograding sedimentary complex in the Sisimiut Basin, offshore West Greenland—stratigraphy and hydrocarbon potential; Marine and Petroleum Geology, v. 24, p. 15–28. https://doi.org/10.1016/j.marpetgeo.2006.10.005

Gregersen, U., Hopper, J.R., and Knutz, P.C., 2013. Basin seismic stratigraphy and aspects of prospectivity in the NE Baffin Bay, Northwest Greenland; Marine and Petroleum Geology, v. 46, p. 1–18. https://doi.org/10.1016/j.marpetgeo.2013.05.013

Gregersen, U., Knutz, P.C., and Hopper, J.R., 2016. New geophysical and geological mapping of the eastern Baffin Bay region, offshore West Greenland; Geological Survey of Denmark and Greenland Bulletin, v. 35, p. 83–86. https://doi.org/10.34194/geusb.v35.4945

Gregersen, U., Andersen, M.S., Nøhr-Hansen, H., Sheldon, E., Kokfelt, T.F., Olivarius, M., Knudsen, C., Jakobsen, K.G., and Adolfssen, J.S., 2018. New subsurface mapping offshore southern West Greenland using geophysical and geological data; Geological Survey of Denmark and Greenland Bulletin, v. 41, p. 57–62. https://doi.org/10.34194/geusb.v41.4342

Gregersen, U., Knutz, P.C., Nøhr-Hansen, H., Sheldon, E., and Hopper, J.R., 2019. Tectonostratigraphy and evolution of the West Greenland continental margin; Bulletin of the Geological Society of Denmark, v. 67, p. 1–21. https://doi.org/10.37570/bgsd-2019-67-01

Grímsson, F., Zetter, R., Halbritter, H., and Grimm, G.W., 2014. *Aponogeton* pollen from the Cretaceous and Paleogene of North America and West Greenland: implications for the origin and palaeobiogeography of the genus; Review of Palaeobotany and Palynology, v. 200, p. 161–187. https://doi.org/10.1016/j.revpalbo.2013.09.005

Grímsson, F., Zetter, R., Grimm, G.W., Pedersen, G.K., Pedersen, A.K., and Denk, T., 2015. Fagaceae pollen from the early Cenozoic of West Greenland: revisiting Engler's and Chaney's Arcto-Tertiary hypotheses; Plant Systematics and Evolution, v. 301, p. 809–832. https://doi.org/10.1007/s00606-014-1118-5

Grímsson, F., Grimm, G.W., Zetter, R., and Denk, T., 2016a. Cretaceous and Paleogene Fagaceae from North America and Greenland: evidence for a Late Cretaceous split between *Fagus* and the remaining Fagaceae; Acta Palaeobotanica, v. 56, no. 2, p. 247–305. https://doi.org/10.1515/acpa-2016-0016

Grímsson, F., Pedersen, G.K., Grimm, G.W., and Zetter, R., 2016b. A revised stratigraphy for the Palaeocene Agatdalen flora (Nuussuaq Peninsula, western Greenland): correlating fossiliferous outcrops, macrofossils, and palynological samples from phosphoritic nodules; Acta Palaeobotanica, v. 56, no. 2, p. 307–327. https://doi.org/10.1515/acpa-2016-0009

Guarnieri, P., Patin, C.A., and Rosa, D., 2016. Palaeovalleys at the basal unconformity of the Palaeoproterozoic Karrat Group, West Greenland; Geological Survey of Denmark and Greenland Bulletin, v. 35, p. 63–66. https://doi.org/10.34194/geusb.v35.4940

Hald, N., 1976. Early Tertiary flood basalts from Hareøen and western Nûgssuaq, West Greenland; Bulletin Grønlands Geologiske Undersøgelse, v. 120, 36 p.

Hald, N. and Larsen, J.G., 1987. Early Tertiary, low-potassium tholeiites from exploration wells on the West Greenland shelf; Grønlands Geologiske Undersøgelse Rapport, v. 136, 25 p.

Hansen, H.J., 1970. Danian foraminifera from Nûgssuaq, West Greenland; Bulletin Grønlands Geologiske Undersøgelse, v. 93, 132 p.

Hansen, J.M., 1980. Stratigraphy and structure of the Paleocene in central West Greenland and Denmark; Ph.D. thesis, University of Copenhagen, Copenhagen, Denmark, 156 p.

Harrison, J.C., Brent, T.A., and Oakey, G.N., 2011. Baffin Fan and its inverted rift system of Arctic eastern Canada: stratigraphy, tectonics and petroleum resource potential; *in* Arctic Petroleum Geology, (ed.) A.M. Spencer, A.F. Embry, D.L. Gautier, A.V. Stoupakova, and K. Sørensen; Geological Society, London, Memoirs, v. 35, p. 595–626. https://doi.org/10.1144/M35.40

Head, M.J., Norris, G., and Mudie, P.J., 1989. Palynology and dinocyst stratigraphy of the Upper Miocene and lowermost Pliocene, ODP Leg 105, Site 646, Labrador Sea; *in* Proceedings of the Ocean Drilling Program, Scientific Results, (ed.) S.P. Srivastava, M.A. Arthur, B. Clement, A. Aksu, J. Baldauf, G. Bohrmann, W. Busch, T. Cederberg, M. Cremer, K. Dadey, A. De Vernal, J. Firth, F. Hall, M. Head, R. Hiscott, R. Jarrard, M. Kaminski, D. Lazarus, A.-L. Monjanel, O.B. Nielsen, R. Stein, F. Thiebault, J. Zachos, and H. Zimmerman; College Station, Texas, v. 105, p. 423– 451. https://doi.org/10.2973/odp.proc.sr.105.1989

Heaman, L.M., Pell, J., Grütter, H., and Creaser, R.A., 2015. U–Pb geochronology and Sr/Nd isotope compositions of groundmass perovskite from the newly discovered Jurassic Chidliak kimberlite field, Baffin Island, Canada; Earth and Planetary Science Letters, v. 415, p. 183–199. https://doi.org/10.1016/j.epsl.2014.12.056

Heer, O., 1883a. Flora fossilis Grönlandica. Die fossile Flora Grönlands. Zweiter Theil; Verlag von J. Wurster and Comp, Zurich, 275 p.

Heer, O., 1883b. Oversigt over Grønlands fossile flora; Meddelelser om Grønland, v. 5, p. 79–202.

Henderson, G., and Pulvertaft, T.C.R., 1967. The stratigraphy and structure of the Precambrian rocks of the Umanak area, West Greenland; Meddelelser fra dansk geologisk Forening, v. 17, p. 1–20.

Henderson, G. and Pulvertaft, T.C.R., 1987. Geological map of Greenland; 1:100 000, Mârmorilik 71 V.2 Syd, Nûgâtsiaq 71 V.2 Nord, Pangnertôq V.2 Syd, descriptive text, 72 p, 3 maps, Copenhagen: Geological Survey of Greenland.

Henderson, G., Rosenkrantz, A., and Schiener, E.J., 1976. Cretaceous–Tertiary sedimentary rocks of West Greenland; *in* Geology of Greenland, (ed.) A. Escher and W.S. Watt; Grønlands Geologiske Undersøgelse, Copenhagen, 341–362 p.

Henriksen, N., Higgins, A.K., Kalsbeek, F., and Pulvertaft, T.C., 2009. Greenland from Archean to Quaternary - Descriptive text to the 1995 Geological map of Greenland 1:2 500 000; geological map of Greenland included; Geological Survey of Denmark and Greenland Bulletin, v. 18, 126 p. (second edition). https://geusbulletin.org/index.php/geusb/issue/view/323

Higgins, A.K., Ineson, J.R., Peel, J.S., Surlyk, F., and Sønderholm, M., 1991. Lower Palaeozoic Franklinian Basin of North Greenland; *in* Sedimentary Basins of North Greenland, (ed.) J.S. Peel and M. Sønderholm; Bulletin of the Geological Survey of Greenland, v. 160, p. 71–139.

Hjortkjær, B.F., 1991. Palynologisk undersøgelse af tertiære skifre fra Disko og Nûgssuaq, Vestgrønland; M.Sc. thesis, University of Copenhagen, Copenhagen, Denmark, 94 p.

Hjuler, M.L., Schovsbo, N.H., Pedersen, G.K., and Hopper, J.R., 2017. Potential hydrocarbon reservoirs of Albian–Paleocene age in the Nuussuaq Basin, West Greenland; Geological Survey of Denmark and Greenland Bulletin, v. 38, p. 49–52. https://doi.org/10.34194/geusb.v38.4408

Hofmann, J.C., Knutz, P.C., Nielsen, T., and Kuijpers, A., 2016. Seismic architecture and evolution of the Disko Bay trough-mouth fan, central West Greenland margin; Quaternary Science Reviews, v. 147, p. 69–90. https://doi.org/10.1016/j.quascirev.2016.05.019

Hofmann, J.C., Knutz, P.C., Kjær, K.H., Nielsen, T., and Ó Cofaigh, C., 2018. Glacial and submarine processes on the shelf margin of the Disko Bay Trough Mouth Fan; Marine Geology, v. 402, p. 33–50. https://doi.org/10.1016/j.margeo.2017.12.001

Hopper, J.R., Pedersen, G.K., Sørensen, E.V., Guarnieri, P., Schovsbo, N.H., Kokfelt, T.F., Hjuler, M.L., and Weng, W.L., 2016. Disko-Nuussuaq: Structural mapping and GIS compilation to better define petroleum exploration targets on Disko and Nuussuaq; Danmarks og Grønlands Geologiske Undersøgelse Rapport 2016/47, 119 p.

Hosseinpour, M., Müller, R.D., Williams, S.E., and Whittaker, J.M., 2013. Full-fit reconstruction of the Labrador Sea and Baffin Bay; Solid Earth, v. 4, p. 461–479. https://doi.org/10.5194/se-4-461-2013

Jackson, H.R. and Reid, I., 1994. Crustal thickness variations between the Greenland and Ellesmere Island margins determined from seismic refraction; Canadian Journal of Earth Sciences, v. 31, p. 1407–1418. https://doi.org/10.1139/e94-124

Japsen, P., Bonow, J.M., Green, P.F., Chalmers, J.A., and Lidmar-Bergström, K., 2006. Elevated, passive continental margins: long-term highs or Neogene uplifts? New evidence from West Greenland; Earth and Planetary Science Letters, v. 248, p. 330–339. https://doi.org/10.1016/j.epsl.2006.05.036

Japsen, P., Bonow, J.M., Green, P.F., Chalmers, J.A., and Lidmar-Bergström, K., 2009. Formation, uplift and dissection of planation surfaces at passive continental margins – a new approach; Earth Surface Processes and Landforms, v. 34, p. 683–699. https://doi.org/10.1002/esp.1766

Jensen, M.A. and Pedersen, G.K., 2010. Architecture of vertically stacked fluvial deposits, Atane Formation, Cretaceous, central West Greenland; Sedimentology, v. 57, issue 5, p. 1280–1314. https://doi.org/10.1111/j.1365-3091.2010.01146.x

Johannessen, P. and Nielsen, L.H., 1982. Aflejringer af flettede floder, Atane Formationen, Øvre Kridt, Pingo, øst Disko; Dansk geologisk Forening, Årsskrift for 1981, p. 13–27.

Johnsen, S.J., Dahl-Jensen, D., Gundestrup, N., Steffensen, J.P., Clausen, H.B., Miller, H., Masson-Delmotte, V., Sveinbjörnsdottir, A.E., and White, J., 2001. Oxygen isotope and palaeotemperature records from six Greenland ice-core stations: Camp Century, Dye-3, GRIP, GISP2, Renland and NorthGRIP; Journal of Quaternary Science, v. 16, p. 299–307. https://doi.org/10.1002/jqs.622

Kaminski, M.A., Gradstein, F.M., Scott, D.B., and Mackinnon, K.D., 1989. Neogene benthic foraminifer biostratigraphy and deep-water history of Sites 645, 646, and 647, Baffin Bay and Labrador Sea; *in* Scientific Results. Ocean Drilling Program, (ed.) S.P. Srivastava, M.A. Arthur, B. Clement, A. Aksu, J. Baldauf, G. Bohrmann, W. Busch, T. Cederberg, M. Cremer, K. Dadey, A. De Vernal, J. Firth, F. Hall, M. Head, R. Hiscott, R. Jarrard, M. Kaminski, D. Lazarus, A.-L. Monjanel, O.B. Nielsen, R. Stein, F. Thiebault, J. Zachos, and H. Zimmerman; College Station, Texas, v. 105, p. 731–756.

Keen, C.E., Dickie, K., and Dafoe, L.T., 2018. Structural characteristics of the ocean-continent transition along the rifted continental margin, offshore central Labrador; Marine and Petroleum Geology, v. 89, p. 443–463. https://doi.org/10.1016/j.marpetgeo.2017.10.012

Kennedy, W.J., Nøhr-Hansen, H., and Dam, G., 1999. The youngest Maastrichtian ammonite faunas from Nuussuaq, West Greenland; Geology of Greenland Survey Bulletin, v. 184, p. 13–17.

King, A.F. and McMillan, N.J., 1975. A Mid-Mesozoic breccia from the coast of Labrador; Canadian Journal of Earth Sciences, v. 12, p. 44–51. https://doi.org/10.1139/e75-005

Klaucke, I., Hesse, R., and Ryan, W.B.F., 1998. Seismic stratigraphy of the Northwest Atlantic Mid-Ocean Channel: growth pattern of a mid-ocean channel-levee complex; Marine and Petroleum Geology, v. 15, p. 575–585. https://doi.org/10.1016/S0264-8172(98)00044-0

Knudsen, C., Gregersen. U., Kokfelt. T.F., Olivarius, M., and Thomsen, T.B., 2020. A mid-Cretaceous alkaline volcano in the Davis Strait; Canadian Journal of Earth Sciences, v. 57, no. 1, p. 69–86. https://doi.org/10.1139/cjes-2018-0307

Knutsen, S.M., Arendt, N.P., Runge, M.K., Stilling, J., and Brandt, M.P., 2012. Structural provinces offshore West Greenland and key geological variations influencing play assessment; First Break, v. 30, p. 43–55. https://doi.org/10.3997/1365-2397.2012021

Knutz, P.C., Gregersen, U., and Hopper, J.R., 2012. Late Paleogene submarine fans in Baffin Bay and NW Greenland margin; 74th European Association of Geoscientists and Engineers, Copenhagen, Denmark, 1 p. (abstract)

Knutz, P.C., Hopper, J.R., Gregersen, U., Nielsen, T., and Japsen, P., 2015. A contourite drift system on the Baffin Bay-West Greenland margin linking Pliocene Arctic warming to poleward ocean circulation; Geology, v. 43, p. 907–910. https://doi.org/10.1130/G36927.1

Knutz, P.C., Newton, A.M.W., Hopper, J.R., Huuse, M., Gregersen, U., Sheldon, E., and Dybkjær, K., 2019. Eleven phases of Greenland Ice Sheet shelf-edge advance over the past 2.7 million years; Nature Geoscience, v. 12, p. 361–368. https://doi.org/10.1038/s41561-019-0340-8

Koch, B.E., 1959. Contribution to the stratigraphy of the non-marine Tertiary deposits on the south coast of the Nûgssuaq peninsula northwest Greenland with remarks on the fossil flora; Bulletin Grønlands Geologiske Undersøgelse, v. 22, 100 p.

Koch, B.E., 1963. Fossil plants from the lower Paleocene of the Agatdalen (Angmârtussut) area, central Nûgssuaq peninsula, northwest Greenland; Bulletin Grønlands Geologiske Undersøgelse, v. 38, 120 p. + 55 plates.

Koch, B.E., 1964. Review of fossil floras and nonmarine deposits of West Greenland; Geological Society of America Bulletin, v. 75, p. 535–548. https://doi.org/10.1130/0016-7606(1964)75[535:ROFFAN]2.0.CO;2

Kollmann, H.A. and Peel, J.S., 1983. Paleocene gastropods from Nûgssuaq, West Greenland; Bulletin Grønlands Geologiske Undersøgelse, v. 146, 115 p.

Koppelhus, E.B. and Pedersen, G.K., 1993. A palynological and sedimentological study of Cretaceous floodplain deposits of the Atane Formation at Skansen and Igdlunguaq, Disko, West Greenland; Cretaceous Research, v. 14, p. 707–734. https://doi.org/10.1006/cres.1993.1048

Korstgård, J.A. and Nielsen, O.B., 1989. Provenance of dropstones in Baffin Bay and Labrador Sea, Leg 105; *in* Proceedings ODP, (ed.) S.P. Srivastava, M.A. Arthur, B. Clement, A. Aksu, J. Baldauf, G. Bohrmann, W. Busch, T. Cederberg, M. Cremer, K. Dadey, A. De Vernal, J. Firth, F. Hall, M. Head, R. Hiscott, R. Jarrard, M. Kaminski, D. Lazarus, A.-L. Monjanel, O.B. Nielsen, R. Stein, F. Thiebault, J. Zachos, and H. Zimmerman; Ocean Drilling Program 1989, Scientific Results Volume 105, College Station, Texas, p. 65–69. https://doi.org/10.2973/odp.proc.sr.105.1989

Lanstorp, J., 1999. En palynologisk undersøgelse af kretassiske og paleocæne sedimenter fra det sydøstlige Nuussuaq, Vestgrønland; Geologisk Tidsskrift, v. 1999, no. 1, p. 13–20.

Larsen, J.G., 1977. Transition from low potassium olivine tholeiites to alkali basalts on Ubekendt Ejland; Meddelelser om Grønland, v. 200, no. 1, 42 p.

Larsen, L.M., 2006. Mesozoic to Palaeogene dyke swarms in West Greenland and their significance for the formation of the Labrador Sea and the Davis Strait; Danmarks og Grønlands Geologiske Undersøgelse Rapport 2006/34, 69 p.

Larsen, L.M. and Dalhoff, F., 2006. Composition, age, and geological and geotectonic significance of igneous rocks dredged from the northern Labrador Sea and the Davis Strait; Danmarks og Grønlands Geologiske Undersøgelse Rapport 2006/43, 51 p + appendices.

Larsen, L.M. and Dalhoff, F., 2007. Composition and significance of igneous rocks dredged in 2006 from the northern Labrador Sea and the Davis Strait; Danmarks og Grønlands Geologiske Undersøgelse Rapport 2007/67, 29 p. + appendix.

Larsen, J.G. and Grocott, J., 1991. Geological Map of Greenland, Svartenhuk 71 V.1 Nord; Geological Survey of Denmark and Greenland, Copenhagen, Denmark, scale 1:100 000.

Larsen, J.G. and Larsen, L.M., 2010. Volcanic rocks in the northern part of the Nuussuaq Basin, West Greenland; Danmarks og Grønlands Geologiske Undersøgelse Rapport 2010/11, 75 p.

Larsen, L.M. and Pedersen, A.K., 2009. Petrology of the Paleocene picrites and flood basalts on Disko and Nuussuaq, West Greenland; Journal of Petrology, v. 50, p. 1667–1711. https://doi.org/10.1093/petrology/egp048

Larsen, J.G. and Pulvertaft, T.C.R., 2000. The structure of the Cretaceous–Palaeogene sedimentary-volcanic area of Svartenhuk Halvø, central West Greenland; Geology of Greenland Survey Bulletin, v. 188, 40 p. https://doi.org/10.34194/ggub.v188.5190

Larsen, L.M. and Williamson, M.-C., 2020. Depleted and ultradepleted basalt and picrite in the Davis Strait: Paleocene volcanism associated with a transform continental margin; Geological Magazine, https://doi.org/10.1017/S0016756820000175

Larsen, L.M., Pedersen, A.K., Pedersen, G.K., and Piasecki, S., 1992. Timing and duration of Early Tertiary volcanism in the North Atlantic: new evidence from West Greenland; Geological Society of London, Special Publications, v. 68, p. 321–333. https://doi.org/10.1144/GSL.SP.1992.068.01.20

Larsen, L.M., Rex, D.C., Watt, W.S., and Guise, P.G., 1999. ^{40}Ar–^{39}Ar dating of alkali basaltic dykes along the south-west coast of Greenland: Cretaceous and Tertiary igneous activity along the eastern margin of the Labrador Sea; Geology of Greenland Survey Bulletin, v. 184, p. 19–29.

Larsen, L.M., Heaman, L.M., Creaser, R.A., Duncan, R.A., Frei, R., and Hutchinson, M., 2009. Tectonomagmatic events during stretching and basin formation in the Labrador Sea and the Davis Strait: evidence from age and composition of Mesozoic to Palaeogene dyke swarms in West Greenland; Journal of the Geological Society, v. 166, p. 999–1012. https://doi.org/10.1144/0016-76492009-038

Larsen, L.M., Pedersen, A.K., Tegner, C., Duncan, R.A., Hald, N., and Larsen, J.G., 2016. Age of Tertiary volcanic rocks on the West Greenland continental margin: volcanic evolution and event correlation to other parts of the North Atlantic Igneous Province; Geological Magazine, v. 153, p. 487–511. https://doi.org/10.1017/S0016756815000515

MacLean, B., Falconer, R.K.H., and Clarke, D.B., 1978. Tertiary basalts of western Davis Strait: bedrock core samples and geophysical data; Canadian Journal of Earth Sciences, v. 15, p. 773–780. https://doi.org/10.1139/e78-083

MacLean, B., Falconer, R.K.H., and Levy, E.M., 1981. Geological, geophysical and chemical evidence for natural seepage of petroleum off the northeast coast of Baffin Island; Bulletin of Canadian Petroleum Geology, v. 29, p. 75–95.

MacRae, R.A., Hills, L.V., and McIntyre, D.J., 1996. The paleoecological significance of new species of *Limbicysta* (Acritarcha) From the Upper Albian of the Canadian Arctic Islands; Canadian Journal of Earth Sciences, v. 33, p. 1475–1486. https://doi.org/10.1139/e96-111

McWhae, J.R.H., Elie, R., Laughton, K.C., and Gunther, P.R., 1980. Stratigraphy and Petroleum Prospects of the Labrador Shelf; Bulletin of Canadian Petroleum Geology, v. 28, no. 4, p. 460–488.

Meese, D.A., Gow, A.J., Alley, R.B., Zielinski, G.A., Grootes, P.M., Ram, M., Taylor, K.C., Mayewski, P.A., and Bolzan, J.F., 1997. The Greenland Ice Sheet Project 2 depth-age scale: Methods and results; Journal of Geophysical Research, v. 102, issue C12, p. 26411–26423. https://doi.org/10.1029/97JC00269

Miall, A.D., 1986. The Eureka Sound Group (Upper Cretaceous-Oligocene), Canadian Arctic Islands; Bulletin of Canadian Petroleum Geology, v. 34, p. 240–270.

Miall, A.D., Balkwill, H.R., and Hopkins, W.S., Jr., 1980. Cretaceous and Tertiary sediments at Eclipse Trough, Bylot Island area, Arctic Canada, and their regional setting; Geological Survey of Canada, Paper 79-23, 20 p.

Midtgaard, H.H., 1996a. Inner-shelf to lower shoreface hummocky sandstone bodies with evidence for geostrophic influenced combined flow, Lower Cretaceous, West Greenland; Journal of Sedimentary Research, v. 66, p. 343–353. https://doi.org/10.1306/D4268342-2B26-11D7-8648000102C1865D

Midtgaard, H.H., 1996b. Sedimentology and sequence stratigraphy of coalbearing synrift sediments on Nuussuaq and Upernivik Ø (Upper Albian - Lower Cenomanian), Central West Greenland; Ph.D. thesis, University of Copenhagen, Copenhagen, Denmark, 175 p. + appendices + plates.

Morlighem, M., Williams, C.N., Rignot, E., An, L., Arndt, J.E., Bamber, J.L., Catania, G., Chauché, N., Dowdeswell, A., Dorschel, B., Fenty, I., Hogan, K., Howat, I., Hubbard, A., Jakobsson, M., Jordan, T.M., Kjeldsen, K.K., Millan, R., Mayer, L., Mouginot, J., Noël, B.P.Y., O'Cofaigh, C., Palmer, S., Rysgaard, S., Seroussi, H., Siegert, M.J., Slabon, P., Straneo, F., van den Broeke, M.R., Weinrebe, W., Wood, M., and Zinglersen, K.B., 2017. BedMachine v3: Complete bed topography and ocean bathymetry mapping of Greenland from multibeam echo sounding combined with mass conservation; Geophysical Research Letters, v. 44, p. 11051–11061. https://doi.org/10.1002/2017GL074954

Müller-Michaelis, A., Uenzelmann-Neben, G., and Stein, R., 2013. A revised Early Miocene age for the instigation of the Eirik Drift, offshore southern Greenland: evidence from high-resolution seismic reflection data; Marine Geology, v. 340, p. 1–15. https://doi.org/10.1016/j.margeo.2013.04.012

Neben, S., Damm, V., Brent, T., and Tessensohn, F., 2006. New multi-channel seismic reflection data from Northwater Bay, Nares Strait: indications for pull-apart tectonics; Polarforschung, v. 74, p. 77–96.

NEEM community members, 2013: Eemian interglacial reconstructed from a Greenland folded ice core; Nature, v. 493, p. 489–494 with supplements. https://doi.org/10.1038/nature11789

Nelson, C.E., Jerram, D.A., Clayburn, J.A.P., Halton, A.M., and Roberge, J., 2015. Eocene volcanism in offshore southern Baffin Bay; Marine and Petroleum Geology, v. 67, p. 678–691. https://doi.org/10.1016/j.marpetgeo.2015.06.002

Newton, A.M.W., Knutz, P.C., Huuse, M., Gannon, P., Brocklehurst, S.H., Clausen, O.R., and Gong, Y., 2017. Ice stream reorganization and glacial retreat on the northwest Greenland shelf; Geophysical Research Letters, v. 44, p. 7826–7835. https://doi.org/10.1002/2017GL073690

Nielsen, T. and Kuijpers, A., 2013. Only 5 southern Greenland shelf edge glaciations since the early Pliocene; Scientific Reports, v. 3, cit. no. 1875. https://doi.org/10.1038/srep01875

Nielsen, T., Andersen, C., Knutz, P.C., and Kuijpers, A., 2011. The Middle Miocene to Recent Davis Strait Drift Complex: implications for Arctic–Atlantic water exchange; Geo-Marine Letters, v. 31, p. 419–426. https://doi.org/10.1007/s00367-011-0245-z

Nøhr-Hansen, H., 1996. Upper Cretaceous dinoflagellate cyst stratigraphy, onshore West Greenland; Bulletin Grønlands Geologiske Undersøgelse, v. 170, 104 p.

Nøhr-Hansen, H., 1997. Palynology of the GRO#3 well, Nuussuaq, West Greenland; Danmarks og Grønlands Geologisk Undersøgelse Rapport 1997/151, 19 p.

Nøhr-Hansen, H., 2003. Dinoflagellate cyst stratigraphy of the Palaeogene strata from the Hellefisk-1, Ikermiut-1, Kangâmiut-1, Nukik-1, Nukik-2 and Qulleq-1 wells, offshore West Greenland; Marine and Petroleum Geology, v. 20, p. 987–1016. https://doi.org/10.1016/S0264-8172(02)00116-2

Nøhr-Hansen, H. and Dam, G., 1997. Palynology and sedimentology across a new Cretaceous–Tertiary boundary section on Nuussuaq, West Greenland; Geology, v. 25, p. 851–854. https://doi.org/10.1130/0091-7613(1997)025%3c0851:PASAAN%3e2.3.CO%3b2

Nøhr-Hansen, H., Sheldon, E., and Dam, G., 2002. A new biostratigraphic scheme for the Paleocene onshore West Greenland and its implications for the timing of the pre-volcanic evolution; *in* The North Atlantic igneous province: stratigraphy, tectonic, volcanic and magmatic processes, (ed.) D.W. Jolley and B.R. Bell; Geological Society, London, Special Publication 197, p. 111–156. https://doi.org/10.1144/GSL.SP.2002.197.01.06

Nøhr-Hansen, H., Williams, G.L., and Fensome, R.A., 2016. Biostratigraphic correlation of the western and eastern margins of the Labrador-Baffin Seaway and implications for the regional geology; Geological Survey of Denmark and Greenland Bulletin, v. 37, 74 p. https://doi.org/10.34194/geusb.v37.4356

Nøhr-Hansen, H., Pedersen, G.K., Knutz, P.C., Bojesen-Koefoed, J.A., Sliwinska, K.K., and Hovikoski, J., 2018. Potential Cretaceous source-rocks from the north-east Baffin Bay, West Greenland; American Association of Petroleum Geologists European Regional Conference, abstract volume, Lisbon, Portugal, p. 29 (abstract).

Nøhr-Hansen, H., Pedersen, G.K., Knutz, P.C., Bojesen-Koefoed, J.A., Śliwińska, K.K., Hovikoski, J., Ineson, J.R., Kristensen, L., and Therkelsen, J., 2021. The Cretaceous succession of northeast Baffin Bay: stratigraphy, sedimentology and petroleum potential; Marine and Petroleum Geology, v. 133, art. no. 105108. https://doi.org/10.1016/j.marpetgeo.2021.105108

Nordenskiöld, A.E., 1871. Redogörelse för en expedition till Grönland år 1870; Kungliga Vetenskapliga-Akademiska Förhandlingar Stockholm 1870, no. 10, p. 973–1082.

Núñez-Betelu, L.K., Hills, L.V., and MacRae, R.A., 1994. Palynostratigraphy and hydrocarbon potential of the Upper Cretaceous Kanguk Formation: an integrated multidisciplinary analysis of the northeastern Canadian Arctic Archipelago; *in* Proceedings of the International Conference on Arctic Margins, (ed.) K.V. Simakov and D.K. Thurston; Magadan, Russia, September 1994, p. 54–61.

Nutman, A.P., Allaart, J.H., Bridgwater, D., Dimroth, E., and Rosing, M., 1984. Stratigraphic and geochemical evidence for the depositional environment of the Early Archaean Isua supracrustal belt, southern West Greenland; Precambrian Research, v. 25, p. 365–396. https://doi.org/10.1016/0301-9268(84)90010-X

Oakey, G.N. and Chalmers, J.A., 2012. A new model for the Palaeogene motion of Greenland relative to North America: plate reconstructions of the Davis Strait and Nares Strait regions between Canada and Greenland; Journal of Geophysical Research, v. 117, p. 1–28, B10401. https://doi.org/10.1029/2011JB008942

Olsen, T., 1993. Large fluvial systems: the Atane Formation, a fluvio-deltaic example from the Upper Cretaceous of central West Greenland; Sedimentary Geology, v. 85, p. 457–473. https://doi.org/10.1016/0037-0738(93)90098-P

Olsen, T. and Pedersen, G.K., 1991. The occurrence of marine fossils in the Upper Cretaceous deltaic sediments at Pautût, central West Greenland; Bulletin of the Geological Society of Denmark, v. 39, p. 111–122.

Payton, C.E. (ed.), 1977. Seismic stratigraphy – applications to hydrocarbon exploration; American Association of Petroleum Geologists, Memoir 26, Tulsa, Oklahoma, U.S.A., 516 p.

Pedersen, K.R., 1968. Angiospermous leaves from the Lower Cretaceous Kome Formation of northern West Greenland; Rapport Grønlands Geologiske Undersøgelse, v. 15, p. 17–18.

Pedersen, K.R., 1976. Fossil floras of Greenland; *in* Geology of Greenland, (ed.) A. Escher and W.S. Watt; Grønlands Geologiske Undersøgelse, Copenhagen, p. 518–535.

Pedersen, G.K. and Bromley, R.G., 2006. *Ophiomorpha irregulaire,* rare trace fossil in shallow marine sandstones, Cretaceous Atane Formation, West Greenland; Cretaceous Research, v. 27, p. 964–972. https://doi.org/10.1016/j.cretres.2006.06.001

Pedersen, A.K. and Larsen, L.M., 2006. The Ilugissoq graphite andesite volcano, central Nuussuaq, West Greenland; Lithos, v. 92, p. 1–19. https://doi.org/10.1016/j.lithos.2006.03.027

Pedersen, G.K. and Nøhr-Hansen, H., 2014. Sedimentary successions and palynoevent stratigraphy from the non-marine Lower Cretaceous to the marine Upper Cretaceous of the Nuussuaq Basin, West Greenland; Bulletin of Canadian Petroleum Geology, v. 62, no. 4, p. 261–288. https://doi.org/10.2113/gscpgbull.62.4.261

Pedersen, A.K. and Peel, J., 1985. Ordovician(?) gastropods from cherts in Cretaceous sandstones, south-east Disko, central West Greenland; Rapport Grønlands Geologiske Undersøgelse, v. 125, p. 30–33.

Pedersen, G.K. and Pulvertaft, T.C.R., 1992. The nonmarine Cretaceous of the West Greenland Basin, onshore West Greenland; Cretaceous Research, v. 13, p. 263–272. https://doi.org/10.1016/0195-6671(92)90002-8

Pedersen, A.K., Larsen, L.M., and Dueholm, K.S., 1993. Geological section along the south coast of Nuussuaq, central West Greenland; Geological Survey of Greenland, Copenhagen, Denmark, scale 1:20 000.

Pedersen, G.K., Larsen, L.M., Pedersen, A.K., and Hjortkjær, B.F., 1998. The syn-volcanic Naajaat lake, Paleocene of West Greenland; *in* Limno-geology – Research and Methods in Ancient and Modern Lacustrine Basins, (ed.) N. Noe-Nygaard; Palaeogeography, Palaeoclimatology, Palaeoecology, v. 140, no. 1–4, p. 271–287.

Pedersen, A.K., Larsen, L.M., Riisager, P., and Dueholm, K.S., 2002. Rates of volcanic deposition, facies changes and movements in a dynamic basin: the Nuussuaq Basin, West Greenland, around the C27n–C26r transition; *in* The North Atlantic Igneous Province: Stratigraphy, Tectonics, Volcanic and Magmatic Processes, (ed.) D.W. Jolley and B.R. Bell; Geological Society, London, Special Publication, v. 197, p. 157–181. https://doi.org/10.1144/GSL.SP.2002.197.01.07

Pedersen, A.K., Larsen, L.M., Pedersen, G.K., Heinesen, M.V., and Dueholm, K.S., 2003. Geological section along the south and south-west coast of Disko, central West Greenland; Geological Survey of Denmark and Greenland, Copenhagen, Denmark, scale 1:20 000.

Pedersen, A.K., Larsen, L.M., Pedersen, G.K., and Dueholm, K.S., 2005. Geological section across north central Disko from Nordfjord to Pingu, central West Greenland; Geological Survey of Denmark and Greenland, Copenhagen, Denmark, scale 1:20 000.

Pedersen, G.K., Andersen, L.A., Lundsteen, E.B., Petersen, H.I., Bojesen-Koefoed, J.A., and Nytoft, H.P., 2006. Depositional environments, organic maturity and petroleum potential of the Cretaceous coal-bearing Atane Formation at Qullissat, Nuussuaq Basin, West Greenland; Journal of Petroleum Geology, v. 29, p. 3–26. https://doi.org/10.1111/j.1747-5457.2006.00003.x

Pedersen, A.K., Larsen, L.M., Pedersen, G.K., Sønderholm, M., Midtgaard, H.H., Pulvertaft, T.C.R., and Dueholm, K.S., 2006a. Geological section along the north coast of the Nuussuaq peninsula, central West Greenland; Geological Survey of Denmark and Greenland, Copenhagen, Denmark, scale 1:20 000.

Pedersen, A.K., Larsen, L.M., Pedersen, G.K., and Dueholm, K.S., 2006b. Five slices through the Nuussuaq Basin, West Greenland; Geological Survey of Denmark and Greenland Bulletin, v. 10, p. 53–56. https://doi.org/10.34194/geusb.v10.4909

Pedersen, A.K., Larsen, L.M., and Pedersen, G.K., 2017. Lithostratigraphy, geology and geochemistry of the volcanic rocks of the Vaigat Formation on Disko and Nuussuaq, Paleocene of West Greenland; Geological Survey of Denmark and Greenland Bulletin, v. 39, 244 p. https://doi.org/10.34194/geusb.v39.4354

Pedersen, A.K., Larsen, L.M., and Pedersen, G.K., 2018. Lithostratigraphy, geology and geochemistry of the volcanic rocks of the Maligât Formation and associated intrusions on Disko and Nuussuaq, Paleocene of West Greenland; Geological Survey of Denmark and Greenland Bulletin, v. 40, 239 p. https://doi.org/10.34194/geusb.v40.4326

Peel, J.S., 2019. Ordovician gastropods from pebbles in Cretaceous fluvial sandstones in south-east Disko, West Greenland; Bulletin of the Geological Society of Denmark, v. 67, p. 75–81. https://doi.org/10.37570/bgsd-2019-67-05

Perch-Nielsen, K., 1973. Danian and Campanian/Maastrichtian coccoliths from Nûgssuaq, West Greenland; Bulletin of the Geological Society of Denmark, v. 22, p. 79–82.

Petersen, G.H. and Vedelsby, A., 2000. An illustrated catalogue of the Paleocene Bivalvia from Nuussuaq, Northwest Greenland: their paleoenvironments and the paleoclimate; Steenstrupia (Copenhagen), v. 25, p. 25–120.

Piasecki, S., 2003. Neogene dinoflagellate cysts from Davis Strait, offshore West Greenland; Marine and Petroleum Geology, v. 20, p. 1075–1088. https://doi.org/10.1016/S0264-8172(02)00089-2

Piasecki, S., Larsen, L.M., Pedersen, A.K., and Pedersen, G.K., 1992. Palynostratigraphy of the Lower Tertiary volcanics and marine clastic sediments in the southern part of the West Greenland Basin: implications for the timing and duration of the volcanism; Rapport Grønlands Geologiske Undersøgelse, v. 154, p. 13–31.

Pulvertaft, T.C.R., 1979. Lower Cretaceous fluvial-deltaic sediments at Kûk, Nûgssuaq, West Greenland; Bulletin of the Geological Society of Denmark, v. 28, p. 57–72.

Pulvertaft, T.C.R. and Chalmers, J.A., 1990. Are there Late Cretaceous unconformities in the onshore outcrops of the West Greenland basin? Rapport Grønlands geologiske Undersøgelse, v. 148, p. 75–82.

Raisbeck, G.M., Yiou, F., Jouzel, J., and Stocker, T.F., 2007. Direct north-south synchronization of abrupt climate change record in ice cores using Beryllium 10; Climate of the Past, v. 3, p. 541–547. https://doi.org/10.5194/cp-3-541-2007

Rasch, M., 2000. Holocene relative sea level changes in Disko Bugt, West Greenland; Journal of Coastal Research, v. 16, p. 306–315.

Rasmussen, T.M., 2002. Aeromagnetic survey in central West Greenland: Project Aeromag 2001; Geology of Greenland Survey Bulletin, v. 191, p. 67–72.

Rasmussen, J.A., Nøhr-Hansen, H., and Sheldon, E., 2003. Palaeoecology and palaeoenvironments of the lower Palaeogene succession, offshore West Greenland; Marine and Petroleum Geology, v. 20, p. 1043–1073. https://doi.org/10.1016/j.marpetgeo.2003.11.001

Rasmussen, S.O., Seierstad, I.K., Andersen, K.K., Bigler, M., Dahl-Jensen, D., and Johnsen, S.J., 2008. Synchronization of the NGRIP, GRIP, and GISP" ice cores across MIS 2 and palaeoclimatic implications; Quaternary Science Reviews, v. 27, p. 18–28. https://doi.org/10.1016/j.quascirev.2007.01.016

Ravn, J.P.J., 1918. De marine Kridtaflejringer i Vest-Grønland og deres fauna; Meddelelser om Grønland, v. 56, no. 9, p. 313–366.

Reid, I. and Jackson, H.R., 1997. Crustal structure of northern Baffin Bay: seismic refraction results and tectonic implications; Journal of Geophysical Research, v. 102, p. 523–542. https://doi.org/10.1029/96JB02656

Ricketts, B.D. and Stephenson, R.A., 1994. The demise of Sverdrup Basin; Late Cretaceous-Paleogene sequence stratigraphy and forward modelling; Journal of Sedimentary Research, v. 64, p. 516–530. https://doi.org/10.1306/d4267ff5-2b26-11d7-8648000102c1865d

Riediger, C.L., Bustin, R.M., and Rouse, G.E., 1984. New evidence for the chronology of the Eurekan Orogeny from south-central Ellesmere Island; Canadian Journal of Earth Sciences, v. 21, p. 1286–1295. https://doi.org/10.1139/e84-133

Rieke, H., McCann, T., Krawczyk, C.M., and Negendank, J.F.W., 2003. Evaluation of controlling factors on facies distribution and evolution in an arid continental environment: an example from the Rotliegend of the NE German Basin; *in* Tracing Tectonic Deformation Using the Sedimentary Record, (ed.) T. McCann and A. Saintot; Geological Society, London, Special Publications, p. 71–94. https://doi.org/10.1144/GSL.SP.2003.208.01.04

Riisager, P. and Abrahamsen, N., 1999. Magnetostratigraphy of Paleocene basalts from the Vaigat Formation of West Greenland; Geophysical Journal International, v. 137, p. 774–782. https://doi.org/10.1046/j.1365-246x.1999.00830.x

Riisager, J., Riisager, P., and Perrin, M., 1999. Palaeodirectional and palaeointensity results of Paleocene and Eocene basalts from West Greenland; Bulletin of the Geological Society of Denmark, v. 46, p. 69–78.

Riisager, J., Riisager, P., and Pedersen, A.K., 2003. Paleomagnetism of large igneous provinces: case-study from West Greenland, North Atlantic igneous province; Earth and Planetary Science Letters, v. 214, p. 409–425. https://doi.org/10.1016/S0012-821X(03)00367-4

Roest, W.R. and Srivastava, S.P., 1989. Sea-floor spreading in the Labrador Sea: A new reconstruction; Geology, v. 17, no. 11, p. 1000–1003. https://doi.org/10.1130/0091-7613(1989)017%3c1000:SFSITL%3e2.3.CO%3b2

Rolle, F., 1985. Late Cretaceous–Tertiary sediments offshore central West Greenland: lithostratigraphy, sedimentary evolution, and petroleum potential; Canadian Journal of Earth Sciences, v. 22, p. 1001–1019. https://doi.org/10.1139/e85-105

Rosa, D., Dewolfe, M.Y., Guarnieri, P., Kolb, J., LaFlamme, C., Partin, C.A., Salhi, S., Sørensen, E.V., Thaarup, S., Thrane, K., and Zimmermann, R., 2017. Architecture and mineral potential of the Palaeoproterozoic Karrat Group, West Greenland. Results of the 2016 season; Danmarks og Grønlands Geologiske Undersøgelse Rapport 2017/5, 112 p.

Rosa, D., Bernstein, S., DeWolfe, M.Y., Dziggel, A., Grocott, J., Guarnieri, P., Kolb, J., Partin, C.A., Sørensen, E.V., and Zimmermann, R., 2018. Architecture and mineral potential of the Palaeoproterozoic Karrat Group, West Greenland. Results of the 2017 season; Danmarks og Grønlands Geologiske Undersøgelse Rapport 2018/23, 102 p.

Rosenkrantz, A., 1970. Marine Upper Cretaceous and lowermost Tertiary deposits in West Greenland; Bulletin of the Geological Society of Denmark, v. 19, p. 406–453.

Rosenkrantz, A. and Pulvertaft, T.C.R., 1969. Cretaceous-Tertiary stratigraphy and tectonics in Northern West Greenland; The American Association of Petroleum Geologists Memoir, v. 12, p. 883–898. https://doi.org/10.1306/M12367C61

Rosing, M.T., Rose, N.M., Bridgwater, D., and Thomsen, H.S., 1996. Earliest part of Earth's stratigraphic record: a reappraisal of the >3.7 Ga Isua (Greenland) supracrustal sequence; Geology, v. 24, p. 43–46. https://doi.org/10.1130/0091-7613(1996)024%3c0043:EPOESS%3e2.3.CO%3b2

Sanford, B.V. and Grant, A.C., 2000. Geological framework of the Ordovician system in the southeast Arctic Platform, Nunavut; *in* Geology and Paleontology of the Southeast Arctic Platform and Southern Baffin Island, Nunavut, (ed.) A.D. McCracken and T.E. Bolton; Geological Survey of Canada, Bulletin 557, p. 13–38. https://doi.org/10.4095/211845

Schenk, C.J., 2011. Geology and petroleum potential of the West Greenland – East Canada Province; *in* Arctic Petroleum Geology, (ed.) A.M. Spencer, A.F. Embry, D.L. Gautier, A.V. Stoupakova, and K. Sørensen; Geological Society, London, Memoirs, v. 35, p. 627–645. https://doi.org/10.1144/M35.41

Scherstén, A. and Sønderholm, M., 2007. Provenance of Cretaceous and Paleocene sandstones in the West Greenland basins based on detrital zircon dating; Geological Survey of Denmark and Greenland Bulletin, v. 13, p. 29–32. https://doi.org/10.34194/geusb.v13.4969

Schmidt, A.G., Riisager, P., Abrahamsen, N., Riisager, J., Pedersen, A., and van der Voo, R., 2005. Palaeomagnetism of Eocene Talerua Member lavas on Hareøen, West Greenland; Bulletin of the Geological Society of Denmark, v. 52, p. 27–38. https://doi.org/10.37570/bgsd-2005-52-04

Secher, K., Heaman, L.M., Nielsen, T.F.D., Jensen, S.M., Schjøth, F., and Creaser, R.A., 2009. Timing of kimberlite, carbonatite, and ultramafic lamprophyre emplacement in the alkaline province located 64°N–67°N in southern West Greenland; Lithos, v. 112, p. 400–406. https://doi.org/10.1016/j.lithos.2009.04.035

Sheldon, E., Gregersen, U., and Andersen, M.S., 2018. Microfossil biostratigraphy of the Cretaceous–Paleocene of recently drilled exploration wells offshore SW Greenland; *in* Conference Proceedings, FORAMS 2018, 17th-22nd June 2018, Edinburgh and St Andrews, 1 p. (abstract)

Símonarsson, L.A., 1981. Upper Pleistocene and Holocene marine deposits and faunas on the north coast of Nuussuaq, West Greenland; Grønlands geologiske Undersøgelse Bulletin, v. 140, 107 p.

Skaarup, N., 2001. Offshore Volcanic Rocks in Baffin Bay. A seismic interpretation of the structures and development of the Palaeogene offshore volcanic rocks in central West Greenland and on the Baffin Island margin eastern Canada; Ph.D. thesis, University of Copenhagen (*also* The Geological Survey of Denmark and Greenland, Copenhagen; Danmarks og Grønlands Geologiske Undersøgelse Rapport 2001/117), 153 p.

Skaarup, N., 2002. Evidence for continental crust in the offshore Palaeogene volcanic province, central West Greenland; Geology of Greenland Survey Bulletin, v. 191, p. 97–102. https://doi.org/10.34194/ggub.v191.5135

Skaarup, N., Jackson, H.R., and Oakey, G., 2006. Margin segmentation of Baffin Bay/Davis Strait, eastern Canada based on seismic reflection and potential field data; Marine and Petroleum Geology, v. 23, p. 127–144. https://doi.org/10.1016/j.marpetgeo.2005.06.002

Slabon, P., Dorschel, B., Jokat, W., Myklebust, R., Hebbeln, D., and Gebhardt, C., 2016. Greenland ice sheet retreat history in the northeast Baffin Bay based on high-resolution bathymetry; Quaternary Science Reviews, v. 154, p. 182–198. https://doi.org/10.1016/j.quascirev.2016.10.022

Smith, M.P. and Bjerreskov, M., 1994. The Ordovician System in Greenland; International Union of Geological Sciences Publication; v. 29, 46 p.

Sønderholm, M., Nøhr-Hansen, H., Bojesen-Koefoed, J.A., Dalhoff, F., and Rasmussen, J.A., 2003. Regional correlation of Mesozoic–Palaeogene sequences across the Greenland–Canada boundary. Regionalgeologisk korrelation af mesozoiske–palæogene sekvenser i det canadisk–grønlandske sokkelområde; Final report for EFP-2001 project ENS J.Nr. 1313/01-0022; Geological Survey of Denmark and Greenland Report 2003/25, 175 p.

Sørensen, A.B., 2006. Stratigraphy, structure and petroleum potential of the Lady Franklin and Maniitsoq Basins, offshore southern West Greenland; Petroleum Geoscience, v. 12, p. 221–234. https://doi.org/10.1144/1354-079305-692

Sørensen, E.V., Hopper, J.R., Pedersen, G.K., Nøhr-Hansen, H., Guarnieri, P., Pedersen, A.K., and Christiansen, F.G., 2017. Inversion structures as potential petroleum exploration targets on Nuussuaq and northern Disko, onshore West Greenland; Geological Survey of Denmark and Greenland Bulletin, v. 38, p. 45–48. https://doi.org/10.34194/geusb.v38.4406

Srivastava, S.P., Arthur, M., and Clement, B. (ed.), 1987. Proceedings ODP, Initial Reports 105; College Station, TX (Ocean Drilling Program). https://doi.org/10.2973/odp.proc.ir.105.1987

St John, K.E.K. and Krissek, L.A., 2002. The late Miocene to Pleistocene ice-rafting history of southeast Greenland; Boreas, v. 31, p. 28–35. https://doi.org/10.1111/j.1502-3885.2002.tb01053.x

St-Onge, M.R., Van Gool, J.A.M., Garde, A.A., and Scott, D.J., 2009. Correlation of Archaean and Palaeoproterozoic units between northeastern Canada and western Greenland: constraining the pre-collisional upper plate accretionary history of the Trans-Hudson orogen; Geological Society of London, Special Publications, v. 318, p. 193–235. https://doi.org/10.1144/SP318.7

Steenstrup, K.J.V., 1883a. Beretning om Undersøgelsesrejserne i Nord-Grønland i Aarene 1878–80; Meddelelser om Grønland, v. 5, p. 1–41.

Steenstrup, K.J.V., 1883b. Om forekomsten af Forsteninger i de kulførende Dannelser i Nord-Grønland; Meddelelser om Grønland, v. 5, p. 43–77.

Steffensen, J.P., Andersen, K.K., Bigler, M., Clausen, H.B., Dahl-Jensen, D., Fischer, H., Goto-Azuma, K., Hansson, M., Johnsen, S.J., Jouzel, J., Masson-Delmotte, V., Popp, T., Rasmussen, S.O., Röthlisberger, R., Ruth, U., Stauffer, B., Andersen, M.-L.S., Sveinbjörnsdóttir, A.E., Svensson, A., and White, J.W.C., 2008. High-resolution Greenland ice core data show abrupt climate change happens in few years; Science, v. 321, no. 5889, p. 680–684. https://doi.org/10.1126/science.1157707

Storey, M., Duncan, R.A., Pedersen, A.K., Larsen, L.M., and Larsen, H.C., 1998. 40Ar/39Ar geochronology of the West Greenland Tertiary volcanic province; Earth and Planetary Science Letters, v. 160, p. 569–586. https://doi.org/10.1016/S0012-821X(98)00112-5

Stouge, S. and Peel, J.S., 1979. Ordovician conodonts from the Precambrian shield of southern West Greenland; Rapport Grønlands Geologiske Undersøgelse, v. 91, p. 105–109.

Stouge, S., Ineson, J.R., Rasmussen, J.A., and Dalhoff, F., 2007. Sedimentary dredge samples from the Davis Strait High: stratigraphic and palaeoenvironmental implications; Danmarks og Grønlands Geologiske Undersøgelse Rapport 2007/19, 49 p.

Strunk, A., Knudsen, M.F., Egholm, D.L., Jansen, J.D., Levy, L.B., Jacobsen, B.H., and Larsen, N.K., 2017. One million years of glaciation and denudation history in west Greenland; Nature Communications, v. 8, p. 14199. https://doi.org/10.1038/ncomms14199

Suckro, S.K., Gohl, K., Funck, T., Heyde, I., Ehrhardt, A., Schreckenberger, B., Gerlings, J., Damm, V., and Jokat, W., 2012. The crustal structure of southern Baffin Bay: implications from a seismic refraction experiment; Geophysical Journal International, v. 190, p. 37–58. https://doi.org/10.1111/j.1365-246X.2012.05477.x

Svensson, A., Andersen, K.K., Bigler, M., Clausen, H.B., Dahl-Jensen, D., Davies, S.M., Johnsen, S.J., Muscheler, R., Parrenin, F., Rasmussen, S.O., Röthlisberger, R., Seierstad, I., Steffensen, J.P., and Vinther, B.M., 2008. A 60 000 year Greenland stratigraphic ice core chronology; Climate of the Past, v. 4, p. 47–57. https://doi.org/10.5194/cp-4-47-2008

Szczechura, J., 1971. Paleocene Ostracoda from Nûgssuaq, West Greenland; Meddelelser om Grønland, v. 193, 42 p.

Tappe, S., Foley, S.F., Stracke, A., Romer, R.L., Kjarsgaard, B.A., Heaman, L.M., and Joyce, N., 2007. Craton reactivation on the Labrador Sea margins: 40Ar/39Ar age and Sr–Nd–Hf–Pb isotope constraints from alkaline and carbonatite intrusives; Earth and Planetary Science Letters, v. 256, p. 433–454. https://doi.org/10.1016/j.epsl.2007.01.036

Tegner, C., Storey, M., Holm, P.M., Þórarinsson, S.B., Zhao, X., Lo, C.-H., and Knudsen, M.F., 2011. Magmatism and Eurekan deformation in the High Arctic Large Igneous Province: 40Ar–39Ar age of Kap Washington Group volcanics, North Greenland; Earth and Planetary Science Letters, v. 303, p. 203–214. https://doi.org/10.1016/j.epsl.2010.12.047

Thomassen, B., 1991. The Black Angel lead-zinc mine 1973–1990; Rapport Grønlands Geologiske Undersøgelse, v. 152, p. 46–50.

Thrane, K., Baker, J., Connelly, J.N., and Nutman, A.P., 2005. Age, petrogenesis and metamorphism of the syn-collisional Prøven Igneous Complex, West Greenland; Contributions to Mineralogy and Petrology, v. 149, p. 541–555. https://doi.org/10.1007/s00410-005-0660-0

Trettin, H.P. (ed.), 1991. Geology of the Innuitian Orogen and Arctic Platform of Canada and Greenland; Geological Survey of Canada, Geology of Canada No. 3, 569 p. (*also* Geological Society of America, The Geology of North America, v. E,). https://doi.org/10.4095/133959

Trettin, H.P., Mayr, U., Long, G.D.F., and Packard, J.J., 1991. Cambrian to Early Devonian basin development, sedimentation, and volcanism, Arctic Islands; Chapter 8 *in* Geology of the Innuitian Orogen and Arctic Platform of Canada and Greenland, (ed.) H.P. Trettin; Geological Survey of Canada, Geology of Canada, No. 3, p. 163–238 (*also* Geological Society of America, The Geology of North America, v. E, Geological Society of America). https://doi.org/10.4095/133959

Umpleby, D.C., 1979. Geology of the Labrador Shelf; Geological Survey of Canada, Paper 79-13, 34 p. https://doi.org/10.4095/105927

Walker, M., Johnsen, S., Rasmussen, S.O., Steffensen, J.P., Popp, T., Gibbard, P., Hoek, W., Lowe, J., Andrews, J., Björck, S., Cwynar, L., Hughen, K., Kershaw, P., Kromer, B., Litt, T., Lowe, D.J., Nakagawa, T., Newnham, R., and Schwander, J., 2008. The Global Stratotype Section and Point (GSSP) for the base of the Holocene Series/Epoch (Quaternary System/Period) in the NGRIP ice core; Episodes, v. 31, no. 2, p. 264–267. https://doi.org/10.18814/epiiugs/2008/v31i2/016

Walker, M.J.C., Berkelhammer, M., Björck, S., and Cwynar, L.C., Fisher, D.A., Long, A.J., Lowe, J.J., Newnham, R.M., Rasmussen, S.O., and Weiss, H., 2012. Formal subdivision of the Holocene Series/Epoch: a discussion paper by a working group of INTIMATE (Integration of ice-core, marine and terrestrial records) and the Subcommission on Quaternary Stratigraphy (International Commission on Stratigraphy); Journal of Quaternary Science, v. 27, no. 7, p. 649–659. https://doi.org/10.1002/jqs.2565

Walker, M., Head, M.J., Berkelhammer, M., Björck, S., Cheng, H., Cwynar, L., Fisher, D., Gkinis, V., Long, A., Lowe, J., Newnham, R., Rasmussen, S.O., and Weiss, H., 2018. Formal ratification of the subdivision of the Holocene Series/Epoch (Quaternary System/Period): two new Global Boundary Stratotype Sections and Points (GSSPs) and three new stages/subseries; Episodes, v. 41, no. 4, p. 213–223. https://doi.org/10.18814/epiiugs/2018/018016

Wangner, D.J., Jennings, A.E., Vermassen, F., Dyke, L.M., Hogan, K.A., Schmidt, S., Kjær, K.H., Knudsen, M.F., and Andresen, C.S., 2018. A 2000-year record of ocean influence on Jakobshavn Isbræ calving activity, based on marine sediment cores; The Holocene, v. 28, no. 11, p. 1731–1744. https://doi.org/10.1177/0959683618788701

Watt, W.S., 1969. The coast-parallel dike swarm of southwest Greenland in relation to the opening of the Labrador Sea; Canadian Journal of Earth Sciences, v. 6, p. 1320–1321. https://doi.org/10.1139/e69-133

Weidick, A. and Bennike, O., 2007. Quaternary glaciation history and glaciology of Jakobshavn Isbræ and the Disko Bugt region, West Greenland: a review; Geological Survey of Denmark and Greenland Bulletin, v. 14, 78 p. https://doi.org/10.34194/geusb.v14.4985

Whittaker, R.C., Hamann, N.E., and Pulvertaft, T.C.R., 1997. A New Frontier Province Offshore Northwest Greenland: Structure, Basin Development, and Petroleum Potential of the Melville Bay Area; American Association of Petroleum Geologists Bulletin, v. 81, p. 978–998.

Williamson, M.-C., Courtney, R.C., Keen, C.E., and Dehler, S.A., 1994. Relationship between crustal deformation and magmatism in rift zones: modelling approach and applications to the eastern Canadian margin; Geological Survey of Canada, Current Research, v. 1994, p. 251–258. https://doi.org/10.4095/194122

Contents

Overview of the stratigraphy, paleoclimate, and paleoceanography of the Labrador–Baffin Seaway

L.T. Dafoe[1*], G.L. Williams[1], K. Dickie[1], U. Gregersen[2], P.C. Knutz[2], G. Dam[2], G.K. Pedersen[2], H. Nøhr-Hansen[2], J.W. Haggart[3], and K.J. DesRoches[1]

Dafoe, L.T., Williams, G.L., Dickie, K., Gregersen, U., Knutz, P.C., Dam, G., Pedersen, G.K., Nøhr-Hansen, H., Haggart, J.W., and DesRoches, K.J., 2022. Overview of the stratigraphy, paleoclimate, and paleoceanography of the Labrador–Baffin Seaway; in *Geological synthesis of Baffin Island (Nunavut) and the Labrador–Baffin Seaway, (ed.) L.T. Dafoe and N. Bingham-Koslowski; Geological Survey of Canada, Bulletin 608, p. 311–339. https://doi.org/10.4095/321853*

Abstract: The tectonic evolution of the Labrador–Baffin Seaway began with Early Cretaceous extension between Greenland and North America, resulting in the development of basins infilled with nonmarine and shallow-marine clastic strata. The Late Cretaceous was a time of continued rifting and local subsidence, with deposition of widespread deeper water marine mud and localized sand deposits. Seafloor spreading began in the south in the Latest Cretaceous and propagated throughout the seaway by the Early Paleocene. Regional seafloor spreading coincided with the onset of significant volcanism in the Davis Strait to central West Greenland region, as well as a regional regression. A change in the spreading direction around the Paleocene–Eocene boundary, was accompanied by strike-slip motion in the Davis Strait and Baffin Bay, deformation and basin inversion, and development of regional unconformities. After seafloor spreading ceased in the late Eocene, the seaway was filled by upper Paleogene to Recent sediments, with clinoform progradation building the modern-day shelves.

Résumé : L'évolution tectonique du bras de mer Labrador-Baffin a débuté au Crétacé précoce par une distension entre le Groenland et l'Amérique du Nord, ce qui a mené subséquemment à la formation de bassins à remplissage de strates détritiques de milieux non marin et marin peu profond. Le Crétacé tardif a été marqué par la poursuite du rifting et une subsidence locale, alors que s'accumulaient sur une vaste étendue des vases marines en eau plus profonde et, localement, des dépôts de sable. L'expansion des fonds marins a débuté au Crétacé terminal dans le sud et, au Paléocène précoce, s'était propagée à l'ensemble du bras de mer. L'expansion régionale des fonds marins a coïncidé avec le début d'un volcanisme d'importance dans la région s'étendant du détroit de Davis jusqu'à la partie centrale de l'ouest du Groenland, ainsi qu'avec une régression régionale. Un changement dans la direction de l'expansion des fonds marins près de la limite Paléocène-Éocène a été accompagné par un mouvement de coulissage dans le détroit de Davis et la baie de Baffin, d'une déformation et d'une inversion de relief du bassin, ainsi que de la formation de discordances régionales. Après l'arrêt de l'expansion des fonds marins à la fin de l'Éocène, le bras de mer a été rempli par des sédiments s'échelonnant du Paléogène supérieur à l'Actuel, et les plates-formes continentales observées de nos jours ont été construites par la progradation de clinoformes.

[1]Geological Survey of Canada, 1 Challenger Drive, P.O. Box 1006, Dartmouth, Nova Scotia B2Y 4A2
[2]Geological Survey of Denmark and Greenland, Øster Voldgade 10, 1350 Copenhagen, Denmark
[3]Geological Survey of Canada, 1500-605 Robson Street, Vancouver, British Columbia V6B 5J3
*Corresponding author: L.T. Dafoe (email: lynn.dafoe@nrcan-rncan.gc.ca)

INTRODUCTION

The Labrador–Baffin Seaway formed during Mesozoic–Cenozoic rifting and encompasses the Labrador Sea, Davis Strait, and Baffin Bay. It includes major basins found primarily in the offshore, as well as onshore areas such as Nuussuaq Basin, the Bylot Island area, and a small region on southeast Baffin Island (Fig. 1). This seaway began forming in the Early Cretaceous as a result of extension within the Laurasia plate between future North America and Greenland (Roest and Srivastava, 1989). Early rifting thinned the crust, forming large grabens and half-grabens across the region (e.g. Balkwill and McMillan, 1990; Chalmers and Pulvertaft, 2001; Dickie et al., 2011; Gregersen et al., 2019). Extension continued into the Late Cretaceous, but was focused farther offshore central Labrador and southern West Greenland, where continental mantle was exhumed and serpentinized (Chian et al., 1995a, b; Keen et al., 2018a, b, this volume). Extension was followed by the onset of seafloor spreading in the Maastrichtian (chron C31) in the central Labrador Sea, and regionally, spreading took place from chron C27n (Danian; Oakey and Chalmers, 2012; Keen et al., 2018a, b). Around the Paleocene–Eocene boundary, between the development of chrons C25n and C24n, the direction of opening changed from northeast–southwest to more northerly. This resulted in significant strike-slip motion through the Davis Strait region along the Ungava Fault Zone and along other major fracture zones (Oakey and Chalmers, 2012; Keen et al., this volume). This change in plate motion also led to convergence of Greenland with Ellesmere Island, resulting in extensive basin inversion in northern Baffin Bay. Creation of oceanic crust ceased by chron C13 near the Eocene–Oligocene boundary (Oakey and Chalmers, 2012). An updated tectonic evolution of the Labrador–Baffin Seaway is presented in Keen et al. (this volume) and new insights into the tectonostratigraphy of the West Greenland margin are described in Gregersen et al. (2019) and summarized in Gregersen et al. (this volume).

The location of the landward limit of oceanic crust from Keen et al. (this volume) is key to restoring plate boundaries and identifying conjugate margin segments, which have been widely separated over time. Inboard of the landward limit of oceanic crust, basement terranes can be correlated into the offshore and across the Labrador–Baffin Seaway (Wasteneys et al., 1996; Chalmers et al., 1999; Hall et al., 2002; St-Onge et al., 2009; Keen et al., this volume). Major crustal blocks include: the Grenville Province of southern Labrador; the Makkovik and Ketilidian orogens; the North Atlantic Craton; the Meta Incognita microcontinent and Nagssugtoqidian Orogen; the Rae Craton; and the Ellesmere–Devon terrane and Inglefield mobile belt (Fig. 1). These Archean and Proterozoic blocks comprise the rifted and thinned continental basement underlying the Mesozoic rift basins (Grant, 1975; MacLean and Falconer, 1979; MacLean et al., 1981; Rolle, 1985; Bell, 1989; MacLean et al., 1990; Wasteneys et al., 1996; Dalhoff et al., 2006; Harrison et al., 2011; Gregersen et al., 2018, 2019; St-Onge et al., this volume). In addition, Proterozoic and Paleozoic sedimentary, metasedimentary, and related volcanic rocks are found both onshore and offshore, or have been hypothesized based on seismic interpretations (Keen and Barrett, 1973; Keen et al., 1974; Grant, 1975; MacLean and Srivastava, 1976; Jansa, 1976; MacLean et al., 1977, 1984, 1990; Rice and Shade, 1982; Bell, 1989; Fader et al., 1989; Moir, 1989; Dawes, 1997; Reid and Jackson, 1997; Dalhoff et al., 2006; Funck et al., 2006; Harrison et al., 2011; Brent et al., 2013; Zhang and Pell, 2014; Zhang et al., 2014; Atkinson et al., 2017; Bingham-Koslowski, 2018, 2019; Nøhr-Hansen et al., 2018; Bingham-Koslowski et al., 2019; Bingham-Koslowski, Zhang, and McCartney, this volume; Gregersen et al., this volume; Turner, this volume).

Overlying pre-rift basement, major Cretaceous–Paleogene sedimentary basins along the Canadian margin (Fig. 1) include the Hopedale and Saglek basins, offshore Labrador (Umpleby, 1979; Balkwill, 1987; Balkwill and McMillan, 1990; Dickie et al., 2011; Dafoe, Dickie, Williams, and McCartney, this volume); the Labrador Sea Basin in the central Labrador Sea overlying oceanic crust (Balkwill and McMillan, 1990; Dafoe, Dickie, Williams, and McCartney, this volume); Cumberland Basin on the southeast Baffin Island Shelf (Balkwill, 1987; Dafoe, DesRoches, and Williams, this volume); Scott and Buchan grabens on the Baffin Shelf (Jackson et al., 1992; Harrison et al., 2011; Dafoe, Dickie, and Williams, this volume); Baffin Basin in the central part of Baffin Bay (Balkwill and McMillan, 1990; Dafoe, Dickie, and Williams, this volume; Gregersen et al., this volume); Eclipse and North Bylot troughs of the Bylot Island area (Jackson et al., 1975; Haggart et al., this volume); and a series of smaller basins in northern Baffin Bay, including Lady Ann Basin (Jackson et al., 1992; Harrison et al., 2011; Dafoe, Dickie, and Williams, this volume). Along the conjugate West Greenland margin, the onshore Nuussuaq Basin preserves Mesozoic–Cenozoic rocks (Fig. 1; Pedersen and Pulvertaft, 1992; Nøhr-Hansen, 1996; Nøhr-Hansen and Dam, 1997; Dam et al., 1998b, 2009; Nøhr-Hansen et al., 2002; Pedersen and Nøhr-Hansen, 2014; Dam and Sønderholm, 2021). Major offshore basins (Fig. 1) include Melville Bay Graben, Kap York Basin, and Kivioq Basin of offshore northern West Greenland (Whittaker et al., 1997; Gregersen et al., 2013, 2019, this volume; Nøhr-Hansen et al., 2018, 2021); Sisimiut Basin, Nuuk Basin, and the Fylla Structural Complex of offshore central West Greenland (Chalmers et al., 1993; Chalmers and Pulvertaft, 2001; Dalhoff et al., 2003; Gregersen and Bidstrup, 2008; Døssing, 2011; Gregersen et al., 2019, this volume); Lady Franklin Basin in central Davis Strait (Chalmers and Pulvertaft, 2001; Sørensen, 2006; Gregersen et al., 2018, this volume; Dafoe, DesRoches, and Williams, this volume); and the relatively narrow Paamiut South Basin on the southern West Greenland margin (Gregersen et al., 2019).

Major volcanism, centred around Davis Strait, began about the same time as the onset of regional seafloor spreading (chron C27n) and has been linked to the arrival of a mantle plume at about 61 Ma (Dam et al., 1998a; Storey et al., 1998, 2007; Larsen et al., 2009). Outpouring of basalt was extensive in the Davis Strait region (e.g. Clarke and Pedersen, 1976; Skaarup, 2001), and Paleocene–Eocene volcanic successions are particularly well documented from the Nuussuaq Basin (Pedersen et al., 2017, 2018). Related magma-rich (volcanic) margins formed in several regions: offshore northern Labrador and its conjugate West Greenland margin (Chalmers, 1997; Sørensen, 2006; Keen et al., 2012, 2018b); offshore Cape Dyer, Baffin Island (Skaarup et al., 2006); and along the central to northern West Greenland margin both offshore and onshore (Skaarup, 2001; Chauvet et al., 2019). These margins exhibit elements of the typical volcano-stratigraphic succession defined by Planke et al. (2000), including seaward-dipping reflectors (SDR), lava delta escarpments, and inner flows. The mapping of these margins is refined in Keen et al. (this volume) and tentatively extrapolated north of the Labrador margin to the Hekja O-71 and Ralegh N-18 wells, as well as north of Cape Dyer toward the Home Bay area along the Baffin Shelf. Seaward-dipping reflectors have been noted elsewhere along the margins and may indicate the presence of other magma-rich margins (Suckro et al., 2012, 2013; Dafoe, DesRoches, and Williams, this volume; Keen et al., this volume). In addition to the magma-rich margins, volcanic eruptive centres have been identified in the Davis Strait at the Gjoa, Hecla, and Maniitsoq highs (Larsen and Dalhoff, 2006; Sørensen, 2006; Dafoe, DesRoches, and Williams, this volume; Keen et al., this volume) and the Cretaceous Atammik Volcano in the Nuuk Basin (Knudsen et al., 2020). Across much of the Davis Strait region and parts of the Labrador Sea and Baffin Bay, thick Paleogene basalt flows mask underlying sedimentary strata and pre-rift basement (Dafoe, DesRoches, and Williams, this volume; Dafoe, Dickie, and Williams, this volume; Dafoe, Dickie, Williams, and McCartney, this volume; Gregersen et al., this volume; Keen et al., this volume). Similar, thick Paleogene basalt units also overlie Cretaceous sedimentary rocks in major outcrops of the elevated Nuussuaq Basin (Dam et al., 2009; Pedersen et al., 2017, 2018).

Within the Labrador–Baffin Seaway, Mesozoic–Cenozoic samples from exploration wells, coreholes, and the seabed have been collected and studied since the 1970s, in addition to examinations of rift-related onshore successions. These have formed the basis for lithostratigraphic assignments of Cretaceous through Pleistocene rocks of the Hopedale and Saglek basins (Umpleby, 1979; McWhae et al., 1980; Moir, 1989; Balkwill and McMillan, 1990; Wielens and Williams, 2009; Dafoe, 2021; Dafoe, Dickie, Williams, and McCartney, this volume), the successions on southeastern Baffin Island (Clarke and

→

Figure 1. a) Labrador–Baffin Seaway study region showing bathymetry (General Bathymetric Chart of the Oceans, 2014), the location of multichannel seismic reflection data (select unreleased data are shown for the Labrador margin; released seismic data up to 2018 is shown for the West Greenland margin), wells, coreholes, GSC cruise samples containing bedrock material (seabed drill cores, dredge samples, and a relevant piston core), and subregion boundaries. Some onshore boreholes in Nuussuaq Basin have been named based on their proximity to geographic locations and their original designations from Shekhar et al. (1982) are as follows: 247701 (Paatût-1), 247801 (Atâ -1), and 247901 (Paatût-2). Offshore basin outlines are from Keen et al. (this volume) and are based on work by Gregersen et al. (2019) and the GSC (this volume), with the Nuussuaq Basin from Dam et al. (2009). Onshore cratonic boundaries are from St-Onge et al. (2009). Inset maps show details of closely spaced wells or coreholes.

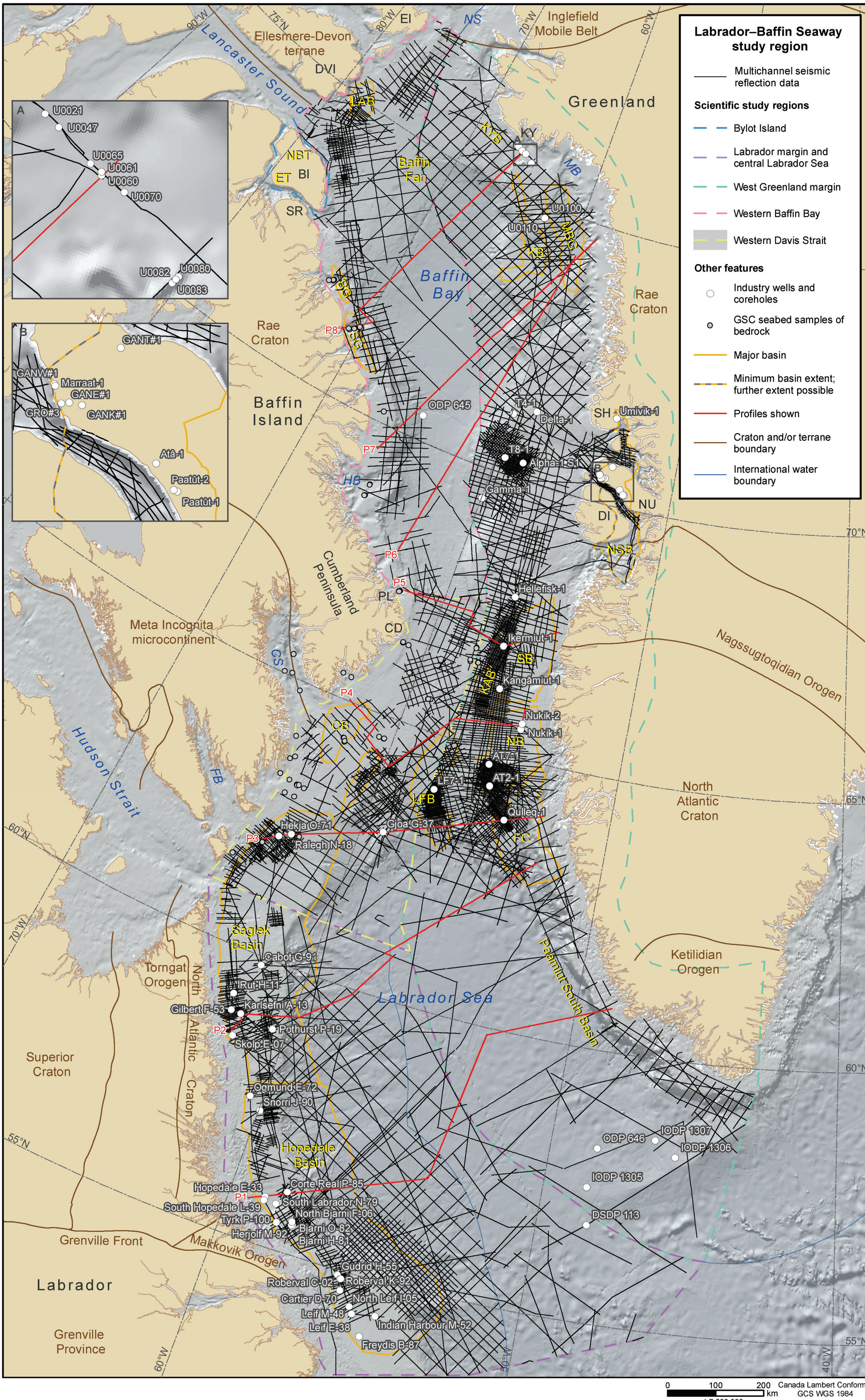
Labrador–Baffin Seaway study region
Multichannel seismic reflection data
Scientific study regions
Bylot Island
Labrador margin and central Labrador Sea
West Greenland margin
Western Baffin Bay
Western Davis Strait
Other features
Industry wells and coreholes
GSC seabed samples of bedrock
Major basin
Minimum basin extent; further extent possible
Profiles shown
Craton and/or terrane boundary
International water boundary
Greenland
Inglefield Mobile Belt
Ellesmere-Devon terrane
Lancaster Sound
Baffin Bay
Baffin Fan
Baffin Island
Rae Craton
Cumberland Peninsula
Meta Incognita microcontinent
Hudson Strait
Nagssugtoqidian Orogen
North Atlantic Craton
Ketilidian Orogen
Labrador Sea
Paamiut South Basin
Saglek Basin
Hopedale Basin
Torngat Orogen
North Atlantic Craton
Superior Craton
Grenville Front
Makkovik Orogen
Labrador
Grenville Province
ODP 645
ODP 646
IODP 1305
IODP 1306
IODP 1307
DSDP 113
Hellefisk-1
Ikermiut-1
Kangamiut-1
Nukik-2
Nukik-1
Qulleq-1
Gjoa G-37
Hekja O-71
Ralegh N-18
Cabot G-91
Rut H-11
Gilbert F-53
Karlsefni A-13
Pothurst P-19
Skolp E-07
Oomund E-72
Snorri J-90
Hopedale E-33
Corte Real P-85
South Hopedale L-39
South Labrador N-79
North Bjarni F-06
Tyrk P-100
Bjarni O-82
Herjolf M-92
Bjarni H-81
Gudrid H-55
Roberval C-02
Roberval K-92
Cartier D-70
North Leif I-05
Leif M-48
Leif E-38
Indian Harbour M-52
Freydis B-87
T4-1
Delta-1
T8-1
Alpha-1 S1
Gamma-1
Umivik-1
AT7-1
AT2-1
LF7-1
U0021
U0047
U0065
U0061
U0060
U0070
U0082
U0080
U0083
U0100
U0110
GANT#1
GANW#1
Marraat-1
GANE#1
GRO#3
GANK#1
Atâ-1
Paatût-2
Paatût-1
0 100 200 km
1:7 500 000
Canada Lambert Conformal
GCS WGS 1984

Basin names

BG – Buchan Graben
CB – Cumberland Basin
ET – Eclipse Trough
FC – Fylla Structural Complex
KAB – Kangâmiut Basin
KB – Kivioq Basin
KYB – Kap York Basin
LAB – Lady Ann Basin
LFB – Lady Franklin Basin
MBG – Melville Bay Graben
NB – Nuuk Basin
NBT – North Bylot Trough
NSB – Nuussuaq Basin
SB – Sisimuit Basin
SG – Scott Graben

Bathymetric names

CS – Cumberland Sound
FB – Frobisher Bay
HB – Home Bay
MB – Melville Bay
NS – Nares Strait

Geological structures

BFZ – Bower Fracture Zone
CA – Cartwright Arch
CFZ – Cartwright Fracture Zone
DSH – Davis Strait High
FZ – Fracture zone
GH – Gjoa High
HFZ – Hudson Fracture Zone
HH – Hecla High
LFA – Lady Franklin Arch
MBR – Melville Bay Ridge
MH – Maniitsoq High
OA – Okak Arch
SFZ – Snorri Fracture Zone
UFZ – Ungava Fault Zone

Onshore place names

BI – Bylot Island
CD – Cape Dyer
DI – Disko Island
DVI – Devon Island
EI – Ellesmere Island
KY – Kap York
NU – Nuussuaq
PL – Paallavvik
SH – Svartenhuk Halvø
SR – Salmon River

Figure 1. b) Common legend of abbreviations in Figures 1a, 8, 9, and 10. Additional projection information is as follows: Central Meridian = 60°W; Standard Parallels = 65°W, 75°W; Latitude of Origin = 65°N.

Upton, 1971; Burden and Langille, 1990; Haggart et al., this volume), the Bylot Island area (Miall et al., 1980; Sparkes, 1989; Waterfield, 1989; Benham and Burden, 1990; Benham, 1991; Wiseman, 1991; Haggart et al., this volume), the Nuussuaq Basin (Henderson et al., 1981; Pedersen and Pulvertaft, 1992; Storey et al., 1998; Dam et al., 2009; Pedersen et al., 2017, 2018), and the West Greenland margin (Rolle, 1985; Nøhr-Hansen, 2003; Gregersen et al., 2013, 2018, 2019, this volume). Age constraints for this framework have relied mostly on biostratigraphy, with major studies including wells along the Labrador margin (Williams and Bujak, 1977a; Barss et al., 1979; Williams, 1986; Bujak Davies Group, 1989; Ainsworth et al., 2014, 2016; Nøhr-Hansen et al., 2016; Dafoe and Williams, 2020a, b), southeast Baffin Island onshore outcrops (Burden and Langille, 1991), outcrops in the Bylot Island area (Miall et al., 1980; Ioannides, 1986; Sparkes, 1989; Benham, 1991), seabed samples of bedrock along western Davis Strait and Baffin Bay (MacLean et al., 2014; Dafoe and Williams, 2020d), outcrops in the Nuussuaq Basin (Nøhr-Hansen, 1996; Nøhr-Hansen et al., 2002; Dam et al., 2009; Pedersen and Nøhr-Hansen, 2014), coreholes in Baffin Bay (G. Acton, G. Claypool, I. Delusina, G. Dunbar, H. Evans, P. Ferretti, G. Guerin, L. Holloway, S. Ishman, P.C. Knutz, L. Krissek, D. Kulhanek, T.L. Insua, J. Lauren, D. Maloney, D. Naafs, H. Nøhr-Hansen, M. Olney, C. Richter, M. Storms, S. Woodard, and J. Wright, unpub. rept., 2012; Nøhr-Hansen et al., 2018, 2021; Dafoe and Williams, 2020c), and wells from the West Greenland margin (Rolle, 1985; Nøhr-Hansen, 2003; Nøhr-Hansen et al., 2016). In the Labrador–Baffin Seaway, palynomorphs from the conjugate margins have been used to develop a regional palynoevent framework (Fig. 2, 3; Nøhr-Hansen et al., 2016).

In addition to the lithostratigraphic and biostratigraphic frameworks, seismic stratigraphy has permitted extrapolation between exploration wells and between subbasins. Along the Labrador margin and into the southeast Baffin Shelf area, the lithostratigraphic framework from the Hopedale and Saglek basins has been applied to seismic interpretation (McWhae, 1981; Balkwill, 1987; Bell, 1989; Balkwill and McMillan, 1990; Jauer et al., 2009, 2014; Dickie et al., 2011; Dafoe, Dickie, Williams, and McCartney, this volume; Dafoe, DesRoches, and Williams, this volume). Further north along the Canadian margin, studies have focused on seismic mapping, relating units to major time slices linked to tectonic activity (McWhae, 1981; Rice and Shade, 1982; Jackson et al., 1992; Harrison et al., 2011; Brent et al., 2013; Atkinson et al., 2017; Dafoe, Dickie, and Williams, this volume). Along the conjugate West Greenland margin, seismic stratigraphy was integral in early studies (Henderson et al., 1981; Chalmers et al., 1993; Chalmers and Pulvertaft, 2001; Sørensen, 2006), and later developed into a regional seismic stratigraphic framework using consistent horizons, which, from youngest to oldest, are A1 through H1 and separate mega-units A through H, with well ties for much of the margin (Gregersen et al., 2013, 2018, 2019, this volume; Knutz et al., 2015, 2019). These horizons (A1 through H1) and packages (units A–H) are referred to extensively below (Fig. 4).

In this bulletin, the stratigraphy of the Canadian side of the Labrador–Baffin Seaway has been documented for a number of subregions including the Labrador margin (Dafoe, Dickie, Williams, and McCartney, this volume), western Davis Strait (Dafoe, DesRoches, and Williams, this volume), western Baffin Bay (Dafoe, Dickie, and Williams, this volume), and the onshore exposures on Bylot and Baffin islands (Haggart et al., this volume). A comprehensive summary of the West Greenland margin also based on subregions has been described by Gregersen et al. (this volume). These papers contain discussions of their subregional data and methods and present summaries of the related stratigraphy in detail (the reader is referred to these papers for more detailed information). Here the stratigraphy for the entire Labrador–Baffin Seaway is summarized and compared based on these papers, with an emphasis on lithostratigraphic and seismic stratigraphic correlations, and distribution of three principal intervals: Cretaceous, lower Cenozoic (Paleocene to Middle Miocene), and upper Cenozoic (Middle Miocene to Pleistocene). Map elements and seismic profiles are combined from relevant papers in this volume that discuss these figures in greater detail, but they are presented as regional compilations here (data shown in maps are contained in the GIS data included with this volume). The seismic stratigraphic framework (units A–H and horizons A1–H1) from the West Greenland margin defined by Gregersen et al. (2013, 2018, 2019, this volume) and Knutz et al. (2015) is used to show regional correlations and is adapted to key horizons on the Canadian side of the seaway from Dickie et al. (2011) and Dafoe, Dickie, Williams, and McCartney (this volume). Using this framework, the Cretaceous interval is capped by the F1 horizon and the Cenozoic is subdivided into lower and upper intervals by the D1 horizon. In the present study, the seismic profiles are considered to show 'conjugate' margins, however, only the southernmost profile forms a true conjugate section (tectonic margin segments are discussed in Keen et al. (this volume)). Finally, a discussion of some of the key paleoclimatic events and paleoceanographic evolution for the region as a whole is presented by bringing together global studies with evidence from samples collected from within the seaway.

REGIONAL STRATIGRAPHIC CORRELATIONS

Regional biostratigraphic events

Stratigraphic correlations across the study region rely on biostratigraphic age control from exploration wells, corehole and seabed samples, and onshore outcrops. Biostratigraphic age control utilized in papers within this volume is based on macrofossils and microfossils, but relies primarily on palynology — mainly spores and pollen (miospores) and dinoflagellate cysts (dinocysts). Rather than biostratigraphic zonations, the present study utilizes the palynoevents as outlined in Nøhr-Hansen et al. (2016). Figures 2 and 3 illustrate the palynostratigraphic event charts for the Cretaceous and Cenozoic of the Labrador–Baffin Seaway developed by these same authors, which highlights palynoevents from 19 offshore wells, as well as the onshore Nuussuaq Basin. These charts include dinocysts, miospores, fungal spores, and elements of the freshwater fern *Azolla*. Nøhr-Hansen et al. (2016), in some cases, included peak occurrences, or acmes of species in their event compilation, but most of the events represent last or youngest occurrences (LOs) as samples are primarily ditch cuttings from exploration wells; in such samples, cavings distort data based on first or oldest occurrences (FOs). Nøhr-Hansen et al. (2016) identified 187 bioevents for the Cretaceous and Cenozoic of the Labrador–Baffin Seaway, but some events are coeval so that there are only 106 individual biohorizons. The LO of a taxon comprise 169 bioevents and the rest represent peak occurrences or abundances of taxa. The Albian to Paleocene strata of the Nuussuaq Basin, onshore West Greenland, include 50 bioevents (44 biohorizons) from Pedersen and Nøhr-Hansen (2014). Neogene strata offshore West Greenland include 22 bioevents (in 13 biohorizons) from Piasecki (2003). Subsequent studies utilize these palynoevents charts and build upon them (e.g. Williams 2017a, b; Dafoe and Williams, 2020a, b, c).

The palynoevents charts show that most bioevents are identified in the Campanian to Rupelian (Fig. 2, 3). This part of the succession is dominated by fine-grained, fully marine sedimentary rocks with resultant good palynomorph preservation. In pre-Campanian rocks, dinocysts are rare, but miospores can be common, especially in the

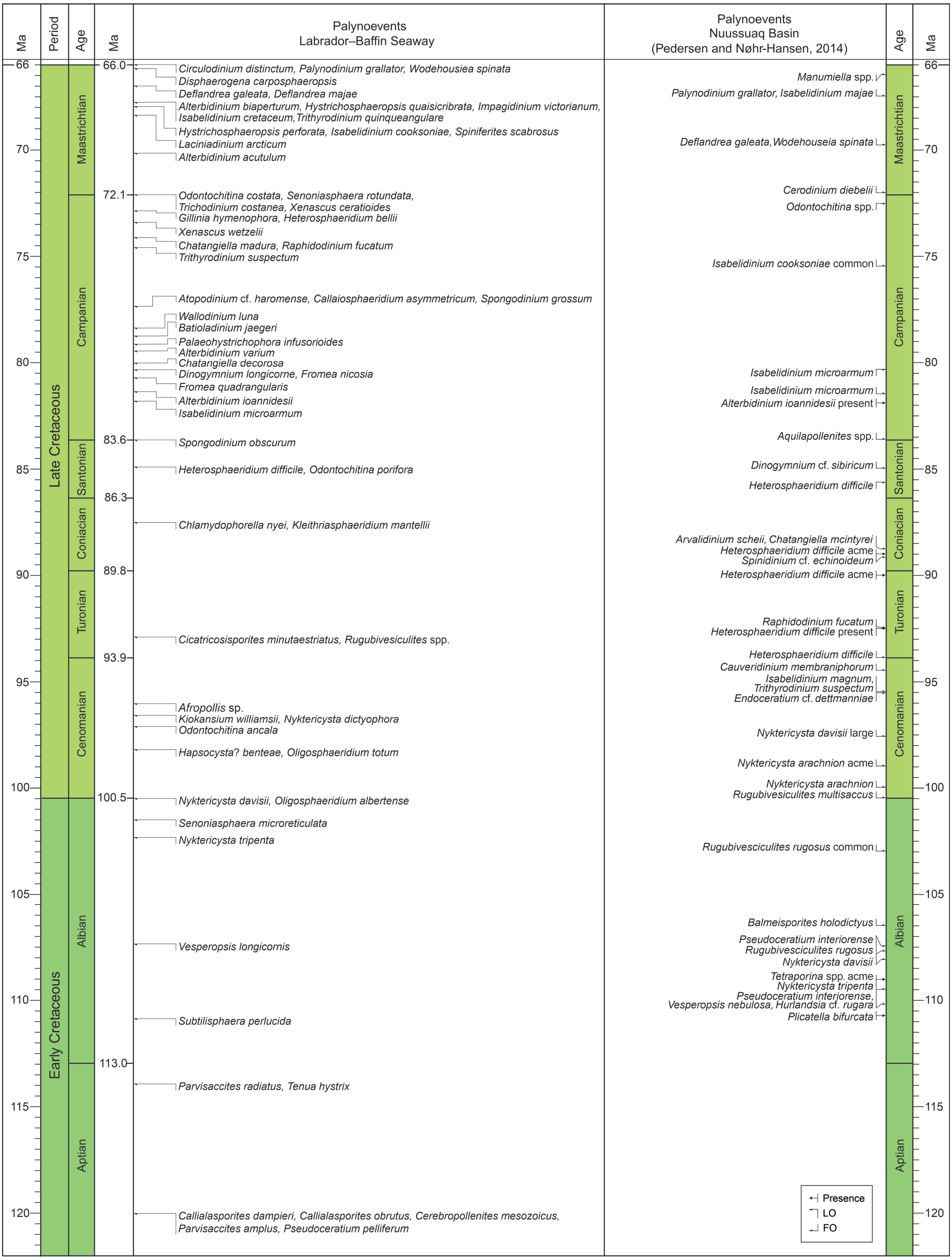

Figure 2. Palynoevents chart from Nøhr-Hansen et al. (2016) for the Cretaceous of the Labrador–Baffin Seaway and Nuussuaq Basin. Time scale is from Gradstein et al. (2012). FO = first occurrence; LO = last occurrence.

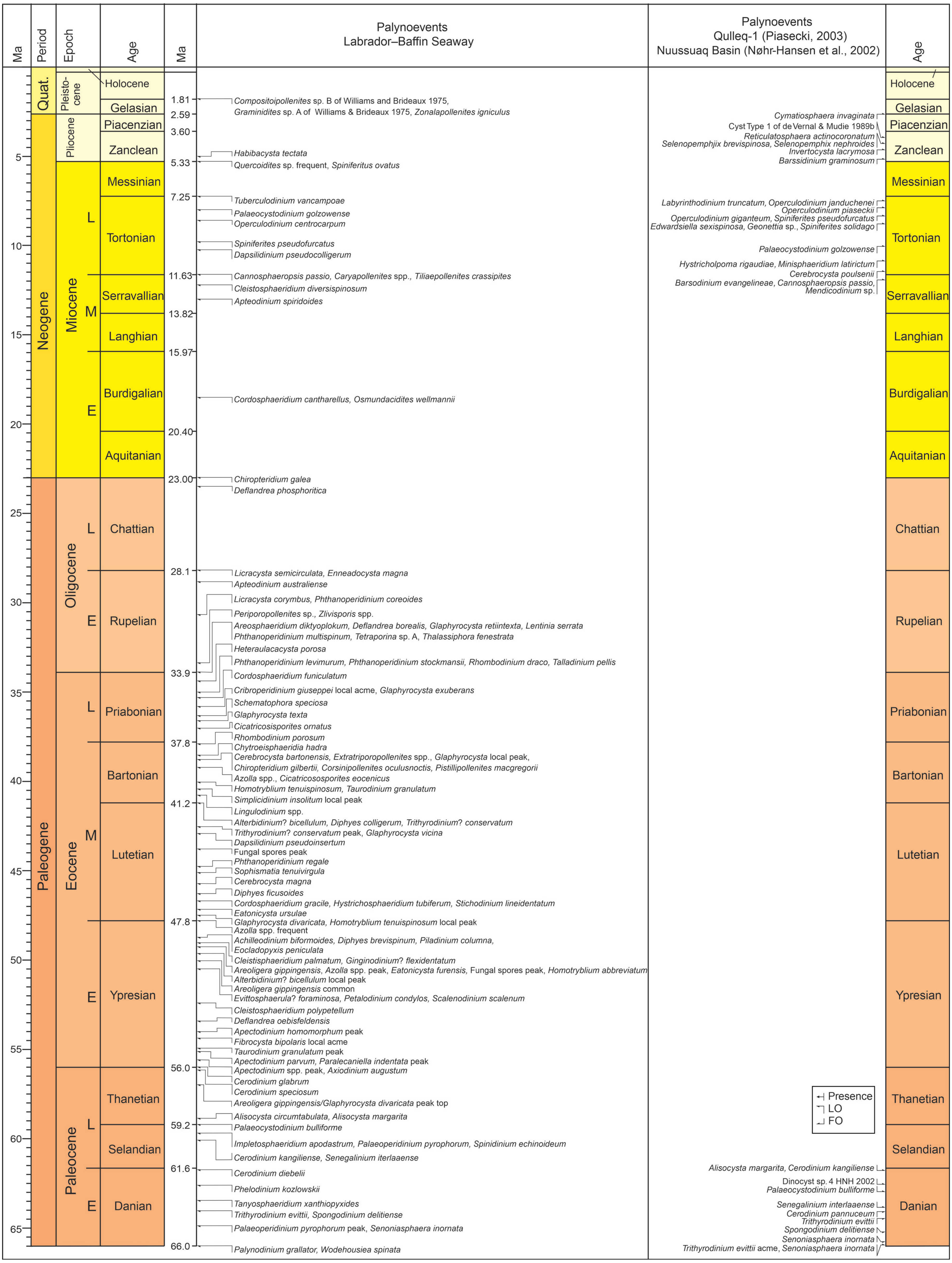

Figure 3. Palynoevents chart from Nøhr-Hansen et al. (2016) for the Cenozoic of the Labrador–Baffin Seaway and the Qulleq-1 well and Nuussuaq Basin. Time scale is from Gradstein et al. (2012). Replace with: FO = first occurrence; HNH 2022 = Nøhr-Hansen et al. (2002); LO = last occurrence; Quat. = Quaternary.

Lower Cretaceous (e.g. Dafoe and Williams, 2020a, b); however, miospore marker taxa are few during this earlier time. Nevertheless, Nøhr-Hansen et al. (2016) were able to identify the oldest rocks sampled in the region as Aptian. Although, sandstone and shale units in conventional cores from the Bjarni H-81 and Herjolf M-92 wells were later identified as Barremian–Aptian by Dafoe and Williams (2020a), indicating the presence of older Lower Cretaceous strata in the seaway. Dinocysts are also sparse in the post-Rupelian strata of the seaway, reflecting the generally coarse-grained nature of the clastic strata in the younger part of the section (a grain size that tends to fragment and destroy palynomorphs) and the inability to obtain cuttings from upper, cased portions of wells. In deeper water strata, however, conditions are more favourable for preservation, such as much of the section sampled in the ODP Site 645 corehole (e.g. Dafoe and Williams, 2020c). Based on their event scheme, Nøhr-Hansen et al. (2016) were able to identify several partly correlative unconformities between the Canadian and West Greenland margins.

Cretaceous interval

Lithostratigraphic columns for subregions of the Labrador–Baffin Seaway are shown together in Figure 4. A more comprehensive, updated lithostratigraphic column for the West Greenland margin is presented in Gregersen et al. (2019) and also shown in Gregersen et al. (this volume; their Fig. 3). The lithostratigraphy is correlated with the seismic stratigraphic framework, with minor discrepancies in the age of horizons between the west and east sides of the seaway due to slight differences between the lithostratigraphy and biostratigraphy of the Labrador and West Greenland margins. The pre-rift basement unit H and its upper boundary, H1, are overlain by the Lower Cretaceous unit G, which is in turn capped by the G1 horizon. Above this, unit F includes Upper Cretaceous to Lower Paleocene (Danian and lower Selandian) sedimentary rocks that are capped by seismic horizon F1. These units are illustrated along seismic profiles that cross the conjugate margins (Fig. 5, 6, 7) and, where present, are mapped as a Cretaceous interval through seismic correlations to well, corehole, or seabed samples (Fig. 8).

Lithostratigraphic correlations

On the west side of the seaway, the Cretaceous section has been sampled and described from exploration wells offshore Labrador and assigned to the following units: the Lower Cretaceous Alexis Formation basalt units; the Lower Cretaceous Bjarni Formation sandstone, shale, and coal units; and the Upper Cretaceous to lower Selandian Markland Formation shale units with Freydis Member sandstone units (Fig. 4; Umpleby, 1979; McWhae et al., 1980; Bell, 1989; Moir, 1989; Balkwill and McMillan, 1990; Dickie et al., 2011; Dafoe, 2021; Dafoe, Dickie, Williams, and McCartney, this volume). Farther north in the offshore, Lower Cretaceous rocks have also been sampled from the seabed in Cumberland Sound and off Paallavvik (island), and numerous Upper Cretaceous rocks have been sampled along the eastern Baffin Island margin (Fig. 8; MacLean et al., 2014; Dafoe and Williams, 2020d; Dafoe, Dickie, and Williams, this volume; Dafoe, DesRoches, and Williams, this volume). Onshore, the stratigraphy of the southeastern Baffin Island area includes the sandstone, shale, and coal units of the Lower to mid-Cretaceous Quqaluit Formation, which are unconformably overlain by the Lower to Middle Paleocene Cape Searle Formation comprising sandstone, mudstone, conglomerate, and volcanic ash (Fig. 4; Jackson, 1998; Burden and Langille, 1990, 1991). Farther north in the Eclipse and North Bylot troughs of Bylot Island and northern Baffin Island, the Lower to mid-Cretaceous, nonmarine to marginal marine sandstone and mudstone units of the Hassel Formation are overlain by Upper Cretaceous marine sandstone and shale units of the informal Byam Martin, Bylot Island, and Sermilik formations and then by the uppermost Cretaceous to Paleocene marine to nonmarine Pond Inlet and Navy Board formations and the lower part of the Aktineq formation (Fig. 4; Miall et al., 1980; Sparkes, 1989; Waterfield, 1989; Wiseman, 1991; Benham, 1991; Haggart et al., this volume).

Onshore in the Nuussuaq Basin, West Greenland, Lower to mid-Cretaceous nonmarine to deltaic deposits of the Kome, Slibestensfjeldet, and Atane formations are overlain by the lower Upper Cretaceous part of the sandstone-dominated Atane Formation and coeval marine shale units of the Itilli Formation (Dam et al., 2009). This is overlain by Upper Cretaceous to Paleocene shale and sandstone units of the marine Itilli (upper part), Kangilia, and Agatdal formations, as well as the nonmarine Quikavsak Formation (Fig. 4; Dam et al., 2000, 2009; Dam and Sønderholm, 2021; Gregersen et al., this volume). Offshore along the West Greenland margin, the stratigraphy is primarily defined from seismic data and includes possible Lower Cretaceous basalt flows and nonmarine deposits of the Lower Cretaceous Kitsissut and Appat sequences (Fig. 4; Chalmers et al., 1993; Chalmers and Pulvertaft, 2001; Sørensen, 2006); however, Aptian to Cenomanian sandstone and mudstone beds have been drilled in northeast Baffin Bay and in Davis Strait (G. Acton, G. Claypool, I. Delusina, G. Dunbar, H. Evans, P. Ferretti, G. Guerin, L. Holloway, S. Ishman, P.C. Knutz, L. Krissek, D. Kulhanek, T.L. Insua, J. Lauren, D. Maloney, D. Naafs, H. Nøhr-Hansen, M. Olney, C. Richter, M. Storms, S. Woodard, and J. Wright, unpub. rept., 2012; Gregersen et al., 2018, 2019, this volume; Nøhr-Hansen et al., 2018, 2021). The Upper Cretaceous of the West Greenland margin is characterized by the Ikermiut Formation shale with thin sandstone units and the sampled Fylla sand unit (Fig. 4; Rolle, 1985; Christiansen et al., 2001; Nøhr-Hansen et al., 2016). These strata are part of the Kangeq sequence interpreted from seismic data offshore southern West Greenland (Chalmers et al., 1993). The Kangeq sequence and much of the Ikermiut Formation are now considered to be part of the major seismic stratigraphic unit F defined along the West Greenland margin (Gregersen et al., 2019). Above this, the Upper Cretaceous to Danian interval is missing within exploration wells along the West Greenland margin (Fig. 4; *see* Fig. 3, Gregersen et al., this volume for a more complete and updated stratigraphic scheme of the West Greenland margin including all exploration wells and the shallow cores of northeast Baffin Bay).

In general, the early syn-rift unit G is characterized by sandstone units throughout the region (Fig. 4). North and east of the Labrador margin, samples of Lower Cretaceous syn-rift rocks are less common and tend to be slightly younger, mostly Aptian–Albian. This may reflect a northward younging of rifting during the Early Cretaceous. Deeply buried strata have yet to be sampled in the northern region, as is the case in the Melville Bay and Scott grabens (Fig. 7b, c). It is unclear why the early rift Alexis Formation alkali basalt units found on the Labrador Shelf have not been sampled elsewhere; however, younger Cenomanian–early Turonian alkaline volcanic rocks (the Atammik Volcano) have been found in the Nuuk Basin on the West Greenland margin in the AT2-1 well (Knudsen et al., 2020). In addition, shallow-marine volcaniclastic rocks in the Bjarni O-82 well have recently been interpreted as middle Albian to Cenomanian (Dafoe and Williams, 2020a), and thus younger than most other volcanic rocks from the Labrador margin (*see* Dafoe, Dickie, Williams, and McCartney, this volume). The rocks of unit G from across the region were deposited in similar nonmarine to shallow-marine paleoenvironments including: fluvial, alluvial, lacustrine, and shallow-marine settings in the Bjarni Formation (Umpleby, 1979; McWhae et al., 1980; Dafoe and Williams, 2020a, b; Dafoe, 2021; Dafoe, Dickie, Williams, and McCartney, this volume), the Quqaluit Formation (Burden and Langille, 1990, 1991; Dafoe, Dickie, and Williams, this volume), the Hassel Formation (Miall et al., 1980; Dafoe et al., 2019; Haggart et al., this volume), and the Kome, Slibestensfjeldet, Atane, and Upernivik Næs formations (Dam et al., 2009; Dam and

Figure 4. Lithostratigraphic columns for regions within and adjacent to the Labrador–Baffin Seaway as modified from Nøhr-Hansen et al. (2016). The Labrador margin is from Dickie et al. (2011). The West Greenland margin is from Gregersen et al. (2013) and Nøhr-Hansen et al. (2016) and based on the studies of Rolle (1985), Nøhr-Hansen (1998, 2003), and Sønderholm et al. (2003), with the subwell section based on Chalmers et al. (1993), Chalmers and Pulvertaft (2001), and Sørensen (2006). The pre-rift basement is from Dalhoff et al. (2006) and Stouge et al. (2007). The column for Nuussuaq Basin is from Gregersen et al. (2013) and Nøhr-Hansen et al. (2016) and based on studies by Storey et al. (1998), Pedersen et al. (2002), Dam et al. (2009), and Larsen et al. (2016). The southeast Baffin Island stratigraphy is modified from Gregersen et al. (2013) and Nøhr-Hansen et al. (2016) and based on the original work by Burden and Langille (1990, 1991). The stratigraphy of Bylot Island is modified from Gregersen et al. (2013) and Nøhr-Hansen et al. (2016) and based on the studies by McWhae et al. (1979), Miall (1986), Waterfield (1989), Harrison et al. (1999), and Haggart et al. (2011), with pre-rift basement from Jackson et al. (1975). Seismic stratigraphy with the approximate timing of horizons is based on Gregersen et al. (2013, 2018, 2019, this volume) with additions for the Canadian margin from Dafoe, Dickie, Williams, and McCartney (this volume, *see* Fig. 6 for additional explanation on the seismic stratigraphy, and dashed lines indicate slight variation in age between margins). A more detailed and updated stratigraphic scheme for the West Greenland margin with all exploration wells and shallow coreholes of northeast Baffin Bay is shown in Figure 3 of Gregersen et al. (this volume). The time scale and magnetostratigraphy are from Gradstein et al. (2012).

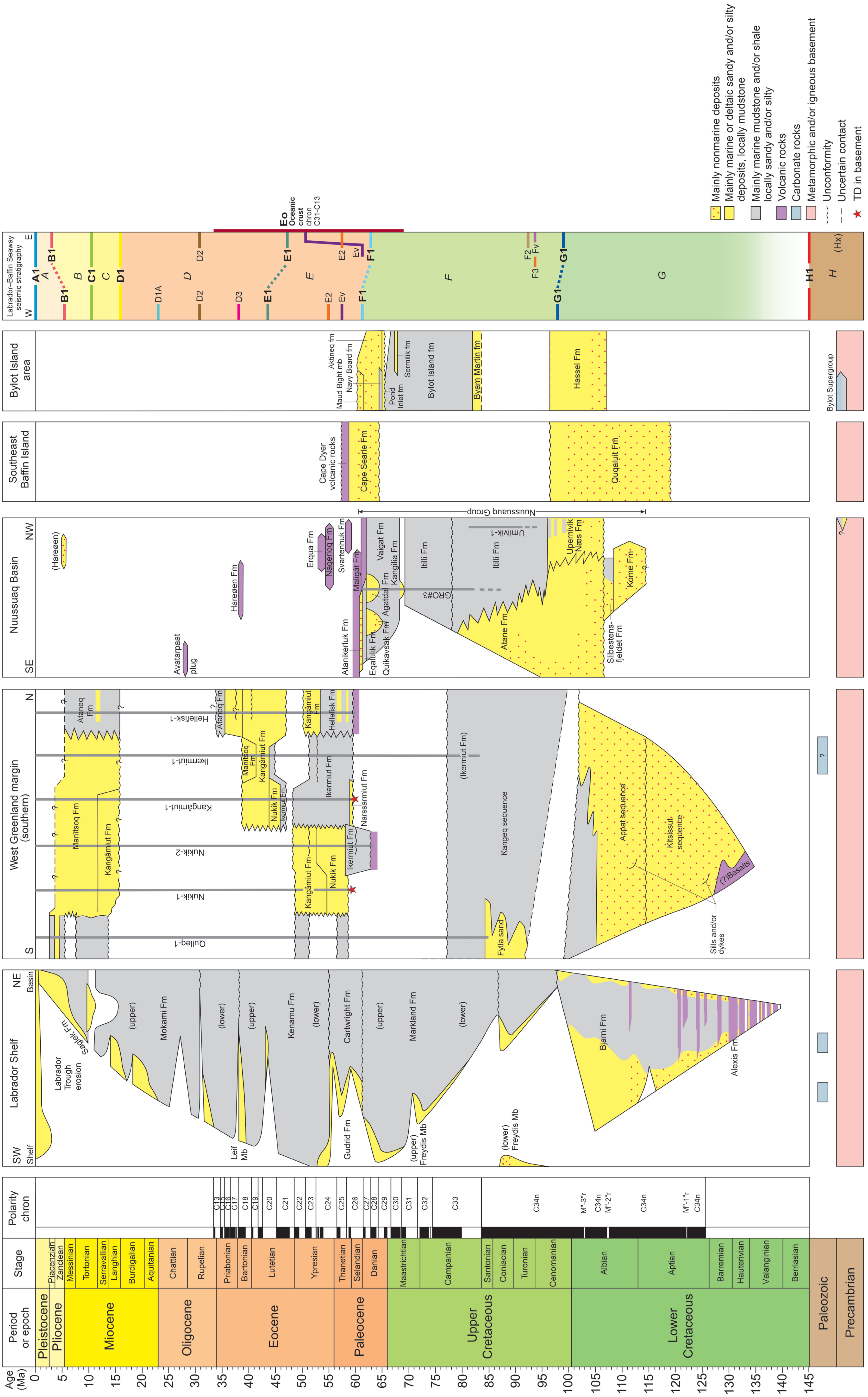
Mainly nonmarine deposits
Mainly marine or deltaic sandy and/or silty deposits, locally mudstone
Mainly marine mudstone and/or shale locally sandy and/or silty
Volcanic rocks
Carbonate rocks
Metamorphic and/or igneous basement
Unconformity
Uncertain contact
TD in basement
Labrador–Baffin Seaway seismic stratigraphy
Bylot Island area
Southeast Baffin Island
Nuussuaq Basin
West Greenland margin (southern)
Labrador Shelf
Polarity chron
Stage
Period or epoch
Age (Ma)
Pleistocene
Pliocene
Miocene
Oligocene
Eocene
Paleocene
Upper Cretaceous
Lower Cretaceous
Paleozoic
Precambrian
Nuussuaq Group
Hassel Fm
Qugaluit Fm
Cape Searle Fm
Bylot Supergroup
Kangeq sequence
Appat sequence
Kitsissut sequence
Markland Fm
Cartwright Fm
Kenamu Fm
Mokami Fm
Bjarni Fm
Alexis Fm

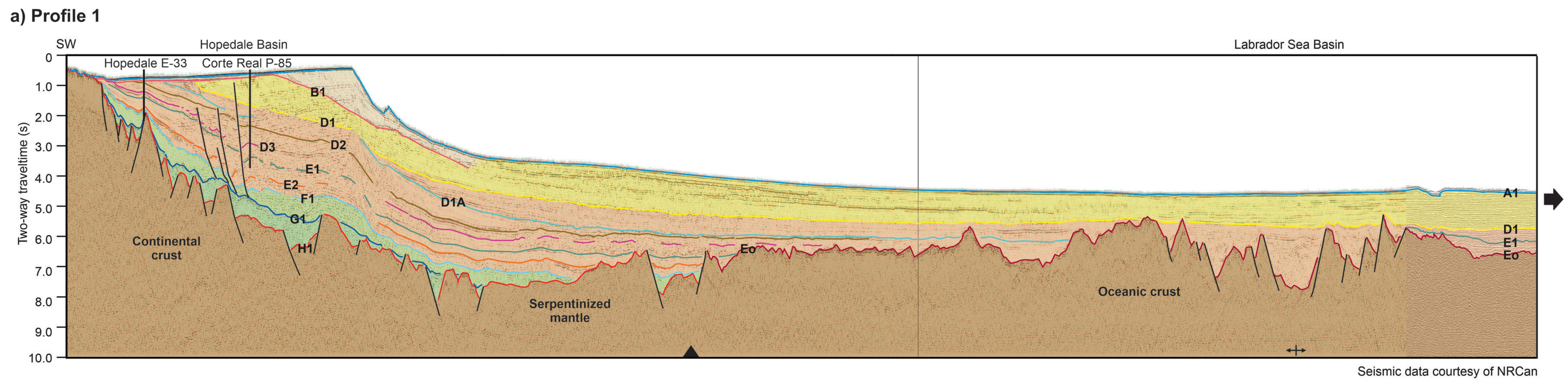

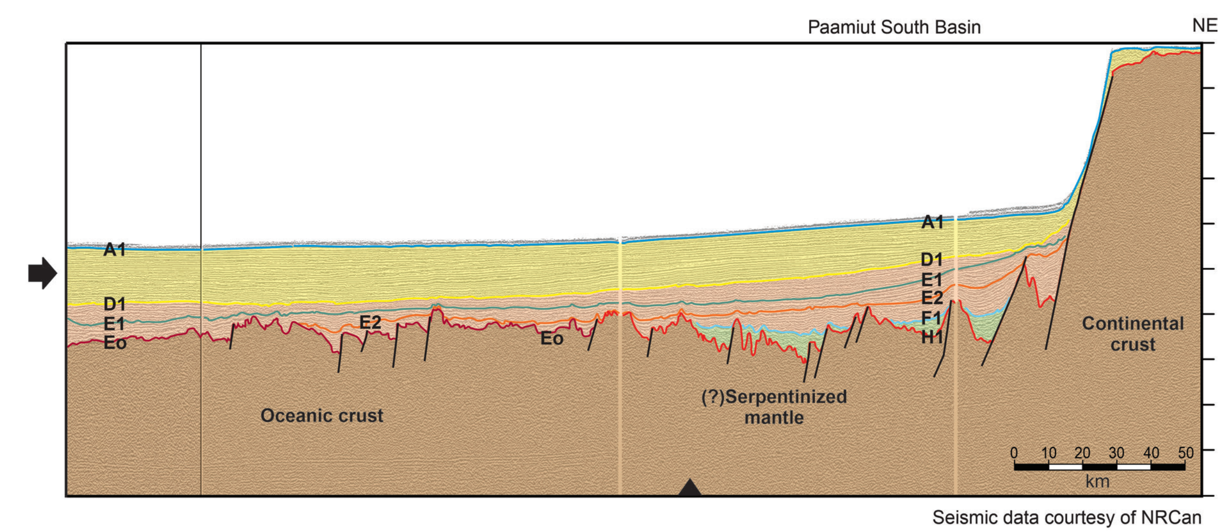

Figure 5. Seismic profiles 1 and 2 across the Labrador Sea showing the geological framework of the Labrador and West Greenland continental margins and the Labrador Sea Basin between them. For line locations and legend, *see* Figures 1 and 6. **a)** Profile 1 with well ties at: Hopedale E-33 and Corte Real P-85. **b)** Profile 2 with well tie at Karlsefni A-13. West Greenland margin parts of the lines are from work by the Geological Survey of Denmark and Greenland (Gregersen et al., 2019, this volume). The location of the landward limit of oceanic crust is from Keen et al. (this volume). Seismic data courtesy of the Federal Institute for Geosciences and Natural Resources Hannover (=DC[3])(lines BGR/77-5 and BGR/77-12), ION Geophysical (=DC[2]), NRCan, and TGS (=DC[1]). SDR = seaward-dipping reflectors.

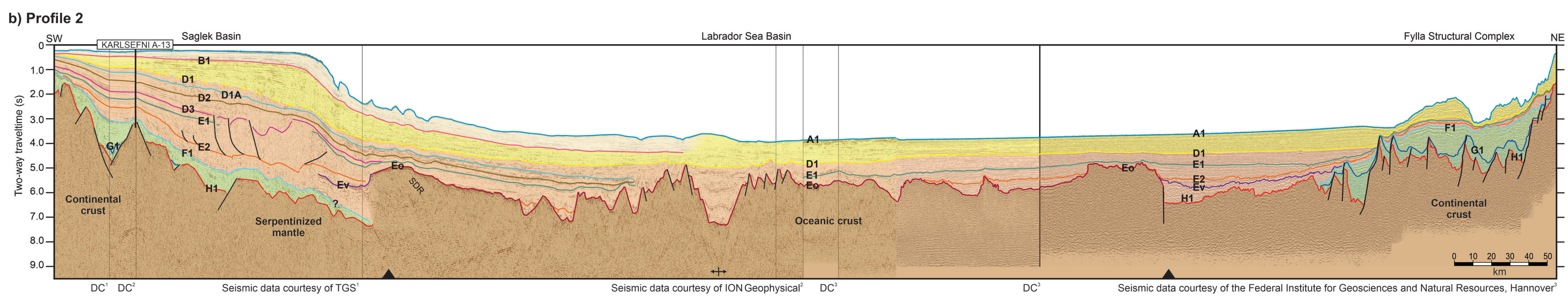

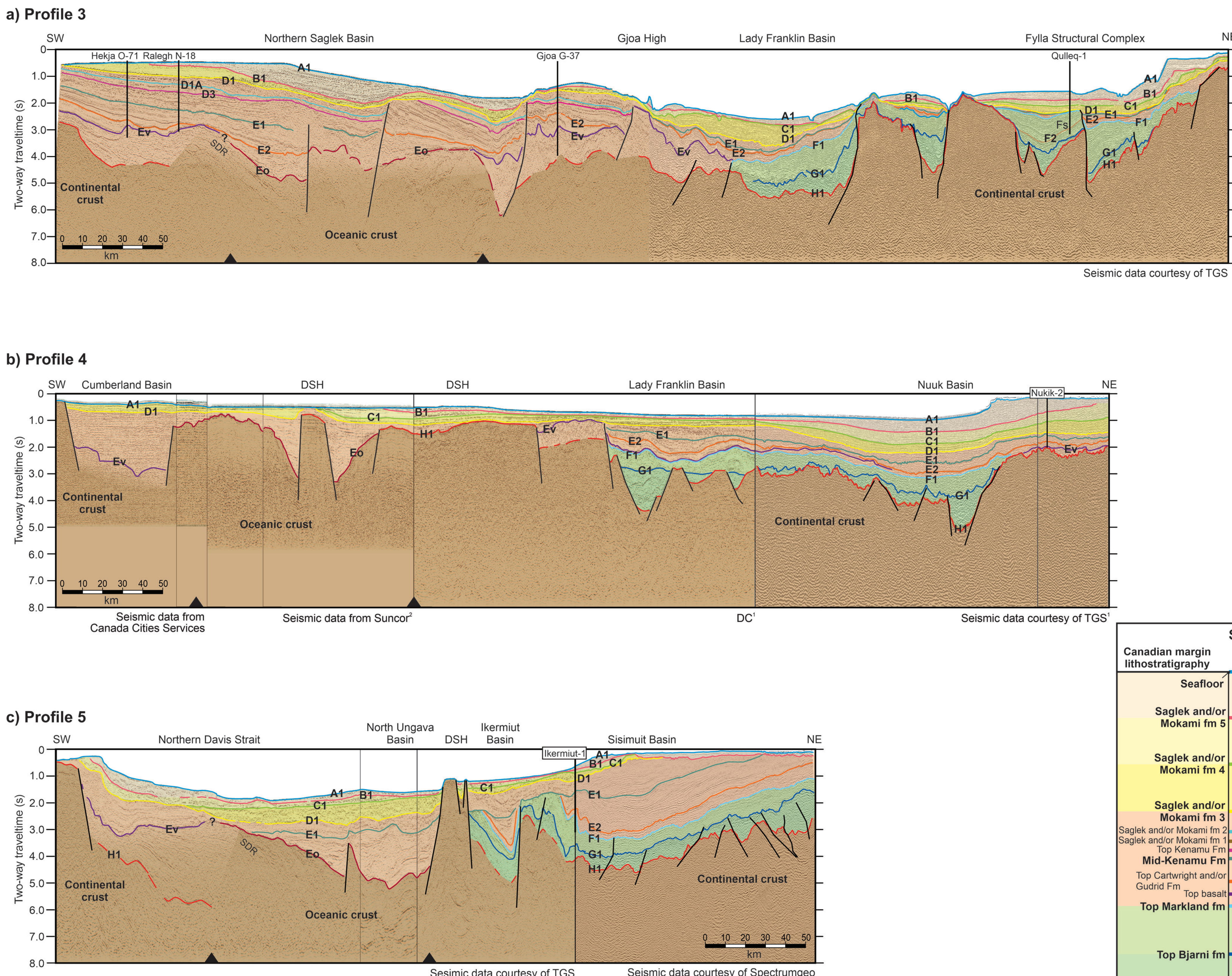

Figure 6. Seismic profiles 3–5 crossing the Davis Strait region showing the geological framework of the margins and narrow oceanic region. For line locations *see* Figure 1. **a)** Profile 3 intersects the Hekja O-71, Ralegh N-18, Gjoa G-37, and Qulleq-1 wells. **b)** Profile 4 with well tie at Nukik-2. **c)** Profile 5 through the Ikermiut-1 well. The West Greenland margin parts of the lines are from work by the Geological Survey of Denmark and Greenland (Gregersen et al., 2019, this volume); location of the landward limit of oceanic crust is from Keen et al. (this volume). Seismic data courtesy of Canada Cities Services, Spectrumgeo, Suncor (=DC²), and TGS (=DC¹). DSH = Davis Strait High; Fs = Fylla Sand, SDR = seaward-dipping reflectors, WGBG = West Greenland Basalt Group, Dist. = Distribution, Cret. = Cretaceous

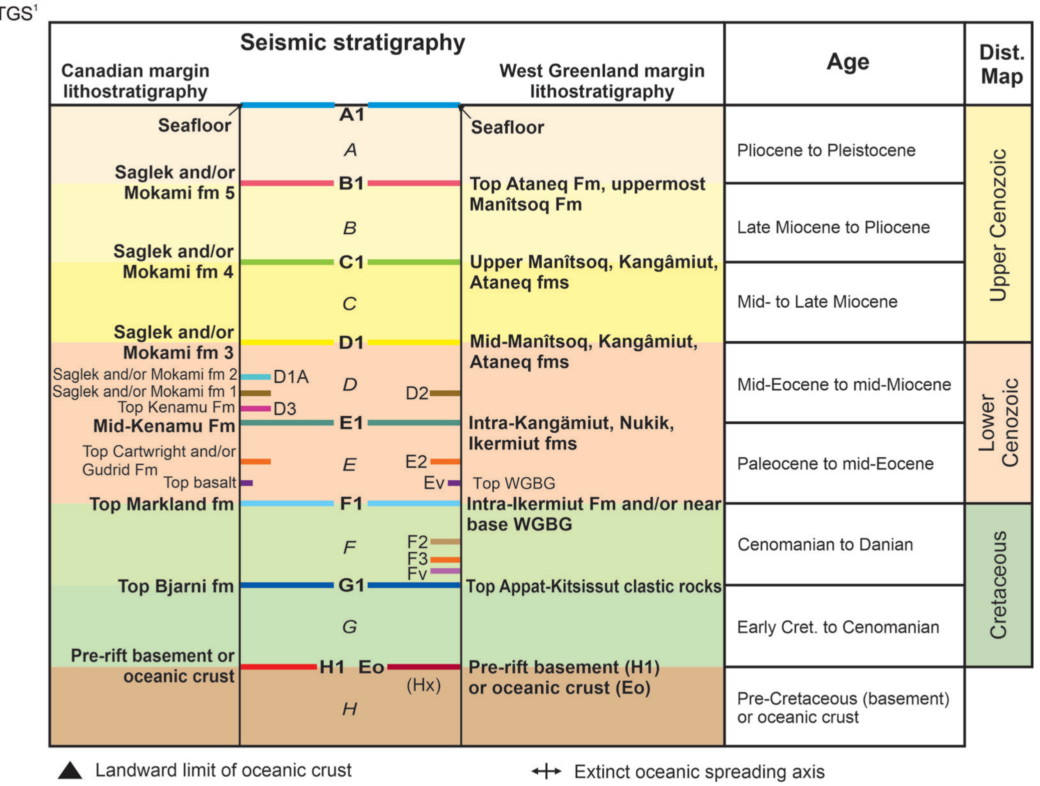

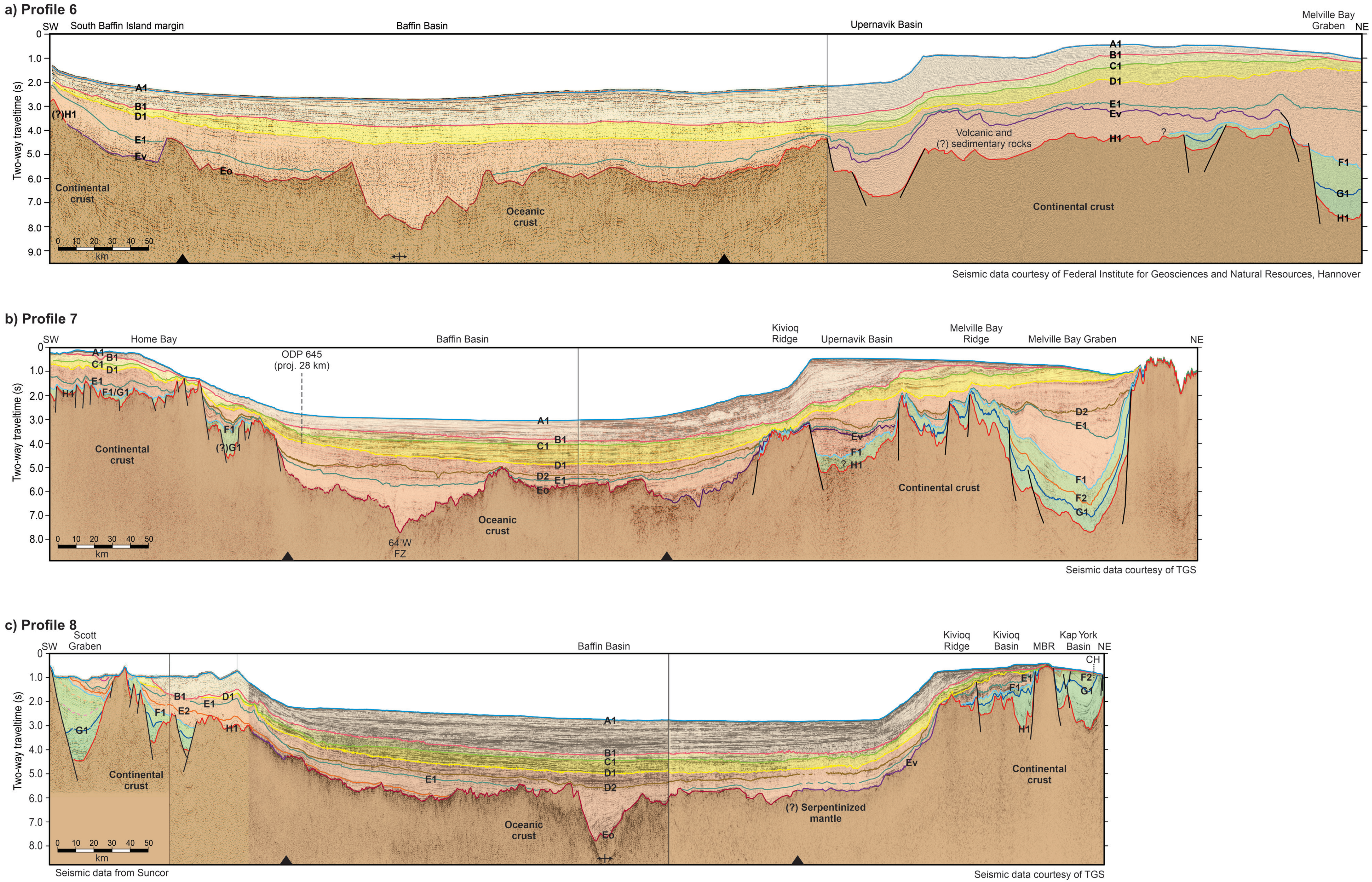

Figure 7. Seismic profiles 6–8 crossing Baffin Bay and showing the geological framework of the Baffin Island and northern West Greenland continental margins and deeper Baffin Basin overlying oceanic crust. For line locations and legend, *see* Figures 1 and 6. **a)** Profile 6 crosses southern Baffin Bay. **b)** Profile 7 shows the asymmetry of the margins, with ODP Site 645 projected onto the profile. **c)** Profile 8 in northern Baffin Bay lies near coreholes in the northeast. Scott Graben is shown as subdivided in the Cretaceous; these details are discussed in Dafoe, Dickie and Williams (this volume). The West Greenland margin parts of the lines are from work by the Geological Survey of Denmark and Greenland (Gregersen et al., 2019, this volume); location of the landward limit of oceanic crust is from Keen et al. (this volume). Seismic data courtesy of or from the Federal Institute for Geosciences and Natural Resources (Hannover; lines BGR08-304 and BGR10-309), Suncor and TGS. CH = corehole, proj. = projected, MBR = Melville Bay Ridge.

Sønderholm, 2021; Gregersen et al., this volume). In addition, Albian nonmarine to shallow-marine sedimentary rocks equivalent to the offshore Appat–Kitsissut clastic rocks have been encountered in coreholes in northern Baffin Bay (Nøhr-Hansen et al., 2018; 2021), as well as in (?)upper Albian to (?)Cenomanian conglomerate units in the AT7-1 well, southern West Greenland (Gregersen et al., 2018). Overall, there is a consistent trend from dominantly nonmarine, generally fluvially dominated successions, to more shallow-marine–dominated strata upward in unit G, typical of an early rift succession (Ravnås and Steel, 1998). The overlying G1 horizon ties to a significant top Bjarni Formation unconformity along the Labrador margin (Fig. 4; McWhae, 1981; Dickie et al., 2011; Dafoe, Dickie, Williams, and McCartney, this volume), and is unconformable over highs between units G (Kitsissut and/or Appat sequences) and F (Kangeq sequence; Gregersen et al., 2013, 2019), with a correlative conformity within basins (Gregersen et al., 2019, this volume). Onshore Nuussuaq Basin, a prominent break is present at the base of the Atane Formation, which is associated with renewed rifting and formation of new sub-basins (Dam and Sønderholm (2021) and may correlate to the G1 horizon in the offshore. Also onshore, a significant hiatus has been proposed to exist above mid- to Lower Cretaceous rocks onshore southeastern Baffin Island and Bylot Island (Fig. 4; Miall et al., 1980; Burden and Langille, 1990, 1991; Haggart et al., this volume).

The overlying unit F is dominated by shale (Fig. 4), as demonstrated by samples encountered in wells described above, and displays a low-amplitude to transparent signature in seismic data (Sørensen, 2006; Dickie et al., 2011; Gregersen et al., 2013). These shale units were formed during a regional marine transgression with depositional settings including shelfal or even deeper water, open-ocean paleoenvironments (but the shelf break was not developed at this time) for the Markland Formation (McWhae et al., 1980; Bell, 1989; Balkwill and McMillan, 1990; Dafoe, 2021; Dafoe, Dickie, Williams, and McCartney, this volume); the Ikermiut Formation (Rolle, 1985; Gregersen et al., this volume); the Itilli and Kangilia formations (Dam et al., 2009; Gregersen et al., this volume); and the Bylot Island formation (Sparkes, 1989; Haggart et al., this volume). Upper Cretaceous marine shale units, some with source-rock potential, are also documented from northeastern Baffin Bay in shallow cores (G. Acton, G. Claypool, I. Delusina, G. Dunbar, H. Evans, P. Ferretti, G. Guerin, L. Holloway, S. Ishman, P.C. Knutz, L. Krissek, D. Kulhanek, T.L. Insua, J. Lauren, D. Maloney, D. Naafs, H. Nøhr-Hansen, M. Olney, C. Richter, M. Storms, S. Woodard, and J. Wright, unpub. rept., 2012; Nøhr-Hansen et al., 2018, 2021). This Late Cretaceous transgressive phase was punctuated by localized shoreline progradational events which developed in proximal regions during the Turonian to Santonian, Campanian to Maastrichtian, and Paleocene intervals. There is a consistent presence of local sandstone in all subregions that reflects deltaic conditions in proximal settings, including the Freydis Member (McWhae et al., 1980; Bell, 1989; Balkwill and McMillan, 1990; Dafoe and Williams, 2020a; Dafoe, 2021; Dafoe, Dickie, Williams, and McCartney, this volume), marine deposits of the Fylla sandstone (Christiansen et al., 2001; Sørensen, 2006), deltaic to shallow-marine strata in the upper part of the Atane Formation (Dam et al., 2009), and basinal to shallow-marine sandstone units in the Byam Martin and Sermilik formations (Sparkes, 1989; Dafoe et al., 2019; Haggart et al., this volume). In the Nuussuaq Basin, the Quikavsak and Agatdal formations, with fluvial and marine sandstone beds filling incised valleys, are thought to have formed in response to plume-related doming in that area (Dam et al., 1998a, 2009). Marine to nonmarine strata of the Cape Searle Formation, Baffin Island (Burden and Langille, 1990, 1991), and of the Pond Inlet, Navy Board, and Aktineq formations on Bylot Island (Waterfield, 1989; Dafoe et al., 2019; Haggart et al., this volume) further suggest a shallowing trend toward the top of unit F in proximal locations. The top of unit F, the F1 horizon, is locally reworked at the base of the overlying Gudrid Formation sandstone units, offshore Labrador (Dickie et al., 2011; Dafoe, Dickie, Williams, and McCartney, this volume). Along the West Greenland margin, however, F1 is a major unconformity with significant missing section, including the Campanian through Danian interval (Rolle, 1985; Nøhr-Hansen et al., 2016; Gregersen et al., 2019, this volume). In general, the F1 horizon forms a regional unconformity which is recognized to varying extent across most regions of the Labrador–Baffin Seaway.

Seismic correlations and mapped distribution

In the Hopedale and southern Saglek basins, offshore Labrador, the Cretaceous interval extends from the basin margin, where it onlaps the basement platform, seaward to near the landward limit of oceanic crust or just basinward of it; the interval may be absent over prominent basement highs (Fig. 5, 8). More specifically, unit G ends inboard of the zone of serpentinized mantle defined by Keen et al. (2018a) that formed during the Late Cretaceous, offshore central Labrador (Fig. 5a). In the southern part of the Saglek Basin, however, unit G appears to be restricted to the deepest parts of grabens and half-grabens (Fig. 5b). The overlying unit F is comparatively seismically transparent and drapes the underlying unit G and basement highs of unit H (Fig. 5). Offshore Labrador, seafloor spreading began in the Maastrichtian (chron C31; Keen et al., 2018a), and unit F extends to the landward limit of oceanic crust on profile 1, but can locally extend beyond the landward limit of oceanic crust where younger unit F strata (latest Maastrichtian and Danian) onlap the oldest oceanic crust. In the southern portion of the Saglek Basin, unit F covers serpentinized mantle (Fig. 5b) and extends to the volcanic margin. In the Paamiut South Basin on the southern West Greenland margin, only Upper Cretaceous unit F is mapped; it is thin relative to its equivalent in the Hopedale Basin, terminating near the landward limit of oceanic crust, and overlying the region of serpentinized mantle (Fig. 5a, 8). In the Fylla Structural Complex, thick strata comprising Cretaceous units G and F terminate inboard of the landward limit of oceanic crust (Fig. 5b, 8), although data in the southern Fylla Structural Complex and further south are sparse (Fig. 1) and volcanic cover (Ev) may mask underlying sedimentary rocks in that region.

Within the western Davis Strait region, Cretaceous rocks are found in seabed samples from Cumberland Sound (unit G) and may also be present in Cumberland Basin and in the northern portion of the Saglek Basin, but interpretation throughout this region is hampered by thick Paleocene basalt flows (Fig. 6, 8, 9; Dafoe, DesRoches, and Williams, this volume). On the conjugate West Greenland margin, thick Cretaceous rocks are present along the southern part of the margin where their presence in several wells allows for more definitive mapping of Cretaceous rocks (Fig. 8; Rolle, 1985; Dam et al., 2009; Nøhr-Hansen et al., 2016; Gregersen et al., 2018, 2019, this volume). In that region, Cretaceous strata generally abut the basement platform and extend into the central Davis Strait region within depocentres such as the Lady Franklin Basin; however, Cretaceous strata are absent above major highs (Fig. 6, 8). Unit G in the Lady Franklin, Nuuk, Sisimiut, and Ikermiut basins, as well as in the Fylla Structural Complex, tends to be confined within basement lows and is draped by a relatively transparent unit F (Fig. 6). The Davis Strait High forms an apparent divide, across which there is an asymmetric distribution of Cretaceous strata shown in Figure 6; but its true extent is difficult to determine due to poor data quality and sample availability, and masking by thick overlying basalt flows.

Along western Baffin Bay, the distribution of Cretaceous rocks can be inferred from the presence of seabed samples of bedrock collected along the margin (Fig. 7, 8; MacLean et al., 2014; Dafoe and Williams, 2020d). The Cretaceous interval overlies the basement platform, and locally extends seaward to near the landward limit of oceanic crust (Fig. 8). Near the volcanic margin south of Home Bay (Fig. 9), Cretaceous rocks are difficult to map (Fig. 7a), but strata showing growth into faults near Home Bay (Fig. 7b) and in Scott Graben

Figure 8. Distribution of the Cretaceous interval along the Labrador–Baffin Seaway with the location of the basement platform and outboard highs. Well, corehole, and relevant seabed samples from GSC marine cruises are also shown (*see* Fig. 1 for well names). Whereas Lower Paleocene rocks from the Bylot Island area are described as part of unit F (and the Cretaceous interval) in the text, only Cretaceous rocks are shown here from Jackson et al. (1975; near Salmon River, Baffin Island), Miall et al. (1980; in Eclipse Trough), and Benham (1991; in North Bylot Trough) as these earlier works did not have the resolution to subdivide the Paleocene in detail. The location of onshore outcrops on southeast Baffin Island are from Burden and Langille (1990, 1991) and Jackson (1998). Onshore igneous outcrops locations are from Tappe et al. (2007) and Peace et al. (2016). The Greenland part of the distribution map is from Gregersen et al. (this volume) with the exposures of onshore Cretaceous and Lower Paleocene rocks in the Nuussuaq Basin from Dam et al. (2009). Offshore basin outlines are from Keen et al. (this volume) and are based on work by Gregersen et al. (2019), Dafoe, Dickie, Williams, and McCartney (this volume), Dafoe, DesRoches, and Williams (this volume), Dafoe, Dickie, and Williams (this volume), and with the Nuussuaq Basin from Dam et al. (2009). The landward limit of oceanic crust is also from Keen et al. (this volume). Fracture zones and the location of the extinct seafloor spreading axis are from Oakey and Chalmers (2012). Inset maps show details of closely spaced wells or coreholes. Additional projection information is as follows: Central Meridian = 60°W; Standard Parallels = 65°W, 75°W; Latitude of Origin = 65°N. *See* Figure 1b for abbreviated names.

Contents

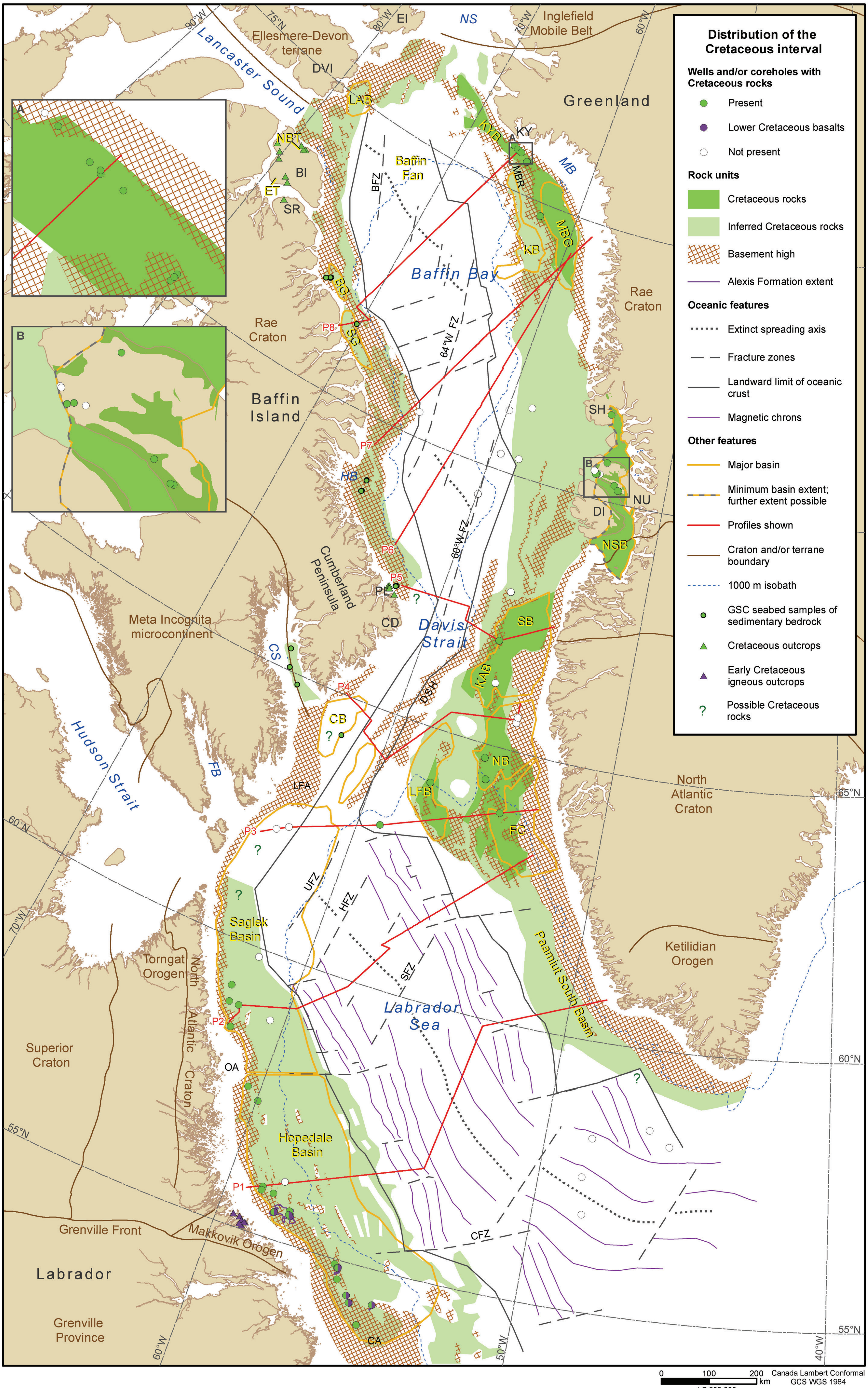
Distribution of the Cretaceous interval
Wells and/or coreholes with Cretaceous rocks
Present
Lower Cretaceous basalts
Not present
Rock units
Cretaceous rocks
Inferred Cretaceous rocks
Basement high
Alexis Formation extent
Oceanic features
Extinct spreading axis
Fracture zones
Landward limit of oceanic crust
Magnetic chrons
Other features
Major basin
Minimum basin extent; further extent possible
Profiles shown
Craton and/or terrane boundary
1000 m isobath
GSC seabed samples of sedimentary bedrock
Cretaceous outcrops
Early Cretaceous igneous outcrops
Possible Cretaceous rocks
A
B
Lancaster Sound
Ellesmere-Devon terrane
DVI
EI
NS
Inglefield Mobile Belt
Greenland
LAB
NBT
BI
ET
SR
Baffin Fan
BFZ
KY
KYB
MB
MBR
MBG
KB
Baffin Bay
BG
SG
P8
Rae Craton
Baffin Island
64°W FZ
P7
HB
SH
NU
DI
NSB
P6
P5
60°W FZ
Cumberland Peninsula
PL
CD
Davis Strait
SB
KAB
DSH
Meta Incognita microcontinent
CS
P4
CB
Hudson Strait
FB
LFA
NB
LFB
North Atlantic Craton
FC
P3
UFZ
HFZ
Saglek Basin
Torngat Orogen
SFZ
Labrador Sea
Paamiut South Basin
Ketilidian Orogen
P2
North Atlantic Craton
Superior Craton
OA
Hopedale Basin
P1
CFZ
Grenville Front
Makkovik Orogen
Labrador
Grenville Province
CA
90°W
80°W
75°N
70°W
60°W
65°N
60°N
55°N
50°W
40°W
0 100 200 km
1:7 500 000
Canada Lambert Conformal
GCS WGS 1984

(Fig. 7c) are assigned to unit G and also possibly unit F. Cretaceous rocks are generally confined to deeper basement structures, as is true for the conjugate West Greenland margin. Distributed along the West Greenland margin, a much wider belt of inferred Cretaceous rocks is interpreted, which have been drilled in the Kap York Basin, the western flank of the Melville Bay Graben (Melville Bay Ridge), and the Nuussuaq Basin (onshore parts; Fig. 8; Gregersen et al., 2019, this volume). Thick Paleocene–Eocene volcanic rocks in the Nuussuaq Basin and west of it (Fig. 9; Skaarup, 2001; Pedersen et al., 2017, 2018) limit seismic interpretation of Cretaceous strata in that region. Units F and G vary in thickness within the Melville Bay Graben and Upernavik, Kivioq, and Kap York basins (Gregersen et al., 2013, 2019), and occur well inboard of the landward limit of oceanic crust and a possible zone of serpentinized mantle (Fig. 7, 8); however, basaltic flows (horizon Ev) may mask underlying Cretaceous strata at the basement hinge line, where the platform ends and basement has subsided into the deeper Baffin Basin (Fig. 7). Several Upper Cretaceous horizons (F2, F3, and Fv) form strong seismic markers along the West Greenland margin, where their distribution has been mapped by Gregersen et al. (2019, this volume; Fig. 6a, 7b, c). Horizon Fv indicates the top of localized Cenomanian–Early Turonian volcanic rocks in the Nuuk Basin (Gregersen et al., 2018; Knudsen et al., 2020).

Lower Cenozoic interval

The lower Cenozoic interval includes the Upper Paleocene through Middle Miocene units E and D (Fig. 4). Unit E is bounded by horizon F1 below and the E1 horizon of Lutetian age above. Within this interval, the Thanetian–Ypresian horizon E2 is mapped, as well as the Ev horizon, a diachronous surface encompassing Paleocene to Lower Eocene volcanic rocks covering much of the Davis Strait and southern Baffin Bay. The overlying unit D is Lutetian to Middle Miocene and is capped by the D1 horizon. On the West Greenland margin, the D2 horizon falls within the Oligocene and a horizon of similar age is recognized along the Canadian margin, as well as horizon D1A (Oligocene–Miocene) and an underlying D3 horizon in the Bartonian. These units are interpreted along seismic profiles that cross the conjugate margins (Fig. 5, 6, 7) and, where they are recognized, are mapped as a lower Cenozoic interval based on sampling and seismic correlations (Fig. 9).

Lithostratigraphic correlations

Lower Cenozoic rocks in the Hopedale and Saglek basins have been sampled and described from exploration wells and assigned to the following: the Selandian to Ypresian Cartwright Formation shale units and Gudrid Formation shallow-marine sandstone units; the Ypresian to Bartonian Kenamu Formation shale units and deltaic Leif Member sandstone units; and the Priabonian to Miocene Mokami Formation shelfal shale and deltaic sandstone units of the lower part of the Saglek Formation (Fig. 4; Umpleby, 1979; McWhae et al., 1980; Bell, 1989; Moir, 1989; Balkwill and McMillan, 1990; Dickie et al., 2011; Dafoe, 2021; Dafoe, Dickie, Williams, and McCartney, this volume). Seabed samples of Paleogene basalt and sedimentary bedrock have also been recovered from the Cumberland Basin, Davis Strait High region, and Scott Graben (Fig. 9; MacLean et al., 2014; Dafoe and Williams, 2020d; Dafoe, DesRoches, and Williams, this volume; Dafoe, Dickie, and Williams, this volume). A thin interval of uppermost unit D is also present at the base of ODP Site 645 (Srivastava et al., 1987; Head et al., 1989a; Knutz et al., 2015; Dafoe and Williams, 2020c; Dafoe, Dickie, and Williams, this volume). On southeastern Baffin Island, the Cape Dyer volcanic rocks form lava deltas and basaltic flows (Clarke and Upton, 1971), with the uppermost Cape Searle Formation possibly also lying at the base of unit E. The upper part of the Aktineq formation and its local Maud Bight member on Bylot Island also lie at the base of unit E as nonmarine sandstone and conglomerate units (Fig. 4; Waterfield, 1989; Benham, 1991; Haggart et al., this volume).

On the central West Greenland margin, in Nuussuaq Basin, are thick Paleocene to Eocene volcanic rocks of the West Greenland Basalt Group. Here unit E includes the Vaigat, Maligât, Svartenhuk, Naqerloq, and Erqua formations (e.g. Clarke and Pedersen, 1976; Larsen, 1977; Storey et al., 1998; Larsen and Pulvertaft, 2000; Pedersen et al., 2017, 2018), with the Eqalulik and Atanikerluk formations comprising mudstone units, tuff beds, and sandstone units at the base of unit E (Dam et al., 2009). There are a few exposures of younger Bartonian volcanic rocks of the Hareøen Formation, and few younger Eocene and Oligocene volcanic rocks and/or intrusions comprising unit D (Fig. 4; e.g. Larsen et al., 2016). A more complete section of unit E is found offshore West Greenland, where it is ascribed to the Paleocene to Middle Eocene Ikermiut and Hellefisk Formation shale units and the sandstone units of the Narssarmiut, Nukik, and Kangâmiut formations (Rolle, 1985; Gregersen et al., this volume). Here, the E1 horizon represents a break in section in the early Lutetian. Elsewhere, a significant section is missing in central West Greenland wells, where a diachronous unconformity from as early as the Ypresian to the Middle Miocene is recognized (Gregersen et al., 2013). Unit D has limited extent and includes shale units of the upper part of the Ikermiut Formation and the Ataneq Formation and sandstone beds of the Nukik, Kangâmiut, and Manîtsoq formations, all Middle to Late Eocene (Rolle, 1985).

Basalt flows near the base of unit E relate to the onset of volcanic outpouring in the region, thought to correlate with the arrival of a mantle plume, the proto-Icelandic plume, around 61 Ma (Storey et al., 1998, 2007; Larsen et al., 2009). In their plate reconstructions, Keen et al. (this volume; their Fig. 15) show that the Cape Dyer volcanic rocks are conjugate to those seen in the Nuussuaq Basin; although volcanism appears to have continued into the Early Eocene in the Nuussuaq Basin, with younger Upper Eocene and Oligocene volcanic rocks also present. This may be due to erosion at Cape Dyer, or to the location of the mantle plume, which had tracked eastward away from Cape Dyer by the Eocene (*see* Keen et al., this volume). Nonmarine to shallow-marine sandstone units appear to have been widespread during the onset of unit E. On Bylot Island, this is represented by the upper part of the nonmarine Aktineq formation and its Maud Bight member (Waterfield, 1989; Benham, 1991; Haggart et al., this volume) and in the Narssarmiut Formation of West Greenland (Rolle, 1985). Similarly, lacustrine mudstone beds and some fluvial sandstone units of the Aktanikerluk Formation include minor marine inundations in the Nuussuaq Basin, although they are more restricted in age (Dam et al., 2009). Along the Labrador margin, shallow-marine shoreface and deltaic sandstone units are locally found in the Gudrid Formation (Umpleby, 1979; Balkwill and McMillan, 1990; Dafoe, 2021; Dafoe, Dickie, Williams, and McCartney, this volume). Following deposition of the Gudrid Formation, transgression ensued with the deposition of the overlying Kenamu Formation (Balkwill and McMillan, 1990; Dickie et al., 2011); a similar Early Eocene transgression has been noted by Rolle (1985) for the West Greenland margin. Overall, the base of unit E suggests an initial period of regional regression, as indicated by several studies (Henderson et al., 1976; Miall et al., 1980; McWhae, 1981; Rolle, 1985; Srivastava, 1986). The Lutetian E1 horizon is interpreted as a flooding event along the Labrador margin (Dafoe, Dickie, Williams, and McCartney, this volume). On the conjugate margin, however, it demarcates a distinct break in section in the mid-Eocene of some West Greenland wells, but amalgamates with the D1 horizon locally, resulting in a significant missing section along parts of that margin (Fig. 4).

Major sandstone units in unit D along the Labrador margin include the Bartonian deltaic Leif Member (Kenamu Formation) and the lowermost shoreline clinothem of the lower part of the Oligocene to Early Miocene Saglek Formation (McWhae et al., 1980; Balkwill

Figure 9. Distribution of the lower Cenozoic (Paleocene–Middle Miocene) interval along the Labrador–Baffin Seaway with the location of the basement platform and outboard highs. Well, corehole, and relevant seabed samples from GSC marine cruises, and the distribution of volcanic rocks are also shown (*see* Fig. 1 for well names). Distribution onshore in the Bylot Island area includes all Paleogene rocks as they are based on older maps that did not separate the Paleocene into stages (Jackson et al., 1975; Miall et al., 1980; Benham, 1991). On northeast Baffin Island, additional outrcrops are shown in Haggart et al. (this volume), and only the most well documented outcrops are shown in this study. The location of onshore outcrops on southeast Baffin Island are from Burden and Langille (1990, 1991) and Jackson (1998). The Greenland part of the distribution map is from Gregersen et al. (this volume) with the distribution of onshore lower Cenozoic volcanic rocks in Nuussuaq Basin from Pedersen et al. (2017, 2018). Offshore basin outlines are from Keen et al. (this volume) and are based on work by Gregersen et al. (2019, this volume), Dafoe, Dickie, Williams, and McCartney (this volume), Dafoe, DesRoches, and Williams (this volume), Dafoe, Dickie, and Williams (this volume), and with the Nuussuaq Basin from Dam et al. (2009). The landward limit of oceanic crust is also from Keen et al. (this volume). Fracture zones and the location of the extinct seafloor spreading axis are from Oakey and Chalmers (2012). Inset map shows details of closely spaced wells or coreholes. Additional projection information is as follows: Central Meridian = 60°W; Standard Parallels = 65°W, 75°W; Latitude of Origin = 65°N. *See* Figure 1b for abbreviated names.

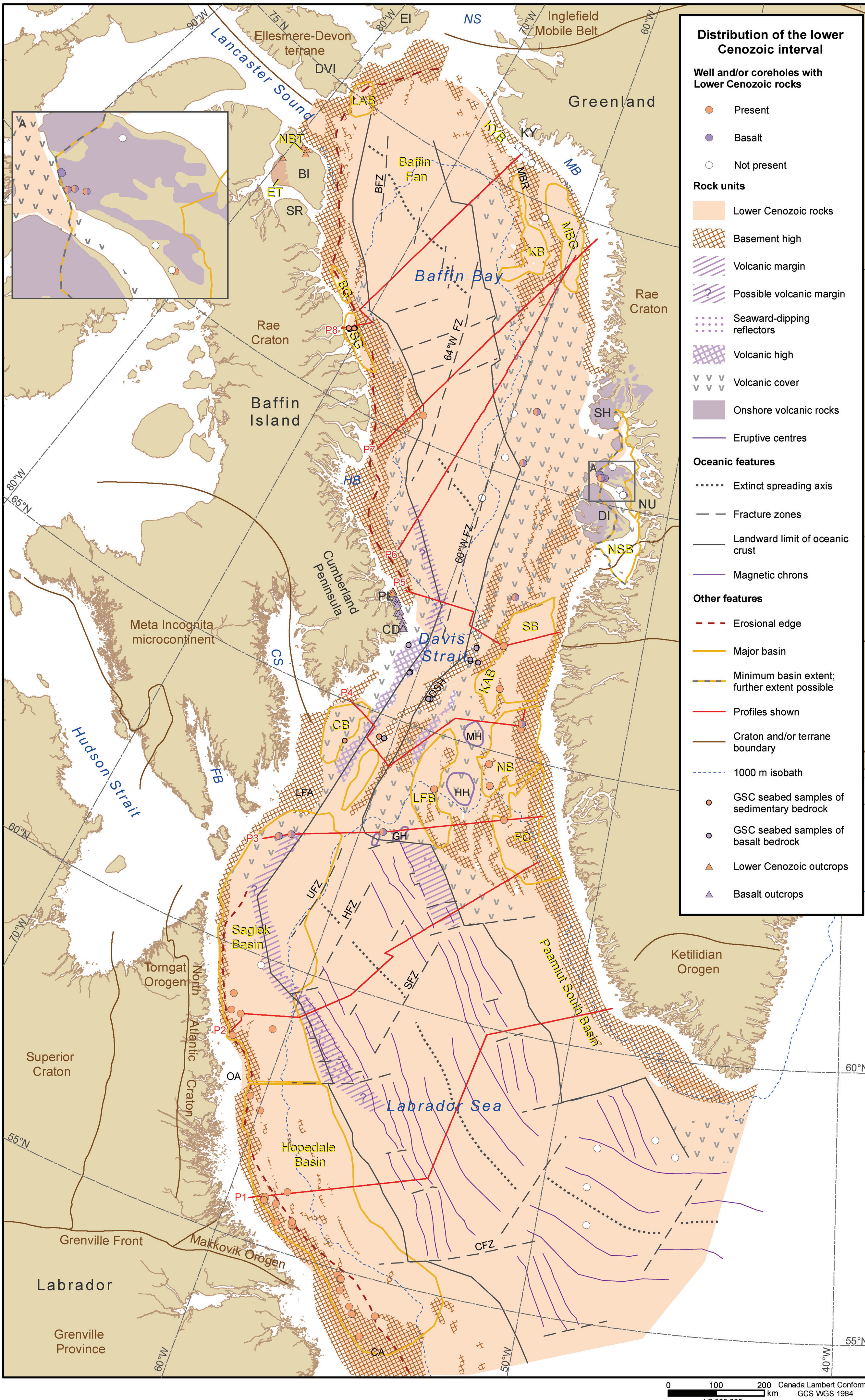
Distribution of the lower Cenozoic interval
Well and/or coreholes with Lower Cenozoic rocks
Present
Basalt
Not present
Rock units
Lower Cenozoic rocks
Basement high
Volcanic margin
Possible volcanic margin
Seaward-dipping reflectors
Volcanic high
Volcanic cover
Onshore volcanic rocks
Eruptive centres
Oceanic features
Extinct spreading axis
Fracture zones
Landward limit of oceanic crust
Magnetic chrons
Other features
Erosional edge
Major basin
Minimum basin extent; further extent possible
Profiles shown
Craton and/or terrane boundary
1000 m isobath
GSC seabed samples of sedimentary bedrock
GSC seabed samples of basalt bedrock
Lower Cenozoic outcrops
Basalt outcrops
Greenland
Inglefield Mobile Belt
Ellesmere-Devon terrane
Lancaster Sound
Baffin Fan
Baffin Bay
Rae Craton
Baffin Island
Cumberland Peninsula
Davis Strait
Meta Incognita microcontinent
Hudson Strait
Torngat Orogen
North Atlantic Craton
Superior Craton
Saglek Basin
Hopedale Basin
Labrador Sea
Paamiut South Basin
Ketilidian Orogen
Grenville Front
Makkovik Orogen
Labrador
Grenville Province
0 100 200 km
1:7 500 000
Canada Lambert Conformal
GCS WGS 1984

and McMillan, 1990; Dickie et al., 2011; Dafoe, 2021; Dafoe, Dickie, Williams, and McCartney, this volume). Sandstone units along offshore West Greenland are more prevalent in the upper portion of unit E and lower part of unit D. Whereas the Kangâmiut Formation denotes deltaic deposition similar to the Leif Member, the Manîtsoq Formation was deposited on a shallow shelf, and the Nukik Formation represents turbidite accumulations (Rolle, 1985; Gregersen et al., this volume). Here, shale and/or claystone units of the Ikermiut Formation are interpreted as fully marine accumulations, but the Hellefisk and Ataneq formations record shallow-marine to delta-plain successions (Rolle, 1985). Shelfal and deeper water mudstone units appear to be more common on the Labrador margin, forming the thick Kenamu and Mokami formations (McWhae et al., 1980; Balkwill and McMillan, 1990; Dickie et al., 2011; Dafoe, 2021; Dafoe, Dickie, Williams, and McCartney, this volume). The presence of deltaic strata along both conjugate margins suggests that regressions took place following the Early Eocene transgression; however, the proximity to sediment sources probably varied and subsidence was likely affected by tectonism during local basin inversion, especially of the West Greenland margin, in the early Cenozoic (Wilson et al., 2006; Gregersen et al., 2013).

Seismic correlations and mapped distribution

In the Labrador–Baffin Seaway, the lower Cenozoic interval onlaps the basement platform, locally at the major basin-bounding faults, such as in the western Davis Strait subregion and Paamiut South Basin, but elsewhere covers the platform, in places extending landward of the seismic data set (Fig. 9). Along the western margin of much of the region, an erosional edge marks the location at which the lower Cenozoic succession is truncated at the seabed (i.e. where the D1 horizon intersects the seafloor); west of this line the section is incomplete. The lower Cenozoic interval is also locally absent above significant basement highs, volcanic highs, and elevated blocks of continental crust forming the Davis Strait High, as well as along parts of the inner margin of West Greenland (Fig. 9).

During the early Cenozoic and within the northern part of the Labrador Sea, magma-rich margins formed with seaward-dipping reflectors, which on the Labrador side, likely overlap a zone of serpentinized mantle (Fig. 5b; Chalmers, 1997; Keen et al., 2012, 2018b, this volume). Here, the locations of the volcanic escarpments tie to the landward limit of oceanic crust, as oceanic crust was forming in this region by the Early Paleocene (Keen et al., 2018b). This volcanic margin has been mapped northward to the Hejka O-71 and Ralegh N-18 wells, where seaward-dipping reflectors are also observed (Fig. 9; Keen et al., this volume; Dafoe, DesRoches, and Williams, this volume). Another volcanic margin, identified by Skaarup et al. (2006), is found east of Cape Dyer and is marked by seaward-dipping reflectors and thick inner flows, and is tentatively mapped farther north toward Home Bay (Fig. 9; Dafoe, Dickie, and Williams, this volume; Keen et al., this volume). Through central Davis Strait is the Davis Strait High, composed of crystalline basement with a thin basalt cover (Funck et al., 2007; Suckro et al., 2013). It forms two main ridge systems which roughly parallel the southeast Baffin Island coastline, with nearby volcanic highs following a similar trend (Fig. 9 ; Dafoe, DesRoches, and Williams, this volume). Seaward-dipping reflectors are also noted from the volcanic high southeast of Cape Dyer (Fig. 9; Suckro et al., 2013). Volcanic cover is widespread in Davis Strait and in southern Baffin Bay, whereas large volcanic eruptive centres formed in southern Davis Strait (Fig. 9). Sedimentary basins on the eastern side of Davis Strait appear to have very thin volcanic cover with improved seismic imaging there. Basalt flows are encountered in several wells in the Davis Strait, as well as in seabed samples of bedrock and onshore outcrops at Cape Dyer (Fig. 9; Clarke and Upton, 1971; Dafoe and Williams, 2020d; Dafoe, DesRoches, and Williams, this volume). Thick basalt flows of the West Greenland Basalt Group are also widespread both onshore (Pedersen et al., 2017, 2018) and offshore of Disko Island, Nuussuaq, and Svartenhuk Halvø (Skaarup, 2001), where they mask underlying structures and strata (Fig. 9; *see* Gregersen et al., this volume). Upper parts of the Paleogene volcanic succession west of the Nuussuaq Basin were drilled in the Alpha-1 S1 and the Delta-1 wells (Fig. 9; Nelson et al., 2015; *see* Fig. 3 in Gregersen et al., this volume).

In the Hopedale and Saglek basins, unit E has a relatively consistent thickness below the present-day shelf, but onlaps oceanic crust basinward, with the E1 horizon terminating against this oceanic basement (Fig. 5a). The package is subdivided by the E2 horizon, which bounds the top of the Gudrid and Cartwright formations. The overlying unit D thickens below the present-day shelf edge and slope; then it thins basinward to cover oceanic crust, except for highly elevated blocks near the extinct spreading axis (Fig. 5). Unit D is subdivided by the D3 horizon (top Kenamu Formation), D2 horizon (Saglek and/or Mokami formation 1), and D1A horizon (Saglek and/or Mokami formation 2; *see* Dafoe, Dickie, Williams, and McCartney, this volume). Units E and D are deformed by Cenozoic faulting below the shelf and slope (Fig. 5), where unit E is overthickened. On the conjugate West Greenland margin, units E and D are thinner, especially over the southern Fylla Structural Complex, where underlying basement inversion is prevalent (Fig. 5b; Døssing, 2011). The units also onlap abruptly against the steep basin-bounding fault in the Paamiut South Basin (Fig. 5a). Along this margin, both horizon Ev (top of Paleogene volcanic succession) and horizon E2 are interpreted, with horizon E2 terminating against oceanic crust.

Within the western Davis Strait region, units E and D comprise much of the sedimentary succession, but thin over oceanic crust, the Davis Strait High, and volcanic highs (Fig. 6). The strata are subdivided by horizon Ev, below which older strata and the basement are difficult to map. Units E and D are further subdivided by horizons E1, E2, D3, and D1A, which can be tied to wells in the northern part of the Saglek Basin (Fig. 6a); elsewhere these horizons can only be mapped locally. Refraction seismic data along profile 3 (Fig. 6a) constrains the presence of oceanic crust and depth to the top of continental basement (Funck et al., 2007; Keen et al., this volume). This is in contrast to the West Greenland margin where several wells constrain the Ev, E2, and E1 horizons (Gregersen et al., 2019, this volume). The stratigraphic interval is very thin to locally absent in the central Fylla Structural Complex (Fig. 6a) and Nuuk Basin (Fig. 6b), but thickens dramatically in the Sisimiut Basin (Fig. 6c). Here, structure is complex, with wrench-style (strike-slip) faulting taking place during development of the Ungava Fault Zone (Wilson et al., 2006), resulting in much of unit E onlapping inverted Cretaceous and older rocks (Fig. 6c), with horizon E1 forming a major unconformity (Gregersen et al., 2019, this volume).

In southern Baffin Bay, horizon E1 appears to onlap against oceanic crust (Fig. 7). The basement low created by the extinct spreading axis is possibly filled with younger Eocene strata of unit D, since spreading ceased near the Eocene–Oligocene boundary (Fig. 7a, c). In general, the lower Cenozoic interval thickens basinward along the southern part of the eastern Baffin Island margin into the extinct spreading axis and then thins slightly before thickening in Upernavik Basin and Melville Bay Graben (Fig. 7a). Unit E contains thick volcanic rocks that partially mask underlying basement and are mapped along much of eastern Baffin Bay, where they may overlie a narrow zone of serpentinized mantle that is thought to be present outboard of Kivioq Ridge (Fig. 7b, c; Keen et al., this volume). In Home Bay, units E and D are relatively thin atop the elevated basement platform, but thicken dramatically into the Eocene 64°W Fracture Zone (Fig. 7b). The lower Cenozoic is exceptionally thick in the Melville Bay Graben, where horizon D1 extends just above the top of basement highs (Fig. 7b). In the Scott Graben, the lower Cenozoic interval is incomplete, with the D3 horizon (top Kenamu Formation) near the seabed (Fig. 7c). Eastward, unit E thickens, with a well defined E2 horizon extending seaward to onlap oceanic crust, and unit D is truncated by slumping that occurred above the B1 horizon and below the present-day shelf edge. Unit D is generally thin, except over the extinct spreading axis, but is also thicker than unit E offshore of Kivioq Ridge, possibly as a result of volcanic cover in that region (Fig. 7c). The lower Cenozoic interval is also relatively thin in Kivioq Basin to absent at Kap York Basin, where coreholes intersect older strata near the seafloor (Fig. 7c, 8; G. Acton, G. Claypool, I. Delusina, G. Dunbar, H. Evans, P. Ferretti, G. Guerin, L. Holloway, S. Ishman, P.C. Knutz, L. Krissek, D. Kulhanek, T.L. Insua, J. Lauren, D. Maloney, D. Naafs, H. Nøhr-Hansen, M. Olney, C. Richter, M. Storms, S. Woodard, and J. Wright, unpub. rept., 2012; Fig. 3: Gregersen et al., 2019, this volume; *see also* Nøhr-Hansen et al., 2021). Finally, horizon D2 is a fairly prominent marker across Baffin Basin and in Melville Bay Graben, but is complicated by mass-transport complexes in the deeper basin (Fig. 7b, c).

Upper Cenozoic interval

The upper Cenozoic section spans the Middle Miocene to Pleistocene and is subdivided into three units: A, B, and C (Fig. 4). The basal unit C, is Middle to Late Miocene and bounded by horizon D1 below and horizon C1 above. The top of unit B (horizon B1) is within the Late Miocene to Pliocene, the age of which has been interpreted somewhat differently on either side of the seaway, due to limited samples and biostratigraphic control in this part of the section (Fig. 4; *see* Nøhr-Hansen et al., 2016). The upper unit A is Pliocene to Pleistocene and capped by the seafloor (horizon A1). These units are interpreted along seismic profiles that cross the conjugate margins (Fig. 5, 6, 7). Maps showing the distribution of upper Cenozoic rocks are based on sampling and from seismic correlations (Fig. 10).

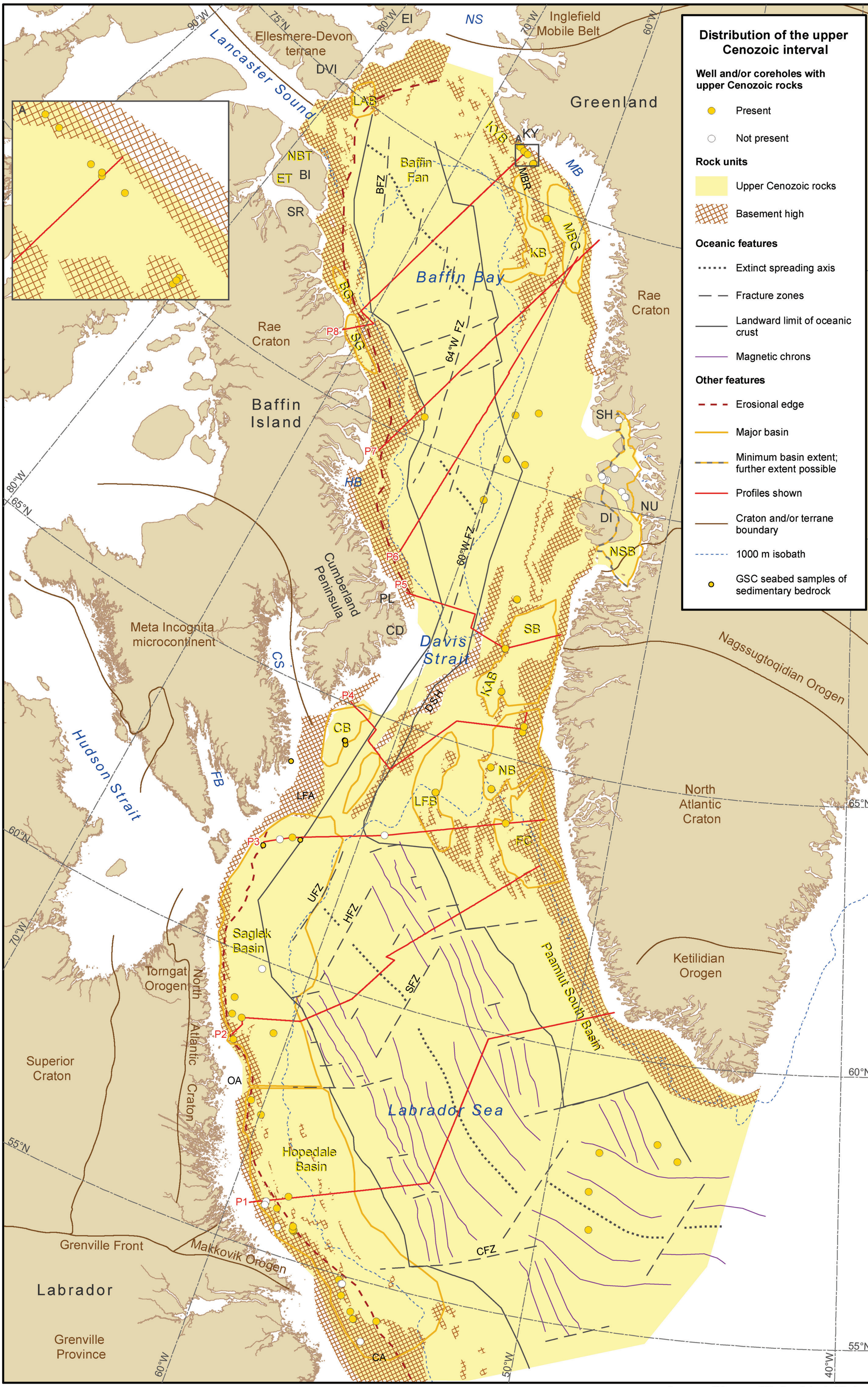
Distribution of the upper Cenozoic interval
Well and/or coreholes with upper Cenozoic rocks
Present
Not present
Rock units
Upper Cenozoic rocks
Basement high
Oceanic features
Extinct spreading axis
Fracture zones
Landward limit of oceanic crust
Magnetic chrons
Other features
Erosional edge
Major basin
Minimum basin extent; further extent possible
Profiles shown
Craton and/or terrane boundary
1000 m isobath
GSC seabed samples of sedimentary bedrock
Greenland
Baffin Bay
Davis Strait
Labrador Sea
Baffin Island
Rae Craton
Lancaster Sound
Ellesmere-Devon terrane
Inglefield Mobile Belt
Baffin Fan
Meta Incognita microcontinent
Cumberland Peninsula
Hudson Strait
Nagssugtoqidian Orogen
North Atlantic Craton
Ketilidian Orogen
Saglek Basin
Hopedale Basin
Paamiut South Basin
Torngat Orogen
North Atlantic Craton
Superior Craton
Grenville Front
Makkovik Orogen
Labrador
Grenville Province
0 100 200 km
1:7 500 000
Canada Lambert Conformal
GCS WGS 1984

Figure 10. Distribution of the upper Cenozoic (Middle Miocene to Pleistocene) interval along the Labrador–Baffin Seaway with the location of the basement platform and outboard highs. Well, corehole, and relevant seabed samples from GSC marine cruises are also shown (*see* Fig. 1 for well names). Offshore basin outlines are from Keen et al. (this volume) and are based on work by Gregersen et al. (2019), Dafoe, Dickie, Williams, and McCartney (this volume), Dafoe, DesRoches, and Williams (this volume), Dafoe, Dickie, and Williams (this volume), and with the Nuussuaq Basin from Dam et al. (2009). The landward limit of oceanic crust is also from Keen et al. (this volume). The Greenland part of the distribution map is from Gregersen et al. (this volume). Fracture zones and the location of the extinct seafloor spreading axis are from Oakey and Chalmers (2012). Inset map shows details of closely spaced wells or coreholes. Additional projection information is as follows: Central Meridian = 60°W; Standard Parallels = 65°W, 75°W; Latitude of Origin = 65°N. *See* Figure 1b for abbreviated names.

Lithostratigraphic correlations

In the Hopedale and Saglek basins, the upper Cenozoic interval is sampled in several wells (Fig. 10). The interval is characterized by the inferred Middle Miocene to (?)Pliocene shelfal to shallow-marine shale units of the upper Mokami Formation (based on seismic interpretation) and the partly inferred Middle Miocene to Pleistocene shoreface and/or deltaic sandstone units of the upper part of the Saglek Formation (partly based on seismic interpretation; Fig. 4, 10; Umpleby, 1979; McWhae et al., 1980; Bell, 1989; Moir, 1989; Balkwill, 1987; Balkwill and McMillan, 1990; Dickie et al., 2011; Dafoe, Dickie, Williams, and McCartney, this volume). Related seabed samples have also been recovered in the northern portion of the Saglek Basin and Cumberland Basin regions, but these are restricted to unit A (Fig. 10; MacLean and Falconer, 1977; MacLean, 1978; Dafoe and Williams, 2020d; Dafoe, DesRoches, and Williams, this volume). Off the Baffin Shelf, ODP Site 645 preserves sandy mudstone and mudstone intervals of units C through A, representing shelf, slope, and open-ocean settings (Srivastava et al., 1987; de Vernal and Mudie, 1989a; Head et al., 1989a; Knutz et al., 2015; Dafoe and Williams, 2020c; Dafoe, Dickie, and Williams, this volume), which are likely distal equivalents of the coarser grained units found on the Labrador Shelf.

At Hareøen, in the Nuussuaq Basin, a thin, local coal bed and a few metres of Neogene clastic sedimentary strata overlie lava flows of the Upper Eocene Talerua Member, Hareøen Formation (Fig. 4; Christiansen et al., 1999). The Neogene strata are further overlain by glaciofluvial deposits. Offshore West Greenland, unit C contains Middle Miocene shallow-marine to deltaic sandstone intervals forming the upper parts of the Kangâmiut, Manîtsoq, and Ataneq formations (Rolle, 1985; Gregersen et al., this volume). The last two formations also comprise units B and A, and Gregersen et al. (2019, this volume) tentatively extended the age of these formations upsection to the end of the Pleistocene. Accordingly, the upper portion of the Manîtsoq Formation is an Upper Miocene to possibly Pleistocene shallow-marine sandstone interval (Rolle, 1985; Piasecki, 2003). The correlative upper part of the Ataneq Formation includes shale and lesser sandstone beds that preserve delta-plain and shallow-marine Upper Miocene to possibly Pleistocene deposits (Rolle, 1985).

Along the Labrador margin, sandstone units of the Saglek Formation form prograding shoreline clinoform systems, with related fans deposited seaward of these features. A Middle Miocene clinoform package sits above the D1 horizon (Fig. 5a; Dafoe, Dickie, Williams, and McCartney, this volume). The B1 horizon forms the base of the uppermost clinoform package which is thought to be Pliocene–Pleistocene, and it displays well developed topsets in some areas outside of the Labrador Trough region, especially in the southern portion of the Saglek Basin (Fig. 5; Dafoe, Dickie, Williams, and McCartney, this volume). The West Greenland margin also contains shallow-marine and deltaic sandstone assigned to the Kangâmiut, Manîtsoq, and Ataneq formations, although these appear to be locally more extensive than equivalents on the Canadian margin (Fig. 4). Recent drilling results from distal wells in the Lady Franklin Basin (LF7-1) and eastern Baffin Basin (e.g. Gamma-1, T8-1), as well as the Qulleq-1 well in the Fylla Structural Complex (Piasecki, 2003; Gregersen et al., 2018, 2019), intersected shale beds similar to those of ODP Site 645. It appears that shoreline progradation was taking place on either side of the seaway, a process responsible for developing the present-day shelves, with distal marine conditions established in the central part of the seaway. The timing of events, however, cannot be fully established due to limited age control within the late Cenozoic. Eustasy, paleoceanography, and glaciation all likely influenced sedimentation during the upper Cenozoic, but the present-day shelves were mainly developed by glacial processes, which included shelf progradation and erosion of pre-Quaternary units. During the Late Miocene and Pliocene, shelf progradation and contourite drift deposition appear to be the principal mechanisms for constructing the shelf and slope regions (Knutz et al., 2015).

With regard to the bounding horizons, D1 is locally erosional in the Hopedale and Saglek basins at the base of Middle Miocene clinoforms (Dickie et al., 2011; Dafoe, DesRoches, and Williams, this volume; Dafoe, Dickie, Williams, and McCartney, this volume), but forms a major unconformity on the West Greenland margin, where strata ranging from upper parts of Eocene to lower parts of the Miocene interval are missing (Nøhr-Hansen et al., 2016; Gregersen et al., 2019, this volume). Offshore Labrador, horizon C1 locally approximates with a horizon demarcating the base of a slumped and channelled interval along this margin (Dickie et al., 2011; Dafoe, Dickie, Williams, and McCartney, this volume), and may be partly correlative to a missing section in eastern Baffin Bay, though unit C is also generally widespread here (Knutz et al., 2015, 2019; Gregersen et al., 2019, this volume). Finally, horizon B1 is relatively mappable throughout the region, underlying the shelf-building Pliocene–Pleistocene clinoform successions that truncate underlying strata in places. This clinothem signalled a major regression triggered by rapid sea-level fall during glaciation of the shelves, locally forming extensive glacial troughs (Dickie et al., 2011; Knutz et al., 2015, 2019; Gregersen et al., this volume).

Seismic correlations and mapped distribution

In proximal regions, the upper Cenozoic interval generally onlaps the basement platform, extending landward beyond the seismic data set in parts of the Labrador Sea, eastern Davis Strait, and Baffin Bay (Fig. 10). In western Davis Strait, the succession terminates locally at the seafloor before reaching the basement platform. Upper Cenozoic strata blankets most of the study region, is thickest near the present-day shelf edge, and forms a thick blanket over oceanic crust. Along the slope and in deep water, mass-transport complexes locally developed (Fig. 5, 6, 7). This section is absent over a few prominent basement highs in Baffin Bay and parts of the Davis Strait High where the basement subcrops at the seafloor, and the interval is also missing in the onshore regions of Nuussuaq Basin, and Bylot and Baffin islands. West of the erosional edge mapped along the Canadian margin (Fig. 10), the upper Cenozoic succession is thin and generally represented by only Pleistocene sediments. Upper Cenozoic strata are intersected by most of the offshore wells in the region, but not in onshore wells and coreholes in the Nuussuaq Basin and some areas of the Labrador Shelf (Fig. 10). Harrison et al. (2011) described and mapped the thick section in northern Baffin Bay (comprised of both lower and upper Cenozoic sedimentary rocks) as the Baffin Fan, which they considered to have resulted from high sediment input through both Lancaster Sound and Nares Strait. Knutz et al. (2019) also described and mapped the latest Pliocene–Pleistocene (during the past 2.7 Ma) sedimentary evolution in eastern Baffin Bay with eleven phases of shelf-edge advance during glaciations on Greenland.

Within the Hopedale and Saglek basins, only the B1 horizon is mapped semiregionally, such that intervals C and B are often represented by a single unit where horizon C1 cannot be defined. The combined units C and B contain a slumped and channellized interval below the present-day shelf in the Hopedale Basin (Fig. 4, 5a), deformation that is less well defined in the Saglek Basin as a result of reduced seismic imaging (Fig. 5b). The overlying unit A forms steep prograding clinoforms and thin topsets that onlap the basement platform (Fig. 5a). To the north, this interval is more aggradational, with well developed topsets and less distinct clinoforms (Fig. 5b). The upper Cenozoic interval has not been subdivided into horizons B1 and C1 on seismic data along the southernmost West Greenland margin (south of the Fylla Structural Complex) due to limited stratigraphic constraints in this region (Fig. 5). The upper Cenozoic succession onlaps the basement platform (Fig. 5a) and has been modified by seabed processes over the southern Fylla Structural Complex (Fig. 5b, 6a) and over large parts of the southern West Greenland margin (Nielsen et al., 2011). Within this succession are major contourites and deposits of other seabottom processes, including the Middle Miocene to Recent Davis Strait Drift Complex (Nielsen et al., 2011), the Miocene to Pleistocene Eirik Drift, and mass flows and spillover from the Northwestern Atlantic Mid-Ocean Channel of the Labrador Sea (Hesse and Chough, 1980). Such upper Cenozoic successions were drilled in the ODP Site 646 southwest of Greenland (Fig. 10; Cremer, 1989).

On the western side of the Davis Strait, horizon B1 and C1 in the upper Cenozoic interval can be mapped locally only, mainly from correlation with the conjugate margin (Dafoe, DesRoches, and Williams, this volume). In the northern portion of the Saglek Basin, horizon B1 separates two major prograding clinoform successions of the Saglek Formation (Fig. 6a). These strata terminate landward where the D1 horizon meets the seafloor, but thicken into the shallow slope before thinning in the region of the Gjoa G-37 well. On the conjugate West Greenland margin, units C and A make up most of the section; unit B is thin to locally absent. At the northeastern end of the Fylla Structural Complex, all three units contain prograding clinoforms, and recent seafloor processes have modified the seabed. In the Cumberland Basin area, units A to C are thin with low-angle progradation above the Davis Strait High (Fig. 6b). In the Nuuk Basin, however, units A to C thicken, forming much of the present-day shelf there. Horizons C1 and B1 are mapped in northern Davis Strait, but are complicated by contourite deposits and channelling above the thick volcanic margin (Fig. 6c). Subtle progradation within units B and A are noted at the edge of the basement platform. The interval thins over the North Ungava Basin and over the conjugate West Greenland margin, with recognizable progradation within unit A, as well as prominent topsets that continue to the east (Fig. 6c).

In Baffin Bay, horizon B1 is a regional marker, but horizon C1 is indistinct off the south Baffin Island margin (Fig. 7). Here, the combined units B and C thicken basinward into Baffin Basin and then thin slightly across the slope into Upernavik Basin and still further over the Melville Bay Graben (Fig. 7a). Notably, unit A is thick within Baffin Basin and is a major component of the present-day shelf on the West Greenland margin, where steep clinoforms developed during the latest Neogene (Fig. 7a). In the Home Bay region, units C to A are relatively thin atop the elevated basement platform and thin over prominent basement highs below the slope, where slumping was prevalent during their deposition (Fig. 7b). These strata thicken basinward into Baffin Basin and further thicken within Upernavik Basin, where unit A forms a major clinoform succession with progradation also evident in the underlying units. Unit A thins to the northeast over Melville Bay Graben, where the upper Cenozoic interval is truncated by glacial trough erosion (Fig. 7b). Continuing the trend, unit A is exceptionally thick in northern Baffin Bay, where the underlying B1 horizon cuts down into units B, D, and E east of Scott Graben (Fig. 7c). Unit A thickens into Baffin Basin and then thins in the Kivioq Basin area, where it forms clinoforms and associated thin topsets. Units B and C also thicken into Baffin Basin, and thin on both conjugate margins where glacial erosion has removed section, as in the Scott Graben and Kap York Basin (Fig. 7c). Knutz et al. (2015) concluded that unit C was composed of large-scale mass-transport deposits, but that unit B included contourite drifts formed by oceanic bottom currents, the timing of which was correlated with ODP Site 645.

Compared to the deep-water Labrador Sea Basin, Baffin Basin contains a much thicker upper Cenozoic interval with the glacially derived shelf edge best developed in Melville Bay. Clinoform development is regionally prominent in unit A and locally also present in units B and C. It appears that similar processes were taking place regionally, and the deposition of upper Cenozoic sediments was shaped by currents, and later, also by glaciation and glacial supply (Li et al., 2011; Knutz et al., 2015), factors influencing the resultant geometry of the margins.

PALEOCLIMATOLOGY AND PALEOCEANOGRAPHY

Fossil assemblages in the wells, coreholes, seabed samples, and onshore outcrops have provided a record of changing paleoclimate and water circulation patterns during the approximately 100 million years of the Labrador–Baffin Seaway's existence. This is especially true of foraminifer and dinocyst assemblages, both groups being particularly sensitive to climatic variations during the Cretaceous and Cenozoic. The distribution of planktonic and benthic foraminifera is dependent on sea-surface and bottom-water temperatures, respectively, resulting in latitudinally restricted biogeographic provinces (Armstrong and Brasier, 2005). Accordingly, oxygen-isotope ratios within the tests (shells) of both benthic and planktonic foraminifera can be used to reconstruct paleoceanographic and paleoclimatic conditions (Armstrong and Brasier, 2005). With regard to palynomorphs, miospores shed light on the composition of terrestrial floras, and regional distribution patterns of modern dinocysts illustrate how these organisms are controlled by latitudinal sea-surface temperature gradients. Such control allows the recognition of 'warm' and 'cold' water taxa that can be used to estimate temperature gradients in the past (Masure and Vrielynck, 2009). The use of foraminifera and palynomorphs can thus shed light on the paleoclimatology and paleoceanography of the Labrador–Baffin Seaway, and allow inferences to be made on the nature of the critical linkage between the North Atlantic and Arctic oceans.

Cretaceous

Global climate studies of the Early Cretaceous are limited, but suggest an overall warming through the Albian (Friedrich et al., 2012), with $\delta^{18}O$ and $\delta^{13}C$ values in the early Albian comparable to those of the Paleocene–Eocene Thermal Maximum (*see* below). Similar to the global studies, major gaps in the understanding of Early Cretaceous paleoclimate and paleoceanography of the Labrador–Baffin Seaway exist due to limited sampling, missing section, and incomplete fossil assemblages in the primarily fluvial to alluvial sedimentary strata. The oldest marine strata in the region are generally Albian to Cenomanian, and reflect marginal marine, often deltaic deposition (Fig. 4; e.g. Dam et al., 2009; Nøhr-Hansen et al., 2016; Dafoe and Williams, 2020a; Dam and Sønderholm, 2021; Nøhr-Hansen et al., 2021; Dafoe, Dickie, Williams, and McCartney, this volume; Gregersen et al., this volume); however, based on palynological analyses, Barremian–Aptian marginal marine shale beds have been recovered from the Labrador margin in core from the Herjolf M-92 well (Dafoe and Williams, 2020a). These Lower Cretaceous strata often contain the dinocyst genus *Nyktericysta* (Fig. 2), considered to be restricted to coastal or marginal marine paleoenvironments (Bint, 1986; Nøhr-Hansen et al., 2016, 2021), settings in which diversity of both dinocysts and planktonic foraminifera is reduced in comparison to distal marine settings (Armstrong and Brasier, 2005). Using a different line of evidence based on analyses of clay mineralogy in Labrador Shelf wells, Hiscott (1984) suggested that the Early Cretaceous of the western part of the Labrador–Baffin Seaway region was characterized by a humid, temperate climate. This agrees well with paleoclimate interpretations based on the flora from the Cenomanian Redmond Formation, found about 400 km inland from the coast of Labrador, which also suggest a warm, temperate, humid climate (Demers-Potvin and Larsson, 2019).

Early Late Cretaceous dinocyst assemblages in the seaway differ somewhat from coeval assemblages of those from the North Atlantic: on the Grand Banks, offshore Newfoundland and the Scotian margin, offshore Nova Scotia (e.g. Williams and Brideaux, 1975). The Labrador–Baffin Seaway assemblages include common *Heterosphaeridium difficile* (Fig. 2) found in the Coniacian of the Bjarni O-82 and South Labrador N-79 wells in the Hopedale Basin (Nøhr-Hansen et al., 2016), in some of the seabed bedrock samples from western Baffin Bay (MacLean et al., 2014), and in Nuussuaq Basin (Pedersen and Nøhr-Hansen, 2014). *Heterosphaeridium difficile* was originally described from Graham Island, Arctic Canada (Manum and Cookson, 1964). The occurrence of this species from other high-latitude localities, such as Bylot Island, Baffin Bay, and the southwestern Barents Sea (Ioannides, 1986; Dam et al., 1998b; Radmacher et al., 2014; Nøhr-Hansen et al., 2016, 2021) and in the Turonian in Baffin Bay (Nøhr-Hansen et al. 2021) suggests that it is a high-latitude species restricted to cooler temperature domains. Conversely, low oxygen-isotope values from global studies suggest that the Cenomanian–Turonian and Santonian ages were warm, with a mid-Cretaceous climate maximum from 97 to 91 Ma (Cenomanian–Turonian), and characterized by $\delta^{18}O$ values apparently lower than those of the Paleocene–Eocene Thermal Maximum (Cramer et al., 2009; Friedrich et al., 2012), suggesting even warmer conditions. The discrepancy between the warm conditions indicated by global studies and cooling suggested by the presence of high-latitude dinocyst species cannot be explained within the scope of the present study, but it may be related to a distinctly different thermal regime in the high latitudes during this time; as well, the limited number of known pre-Campanian palynoevents from the seaway may play a role.

During the late Late Cretaceous, provincialism of Campanian dinocysts was demonstrated by Lentin and Williams (1980), who defined assemblages related to climatic belts. One of these was the McIntyre or Boreal suite, characterized by *Laciniadinium* and large species of the genus *Chatangiella* (Fig. 2). Regions where this assemblage is found include Arctic Canada (Manum and Cookson, 1964; Mcintyre, 1975; Lentin and Williams, 1980; Ioannides, 1986), western Baffin Bay (MacLean et al., 2014), and West Greenland (Nøhr-Hansen, 1996). Accordingly, this suite is representative of high latitudes and cooler temperate climates. MacLean et al. (2014) further noted that *Chlamydophorella grossa*, *Endoscrinium obscurum*, *Heterosphaeridium difficile*, and *Heterosphaeridium heteracanthum* were significant elements associated with the McIntyre suite. These taxa, as well as *Laciniadinium* and *Chatangiella*, have also been found in Coniacian–Santonian and Maastrichtian samples from the Labrador–Baffin Seaway (Fig. 2; MacLean et al., 2014), indicating that cooler temperatures may have persisted prior to, and following the Campanian. In contrast, the Williams suite — which contains smaller species of *Chatangiella*, *Isabelidinium*, and *Alterbidinium* — is found in warm-temperate regions such as the Grand Banks and Scotian margin (Lentin and Williams, 1980). Taxa characteristic of the Williams suite are found along the Labrador margin and also in some of the Baffin Bay samples (Fig. 2; Nøhr-Hansen et al., 2016), indicating that the climate during part of the Campanian was also warm temperate. Global stable oxygen curves suggest a cooling from the Turonian into the later part of the Cretaceous, with $\delta^{18}O$ values similar to those of the Albian, but with some fluctuations over time (Cramer et al., 2009; Friedrich et al., 2012). This would appear to be consistent with the mix of warm and cooler water dinocysts described above.

Toward the end of the Cretaceous, the dinocyst *Isabelidinium cretaceum* is present in some of the Maastrichtian samples of the Labrador Shelf wells (Fig. 2; Nøhr-Hansen et al., 2016). According to Mohr and Mao (1997), *Isabelidinium cretaceum* subsp. *gravidum* is a higher latitude taxon that occurs in the Maastrichtian of the Southern (Antarctic) Ocean. Likewise, Nøhr-Hansen and Dam (1997, 1999), in their studies of uppermost Maastrichtian rocks from onshore West Greenland, noted a similar relationship between their dinocyst assemblages and those of Seymour Island, Antarctica. In regards to foraminifer assemblages, planktonic foraminifera in marine Campanian–Maastrichtian shale beds from Nuussuaq, West Greenland, show affinities with North Atlantic assemblages, suggesting warmer surface waters and temperate climatic conditions (Gradstein and Srivastava, 1980). Based on this observation, Atlantic surface waters may have periodically extended as far as present-day latitude 70°N (paleolatitude 65°N during the Cretaceous; Gradstein and Srivastava, 1980). Whereas a Campanian warm-temperate climate is relatively consistent from both dinocyst and foraminiferal evidence, there is less agreement in the Maastrichtian, with dinocysts suggesting cooler climates. These results from dinocysts in the Maastrichtian are in accord with the global oxygen-isotope curves, which indicate an early Maastrichtian cooling (Cramer et al., 2009; Friedrich et al., 2012) and possible link to glaciation during that time (Miller et al., 1999).

In terms of Late Cretaceous paleoceanography of the seaway, Miller and Bell (1989) suggested that a lack of Boreal affinity of foraminifera within the Albian to Santonian of the Labrador margin indicated that a connection only with the Atlantic was probable at that time; however, this interpretation conflicts with evidence from Cenomanian–Turonian to Maastrichtian ammonite faunas from onshore Nuussuaq Basin. The fauna are similar to coeval assemblages from the Western Interior Seaway of North America, suggesting a marine connection between these areas either through the Arctic Ocean, the Hudson Seaway, or over the Canadian Shield, possibly in the vicinity of the James Bay Lowlands (Birkelund, 1965; Jeletzky, 1971; Williams and Stelck, 1975; White et al., 2000; Schröder-Adams, 2014). For the late Late Cretaceous, however, there is more of a paleoceanographic consensus. Teichert *in* Ruedemann and Balk (1939) postulated a connection between Baffin Bay and the Western Interior Seaway of North America during the Campanian. This is consistent with the presence of Campanian–Maastrichtian ammonites from West Greenland that show affinities with coeval assemblages from the Western Interior Seaway and the Atlantic, but also with North Pacific forms, suggesting that all three areas were connected by marine waters (Williams and Stelck, 1975). A connection between the Atlantic and Arctic oceans in the Campanian–Maastrichtian is further supported by the presence of specific planktonic foraminifera in Nuussuaq Basin shale beds (Gradstein and Srivastava, 1980). Dinocysts from samples along western Baffin Bay also support this connection, based on the presence of forms from both the Williams (warm-temperate) and McIntyre (Boreal) suites (MacLean et al., 1990, 2014), but this connection could have existed as early as the Coniacian–Santonian. A Campanian marine linkage is also indicated beyond the present study region in the Greenland–Norwegian Seaway where Radmacher et al. (2020) proposed a connection through the Hudson Seaway based on model simulations and integration with palynological data.

Cenozoic

Global climate fluctuations during the Cenozoic have been well established through oxygen-isotope curves, which reveal a continuous shift through time between ice-free conditions and extreme cold (Zachos et al., 2001), and these changing conditions are reflected in the microfossil record. The use of dinocysts in assessing Paleogene paleoclimates has made significant advances in recent years (Williams and Bujak, 1977b; Jaramillo and Oboh-Ikuenobe, 1999; Sluijs et al., 2005, 2006, 2008; Sluijs and Brinkhuis, 2009). These studies have focused on lower latitude assemblages, but higher latitude taxa also show significant changes. One such genus is *Trithyrodinium*, which is common to abundant in the Danian of several Labrador Shelf wells (Fig. 3; Nøhr-Hansen et al., 2016), particularly the species *Trithyrodinium evittii*, which is periodically abundant in the Danian of the Nuussuaq Basin (Fig. 3; Nøhr-Hansen and Dam, 1997, 1999; Nøhr-Hansen et al., 2002). Lentin and Williams (1980) included this taxon in the Williams suite, but established their suites based on occurrences solely in the Campanian. According to Smit and Brinkhuis (1996) and Nøhr-Hansen and Dam (1997, 1999), *Trithyrodinium evittii* favoured lower latitudes in the Late Cretaceous, but migrated later to higher latitudes, perhaps because of warmer water conditions in the Early Paleocene. Previous studies have confirmed this abundance at higher latitudes during this time (Nøhr-Hansen et al., 2002; Willumsen and Vajda, 2010; Bowman et al., 2012). In support of this, Gradstein and Srivastava (1980) considered that foraminifera implied temperate (warmer) conditions in the Labrador Sea region during the Danian.

At about 55.5 Ma, increased carbon in the atmosphere led to a rapid increase in global temperatures and an event known as the Paleocene–Eocene Thermal Maximum (PETM; Kennett and Stott, 1991; Koch et al., 1992; Zachos et al., 2008; Moran, 2009; Schaller, 2015). The effect of the Paleocene–Eocene Thermal Maximum warming episode in the seaway is reflected by the presence of diverse calcareous nannofossils in the Kangâmiut-1 well (Sheldon, 2003), microfossils that are also latitudinally dependent. Additional evidence for this warm episode is the abundant occurrences of species of the dinocyst *Apectodinium*, especially *Apectodinium homomorphum*, close to the Paleocene–Eocene boundary in a number of wells in the Labrador–Baffin Seaway (Fig. 3; Nøhr-Hansen et al., 2016). Bujak and Brinkhuis (1998) postulated that *Apectodinium homomorphum* was a warmer water species and their findings were confirmed by stable isotope studies and biogeochemical paleotemperature indicators (Sluijs et al., 2006; Zachos et al., 2006; Schoon et al., 2013). The earliest appearance of *Apectodinium*-dominated assemblages appears to be synchronous worldwide (Crouch et al., 2001), with one peak equating with the Paleocene–Eocene Thermal Maximum. Accordingly, the *Apectodinium* influx represents higher sea-surface temperatures, with a significant increase in productivity in marginal marine, surface-water settings (Crouch et al., 2001). In the Labrador–Baffin Seaway, there is a marked decline in *Apectodinium* abundances at the end of the Paleocene–Eocene Thermal Maximum (Nøhr-Hansen et al., 2016), a trend noted elsewhere (Iakovleva et al., 2001; Crouch et al., 2003; Sluijs et al., 2008); presumably this reflects a reduction in sea-surface temperature.

The global Paleocene–Eocene Thermal Maximum climatic peak is succeeded by climatic fluctuations, tropical in the Early Eocene during the Eocene Thermal Maximum 2 and the Early Eocene Climatic Optimum, generally warmer, but not tropical in the Middle Eocene, and somewhat cooler in the Late Eocene (Sluijs et al., 2008; Zachos et al., 2008; Schoon et al., 2013). Dinocyst taxa known to be warmer water indicators, such as *Apectodinium homomorphum, Axiodinium augustum, Homotryblium abbreviatum*, and *Homotryblium tenuispinosum,* are found in the Ypresian in several Labrador Shelf wells (Fig. 3; Nøhr-Hansen et al., 2016). *Homotryblium* is noted most frequently in restricted environments, such as inshore lagoonal settings with increased salinity (Brinkhuis, 1992, 1994; de Verteuil and Norris, 1996; Dybkjær, 2004). Elements of the fern *Azolla* are found at the top of the Ypresian in some wells (Fig. 3; Nøhr-Hansen et al., 2016), suggesting that the Labrador–Baffin Seaway was warm, but humid, during the Ypresian and Lutetian (Nøhr-Hansen et al., 2016). These ferns are freshwater to brackish-water forms (van Kempen et al., 2012), and modern examples are found in comparatively warmer waters than that of the present-day Labrador–Baffin Seaway (Nøhr-Hansen et al., 2016). Brinkhuis et al. (2006) suggested that Ypresian *Azolla* found in the Labrador–Baffin Seaway were likely derived from freshwater overspill from the Arctic Ocean, based on the presence of specimens of the fern found at the Lomonosov Ridge. Nøhr-Hansen et al. (2016), however, subsequently suggested that establishment of these ferns in surface waters within such a large oceanic body of water was quite unlikely, and that specimens found in the Labrador–Baffin Seaway were more likely to have been derived from large rivers draining into the seaway at that time. Planktonic foraminifera in the Labrador–Baffin Seaway also indicate warm temperate conditions in the Early–Middle Eocene (Gradstein and Srivastava, 1980). The disappearance, however, of *Homotryblium* species in the Middle Eocene (Fig. 3), and their absence from younger rocks in the seaway, support a climatic cooling, further suggested by a decline in dinocyst diversity along the Labrador margin at this time (Nøhr-Hansen et al., 2016). In general, diversity and abundance of dinocysts continued to decline throughout the rest of the Cenozoic (Nøhr-Hansen et al., 2016), possibly reflecting the global transition from a greenhouse to an icehouse world (Zachos et al., 2001, 2008).

Other evidence for climatic conditions in the Eocene–Oligocene can be gleaned from the strata of ODP Site 647A in the southern Labrador Sea, just outside of the present study region. Head and Norris (1989) concluded that there was evidence for a proto-Gulf Stream at this locality in the Middle Eocene, based on the presence of dinocyst taxa known previously only from the southwestern Atlantic, eastern United States, Norwegian Sea, Belgium, and Australia. Head and Norris (1989) suggested that the best explanation for this distribution is that it mirrors the northward circulation of oceanic currents bringing warmer waters from the proto-North Atlantic at that time; however, these authors further noted an influx of colder water taxa, including *Gelatia inflata* and *Svalbardella* (e.g. Śliwińska, 2019) into the southern Labrador Sea region in the Late Eocene–Oligocene. These taxa presumably indicate a cooling trend, consistent with the global climate trend recognized by Zachos et al. (2001).

A decline in angiosperm pollen species in samples from the Labrador–Baffin Seaway correlates with the general drop in dinocyst species richness in the Oligocene–Neogene (Williams, 1986), but conifer pollen, primarily *Pinuspollenites*, is common in the Neogene (Nøhr-Hansen et al., 2016), reflecting well developed coniferous forests onshore. There seems to have been widespread cooling in the Labrador–Baffin Seaway during most of the Neogene, partly reflecting oceanic circulation patterns. A common taxon found in ODP Site 646 is *Impagidinium pallidum* (Head et al., 1989b), which is restricted primarily to higher latitudes such as the Arctic (Zonneveld et al., 2013). Species of *Impagidinium* are also common in ODP Site 645E (Head et al., 1989a; Dafoe and Williams, 2020c). Head et al. (1989a, b) recorded taxa with high-latitude North Atlantic affinities, especially in ODP Site 646, and considered these Early to Middle Miocene dinocyst assemblages to indicate temperate to cool surface waters with circulation patterns in Baffin Bay similar to today, possibly including development of a proto-East Greenland Current. As far back as the Middle Miocene, poleward geostrophic currents were operating in Baffin Bay during deposition of unit C, as suggested by Knutz et al. (2015).

The Middle and Upper Miocene succession in ODP Site 645E shows another marked drop in dinocyst species richness, although some remaining forms still possess North Atlantic affinities, indicating continued temperate to cool surface waters (Head et al., 1989a). The mixing of Arctic and Atlantic water masses is even more prevalent as shown by dinocyst assemblages during this time in ODP Site 646, further indicating temperate to cool surface waters in the southern portion of the Labrador–Baffin Seaway (Head et al., 1989b). Supporting evidence includes the presence of the dinocyst *Dapsilidinium pastielsii* (or the related *Dapsilidinium pseudocolligerum*) in the Middle to Late Miocene (Fig. 3; Head et al., 1989a, b). Head and Westphal (1999) found this form to be a warm-temperate species present at much lower latitudes. Assessing foraminifera, however, Kaminski et al. (1989) reported only boreal benthic species in the Middle Miocene of ODP Site 645. Piasecki (2003) also described a mix of North Atlantic and high-latitude dinocysts in the Neogene of the Qulleq-1 well on the West Greenland margin, with warmer water species in Serravallian strata presumably becoming established following the mid-Miocene Climatic Optimum, around 17 to 15 Ma (Zachos et al., 2001).

The mid-Miocene Climatic Optimum was followed by gradual cooling and a re-establishment of ice-sheets in the Antarctic and Arctic (Zachos et al., 2001), with a shift to a cooler climate in the Labrador–Baffin Seaway. Based on lithological analyses of ODP Site 645, Srivastava et al. (1987) suggested that seasonal sea ice began forming as early as 8 Ma (within the Late Miocene), and Head et al. (1989a) arrived at a similar time frame based on palynology and sedimentation rates (9.5–7.4 Ma). Dafoe and Williams (2020c) further suggested that based on evidence in the same corehole, ice rafting began as early as the latest Serravallian based on reported depths of ice-rafted clasts (e.g. Srivastava et al., 1987) and their revised biostratigraphic age constraints. Compared to the Miocene, depleted dinocyst assemblages in the Pliocene of the Qulleq-1 well also indicate a change to cooler climatic conditions (Piasecki, 2003). Similarly, calcareous microfossil data show a general southward migration of warm-temperate foraminifera near the Miocene–Pliocene boundary (Gradstein et al., 1990), especially in ODP Site 646 (Aksu and Kaminski, 1989). Head and Westphal (1999) attributed the decline of *Dapsilidinium pastielsii* in the latest Miocene to Pliocene, such as in ODP Site 646, to the cooling of the North Atlantic and the development of the cold Labrador Current. Gradstein and Srivastava (1980) also postulated a reversal in ocean circulation from the Arctic to Atlantic, forming the Labrador Current. In addition to geostrophic currents in the Late Miocene to Pliocene (during deposition of unit B), Knutz et al. (2015) indicated that ocean-bottom currents were active, resulting in development of significant contourite drift accumulations.

The Pliocene was marked by a subtle warming from about 3.3 to 3.0 Ma, and this was especially notable in mid- to high latitudes; this warming was a result of greenhouse forcing and a change in ocean heat transport (Zachos et al., 2001; Dowsett et al., 2005). Based on current-induced deposition in the Labrador–Baffin Seaway, water-mass circulation via intense geostrophic currents through Baffin Bay may have added to warming during the Pliocene (Knutz et al., 2015). Reflecting this warming, tropical planktonic foraminifera have been documented in the southern Labrador Sea until about the Middle Pliocene, when they were replaced by subpolar forms (Gradstein et al., 1990). Similarly, in the Pliocene and Pleistocene of ODP Site 646 and Site 647, de Vernal and Mudie (1989b) noted a few warm-temperate indicators (*Impagidinium* and *Polyspaeridium zoharyi*), implying northward advection of warm surface-water currents (North Atlantic Drift) into the southern Labrador Sea, but otherwise the dinocysts were dominated by boreal forms. In contrast, planktonic foraminifera and the presence of ice-rafted detritus in ODP Site 646 argue against significant Pliocene warming (Dowsett and Poore, 1991). The waning influence of the Gulf Stream in the Middle–Late Pliocene (Poore and Berggren, 1974) may have been a contributing factor in this region.

Evidence for significant amounts of land-based ice approximately corresponds to the Pliocene–Pleistocene boundary (around 2.5 Ma). Within ODP Site 645, the onset of ice rafting may date back to the latest Serravallian (Dafoe and Williams, 2020c) within unit IIIA; however, enhanced ice-rafting at the base of unit II (Srivastava et al., 1987) occurred in the Early Pliocene (Dafoe and Williams, 2020c) and appears to demarcate a change to major continental glaciation. Also at this site, a well established boreal palynomorph assemblage dominated by the acritarch *Cymatiosphaera* (Fig. 3) and peridiniacean dinocysts occurs in the upper Pliocene to lowest Pleistocene strata, but in the late Early Pleistocene to Holocene the marine palynoflora are depauperate, indicating cold, dry, high-arctic conditions except for brief interglacial episodes (de Vernal and Mudie, 1989a). To the south, in ODP Site 646 and Site 647, de Vernal and Mudie (1989b) indicated that dinocysts and acritarchs in the Pliocene suggest high primary productivity, but this decreased in the Pliocene–early Pleistocene, marking a change from cool-temperate to subarctic conditions. Following the Middle Pliocene in the southern Labrador Sea, subpolar planktonic foraminifera took over (Gradstein et al., 1990) and polar faunas and floras with low species diversity were well established in ODP Site 646 by the Pleistocene (Aksu and Kaminski, 1989). Benthic foraminifera with Arctic affinities first appeared in ODP Site 646 in the Early Pleistocene, but based on a change in species composition, Kaminski et al. (1989) noted a switch from preglacial to glacial conditions in the Pliocene. Clinoforms developed in the Pliocene in Baffin Bay likely formed during the onset of trough-mouth fan development and early glacial advances as geostrophic currents began to decline (Knutz et al., 2015, 2019). Onshore, in the Late Pliocene to Pleistocene, coniferous, boreal forest, and forest tundra surrounded Baffin Bay during cool-temperate to subarctic climatic conditions (de Vernal and Mudie, 1989a). Farther south, near ODP Site 646 and Site 647, cool-temperate and temperate forests were replaced by coniferous boreal forests in the Late Pliocene as glaciation became well established (de Vernal and Mudie, 1989b).

CONCLUSIONS

The Labrador–Baffin Seaway is characterized by a lithologically and paleontologically diverse stratigraphic succession, reflecting a great variety of changing depositional environments and evolving plant communities from late Early Cretaceous through Cenozoic. The history of deposition in the basin is informed by numerous offshore wells and an extensive network of seismic data, and supplemented by coreholes and seabed samples, as well as onshore exposures of correlative strata. Synthesizing data sets from conjugate margins of the seaway provides a unique view of the geological evolution of the region.

Palynological events identified within the Labrador–Baffin Seaway provide a robust biostratigraphic framework, with the Campanian to Rupelian possessing the richest assemblages and the greatest number of palynoevents. Barremian–Aptian strata are the oldest rocks sampled in the region and the late Neogene section is the least constrained interval. The age framework provided by the palynoevents allows for construction and comparison of lithostratigraphic columns for conjugate margins that are tied to the regional seismic-stratigraphic framework, comprising units H (pre-rift basement) to A, with intervening horizons H1 through A1.

The mostly Lower Cretaceous unit G, is sandstone dominated, with local basalt flows and sills and it is known from the Labrador Shelf, Cumberland Basin, onshore exposures on Bylot and Baffin islands, the Nuuk Basin, and northeast Baffin Bay (Fig. 4; *see* Fig. 3 in Gregersen et al., this volume). These strata were deposited in nonmarine fluvial, alluvial, and lacustrine settings, becoming shallow marine in the upper part of the section. The G1 horizon appears to represent an unconformity along the Canadian margin, but is more conformable along the West Greenland margin, except over highs. In contrast to the sandstone beds of unit G, the overlying Upper Cretaceous to Lower–Middle Paleocene unit F includes shelfal and distal marine shale deposits associated with a significant regional transgression; however, Early Paleocene shallowing is evident especially in proximal regions, with some renewed sandstone development at the top of unit F. Horizon F1 of about Middle Paleocene age is locally unconformable on the Labrador margin and in Canadian onshore exposures, but forms a major stratigraphic break along the West Greenland margin, and is demarcated by vast incised valleys in the Nuussuaq Basin, all reflecting the onset of regressive conditions. The seaward extent of Cretaceous rocks lies near the landward limit of oceanic crust, and in proximal regions, these units onlap the basement platform and may be absent over prominent basement highs. Their true extent may be masked by thick volcanic cover, especially in Davis Strait and southeastern Baffin Bay. Growth faulting is associated with deposition of the Lower Cretaceous unit G, but the Upper Cretaceous to Middle Paleocene unit F is generally more seismically transparent than unit D, draping structures in the Labrador Sea and generally confined to grabens and half-grabens in Baffin Bay.

The lower Cenozoic section is composed of units E and D, which are Selandian through Middle Miocene and blanket much of the region, except for the most prominent basement and volcanic highs. Basalt flows of unit E are correlated with the arrival of a mantle plume in Davis Strait, the onset of regional seafloor spreading, and formation of magma-rich margins. The overall depositional setting in the Middle to Late Paleocene is nonmarine to shallow marine, suggesting a regional regressive phase. A significant marine transgression ensued in the Early Eocene. Later in the Eocene, local deltaic settings were established in the Labrador–Baffin Seaway region, although more distal shelf to bathyal settings are recorded in wells along the Labrador Shelf until the later part of the Middle Eocene. The lower Cenozoic interval shows variable thickness across the region, with the thickest strata below the Labrador Shelf, within the extinct spreading axis and major fracture zones, locally in Davis Strait, and in the Melville Bay Graben. The E1 horizon represents a flooding event on the Labrador margin, but appears to be an unconformity on the West Greenland margin. The D1 horizon is unconformable below a major clinoform succession along the Labrador margin, and correlates with significant missing section along West Greenland.

After the Middle Miocene, the Upper Cenozoic section is divided into three intervals: C, B, and A. During that time, several major clinoform systems prograded across both margins, resulting in build up of the present-day shelves. The timing of some of these progradational episodes is less clear, making direct correlations difficult. Much like lower Cenozoic strata, the upper Cenozoic interval blankets the region, except for a few basement promontories. Locally, the upper Cenozoic section can be subdivided, but often only a single interval is mapped. In Baffin Bay, the upper Cenozoic package is exceptionally thick, especially over northern Baffin Basin and the West Greenland outer shelf. The unit is of more moderate thickness in the Labrador Sea, and is generally thin in Davis Strait. Global sea-level fall and paleoceanographic currents were likely driving some of this sedimentation, with glacial processes dominant in the Pliocene–Pleistocene.

A lack of marine fossils in the Lower Cretaceous of the Labrador–Baffin Seaway precludes detailed paleoclimate analyses, but clay mineralogy and onshore floras suggest humid, warm-temperate conditions. Dinocysts indicate a cooling into the early Late Cretaceous of the seaway that may have continued into the Coniacian–Santonian to Campanian, although global paleoclimate studies suggest warming in the early Late Cretaceous. Some warm-temperate episodes in the Campanian are suggested by both dinocyst and foraminiferal assemblages, with a return to cooler conditions in the Maastrichtian indicated by dinocyst suites and global oxygen-isotope curves. There is some disagreement regarding ties to the Arctic Ocean in the late Early to early Late Cretaceous, but this connection appears to have been well established by the Campanian, based on ammonites, dinocysts, and planktonic foraminifera.

Dinocysts, foraminifera, and macrofossils all suggest warmer sea-surface temperatures in the Danian. Warm conditions peaked at the Paleocene–Eocene Thermal Maximum based on the dinocyst *Apectodinium*. The Eocene Thermal Maximum 2 and Early Eocene Climatic Optimum appear to be recognized in the seaway, based on dinocyst assemblages, and the presence of *Azolla* indicates warm conditions during the Ypresian–Lutetian. Dinocyst diversity declines in the Middle Eocene, indicating a subsequent cooling, which is also mirrored in the presence of cold-water foraminifera during the Late Eocene–Oligocene. Cooling continued into the Neogene, and dinocysts in the Early–Middle Miocene indicate that circulation patterns in Baffin Bay may have been similar to those of the present day. Temperate to cool surface waters continued into the Middle–Late Miocene, but the presence of some dinocysts and foraminifera of North Atlantic affinity may equate with the mid-Miocene Climatic Optimum. In the Pliocene, dinocysts show a marked decline, and warm-temperate calcareous microfossils migrated southward, potentially linked with development of geostrophic currents like the Labrador Current. The Pliocene warming from 3.3 to 3.0 Ma is not as apparent in the Labrador–Baffin Seaway fossil record as elsewhere, except for the presence of a few warmer water foraminifera and dinocysts. Continental glaciation was well established by the Pleistocene, evidenced by ice-rafted detritus, changes in dinocyst, acritarch, and foraminiferal assemblages, and thick accumulations of trough-mouth fan deposits.

ACKNOWLEDGMENTS

The authors would like to acknowledge support of this work through the Baffin Island and the Labrador–Baffin Seaway Geological Synthesis activity under the Geo-mapping for Energy and Minerals program (GEM-2). The authors thank the Federal Institute for Geosciences and Natural Resources (Hannover), the Geological Survey of Denmark and Greenland (GEUS), ION Geophysical, NRCan, Spectrumgeo, and TGS for allowing us to show the seismic data. The authors further acknowledge the use of Canada Cities Services and Suncor data in seismic compilations. Thanks to R. Fensome and D. Piper for their thoughtful reviews of an earlier draft. A special thanks to Leith MacLeod for design and compilation of the maps. Also thanks to Paul Champagne for his work drafting the merged seismic profiles to form the conjugate margin sections.

REFERENCES

Ainsworth, N.R., Riley, L.A., Bailey, H.W., and Gueinn, K.J., 2014. Cretaceous–Tertiary stratigraphy of the Labrador Shelf; Riley Geoscience Ltd.; on file with the Canada–Newfoundland and Labrador Offshore Petroleum Board, St. John's, Newfoundland and Labrador, 56 p.

Ainsworth, N.R., Riley, L.A., Bailey, H.W., and Gueinn, K.J., 2016. Cretaceous–Tertiary stratigraphy of the Labrador Shelf; Riley Geoscience Ltd.; on file with the Canada–Newfoundland and Labrador Offshore Petroleum Board, St. John's, Newfoundland and Labrador, 31 p.

Aksu, A.E. and Kaminski, M.A., 1989. Neogene and Quaternary planktonic foraminifer biostratigraphy and biochronology in Baffin Bay and the Labrador Sea; *in* Proceedings of the Ocean Drilling Program: Scientific Results, v. 105, p. 287–304.

Armstrong, H.A. and Brasier, M.D., 2005. Microfossils; Blackwell Publishing, Oxford, United Kingdom, 296 p. (second edition).

Atkinson, E.A., Fustic, M., Hanna, M.C., and Lister, C.J., 2017. Qualitative assessment of petroleum potential in Lancaster Sound region, Nunavut; Geological Survey of Canada, Open File 8297, 18 p. https://doi.org/10.4095/305321

Balkwill, H.R., 1987. Labrador basin: structural and stratigraphic style; *in* Sedimentary Basins and Basin-Forming Mechanisms, (ed.) C. Beaumont and A.J. Tankard; Canadian Society of Petroleum Geologists, Memoir, v. 12, p. 17–43.

Balkwill, H.R. and McMillan, N.J., 1990. Mesozoic-Cenozoic geology of the Labrador Shelf; *in* Chapter 7 of Geology of the Continental Margin of Eastern Canada, (ed.) M.J. Keen and G.L. Williams; Geological Survey of Canada, Geology of Canada, no. 2, p. 295–324 (*also* Geological Society of America, The Geology of North America, v. I-1, p. 295–324). https://doi.org/10.4095/132708

Bell, J.S. (co-ord.), 1989. Labrador Sea / Mer du Labrador; Geological Survey of Canada, East Coast Basin Atlas Series, 135 p. https://doi.org/10.4095/127152

Benham, P.H., 1991. Stratigraphy and palynology of Cretaceous and Tertiary rocks, North Bylot Trough, Bylot Island, Northwest Territories, Canada; M.Sc. thesis, Memorial University of Newfoundland, St. John's, Newfoundland and Labrador, 361 p.

Benham, P.H. and Burden, E.T., 1990. Stratigraphy of Cretaceous–Tertiary rocks of North Bylot Trough, Bylot Island, N.W.T.; *in* Current Research, Part D; Geological Survey of Canada, Paper 90-1D, p. 179–185.

Bingham-Koslowski, N., 2018. Descriptions of drill-cores and thin sections from lower Paleozoic strata, southeastern Baffin Island shelf, Nunavut; Geological Survey of Canada, Open File 8409, 78 p. https://doi.org/10.4095/308354

Bingham-Koslowski, N., 2019. Descriptions of Paleozoic cores and thin sections from the Gudrid H-55, Roberval K-92, Indian Harbour M-52, and Freydis B-87 wells, offshore Labrador (Newfoundland and Labrador); Geological Survey of Canada, Open File 8543, 142 p. https://doi.org/10.4095/313573

Bingham-Koslowski, N., Miller, M.A., McCartney, T., and Carey, J.S., 2019. Revised biostratigraphic and thermal alteration interpretations for the Paleozoic of the Hopedale Basin, offshore Labrador, Canada; Bulletin of Canadian Petroleum Geology, v. 67, p. 185–213.

Bint, A.N., 1986. Fossil ceratiaceae: a restudy and new taxa from the mid-Cretaceous of the western interior, U.S.A.; Palynology, v. 10, no. 1, p. 135–180. https://doi.org/10.1080/01916122.1986.9989307

Birkelund, T., 1965. Ammonites from the Upper Cretaceous of West Greenland; Meddelelser om Grønland, v. 179, no. 7, 192 p.

Bowman, V.E., Francis, J.E., Riding, J.B., Hunter, S.J., and Haywood, A.M., 2012. A latest Cretaceous to earliest Paleogene dinoflagellate cyst zonation from Antarctica, and implications for phytoprovincialism in the high latitudes; Review of Palaeobotany and Palynology, v. 171, p. 40–56. https://doi.org/10.1016/j.revpalbo.2011.11.004

Brent, T.A., Chen, Z., Currie, L.D., and Osadetz, K., 2013. Assessment of the conventional petroleum resource potential of Mesozoic and younger structural plays within the proposed National Marine Conservation Area, Lancaster Sound, Nunavut; Geological Survey of Canada, Open File 6954, 44 p. https://doi.org/10.4095/289615

Brinkhuis, H., 1992. Late Eocene to early Oligocene dinoflagellate cysts from central and northeast Italy; Ph.D. thesis, University of Utrecht, Utrecht, The Netherlands, 169 p.

Brinkhuis, H., 1994. Late Eocene to early Oligocene dinoflagellate cysts from the Priabonian type-area (Northeast Italy): biostratigraphy and paleoenvironmental interpretation; Palaeogeography, Palaeoclimatology, Palaeoecology, v. 107,no. 1-2,p. 121–163.https://doi.org/10.1016/0031-0182(94)90168-6

Brinkhuis, H., Schouten, S., Collinson, M.E., Sluijs, A., Sinninghe-Damste, J.S., Dickens, G.R., Huber, M., Cronin, T.M., Onodera, J., Takahashi, K., Bujak, J.P., Stein, R., van der Burgh, J., Eldrett, J.S., Harding, I.C., Lotter, A.F., Sangiorgi, F., van Konijnenburg-van Cittert, H., de Leeuw, J.W., and the Expedition 302 Scientists, 2006. Episodic fresh surface waters in the early Eocene Arctic Ocean; Nature, v. 441, no. 7093, p. 606–609. https://doi.org/10.1038/nature04692

Bujak, J.P. and Brinkhuis, H., 1998. Global warming and dinocyst changes across the Paleocene/Eocene epoch boundary; *in* Late Paleocene–early Eocene Climatic and Biotic Events in the Marine and Terrestrial Records, (ed.) M.-P. Aubry, S.G. Lucas, and W.A. Berggren; Columbia University Press, New York, New York, p. 277–295.

Bujak Davies Group, 1989. Biostratigraphy and Maturation of 17 Labrador and Baffin Shelf wells, volume 1: scope, methodology, format and recommendations; Geological Survey of Canada, Open File 1929, 92 p. https://doi.org/10.4095/130622

Burden, E.T. and Langille, A.B., 1990. Stratigraphy and sedimentology of Cretaceous and Paleocene strata in half-grabens on the southeast coast of Baffin Island, Northwest Territories; Bulletin of Canadian Petroleum Geology, v. 38, p. 185–196.

Burden, E.T. and Langille, A.B., 1991. Palynology of Cretaceous and Tertiary strata, northeast Baffin Island, Northwest Territories, Canada: implications for the history of rifting in Baffin Bay; Palynology, v. 15, p. 91–114. https://doi.org/10.1080/01916122.1991.9989392

Chalmers, J.A., 1997. The continental margin off southern Greenland: along-strike transition from an amagmatic to a volcanic margin; Journal of the Geological Society, v. 154, p. 571–576. https://doi.org/10.1144/gsjgs.154.3.0571

Chalmers, J.A. and Pulvertaft, T.C.R., 2001. Development of the continental margins of the Labrador Sea: a review; *in* Non-Volcanic Rifting of Continental Margins: A Comparison of Evidence from Land and Sea, (ed.) R.C.L. Wilson, R.B. Whitmarsh, B. Taylor, and N. Froitzhelm; Geological Society, London, Special Publications 187, p. 77–105. https://doi.org/10.1144/GSL.SP.2001.187.01.05

Chalmers, J.A., Pulvertaft, T.C.R., Christiansen, F.G., Larsen, H.C., Laursen, K.H., and Ottesen, T.G., 1993. The southern West Greenland continental margin: rifting history, basin development, and petroleum potential; *in* Petroleum Geology of NW Europe: Proceedings of the 4th Conference, (ed.) J.R. Parker; March 29–April 1, 1992, London, United Kingdom; Geological Society, London, United Kingdom, p. 915–931.

Chalmers, J.A., Pulvertaft, T.C.R., Marcussen, C., and Pedersen, A.K., 1999. New insight into the structure of the Nuussuaq Basin, central West Greenland; Marine and Petroleum Geology, v. 16, p. 197–224. https://doi.org/10.1016/S0264-8172(98)00077-4

Chauvet, F., Geoffrey, L., Guillou, H., Maury, R.C., Le Gall, B., Agranier, A., and Viana, A., 2019. Eocene continental breakup in Baffin Bay; Tectonophysics, v. 757, p. 170–186. https://doi.org/10.1016/j.tecto.2019.03.003

Chian, D., Louden, K.E., and Reid, I., 1995a. Crustal structure of the Labrador Sea conjugate margin and implications for the formation of nonvolcanic continental margins; Journal of Geophysical Research, v. 100, no. B12, p. 24239–24253. https://doi.org/10.1029/95JB02162

Chian, D., Keen, C., Reid, I., and Louden, K.E., 1995b. Evolution of nonvolcanic rifted margins: new results from the conjugate margins of the Labrador Sea; Geology, v. 23, p. 589–592. https://doi.org/10.1130/0091-7613(1995)023%3c0589:EONRMN%3e2.3.CO%3b2

Christiansen, F.G., Boesen, A., Bojesen-Koefoed, J.A., Chalmers, J.A., Dalhoff, F., Dam, G., Hjortkær, B.F., Kristensen, L., Larsen, L.M., Marcussen, C., Mathiesen, A., Nøhr-Hansen, H., Pedersen, A.K., Pedersen, G.K., Pulvertaft, T.C.R., and Sønderholm, M., 1999. Petroleum geological activities in West Greenland in 1998; Geology of Greenland Survey Bulletin, v. 183, p. 46–56. https://doi.org/10.34194/ggub.v183.5204

Christiansen, F.G., Bojesen-Koefoed, J.A., Chalmers, J.A., Dalhoff, F., Mathiesen, A., Sønderholm, M., Dam, G., Gregersen, U., Marcussen, C., Nøhr-Hansen, H., Piasecki, S., Preuss, T., Pulvertaft, T.C.R., Rasmussen, J.A., and Sheldon, E., 2001. Petroleum geological activities in West Greenland in 2000; Geology of Greenland Survey Bulletin, v. 189, p. 24–33. https://doi.org/10.34194/ggub.v189.5150

Clarke, D.B. and Pedersen, A.K., 1976. Tertiary volcanic province of West Greenland; *in* Geology of Greenland, (ed.) A. Esher and W.S. Watt; Geological Survey of Greenland, Copenhagen, Denmark, p. 364–385.

Clarke, D.B. and Upton, B.G.J., 1971. Tertiary basalts of Baffin Island: field relations and tectonic setting; Canadian Journal of Earth Sciences, v. 8, p. 248–258. https://doi.org/10.1139/e71-025

Cramer, B.S., Toggweiler, J.R., Wright, J.D., Katz, M.E., and Miller, K.G., 2009. Ocean overturning since the Late Cretaceous: inferences from a new benthic foraminiferal isotope compilation; Paleoceanography, v. 24, no. 4, cit. no. PA4216. https://doi.org/10.1029/2008PA001683

Cremer, M., 1989. Texture and microstructure of Neogene–Quaternary sediments, ODP Sites 645 and 646, Baffin Bay and Labrador Sea; *in* Proceedings of the Ocean Drilling Program, Scientific Results, v. 105, p. 7–20.

Crouch, E.M., Heilmann-Clausen, C., Brinkhuis, H., Morgans, H.E.G., Rogers, K.M., Egger, H., and Schmitz, B., 2001. Global dinoflagellate event associated with the late Paleocene thermal maximum; Geology, v. 29, no. 4, p. 315–318. https://doi.org/10.1130/0091-7613(2001)029%3c0315:GDEAWT%3e2.0.CO%3b2

Crouch, E.M., Dickens, G.R., Brinkhuis, H., Aubry, M.-P., Hollis, C.J., Rogers, K.M., and Visscher, H., 2003. The *Apectodinium* acme and terrestrial discharge during the Paleocene–Eocene thermal maximum: new palynological, geochemical and calcareous nannoplankton observations at Tawanui, New Zealand; Palaeogeography, Palaeoclimatology, Palaeoecology, v. 194, p. 387–403. https://doi.org/10.1016/S0031-0182(03)00334-1

Dafoe, L.T., 2021. Paleoenvironmental analyses and revised lithostratigraphic assignments for 28 wells of the Hopedale and Saglek basins, offshore eastern Canada; Geological Survey of Canada, Open File 8810, 209 p. https://doi.org/10.4095/328477

Dafoe, L.T. and Williams, G.L., 2020a. Lithological, sedimentological, ichnological, and palynological analysis of 37 conventional core intervals from 15 wells, offshore Labrador (Newfoundland and Labrador) and southeast Baffin Island (Nunavut); Geological Survey of Canada, Bulletin 613, 146 p. https://doi.org/10.4095/315362

Dafoe, L.T. and Williams, G.L., 2020b. Palynological analysis of the two Labrador Shelf wells, Petro-Canada et al. North Leif I-05 and Total Eastcan et al. Skolp E-07, offshore eastern Canada: new age, paleoenvironmental and lithostratigraphic interpretations; Geological Survey of Canada, Open File 8670, 103 p. https://doi.org/10.4095/321502

Dafoe, L.T. and Williams, G.L., 2020c. Palynostratigraphic and integrated paleoenvironmental assessment of the ODP Site 645 corehole in Baffin Bay, offshore Nunavut; Geological Survey of Canada, Open File 8701, 61 p. https://doi.org/10.4095/321736

Dafoe, L.T. and Williams, G.L., 2020d. A reassessment of Mesozoic–Cenozoic seabed samples of bedrock from the western Davis Strait and eastern Baffin Island margin, offshore Nunavut: new insights into their lithology, age, and paleoenvironment of deposition; Geological Survey of Canada, Open File 8702, 41 p. https://doi.org/10.4095/321758

Dafoe, L.T., Haggart, J., Williams, G., and Stimson, M., 2019. Ichnology and paleoenvironmental interpretations of the Cretaceous—Paleocene rift succession of northeast Baffin Island region, Nunavut, Canada; AAPG Datapages, Search and Discovery Article no. 90350, 2 p. (abstract).

Dalhoff, F., Chalmers, J.A., Gregersen, U., Nøhr-Hansen, H., Rasmussen, J.A., and Sheldon, E., 2003. Mapping and facies analysis of Paleocene–mid-Eocene seismic sequences, offshore southern West Greenland; Marine and Petroleum Geology, v. 20, p. 935–986. https://doi.org/10.1016/j.marpetgeo.2003.09.004

Dalhoff, F., Larsen, L.M., Ineson, J.R., Stouge, S., Bojesen-Koefoed, J.A., Lassen, S., Kuijpers, A., Rasmussen, J.A., and Nøhr-Hansen, H., 2006. Continental crust in the Davis Strait: new evidence from seabed sampling; Geological Survey of Denmark and Greenland Bulletin, v. 10, p. 33–36. https://doi.org/10.34194/geusb.v10.4901

Dam, G. and Sønderholm, M., 2021. Tectonostratigraphic evolution, palaeogeography and main petroleum plays of the Nuussuaq Basin: an outcrop analogue for the Cretaceous–Palaeogene rift basins offshore West Greenland; Marine and Petroleum Geology, v. 129, p. 1–33. https://doi.org/10.1016/j.marpetgeo.2021.105047

Dam, G., Larsen, M., and Sønderholm, M., 1998a. Sedimentary response to mantle plumes: implications from Palaeocene onshore successions, West and East Greenland; Geology, v. 26, p. 207–210. https://doi.org/10.1130/0091-7613(1998)026%3c0207:SRTMPI%3e2.3.CO%3b2

Dam, G., Nøhr-Hansen, H., Christiansen, F.G., Bojesen-Koefoed, J.A., and Laier, T., 1998b. The oldest marine Cretaceous sediments in West Greenland (Umiivik-1 borehole) – record of the Cenomanian–Turonian Anoxic Event; Geology of Greenland Survey Bulletin, v. 180, p. 128–137. https://doi.org/10.34194/ggub.v180.5096

Dam, G., Nøhr-Hansen, H., Pedersen, G.K., and Sønderholm, M., 2000. Sedimentary and structural evidence of a new early Campanian rift phase in the Nuussuaq Basin, West Greenland; Cretaceous Research, v. 21, p. 127–154. https://doi.org/10.1006/cres.2000.0202

Dam, G., Pedersen, G.K., Sønderholm, M., Midtgaard, H., Larsen, L.M., Nøhr-Hansen, H., and Pedersen, A.K., 2009. Lithostratigraphy of the Cretaceous-Paleocene Nuussuaq Group, Nuussuaq Basin, West Greenland; Geological Survey of Denmark and Greenland, Bulletin 19, 171 p.

Dawes, P.R., 1997. The Proterozoic Thule Supergroup, Greenland and Canada: history, lithostratigraphy and development; Bulletin Grønlands Geologiske Undersøgelse, v. 174, 150 p.

de Vernal, A. and Mudie, P.J., 1989a. Late Pliocene to Holocene palynostratigraphy at ODP Site 645, Baffin Bay; *in* Proceedings of the Ocean Drilling Program: Scientific Results, v. 105, p. 387–397. https://doi.org/10.2973/odp.proc.sr.105.133.1989

de Vernal, A. and Mudie, P.J., 1989b. Pliocene and Pleistocene palynostratigraphy at ODP sites 646 and 647, eastern and southern Labrador Sea; *in* Proceedings of the Ocean Drilling Program: Scientific Results, v. 105, p. 401–422. https://doi.org/10.2973/odp.proc.sr.105.134.1989

de Verteuil, L. and Norris, G., 1996. Middle to upper Miocene *Geonettia clineae*, an opportunistic coastal embayment dinoflagellate of the *Homotryblium* complex; Micropaleontology, v. 42, p. 263–284. https://doi.org/10.2307/1485875

Demers-Potvin, A.V. and Larsson, H.C.E., 2019. Palaeoclimatic reconstruction for a Cenomanian-aged angiosperm flora near Schefferville, Labrador; Palaeontology, v. 62, no. 6, p. 1027–1048. https://doi.org/10.1111/pala.12444

Dickie, K., Keen, C.E., Williams, G.L., and Dehler, S.A., 2011. Tectonostratigraphic evolution of the Labrador margin, Atlantic Canada; Marine and Petroleum Geology, v. 28, p. 1663–1675. https://doi.org/10.1016/j.marpetgeo.2011.05.009

Døssing, A., 2011. Fylla Bank: structure and evolution of a normal-to-shear rifted margin in the northern Labrador Sea; Geophysical Journal International, v. 187, p. 655–676. https://doi.org/10.1111/j.1365-246X.2011.05184.x

Dowsett, H.J. and Poore, R.Z., 1991. Pliocene sea surface temperatures of the North Atlantic Ocean at 3.0 Ma; Quaternary Science Reviews, v. 10, p. 189–204. https://doi.org/10.1016/0277-3791(91)90018-P

Dowsett, H.J., Chandler, M.A., Cronin, T.M., and Dwyer, G.S., 2005. Middle Pliocene sea surface temperature variability; Paleoceanography, v. 20, no. 2, cit. no. PA2014. https://doi.org/10.1029/2005PA001133

Dybkjær, K., 2004. Morphological and abundance variations in *Homotryblium*-cyst assemblages related to depositional environments; uppermost Oligocene–Lower Miocene, Jylland, Denmark; Palaeogeography, Palaeoclimatology, Palaeoecology, v. 206, p. 41–58. https://doi.org/10.1016/j.palaeo.2003.12.021

Fader, G.B., Cameron, G.D.M., and Best, M.A., (comp.), 1989. Geology of the continental margin of eastern Canada; Geological Survey of Canada, Map 1705A, scale 1:5 000 000. https://doi.org/10.4095/127347

Friedrich, O., Norris, R.D., and Erbacher, J., 2012. Evolution of middle to Late Cretaceous oceans — a 55 m.y. record of Earth's temperature and carbon cycle; Geology, v. 40, no. 2, p. 107–110. https://doi.org/10.1130/G32701.1

Funck, T., Jackson, H.R., Dehler, S.A., and Reid, I.D., 2006. A refraction seismic transect from Greenland to Ellesmere Island, Canada: the crustal structure in southern Nares Strait; Polarforschung, v. 74, no. 1–3, p. 97–112. https://doi.org/10013/epic.29927.d001

Funck, T., Jackson, H.R., Louden, K.E., and Klingelhöfer, F., 2007. Seismic study of the transform-rifted margin in Davis Strait between Baffin Island (Canada) and Greenland: what happens when a plume meets a transform; Journal of Geophysical Research, v. 112, no. B4, cit. no. B04402. https://doi.org/10.1029/2006JB004308

General Bathymetric Chart of the Oceans, 2014. GEBCO 2014 Grid; International Hydrographic Organization and the Intergovernmental Oceanographic Commission (of UNESCO). <www.gebco.net> [accessed May 10, 2015]

Gradstein, F.M. and Srivastava, S.P., 1980. Aspects of Cenozoic stratigraphy and paleoceanography of the Labrador Sea and Baffin Bay; Palaeogeography, Palaeoclimatology, Palaeoecology, v. 30, no. 3-4, p. 261–295. https://doi.org/10.1016/0031-0182(80)90061-9

Gradstein, F.M., Jansa, L.F., Srivastava, S.P., Williamson, M.A., Bonham Carter, G., and Stam, B., 1990. Aspects of North Atlantic paleo-oceanography; Chapter 8 *in* Geology of the Continental Margin of Eastern Canada, (ed.) M.J. Keen and G.L. Williams; Geological Survey of Canada, Geology of Canada, no. 2, p. 351–389. (*also* Geological Society of America, The Geology of North America, v. I-1, p. 351–389). https://doi.org/10.4095/132712

Gradstein, F.M., Ogg, J.G., Schmitz, M., and Ogg, G., 2012. The Geologic Time Scale 2012; Elsevier B.V., Oxford, United Kingdom, 1144 p.

Grant, A.C., 1975. Geophysical results from the continental margin off southern Baffin Island; *in* Canada's Continental Margins and Offshore Petroleum Exploration, (ed.) D.J. Yorath and E.R. Parker; Canadian Society of Petroleum Geologists, Memoir 4, p. 411–431.

Gregersen, U. and Bidstrup, T., 2008. Structures and hydrocarbon prospectivity in the northern Davis Strait area, offshore West Greenland; Petroleum Geoscience, v. 14, p. 151–166. https://doi.org/10.1144/1354-079308-752

Gregersen, U., Hopper, J.R., and Knutz, P., 2013. Basin seismic stratigraphy and aspects of prospectivity in the NE Baffin Bay, northwest Greenland; Marine and Petroleum Geology, v. 46, p. 1–18. https://doi.org/10.1016/j.marpetgeo.2013.05.013

Gregersen, U., Andersen, M.S., Nøhr-Hansen, H., Sheldon, E., Kokfelt, T.F., Olivarius, M., Knudsen, C., Jakobsen, K.G., and Adolfssen, J.S., 2018. New subsurface mapping offshore southern West Greenland using geophysical and geological data; Geological Survey of Denmark and Greenland Bulletin, v. 41, p. 57–62. https://doi.org/10.34194/geusb.v41.4342

Gregersen, U., Knutz, P.C., Nøhr-Hansen, H., Sheldon, E., and Hopper, J.R., 2019. Tectonostratigraphy and evolution of the West Greenland continental margin; Bulletin of the Geological Society of Denmark, v. 67, p. 1–21.

Haggart, J.W., Sweet, A.R., Williams, G.L., Currie, L., McNicoll, V., Burden, E.T., Benham, P.H., and Galloway, J., 2011. Paleoenvironments and correlation of Cretaceous–Paleogene strata, Bylot Island, Nunavut; American Association of Petroleum Geologists, 3P Arctic, The Polar Petroleum Potential Conference & Exhibition, Official Program, Halifax, Nova Scotia, 30 August–2 September, 2011, AAPG Search and Discovery Article, 1 p. (abstract). <https://www.searchanddiscovery.com/abstracts/html/2011/3Parctic/abstracts/haggart.htm>

Hall, J., Louden, K.E., Funck, T., and Deemer, S., 2002. Geophysical characteristics of the continental crust along the Lithoprobe Eastern Canadian Shield Onshore-Offshore Transect (ECSOOT): a review; Canadian Journal of Earth Sciences, v. 39, no. 5, p. 569–587. https://doi.org/10.1139/e02-005

Harrison, J.C., Mayr, U., McNeil, D.H., Sweet, A.R., McIntyre, D.J., Eberle, J.J., Harington, C.R., Chalmers, J.A., Dam, G., and Nøhr-Hansen, H., 1999. Correlation of Cenozoic sequences of the Canadian Arctic region and Greenland; implications for the tectonic history of northern North America; Bulletin of Canadian Petroleum Geology, v. 47, p. 223–254.

Harrison, J.C., Brent, T.A., and Oakey, G.N., 2011. Baffin Fan and its inverted rift system of Arctic eastern Canada: stratigraphy, tectonics and petroleum resource potential; *in* Arctic Petroleum Geology, (ed.) A.M. Spencer, A.F. Embry, D.L. Gautier, A.V. Stoupakova, and K. Sørensen; Geological Society, London, Memoir 35, p. 595–626. https://doi.org/10.1144/M35.40

Head, M.J. and Norris, G., 1989. Palynology and dinocyst stratigraphy of the Eocene and Oligocene in ODP Leg 105, Hole 647A, Labrador Sea. *in* Proceedings of the Ocean Drilling Program: Scientific Results, v. 105, p. 515–550. https://doi.org/10.2973/odp.proc.sr.105.178.1989

Head, M.J. and Westphal, H., 1999. Palynology and paleoenvironments of a Pliocene carbonate platform: the Clino core, Bahamas; Journal of Paleontology, v. 73, no. 1, p. 1–25. https://doi.org/10.1017/S0022336000027505

Head, M.J., Norris, G., and Mudie, P.J., 1989a. Palynology and dinocyst stratigraphy of the Miocene in ODP Leg 105, Hole 645E, Baffin Bay; *in* Proceedings of the Ocean Drilling Program: Scientific Results, v. 105, p. 467–514. https://doi.org/10.2973/odp.proc.sr.105.137.1989

Head, M.J., Norris, G., and Mudie, P.J., 1989b. Palynology and dinocyst stratigraphy of the upper Miocene and lowermost Pliocene, ODP Leg 105, Site 646, Labrador Sea; *in* Proceedings of the Ocean Drilling Program: Scientific Results, v. 105, p. 423–451. https://doi.org/10.2973/odp.proc.sr.105.135.1989

Henderson, G., Rosenkrantz, A., and Schiener, E.J., 1976. Cretaceous-Tertiary sedimentary rocks of West Greenland; *in* Geology of Greenland, (ed.) A. Esher and W.S. Watt; Grønlands Geologiske Undersøgelse, Copenhagen, Denmark, p. 340–362.

Henderson, G., Schiener, E.J., Risum, J.B., Croxton, C.A., and Andersen, B.B., 1981. The West Greenland basin; *in* Geology of the North Atlantic Borderlands, (ed.) J.W. Kerr, A.J. Fergusson, and L.C. Machan; Canadian Society of Petroleum Geologists, Memoir 7, p. 399–428.

Hesse, R. and Chough, S.K., 1980. The Northwest Atlantic Mid-Ocean Channel of the Labrador Sea: II. Deposition of parallel laminated levee-muds from the viscous sublayer of low density turbidity currents; Sedimentology, v. 27, p. 697–711. https://doi.org/10.1111/j.1365-3091.1980.tb01656.x

Hiscott, R.N., 1984. Clay mineralogy and clay-mineral provenance of Cretaceous and Paleogene strata, Labrador and Baffin shelves; Bulletin of Canadian Petroleum Geology, v. 32, no. 3, p. 272–280.

Iakovleva, A.I., Brinkhuis, H., and Cavagnetto, C., 2001. Late Palaeocene–early Eocene dinoflagellate cysts from the Turgay Strait, Kazakhstan; correlations across ancient seaways; Palaeogeography, Palaeoclimatology, Palaeoecology, v. 172, p. 243–268. https://doi.org/10.1016/S0031-0182(01)00300-5

Ioannides, N.S., 1986. Dinoflagellate cysts from Upper Cretaceous-lower Tertiary sections, Bylot and Devon islands, Arctic Archipelago; Geological Survey of Canada, Bulletin 371, 99 p. https://doi.org/10.4095/123641

Jackson, G.D., 1998. Geology, Okoa Bay-Padloping Island area, District of Franklin, Northwest Territories; Geological Survey of Canada, Open File 3532, scale 1:250 000. https://doi.org/10.4095/209911

Jackson, G.D., Davidson, A., and Morgan, W.C., 1975. Geology of the Pond Inlet map-area, Baffin Island, District of Franklin; Geological Survey of Canada, Paper 74-25, 33 p. https://doi.org/10.4095/102498

Jackson, H.R., Dickie, K., and Marillier, F., 1992. A seismic reflection study of northern Baffin Bay: implication for tectonic evolution; Canadian Journal of Earth Sciences, v. 29, p. 2353–2369. https://doi.org/10.1139/e92-184

Jansa, L.F., 1976. Lower Paleozoic radiolaria-bearing limestones from the Baffin Island shelf; *in* Report of Activities, Part B; Geological Survey of Canada, Paper 76-1B, p. 99–105. https://doi.org/10.4095/104085

Jaramillo, C.A. and Oboh-Ikuenobe, F.E., 1999. Sequence stratigraphic interpretations from palynofacies, dinocyst and lithological data of upper Eocene – lower Oligocene strata in southern Mississippi and Alabama, US Gulf Coast; Palaeogeography, Palaeoclimatology, Palaeoecology, v. 145, p. 259–302. https://doi.org/10.1016/S0031-0182(98)00126-6

Jauer, C., Wielens, H., and Williams, G., 2009. Hydrocarbon prospectivity of Davis Strait and Labrador Shelf: seismic setting and stratigraphy for Gjoa G-37, Hekja O-71, Rut H-11, Gilbert F-53, Karlsefni A-13, and Skolp E-07; Geological Survey of Canada, Open File 5910, 6 sheets. https://doi.org/10.4095/247336

Jauer, C.D., Oakey, G.N., Williams, G., and Wielens, J.B.W.H., 2014. Saglek Basin in the Labrador Sea, east coast Canada; stratigraphy, structure and petroleum systems; Bulletin of Canadian Petroleum Geology, Baffin Bay special issue, v. 62, no. 4, p. 232–260. https://doi.org/10.2113/gscpgbull.62.4.232

Jeletzky, J.A., 1971. Marine Cretaceous biotic provinces and paleogeography of western and Arctic Canada: illustrated by a detailed study of ammonites; Geological Survey of Canada, Paper 70-22, 92 p. https://doi.org/10.4095/100663

Kaminski, M.A., Gradstein, F.M., Scott, D.B., and Mackinnon, K.D., 1989. Neogene benthic foraminifer biostratigraphy and deep-water history of Sites 645, 646, and 647, Baffin Bay and Labrador Sea; *in* Proceedings of the Ocean Drilling Program: Scientific Results, v. 105, p. 731–756. https://doi.org/10.2973/odp.proc.sr.105.123.1989

Keen, C.E. and Barrett, D.L., 1973. Structural characteristics of some sedimentary basins in northern Baffin Bay; Canadian Journal of Earth Sciences, v. 10, p. 1267–1278. https://doi.org/10.1139/e73-112

Keen, C.E., Keen, M.J., Ross, D.I., and Lack, M., 1974. Baffin Bay; small ocean basin formed by seafloor spreading; The American Association of Petroleum Geologists Bulletin, v. 58, p. 1089–1108.

Keen, C.E., Dickie, K., and Dehler, S., 2012. The volcanic margins of the northern Labrador Sea: insights to the rifting process; Tectonics, v. 31, cit. no. TC1011. https://doi.org/10.1029/2011TC002985

Keen, C.E., Dickie, K., and Dafoe, L.T., 2018a. Structural characteristics of the ocean-continent transition along the rifted continental margin, offshore central Labrador; Marine and Petroleum Geology, v. 89, p. 443–463. https://doi.org/10.1016/j.marpetgeo.2017.10.012

Keen, C.E., Dickie, K., and Dafoe, L.T., 2018b. Structural evolution of the rifted margin off northern Labrador: the role of hyperextension and magmatism; Tectonics, v. 37, p. 1955–1972. https://doi.org/10.1029/2017TC004924

Kennett, J.P. and Stott, L.D., 1991. Abrupt deep-sea warming, palaeoceanographic changes and benthic extinctions at the end of the Palaeocene; Nature, v. 353, p. 225–229. https://doi.org/10.1038/353225a0

Knudsen, C., Gregersen, U., Kokfelt, T.F., Olivarius, M., and Thomsen, T.B., 2020. A mid-Cretaceous alkaline volcano in the Davis Strait; Canadian Journal of Earth Sciences, v. 57, p. 69–86. https://doi.org/10.1139/cjes-2018-0307

Knutz, P.C., Hopper, J.R., Gregersen, U., Nielsen, T., and Japsen, P., 2015. A contourite drift system on the Baffin Bay–West Greenland margin linking Pliocene Arctic warming to poleward ocean circulation; Geology, v. 43, p. 907–910. https://doi.org/10.1130/G36927.1

Knutz, P.C., Newton, A.M.W., Hopper, J.R., Huuse, M., Gregersen, U., Sheldon, E., and Dybkjær, K., 2019. Eleven phases of Greenland Ice Sheet shelf-edge advance over the past 2.7 million years; Nature Geoscience, v. 12, p. 361–368. https://doi.org/10.1038/s41561-019-0340-8

Koch, P.L., Zachos, J.C., and Gingerich, P.D., 1992. Correlation between isotope records in marine and continental carbon reservoirs near the Palaeocene–Eocene boundary; Nature, v. 358, p. 319–322. https://doi.org/10.1038/358319a0

Larsen, J.G.,1977. Transition from low potassium olivine tholeiites to alkali basalts on Ubekendt Ejland; Meddelelser om Grønland, v. 200, no. 1, 42 p.

Larsen, L.M., and Dalhoff, F., 2006. Composition, age, and geological and geotectonic significance of igneous rocks dredged from the northern Labrador Sea and the Davis Strait; Danmarks og Grønlands Geologiske Undersøgelse Rapport, 2006/43, 67 p.

Larsen, J.G. and Pulvertaft, T.C.R., 2000. The structure of the Cretaceous–Palaeogene sedimentary-volcanic area of Svartenhuk Halvo, central West Greenland; Geology of Greenland Survey Bulletin, v. 188, 40 p.

Larsen, L.M., Heaman, L.M., Creaser, R.A., Duncan, R.A., Frei, R., and Hutchinson, M., 2009. Tectonomagmatic events during stretching and basin formation in the Labrador Sea and the Davis Strait: evidence from age and composition of Mesozoic to Palaeogene dyke swarms in West Greenland; Journal of the Geological Society, v. 166, p. 999–1012. https://doi.org/10.1144/0016-76492009-038

Larsen, L.M., Pedersen, A.K., Tegner, C., Duncan, R.A., Hald, N., and Larsen, J.G., 2016. Age of Tertiary volcanic rocks on the West Greenland continental margin: volcanic evolution and event correlation to other parts of the North Atlantic Igneous Province; Geological Magazine, v. 153, no. 3, p. 487–511. https://doi.org/10.1017/S0016756815000515

Lentin, J.K. and Williams, G.L., 1980. Dinoflagellate provincialism with emphasis on Campanian peridiniaceans; American Association of Stratigraphic Palynologists Contribution Series, v. 7, p. 1–47.

Li, G., Piper, D.J.W., and Campbell, D.C., 2011. The Quaternary Lancaster Sound trough-mouth fan, NW Baffin Bay; Journal of Quaternary Science, v. 26, no. 5, p. 511–522. https://doi.org/10.1002/jqs.1479

MacLean, B., 1978. Marine geological-geophysical investigations in 1977 of the Scott Inlet and Cape Dyer-Frobisher Bay areas of the Baffin Island continental shelf; *in* Current Research, Part B; Geological Survey of Canada, Paper 78-1B, p. 13–20. https://doi.org/10.4095/103568

MacLean, B. and Falconer, R.K.H., 1977. Baffin Island shelf – shallow corehole drilling, 1976; *in* Report of Activities, Part B; Geological Survey of Canada, Paper 77-1B, p. 125–127. https://doi.org/10.4095/102768

MacLean, B. and Falconer, R.K.H., 1979. Geological/geophysical studies in Baffin Bay and Scott Inlet – Buchan Gulf and Cape Dyer-Cumberland Sound areas of the Baffin Island Shelf; *in* Current Research, Part B; Geological Survey of Canada, Paper 79-1B, p. 231–244. https://doi.org/10.4095/105432

MacLean, B. and Srivastava, S.P., 1976. Shallow corehole drilling on the Baffin Island shelf; *in* Report of Activities, Part A; Geological Survey of Canada, Paper 76-1A, p. 141–143. https://doi.org/10.4095/104182

MacLean, B., Jansa, L.F., Falconer, R.K.H., and Srivastava, S.P., 1977. Ordovician strata on the southeastern Baffin Island shelf revealed by shallow drilling; Canadian Journal of Earth Sciences, v. 14, p. 1925–1939. https://doi.org/10.1139/e77-163

MacLean, B., Falconer, R.K.H., and Levy, E.M., 1981. Geological, geophysical and chemical evidence for natural seepage of petroleum off the northeast coast of Baffin Island; Bulletin of Canadian Petroleum Geology, v. 29, p. 75–95.

MacLean, B., Woodside, J.M., and Girouard, P., 1984. Geological and geophysical investigations in Jones Sound, District of Franklin; *in* Current Research, Part A; Geological Survey of Canada, Paper 84-1A, p. 359–365. https://doi.org/10.4095/119685

MacLean, B., Williams, G.L., and Srivastava, S.P., 1990. Geology of Baffin Bay and Davis Strait; *in* Chapter 7 of Geology of the Continental Margin of Eastern Canada, (ed.) M.J. Keen and G.L. Williams; Geological Survey of Canada, Geology of Canada, no. 2, p. 325–348 (*also* Geological Society of America, The Geology of North America, v. I-1).

MacLean, B., Williams, G., and Zhang, S., 2014. New insights into the stratigraphy and petroleum potential of the Baffin shelf's Cretaceous rocks; Bulletin of Canadian Petroleum Geology, Baffin Bay Special Issue, v. 62, no. 4, p. 289–310. https://doi.org/10.2113/gscpgbull.62.4.289

Manum, S.B. and Cookson, I.C., 1964. Cretaceous microplankton in a sample from Graham Island, Arctic Canada, collected during the second "Fram"-expedition (1898–1902). With notes on microplankton from the Hassel Formation, Ellef Ringnes Island; Norske Videnskaps-Akademi i Oslo, I. Matematisk-Naturvidenskapelig Klasse, Skrifter, Ny Serie, no. 17, 36 p.

Masure, E. and Vrielynck, B., 2009. Late Albian dinoflagellate cyst paleobiogeography as indicator of asymmetric sea surface temperature gradient on both hemispheres with southern high latitudes warmer than northern ones; Marine Micropaleontology, v. 70, p. 120–133. https://doi.org/10.1016/j.marmicro.2008.11.004

Mcintyre, D.J., 1975. Morphologic changes in *Deflandrea* from a Campanian section, District of Mackenzie, N.W.T., Canada; Geoscience and Man, v. 11, p. 61–76. https://doi.org/10.1080/00721395.1975.9989756

McWhae, J.R.H., 1981. Structure and spreading history of the northwestern Atlantic region from the Scotian Shelf to Baffin Bay; *in* Geology of the North Atlantic Borderlands, (ed.) J.W. Kerr, A.J. Fergusson, and L.C. Machan; Canadian Society of Petroleum Geologists, Memoir 7, p. 299–332.

McWhae, J.R.H., Gunther, P.R., and Shade, B., 1979. Canadian Arctic Islands geological field operation (Lancaster Sound segment); Indian and Northern Affairs Department, Canada, Canadian Oil and Gas Lands Administration Report, 319 p.

McWhae, J.R.H., Elie, R., Laughton, K.C., and Gunther, P.R., 1980. Stratigraphy and petroleum prospects of the Labrador Shelf; Bulletin of Canadian Petroleum Geology, v. 28, p. 460–488.

Miall, A.D., 1986. The Eureka Sound Group (Upper Cretaceous - Oligocene), Canadian Arctic Islands; Bulletin of Canadian Petroleum Geology, v. 34, no. 2, p. 240–270.

Miall, A.D., Balkwill, H.R., and Hopkins, W.S., Jr., 1980. Cretaceous and Tertiary sediments of Eclipse Trough, Bylot Island area, Arctic Canada, and their regional setting; Geological Survey of Canada, Paper 79-23, 20 p. https://doi.org/10.4095/102162

Miller, P.E. and Bell, J.S., 1989. Paleogeography, I, Labrador sea, Early to middle Albian and Turonian to Santonian paleoenvironments / Paléogéographie, I, Mer du Labrador, Paléoenvironnements de l'Albien moyen inférieur et du Turonien au Santonien; *in* Labrador Sea / Mer du Labrador, (co-ord.) J.S. Bell; Geological Survey of Canada, East Coast Basin Atlas Series, p. 78–79. https://doi.org/10.4095/127192

Miller, K.G., Barrera, E., Olsson, R.K., Sugarman, P.J., and Savin, S.M., 1999. Does ice drive early Maastrichtian eustasy; Geology, v. 27, no. 9, p. 783–786. https://doi.org/10.1130/0091-7613(1999)027%3c0783:DIDEME%3e2.3.CO%3b2

Mohr, B.A.R. and Mao, S., 1997. Maastrichtian dinocyst floras from Maud Rise and Georgia Basin (Southern Ocean): their stratigraphic and paleoenvironmental implications; Palynology, v. 21, p. 41–65. https://doi.org/10.1080/01916122.1997.9989486

Moir, P.N., 1989. Lithostratigraphy I, Labrador sea, Review and type sections / Lithostratigraphie I, Mer du Labrador, Revue et sections types; *in* Labrador Sea / Mer du Labrador, (co-ord.) J.S. Bell; Geological Survey of Canada, East Coast Basin Atlas Series, p. 26–27. https://doi.org/10.4095/127166

Moran, K., 2009. The Geoscience of Climate and Energy 3. The Cenozoic Arctic Ocean Climate; Geoscience Canada, v. 36, no. 2, p. 55–59.

Nelson, C.E., Jerram, D.A., Clayburn, J.A.P., Halton, A.M., and Roberge, J., 2015. Eocene volcanism in offshore southern Baffin Bay; Marine and Petroleum Geology, v. 67, p. 678–691. https://doi.org/10.1016/j.marpetgeo.2015.06.002

Nielsen, T., Andersen, C., Knutz, P.C., and Kuijpers, A., 2011. The Middle Miocene to Recent Davis Strait Drift Complex: implications for Arctic–Atlantic water exchange; Geo-Marine Letters, v. 31, p. 419–426. https://doi.org/10.1007/s00367-011-0245-z

Nøhr-Hansen, H., 1996. Upper Cretaceous dinoflagellate cyst stratigraphy, onshore West Greenland; Grønlands Geologiske Undersøgelse, Bulletin 170, 104 p.

Nøhr-Hansen, H., 1998. Dinoflagellate cyst stratigraphy of the Upper Cretaceous to Palaeogene strata from the Hellefisk-1, Ikermiut-1, Kangâmiut-1 and Nukik-1 wells, offshore central West Greenland; Danmarks og Grønlands Geologiske Undersøgelse, Rapport 1998/54, 58 p.

Nøhr-Hansen, H., 2003. Dinoflagellate cyst stratigraphy of the Palaeogene strata from the Hellefisk-1, Ikermiut-1, Kangâmiut-1, Nukik-1, Nukik-2 and Qulleq-1 wells, offshore West Greenland; Marine and Petroleum Geology, v. 20, p. 987–1016. https://doi.org/10.1016/S0264-8172(02)00116-2

Nøhr-Hansen, H. and Dam, G., 1997. Palynology and sedimentology across a new marine Cretaceous–Tertiary boundary section on Nuussuaq, West Greenland; Geology, v. 25, p. 851–854. https://doi.org/10.1130/0091-7613(1997)025%3c0851:PASAAN%3e2.3.CO%3b2

Nøhr-Hansen, H. and Dam, G., 1999. *Trithyrodinium evittii* Drugg 1967 and T. fragile Davey 1969 an artificially split [sic] of one dinoflagellate cyst species - stratigraphic and palaeoenvironmental importance; Grana, v. 38, no. 2/3, p. 125–133.

Nøhr-Hansen, H., Sheldon, E., and Dam, G., 2002. A new biostratigraphic scheme for the Paleocene onshore West Greenland and its implications for the timing of the pre-volcanic evolution; *in* The North Atlantic Igneous Province: Stratigraphy, Tectonic, Volcanic and Magmatic Processes, (ed.) D.W. Jolley and B.R. Bell; Geological Society London, Special Publications, v. 197, p. 111–156.

Nøhr-Hansen, H., Williams, G.L., and Fensome, R.A., 2016. Biostratigraphic correlation of the western and eastern margins of the Labrador—Baffin Seaway and implications for the regional geology; Geological Survey of Denmark and Greenland, GEUS Bulletin 37, 74 p. https://doi.org/10.34194/geusb.v37.4356

Nøhr-Hansen, H., Pedersen, G.K., Knutz, P., Bojesen-Koefoed, J., Sliwinska, K.K., and Hovikoski, J., 2018. Potential Cretaceous source-rocks from the north-east Baffin Bay, West Greenland; American Association of Petroleum Geologists Europe Regional Conference, Lisbon, Portugal, May 2–3, 2018, article 90325, 1 p. (abstract).

Nøhr-Hansen, H., Pedersen, G.K., Knutz, P.C., Bojesen-Koefoed, J.A., Śliwińska, K.K., Hovikoski, J., Ineson, J.R., Kristensen, L., and Therkelsen, J., 2021. The Cretaceous succession of northeast Baffin Bay: Stratigraphy, sedimentology and petroleum potential; Marine and Petroleum Geology, v. 133, 105108. https://doi.org/10.1016/j.marpetgeo.2021.105108

Oakey, G.N. and Chalmers, J.A., 2012. A new model for the Paleogene motion of Greenland relative to North America: plate reconstructions of the Davis Strait and Nares Strait regions between Canada and Greenland; Journal of Geophysical Research, v. 117, cit. no. B10401. https://doi.org/10.1029/2011JB008942

Peace, A.L., McCaffrey, K.J.W., Imber, J., Phethean, J., Nowell, G., Gerdes, K., and Dempsey, E., 2016. An evaluation of Mesozoic rift-related magmatism on the margins of the Labrador Sea: implications for rifting and passive margin asymmetry; Geosphere, v. 12, no. 6, p. 1701–1724. https://doi.org/10.1130/GES01341.1

Pedersen, G.K. and Nøhr-Hansen, H., 2014. Sedimentary successions and palynoevent stratigraphy from the non-marine Lower Cretaceous to the marine Upper Cretaceous of the Nuussuaq Basin, West Greenland; Bulletin of Canadian Petroleum Geology, v. 62, no. 4, p. 261–288. https://doi.org/10.2113/gscpgbull.62.4.261

Pedersen, G.K. and Pulvertaft, T.C.R., 1992. The nonmarine Cretaceous of the West Greenland Basin, onshore West Greenland; Cretaceous Research, v. 13, p. 263–272. https://doi.org/10.1016/0195-6671(92)90002-8

Pedersen, A.K., Larsen, L.M., Riisager, P., and Dueholm, K.S., 2002. Rates of volcanic deposition, facies changes and movements in a dynamic basin: the Nuussuaq Basin, West Greenland, around the C27n-C26r transition; *in* The North Atlantic Igneous Province: Stratigraphy, Tectonic, Volcanic and Magmatic Processes, (ed.) D.W. Jolley and B.R. Bell; Geological Society of London, Special Publication 197, p. 157–181.

Pedersen, A.K., Larsen, L.M., and Pedersen, G.K., 2017. Lithostratigraphy, geology and geochemistry of the volcanic rocks of the Vaigat Formation on Disko and Nuussuaq, Paleocene of West Greenland; Geological Survey of Denmark and Greenland, GEUS Bulletin 39, 244 p. https://doi.org/10.34194/geusb.v39.4354

Pedersen, A.K., Larsen, L.M., and Pedersen, G.K., 2018. Lithostratigraphy, geology and geochemistry of the volcanic rocks of the Maligât Formation and associated intrusions on Disko and Nuussuaq, Paleocene of West Greenland; Geological Survey of Denmark and Greenland Bulletin, GEUS Bulletin 40, 239 p.

Piasecki, P., 2003. Neogene dinoflagellate cysts from Davis Strait, offshore West Greenland; Marine and Petroleum Geology, v. 20, p. 1075–1088. https://doi.org/10.1016/S0264-8172(02)00089-2

Planke, S., Symonds, P.A., Alvestad, E., and Skogseid, J., 2000. Seismic volcanostratigraphy of large volume basaltic extrusive complexes on rifted margins; Journal of Geophysical Research, v. 105, p. 19335–19351. https://doi.org/10.1029/1999JB900005

Poore, R.Z. and Berggren, W.A., 1974. Pliocene biostratigraphy of the Labrador Sea: calcareous plankton; Journal of Foraminiferal Research, v. 4, no. 3, p. 91–108. https://doi.org/10.2113/gsjfr.4.3.91

Radmacher, W., Tyszka, J., and Mangerud, G., 2014. Distribution and biostratigraphical significance of *Heterosphaeridium bellii* sp. nov. and other Late Cretaceous dinoflagellate cysts from the southwestern Barents Sea; Review of Palaeobotany and Palynology, v. 201, p. 29–40. https://doi.org/10.1016/j.revpalbo.2013.10.003

Radmacher, W., Niezgodzki, I., Tyszka, J., Mangerud, F., and Pearce, M.A., 2020. Palynology vs. model simulation: oceanographic reconstruction of incomplete data from the Cretaceous Greenland–Norwegian Seaway; Newsletters on Stratigraphy, v. 53, no. 1, p. 93–120. https://doi.org/10.1127/nos/2019/0527

Ravnås, R. and Steel, R.J., 1998. Architecture of marine rift-basin successions; The American Association of Petroleum Geologists Bulletin, v. 82, no. 1, p. 110–146.

Reid, I. and Jackson, H.R., 1997. Crustal structure of northern Baffin Bay: seismic refraction results and tectonic implications; Journal of Geophysical Research, v. 102, no. B1, p. 523–542. https://doi.org/10.1029/96JB02656

Rice, P.D. and Shade, B.D., 1982. Reflection seismic interpretation and seafloor spreading history of Baffin Bay; *in* Arctic Geology and Geophysics, (ed.) A.F. Embry and H.R. Balkwill; Proceedings of the Third International Symposium on Arctic Geology, Canadian Society of Petroleum Geologists, Memoir 8, p. 245–265.

Roest, W.R. and Srivastava, S.P., 1989. Sea-floor spreading in the Labrador Sea: A new reconstruction; Geology, v. 17, p. 1000–1003. https://doi.org/10.1130/0091-7613(1989)017%3c1000:SFSITL%3e2.3.CO%3b2

Rolle, F., 1985. Late Cretaceous – Tertiary sediments offshore central West Greenland: lithostratigraphy, sedimentary evolution, and petroleum potential; Canadian Journal of Earth Sciences, v. 22, p. 1001–1019. https://doi.org/10.1139/e85-105

Ruedemann, R. and Balk, R. (ed.), 1939. Geology of North America, volume 1; Verlag von Gebrüder Borntraeger, Berlin, Germany, 643 p.

Schaller, M.F., 2015. Corrosive circulation; Nature Geoscience, v. 8, p. 429–430. https://doi.org/10.1038/ngeo2446

Schoon, P.L., Heilmann-Clausen, C., Pagh Schultz, B., Sluijs, A., Sinninghe Damsté, J.S., and Schouten, S., 2013. Recognition of early Eocene global carbon isotope excursions using lipids of marine Thaumarchaeota; Earth and Planetary Science Letters, v. 373, p. 160–168. https://doi.org/10.1016/j.epsl.2013.04.037

Schröder-Adams, C., 2014. The Cretaceous Polar and Western Interior seas: paleoenvironmental history and paleoceanographic linkages; Sedimentary Geology, v. 301, p. 26–40. https://doi.org/10.1016/j.sedgeo.2013.12.003

Shekhar, S.C., Frandsen, N., and Thomsen, E., 1982. Coal on Nûgssuaq, West Greenland; Geological Survey of Greenland, Copenhagen, 82 p.

Sheldon, E., 2003. Palaeogene nannofossil biostratigraphy of the Kangâmiut-1 and Nukik-2 wells, offshore West Greenland; Marine and Petroleum Geology, v. 20, no. 9, p. 1031–1041. https://doi.org/10.1016/S0264-8172(02)00119-8

Skaarup, N., 2001. Offshore Volcanic Rocks in Baffin Bay: A seismic interpretation of the structures and development of the Palaeogene offshore volcanic rocks in central West Greenland and on the Baffin Island margin eastern Canada; Ph.D. thesis, The Geological Survey of Denmark and Greenland, Copenhagen, Danmarks og Grønlands Geologiske Undersøgelse Rapport 2001/117, 154 p.

Skaarup, N., Jackson, H.R., and Oakey, G., 2006. Margin segmentation of Baffin Bay/Davis Strait, eastern Canada based on seismic reflection and potential field data; Marine and Petroleum Geology, v. 23, p. 127–144. https://doi.org/10.1016/j.marpetgeo.2005.06.002

Śliwińska, K.K., 2019. Early Oligocene dinocysts as a tool for palaeoenvironment reconstruction and stratigraphical framework – a case study from a North Sea well; Journal of Micropalaeontology, v. 38, p. 143–176. https://doi.org/10.5194/jm-38-143-2019

Sluijs, A. and Brinkhuis, H., 2009. A dynamic climate and ecosystem state during the Paleocene–Eocene Thermal Maximum: inferences from dinoflagellate cyst assemblages on the New Jersey shelf; Biogeosciences, v. 6, p. 1755–1781. https://doi.org/10.5194/bg-6-1755-2009

Sluijs, A., Pross, J., and Brinkhuis, H., 2005. From greenhouse to icehouse; organic-walled dinoflagellate cysts as paleoenvironmental indicators in the Paleogene; Earth-Science Reviews, v. 68, no. 3-4, p. 281–315. https://doi.org/10.1016/j.earscirev.2004.06.001

Sluijs, A., Schouten, S., Pagani, M., Woltering, M., Brinkhuis, H., Sinninghe Damsté, J.S., Dickens, G.R., Huber, M., Reichart, G.-J., Stein, R., Matthiessen, J., Lourens, L.J., Pedentchouk, N., Backman, J., and Moran, K., and the Expedition 302 Scientists, 2006. Subtropical Arctic Ocean temperatures during the Palaeocene–Eocene thermal maximum; Nature, v. 441, p. 610–613. https://doi.org/10.1038/nature04668

Sluijs, A., Brinkhuis, H., Crouch, E.M., John, C.M., Handley, L., Munsterman, D., Bohaty, S.M., Zachos, J.C., Reichart, G.-J., Schouten, S., Pancost, R.D., Sinninghe Damsté, J.S., Welters, N.L.D., Lotter, A.F., and Dickens, G.R., 2008. Eustatic variations during the Paleocene–Eocene greenhouse world; Paleoceanography, v. 23, no. 4, cit. no. PA4216. https://doi.org/10.1029/2008PA001615

Smit, J. and Brinkhuis, H., 1996. The Geulhemmerberg Cretaceous/Tertiary boundary section (Maastrichtian type area, SE Netherlands); *in* Summary of Results and a Scenario of Events; (ed.) H. Brinkhuis and J. Smit; Geologie en Mijnbouw, v. 75, no. 2/3, p. 283–293.

Sønderholm, M., Nøhr-Hansen, H., Bojesen-Koefoed, J.A., Dalhoff, F., and Rasmussen, J.A., 2003. Regional correlation of Mesozoic–Palaeogene sequences across the Greenland–Canada boundary; Danmarks og Grønlands Geologiske Undersøgelse, Rapport 2003/25, 175 p.

Sørensen, A.B., 2006. Stratigraphy, structure and petroleum potential of the Lady Franklin and Maniitsoq basins, offshore southern West Greenland; Petroleum Geoscience, v. 12, p. 221–234. https://doi.org/10.1144/1354-079305-692

Sparkes, K.E., 1989. Stratigraphy and terrestrial palynology of Late Cretaceous Eclipse Group strata, Bylot Island, Northwest Territories, Canada; M.Sc. thesis, Memorial University of Newfoundland, St. John's, Newfoundland and Labrador, 195 p.

Srivastava, S.P., 1986. Geophysical maps and geological sections of the Labrador Sea; Geological Survey of Canada, Paper 85-16, 11 p. https://doi.org/10.4095/120602

Srivastava, S.P., Arthur, M., Clement, B., 1987. Proceedings of the Ocean Drilling Program, Initial Reports, v. 105. https://doi.org/10.2973/odp.proc.ir.105.1987

St-Onge, M.R., Van Gool, J.A.M., Garde, A.A., and Scott, D.J., 2009. Correlation of Archean and Paleoproterozoic units between northeastern Canada and western Greenland: constraining the pre-collisional upper plate accretionary history of the trans-Hudson orogen; *in* Earth Accretionary Systems in Space and Time, (ed.) P.A. Cawood and A. Kroner; Geological Society, London, Special Publication 318, p. 193–235. https://doi.org/10.1144/SP318.7

Storey, M., Duncan, R.A., Pedersen, A.K., Larsen, L.M., and Larsen, H.C., 1998. $^{40}Ar/^{39}Ar$ geochronology of the West Greenland Tertiary volcanic province; Earth and Planetary Science Letters, v. 160, p. 569–586. https://doi.org/10.1016/S0012-821X(98)00112-5

Storey, M., Duncan, R.A., and Tegner, C., 2007. Timing and duration of volcanism in the North Atlantic Igneous Province: implications for geodynamics and links to the Iceland hotspot; Chemical Geology, v. 241, no. 3-4, p. 264–281. https://doi.org/10.1016/j.chemgeo.2007.01.016

Stouge, S., Ineson, J.R., Rasmussen, J.A., and Dalhoff, F., 2007. Sedimentary dredge samples from the Davis Strait High: stratigraphic and palaeoenvironmental implications; Danmarks og Grønlands Geologiske Undersøgelse, Rapport 2007/19, 49 p.

Suckro, S.K., Gohl, K., Funck, T., Heyde, I., Ehrhardt, A., Schreckenberger, B., Gerlings, J., Damm, V., and Jokat, W., 2012. The crustal structure of southern Baffin Bay: implications from a seismic refraction experiment; Geophysical Journal International, v. 190, no. 1, p. 37–58. https://doi.org/10.1111/j.1365-246X.2012.05477.x

Suckro, S.K., Gohl, K., Funck, T., Heyde, I., Schreckenberger, B., Gerlings, J., and Damm, V., 2013. The Davis Strait crust—a transform margin between two oceanic basins; Geophysical Journal International, v. 193, no. 1, p. 78–97. https://doi.org/10.1093/gji/ggs126

Tappe, S., Foley, S.F., Stracke, A., Romer, R.L., Kjarsgaard, B.A., Heaman, L.M., and Joyce, N., 2007. Craton reactivation on the Labrador Sea margins: $^{40}Ar/^{39}Ar$ age and Sr-Nd-Hf-Pb isotope constraints from alkaline and carbonatite intrusives; Earth and Planetary Science Letters, v. 256, no. 3-4, p. 433–454. https://doi.org/10.1016/j.epsl.2007.01.036

Umpleby, D.C., 1979. Geology of the Labrador Shelf; Geological Survey of Canada, Paper 79-13, 40 p. https://doi.org/10.4095/105927

van Kempen, M.M.L., Smolders, A.J.P., Lamers, L.P.M., and Roelofs, J.G.M., 2012. Micro-halocline enabled nutrient recycling may explain extreme *Azolla* event in the Eocene Arctic Ocean; PLoS One, v. 7, cit. no. e50159. https://doi.org/10.1371/journal.pone.0050159

Wasteneys, H.A., Wardle, R.J., and Krogh, T.E., 1996. Extrapolation of tectonic boundaries across the Labrador Shelf: U-Pb geochronology of well samples; Canadian Journal of Earth Sciences, v. 33, no. 9, p. 1308–1324. https://doi.org/10.1139/e96-099

Waterfield, J.J., 1989. Stratigraphy, sedimentology and palynology of Cretaceous and Tertiary strata, southwest Bylot Island, Northwest Territories, Canada; M.Sc. thesis, Memorial University of Newfoundland, St. John's, Newfoundland and Labrador, 260 p.

White, T.S., Witzke, B.J., and Ludvigson, G.A., 2000. Evidence for an Albian Hudson arm connection between the Cretaceous Western Interior Seaway of North American and the Labrador Sea; Geological Society of America Bulletin, v. 112, no. 9, p. 1342–1355. https://doi.org/10.1130/0016-7606(2000)112%3c1342:EFAAHA%3e2.0.CO%3b2

Whittaker, R.C., Hamann, N.E., and Pulvertaft, T.C.R., 1997. A new frontier province offshore northwest Greenland: structure, basin development, and petroleum potential of the Melville Bay area; American Association of Petroleum Geologists, AAPG Bulletin, v. 81, p. 978–998.

Wielens, J.B.W. and Williams, G.L., 2009. Stratigraphic cross section Gjoa-Snorri, Saglek – Hopedale Basin, in the Labrador Sea on the east coast of Canada, from north to south; Geological Survey of Canada, Open File 5903, 1 poster. https://doi.org/10.4095/247636

Williams, V.E., 1986. Palynological studies of the continental shelf sediments of the Labrador Sea; Ph.D. thesis, University of British Columbia, Vancouver, British Columbia, 210 p.

Williams, G.L., 2017a. Palynological analyses of the two Labrador Shelf wells, Petro-Canada et al. Corte Real P-85 and Petro-Canada et al. Pothurst P-19, offshore Newfoundland and Labrador; Geological Survey of Canada, Open File 8182, 50 p. https://doi.org/10.4095/299653

Williams, G.L., 2017b. Palynological analysis of the two Labrador Shelf wells, Petro-Canada et al. Roberval C-02 and Total Eastcan et al. Roberval K-92, offshore Newfoundland and Labrador; Geological Survey of Canada, Open File 8183, 63 p. https://doi.org/10.4095/299645

M.S. Barss, J.P. Bujak, and G.L. Williams, 1979; Palynological zonation and correlation of sixty-seven wells, eastern Canada; Geological Survey of Canada, Paper 78-24, p. 91. https://doi.org/10.4095/104894

Williams, G.L. and Brideaux, W.W., 1975. Palynological analyses of upper Mesozoic and Cenozoic rocks of the Grand Banks, Atlantic continental margin; Geological Survey of Canada, Bulletin 236, 163 p. https://doi.org/10.4095/103982

Williams, G.L. and Bujak, J.P., 1977a. Cenozoic palynostratigraphy of offshore eastern Canada; American Association of Stratigraphic Palynologists, Contribution Series 5A, p. 14–47.

Williams, G.L. and Bujak, J.P., 1977b. Distribution patterns of some North Atlantic Cenozoic dinoflagellate cysts; Marine Micropaleontology, v. 2, p. 223–233. https://doi.org/10.1016/0377-8398(77)90012-3

Williams, G.D. and Stelck, C.R., 1975. Speculations on the Cretaceous palaeogeography of North America; *in* The Cretaceous System in the Western Interior of North America, (ed.) W.G.E. Caldwell; Geological Association of Canada, Special Paper 13, p. 1–20.

Willumsen, P.S. and Vajda, V., 2010. A new early Paleocene dinoflagellate cyst species, *Trithyrodinium partridgei*: its biostratigraphic significance and palaeoecology; Alcheringa, v. 34, no. 4, p. 523–538. https://doi.org/10.1080/03115518.2010.519258

Wilson, R.W., Klint, K.E.S., van Gool, J.A.M., McCaffrey, K.J.W., Holdsworth, R.E., and Chalmers, J.A., 2006. Faults and fractures in central West Greenland: onshore expression of continental break-up and sea-floor spreading in the Labrador–Baffin Bay sea; Geological Survey of Denmark and Greenland Bulletin, v. 11, p. 185–204. https://doi.org/10.34194/geusb.v11.4931

Wiseman, T.R., 1991. Sedimentology of the Maastrichtian, Pond Inlet formation (channelized turbidite system), Bylot Island, Northwest Territories, Canada; B.Sc. thesis, Memorial University of Newfoundland, St. John's, Newfoundland and Labrador, 133 p.

Zachos, J., Pagani, M., Sloan, L., Thomas, E., and Billups, K., 2001. Trends, rhythms, and aberrations in global climate 65 Ma to present; Science, v. 292, no. 5517, p. 686–693. https://doi.org/10.1126/science.1059412

Zachos, J.C., Schouten, S., Bohaty, S., Quattlebaum, T., Sluijs, A., Brinkhuis, H., Gibbs, S.J., and Bralower, T.J., 2006. Extreme warming of mid-latitude coastal ocean during the Paleocene–Eocene Thermal Maximum: inferences from TEX86 and isotope data; Geology, v. 34, no. 9, p. 737–740. https://doi.org/10.1130/G22522.1

Zachos, J.C., Dickens, G.R., and Zeebe, R.C., 2008. An early Cenozoic perspective on greenhouse warming and carbon-cycle dynamics; Nature, v. 451, p. 279–283. https://doi.org/10.1038/nature06588

Zhang, S. and Pell, J., 2014. Conodonts recovered from the carbonate xenoliths in the kimberlites confirm the Paleozoic cover on the Hall Peninsula, Nunavut; Canadian Journal of Earth Sciences, v. 51, p. 142–155. https://doi.org/10.1139/cjes-2013-0171

Zhang, S., Creaser, R.A., and Pell, J., 2014. Discovery of organic-rich black shale xenolith from kimberlite on the Hall Peninsula, Nunavut and its implication for petroleum potential in Cumberland Sound; Bulletin of Canadian Petroleum Geology, v. 62, p. 125–131.

Zonneveld, K.A.F., Marret, F., Versteegh, G.J.M., 2013. Atlas of modern dinoflagellate cyst distribution based on 2405 data points; Review of Palaeobotany and Palynology, v. 191, p. 1–197. https://doi.org/10.1016/j.revpalbo.2012.08.003

Contents

Rifting and evolution of the Labrador–Baffin Seaway

C.E. Keen[1], K. Dickie[1], L.T. Dafoe[1*], T. Funck[2], J.K. Welford[3], S.A. Dehler[4], U. Gregersen[2], and K.J. DesRoches[1]

with contributions by P.C. Knutz[2], G.N. Oakey[1], J.R. Hopper[2], Q. Li[1], and T.A. Brent[4]

Keen, C.E., Dickie, K., Dafoe, L.T., Funck, T., Welford, J.K., Dehler, S.A., Gregersen, U., and DesRoches, K.J., 2022. Rifting and evolution of the Labrador–Baffin Seaway; in *Geological synthesis of Baffin Island (Nunavut) and the Labrador–Baffin Seaway, (ed.) L.T. Dafoe and N. Bingham-Koslowski; Geological Survey of Canada, Bulletin 608, p. 341–377. https://doi.org/10.4095/321854*

Abstract: The evolution of the 2000 km long Mesozoic rift system underlying the Labrador–Baffin Seaway is described, with emphasis on results from geophysical data sets, which provide the timing, sediment thickness, and crustal structure of the system. The data sets include seismic reflection and refraction, gravity, and magnetic data, with additional constraints provided by near-surface geology and well data. Many features that characterize rift systems globally are displayed, including: wide and narrow rift zones; magma-rich and magma-poor margin segments; exhumation of continental mantle in distal, magma-poor zones; and occurrences of thick basalts, associated with the development of seaward-dipping reflectors, and magmatic underplating. The magma-rich regions were affected by Paleogene volcanism, perhaps associated with a hotspot or plume. Plate reconstructions help elucidate the plate tectonic history and modes of rifting in the region; however, many questions remain unanswered with respect to this rift system.

Résumé : Nous décrivons l'évolution du système de rift mésozoïque long de 2 000 km qui occupe le sous-sol du bras de mer Labrador-Baffin, en mettant l'accent sur les résultats tirés d'ensembles de données géophysiques, lesquels fournissent de l'information sur la chronologie, l'épaisseur des sédiments et la structure crustale du système. Les ensembles de données comprennent des données de sismique-réflexion et de sismique-réfraction ainsi que des données gravimétriques et magnétiques. Des contraintes additionnelles sont fournies par la géologie de la proche surface et des données sur les puits. Nombre d'éléments qui caractérisent les systèmes de rift à l'échelle planétaire se manifestent ici, dont les suivants : des zones de rift tantôt larges, tantôt étroites; des segments de marge riches en magma et d'autres pauvres en magma; une exhumation du manteau continental dans les zones distales pauvres en magma; et l'existence d'épaisses accumulations de basalte, auxquelles sont associés des réflecteurs inclinés vers le large et un sous-placage magmatique. Les secteurs riches en magma ont été touchés par un volcanisme paléogène, qui pourrait avoir été associé à un point chaud ou panache mantellique. Les reconstitutions de plaques aident à tirer au clair l'histoire de la tectonique des plaques et les modes de rifting dans la région. Cependant, de nombreuses questions subsistent au sujet de ce système de rift.

[1]Geological Survey of Canada, 1 Challenger Drive, Dartmouth, Nova Scotia B2Y 4A2
[2]Geological Survey of Denmark and Greenland, Øster Voldgade 10, 1350 Copenhagen, Denmark
[3]Department of Earth Sciences, Memorial University of Newfoundland, St. John's, Newfoundland and Labrador A1C 5S7
[4]Geological Survey of Canada, 3303-33rd Street NW, Calgary, Alberta T2L 2A7
*Corresponding author: L.T. Dafoe (email: lynn.dafoe@nrcan-rncan.gc.ca)

INTRODUCTION

The Labrador–Baffin Seaway (Fig. 1) formed as a result of extension and rifting of the ancient North American Craton during the Mesozoic. By the Early Cenozoic, the Greenland Plate had separated from North America and seafloor spreading was forming the oceanic crust that now underlies much of Baffin Bay and the Labrador Sea. Opening ceased by the end of the Eocene and Greenland once again became part of the North American Plate. The Labrador–Baffin Seaway region plays an important role as a major link between plate motions in the Atlantic and Arctic oceans.

Early attempts to determine the tectonic history of the Labrador–Baffin Seaway began in the late 1960s with studies of the marine geology and geophysics that characterized the region (Hood et al., 1967; Keen and Barrett, 1972; Hyndman, 1973; Keen et al., 1974; Hood and Bower, 1975; Van der Linden, 1975; Srivastava, 1978; Srivastava et al., 1982; MacLean et al., 1990). In addition, there was increasing interest in the adjacent onshore geology during this period (Kerr, 1967; Clarke and Pedersen, 1976; Dawes, 1976; Henderson, 1976). The early marine analyses were hindered by the limited availability of data, a lack of modern instrumentation and the presence of thick sediments that blanketed much of the region. Nevertheless, significant progress was made in understanding the plate tectonic evolution, although much remained controversial. For example, there was major disagreement about whether Nares Strait was the locus of a large-offset transform during opening (Srivastava, 1978; Dawes and Kerr, 1982). Later, the position of the landward limit and age of the oldest oceanic crust in the Labrador Sea was hotly debated (Chalmers and Laursen, 1995; Srivastava and Roest, 1999). In Baffin Bay, the absence of clear magnetic isochrons still leads to some uncertainty regarding the age of the onset of seafloor spreading, although understanding of plate motions in the region has greatly improved (e.g. Srivastava, 1978; Roest and Srivastava, 1989; Lawver et al., 1990; Oakey and Chalmers, 2012; Hosseinpour et al., 2013; Gion et al., 2017). Some of these issues are still contentious, but there is now generally more of a consensus about the tectonic history. This is in part due to a more complete understanding of passive-margin development, both globally and locally, especially where modern data gathered from digital imaging of the deep crustal structure are integrated with other geological and geophysical data.

The onshore geology reveals much about the nature of the pre-rift continental basement and the main structural trends, which might have influenced development of the rift. The rocks surrounding the seaway are primarily composed of Archean crustal blocks assembled during the Paleoproterozoic (Fig. 1; St-Onge et al., 2009, this volume). The Paleoproterozoic mobile belts and sutures, as well as the Mesoproterozoic Grenville Province, are strongly correlated across the conjugate margins (St-Onge et al., 2009). Some of these onshore boundaries have been traced offshore using geophysical data (Chalmers et al., 1999; Hall et al., 2002). Basement rocks sampled in onshore and offshore regions indicate that pre-Mesozoic basement includes: Precambrian crystalline rocks (Wasteneys et al., 1996; St-Onge et al., 2009; Gregersen et al., 2018); remnants of Paleoproterozoic basins, both offshore and onshore around northern Baffin Bay (Jackson and Iannelli, 1981; Dawes, 1997); and Paleozoic sedimentary rocks offshore Labrador (Balkwill and McMillan, 1990), onshore Baffin Island (MacLean et al., 1986, 1990), and offshore Davis Strait and Cumberland Sound (Dalhoff et al., 2006; Stouge et al., 2007; MacLean et al., 2014). Igneous dykes of Triassic to Early Cretaceous age may indicate preconditioning, weakening, and thinning of the cold, thick cratonic lithosphere prior to rifting (Tappe et al., 2007; Larsen et al., 2009; Secher et al., 2009). Offshore, Early Cretaceous alkali basalt was sampled on the Labrador margin (Balkwill and McMillan, 1990).

The early rifting phase thinned and extended the continental crust under the Labrador–Baffin Seaway during the Early Cretaceous, producing large half-grabens and graben structures in basement rocks (Balkwill and McMillan, 1990; Chalmers and Pulvertaft, 2001; Dickie et al., 2011; Gregersen et al., 2019). During the Late Cretaceous–Paleocene, breakup of the continental crust occurred in some regions (the central Labrador Sea is the best example) and part of the continental mantle was exhumed and serpentinized (Keen et al., 2018a, b). Other regions, particularly in the north, show evidence of renewed extensional and rotational block faulting in the Late Cretaceous to early Paleocene (Chalmers et al., 1999; Døssing, 2011; Gregersen et al., 2019).

The geometry and timing of plate motions in the region is defined by the position of the seafloor-spreading axis, and identification of the magnetic isochrons and fracture zones preserved within oceanic crust (Srivastava, 1978; Roest and Srivastava, 1989; Oakey and Chalmers, 2012). Most of the oceanic crust is Paleocene to Eocene in age; plate motions ceased around the end of the Eocene (Srivastava, 1978). In the Labrador Sea, spreading began earlier (Late Cretaceous/magnetic polarity chron C31; Keen et al., 2018a) than in Baffin Bay, which opened around chron C27 (Oakey and Chalmers, 2012) or later (Chauvet et al., 2019). Thus, the onset of seafloor spreading was diachronous within the Labrador Sea (Srivastava and Roest, 1999), with the oldest seafloor having formed in the south.

The onset of seafloor spreading in the Baffin Bay region (chron C27) may have occurred almost simultaneously with the onset of major volcanism in the Davis Strait region (Clarke, 1970; Clarke and Pedersen, 1976; Larsen and Dalhoff, 2006; Larsen et al., 2009). This large volcanic province is thought to be related to the arrival of a mantle plume or hotspot around 61 Ma, which resulted in the production of similar basalts across the region, from Cape Dyer (Baffin Island) in the west to as far east as the British Isles (North Atlantic Igneous Province; Storey et al., 2007b). The 'plume theory' has been disputed, however, by some (Nielsen et al., 2007; Peace et al., 2017). Whatever its source, the magmatism was very intense, providing excess magma to the regions bordering Davis Strait and overprinting much of the earlier margin structure.

In this paper, some of the main tectonic elements of the Labrador–Baffin Seaway region are re-examined in light of current concepts of rifting and rifted and transform margins, as well as by integrating pre-existing data with new mapping of seismic reflection data and new compilations, and analysis of potential-field data and seismic refraction data.

DATA

Seismic reflection data

Western Labrador Sea

The two-dimensional multichannel seismic reflection line coverage used in the interpretation along the Labrador margin includes over 128 000 line-kilometres of data (Fig. 2). Sixty percent of these data are modern (collected since 2000) and form a regional grid with line spacing generally ranging from 10 to 30 km and with recording depths of 9 to 15 s two-way traveltime (twt). These data were acquired using long streamers (generally 8 km or more) and processed with modern demultiple removal algorithms (e.g. 'Radon') and prestack time migration. Major data sets used in this study were collected by several organizations: the Geological Survey of Canada (https://basin.gdr.nrcan.gc.ca/), the Geological Survey of Denmark and Greenland (https://www.eng.geus.dk/), ION Geophysical (https://www.iongeo.com/), and TGS-NOPEC Geophysical Company ASA (TGS; https://www.tgs.com).

Vintage data sets (1972–1992) form the remainder of the multichannel seismic reflection data set on the Labrador margin; these were acquired using shorter streamers and with only 6 to 8 s two-way traveltime of data. They were processed using older demultiple algorithms and poststack migration was applied rather than prestack migration. These data were used to cover gaps in the modern seismic-data coverage, primarily north of latitude 58°N, where the modern seismic-data coverage was reduced to a line spacing of 30 km or more. More information regarding seismic surveys on the Labrador margin can be found on the Canada–Newfoundland and Labrador Offshore Petroleum Board's website (https://www.cnlopb.ca).

Western Davis Strait

Approximately 75 000 line-kilometres of publicly released multichannel seismic reflection data constitute the bulk of the data used in the western Davis Strait region of this study (Fig. 2). Of these data,

Figure 1. a) Major basins of the Labrador–Baffin Seaway are outlined based on the sediment thickness map shown in Figure 8, except for the Nuussuaq Basin, which is from Dam et al. (2009). Major Precambrian boundaries are *modified from* St-Onge et al. (2009) and bathymetry is *after* the International Hydrographic Organization and Intergovernmental Oceanographic Commission (2014). *See* Figure 1b for abbreviations of feature names. Additional projection information for all maps in this paper is as follows: Central Meridian = 60°W; Standard Parallels = 65, 75°W; Latitude of Origin = 65°N.

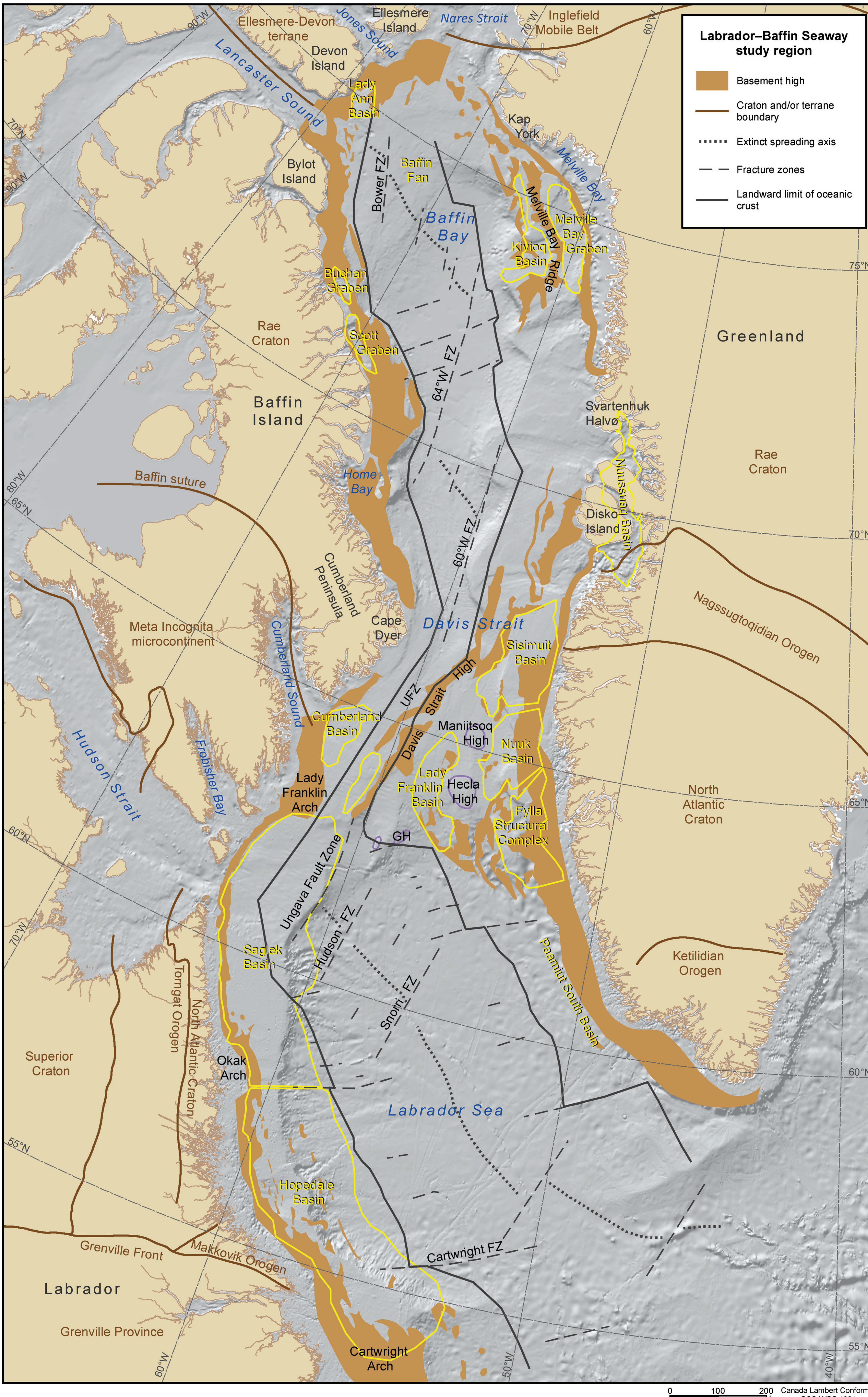
Labrador–Baffin Seaway study region
Basement high
Craton and/or terrane boundary
Extinct spreading axis
Fracture zones
Landward limit of oceanic crust
Ellesmere-Devon terrane
Ellesmere Island
Nares Strait
Inglefield Mobile Belt
Jones Sound
Devon Island
Lancaster Sound
Lady Ann Basin
Kap York
Melville Bay
Bylot Island
Bower FZ
Baffin Fan
Baffin Bay
Melville Bay Ridge
Melville Bay Graben
Kivioq Basin
Buchan Graben
Scott Graben
Rae Craton
Greenland
64°W FZ
Baffin Island
Svartenhuk Halvø
Rae Craton
Home Bay
Baffin suture
Nuussuaq Basin
Disko Island
60°W FZ
Cumberland Peninsula
Cape Dyer
Davis Strait
Nagssugtoqidian Orogen
Meta Incognita microcontinent
Cumberland Sound
Sisimiut Basin
UFZ
Davis Strait High
Cumberland Basin
Maniitsoq High
Nuuk Basin
Hudson Strait
Frobisher Bay
Lady Franklin Arch
Lady Franklin Basin
Hecla High
North Atlantic Craton
Fylla Structural Complex
GH
Ungava Fault Zone
Hudson FZ
Saglek Basin
Snorri FZ
Paamiut South Basin
Ketilidian Orogen
Torngat Orogen
North Atlantic Craton
Superior Craton
Okak Arch
Labrador Sea
Hopedale Basin
Grenville Front
Makkovik Orogen
Cartwright FZ
Labrador
Grenville Province
Cartwright Arch
90°W
70°W
60°W
80°W
50°W
40°W
75°N
70°N
65°N
60°N
55°N
0 100 200 km
1:7 500 000
Canada Lambert Conformal
GCS WGS 1984

Sedimentary basin names

BF – Baffin Fan
BG – Buchan Graben
CB – Cumberland Basin
FC – Fylla Structural Complex
HDB – Hopedale Basin
KB – Kivioq Basin
LAB – Lady Ann Basin
LFB – Lady Franklin Basin
MBG – Melville Bay Graben
NB – Nuuk Basin
NSB – Nuussuaq Basin
PSB – Paamiut South Basin
SB – Sisimuit Basin
SG – Scott Graben
SGB – Saglek Basin

Bathymetric names

CS – Cumberland Sound
FB – Frobisher Bay
HB – Home Bay
JS – Jones Sound
MB – Melville Bay
NS – Nares Strait

Geological structures

BFZ – Bower Fracture Zone
CA – Cartwright Arch
CFZ – Cartwright Fracture Zone
DSH – Davis Strait High
FZ – Fracture zone
GH – Gjoa High
HFZ – Hudson Fracture Zone
HH – Hecla High
LFA – Lady Franklin Arch
MBR – Melville Bay Ridge
MH – Maniitsoq High
OA – Okak Arch
SFZ – Snorri Fracture Zone
UFZ – Ungava Fault Zone

Onshore place names

CD – Cape Dyer
CP – Cumberland Peninsula
DI – Disko Island
DVI – Devon Island
EI – Ellesmere Island
KY – Kap York
SH – Svartenhuk Halvø

Figure 1. b) Abbreviations of key place names and features for Figures 1a, 3, 7, 8, and 14.

most were collected in the 1970s and early 1980s (https://basin.gdr.nrcan.gc.ca). They were collected by Imperial Oil, Bundesanstalt für Geowissenschaften und Rohstoffe, Aquitaine, Compagnie Générale de Géophysique, Petro-Canada, Eureka Exploration, Canterra Energy, Gulf Canada, Esso Resources, and Shell Canada. These data are mainly regional lines varying in penetration from 5 to 7 s two-way traveltime. Most of the data are not migrated, but critical lines and surveys were migrated using a single-velocity, finite-difference migration to improve interpretation (Dafoe et al., 2016a, b). Much of the data were converted to digital SEG-Y files from analogue plots and suffer from relatively limited frequency content as a result. The remainder of the multichannel seismic reflection data used in this study is a more modern data set consisting of approximately 5000 line-kilometres of high-quality data collected by TGS in 2001 and 2002. These lines were shot using a 6 km long streamer and recorded 8 s two-way traveltime of data.

Western Baffin Bay

The multichannel seismic reflection data set used for interpretation along the Baffin Island margin consists of over 32 000 line-kilometres of seismic data (Fig. 2) with the bulk of this being vintage data sets acquired between 1968 and 1982. A loose grid of modern seismic data, with over 2700 line-kilometres and a spacing of about 300 km, was acquired by TGS in Baffin Bay in 2008. The seismic acquisition and processing techniques applied to the vintage and modern data sets are the same as those described above for the Labrador margin; however, in Baffin Bay, over half of the vintage lines were not migrated following their acquisition, so poststack migrations were conducted on key surveys (Dafoe et al., 2016a, b).

West Greenland

The released seismic reflection data sets along the West Greenland margin are processed multichannel seismic reflection data collected between 1977 and 2008 (Fig. 2). Most older data were acquired with streamers over 2 km long, whereas modern streamers are over 8 km long. A total of about 95 000 line-kilometres was used and the line spacing ranges from 5 to 20 km (Fig. 2). Most of the seismic data sets used were acquired by institutions, companies, and contractors including mainly Bundesanstalt für Geowissenschaften und Rohstoffe, Cairn Energy/Capricorn, Dansk Olie og Naturgas A/S, Fugro-Geoteam, Geological Survey of Denmark and Greenland, KANUMAS Group (consortium of seven oil companies), NUNAOIL A/S, Phillips Petroleum, Statoil (now Equinor), and TGS. Others also acquired data both as part of exclusive exploration licences and nonexclusive prospecting licences (*see* https://www.govmin.gl). Additional information on the seismic data is available from the Geological Survey of Denmark and Greenland (https://eng.geus.dk/products-services-facilities/archives/the-subsurface-archive) and the Greenland National Petroleum Data Repository (https://www.greenpetrodata.gl).

Seismic refraction data

A compilation of post-1986 seismic refraction data is shown in Figure 3. From 1987 to 1991, Dalhousie University and the Atlantic division of the Geological Survey of Canada conducted four surveys in the study area utilizing the vessel *CCGS Hudson*. The number of seismic receivers was limited and varied between four and eleven ocean-bottom seismometers (OBS). Some of the lines were supplemented by sonobuoys. The surveys were conducted on the Labrador continental margin (lines 90-R1 to 90-R3; Chian et al., 1995a; Reid, 1996), the conjugate southwestern Greenland margin (lines 88-R1 and 88-R2; Chian and Louden, 1992, 1994), at the extinct Labrador Sea spreading axis (lines R1, R2; Osler and Louden, 1992, 1995), and in northern Baffin Bay at the entrance to Nares Strait (lines 1991-1 to 1991-4; Jackson and Reid, 1994; Reid and Jackson, 1997).

These initial experiments were followed by three surveys that focused on the crustal structure of the continents bordering the Labrador Sea and Davis Strait. These were combined onshore-offshore experiments using air guns as seismic sources and land seismometers as receivers, which often were supplemented by some ocean-bottom seismometers. In 1989, Gohl and Smithson (1993) acquired a 400 km line along the coast of Greenland, in the Davis Strait area (line GR89-WA). The Canadian LITHOPROBE research program completed two dedicated surveys along the coast of Labrador as part of the Eastern Canadian Shield Onshore-Offshore Transect project in 1992 and 1996. During the first survey in 1992, multichannel seismic reflection data were acquired that were recorded by six land seismometers. In 1996, seven dedicated seismic refraction lines were acquired (Funck and Louden, 1998, 1999; Funck et al., 2000a, 2001, 2008), including crustal-scale, three-dimensional tomography in the Torngat Mountains in northern Labrador (Funck et al., 2000b). Another combined onshore-offshore experiment was carried out across southern Nares Strait in 2001 (line PASSAGE-3; Funck et al. 2006).

Davis Strait and the southern and central parts of Baffin Bay were not studied by any modern seismic refraction experiments until 2003. In that year, the vessel *CCGS Hudson* acquired two lines (NUGGET-1 and -2) in southern Davis Strait (Funck et al., 2007; Gerlings et al., 2009). These lines were tied to four wells (Fig. 2) and relied on up to 28 ocean-bottom seismometers, through which the lateral resolution of the velocity models was significantly improved when compared to most of the previous experiments. Two German expeditions led by the Alfred Wegener Institute with the research vessels RV *Maria S. Merian* and RV *Polarstern* were conducted in 2008 and 2010, respectively. The 2008 data (AWI-2008 lines; Funck et al., 2012a; Suckro et al., 2012, 2013) comprise three transects from Baffin Island to Greenland using between 12 and 24 ocean-bottom seismometers. The 2010 lines cover the Melville Bay area and the entrance to Nares

Figure 2. Location of released multichannel seismic reflection data and wells in the Labrador–Baffin Seaway (select unreleased data is also shown for the Labrador margin and released data up to 2018 is shown for the West Greenland margin). Names of wells mentioned in the text are shown.

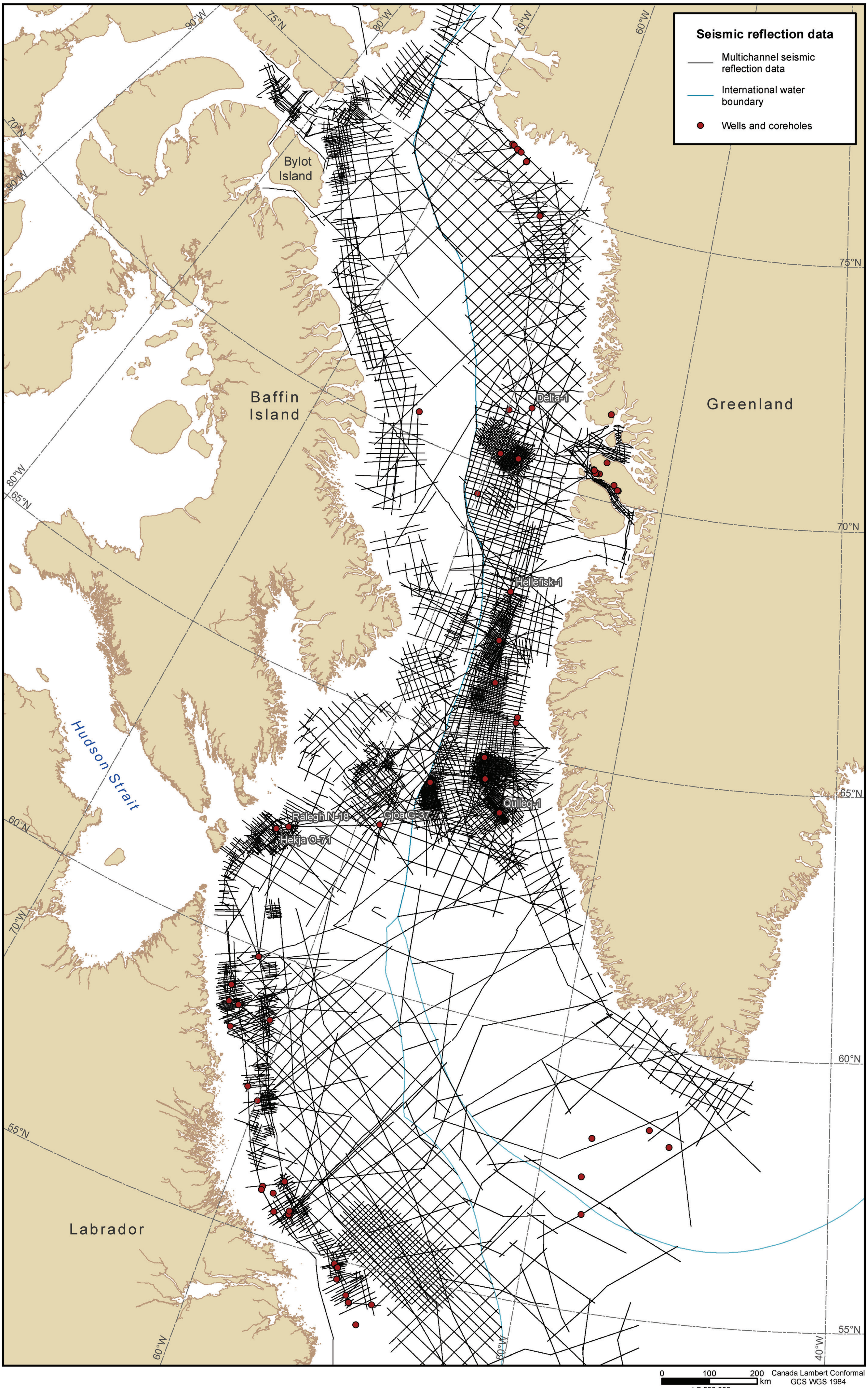
Seismic reflection data
Multichannel seismic reflection data
International water boundary
Wells and coreholes
Bylot Island
Baffin Island
Greenland
Hudson Strait
Labrador
Delta-1
Hellefisk-1
Qulleq-1
Ralegh N-18
Gjoa G-37
Hekja O-71
75°N
70°N
65°N
60°N
55°N
90°W
80°W
75°N
70°W
60°W
40°W
0 100 200 km
1:7 500 000
Canada Lambert Conformal
GCS WGS 1984

Strait (AWI-2010 lines; Suckro et al., 2012; Altenbernd et al., 2014, 2015, 2016), but are restricted to the Greenland side of Baffin Bay; between 17 and 28 OBS were used along the four lines collected during that cruise.

In 2009, the extended continental-shelf programs of Canada and the Kingdom of Denmark conducted a joint cruise on board the vessel *CCGS Hudson* to acquire two additional seismic refraction lines in the area of the extinct Labrador Sea spreading axis (Delescluse et al., 2015), and two lines across and along the axis of the Eirik Drift off south Greenland (the SIGNAL lines; Funck et al., 2012b); on these lines, between 10 and 24 ocean-bottom seismometers were used. Another line studying the magma-rich eastern Greenland continental margin was acquired in 1996, close to the Eirik Drift (line SIGMA-4; Holbrook et al., 2001).

Gravity data

The free-air gravity anomaly at sea and Bouguer gravity anomaly on land shown on Figure 4 represent a compilation of four maps covering the Labrador–Baffin Seaway region gridded at a resolution of 5 km (Oakey et al., 2001e, f, g, h). The data set used in the development of the maps includes both land stations and marine surface measurements with observations at a spacing of 5 to 10 km and 5 to 30 km, respectively. The Bouguer correction on land was calculated using a rock density of 2670 kg/m^3 and densities of 1000 kg/m^3 and 900 kg/m^3 for onshore water and ice, respectively. An additional terrain correction was applied to some coastal regions, where observations were made next to rugged terrain such as fjords.

The filtered Bouguer map (Fig. 5) was generated to compensate for the effects of bathymetry on the marine free-air anomaly. The gridded physiography data from Oakey et al. (2001a, b, c, d) were used in the marine Bouguer gravity correction. The mass of the water column was replaced with a rock density of 2600 kg/m^3. The physiography data were used at their original 2 km gridded resolution (rather than the final regridded resolution of 1 km in the published maps) for the correction, then regridded to match the free-air data (Oakey et al., 2001e, f, g, h). A 200 km high-pass filter was applied to remove long wavelength effects of the Bouguer correction.

Magnetic data

The magnetic anomaly map (Fig. 6) is a compilation of four data sets, numbered 1 to 4 on the inset map. In the Labrador Sea, Davis Strait, and southern Greenland regions, two data sets have been merged: the Atlantic region data from Oakey and Dehler (1998), gridded at 1 km, and the Labrador Sea and Davis Strait magnetic data set from Oakey et al. (2001i, j), gridded at 2 km. The two were combined and regridded at 2 km. It should be noted that marine shipborne data were collected at a 2 to 20 km track spacing. Data set 3 (Miles and Oneschuk, 2016) covers the onshore Canadian side of the map, the contiguous offshore areas, and Baffin Bay. This data set was compiled at a higher resolution (1 km) grid; however, limited shipborne data are available from the Baffin Bay region, resulting in poorly defined magnetic anomalies there (cf. Verhoef et al., 1996). Data set 4 covers the northern half of Greenland using an older compilation of data at 7 km grid spacing (Verhoef et al., 1996).

METHODS AND RESULTS

Depth to basement and sediment thickness

Methods

In this section, updated maps of depth to basement (Fig. 7) and sediment thickness (Fig. 8) constructed from the interpretation of the available two-dimensional multichannel seismic reflection data are presented. Different time-depth conversion functions were used for three subregions, as described below. The West Greenland portion of the maps in Figures 7 and 8 is based on work by Gregersen et al. (2019), who published a thickness map (in twt) for that margin, with Cretaceous depocentres shown in Gregersen et al. (this volume). This was combined with new maps for the Canadian side, including the western Labrador Sea, western Davis Strait, and western Baffin Bay (*see* 'Data' section). Major sedimentary basins were then outlined using the sediment thickness.

Other maps of depth to basement and sediment thickness were compiled previously and published by Oakey and Stark (1995) from older data (Grant, 1990). Louden et al. (2004) used these and other data to present maps of anomalous basement topography, corrected for sediment loading and age. Welford et al. (2018) showed an early version of the sediment thickness presented here for the western side of Baffin Bay.

The acoustic basement and seafloor horizons were interpreted along the two-dimensional seismic reflection data set (Fig. 2). The distribution of these data is uneven, reflecting where exploration efforts have been concentrated: the Canadian margin in the Labrador Sea, whereas exploration has focused on the West Greenland margin in Davis Strait and Baffin Bay. Acoustic basement was tied to the wells that intersected basement.

The prerift acoustic-basement horizon generally forms a strong, fairly continuous reflection, which indicates a major increase in the reflection coefficient across this boundary, with layering above and chaotic to transparent seismic facies below. This is the typical signature for Precambrian crystalline basement, as well as possible volcanic rocks and other supracrustal rocks (Gregersen et al., 2019). There are also remnants of sedimentary basins, which predate Mesozoic rifting. Paleozoic strata were encountered in six exploration wells on the central Labrador margin, in several shallow boreholes, and in dredge samples collected within Davis Strait (MacLean et al., 1990; Dalhoff et al., 2006; Stouge et al., 2007). These rocks may exhibit weak layering, folding and/or angular unconformities beneath a more continuous, stronger acoustic-basement reflection. Remnants of a Mesoproterozoic–Neoproterozoic (Thule Supergroup) sedimentary basin have also been drilled offshore northwestern Greenland in the Kap York region, where locally they form a thick, layered interval (Gregersen et al., 2019, this volume).

Oceanic basement rocks, comprising the deeper, central parts of the region, can be difficult to distinguish from other basement rock types, but may have a more hummocky appearance, and their presence is constrained, where possible, by seismic refraction and potential-field data. In regions where igneous rocks form magma-rich margins, seaward-dipping reflectors and other features typical of this type of margin (Planke et al., 2000) can be observed below the top of the interpreted acoustic basement. Between oceanic and continental crust, there is a transition zone floored by serpentinized mantle in parts of the study region. The transition zone is primarily identified by its anomalous velocity structure on seismic refraction profiles (*see* 'Crustal structure' section), although Keen et al. (2018a, b) indicated this basement may exhibit some distinguishing characteristics on seismic reflection data.

A final category of acoustic basement consists of Paleogene volcanic rocks. These have been mapped as 'basement' in regions where they mask underlying prerift sediments and basement. This relationship between volcanic rocks and underlying rift basins is known from outcrops in the Nuussuaq Basin (Dam et al., 2009) and Cape Dyer (Clarke and Upton, 1971). Therefore, it is not always possible to discriminate between basement types except locally (Skaarup, 2002). In regions of intense volcanism, such as Davis Strait and offshore southeastern Baffin Bay, the mapped basement depths and sediment thicknesses represent minimum values.

The seafloor reflection also forms a strong positive signal on seismic sections. This horizon was interpreted throughout the region and subtracted from the basement horizon to derive sediment thickness. Both the basement horizon and the sediment thickness were gridded (5 by 5 km) using Schlumberger's GeoFrame © (2012) software on the Canadian side and Schlumberger's Petrel © (2017) software for the West Greenland margin, and followed by smoothing within each subregion; no interpolation or smoothing was carried out between these subregions.

The relationship between seismic reflection traveltime and depth was derived using sonic logs and checkshot surveys from the industry boreholes, as well as refraction/wide-angle reflection (RWAR); details regarding this methodology can be found in Keen (2019). The region was divided into three subregions: Labrador Sea, Davis Strait, and Baffin Bay based on geology and data availability (these areas differ slightly from those presented in other papers in this volume). In each subregion, the availability and quality of the above data sets vary; however, all data sets were edited to remove bad

Figure 3. Location of seismic refraction data collected after 1986 in the Labrador–Baffin Seaway. Major Precambrian boundaries are *modified from* St-Onge et al. (2009) and bathymetry is *after* the International Hydrographic Organization and Intergovernmental Oceanographic Commission (2014). *See* Figure 1b for abbreviations of feature names.

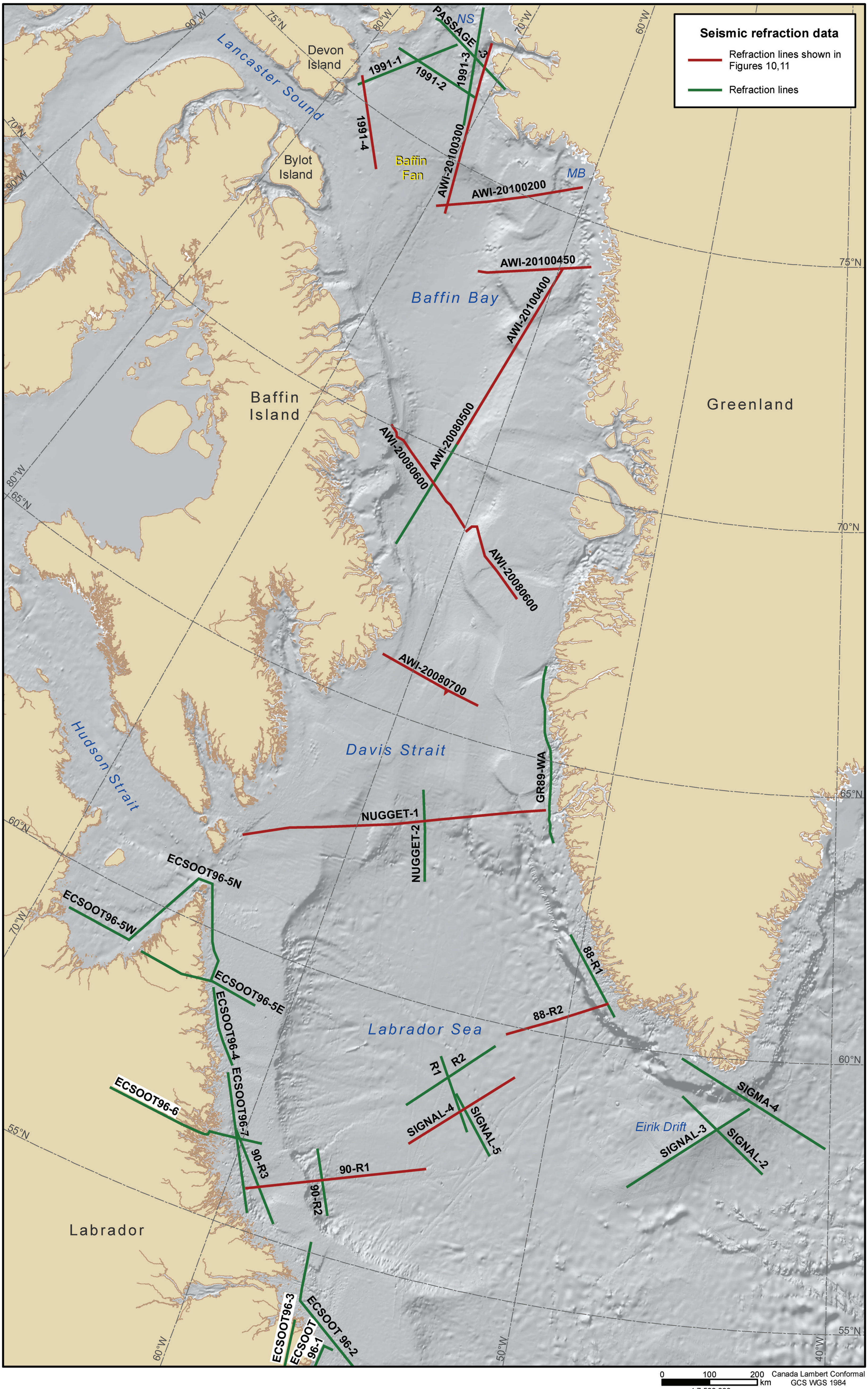
Seismic refraction data
Refraction lines shown in Figures 10,11
Refraction lines
Devon Island
Lancaster Sound
Bylot Island
Baffin Fan
Baffin Bay
Baffin Island
Greenland
Davis Strait
Hudson Strait
Labrador Sea
Labrador
Eirik Drift
NS
MB
PASSAGE-3
1991-1
1991-2
1991-3
1991-4
AWI-20100300
AWI-20100200
AWI-20100450
AWI-20100400
AWI-20080500
AWI-20080600
AWI-20080700
GR89-WA
NUGGET-1
NUGGET-2
ECSOOT96-5N
ECSOOT96-5W
ECSOOT96-5E
ECSOOT96-4
ECSOOT96-7
ECSOOT96-6
ECSOOT96-3
ECSOOT 96-1
ECSOOT 96-2
88-R1
88-R2
R1
R2
SIGNAL-4
SIGNAL-5
SIGMA-4
SIGNAL-3
SIGNAL-2
90-R1
90-R2
90-R3
0 100 200 km
1:7 500 000
Canada Lambert Conformal
GCS WGS 1984

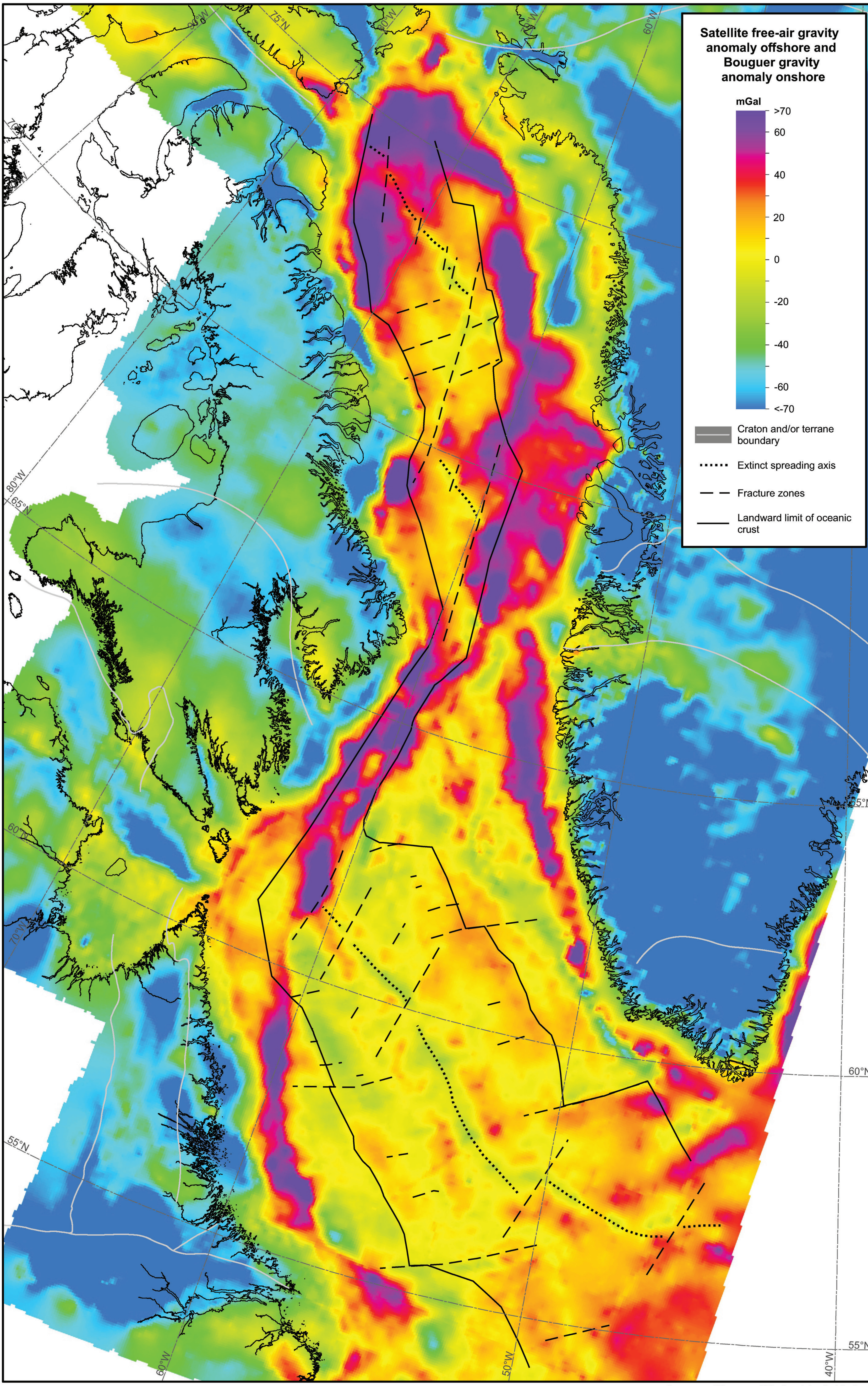
Satellite free-air gravity anomaly offshore and Bouguer gravity anomaly onshore
mGal
>70
60
40
20
0
-20
-40
-60
<-70
Craton and/or terrane boundary
Extinct spreading axis
Fracture zones
Landward limit of oceanic crust
75°N
70°N
65°N
60°N
55°N
80°W
70°W
60°W
50°W
40°W
0
100
200
km
1:7 500 000
Canada Lambert Conformal
GCS WGS 1984

Figure 4. Satellite free-air gravity anomaly at sea and Bouguer gravity anomaly on land (*after* Oakey et al., 2001e, f, g, h). *See* Figure 1 for nomenclature associated with the onshore and offshore features of the Labrador–Baffin Seaway.

data points or values from nonsedimentary units (e.g. basement or volcanic rocks). Although the log and checkshot data may provide the best results near individual wells, they are limited to the upper 3000 to 4500 m of the sedimentary column and are more difficult to extrapolate regionally than the RWAR data. The ability of the derived time-depth functions to accurately predict depths to key horizons was assessed in both the Davis Strait and Labrador Shelf regions by comparing results to measured well depths. The time-depth relationships from the different data sets were compared for consistency and estimates of possible errors.

In Baffin Bay, there were no released wells available for this analysis, except for Ocean Drilling Program site ODP 645, which is relatively shallow and for which no high-quality sonic-log data are available. Therefore, high-quality RWAR data collected since 2000 were used to determine sediment-velocity variations with depth and position along the refraction lines (*see* Fig. 3, all lines with 'AWI' prefixes, except line AWI-20080700; *see also* RWAR data descriptions in 'Crustal structure' section). These RWAR data provided a very consistent time-depth relationship.

In the Davis Strait region, several data sets were available; RWAR data (NUGGET lines and line AWI-20080700; Fig. 3), checkshot surveys and sonic logs were separately used to derive and compare time-depth relationships. Results for the three data sets in Davis Strait show more divergence (up to 600 m at 4000 m depth), which is addressed further in Keen (2019). This is partly a result of the geographical distribution of the wells versus the RWAR data, and perhaps also reflects structural complexity along with varying amounts of erosion during times of uplift in this region (Japsen et al., 2012). As the RWAR seismic and checkshot results are very similar, the checkshots were used for time-depth conversion.

In the Labrador Sea, the focus was mainly on the Labrador Shelf, where checkshots and sonic logs from 21 wells were analyzed. The checkshot results, shown in Figure 9, are almost identical to the sonic-log results (not shown; *see* Keen (2019)). The Labrador Sea curve of Li et al. (2015) is also shown, which was derived using additional sonobuoy data in the deep-water Labrador Sea Basin. This curve diverges from the checkshot results by about 250 m within the upper 5000 m depth range. The RWAR data in this region are sparse and do not provide sufficiently high-resolution results within the sediments to derive a separate time-depth curve (*see* 'Seismic refraction data' section); however, they were used for comparison at depths greater than those observed in the wells. The RWAR depths to basement match the checkshot time to depth results within about 500 m, when the latter are extrapolated to depths of 5 to 9 km (Keen, 2019). Based on this analysis, the checkshot results were used in the time-depth conversion.

The results are expressed as the best-fitting, second-degree polynomial: $z = a+bt+ct^2$ (where z = depth and t is the one-way reflection time). Table 1 shows the resulting constants for the time-depth functions and indicates which data set was used to derive each of them. Figure 9 shows a comparison of a subset of the time-depth curves for all three subregions (*see* Keen (2019) for more details).

The difference between the predicted depths and those measured at the wells gives root mean-square errors of 128 m for the Labrador margin and 205 m for the Davis Strait checkshots. The resulting maps display two junctures on either side of Davis Strait, indicating the three subregions where these different velocity functions were applied (*see* inset maps in Fig. 7, 8). Features compared across these junctures match up well, thus providing an additional degree of confidence in the method used for depth conversion. There are a few mismatches along the international boundary; these relate primarily to differences in distribution of multichannel seismic reflection data (Fig. 2) and data quality on either side of the boundary.

Results

Basement depths range from 0 to 100 m near the coast to a maximum depth of about 16 000 m (approximately 15 000 m of sediment infill) offshore northwestern Greenland in the Melville Bay Graben (Fig. 7, 8). This graben averages about 14 000 m depth and contains substantially thicker sediments than elsewhere within the region (it should be noted that the scale bar is restricted). Other major sedimentary depocentres occur in the region, most notably in the Hopedale and Saglek basins (Balkwill, 1987) and the Baffin Fan (Harrison et al., 2011). There is a moderate degree of asymmetry across the entire region, but this is most striking in the Labrador Sea, where deep basins lie predominantly along the Canadian margin.

Shallow basement platforms (generally <3500 m) line the coastline, extending an average distance of around 100 km offshore (Fig. 7). Off northern Labrador and northwestern Greenland, the basement dips steeply into deep, nearshore grabens. Basement also dips steeply into Scott and Buchan grabens along the central Baffin Island margin, although these are shallower and narrower than the others. Along the edges of the Labrador Sea, the platform is relatively straight and narrow compared to that along Davis Strait and Baffin Bay. In the south-central Labrador Sea, there is less sediment cover over oceanic crust than in the northern Labrador Sea region adjacent to Hudson Strait, where there was an ample source of sediment from the continent (Sears, 2013). In Baffin Bay, there is both a deep basement and thick sedimentary package overlying oceanic crust, some of which is sourced from Lancaster Sound (the Baffin Fan) and other continental regions to the north (Harrison et al., 2011).

In the centre of the Labrador Sea, a thin, linear basement low outlines the location of the buried and extinct seafloor-spreading axis (Fig. 8). Similarly, in central Baffin Bay, deeper, thicker sediments mark both the axis and a major transform fault (64°W fracture zone (FZ)). These features appear less continuous than in the Labrador Sea, largely due to poor data coverage in Baffin Bay. In Davis Strait, basement is shallow and irregular in shape, with the thickest depocentre (over 8 km) in the Sisimiut Basin. The northeast-trending Davis Strait high (DSH) is over 400 km long and trends in the direction of the Ungava Fault Zone (UFZ; Oakey and Chalmers, 2012). Several roughly circular basement highs (Hecla, Maniitsoq, and Gjoa) are situated in southeastern Davis Strait; these may be volcanic eruption centres (Sørensen, 2006).

The underlying position of the shallow-basement platform is mirrored to a certain extent in the bathymetry (Fig. 3) except, most notably, in northern Baffin Bay and the east of Hudson Strait. In these regions, the bathymetric shelf edge (approximately 1000 m) extends over 100 km further offshore than the shallow-basement platform and a thick wedge of sediments obscures the underlying basement configuration. Numerous troughs cut across the bathymetric shelves, a result of Pleistocene glaciation, and now reach water depths between 500 to 1000 m.

Labrador Sea

Deep basement and thick sediments form a distinct linear and gently curving trend along the Labrador margin. The Okak and Cartwright arches (Fig. 7, 8) form promontories along this margin and bound the Hopedale Basin depocentre. These offsets align with prominent geological terrane boundaries identified onshore; the Grenville Front underlies the Cartwright Arch and shear zones in the Makkovik Province extend toward the central Hopedale embayment, where there are nine boreholes and several gas discoveries (Dickie et al., 2011). The southern Hopedale Basin depocentre is shallower than the northern portion and the basement platform widens southward onto the Cartwright Arch. East and south of the arch, the depocentre shallows significantly and connects with other basins to the south of the study area.

North of the Okak Arch lies the Saglek Basin, the depocentre of which appears to be the deepest in the Labrador Sea region. The main depocentre of the Saglek Basin cuts across the inner and outer shelf (Keen et al., 2012), whereas the main depocentre in the Hopedale Basin lies along the outer shelf. A region of deep basement extends seaward of the main Saglek Basin depocentre, possibly overlying ocean crust in a setting reminiscent of the Baffin Fan in northern Baffin Bay. Southeast of the Hudson Fracture Zone, basement shallows onto oceanic crust.

Figure 5. Filtered Bouguer gravity anomaly with a 200 km high-pass filter generated for this study. *See* Figure 1 for nomenclature associated with the onshore and offshore features of the Labrador–Baffin Seaway.

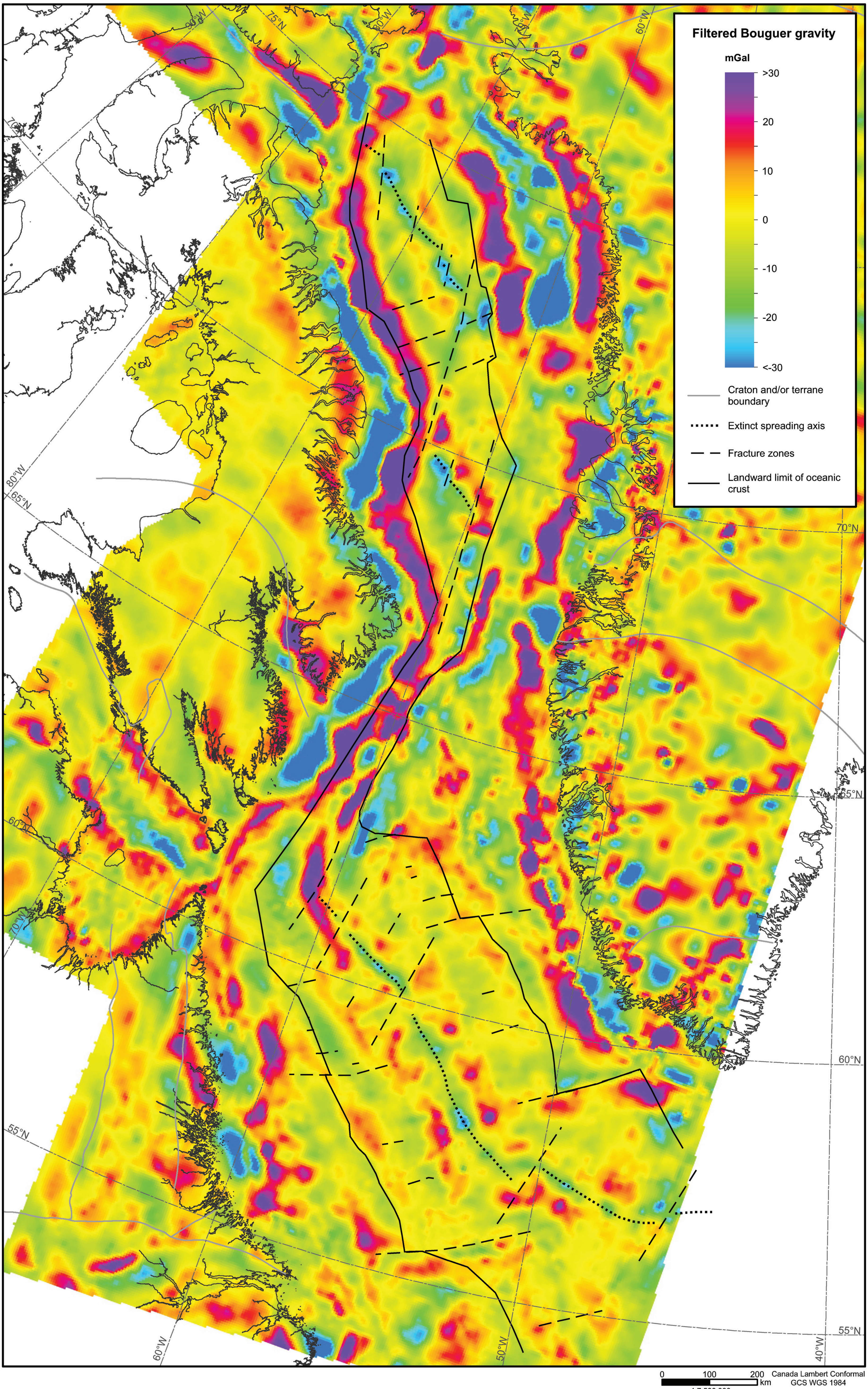
Filtered Bouguer gravity
mGal
>30
20
10
0
-10
-20
<-30
Craton and/or terrane boundary
Extinct spreading axis
Fracture zones
Landward limit of oceanic crust
70°N
65°N
60°N
55°N
80°W
75°N
60°W
50°W
40°W
0
100
200
km
1:7 500 000
Canada Lambert Conformal
GCS WGS 1984

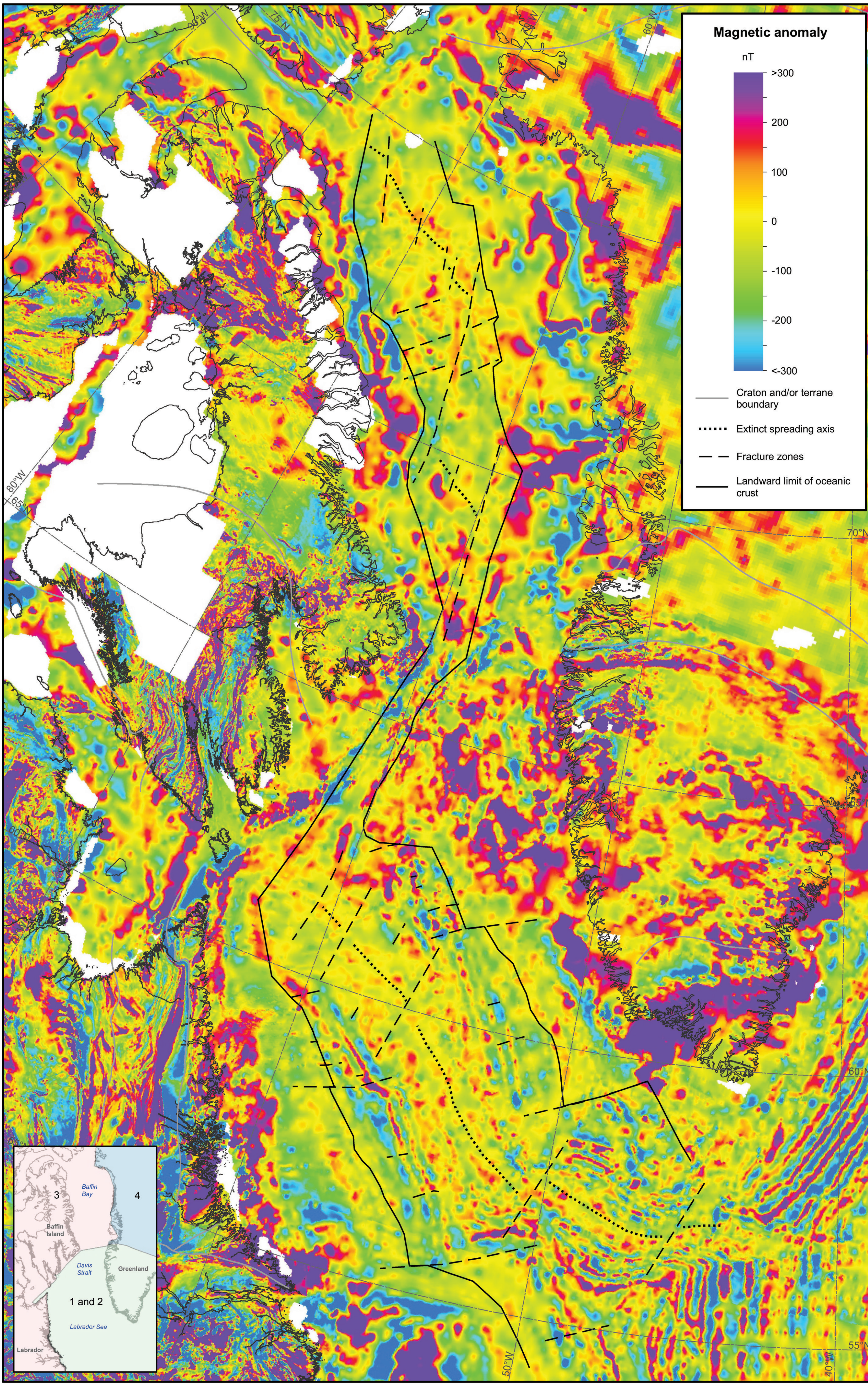
Magnetic anomaly
nT
>300
200
100
0
-100
-200
<-300
Craton and/or terrane boundary
Extinct spreading axis
Fracture zones
Landward limit of oceanic crust
75°N
70°N
65°N
60°N
55°N
80°W
60°W
50°W
40°W
Baffin Bay
Baffin Island
Davis Strait
Greenland
Labrador Sea
Labrador
3
4
1 and 2
0
100
200
km
1:7 500 000
Canada Lambert Conformal
GCS WGS 1984

Figure 6. Magnetic-anomaly map compilation. Inset map shows the data sets used: 1) Oakey and Dehler (1998) merged with 2) Oakey et al. (2001i, j) at 2 km grid spacing for the Labrador Sea, Davis Strait and southern Greenland; 3) Miles and Oneschuk (2016) at 1 km grid spacing for Baffin Bay and eastern Canada; and 4) Verhoef et al. (1996) at 7 km grid spacing for northern Greenland.

East of the main depocentres in Hopedale and Saglek basins, basement shallows onto oceanic crust and sedimentary cover becomes thin, reaching less than 1000 m in the southeastern part of the Labrador Sea. Along the eastern side of the Labrador Sea, the basement platform forms a gently curving, narrow, shallow feature that parallels the southwestern Greenland coastline. Sediments are thin along this margin, reaching about 4000 m in a few deeper grabens within the elongated Paamiut South Basin.

Davis Strait

Unlike Baffin Bay to the north and Labrador Sea to the south, the depth-to-basement and sediment thickness in western Davis Strait are much shallower and thinner, respectively (Fig. 7, 8). North of Hudson Strait, the basement platform widens northeastward toward the mouth of Cumberland Sound, where it swings north-northwest, forming the Lady Franklin Arch. Basement deepens southeast of the platform into the northern Saglek Basin, which contains the thickest sediments in the region (8000 m in the south) and is the site of the Hekja O-71 discovery well (Fig. 2). Farther north, off Cumberland Sound, the basement platform trends northerly and lies inboard of most of the seismic coverage. The northerly trending Cumberland Basin (Balkwill, 1987) forms a relatively small, shallow depocentre off the mouth of Cumberland Sound.

The eastern edge of the Cumberland Basin is bounded by a volcanic high that roughly parallels the north-northeast-trending Davis Strait high farther to the east. This trend links with the shallow basement offshore of Cape Dyer, where volcanic rocks are found near the seabed (Skaarup et al., 2006). The Davis Strait High is a prominent, shallow, fault-bounded Precambrian ridge 20 to 80 km wide, which extends over 400 km through central Davis Strait. Offshore from the Cumberland Peninsula, between the Davis Strait High and the basement platform, lies a narrow, unnamed basin, which extends north-northeast for about 200 km.

Along the southeastern edge of the Davis Strait High is the Lady Franklin Basin, which contains sediments more than 5000 m thick. The thickest sediments in the region, over 8000 m, are found in the Sisimiut Basin, east of the northern Davis Strait High. Sediments in the basins along the eastern edge of Davis Strait, the Fylla Structural Complex, and the Nuuk Basin locally reach over 5000 m in thickness. Thin sediments (<1000 m) cover the Paleogene volcanic highs (Gjoa, Hecla, and Maniitsoq) and the uplifted western margin west of the Fylla Structural Complex.

Baffin Bay

The basement platform (<3500 m) off central Baffin Island generally forms large continental basement blocks, which step steeply down toward the ocean basin to the east. The margin displays two northwest-trending segments separated by a north-trending segment at Home Bay, which aligns with the north-trending fracture zones in the deep ocean basin (Oakey and Chalmers, 2012). The northwest trend continues as far as the mouth of Lancaster Sound, where the margin then follows a more northerly trend. North of the Buchan Graben, the margin becomes narrow and approaches the coastline, and, in general, the Baffin Island margins are narrow by comparison with their West Greenland conjugates.

The thick Baffin Fan, mapped by Harrison et al. (2011) is located offshore Devon Island. They interpreted the fan as comprising over 10 000 m of relatively young, Eocene to Pleistocene sedimentary rocks that onlap oceanic crust. Sediments are relatively thin along the western Baffin Bay continental margin, except for the Baffin Fan. Basins are also much smaller compared to those on the eastern side of Baffin Bay. Melville Bay Graben and Kivioq Basin, which contain in excess of 10 000 m of sediment, are separated by ridges, which are covered by less than 1000 m of sediment. South of these depocentres, shallow basement is related to thick volcanic rocks, which cover a large region offshore of Disko Island (Gregersen and Bidstrup, 2008; Gregersen et al., 2013).

Crustal structure

The full width of the continental margins off Labrador and southwestern Greenland are only imaged by one seismic refraction line each. Both lines are roughly conjugate and were acquired in 1990 (line 90-R1 off Labrador) and 1988 (line 88-R2 off Greenland), and have a low lateral resolution due to the limited number of seismic receivers that were used. The lack of well-resolved crustal-velocity models along the margins resulted in some uncertainty about the breakup age in the Labrador Sea, which was based primarily on the interpretation of magnetic anomalies. Initially, Roest and Srivastava (1989) proposed magnetic chron C33 to be the oldest seafloor-spreading anomaly. Later, based on magnetic modelling along seismic reflection lines, Chalmers and Laursen (1995) concluded that chron C27n was the oldest anomaly. Since then, knowledge on magma-poor continentalmargins has increased significantly. Sibuet et al. (2007) documented that the serpentinization process during mantle exhumation in the continent-ocean transition zone can create magnetic anomalies similar to seafloor-spreading anomalies. Serpentinized mantle is documented on both margins bounding the Labrador Sea (Chian and Louden, 1994; Chian et al., 1995a) and the magnetic anomaly interpreted as chron C33 (Roest and Srivastava, 1989) is within the zone of exhumed and serpentinized mantle (Fig. 10a). The adjacent magnetic anomaly is interpreted as chron C31 and is located close to the seaward limit of the region with serpentinized mantle (Chian and Louden, 1994; Chian et al., 1995a). As both refraction lines have a rather low lateral resolution due to a wide receiver spacing of 40 to 50 km, there remains some uncertainty with respect to the exact location of the initial oceanic crust. Keen et al. (2018a) looked at additional modern seismic reflection lines and potential-field data; they interpreted the location of chron C31 as corresponding roughly with the transition from exhumed mantle to the initial oceanic crust. Thus, chron C31 (69 Ma using the time scale of Ogg (2012)) seems to be the best approximation for the start of seafloor spreading in the Labrador Sea. Furthermore, Keen et al. (2018a) interpreted the crust that formed between chrons C31 and C27 as embryonic oceanic crust (cf. Gillard et al., 2017), where the crust was emplaced in a more random and less vigorous way than in the later stage of steady-state seafloor spreading.

The thickness of the oceanic crust in the Labrador Sea rarely exceeds the global average of 7 km (White et al., 1992), apart from the northern area, where 14 km thick crust is observed on NUGGET line 2 (Gerlings et al., 2009). This area is influenced by the widespread Paleocene and Eocene volcanism observed in the Davis Strait area in association with the formation of the North Atlantic Igneous Province (Storey et al., 2007a, b). This contrasts with the 3.5 km thick crust (Fig. 10b) that was formed during Eocene ultraslow seafloor spreading in the vicinity of the now extinct spreading axis (Osler and Louden, 1992, 1995; Delescluse et al., 2015). Delescluse et al. (2015) also imaged an oceanic core complex on early Eocene crust and underlain by partially serpentinized mantle (Fig. 10b). These complexes develop by slow and asymmetric spreading, when lower crustal and mantle rocks are unroofed along oceanic detachment faults (MacLeod et al., 2009).

The nature of the crust underlying Davis Strait was disputed for a long time. Based on a seismic refraction profile, Keen and Barrett (1972) suggested the presence of oceanic crust 20 km thick in the centre of the strait. In contrast, Chalmers and Pulvertaft (2001) concluded from seismic reflection records and the age of drilled sediments that there should be continental crust in the central part of Davis Strait. The first modern seismic refraction line was acquired in southern Davis Strait through Hekja O-71, Ralegh N-18, Gjoa G-37, and Qulleq-1 (NUGGET-line 1; Fig. 2, 10c), and here Funck et al. (2007) reported

Figure 7. Depth-to-basement map from the interpretation of seismic reflection data, showing oceanic and onshore geological features. The map areas of the three subregions shown in the inset were converted to depth using different velocity functions. The Greenland part of the map is based on work by Gregersen et al. (2019) and the Canadian part is from this study. Major Precambrian boundaries are *modified from* St-Onge et al. (2009). *See* Figure 1b for abbreviations of feature names.

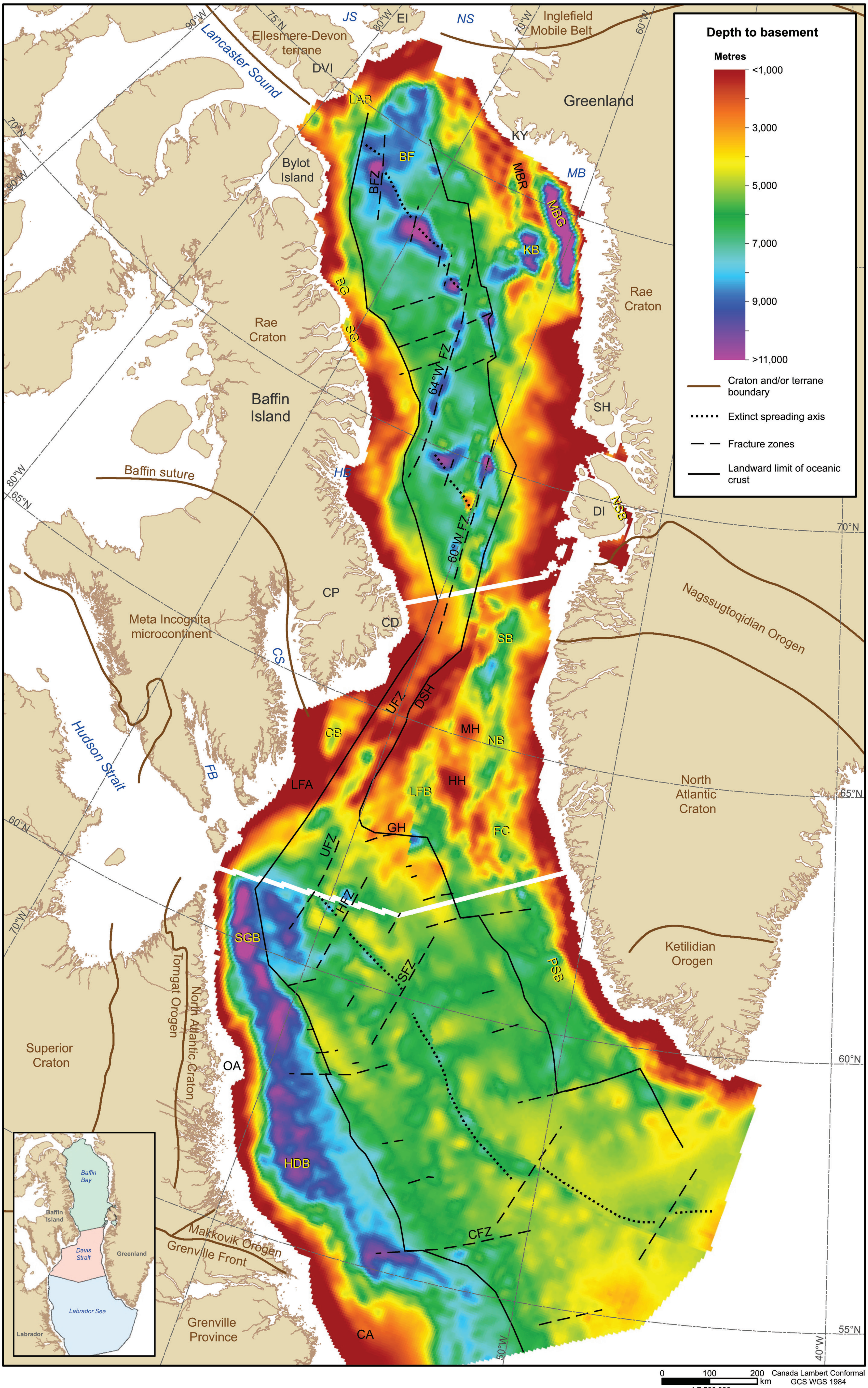
Depth to basement
Metres
<1,000
3,000
5,000
7,000
9,000
>11,000
Craton and/or terrane boundary
Extinct spreading axis
Fracture zones
Landward limit of oceanic crust
Lancaster Sound
Ellesmere-Devon terrane
DVI
EI
JS
NS
Inglefield Mobile Belt
Greenland
KY
MB
MBR
MBG
KB
LAB
BF
BFZ
Bylot Island
BG
SG
Rae Craton
Baffin Island
64°W FZ
60°W FZ
SH
DI
NSB
HB
Baffin suture
CP
CD
Meta Incognita microcontinent
CS
Nagssugtoqidian Orogen
SB
UFZ
DSH
CB
MH
NB
HH
LFA
LFB
GH
FC
Hudson Strait
FB
North Atlantic Craton
UFZ
HFZ
SGB
SFZ
PSB
Ketilidian Orogen
Torngat Orogen
North Atlantic Craton
Superior Craton
OA
HDB
CFZ
Makkovik Orogen
Grenville Front
Grenville Province
CA
Baffin Bay
Baffin Island
Davis Strait
Greenland
Labrador Sea
Labrador
90°W
75°N
80°W
70°W
60°W
70°N
65°N
60°N
55°N
50°W
40°W
0
100
200
km
1:7 500 000
Canada Lambert Conformal
GCS WGS 1984

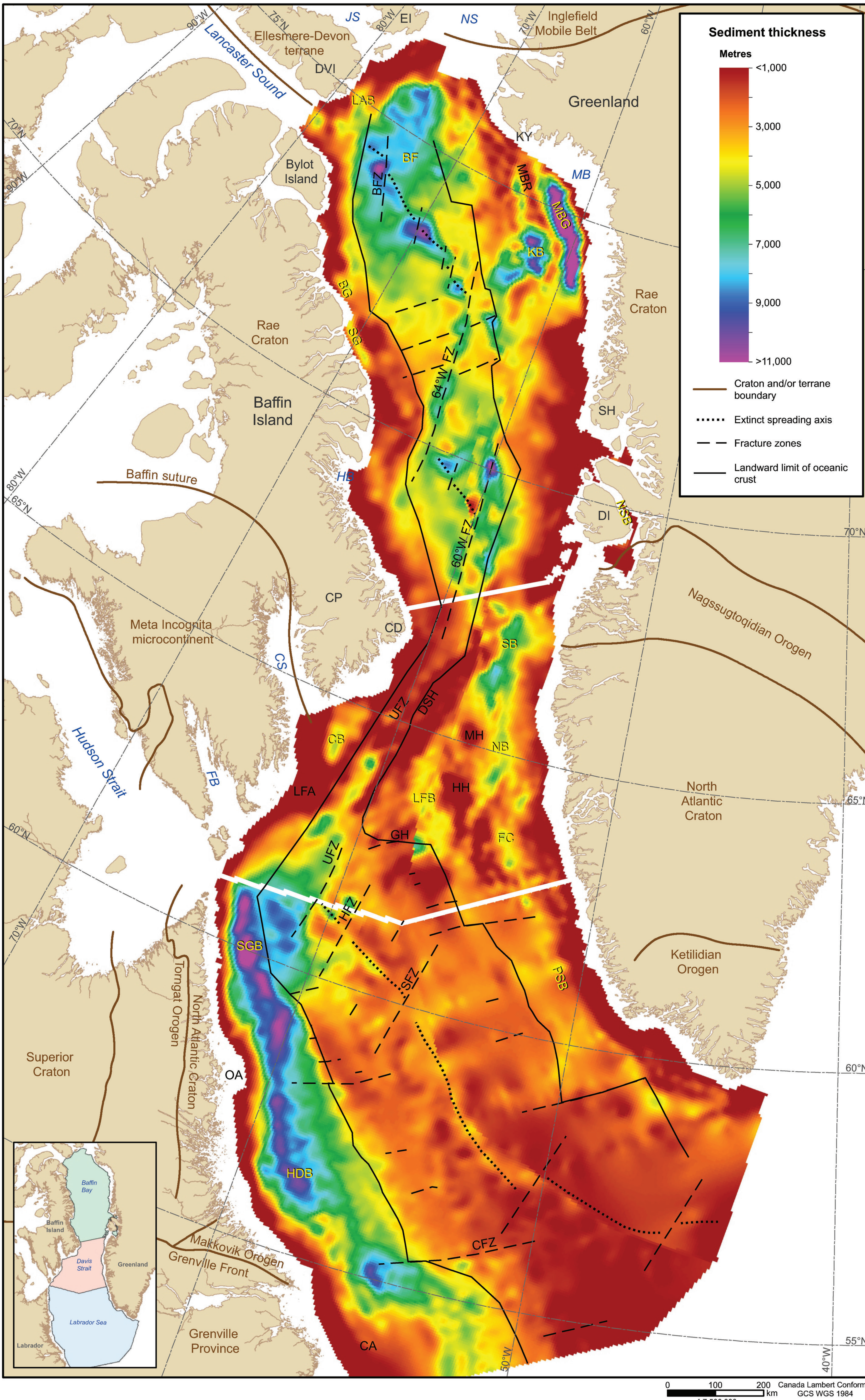
Sediment thickness
Metres
<1,000
3,000
5,000
7,000
9,000
>11,000
Craton and/or terrane boundary
Extinct spreading axis
Fracture zones
Landward limit of oceanic crust
Ellesmere-Devon terrane
DVI
EI
JS
NS
Inglefield Mobile Belt
Lancaster Sound
Greenland
LAB
KY
BF
BFZ
MBR
MB
MBG
KB
Bylot Island
Rae Craton
BG
SG
Rae Craton
64°W FZ
Baffin Island
SH
Baffin suture
HB
DI
NSB
60°W FZ
Meta Incognita microcontinent
CP
CD
CS
SB
Nagssugtoqidian Orogen
Hudson Strait
UFZ
DSH
CB
MH
NB
FB
LFA
HH
LFB
North Atlantic Craton
GH
FC
UFZ
HFZ
SGB
SFZ
PSB
Ketilidian Orogen
Torngat Orogen
North Atlantic Craton
Superior Craton
OA
HDB
CFZ
Makkovik Orogen
Grenville Front
Grenville Province
CA
Baffin Bay
Baffin Island
Davis Strait
Greenland
Labrador Sea
Labrador
75°N
70°N
65°N
60°N
55°N
90°W
80°W
70°W
60°W
50°W
40°W
0
100
200
km
1:7 500 000
Canada Lambert Conformal
GCS WGS 1984

Figure 8. Sediment-thickness map from the interpretation of seismic reflection data, showing oceanic and onshore geological features. The map areas of the three subregions shown in the inset were converted to depth using different velocity functions. The Greenland part of the map is based on work by Gregersen et al. (2019) and the Canadian part is from this study. Major Precambrian boundaries are *modified from* St-Onge et al. (2009). *See* Figure 1b for abbreviations of feature names.

a zone 140 km wide with igneous crust bordered by thinned continental crust on either side. Both the igneous crust and the adjacent continental crust are underlain by a high-velocity, lower crustal layer up to 8 km thick, with velocities of 7.4 km/s. In the western part of the igneous crust, seaward-dipping reflectors are recognized and indicate a volcanic overprint of the northernmost continental margin in the Labrador Sea. Keen et al. (2012) showed that this may extend south as far as the Okak Arch along the Labrador margin. The Paleocene and Eocene volcanic activity is also imaged by sequences of volcanic rocks up to 5 km thick, partly interbedded with sediments and underlain in places by prevolcanic sediments. The uppermost section of the volcanic unit was drilled at three locations along the refraction line (wells Hekja O-71, Ralegh N-18, and Gjoa G-37 in Fig. 10c; Canterra Energy Ltd., 1982; Klose et al., 1982).

The high-velocity lower crust (HVLC) in southern Davis Strait is restricted to the areas with thinned continental or igneous crust (Fig. 10c), but is not observed beneath the thicker crust off Greenland (Funck et al., 2007). To explain the distribution of the high-velocity lower crust, Funck et al. (2007) utilized the explanation presented by Nielsen et al. (2002), in which material related to the Iceland plume is guided by the relief at the base of the lithosphere. Plume material is channelled along lithospheric thin spots and extracted melt is then ponded as high-velocity lower crust beneath the original crust. Where the continental crust is thicker, such as off Greenland, the lithosphere is thicker as well, and hence, the plume material did not propagate into that zone. Contradicting this model is the observation that a high-velocity lower crust up to 10 km thick exists beneath a refraction line parallel to the coast of Greenland in Davis Strait (GR89-WA; Gohl and Smithson, 1993), which is only 10 km away from the eastern end of NUGGET line 1. The seismic resolution along the coast-parallel line is low as there were only four onshore seismic receivers with a lateral offset of about 20 km to the airgun shots offshore. Out-of-plane reflections from the Moho may mimic a double reflection, which is typical for a high-velocity lower crust with large impedance contrasts both at the top and base of the layer; however, this is difficult to verify as these effects cannot be incorporated in the two-dimensional modelling programs. A constrained three-dimensional gravity inversion for the Labrador Sea (Welford and Hall, 2013) reveals the Moho at a depth that corresponds to the top of the high-velocity lower crust of Gohl and Smithson (1993), which would support the hypothesis of an absent high-velocity lower crust.

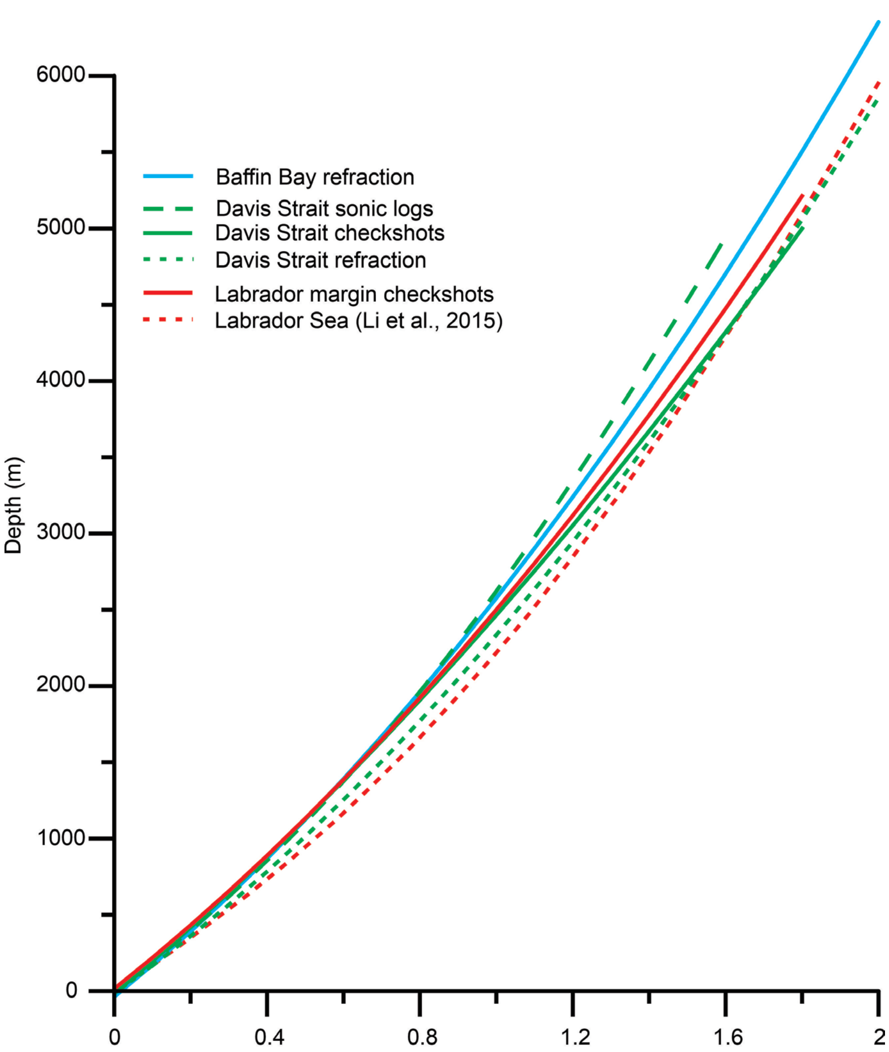

Figure 9. Comparison of time-depth functions for Baffin Bay, Davis Strait, and the Labrador Sea. Checkshot surveys, sonic logs, and wide-angle seismic-velocity data sets were used to define these functions (parameters are listed in Table 1). The time-depth curve for the central Labrador Sea *after* Li et al. (2015) is also shown. The functions selected as best representing the time-depth distribution in each of these three subregions are shown as solid lines.

Although the plume hypothesis is widely used to explain the magmatism in Davis Strait (Nielsen et al., 2002; Funck et al., 2007; Storey et al. 2007b), other models exist. For example, Peace et al. (2017) proposed that a thick continental lithospheric keel of orogenic origin beneath Davis Strait blocked the northward-propagating Labrador Sea rift, which then resulted in locally enhanced magmatism. Foulger and Anderson (2005) attributed the enhanced magmatism to high local mantle fertility from subducted Iapetus oceanic crust trapped in the Laurasian continental-mantle lithosphere within the collision zone associated with the Caledonian suture.

There is no evidence for oceanic crust in Davis Strait that formed by normal seafloor-spreading processes, although during the first phase of major plate motions during the Paleocene, there may have been oblique spreading in the region of the Ungava Fault Zone, coupled with hotspot activity. Funck et al. (2007) proposed that the Ungava Fault Zone acted as a leaky transform fault during phases of transtension, and the observed igneous crust is explained with the strait being part of a transform margin, as well as the site of hotspot activity. Palynological evidence from interbedded and overlying sedimentary rocks places the basalts within the Gjoa G-37, Ralegh N-18, and Hejka O-71 wells as Paleocene in age (Danian–Thanetian; Nøhr-Hansen et al., 2016). This is consistent with the observation that the seaward-dipping reflectors and thick igneous crust off the northern Labrador margin (Keen et al., 2012) are associated with magnetic chron C27n. In the central part of Davis Strait, Suckro et al. (2013) reported a zone 60 km wide with increased crustal velocities in the area of the Ungava Fault Zone (Fig. 10d), which was interpreted as intruded continental crust or new igneous crust that can be correlated with the igneous crust on NUGGET line 1 in southern Davis Strait (Fig. 10c). Similarly, Funck et al. (2012a) observed a 25 km wide zone with igneous crust in northern Davis Strait on seismic line AWI-20080600 (Fig. 10e). Here the crust is up to 23 km thick, including a sequence of volcanic rocks up to 3 km thick. In the nearby Hellefisk-1 well (Fig. 2), volcanic rocks have a Paleocene age (Larsen et al., 2016); the well is located on thinned continental crust that is underlain by a high-velocity lower crust. The northward movement of Greenland relative to North America started at magnetic chron C25n (Oakey and Chalmers, 2012) in the late Paleocene, which postdates the lava flows at the Hellefisk-1 well by 2 to 3 Ma (Larsen et al., 2016). Hence, some of the interpreted igneous crust in the area of the Ungava Fault Zone may have formed prior to the development of the transform margin in Davis Strait.

Apart from some older lines in the northernmost Baffin Bay and Nares Strait (Jackson and Reid, 1994; Reid and Jackson, 1997; Funck et al., 2006), very little was known about the crustal structure in Baffin Bay until two major seismic refraction experiments were carried out in 2008 and 2010. The line coverage was better on the continental margin of Greenland than on the conjugate Canadian side; however, the new data greatly improved the understanding of the opening of Baffin Bay. The new models are presented here, from south to north, and include some remarks on possible alternative interpretations of the velocity models.

Table 1. Parameters describing the time-depth conversion for various data sets.

Region	Data set	a*	b*	c*
Labrador	All lithologies, sonic logs	9.076	1779.96	634.21
Labrador	Sand only, sonic logs	29.307	1543.34	1136.006
Labrador	Checkshots	-14.562	1983.42	502.628
Davis Strait	All lithologies, sonic logs	-1.018	1822.47	800.247
Davis Strait	Checkshots	-18.389	2101.92	381.189
Davis Strait	RWAR (NUGGET 1 and 2 and AWI-20080700)	-16.853	1766.21	585.583
Baffin Bay	RWAR (AWI-20100200, ..300, ..400, ..450, AWI-20080500, ..600)	-39.728	2037.08	579.745

*a, b, c are constants in 2nd order polynomial $z=a+bt+ct^2$, where z is depth in metres and t is one-way traveltime in seconds.

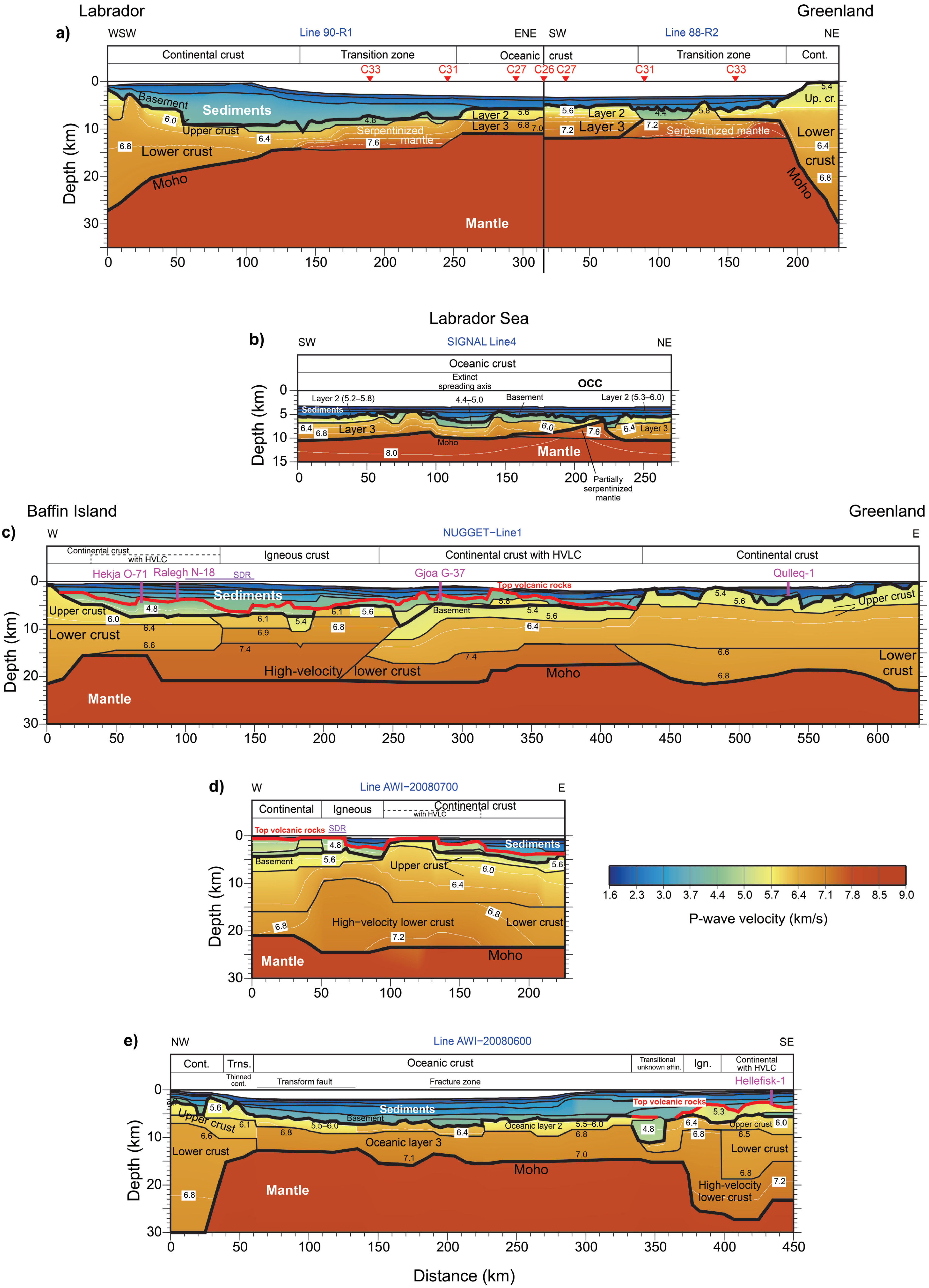

Figure 10. P-wave velocity models for the Labrador Sea and Davis Strait: **a)** conjugate seismic refraction profiles 90-R1 and 88-R2 across the Labrador and southwestern Greenland continental margins, respectively (velocity models *after* Chian and Louden (1994) and Chian et al. (1995a); red triangles mark location of interpreted magnetic anomalies *after* Roest and Srivastava (1989)), and conjugate profiles merged at magnetic chron C26; **b)** seismic-refraction profile 4 of the SIGNAL experiment across the extinct spreading axis in the Labrador Sea (*after* Delescluse et al., 2015); **c)** line 1 of the NUGGET experiment (Funck et al., 2007) in southern Davis Strait; **d)** seismic line AWI-20080700 (Suckro et al., 2013) in central Davis Strait; **e)** seismic line AWI-20080600 (Funck et al., 2012a) in northern Davis Strait and southern Baffin Bay. Velocities are given in kilometres per second and white lines are velocity contours with a spacing of 0.4 km/s. Location of seismic-refraction profiles is shown on Figure 3 and wells on Figure 2. affin. = affinity; Cont. = continental crust; HVLC = high-velocity lower crust; Ign. = igneous crust; OCC = oceanic-core complex; SDR = seaward-dipping reflectors; Trns. = transition zone; Up. Cr. = Upper crust.

The southernmost seismic line (AWI-20080600 in Fig. 10e) in Baffin Bay was discussed above in reference to Davis Strait, but the line crosses southern Baffin Bay parallel to the interpreted location of the extinct spreading axis (Oakey and Chalmers, 2012) at a distance of 40 km. Funck et al. (2012a) observed oceanic crust with a variable thickness along the line. In the southeast, the oceanic crust is 9 km thick, which is more than the global average of 7 km (White et al., 1992), indicating an ample magma supply. This may be related to the proximity of the area to the Davis Strait region with its widespread Paleogene magmatism. Thinner oceanic crust is only observed within a fracture zone (6 km) and in the northwest, where the crust is 7 km thick in a zone that is interpreted as a north-south–oriented transform fault based on gravity data (Chalmers and Pulvertaft, 2001; Funck et al., 2012a). The Baffin Island continental margin is only poorly covered by the available seismic data, but what evidence is available indicates a sharp transition between oceanic and thinned continental crust. The crustal thickening occurs over a very narrow zone of 30 km, which Funck et al. (2012a) interpreted as being compatible with a transform margin, where major crustal thinning often occurs over lateral distances of less than 20 to 30 km (e.g. Edwards et al., 1997). The crust in the narrow transition zone is highly faulted and displays velocities typical for continental crust.

Figure 11a shows the northern part of the velocity model that Suckro et al. (2012) developed from the data along seismic lines AWI-20080500 and AWI-20100400. The profile did not reach continental crust at the Baffin Island margin, which is why the southern portion of the line is not shown here. The oceanic crust along the line has an average thickness of 7.5 km (Suckro et al., 2012). Between kilometre 380 and 500 at the Greenland margin, Suckro et al. (2012) interpreted a transition zone that thickens from 7.5 to 17 km. Volcanic material overlies the transition zone, including some seaward-dipping reflectors (Block et al., 2012; Suckro et al., 2012). Lower crustal velocities in the transition zone reach 7.2 km/s, which Suckro et al. (2012) interpreted to be related to mafic intrusions. Northward of kilometre 500, three crustal layers can be distinguished with a total thickness of up to 25 km overlain by volcanic rocks in most areas. Although Suckro et al. (2012) interpreted the lower crust in this zone as continental (yellow dashed line in Fig. 11a), it could equally well be a zone of high-velocity lower crust; there are several observations that support such an alternative interpretation. First, the model indicates velocities of 6.9 to 7.0 km/s in the lower crust, which would correspond to a density of 2940 kg/m^3 using the empirical velocity-density relationship of Ludwig et al. (1970). In the final gravity model, however, Suckro et al. (2012) increased the density in that zone to 3050 kg/m^3, which would correspond to a velocity of 7.25 km/s; such a velocity would clearly be categorized as high-velocity lower crust. Second, velocities in the lower crust are not well constrained as there are no observed lower crustal refractions. Hence, the velocities solely rely on the moveout time of Moho reflections, which are much less sensitive to velocity changes than refractions. Furthermore, there are several strong reflections from the top of the lower crust, which is surprising as the velocity model only shows a velocity increase of 0.15 km/s across this boundary. Such strong reflections would indeed be more compatible with those from the top of a high-velocity lower crust. It is also unusual to see a substantial amount of extrusive volcanic rocks without any mafic addition at deeper crustal levels. A comparison with the crust in the central part of NUGGET line 1 in southern Davis Strait (Fig. 10c) shows a very good correspondence with volcanic rocks at the top, two crustal layers with very similar velocities to the ones modelled by Suckro et al. (2012), and a high-velocity lower crust the velocity of which is constrained by refractions.

Seismic lines AWI-20080500–AWI-20100400 (Fig. 11a) cross line AWI-20100450 (Fig. 11b) in the Melville Bay Graben. The lower crustal velocities on line AWI-20100450 are 6.6 to 6.9 km/s (Altenbernd et al., 2015) at the intersection, which would argue against the proposed alternative of a high-velocity lower crust on lines AWI-20080500–AWI-20100400, unless only portions of the lower crust are characterized by higher velocities. Such a lateral change may occur at kilometre 670, where a pronounced change in thickness of the lower crust is observed.

Line AWI-20100450 (Fig. 11b) is a dip line along the Melville Bay continental margin that crosses both the Melville Bay Graben and Melville Bay Ridge. The velocity model of Altenbernd et al. (2015) shows a sedimentary infill 11 km thick in the graben, the thickest layer of which (up to 6 km) is interpreted as synrift sediments. On the crossing line (Fig. 11a, AWI-20080500/AWI-20100400), Suckro et al. (2012) have divided this unit into two layers and proposed a composition of sedimentary and volcanic rocks. On the Melville Bay Ridge and its northeastern flank (Fig. 11b), a layer 3 km thick with velocities of 4.5 to 5.2 km/s is present. These velocities are not constrained by refractions as it is a low-velocity zone and Altenbernd et al. (2015) suggested a composition of sedimentary rocks or basalt. The velocities could also be compatible with those found in the Proterozoic Thule Supergroup (Funck et al., 2006).

The continental crust on seismic line AWI-20100450 is divided into three layers (Fig. 11b). Upper crustal velocities change across the Melville Bay Fault from 5.6 to 5.9 km/s in the southwest to 5.8 to 6.2 km/s in the northeast, whereas middle and lower crustal velocities remain unchanged. The Moho depth beneath the shelf is 31 km, shallows to 27 km beneath the Melville Bay Graben, and increases again to 33 km beneath the Melville Bay Ridge. The model is not in isostatic balance between the ridge and the shelf region, but then the Moho is not constrained seismically beneath the shelf. Another way of compensating the isostatic imbalance could be to replace some of the lower crustal root beneath the ridge with mafic material with a higher velocity and density. Similar to seismic lines AWI-20080500 and AWI-20100400, the velocity control in the lower crust is reduced and there are also some observed strong reflections from the top of the lower crust, which could be more compatible with a high-velocity lower crust. In addition, Altenbernd et al. (2015) noticed a velocity increase in the lower crustal layer of the adjacent transition zone, which they think could indicate an intrusion. This zone correlates with a strong positive gravity anomaly immediately to the south, which Whittaker et al. (1997) interpreted as a mafic or ultramafic intrusion. Although there is some indication that there could be a high-velocity lower crust beneath the Melville Bay Ridge, any attempt to reach a more affirmative conclusion would require a careful re-examination of the seismic data.

The transition zone on line AWI-20100450 extends from kilometre 57 to 135 (Fig. 11b) and is composed of two layers with a combined thickness of 7 to 13 km. Outside the area with the possible intrusion, velocities range from 4.8 to 5.2 km/s and 6.2 to 6.5 km/s in the upper and lower layers, respectively. Altenbernd et al. (2015) did not provide a detailed analysis of the continent-ocean transition. They state that the latter does not resemble those of magma-poor margins due to the lack of peridotite ridges and exhumed mantle. On the other hand, they did not observe seaward-dipping reflectors or magmatic underplating typical for magma-rich continental margins apart from a possible lower crustal intrusion. Therefore, they suggested that the margin in this area developed essentially as a magma-poor margin with some magmatic addition related to the Iceland plume.

From kilometre 0 to 57, Altenbernd et al. (2015) interpreted oceanic crust on seismic line AWI-20100450 (Fig. 11b). This interpretation contradicts the plate reconstruction of Oakey and Chalmers (2012), who showed the northeastern half of this zone as transitional crust (from approximately kilometre 27 to 57). For this reason, a second look at the velocity model of Altenbernd et al. (2015) seems worthwhile. There are indeed some lateral changes that may support an alternative interpretation. The velocity model and the coincident seismic reflection data shows a very pronounced lateral change in the basement character. Between kilometre 0 and 25, there is a rough basement morphology (0.7 s two-way traveltime), whereas the basement is fairly smooth between kilometre 25 and 57. A rough oceanic basement is often observed in areas with slow and ultraslow spreading systems with limited magma supply and faults created by extension. Examples for a rough oceanic basement can be found, for instance, in the Eurasia Basin in the Arctic Ocean (Jokat and Micksch, 2004), where it formed by ultraslow spreading and in the initial oceanic crust formed after breakup of the eastern Canadian margin off Nova Scotia (Funck et al., 2004; Lau et al., 2018). This rough oceanic basement off Nova Scotia is adjacent to smoother transitional basement that is interpreted as serpentinized mantle. Hence, the smooth basement on seismic line AWI-20100450 may similarly be serpentinized mantle rather than oceanic crust. A further argument for this is the observed intracrustal reflection between the upper and lower crustal layer. This is not typical for oceanic crust and is indeed not observed in the zone with the rough basement, where the oceanic crust is not disputed.

Another dip line across the Melville Bay continental margin off northwestern Greenland is seismic line AWI-20100200 (Fig. 11c; Altenbernd et al., 2014) approximately 150 km to the north of line AWI-2010450. Within the continental domain, the Moho depth shows little change and varies mostly between 24 and 26 km before it starts to rise more significantly seaward of kilometre 160. Two major sedimentary basins are imaged beneath the shelf: the Kivioq Basin, with a sediment thickness of 5 km, and the Melville Bay Graben, with a sedimentary infill of 11 km. There is no isostatic compensation for the 80 km wide Melville Bay Graben. Instead of a shallower Moho, a slight deepening of the Moho is observed. The velocity model has some problems with fitting the deeper crustal arrivals in the area of the Melville Bay Graben (*see* Fig. 6 in Altenbernd et al. 2014). The picked (observed) arrival times for the Moho (the P_mP phase) in the

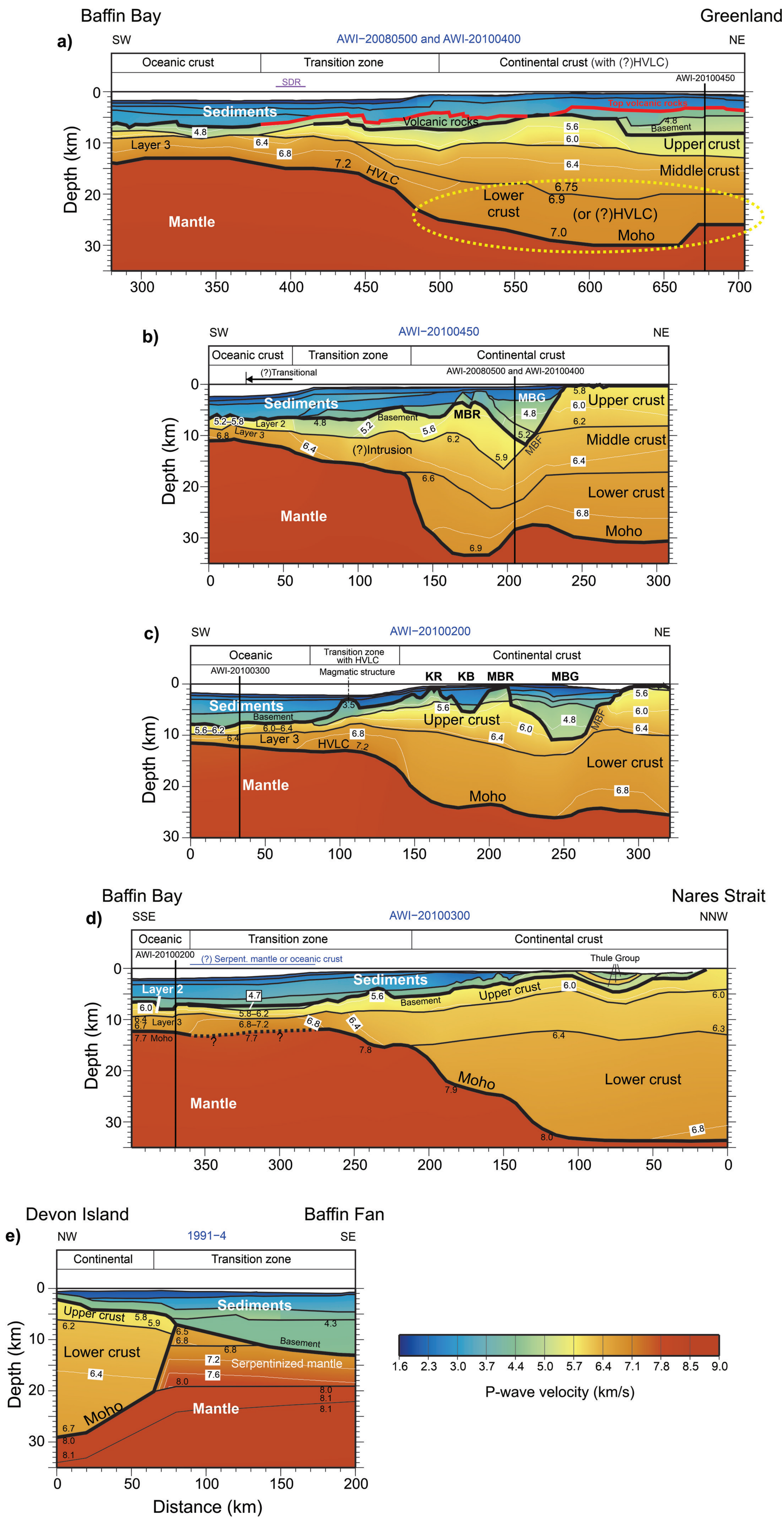
Baffin Bay
Greenland
a)
SW
AWI−20080500 and AWI-20100400
NE
Oceanic crust
Transition zone
Continental crust (with (?)HVLC)
SDR
AWI-20100450
Sediments
Top volcanic rocks
Volcanic rocks
Basement
Layer 3
Upper crust
Middle crust
HVLC
Lower crust
(or (?)HVLC)
Moho
Mantle
Depth (km)
b)
SW
AWI−20100450
NE
Oceanic crust
Transition zone
Continental crust
(?)Transitional
AWI-20080500 and AWI-20100400
Sediments
Layer 2
Layer 3
Basement
MBR
MBG
MBF
(?)Intrusion
Upper crust
Middle crust
Lower crust
Moho
Mantle
c)
SW
AWI−20100200
NE
Oceanic
Transition zone with HVLC
Continental crust
AWI-20100300
Magmatic structure
KR
KB
MBR
MBG
Sediments
Basement
Layer 3
HVLC
Upper crust
MBF
Lower crust
Moho
Mantle
Baffin Bay
Nares Strait
d)
SSE
AWI−20100300
NNW
Oceanic
Transition zone
Continental crust
AWI-20100200
(?) Serpent. mantle or oceanic crust
Thule Group
Layer 2
Sediments
Basement
Upper crust
Layer 3
Moho
Lower crust
Mantle
Devon Island
Baffin Fan
e)
NW
1991−4
SE
Continental
Transition zone
Sediments
Upper crust
Basement
Lower crust
Serpentinized mantle
Moho
Mantle
Distance (km)
P-wave velocity (km/s)

model lie about 1 s ahead of the calculated arrival times. This could mean that there is a reflector that would lie some 3 to 4 km above the Moho shown in the model, which could either be a shallower Moho or the top of a high-velocity lower crust. Altenbernd et al. (2016) attributed the misfit to a complex geological structure beneath the steep Melville Bay Fault. Given that the depth of the Moho beneath the Melville Bay Graben is also constrained by some other seismic stations, a high-velocity lower crust in that region may reconcile some of the conflicting observations.

Increased lower crustal velocities of up to 7.2 km/s are observed in the transition zone farther seaward (Fig. 11c). The 50 km wide high-velocity lower crust is in an area where a 4 km high seamount-shaped magmatic structure was observed (Altenbernd et al., 2014). The exact landward limit of oceanic crust within the transition zone cannot be determined. Clear oceanic crust is found between kilometre 0 and 80. The initial oceanic crust has a thickness of 6 km, but thins to 3.5 km at the southwestern end of the line. This is less than the global average of 7 km (White et al., 1992) or the 9 km thick oceanic crust in southern Baffin Bay (Fig. 10e; Funck et al., 2012a). Within the interpreted oceanic-crust domain, a lateral change in velocity and basement roughness occurs at kilometre 40, which could suggest the presence of serpentinized mantle between kilometre 40 and 80 similar to that in the zone of smooth basement on seismic line AWI-20100300 (Fig. 11d; Altenbernd et al., 2016) between kilometre 270 and 360. The presence of Moho reflections on line AWI-20100200, however, are more consistent with oceanic crust.

The northernmost seismic line in Baffin Bay presented here is line AWI-20100300 (Fig. 11d; Altenbernd et al., 2016) that extends into the southern Nares Strait. Between kilometre 0 and 210, a three-layered continental crust is observed, which thins from 33 km in the north to 10 km in the south. Velocities range from 5.6 to 6.9 km/s. An up to 3 km thick basin in the north is interpreted as part of the Proterozoic Thule Basin (Altenbernd et al., 2016). Further to the south up to kilometre 270 in the model, Altenbernd et al. (2016) described the crust as transitional, beyond which they interpreted oceanic crust. A possible alternative interpretation is one in which the oceanic crust does not start before kilometre 360. Crustal velocities between kilometre 270 and 360 are distinctly different from those between kilometre 360 and 399. Interestingly, the plate reconstruction of Oakey and Chalmers (2012) also suggests the onset of oceanic crust at kilometre 360. In the zone of dispute (kilometre 270 to 360), a very flat basement with a velocity of 4.7 km/s is observed, which is consistent with mantle peridotite that is fully serpentinized (Christensen, 2004). As described in more detail above for line AWI-20100450, a flat basement in an area of reduced magma supply would be inconsistent with oceanic crust. The seismic record that Altenbernd et al. (2016) presented for this zone does not show a convincing Moho reflection (*see* observations to the north-northwest in Fig. 7 in Altenbernd et al. (2016)). Hence, it remains unclear if there really is a sharp velocity contrast across the interpreted Moho or if the travel times could also be fitted with a smooth transition into normal-mantle velocities. The latter case would be compatible with a downward decrease in serpentinization rate, where the interpreted two lower basement layers consist of partially serpentinized mantle peridotite.

For the interpretation of the 6.8 km/s layer on seismic line AWI-20100300 (Fig. 11d), a comparison with line 1991-4 (Fig. 11e) is quite enlightening. Line 1991-4 runs from Devon Island into the Baffin Fan, where it is underlain by Eocene oceanic crust according to the plate reconstruction of Oakey and Chalmers (2012), whereas Harrison et al. (2011) called it 'oceanized crust'. In contrast, Reid and Jackson (1997), who modelled the seismic refraction data along the line, reported a basement layer with velocities of 6.8 km/s below a 12 km thick blanket of sedimentary rocks and interpreted it as serpentinized mantle. Although velocities of 6.8 km/s are compatible with oceanic layer 3 (White et al., 1992), Reid and Jackson (1997) listed several arguments why the basement is not oceanic. These arguments include the lack of an oceanic layer 2 as well as a high-velocity gradient with no distinct reflection from a Moho, suggesting a smooth transition into normal-mantle velocities. Furthermore, with S-wave velocities of 3.6 km/s in that layer, the combination of P- and S-wave velocities is more compatible with partially serpentinized mantle than with gabbroic oceanic layer 3 (Christensen, 2004). Although there are many similarities between lines 1991-4 and AWI-20100300, the differences should nevertheless not be ignored. Line 1991-4 is missing the two upper basement layers (4.7 and 5.6 km/s) observed on line AWI-20100300. The thick sedimentary column in the Baffin Fan with a very complex velocity structure, as evidenced by the presence of at least one low-velocity zone, may prohibit or mask refractions from such basement layers with velocities not too different from the deeper portions of the sedimentary basin. In summary, the velocity models in the northernmost part of Baffin Bay leave room for the interpretation that exhumed and serpentinized mantle peridotite could be present in the continent-ocean transition zone. This would also be consistent with the magma-poor margins in the southern Labrador Sea (Fig. 10a).

Potential-field maps

Gravity- and magnetic-anomaly maps (Fig. 4–6) are basic tools in supporting geological and geodynamic interpretations throughout the region. Below the shelves, they have been used to trace onshore coastal geological features into adjacent offshore regions (e.g. MacLean et al., 1982; Hall et al., 2002; Wardle et al., 2002). They have also been used to define the landward limit of oceanic crust (Chalmers and Laursen, 1995; Srivastava and Roest, 1999) and the nature of the transition from oceanic to continental crust (Keen et al., 2018a). Finally, they are used to define the extinct spreading centre in the Labrador Sea and Baffin Bay, as well as magnetic isochrons, particularly in the Labrador Sea (Oakey and Chalmers, 2012).

The gravity map (Fig. 4), showing free-air anomalies offshore and Bouguer anomalies onshore, generally exhibits negative anomalies on land, representing thick, prerift continental crust and lithosphere. Within the onshore region, some of the major boundaries between Precambrian terranes can be correlated using the gravity-anomaly map. A clear example of this is the Grenville Front, where the anomaly is lower than average. Another example is the Paleoproterozoic Nagssugtoqidian Orogen, which in coastal West Greenland manifests itself as a reduction in the gravity low.

Offshore, the gravity anomaly is characterized by a band of high-amplitude gravity anomalies, ranging from about 20 to greater than 70 mGals, which generally lie over the outer continental-shelf regions. This 'edge effect' anomaly is a signature feature of most rifted margins and is commonly observed along the Atlantic margins (Keen and Beaumont, 1990). The anomaly is mainly caused by the competing effects of crustal thinning and subsidence across the margin: toward the deep ocean basin, the crust thins, bringing high-density mantle to shallower depths, whereas the overlying low-density water and sedimentary layers increase in thickness. These competing contributions to the free-air gravity anomaly tend to cancel each other except where the changes in structure are very rapid, corresponding to the observed high amplitudes near the edge of the continental shelf. The amplitude and wavelength of the gravity anomaly will change, depending in part on the strength of the lithosphere that provides isostatic adjustment as these layers vary in thickness (Keen and Beaumont, 1990; Keen and Dehler, 1997; Watts, 2001). In the Labrador–Baffin Seaway region, the wavelengths and amplitude of this anomaly are comparable to those observed over younger, presumed hotter and weaker continental lithosphere offshore of the eastern Canadian margin to the south (Geological Survey of Canada, 1988).

In Davis Strait, the major offset along the Ungava Fault Zone is also characterized by a positive anomaly. Funck et al. (2007) showed that this was due to a similar combination of factors, with the added complexity of magmatic additions to the crust in this region. The West Greenland margin, where Paleogene volcanic rocks occupy a

Figure 11. P-wave velocity models in Baffin Bay: **a)** combined seismic lines AWI-20080500 and AWI-20100400 (Suckro et al., 2012) in southern Baffin Bay, extending from Baffin Island to Melville Bay (dashed yellow line marks a lower crustal zone that is discussed in the text); **b)** line AWI-20100450 (Altenbernd et al., 2015) in northern Baffin Bay; **c)** line AWI-20100200 (Altenbernd et al., 2014) in northern Baffin Bay; **d)** line AWI-20100300 (Altenbernd et al., 2016) in northern Baffin Bay and southern Nares Strait; **e)** line 1991-4 (Reid and Jackson, 1997) in northern Baffin Bay, extending from Devon Island into the Baffin Fan region. Velocities for all lines except 1991-4 are given in kilometres per second and white lines are velocity contours with a spacing of 0.4 km/s starting with 4.8 km/s. Velocities for line 1991-4 are given in kilometres per second and white lines are velocity contours with a spacing of 0.4 km/s starting with 6.4 km/s. Vertical black lines show the location of intersecting lines. Location of seismic refraction profiles is shown on Figure 3. HVLC = high-velocity lower crust; KB = Kivioq Basin; KR = Kivioq Ridge; MBF = Melville Bay Fault; MBG = Melville Bay Graben; MBR = Melville Bay Ridge; SDR = seaward-dipping reflectors; serpent. = serpentinized.

large offshore area, also exhibits a very broad region with positive free-air anomalies (Skaarup, 2002). Further north, positive free-air anomalies characterize the region encompassed by the Baffin Fan, a package of thick, young sedimentary rocks (Harrison et al., 2011). Gravity anomalies in these regions tend to be more complex than the simpler 'edge effect' anomalies elsewhere in the Labrador–Baffin Seaway.

The oceanic regions are characterized by generally lower amplitude anomalies. Nevertheless, a few very important features have been identified, including a gravity low over the extinct spreading axis in the Labrador Sea and Baffin Bay (Srivastava, 1978; Jackson et al., 1979; Whittaker et al., 1997). Furthermore, the large Eocene fracture zones (64°W and 60°W) visibly offset the axis and form lineaments with generally low gravity anomalies. Definition of these features in Baffin Bay has allowed the development of a much-improved plate-tectonic model for the region (Oakey and Chalmers, 2012).

The filtered Bouguer anomaly map (Fig. 5) is useful because it accounts for the effects of changes in water depth. This map shows trends of the crustal and sedimentary features and is particularly useful for this reason in the Davis Strait region for mapping the complex structural deformation and volcanism (e.g. Sørensen, 2006; Funck et al., 2007; Jauer et al., 2019). Linear trends in the oceanic region in the Labrador Sea are clearly observed, but are less clearly defined in Baffin Bay. Along the Baffin Island margin, north of Frobisher Bay, this map shows a paired band of low and high anomalies bordering the margin. There are several major changes in the trend of these bands along strike, suggesting comparable changes in the strike of the margin, and possible margin segmentation. Similar features are not well defined on the Greenland margin.

Magnetic anomalies (Fig. 6) have been used to define seafloor-spreading magnetic isochrons and fracture zones in the Labrador Sea (Srivastava, 1978; Roest and Srivastava, 1989), which are some of the major factors used in defining the Paleogene history of plate motions between Greenland and North America. Attempts have been made to define similar features in Baffin Bay, but without success. Identification of specific magnetic isochrons is still difficult there (Jackson et al., 1979; Oakey and Chalmers, 2012) and, as noted above, gravity data provide most of the information to date on positions of fracture zones and the ridge axis. This axis can vaguely be discerned in the magnetic-anomaly field as offsets in trends, but it is less clear than the gravity signature.

Some of the sedimentary basin depocentres appear as negative anomalies relative to the surrounding positives. This can be clearly seen in the Melville Bay Graben. In Davis Strait, parts of the Ungava Fault Zone are clearly defined as a magnetic low. The prominent northeast-trending negative anomaly at the mouth of Frobisher Bay may be the southern continuation of this fault zone during the Paleocene, based on a similar orientation of Paleocene fracture zones. Offshore Paleogene basalts appear to have a variable signature. Some of the high-amplitude magnetic anomalies may correspond to the presence of basalt, where it is not too deeply buried by sedimentary rocks and water. These anomalies are seen, for example, offshore Cape Dyer, Baffin Island and near Disko Island, West Greenland. The character of magnetic anomalies over the Paleogene basalts cannot, however, be clearly differentiated from that over other types of basement and therefore magnetic anomalies are not a definitive marker of the distribution of Paleogene volcanism.

On the Labrador Sea margins, Chalmers and Laursen (1995) used the magnetic anomalies along seismic reflection lines to show that regions that were once thought to be occupied by the oldest oceanic crust might be continental instead. This was later supported by seismic refraction studies (Fig. 10a). Keen et al. (2018a, b) extended the postulated serpentinized- and exhumed-mantle zone along the margin, using the magnetic character, as well as seismic and gravity data (*see also* 'Crustal structure' section).

Some of the magnetic signatures on land and adjacent marine areas are quite prominent. These clearly define major terrane boundaries, such as: the Grenville Front and its offshore extension toward the Cartwright Fracture Zone; the north-trending Torngat Orogen in northern Labrador; the arcuate fabric of the Nagssugtoqidian Orogen in West Greenland; and the southern termination of the North Atlantic Craton in West Greenland. More complex north-trending anomalies occur within Hudson Strait, linking the Torngat Orogen to southwestern Baffin Island. The northeastward trend through this region observed across the mouth of Frobisher Bay into southern Davis Strait may also be related to these prerift structures. Onshore terrane boundaries bordering Baffin Bay are not as well defined. On the Labrador and conjugate West Greenland shelves, other large positive magnetic anomalies appear to extend seaward from the onshore coastal regions. Most of these are not clearly aligned with the oceanic features and are diminished where basement deepens significantly.

Crustal thickness and depth to Moho from gravity inversion

The crustal variations that resulted from rifting and extension as part of the separation of North America and Greenland are reflected in the gravity-anomaly signature. Regional three-dimensional gravity inversion was used to provide large-scale depth to Moho, crustal-density distribution and crustal-thickness estimates over the Labrador Sea (Welford and Hall, 2013) and Baffin Bay (Welford et al., 2018). These inversions were constrained by bathymetry and sediment-thickness information. Sparse, localized seismic studies have been used to ensure that the inversion results provide geologically reasonable results.

The GRAV3D inversion algorithm, developed by Li and Oldenburg (1996, 1998), was used in both studies to invert gravity observations at the Earth's surface and generate a subsurface three-dimensional density-anomaly model (relative to a reference density of 2950 kg/m^3) able to reproduce the observations. Model meshes for the inversions consisted of flattened cubes, each with lateral dimensions of 5 by 5 km and 500 m thick; the total mesh depth for both studies was 40 km.

To estimate Moho depth (Fig. 12) across the modelled regions, a specific density contrast, or isosurface, was chosen as a Moho-proxy such that the isosurface showed the best and most consistent match with available seismic constraints of Moho depth. The chosen isosurface of 70 kg/m^3 for both regions corresponded to a density of 3020 kg/m^3. Once estimates of Moho depth had been extracted from the inverted density-anomaly volumes, the crustal thicknesses were derived by taking the difference between the Moho depths and the depths to basement obtained from regional compilations.

Inversions for the Labrador Sea revealed Moho structures with a depth to Moho of 12 km beneath the central portions of the Labrador Sea, increasing to 20 km and greater toward Davis Strait and beneath the offshore extension of the Grenville Province of southeastern Labrador. Comparison with seismic refraction and wide-angle-reflection profiles shows generally good agreement between seismically derived Moho depths and the inverted Moho-proxies. In locations such as Davis Strait, however, where high-velocity lower crust or underplating is present, the Moho-proxy tended to identify the top of these zones and therefore likely underestimated the total depth to seismic Moho.

Crustal-thickness estimates (Fig. 13), derived from the inverted depth-to-Moho estimates in combination with depth-to-basement constraints, reveal that the crust of the central Labrador Sea is generally 5 to 10 km thick, but thickens to approximately 20 to 25 km toward Davis Strait and beneath the offshore extension of the Grenville Province. The magma-rich margin below the northern Labrador Sea (Keen et al., 2012) is represented by a band of thicker igneous crust that trends northwest toward Hudson Strait.

Assuming an initial crustal thickness of 35 to 40 km, which is typical of the region (Chian and Louden, 1992; Hall et al., 2002), the crustal thicknesses of 10 and 20 km highlighted on the map (Fig. 13) correspond to stretching factors of β = 3.5–4.0 and β = 1.75–2.0, respectively. Welford and Hall (2013) suggested that β = 3.5 corresponds to the onset of hyperextended crust; however, they noted that variable initial crustal thickness will modify the β value. Also, the addition of magmatic underplating can thicken the crust significantly and overprint the original stretching profile across the margins. For the south-central magma-poor Labrador margin and conjugate southwestern Greenland margins, the crustal thicknesses show that these margins, landward of oceanic crust, have experienced a very large degree of extension (β >3.5). There may be embrittlement of the entire crust and serpentinization of the upper mantle in these regions landward of known oceanic crust (Pérez-Gussinyé and Reston, 2001; *see* Welford and Hall, 2013). This is consistent with seismic and other

Figure 12. Map of depth to inferred Moho of the study area from three-dimensional gravity inversion *modified from* Welford and Hall (2013) for the Labrador Sea and Davis Strait, and Welford et al. (2018) for Baffin Bay. Major Precambrian boundaries are *modified from* St-Onge et al. (2009).

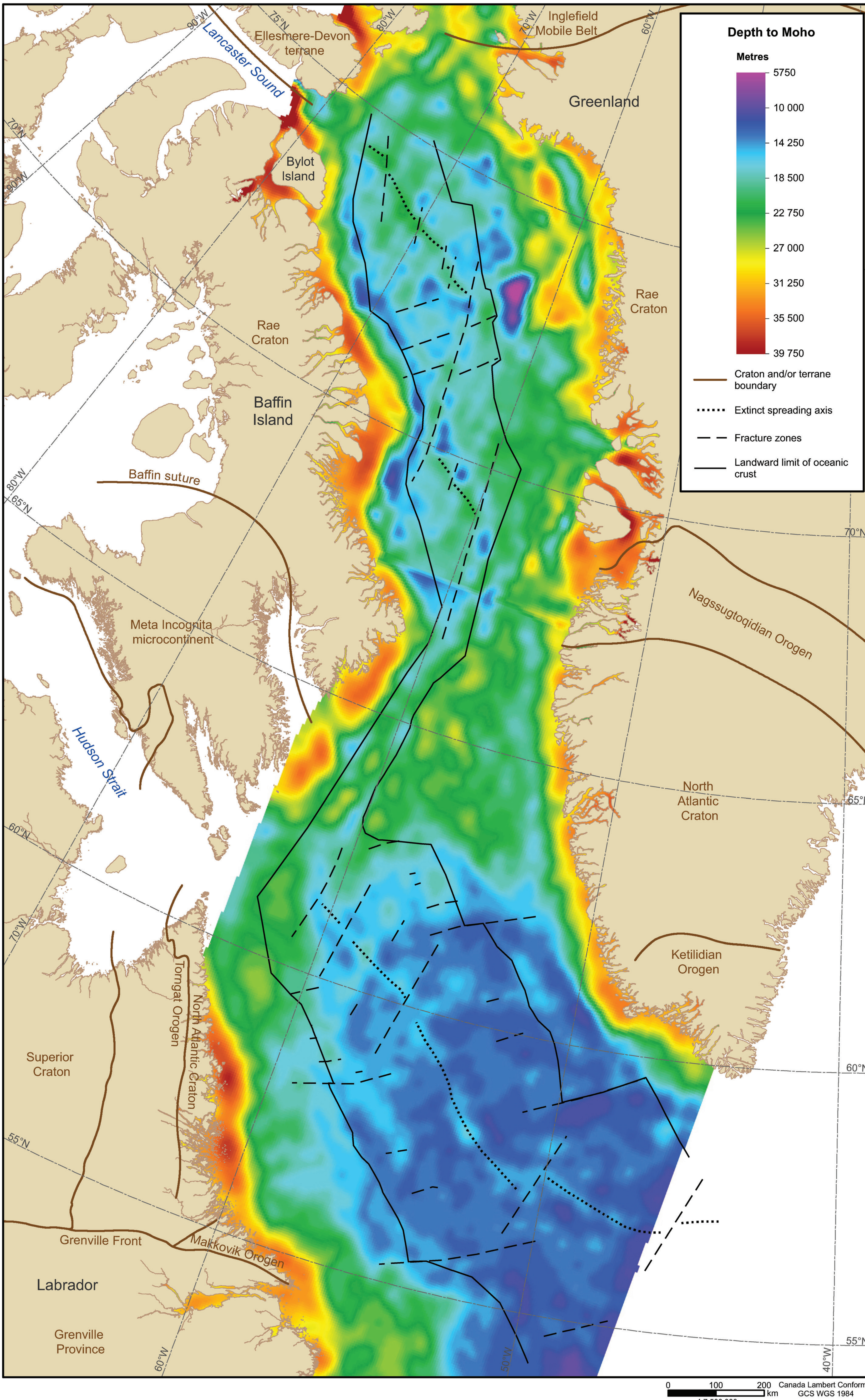
Depth to Moho
Metres
5750
10 000
14 250
18 500
22 750
27 000
31 250
35 500
39 750
Craton and/or terrane boundary
Extinct spreading axis
Fracture zones
Landward limit of oceanic crust
Lancaster Sound
Ellesmere-Devon terrane
Inglefield Mobile Belt
Greenland
Bylot Island
Rae Craton
Rae Craton
Baffin Island
Baffin suture
Meta Incognita microcontinent
Hudson Strait
Nagssugtoqidian Orogen
North Atlantic Craton
Ketilidian Orogen
Torngat Orogen
North Atlantic Craton
Superior Craton
Grenville Front
Makkovik Orogen
Labrador
Grenville Province
75°N
70°N
65°N
60°N
55°N
90°W
80°W
70°W
60°W
50°W
40°W
0
100
200
km
1:7 500 000
Canada Lambert Conformal
GCS WGS 1984

potential-field studies in this region (Chian et al., 1995a; Keen et al., 2018a). South of the offshore extension of the Grenville Front, where unstretched crustal thicknesses are about 50 km (Hall et al., 2002), there will be discrepancies in the stretching values obtained (Welford and Hall, 2013). This discrepancy will produce β values that are too low in this region, unless the initial crustal thickness is increased. Furthermore, the northern Labrador Sea margins may have been modified by a large magmatic component added to the crust (Keen et al., 2012), reducing the validity of the apparent stretching factors.

Baffin Bay is partially underlain by oceanic crust with zones of extended continental crust of variable width along its margins. Generally, the Moho depth beneath the margins of Baffin Bay landward of the oceanic region is approximately 25 to 30 km, whereas an average Moho depth of 15 km was derived beneath the west-central part of the margins. Depths-to-Moho of approximately 25 km are observed to the north in Nares Strait and to the south through Davis Strait.

The three-dimensional density models for this region reveal an asymmetric distribution of extended continental crust, approximately 25 to 30 km thick, along both margins of Baffin Bay, with a wider extended zone on the Greenland margin. Central Baffin Bay is underlain by a zone of oceanic crust 5 to 13 km thick, with the thinnest crust (5 km thick) aligning with Eocene spreading centres. Seismic constraints show a generally good match between observed seismic Moho and the Moho-proxy beneath much of Baffin Bay, with most discrepancies corresponding to zones of higher density lower crust in Nares Strait, along the Greenland margin, and in Davis Strait. In the last two regions, the seismic data indicate magmatic underplating and intrusion of the thinned continental crust (Fig. 10, 11), and the Moho-proxy in some regions follows the base of this thinned continental layer, rather than the base of the underplated layer at the seismic Moho (Welford et al., 2018). A very thin region seaward of Melville Bay is probably an artifact as it is the site of a large intrusion (Whittaker et al., 1997) giving rise to a large gravity high (Fig. 11b). The variability in prerift crustal thickness from south to north in Baffin Bay (Dahl-Jensen et al., 2003; Darbyshire, 2003; Darbyshire et al., 2017, 2018), as well as the uncertainties in magmatic effects along the magma-rich margin segments, indicate that crustal-thickness variations result from more factors than extension alone.

Plate reconstructions

The open-source software GPlates (version 2.1.0) provided a tool to determine and visualize the latest plate reconstructions for Greenland relative to North America during the creation of the Labrador Sea and Baffin Bay (Seton et al., 2012; Hosseinpour et al., 2013; Müller et al., 2016; Gion et al., 2017; Barnett-Moore et al., 2018). There are many sets of poles of rotation that have provided credible plate motions for the region. Most are based on reconstruction of the seafloor-spreading isochrons and the direction of transform faults in the Labrador Sea region (Roest and Srivastava, 1989; Srivastava and Roest, 1999), and, more recently, include geophysical data in Baffin Bay (Oakey and Chalmers, 2012), as well as geological data from the eastern Canadian Arctic Islands (Gion et al., 2017). The recent work undertaken by Gion et al. (2017) allows for motions between parts of the Canadian Arctic Islands region, which is divided into microplates, relative to Greenland and Baffin Island (*see also* Lawver et al., 1990). This enables convergence between Ellesmere Island and Greenland (Oakey and Stephenson, 2008; Oakey and Chalmers, 2012), and rifting in Lancaster Sound during the opening of Baffin Bay (Oakey and Chalmers, 2012). Although discussion of plate motions here is limited to the Labrador–Baffin Seaway region, it is important to note that constraints in the peripheral regions are also reasonably satisfied. This study focuses mostly on relative motions between the plates and, therefore, absolute plate motions are not considered.

The reconstruction poles of Oakey and Chalmers (2012) were used for the plate motions from 33 Ma (chron C13, the cessation of seafloor spreading) to 62 Ma (chron C27n), and the full-fit reconstruction pole of Hosseinpour et al. (2013) was used for 120 Ma. Between 62 and 120 Ma, there is little data within the study area to constrain plate motions; however, south of the Cartwright Fracture Zone, seafloor spreading between Rockall and North America started near chron C34 (83.5 Ma), as discussed by Barnett-Moore et al. (2018). In that work, the authors presented full-fit reconstructions at chron C34, which are based on the Hosseinpour et al. (2013) results for the Labrador Sea region, and included the complex multiplate motions and plate deformations that occurred in the North Atlantic to the south. Their results were used for the poles of rotation between Greenland and North America during the Late Cretaceous. These poles are listed in Table 2.

The reconstructions use the 'average deformable plate boundary' method described by Hosseinpour et al. (2013) and Ady and Whittaker (2018). The present-day continent-ocean boundary is defined as the landward limit of oceanic crust. Landward of the oceanic regions in parts of the Labrador Sea and possibly Baffin Bay, there are regions occupied by serpentinized and exhumed continental mantle. These can also be closed, as if the crust were oceanic, because there is infinite crustal stretching there.

Previous work of Oakey and Chalmers (2012) provides a detailed analysis of fracture zones and seafloor-spreading magnetic anomalies. Their analysis of the extent of oceanic crust also provided a starting point for defining the landward limit of oceanic crust, which was then updated using all of the recent seismic refraction and reflection data and potential-field data, described herein, as well as a new understanding of the age of onset of seafloor spreading in the central Labrador Sea (Keen et al., 2018a). The inclusion of seismic refraction and reflection data in choosing the landward limit of oceanic crust may provide a better result than gravity-inversion methods alone, since igneous additions to the crustal thickness and zones of exhumed mantle are difficult to identify using only gravity data (Hosseinpour et al., 2013; Welford et al., 2018).

Estimates of the prerift positions of the restored continent-ocean boundary on each plate removes the average deformation of the extended continental lithosphere and provides the prerift locations of the plate boundaries. During a reconstruction, overlap of the deformed continental plates is 'allowed' until the restored continent-ocean boundary of the plates overlap. Since this is not a palinspastic reconstruction, features such as sedimentary basins, which lie within the deformed zone on each plate boundary, are not restored to earlier configurations. They are displayed in the reconstructions with their present shapes, which may overlap other features. Hosseinpour et al. (2013) obtained the restored continent-ocean boundary from gravity modelling of crustal thickness. They showed that it is not strongly dependent on the position of the landward limit of oceanic crust within the range of reasonable models. In this study, the Hosseinpour et al. (2013) restored continent-ocean boundary from their model 3 is used, but other models they considered could also be used without significantly changing the results. Final plate reconstructions are discussed in the next section.

REGIONAL INTERPRETATION

Tectonic features

The tectonic elements map (Fig. 14) reveals the highly segmented nature of the Labrador–Baffin Seaway, which formed during Mesozoic rifting and subsequent seafloor spreading. Basement faulting along the continental margins reflects the timing and direction of rifting. The variation in depicted faulting style may be related in part to the merging of different interpretations and differing data coverage. Shallow basement platforms line the coastline (generally <3500 m deep; Fig. 7, 8). In the Labrador Sea and Baffin Bay, faults straddle the seaward edge of the basement platform, where basement tends to form a hinge, dipping steeply seaward under the thickening sedimentary wedge. Seaward of these platforms, basement highs are generally deeper than the platforms themselves; however, in Davis Strait, basement and volcanic rocks can be shallower and faults show a variety of orientations. Inboard of the 1000 m basement depth, there are few faults that were active in Mesozoic and Cenozoic time, and the continental crust is probably close to its original thickness.

Most of the faults along the edge of the basement platforms reflect Early Cretaceous, southwest-northeast extension. Seaward of the platforms, faults are more difficult to map due to thick sediment cover and locally overlying Paleogene volcanic rocks. Faulting is very complex along regions subjected to strike-slip motion, most notably in Davis Strait. Here, the large-offset Ungava Fault Zone has created both transtensional and transpressional structures along its

Figure 13. Crustal-thickness map of the study area from gravity inversion *modified from* Welford and Hall (2013) for the Labrador Sea and Davis Strait, and Welford et al. (2018) for Baffin Bay. Major Precambrian boundaries are *modified from* St-Onge et al. (2009). Contours of 10 and 20 km values are shown and approximate β-values of 2 and 4 assuming an initial crustal thickness of 40 km.

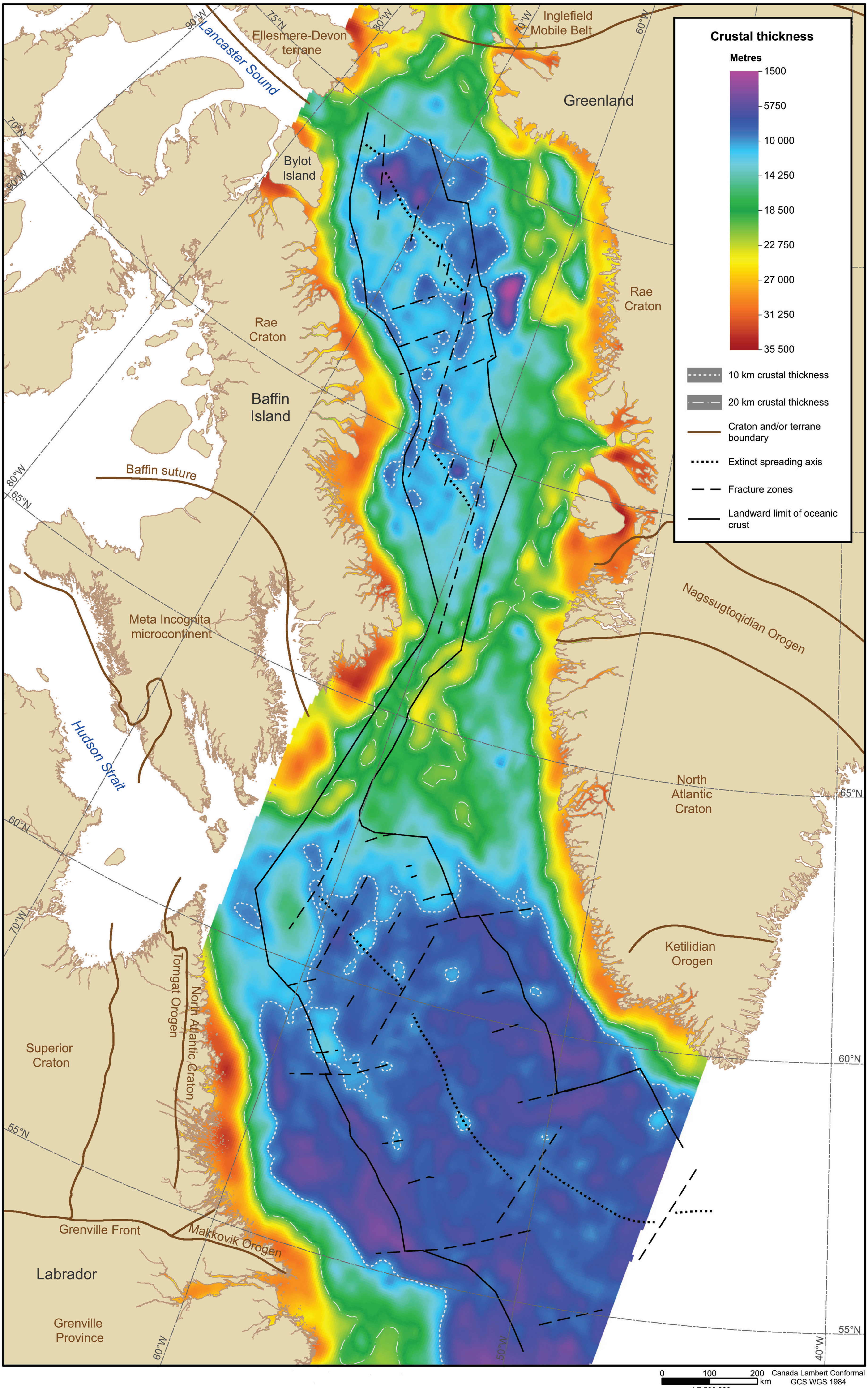
Crustal thickness
Metres
1500
5750
10 000
14 250
18 500
22 750
27 000
31 250
35 500
10 km crustal thickness
20 km crustal thickness
Craton and/or terrane boundary
Extinct spreading axis
Fracture zones
Landward limit of oceanic crust
Lancaster Sound
Ellesmere-Devon terrane
Inglefield Mobile Belt
Greenland
Bylot Island
Rae Craton
Rae Craton
Baffin Island
Baffin suture
Meta Incognita microcontinent
Nagssugtoqidian Orogen
Hudson Strait
North Atlantic Craton
Ketilidian Orogen
Torngat Orogen
North Atlantic Craton
Superior Craton
Grenville Front
Makkovik Orogen
Labrador
Grenville Province
75°N
70°N
65°N
60°N
55°N
90°W
80°W
70°W
60°W
50°W
40°W
0
100
200
km
1:7 500 000
Canada Lambert Conformal
GCS WGS 1984

Table 2. Poles of rotation associated with the plate motions of Greenland relative to North America.

Time (Ma)	Latitude (°N)	Longitude (°W)	Angle	Source and age
33.1	90.0	0.0	0.0	No motion after this time chron C13
46.2	53.2	112.9	-1.65	Oakey & Chalmers (2012) chron C21n
53.0	53.2	112.9	-3.75	Oakey & Chalmers (2012) chron C24n
56.8	24.5	137.3	-3.12	Oakey & Chalmers (2012) chron C25n
58.5	26.3	143.8	-3.4	Oakey & Chalmers (2012) chron C26n
61.8	27.8	150.0	-3.75	Oakey & Chalmers (2012) chron C27n
79.1	57.73	138.96	-8.0	Barnett Moore et al. (2018) chron C33
83.5	61.42	132.01	-9.76	Barnett-Moore et al. (2018) chron C34
120.0	62.82	129.87	-11.28	Hosseinpour et al. (2013)
250.0	62.82	129.87	-11.28	Hosseinpour et al. (2013)

length (Wilson et al., 2006). Severe deformation along the northern margin of Baffin Bay is also recognized (Jackson et al., 1992; Oakey and Chalmers, 2012; Gion et al., 2017). Underlying this region is a complex and diffuse plate boundary formed as a result of the northwest motion of Greenland with respect to North America during the Paleogene.

The timing of rift-related faulting varies in different areas. Although Cretaceous extensional faulting is observed in the region, little extensional faulting appears to have occurred after the Early Cretaceous along the inner Labrador margin (Dickie et al., 2011). In contrast, other regions record both Early and Late Cretaceous extensional faulting, such as the Lady Franklin Basin (Sørensen, 2006), the Fylla Structural Complex (Døssing, 2011), and the Melville Bay Graben (Gregersen et al., 2013). The younger fault trend appears to be oriented north or northeast, more consistent with Eocene plate motions. Døssing (2011) suggested that older, Precambrian structures influenced the northeasterly trend during a period of Late Cretaceous faulting in the Fylla Structural Complex, and Chalmers et al. (1999) found a similar pattern in the Nuussuaq Basin of West Greenland.

Six major tectonic segments underlie the Labrador–Baffin region (coloured bands along the coastlines in Fig. 14). These are defined first by their plate-tectonic type, as either rifted- or transform-margin segments, and second by whether they are magma-poor or magma-rich. Features of magma-rich (or volcanic) margins have been described by Planke et al. (2000), and include a volcanic plateau associated with seaward-dipping reflectors and a thick igneous crust. Magma-poor margins, in contrast, may be occupied by zones of hyperextended continental crust and by zones of exhumed continental-mantle lithosphere (Pérez-Gussinyé and Reston, 2001; Reston, 2009; Bayrakci et al., 2016).

Segment 1

The southern Labrador Sea extensional segment (south of the Snorri Fracture Zone) is considered a magma-poor margin. The Hopedale Basin, offshore Labrador, which formed as a result of rift-related subsidence starting in the Early Cretaceous, is a major feature of this segment, and is not matched by a comparable basin on the conjugate West Greenland margin (the Paamiut South Basin contains less than 4 km of sediment accumulation). Extension continued into the Late Cretaceous, resulting in crustal hyperextension below the present-day outer-shelf and upper-slope region as predicted by gravity models, as well as seismic refraction data (Chian et al., 1995a; Welford and Hall, 2013). Mantle exhumation would have followed the rupture of the continental crust in the Late Cretaceous, forming a transition zone of serpentinized continental mantle along the landward edge of the landward limit of oceanic crust (Chian et al., 1995a; Keen et al., 2018a). As a provisional hypothesis, it could be inferred that exhumed mantle extends south of the Cartwright Fracture Zone. On the West Greenland margin, the magma-poor margin continues south, to the southern tip of Greenland, where it later became buried by basalt associated with the opening of the Northeast Atlantic in the Eocene (Funck et al., 2012b). The oldest oceanic crust in this region formed during the Late Cretaceous (chron C31).

Major offsets in this margin segment include the Cartwright Fracture Zone, the landward prolongation of which corresponds to the Grenville Front (Hall et al., 2002), separating the Grenville Province and Makkovik Orogen. The basement platform is also offset in the region of the Bjarni wells (Dickie et al., 2011), where a major shear zone can be projected from the Makkovik Orogen (Hall et al., 2002). Another offset is seen at the Okak Arch, located at the northern end of the Hopedale Basin, where the Snorri Fracture Zone intersects the margin. Both these offsets are also associated with complex basement faulting and possible structural inversion of Lower Cretaceous sediments. South of the Cartwright Fracture Zone, the margin is also extensional and shares a similar rifting history; however, the Hopedale Basin is generally not carried south of the Cartwright Arch (Balkwill and McMillan, 1990).

Segment 2

The northern Labrador Sea extensional segment extends north of the Snorri Fracture Zone to Hudson Strait on the western side, and to the Sisimuit Basin on the eastern side (Fig. 14). This is a magma-rich margin segment probably due to the arrival of the hotspot in Davis Strait in the mid-Paleocene (Storey et al., 1998). The volcanism may have overprinted an older magma-poor segment that could have formed concurrently with the margin segment to the south (Keen et al., 2018b), and the serpentinized mantle (segment 1) is provisionally shown extending northward into this region. Regions of excess volcanism are characterized by a volcanic plateau with seaward-dipping reflectors (Keen et al., 2012). Based on seismic reflection data, a possible volcanic region extending north into the Davis Strait has been mapped, but the evidence is inconclusive. Here, the orientation of the possible volcanic plateau turns northeastward near the mouth of Hudson Strait, where it becomes aligned with the trend of the Ungava Fault Zone. At the southern end of this segment, where the magma-rich and magma-poor segments meet (Fig. 14), seaward-dipping reflectors are not as prevalent and the igneous crust thins south of the Snorri Fracture Zone. Paleocene magmatism, however, has affected the crust south of this fracture zone (Keen et al., 2018a), where there appears to be some ‘spillover’ of magma onto the magma-poor segment. It appears that the southern extent of magmatism was only partially restricted by the fracture zone. On the conjugate West Greenland margin, Early Paleocene volcanism formed volcanic eruptive centres, such as the Gjoa, Maniitsoq, and Hecla highs (Larsen and Dalhoff, 2006; Sørensen, 2006).

On the Canadian side, the magma-rich margin segment is occupied by the southern part of the Saglek Basin, which is very deep (over 10 km), and relatively little data are available for this basin compared to the Hopedale Basin. The conjugate margin does not show a similar, deep basin off West Greenland (Fig. 7), but seaward-dipping reflectors and thick igneous crust have been mapped there (Chalmers, 1997; Chalmers and Pulvertaft, 2001; Gerlings et al., 2009). This volcanic margin may merge with the Gjoa High (Sørensen, 2006) in southern Davis Strait, where refraction measurements show thinned continental crust, underlain by an underplated igneous layer (Fig. 10c; Funck et al., 2007). The Fylla Structural Complex and Lady Franklin Basin are conjugate to the southern Saglek Basin (Døssing, 2011; Keen et al., 2018b; *see* ‘Plate reconstructions’ section below). The Fylla Structural Complex is highly structured with faults trending

Figure 14. Regional tectonic elements map from the interpretation of seismic reflection data, showing oceanic and onshore geological features. The general location of the six conjugate margin segments are indicated as numbered and coloured bands along the coastlines. The map shows crustal types (e.g. oceanic, serpentinized mantle), as well as the outline of the major sedimentary basins and faults in basement. The Greenland part of the map is *modified from* Gregersen et al. (2019, this volume). The Canadian part is from this study. The Nuussuaq Basin outline is from Dam et al. (2009). Major Precambrian boundaries are *modified from* St-Onge et al. (2009). *See* Figure 1b for abbreviations of feature names.

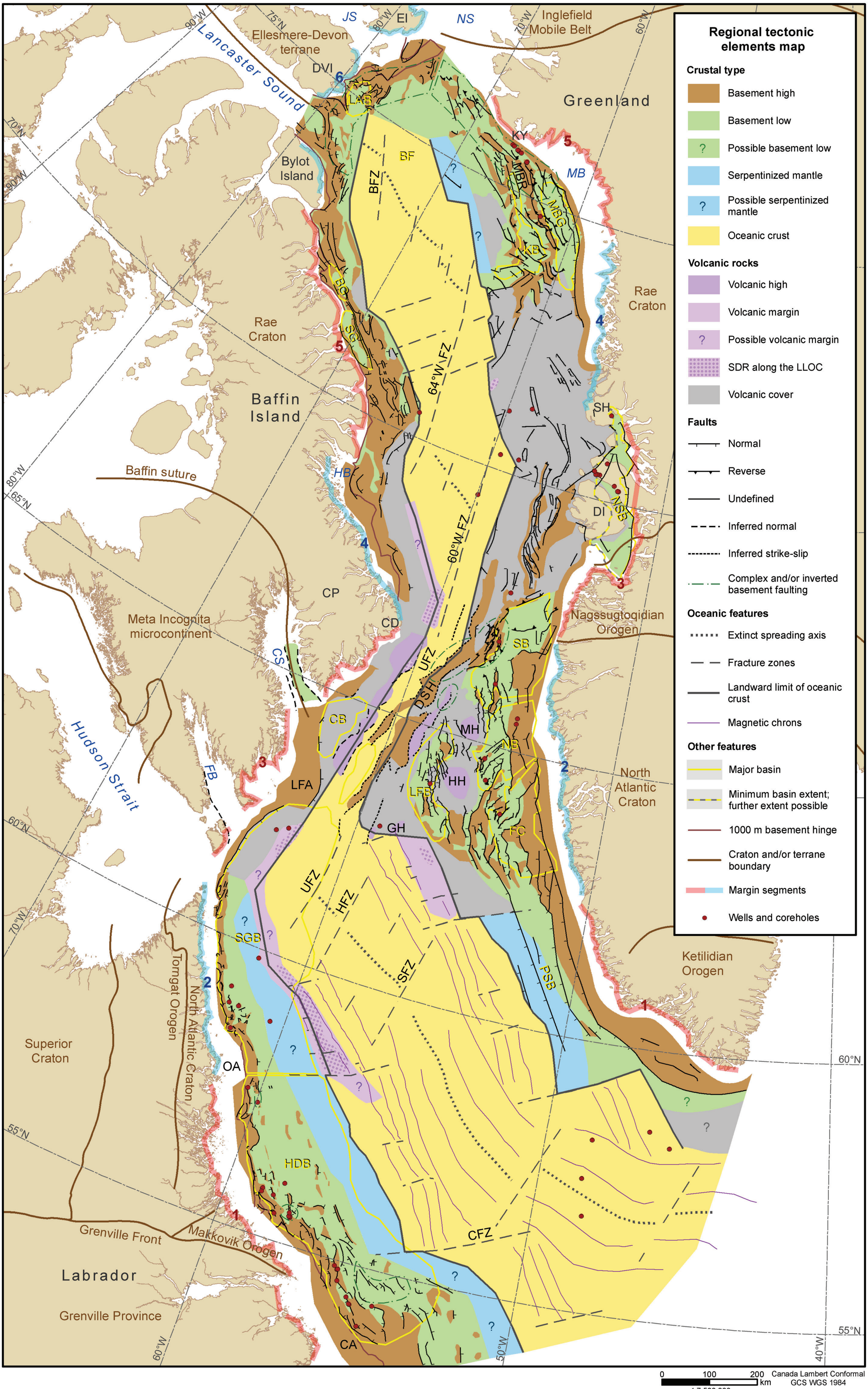
Regional tectonic elements map
Crustal type
Basement high
Basement low
Possible basement low
Serpentinized mantle
Possible serpentinized mantle
Oceanic crust
Volcanic rocks
Volcanic high
Volcanic margin
Possible volcanic margin
SDR along the LLOC
Volcanic cover
Faults
Normal
Reverse
Undefined
Inferred normal
Inferred strike-slip
Complex and/or inverted basement faulting
Oceanic features
Extinct spreading axis
Fracture zones
Landward limit of oceanic crust
Magnetic chrons
Other features
Major basin
Minimum basin extent; further extent possible
1000 m basement hinge
Craton and/or terrane boundary
Margin segments
Wells and coreholes
Greenland
Inglefield Mobile Belt
Ellesmere-Devon terrane
Lancaster Sound
Bylot Island
Baffin Island
Rae Craton
Baffin suture
Meta Incognita microcontinent
Hudson Strait
Superior Craton
Torngat Orogen
North Atlantic Craton
Nagssugtoqidian Orogen
Ketilidian Orogen
Grenville Front
Makkovik Orogen
Labrador
Grenville Province
JS
NS
EI
DVI
LAB
BF
BFZ
KY
MB
MBR
MBG
KB
BG
SG
SH
DI
NSB
HB
CP
CD
CS
FB
64°W FZ
60°W FZ
UFZ
DSH
SB
CB
MH
NB
HH
LFA
LFB
GH
FC
HFZ
SFZ
SGB
PSB
OA
HDB
CFZ
CA
75°N
70°N
65°N
60°N
55°N
90°W
80°W
70°W
60°W
50°W
40°W
0 100 200 km
1:7 500 000
Canada Lambert Conformal
GCS WGS 1984

from northwest to north-northeast, suggesting polyphase rifting from Early Cretaceous to early Cenozoic time with both extensional and strike-slip components. This differs from the conjugate offshore northern Labrador margin, which is much deeper, appears to lack a significant phase of Late Cretaceous extension, and primarily exhibits northwest-trending faults.

Segment 3

The Davis Strait transform-margin segment records both an extensional phase of faulting and later strike-slip wrench faulting (Wilson et al., 2006). It was created by plate motions along the Ungava Fault Zone and related zones of accommodation, and extends from the northern termination of the Labrador Sea spreading centre to the resumption of seafloor spreading in southern Baffin Bay. In the Early Cretaceous through early Paleocene, the region recorded primarily southwest-northeast extension between Greenland and North America (Oakey and Chalmers, 2012) reflected in northwest-trending extensional faults that are roughly parallel to the Greenland coastline and to the trend of Cumberland Sound, on the southeastern Baffin Island margin.

Early Paleocene volcanism is seen onshore Cape Dyer and in the Nuussuaq Basin, which also records the later Eocene phase of volcanism (Clarke and Upton, 1971; Skaarup, 2002; Larsen et al., 2016; Chauvet et al., 2019). Seaward-dipping reflectors are observed locally, especially offshore Baffin Island at the Hekja O-71 and Ralegh N-18 wells (Fig. 2; Keen et al., 2012), and further north along that margin (Suckro et al., 2013). A volcanic ridge appears to mark the more northern occurrences that trend north-northeast offshore Cumberland Peninsula. The late Paleocene change in the direction of plate motion led to the northward displacement of Greenland by about 290 km along the sinistral Ungava Fault Zone, where basement and older sediments were highly structured during the Eocene (Oakey and Chalmers, 2012). This transform-fault zone has also been described as ‘leaky,’ and one along which voluminous Paleogene basalts were extruded (Funck et al., 2007).

The Paleocene–Eocene outpouring of basalts obscures much of the deeper structure on seismic reflection lines. Some near-vertical discontinuities, associated with strike-slip faults, can be observed on sections, along with inversion of older rift basins (Funck et al., 2012a; Gregersen et al., 2013). The Davis Strait High is an example of a predominantly transpressional basement high related to Eocene plate motion (Oakey and Chalmers, 2012) with a zone of intense compression seen at the northern end. A region of complete rupture of the continental lithosphere may occur, as observed on seismic refraction profiles (Fig. 10c; Funck et al., 2007). This region is now filled with igneous crust over 15 km thick. Elsewhere the thinned continental crust is underplated and/or intruded by igneous rocks (Fig. 10d; Suckro et al., 2013). Much of the landward limit of oceanic crust, mapped in Davis Strait across the region of igneous crust, is supported by potential-field trends, as well as seismic refraction data.

Segment 4

The southern Baffin Bay extensional margin includes the Home Bay region off Baffin Island and extends from Svartenhuk Halvø to Kivioq Basin on the West Greenland margin. This segment is highly asymmetric, with a narrow margin along Home Bay conjugate to a wider margin off West Greenland. Both sides appear to be magma-rich with some evidence of seaward-dipping reflectors and a volcanic plateau (Skaarup et al., 2006; Suckro et al., 2012). Due to poor resolution of the seismic data along the Home Bay segment, only a tentative attempt to map the extent of this magma-rich margin has been made. This interpretation is also supported by the seismic refraction data off West Greenland, showing a volcanic layer, as well as a possible igneous underplated layer.

The faults and distribution of volcanic rocks in northern Davis Strait (segment 3) follow the northerly trending Ungava Fault Zone, but trends become northwest along this margin segment. On the Canadian margin, the basement platform in Home Bay also trends northwest, but is offset abruptly toward the northeast, following the trend of the coastline. Here, the margin offset is interpreted as a transform margin on the refraction line across it (Fig. 10e; Funck et al., 2012a). This transform margin marks the boundary along western Baffin Bay between this extensional margin segment and the next segment to the north.

Northwest of Svartenhuk Halvø, the conjugate West Greenland margin is covered by volcanic rocks that obscure many of the prevolcanic margin features. The 64°W fracture zone, when extrapolated in the direction of Paleocene spreading (southwest-northeast), follows the southern end of the Kivioq Basin, offshore West Greenland, in the region where Whittaker et al. (1997) mapped a large intrusive igneous body (Fig. 11b). Similarly, extrapolating this fracture zone toward the Canadian margin aligns it with the transform margin in Home Bay.

Segment 5

Further north, the Baffin Bay segment extends from the 64°W fracture zone to the Bower Fracture Zone, including offshore northeastern Baffin Island and the Melville Bay region, offshore West Greenland. These conjugate margin segments are extensional and generally magma-poor. Although high-amplitude reflections observed along this segment suggest volcanic rocks are present within the sedimentary section landward of the landward limit of oceanic crust, there are no well defined seaward-dipping reflectors or other features normally associated with magma-rich margins. The northernmost extent of the seafloor-spreading axis lies near the mouth of Lancaster Sound, but is not well defined (Oakey and Chalmers, 2012). The location of the landward limit of oceanic crust on the Canadian side has been estimated from older seismic refraction results (Jackson et al., 1977; Reid and Jackson, 1997) whereas several modern refraction lines cross the Greenland margin. These modern data indicate that continental crust thins toward the ocean basin. There may be an intervening transition zone of serpentinized mantle (*see* ‘Crustal structure’ section).

This segment contains the deep Kivioq Basin and Melville Bay Graben on the Greenland margin and the deepest grabens on the Canadian margin: Scott and Buchan grabens. Faults have a dominantly northwest trend within this segment and the Greenland margin is much wider than the Canadian margin. Older extensional faults have been subject to Eocene compression within the Kap York region (Fig. 14). This is due to the convergence of Greenland with Ellesmere Island during the Eocene (Oakey and Chalmers, 2012), an event that manifests itself as complex folding and faulting, as observed on seismic reflection lines (Whittaker et al., 1997; Gregersen et al., 2019). The Canadian side of this margin segment does not appear to be similarly affected.

Segment 6

Around the edges of northern Baffin Bay, the most northern tectonic segment is covered by the large Baffin Fan (Harrison et al., 2011). From offshore Bylot Island, along the mouth of Lancaster Sound and offshore Devon Island, faults trend more northerly than along the segment to the south. This region forms a transform margin parallel to the Bower Fracture Zone defined by Oakey and Chalmers (2012). There is evidence of structural inversion along this margin (Fig. 14), which has been documented by Jackson et al. (1992) and Harrison et al. (2011). Fault trends generally become more northeasterly offshore Devon Island, where the depocentre of the small Lady Ann Basin is located. Off the mouth of Jones Sound, a northerly trending basement ridge described as a ‘flower structure’ was interpreted as evidence of possible transform motion along Nares Strait (Jackson et al., 1992). The tectonic interpretation of this margin has been in dispute (Dawes and Kerr, 1982); however, some of the controversy has been resolved by Oakey and Chalmers (2012). They proposed that much of the transform motion required along this margin could be taken up by movement along a complex fault zone that extends north-northwest crossing Lady Ann Basin, and then turns north-northeast through the orogenic belt on Ellesmere Island, rather than through Nares Strait. Much about this segment remains a mystery due to the degree of structural complexity, thick sedimentary cover, and sparse seismic coverage.

Crustal thinning, magmatism, and basin development

The depth-to-basement map (Fig. 7) shows that the Hopedale Basin is very deep and occupied by thick sediments. In contrast, there is very little basin development on the offshore conjugate southwestern Greenland margin, which is relatively narrow. Farther north, the West Greenland basins of tectonic segment 2 (Fig. 14) in southern Davis Strait, are relatively shallow with respect to the deep Saglek Basin along the northern Labrador margin. There may have been some erosion of these Davis Strait basins (Dam et al., 1998; Chalmers et al., 1999; McGregor et al., 2012) during development of regional unconformities of mid-Paleocene and mid-Eocene age, but erosion alone is unlikely to explain the large differences in sediment thickness.

The crustal structure (Fig. 10a) across the conjugate margins of segment 1 suggests asymmetry in the modes of crustal extension and thinning (Chian et al., 1995b; Keen et al., 2018b). The crustal profiles across the Labrador Sea conjugate margins of segment 1 exhibit a much wider zone of highly extended continental crust offshore Labrador than that below the West Greenland conjugate margin (Fig. 10a). Seaward of the extended crust lie approximately symmetric zones of exhumed mantle (Fig. 4). The gravity inversion (Fig. 13) also shows very thin crust landward of the oceanic crust, over a zone 100 to 150 km wide offshore central Labrador, and about 100 km off the West Greenland margin. Although mapped as very thin crust, this zone would also include serpentinized and exhumed mantle as the gravity inversion is not able to resolve the total absence of crust.

The zone of thin crust and/or exhumed mantle is also seen to extend below the offshore northern Labrador segment (segment 2), narrowing to the north (Fig. 13). This zone is bordered to the east by thicker igneous crust of the magma-rich margin off northern Labrador, creating a region of thin crust or mantle inboard of the thicker oceanic and/or igneous crust. This is not as evident off the conjugate West Greenland margin (Keen et al., 2018b), which exhibits a broad zone of only moderately thinned crust (Fig. 10c). Most importantly, along segment 2, unlike segment 1, the wider margin lies on the West Greenland side. In Baffin Bay, the entire length of the Baffin Island margin (segments 4 and 5) is narrower than the West Greenland margin. Such asymmetries in margin width are observed on many rifted margins globally (e.g. Brune et al., 2017). In Davis Strait and Baffin Bay, however, Paleogene magmatic events modified observed crustal thicknesses (Fig. 10) and may have obscured the distribution of premagmatic crustal stretching on these margin segments.

The mechanisms for formation of the deep Hopedale and Saglek basins on the Labrador margin, in contrast to the relatively shallow West Greenland conjugate basins, are not well understood. Since they lie over very thin crust and exhumed mantle, subsidence due to crustal thinning will be maximized. Possible asymmetries in the mode of lithospheric deformation during rifting may have resulted in less subsidence on the West Greenland side (e.g. Huismans and Beaumont, 2014; Brune et al., 2017). The relationship between the wider Labrador margin with the deep Hopedale Basin of segment 1, however, is reversed in segment 2, where the deeper Saglek Basin is associated with the narrower margin. Assuming that crustal-scale simple shear extension was responsible for these observations (Chian et al., 1995b) and that the polarity of the simple shear zone is reversed between segments 1 and 2, then the Saglek Basin should not be so deep.

The nature of deformation of the lithospheric mantle during extension and the influence of plate-scale tectonic inheritance are important factors in creating the observed asymmetries. The southwestern Greenland onshore coastal region of segment 1 exhibited more active Mesozoic rift-related magmatism than onshore coastal Labrador, suggesting that the mantle lithosphere was thinnest on the eastern side of the rift system (Peace et al., 2016). This might imply simple shear deformation through the entire lithosphere (Peace et al., 2016). Most of the effects of the magmatism on the Labrador side, however, may be buried below the sedimentary basins and thus remain unrecognized. Tectonic inheritance of alternating strong and weak lithosphere, reflecting the presence of weaker Paleoproterozoic orogenic belts linking the stronger cratons may be another important factor, which has been suggested to explain the presence of the large-offset Ungava Fault Zone situated between two ocean basins (Heron et al., 2019). This could account for other along-strike variations in rift geometry as well.

In addition to lithospheric processes, Andrés-Martinez et al. (2019) have recently shown that the timing and magnitude of erosion and sedimentation modify the mechanical and thermal properties of the lithosphere and provide an important feedback to its deformation, including asymmetries in basin development. Sediment supply may have been much higher on the western side of the rift, which had access to a large region of North America as its source (Hinz et al., 1979). The influence of different rates of sedimentation in space and time requires further consideration within the region. Louden et al. (2004) also showed asymmetry in the sediment- and age-corrected depths-to-basement around the margins of the Labrador Sea, with present-day basement on the southwestern Greenland margin anomalously shallow. Therefore, another possibility to explain the asymmetries is that dynamic topography, created by mantle density variations, has sustained a shallower basement on the Greenland margin (Louden et al., 2004). At present, it is not possible to distinguish which of these factors are more important, but the observations likely reflect the large role played by deep lithosphere-scale processes.

Paleogene magmatism in the Davis Strait region and related underplating will cause isostatic uplift due to thickening of the crust. Uplift of about 280 to 560 m, relative to depths prior to magmatism, corresponds to underplated thicknesses of 5 and 10 km, respectively, assuming densities of 3000 and 3180 kg/m^3 for the underplated material and asthenosphere. Crustal additions from the near-surface extrusion of magma, will add more to the uplift. The above range of thicknesses of underplated material is comparable to that observed in Davis Strait and adjacent regions (Fig. 10), and the resulting uplift is similar to that required by Dam et al. (1998) to explain the depositional history of Upper Cretaceous (Maastrichtian) to Paleocene strata preserved on coastal West Greenland, where about 1.3 km of erosional denudation is thought to have occurred.

The lithospheric thermal anomaly related to rifting and magmatism will decay during postrift time, causing thermal subsidence. In contrast, the relative uplift due to crustal additions from both underplating and extrusion of thick basalt would be permanent, affecting the subsidence and stratigraphy of Davis Strait and adjacent regions from the time of occurrence of the magmatic event in the Paleocene. Therefore, the basins in the Davis Strait region should remain at shallower depths overall, compared to those not affected by magmatism; Prior to magmatism, however, the basins did subside during Late Cretaceous rifting. If they were filled with sediments by the Early Paleocene, an erosional unconformity would be predicted to develop during Paleogene magmatism due to the associated uplift. McGregor et al. (2012) and Gregersen et al. (2013, this volume) have mapped a latest Cretaceous to mid-Paleocene regional unconformity through much of this region. The development of this unconformity would have been followed by renewed subsidence after the cessation of volcanism (Jess et al., 2018).

There has been controversy concerning the age of the present-day uplift of coastal regions around the Labrador–Baffin Seaway, notably along the West Greenland margin (Japsen et al., 2005, 2012; McGregor et al., 2012; Jess et al., 2018). Marine sediments of Late Cretaceous and Paleocene age now lie several hundred metres above sea level (Dam et al., 1998; Harrison et al., 2011). Many studies have attempted to explain this uplift by a series of Neogene episodic burial and exhumation events. Other studies, particularly those carried out in offshore regions (McGregor et al., 2012; Jess et al., 2018), suggested that there is no requirement for these postrift vertical motions, and that glacial isostatic uplift and erosion during the Quaternary, plus the pre-existing topography, were sufficient to create the uplift on land. The coastal regions of Baffin Island and northern Labrador are also elevated with respect to the continental interior (McGregor et al., 2013; Japsen et al., 2018), although the evidence is sparse for the timing of the uplift. At present, there is no convincing tectonic mechanism to explain these observations and the issue remains unresolved.

Plate reconstructions

Plate reconstructions are shown in Figure 15 and the features shown are described in previous sections. At 120 Ma (Fig. 15a), the onset of rifting, there is a good fit of the restored continent-ocean boundary, with the only major overlap (approximately 80 km) occurring near Cape Dyer. There are other small gaps and overlaps, which are likely caused by errors in the estimated amount of crustal extension used to derive the position of the restored continent-ocean boundary (Hosseinpour et al., 2013). This is especially true of the largest overlap, where thick igneous rocks obscure the measurement of crustal extension. Details regarding the poles of rotation or positions of the ocean-continent boundaries or transition zones do not change these results significantly, as shown by other studies that provided a similar result (e.g. Ady and Whittaker, 2018). As noted by Hosseinpour et al. (2013), although the exact locations of the offshore extensions of major Precambrian terrane boundaries are unknown, there is a good prerift correlation across their opposing coastal positions.

Between 120 and 100 Ma, Early Cretaceous rift basins were developing, with deposition of the Bjarni and Kome formations and the Appat and Kitsissut clastic successions. There was a period of relative quiescence at about 100 Ma (Fig. 15b), with a renewed period of rifting in the early Campanian (Fig. 15c, 80 Ma; Dam et al., 2009; Døssing, 2011; Gregersen et al., 2019), which appears to have been absent on the south-central Labrador Sea margin (Dickie et al., 2011). The major sedimentary basins on the shelves surrounding northern Baffin Bay (Melville Bay Graben, Kivioq Basin, and Buchan and Scott grabens) formed a narrow swath along the rift axis through much of the Cretaceous, and are located within the same Archean terrane, the Rae Craton. Early Cretaceous rifting may also have influenced the formation of some of the peripheral bathymetric features. Lancaster Sound in northern Baffin Bay and Hudson Strait, Frobisher Bay, and Cumberland Sound, in the Davis Strait region, have a west or northwest trend, which is probably due to glacial erosion along Early Cretaceous rift-related features. Lower Cretaceous sedimentary rocks occur within Cumberland Sound (Fig. 14) and probably within Lancaster Sound (Oakey and Chalmers, 2012; Brent et al., 2013).

As mentioned earlier (*see* ‘Methods and results’ section), the overlap of many basins at 100 to 80 Ma in the Davis Strait and northern Labrador Sea is an artifact since the geometry of these basins has not been restored to remove later deformation, but their proximity indicates that they were once kinematically linked and formed within the same terrane, the North Atlantic Craton. There are, however, important exceptions such as the Nuussuaq Basin (onshore West Greenland), and the Hopedale Basin (offshore Labrador). The latter overlies the North Atlantic Craton, as well as the Paleoproterozoic Makkovik Orogen and Mesoproterozoic Grenville Province, whereas the former appears to lie close to the boundary between the Paleoproterozoic Nagssugtoqidian Orogen and the Archean Rae Craton. Many of these prerift boundaries cross the rift basins at high angles, unlike, for example, many of the rifted margins of the North and South Atlantic (Salazar-Mora et al., 2018).

In contrast, the Ungava Fault Zone appears to have formed primarily within the region of Paleoproterozoic orogens, which occupy Hudson Strait, southern Baffin Island, and central West Greenland (St-Onge et al., 2009; Darbyshire et al., 2017). The prerift crust is thicker there than elsewhere in the region (Dahl-Jensen et al., 2003; Darbyshire, 2003; Darbyshire et al., 2017) and thick-skinned orogenic suturing may have provided a prerift zone of weak lithosphere or ‘mantle scar’ for nucleation of this fault zone (Heron et al., 2019). Furthermore, as outlined below, the fault zone was initially a region of Early Cretaceous–Paleocene continental extension and emplacement of igneous crust, so these rift-related processes may have weakened the region prior to formation of the Ungava Fault Zone in Eocene time.

Late Cretaceous rifting phases are documented in stratigraphic and structural studies of Davis Strait and offshore West Greenland, as well as onshore on Bylot Island and West Greenland (Whittaker et al., 1997; Chalmers et al., 1999; Larsen and Pulvertaft, 2000; Døssing, 2011; Harrison et al., 2011; Gregersen et al., 2019). In contrast, basins on the south-central Labrador margin show less evidence for Late Cretaceous rifting below the shelf. This is compatible with rifting events concentrating farther offshore, and with sag-basin development in proximal regions (Markland Formation; Dickie et al., 2011), whereas exhumed continental mantle formed in more distal zones (Péron-Pinvidic and Manatschal, 2009).

Crustal hyperextension on the Labrador Sea margins probably occurred prior to 80 Ma, with crustal breakup occurring shortly after 80 Ma. Between 80 and 69 Ma, continued extension created regions of serpentinized and possibly exhumed continental mantle on both conjugate margins, with final lithospheric breakup and seafloor spreading beginning at 69 Ma (Fig. 15d; chron C31; Keen et al., 2018a). Thus, rifting and early seafloor spreading was generally more advanced in the south-central Labrador Sea region. In the northern Labrador Sea and Baffin Bay, breakup occurred later at chron C27n (62 Ma). In Davis Strait, Late Cretaceous rifting and plate separation affected a broad region, as indicated by the distribution of basins at 69 Ma. This region continued to open under the impetus of southwest-northeast extension until 56 Ma and includes the zone that later became the Ungava Fault Zone.

At 62 Ma (Fig. 15e), which is the approximate age of the oldest Paleogene volcanic rocks (Storey et al., 1998), intense magmatism affected the region, with the centre of magmatism located in Davis Strait. Magmatism propagated outward from there to affect the northern Labrador Sea and southern Baffin Bay regions (tectonic segments 2 and 4). The distribution of major centres of Paleogene volcanism are shown on the 62 Ma reconstruction, whereas in fact it occurred over a finite period, with the main pulse of volcanism occurring between about 62 and 58 Ma (Abdelmalak et al., 2019). The reconstruction for this time shows the close match and juxtaposition of the magma-rich margins and volcanic highs along these margin segments, but which are now widely separated. The northern Labrador volcanic margin (segment 2), where seaward-dipping reflectors and a large igneous plateau are mapped, is collinear with the Gjoa High, which now forms part of the volcanic margin segment on the West Greenland side. The Cape Dyer volcanic rocks and the large volcanic province on the West Greenland margin are also contiguous (Larsen et al., 2016). Breakup may have occurred in Baffin Bay, and probably in parts of Davis Strait, at this time, but seafloor spreading had already begun earlier (around 69 Ma) in the Labrador Sea. In the northern Labrador Sea and Davis Strait, volcanism, magmatic intrusion, and crustal underplating thickened the crust by up to approximately 15 km (Fig. 10c; Funck et al., 2007; Suckro et al., 2013), imposing significant new characteristics upon a previously magma-poor rift. The magmatic underplating would have been concentrated within regions of previously thinned continental crust (Keen et al., 2012), possibly coinciding with extrusion centres of volcanic rocks.

In northern Baffin Bay, the presence of serpentinized and possibly exhumed mantle is not well established (*see* discussion in ‘Crustal structure’ section). Plate reconstructions suggest that if serpentinized mantle zones were present, they would have formed close to the time of breakup, at 62 Ma (Fig. 15e). The exhumed mantle on the western side of Baffin Bay is not shown on the plate reconstructions because the seismic refraction data for that region is unresolved (*see* ‘Crustal structure’ section) and lies on the diffuse, and structurally complex, plate boundary extending from the northern end of the extinct ridge axis onto the continental shelf (Oakey and Chalmers, 2012).

At 56 Ma (Fig. 15f), the region of oceanic crust in Davis Strait reached its maximum width; after this time, the direction of plate motions changed to become almost north-south and transpression along the Ungava Fault Zone caused local inversion of structures and partial closure of the oceanic region (Oakey and Chalmers, 2012). This is most clearly expressed in the Davis Strait High (DHS; Fig. 14). There has been almost 300 km of sinistral strike-slip offset between the plates on either side of this Eocene fracture zone. This is an important consideration in comparing stratigraphic data and crustal structure across the current margins, as conjugate profiles are now widely separated. Cretaceous stratigraphy below the northern Labrador margin and many of the West Greenland and Davis Strait basins should be similar, becoming progressively less so in the Paleocene–Eocene. The West Greenland margin was, relative to present-day Labrador, much farther south when most of the crustal thinning, basement faulting and subsidence occurred during the Cretaceous. Therefore, care must be taken when comparing structure and stratigraphy across the present-day margins (Fig. 15g).

The reconstructions show the inferred track of the proto-Iceland hotspot through the Cretaceous (Whittaker et al., 2015), where it appears to have travelled south down Baffin Bay near Melville Bay at 100 Ma to coastal West Greenland at 80 Ma. This apparent southward track is consistent with studies of absolute plate motions, which suggest northward motion of North America and Greenland through Late Mesozoic–Cenozoic time (Müller et al., 2016). At 62 Ma the hotspot is predicted to lie further east under the thicker Greenland lithosphere, about 200 km east of Svartenhuk Halvø. There is no evidence of hotspot influence in the Melville Bay region, suggesting that it had not impinged on the base of the lithosphere in Cretaceous time. The onset of magmatism at 62 Ma, when the plume is shown below Greenland, may, in part, explain why the igneous addition to continental crust under the West Greenland margin appears generally more voluminous than under the Canadian conjugate margin, according to seismic refraction results (Fig. 10, 11). Also, wells drilled in southern Davis Strait do not appear to contain the younger sequence of Eocene volcanic rocks (Wielens and Williams, 2009; Nøhr-Hansen

Figure 15. Plate reconstructions, as produced by open-source software GPlates, showing snapshots of the relative positions of Greenland and North America at various times. The present-day configuration of the Labrador Sea–Baffin Bay region outlines some of the major features related to the reconstructions and described in the text: major sedimentary basins, the volcanic features and margins, the restored continent-ocean boundary (RCOB; Hosseinpour et al., 2013), the landward limit of oceanic crust (LLOC), oceanic fracture zones, and extinct-rift axis. Overlap of features is shown by a darker colour. Major Precambrian boundaries are *modified from* St-Onge et al. (2009). Fracture zones and extinct spreading axis are *after* Oakey and Chalmers (2012). The motion paths are shown for Greenland with respect to North America (Fig. 15g), with arrows marking the following times: 100, 80, 69, 62, 56, and 0 to 33 Ma. Plate reconstructions are shown for: **a)** 120 Ma: early continental rifting with the formation of faulted basement blocks and deposition of synrift sediments; **b)** 100 Ma: continued continental extension; **c)** 80 Ma: Late Crectaceous rifting with extension probably focused below the more distal regions off Labrador and southwestern Greenland (Keen et al., 2012); **d)** 69 Ma: onset of seafloor spreading in the Labrador Sea (chron C31; Keen et al., 2018a); **e)** 62 Ma: onset of Paleocene volcanism and continental breakup in Baffin Bay (chron C27n; Oakey and Chalmers, 2012); **f)** 56 Ma: change in direction of plate motion and onset of northward motion of the Greenland Plate relative to North America (chron C25n–C24n); **g)** 0 to 33 Ma: structure across present-day margins. *See* Figure 1b for abbreviations of feature names.

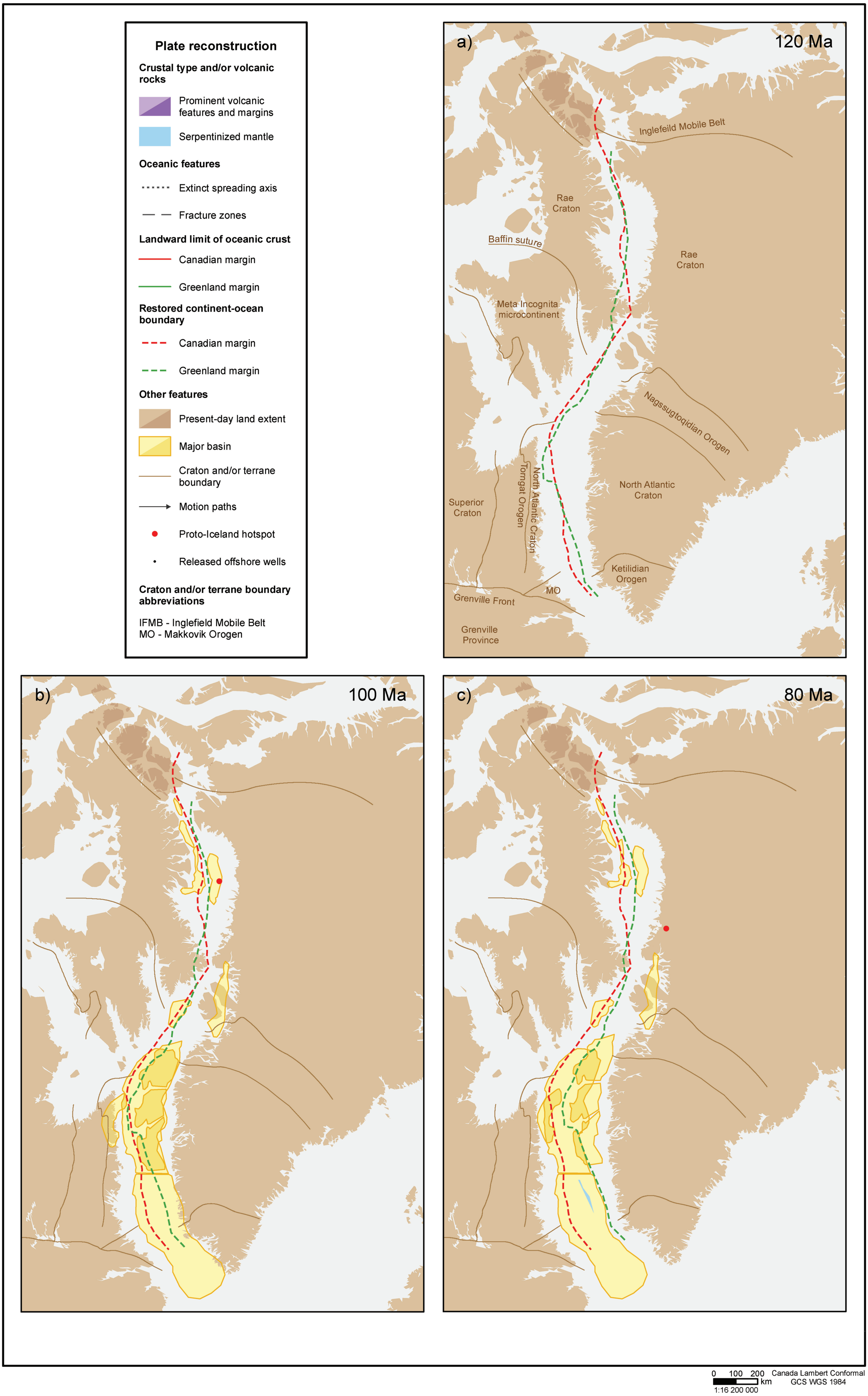
Plate reconstruction
Crustal type and/or volcanic rocks
Prominent volcanic features and margins
Serpentinized mantle
Oceanic features
Extinct spreading axis
Fracture zones
Landward limit of oceanic crust
Canadian margin
Greenland margin
Restored continent-ocean boundary
Canadian margin
Greenland margin
Other features
Present-day land extent
Major basin
Craton and/or terrane boundary
Motion paths
Proto-Iceland hotspot
Released offshore wells
Craton and/or terrane boundary abbreviations
IFMB - Inglefield Mobile Belt
MO - Makkovik Orogen
a)
120 Ma
Inglefeild Mobile Belt
Rae Craton
Rae Craton
Baffin suture
Meta Incognita microcontinent
Nagssugtoqidian Orogen
North Atlantic Craton
Superior Craton
Torngat Orogen
North Atlantic Craton
Ketilidian Orogen
MO
Grenville Front
Grenville Province
b)
100 Ma
c)
80 Ma
0 100 200 km
1:16 200 000
Canada Lambert Conformal
GCS WGS 1984

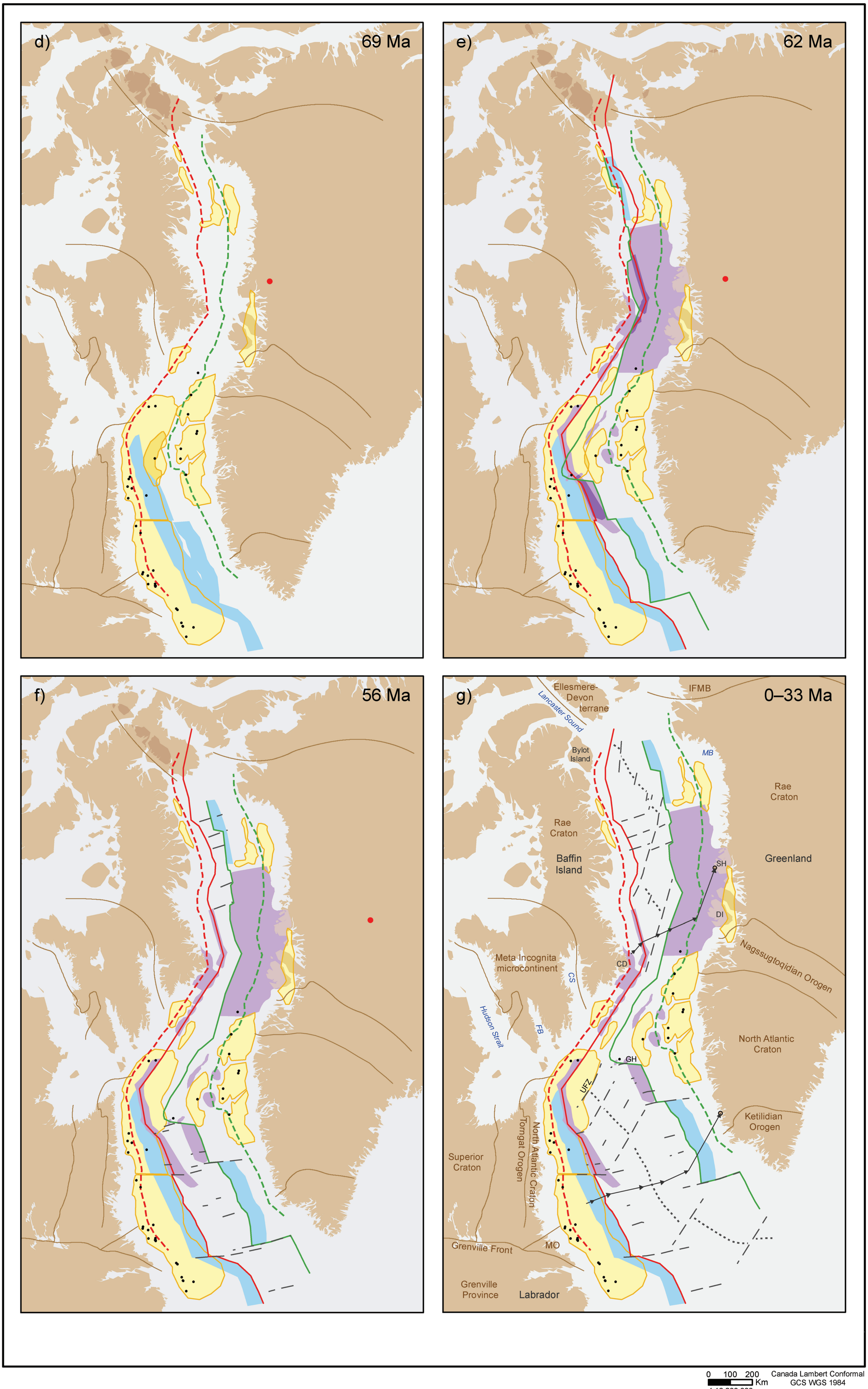
d)
69 Ma
e)
62 Ma
f)
56 Ma
g)
0–33 Ma
Ellesmere-
Devon
terrane
Lancaster Sound
IFMB
Bylot
Island
MB
Rae
Craton
Rae
Craton
Baffin
Island
Greenland
SH
DI
Nagssugtoqidian Orogen
Meta Incognita
microcontinent
CD
CS
Hudson Strait
FB
North Atlantic
Craton
GH
UFZ
Ketilidian
Orogen
Superior
Craton
Torngat Orogen
North Atlantic Craton
Grenville Front
MO
Grenville
Province
Labrador
0 100 200
Km
1:16,200,000
Canada Lambert Conformal
GCS WGS 1984

et al., 2016), but these are observed onshore in the Disko Island–Svartenhuk Halvø region of West Greenland and offshore in the Delta-1 well (Fig. 2; Nelson et al., 2015; Abdelmalak et al., 2019).

Some geochemical studies and radiometric dates of Paleocene basalt in Davis Strait suggested that the potential temperature of the mantle was 200° C higher than the ambient temperature and that the lithosphere was thin (90 km or less) at the time of magmatism (Larsen and Dalhoff, 2006; Hole and Millett, 2016; Larsen et al., 2016; Abdelmalak et al., 2019). These results supported the occurrence below Davis Strait of a thermal anomaly similar and slightly hotter than that below present-day Iceland, and were consistent with the presence of a proto-Iceland mantle plume as the source of magmatism. Nevertheless, lithospheric thinning also appeared to have played an important role in determining the geographic variation in the geochemistry of the basalt (Hole and Millett, 2016). Others disputed the necessity of a plume and suggested instead that lithospheric deformation was wholly responsible for this variation. Most recently Clarke and Beutel (2019) have argued that tectonic inheritance, involving the reactivation of a Paleoproterozoic suture in the Davis Strait region during rifting, created pathways for rapid ascent of the early picritic magmatism, an interpretation that does not require high mantle temperatures.

Plate velocities for Greenland relative to North America increased dramatically between 85 and 75 Ma (early- to mid-Campanian). In the central Labrador Sea, low velocities of about 0.2 cm/a are observed from 120 to 84 Ma increasing to about 1.3 cm/a (full rate) by 73 Ma. Slightly lower values apply to Baffin Bay over the same time periods, increasing between 84 to 73 Ma to 0.75 cm/a. This pronounced increase in plate velocity is like that reported by Roest and Srivastava (1989) and Brune et al. (2016) for these plates. Brune et al. (2016) suggested that this occurs at many rifted margins and reflects a rapid drop in the strength of the lithosphere well before breakup. On the Labrador and West Greenland margins, this is supported by a rapid increase in the subsidence rate between 85 and 75 Ma (Dickie et al., 2011; Døssing, 2011; McGregor et al., 2012), before the arrival of the plume or hotspot in the region. The sustained higher rate of plate separation, which reached about 2 cm/a at 62 Ma in the Davis Strait region, would enhance the upwelling of melt into the rift (Larsen et al., 2016).

CONCLUSIONS

The Labrador–Baffin Seaway represents a complex rift system of great length (about 2000 km), which is only now beginning to be understood in terms of its variability in both space and time. Many types of passive margins are represented: rifted and transform, and with magma-poor and magma-rich segments. Rifting began in the Early Cretaceous throughout the region, but breakup in Late Cretaceous and Paleocene time was diachronous and generally later in the north than in the south. Rifting was more advanced in the south and by Late Cretaceous time, extension had migrated farther offshore into deep-water regions, where zones of hyperextension and mantle exhumation are present. The more proximal basins in the south are sag basins and exhibit little or no Late Cretaceous rift-related stratigraphic events. The large-scale, Paleocene–Eocene magmatic event centred on Davis Strait added an extra degree of complexity, as it modified both the crustal structure and the overlying basin fill. Margins from the northern Labrador Sea to southern Baffin Bay are most affected by this event. Igneous rocks are thickest where the continental crust had already been extended and thinned. Presumably, the lower mantle lithosphere was also thinner in these regions and might have acted as a channel along which melts could travel. These magma-rich margins were probably magma-poor before Paleogene magmatism, and relicts of the magma-poor margin can be seen along the northern Labrador region. In northern Baffin Bay and the southern Labrador Sea, the margins are mostly magma-poor in nature.

In Eocene time, there was a major change in the direction of plate motion as seafloor spreading began in the Northeast Atlantic. This led to the convergence of northern Greenland and North America, which resulted in transpression and transtension along the northern Baffin Bay margin and the adjacent landmasses. The high degree of structural complexity prevents the clear definition of the plate boundaries in that region. The change in plate motion also produced a large offset along the Ungava Fault Zone through Davis Strait and the zone is associated with many strike-slip structures.

Both the magmatism and the change in regional stress patterns present additional challenges to determining the evolution of the rift in space and time. Sedimentary basins developed in response to local lithospheric conditions and reflect the deeper deformation, thermal state, and magmatism that affected the region. They vary in subsidence and size, both across conjugate margins and along the strike of the rift system in ways that are not easily explained. This highlights the need for a better understanding of the role of the deep lithospheric mantle in controlling rift evolution, and the interactions of deep and shallow processes, including what sedimentary basins can reveal about the deeper structure and vice versa. Although many questions remain, the purpose of this study has been to present an overview of the evolution of the Labrador–Baffin system as a whole so that important comparisons and connections can be made.

ACKNOWLEDGMENTS

The authors are grateful to M.H. Salisbury and D.J.W. Piper for their reviews of the manuscript and their many helpful suggestions. They also thank S. Hynes who assisted with the data compilation, L. MacLeod who used her extensive GIS mapmaking skills to produce the maps, and P. Lake who helped with editing the manuscript.

REFERENCES

Abdelmalak, M.M., Planke, S., Polteau, S., Hartz, E.H., Faleide, J.I., Tegner, C., Jerram, D.A., Millett, J.M., and Myklebust, R., 2019. Breakup volcanism and plate tectonics in the NW Atlantic; Tectonophysics, v. 760, p. 267–296. https://doi.org/10.1016/j.tecto.2018.08.002

Ady, B.E. and Whittaker, R.C., 2018. Examining the influence of tectonic inheritance on the evolution of the North Atlantic using a palinspastic deformable plate reconstruction; *in* Fifty years of the Wilson Cycle concept in plate tectonics, (ed.) R.W. Wilson, G.A. Housemen, K.J.W. McCaffery, A.G. Doré, and S.J.H. Buiter; Geological Society of London, Special Publications, v. 470. https://doi.org/10.1144/SP470.9

Altenbernd, T., Jokat, W., Heyde, I., and Damm, V., 2014. A crustal model for northern Melville Bay, Baffin Bay; Journal of Geophysical Research, v. 119, no. 12, p. 8610–8632. https://doi.org/10.1002/2014JB011559

Altenbernd, T., Jokat, W., Heyde, I., and Damm, V., 2015. Geophysical evidence for the extent of crustal types and the type of margin along a profile in the northeastern Baffin Bay; Journal of Geophysical Research, v. 120, no. 11, p. 7337–7360. https://doi.org/10.1002/2015JB012307

Altenbernd, T., Jokat, W., Heyde, I., and Damm, V., 2016. Insights into the crustal structure of the transition between Nares Strait and Baffin Bay; Tectonophysics, v. 691 pt. A, p. 31–47. https://doi.org/10.1016/j.tecto.2016.04.001

Andrés-Martínez, M., Perez-Gussinye, M., Armitage, J., and Morgan, J.P., 2019. Thermo-mechanical implications of sediment transport for the architecture and evolution of continental rifts and margins; Tectonics, v. 38, p. 641–665. https://doi.org/10.1029/2018TC005346

Balkwill, H.R., 1987. Labrador basin: structural and stratigraphic style; *in* Sedimentary basins and basin-forming mechanisms, (ed.) C. Beaumont and A.J. Tankard; Canadian Society of Petroleum Geologists, Memoir, v. 12, p. 17–43.

Balkwill, H.R., McMillan, N.J., MacLean, B., Williams, G.L., and Srivastava, S.P., 1990. Geology of the Labrador Shelf, Baffin Bay, and Davis Strait, Part 1: Mesozoic–Cenozoic geology of the Labrador Shelf; *in* Chapter 7 of Geology of the continental margin of Eastern Canada, Geology of Canada, (ed.) M.J. Keen and G.L. Williams, Geological Survey of Canada, Geology of Canada no. 2, p. 295–324 (*also* Geological Society of America, The Geology of North America, v. I-1). https://doi.org/10.4095/132690

Barnett-Moore, N., Müller, R.D., Williams, S.E., Skogseid, J., and Seton, M., 2018. A reconstruction of the North Atlantic since the earliest Jurassic; Basin Research, v. 30, suppl. 1, p. 160–185. https://doi.org/10.1111/bre.12214

Bayrakci, G., Minshull, T.A., Sawyer, D.S., Reston, T.J., Klaeschen, D., Papenberg, C., Ranero, C., Bull, J.M., Davy, R.G., Shillington, D.J., Pérez-Gussinyé, M., and Morgan, J.K., 2016. Fault-controlled hydration of the upper mantle during continental rifting; Nature Geoscience, v. 9, p. 384–388. https://doi.org/10.1038/ngeo2671

Block, M., Damm, V., Ehrhardt, A., Berglar, K., Schnabel, M., and Altenbernd, T., 2012. Characteristics of the West Greenland margin in the southern Baffin Bay; 74th EAGE Conference, Copenhagen, June 4–7, 2012, extended abstract. https://doi.org/10.3997/2214-4609.20148225

Brent, T.A., Chen, Z., Currie, L.D., and Osadetz, K., 2013. Assessment of the conventional petroleum resource potential of Mesozoic and younger structural plays within the proposed National Marine Conservation Area, Lancaster Sound, Nunavut; Geological Survey of Canada, Open File 6954, 54 p. https://doi.org/10.4095/289615

Brune, S., Williams, S.E., Butterworth, N.P., and Müller, R.D., 2016. Abrupt plate accelerations shape rifted continental margins; Nature, v. 536, p. 201–204. https://doi.org/10.1038/nature18319

Brune, S., Heine, C., Clift, P.D., and Pérez-Gussinyé, M., 2017. Rifted margin architecture and crustal rheology: reviewing Iberia–Newfoundland, Central South Atlantic, and South China Sea; Marine and Petroleum Geology, v. 79, p. 257–281. https://doi.org/10.1016/j.marpetgeo.2016.10.018

Canterra Energy Ltd., 1982. Well history report–Ralegh N-18; prepared by Canterra Energy Ltd. for the Canada-Newfoundland and Labrador Offshore Petroleum Board, 146 p.

Chalmers, J.A., 1997. The continental margin off southern Greenland: along strike transition from an amagmatic to a volcanic margin; Geological Society of London, Journal, v. 154, p. 571–576. https://doi.org/10.1144/gsjgs.154.3.0571

Chalmers, J.A. and Laursen, K.H., 1995. Labrador Sea: the extent of continental and oceanic crust and the timing of the onset of seafloor spreading; Marine and Petroleum Geology, v. 12, no. 2, p. 205–217. https://doi.org/10.1016/0264-8172(95)92840-S

Chalmers, J.A. and Pulvertaft, T.C.R., 2001. Development of the continental margins of the Labrador Sea: a review; Geological Society of London, Special Publications, v. 187, no. 1, p. 77–105. https://doi.org/10.1144/GSL.SP.2001.187.01.05

Chalmers, J.A., Pulvertaft, T.C.R., Marcussen, C., and Pedersen, A.K., 1999. New insight into the structure of the Nuussuaq Basin, central West Greenland; Marine and Petroleum Geology, v. 16, p. 197–211, 213–224. https://doi.org/10.1016/S0264-8172(98)00077-4

Chauvet, F., Geoffrey, L., Guillou, H., Maury, R.C., Le Gall, B., Agranier, A., and Viana, A., 2019. Eocene continental breakup in Baffin Bay; Tectonophysics, v. 757, p. 170–186. https://doi.org/10.1016/j.tecto.2019.03.003

Chian, D. and Louden, K., 1992. The structure of Archean–Ketilidian crust along the continental shelf of southwestern Greenland from a seismic refraction profile; Canadian Journal of Earth Sciences, v. 29, no. 2, p. 301–313. https://doi.org/10.1139/e92-027

Chian, D. and Louden, K.E., 1994. The continent-ocean crustal transition across the southwest Greenland margin; Journal of Geophysical Research, v. 99, no. B5, p. 9117–9135. https://doi.org/10.1029/93JB03404

Chian, D., Louden, K.E., and Reid, I., 1995a. Crustal structure of the Labrador Sea conjugate margin and implications for the formation of nonvolcanic continental margins; Journal of Geophysical Research, v. 100, no. B12, p. 24 239–24 253. https://doi.org/10.1029/95JB02162

Chian, D., Keen, C., Reid, I., and Louden, K.E., 1995b. Evolution of nonvolcanic rifted margins: new results from the conjugate margins of the Labrador Sea; Geology, v. 23, p. 589–592. https://doi.org/10.1130/0091-7613(1995)023%3c0589:EONRMN%3e2.3.CO%3b2

Christensen, N.I., 2004. Serpentinites, peridotites, and seismology; International Geology Review, v. 46, no. 9, p. 795–816. https://doi.org/10.2747/0020-6814.46.9.795

Clarke, D.B., 1970. Tertiary basalts in Baffin Bay: possible primary magma from the mantle; Contributions to Mineralogy and Petrology, v. 25, p. 203–224. https://doi.org/10.1007/BF00371131

Clarke, D.B. and Beutel, E.K., 2019. Davis Strait Paleocene picrites: products of a plume or plates?; Earth-Science Reviews, v. 206. https://doi.org/10.1016/j.earscirev.2019.01.012

Clarke, D.B. and Pedersen, A.K., 1976. Tertiary volcanic province of West Greenland; *in* Geology of Greenland, (ed.) A. Esher and W.S. Watt; Geological Survey of Greenland, Copenhagen, Denmark, p. 364–385.

Clarke, D.B. and Upton, B.G.J., 1971. Tertiary basalts of Baffin Island: field relations and tectonic setting; Canadian Journal of Earth Sciences, v. 8, p. 248–258. https://doi.org/10.1139/e71-025

Dafoe, L.T., Dickie, K., Williams, G.L., Jauer, C.D., Hynes, S., Brent, T.A., Li, Q., Oakey, G.N., Potter, D.P., Haggart, J.W., Smyth, H.R., Currie, L.D., Sweet, A.R., DesRoches, K., and Szlavko, B., 2016a. Report of activities for the stratigraphic and tectonic framework for the Baffin Bay Petroleum Systems, craton 2 Baffin Project; Geological Survey of Canada, Open File 7960, 10 p. https://doi.org/10.4095/297248

Dafoe, L.T., Dickie, K., Williams, G.L., Jauer, C.D., Li., Q., Dehler, S., Potter, D.P., Hynes, S., Patton, E., Bates, J., Haggart, J.W., and Clark, K., 2016b. Report of activities for the stratigraphic and tectonic framework for the Baffin Bay Petroleum Systems (2016), GEM-2 Baffin Project; Geological Survey of Canada, Open File 8144, 10 p. https://doi.org/10.4095/299240

Dahl-Jensen, T., Larsen, T.B., Woelbern, I., Bach, T., Hanka, W., Kind, R., Gergersen, S., Mosegaard, K., Voss, P., and Gudmundsson, O., 2003. Depth to Moho in Greenland: receiver-function analysis suggests two Proterozoic blocks in Greenland; Earth and Planetary Science Letters, v. 205, no. 3–4, p. 379–393. https://doi.org/10.1016/S0012-821X(02)01080-4

Dalhoff, F., Larsen, L.M., Ineson, J.R., Stouge, S., Bojesen-Koefoed, J.A., Lassen, S., Kuijpers, A., Rasmussen, J.A., and Nøhr-Hansen, H., 2006. Continental crust in the Davis Strait: new evidence from seabed sampling; Geological Survey of Denmark and Greenland Bulletin, v. 10, p. 33–36. https://doi.org/10.34194/geusb.v10.4901

Dam, G., Larsen, M., and Sørensen, J.C., 1998. Sedimentary response to mantle plumes: implications from Palaeocene onshore successions, West and East Greenland; Geology, v. 26, p. 207–210. https://doi.org/10.1130/0091-7613(1998)026%3c0207:SRTMPI%3e2.3.CO%3b2

Dam, G., Pedersen, G.K., Sønderholm, M., Midtgaard, H., Larsen, L.M., Nøhr-Hansen, H., and Pedersen, A.K., 2009. Lithostratigraphy of the Cretaceous–Paleocene Nuussuaq Group, Nuussuaq Basin, West Greenland; Geological Survey of Denmark and Greenland Bulletin, v. 19, 171 p. https://doi.org/10.34194/geusb.v19.4886

Darbyshire, F.A., 2003. Crustal structure across the Canadian High Arctic region from teleseismic receiver function analysis; Geophysical Journal International, v. 152, p. 372–391. https://doi.org/10.1046/j.1365-246X.2003.01840.x

Darbyshire, F.A., Bastow, I.D., Petrescu, L., Gilligan, A., and Thompson, D.A., 2017. A tale of two orogens: crustal processes in the Proterozoic Trans-Hudson and Grenville orogens, eastern Canada; Tectonics, v. 36, p. 1633–1659. https://doi.org/10.1002/2017TC004479

Darbyshire, F.A., Dahl-Jensen, T., Larsen, T.B., Voss, P.H., and Jayal, G., 2018. Crustal and uppermost-mantle structure of Greenland and the Northwest Atlantic from Rayleigh wave group velocity tomography; Geophysical Journal International, v. 212, p. 1546–1569. https://doi.org/10.1093/gji/ggx479

Dawes, P.R., 1976. Precambrian to Tertiary of northern Greenland; *in* Geology of Greenland, (ed.) A. Escher and W.S. Watt; Geological Survey of Greenland, Copenhagen, Denmark, p. 248–303.

Dawes, P.R., 1997. The Proterozoic Thule Supergroup, Greenland and Canada: history, lithostratigraphy and development; Geological Survey of Denmark and Greenland, Geology of Greenland Survey, Bulletin 174, 150 p.

Dawes, P.R. and Kerr, J.W., 1982. The case against major displacement along Nares Strait; *in* Nares Strait and the drift of Greenland: a conflict in plate tectonics. Meddelelser om Grønland, (ed.) P.R. Dawes and J.W. Kerr; Geoscience, v. 8, p. 369–386.

Delescluse, M., Funck, T., Dehler, S.A., Louden, K.E., and Watremez, L., 2015. The oceanic crustal structure at the extinct, slow to ultraslow Labrador Sea spreading center; Journal of Geophysical Research, v. 120, no. 7, p. 5249–5272. https://doi.org/10.1002/2014JB011739

Dickie, K., Keen, C.E., Williams, G.L., and Dehler, S.A., 2011. Tectonostratigraphic evolution of the Labrador margin, Atlantic Canada; Marine and Petroleum Geology, v. 28, p. 1663–1675. https://doi.org/10.1016/j.marpetgeo.2011.05.009

Døssing, A., 2011. Fylla bank: structure and evolution of a normal-to-shear rifted margin in the northern Labrador Sea; Geophysical Journal International, v. 187, p. 655–676. https://doi.org/10.1111/j.1365-246X.2011.05184.x

Edwards, R.A., Whitmarsh, R.B., and Scrutton, R.A., 1997. The crustal structure across the transform continental margin off Ghana, eastern equatorial Atlantic; Journal of Geophysical Research, v. 102, no. B1, p. 747–772. https://doi.org/10.1029/96JB02098

Foulger, G.R. and Anderson, D.L., 2005. A cool model for the Iceland hotspot; Journal of Volcanology and Geothermal Research, v. 141, no. 1–2, p. 1–22. https://doi.org/10.1016/j.jvolgeores.2004.10.007

Funck, T. and Louden, K.E., 1998. Wide-angle seismic imaging of pristine Archean crust in the Nain Province, Labrador; Canadian Journal of Earth Sciences, v. 35, no. 6, p. 672–685. https://doi.org/10.1139/e98-019

Funck, T. and Louden, K.E., 1999. Wide-angle seismic transect across the Torngat Orogen, northern Labrador: evidence for a Proterozoic crustal root; Journal of Geophysical Research, v. 104, no. B4, p. 7463–7480. https://doi.org/10.1029/1999JB900010

Funck, T., Louden, K.E., and Reid, I.D., 2000a. Wide-angle seismic imaging of a Mesoproterozoic anorthosite complex: the Nain Plutonic Suite in Labrador, Canada; Journal of Geophysical Research, v. 105, no. B11, p. 25 693–25 707. https://doi.org/10.1029/2000JB900237

Funck, T., Louden, K.E., Wardle, R.J., Hall, J., Hobro, J.W., Salisbury, M.H., and Muzzatti, A.M., 2000b. Three-dimensional structure of the Torngat Orogen (NE Canada) from active seismic tomography; Journal of Geophysical Research, v. 105, no. B10, p. 23 403–23 420. https://doi.org/10.1029/2000JB900228

Funck, T., Louden, K.E., and Reid, I.D., 2001. Crustal structure of the Grenville Province in southeastern Labrador from refraction seismic data: evidence for a high-velocity lower crustal wedge; Canadian Journal of Earth Sciences, v. 38, no. 10, p. 1463–1478. https://doi.org/10.1139/e01-026

Funck, T., Jackson, H.R., Louden, K.E., Dehler, S.A., and Wu, Y., 2004. Crustal structure of the northern Nova Scotia rifted continental margin (eastern Canada); Journal of Geophysical Research, v. 109, no. B9, 19 p. https://doi.org/10.1029/2004JB003008

Funck, T., Jackson, H.R., Dehler, S.A., and Reid, I.D., 2006. A refraction seismic transect from Greenland to Ellesmere Island, Canada: the crustal structure in southern Nares Strait; Polarforschung, v. 74, no. 1–3, p. 97–112. https://doi.org/10013/epic.29927.d001

Funck, T., Jackson, H.R., Louden, K.E., and Klingelhöfer, F., 2007. Seismic study of the transform-rifted margin in Davis Strait between Baffin Island (Canada) and Greenland: what happens when a plume meets a transform; Journal of Geophysical Research, v. 112, no. B4, 22 p. https://doi.org/10.1029/2006JB004308

Funck, T., Hansen, A.K., Reid, I.D., and Louden, K.E., 2008. The crustal structure of the southern Nain and Makkovik provinces of Labrador derived from refraction seismic data; Canadian Journal of Earth Sciences, v. 45, no. 4, p. 465–481. https://doi.org/10.1139/E08-007

Funck, T., Gohl, K., Damm, V., and Heyde, I., 2012a. Tectonic evolution of southern Baffin Bay and Davis Strait: results from a seismic refraction transect between Canada and Greenland; Journal of Geophysical Research, v. 117, no. B4, 24 p. https://doi.org/10.1029/2011JB009110

Funck, T., Andrup-Henriksen, G., Dehler, S.A., and Louden, K.E., 2012b. The crustal structure of the Eirik Ridge at the southern Greenland continental margin; Geological Association of Canada–Mineralogical Association of Canada, St. John's, Newfoundland, May 27–29, 2012, Abstracts, v. 35, p. 47.

Geological Survey of Canada, 1988. Gravity anomaly map of the continental margin of Eastern Canada (Bouguer on land; free-air at sea); Geological Survey of Canada, Map 1708A, scale 1:5 000 000. https://doi.org/10.4095/125186

Gerlings, J., Funck, T., Jackson, H.R., Louden, K.E., and Klingelhöfer, F., 2009. Seismic evidence for plume-derived volcanism during formation of the continental margin in southern Davis Strait and northern Labrador Sea; Geophysical Journal International, v. 176, no. 3, p. 980–994. https://doi.org/10.1111/j.1365-246X.2008.04021.x

Gillard, M., Sauter, D., Tugend, J., Tomasi, S., Epin, M.-E., and Manatschal, G., 2017. Birth of an oceanic spreading center at a magma-poor rift system; Scientific Reports, v. 7, no. 1, 6 p. https://doi.org/10.1038/s41598-017-15522-2

Gion, A.M., Williams, S.E., and Müller, R.D., 2017. A reconstruction of the Eurekan Orogeny incorporating deformation constraints; Tectonics, v. 36, p. 304–320. https://doi.org/10.1002/2015TC004094

Gohl, K. and Smithson, S.B., 1993. Structure of Archean crust and passive margin of southwest Greenland from seismic wide-angle data; Journal of Geophysical Research, v. 98, no. B4, p. 6623–6638. https://doi.org/10.1029/93JB00016

Grant, A.C., 1990. Depth to basement of the continental margin of eastern Canada; *in* Geology of the continental margin of Eastern Canada, (ed.) M.J. Keen and G.L. Williams, Geological Survey of Canada, Geology of Canada no. 2, Map 1707a, scale 1:5 000 000 (*also* Geological Society of America, The Geology of North America, v. I-1). https://doi.org/10.4095/132690

Gregersen, U. and Bidstrup, T., 2008. Structures and hydrocarbon prospectivity in the northern Davis Strait area, offshore West Greenland; Petroleum Geoscience, v. 14, p. 151–166. https://doi.org/10.1144/1354-079308-752

Gregersen, U., Hopper, J.R., and Knutz, P.C., 2013. Basin seismic stratigraphy and aspects of prospectivity in the NE Baffin Bay, northwest Greenland; Marine and Petroleum Geology, v. 46, p. 1–18. https://doi.org/10.1016/j.marpetgeo.2013.05.013

Gregersen, U., Andersen, M.S., Nøhr-Hansen, H., Sheldon, E., Kokfelt, T.F., Olivarius, M., Knudsen, C., Jakobsen, K.G., and Adolfssen, J.S., 2018. New subsurface mapping offshore southern West Greenland using geophysical and geological data; Geological Survey of Denmark and Greenland, Bulletin, v. 41, p. 57–62. https://doi.org/10.34194/geusb.v41.434

Gregersen, U., Knutz, P.C., Nøhr-Hansen, H., Sheldon, E., and Hopper, J.R., 2019. Tectonostratigraphy and evolution of the West Greenland continental margin; Bulletin of the Geological Society of Denmark, v. 67, p. 1–21. https://doi.org/10.37570/bgsd-2019-67-01

Hall, J., Louden, K.E., Funck, T., and Deemer, S., 2002. Geophysical characteristics of the continental crust along the Lithoprobe Eastern Canadian Shield Onshore–Offshore Transect (ECSOOT): a review; Canadian Journal of Earth Sciences, v. 39, p. 569–587. https://doi.org/10.1139/e02-005

Harrison, J.C., Brent, T.A., and Oakey, G.N., 2011. Baffin Fan and its inverted rift system of Arctic eastern Canada: stratigraphy, tectonics and petroleum resource potential; Chapter 40 *in* Arctic petroleum geology, (ed.) A.M. Spencer, A.F. Embry, D.L. Gautier, A.V. Stoupakova, and K. Sørensen; Geological Society of London, Memoirs, v. 35, no. 1, p. 595–626. https://doi.org/10.1144/m35.40

Henderson, G., 1976. Petroleum Geology; *in* Geology of Greenland, (ed.) A. Escher and W.S. Watt; Geological Survey of Greenland, Copenhagen, Denmark, p. 488–505.

Heron, P.J., Peace, A.L., McCaffery, K.J.W., Welford, J.K., Wilson, R., van Hunen, J., and Pysklywec, R.N., 2019. Segmentation of rifts through structural inheritance: creation of the Davis Strait; Tectonics, v. 38, p. 2411–2430. https://doi.org/10.1029/2019TC005578

Hinz, K., Schluter, H.-U., Grant, A.C., Srivastava, S.P., Umpleby, D., and Woodside, J., 1979. Geophysical transects of the Labrador Sea: Labrador to southwest Greenland; Tectonophysics, v. 59, p. 151–183. https://doi.org/10.1016/0040-1951(79)90043-X

Holbrook, W.S., Larsen, H.C., Korenaga, J., Dahl-Jensen, T., Reid, I.D., Kelemen, P.B., Hopper, J.R., Kent, G.M., Lizzaralde, D., Bernstein, S., and Detrick, R.S., 2001. Mantle thermal structure and active upwelling during continental breakup in the North Atlantic; Earth and Planetary Science Letters, v. 190, no. 3–4, p. 251–266. https://doi.org/10.1016/S0012-821X(01)00392-2

Hole, M.J. and Millett, J.M., 2016. Controls of mantle potential temperature and lithospheric thickness on magmatism in the North Atlantic Igneous Province; Journal of Petrology, v. 57, p. 417–436. https://doi.org/10.1093/petrology/egw014

Hood, P. and Bower, M.E., 1975. Aeromagnetic reconnaissance of Davis Strait and adjacent areas; *in* Canada's continental margins and offshore petroleum explorations, (ed.) C.J. Yorath, E.R. Parker, and D.J. Glass, Canadian Society of Petroleum Geologists, Memoir 4, p. 433–451.

Hood, P.J., Sawatzky, P., and Bower, M.E., 1967. Progress report on low-level aeromagnetic profiles over the Labrador Sea, Baffin Bay and across the North Atlantic Ocean; Geological Survey of Canada, Paper 66-58, 11 p. https://doi.org/10.4095/103341

Hosseinpour, M., Muller, R.D., Williams, S.E., and Whittaker, J.M., 2013. Full-fit reconstruction of the Labrador Sea and Baffin Bay; Solid Earth, v. 4, p. 461–479. https://doi.org/10.5194/se-4-461-2013

Huismans, R.S. and Beaumont, C., 2014. Rifted continental margins: the case for depth-dependent extension; Earth and Planetary Science Letters, v. 407, p. 148–162. https://doi.org/10.1016/j.epsl.2014.09.032

Hyndman, R.D., 1973. Evolution of the Labrador Sea; Canadian Journal of Earth Sciences, v. 10, p. 637–644. https://doi.org/10.1139/e73-064

International Hydrographic Organization and Intergovernmental Oceanographic Commission, 2014. General bathymetric chart of the oceans; International Hydrographic Organization and Intergovernmental Oceanographic Commission. <www.gebco.net> [accessed May 2015]

Jackson, G.D. and Iannelli, T.R., 1981. Rift-related cyclic sedimentation in the Neohelikian Borden Basin, northern Baffin Island; *in* Proterozoic basins of Canada, (ed.) F.H.A. Campbell, Geological Survey of Canada, Paper 81-10, p. 269–302.

Jackson, H.R. and Reid, I., 1994. Crustal thickness variations between the Greenland and Ellesmere Island margins determined from seismic refraction; Canadian Journal of Earth Sciences, v. 31, no. 9, p. 1407–1418. https://doi.org/10.1139/e94-124

Jackson, H.R., Keen, C.E., and Barrett, D.L., 1977. Geophysical studies on the eastern continental margin of Baffin Bay and Lancaster Sound; Canadian Journal of Earth Sciences, v. 14, p. 1991–2001. https://doi.org/10.1139/e77-170

Jackson, H.R., Keen, C.E., Falconer, R.K.H., and Appleton, K.P., 1979. New geophysical evidence for sea-floor spreading in central Baffin Bay; Canadian Journal of Earth Sciences, v. 16, p. 2122–2135. https://doi.org/10.1139/e79-200

Jackson, H.R., Dickie, K., and Marillier, F., 1992. A seismic reflection study of northern Baffin Bay: implication for tectonic evolution; Canadian Journal of Earth Sciences, v. 29, p. 2353–2369. https://doi.org/10.1139/e92-184

Japsen, P., Green, P.F., and Chalmers, J.A., 2005. Separation of Palaeogene and Neogene uplift on Nuussuag, West Greenland; Journal of the Geological Society, v. 162, p. 299–314. https://doi.org/10.1144/0016-764904-038

Japsen, P., Chalmers, J.A., Green, P.F., and Bonow, J.M., 2012. Elevated, passive continental margins: not rift shoulders, but expressions of episodic, post-rift burial and exhumation; Global and Planetary Change, v. 90–91, p. 73–86. https://doi.org/10.1016/j.gloplacha.2011.05.004

Japsen, P., Green, P.F., Bonow, J.M., Wilton, D.H.C., and Hinchey, A.M., 2018. Burial and exhumation history of the Labrador–Newfoundland margin and implications for hydrocarbon exploration on the Grand Banks and on the Labrador Shelf; Association of American Petroleum Geologists, Search and Discovery Article #30543, 15 p.

Jauer, C.D., Oakey, G.N., and Li, Q., 2019. Western Davis Strait, a volcanic transform margin with petroliferous features; Marine and Petroleum Geology, v. 107, p. 59–80. https://doi.org/10.1016/j.marpetgeo.2019.05.004

Jess, S., Stephenson, R., and Brown, R., 2018. Evolution of the central West Greenland margin and the Nuussuaq Basin: localised basin uplift along a stable continental margin proposed from thermochronological data; Basin Research, v. 30, p. 1230–1246. https://doi.org/10.1111/bre.12301

Jokat, W. and Micksch, U., 2004. Sedimentary structure of the Nansen and Amundsen basins, Arctic Ocean; Geophysical Research Letters, v. 31, no. 2, 4 p. https://doi.org/10.1029/2003GL018352

Keen, C.E., 2019. Conversion of seismic-reflection time to depth for the Labrador margin, Davis Strait, and Baffin Bay, offshore northern Canada and Greenland, using sonic logs, checkshot surveys, and wide-angle seismic velocities; Geological Survey of Canada, Open File 8617, 42 p. https://doi.org/10.4095/315016

Keen, C.E. and Barrett, D.L., 1972. Seismic refraction studies in Baffin Bay: an example of a developing ocean basin; Geophysical Journal of the Royal Astronomical Society, v. 30, no. 3, p. 253–271. https://doi.org/10.1111/j.1365-246X.1972.tb05812.x

Keen, C.E. and Beaumont, C., 1990. Geodynamics of rifted continental margins; *in* Chapter 9 of Geology of the continental margin of Eastern Canada, (ed.) M.J. Keen and G.L. Williams; Geological Survey of Canada, Geology of Canada no. 2, p. 393–472 (*also* Geological Society of America, The Geology of North America, v. I-1). https://doi.org/10.4095/132690

Keen, C.E. and Dehler, S.A., 1997. Extensional styles and gravity anomalies at rifted continental margins: some North Atlantic examples; Tectonics, v. 16, p. 744–754. https://doi.org/10.1029/97TC01765

Keen, C.E., Keen, M.J., Ross, D.I., and Lack, M., 1974. Baffin Bay: small ocean basin formed by sea-floor spreading; American Association of Petroleum Geologists, Bulletin, v. 58, p. 1089–1108.

Keen, C.E., Dickie, K., and Dehler, S.A., 2012. The volcanic margins of the northern Labrador Sea: insights to the rifting process; Tectonics, v. 31, no. 1, 13 p. https://doi.org/10.1029/2011TC002985

Keen, C.E., Dickie, K., and Dafoe, L.T., 2018a. Structural characteristics of the ocean-continent transition along the rifted continental margin, offshore central Labrador; Marine and Petroleum Geology, v. 89, pt. 2, p. 443–463. https://doi.org/10.1016/j.marpetgeo.2017.10.012

Keen, C.E., Dickie, K., and Dafoe, L.T., 2018b. Structural evolution of the rifted margin off northern Labrador: the role of hyper-extension and magmatism; Tectonics, v. 37, p. 1955–1972. https://doi.org/10.1029/2017TC004924

Kerr, J.W., 1967. A submerged continental remnant beneath the Labrador Sea; Earth and Planetary Science Letters, v. 2, p. 283–289. https://doi.org/10.1016/0012-821X(67)90143-4

Klose, G.W., Malterre, E., McMillan, N.J., and Zinkan, C.G., 1982. Petroleum exploration offshore southern Baffin Island, northern Labrador Sea, Canada; *in* Arctic geology and geophysics, Proceedings of the Third International Symposium on Arctic Geology, (ed.) A.F. Embry and H.R. Balkwill; Canadian Society of Petroleum Geologists, Memoir 8, p. 233–244.

Larsen, L.M., and Dalhoff, F., 2006. Composition, age, and geological and geotectonic significance of igneous rocks dredged from the northern Labrador Sea and the Davis Strait; Danmarks og Grønlands Geologiske Undersøgelse Rapport 2006/43, 67 p.

Larsen, J.G. and Pulvertaft, T.C.R., 2000. The structure of the Cretaceous–Paleogene sedimentary–volcanic area of Svertenhuk Halvø, central West Greenland; Geology Survey of Greenland, Bulletin, v. 188, 40 p.

Larsen, L.M., Heaman, L.M., Creaser, R.A., Duncan, R.A., Frei, R., and Hutchison, M., 2009. Tectonomagmatic events during stretching and basin formation in the Labrador Sea and the Davis Strait: evidence from age and composition of Mesozoic to Palaeogene dyke swarms in West Greenland; Journal of the Geological Society, v. 166, p. 999–1012. https://doi.org/10.1144/0016-76492009-038

Larsen, L.M., Pedersen, A.K., Tegner, C., Duncan, R.A., Hald, N., and Larsen, J.G., 2016. Age of Tertiary volcanic rocks on the West Greenland continental margin: volcanic evolution and event correlation to other parts of the North Atlantic Igneous Province; Geological Magazine, v. 153, no. 3, p. 487–511. https://doi.org/10.1017/S0016756815000515

Lau, K.W.H., Nedimović, M.R., and Louden, K.E., 2018. Continent-ocean transition across the northeastern Nova Scotian margin from a dense wide-angle seismic profile; Journal of Geophysical Research, v. 123, no. 5, p. 4331–4359. https://doi.org/10.1029/2017JB015282

Lawver, L.A., Müller, R.D., Srivastava, S.P., and Roest, W., 1990. The opening of the Arctic Ocean; *in* Geological History of the Polar Oceans: Arctic versus Antarctic, (ed.) U. Bleil and J. Thiede; NATO ASI Series, v. 308, Springer, Dordrecht, The Netherlands, p. 29–62. https://doi.org/10.1007/978-94-009-2029-3_3

Li, Y. and Oldenburg, D.W., 1996. 3-D inversion of magnetic data; Geophysics, v. 61, no. 2, p. 394–408. https://doi.org/10.1190/1.1443968

Li, Y. and Oldenburg, D.W., 1998. 3-D inversion of gravity data; Geophysics, v. 63, p. 109–119. https://doi.org/10.1190/1.1444302

Li, Q., Shimeld, J., Dickie, K., Dehler, S.A., Mosher, D., and Desroches, K., 2015. Seismic velocity modelling, fixed point optimization, and evaluation of positioning uncertainty in the central Labrador Sea region: methods, a software tool, and an application; Geological Survey of Canada, Open File 7665, 116 p. https://doi.org/10.4095/295859

Louden, K.E., Tucholke, B.E., and Oakey, G.N., 2004. Regional anomalies of sediment thickness, basement depth and isostatic crustal thickness in the North Atlantic Ocean; Earth and Planetary Science Letters, v. 224, p. 193–211. https://doi.org/10.1016/j.epsl.2004.05.002

Ludwig, W.J., Nafe, J.E., and Drake, C.L., 1970. Seismic refraction; *in* The Sea, volume 4, (ed.) A.E. Maxwell; Wiley-Interscience, New York, New York, p. 53–84.

MacLean, B., Srivastava, S.P., and Haworth, R.T., 1982. Bedrock structures off Cumberland Sound, Baffin Island shelf: core sample and geophysical data; *in* Arctic geology and geophysics, Proceedings of the Third International Symposium on Arctic Geology, (ed.) A.F. Embry and H.R. Balkwill; Canadian Society of Petroleum Geologists, Memoir 8, p. 279–295.

MacLean, B., Jennings, A., and Blakeney, C., 1986. Bedrock and surficial geology of Cumberland Sound, N.W.T.; *in* Current research, Part B; Geological Survey of Canada, Paper 86-1B, p. 605–615. https://doi.org/10.4095/120672

MacLean, B., Williams, G.L., and Srivastava, S.P., 1990. Geology of Baffin Bay and Davis Strait; *in* Chapter 7 (Part 2) of Geology of the continental margin of Eastern Canada, (ed.) M.J. Keen and G.L. Williams, Geological Survey of Canada, Geology of Canada, no. 2, p. 325–348 (*also* Geological Society of America, The Geology of North America, v. I-1). https://doi.org/10.4095/132690

MacLean, B., Williams, G., and Zhang, S., 2014. New insights into the stratigraphy and petroleum potential of the Baffin shelf's Cretaceous rocks; Bulletin of Canadian Petroleum Geology, v. 62, p. 289–310. https://doi.org/10.2113/gscpgbull.62.4.289

MacLeod, C.J., Searle, R.C., Murton, B.J., Casey, J.F., Mallows, C., Unsworth, S.C., Achenbach, K.L., and Harris, M., 2009. Life cycle of oceanic core complexes; Earth and Planetary Science Letters, v. 287, no. 3–4, p. 333–344. https://doi.org/10.1016/j.epsl.2009.08.016

McGregor, E.D., Nielsen, S.B., Stephenson, R.A., Clausen, R., Petersen, K.D., and MacDonald, D.I.M., 2012. Evolution of the west Greenland margin: offshore thermostratigraphic data and modelling; Geological Society of London, Journal, v. 169, p. 515–530. https://doi.org/10.1144/0016-76492011-139

McGregor, E.D., Nielsen, S.B., Stephenson, R.A., Petersen, K.D., and MacDonald, D.I.M., 2013. Long-term exhumation of a Palaeoproterozoic orogen and the role of pre-existing heterogeneous thermal crustal properties: a fission-track study of SE Baffin Island; Geological Society of London, Journal, v. 170, p. 877–891. http://doi.org/10.1144/jgs2012-146

Miles, W. and Oneschuk, D., 2016. Magnetic anomaly map, Canada; Geological Survey of Canada, Open File 7799, scale 1:7 500 000. https://doi.org/10.4095/297337

Müller, R.D., Seton, M., Zahirovic, S., Williams, S.E., Matthews, K.J., Wright, N.M., Shephard, G.E., Maloney, K.T., Barnett-Moore, N., Hosseinpour, M., Bower, D.J., and Cannon, J., 2016. Ocean basin evolution and global-scale plate reorganization events since Pangea breakup; Annual Review of Earth and Planetary Sciences, v. 44, p. 107–138. https://doi.org/10.1146/annurev-earth-060115-012211

Nelson, C.E., Jerram, D.A., Clayburn, J.A.P., Halton, A.M., and Roberge, J., 2015. Eocene volcanism in offshore southern Baffin Bay; Marine and Petroleum Geology, v. 67, p. 678–691. https://doi.org/10.1016/j.marpetgeo.2015.06.002

Nielsen, T.K., Larsen, H.C., and Hopper, J.R., 2002. Contrasting rifted margin styles south of Greenland: implications for mantle plume dynamics; Earth and Planetary Science Letters, v. 200, no. 3–4, p. 271–286. https://doi.org/10.1016/S0012-821X(02)00616-7

Nielsen, S.B., Stevenson, R., and Thomsen, E., 2007. Dynamics of mid-Palaeocene North Atlantic rifting linked with European intra-plate deformations; Nature, v. 450, p. 1071–1074. https://doi.org/10.1038/nature06379

Nøhr-Hansen, H., Williams, G.L., and Fensome, R.A., 2016. Biostratigraphic correlation of the western and eastern margins of the Labrador–Baffin Seaway and implications for the regional geology; Geological Survey of Denmark and Greenland, Bulletin 37, 74 p. https://doi.org/10.34194/geusb.v37.4356

Oakey, G.N. and Chalmers, J.A., 2012. A new model for the Paleogene motion of Greenland relative to North America: plate reconstructions of the Davis Strait and Nares Strait regions between Canada and Greenland; Journal of Geophysical Research, v. 117, no. B10401, 28 p. https://doi.org/10.1029/2011JB008942

Oakey, G.N. and Dehler, S.A., 1998. Magnetic anomaly map, Atlantic region, Canada; Geological Survey of Canada, Open File 3659, scale 1:3 000 000. https://doi.org/10.4095/209979

Oakey, G.N. and Stark, A., 1995. A digital compilation of depth to basement and sediment thickness for the North Atlantic and adjacent coastal land areas; Geological Survey of Canada, Open File 3039, 53 p. https://doi.org/10.4095/203476

Oakey, G.N. and Stephenson, R., 2008. Crustal structure of the Innuitian region of Arctic Canada and Greenland from gravity modelling: implications for the Palaeogene Eurekan orogeny; Geophysical Journal International, v. 173, no. 3, p. 1039–1063. https://doi.org/10.1111/j.1365-246X.2008.03784.x

Oakey, G.N., Ekholm, S., Jackson, H.R., and Marcussen, C., 2001a. Physiography of the Baffin Bay region, Canadian and Greenland Arctic; Geological Survey of Canada, Open File 3933C, scale 1:1 500 000. https://doi.org/10.4095/212000

Oakey, G.N., Ekholm, S., Jackson, H.R., and Marcussen, C., 2001b. Physiography of the Davis Strait region, Canadian and Greenland Arctic; Geological Survey of Canada, Open File 3933B, scale 1:1 500 000. https://doi.org/10.4095/211999

Oakey, G.N., Ekholm, S., and Jackson, H.R., 2001c. Physiography of the Innuitian region, Canadian and Greenland Arctic; Geological Survey of Canada, Open File 3933D, scale 1:1 500 000. https://doi.org/10.4095/212001

Oakey, G.N., Ekholm, S., Jackson, H.R., and Marcussen, C., 2001d. Physiography of the Labrador Sea region, Canadian and Greenland Arctic; Geological Survey of Canada, Open File 3933A, scale 1:1 500 000. https://doi.org/10.4095/211998

Oakey, G.N., Forsberg, R., and Jackson, H.R., 2001e. Gravity anomaly map of the Baffin Bay region, Canadian and Greenland Arctic; Geological Survey of Canada, Open File 3934C, scale 1:1 500 000. https://doi.org/10.4095/212062

Oakey, G.N., Forsberg, R., and Jackson, H.R., 2001f. Gravity anomaly map of the Davis Strait region, Canadian and Greenland Arctic; Geological Survey of Canada, Open File 3934B, scale 1:1 500 000. https://doi.org/10.4095/212061

Oakey, G.N., Forsberg, R., and Jackson, H.R., 2001g. Gravity anomaly map of the Innuitian region, Canadian and Greenland Arctic; Geological Survey of Canada, Open File 3934D, scale 1:1 500 000. https://doi.org/10.4095/212064

Oakey, G.N., Forsberg, R., and Jackson, H.R., 2001h. Gravity anomaly map of the Labrador Sea region, Canadian and Greenland Arctic; Geological Survey of Canada, Open File 3934A, scale 1:1 500 000. https://doi.org/10.4095/212060

Oakey, G.N., Miles, W., and Jackson, H.R., 2001i. Magnetic anomaly map of the Davis Strait region, Canadian and Greenland Arctic; Geological Survey of Canada, Open File 3935B, scale 1:1 500 000. https://doi.org/10.4095/212102

Oakey, G.N., Miles, W., and Jackson, H.R., 2001j. Magnetic anomaly map of the Labrador Sea region, Canadian and Greenland Arctic; Geological Survey of Canada, Open File 3935A, scale 1:1 500 000. https://doi.org/10.4095/212100

Ogg, J.G., 2012. Geomagnetic polarity time scale; Chapter 5 *in* The Geologic Time Scale, (ed.) F.M. Gradstein, J.G. Ogg, M. Schmitz, and G. Ogg; Elsevier, Boston, Massachusetts, p. 85–113. https://doi.org/10.1016/B978-0-444-59425-9.00005-6

Osler, J.C. and Louden, K.E., 1992. Crustal structure of an extinct rift axis in the Labrador Sea: preliminary results from a seismic refraction survey; Earth and Planetary Science Letters, v. 108, no. 4, p. 243–258. https://doi.org/10.1016/0012-821X(92)90026-R

Osler, J.C. and Louden, K.E., 1995. Extinct spreading center in the Labrador Sea: crustal structure from a two-dimensional seismic refraction velocity model; Journal of Geophysical Research, v. 100, no. B2, p. 261–2278. https://doi.org/10.1029/94JB02890

Peace, A., McCaffrey, K., Imber, J., Phethean, J., Nowell, G., Gerdes, K., and Dempsey, E., 2016. An evaluation of Mesozoic rift-related magmatism on the margins of the Labrador Sea: implications for rifting and passive margin asymmetry: Geosphere, v. 12, no. 6, p. 1701–1724. https://doi.org/10.1130/GES01341.1

Peace, A.L., Foulger, G.R., Schiffer, C., and McCaffrey, K.J.W., 2017. Evolution of Labrador Sea–Baffin Bay: plate or plume processes?; Geoscience Canada, v. 44, p. 91–102. https://doi.org/10.12789/geocanj.2017.44.120

Pérez-Gussinyé, M. and Reston, T., 2001. Rheological evolution during extension at nonvolcanic rifted margins: onset of serpentinization and development of detachments leading to continental breakup; Journal of Geophysical Research, v. 106, no. B3, p. 3961–3975. https://doi.org/10.1029/2000JB900325

Péron-Pinvidic, G. and Manatschal, G., 2009. The final rifting evolution at deep magma-poor passive margins from Iberia–Newfoundland: a new point of view; International Journal of Earth Sciences, v. 98, p. 1581–1597. https://doi.org/10.1007/s00531-008-0337-9

Planke, S., Symonds, P.A., Alvestad, E., and Skogseid, J., 2000. Seismic volcanostratigraphy of large volume basaltic extrusive complexes on rifted margins; Journal of Geophysical Research, v. 105, p. 19 335–19 351. https://doi.org/10.1029/1999JB900005

Reid, I., 1996. Crustal structure across the Nain–Makkovik boundary on the continental shelf off Labrador from seismic refraction data; Canadian Journal of Earth Sciences, v. 33, no. 3, p. 460–471. https://doi.org/10.1139/e96-036

Reid, I. and Jackson, H.R., 1997. Crustal structure of northern Baffin Bay: seismic refraction results and tectonic implications; Journal of Geophysical Research, v. 102, no. B1, p. 523–542. https://doi.org/10.1029/96JB02656

Reston, T.J., 2009. The structure, evolution and symmetry of the magma-poor rifted margins of the North and Central Atlantic: a synthesis; Tectonophysics, v. 468, p. 6–27. https://doi.org/10.1016/j.tecto.2008.09.002

Roest, W.R. and Srivastava, S.P., 1989. Sea-floor spreading in the Labrador Sea: a new reconstruction; Geology, v. 17, no. 11, p. 1000–1003. https://doi.org/10.1130/0091-7613(1989)017%3c1000:SFSITL%3e2.3.CO%3b2

Salazar-Mora, C.A., Huismans, R.S., Fossen, H., and Egydio-Silva, M., 2018. The Wilson cycle and effects of tectonic structural inheritance on rifted passive margin formation; Tectonics, v. 37, p. 3085–3101. https://doi.org/10.1029/2018TC004962

Sears, J., 2013. Late Oligocene–early Miocene Grand Canyon: a Canadian connection; GSA Today, v. 23, no. 11, p. 4–10. https://doi.org/10.1130/GSATG178A.1

Secher, K., Heaman, L.M., Nielsen, T.F.D., Jensen, S.M., Schjøth, F., and Creaser, R.A., 2009. Timing of kimberlite, carbonatite, and ultramafic lamprophyre emplacement in the alkaline province located 64°–67° N in southern West Greenland; Lithos, v. 112, suppl. 1, p. 400–406. https://doi.org/10.1016/j.lithos.2009.04.035

Seton, M., Müller, R.D., Zahirovic, S., Gaina, C., Torsvik, T., Shephard, G., Talsma, A., Gurnis, M., Turner, M., Maus, S., and Chandler, M., 2012. Global continental and ocean basin reconstructions since 200 Ma; Earth-Science Reviews, v. 113, p. 212–270. https://doi.org/10.1016/j.earscirev.2012.03.002

Sibuet, J.-C., Srivastava, S., and Manatschal, G., 2007. Exhumed mantle-forming transitional crust in the Newfoundland–Iberia rift and associated magnetic anomalies; Journal of Geophysical Research, v. 112, no. B6, 23 p. https://doi.org/10.1029/2005JB003856

Skaarup, N., 2002. Evidence for continental crust in the offshore Palaeogene volcanic province, central West Greenland; Geology of Greenland Survey Bulletin, v. 191, p. 97–102. https://doi.org/10.34194/ggub.v191.5135

Skaarup, N., Jackson, H.R., and Oakey, G., 2006. Margin segmentation of Baffin Bay/Davis Strait, eastern Canada based on seismic reflection and potential field data; Marine and Petroleum Geology, v. 23, p. 127–144. https://doi.org/10.1016/j.marpetgeo.2005.06.002

Sørensen, A.B., 2006. Stratigraphy, structure and petroleum potential of the Lady Franklin and Maniitsoq basins, offshore southern West Greenland; Petroleum Geoscience, v. 12, p. 221–234. https://doi.org/10.1144/1354-079305-692

Srivastava, S.P., 1978. Evolution of the Labrador Sea and its bearing on the early evolution of the North Atlantic; Geophysical Journal International, v. 52, p. 313–357. https://doi.org/10.1111/j.1365-246X.1978.tb04235.x

Srivastava, S.P. and Roest, W.R., 1999. Extent of oceanic crust in the Labrador Sea; Marine and Petroleum Geology, v. 16, p. 65–84. https://doi.org/10.1016/S0264-8172(98)00041-5

Srivastava, S.P., MacLean, B., Macnab, R.F., and Jackson, H.R., 1982. Davis Strait: structure and evolution as obtained from a systematic geophysical survey; *in* Arctic geology and geophysics, Proceedings of the Third International Symposium on Arctic Geology, (ed.) A.F. Embry and H.R. Balkwill; Canadian Society of Petroleum Geologists, Memoir 8, p. 267–278.

St-Onge, M.R., Van Gool, J.A., Garde, A.A., and Scott, D.J., 2009. Correlation of Archaean and Palaeoproterozoic units between northeastern Canada and western Greenland: constraining the pre-collisional upper plate accretionary history of the Trans-Hudson orogen; Geological Society of London, Special Publications, v. 318, p. 193–235. https://doi.org/10.1144/SP318.7

Storey, M., Duncan, R.A., Pedersen, A.K., Larsen, L.M., and Larsen, H.C., 1998. $^{40}Ar/^{39}Ar$ geochronology of the West Greenland Tertiary volcanic province; Earth and Planetary Science Letters, v. 160, p. 569–586. https://doi.org/10.1016/S0012-821X(98)00112-5

Storey, M., Duncan, R.A., and Swisher, C.C., 2007a. Paleocene–Eocene thermal maximum and the opening of the Northeast Atlantic; Science, v. 316, no. 5824, p. 587–589. https://doi.org/10.1126/science.1135274

Storey, M., Duncan, R.A., and Tegner, C., 2007b. Timing and duration of volcanism in the North Atlantic Igneous Province: implications for geodynamics and links to the Iceland hotspot; Chemical Geology, v. 241, no. 3–4, p. 264–281. https://doi.org/10.1016/j.chemgeo.2007.01.016

Stouge, S., Ineson, J.R., Rasmussen, J.A., and Dalhoff, F., 2007: Sedimentary dredge samples from the Davis Strait High: stratigraphic and palaeoenvironmental implications; Danmarks og Grønlands Geologiske Undersøgelse Rapport 2007/19, 49 p.

Suckro, S.K., Gohl, K., Funck, T., Heyde, I., Ehrhardt, A., Schreckenberger, B., Gerlings, J., Damm, V., and Jokat, W., 2012. The crustal structure of southern Baffin Bay: implications from a seismic refraction experiment; Geophysical Journal International, v. 190, no. 1, p. 37–58. https://doi.org/10.1111/j.1365-246X.2012.05477.x

Suckro, S.K., Gohl, K., Funck, T., Heyde, I., Schreckenberger, B., Gerlings, J., and Damm, V., 2013. The Davis Strait crust—a transform margin between two oceanic basins; Geophysical Journal International, v. 193, no. 1, p. 78–97. https://doi.org/10.1093/gji/ggs126

Tappe, S., Foley, S.F., Stracke, A., Romer, R.L., Kjarsgaard, B.A., Heaman, L.M., and Joyce, N., 2007. Craton reactivation on the Labrador Sea margins: $^{40}Ar/^{39}Ar$ age and Sr-Nd-Hf-Pb isotope constraints from alkaline and carbonatite intrusives; Earth and Planetary Science Letters, v. 256, p. 433–454. https://doi.org/10.1016/j.epsl.2007.01.036

Van der Linden, W.J.M., 1975. Crustal attenuation and sea-floor spreading in the Labrador Sea; Earth and Planetary Science Letters, v. 27, p. 409–423. https://doi.org/10.1016/0012-821X(75)90060-6

Verhoef, J., Roest, W.R., Macnab, R., Arkani-Hamed, J., and Members of the Project Team, 1996. Magnetic anomalies of the Arctic and North Atlantic oceans and adjacent land areas; Geological Survey of Canada, Open File 3125, 225 p. https://doi.org/10.4095/207789

Wardle, R.J., James, D.T., Scott, D.J., and Hall, J., 2002. The southeastern Churchill Province: synthesis of a Paleoproterozoic transpressional orogeny; Canadian Journal of Earth Sciences, v. 39, no. 5, p. 639–663. https://doi.org/10.1139/e02-004.

Wasteneys, H.A., Wardle, R.J., and Krogh, T.E., 1996. Extrapolation of tectonic boundaries across the Labrador shelf: U-Pb geochronology of well samples; Canadian Journal of Earth Sciences, v. 33, p. 1308–1324. https://doi.org/10.1139/e96-099

Watts, A.B., 2001. Gravity anomalies, flexure, and crustal structure at the Mozambique rifted margin; Marine and Petroleum Geology, v. 18, p. 445–455. https://doi.org/10.1016/S0264-8172(00)00079-9

Welford, J.K. and Hall, J., 2013. Lithospheric structure of the Labrador Sea from constrained 3-D gravity inversion; Geophysical Journal International, v. 195, no. 2, p. 767–784. https://doi.org/10.1093/gji/ggt296

Welford, J.K., Peace, A.L., Geng, M., Dehler, S.A., and Dickie, K., 2018. Crustal structure of Baffin Bay from constrained three-dimensional gravity inversion and deformable plate tectonic models; Geophysical Journal International, v. 214, p. 1281–1300. https://doi.org/10.1093/gji/ggy193

White, R.S., McKenzie, D., and O'Nions, R.K., 1992. Oceanic crustal thickness from seismic measurements and rare earth element inversions; Journal of Geophysical Research, v. 97, no. B13, p. 19 683–19 715. https://doi.org/10.1029/92JB01749

Whittaker, R.C., Hamann, N.E., and Pulvertaft, T., 1997. A new frontier province offshore northwest Greenland: structure, basin development, and petroleum potential of the Melville Bay area; American Association of Petroleum Geologists Bulletin, v. 81, p. 978–998. https://doi.org/10.1306/522B49B5-1727-11D7-8645000102C1865D

Whittaker, J., Afonso, J., Masterton, S., Müller, R., Wessel, P., Williams, S., and Seton, M., 2015. Long-term interaction between mid-ocean ridges and mantle plumes; Nature Geoscience, v. 8, no. 6, p. 479–483. https://doi.org/10.1038/ngeo2437

Wielens, H.J. and Williams, G.L., 2009. Stratigraphic cross section Gjoa–Snorri, Saglek–Hopedale Basin, in the Labrador Sea on the east coast of Canada, from North to South; Geological Survey of Canada, Open File 5903, 1 plot. https://doi.org/10.4095/247636

Wilson, R.W., Klint, K.E.S., van Gool, J.A.M., McCaffrey, K.J.W., Holdsworth, R.E., and Chalmers, J.A., 2006. Faults and fractures in central West Greenland: onshore expression of continental break-up and sea-floor spreading in the Labrador–Baffin Bay Sea; Geological Survey of Denmark and Greenland, Bulletin, v. 11, p. 185–204. https://doi.org/10.34194/geusb.v11.4931

Contents

Seismicity in the Labrador–Baffin Seaway and surrounding onshore regions

A.L. Bent[1]* and P. Voss[2]

Bent, A.L. and Voss, P., 2022. Seismicity in the Labrador–Baffin Seaway and surrounding onshore regions; in *Geological synthesis of Baffin Island (Nunavut) and the Labrador–Baffin Seaway, (ed.) L.T. Dafoe and N. Bingham-Koslowski; Geological Survey of Canada, Bulletin 608, p. 379–387. https://doi.org/10.4095/321857*

Abstract: Studying earthquakes in Baffin Bay and the surrounding regions is challenging. There is no knowledge of earthquake activity in this region prior to 1933 when a moment magnitude (M_W) 7.4 earthquake occurred in Baffin Bay. With improved instrumentation, increased seismograph coverage in the north, and modern analysis techniques, knowledge and understanding of earthquakes in the Baffin region is improving. Active seismic zones include Baffin Bay, the east coast of Baffin Island, and the Labrador Sea, separated by areas of low seismicity. Focal-mechanism solutions show a mix of faulting styles, predominantly strike-slip and thrust. Regional stress-axes orientations show more consistency, which suggests that activity is occurring on previously existing structures in response to the current stress field. There is little correlation between earthquake epicentres in Baffin Bay and mapped structures. Glacial isostatic adjustment may be a triggering mechanism for earthquakes in the Baffin region, but modelling efforts have yielded equivocal results.

Résumé : L'étude des tremblements de terre dans la baie de Baffin et les régions avoisinantes représente un défi de taille. On ne connaît pas l'activité sismique dans cette région avant 1933, année où un tremblement de terre de magnitude de moment (M_W) de 7,4 s'est produit dans la baie de Baffin. Grâce à l'amélioration de l'instrumentation, à l'augmentation de la couverture sismographique dans le Nord et aux techniques d'analyse modernes, notre connaissance et notre compréhension des tremblements de terre dans la région de Baffin s'améliorent. Les zones sismiques actives comprennent la baie de Baffin, la côte est de l'île de Baffin et la mer du Labrador, séparées par des zones de faible sismicité. Les solutions des mécanismes au foyer révèlent un mélange de styles de failles, principalement de coulissage et de chevauchement. Les orientations des axes des contraintes régionales sont plus cohérentes, ce qui donne à penser que l'activité se produit sur des structures préexistantes en réponse au champ de contraintes actuel. Il y a peu de corrélation entre les épicentres sismiques dans la baie de Baffin et les structures cartographiées. L'ajustement isostatique glaciaire pourrait être un mécanisme déclencheur des tremblements de terre dans la région de Baffin, mais les efforts de modélisation n'ont donné jusqu'ici que des résultats équivoques.

[1]Natural Resources Canada, 7 Observatory Crescent, Ottawa, Ontario K1A 0Y3
[2]Geological Survey of Denmark and Greenland, Øster Voldgade 10, 1350 Copenhagen, Denmark
*Corresponding author: A.L. Bent (email: allison.bent@nrcan-nrcan.gc.ca)

INTRODUCTION

Baffin Bay as well as the Labrador Sea and east coast of Baffin Island are all active seismic zones with moderate to high hazard from earthquakes as can be seen in the most recent seismic-hazard maps for Canada (http://www.earthquakescanada.nrcan.gc.ca/hazard-alea/simphaz-en.php). Monitoring and studying earthquakes in this region are challenging tasks for several reasons, most of them stemming from a combination of the remoteness and large size of the region combined with the sparse population. Many areas are inaccessible and infrastructure, in particular power and telecommunications, are not available outside of communities, which are separated by large distances and not connected by road.

There is no knowledge of earthquakes in the Baffin region until 1933, when a magnitude (M_W) 7.4 earthquake occurred in Baffin Bay and was recorded by seismograph stations worldwide with the closest being 1600 km away in Ivigtut, Greenland. No stations were installed in the Canadian Arctic until 1950 and all knowledge of earthquakes in this region between 1933 and 1950 is derived from teleseismic data. Beginning in the 1960s and continuing to the present, the number of seismograph stations in the Arctic has increased and the quality of the instrumentation has improved. Improved data quality and quantity, combined with the development of new analysis techniques, has led to an increased understanding of earthquakes in the Labrador–Baffin Seaway and elsewhere in the Arctic.

Nevertheless, there are many unresolved issues regarding Labrador–Baffin earthquakes. Seismicity in the Labrador Sea appears to be linked to the extinct ridge and fracture zones in the region (*see* Keen et al., this volume). There is no clear correlation between earthquake activity in Baffin Bay and mapped structures or other geophysical anomalies. In eastern North America as a whole, it is difficult to associate any given earthquake with a specific fault, but in most regions, as is the case with the Labrador Sea, it is possible to associate earthquake activity with larger scale regional features. Glacial isostatic adjustment has been proposed as a possible triggering mechanism for earthquakes in the Baffin region, together with plate tectonic stresses (Gregersen and Basham, 1989). Efforts to model and link glacial isostatic adjustment and earthquake activity have produced equivocal results, which will be discussed in more detail in this paper.

Note that throughout this paper, compound adjectives have been hyphenated when they are placed before the noun they modify — e.g. 'fault-plane solutions'.

DATA AND METHODS

Prior to 1950, when a seismograph was installed in Resolute, there were no seismograph stations in the Canadian Arctic, although a station at Qeqertarsuaq on the west coast of Greenland was in operation from 1907 to 1912 and another at Ivigtut on the southwest coast of Greenland was established in 1929 (http://seis.geus.net/papers/harboe-disko-1911.pdf), both providing some coverage of the Baffin region. No additional northern Canadian stations were installed until the early 1960s when a truly national network was established. As a result, historical earthquakes were located using data primarily from distant or teleseismic stations and only the largest would have been detected. Thus, there are only a few small northern earthquakes in the Canadian National Earthquake Database (http://www.earthquakescanada.nrcan.gc.ca/stndon/NEDB-BNDS/bulletin-en.php) prior to the 1960s and no eastern Arctic events of any size until the occurrence of a magnitude 7.4 earthquake in Baffin Bay in 1933 (Bent, 2002). There are considerable uncertainties (of the order of tens of kilometres) associated with the locations of the historical earthquakes that are in the database. The Canadian National Seismograph Network is still sparse in the north relative to southern Canada, but with the current Canadian National Seismograph Network configuration (Fig. 1), realtime access to data from seismograph stations on Greenland, and modern instruments, which are much more sensitive than their historical counterparts, the Canadian National Earthquake Database is complete in recent years for magnitude 3.5 and higher throughout the Arctic. Although smaller northern earthquakes are in the Canadian National Earthquake Database as seen in Figure 1, there are likely many others that were not detected. For recent earthquakes above the 3.5 magnitude threshold, epicentral uncertainties in Baffin Bay are of the order of 10 km, but may be greater or smaller for any given earthquake. Uncertainties are likely to be higher for smaller earthquakes or for any earthquakes for which data from one or more of the few closest stations are not available. If the earthquake was not located using data from stations on both Baffin Island and Greenland, the uncertainty will be higher because the data will cover only a narrow range of azimuths.

Figure 1 shows seismic activity and seismograph stations in the Labrador–Baffin Seaway and surrounding onshore regions. The epicentres and magnitudes were obtained from the Canadian National Earthquake Database. Further seismicity data are available from the Geological Survey of Denmark and Greenland (http://www.eng.geus.dk/nature-and-climate/earthquakes-and-seismology/). Focal-mechanism data were compiled for earthquakes of magnitude 4.0 and greater. More detailed information regarding both the earthquakes and derived focal mechanisms is found in subsequent sections of this chapter and within the GIS data included with this volume. Depths are not included as they have not been determined for most of the events primarily because the seismograph density in the north is too sparse for depths to be determined reliably as part of the earthquake location process. Instead, earthquakes are located assuming a fixed depth, the default value of which is 18 km, but other values may be used in some cases. For example, the presence of a strong Rg phase would indicate that the earthquake was very shallow, in which case a fixed depth of 1 or 5 km would be used. If there is *a priori* information about depths of earthquakes in a given region, then the average value for that region might be used instead. Having said that, it is extremely rare in the Baffin region for the depth in the Canadian National Earthquake Database to be listed as anything other than 18 km for earthquakes since the late 1960s. A perusal of the database shows that 0 km was the default depth until about 1968.

Several different magnitude scales are used to determine the size of an earthquake. All are logarithmic in nature and consider the attenuation of the earthquake signal with distance from the source. One magnitude scale may be preferred over another, depending on such factors as the tectonic regime in which the earthquake occurs, the distance of the recording station from the earthquake, and the frequency at which the amplitude is measured. Moment magnitude (M_W; Kanamori, 1977) is generally considered to be the best measure of earthquake size as it does not saturate for large earthquakes and can be related to the physical properties of the fault rupture. It is, however, a relatively new magnitude scale and therefore M_W has not been calculated for most historical earthquakes; there are a few exceptions, such as those earthquakes that were part of in-depth studies. It is difficult to calculate M_W for smaller earthquakes as it is a long-period magnitude scale and smaller (M_W <4.0) earthquakes have a limited long-period signature. The teleseismic magnitudes M_S (Gutenberg, 1945) and m_b (Gutenberg and Richter, 1956) are most often used for larger, historical earthquakes. Magnitudes based on data recorded at regional distances are more commonly used for smaller earthquakes in recent decades. In the eastern Arctic and southeastern Canada, M_N (Nuttli, 1973), as adapted for use in eastern Canada (Bent and Greene, 2014), is most often used for earthquakes occurring in continental crust and the original Richter (1935) M_L scale, for earthquakes occurring in oceanic crust. The M_N scale is based on the Lg phase and cannot be used for offshore earthquakes as Lg does not propagate in oceanic crust. Wetmiller (1974) specifically commented on the absence of a Lg phase from seismic waves crossing the deepest part of Baffin Bay. For some events, M_L magnitudes using a version of the scale adapted for Greenland (Gregersen, 1999) are also available; M_L (Greenland) magnitudes were obtained from the Geological Survey of Denmark and Greenland and M_W magnitudes, from the references associated with the earthquakes in the GIS data included with this volume. All others are as noted in the Canadian National Earthquake Database although some may have been calculated by an external agency. Not all magnitude types are available for every earthquake.

The focal mechanisms (fault-plane solutions) and stress axes derived from them for earthquakes of magnitude 4.0 and greater were obtained from the published literature. Focal mechanisms were not determined for every event; the more recent the earthquake, the more likely that a focal-mechanism solution is available. Table 1 explains the reference codes used in the GIS data included with this volume. Focal mechanisms were determined using a variety of methods, which fall into two broad categories: waveform modelling and first

Figure 1. Seismicity and stations in the Labrador–Baffin region. Earthquakes of magnitude 2.0–3.9 (black dots) are from the period 2000 to present. All known earthquakes of magnitude 4.0 and greater (blue dots) are plotted. Red circles indicate seismograph stations. More details about the stations and the magnitude 4.0 and greater earthquakes are found in the GIS data included with this volume.

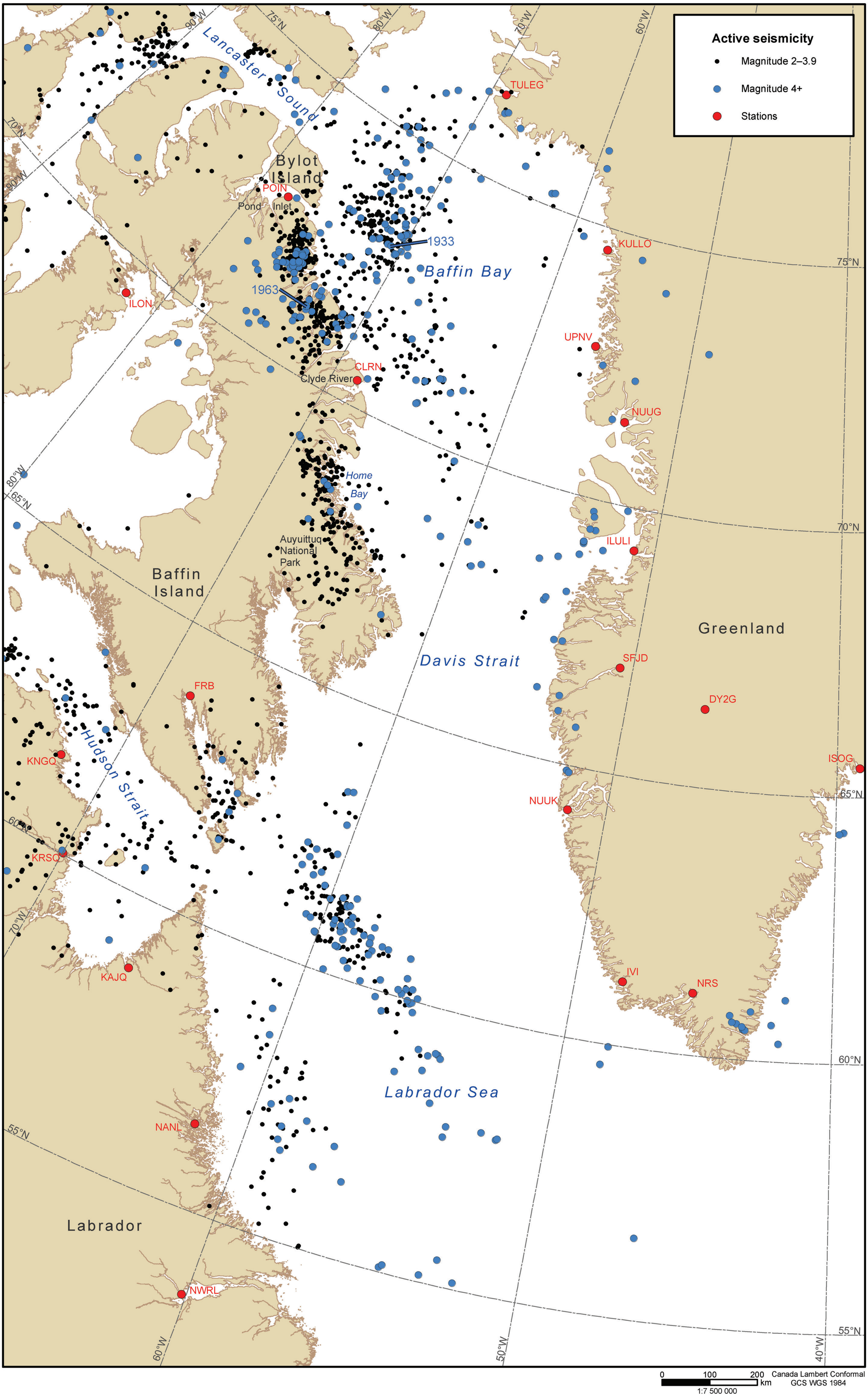
Active seismicity
Magnitude 2–3.9
Magnitude 4+
Stations
Lancaster Sound
Bylot Island
Pond Inlet
POIN
1933
1963
Baffin Bay
ILON
CLRN
Clyde River
TULEG
KULLO
UPNV
NUUG
Home Bay
Auyuittuq National Park
Baffin Island
ILULI
Greenland
Davis Strait
SFJD
DY2G
FRB
Hudson Strait
KNGQ
ISOG
NUUK
KRSC
KAJQ
IVI
NRS
Labrador Sea
NANL
Labrador
NWRL
75°N
70°N
65°N
60°N
55°N
90°W
80°W
70°W
60°W
50°W
40°W
0 100 200 km
1:7 500 000
Canada Lambert Conformal
GCS WGS 1984

Table 1. References for focal-mechanism solutions included with GIS data.

Code in GIS metadata	Reference
A91	Adams, 1991
B02	Bent, 2002
B15a	Bent, 2015a
B15b	Bent, 2015b
B17	Bent, 2017
B19a	Bent, 2019a
B19b	Bent, 2019b
B94	Bent, 1994
B96	Bent, 1996
BDP03	Bent et al., 1993
BH92	Bent and Hasegawa, 1992
H73	Hashizume, 1973
H77	Hashizume, 1977
K+12	Kao et al., 2012

motions. If a focal mechanism was determined by waveform modelling, it may also have been possible to determine the depth of the earthquake and interested readers should consult the appropriate references. The method used is indicated in the GIS data included with this volume with RCMT referring to regional centroid moment tensors, WM referring to any other method based on waveform modelling, and 1st M indicating that the solution was derived from first motions or the polarity of the P-wave onset. Because the earthquake source is a double couple, the focal mechanism has two nodal planes, one of which should be the fault plane. From the focal-mechanism solution alone, it cannot be determined which nodal plane is the fault plane. Thus, data for both nodal planes are listed. The strike direction is measured from the north, the dip angle from the horizontal, and the dip direction is the strike plus 90°. 'Rake' is sometimes referred to as slip angle; it indicates the motion of the hanging wall relative to the strike. For those unfamiliar with rake, 0° indicates pure left-lateral strike slip, 180° pure right-lateral strike slip, 90° pure thrust and −90° pure normal faulting. Solutions with roughly equal parts dip-slip and strike-slip motion are generally referred to as oblique. Stress axes are defined by trend (azimuth) and plunge (measured relative to the horizontal), and are derived from the focal mechanism.

SEISMICITY IN THE BAFFIN REGION

Seismic-hazard maps of Canada (http://www.earthquakescanada.nrcan.gc.ca/hazard-alea/simphaz-en.php#CA) indicate moderate to high seismic hazard along the northeastern margin of Canada from the Labrador Sea through northern Baffin Bay. Typically, 3 to 4 earthquakes of magnitude 4.0 or greater occur somewhere in the Baffin region each year with frequent smaller earthquakes and occasional larger ones; however, the seismicity is not evenly distributed but is concentrated in several active zones (Fig. 1) separated by regions of little or no activity.

The most active region, which is also the one in which most of the largest earthquakes have occurred, is referred to as the Baffin Bay Seismic Zone (Basham et al., 1982). The 1933 M_W 7.4 earthquake (Bent, 2002), the largest known Canadian earthquake east of the Rockies and one of the largest earthquakes worldwide north of the Arctic Circle, occurred in this zone. Earthquakes of magnitude 6.0 or greater also occurred in 1934, 1945, 1947, and 1957. The first three occurred close to the epicentre of the 1933 earthquake and are likely aftershocks. The 1957 earthquake occurred about 130 km to the south. In terms of its north-south extent, the Baffin Bay Seismic Zone corresponds to the deepest part of Baffin Bay, where sediments are very thick, but most of the activity occurs toward the Baffin Island side of the 1000 m isobath (Basham et al., 1977; Adams and Basham, 1989a, b) and cannot be directly tied to the extinct spreading centre and related fracture zones (*see* Keen et al., this volume). In this region, it is difficult to correlate the seismic activity with any geological or geophysical features.

Davis Strait experiences only a moderate level of seismicity. Further south, the Labrador Sea is considered an active seismic zone (Basham et al., 1982). Although the Labrador Sea is active in terms of the overall number of earthquakes, these are generally small to moderate in size and there are no known earthquakes of magnitude 6.0 or greater; however, knowledge of seismicity in this region is based on less than a century of data and the occurrence of larger, pre-instrumental earthquakes cannot be ruled out.

Seismicity on Baffin Island occurs almost exclusively in the coastal regions on the Baffin Bay side of the island (Fig. 1) and is concentrated in two regions. The northern region, which is often referred to as the Baffin Island Seismic Zone (Basham et al., 1982) lies roughly between Clyde River and Pond Inlet. The largest earthquakes on Baffin Island, including the only known event of magnitude 6.0 or greater (M_W 6.1 in 1963), have occurred within this zone. The Baffin Island Seismic Zone is adjacent to the Baffin Bay Seismic Zone, but the two are separated by a region of low activity. There is also a zone of moderate activity further south on Baffin Island near Home Bay and to the north of Auyuittuq National Park. These two active regions appear to be separated by a relatively aseismic zone. Given the relatively sparse seismograph network in the north (*see* 'Data and methods' section) and the short time period for which instrumental data are available, it is possible that small earthquakes occurred in the apparently aseismic zones, but were not recorded.

The west coast of Greenland experiences a moderate level of seismic activity. Chung (2002), Gregersen (2006), and Larsen et al. (2006) noted that there is a good spatial correlation between seismicity and deglaciation. Almost all activity occurs along the deglaciated margin, whereas the interior, still covered by a substantial ice cap, is aseismic, consistent with the theory presented in Johnston (1987) that seismicity is suppressed by the weight of the ice cap. In contrast, the papers involving Gregersen have emphasized that the stresses may well be caused by plate tectonics.

Although instrumental data are crucial for determining precise earthquake locations and other source parameters, the effects of earthquakes may be best described by people who felt them and by post-earthquake assessments of damage. Felt reports supplement the instrumental data for modern earthquakes and provide most of the known information about earthquakes preceding the instrumental era. Natural Resources Canada receives occasional felt reports for earthquakes in the Canadian Arctic, as does the Geological Survey of Denmark and Greenland for Greenland. Neither organization has attempted to produce isoseismal maps for earthquakes in these regions as the population density is too sparse. To date, neither the Geological Survey of Denmark and Greenland nor National Resources Canada has received reports of structural damage in Greenland or the Canadian Arctic resulting from an earthquake.

The historical record for these regions is relatively sparse primarily due to the low population density and short time period for which written records have been produced. Nevertheless, there is some documentation of felt earthquakes in the historical record. In a recent paper based on journals and newspapers written by Danish and Moravian missionaries in Greenland and Labrador, Demarée at al. (2019) found evidence for several felt earthquakes in both locations during the 18th and 19th centuries. They noted that they found no evidence that the same earthquake was felt both in Labrador and on Greenland. The only earthquake known to have been felt on both sides of Baffin Bay is the 1933 Baffin Bay earthquake. It was long known, as shown by a report in the *London Times* (28 November 1933), that the earthquake had been felt in the region from Upernavik to southern Upernavik on Greenland, approximately 550 km from the epicentre. In the report, no note was made of damage, but it was explicitly stated that the earthquake had not been reported felt in either Diskofjord or Thule, 480 km south and 560 km north of Upernavik, respectively. Although the earthquake would likely have been felt in communities on the northeastern coast of Baffin Island, no concerted effort was made at the time to collect felt reports from Baffin Island to verify this. Recent access to a log for the Hudson Bay Company post at Clyde River (Hudson Bay Company Archives, 1933), however, uncovered a clear statement that the earthquake had been felt in Clyde River and it is explicitly mentioned that there had been no damage.

FOCAL MECHANISMS

Focal mechanisms, also known as fault-plane solutions, provide information about the orientation of the fault on which the earthquake occurred, the style of slip (e.g. thrust, normal, strike-slip), and the inferred stress field. There are many methods by which they can be determined, but most fall into the realm of either waveform modelling or first motions (*see* 'Data and methods' section). For the Baffin region, most focal mechanisms determined prior to the early 2000s (Stein et al., 1979; Adams, 1991; Bent et al., 2003) were derived from first motions using the grid-search algorithm of Snoke et al. (1984). The first arriving wave at a seismograph station will be a P-wave or a regional variation of it (Pg, Pn). It will be either compressional or dilatational, appearing as either an upward or downward motion, respectively, on the seismogram. The nodal planes (*see* 'Data and methods' section) show the boundaries between dilatational and compressional quadrants. A well constrained focal mechanism derived from first motions requires clear, unambiguous polarities at many stations, which is one of the reasons that focal mechanisms were not determined for many earthquakes in the Baffin region. Most of the recent focal mechanisms were derived from regional moment tensor analysis (Kao et al., 2012; Bent 2015a, b, 2017, 2019a, b) using the method of Kao et al. (1998, 2001). Other modelling methods have been used for some of the larger earthquakes of particular interest and are discussed further in the publications on these earthquakes (Hashizume 1973, 1977; Bent and Hasegawa, 1992; Bent, 1994, 1996, 2002). Modelling methods evaluate longer portions of the seismograms than do first-motion methods and, therefore, can often obtain reliable solutions with data from fewer stations. Many of the waveform-modelling studies also evaluated the available first-motion data as a secondary form of analysis to verify consistency with the modelled solutions.

Early attempts to understand the seismicity of the Canadian Arctic (e.g. Basham et al., 1977; Stein et al., 1979; Adams and Basham, 1989a, b; Gregersen and Basham, 1989; N.H. Sleep, G. Kroeger, and S. Stein, unpub. rept., 1989) were based on a very small number of focal mechanisms, which suggested that Baffin Bay was dominated by thrust faulting and Baffin Island by normal faulting. This difference was the primary factor that led to the proposal that glacial isostatic adjustment was an underlying cause of earthquakes on Baffin Island (*see* 'Relationship between earthquakes, earth structure, and ice history' section). The much larger suite of focal-mechanism solutions now available (Fig. 2) has introduced added complexity to the picture. Focal-mechanism solutions for Baffin Bay show a complex mix of strike-slip and thrust faulting events, with many of the largest, such as the M_W 7.4 earthquake of 1933 and its large aftershocks, being associated with strike-slip faulting (Bent, 2002). Thrust faulting appears to be more dominant toward the northern part of Baffin Bay, but is not exclusive to that region. An examination of the P axis directions for Baffin Bay (Fig. 2), however, shows that the maximum compressive stress direction is generally northwest–southeast regardless of the focal-mechanism type, which suggests that the style of faulting may be controlled by pre-existing structures responding to the current stress field. Similar northwest–southeast compression is also observed in the passive-margin regions to the north (Ellesmere Island) and south (Labrador Sea).

Baffin Island also shows a of mix of faulting styles (Fig. 2). The largest event, the 1963 M_W 6.1 earthquake (Bent, 1996), is a normal faulting event, but both strike-slip and thrust faulting events have occurred. In terms of stress orientations (Fig. 2), focal mechanisms of a few events are indicative of northwest–southeast compression, as observed in Baffin Bay; however, a larger number imply northeast–southwest compression, the orientation of which is more consistent with observations from the central Arctic and southern Canada.

Focal mechanisms in the Labrador Sea show various faulting styles and orientations (Fig. 2), which may be at least partially explained by the combination of ridge and transform faults in the region (*see* Keen et al., this volume). Although P axes are generally oriented northwest–southeast along the margin (Fig. 2), they tend to be closer to east–west in the case of events further offshore.

Only a small number of focal mechanisms have been determined for Greenland, in part because there have not been any particularly large earthquakes along the west coast of Greenland. The focal mechanisms that are available are normal faulting in nature (Chung and Gao, 1997; Chung, 2002; Gregersen, 2006; Larsen et al., 2006)

The predominance of northwest–southeast compression along the passive margin contrasts sharply with southeastern Canada and the northeastern United States, where the maximum compression is oriented northeast–southwest (e.g. Adams and Bell, 1991; Zoback, 1992; Bent et al., 2003). The stress field in Baffin Bay and the northern Labrador Sea inferred from focal mechanisms is consistent with industry-well breakout data from the Labrador Shelf compiled in the Canadian crustal stress database (Adams, 1995). A change in stress orientation north of 50°N latitude, as observed in the focal-mechanism solutions, is consistent with models of the tectonic forces acting on the North American Plate (Richardson and Reding, 1991) and, thus, the north–south change (i.e. Baffin–Labrador Sea vs. southeastern Canada) in stress field appears to be largely dominated by stresses associated with plate tectonics. The east–west change (i.e. Baffin regions vs. central Arctic) appears to be dominated by glacial isostatic-adjustment stresses due to the retreat of the ice sheet (e.g. James and Schamehorn, 2016).

RELATIONSHIP BETWEEN EARTHQUAKES, EARTH STRUCTURE, AND ICE HISTORY

It is not currently possible to associate any earthquake in the Baffin region with rupture on a specific fault. None of these earthquakes are known to have produced surface faulting, which is not unusual for eastern North America. The 1989 Ungava earthquake is the only historical eastern North American earthquake with a confirmed surface rupture (Adams et al., 1991; Bent, 1994). Uncertainty in epicentral locations (*see* 'Data and methods' section), combined with the relatively large size of symbols used on most seismicity maps relative to the map scale, may give the appearance that an earthquake occurred on a specific fault, but without corroborative evidence, it should not be considered conclusive. Conversely, the uncertainty in location means that an event that does not plot on a mapped fault could have occurred on it. Additionally, the epicentre of an earthquake occurring at depth on a shallowly dipping fault would not necessarily plot on the surface trace of the fault on which it occurred. These caveats notwithstanding, seismicity in the Labrador Sea and Davis Strait (Fig. 1) appears to be associated with extinct ridge and fracture zones (Adams and Basham, 1989a, b; *see also* Keen et al., this volume), whereas the seismicity in the most active region of Baffin Bay does not appear to correlate with any mapped structures (Fig. 1).

Globally, most earthquakes occur at plate boundaries and are explained by plate tectonics. There are, however, a smaller yet significant number of earthquakes, known as intraplate earthquakes, that occur far from plate boundaries. Earthquakes in Baffin Bay and adjacent regions fall into this category. The underlying reasons for the occurrence of intraplate earthquakes are not completely understood. A high percentage of intraplate earthquakes occur on ancient rifts and most of the rest at cratonic boundaries (Mooney et al., 2012; Talwani, 2014). In broad terms, the occurrence of seismic activity in the Labrador–Baffin Seaway is consistent with this observation (*see* Keen et al., this volume). As suggested in the previous section, however, a detailed examination reveals a more complex situation.

Although intraplate earthquakes occur far from plate boundaries, the forces acting at the plate boundaries may play a significant role in their occurrence. Zoback (1992) demonstrated that intraplate stress fields are dominated by a relatively uniform stress field associated with forces at plate boundaries. Ziegler (1987) showed that stresses can be transmitted over thousands of kilometres through the lithosphere. These stresses may be supplemented by others derived from regional features and processes, including local geology and loading or unloading of the crust through processes such as deglaciation, erosion, and sediment deposition. Some of these may play a role in the generation of earthquakes and will be explored further, with an emphasis on deglaciation.

At the time of the Last Glacial Maximum (24–14 14C ka BP; Simon et al., 2016), much of North America as well as Greenland, northern Europe, and Antarctica was covered by large ice sheets. There is some debate over the extent of the ice sheets (Simon et al., 2015, 2016), but it is focused on regions beyond the area of interest for this paper. The weight of the ice sheets caused depression of the Earth's crust. As the ice melted, the land beneath and near the ice sheets was uplifted and relative sea levels decreased; this process is known as glacial isostatic adjustment.

The concept of a causal relation between glacial isostatic adjustment and earthquakes was proposed in the 1970s. Basham et al. (1977) suggested that seismicity in the Baffin Island–Foxe Basin region occurred in response to differential rates of uplift along the boundaries of this zone with respect to Hudson Bay. Stein et al. (1979) developed a model based on glacial isostatic adjustment that accounted for variations in focal mechanisms between Baffin Bay and Baffin Island; the model also proposed that thrust faulting should occur along the entire North Atlantic passive margin seaward of the 1000 m isobath and normal faulting landward; however, this does not appear to be the case based on the complex faulting styles in the Baffin and Labrador Sea regions seen from the larger number of focal mechanisms now available (*see* 'Focal mechanism' section).

Figure 2. Fault-plane solutions for earthquakes in the Baffin region. Focal mechanisms are shown as lower hemisphere projections with shaded regions representing compressional quadrants. The P and T axes are shown as shaded and white dots, respectively. Unidentified fault type indicates that the designation is dependent upon which nodal plane is the fault plane. All of these show both a strike-slip and dip-slip component of faulting. The complete focal mechanisms are available in the GIS data included with this volume.

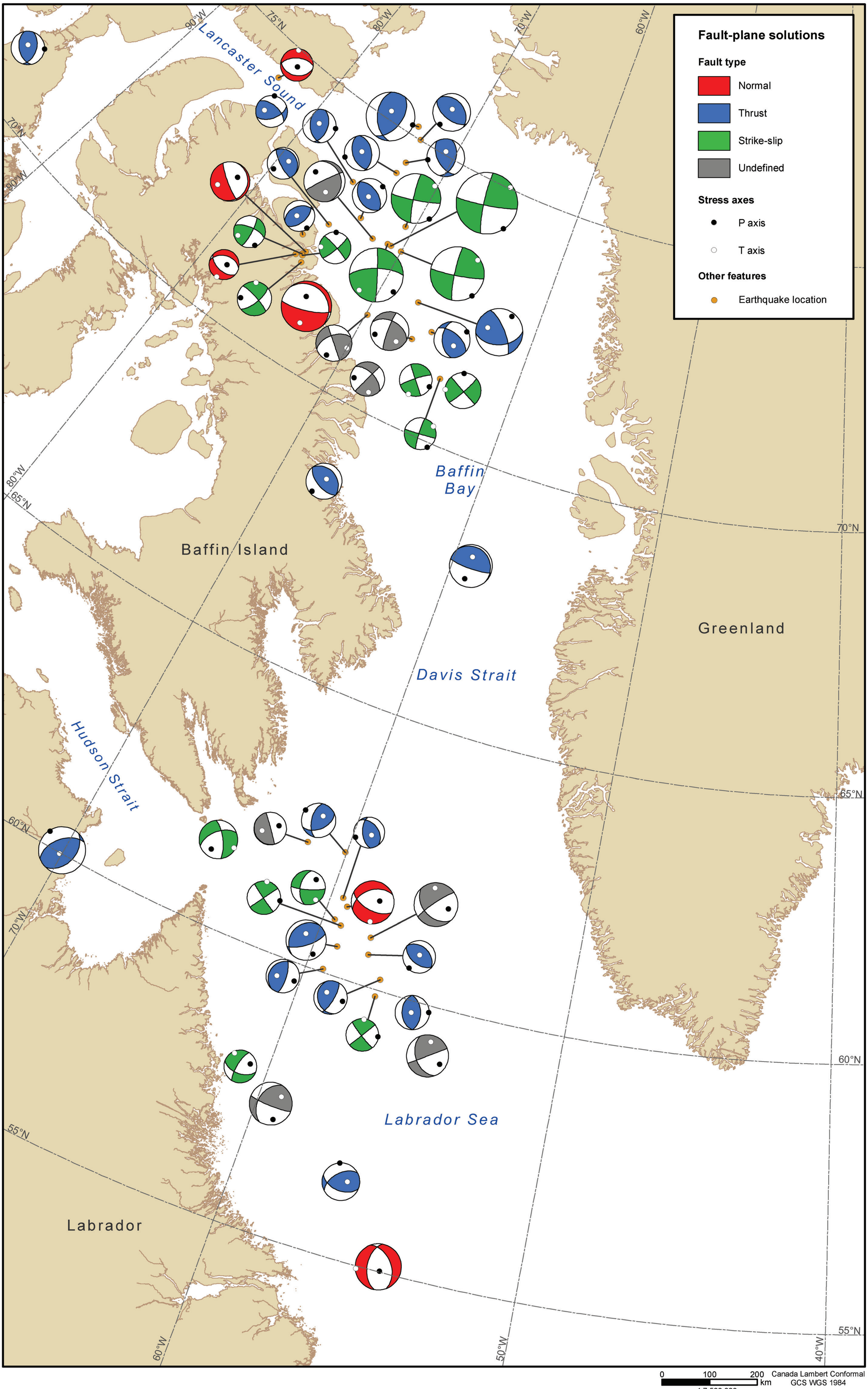
Fault-plane solutions
Fault type
Normal
Thrust
Strike-slip
Undefined
Stress axes
P axis
T axis
Other features
Earthquake location
Lancaster Sound
Baffin Bay
Baffin Island
Davis Strait
Greenland
Hudson Strait
Labrador Sea
Labrador
90°W
80°W
70°W
60°W
50°W
40°W
75°N
70°N
65°N
60°N
55°N
0
100
200
km
1:7 500 000
Canada Lambert Conformal
GCS WGS 1984

For completeness, neither does the proposed normal-thrust faulting pattern suggested by Stein et al. (1979) hold up along the passive margin of southeastern Canada, where the largest earthquake (i.e. the 1929 M_W 7.2 Grand Banks earthquake) was a strike-slip event (Bent, 1995) and where normal faulting is not common. Almost all events on- and offshore are either thrust or strike-slip (examples include, but are not limited to, Bent et al., 2003, Bent 2015a, b, 2017, 2019a, b).

A more complex model for the north was developed by Stein et al. (1989) and others (N.H. Sleep, G. Kroeger, and S. Stein, unpub. rept., 1989), but reached essentially the same conclusions as Stein et al. (1979). Others, such as Quinlan (1984), agreed that glacial isostatic adjustment was a potential cause of earthquakes, but were sceptical that it controlled the style of faulting.

Subsequent modelling of glacial isostatic-adjustment strain rates based on detailed ice-sheet loading histories and realistic Earth properties (mantle viscosity, crustal thickness), and comparisons with seismic strain rates (Spada et al., 1991; James and Bent, 1994) showed that the glacial isostatic-adjustment strain rates are orders of magnitude greater than seismic strain rates both within and beyond the glaciated region. Thus, glacial isostatic-adjustment strain rates are more than adequate to generate the observed seismicity. The fact that there are fewer earthquakes than would be predicted by glacial isostatic adjustment alone suggests that the orientation of the crustal strain induced by glacial isostatic adjustment is not ideally oriented to enhance the deviatoric-stress field.

Recently developed sheet histories for the Innuitian (Simon et al., 2015) and Laurentide (Simon et al., 2016) ice sheets that covered northern Canada were an improvement over earlier models with respect to their fit to crustal motions obtained from GPS data and to relative sea-level measurements. Additionally, a new model of the Earth's viscosity structure (Peltier et al., 2015) provided an improved fit to horizontal crustal motions for North America relative to previous models. Combining these two, James and Schamehorn (2016) modelled glacial isostatic adjustment strain rates and velocities over nine regions in northern Canada.

They found a good correlation between glacial isostatic adjustment and seismicity in the Baffin region, where high compressional glacial isostatic-adjustment strain rates occur in the Baffin Bay Seismic Zone, and where both the overall seismicity rate and the number of large earthquakes is high. The correlation was not strong in other regions where high glacial isostatic-adjustment strain rates correlated with low seismicity (e.g. southern Greenland) or vice versa (e.g. Ungava). Thus, although the glacial isostatic adjustment–earthquake relation is intriguing, the subject is far from closed. James and Schamehorn (2016) provided suggestions for future research, such as the evaluation of stress rates and a comparison of stress orientations derived from earthquake data, such as focal mechanisms, to glacial isostatic-adjustment stresses. In the attempt to distinguish earthquakes that are a result of glacial isostatic adjustment from those that are caused by large-scale plate motion, the fact that glacial isostatic adjustment will affect the stress field caused by plate motion and possibly trigger earthquakes prematurely must be considered.

The unloading of the Earth's crust in areas of rapid erosion can create differential stress fields in a manner like that resulting from deglaciation; however, James and Bent (1994) commented that the strain rates due to erosion (Anderson, 1986) in the continental United States are considerably smaller than the glacial isostatic-adjustment strain rates within the area of deglaciation and extending to several hundred kilometres beyond. Thus, erosion may not be a dominant mechanism for earthquake generation in the Baffin region.

In their paper discussing the possible relation between glacial isostatic adjustment and earthquakes in the Baffin region, Stein et al. (1979) also mentioned sediment loading as a possible earthquake trigger; however, they and subsequent researchers (Cloetingh et al., 1984; Stein et al., 1987) noted that, except in areas of rapid sedimentation, sediment loads are generally in place for long enough periods of time for the stresses to relax and would therefore be inefficient at generating earthquakes. The sediment-loading hypothesis has been largely dismissed for northern Canada. Maps of seafloor sediments (*see* Keen at al., this volume) show thick sediments in much of Baffin Bay and thicknesses in excess of 10 000 m along much of the Labrador coast as well as the north coasts of Baffin Island and Greenland. Although these sediments are not likely to be contributing to the occurrence of earthquakes, their presence raises some issues in terms of tsunami hazard. A tsunami that devastated much of the Burin Peninsula of Newfoundland following the 1929 Grand Banks earthquake was generated not directly by the earthquake, but by a huge submarine landslide that had been triggered by the earthquake (cf. Bent, 1995). This raises the possibility that coastal areas with high sediment loads may be at risk from tsunamis. The tsunamis triggered by onshore landslides in West Greenland in 2000 (Dahl-Jensen et al., 2004) and 2017 (Clinton et al., 2017) show that onshore sediments also present a possible risk. The multiple landslides triggered by the recent magnitude 6.7 earthquake in Hokkaido, Japan (Yamagishi and Yamazaki, 2018), an earthquake comparable to the 1933 event, show that repeated landslides may also be triggered in the Baffin Bay region.

The present authors are in no way speculating on or predicting the occurrence of a future large earthquake or tsunami in any of these regions, but rather, the authors are raising the possibility that areas along the continental slope where sediment accumulations are thickest may be at higher risk from landslide generated tsunamis than regions where the sediment load is thinner, regardless of whether the landslide is triggered by an earthquake. Complete resolution of this issue is beyond the scope of this paper.

CONCLUSION

The known history of earthquakes in the Labrador–Baffin Seaway spans less than a century owing to the lack of instrumental coverage of northern Canada prior to the second half of the 20th century. As the number of seismograph stations increases and new analysis techniques emerge, the understanding of earthquakes in this region is improving, but many questions remain. Successes include a lowering of the magnitude threshold at which earthquakes can be detected and located, and the ability within the last decade to determine focal mechanisms for a much higher percentage of moderate to large earthquakes than in the past. At the same time, the increased data set has shown that earthquake activity in the Baffin region is more complex than previously thought. For example, the observation that earthquakes in Baffin Bay were predominantly thrust-faulting events, whereas those on Baffin Island were normal-faulting events is not as clear cut as it once appeared. Correlating seismicity and structure in Baffin Bay has been, and remains, challenging. A possible relation between glacial isostatic adjustment and earthquake occurrence is intriguing, but has not been fully resolved.

ACKNOWLEDGMENTS

The authors thank Lynn Dafoe, Charlotte Keen, Soren Gregersen, Stephen Halchuk, and Tom James for their comments and reviews on various iterations of the manuscript. Leith MacLeod's assistance in drafting the figures and converting the data to GIS format was invaluable. They also thank Ed Picco for directing them to the Hudson Bay Company Archives for a report on the 1933 earthquake.

REFERENCES

Adams, J., 1991. New focal mechanisms for Eastern Canada; Geological Survey of Canada, Open File 2430, 188 p. https://doi.org/10.4095/132673

Adams, J., 1995. The Canadian crustal stress database: a compilation to 1994; Geological Survey of Canada, Open File 3122, 38 p. https://doi.org/10.4095/205058

Adams, J. and Basham, P.W., 1989a. The seismicity and seismotectonics of Canada east of the Cordillera; Geoscience Canada, v. 16, p. 3–16.

Adams, J. and Basham, P.W., 1989b. Seismicity and seismotectonics of Canada's eastern margin and craton; *in* Earthquakes at North Atlantic Passive Margins: Neotectonics and Postglacial Rebound, (ed.) S. Gregersen and P.W. Basham; Kluwer Academic Publishers, Dordrecht, The Netherlands, NATO ASI Series C, v. 266, p. 355–370.

Adams, J. and Bell, S., 1991. Crustal stresses in Canada; *in* Neotectonics of North America, (ed.) D.B. Slemmons, E.R. Engdahl, M.D. Zoback, and D.D. Blackwell; Geology Society of America, Boulder, Colorado, Geology of North America Decade Map, v. 1, p. 376–386.

Adams, J., Wetmiller, R.J., Hasegawa, H.S., and Drysdale, J., 1991. The first surface faulting from a historical intraplate earthquake in North America; Nature, v. 352, p. 617–619. https://doi.org/10.1038/352617a0

Anderson, J.G., 1986. Seismic strain rates in the central and eastern United States; Seismological Society of America, Bulletin, v. 76, p. 273–290.

Basham, P.W., Forsyth, D.A., and Wetmiller, R.J., 1977. The seismicity of northern Canada; Canadian Journal of Earth Sciences, v. 14, p. 1646–1667. https://doi.org/10.1139/e77-140

Basham, P.W., Weichert, D.H., Anglin F.M., and Berry, M.J., 1982. New probabilistic strong seismic ground motions maps of Canada: a compilation of earthquake source zones, methods and results; Earth Physics Branch, Open File 82-33, 206 p. https://doi.org/10.4095/8869

Bent, A.L., 1994. The 1989 (MS 6.3) Ungava, Quebec earthquake: a complex intraplate event; Bulletin of the Seismological Society of America, v. 84, p. 1075–1088.

Bent, A.L., 1995. A complex double-couple source mechanism for the MS 7.2 1929 Grand Banks earthquake; Bulletin of the Seismological Society of America, v. 85, p. 1003–1020.

Bent, A.L., 1996. Another look at the 1963 MW 6.1 Baffin Island earthquake; Seismological Research Letters, v. 67, p. 64–71. https://doi.org/10.1785/gssrl.67.6.64

Bent, A.L., 2002. The 1933 Ms 7.3 Baffin Bay earthquake: strike-slip faulting along the northeastern Canadian passive margin; Geophysical Journal International, v. 150, p. 724–736. https://doi.org/10.1046/j.1365-246X.2002.01722.x

Bent, A.L., 2015a. Regional centroid moment tensor solutions for eastern Canadian earthquakes: 2011–2013; Geological Survey of Canada, Open File 7726, 71 p. https://doi.org/10.4095/296795

Bent, A.L., 2015b. Regional centroid moment tensor solutions for eastern Canadian earthquakes: 2014; Geological Survey of Canada, Open File 7834, 35 p. https://doi.org/10.4095/296822

Bent, A.L., 2017. Regional centroid moment tensor Solutions for eastern Canadian earthquakes: 2015; Geological Survey of Canada, Open File 8050, 26 p. https://doi.org/10.4095/299816

Bent, A.L., 2019a. Regional centroid moment tensor solutions for eastern Canadian earthquakes: 2016; Geological Survey of Canada, Open File 8226, 24 p. https://doi.org/10.4095/314592

Bent, A.L., 2019b. Regional centroid moment tensor solutions for eastern Canadian earthquakes: 2017; Geological Survey of Canada, Open File 8466, 27 p. https://doi.org/10.4095/314591

Bent, A.L. and Greene, H., 2014. Toward an improved understanding of the MN-MW time dependence in eastern Canada; Bulletin of the Seismological Society of America, v. 104, p. 2125–2132. https://doi.org/10.1785/0120140031

Bent, A.L. and Hasegawa, H.S., 1992. Earthquakes along the northwestern boundary of the Labrador Sea; Seismological Research Letters, v. 63, p. 587–602. https://doi.org/10.1785/gssrl.63.4.587

Bent, A.L., Drysdale, J., and Perry, H.K.C., 2003. Focal mechanisms for eastern Canadian earthquakes: 1994–2000; Seismological Research Letters, v. 74, p. 452–468. https://doi.org/10.1785/gssrl.74.4.452

Chung, W.-Y., 2002. Earthquakes along the passive margin of Greenland: evidence for postglacial rebound control; Pure and Applied Geophysics, v. 159, p. 2567–2584. https://doi.org/10.1007/s00024-002-8748-1

Chung, W.-Y. and Gao, H., 1997. The Greenland earthquake of 11 July 1987 and postglacial fault reactivation along a passive margin; Bulletin of the Seismological Society of America, v. 87, p. 1058–1068.

Clinton, J., Larsen, T.B., Dahl-Jensen, T., Voss, P., and Nettles, M., 2017. Seismic observations from Nuugatsiaq slide/tsunami, https://ds.iris.edu/ds/nodes/dmc/specialevents/2017/06/22/nuugaatsiaq-greenland-landslide-and-tsunami/ [accessed July 24, 2019]

Cloetingh, S., Wortel, M.J.R., and Vlaar, N.J., 1984. Passive margin evolution, initiation of subduction and the Wilson cycle; Tectonophysics, v. 109, p. 147–163. https://doi.org/10.1016/0040-1951(84)90175-6

Dahl-Jensen, T., Larsen, L.M., Pedersen, S.A.S., Pedersen, J., Jepsen, H.F., Pedersen, G.K., Nielsen, T., Pedersen, A.K., von Platen-Hallermund, F., and Wenig, W., 2004. Landslide and tsunami 21 November 2000 in Paatut, West Greenland; Natural Hazards, v. 31, p. 277–287. https://doi.org/10.1023/B:NHAZ.0000020264.70048.95

Demarée, G.R., Ogilvie, A.E.J., and Kusman, D., 2019. Historical records of earthquakes for Greenland and Labrador in Moravian missionary journals; Journal of Seismology, v. 23, p. 123–133. https://doi.org/10.1007/s10950-018-9796-z

Gregersen, S., 1999. National Survey and Cadastre (KMS), Copenhagen, Denmark; European-Mediterranean Seismological Centre Newsletter, v. 15, p. 3.

Gregersen, S., 2006. Intraplate earthquakes in Scandinavia and Greenland. Neotectonics or postglacial uplift; Journal of the Indian Geophysical Union, v. 10, p. 25–30.

Gregersen, S. and Basham, P.W. (ed.), 1989. Earthquakes at North-Atlantic Passive Margins: Neotectonics and Postglacial Rebound; Kluwer Academic Publishers, Dordecht, The Netherlands. NATO ASI Series C, v. 266, 716 p. https://doi.org/10.1007/978-94-009-2311-9

Gutenberg, B., 1945. Amplitudes of surface waves and magnitudes of shallow earthquakes; Bulletin of the Seismological Society of America, v. 35, p. 3–12.

Gutenberg, B. and Richter, C.F., 1956. Magnitude and energy of earthquakes; Annali di Geofisica, v. 9, p. 1–15.

Hashizume, M., 1973. Two earthquakes on Baffin Island and their tectonic implications; Journal of Geophysical Research, v. 78, p. 6069–6081. https://doi.org/10.1029/JB078i026p06069

Hashizume, M., 1977. Surface-wave study of the Labrador Sea earthquake 1971 December; Geophysical Journal International, v. 51, p. 149–168. https://doi.org/10.1111/j.1365-246X.1977.tb04194.x

Hudson Bay Company Archives, 1933. Clyde River Post Journal, Document references B.403/a/1–3 and B.403/a/3–6 of period 1930–1939, microfilm.

James, T.S. and Bent, A.L., 1994. A comparison of eastern North American seismic strain-rates to glacial rebound strain-rates; Geophysical Research Letters, v. 21, p. 2127–2130. https://doi.org/10.1029/94GL01854

James, T.S. and Schamehorn, T.D., 2016. A comparison of seismicity to the crustal deformation predicted by a glacial isostatic adjustment model in northern Canada and western Greenland; Geological Survey of Canada, Open File 8106, 18 p. https://doi.org/10.4095/299098

Johnston, A.C., 1987. Suppression of earthquakes by large continental ice sheets; Nature, v. 330, p. 467–469. https://doi.org/10.1038/330467a0

Kanamori, H., 1977. The energy release in great earthquakes; Journal of Geophysical Research, v. 82, p. 2981–2987. https://doi.org/10.1029/JB082i020p02981

Kao, H., Juan, P.-R., Ma, K.-F., Huang, B.-S., and Liu, C.-C., 1998. Moment-tensor inversion for offshore earthquakes east of Taiwan and their implications to regional collision; Geophysical Research Letters, v. 25, p. 3619–3622. https://doi.org/10.1029/98GL02803

Kao, H., Liu, Y.-H., and Jian, P.-R., 2001. Source parameters of regional earthquakes in Taiwan: January–December 1997; Terrestrial, Atmospheric and Oceanic Sciences Journal, v. 12, p. 431–439. https://doi.org/10.3319/TAO.2001.12.2.431(T)

Kao, H., Shan, S.-J., Bent, A., Woodgold, C., Rogers, G., Cassidy, J.F., and Ristau, J., 2012. Regional centroid-moment tensor analysis for earthquakes in Canada and adjacent regions: an update; Seismological Research Letters, v. 83, p. 505–515. https://doi.org/10.1785/gssrl.83.3.505

Larsen, T.B., Dahl-Jensen, T., Voss, P., Jørgensen, T.M., Gregersen, S., and Rasmussen, H.P., 2006. Earthquake seismology in Greenland–improved data with multiple applications; Geological Survey of Denmark and Greenland, Bulletin 10, p. 57–60.

Mooney, W.D., Ritsema, J., and Hwang, Y.K., 2012. Crustal seismicity and earthquakes catalog maximum moment magnitude (M_{CMAX}) in stable continental regions (SCRS): correlation with the seismic velocity of the lithosphere; Earth and Planetary Science Letters, v. 357–358, p. 78–83. https://doi.org/10.1016/j.epsl.2012.08.032

Nuttli, O.W., 1973. Seismic wave attenuation and magnitude relations for eastern North America; Journal of Geophysical Research, v. 78, p. 876–885. https://doi.org/10.1029/JB078i005p00876

Peltier, W.R., Argus, D.F., and Drummond, R., 2015. Space geodesy constrains ice-age terminal deglaciation: the global ICE-6G_C (VM5a) model; Journal of Geophysical Research–Solid Earth, v. 120, p. 450–487. https://doi.org/10.1002/2014JB011176

Quinlan, G., 1984. Postglacial rebound and the focal mechanisms of eastern Canadian earthquakes; Canadian Journal of Earth Sciences, v. 21, p. 1018–1023. https://doi.org/10.1139/e84-106

Richardson, R.M. and Reding, L.M., 1991. North American plate dynamics; Journal of Geophysical Research, v. 96, p. 12201–12223. https://doi.org/10.1029/91JB00958

Richter, C.F., 1935. An instrumental earthquake magnitude scale; Bulletin of the Seismological Society of America, v. 25, p. 1–32.

Simon, K.M., James, T.S., and Dyke, A.S., 2015. A new glacial isostatic adjustment model of the Innutian Ice Sheet; Quaternary Science Reviews, v. 119, p. 11–21. https://doi.org/10.1016/j.quascirev.2015.04.007

Simon, K.M., James, T.S., Henton, J.A., and Dyke, A.S., 2016. A glacial isostatic adjustment model for the central and northern Laurentide Ice Sheet based on relative sea level and GPS measurements; Geophysical Journal International, v. 205, p. 1618–1636. https://doi.org/10.1093/gji/ggw103

Snoke, J.A., Munsey, J.W., Teague, A.G., and Bollinger, G.A., 1984. A program for focal mechanism determination by combined use of polarity and SV-P amplitude data; Earthquake Notes, v. 55, p. 15.

Spada, G., Yuen, D.A., Sabatini, R., and Boschi, E., 1991. Lower-mantle viscosity constrained by seismicity around deglaciated regions; Nature, v. 351, p. 53–55. https://doi.org/10.1038/351053a0

Stein, S., Sleep, N.H., Geller, R.J., Wang, S.-C., and Kroeger, G.C., 1979. Earthquakes along the passive margin of eastern Canada; Geophysical Research Letters, v. 6, p. 537–540. https://doi.org/10.1029/GL006i007p00537

Stein, S., Okal, E.A., and Wiens, D., 1987. Application of modern techniques to analysis of historical earthquakes; *in* Historical Seismograms and Earthquakes of the World, (ed.) W.H.K Lee, H. Meyers, and K. Shimataki; Academic Press, London, United Kingdom, p. 85–104.

Stein, S., Cloetingh, S., Sleep, N., and Wortel, R., 1989. Passive margin earthquakes, stresses and rheology; *in* Earthquakes at North Atlantic Passive Margins: Neotectonics and Postglacial Rebound, (ed.) S. Gregersen and P.W. Basham; Kluwer Academic Publishers, Dordrecht, The Netherlands, NATO ASI Series C, v. 266, p. 231–259. https://doi.org/10.1007/978-94-009-2311-9_14

Talwani, P., 2014. Unified model for intraplate earthquakes; *in* Intraplate Earthquakes, (ed.) P. Talwani; Cambridge University Press, Cambridge, United Kingdom, p. 275–302. https://doi.org/10.1017/CBO9781139628921.012

Wetmiller, R.J., 1974. Crustal structure of Baffin Bay from the earthquake-generated Lg phase; Canadian Journal of Earth Sciences, v. 11, p. 123–130. https://doi.org/10.1139/e74-011

Wood, H.O. and Neumann, F., 1931. Modified Mercalli Intensity Scale of 1931; Bulletin of the Seismological Society of America, v. 21, p. 277–283.

Yamagishi, H. and Yamazaki, F., 2018. Landslides by the 2018 Hokkaido Iburi-Tobu earthquake on September 6; Landslides, v. 15, p. 2521–2524. https://doi.org/10.1007/s10346-018-1092-z

Ziegler, P.A., 1987. Late Cretaceous and Cenozoic intra-plate compressional deformations in the Alpine foreland- a geodynamic model; Tectonophysics, v. 137, p. 389–420. https://doi.org/10.1016/0040-1951(87)90330-1

Zoback, M.L., 1992. Stress field constraints on intraplate seismicity in eastern North America; Journal of Geophysical Research, v. 97, p. 11 761–11 782. https://doi.org/10.1029/92JB00221

Contents

Mineral and carving-stone resources of Baffin Island

J.C. Harrison[1, 2*], B.M. Saumur[1, 3], and D.R. Skipton[1, 4]

Harrison, J.C., Saumur, B.M., and Skipton, D.R., 2022. Mineral and carving-stone resources of Baffin Island; in *Geological synthesis of Baffin Island (Nunavut) and the Labrador–Baffin Seaway, (ed.) L.T. Dafoe and N. Bingham-Koslowski; Geological Survey of Canada, Bulletin 608, p. 389–407. https://doi.org/10.4095/321858*

Abstract: Mineral resources of Baffin Island include iron (Mary River), diamonds, carbonate-hosted zinc and lead (Nanisivik), nickel, copper, platinum group elements, uranium, thorium, gemstones (sapphire, spinel, lapis lazuli), carving stone, and coal.

Iron deposits include the Mary River No. 1 to 4 deposits of northern Baffin Island, which came into production in 2015 and contain 586 Mt grading 66% Fe. The Mesoproterozoic Borden Basin hosts the Nanisivik deposit, mined between 1976 and 2002; this is a Mississippi Valley–type deposit and contains 9.0% Zn, 0.7% Pb, and 41 ppm Ag. Diamond-rich kimberlite occurs as sheets and small pipes at Chidliak on Hall Peninsula; largest by area is the CH-1 (6 ha) pipe. At least 32 carving-stone localities are known; 7 communities on Baffin Island have good access to quarried material. Coal occurs in the Cretaceous–Paleogene Eclipse Trough of Bylot and northwestern Baffin islands. Exposures near Pond Inlet have been excavated for local use.

Résumé : Parmi les ressources minérales de l'île de Baffin, on compte du fer (Mary River), des diamants, du zinc et du plomb dans des roches carbonatées (Nanisivik), du nickel, du cuivre, des éléments du groupe du platine, de l'uranium, du thorium, des pierres précieuses (saphir, spinelle, lapis-lazuli), de la pierre à sculpter et du charbon.

Les gîtes de fer comprennent les gisements n[os] 1-4 de Mary River, dans le nord de l'île de Baffin, qui contiennent 586 mT de minerai titrant 66 % de Fe et dont l'exploitation a débuté en 2015. Le bassin de Borden du Mésoprotérozoïque renferme le gisement de Nanisivik, qui a été exploité de 1976 à 2002. Ce gisement est de type Mississippi-Valley et consiste en une minéralisation à 9,0 % de Zn, 0,7 % de Pb et 41 ppm de Ag. À Chidliak, dans la péninsule Hall, de la kimberlite riche en diamants se présente sous forme de feuillets et de petites cheminées; la kimberlite la plus étendue (6 ha) est la cheminée CH-1. Au moins 32 sites de pierre à sculpter sont connus; 7 collectivités de l'île de Baffin ont une bonne accessibilité aux matériaux extraits de carrières. Du charbon est présent dans la cuvette d'Eclipse du Crétacé-Paléogène, dans l'île Bylot et le nord-ouest de l'île de Baffin. Près de Pond Inlet, du charbon a été extrait d'affleurements en vue d'une utilisation locale.

[1]Geological Survey of Canada, 601 Booth Street, Ottawa, Ontario K1A 0E8
[2]Present address: 83 Metcalfe Street, Guelph, Ontario N1E 4X8 (retired)
[3]Present address: Université du Québec à Montréal, 201, avenue du Président-Kennedy, Montréal, Quebec H2X 3Y7
[4]Present address: Yukon Geological Survey, Government of Yukon, P.O. Box 2703, Whitehorse, Yukon Y1A 2C6
[*]Corresponding author: J.C. Harrison (email: blackswn10@gmail.com)

INTRODUCTION

Baffin Island, like the rest of Canada's Arctic Archipelago, is part of the last frontier of mineral exploration in North America. Factors such as remoteness, the lack of infrastructure, complicated logistics, short field seasons, and high operational costs have all played a role in hindering exploration investment. Nevertheless, Baffin Island consists of geological units that formed in environments where mineralization is known to develop. Further, known correlations exist with well endowed geological provinces on the mainland areas of Nunavut, Greenland, and Nunavik (northern Quebec). as the world's fifth largest island, Baffin's sheer size (~507 000 km^2) rivals that of Manitoba and northern Ontario. It is therefore reasonable to assume that, although as only a handful of significant discoveries have been made there over the last half century, Baffin Island remains largely untapped in terms of mineral potential.

With the completion of the Geological Survey of Canada's Geo-mapping for Energy and Minerals (GEM) program and the compilation of multiple new bedrock-geology maps between 2005 and 2019 (*see* St-Onge et al., this volume) a modern, publicly available geological framework has been established for the majority of the surface area of the island. A proper knowledge base is thus in place to encourage new mineral exploration. In this paper, known mineral deposits and showings of Baffin Island are described. The aim of this compilation is to demonstrate that Baffin Island has known resources for numerous commodities, including iron, diamonds, gemstones, carbonate-hosted zinc and lead (Mississippi Valley type), magmatic nickel, copper and platinum-group elements (Ni-Cu-PGE), uranium, thorium, as well as carving stone and coal. The information provided in this paper, along with that from other GEM program contributions on Baffin Island, will hopefully help to highlight the wealth of Baffin Island and target mineral sector investment, as well as contribute to land-use decisions of benefit to both industry and northern stakeholders.

A comprehensive database of past exploration efforts and available assessment reports related to mineral prospects of Baffin Island are publicly available through Nunavut Minerals (NUMIN), a mineral occurrence database managed by the Government of Nunavut. Highlights are presented and summarized herein; the reader is referred to NUMIN for further information on mineral prospects and past exploration.

The location and distribution of mineral deposits and showings discussed herein is shown in Figure 1a, b. This review is divided by commodity type: 1) iron ore (e.g. Mary River district); 2) base and precious metals (e.g. Nanisivik); 3) diamond (e.g. Chidliak); 4) gemstones (e.g. Kimmirut); 5) uranium and thorium; 6) coal; and 7) carving stone. For further details on the geology of the areas discussed by commodity, the reader is invited to consult other chapters of this synthesis volume (e.g. St-Onge et al., this volume).

Iron ore

Mary River, northern Baffin Island, Borden Basin

Jackson (2000) and Iannelli et al. (2013b) provided a summary of past exploration efforts in the Mary River area (Fig. 2, 3). Mining exploration activities in the area have been sporadic since the discovery of Deposit No. 1 at Mary River (locality 1) by M. Watts and R. Sheardown in 1962 (Guimond, 1963). The presence of iron ore of commercial significance was proven by drilling as early as 1965. There was no new interest until 2004, when additional drilling was completed. The current owner, Baffinland Iron Mines Corporation,

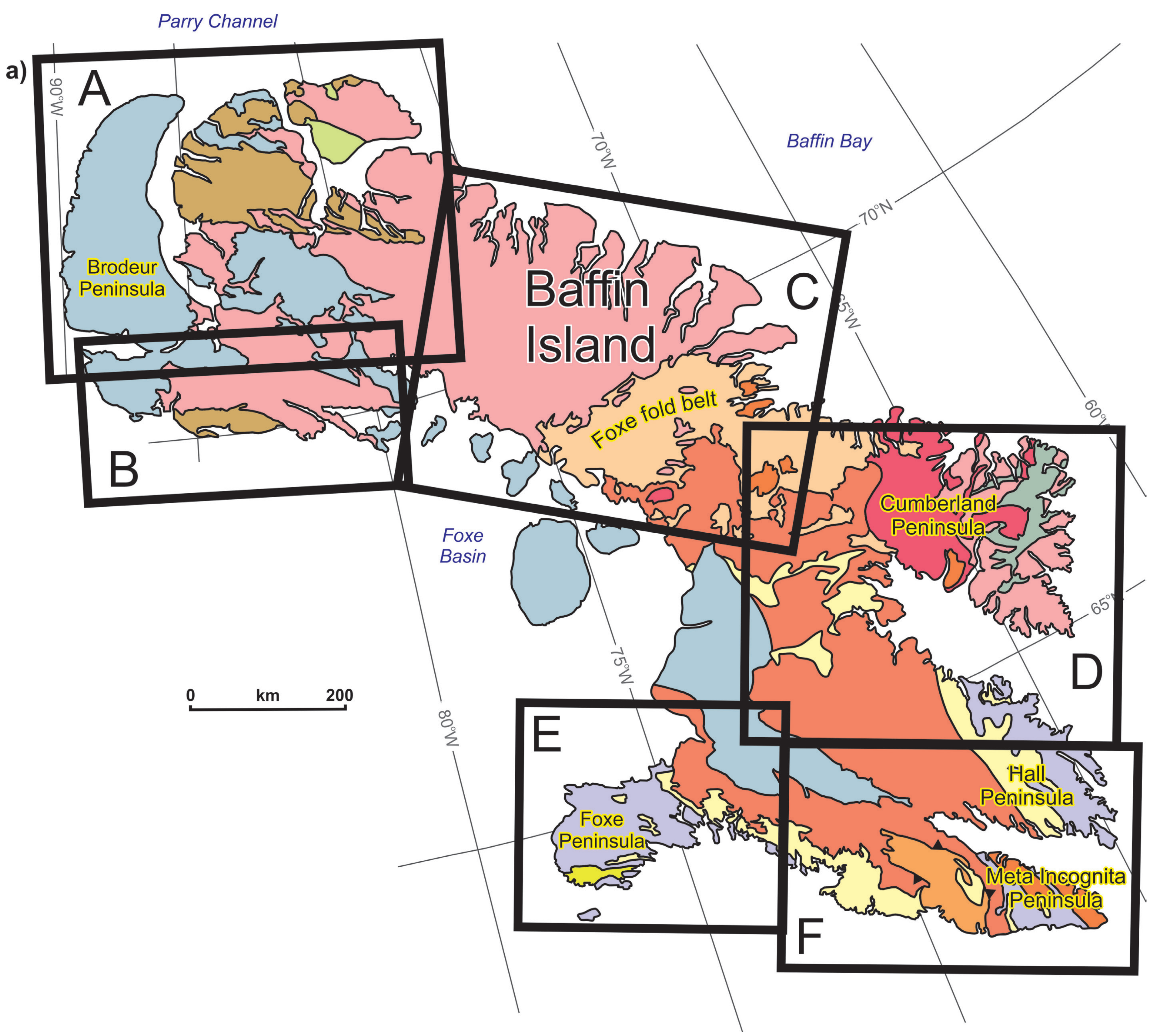

Figure 1. Mineral localities of Baffin Island (numbered localities are described in the text): **a)** index to map areas.

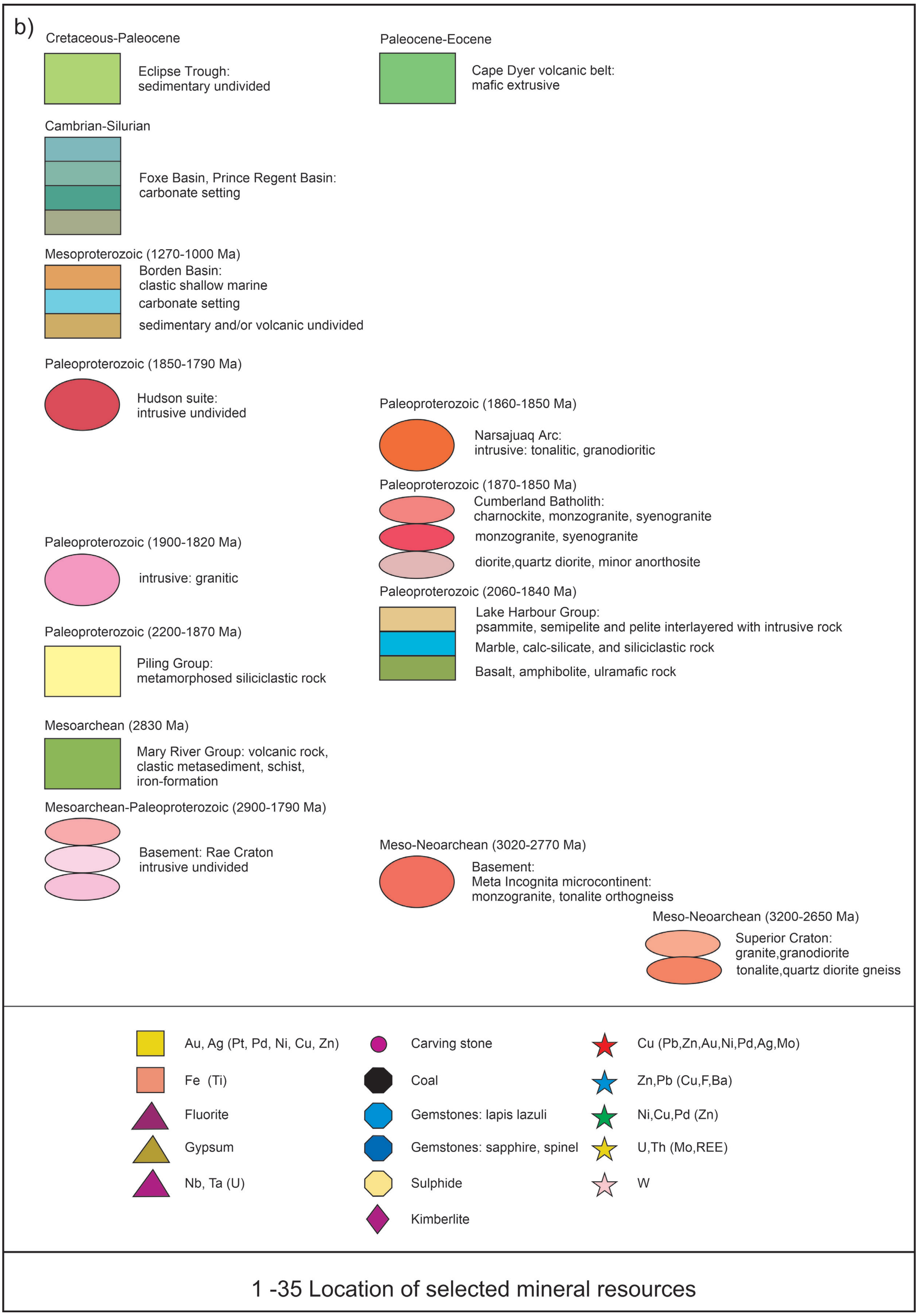

Figure 1. (cont.) b) geological legend, and mineral-resource symbols and locations.

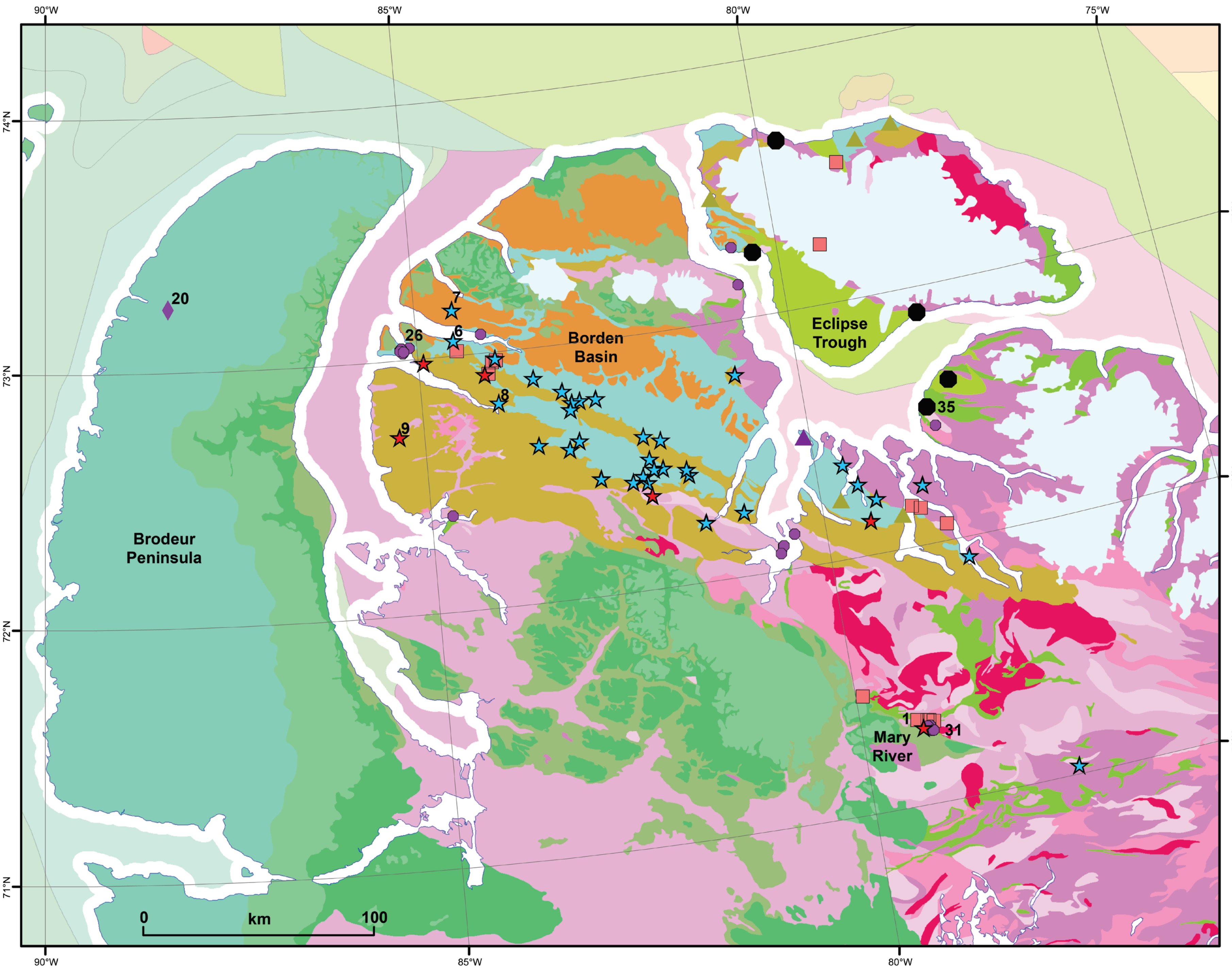

Figure 2. Mary River area, Borden Basin, Eclipse Trough, northwestern Baffin Island (*see* Fig. 1a, b for legend, and mineral-resource symbols and location).

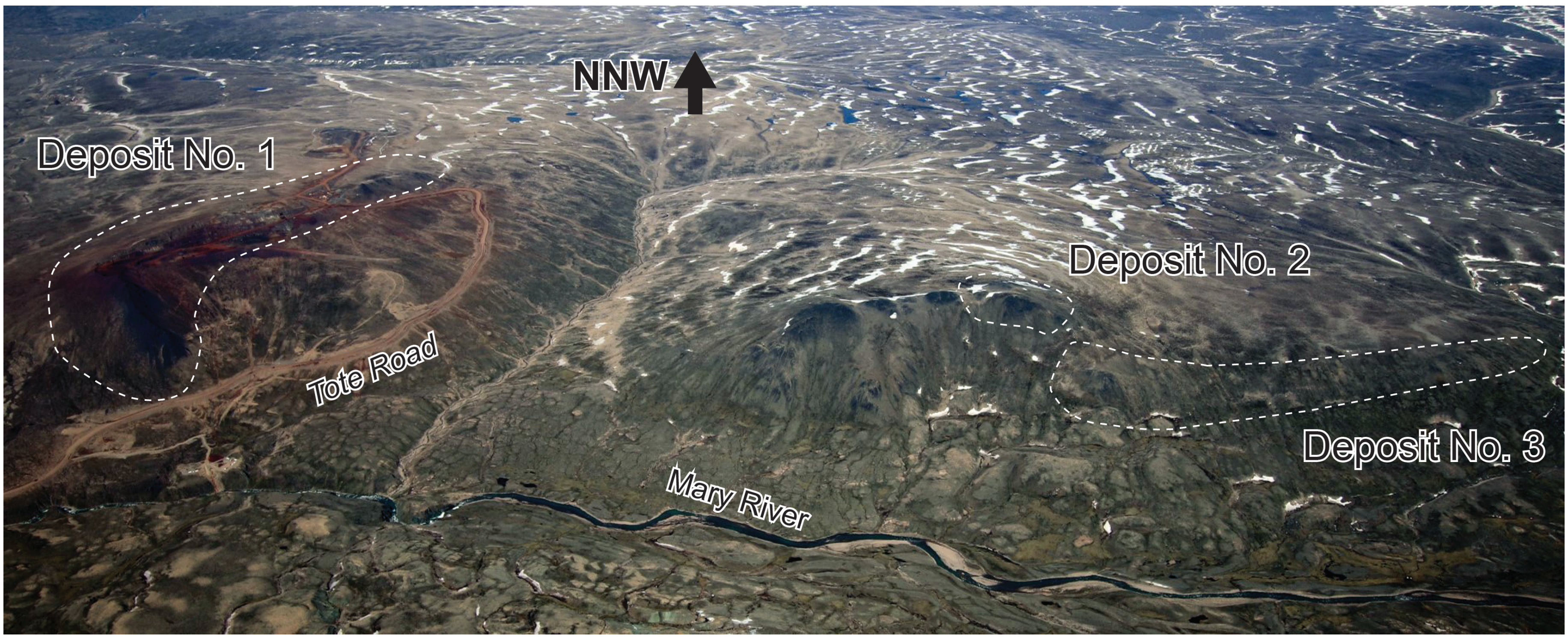

Figure 3. Panoramic aerial view of Mary River Deposits No. 1, 2, and 3 (Iannelli, 2018), northern Baffin Island (field of view is 6 km). Photograph by T. Iannelli, courtesy of Baffinland Iron Mines Corporation.

provided the following National Instrument 43-101 compliant resource figures (G.H. Wahl, R. Gharapetian, J.E. Jackson, V. Khera, and G.G. Wortman, unpub. report, 2011) for the combined No. 1, 2, and 3 deposits: 444 Mt grading 66.2% measured and indicated Fe, as well as 549 Mt of 66.3% inferred Fe. In addition to these resources, there are two other drilled deposits (Deposit No. 4 and Deposit No. 5) and four more (>60% Fe) discovered in 2010 for a total strike length of 160 km of iron-formation (Campbell and MacLeod, 2014). Production from Deposit No. 1 started in 2014, with a target mining rate set at 18 Mt/a. Mary River ore is currently hauled by road 100 km to Milne Inlet, where it is stockpiled and then transferred to bulk carriers. The first ore was shipped to European markets in July 2015. Further details are available from assessment reports recently released by Baffinland (Iannelli et al., 2013a, b, c), which are available in the public domain via NUMIN.

The Mary River Group (ca. 2.83 Ga and ca. 2.76 –2.72 Ga; available ages from Young et al., 2007, Skipton et al., 2017) is comprised of supracrustal outliers in the northwestern part of Baffin Island, which overlie Mesoarchean to Neoarchean basement. With respect to regional architecture, Fe deposits of the Mary River Group tend to occur within tight 10 km-scale folds that are broadly oriented consistently with the northwest- to west-trending structural grain (Young et al., 2004; Johns and Young, 2006). The area is strongly polydeformed; Skipton et al. (2017) and Saumur et al. (2018) summarized the current state of understanding of the structural framework of the area. Jackson (2000) and Johns and Young (2006) have correlated the Mary River Group with the Prince Albert and Woodburn groups of Melville Peninsula, and with similar rocks in northwestern Greenland, a tectonic entity that they identified as the ‘Committee Orogen’ (Jackson, 1969, 2000). However, these relationships are currently being tested by new research stemming from the GEM mapping program (Skipton et al., 2017; Saumur et al., 2018; Skipton et al., 2020a, b). The Mary River Group overlies a basement complex that includes foliated to strongly gneissose monzogranitic to tonalitic orthogneiss (ca. 3.9–2.8 Ga; Campbell and MacLeod, 2014; Skipton et al., 2017; Saumur et al., 2018). The contact relationship is thought to be unconformable, but in places is faulted, mylonitic, intrusive, and migmatitic (e.g. Bros and Johnston, 2017; Skipton et al., 2017). This highlights the different and locally ambiguous relationships with the multiple granitoid units occurring in the area, some of which are as young as ca. 2.7 Ga (Jackson et al., 1990; Bethune and Scammell, 2003). The Mary River Group is succeeded regionally by the Paleoproterozoic Piling Group (central Baffin Island), generally unmetamorphosed Mesoproterozoic strata of the Borden Basin, diabase dykes of the Franklin (720 Ma) swarm, and flat-lying to slightly tilted Ordovician carbonate and siliciclastic strata (Skipton et al., 2017; Saumur et al., 2018).

Previous reconnaissance-scale mapping (e.g. Jackson and Morgan, 1978; Jackson et al., 1978; Davidson et al., 1979) identified extensive tracts of Mary River Group in the surroundings of the Mary River Mine (Deposit No. 1) and north of the Barnes Ice Cap, as well as numerous smaller (1–10 km scale) exposures. Recent targeted mapping by personnel of the Geological Survey of Canada (Skipton et al., 2018, 2020a, b; Saumur et al., 2020a, b) has shown that the Mary River Group is less extensive than previously suggested at the regional scale; areas previously mapped as such are instead dominantly underlain by tonalitic to monzogranitic gneiss and/or monzogranitic to granodioritic plutons. Nevertheless, the thickness of the Mary River Group in the vicinity of the iron deposits varies between 2000 and 4000 m (Jackson, 2000). The regional metamorphic grade on northern Baffin Island ranges from greenschist to granulite facies, and amphibolite facies conditions prevail in the area of the Mary River iron deposits (Jackson, 2000; Jackson and Berman, 2000; Skipton et al., 2017; Saumur et al., 2018).

The Mary River Group comprises mafic–intermediate metavolcanic rocks with lesser ultramafic rocks, psammite to pelite, and iron-formation. Jackson (2000) identified five units within the Mary River Group, which include, from the stratigraphic base:

- pelite, mafic metavolcanic rocks; lenses of metaconglomerate
- quartzite; metarhyolite, metadacite (2718 +5/-3 Ma; Jackson et al., 1990), mafic metavolcanic rocks; oxide-facies iron-formation (and ore deposits)
- metaconglomerate and breccias; metagreywacke, pelite; metavolcanic rocks; metabasites; iron-formation
- local metaconglomerate and breccias; metagreywacke, pelite
- local metaconglomerate, breccia; metavolcanic strata with meta-anorthosite, metagabbro, and granulite-facies mafic rocks

Local unconformities have been proposed under the metaconglomerate within each unit. Layering of iron-formation with other lithofacies is common and has been attributed to a mixture of both depositional-facies variation and tectonic interleaving (Jackson, 2000).

Varieties of facies found in the Mary River Group include oxide-facies, silicate-facies, pelitic and carbonate-facies (calcitic and/or ferroan dolomitic), and locally pelitic and/or aluminosilicate-facies iron-formation, such as in the Rowley River prospect (Fig. 4e; Hey et al., 2015). Oxide- and pelitic-facies iron-formation also contain small amounts of disseminated pyrite and pyrrhotite. The greatest thickness of iron-formation occurs in the vicinity of the main orebodies: 52 to 195 m thick and traceable for up to 3.8 km (Fig. 4a–f). However, the ore zones are generally lenticular in shape; ore zone mineralogy is mostly hematite-magnetite grading to hematite and specularite. These high-grade zones often commonly comprise oxide- to silicate-facies iron-formation grading into or interlayered with quartzite, quartz-mica schist, or chlorite-schist (Iannelli et al., 2013a, b, c). Subsidiary phases within banded iron-formation (BIF) include grunerite, anthophyllite, clinochlore, quartz, garnet, pyrite, pyrrhotite, chalcopyrite, and covellite (G.H. Wahl, R. Gharapetian, J.E. Jackson, V. Khera, and G.G. Wortman, unpub. report, 2011). Upgrading of iron orebodies is attributed to pervasive metasomatism causing desilicification of oxide- and silicate-facies banded iron-formation, which has been linked to the Trans-Hudson Orogen (MacLeod, 2012). The Mary River Group in the area is also strongly polydeformed (*see* Young et al., 2004); thus deformation may also have played a role in the distribution and upgrading of iron ore, as was the case in other camps such as Hamersley, Australia (Egglseder et al., 2017).

Other Archean iron prospects of northern Baffin Island

Other iron-formation prospects in the larger Mary River district include Glacier Lake (Deposit No. 6), Turner River (Deposit No. 7), North Cockburn River (Deposit No. 8), North Rowley River (Deposit No. 9), Cockburn-Rowley, North Isortoq, South Isortoq, and Eqe Bay (Iannelli et al., 2013a; Campbell and MacLeod, 2014). The Glacier Lake deposit (locality 2) also contains base- and precious-metal occurrences (Iannelli et al., 2013b); other minor showings are highlighted by Skipton et al. (2017) and Saumur et al. (2018). Oxide-facies iron-formation (including hematite pseudomorphs after magnetite) occurs in Mary River Group belts up to 300 m in width and in excess of 1000 m in strike length. Channel samples have been collected from magnetite iron-formation grading 64% Fe over widths of 20 and 22 m at the Knob Hill and River Bend (Iannelli, 2018) prospects (locations uncertain), and grading 65% Fe over 54 m at the BIM (Baffinland Iron Mines) Island hematite iron-formation prospect (location uncertain; Campbell and MacLeod, 2014).

Additional iron-formation deposits, documented in the Eqe Bay belt, were largely explored by personnel of the Patino Mining Corporation (Eqe Bay area deposits 1 to 7 at locality 3; Boyd, 1969). Deposit 1 consists of banded hematite and magnetite interbedded with mafic to intermediate volcanic rocks. Resources quoted from the assessment report compiled by Boyd (1969) for deposits 1, 2, 3, and 4 combined are 236 Mt, with an additional 350 Mt of inferred resource. Probable resource in deposits 5, 6, and 7 amounts to 150 Mt (Boyd, 1969). The lithostratigraphy, structure, and age of supracrustal rocks that host iron-formation at Eqe Bay were studied during targeted mapping campaigns by the Geological Survey of Canada in the 1990s (Bethune and Scammell, 1997, 2003). Ages of the supracrustal rocks range between 2740 and 2725 Ma (Bethune and Scammell, 2003).

Banded iron-formations of the Piling Group, north-central Baffin Island

Showings of BIF are locally reported within the Astarte River formation of the Paleoproterozoic Piling Group (ca. 2160–1883 Ma; Fig. 5; Wodicka et al., 2014); such as an occurrence mapped approximately 30 km east of Steensby Inlet and discovered through helicopter-supported reconnaissance (Jackson and Morgan, 1978). A more complete study of the Piling Group was completed in 2000–2002, followed by the release of six new maps (St-Onge et al., 2005a–f). Recent traverse-supported fieldwork in this area, which covered the northernmost extent of the Piling Group on Baffin Island (Skipton et al., 2019, 2020b), found that BIFs in the Piling Group are neither extensive nor common. Unlike those of the Archean Mary River Group, Piling Group BIFs are considered sub- to uneconomic.

Foxe Basin: Cape Dorset area

Iron prospects are also documented in the Cape Dorset area on southwestern Baffin Island, including Maltby Lake, Chorkbak Inlet (four deposits; locality 4), and Korok Inlet (locality 5). The Maltby

Figure 4. Banded iron-formation, ironstone and iron ore of the Mary River district: **a)** view to the northwest of Mary River Deposit No. 1, which is 2.5 km long and consists of hematite and magnetite with average 68.2% iron content. Photograph by B. Saumur. NRCan photo 2019-255; **b)** outcrop of strongly foliated iron-formation 11 km east-northeast of Mary River Deposit No. 1. Photograph by B. Saumur, NRCan photo 2019-256; **c)** disharmonic folding in quartz garnet iron-formation with inter-bedded dacite and amphibolite located near Mary River Deposit No. 4. Photograph courtesy of H. Sandeman, Department of Natural Resources, Government of Newfoundland and Labrador; **d)** strongly lineated banded iron-formation at the Turner River prospect, 36 km northeast of Mary River Deposit No. 1. Photograph by B. Saumur. NRCan photo 2019-258; **e)** aluminosilicate-facies ironstone (grunerite+garnet+cordierite+magnetite±sillimanite) at the Rowley River prospect. Photograph by B. Saumur. NRCan photo 2019-259; **f)** recumbently folded banded iron-formation at the Nivalis Lake showing, near Barnes Ice Cap (NTS 37-E). Photograph by B. Saumur. NRCan photo 2018-334

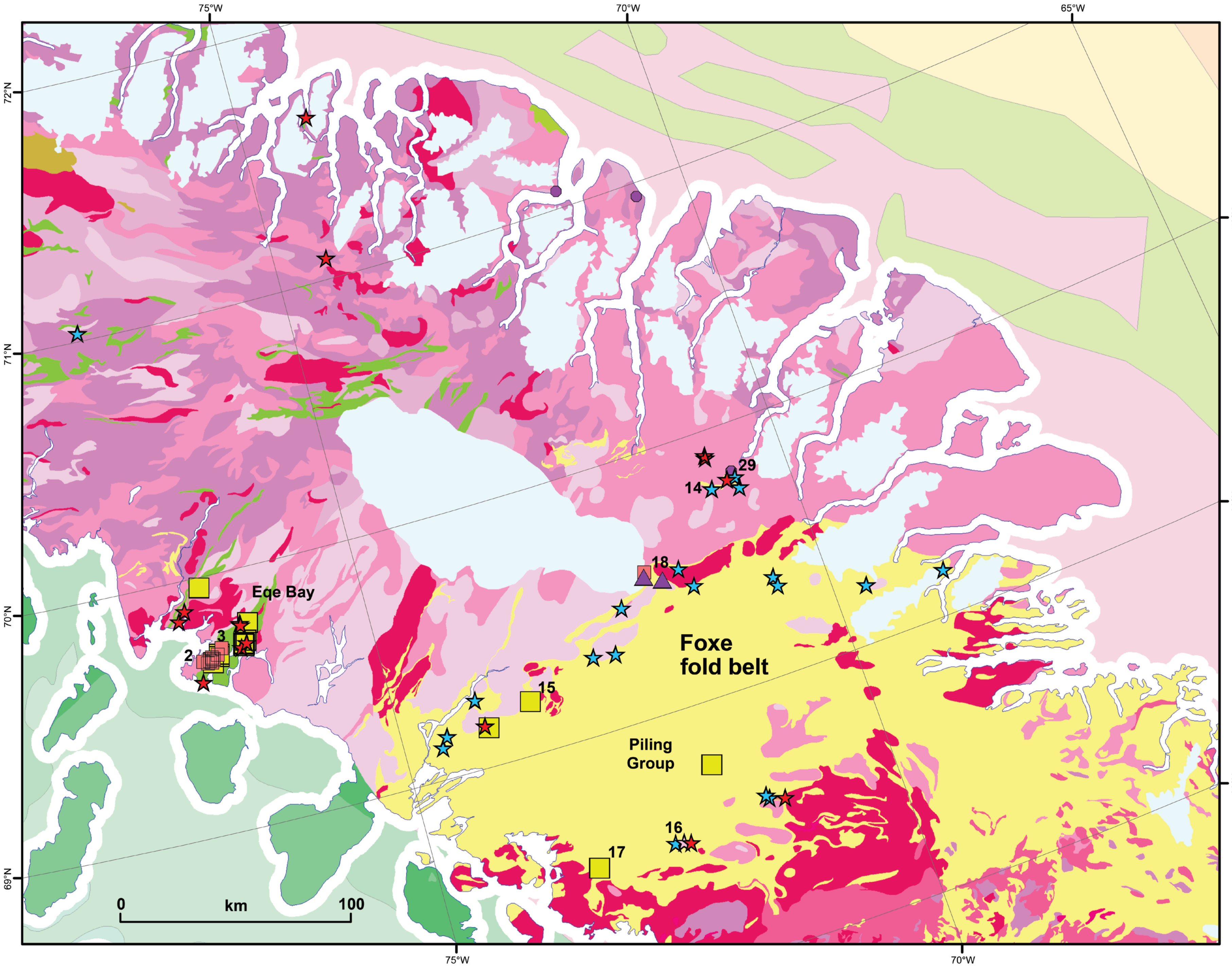

Figure 5. Piling Group and Foxe fold belt, central Baffin Island (*see* Fig. 1a, b for legend, and mineral-resource symbols and location).

Lake deposit, discovered and assessed by the Oceanic Iron Ore Corp., is generally disregarded as a potentially economic resource due to low grades (20–24% Fe in magnetite) and low tonnage (200 Mt; Siegel, 1956). While the Chorkbak Inlet prospects 1 to 3 of Ultra-Shawkey Mines Ltd. consist primarily of low-grade disseminated magnetite in garnet amphibolite, prospect 4 at Chorkbak Inlet is described as magnetite iron-formation (Labow, 1957). In contrast to the Chorkbak Inlet properties, magnetite at Korok Inlet features an intrusive relationship into gneissic country rock; however, the tonnage (7 Mt in four lenses) is not significant (Labow, 1957).

Base and precious metals

Nanisivik Mississippi Valley–type Zn-Pb, Arctic Bay area, northern Baffin Island

The Mesoproterozoic rocks of the Borden Basin on northern Baffin Island host the Nanisivik deposit (Fig. 6a–c; locality 6). Borden Basin is interpreted as the result of rifting that happened ca. 1270 Ma, with episodic extensional faulting occurring during basin evolution (Jackson, 2000). Sedimentation was terminated by inversion at ca. 1000 Ma (Turner, 2009). The Nanisivik mineralization is hosted in the Nanisivik and Ikpiarjuk formations, which were formerly grouped together in the Society Cliffs Formation (*see* Turner, 2009, 2011 for updated stratigraphy). These formations consist mainly of dolostone (>1000 m thick) featuring deep-water laminates and deep-water carbonate mounds in the western part of Borden Basin. In the eastern part of the basin, the (former) Society Cliffs formation is dolostone forming peritidal cycles reaching 250 m in thickness. Radiometric dating using the Pb-Pb (common lead) method indicates a sedimentation age of 1199 Ma (Dewing et al., 2007).

Prospecting in the vicinity of Strathcona Sound and the Nanisivik ore deposit was first carried out by prospector A. English, who accompanied an Arctic Expedition of 1910 (Bernier, 1911). A vein of pyrite and quartz 12 m thick was discovered, traceable for “several miles”; the site was noted as “metallic rocks” on an accompanying map. Years later, Blackadar and Lemon (1963) reported that A. English had also located a deposit of pyrite with sphalerite and galena in an exposure of four 1–10 m thick veins collectively exposed across a width of approximately 90 m. The occurrence of an erratic sample of silver and nickel ore was also reported; however, the bedrock source of this material has not been located. Similarly, near Arctic Bay, rusty dolostone containing small quantities of copper sulphides was discovered. The Nanisivik deposit was subsequently staked by Texas Gulf Sulphur Company in 1957 and was mined from 1976 to 2002; the community of Nanisivik, now abandoned, was built to support the mine and its workers. The other nearest settlement, Arctic Bay, was accessed from the mine and airport by an all-weather gravel road. Concentrate was removed by ship from a purpose-built port in the immediate vicinity of the mine.

Local features of the orebody, which occurs in a horst block that is part of a zone of east-striking normal faults, include a laminated dolostone host rock. The orebody is 3 km long, 100 to 200 m wide, 10 to 30 m thick, and contains 17 Mt grading 9.0% Zn, 0.7% Pb and 41 ppm Ag; in addition, there is an ore-zone keel 65 m deep and 5 to 30 m wide. The ore is mostly pyrite with zones rich in sphalerite, galena, and dolospar. The age of the orebody is unresolved, but determinations range from 1095 Ma (paleomagnetic dating of hydrothermally altered dolomite) to 461 Ma (dating of feldspathic alteration; Dewing et al., 2007). The latter age is unlikely as the deposit is cut by dykes of the 723 Ma Franklin swarm (Dewing et al., 2007). Early genetic models emphasized a void-filling, karst-related origin for the Nanisivik deposit (Dewing et al., 2007). More recent models emphasize staged replacement of host rocks involving a gas cap trapped beneath overlying Victor Bay Formation shale, with only minor, initial karst-related porosity in the Society Cliffs. Turner (2011) showed that hydrothermal mineralization is controlled by faults and fractures, as well as stratigraphic controls acting as barriers to fluid migration.

Other base-metal prospects of the Borden Basin

Exploration in the Arctic Bay, Nanisivik, and Pond Inlet region of northern Baffin Island has been the focus of Nanisivik, Mines Ltd. in the Society Cliffs Formation (Thorpe and Thalenhorst, 1981; Sutherland and Dumka, 1995), Petro-Canada in the Nauyat Formation

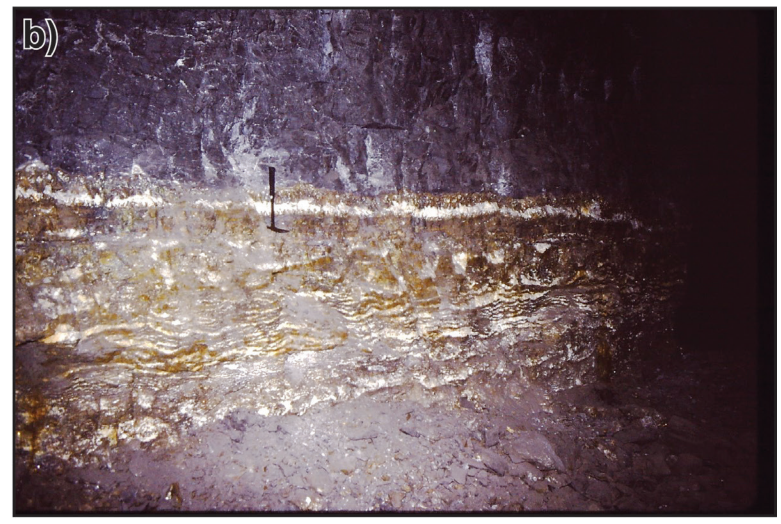

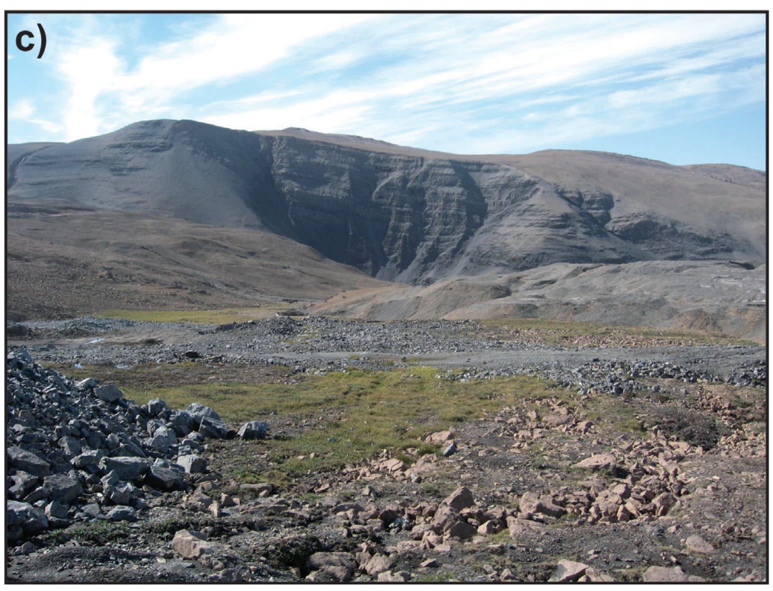

Figure 6. Photographs of the Nanisivik Mississippi Valley–type deposit area: **a)** Nanisivik townsite (single-family dwellings), with mill and port. Photograph courtesy of E. Turner, Laurentian University; **b)** Nanisivik underground ore face under dolostone. Photograph courtesy of R. Sherlock, Laurentian University; **c)** former Nanisivik mine site, with dolostone of the (former) Society Cliffs formation exposed in the hill in the background, which is approximately 50 m high. Photograph courtesy of E. Turner, Laurentian University.

basalt and Adams Sound Formation quartz arenite (Moffatt and Donald, 1985; Moffatt, 1986), and Noranda Exploration Company Ltd. in the Nauyat Formation (Wunder, 1994).

Apart from the Nanisivik mine, showings of sphalerite and galena or of anomalous metals (Zn, Pb, Ag, and locally Cu) are primarily located in the Society Cliffs Formation, between Strathcona Sound and Arctic Bay (13 showings). Additional mineralization has been located over a distance of 118 km to the east-southeast of the Nanisivik mine (9 showings). Notable separate showings include a site north of Strathcona Sound, which intersected stringers, vugs, and cavity fills in the Society Cliffs Formation with assay values of up to 5% Zn and 2% Pb (Sutherland, 1999; locality 7). In a separate locality east of the head of Arctic Bay, grab samples from a 200 m long interval of the Society Cliffs Formation returned assay values of 13.5% Pb and 10% Zn (Moffatt and Donald, 1985; locality 8).

Petro-Canada primarily focused its activities on quartz arenite of the Adams Sound Formation (Moffatt and Donald, 1985; Moffatt, 1986) in the 1980s. This included the discovery of disseminated malachite at a site near the northern shore of Arctic Bay, and barite and pyrite (up to 32%) at a site east of Arctic Bay. The mineralogy of a cluster of ten showings located east of Elwin Inlet consisted of galena and barite, with anomalous silver.

Mineralization was also found in shale intervals within the Nauyat Formation basalt. Noranda Exploration Company Ltd. reported copper from two showings south of Arctic Bay, with grab samples grading up to 7.1% Cu (Wunder, 1994; locality 9).

Minor subeconomic showings of sphalerite and galena have been documented near Tay Sound, within the Iqqittuq Formation on the hanging wall of the White Bay fault zone, roughly 75 km southwest of Pond Inlet (Young et al., 2004).

Mafic–ultramafic systems of the Kimmirut area

Twenty-six base- and precious-metal prospects were investigated by Rubicon Minerals Corporation in 1998 and 1999 west and north of the village of Kimmirut, near the southern coast of Baffin Island (Vande Guchte, 1998; Vande Guchte and Gray, 1999; showings in the vicinity of locality 10). All have broadly similar geological and metallogenic characteristic host rocks: psammite and semipelite of the Lake Harbour Group, specifically sulphidic and graphitic metasedimentary rocks. These are intruded by mafic–ultramafic sills, with phases including pyroxenite and peridotite. Sulphide mineralization occurs within the Lake Harbour Group strata or within the sills. Often, there are no sills in the vicinity of the mineralized sediments. Commodities in anomalous concentrations include nickel, copper, palladium, platinum, and sometimes gold, silver, and zinc. Pod-shaped sulphide bodies can be only a few metres long, but are contained within larger gossans measuring up to 100 m (West-1 and West-2 showings; locality 10), 150 m (MD showing; locality 11), 400 m (Blue Lake showing; locality 12), and 700 m (Elephant Island property; locality 13). Favourable comparisons, in terms of analogous geological environments and mineral associations, have been made with base-metal deposits of Thompson, Manitoba (Vande Guchte, 1998; Vande Guchte and Gray, 1999). International Capri Resources Ltd. (Larouche, 1997; Lichtblau, 1997) investigated five similar showings of disseminated mineralization in the Kimmirut area hosted in diorite, tonalite, gabbro, and pyroxenite.

Base-metal showings of the Piling Group, central Baffin Island

Exploration centred on the Paleoproterozoic Piling Group was carried out by Cominco Ltd. (Armstrong et al., 1976), Petro-Canada Limited (Moffatt, 1986), Savanna Resources Ltd. (Durocher, 1994, 1995), Comaplex Minerals Corp. (McPherson, 1992), and Commander Resources Ltd. (Sexton, 2008; Fleming and Sexton, 2010).

Cominco Ltd. targeted the Flint Lake formation along the northern margin of the Piling Group (St-Onge et al., 2005a), with the expectation of finding carbonate-hosted mineralization like that of the Black Angel deposit of west-central Greenland. Better prospects, also in the Flint Lake formation, included the Miki Maku Lake prospect (locality 14), in which sphalerite and galena occur parallel to bedding in marble over a distance of 1.5 km and reach a thickness of 10 to 20 cm. Elsewhere, up to 5% sphalerite occurs in dolomitic marble, and disseminated pyrite, pyrrhotite, and chalcopyrite are hosted in grey marble. Cominco Ltd. also identified rusty and graphitic schist (Astarte formation?) with variably anomalous Zn, Ni, and Cu. Petro-Canada Limited documented sulphide-bearing boulders in three localities with anomalous Zn, Ni, and Cu, potentially derived from the Astarte formation. At a fourth locality, a gossan in amphibolite with anomalous Cu was identified.

The exploration activities of Savanna Resources Ltd. focused on the Astarte formation exposed in the western part of the Piling Group (St-Onge et al., 2005a, b). Eight prospects are recorded (in the vicinity of locality 15) consisting of the following dominant rock units: 1) pyritic graphitic meta-argillite; 2) sulphide breccia; and 3) quartzite and metasiltstone. Dominant elements vary between showings. However, typical anomalies in pyritic argillite include As, Pb, Ag, and Cd with 20 to 70% pyrite and pyrrhotite. Sulphide breccia contains anomalous Ag, Zn, Cu, Mn, Cd, As, Pb, and Ni. Breccia clasts consist of sandstone and argillite in a matrix of 20 to 100% pyrite and pyrrhotite. Sandstone and siltstone exposed in the vicinity of argillite and breccia also contain locally massive sulphides (up to 30%) and anomalous concentrations of Ba, Mn, Ag, Ni, and Cu.

Comaplex Mineral Corp. focused its exploration activities in the southern and southwestern Piling Group on gossans developed in the Astarte formation. Typical showings (near locality 16) include massive to pod-shaped pyrrhotite and pyrite, and pyritic graphitic argillite with variably anomalous Zn, Ag, Cu, and Ni. Comaplex also documented a tungsten showing in the same general area.

Commander Resources Ltd. located five showings in the southern Piling Group. The best of these is the Tuktu prospect (locality 17), which is hosted by mafic metavolcanic rocks of the Bravo Lake formation, itself the host of semimassive sulphide-containing sphalerite, galena, pyrite, and pyrrhotite. Assays returned values up to 0.55 g/t Au, 513.3 g/t Ag, 0.14% Cu, 11.34% Pb, and 18.6% Zn.

Rounding out the mineral occurrences in the Piling Group are two properties featuring niobium and tantalum. The first of these is an occurrence on the Barnes Ice Cap (locality 18) consisting of radioactive columbite and tantalite in pegmatite (Lang et al., 1962); no other details are provided. The occurrence reported at the second property consists of columbite in pegmatite and is located on the Plex claim block owned by Cominco Ltd. (LeCouteur, 1979).

Northern Baffin Island

Sparse showings and potential for Ni-Cu-PGEs and precious metals have been noted for the greenstone belts of the Mary River district (Young et al., 2004; Johns and Young, 2006) and the Kangiqłuruluk layered mafic–ultramafic intrusion, 50 km west of Pond Inlet (Skipton et al., 2017). Minor showings of Cu and Mo have been documented along the shores of Quernbiter Fiord and Royal Society Fiord (Jackson, 1969), roughly 200 km northwest of Clyde River; these are probably associated with units of intrusive granitic basement.

Diamond-bearing kimberlite

Chidliak, southern Baffin Island

The Chidliak property (locality 19), initially held by Peregrine Diamonds Ltd. and now by De Beers Canada, consists of 60 prospecting permits located on Hall Peninsula (southern Baffin Island), approximately 150 km northeast of Iqaluit.

Bedrock on Hall Peninsula (Fig. 7, 8) includes Archean orthogneissic basement (ca. 2920–2701 Ma; Scott, 1999; Rayner, 2014, 2015) that is generally considered to form part of the Meta Incognita microcontinent (*see* St-Onge et al., 2009). Various cratonic affinities have been proposed for the basement, including: the Rae, Superior, or Nain craton; the Aasiaat domain in western Greenland; or the Core Zone in Labrador (Jackson et al., 1990; Scott, 1999; St-Onge et al., 2009). Archean orthogneissic basement is unconformably overlain by Paleoproterozoic cover strata, with a maximum depositional age of ca. 1960 Ma (Rayner, 2014, 2015) and which are considered to form part of the Lake Harbour Group (*see* St-Onge et al., 2009), or, alternatively, the northern extent of the Tasiuyak gneiss (*see* Scott et al., 2002). On western Hall Peninsula, these strata host orthopyroxene-bearing felsic intrusions (ca. 1890–1852 Ma; Rayner, 2014, 2015) that mostly represent the eastern margin of the Paleoproterozoic Cumberland batholith (*see* Whalen et al., 2010). Hall Peninsula underwent regional middle amphibolite- to granulite-facies metamorphism and crustal shortening ca. 1860 to 1820 Ma, followed by post-thermal peak folding and intrusions of pegmatitic dykes ca. 1800 to 1750 Ma (Skipton et al., 2016a, b).

The bulk of the Chidliak property consists of Archean ortho-gneiss (3019–2784 Ma; J. Pell, unpub. report, 2008). North-trending belts of the Lake Harbour Group are also present, which comprise psammite, quartzite, semipelite, pelite, minor marble, calc-silicate, and leucogranite. Additionally, leucodiorite, peridotite, pyroxenite, and dunite occur as basement-sourced units. All units experienced peak mid-amphibolite-facies metamorphism (J. Pell, unpub. report, 2008; Skipton et al., 2016a).

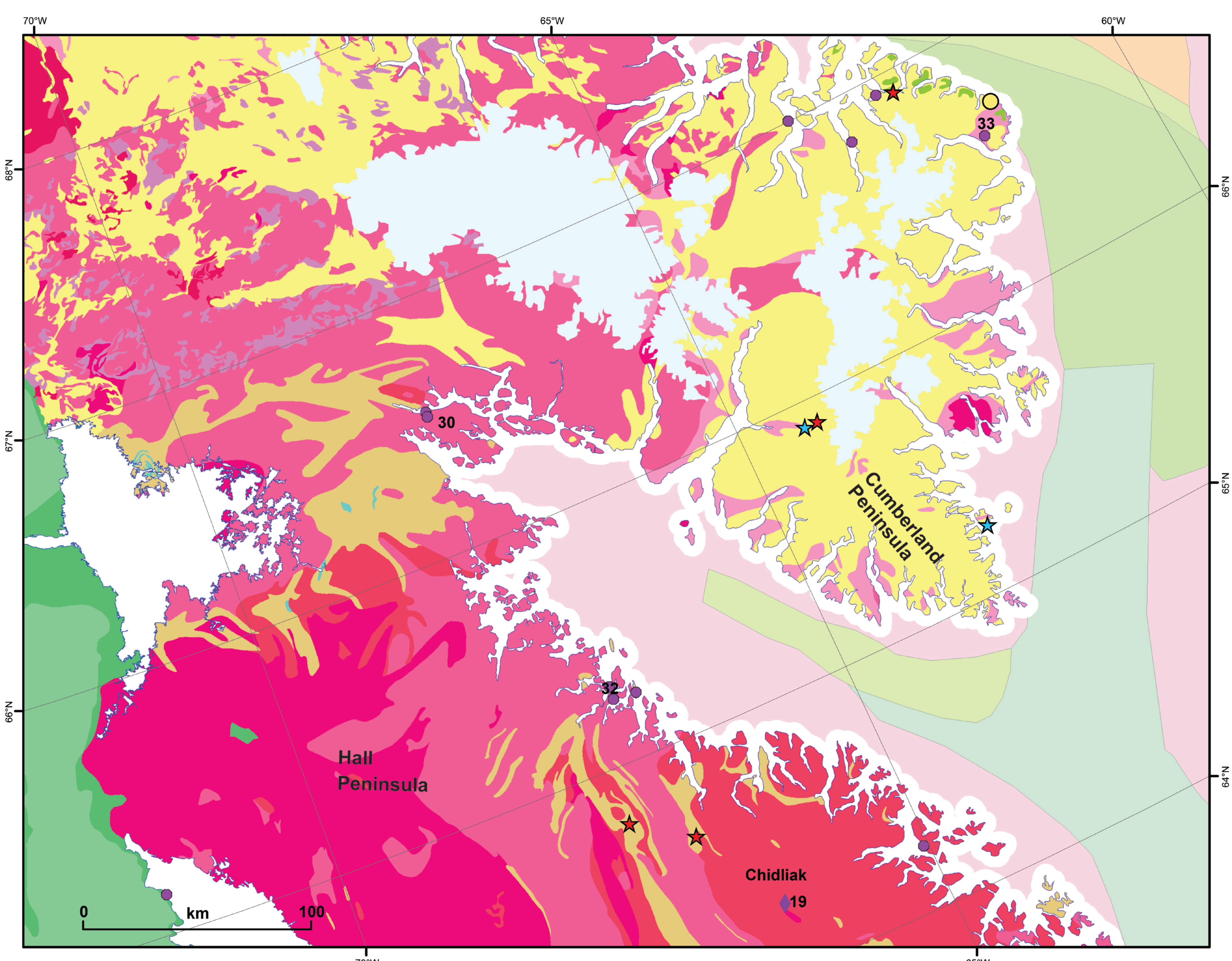

Figure 7. Cumberland Peninsula and northern Hall Peninsula, eastern Baffin Island (*see* Fig. 1a, b for legend, and mineral-resource symbols and location).

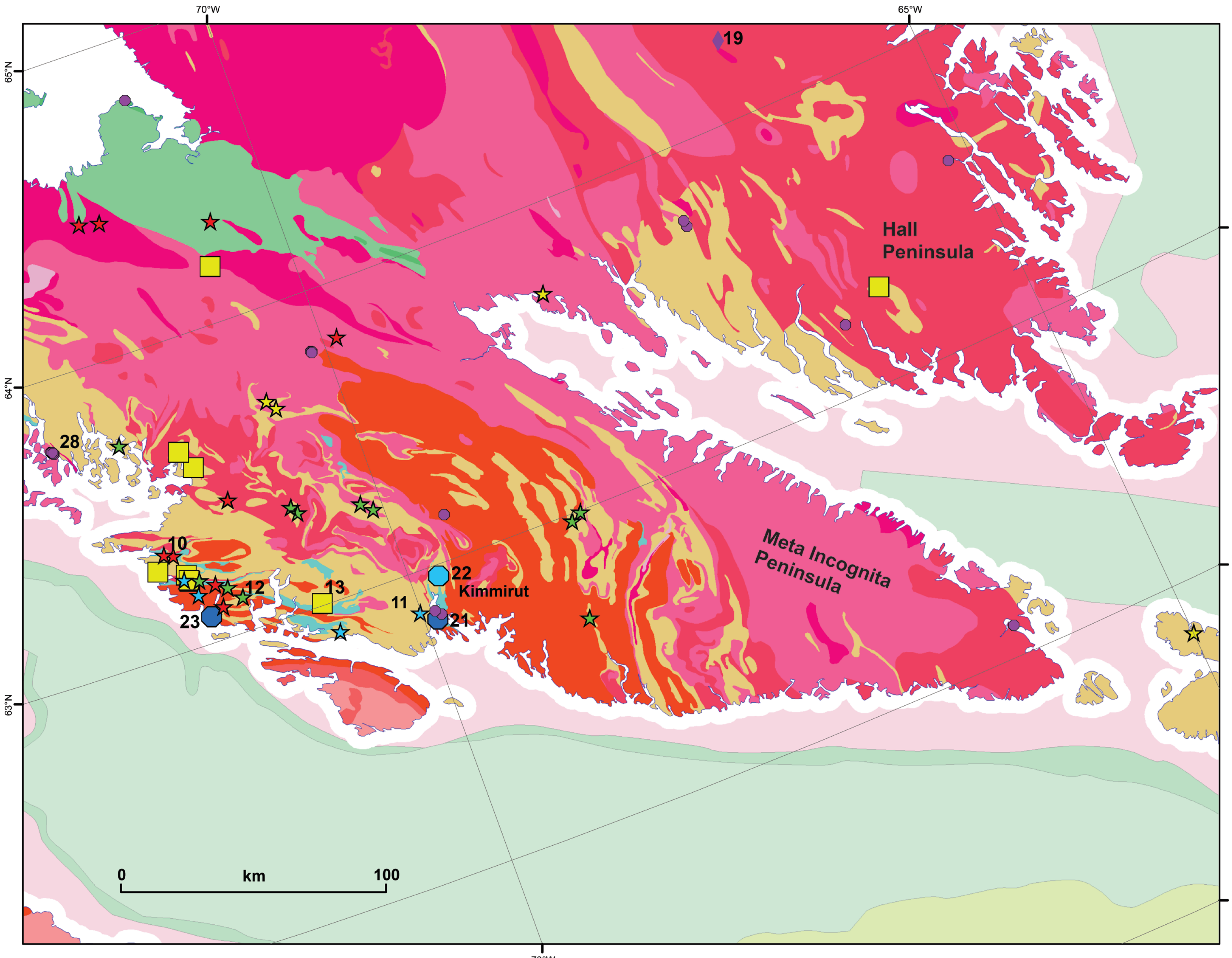

Figure 8. Southern Hall Peninsula and Meta Incognita Peninsula, southern Baffin Island (*see* Fig. 1a, b for legend, and mineral-resource symbols and location).

Kimberlites on the Chidliak property include sheets and pipe-like bodies up to 6 ha in area. The sheet-like bodies consist of hypabyssal (coherent) kimberlite with basement xenoliths. The kimberlite pipes contain basement xenoliths and fragments of carbonate and clastic rock of Late Ordovician to early Silurian age (Zhang and Pell, 2013). As these rocks are not encountered at the surface, it is presumed that the Ordovician–Silurian was a former cover on Hall Peninsula (Zhang and Pell, 2013). The kimberlites provide a U-Pb age range on perovskite of 156.7 to 138.9 Ma (Kimmeridgian to Valanginian; Heaman et al., 2015). Kimberlite facies at the Chidliak property are distinguished as volcanic kimberlite, hypabyssal kimberlite, coherent kimberlite, and pyroclastic kimberlite. All of these contain mantle xenoliths; however, some contain clasts of Archean gneissic basement but none of lower Paleozoic age.

The most prospective kimberlites for diamonds are CH-1, CH-6, CH-7, and CH-44. The CH-1 kimberlite covers an area of close to 6 ha and consists of coherent (magmatic) kimberlite with pyrope garnet, chrome diopside, olivine phenocrysts up to 0.1 m across, eclogite, and peridotite xenoliths (Pell, 2008). It is exposed as cobbles in frost boils. The CH-6 kimberlite underlies an area of approximately 1 ha and consists of carbonate-clast-bearing kimberlite. Deeper in the pipe, there are kimberlite facies that are either carbonate-poor or carbonate-rich. Basement xenoliths are also rare. It is unclear whether this is facies of the kimberlite-bearing carbonate xenoliths or whether it is a distinct and separate phase (Farrow et al., 2015). The CH-7 kimberlite, also measuring about 1 ha across, consists of two distinct lobes, the smaller of which comprises coherent kimberlite and the other, apparently coherent kimberlite and volcanic kimberlite, with clasts of carbonate and basement (Farrow et al., 2015). The CH-44 kimberlite covers 0.5 ha with apparently coherent kimberlite in the upper part and volcanic kimberlite or pyroclastic kimberlite at greater depths.

Jackson Inlet, Brodeur Peninsula, northern Baffin Island

Brodeur Peninsula (locality 20) has been notably active for kimberlite exploration in recent years, as carried out specifically by Twin Mining Corporation, Mountain Province Diamonds, and Kennecott Canada Exploration Inc. The most favourable prospect was the kimberlite swarm discovered near Jackson Inlet by F. Tatarnic in 1998, worked by Twin Mining Corp., and reported by Dalmin Corporation (Davis, 2000).

Brodeur Peninsula is underlain by flat-lying Ordovician and Silurian carbonate rocks and a blanket of till. The exposed kimberlites near Jackson Inlet show up as three dark brown patches within a halo of tan-brown altered carbonate. Sixteen kimberlite pipes have been outlined in an oval-shaped (580 by 430 m) area; five pipes have been subjected to trenching. Olivine, garnet, and phlogopite are the dominant phenocryst phases set in 20 to 30% groundmass. In addition, there are host rock xenoliths of limestone, shale, gneiss, lapilli, and mantle-derived peridotite. Trench sampling results indicate good diamond grades, although the pipes are relatively small in diameter (15–60 m each).

Steensby Inlet, northern Baffin Island

Kimberlitic diamond-exploration campaigns south and southwest of Mary River by De Beers (P. Hundt., unpub. assessment report, 2004; D. Wiznar and J. McKenzie, unpub. assessment report, 2005; B. McMonnies, J. McKenzie, N. Januszczac, and D. Chartier, unpub. assessment report, 2007), which included airborne aeromagnetic surveys, did not yield significant prospects.

Gemstones

The Kimmirut area is well endowed in gemstones (sapphire, lapis lazuli, gem-quality spinel), all of which occur within metasedimentary rocks of the mid-Paleoproterozoic Lake Harbour Group (ca. 1.93–1.86 Ga; Scott et al., 2002) that was affected by high-grade granulite-facies metamorphism.

Sapphire (Kimmirut area, southern Baffin Island)

The NUMIN file entry indicates that Canadian Arctic sapphires were first discovered in the vicinity of Kimmirut on southern Baffin Island (locality 21) by a local prospector, N. Aqpik, in 2002. An option agreement was drawn up with True North Gems Inc. in 2003, which subsequently acquired a 100% right to the property. Two additional small showings have been located 100 km to the west, in the vicinity of Beaumont Harbour and Crooks Inlet (Lepage, et al., 2012). Assessment of resource potential included property-scale mapping (2006–2008), prospecting with an ultraviolet lamp (2007–2008), and bulk sampling (2004–2008). During and after 2006, 27 additional localities were discovered in the vicinity of the main (Beluga) showing, including Beluga South, Aqpik, Mark Ruby, and Narwhal.

The sapphires near Kimmirut (Fig. 9a–c) occur within the Lake Harbor Group, which is exposed over a strike length exceeding 500 km from Cape Dorset in the west to Kimmirut in the east. Units of the Lake Harbour Group include: 1) semipelite and garnet psammite; 2) garnet psammite and quartzite; and 3) marble and calc-silicate schist, which is host to the sapphire showings. The marble contains phlogopite and graphite, whereas the calc-silicate contains diopside and lesser phlogopite, wollastonite, tremolite, titanite, and apatite. Common association of sapphire with calc-silicate includes scapolite, spinel, tourmaline, and apatite. The main discovery area (Beluga) extends over 1000 m, with specific occurrences located in detached blocks. The most prospective rocks feature 10% sapphire as euhedral and subhedral crystals, many averaging 1.5 cm in length and some reaching 7 cm. Gangue phases include anorthite, calcite, scapolite, phlogopite, and pyroxene. It has been suggested that the occurrence of scapolite may indicate an origin linked to the regional metamorphism of impure evaporites (Lepage, et al., 2012). Alternatively, recent work has indicated that the protolith was most likely dolomitic argillaceous marl, and that sapphire formed as a result of retrograde replacement and breakdown of the peak granulite-facies metamorphic mineral assemblage (Belley et al., 2017).

Lapis lazuli (Kimmirut area, southern Baffin Island)

The local Inuit have known for some decades of the occurrence of lapis lazuli 15 km north of Kimmirut, on southern Baffin Island (locality 22; Hogarth, 1971). The host rock is white to grayish marble of the Paleoproterozoic Lake Harbour Group containing minor components of phlogopite and graphite. Occurrences are located in a northeast-plunging regional synform, with the favourable area totalling 3500 m^2. Two outcrop areas, 1.6 km apart, are known as the Main and North occurrences. Commercially significant material consists of haüyne, diopside, nepheline, plagioclase, and phlogopite; the association of haüyne with pyrite is considered to be the origin of the lazurite in lapis lazuli (Rogers, 1938; Deer et al., 1966; Hogarth, 1971). The most common texture in Kimmirut lapis lazuli consists of granoblastic diopside in a lazurite matrix. Mineralogy of enclosing gneiss indicates regional granulite-facies metamorphism (St-Onge et al., 2007). The original model for the genesis of the Lake Baikal lapis lazuli involved metasomatism associated with pegmatite emplacement (Korzhinskii, 1947). However, the favoured and more current model suggests that the lapis lazuli originated from regional granulite-facies metamorphism of an evaporite-dolomite-shale sequence and the removal of large volumes of Na and Cl from the evaporite (Hogarth and Griffin, 1978).

Although some lapis lazuli could be considered valuable as an unusual source of carving stone, Hogarth (1971) has described the Kimmirut lapis lazuli as "not as attractive as that of specimens from Afghanistan and Siberia."

Gem-quality spinel and cobalt-blue spinel, southern Baffin Island

Recent research by Belley and Groat (2019) has documented the presence of gem-quality spinel and cobalt-blue spinel (locality 23) at 14 localities within metasedimentary (metamarl, marble,

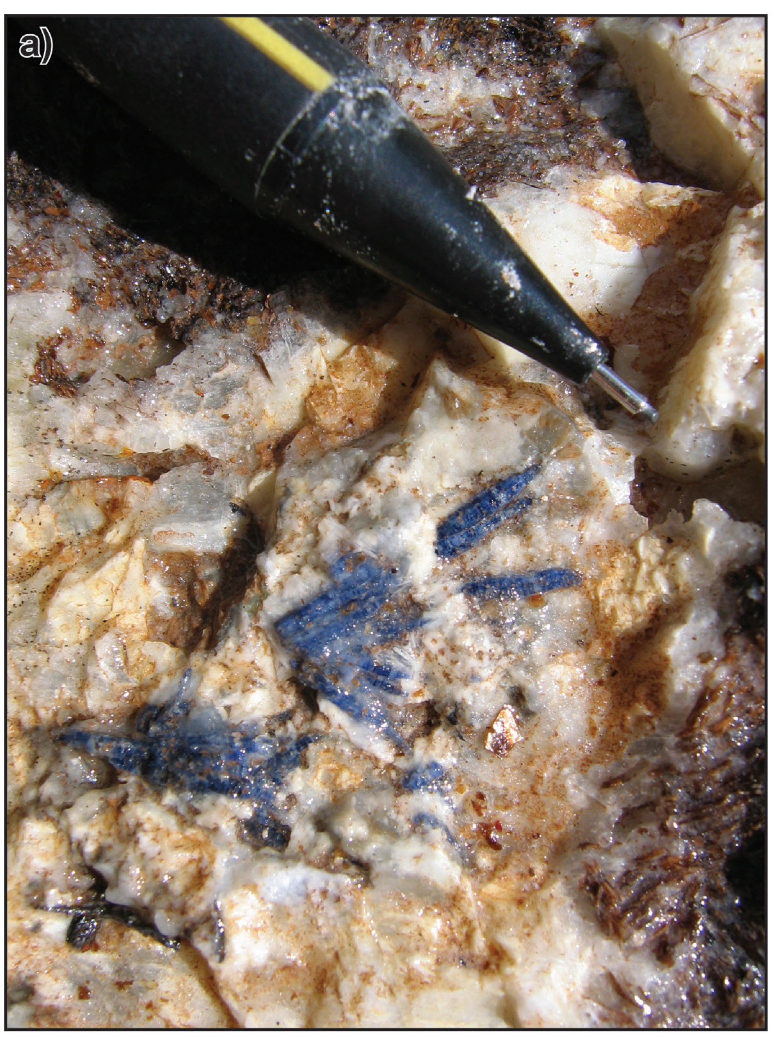

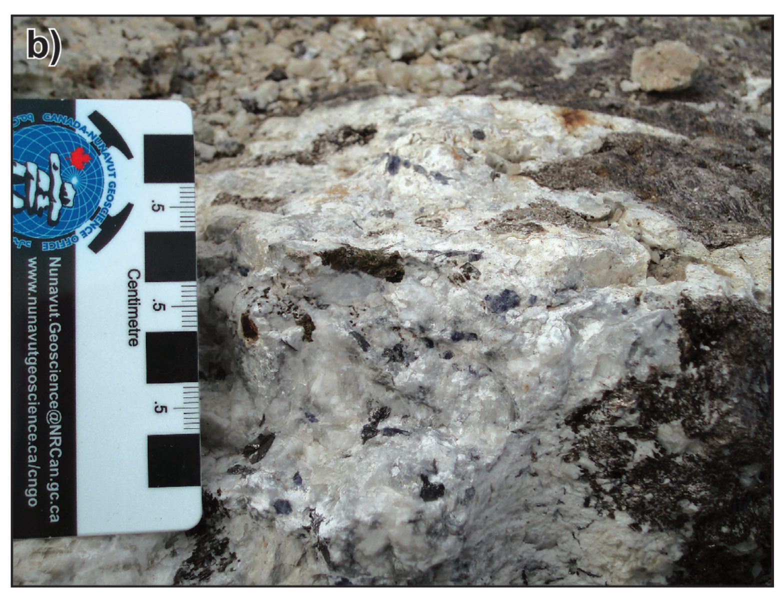

Figure 9. Gemstones of the Kimmirut area, within Lake Harbour Group metasedimentary rocks: **a)** blue sapphires in outcrop, pen tip for scale. **b)** blue sapphires in outcrop. **c)** cobalt-blue spinel in metamarl. All photographs courtesy of A. Bigio, Crown-Indigenous Relations and Northern Affairs Canada.

calc-silicate) rocks of the Lake Harbour Group, notably at Markham Bay, Glencoe Island, Waddell Bay, and the Kimmirut area. Granulite-facies metamorphism yields a stable assemblage of calcite, dolomite, phlogopite, pargasite, diopside, humite, forsterite, scapolite, anorthite, graphite, spinel, and pyrrhotite. The presence of gem-quality and cobalt-blue spinel is strongly dependent on the composition of the protolith, requiring a low Si/Al ratio, low K activity, low X_{CO_2} in marble, and relatively low Mg content. Belley and Groat (2019) noted that the strong partitioning of Fe into pyrrhotite decreases its amount in spinel, thus making the spinel clearer and more attractive.

Uranium–thorium

Foxe Peninsula–Cape Dorset area

Airborne and ground radiometric surveys in 1967 and afterwards by Borealis Exploration Ltd. (Henderson, 1969) and Esso Minerals Canada (Garvey, 1978) uncovered eleven showings of uranium and thorium in the Foxe Peninsula–Cape Dorset area (locality 24; Fig. 10). Host rocks consist of pegmatite (six showings), biotite gneiss (three showings), granite and granitic gneiss (two showings), quartzite (one showing), and grey gneiss (one showing). Four properties were drill tested. However, results of drilling and grab-sample assaying were deemed to be either low grade or too small to be economically significant.

More recently, property work was done by Peregrine Diamonds Ltd. on the Kimmirut and Kimmirut-B claims. Uranium and thorium were found to occur in a small area in dark green silicates of altered amphibolite (Nielson and Pell, 2009).

Other properties in the Kimmirut region include two prospects of uranium and thorium in pegmatites explored by Borealis Exploration Ltd. (Henderson, 1969).

Fury and Hecla Basin, northern Baffin Island

Uranium and thorium prospects are located close to the northern contact of the Mesoproterozoic Fury and Hecla Basin of northwestern Baffin Island (locality 25; Fig. 11). A western cluster of nine showings occur in Neoarchean pegmatite intruding gneiss in close proximity to small bodies of late-phase granite. Pegmatite intrusions are seldom traceable for more than a few metres and none are commercially significant (Maurice, 1982; Chandler, 1988). An eastern cluster of eight unconformity-related showings includes occurrences discovered by Geological Survey of Canada personnel during follow-up of an airborne radiometric survey (Chandler et al., 1980). These prospects are associated with a single, large granite body near the sub-Fury and Hecla Basin unconformity surface. Additional showings were discovered in this area by Dejour Mines Ltd. along a faulted contact between Fury and Hecla Group sandstone and basement granite (Fisher, 1981; Fisher and Kwiecien, 1981). Likewise, a showing discovered by Noranda Exploration Ltd. is adjacent to a quartz vein in Fury and Hecla Group sandstone (Prest, 1977).

As part of recent bedrock mapping conducted in the Fury and Hecla Strait area by personnel of the Canada-Nunavut Geoscience Office (*see* Steenkamp et al., 2018), hand-held gamma-ray spectrometry measurements were taken throughout the Fury and Hecla Group and along the unconformity with Archean metaplutonic rocks to quantify radioactive U, Th, and K concentrations (Patzke et al., 2018). No new anomalous values were obtained during fieldwork, although interpretation of new radiometric-survey data suggests the occurrence of relatively high radioactive signatures north of the basin (Steenkamp et al., 2018).

Carving stone

At least 32 localities of carving stone are located in the Baffin Island (Qikiqtaaluk) region. Seven communities are well served and have good access to carving-stone localities. These include Arctic Bay, Cape Dorset, Clyde River, Iqaluit, Kimmirut, Pangnirtung, and Pond Inlet. Typical carving-stone material includes serpentinite (antigorite), marble, and argillite.

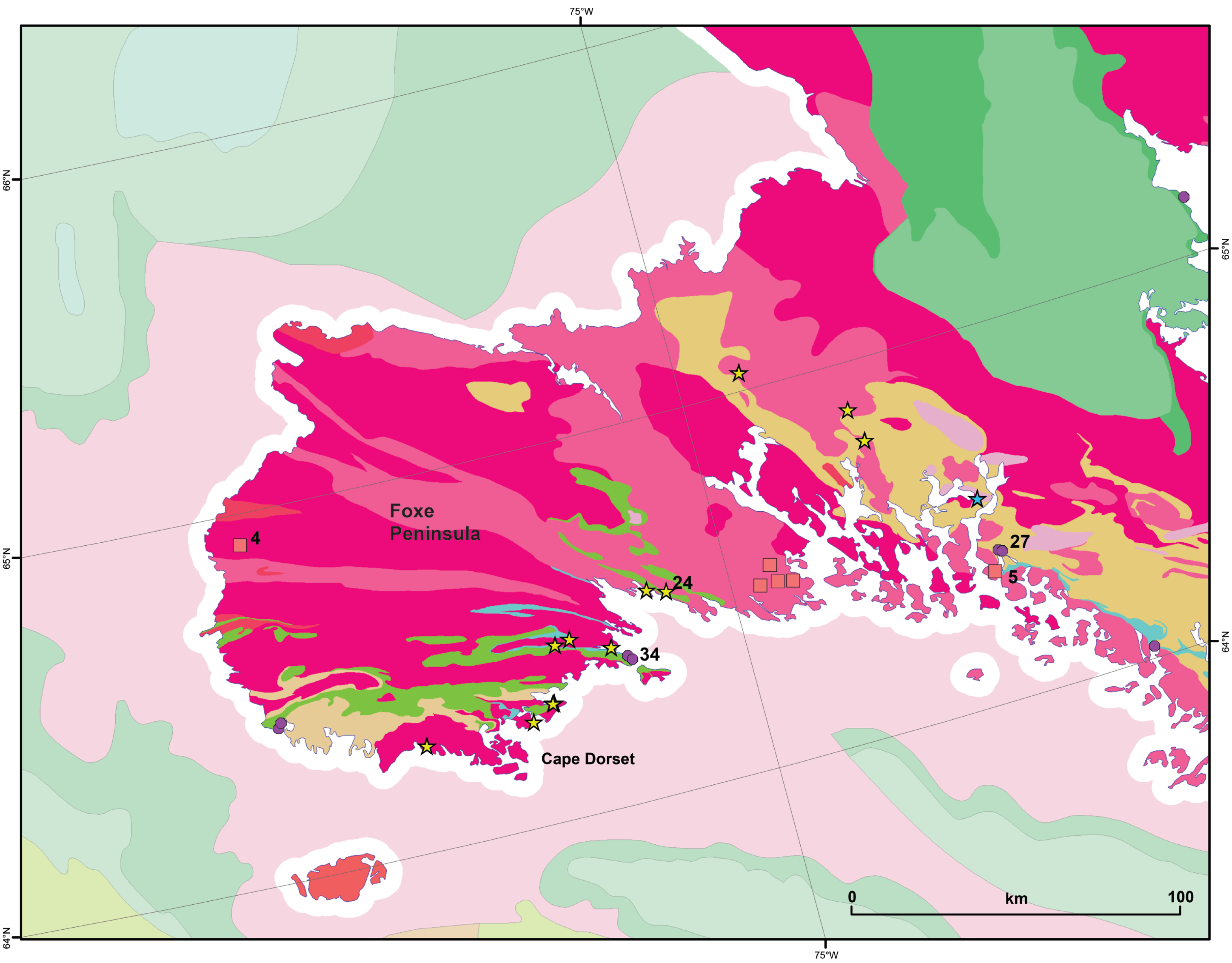

Figure 10. Foxe Peninsula, southwestern Baffin Island (*see* Fig. 1a, b for legend, and mineral-resource symbols and location).

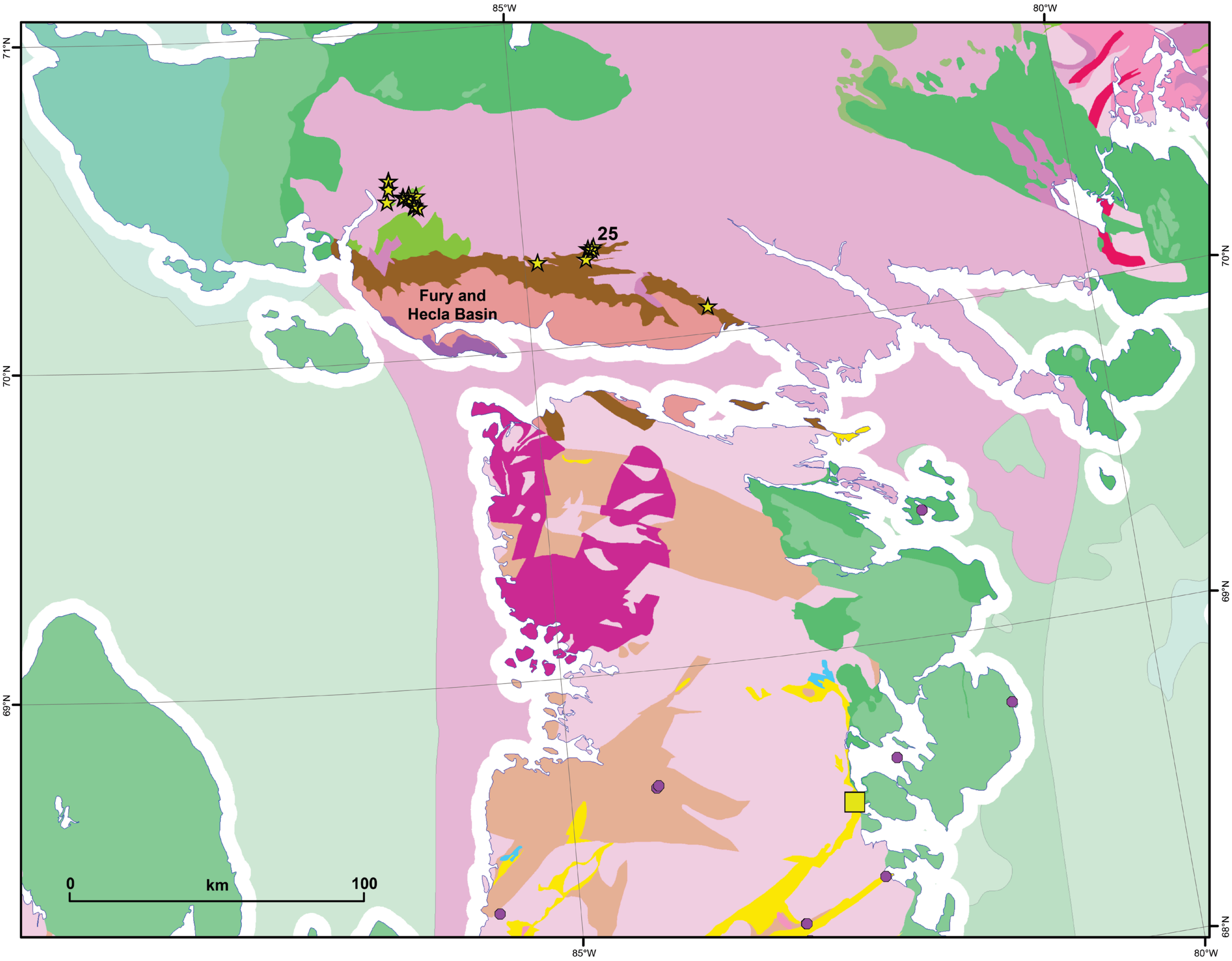

Figure 11. Fury and Hecla Basin, western Baffin Island (*see* Fig. 1a, b for legend, and mineral-resource symbols and location).

The deposits near Arctic Bay (locality 26) consist of eight sites of Mesoproterozoic carbonate altered to marble in contact-metamorphic proximity to Franklin dykes, one site of serpentinite, and one site of ilmenite-bearing kimberlite near Fabricius Fiord (McDermott, 1992; Beauregard and Ell, 2015).

The Kangiqsukutaaq deposit (15 500 t extracted) is located near the northeastern shore of Korok Inlet on the southern coast of Baffin Island, 160 km east of Cape Dorset (Fig. 12a; locality 27; Steenkamp et al., 2014) and consists of two quarries. The lower southern pit is a large deposit, now exhausted, of serpentinized magnesian marble of the Lake Harbour Group, iron-rich serpentinite, and antigorite serpentinite (total production since the 1960s was 15 400 t at a rate of 301 t/a; Elgin, 2017). The upper (northern) pit, consisting of serpentinized magnesian carbonate, continues to provide good material and may have 2880 t or 10 years of production remaining (Elgin, 2017).

There are two carving-stone quarries on Aberdeen Bay, 160 km west of Kimmirut (locality 8; Beauregard et al., 2013; Elgin, 2017). The Tatsiituk (Ujaraniarvik) deposit is of modest size (3000 t) and consists of apple green serpentinized magnesian marble of the Lake Harbour Group intruded by ultramafic rocks and monzogranite of the Cumberland batholith (Fig. 12b; Beauregard and Ell, 2015; Elgin, 2017). This site has been active since the 1950s, with production of 4.2 to 10.6 t/a (Elgin, 2017). The nearby Tatsiituk Taniinya deposit consists of altered ultramafic rocks (Beauregard, 2014). Total remaining resource is estimated to be a maximum of 2237 t (Elgin, 2017).

Locality 29, 80 km from the hamlet of Clyde River, is a large deposit of pink marble (Beauregard et al., 2013). Other carving-stone materials include black and green serpentinized dolomitic marble (Fig. 12c).

The Ikatuyak deposit (locality 30) is located near Clearwater Fiord and Iqaluit. This is a modest-size deposit of coarse-grained, partly serpentinized peridotite (Fig. 12d).

The Koonark deposit (locality 31; Beauregard et al., 2013) is located 5 km southeast of the Mary River iron mine and is accessible by road from Pond Inlet. Carving stone is green and black soapstone, and consists of three undeveloped small deposits (Valley Side, Upper Koonark, and Scree Slope; Fig. 12e; Steenkamp et al., 2017) and one of large size (Koonark Mountain: 63 000 t), which collectively represent a total resource of 80 240 t (Steenkamp et al., 2017).

The modest-size Opingivik deposit (locality 32; Steenkamp et al., 2015) is located on the southwestern shore of Cumberland Sound, 112 km southwest of Pangnirtung. It lies midway between Ikpit Bay (to the north) and Robert Peel Inlet (to the south). The quarry-hosted talc-altered (steatite; Fig. 12f) ultramafic rock and serpentinite (Fig. 12g) occur within a fault-bounded ultramafic boudin enclosed in monzogranite. It has been suggested that this talus-impacted hillside quarry may one day be able to supply carving-stone material to other communities in the Baffin Island region.

Other noteworthy carving-stone localities include a resource site near Cape Dyer (locality 33) and a marble exposure located on the western side of Andrew Gordon Bay, 40 km east of Cape Dorset (locality 34; Beauregard et al., 2013).

Coal

Coal seams have been reported to occur in Cretaceous strata on Bylot Island and on adjacent parts of northern Baffin Island, the first accounts of which were those of McMillan (1910). Coal seams, up to 2 m thick, occur at the eastern end of the basin on Bylot Island and near the settlement of Pond Inlet, where some local use excavation work has occurred (locality 35). The presence of thin coal seams has also been noted in western and northern Bylot Island. Host strata, located in the lower part of Eclipse Trough, are assigned to the Albian Cenomanian Hassel Formation (Miall et al., 1980).

SUMMARY

Baffin Island has a proven track record of large-scale mining, both at present at the Mary River mine and formerly for zinc, lead, and silver at Nanisivik. Small-scale quarrying operations for carving stone have been important for nearby communities at many locations and new discoveries indicate that the activity will continue

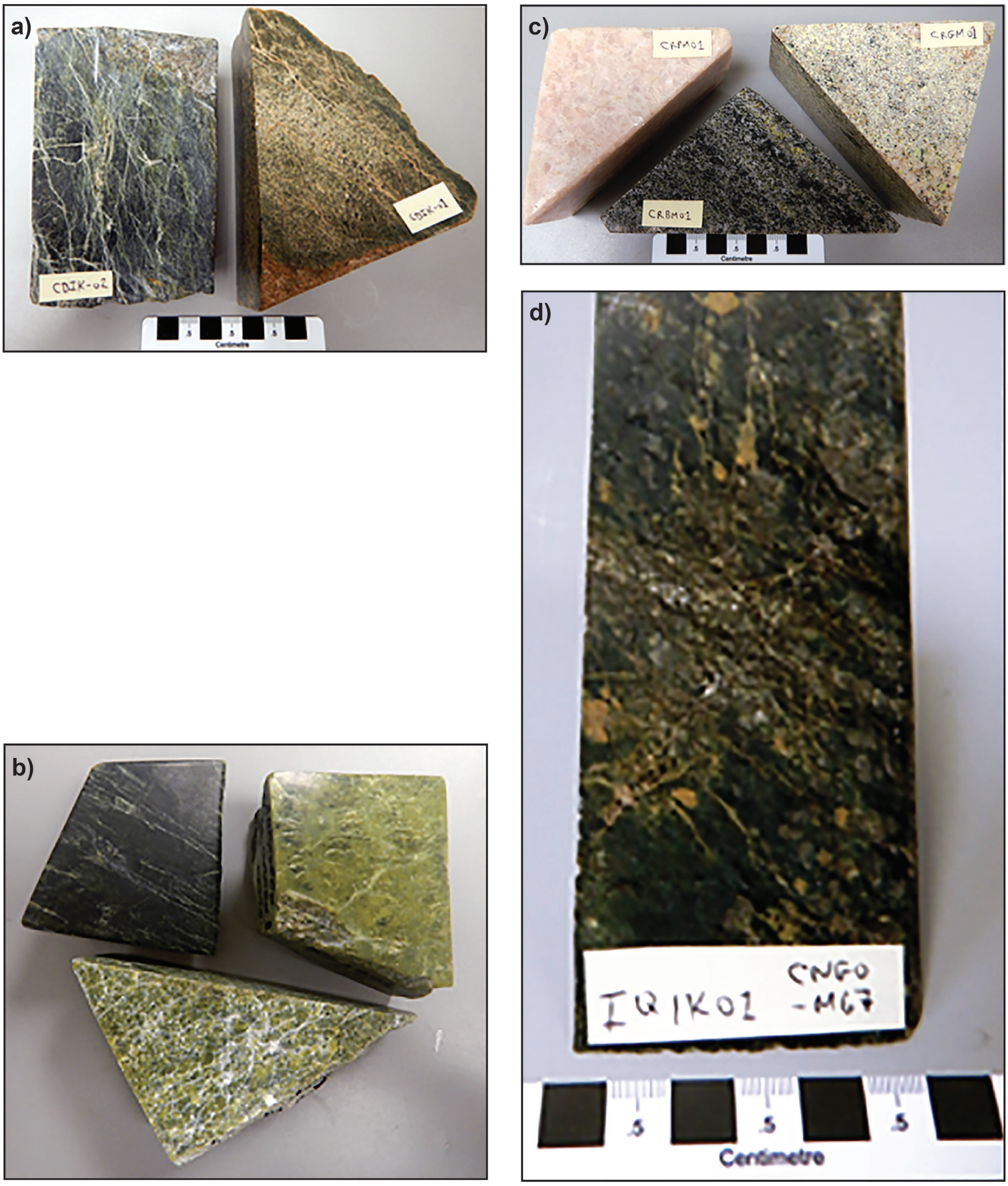

Figure 12. Photographs from carving-stone localities on Baffin Island, Nunavut. **a)** Polished carving stone, from the Kangiqsukutaaq quarry at Korok Inlet on southern Baffin Island, varies greatly in colour and texture throughout the deposit; these 2011 polished samples of excellent-quality serpentine+magnetite-altered marble were collected from the active upper pit (green stone on the left) and inactive lower pit (slightly weathered and iron-stained yellowish-green stone on the right), respectively. **b)** Hand-sized polished demonstration samples approximately 15 cm in length of Ujaraniarvik serpentinized marble from Aberdeen Bay, southern Baffin Island; shown at the top left is an excellent-quality, dark green soapstone; at the top right, an excellent-quality, vibrant green soapstone; and at the bottom is a good-quality, surface-altered, lime green soapstone. **c)** Clyde River community quarry, Clyde River drainage, north-central Baffin Island; polished hand samples of good-quality, coarsely crystalline pink marble (the quarry's traditional carving stone) on the left, excellent-quality serpentine-altered black marble at the bottom, and good-quality serpentine-altered green marble on the right. **d)** Ikatuyak quarry, Hall Peninsula, eastern Baffin Island; polished sample of excellent-quality, medium-hard, partially serpentinized peridotite from the Ikatuyak soapstone deposit.

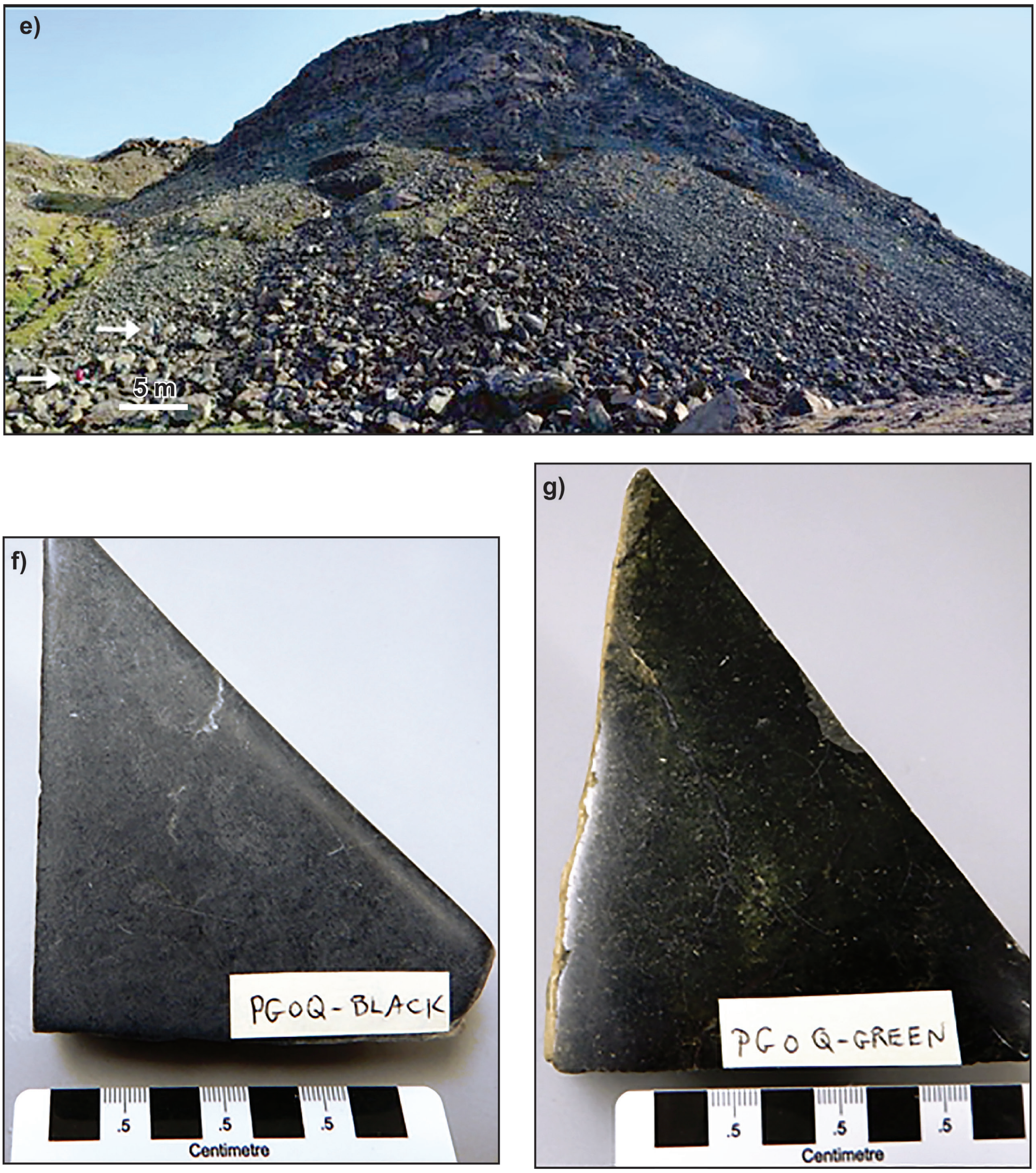

Figure 12. (cont.) e) Panorama of the large Koonark carving-stone deposit in the Mary River area, northwestern Baffin Island; good- to excellent-quality serpentinite of medium hardness is exposed on the hillside and talus slope; east-facing view taken in 2017. Photograph courtesy of the Canada-Nunavut Geoscience Office. **f)** and **g)** Opingivik quarry, at Cumberland Sound in eastern Baffin Island, polished hand samples of a soft, black, talcose-altered ultramafic rock (steatite) in (f) and a dark green, medium-hard serpentinite in (g); both demonstration samples are excellent-quality carving stone). All photographs, except (e), courtesy of the Government of Nunavut, Department of Economic Development and Transportation.

for years to come. The future of iron mining is promising as many high-grade deposits have been discovered and exploration for viable resources is still in its infancy. Also promising is the potential for commercial diamond in kimberlite, most notably at Chidliak on Hall Peninsula. Nickel-copper-PGE occurrences are common in mafic–ultramafic sills in the Lake Harbour group and may one day lead to the discovery of one or more commercial deposits, as was the case for the Raglan-area deposits of northern Quebec. Other commodities of lesser importance include uranium, thorium, tungsten, niobium, tantalum, gemstones, and coal.

ACKNOWLEDGMENTS

The authors would like to thank M. Beauregard for providing extensive literature on carving-stone properties of Baffin Island and for photographs of the principal carving-stone localities. They would also like to thank the following for providing locality photographs as illustrated in this paper: T. Iannelli from Baffinland Iron Mines Limited; the Department of Economic Development and Transportation of the Government of Nunavut; the Canada-Nunavut Geoscience Office; H. Sandeman; E. Turner; R. Sherlock; and A. Bigio. They are also indebted to A. Ford for preparing the map figures. The critical review comments provided by J. Smith, M. St-Onge, and M. Beauregard significantly improved the manuscript.

REFERENCES

Armstrong, R.C., Das Gupta, U., Downes, M.J., Grosl, V., and Lecouteur, P.C., 1976. Baffin Recce – 1976 assessment report; Aboriginal Affairs and Northern Development Canada, Assessment Report 061531. <http://nunavutgeoscience.ca/pages/en/numin.html> [accessed January 2020].

Beauregard, M.A., 2014. Highlights from a four-year evaluation of carving stone resources in Kitikmeot, Kivalliq and Qikiqtaaluk regions, Nunavut, Canada; presentation at the 2014 Nunavut Mining Symposium, Nunavut Department of Economic Development and Transportation, Iqaluit, April 9–10, 2014, 36 p. <https://www.nunavutminingsymposium.ca/2014-presentations> [accessed April 2014].

Beauregard, M.A. and Ell, J., 2015. Nunavut Carving Stone Deposit Evaluation Program: 2015 fieldwork at Rankin Inlet, Cumberland Sound and Arctic Bay, Nunavut; *in* Summary of Activities 2015, Canada-Nunavut Geoscience Office, p. 183–192.

Beauregard, M.A., Ell, J., Pikor, R.K., and Ham, L.J., 2013. Nunavut carving stone deposit evaluation program (2010-2013): third year results; *in* Summary of Activities 2012, Canada-Nunavut Geoscience Office, p. 151–162.

Belley, P.M. and Groat, L.A., 2019. Metacarbonate-hosted spinel on Baffin Island, Nunavut, Canada: insights into the origin of gem spinel and cobalt-blue spinel; Canadian Mineralogist, v. 57, p. 147–200. https://doi.org/10.3749/canmin.1800060

Belley, P.M., Dzikowski, T.J., Fagan, A., Cempírek, J., Groat, L.A., Mortenson, J.K., Giuliani, G., Fallick, A.E., and Gertzbein, P., 2017. Origin of scapolite-hosted sapphire (corundum) near Kimmirut, Baffin Island, Nunavut, Canada; Canadian Mineralogist, v. 55, p. 669–699. https://doi.org/10.3749/canmin.1700018

Bernier, J.E., 1911. Report on the Dominion Government expedition to the northern waters and Arctic Archipelago of the D.G.S. "Arctic" in 1910; Department of Marine and Fisheries, 157 p.

Bethune, K.M. and Scammell, R.J., 1997. Precambrian geology, Koch Island area (part of NTS 37C), District of Franklin, Northwest Territories; Geological Survey of Canada, Open File 3391, scale 1:50 000. https://doi.org/10.4095/208509

Bethune, K.M. and Scammell, R.J., 2003. Geology, geochronology, and geochemistry of Archean rocks in the Eqe Bay area, north-central Baffin Island, Canada: constraints on the depositional and tectonic history of the Mary River Group of northeastern Rae Province; Canadian Journal of Earth Sciences, v. 40, p. 1137–1167. https://doi.org/10.1139/e03-028

Blackadar, R.G. and Lemon, R.R.H., 1963. Admiralty Inlet area, Baffin Island, District of Franklin; Geological Survey of Canada, Memoir 328, 84 p. https://doi.org/10.4095/100662

Boyd, J.A., 1969. Report of geological and geophysical investigations of the Eqe Bay claims group, Eqe Bay, Baffin Island. Patino Mining Corp. Aboriginal Affairs and Northern Development Canada Assessment Report 019501. <http://nunavutgeoscience.ca/pages/en/numin.html> [accessed January 2020].

Bros, E.R. and Johnston, S.T., 2017. Field observations of the Mary River Group south of Tay Sound, northern Baffin Island, Nunavut: stratigraphy and structure of supracrustal sequences and surrounding plutonic units; *in* Summary of Activities 2017, Canada-Nunavut Geoscience Office, p. 69–80.

Campbell, H. and MacLeod, M., 2014. Mary River project: 2013 exploration program highlights and outline of 2014 program; presentation at the 2014 Nunavut Mining Symposium, Nunavut Department of Economic Development and Transportation, Iqaluit, April 9–10, 2014, 37 p. <https://www.nunavutminingsymposium.ca/2014-presentations> [accessed January 2017].

Chandler, F.W., 1988. Geology of the late Precambrian Fury and Hecla Group, northwest Baffin Island, District of Franklin; Geological Survey of Canada, Bulletin 370, 30 p. https://doi.org/10.4095/126938

Chandler, F.W., Charbonneau, B.W., Ciesielski, A., Maurice, Y.T., and White, S., 1980. Geological studies of the Late Precambrian supracrustal rocks and underlying granitic basement, Fury and Hecla Strait area, Baffin Island, District of Franklin (80-1AP125); *in* Current Research, Part A; Geological Survey of Canada, Paper 80-1A, p. 125–132. https://doi.org/10.4095/106192

Davidson, A., Jackson, G.D., and Morgan, W.C., 1979. Geology, Icebound Lake, District of Franklin; Geological Survey of Canada, Map 1451A, scale 1:250 000. https://doi.org/10.4095/109161

Davis, D.W., 2000. Report of representation work on behalf of Fred Tatarnic (Licence number N30953), Mineral claim: Freightrain – tag number F65593, Brodeur Peninsula, Baffin Island, Nunavut; Aboriginal Affairs and Northern Development Canada, Assessment Report 084331. <http://nunavutgeoscience.ca/pages/en/numin.html> [accessed January 2020].

Deer, W.A., Howie, R.A., and Zussman, J., 1966. An introduction to the rock-forming minerals; John Wiley and Sons, New York, New York, 528 p.

Dewing, K., Turner, E., and Harrison, J.C., 2007. Geological history, mineral occurrences, and mineral potential of the sedimentary rocks of the Canadian Arctic Archipelago; *in* Mineral deposits of Canada: a synthesis of major deposit-types, district metallogeny, the evolution of geological provinces, and exploration methods, (ed.) W.D. Goodfellow; Geological Association of Canada, Special Publication 5, p. 733–753.

Durocher, M., 1994. Report on Savanna Resources Limited Foxe project – 1993 exploration program; Aboriginal Affairs and Northern Development Canada, Assessment Report 083350. <http://nunavutgeoscience.ca/pages/en/numin.html> [accessed January 2020].

Durocher, M., 1995. Report on [Savanna Resources Limited] 1994 prospecting and lithogeochemical sampling program; Aboriginal Affairs and Northern Development Canada, Assessment Report 083477. <http://nunavutgeoscience.ca/pages/en/numin.html> [accessed January 2020].

Egglseder, M.S., Cruden, A.R., Dalstra, H.J., and Nicholas, L., 2017. The role of deformation in the formation of banded iron formation-hosted high-grade iron deposits, Hamersley Province (Australia); Precambrian Geology, v. 296, p. 62–77. https://doi.org/10.1016/j.precamres.2017.04.034

Elgin, R.A., 2017. Status and implications of reserves at carving stone quarries within the Qikiqtaaluk Region of Nunavut; *in* Summary of Activities 2017, Canada-Nunavut Geoscience Office, p. 151–158.

Farrow, D., Fitzgerald, C., and Pell, J., 2015. 2015 technical report for the Chidliak Project, Baffin Region, Nunavut; NI 43-101 Technical Report, Geostrat Consulting Services Inc., 2015-02-23, 176 p.

Fisher, D., 1981. Fury and Hecla uranium project; geological reconnaissance and prospecting report – 1979 exploration programme [Dejour Mines Ltd.]; Aboriginal Affairs and Northern Development Canada, Assessment Report 081302. <http://nunavutgeoscience.ca/pages/en/numin.html> [accessed January 2020].

Fisher, D. and Kwiecien, B.S., 1981. Report on 1980 exploration programme [Dejour Mines Ltd.]; Aboriginal Affairs and Northern Development Canada, Assessment Report 081218. <http://nunavutgeoscience.ca/pages/en/numin.html> [accessed January 2020].

Fleming, D.B. and Sexton, A., 2010. Assessment report on 2010 exploration program [Commander Resources Ltd.]; Aboriginal Affairs and Northern Development Canada, Assessment Report 085594. <http://nunavutgeoscience.ca/pages/en/numin.html> [accessed January 2020].

Garvey, R.T., 1978. Radiometric surveying and diamond drilling on the HEW, TED and RAY claims [Esso Minerals Canada]; Aboriginal Affairs and Northern Development Canada, Assessment Report 080938. <http://nunavutgeoscience.ca/pages/en/numin.html> [accessed January 2020].

Guimond, R., 1963. Exciting iron ore discovery on the Baffin Island; Precambrian, v. 36, no. 1, p. 6–8.

Heaman, L.M., Pell, J., Gruetter, H.S., and Creaser, R.A., 2015. U-Pb geochronology and Sr/Nd isotope compositions of groundmass perovskite from the newly discovered Jurassic Chidliak kimberlite field, Baffin Island, Canada; Earth and Planetary Science Letters, v. 415, p. 183–199. https://doi.org/10.1016/j.epsl.2014.12.056

Henderson, J.R., 1969. Mineral exploration on southern Baffin Island [Borealis Exploration Ltd.]; Aboriginal Affairs and Northern Development Canada, Assessment Report 019944. <http://nunavutgeoscience.ca/pages/en/numin.html> [accessed January 2020].

Hey, J., Duke, N., Moser, D., and Iannelli, T., 2015. A metallogenic study of high-grade iron ores on north Baffin Island in the "granulite facies" domain south of the Central Borden Fault Zone; *in* Conference Proceedings, SEG 2015: World-Class Ore Deposits: Discovery to Recovery, Society of Exploration Geophysicists, September 27–30, Hobart, Australia. <https://www.segweb.org/SEG/_Events/Conference_Archive/2015/Conference_Proceedings/files/pdf/Oral-Presentations/Abstracts/Hey.pdf>

Hogarth, D.D., 1971. Lapis lazuli near Lake Harbour, southern Baffin Island, Canada; Canadian Journal of Earth Sciences, v. 8, p. 1210–1217. https://doi.org/10.1139/e71-112

Hogarth, D.D. and Griffin, W.L., 1978. Lapis lazuli from Baffin Island – a Precambrian meta-evaporite; Lithos, v. 11, p. 37–60. https://doi.org/10.1016/0024-4937(78)90030-0

Iannelli, T., 2018. Baffinland Iron Mines–Exploration Review; presentation at the 2018 Nunavut Mining Symposium; Nunavut Department of Economic Development and Transportation, Iqaluit, April 10–11, 2018, 36 p. <https://www.nunavutminingsymposium.ca/2018> [accessed April 2018].

Iannelli, T., Robatian, M., Breckon, S., Campbell, H., Dao, P., and MacLeod, M., 2013a. Baffinland–Assessment Report: rock sampling, prospecting, geological mapping and geophysical surveying; unpublished report prepared for Indian and Northern Affairs Canada, Assessment Report 085816. <http://nunavutgeoscience.ca/pages/en/numin.html> [accessed January 2020].

Iannelli, T., Robatian, M., Breckon, S., Campbell, H., Dao, P., and MacLeod, M., 2013b. Baffinland–Assessment Report: rock sampling, prospecting, geological mapping, and geophysical surveying; unpublished report prepared for Indian and Northern Affairs Canada, Assessment Report 085823. <http://nunavutgeoscience.ca/pages/en/numin.html> [accessed January 2020].

Iannelli, T., Robatian, M., Breckon, S., and Iannelli, E., 2013c. Baffinland–Mary River Project Assessment Report: rock sampling, prospecting, geological mapping and geophysical surveying; unpublished report prepared for Indian and Northern Affairs Canada, Assessment Report 085842. <http://nunavutgeoscience.ca/pages/en/numin.html> [accessed January 2020].

Jackson, G.D., 1969. Reconnaissance of north-central Baffin Island (27C-G, 37C-H, 38A-C, parts of 48A); *in* Report of Activities, Part A; Geological Survey of Canada, Paper 69-1A, p. 171–176. https://doi.org/10.4095/119856

Jackson, G.D., 2000. Geology of the Clyde-Cockburn Land map area, north-central Baffin Island, Nunavut; Geological Survey of Canada, Memoir 440, 316 p. https://doi.org/10.4095/211268

Jackson, G.D. and Berman, R.G., 2000. Precambrian metamorphic and tectonic evolution of northern Baffin Island, Nunavut, Canada; Canadian Mineralogist, v. 38, p. 399–421. https://doi.org/10.2113/gscanmin.38.2.399

Jackson, G.D. and Morgan, W.C., 1978. Geology, Conn Lake, District of Franklin; Geological Survey of Canada, Map 1458A, scale 1:250 000. https://doi.org/10.4095/109162

Jackson, G.D., Morgan, W.C., and Davidson, A., 1978. Geology, Steensby Inlet, District of Franklin; Geological Survey of Canada, Map 1450A, scale 1:250 000. https://doi.org/10.4095/109160

Jackson, G.D., Hunt, P.A., Loveridge, W.D., and Parrish, R.R., 1990. Reconnaissance geochronology of Baffin Island, N.W.T.; *in* Radiogenic age and isotopic studies report 3; Geological Survey of Canada, Paper 89-2, p. 123–148. https://doi.org/10.4095/129079

Johns, S.M. and Young, M.D., 2006. Bedrock geology and economic potential of the Archean Mary River group, northern Baffin Island, Nunavut; Geological Survey of Canada, Current Research 2006-C5, 13 p. https://doi.org/10.4095/222954

Korzhinskii, D.S., 1947. Bimetasomatic phlogopite and lazurite occurrences from the Archean of the Baikal area; Trudy In-ta Geologicheskikh Nauk 29, Petrograf Series 10, 164 p. (in Russian).

Labow, L.F., 1957. Report on geological and mapping program, Foxe Peninsula, Baffin Island; Ultra Shawkey Mines Ltd. Aboriginal Affairs and Northern Development Canada Assessment Report 017004. <http://nunavutgeoscience.ca/pages/en/numin.html> [accessed January 2020].

Lang, A.H., Griffith, J.W., and Steacy, H.R., 1962. Canadian deposits of uranium and thorium; Geological Survey of Canada, Economic Geology Series 16, 342 p. https://doi.org/10.4095/102450

Larouche, C., 1997. Prospecting, mapping, sampling and geophysical test surveys [International Capri Resources Ltd]; Aboriginal Affairs and Northern Development Canada, Assessment Report 083972. <http://nunavutgeoscience.ca/pages/en/numin.html> [accessed January 2020].

LeCouteur, P.C., 1979. Geological survey on Plex claim group [Cominco Ltd]; Aboriginal Affairs and Northern Development Canada, Assessment Report 081247. <http://nunavutgeoscience.ca/pages/en/numin.html> [accessed January 2020].

Lepage, L., Fagan, A.J., Miller, E., and Weston, B., 2012. 2007–2009 assessment report describing geological mapping, UV surveying and geological sampling at the Beluga sapphire project, Baffin Island, Nunavut territory, Canada; Aboriginal Affairs and Northern Development Canada, Assessment Report 085511. <http://nunavutgeoscience.ca/pages/en/numin.html> [accessed January 2020].

Lichtblau, A., 1997. Baffin Island project – Report of work [International Capri Resources Ltd]; Aboriginal Affairs and Northern Development Canada, Assessment Report 083824. <http://nunavutgeoscience.ca/pages/en/numin.html> [accessed January 2020].

MacLeod, M., 2012. Metallogenic setting of high-grade iron ores, Mary River District, north Baffin Island, Nunavut; M.Sc. thesis, University of Western Ontario, London, Ontario, 285 p.

Maurice, Y.T. (ed.), 1982. Uranium in granites; Geological Survey of Canada, Paper 81-23, 173 p. https://doi.org/10.4095/111360

McDermott, G., 1992. Carving stone occurrences in the Northwest Territories; Economic Geology Series 1992-15, Department of Indian Affairs and Northern Development, 128 p.

McMillan, J.G., 1910. Geologist's report on the Arctic Expedition, 1908–1909; *in* Cruise of the Arctic, 1908–1909, (ed.) J.E. Bernier, 529 p.

McPherson, R.L., 1992. Geological, geochemical and prospecting in the central Baffin Island area [Comaplex Minerals Corp.]; Aboriginal Affairs and Northern Development Canada, Assessment Report 084078. <http://nunavutgeoscience.ca/pages/en/numin.html> [accessed January 2020].

Miall, A.D., Balkwill, H.R., and Hopkins, W.S., 1980. Cretaceous and tertiary sediments of Eclipse Trough, Bylot Island area, Arctic Canada, and their regional setting; Geological Survey of Canada, Paper 79-23, 20 p. https://doi.org/10.4095/102162

Moffatt, L., 1986. Dewar Lakes, mineral inventory year end report, 1985. [Petro-Canada Resources Ltd.]; Aboriginal Affairs and Northern Development Canada, Assessment Report 082051. <http://nunavutgeoscience.ca/pages/en/numin.html> [accessed January 2020].

Moffatt, L. and Donald, K.G., 1985. Geological/geochemical report [Petro-Canada Resources Ltd.]; Aboriginal Affairs and Northern Development Canada, Assessment Report 081834. <http://nunavutgeoscience.ca/pages/en/numin.html> [accessed January 2020].

Nielson, S. and Pell, J., 2009. Satellite photo terrain mapping, heavy mineral sampling, and till geochemistry in the Kimmirut area. [Peregrine Diamonds Ltd.]; Aboriginal Affairs and Northern Development Canada, Assessment Report 085421. <http://nunavutgeoscience.ca/pages/en/numin.html> [accessed January 2020].

Patzke, M., Greenman, J.W., Ielpi, A., and Halverson, G.P., 2018. Sedimentology of the sandstone-dominated units in the Fury and Hecla Basin, northern Baffin Island, Nunavut; *in* Summary of Activities 2018, Canada-Nunavut Geoscience Office, p. 75–84.

Prest, S.E., 1977. Geological and geochemical investigations of prospecting permits 385 and 386 [Noranda Exploration Company Ltd.]; Aboriginal Affairs and Northern Development Canada, Assessment Report 061534. <http://nunavutgeoscience.ca/pages/en/numin.html> [accessed January 2020].

Rayner, N.M., 2014. New U-Pb geochronological results from Hall Peninsula, Baffin Island, Nunavut; *in* Summary of Activities 2013, Canada-Nunavut Geoscience Office, p. 39–52.

Rayner, N.M., 2015. New (2013–2014) U-Pb geochronological results from northern Hall Peninsula, southern Baffin Island, Nunavut; *in* Summary of Activities 2014, Canada-Nunavut Geoscience Office, p. 31–44.

Rogers, A.F., 1938. Lapis lazuli from San Bernardino County, California; American Mineralogist, v. 23, p. 111–114.

Saumur, B.M., Skipton, D.R., St-Onge, M.R., Bros, E.R., Acosta-Gongora, P., Kelly, C.J., Morin, A., O'Brien, M.E., Johnston, S.T., and Weller, O.M., 2018. Precambrian geology of the surroundings of Steensby Inlet and western Barnes Ice Cap (parts of NTS 37E, 37F, 37G), Baffin Island, Nunavut; *in* Summary of Activities 2018, Canada-Nunavut Geoscience Office, p. 29–45.

Saumur, B.M., Skipton, D.R., St-Onge, M.R., Jackson, G.D., Wodicka, N., Bros, E.R., Weller, O.M., and Johnston, S.T., 2020a. Bedrock geology, Angijurjuk-Mary River, Baffin Island, Nunavut, NTS 37-G west; Geological Survey of Canada, Canadian Geoscience Map 403, scale 1:100 000. https://doi.org/10.4095/321794

Saumur, B.M., Skipton, D.R., Zhang, S., St-Onge, M.R., Bros, E.R., Acosta-Gongora, P., Kelly, C.J., O'Brien, M.E., Weller, O.M., and Johnston, S.T., 2020b. Bedrock geology, Nina Bang Lake, Nunavut, NTS 37F west and parts of NTS 37C; Geological Survey of Canada, Canadian Geoscience Map 404, scale 1:100 000. https://doi.org/10.4095/314876

Scott, D.J., 1999. U-Pb geochronology of the eastern Hall Peninsula, southern Baffin Island, Canada: a northern link between the Archean of West Greenland and the Paleoproterozoic Torngat Orogen of northern Labrador; Precambrian Research, v. 93, p. 5–26. https://doi.org/10.1016/S0301-9268(98)00095-3

Scott, D.J., Stern, R.A., St-Onge, M.R., and McMullen, S.M., 2002. U-Pb geochronology of detrital zircons in metasedimentary rocks from southern Baffin Island; implications for the Paleoproterozoic tectonic evolution of northeastern Laurentia; Canadian Journal of Earth Sciences, v. 39, p. 611–623. https://doi.org/10.1139/e01-093

Sexton, A., 2008. Assessment report on 2008 exploration program [Commander Resources Ltd.]; Aboriginal Affairs and Northern Development Canada, Assessment Report 085400. <http://nunavutgeoscience.ca/pages/en/numin.html> [accessed January 2020].

Siegel, H.O., 1956. Small geophysical report, [Maltby Lake Iron deposit], Foxe Basin, Baffin Island. Oceanic Iron Ore Company of Canada; Aboriginal Affairs and Northern Development Canada, Assessment Report 017003. <http://nunavutgeoscience.ca/pages/en/numin.html> [accessed January 2020].

Skipton, D.R., St-Onge, M.R., Schneider, D.A., and McFarlane, C.R.M., 2016a. Tectonothermal evolution of the middle crust in the Trans-Hudson Orogen, Baffin Island, Canada: evidence from petrology and monazite geochronology of sillimanite-bearing migmatites; Journal of Petrology, v. 57, no. 8, p. 1437–1462. https://doi.org/10.1093/petrology/egw046

Skipton, D.R., Schneider, D.A., McFarlane, C.R.M., St-Onge, M.R., and Jackson, S.E., 2016b. Multi-stage zircon and monazite growth revealed by depth profiling and in situ U-Pb geochronology: resolving the Paleoproterozoic tectonics of the Trans-Hudson Orogen on southeastern Baffin Island, Canada; Precambrian Research, v. 285, p. 272–298. https://doi.org/10.1016/j.precamres.2016.09.002

Skipton, D.R., Saumur, B.M., St-Onge, M.R., Wodicka, N., Bros, E.R., Morin, A., Brouillette, P., Weller, O.M., and Johnston, S.T., 2017. Precambrian bedrock geology of the Pond Inlet–Mary River area, northern Baffin Island, Nunavut; *in* Summary of Activities 2017, Canada-Nunavut Geoscience Office, p. 49–68.

Skipton, D.R., Saumur, B.M., St-Onge, M.R., Wodicka, N., Bros, E.R.,Currie, L.D., Haggart, J.W., and Weller, O.M., 2018. Bedrock geology, Pond Inlet, Nunavut, part of NTS 38-B; Geological Survey of Canada, Canadian Geoscience Map 347, scale 1:100 000. https://doi.org/10.4095/306578

Skipton, D.R., Saumur, B.M., St-Onge, M.R., Bros, E.R., Acosta-Gongora, P., Kelly, C.J., O'Brien, M.E., Weller, O.M., and Johnston, S.T., 2020a. Bedrock geology, Barnes Ice Cap northwest, Baffin Island, Nunavut, NTS 37-E west; Geological Survey of Canada, Canadian Geoscience Map 402, scale 1:100 000. https://doi.org/10.4095/314657

Skipton, D.R., Saumur, B.M., St-Onge, M.R., Bros, E.R., Acosta-Gongora, P., Kelly, C.J., O'Brien, M.E., Johnston, S.T., and Weller, O.M., 2020b. Bedrock Geology, Rowley River–Isortoq River, Baffin Island, Nunavut, NTS 37-F east; Geological Survey of Canada, Canadian Geoscience Map 406, scale 1:100 000. https://doi.org/10.4095/315401

Steenkamp, H.M., Pizzo-Lyall, M., Wallace, C.J., Beauregard, M.A., and Dyck, B.J., 2014. Geology, history and site-management planning of the Kangiqsukutaaq carving stone quarry, southern Baffin Island; *in* Summary of Activities 2013, Canada-Nunavut Geoscience Office, p. 193–200.

Steenkamp, H.M., Beauregard, M.A., and Mate, D.J., 2015. Carving stone and mineral resource potential of the Opingivik deposit, southern Baffin Island; *in* Summary of Activities 2014, Canada-Nunavut Geoscience Office, p. 153–162.

Steenkamp, H.M., Elgin, R.A., and Therriault, I., 2017. Geological mapping and resource evaluation of the Koonark carving stone deposit, northern Baffin Island, Nunavut; *in* Summary of Activities 2017, Canada-Nunavut Geoscience Office, p. 139–150.

Steenkamp, H.M., Bovingdon, P.J., Dufour, F., Généreux, C.-A., Greenman, J.W., Halverson, G.P., Ielpi, A., Patzke, M., and Tinkham, D.K., 2018. New regional mapping of Precambrian rocks north of Fury and Hecla Strait, northwestern Baffin Island, Nunavut; *in* Summary of Activities 2018, Canada-Nunavut Geoscience Office, p. 47–62.

St-Onge, M.R., Scott, D.J., Corrigan, D., and Wodicka, N., 2005a. Geology, Ikpik Bay, Baffin Island, Nunavut; Geological Survey of Canada, Map 2077A, scale 1:100 000. https://doi.org/10.4095/221054

St-Onge, M.R., Scott, D.J., Corrigan, D., and Wodicka, N., 2005b. Geology, Flyway Lake, Baffin Island, Nunavut; Geological Survey of Canada, Map 2078A, scale 1:100 000. https://doi.org/10.4095/221091

St-Onge, M.R., Scott, D.J., Corrigan, D., and Wodicka, N., 2005c. Geology, Clyde River, Baffin Island, Nunavut; Geological Survey of Canada, Map 2079A, scale 1:100 000. https://doi.org/10.4095/221092

St-Onge, M.R., Scott, D.J., Corrigan, D., and Wodicka, N., 2005d. Geology, Clyde River, Baffin Island, Nunavut; Geological Survey of Canada, Map 2080A, scale 1:100 000. https://doi.org/10.4095/221093

St-Onge, M.R., Scott, D.J., Corrigan, D., and Wodicka, N., 2005e Geology, Straits Bay, Baffin Island, Nunavut; Geological Survey of Canada, Map 2081A, scale 1:100 000. https://doi.org/10.4095/221094

St-Onge, M.R., Scott, D.J., Corrigan, D., and Wodicka, N., 2005f. Geology, Dewar Lakes, Baffin Island, Nunavut; Geological Survey of Canada, Map 2082A, scale 1:100 000. https://doi.org/10.4095/221095

St-Onge, M.R., Wodicka, N., and Ijewliw, O., 2007. Polymetamorphic evolution of the Trans-Hudson Orogen, Baffin Island, Canada; integration of petrological, structural and geochronological data; Journal of Petrology, v. 48, no. 2, p. 271–302. https://doi.org/10.1093/petrology/egl060

St-Onge, M.R., van Gool, J.A.M., Garde, A.A., and Scott, D.J., 2009. Correlation of Archaean and Palaeoproterozoic units between northeastern Canada and western Greenland: constraining the pre-collisional upper plate accretionary history of the Trans-Hudson Orogen; Geological Society of London, Special Publications, v. 318, p. 193–235. <https://doi.org/10.1144/SP318.7>

Sutherland, R., 1999. Diamond drilling report for the BB1 and BB2 claims, Nanisivik mine area, Nunavut; Aboriginal Affairs and Northern Development Canada, Assessment Report 084196. <http://nunavutgeoscience.ca/pages/en/numin.html> [accessed January 2020].

Sutherland, R.A. and Dumka, D., 1995. Geology of Nanisivik mine, N.W.T., Canada; *in* Carbonate-hosted lead-zinc-fluorite-barite deposits of North America, (ed.) K.C. Misra; Society of Economic Geologists, Guidebook Series 22, p. 4–12.

Thorpe, L. and Thalenhorst, H., 1981. Report on exploration results, 1979 and 1980, on the Nanisivik mine property [Nanisivik Mines Ltd]; Aboriginal Affairs and Northern Development Canada, Assessment Report 082447. <http://nunavutgeoscience.ca/pages/en/numin.html> [accessed January 2020].

Turner, E.C., 2009. Mesoproterozoic carbonate systems in the Borden Basin, Nunavut; Canadian Journal of Earth Sciences, v. 46, p. 915–938. <https://doi.org/10.1139/E09-062>

Turner, E.C., 2011. Structural and stratigraphic controls on carbonate-hosted base metal mineralization in the Mesoproterozoic Borden Basin (Nanisivik District), Nunavut; Economic Geology, v. 106, p. 1197–1223. <https://doi.org/10.2113/econgeo.106.7.1197>

Vande Guchte, M.J., 1998. Geological, geochemical and geophysical report on the Incognito joint venture project [Rubicon Minerals Corp.]; Aboriginal Affairs and Northern Development Canada, Assessment Report 084053. <http://nunavutgeoscience.ca/pages/en/numin.html> [accessed January 2020].

Vande Guchte, M.J. and Gray, M.J., 1999. Geological, geochemical and diamond drilling report on the Incognito joint venture project, 1997 exploration program [Rubicon Minerals Corp.]; Aboriginal Affairs and Northern Development Canada, Assessment Report 084168. <http://nunavutgeoscience.ca/pages/en/numin.html> [accessed January 2020].

Whalen, J.B., Wodicka, N., Taylor, B.E., and Jackson, G.D., 2010. Cumberland Batholith, Trans-Hudson Orogen, Canada: petrogenesis and implications for Paleoproterozoic crustal and orogenic processes; Lithos, v. 117, p. 99–118. <https://doi.org/10.1016/j.lithos.2010.02.008>

Wodicka, N., St-Onge, M.R., Corrigan, D., Scott, D.J., and Whalen, J.B., 2014. Did a proto-ocean basin form along the southeastern Rae cratonic margin? Evidence from U-Pb geochronology, geochemistry (Sm-Nd and whole-rock), and stratigraphy of the Paleoproterozoic Piling Group, northern Canada; Geological Society of America, Bulletin, v. 126, no. 11–12, p. 1625–1653. <https://doi.org/10.1130/B31028.1>

Wunder, M., 1994. Summary report on the Adams Sound project [Noranda Exploration Company Ltd.]; Aboriginal Affairs and Northern Development Canada, Assessment Report 083230. <http://nunavutgeoscience.ca/pages/en/numin.html> [accessed January 2020].

Young, M.D., Sandeman, H., Berniolles, F., and Gertzbein, P.M., 2004. A preliminary stratigraphic and structural geology framework for the Archean Mary River Group, northern Baffin Island, Nunavut; Geological Survey of Canada, Current Research 2004-C1, 14 p. <https://doi.org/10.4095/215376>

Young, M.D., McNicoll, V., Sandeman, H., Creaser, R., and James, D., 2007. Meso- to Neoarchean crustal growth and recycling on northern Baffin Island and correlation of Rae Province rocks across mainland Nunavut and Greenland; Geological Association of Canada–Mineralogical Association of Canada Annual Meeting, Yellowknife, May 23–25, 2007, Abstract Volume 32, p. 89.

Zhang, S. and Pell, J., 2013. Conodonts from carbonate xenoliths in Chidliak kimberlites confirm the previous existence of lower Paleozoic cover on Hall Peninsula, Nunavut and provide temperature estimates; *in* Summary of Activities 2012, Canada-Nunavut Geoscience Office, p. 107–112.

Contents

Hydrocarbon resource potential in the Labrador–Baffin Seaway and onshore West Greenland

N. Bingham-Koslowski[1], T. McCartney[2], and J. Bojesen-Koefoed[3]; with contributions by C. Jauer[2]

Bingham-Koslowski, N., McCartney, T., and Bojesen-Koefoed, J., 2022. Hydrocarbon resource potential in the Labrador–Baffin Seaway and onshore West Greenland; in *Geological synthesis of Baffin Island (Nunavut) and the Labrador–Baffin Seaway, (ed.) L.T. Dafoe and N. Bingham-Koslowski; Geological Survey of Canada, Bulletin 608, p. 409–432. https://doi.org/10.4095/321859*

Abstract: Exploration for hydrocarbons began in the Labrador–Baffin Seaway in the 1960s; activity along the Labrador margin is still ongoing. A moratorium on exploration activities in the Canadian Arctic was enacted in 2016, halting drilling and data acquisition in western Davis Strait and along the Baffin Island margin. The exploration for hydrocarbons along the West Greenland margin ceased in 2021. Despite the presence of all hydrocarbon system elements as well as direct indicators of at least one working hydrocarbon system (e.g. slicks and/or seeps, oil and/or gas shows), no commercially viable accumulations of hydrocarbons have been discovered in the region. Potential sea-surface hydrocarbon slicks have been identified throughout the study region using synthetic aperture radar, but only the slick offshore Scott Inlet (Nunavut) has been directly linked to seafloor hydrocarbon seepage.

Résumé : La recherche de gisements d'hydrocarbures dans le bras de mer Labrador–Baffin a commencé dans les années 1960, et encore à ce jour, des activités d'exploration ont lieu le long de la marge du Labrador. Un moratoire sur les activités d'exploration dans l'Arctique canadien est entré en vigueur en 2016, celui-ci interdisant toute activité de forage et d'acquisition de données dans la partie ouest du détroit de Davis et le long de la marge de l'île de Baffin. La recherche d'hydrocarbures le long de la marge de l'ouest du Groenland a cessé en 2021. Malgré la présence de tous les éléments caractéristiques d'un système pétrolier et d'indicateurs directs témoignant de la présence d'au moins un système pétrolier actif (p. ex., nappes ou suintements d'hydrocarbures, indices de pétrole ou de gaz), aucune accumulation commercialement viable d'hydrocarbures n'a été découverte dans la région. De possibles nappes d'hydrocarbures à la surface de la mer ont été repérées dans toute la région étudiée à l'aide d'un radar à synthèse d'ouverture, mais seule une nappe au large du bras Scott (Nunavut) a été directement liée à un suintement d'hydrocarbures sur le fond marin.

[1]Geological Survey of Canada, 601 Booth Street, Ottawa, Ontario K1A 0E8
[2]Geological Survey of Canada, 1 Challenger Drive, P.O. Box 1006, Dartmouth, Nova Scotia B2Y 4A2
[3]Geological Survey of Denmark and Greenland, Øster Voldgade 10, 1350 Copenhagen, Denmark
*Corresponding author: N. Bingham-Koslowski (email: nikole.bingham-koslowski@nrcan-rncan.gc.ca)

INTRODUCTION

The Labrador–Baffin Seaway is a tectonically complex region involving rifting, transpression, transtension, seafloor spreading, inversion, and plate rotation (Schenk, 2011; *see* Keen et al., this volume). The rifted margins in the Labrador Sea and Baffin Bay are separated by the transform margin associated with the Ungava Fault Zone (Wilson et al., 2006; *see* Fig. 14, Keen et al., this volume). The breadth of structural configurations and stratigraphic settings of the Mesozoic and Cenozoic basins in the Labrador–Baffin Seaway (as discussed by Dafoe, Williams et al., this volume and Keen et al., this volume) reflect the complex development typical of rifted continental margins (Nemčok et al., 2016). Analogous margins around the world where hydrocarbon exploration is commercially viable suggest that the Labrador–Baffin Seaway has potential as a hydrocarbon province. For example, the Campos and the Espirito Santo basins, offshore Brazil, are part of a major hydrocarbon province on a passive margin that may be analogous to the Labrador margin (Charpentier et al., 2008) and offshore Indonesia may be an analogue for the Baffin Bay Basin (Schenk, 2017). Transform margins (e.g. the Davis Strait and the Davie Fracture Zone, offshore east Africa) are increasingly becoming the focus of hydrocarbon exploration (Nemčok et al., 2016).

The hydrocarbon (oil and gas) potential of the Labrador–Baffin Seaway has been recognized since the 1960s. Hydrocarbons have been discovered in exploration wells on the Labrador margin, in western Davis Strait, and along the West Greenland margin (Table 1); however, not in economically viable quantities. The presence of a confirmed hydrocarbon seafloor seep along the Baffin Island margin offshore Scott Inlet, along with numerous potential oil slicks identified via satellite imagery across the region, implies the existence of an active, albeit elusive, hydrocarbon system in the area. Other notable Arctic regions of hydrocarbon significance include the Sverdrup Basin to the west (Bent Horn oil field) and the West Greenland margin to the east (Embry, 2011; Harrison et al., 2011).

Resource assessments by the Government of Canada have been conducted in Lancaster Sound (Smith et al., 1989; Brent et al., 2013; Atkinson et al., 2017), eastern Hudson Bay and James Bay (Hanna et al., 2019), western Hudson Bay, Foxe Channel, and Repulse Bay (Hanna et al., 2018), Peel Sound, Bellot Strait, Gulf of Boothia, Fury and Hecla Strait, and Foxe Basin (Fustic et al., 2018), as well as on the Labrador margin (Carey et al., 2020), but are absent in Baffin Bay and western Davis Strait. This lack leaves a substantial gap in coverage and, subsequently, a gap in the current understanding of the presence and possible extent of hydrocarbons along Canada's eastern margin. The acquisition of geophysical (seismic, gravity, and magnetic) data from western Davis Strait and the Baffin Island margin from 2000 to 2016 could support a meaningful resource assessment for these regions, filling the void between Lancaster Sound and the Labrador margin. The hydrocarbon potential of western Davis Strait and Baffin Bay is discussed here; however, no attempts are made to provide new resource assessments as this work is beyond the scope of this volume.

This paper summarizes the current understanding of the known and potential hydrocarbon resources offshore in the Labrador–Baffin Seaway and onshore west Greenland (Fig. 1). It divides the Labrador–Baffin Seaway into five regions for a detailed discussion of the hydrocarbon potential: the Labrador margin (between latitudes 53°N and 61°N); western Davis Strait and the southeast Baffin Shelf (between latitudes 61°N and 67°N); the northeast Baffin Shelf and western Baffin Bay (between latitudes 67°N and 77°N); the onshore West Greenland margin; and the offshore West Greenland margin. An overview of hydrocarbon slicks and seeps from the Canadian margin is provided in a separate section. This paper presents information directly related to hydrocarbon potential in the Labrador–Baffin Seaway and onshore West Greenland. For stratigraphic and tectonic context, readers are referred to other papers in this volume including Bingham-Koslowski, Zhang, and McCartney (Paleozoic); Dafoe, Dickie, Williams, and McCartney (Mesozoic–Cenozoic stratigraphy of the Labrador margin); Dafoe, DesRoches, and Williams (Mesozoic–Cenozoic stratigraphy of western Davis Strait); Dafoe, Dickie, and Williams (Mesozoic–Cenozoic stratigraphy of the Baffin Island margin); Gregersen et al. (Mesozoic–Cenozoic stratigraphy of the West Greenland margin); Dafoe, Williams et al. (stratigraphic summary of the Labrador–Baffin Seaway); and Keen et al. (rifting and evolution of the Labrador–Baffin Seaway).

EXPLORATION HISTORY

Labrador margin

A detailed exploration history of the Labrador Shelf up to 1990, is found in Bell and Campbell (1990) and summarized here. Exploration on the Labrador Shelf began in the late 1960s with aeromagnetic and seismic reflection surveys conducted by Tenneco. More than 75 000 km of 2-D seismic reflection data were collected on the Labrador margin between 1968 and 1984 (Fig. 2). Tenneco et al. Leif E-38 was the first well drilled on the margin in 1971 (Table 2; Fig. 2). Over the next eleven years, 23 exploration wells and two delineation wells followed (Table 2; Fig. 2). The exploration programs resulted in five gas

Table 1. Conventional hydrocarbon occurrences in the Canadian waters of the Labrador–Baffin Seaway.

Well name	Spud year	Hydrocarbons	Gas estimate (trillion cubic feet)[1]	Natural gas liquid estimate (million barrels)[1]	Reservoir formation[2]	Net pay[2] (m)	Average porosity[2] (%)	Average max test rate[2] ($10^3 m^3/d$)
Eastcan et al. Bjarni H-81	1973	Significant discovery–gas	0.863	31	Bjarni	86	20	567
Eastcan et al. Gudrid H-55	1974	Significant discovery–gas	0.924	6	Paleozoic	64	10	567
Eastcan et al. Snorri J-90	1975	Significant discovery–gas	0.105	2	Cartwright	24	18	278
					(Gudrid sand)			
Chevron et al. Hopedale E-33	1978	Significant discovery–gas	0.105	2	Paleozoic	12	8	553
					Bjarni	11	11	402
Total Eastcan et al. Bjarni O-82	1979	Gas–part of Bjarni H-81 discovery acreage	n.a.	n.a.	n.a.	n.a.	n.a.	n.a.
Petro Canada et al. North Leif I-05	1980	Oil show	n.a.	n.a.	n.a.	n.a.	n.a.	n.a.
Petro Canada et al. North Bjarni F-06	1980	Significant discovery–gas	2.247	82	Bjarni	194	19	n.a.
Well name	**Spud year**	**Hydrocarbons**	**Gas estimate (trillion cubic feet)[3]**	**Natural gas liquid estimate (million barrels)[1]**	**Reservoir formation**	**Net pay[3] (m)**	**Porosity[3]**	**Permeability[3] (mD)**
Aquitaine et al. Hekja O-71	1979	Discovery–wet gas	2.3	n.a.	"Gudrid"	44	16	10

[1](Canada-Newfoundland and Labrador Offshore Petroleum Board, 2019g)
[2](Canada-Newfoundland and Labrador Offshore Petroleum Board, 2003)
[3](Klose et al., 1982)

Figure 1. Map of the Labrador–Baffin Seaway. Additional details, including well names, can be found in Figures 3, 6, 7, and 8. Additional projection information for all maps in this paper include: Central Meridian = 60°W; Standard Parallels = 65, 75°W; Latitude of Origin = 65°N.

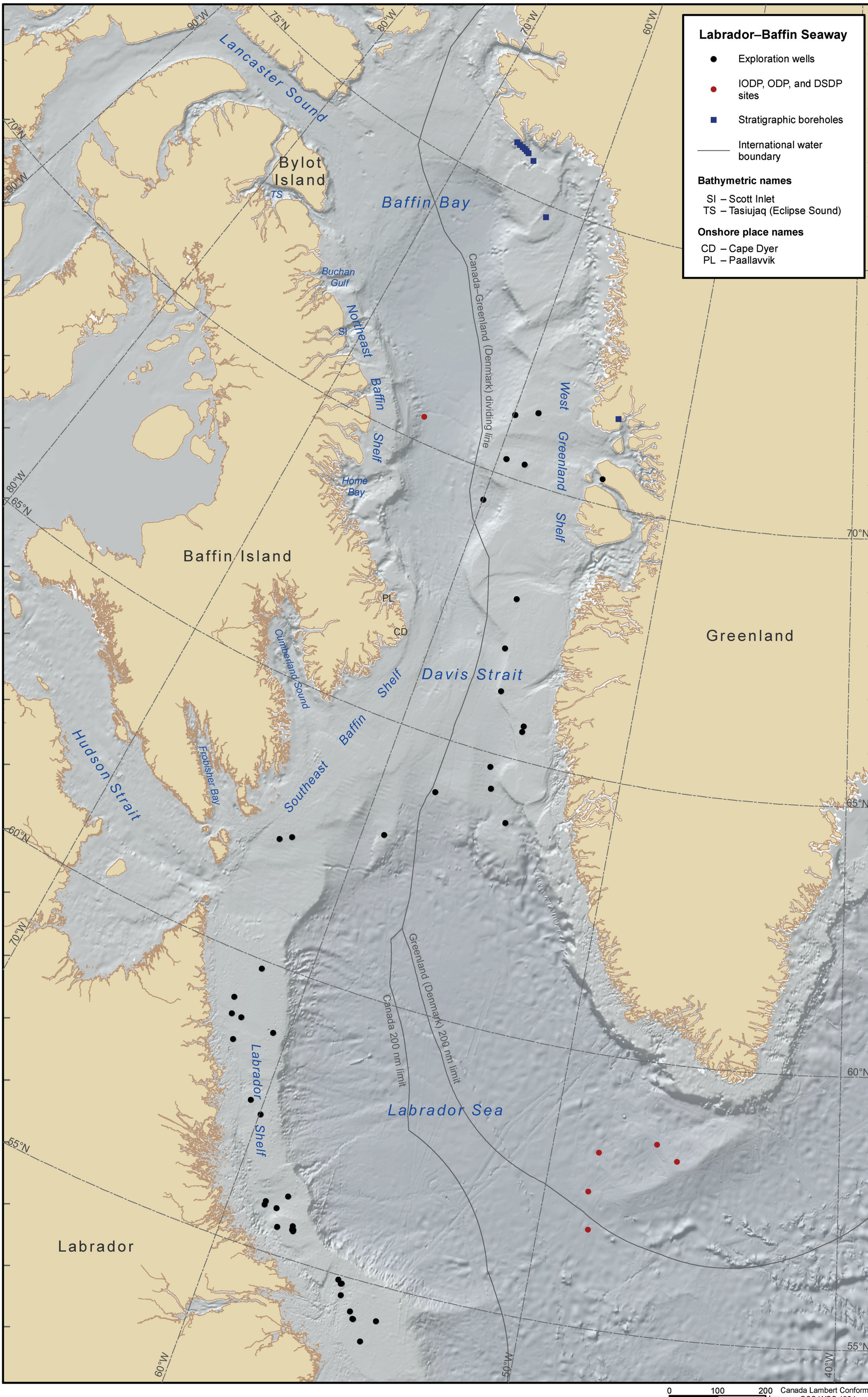
Labrador–Baffin Seaway
Exploration wells
IODP, ODP, and DSDP sites
Stratigraphic boreholes
International water boundary
Bathymetric names
SI – Scott Inlet
TS – Tasiujaq (Eclipse Sound)
Onshore place names
CD – Cape Dyer
PL – Paallavvik
Lancaster Sound
Bylot Island
TS
Baffin Bay
Buchan Gulf
SI
Northeast Baffin Shelf
Home Bay
Canada–Greenland (Denmark) dividing line
West Greenland Shelf
Baffin Island
PL
CD
Cumberland Sound
Davis Strait
Southeast Baffin Shelf
Hudson Strait
Frobisher Bay
Greenland
Labrador Shelf
Canada 200 nm limit
Greenland (Denmark) 200 nm limit
Labrador Sea
Labrador
90°W
80°W
75°N
70°W
60°W
50°W
40°W
70°N
65°N
60°N
55°N
0
100
200
km
1:7 500 000
Canada Lambert Conformal
GCS WGS 1984

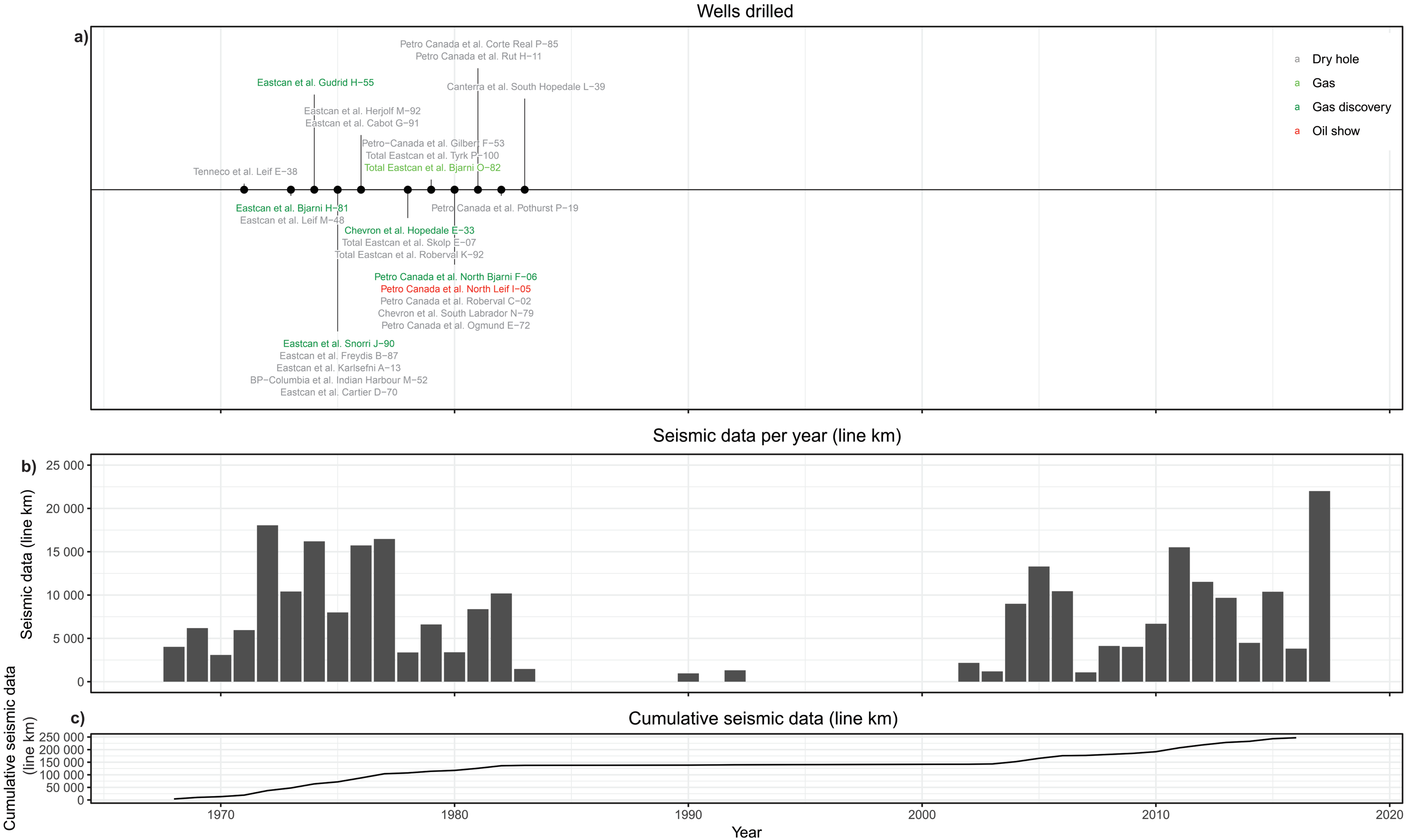

Figure 2. Exploration history of the Labrador margin (latitude 53°N–61°N). Data are sourced from well and seismic reports on file at the Canada-Newfoundland and Labrador Offshore Petroleum Board. **a)** Exploration wells drilled on the Labrador margin; **b)** line kilometres of seismic data collected per year on the Labrador margin (line kilometres for 2017 includes Orphan Basin, outside of study area); and **c)** cumulative line kilometres of sismic collected on the Labrador margin.

Table 2. Summary of exploration wells on the Labrador and southeast Baffin shelves.

Well name	UWI	Spud date (year-month-day)	Well class	Water depth (m)	TD (m)	Status	Gas	Oil
53˚N–61˚N[1]								
Tenneco et al. Leif E-38	300 E38 54200 55000	1971-08-13	Exploratory	167.6	1084.2	Abandoned	Unrated	Unrated
Eastcan et al. Leif M-48	300 M48 54200 55000	1973-08-01	Exploratory	165.2	1879.1	Abandoned	Unrated	Unrated
Eastcan et al. Bjarni H-81	300 H81 55400 57300	1973-08-29	Exploratory	140.2	2514.6	Abandoned	Significant discovery	Unrated
Eastcan et al. Gudrid H-55	300 H55 55000 55450	1974-07-14	Exploratory	299.3	2838.0	Abandoned	Significant discovery	Unrated
Eastcan et al. Freydis B-87	300 B87 54000 54300	1975-07-02	Exploratory	178.6	2314.1	Abandoned	Unrated	Unrated
Eastcan et al. Snorri J-90	300 J90 57200 59450	1975-07-28	Exploratory	140.8	3209.9	Abandoned	Significant discovery	Unrated
Eastcan et al. Karlsefni A-13	300 A13 59000 61450	1975-08-10	Exploratory	174.7	3284.0	Abandoned	Unrated	Unrated
BP-Columbia et al. Indian Harbour M-52	300 M52 54300 54150	1975-08-21	Exploratory	197.8	2361.1	Abandoned	Unrated	Unrated
Eastcan et al. Cartier D-70	300 D70 54400 55330	1975-09-27	Exploratory	310.0	1927.0	Abandoned	Unrated	Unrated
Eastcan et al. Cabot G-91	300 G91 60000 61300	1976-07-31	Exploratory	179.8	0289.9	Abandoned	Unrated	Unrated
Eastcan et al. Herjolf M-92	300 M92 55400 57300	1976-08-31	Delineation	139.0	4086.2	Abandoned	Unrated	Unrated
Total Eastcan et al. Skolp E-07	300 E07 58300 61450	1978-07-22	Exploratory	166.5	2992.0	Abandoned	Unrated	Unrated
Chevron et al. Hopedale E-33	300 E33 56000 58450	1978-08-09	Exploratory	549.8	2069.4	Abandoned	Significant discovery	Unrated
Total Eastcan et al. Roberval K-92	300 K92 55000 55300	1978-10-02	Exploratory	268.5	3874.0	Abandoned	Unrated	Unrated
Total Eastcan et al. Tyrk P-100	300 P00 55300 58000	1979-07-19	Exploratory	117.0	1739.0	Abandoned	Unrated	Unrated
Total Eastcan et al. Bjarni O-82	300 O82 55400 57300	1979-07-30	Delineation	142.6	2650.0	Abandoned	Show	Unrated
Petro Canada et al. Gilbert F-53	300 F53 59000 62000	1979-09-10	Exploratory	183.0	1728.0	Abandoned	Unrated	Unrated
Petro Canada et al. Roberval C-02	300 C02 55000 55450	1980-07-07	Exploratory	276.0	2823.0	Abandoned	Unrated	Unrated
Chevron et al. South Labrador N-79	300 L39 55500 58450	1980-08-03	Exploratory	499.9	3571.0	Abandoned	Unrated	Unrated
Petro Canada et al. Ogmund E-72	300 E72 57400 60150	1980-08-16	Exploratory	156.2	3094.0	Abandoned	Unrated	Unrated
Petro Canada et al. North Leif I-05	300 I05 54300 55150	1980-09-14	Exploratory	144.0	3513.0	Abandoned	Unrated	Show
Petro Canada et al. North Bjarni F-06	300 F06 55400 57450	1980-09-28	Exploratory	150.0	2813.0	Abandoned	Significant discovery	Unrated
Petro Canada et al. Rut H-11	300 H11 59200 62150	1981-07-14	Exploratory	124.0	3527.0	Abandoned	Unrated	Unrated
Petro Canada et al. Corte Real P-85	300 P85 46100 58000	1981-10-05	Exploratory	438.0	0770.0	Abandoned	Unrated	Unrated
Petro Canada et al. Pothurst P-19	300 P19 58500 60300	1982-07-13	Exploratory	193.0	3843.0	Abandoned	Unrated	Unrated
Canterra et al. South Hopedale L-39	300 L39 55500 58450	1983-07-13	Exploratory	580.0	2364.0	Abandoned	Unrated	Unrated
61˚N–67˚N[2]								
Esso–H.B. Gjoa G-37	300 G37 63000 59000	1979-07-12	Exploratory	1000.0	3998.0	Abandoned	Unrated	Unrated
Aquitaine et al. Hekja O-71	300 O71 62200 62450	1979-07-17	Exploratory	250.8	4566.0	Abandoned	Gas discovery	Unrated
Canterra et al. Ralegh N-18	300 N18 62200 62300	1982-08-01	Exploratory	339.0	3858.0	Abandoned	Unrated	Unrated

[1]Canada-Newfoundland and Labrador Offshore Petroleum Board (2007)
[2]Data from well reports on file at the Canada-Newfoundland and Labrador Offshore Petroleum Board

discoveries, one gas show, and one oil show (North Leif I-05, since shown to be only in the early part of the oil window; Fowler et al., 2019) (Table 1).

The Canada-Newfoundland and Labrador Offshore Petroleum Board (C-NLOPB) was established in 1985 with the signing of the Atlantic Accord. The Board's mandate is to regulate and licence offshore activities so that the provisions set out by the Atlantic Accord are met (Canada-Newfoundland and Labrador Offshore Petroleum Board, 2019d). A significant discovery, as defined by the Canada-Newfoundland and Labrador Offshore Petroleum Board, is one "… indicated by the first well on a geological feature that demonstrates by flow testing the existence of hydrocarbons in that feature and, having regard to geological and engineering factors, suggests the existence of an accumulation of hydrocarbons that has potential for sustained production" (Canada-Newfoundland and Labrador Offshore Petroleum Board, 2019b). Significant Discovery Licences have been issued for five offshore Labrador wells: Gudrid H-55, Bjarni H-81, North Bjarni F-06, Snorri J-90, and Hopedale E-33 (Table 1; Fig. 3) (Canada-Newfoundland and Labrador Offshore Petroleum Board, 2019c).

Between 1984 and 2002, two deep seismic programs were conducted on the Labrador margin, both by the Geological Survey of Canada (Atlantic), as part of the National LITHOPROBE project. These surveys, along with increased market demand, renewed interest in hydrocarbon exploration in the region (Clowes, 2010). From 2002 to 2008, 41 271 km of 2-D seismic reflection data were acquired by industry.

In 2008, a call for bids in the Labrador Offshore Region resulted in four successful bids on four parcels on the Labrador Shelf (Canada-Newfoundland and Labrador Offshore Petroleum Board, 2009). Although seismic acquisition on the margin has increased since then (Fig. 2) no new licences have been issued for the margin, and no bids were received during the 2021 Call for Bids in the Labrador South region (Canada-Newfoundland and Labrador Offshore Petroleum Board, 2019a, f, 2021).

Baffin Island margin

North of latitude 61°N, offshore exploration is regulated by the National Energy Board (NEB). Between 1969 and 1982, 70 344 line kilometres of seismic data were acquired north of latitude 61°N in the Labrador–Baffin Seaway (Fig. 4). Three exploratory wells were drilled on the southeast Baffin Shelf between 1979 and 1982 (Table 2). Gjoa G-37 and Ralegh N-18 were abandoned as dry holes, but a significant discovery was made at Hekja O-71 (Table 1). Since 1990, an additional 72 690 line kilometres of seismic data were acquired north of latitude 61°N, primarily on the West Greenland Shelf. Data acquisition in Canadian waters ceased in 2016 when the Government of Canada announced a moratorium on new oil and gas exploration licences in Arctic waters; the moratorium is indefinite, and subject to science-based reviews and consultation with northern partners every five years (Government of Canada, 2018).

West Greenland margin

The West Greenland margin, both onshore and offshore, was the target of hydrocarbon assessment and exploration since the 1970s (Gregersen et al., 2018); however, in the summer of 2021, in light of the ongoing climate crisis, the government of Greenland (Naalakkersuisut) stopped issuing new licenses for hydrocarbon exploration in Greenland. The first sufficiently nondegraded oil samples recovered for geochemical analyses from onshore oil seeps in West Greenland were collected in 1992 from western Nuussuaq at Maarrat (Bojesen-Koefoed et al., 1999, 2004). Fieldwork during 1993 and 1994, in conjunction with geophysical programs directed by the Geological Survey of Denmark and Greenland (GEUS), expanded the area of known onshore oil occurrences to approximately 40 km^2 (Bojesen-Koefoed et al., 1999). Five shallow core holes (less than 700 m in depth) were drilled by grønArctic Energy Inc. in the 1990s: Marrat-1 (1994), GANW-1 (1994), GANE-1 (1995), GANK-1 (1995), and GANT-1 (1995). Oil was found in the cores recovered from these wells and in surface seeps in close proximity to the drill sites. GrønArctic Energy Inc. drilled the 1200 m deep Umiivik-1 borehole in 1995 on Svartenhuk Halvø (Dam et al., 1998; Sønderholm et al., 2003). A wildcat exploration well, GRO-3, was drilled by grønArctic Energy Inc. on western Nuussuaq in 1996 to a depth of 2996 m, which exhibited oil shows at multiple intervals (Bojesen-Koefoed, 2011; Sørensen et al., 2017). The current region of known oil occurrences from onshore West Greenland spans approximately 150 km from northern Disko Island, across the Nuussuaq Peninsula, to the north of the southern section of Svartenhuk Halvø, and includes several small islands in the vicinity (Bojesen-Koefoed et al., 1999).

As of the summer of 2021, fourteen offshore exploration wells have been drilled along the West Greenland margin between 1976 (Kangamiut-1) and 2011 (Delta-1 and Gamma-1) (Table 3; Fig. 4). Seismic surveys by industry in 1971 and again in 1975, resulted in the awarding of 13 exclusive concessions for hydrocarbon exploration in the central West Greenland region covering an area of 19 082 km^2 (Rolle, 1985). This led to the drilling of five offshore wildcat exploration wells on the West Greenland Shelf between 1976 and 1977: Kangamiut-1, Hellefisk-1, Ikermiut-1, Nukik-1, and Nukik-2 (Table 3; Fig. 4). All of these wells were dry, and as such, all concessions were relinquished by the spring of 1979.

Exploration activity by industry was largely at a standstill until new seismic data acquired in the early to mid-1990s renewed interest in the region (Gregersen and Bidstrup, 2008). Two exploration and exploitation licences were awarded in 1996, resulting in the drilling of the Quelleq-1 exploration well in 2000 (Table 3; Fig. 4) (Nøhr-Hansen, 2003; Gregersen and Bidstrup, 2008). Additional high-resolution seismic surveys were conducted in the late 1990s and early 2000s. This resulted in the issuance of exploration licences by the Greenland authorities in 2002 and 2004 (Gregersen et al., 2018). An additional three wells (T4-1, T8-1, and Alpha-1S1) were drilled in 2010 and another five in 2011 (Delta-1, Gamma-1, AT2-1, AT7-1, and LF7-1) (Table 3; Fig. 4). The well data for these wells have not yet been released. Additionally, 11 shallow (up to 260 m) stratigraphic boreholes were drilled by a consortium of eight petroleum companies in 2012 in northeastern Baffin Bay (Fig. 1) (Nøhr-Hansen et al., 2018; Gregersen et al., 2019). Despite some gas kicks and oil shows in the offshore wells, no commercially viable accumulations of hydrocarbons have been discovered.

HYDROCARBON POTENTIAL

Labrador margin

A 1984 assessment of the regional hydrocarbon potential on the Labrador Shelf by the Geological Survey of Canada produced source-rock analyses and maturation indices from 23 wells on the shelf (Nantais, 1984). Nantais (1984) concluded that because the source rocks in wells on the Labrador Shelf were immature to marginally mature (e.g. McWhae et al., 1980) the potential for gas or condensate on the Labrador Shelf is much greater than the potential for oil.

In recent years, resource assessments have adopted a "play fairway" methodology for analyzing regional hydrocarbon systems. A play is identified and the key elements of the play (trap, seal, source, reservoir) are mapped as polygons so that the extent, or fairway, of the play can be mapped and risk can be assigned (Fraser and Gawthorpe, 2003). The most recent resource assessment on the Labrador margin, by Carey et al. (2020), is part of a series of resource assessments completed in support of the Government of Canada's commitment to protect 10% of Canada's marine and coastal areas by 2020. These Marine Conservation Targets (MCT) resource assessments applied the probabilistic fairway approach described by Lister et al. (2018), where the Area of Interest (AOI) is divided into plays, which are composed of four elements: source, reservoir, seal, and trap. For each element, the Area of Interest is divided into polygons and a chance of success (COS), between 0 and 1, and accounting for data limitations (Lister et al., 2018), is assigned to each polygon. The combined chance of success (CCOS) for each play is the product of the chance of success for each element in the play. A global scale factor is assigned to the combined chance of success, to compare the combined chance of success to that of a known world-class reservoir, producing a technical combined chance of success (TCCOS) for the play. The technical combined chance of success maps for all plays in the Area of Interest are stacked to produce a final stacked technical combined chance of success (STCCOS) map for the Area of Interest.

The Carey et al. (2020) resource assessment identified six regional plays on the Labrador margin. Following the stratigraphic framework already established on the margin (e.g. Dickie et al., 2011; Dafoe, Dickie, Williams, and McCartney, this volume), the identified plays are associated with the Paleozoic, Bjarni, Markland, Cartwright, Kenamu, and Mokami formations (Fig. 5) (Carey et al., 2020). Although ages were assigned to the sequence boundaries for modelling thermal maturity, the sequences are unconformity-bounded and are diachronous on a regional scale (Dickie et al., 2011; Carey et al., 2020). The remainder of this section is summarized from Carey et al. (2020).

The oldest play on the Labrador margin is the Paleozoic play. Whereas the younger Bjarni sequence is the source for the Paleozoic discoveries (with hydrocarbons migrating updip into Paleozoic dolostone strata), any Paleozoic strata preserved beneath the undrilled Bjarni (Cretaceous) depocentres could contain mature source rock. The best reservoir rocks in the Paleozoic play are the dolostone rocks, however limestone and clastic rocks may also be good reservoir candidates if they have associated fracturing and/or diagenesis. In the localities where Alexis Formation volcanic rocks overlie Paleozoic strata (*see* Bingham-Koslowski, Zhang, and McCartney, this volume; Dafoe, Dickie, Williams, and McCartney, this volume), the volcanic rocks may provide a seal for Paleozoic reservoirs; however, a more likely seal is the fine-grained strata of the Upper Cretaceous Markland sequence.

The source rocks of the Bjarni sequence can be divided into two types: coaly beds and carbonaceous shale units. These represent important source rocks in the Hopedale Basin; whereas gas-prone source rocks are the most common, oil-prone source rocks are present, and mature source rocks likely occur in the undrilled depocentres. For the purposes of their resource assessment, Carey et al. (2020) considered each Bjarni depocentre as a structurally trapped reservoir sealed by the overlying Markland sequence.

The predominantly fine-grained Markland sequence is not particularly organic-rich and was therefore not considered a promising source rock by Carey et al. (2020). Coarse clastic rocks with good

Figure 3. Labrador margin from latitude 53°N to 61°N. Significant Discovery Licence acreages are from the Canada-Newfoundland and Labrador Offshore Petroleum Board (2019e). Modern bathymetric features are *modified from* Carey et al. (2020).

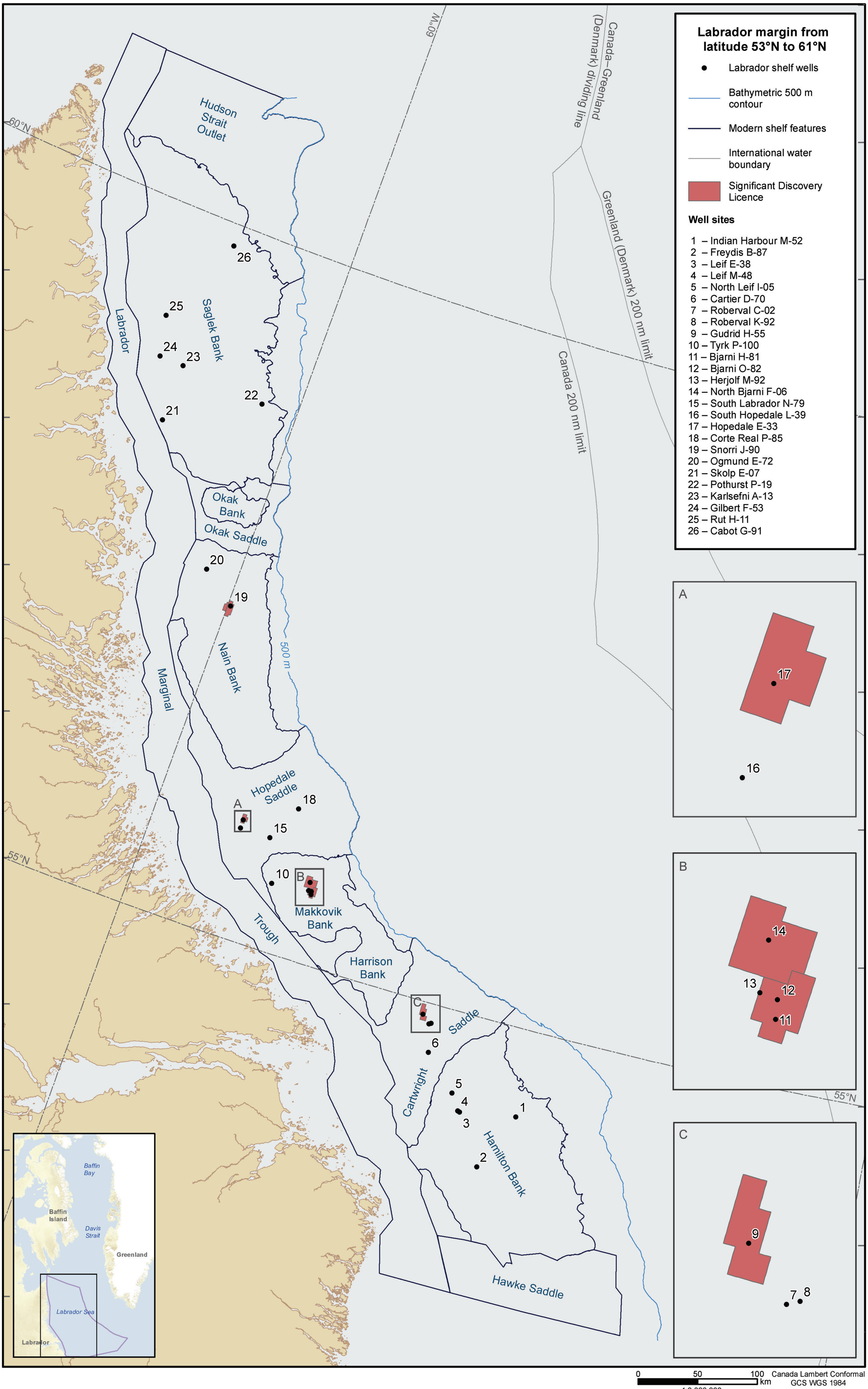
Labrador margin from latitude 53°N to 61°N
Labrador shelf wells
Bathymetric 500 m contour
Modern shelf features
International water boundary
Significant Discovery Licence
Well sites
1 – Indian Harbour M-52
2 – Freydis B-87
3 – Leif E-38
4 – Leif M-48
5 – North Leif I-05
6 – Cartier D-70
7 – Roberval C-02
8 – Roberval K-92
9 – Gudrid H-55
10 – Tyrk P-100
11 – Bjarni H-81
12 – Bjarni O-82
13 – Herjolf M-92
14 – North Bjarni F-06
15 – South Labrador N-79
16 – South Hopedale L-39
17 – Hopedale E-33
18 – Corte Real P-85
19 – Snorri J-90
20 – Ogmund E-72
21 – Skolp E-07
22 – Pothurst P-19
23 – Karlsefni A-13
24 – Gilbert F-53
25 – Rut H-11
26 – Cabot G-91
Hudson Strait Outlet
Saglek Bank
Labrador
Okak Bank
Okak Saddle
Nain Bank
Marginal
500 m
Hopedale Saddle
Makkovik Bank
Trough
Harrison Bank
Saddle
Cartwright
Hamilton Bank
Hawke Saddle
60°N
55°N
60°W
Canada–Greenland (Denmark) dividing line
Greenland (Denmark) 200 nm limit
Canada 200 nm limit
A
B
C
Baffin Bay
Baffin Island
Davis Strait
Greenland
Labrador Sea
Labrador
0
50
100
km
1:3 000 000
Canada Lambert Conformal
GCS WGS 1984

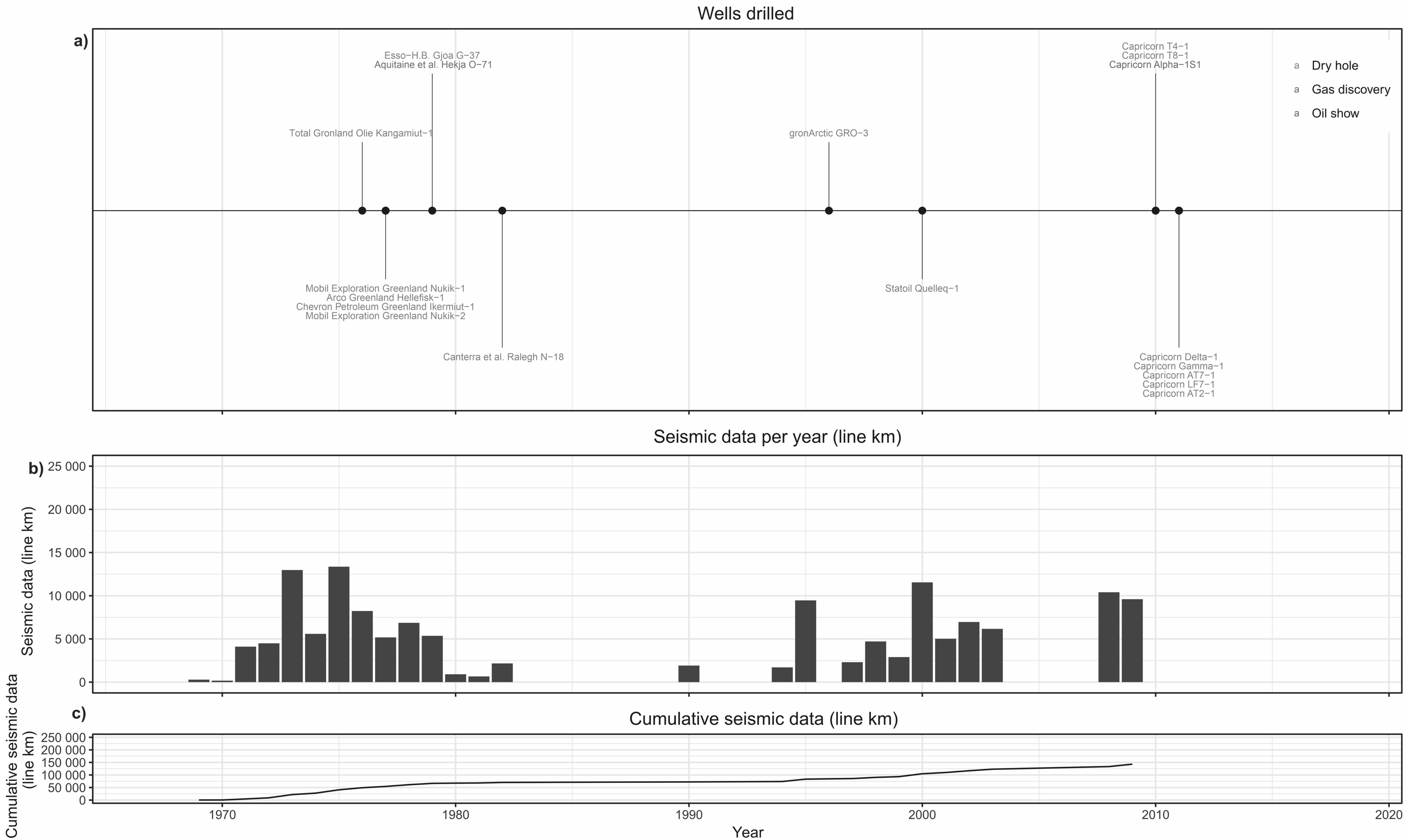

Figure 4. Exploration history for the Labrador–Baffin Seaway, north of latitude 61°N, including West Greenland, derived from well and seismic reports held in confidence by the Geological Survey of Canada: **a)** exploration wells drilled north of latitude 61°N; **b)** line kilometres of seismic data collected per year north of latitude 61°N; and **c)** cumulative line kilometres of seismic data collected north of latitude 61°N.

Table 3. Summary of exploration wells on the West Greenland margin.

Well name	Operator	Spud year	TD (m)	Well class	Location	Latitude and longitude	Notes
Delta-1	Cairn (Capricorn)	2011	2977 m	Exploration	Baffin Bay	71°18'25.65"N; 58°40'08.14"W	Dry; abandoned 2011. TD in Tertiary volcanic rocks[2].
T4-1	Cairn (Capricorn)	2010	3312 m	Exploration	Baffin Bay	71°07'44.82"N; 59°54'10.48"W	Dry; plugged and abandoned October 2010[2].
T8-1	Cairn(Capricorn)	2010	3250 m	Exploration	Baffin Bay	70°18'02.86"N; 59°31'53.58"W	Plugged and abandoned August 2010. Gas in thin sand beds[2].
Alpha-1S1	Cairn (Capricorn)	2010	4801 m	Exploration	Baffin Bay	70°18'54.154"N; 58°28'42.215"W	Suspended 2010; hydrocarbons present with two different origins and maturities[2].
Gamma-1	Cairn (Capricorn)	2011	2680 m	Exploration	Davis Strait	69°26'40.401"N; 59°58'05.414"W	Dry; abandoned 2011[2].
Hellefisk-1	Arco Greenland Inc.	1977	3189 m	Exploration	Davis Strait	67°52'40.60"N; 56°44'20.98"W	Dry. Terminated in Paleocene basalt[1].
Ikermiut-1	Chevron Petroleum Co. of Greenland	1977	3607 m	Exploration	Davis Strait	66°56'11.66"N; 56°35'26.45"W	Terminated in Campanian shale[1]. Hydrocarbon fluid inclusions present[2].
Kangamiut-1	Total Grønland Olie A/S	1976	3862 m	Exploration	Davis Strait	66°09'00.92"N; 56°11'24.28"W	Terminated in Precambrian basement[1]. Gas in lower part of sedimentary interval[2].
Nukik-1	Mobil Exploration Greenland Inc.	1977	2339 m	Exploration	Davis Strait	65°31'60.32"N; 54°45'62.98"W	Terminated in Precambrian basement[1].
Nukik-2	Mobil Exploration Greenland Inc.	1977	2670 m	Exploration	Davis Strait	65°37'54.39"N; 54°46'00.59"W	Terminated in basalt[2].
AT2-1	Cairn (Capricorn)	2011	4847 m	Exploration	Davis Strait	64°44'33.15"N; 55°42'30.86"W	Abandoned; minor oil shows[2].
AT7-1	Cairn (Capricorn)	2011	4846.5 m	Exploration	Davis Strait	64°21'24.92"N; 55°25'34.52"W	Abandoned; traces of oil and gas.
LF7-1	Cairn (Capricorn)	2011	3360 m	Exploration	Davis Strait	64°00'02.899"N; 57°39'44.792"W	Abandoned.
Quelleq-1	Statoil	2000	2937 m	Exploration	Davis Strait	63°48'48.03"N; 54°27'06.61"W	Dry[2]. Terminated in (?) Upper Santonian sandstone[1].
GRO-3	grønArctic Energy Inc.	1996	2996.2 m	Exploration	Onshore West Greenland	70°27'48.128"N; 54°02'25.331"W	

[1]Nøhr-Hansen (2003)
[2]Knutsen et al. (2012)

reservoir potential have only been identified at the Freydis B-87, Skolp E-07, and Gilbert F-53 wells (Fig. 3), and the extent of these units is limited. Where Markland reservoir rocks exist, they are sealed by overlying fine-grained Markland strata and are structurally trapped by syndepositional and blind faults (cf. Baudon and Cartwright, 2008).

The Cartwright sequence contains fine-grained sediments that are a good source for gas, but poor for oil. Cartwright strata that are sufficiently buried are thought to be the most likely mature source rock on the slope and beyond. The Gudrid sands of this sequence are important reservoirs as they have high net-to-gross ratios and high porosity; they are sealed by Kenamu shales in the south and interbedded sand and/or shale in the north. The Cartwright sequence marks a transition on the Labrador margin from dominantly structural traps to dominantly stratigraphic traps.

Whereas the Kenamu sequence is interpreted to have good source-rock potential, modelling suggested that maturity is limited to the outer shelf and slope. The Leif sands of the Kenamu sequence are thickest at Karlsefni A-13; elsewhere they are thin, sheet-like sand units; however, stacked reservoirs of these sand units are possible. The sand units in the lower Kenamu sequence are sealed by fine-grained upper Kenamu strata. Stratigraphic traps (lateral facies changes) are the most likely trap type on the shelf for the Kenamu play; however, later faults that propagated through the Kenamu sequence on the outer shelf, the slope, and in the deep water could provide structural traps.

The organic-rich mud layers of the Mokami sequence are interpreted to have excellent source-rock potential, but they are not sufficiently buried to have matured. Sand intervals within this sequence were identified by Carey et al. (2020) as potential reservoirs for migrating hydrocarbons, but only if they are sealed by overlying fine-grained strata within the Mokami sequence. Structural traps in the deep water, corresponding to the southern Hopedale Basin, are proposed to yield the most prospective plays in this sequence, however, no ground-truthing is available in the Labrador deep water.

The final stacked technical combined chance of success (STCCOS) map produced for the Labrador margin (Carey et al., 2020) demonstrates that the highest potential for hydrocarbon success is on the shelf, associated with the known discoveries (Table 1; Fig. 3). A moderate chance of success is expected along most of the length of the outer shelf, on the slope, and in deep-water areas; it is expected this potential will increase as more data becomes available in these areas (Carey et al., 2020). The Carey et al. (2020) resource assessment is a qualitative assessment that provides a framework for future quantitative studies, including phase discrimination, volumetrics, and ultimately, economic prospectivity.

Western Davis Strait and southeast Baffin Shelf

The Government of Nunavut identifies four Canadian offshore regions that fall within the Baffin–Labrador Seaway between latitudes 61°N and 67°N, which have hydrocarbon potential (Government of Nunavut, 2018): Cumberland Basin, Davis Strait Shelf Basin, Frobisher Bay Basin, and Saglek Basin (Fig. 6). Klose et al. (1982) proposed three types of exploration plays supported by geophysical interpretation in western Davis Strait: 1) wrench-related structures above Upper Cretaceous to lower Paleocene volcanic rocks; 2) Lower Cretaceous reservoirs associated with horst blocks; and 3) isolated Paleozoic reservoirs. Only the first type has been proven.

The Saglek Basin extends from the Okak Arch (*see* Keen et al., this volume) on the Labrador margin to about latitude 62°30′N in the Davis Strait. Okak Bank (Fig. 3) is the modern bathymetric expression of the Okak Arch. This section focuses on the area of the basin north of latitiude 61°N, where two wells have been drilled, Hekja O-71 in 1979 and Ralegh N-18 in 1982 (Fig. 6). Whereas Hekja O-71 resulted in a significant discovery (Table 1), Ralegh N-18 was a dry hole. The Hekja gas discovery is in a structurally trapped, coarse-grained Paleocene sandstone reservoir with a 76 m gross sand interval (Klose et al., 1982). The equivalent sand interval at Ralegh N-18 was water-bearing (Canterra Energy Ltd., 1982). The source of the gas condensate at Hekja O-71 is thought to be a resinite-bearing zone of coaly siliciclastic strata and coal units (Klose et al., 1982; Fowler et al., 2005, 2019; Jauer and Budkewitsch, 2010). Rock-Eval data from Fowler et al. (2019) is in agreement with vitrinite reflectance data (Avery, 2005), indicating that the source rock interval in the lower Paleogene section is mature. Wielens and Jauer's (2009) 4-D basin model suggests the condensate-rich deposit at Hekja O-71 could be the result of a multiphase thermal history with migration of lighter hydrocarbons to the Hekja reservoir. A proposed Paleocene sand fairway extending southwest from Ralegh N-18 and Hekja O-71 (Jauer et al., 2014) provides possible locations for additional structurally trapped reservoirs.

Figure 5. Stratigraphic column for the Labrador–Baffin Seaway, Baffin Island, Bylot Island, and West Greenland (Dafoe, Williams et al., this volume, Fig. 4).


Age (Ma)
Period or epoch
Stage
Polarity chron
Labrador Shelf
West Greenland margin (southern)
Nuussuaq Basin
Southeast Baffin Island
Bylot Island area
Labrador–Baffin Seaway seismic stratigraphy
Pleistocene
Pliocene
Miocene
Oligocene
Eocene
Paleocene
Upper Cretaceous
Lower Cretaceous
Paleozoic
Precambrian
Piacenzian
Zanclean
Messinian
Tortonian
Serravallian
Langhian
Burdigalian
Aquitanian
Chattian
Rupelian
Priabonian
Bartonian
Lutetian
Ypresian
Thanetian
Selandian
Danian
Maastrichtian
Campanian
Santonian
Coniacian
Turonian
Cenomanian
Albian
Aptian
Barremian
Hauterivian
Valanginian
Berriasian
Saglek Fm
Labrador Trough erosion
Mokami Fm
Kenamu Fm
Cartwright Fm
Markland Fm
Bjarni Fm
Alexis Fm
Leif Mb
Gudrid Fm
(upper) Freydis Mb
(lower) Freydis Mb
Manitsoq Fm
Kangâmiut Fm
Ataneq Fm
Nukik Fm
Ikermiut Fm
Hellefisk Fm
Narssarmiut Fm
Kangeq sequence
Appat sequence
Kitsissut sequence
(?)Basalts
Sills and/or dykes
Fylla sand
Qulleq-1
Nukik-1
Nukik-2
Kangâmiut-1
Ikermiut-1
Hellefisk-1
(Hareøen)
Hareøen Fm
Avatarpaat plug
Erqua Fm
Naqerloq Fm
Svartenhuk Fm
Vaigat Fm
Maligât Fm
Kangilia Fm
Atanikerluk Fm
Eqalulik Fm
Agatdal Fm
Quikavsak Fm
Itilli Fm
GRO#3
Umiivik-1
Upernivik Næs Fm
Atane Fm
Kome Fm
Slibestensfjeldet Fm
Nuussuaq Group
Cape Dyer volcanic rocks
Cape Searle Fm
Quqaluit Fm
Aktineq fm
Maud Bight mb
Navy Board fm
Pond Inlet fm
Sermilik fm
Bylot Island fm
Byam Martin fm
Hassel Fm
Bylot Supergroup
Eo Oceanic crust chron C31-C13
Mainly nonmarine deposits
Mainly marine or deltaic sandy and/or silty deposits, locally mudstone
Mainly marine mudstone and/or shale locally sandy and/or silty
Volcanic rocks
Carbonate rocks
Metamorphic and/or igneous basement
Unconformity
Uncertain contact
TD in basement

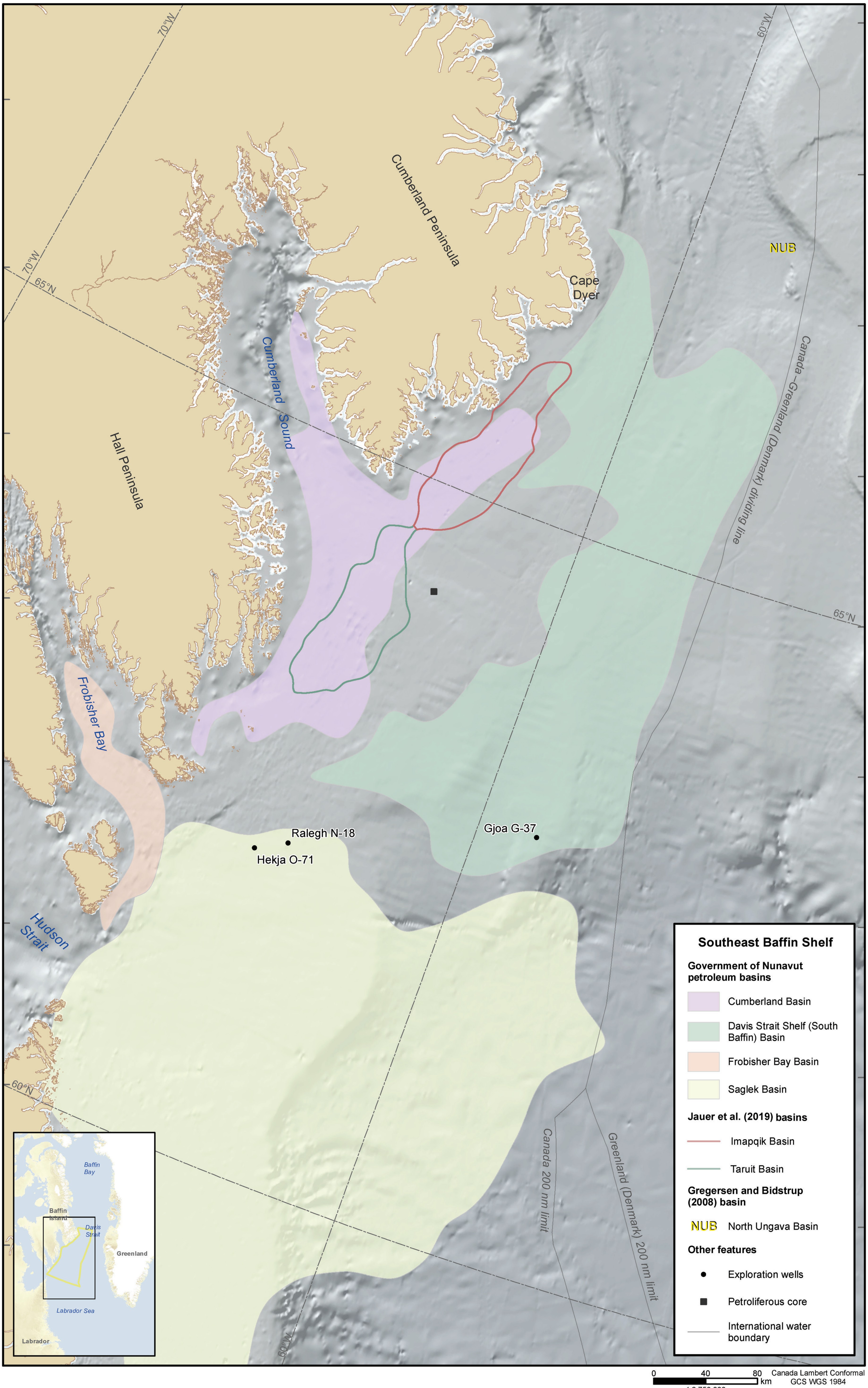
Cumberland Peninsula
Cape Dyer
Cumberland Sound
Hall Peninsula
Frobisher Bay
Hudson Strait
NUB
Canada–Greenland (Denmark) dividing line
65°N
60°N
70°W
60°W
Ralegh N-18
Hekja O-71
Gjoa G-37
Canada 200 nm limit
Greenland (Denmark) 200 nm limit
Southeast Baffin Shelf
Government of Nunavut petroleum basins
Cumberland Basin
Davis Strait Shelf (South Baffin) Basin
Frobisher Bay Basin
Saglek Basin
Jauer et al. (2019) basins
Imapqik Basin
Taruit Basin
Gregersen and Bidstrup (2008) basin
NUB North Ungava Basin
Other features
Exploration wells
Petroliferous core
International water boundary
Baffin Bay
Baffin Island
Davis Strait
Greenland
Labrador Sea
Labrador
0 40 80 km
1:2 750 000
Canada Lambert Conformal
GCS WGS 1984

Figure 6. Basins on the southeastern Baffin Shelf (between latitudes 61°N and 67°N). Basins are based on published reports by the Government of Nunavut (2018), Jauer et al., 2019, as well as Gregersen and Bidstrup (2008).

The southeast Baffin Shelf hydrocarbon region, as defined by the Government of Nunavut (2018), also includes the North Ungava Basin (Fig. 6), which is on Paleocene crust (Oakey and Chalmers, 2012; *see* Keen et al., this volume) and therefore cannot contain Mesozoic and older hydrocarbon elements. Although undrilled, the North Ungava Basin is a potential hydrocarbon 'kitchen' for Paleogene and Neogene source rocks due to its dimension and depth, provided source rock is present (Gregersen et al., 2007). Approximately 200 km from Hekja O-71 and Ralegh N-18, is Gjoa G-37 (Fig. 6), which is structurally separated from these wells by the Ungava Fault Zone (Oakey and Chalmers, 2012; Nøhr-Hansen et al., 2016). This dry hole was drilled on a bathymetric rise, interpreted at time of drilling as a wrench-related anticline (Klose et al., 1982). The National Oceanic and Atmospheric Administration (NOAA) sediment thickness map (Whittaker et al., 2013) suggests this region is connected to the Saglek Basin, however the crust between Ralegh N-18 and Gjoa G-37 is Eocene (Nøhr-Hansen et al., 2016) and thus any connection to the Saglek Basin is relatively young. The NOAA sediment thickness map may therefore be reflecting the Eocene volcanic rocks that are mapped across this region (Jauer and Budkewitsch, 2010). The base of the Gjoa G-37 well is in a Danian section (Nøhr-Hansen et al., 2016) and Fowler et al. (2019) found no significant hydrocarbon potential between 1450 and 3998 m. Older strata may exist beneath the Paleocene section at Gjoa G-37, as it is thought to sit on continental crust (Sørensen, 2006), and therefore the presence of deeper source and/or reservoir rocks cannot be ruled out.

Cretaceous black shale and mudstone on the northeastern side of Cumberland Sound contain Type III kerogen, indicating a potential gas source; however, samples collected from a bedrock coring program by the Geological Survey of Canada are immature for hydrocarbon generation and therefore, source rocks for a Cumberland Sound hydrocarbon system must be more deeply buried (MacLean et al., 2014). A black shale xenolith on the Hall Peninsula indicates Paleozoic source rocks are more likely than Mesozoic (Zhang et al., 2014; *see* Bingham-Koslowski, Zhang, and McCartney, this volume). Silurian brecciated carbonate rocks and Mesozoic clastic rocks in the region are good candidates for reservoir rocks (Zhang et al., 2014). Six drill-core samples from the southwest entrance to Cumberland Sound yielded Paleozoic limestone (Bingham-Koslowski, 2018; *see* Bingham-Koslowski, Zhang, and McCartney, this volume) and therefore Jauer et al.'s (2019) Taruit and Imapqik basins (Fig. 6) could contain Paleozoic successions that house potential source rocks, whereas overlying Mesozoic clastic strata in the deeper parts of these small basins may be possible reservoirs (Jauer et al., 2019). MacLean et al. (2014) described a northeast-trending ridge of strata uplifted during dyke emplacement east of Cumberland Sound (northwest of Jauer et al.'s (2019) Taruit Basin), and suggested that this structure may be capable of trapping hydrocarbons. Their hypothesis was later confirmed when a 65 cm long petroliferous (gas-saturated; the source of which has not yet been determined) drill core composed of late Paleocene to early Eocene mudstone was recovered from the western edge of the structure during a Geological Survey of Canada cruise in 1980 (MacLean and Srivastava, 1981; MacLean et al., 1982). A mafic sill network in the northern Imapqik Basin may represent an additional element for trapping hydrocarbons in this region (Jauer et al., 2019).

Oakey and Chalmers (2012) mapped an extension of the Cambrian–Devonian Arctic Platform (a tectonic province that has a thin Paleozoic sedimentary succession above it in the southeast Arctic; Dawes and Christie, 1991) in Frobisher Bay. Nøhr-Hansen et al. (2016) did not recognize a large basin in Frobisher Bay and, as such, the Arctic Platform may only locally be covered by sediments. The possible presence of additional Paleozoic strata in Frobisher Bay implies that the same extrapolations from Hall Peninsula to Cumberland Sound discussed above could also apply here. Therefore, a deeply buried hydrocarbon system is possible in the subsurface of Frobisher Bay where sufficient thicknesses are found.

Northeast Baffin Shelf and western Baffin Bay

The northeast Baffin Shelf extends northwest from Cape Dyer to Lancaster Sound and widens appreciably beneath the Baffin Fan, the third largest Cenozoic delta in the Arctic (Harrison et al., 2011), which extends farther north and east. The northeast Baffin Shelf and Baffin Bay contain several sedimentary basins (e.g. Lady Ann Basin, Jones Sound Basin, Carey Basin, Scott Trough, Scott Graben, Buchan Trough, Buchan Graben, and Eclipse Trough) that are filled with synrift to postrift strata (Harrison et al., 2011; Schenk, 2011; Brent et al., 2013). The following geological interpretations, and therefore hydrocarbon estimates, for the northeast Baffin Shelf and western Baffin Bay are compiled from previously acquired industry and government reflection and seismic refraction surveys, bottom sampling results, ODP site 645E, studies from the West Greenland margin, as well as onshore analogues (Harrison et al., 2011).

The northeast Baffin Shelf contains numerous structures related to Cretaceous and early Paleogene extensional events that provide ample structural traps along the shelf. Potential source rocks are Ordovician mudstone units, lower Cretaceous synrift shale units, Upper Cretaceous marine shale units associated with thermal subsidence, and Paleogene shale units related to sag basin formation (Schenk, 2011; Spencer et al., 2011). Reservoir units are postulated to consist of Upper Cretaceous postrift marine sandstone strata as well as Paleogene and Neogene orogenic-sourced clastic sediments associated with slope and fan deposits. Competent sealing units are largely unknown and represent a regional risk for hydrocarbon exploration, but intraformational mudstone rocks may provide localized sealing (Nassichuk, 1983; Schenk, 2011). Oil generation along the northeast Baffin Shelf is estimated to have begun in the Late Cretaceous–early Paleogene with hydrocarbons later migrating into synrift and postrift reservoirs (Schenk, 2011). Cretaceous shale and mudstone rocks were sampled by the Geological Survey of Canada along the northeast Baffin Shelf in the regions of Padloping Island, Home Bay, Scott Inlet, and Buchan Gulf all of which contained gas-prone Type III terrestrial kerogen (Fig. 1) (Zhang, 2012, 2013; MacLean et al., 2014), with total organic carbon (TOC), hydrogen indices (HI), maximum temperature (T_{max}) values, and vitirinite reflectance (%R_o) values (Table 4) indicating that the Cretaceous shale strata are immature to marginally mature (MacLean et al., 2014).

The Baffin Fan is a sedimentary wedge structure in northwestern Baffin Bay that encompasses 92 447 km^2 (Harrison et al., 2011; Spencer et al., 2011). The fan contains approximately 12 km of Eocene to Pleistocene sediments and is estimated to have a similar resource potential to the Beaufort-Mackenzie Basin (Harrison et al., 2011). The Baffin Fan complex has yet to be tested by wells, therefore resource estimates vary greatly with mean oil reserves estimated between 0 and 10.1 BBL (billion barrels) and mean gas reserves between 0 and 57 × 10^{12} scf (standard cubic feet) (Schenk et al., 2008; Harrison et al., 2011). Harrison et al. (2011) identified more than 40 hydrocarbon targets within the Baffin Fan complex and the underlying rift system based on a depth to basement structure contour map. The majority of the structures are located north of Bylot Island in the mouth of Lancaster Sound or in western Baffin Bay between Bylot Island and Coburg Island (Harrison et al., 2011). Play types identified include those related to structural (horsts, inversion anticlines, etc.) and stratigraphic (canyon fills, clinoforms and/or clinothems, lateral facies change, unconformities, etc.) traps. The top of the oil window is tentatively proposed to have been entered during the Selandian in the nearshore and in the Miocene in the offshore (Harrison et al., 2011).

Potential source and reservoir rock candidates were identified by Harrison et al. (2011) in the Baffin Fan complex based on correlative deposits in the Sverdrup Basin, the Beaufort-Mackenzie Basin, along the West Greenland margin, and from an oil seep along the northeast Baffin Shelf (offshore Scott Inlet). Due to the lack of sampling in the subsurface of Baffin Bay, the presence of these cannot be confirmed;

Table 4. Hydrocarbon geochemistry for the Cretaceous shale strata from locations along the northeast Baffin Shelf (summarized from MacLean et al., 2014).

Region	Average TOC[1] (%)	Average HI[2]	Average T_{max}[3] (°C)	R_o[4]
Padloping	6.7	29	426.3	0.44-0.47
Home Bay	4.0	46	407.4	0.5
Scott Inlet	1.6	111	434.5	0.5-0.52
Buchan Gulf	1.05	93.5	423-432	n.a.

[1]Total organic content
[2]Hydrogen index
[3]Temperature at which maximum rate of hydrocarbon generation occurs
[4]Vitrinite reflectance

however, potential source-rock candidates for oil generation include equivalents to the Cenomanian–Turonian Kanguk Formation as well as an unnamed Eocene shale unit. The offshore equivalents of the Barremian–Aptian Isachsen, Albian–Cenomanian Hassel, Selandian Mount Bell, and the Eocene Margaret formations are all thought to have potential to generate gas in the Baffin Fan complex (Harrison et al., 2011). Potential reservoir units in the fan complex include interbedded sand units within offshore equivalents of the Isachsen and Hassel formations, along with Danian–Selandian fluvial sandstone units and Thanetian–Eocene fault-related conglomerate units. Possible seal units include Lower Cretaceous mudstone units along with synrift Danian and postrift Selandian shale and siltstone units (Harrison et al., 2011). There is also the potential for plays beneath the Baffin Fan complex related to plays identified in Lancaster Sound (Atkinson et al., 2017).

The 2013 resource assessment for Lancaster Sound estimated up to 4.5 billion barrels of crude oil in place and 13 Tcf (trillion cubic feet) of total aggregated natural gas (Brent et al., 2013). The most likely source rocks are Upper Cretaceous shale strata associated with global episodes of oil-prone source-rock deposition including equivalents of the Albian Hassel Formation and the Cenomanian–lower Turonian Kanguk Formation (Creaney and Sullivan, 2011; Brent et al., 2013). Identified reservoir units include Proterozoic clastic rocks, Paleozoic clastic and carbonate strata, as well as equivalents of the Lower Cretaceous Hassel Formation, the Upper Cretaceous Kanguk Formation, and the Cenozoic Eureka Sound Formation (Smith et al., 1989; Atkinson et al., 2017). Atkinson et al. (2017) identified 15 play types associated with three geological megasequences: Proterozoic, Paleozoic, and Mesozoic–Cenozoic clastic sediment. The greatest potential for conventional hydrocarbon resources was postulated to be in the Mesozoic–Cenozoic clastic plays associated with structural and stratigraphic traps in eastern Lancaster Sound and Baffin Bay (within the Baffin Fan complex) (Smith et al., 1989; Atkinson et al., 2017). Plays associated with Paleozoic carbonate rocks and salt deposits in western Lancaster Sound were also identified as areas with the potential for hydrocarbon resources (Atkinson et al., 2017).

In the Baffin Bay Basin, oil generation is suggested to have occurred in the late Paleogene or Neogene, before hydrocarbons migrated into reservoirs associated with incised valley systems, shelf-edge deltaic systems, shoreline systems, as well as slope and basin floor (fan) systems (Schenk, 2011). Traps in the Baffin Bay Basin are thought to be associated with listric faults, rollover structures, and changes in lithology such as slope and fan sandstone units encased in mud (stratigraphic traps) (Harrison et al., 2011; Schenk, 2011).

The northeastern Canada rifted margin assessment unit identified by Schenk et al. (2008) encompasses the northeast Baffin Shelf, an area of approximately 111 000 km^2 from the Baffin Island coast to the edge of the Baffin Bay Basin. A median of 11 undiscovered oil fields and a median of 9 undiscovered gas fields are calculated (based on a median field density of 0.21 fields/1000 km^2 and an area of 111 000 km^2) to exist within this assessment unit with an estimated mean of 1431 million barrels of undiscovered oil and a mean of 7369 billion cubic feet of undiscovered gas (Schenk et al., 2008; Schenk, 2011). A median of 40 undiscovered oil and gas fields (median of 20 for oil and a median of 20 for gas; based on a median field density of 0.15 fields/1000 km^2 and an area of 252 000 km^2; Schenk, 2011) are predicted to exist in the Baffin Bay assessment unit which encompasses both the Canadian and Greenland sides of the Baffin Bay Basin (Schenk et al., 2008). A mean 1555 million barrels of undiscovered oil and a mean 9338 billion cubic feet of undiscovered gas has been estimated for this region (Schenk et al., 2008; Gautier et al., 2011; Schenk, 2011). The Baffin Bay Basin is estimated to have a 50% chance of containing at least one oil accumulation with recoverable volumes in excess of 1 BBO (billion barrels of oil) (Gautier et al., 2011).

Onshore West Greenland margin

Surface oil seeps associated with Mesozoic to Cenozoic strata are common and widespread onshore West Greenland and have been reported from several locations, including on the Nuussuaq Peninsula, Disko Island, Svartenhuk Halvø, Hareøen, Qeqertat (Schades Øer), and Ubekendt Ejland (Fig. 7) (Bojesen-Koefoed, 2011). Hydrocarbons are primarily found plugging available porosity in volcanic units (picritic lavas or haloclastite rocks), but have also been recorded in sandstone units and carbonate veins associated with fracture systems and dykes. The amount of oil present can vary from minor staining along dykes (common in localities in northwestern Disko Island, Hareøen, westernmost Nuussuaq, Ubekendt Ejland, Qeqertat, and Svartenhuk Halvø), to significant volumes approaching reservoir-like accumulations such as those noted at locations near Nuussuaq-Marraat and Sikillingi (nondegraded, early mature oil) (Bojesen-Koefoed et al., 1999; Bojesen-Koefoed, 2011). Oil degradation appears to intensify inland due to increased interactions with water produced via continuous freezing-thawing processes that dilute and/or wash away hydrocarbons. Based on known occurrences, oil seepage and staining are more common (though not limited to) at localities that:

- include the lower part of the Paleocene Vaigat Formation, the lowermost succession of the volcanic rocks (Fig. 5);
- are located near or within regional fracture and dyke zones;
- contain several fractures and mineralized veins (particularly ones that contain quartz and calcite);
- have a high primary porosity such as that characteristic of vesicular lava flows, hyaloclastite rocks, or volcanoclastic conglomerate units; and
- exhibit a silica-enriched composition such as silica-rich basalt and hyaloclastite rocks (Bojesen-Koefoed et al., 1999; Bojesen-Koefoed, 2011).

Geochemical and biomarker analyses conducted on the oil occurrences throughout the Disko-Nuussuaq-Svartenhuk Halvø region have identified five distinct different oil types (Table 5). The distribution of these five oil types, their wax content, and the presence or absence of certain biomarkers (specifically those associated with angiosperms, which did not evolve until approximately the Santonian) have been used to identify potential source-rock candidates for the different oil types. Of the five oil types identified, three contain a high wax content and are interpreted to be sourced from deltaic source rocks with a significant input of terrigenous organic matter (the Marraat, Niaqornaarsuk, and Kuugannguaq oil types) (Bojesen-Koefoed et al., 2007; Bojesen-Koefoed, 2011). A fourth type, the Itilli oil type, is sourced from Cenomanian–Turonian or older marine shale rocks. The source rock of the fifth and final type, the Eqalulik oil type, is unknown. The occurrence of five oil types with various distributions and source rocks, suggests the presence of multiple, active hydrocarbon systems in the region (Bojesen-Koefoed et al., 1999, 2004).

The Marraat oil type is named for the place where it was first discovered along the southern coast of the Nuussuaq Peninsula (Bojesen-Koefoed, 2011). The oil type was first identified in 1993 and was the first oil type defined for the region (Christiansen et al., 1996). It has a widespread distribution and is commonly found in relatively large volumes. Surface seeps composed of the Marraat oil type have been observed in and around Marraat (including in the Marrat-1, GANW-1, GANK-1, and GANE-1 shallow onshore wells; Fig. 7f), on the northern coast of Disko Island, on Hareøen, as well as on a small, rocky island off the coast of Hareøen (Fig. 7a) (Bojesen-Koefoed et al., 1999; Bojesen-Koefoed, 2011). Marraat oil is typically found in pores, cracks, and veins associated with volcanic beds (basalt layers and hyaloclastite rocks) that may be laterally continuous over several kilometres.

The Marraat oil type is an oil with high wax content, with abundant long-chain normal alkanes and saturated components (Bojesen-Koefoed et al., 1999; Pedersen et al., 2006; Bojesen-Koefoed, 2011). It has been classified as a deltaic oil that was sourced from sediments with a predominantly terrigenous organic component. The presence of abundant angiosperm-derived biological markers in the oil suggests that Marraat oil was generated from Paleocene mudstone with the most likely candidates attributed to the Danian Eqalulik Formation (Fig. 5). Marraat oil seeps (both pure and mixtures) can be traced over an area of approximately 7500 km^2, implying that the Paleocene source rocks from which it is derived share a similar widespread distribution (Bojesen-Koefoed, 2011). This further suggests that paleoenvironments in the Paleocene, at least on a regional scale, promoted the extensive deposition of organic-rich, oil-prone mudstone source rocks, which may have the potential to generate significant volumes of oil both onshore and offshore.

The Niaqornaarsuk oil type is named for the location on the southern coast of the Nuussuaq Peninsula at which the oil is found (Fig. 7b) (Bojesen-Koefoed, 2011). The oil occurs as surface seeps in a fracture and/or fault zone west of the Kuugannguaq-Qunnilik Fracture Zone. Niaqornaarsuk oil has a high wax content and is characterized by the presence of long-chain normal alkanes (*n*C22+) and saturated components (Bojesen-Koefoed et al., 1999; Bojesen-Koefoed, 2011). The oil was likely sourced from deltaic marine shale units with significant terrigenous organic matter. Dam et al. (2009) found biological markers from Campanian shale units from the GANT-1 well (Fig. 7f) that are similar to those found in the Niaqornaarsuk oil and suggested that these shale units may have generated this oil type with maturity

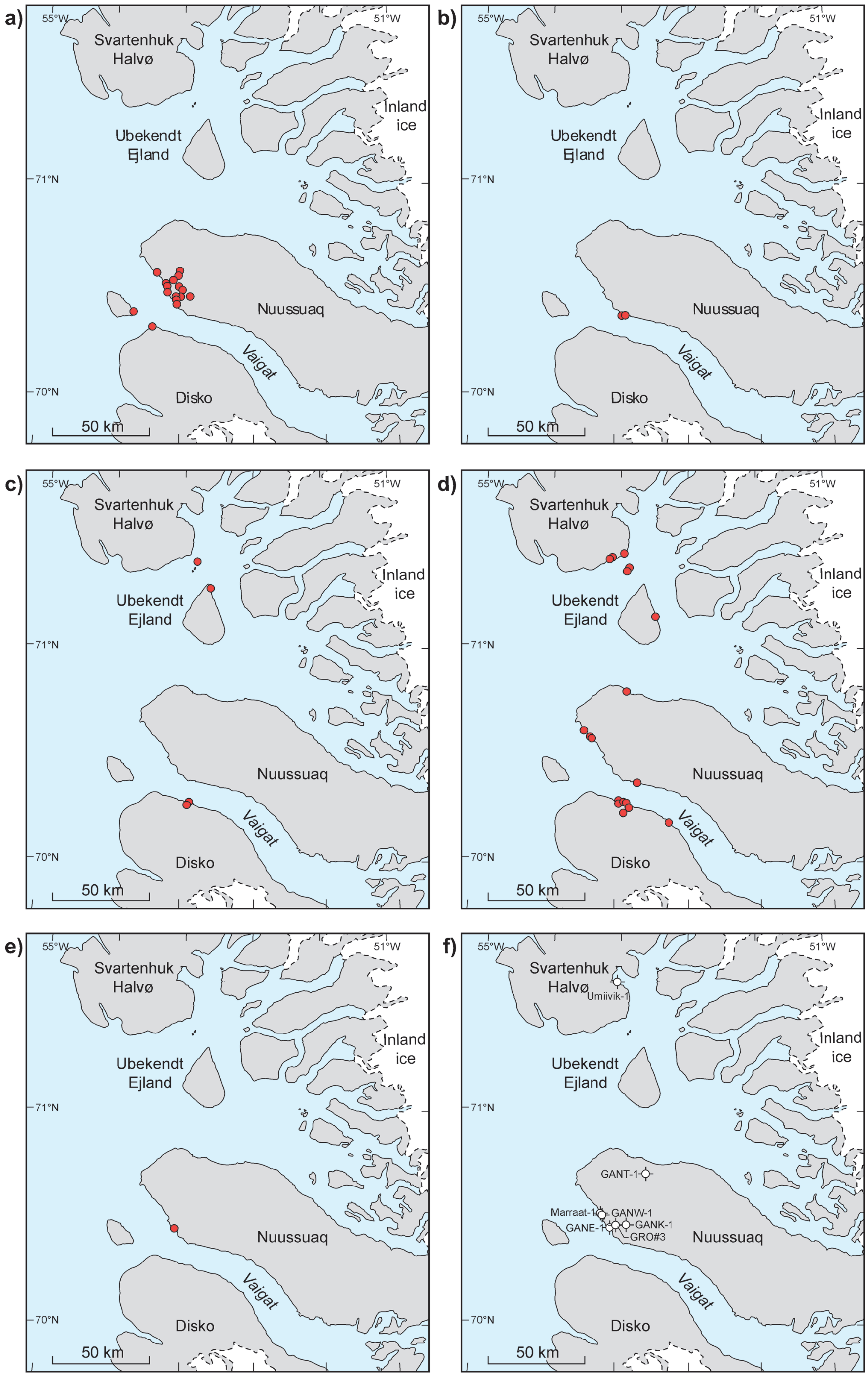

Figure 7. Location map showing distribution of surface seepages of petroleum and boreholes in the Nuussuaq Basin, central West Greenland. **a)** The Marraat oil type; **b)** the Niaqornaarsuk oil type; **c)** the Kuugannguaq oil type; **d)** the Itilli oil type; **e)** the Eqalulik oil type; **f)** wells and boreholes in the Nuussuaq Basin. Compiled from various sources, primarily Bojesen-Koefoed et al. (1999).

occurring locally in and around the fault zone. The limited extent of the Niaqornaarsuk oil type implies a rather restricted distribution for the source rock and therefore limits the importance of this oil type for hydrocarbon exploration (Bojesen-Koefoed, 2011).

The Kuugannguaq oil type was named for a place on the north coast of Disko Island where the oil was originally discovered and where the greatest occurrence of the oil can be found (Fig. 7c) (Bojesen-Koefoed, 2011). This oil type solely occurs as surface seeps and is known from a rather restricted area located in close proximity to the mouth of the Kuugannguaq valley, east of the Kuugannguaq Fault Zone. Kuugannguaq oil is primarily identified by negative criteria (e.g. the absence of certain compounds and biomarkers), and therefore its presence in oil mixtures is very difficult to recognize (Bojesen-Koefoed et al., 1999; Bojesen-Koefoed, 2011).

Kuugannguaq oil has a high wax content and contains long-chain (*n*C22+) normal alkanes and saturated components (Bojesen-Koefoed et al., 1999; Pedersen et al., 2006; Bojesen-Koefoed, 2011). The oil has a high pristane/phytane ratio, but lacks biomarkers derived from angiosperms placing the age of the source rock no younger than Santonian. Kuugannguaq oil has defining characteristics of terrigenous oil and is thought to be sourced from Lower Cretaceous (Albian–Cenomanian) coal and carbonaceous shale units of the Atane Formation (Fig. 5) (Bojesen-Koefoed et al., 1999; Pedersen et al., 2006; Bojesen-Koefoed, 2011). Coaly Type III source rocks of the Atane Formation have been interpreted by Pedersen et al. (2006) to have undergone sufficient burial in the Vaigat Strait to achieve thermal maturity and therefore are a viable candidate for the source rocks that produced the Kuugannguaq oil type. The paucity of Kuugannguaq oil implies a rather restricted distribution of its source rock and therefore the oil has minimal relevance for hydrocarbon exploration (Bojesen-Koefoed et al., 1999; Bojesen-Koefoed, 2011).

The Itilli oil type was named after the Itilli valley in western Nuussuaq where it was first discovered (Bojesen-Koefoed, 2011). Itilli oil surface seeps are widespread, and have been reported from the Nuussuaq Peninsula (more common along the southern coast, though one sample has been collected from the north coast), Disko Island (north coast; reported from the Kuugannguaq valley and Asuk), as well as from Nuussuaq, northward to Svartenhuk Halvø, including Ubekjendt Ejand and Schades Øer (Fig. 7d) (Bojesen-Koefoed et al.,

Table 5. Onshore oil types from central West Greenland.

Oil type	Description	Distribution	Age of oil	Possible source rocks
Marraat oil type	High wax content[1]	Widespread distribution. Identified in Marraat-1, GANW-1, GANE-1, and the GANK-1 wells[1,3].	Latest Cretaceous or younger	Most likely Paleocene deltaic mudstone[3].
Niaqornaarsuk oil type	High wax content[1]	Local occurrences in southern Nuussuaq[3].	Campanian	Most likely deltaic marine shale.
Kuugannguaq oil type	High wax content[1]	Local occurrences on northern Disko Island[3].	Santonian or older	Most likely Lower Cretaceous coal and Atane Formation shale[1,3].
Itilli oil type	Low wax content[1]	Widespread distribution[1,3].	Late Cretaceous	Unknown. Most likely marine shale[1,2,3].
Eqalulik oil type	Low to moderate wax content[1]	Limited local distribution with occurrences in the GANE-1 well[3].	Santonian or older	Unknown source rocks of possibly lagoonal or lacustrine origin[1].

[1]Bojesen-Koefoed et al. (1999)
[2]Bojesen-Koefoed et al. (1997)
[3]Bojesen-Koefoed (2011)

1999, 2007; Bojesen-Koefoed, 2011). On the Nuussuaq Peninsula, the oil is typically found west of the Itilli Fault Zone (west of the Kuugannguaq-Qunnillik Fault) within carbonate-filled fractures and veins in basalt rocks associated with major dykes and fractures.

Itilli oil is characterized by a low to moderate wax content and exhibits a light end–skewed normal alkane distribution with a variable pristane/phytane ratio (0.8 to 3.0) (Bojesen-Koefoed et al., 1999, 2007; Bojesen-Koefoed, 2011). This oil type has been described by Bojesen-Koefoed et al. (1999, 2007) as having characteristics typical of oil sourced from a marine black shale. Biomarkers, including the absence of any related to angiosperms, suggest a Cenomanian–Turonian marine source rock. No source rock has been identified in the vicinity of the Itilli oil seeps that meets the age, compositional, and geochemical requirements; however, marine shale units equivalent to those of the Kanguk Formation on Ellesmere Island (Nunavut, Canada) or older marine mudstone units, are favoured as potential source-rock candidates (Bojesen-Koefoed et al., 1999; Bojesen-Koefoed, 2011; Sørensen et al., 2017). The widespread distribution of Itilli oil implies a similar extent to the source rock.

The Eqalulik oil type is only known in its pure form from Paleocene sandstone strata of the Agatdalen Formation in the deeper section (approximately 600–700 m) of the GANE-1 (GrønArctic Nuussuaq Eqalulik-1) shallow well on the Nuussuaq Peninsula (Fig. 7e) (Bojesen-Koefoed, 2011). The oil is found plugging porosity in turbidite and sandstone units as well as in the overlying volcanic rocks. Eqalulik oil commonly occurs in mixtures with other oil types that have been reported from the southern coast of the Nuussuaq Peninsula, as well as on Ubkjendt Ejland and Svartenhuk Halvø (Bojesen-Koefoed et al., 1999; Bojesen-Koefoed, 2011).

Eqalulik oil has a low to moderate wax content with a unique and easily recognizable composition that is rich in acyclic isoprenoids, sesquiterpanes, and pentacyclic triterpene and sterane biomarkers (Bojesen-Koefoed et al., 1999; Bojesen-Koefoed, 2011). Its distinct composition enables it to be readily detected in multi-oil type mixtures. The source rock for the Eqalulik oil type is unknown. The oil lacks biomarkers derived from angiosperms, implying that the source rock that generated it is no younger than Santonian. The low wax content of the oil suggests a marine (possibly lagoonal) or lacustrine origin (Bojesen-Koefoed et al., 1999). To date, no known source rocks have been found that would account for the distinct characteristics of the Eqalulik oil type, making it of minimal importance for hydrocarbon exploration.

Due to overlapping distributions of the five oil types, mixtures containing two or more oil types are common. Marraat and Eqalulik oil mixtures occur frequently as surface seeps along the southern coast of the Nuussuaq Peninsula, west of Niaqornaarsuk (Bojesen-Koefoed et al., 1999; Bojesen-Koefoed, 2011). Mixtures containing elements of Itilli and Eqalulik oil types are also abundant, especially on the eastern coast of Ubekjendt Ejland (Bojesen-Koefoed, 2011). Other reported oil mixtures from the West Greenland margin include mixtures of Itilli and Marraat oils (found in close proximity to the Itilli Fault Zone on the southern coast of Nuussuaq) as well as Niaqornaarsuk and Eqalulik oils (Bojesen-Koefoed et al., 1999; Bojesen-Koefoed, 2011). The presence of the Kuugannguaq oil type in multi-oil mixtures would be nearly impossible to determine as the oil does not contain any distinguishing characteristics and is identified based on the absence of certain biomarkers.

Reservoir candidates for the onshore include the Atane, Itilli, Kangilia, Agatdal, and Vaigat formations (Table 6; Fig. 5) based on surface oil-seep occurrences and onshore well data (Sønderholm and Dam, 1998; Hopper et al., 2016). Additionally, Cretaceous–Cenozoic sandstone strata, and possibly Ordovician carbonate rocks, have been proposed as potential reservoir candidates in both onshore and offshore regimes.

Oil stains and potential source-rock candidates associated with Paleozoic rocks have been identified from the Disko–Nuussuaq–Svartenhuk Halvø region. A review of their occurrences was published by Bojesen-Koefoed in 2011 and is summarized here. Oil has been recovered from several Ordovician carbonate rocks in the region, both onshore and offshore (Bojesen-Koefoed, 2011). Each oil appears to have a slightly different composition, complicating the determination of potential lower Paleozoic source-rock candidates. A

Table 6. Potential reservoir units from the West Greenland margin.

Potential reservoir	Known reservoir occurrences
Atane Formation	Medium- to coarse-grained flood-plain deposits on Disko Island grade into delta-front and -plain deposits. Porosity of sandstone units in onshore Ataata Kuua well range from 5–25% (average of 17%) with a net to gross ratio of 50%. Permeability ranges between 0.5 mD and 150 mD.[4]
Itilli Formation	Interbedded, medium- to coarse-grained turbidite and channel sandstone units up to 100 m thick in the GRO-3 well. Porosities range up to 10% near Itilli Fault with permeability below 1 mD.[1,4]
Kangilia Formation	Submarine canyon conglomerate and sandstone units in the Nuussuaq Basin with porosities ranging from 5.7–17.5% and permeability readings up to 219 mD. Over 240 m thick potential reservoir units in the GRO-3 well. [1,4]
Agatdal Formation	Coarse to very coarse, gas-bearing, channellized sandstone units encountered in the GANE-1 well with porosities of 6.4–20.6% and permeability up to 10 mD. Formation is 295 m thick in the GRO-3 well where sandstone beds are up to 30 m thick with an average porosity of 9.0%.[4]
Vaigat Formation	Porosity associated with volcanic hyaloclastite deposits. Formation is 303 m thick in GRO-3 well.[4]
Mega-unit F	Late Cretaceous to Paleocene sandstone and conglomerate units. AT7-1 well contains conglomerate units with good reservoir qualities in its lower succession as well as sandstone and diatomite with high porosities, but medium to low permeability. Late Santonian potential reservoir sandstone (Fylla sands) were reported from Quelleq-1. Other Cretaceous intervals with potential reservoir-quality units (lower than that of AT7-1) were encountered in AT2-1 and LF7-1 wells. [2,3,4,5]

[1]Sønderholm and Dam (1998)
[2]Gregersen and Bidstrup (2008)
[3]Schenk (2011)
[4]Hopper et al. (2016)
[5]Gregersen et al. (2018)

small, erosional remnant composed of Ordovician carbonate rocks, referred to as the Fossilik inlier, is located north of Nuuk (Bojesen-Koefoed, 2011). The Ordovician carbonate inlier is grey and contains small droplets of undegraded oil. Biological markers suggest that the oil was generated from a carbonate source rock, the origin of which has yet to be determined, as no units with hydrocarbon potential are known from the area. An oil sample collected from the Aleqatsiaq Fjord Formation in northern Greenland is also Ordovician and shows some similarities in composition to the oil retrieved from the Fossilik inlier; however, its hydrocarbon potential is thought to be somewhat lower than the inlier (Bojesen-Koefoed, 2011). A 2003 TTR cruise dredged a centimetre-scale sample of brownish-black Ordovician carbonate from Canyon A offshore southwest Greenland, in the Davis Strait. Analyses demonstrated that the rock was organic-rich (TOC close to 2% and hydrogen indices 400–500) and oil prone (Bojesen-Koefoed, 2011). The origin of the Canyon A Ordovician carbonate is interpreted as marine; however, its biomarker assemblage exhibits several lacustrine characteristics. Another occurrence of Ordovician carbonate was recovered from a dredge of the Davis Strait High (Dalhoff et al., 2006). This second piece of carbonate was oil stained, with the oil exhibiting a relative wax-rich distribution of normal alkanes, although the pristane/phytane ratio was rather low (Bojesen-Koefoed, 2011). The composition of the oil appears to be dissimilar to that of the oil at the Fossilik inlier, the Canyon A sample, and the Aleqatsiaq Fjord Formation sample. Organic-rich Silurian shale strata of the Lafayette Bugt Formation and the Tors Fjord Member of the Wulff Land Formation are considered to have hydrocarbon generation potential (Bojesen-Koefoed, 2011). These shale rocks are widespread in northern Greenland and may be present in offshore basins, including those along the West Greenland margin, throughout Davis Strait, and along the Baffin Island margin.

Offshore West Greenland margin

The majority of the offshore western Greenland basins and structural highs described by Gregersen et al. (this volume), are untested by wells. The Mesozoic and Cenozoic sediments that have accumulated in these depocentres (kilometers to, in some cases, in excess of 10 km in thickness) include potential source, reservoir, and seal rocks (Gregersen and Bidstrup, 2008; Bojesen-Koefoed, 2011; Gregersen et al., 2018). Despite evidence of active hydrocarbon systems on the margin (e.g. onshore seeps), the specific offshore hydrocarbon system components have yet to be identified.

Offshore basins are disconnected as a result of the tectonic history of the region. During the Cenozoic, varying degrees of tectonic and volcanic activity affected these basins, resulting in differences in platform development, sediment thickness, thermal maturation related to localized volcanism, and burial histories involving Cenozoic uplift and exhumation (Knutsen et al., 2012). The disparate tectonic and volcanic histories of the basins have also had ramifications for the evolution and presence of potential hydrocarbon systems along the West Greenland margin. To complicate matters further, correlation between formal lithostratigraphic formations identified onshore and strata found in offshore depocentres is limited by the lack of well coverage. Where well data are not available to ground truth the seismic reflection interpretation, informal seismic stratigraphic mega-units have been defined (Table 7) (Gregersen et al., 2019).

Source rocks of Upper Cretaceous (Cenomanian–Turonian and Campanian) and Paleogene age are interpreted to occur along the West Greenland margin (Bojesen-Koefoed, 2011; Schenk, 2011). Based on onshore outcrops, drill cores, and well data, organic-rich shale units associated with the Upper Cretaceous Itilli, the Paleocene Eqalulik, and possibly the Paleocene Kangilia and the Paleocene to Eocene Ikermiut and Nukik formations represent the most likely source rocks for the hydrocarbon systems in the area (Table 8; Fig. 5) (Rolle, 1985; Hopper et al., 2016). In the offshore, these formations may be present in mega-units F (Itilli and Kagilia formation equivalent), E (Eqalulik, Kangilia, Ikermiut, and Nukik formation equivalents), and D (Ikermiut and Nukik formation equivalents) (Table 7; Fig. 5). Possible older source rocks, some of which may be obscured by volcanic rocks, include synrift lacustrine mudstone units associated with the Lower Cretaceous Kome Formation and the Lower to Upper Cretaceous Atane Formation (mega-units G and F; Table 7; Fig. 5) (equivalent to the Bjarni Formation in eastern Canada) as well as Ordovician shale strata (Schenk, 2011), however, these have not been sampled or tested by wells. Boreholes drilled in the Kap York Basin, northeast Baffin Bay (Fig. 1), encountered Lower and Upper Cretaceous strata (Nøhr-Hansen et al., 2018). The Lower Cretaceous succession, which sits unconformably on Proterozoic rocks, is interpreted to have been deposited in a nonmarine to brackish environment and contains immature to marginally mature Type III and/or IV kerogen. The Upper Cretaceous succession contains black marine mudstone units with TOC values of 3% to 6% and hydrogen indicies (HIs) of 200 to 350 (Nøhr-Hansen et al., 2018). Predictions based on seismic interpretation and modelling suggest that mid-Cretaceous successions present in deep basins (e.g. Sisimiut and Aasiaat basins, the Aasiaat Structural Trend, and the Ilulissat Graben) entered the oil window after the mid-Miocene, which postdates the formation of traps and closures (Gregersen and Bidstrup, 2008). Other estimations suggest that maturation may have begun as early as the Eocene for these deep successions (Gregersen et al., 2013).

Synrift and sag-related sandstone and conglomerate units associated with fluvial, flood plain, channel, delta, slope (turbidite deposits), and fan depositional systems from the West Greenland margin have been shown to have poor to good reservoir quality (Table 6) (Schenk, 2011; Hopper et al., 2016). Coarse-grained facies are common in channels and have the highest porosities and permeabilities, whereas finer grained units (such as turbidite deposits) are associated with deposition that is more distal and register the lowest porosities and permeabilities of potential reservoir intervals (Hopper et al., 2016). Hydrocarbon shows have been reported from coarser grained, high porosity and/or permeability strata, both onshore and offshore.

Sandstone and conglomerate units with reservoir potential are present locally in almost all Cretaceous to Paleocene sedimentary and volcanic sequences noted in onshore wells and outcrops (Hopper et al., 2016). These include units from the Kome, Slibestensfjeldet, Upernivik Naes, Atane (Qilakitsoq, Kinittoq, Ravn Kløft, and Skansen members), Itilli (interbedded sand units; Umiivik member), Kangilia (Annertuneq conglomerate), Agatdal, Quikavsak (Tupaasat and Patuutkløften members), Vaigat (Annaanaa member), Eqalulik, and Atanikerluk formations (Table 7; Fig. 5) (Hopper et al., 2016). Offshore, these units correspond to mega-units G, F, and E. The composition, quality, and thickness of each unit varies across the region, making their potential as a reservoir unit only locally important. Of these units, the Atane, Itilli, Kangilia, Agatdal, and Vaigat formations, along with offshore equivalents of mega-unit F (Table 7), have been identified as the best possible candidates for reservoir units (Table 6) (Bojesen-Koefoed, 2011; Schenk, 2011). Also of note is the presence of over 100 m of Lower Cretaceous sandstone with estimated porosities of 25% in the Kap York Basin boreholes (northeastern Baffin Bay) (Nøhr-Hansen et al., 2018). In deeper grabens and basins that have been untested by wells, Proterozoic sandstone, Paleozoic carbonate, and Lower Cretaceous sandstone with reservoir properties are also possible (Bojesen-Koefoed, 2011; Schenk, 2011).

Both Upper Cretaceous and Paleogene mudstone units and Paleocene subaerial lava flows represent viable seal units in the region (Table 8). Mudstone strata associated with the Itilli, Kangilia, and Eqalulik formations and their offshore counterparts (mega-units G-E) (Fig. 5) are widespread, occurring in thick (several hundred metres) accumulations especially in offshore basins (Hopper et al.,

Table 7. Onshore formations from the West Greenland margin and their offshore mega-unit equivalents.

Formation	Age	Mega-unit
Ataneq Formation	Late Eocene to Pliocene	Mega-units A, B, and C
Manîtosoq Formation	Mid-Eocene to Pliocene	Mega-units A, B, and C
Kangâmiut Formation	Eocene to mid-Miocene	Mega-units D and E
Hellefisk Formation	Paleocene to early Eocene	Mega-unit E
Nukik Formation	Paleocene to Eocene	Mega-units D and E
Ikermiut Formation	Paleocene to Eocene	Mega-units D and E
Narssamiut Formation	Paleocene	Mega-unit E
Atanikerluk Formation	Paleocene	Mega-unit E
Eqalulik Formation	Paleocene	Mega-unit E
Vaigat Formation	Paleocene	Mega-unit E
Quikavsak Formation	Paleocene	Mega-unit F
Agatdal Formation	Paleocene	Mega-unit F
Kangilia Formation	Paleocene (mostly Danian)	Mega-unit F-E
Itilli Formation	Late Cretaceous	Mega-unit F
Atane Formation	Early to Late Cretaceous (Albian to Campanian)	Mega-units G and F
Upernivik Naes Formation	Early to Late Cretaceous (Albian to Cenomanian)	Mega-units G and F
Slibestensfjeldet Formation	Early Cretaceous	Mega-unit G
Kome Formation	Early Cretaceous	Mega-unit G

Table 8. Potential hydrocarbon system elements (potential source rock, reservoir and seal units) from the West Greenland margin.

Petroleum system element	Formation name	Description	Possible offshore presence	Onshore occurrences
Potential source rock	Itilli Formation	Possible source of the Itilli and Niaqornaarsuk oil types	Upper Cretaceous mudstone units associated with mega-unit F	Encountered in the Umiivik-1, GANT-1, and GRO-3 wells
Potential source rock	Atane Formation	Possible source of the Kuugannguaq oil	Lower to Upper Cretaceous mudstone units associated with mega-units G-F	Disko Island local to occurrences of Kuugannguaq oil seeps
Potential source rock	Eqalulik Formation	Possible source of the Marraat oil type	Paleocene mudstone units associated with mega-unit E	Encountered in the GRO-3 well
Potential source rock	Kangilia Formation	Possible source of the Marraat oil type	Paleocene mudstone units associated with mega-unit F-E	Encountered in the GRO-3 well
Potential reservoir unit	Itilli Formation	Sandstone packages interbedded with mudstone in the Anariartorfik Member	Interbedded Upper Cretaceous sandstone units associated with mega-unit F	Encountered in the Umiivik-1, GANT-1, and GRO-3 wells
Potential reservoir unit	Atane Formation	Fluvial or shallow-marine delta-front sandstone units	Lower to Upper Cretaceous sandstone units associated with mega-units G-F	Encountered in the Ataata Kuua well
Potential reservoir unit	Kangilia Formation	Local potential in the conglomeritic Annertuneq Member	Paleocene sandstone and conglomerate units associated with mega-unit F-E	Encountered in the GANT-1, GANK-1, and GRO-3 wells
Potential reservoir unit	Agatdal Formation	Channel sandstone units	Paleocene sandstone units associated with mega-unit F	Encountered in the GANE-1 and GRO-3 wells
Potential reservoir unit	Vaigat Formation (Anaanaa Member)	Hyaloclastite deposits	Paleocene volcanic rocks associated with mega-unit E	Encountered in the Gane-1, GANK-1, GANW-1, Marraat-1, and GRO-3 wells
Potential seal	Vaigat Formation	Subaerial lava flows	Paleocene volcanic rocks associated with mega-unit E	Encountered in the Gane-1, GANK-1, GANW-1, Marraat-1, and GRO-3 wells
Potential seal	Maligât Formation	Subaerial lava flows	Paleocene volcanic rocks associated with mega-unit E	Only preserved on Disko Island
Potential seals	Itilli, Kangilia, and Eqalulik formations	Mudstone units of the Itilli, Kangilia, and Eqalulik formations may attain sufficient thicknesses to form seals	Mudstone units associated with mega-units F-E	Encountered in the Umiivik-1, GANT-1, and GRO-3 wells

2016). More than 1.7 km of lower Campanian to lower Eocene shale was encountered in the Ikermiut-1 offshore well, with other wells to the south showing potentially competent seal successions of Campanian (Quelleq-1, Ikermiut-1) and Paleogene (Kangamiut-1) mudstone units (Fig. 5) (Gregersen and Bidstrup, 2008). Seals may also be present as intraformational mudstone, encasing interbedded, localized reservoir units (Schenk, 2011). Subaerial lava flows of the Vaigat and Maligât (only preserved on Disko Island) formations, as well as offshore volcanic sequences associated with mega-unit E (Fig. 5), may also represent potential seal units onshore and offshore West Greenland (Hopper et al., 2016).

Several possible trap types typical of rifted margins, including several four-way closures identified in seismic reflection data, are present in the offshore of western Greenland such as those related to rift blocks, compressional ridges, drapes, faults, and folds (Schenk, 2011; Gregersen et al., 2013; Hopper et al., 2016). There is also the potential for stratigraphic traps, particularly within the interbedded sandstone and mudstone units of the Itilli Formation and its offshore equivalent (mega-unit F).

HYDROCARBON SLICKS AND SEEPS IN THE LABRADOR–BAFFIN SEAWAY

Hydrocarbons generated at depth migrate upward through the subsurface until they are either trapped and begin to accumulate or they escape into the water column at the seafloor. Oil seeping out at the seafloor will ascend through the water column as droplets, or entrained in bubbles, and burst on the sea surface causing the oil to disperse and create an oil slick. These oil slicks may be visible from ships or via aerial surveillance when sea-surface conditions are favourable (i.e. minimal wind and wave action). They are also detectable using Synthetic Aperture Radar (SAR) imaging because oil has a higher surface tension than water, and therefore produces a smoother sea surface than uncontaminated ocean. Radar backscatter is attenuated by surface slicks, resulting in a dark patch in the image where the slick occurs, referred to as a dark target (Jauer and Budkewitsch, 2010; Fustic et al., 2017; Najoui et al., 2018). The study and detection of oil slicks using SAR imaging is of interest to the exploration industry as it may indicate the presence of an active hydrocarbon system in a region; however, caution is encouraged as dark targets in SAR images may also have nonhydrocarbon origins including algae and/or phytoplankton blooms, upwelling, fresh-water inputs, wind shadows, the presence of internal waves, as well as current shear zones (Jauer and Budkewitsch, 2010; Najoui et al., 2018). Additionally, not all detected oil slicks are the result of natural oil seeping from the seafloor. Anthropogenic surface slicks caused by oil leaking from ships, oil rigs, or pipelines can also produce SAR dark targets.

If an oil slick is indeed composed of natural oil, determining its point of origin on the seafloor is a complicated process as oil slicks can be displaced hundreds to thousands of metres from the seafloor seep from which they originated (Najoui et al., 2018). The distance the oil has travelled, its vertical drift, depends on the water depth and the upward velocity of the oil through the water column, which affects the length of time the oil spends in the water column where it can be subjected to lateral marine currents (Najoui et al., 2018). The residence time of the oil is, in turn, impacted by the composition of the oil, its density, and the size of the droplets. The longer the oil takes to traverse the water column, the more distance it can be carried if lateral currents are present. Additionally, once at surface, an oil slick can also be pushed by wind and wave action.

Since trying to determine the presence of an active seep on the seafloor to confirm the existence of a hydrocarbon system is very difficult, other features that may indicate seafloor hydrocarbon seepage are sought. Pockmarks are cone-shaped, metre-scale, seafloor depressions that are identifiable using multibeam sonar (Fader, 1991). They were first associated with hydrocarbon seeps offshore Nova Scotia in 1970 (King and MacLean, 1970) and are thought to form via the migration of fluids (including hydrocarbons) through the sediment. Positive relief structures (e.g. mounds and/or vents) observed using multibeam sonar and seismic data might be the result of hydrocarbons venting at the seafloor (Fader, 1991; Jauer et al., 2014). Acoustic anomalies in seismic data, such as pipes (up to a few hundred metres in diameter) or chimneys (kilometre-scale), may be associated with these positive relief structures and are thought to indicate the migration of fluids in the subsurface (Fader, 1991; Jauer and Budkewitsch, 2010; Jauer et al., 2014; Jatiault et al., 2019). Anomalously high dissolved levels of methane in the water column have also been linked to the possible presence of hydrocarbon seepage (Punshon et al., 2014; Jauer, 2019; Punshon et al., 2019). Fuzzy, white patches of filamentous bacteria, including species of the sulphur-oxidizing *Beggiatoa* genus, have been found in association with seafloor hydrocarbon seeps (Fader, 1991). These bacteria patches have been observed in clusters on the sandy substrate or within pockmarks, and may form weakly cemented crusts. Biological cold-seep communities predominantly composed of filter-feeders, such as cool-water corals and thyasirid bivalves, have been proposed as having an association with seafloor hydrocarbon seepage (Fader, 1991; Jauer and Budkewitsch, 2010; Jauer et al., 2014; Fustic et al., 2017). It is thought that these organisms are either feeding on bacteria that consume hydrocarbons or that they have an endosymbiotic relationship with chemoautotrophic micro-organisms that live in their tissues (Jauer and Budkewitsch, 2010). Unfortunately, none of these features on their own represent a 'smoking gun' in terms of locating seafloor hydrocarbon seeps as each feature may have a nonhydrocarbon origin. Therefore, the majority of research on slicks and seeps is speculative and should be treated as such.

The only proven oil slick–oil seep relationship in the Labrador–Baffin Seaway is the slick offshore of Scott Inlet (Fig. 8), which is formed by oil that has been visually confirmed to be seeping from the seafloor in the Scott Trough (MacLean, 1981; Grant et al., 1986; MacLean et al., 2014). Potential hydrocarbon slicks are pervasive throughout the Labrador–Baffin Seaway (Fig. 8), with three main areas of consistent slick activity being here identified in the study region that may indicate the presence of multiple offshore hydrocarbon systems: offshore Cape Chidley (Labrador margin), the western Davis Strait region, and northern Baffin Bay including Scott Inlet and Buchan Gulf (Fig. 8).

Labrador margin

Potential sea-surface oil slicks were tentatively proposed off the northern coast of Labrador, offshore Cape Chidley based on dark targets in SAR images as well as possible chimney and/or pipe features noted in 2-D seismic data (Fig. 8) (Jauer and Budkewitsch, 2010). Cold-water coral colonies have been documented in the region (Wareham, 2009 as reported in Jauer and Budkewitsch, 2010) and some mound-like features, thought to reflect carbonate buildups associated with these coral colonies, were identified on the seafloor in 2-D seismic data by Jauer and Budkewitsch (2010), tentatively supporting their hypothesis that an active hydrocarbon seep is present in the area (Jauer and Budkewitsch, 2010; Jauer et al., 2014). A 2016 Geological Survey of Canada–led research cruise aboard the *CCGS Amundsen* investigated two locations offshore Cape Chidley and confirmed that the dark targets were legitimate oil slicks and may have been created by an active oil seep in the region; however, multibeam sonar and subbottom profiling failed to find evidence of active hydrocarbon seepage at the seafloor (Fustic et al., 2017; Jauer, 2019). An abundance of thyasirid bivalves were imaged below the oil slick and box core samples were collected; examination is ongoing to determine whether the bivalves contain chemoautotrophic sulphur-oxidizing or methanotrophic bacteria symbionts in their tissues (Fustic et al., 2017). A second location was investigated nearby during the 2016 cruise based on dark targets in SAR images and the tentative identification of a mound structure in seismic data (Jauer and Budkewitsch, 2010; Jauer et al., 2014); however, no indications of an active seep or surface slick were observed at the second site and seafloor investigations determined that the mound, previously thought to be a carbonate buildup related to hydrocarbon seepage, was in fact a glacial structure (Fustic et al., 2017). Methane in the water column was found to be modestly elevated in the region (over 300% above background at 300 m water depth; Punshon et al., 2019), supporting the notion that an active seafloor seep exists offshore northern Labrador. The lack of direct evidence for a seafloor hydrocarbon seep has been attributed by Jauer et al. (2014) to seismic activity along the Labrador margin that may lead to sporadic venting of hydrocarbons, resulting in ephemeral oil slicks that may or may not be observed either on site or via SAR imaging. Alternatively, the lack of a consistent oil slick may be due to possible buildup and episodic releases of hydrocarbons in the area.

Western Davis Strait

Numerous dark targets have been identified using SAR imaging taken in the fall of 2003 and 2004 in the western Davis Strait region, of which only a very small percentage may represent actual oil slicks (Fig. 8) (Budkewitsch et al., 2013). Anomalously high levels of dissolved methane have been measured by Punshon et al. (2014, 2019) in the water column offshore Cape Dyer in a region containing multiple dark targets identified in SAR images (Fig. 8) (Jauer, 2019). A Geological Survey of Canada–led research cruise in 2018 traversed the region east of Cape Dyer in an attempt to confirm the occurrence of active hydrocarbon seepage (Normandeau et al., 2018; Jauer, 2019). Unfortunately, the presence of hydrocarbons could not be visually confirmed either actively seeping from the seafloor or as slicks on the ocean's surface. No mound or vent-like features were detected using multibeam sonar, but some pockmark-like features were noted and preferentially targeted for sampling and imaging (Normandeau et al., 2018). Water-column measurements from samples collected with a CTD (conductivity, temperature, and density) rosette did confirm elevated levels of dissolved methane (1000% above background) (Punshon et al., 2014, 2019); Normandeau et al., 2018; Jauer, 2019; however, it is unknown whether the methane has an abiotic or biotic origin. An underwater camera was used to capture benthic ecosystems, which showed a predominance of filter-feeding organisms. More work is needed to determine whether there is any relationship between the filter feeders and the possibility of seafloor hydrocarbon seepage or the elevated levels of dissolved methane in the water column (Jauer, 2019).

Jauer and Budkewitsch (2010) identified three potential hydrocarbon seep sites in the western Davis Strait region in close proximity to the Hekja O-71, Ralegh N-18, and Gjoa G-37 wells based primarily on the consistent presence of dark targets in SAR images. The authors also attempted to correlate these dark targets to seafloor and subsurface features thought to be associated with hydrocarbon seeps (such as positive relief mounds or chimney and/or pipe anomalies observed in seismic data) (Jauer and Budkewitsch, 2010; Jauer et al., 2019). No direct evidence of hydrocarbons has been observed in these areas either as surface oil slicks or seafloor seeps and as such, these sites remain highly speculative. The first potential oil slick and/or seep site identified by Jauer and Budkewitsch (2010) is located 150 km from the Hekja O-71 well, near the seafloor shelf break, where the persistent dark target appeared to be associated with a prominent seafloor mound structure with an underlying chimney-like seismic signature. The second site described by the authors is located to the south of the first site and correlates with the presence of two positive-relief mound-like structures on the seafloor. The third site is located 60 km east of the Gjoa G-37 well within the volcanically dominated Gjoa eruptive centre. Dark targets occur consistently in this region; however, no additional indicators of possible seafloor seepage have been noted on the seafloor (e.g. positive relief structures) or in the thin sedimentary succession (e.g. chimney and/or pipe-like acoustic signatures) (Jauer and Budkewitsch, 2010). Other mound-like structures and pockmark features have been identified in the area, but have not been directly correlated with dark targets identified in SAR images (Jauer, 2009). Numerous potential sea-surface hydrocarbon slicks identified in Cumberland Sound (Budkewitsch et al., 2013) suggest an active hydrocarbon system exists in the subsurface; however, identifying the source remains problematic (Fig. 8) (Zhang, 2012; Zhang et al., 2014).

Baffin Bay

There are two main areas of consistent oil-slick activity in northern Baffin Bay: Scott Trough and Buchan Trough (Fig. 8). An oil slick offshore Scott Inlet was first reported by a Geological Survey of Canada research cruise in 1976, which observed oil slicks in the water ahead of the boat and globules of low viscosity, biodegraded oil rising to the sea surface and dispersing at an approximate rate of one every 3 to 5 minutes (Loncarevic and Falconer, 1977). This oil slick has since been explored on numerous occasions by the Geological Survey of Canada (e.g. MacLean, 1978; MacLean et al., 1981) and by the Department of Fisheries and Oceans (Levy, 1978, 1979). Oil slicks, some in excess of 40 km in length, have been reported by subsequent expeditions to the region as well as consistently observed in aerial and radar imaging (Loncarevic and Falconer, 1977; Levy, 1978, 1979; Levy and MacLean, 1981; MacLean et al., 1981; Budkewitsch et al., 2013; Decker et al., 2013). Additionally, both gas bubbles and oil droplets have been observed rising through the water column and bursting at surface on several occasions; further evidence for the presence of hydrocarbon seepage at the seafloor (Levy, 1978; Levy and MacLean, 1981).

The Scott Trough is a 200 to 300 km long by 25 to 50 km wide, northwest-southeast feature that cuts across the northeast Baffin Shelf and exhibits relief up to 700 m with more than 6 km of Cretaceous and younger strata present (MacLean et al., 1981; Grant et al., 1986; Moir et al., 2012). The walls of the trough consist of flat-bedded strata, whereas the floor of the trough is, in part, folded and faulted (MacLean, 1978). The truncation of the beds that compose the walls of the trough may contain additional hydrocarbon seep sites (MacLean, 1978; MacLean and Falconer, 1979; MacLean et al., 2014); however, oil slicks are most consistently observed toward the seaward end of Scott Trough, adjoining a basement high beneath the outer south wall of the trough (MacLean and Falconer, 1979; Levy and MacLean, 1981). Hydrocarbon migration is postulated to occur updip through the strata flanking the basement high or along the contact between the flanking strata and the basement high (MacLean and Falconer, 1979).

Figure 8. Possible hydrocarbon slick locations based on SAR image analyses and visual confirmation. Information sourced from Jauer and Budkewitsch (2010), Brent et al. (2013), Budkewitsch et al. (2013), Decker et al. (2013), Jauer et al., (2014), and Atkinson et al. (2017).

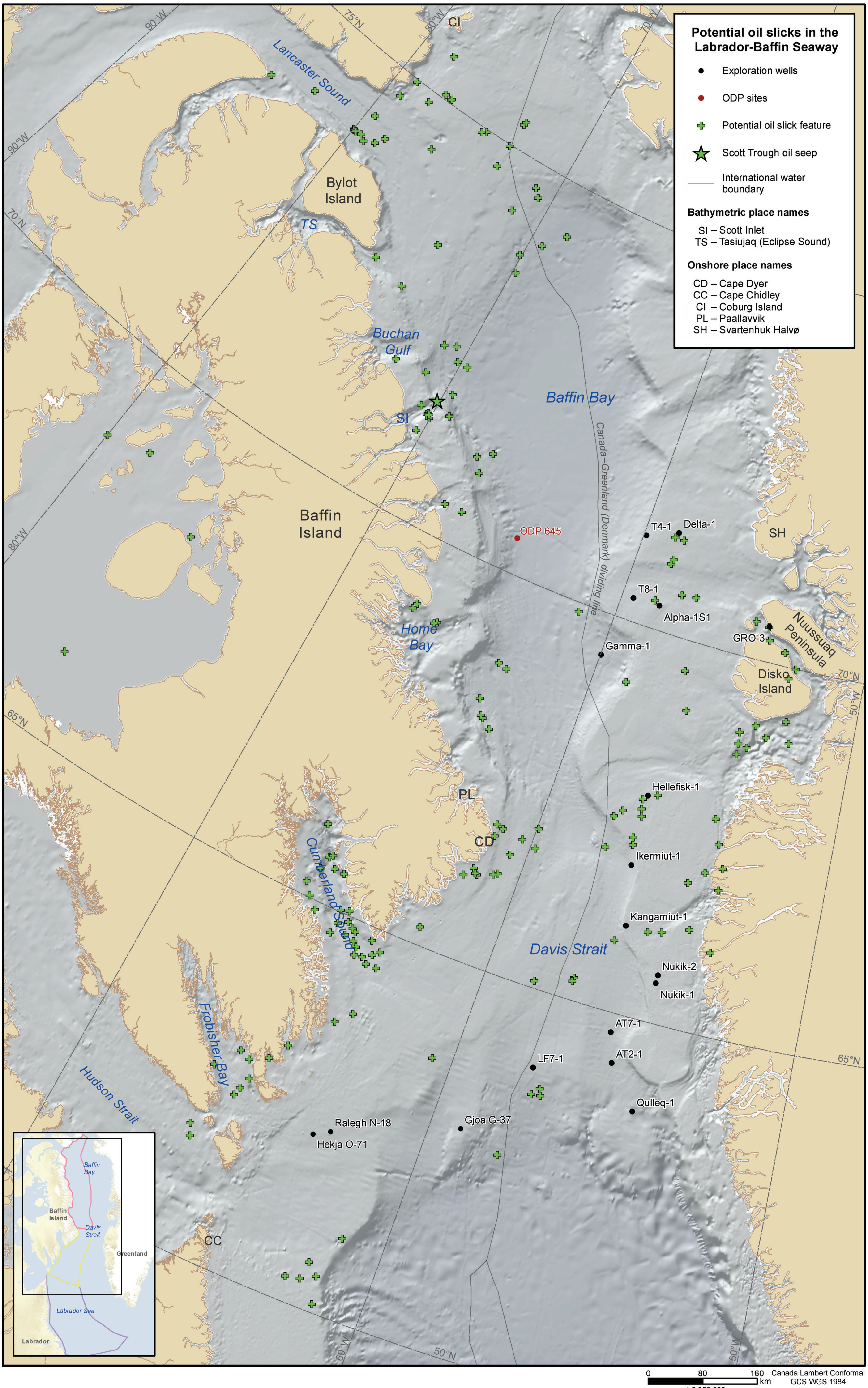
Potential oil slicks in the Labrador-Baffin Seaway
Exploration wells
ODP sites
Potential oil slick feature
Scott Trough oil seep
International water boundary
Bathymetric place names
SI – Scott Inlet
TS – Tasiujaq (Eclipse Sound)
Onshore place names
CD – Cape Dyer
CC – Cape Chidley
CI – Coburg Island
PL – Paallavvik
SH – Svartenhuk Halvø
Lancaster Sound
Bylot Island
TS
Buchan Gulf
SI
Baffin Bay
Baffin Island
Canada–Greenland (Denmark) dividing line
ODP 645
T4-1
Delta-1
SH
T8-1
Alpha-1S1
GRO-3
Nuussuaq Peninsula
Gamma-1
Disko Island
Home Bay
PL
CD
Hellefisk-1
Ikermiut-1
Cumberland Sound
Kangamiut-1
Davis Strait
Nukik-2
Nukik-1
Frobisher Bay
AT7-1
AT2-1
LF7-1
Hudson Strait
Qulleq-1
Ralegh N-18
Gjoa G-37
Hekja O-71
CC
CI
Baffin Bay
Baffin Island
Davis Strait
Greenland
Labrador Sea
Labrador
90°W
75°N
80°W
70°W
70°N
65°N
80°W
60°W
50°N
50°W
0 80 160 km
1:5 250 000
Canada Lambert Conformal
GCS WGS 1984

Submersible investigations of Scott Inlet and the trough were undertaken as part of a Geological Survey of Canada research program in 1981 and 1985 using the Pisces IV submersible vehicle (MacLean, 1981; Grant et al., 1986). No seafloor hydrocarbon seeps were observed in 1981, but numerous white fuzzy patches of bacteria were noted throughout the inlet on the seafloor and were thought to be composed of bacteria that fed on hydrocarbons (MacLean, 1981; Grant et al., 1986) (these patches were later discovered to be confined to the area of the seep). The bacterial patches were sampled during a submersible dive in 1985 along with weakly cemented crusts associated with the patches (Grant et al., 1986). When a sample of the cemented crust was brought to surface, several cubic centimetres of a dark brown, medium viscosity oil seeped from the crust, confirming that the white patches were related to the seepage of hydrocarbons. The 1985 dive also noted a concentration of these bacteria patches and associated crusts within circular, saucer-like depressions similar in scale to pockmarks (approximately 30 m wide by 2–3 m deep), features that have since been identified on several occasions on the floor of Scott Trough using multibeam sonar (Moir et al., 2012; Oakey et al., 2012). Unlike other proposed seep sites offshore Labrador and in the western Davis Strait region, no mound-like features have been detected in the region of the Scott Trough seep. Water column methane saturations in excess of 1600% near the bottom of the Scott Trough measured by Punshon et al. (2019) further imply the presence of an active hydrocarbon seep. Elevated dissolved methane levels (greater than 400%) were also detected in Home Bay south of Scott Inlet by Punshon et al. (2019), who attributed the methane to the offshore Scott Inlet seep and the southward-flowing current. MacLean et al. (2014) described Cretaceous petroliferous strata in Home Bay and proposed that these rocks may also contribute locally to the elevated methane levels.

Palynological analyses of black shale rocks collected near the Scott Trough seep were assigned a Late Cretaceous age (MacLean et al., 2014) (Turonian to Coniacian; Moir et al., 2012). Geochemical analyses of these shale units yielded total organic carbon (TOC) values of 1.5 to 1.9% (average of 1.6%), hydrogen indices of 90 to 149 (average of 111), and T_{max} values between 433°C and 436°C (average of 434.5°C), indicating a marginally mature source rock (Table 4) (MacLean et al., 2014). Organic geochemical analyses of the biomarker assemblage of the biodegraded, mature oil also support an Upper Cretaceous source rock for the oil offshore Scott Inlet with similarities drawn with the Itilli oil type identified onshore West Greenland (Fowler et al., 2005; Blasco, et al., 2010; Moir et al., 2012; Oakey et al., 2012).

The Scott Trough oil slick is the only oil slick from the Labrador–Baffin Seaway to be directly connected to a site of hydrocarbon seepage on the seafloor (Grant et al., 1986). The rate of flow of hydrocarbon seafloor seepage at the Scott Trough locality is such that a slick can be maintained in 25 knot (45 km/h) winds (B. MacLean, pers. comm., 2019). Attempts have been made to calculate the size of the Scott Trough oil slick and the volume of oil required to achieve and sustain the oil slick based on SAR images taken in 2005 and 2010 (Budkewitsch et al., 2013). These estimates are highly speculative as the size of the slick on any given day is influenced by a number of factors (flow rate, wind, sea-surface conditions, water-column currents, etc.) that also affect the ability of SAR imaging to detect the slick. Under optimal wind and surface conditions, a slick with a thickness of 0.1 µm may be detected by SAR imaging (Budkewitsch et al., 2013). The size of the slick offshore Scott Inlet was estimated to be around 6788 ha which would require approximately 90 000 L (using a lower thickness limit of 0.1 µm) to 1 130 000 L of oil (using thicknesses of 15 to 20 µm based on results from SAR slick detection in the North Sea) to create (Budkewitsch et al., 2013). Furthermore, given a possible residence time of 48 h at the sea surface before dispersion of the oil, an estimated flow rate of 200 L/h to over 20 000 L/h would be needed to sustain the oil slick.

The submarine Buchan Trough is located 87 km northwest of Scott Inlet near the northern boundary of the northeast Baffin Shelf (Fig. 8) (MacLean, 1978; MacLean et al., 1981, 2014). The trough has a relief of 600 to 700 m, with a similar geometry and length to the Scott Trough, but a thinner sedimentary cover (MacLean and Falconer, 1979; MacLean et al., 1981). The Buchan Trough became an area of interest with respect to hydrocarbon occurrences in 1977 during a reconnaissance investigation of the oil slick offshore Scott Inlet. A second slick was noted to the north of Scott Inlet and, with south-flowing currents in the area, it was surmised that hydrocarbons must have been seeping from additional areas to the north (Levy, 1978, 1979; MacLean, 1978; Moir et al., 2012). Oil slicks in the vicinity between Buchan Gulf and Scott Inlet have been observed by the majority of research expeditions to the region (MacLean and Falconer, 1979; Levy and MacLean, 1981; Moir et al., 2012). The occasional absence of slicks in this region may be related to adverse sea conditions, changes in wind or water column currents, or episodic seepage. Drill cores collected from the floor of the Buchan Trough by the Geological Survey of Canada consist of Upper Cretaceous marine siltstone and shale (MacLean and Falconer, 1979; Levy and MacLean, 1981; MacLean et al., 2014). The samples collected in the 1970s and 1980s from the Buchan Trough were re-examined more recently, resulting in total organic carbon values of 0.51 to 1.8% (average TOC of 1.05%), hydrogen indices of 72 to 153 (average of 93.5), and T_{max} values ranging from 423°C to 432°C, suggesting that the majority of these rocks are immature (Table 4) (Zhang, 2013; MacLean et al., 2014).

Pockmarks and mound structures have been identified in Lancaster Sound using multibeam sonar, but have not been directly correlated with any specific hydrocarbon slicks (Brent et al., 2013). Possible slicks have also been identified in this region (Fig. 8) from SAR images, but the presence and origin of such features has not yet been confirmed.

SUMMARY

- Despite the evidence for an active hydrocarbon system offshore Labrador, no production licences have been granted.
- A Significant Discovery Licence (SDL) was awarded at Hekja O-71, proving the existence of hydrocarbons in the western Davis Strait region; however, no formal hydrocarbon assessments have been conducted in the western Davis Strait and southeastern Baffin Shelf areas.
- The northeast Baffin Shelf and western Baffin Bay have been untested by wells, but the region is estimated to have a 50% chance of containing at least one oil accumulation in excess of 1 billion barrels of oil (BBO) (Gautier et al., 2011). The highest potential for hydrocarbons in the area is considered to be associated with the Baffin Fan complex.
- The presence of five oil types associated with onshore oil seeps and the identification of at least three sources suggests multiple working hydrocarbon systems for onshore West Greenland.
- Tectonic and magmatic processes have affected the offshore West Greenland margin to varying degrees, resulting in disparate thermal maturities and hydrocarbon potential along the margin. Though no economically viable discoveries of hydrocarbons have been made, oil and gas shows in six of the offshore wells indicate the presence of a working hydrocarbon system.
- Persistent slick activity occurs in three main regions along the Canadian margin of the Labrador–Baffin Seaway (Fig. 8): offshore Cape Chidley (Labrador margin), western Davis Strait, and northeastern Baffin Shelf–western Baffin Bay; only the slick offshore Scott Inlet is linked directly to seafloor hydrocarbon seepage and therefore definitively indicates the existence of hydrocarbon systems along the northeastern Baffin Shelf.

ACKNOWLEDGMENTS

This paper is part of *Geological synthesis of Baffin Island (Nunavut) and the Labrador–Baffin Seaway*, a Geo-mapping for Energy and Minerals (GEM-2) product. Contributions for this paper were provided by C. Jauer (Geological Survey of Canada). Thanks are owed to the Natural Resources Canada (GEM and Marine Conservation Targets programs) and the Geological Survey of Denmark and Greenland (GEUS) initiatives that helped facilitate the research summarized within. Thank you to L. MacLeod for producing the maps; to P. Champagne for doing the layout; to E. Inglis for editing; and to M. Enachescu, B. MacLean, and the Canada-Newfoundland and Labrador Offshore Petroleum Board for reviewing the paper and providing feedback.

This paper is dedicated to the memory of Brian MacLean (September 3, 1929–April 30, 2021). Brian was instrumental in advancing our knowledge of the offshore geology around Baffin Bay, having led several research cruises to Davis Strait, Hudson Strait, and Baffin Bay in the 1970s and 1980s. He published several reports and articles about his findings in the North, and co-authored countless more, many of which are cited in this paper. Brian was a prominent scientist at the Geological Survey of Canada Atlantic office in Dartmouth, Nova Scotia, and despite his emeritus status, he remained actively engaged in ongoing offshore research, and provided mentorship and guidance to the new generation of geologists. We are grateful to have known Brian and to have had him as a reviewer of this paper prior to his passing.

REFERENCES

Atkinson, E.A., Fustic, M., Hanna, M.C., and Lister, C.J., 2017. Qualitative assessment of petroleum potential in Lancaster Sound region, Nunavut; Geological Survey of Canada, Open File 8297, 18 p. https://doi.org/10.4095/305321

Avery, M.P., 2005. Vitrinite reflectance data for Aquitaine et al Hekja 0-71; Geological Survey of Canada, Open File 4842, 16 p. https://doi.org/10.4095/220357

Baudon, C. and Cartwright, J.A., 2008. 3D seismic characterisation of an array of blind normal faults in the Levant Basin, Eastern Mediterranean; Journal of Structural Geology, v. 30, no. 6, p. 746–760. https://doi.org/10.1016/j.jsg.2007.12.008

Bell, J.S. and Campbell, G.R., 1990. Petroleum Resources; Chapter 12 *in* Geology of the Continental Margin of Eastern Canada, (ed.) M. Keen, and G. Williams; Geological Survey of Canada, Geology of Canada, no. 2, p. 677–720 (*also* Geological Society of America, The Geology of North America, v. I-1. https://doi.org/10.4095/132720

Bingham-Koslowski, N., 2018. Descriptions of drill cores and thin sections from lower Paleozoic strata, southeastern Baffin Island shelf, Nunavut; Geological Survey of Canada, Open File 8409, 80 p. https://doi.org/10.4095/308354

Blasco, K.A., Blasco, S.M., Bennett, R., MacLean, B., Rainey, W.A., and Davies, E.H., 2010. Seabed geologic features and processes and their relationship with fluid seeps and the benthic environment; Geological Survey of Canada, Open File 6438, 58 p. https://doi.org/10.4095/287316

Bojesen-Koefoed, J.A., 2011. West Greenland petroleum systems: An overview of source rocks and oil seepages and their implications for offshore petroleum exploration; Danmarks og Grønlands Geologiske Undersøgelse Rapport, 2011/42, 49 p.

Bojesen-Koefoed, J.A., Christiansen, F.G., Nytoft, H.P., and Pedersen, A.K., 1997. Seep data from onshore West Greenland; Danmarks og Grønlands Geologiske Undersøgelse Rapport, 1997/34, 7 p.

Bojesen-Koefoed, J.A., Christiansen, F.G., Nytoft, H.P., and Pedersen, A.K., 1999. Oil seepage onshore West Greenland: evidence of multiple source rocks and oil mixing; *in* Petroleum Geology of Northwest Europe: Proceedings of the 5th Conference, (ed.) A.J. Fleet and S.A.R. Boldy; Geological Society, London, p. 305–314.

Bojesen-Koefoed, J.A., Nytoft, H.P., and Christiansen, F.G., 2004. Age of oils in West Greenland: was there a Mesozoic seaway between Greenland and Canada; Geological Survey of Denmark and Greenland Bulletin, v. 4, p. 49–52.

Bojesen-Koefoed, J.A., Bidstrup, T., Christiansen, F.G., Dalhoff, F., Gregersen, U., Nytoft, H.P., Nøhr-Hansen, H., Pedersen, A.K., and Sønderholm, M., 2007. Petroleum seepages at Asuk, Disko, West Greenland: implications for regional petroleum exploration; Journal of Petroleum Geology, v. 30, p. 219–236. https://doi.org/10.1111/j.1747-5457.2007.00219.x

Brent, T.A., Chen, Z., Currie, L.D., and Osadetz, K., 2013. Assessment of the conventional petroleum resource potential of Mesozoic and younger structural plays within the proposed National Marine Conservation area, Lancaster Sound, Nunavut; Geological Survey of Canada, Open File 6954, 54 p. https://doi.org/10.4095/289615

Budkewitsch, P., Pavlic, G., Oakey, G., Jauer, C., and Decker, V., 2013. Reconnaissance mapping of suspect oil seep occurrences in Baffin Bay and Davis Strait using satellite radar: preliminary results; Geological Survey of Canada, Open File 7068. https://doi.org/10.4095/292280

Canada-Newfoundland and Labrador Offshore Petroleum Board, 2003. Properties of gas bearing reservoirs; Canada-Newfoundland and Labrador Offshore Petroleum Board, St. John's, Newfoundland and Labrador, p. 1. <https://www.cnlopb.ca/wp-content/uploads/gas_prop.pdf> [accessed June 26, 2019]

Canada-Newfoundland and Labrador Offshore Petroleum Board, 2007. C-NLOPB schedule of wells: St. John's, Newfoundland. <http://www.cnlopb.ca/wells/> [accessed August 20, 2018]

Canada-Newfoundland and Labrador Offshore Petroleum Board, 2009. Canada-Newfoundland and Labrador Offshore Petroleum Board Annual Report 2008–2009; Canada-Newfoundland and Labrador Offshore Petroleum Board, St. John's, Newfoundland and Labrador, 60 p.

Canada-Newfoundland and Labrador Offshore Petroleum Board, 2019a. Land issuance - Active Call for Bids; Canada-Newfoundland and Labrador Offshore Petroleum Board, St. John's, Newfoundland and Labrador. <www.cnlopb.ca/exploration/issuance/#bids-active> [accessed May 16, 2019]

Canada-Newfoundland and Labrador Offshore Petroleum Board, 2019b. Land rights issuance process; Canada-Newfoundland and Labrador Offshore Petroleum Board, St. John's, Newfoundland and Labrador. <https://www.cnlopb.ca/exploration/issuanceprocess/> [accessed June 3, 2019]

Canada-Newfoundland and Labrador Offshore Petroleum Board, 2019c. Licence information tables; Canada-Newfoundland and Labrador Offshore Petroleum Board, St. John's, Newfoundland and Labrador. <www.cnlopb.ca/exploration/tables> [accessed June 3, 2019]

Canada-Newfoundland and Labrador Offshore Petroleum Board, 2019d. Mandate; Canada-Newfoundland and Labrador Offshore Petroleum Board, St. John's, Newfoundland and Labrador. <https://www.cnlopb.ca/about/mandate/> [accessed April 24, 2019]

Canada-Newfoundland and Labrador Offshore Petroleum Board, 2019e. Mapping information and shapefiles; Canada-Newfoundland and Labrador Offshore Petroleum Board, St. John's, Newfoundland and Labrador. <https://www.cnlopb.ca/information/shapefiles/> [accessed July 26, 2019]

Canada-Newfoundland and Labrador Offshore Petroleum Board, 2019f. News releases 2019; Canada-Newfoundland and Labrador Offshore Petroleum Board, St. John's, Newfoundland and Labrador. <www.cnlopb.ca/news/nr20190205> [accessed May 16, 2019]

Canada-Newfoundland and Labrador Offshore Petroleum Board, 2019g. Petroleum reserves and resources Newfoundland offshore area; Canada-Newfoundland and Labrador Offshore Petroleum Board, St. John's, Newfoundland and Labrador, p. 1. <https://www.cnlopb.ca/wp-content/uploads/disc_rr.pdf> [accessed June 26, 2019]

Canada-Newfoundland and Labrador Offshore Petroleum Board, 2021. News releases 2021: C-NLOPB announces results of Call for Bids in the Labrador South region; Canada–Newfoundland and Labrador Offshore Petroleum Board, St. John's, Newfoundland and Labrador, p. 1. <https://www.cnlopb.ca/news/c-nlopb-announces-results-of-call-for-bids-in-the-labrador-south-region/> [accessed May 5, 2022]

Canterra Energy Ltd., 1982. Canterra et al Ralegh N-18; Well history report; <https://basin.gdr.nrcan.gc.ca/index_e.php> [accessed May 15, 2019]

Carey, J.S., McCartney, T., Hanna, M.C., Lister, C., and Keng, L.E., 2020. Qualitative petroleum resource assessment of the Labrador margin; Geological Survey of Canada, Open File 8535, 104 p. https://doi.org/10.4095/326017

Charpentier, R.R., Klett, T.R., and Attanasi, E.D., 2008. Database for assessment unit-scale analogs (exclusive of the United States); U.S. Geological Survey, Open-File Report 2007-1404, 61 p. https://doi.org/10.3133/ofr20071404

Christiansen, F.G., Boesen, A., Dalhoff, F., Pedersen, A.K., Pedersen, G.K., Riisager, P., and Zinck-Jorgensen, K., 1996. Petroleum geological activities onshore West Greenland in 1996, and drilling of a deep exploration well; Geology of Greenland Survey Bulletin, v. 176, p. 17–23.

Clowes, R.M., 2010. Initiation, development, and benefits of Lithoprobe — shaping the direction of Earth science research in Canada and beyond; Canadian Journal of Earth Sciences, v. 47, no. 4, p. 291–314. https://doi.org/10.1139/E09-074.

Creaney, S. and Sullivan, M.A., 2011. The genetic evolution of Arctic North American and Greenland and implications for petroleum systems; Chapter 30 *in* Arctic Petroleum Geology, (ed.) M. Spencer, A.F. Embry, D.L. Gautier, A.V. Stoupakova, and K. Sørensen; Geological Society of London Memoirs, v. 35, p. 451–462.

Dalhoff, F., Larsen, L.M., Ineson, J.R., Stouge, S., Bojesen-Koefoed, J.A., Lassen, S., Kuijpers, A., Rasmussen, J.A., and Nohr-Hansen, H., 2006. Continental crust in the Davis Strait: new evidence from seabed sampling; Geological Survey of Denmark and Greenland Bulletin, v. 10, p. 33–36.

Dam, G., Nøhr-Hansen, H., Christiansen, F.G., Bojesen-Koefoed, J.A., and Laier, T., 1998. The oldest marine Cretaceous sediments in west Greenland (Umiivik-1 borehole) — record of the Cenomanian–Turonian Anoxic Event; Geology of Greenland Survey Bulletin, v. 180, p. 128–137.

Dam, G., Pedersen, G.K., Sønderholm, M., Midtgaard, H., Larsen, L.M., Nøhr-Hansen, H., and Pedersen, A.K., 2009. Lithostratigraphy of the Cretaceous-Paleocene Nuussuaq Group, Nuussuaq Basin, West Greenland; Geological Survey of Denmark and Greenland Bulletin, v. 19, 171 p.

Dawes, P.R. and Christie, R.L., 1991. Geomorphic regions; Chapter 3 *in* Geology of the Innuitian Orogen and Arctic Platform of Canada and Greenland, (ed.) H.P. Trettin; Geological Survey of Canada, Geology of Canada, no. 3, p. 29–56; (*also* Geological Society of America, The Geology of North America, v. E). https://doi.org/10.4095/133962

Decker, V., Budkewitsch, P., and Tang, W., 2013. Database of suspect oil seeps in the marine environment of Baffin Bay and Davis Strait, Nunavut, identified from a survey of RADARSAT-2 data; Geological Survey of Canada, Open File 7404, 12 p. https://doi.org/10.4095/292761

Dickie, K., Keen, C.E., Williams, G.L., and Dehler, S.A., 2011. Tectonostratigraphic evolution of the Labrador margin, Atlantic Canada; Marine and Petroleum Geology, v. 28, no. 9, p. 1663–1675. https://doi.org/10.1016/j.marpetgeo.2011.05.009

Embry, A., 2011. Petroleum prospectivity of the Triassic-Jurassic succession of Sverdrup Basin, Canadian Arctic Archipelago; Chapter 36 *in* Arctic Petroleum Geology, (ed.) M. Spencer, A.F. Embry, D.L. Gautier, A.V. Stoupakova, and K. Sørensen; Geological Society of London Memoirs, p. 545–558. https://doi.org/10.1144/M35.36

Fader, G.B.J., 1991. Gas-related sedimentary features from the eastern Canadian continental shelf; Continental Shelf Research, v. 11, no. 8–10, p. 1123–1153. https://doi.org/10.1016/0278-4343(91)90094-M

Fowler, M.G., Stasiuk, L.D., and Avery, M., 2005. Potential petroleum systems in the Labrador and Baffin Shelf areas, offshore eastern Canada; *in* Geological Association of Canada–Mineralogical Association of Canada–Canadian Society of Petroleum Geologists–Canadian Society of Soil Science Halifax 2005, Abstracts, Halifax, Nova Scotia, May 2005, Geological Association of Canada, Contribution Series 2004330. (abstract)

Fowler, M.G., Obermajer, M., and Jiang, C., 2019. Rock-Eval/TOC data for twelve wells from the Labrador Shelf, Eastern Canada, offshore Newfoundland and Labrador; Geological Survey of Canada, Open File 8570, 12 p. https://doi.org/10.4095/314722

Fraser, A.J. and Gawthorpe, R.L., 2003. Play fairway analysis; *in* An Atlas of Carboniferous Basin Evolution in Northern England; Geological Society of London Memoirs, v. 28, p. 51–69.

Fustic, M., Neves, B., Dove, R., Mort, A., Fowler, M., Chakraborty, A., Ellefson, E., Herder, E., Wareham, V., Dufour, S., and Edinger, E., 2017. Saglek Basin macro- and micro-hydrocarbon seeps–new evidence, reinterpretation, and emerging exploration tools; GeoConvention, annual joint Canadian Society of Petroleum Geologists–Canadian Society of Exploration Geophysicists–Canadian Well Logging Society convention, May 15–19, 2017, Calgary, Alberta, 5 p. (abstract).

Fustic, M., Hanna, M.C., Lister, C.J., King, H.M., Atkinson, E.A., and Dewing, K.E., 2018. Qualitative petroleum resource assessment of Peel Sound, Bellot Strait, Gulf of Boothia, Fury and Hecla Strait, and Foxe Basin, Nunavut; Geological Survey of Canada, Open File 8439, 29 p. https://doi.org/10.4095/308495

Gautier, D.L., Bird, K.J., Charpentier, R.R., Grantz, A., Houseknecht, D.W., Klett, T.R., Moore, T.E., Pitman, J.K., Schenk, C.J., Schuenemeyer, J.H., Sørensen, K., Tennyson, M.E., Valin, Z.C., and Wandrey, C.J., 2011. Oil and gas resource potential north of the Arctic Circle; Chapter 9 *in* Arctic Petroleum Geology, (ed.) M. Spencer, A.F. Embry, D.L. Gautier, A.V. Stoupakova, and K. Sørensen; Geological Society of London Memoirs, v. 35, p. 151–161. https://doi.org/10.1144/M35.9

Government of Canada, 2018. Arctic offshore oil and gas; Government of Canada, Ottawa, Ontario. <www.rcaanc-cirnac.gc.ca/eng/1535571547022/1538586415269> [accessed May 23, 2019]

Government of Nunavut, 2018. Nunavut Petroleum Sedimentary Basins. Government of Nunavut Department of Economic Development and Transportation, 2 p. <https://gov.nu.ca/sites/default/files/nunavut_petroLEUM_basins_geology_map.pdf> [accessed May 17, 2019]

Grant, A.C., Levy, E.M., Lee, K., and Moffat, J.D., 1986. Pisces IV research submersible finds oil on Baffin Shelf; *in* Current Research, Part A; Geological Survey of Canada, Paper 86-1A, p. 65–69. https://doi.org/10.4095/120351

Gregersen, U. and Bidstrup, T., 2008. Structures and hydrocarbon prospectivity in the northern Davis Strait area, offshore West Greenland; Petroleum Geoscience, v. 14, p. 151–166. https://doi.org/10.1144/1354-079308-752

Gregersen, U., Bidstrup, T., Bojesen-Koefoed, J.A., Christiansen, F.G., Dalhoff, F., and Sønderholm, M., 2007. Petroleum systems and structures offshore central West Greenland: implications for hydrocarbon prospectivity; Geological Survey of Denmark and Greenland Bulletin, v. 13, p. 25–28.

Gregersen, U., Hopper, J.R., and Knutz, P.C., 2013. Basin seismic stratigraphy and aspects of prospectivity in the NE Baffin Bay, Northwest Greenland; Marine and Petroleum Geology, v. 46, p. 1–18. https://doi.org/10.1016/j.marpetgeo.2013.05.013

Gregersen, U., Andersen, M.S., Nøhr-Hansen, H., Sheldon, E., Kokfelt, T.F., Olivarius, M., Knudsen, C., Jakobsen, K.G., and Adolfssen, J.S., 2018. New subsurface mapping offshore southern West Greenland using geophysical and geological data; Geological Survey of Denmark and Greenland Bulletin, v. 41, p. 57–62. https://doi.org/10.34194/geusb.v41.4342

Gregersen, U., Knutz, P.C., Nøhr-Hansen, H., Sheldon, E., and Hopper, J.R., 2019. Tectonostratigraphy and evolution of the West Greenland continental margin; Bulletin of the Geological Society of Denmark, v. 67, p. 1–21.

Hanna, M.C., Lister, C.J., Kublik, K., King, H.M., Kung, L.E., McCarthy, W.M., McDannell, K.T., and Jassim, Y., 2018. Qualitative petroleum resource assessment of western Hudson Bay, Foxe Channel, and Repulse Bay, Manitoba, Nunavut, Ontario, and Quebec; Geological Survey of Canada, Open File 8434, 31 p. https://doi.org/10.4095/311260

Hanna, M.C., King, H.M., and Lister, C.J., 2019. Qualitative petroleum resource assessment of eastern Hudson Bay and James Bay, Nunavut, Ontario, and Quebec; Geological Survey of Canada, Open File 8344 (ed. revised), 21 p. https://doi.org/10.4095/313398

Harrison, J.C., Brent, T.A., and Oakey, G.N., 2011. Baffin Fan and its inverted rift system of Arctic eastern Canada: stratigraphy, tectonics and petroleum resource potential; Chapter 40 *in* Arctic Petroleum Geology, (ed.) M. Spencer, A.F. Embry, D.L. Gautier, A.V. Stoupakova, and K. Sørensen; Geological Society of London Memoirs, v. 35, p. 595–626. https://doi.org/10.1144/M35.40

Hopper, J.R., Pedersen, G.K., Sørensen, E.V., Guarnieri, P., Schovsbo, N.H., Kokfelt, T.F., Hjuler, M.L., and Weng, W.L., 2016. Disko-Nuussuaq: structural mapping and GIS compilation to better define petroleum exploration targets on Disko and Nuussuaq; Danmarks og Grønlands Geologiske Undersøgelse Rapport, 2016/47, 119 p.

Jatiault, R., Loncke, L., Dhont, D., Dubucq, D., and Imbert, P., 2019. Geophysical characterisation of active thermogenic oil seeps in the salt province of the lower Congo basin. Part II: a regional validation; Marine and Petroleum Geology, v. 103, p. 773–791. https://doi.org/10.1016/j.marpetgeo.2019.02.002

Jauer, C.D., 2009. Hekja O-71, a major stranded gas discovery offshore Baffin Island with seismic examples of probable gas vents; Geological Survey of Canada, Open File 6432, 1 p. https://doi.org/10.4095/248252

Jauer, C.D., 2019. *CCGS Hudson* Expedition 2018042 GEM-2 Baffin marine survey activity report with preliminary results; Geological Survey of Canada, Open File 8542, 20 p.

Jauer, C.D. and Budkewitsch, P., 2010. Old marine seismic and new satellite radar data: petroleum exploration of north west Labrador Sea, Canada; Marine and Petroleum Geology, v. 27, p. 1379–1394. https://doi.org/10.1016/j.marpetgeo.2010.03.003

Jauer, C.D., Oakey, G.N., Williams, G., and Wielens, J.B.W.H., 2014. Saglek Basin in the Labrador Sea, east coast Canada; stratigraphy, structure and petroleum systems; Bulletin of Canadian Petroleum Geology; Baffin Bay Special Issue, v. 62, no. 4, p. 232–260.

Jauer, C.D., Oakey, G.N., and Li, Q., 2019. Western Davis Strait, a volcanic transform margin with petroliferous features; Marine and Petroleum Geology, v. 107, May, p. 59–80. https://doi.org/10.1016/j.marpetgeo.2019.05.004

King, L.H. and MacLean, B., 1970. Pockmarks on the Scotian shelf; Geological Society of America Bulletin, v. 81, no. 10, p. 3141–3148. https://doi.org/10.1130/0016-7606(1970)81[3141:POTSS]2.0.CO%3b2

Klose, G.W., Maltere, E., McMillian, N., and Zinkan, C.G., 1982. Petroleum exploration offshore southern Baffin Island, northern Labrador Sea, Canada; *in* Arctic Geology and Geophysics; Canadian Society of Petroleum Geologists, Memoir 8, p. 233–244.

Knutsen, S.M., Arendt, N.P., Runge, M.K., Stilling, J., and Brandt, M.P., 2012. Structural provinces offshore West Greenland and key geological variations influencing play assessment; First Break, v. 30, p. 43–55. https://doi.org/10.3997/1365-2397.2012021

Levy, E.M., 1978. Visual and chemical evidence for a natural seep at Scott Inlet, Baffin Island, District of Franklin; *in* Current Research, Part B; Geological Survey of Canada, Paper 78-1B, p. 21–26. https://doi.org/10.4095/103569

Levy, E.M., 1979. Further chemical evidence for natural seepage on the Baffin Island Shelf; *in* Current Research, Part B; Geological Survey of Canada, Paper 79-1B, p. 379–383. https://doi.org/10.4095/105445

Levy, E.M. and MacLean, B., 1981. Natural hydrocarbon seepage at Scott Inlet and Buchan Gulf, Baffin Island Shelf: 1980 update; *in* Current Research, Part A; Geological Survey of Canada, Paper 81-1A, p. 401–403. https://doi.org/10.4095/109550

Lister, C.J., King, H.M., Atkinson, E.A., Kung, L.E., and Nairn, R., 2018. A probability-based method to generate qualitative petroleum potential maps: adapted for and illustrated using ArcGIS; Geological Survey of Canada, Open File 8404, 50 p. https://doi.org/10.4095/311225

Loncarevic, B.D. and Falconer, R.K., 1977. An oil slick occurrence off Baffin Island; *in* Report of Activities, Part A; Geological Survey of Canada, Paper 77-1A, p. 523–524. https://doi.org/10.4095/102743

MacLean, B., 1978. Marine Geological-geophysical investigations in 1977 of the Scott Inlet and Cape Dyer–Frobisher Bay areas of the Baffin Island continental shelf; *in* Current Research, Part B; Geological Survey of Canada, Paper 78-1B, p. 13–20. https://doi.org/10.4095/103568

MacLean, B., 1981. Investigations of Baffin Island Shelf from surface ship and research submersible in 1981; *in* Current Research, Part A; Geological Survey of Canada, Paper 82-1A, p. 445–447. https://doi.org/10.4095/111342

MacLean, B. and Falconer, R.K.H., 1979. Geological/geophysical studies in Baffin Bay and Scott Inlet-Buchan Gulf and Cape Dyer-Cumberland Sound areas of the Baffin Island Shelf; *in* Current Research, Part B; Geological Survey of Canada, Paper 79-1B, p. 231–244. https://doi.org/10.4095/105432

MacLean, B. and Srivastava, S.P., 1981. Petroliferous core from a diaper east of Cumberland Sound, Baffin Island; *in* Current Research, Part A; Geological Survey of Canada, Paper 81-1A, p. 399–400. https://doi.org/10.4095/109551

MacLean, B., Falconer, R.K.H., and Levy, E.M., 1981. Geological, geophysical and chemical evidence for natural seepage of petroleum off the Northeast coast of Baffin Island; Bulletin of Canadian Petroleum Geology, v. 29, no. 1, p. 75–95.

MacLean, B., Srivastava, S.P., and Haworth, R.T., 1982. Bedrock structures off Cumberland Sound, Baffin Island Shelf: core sample and geophysical data; Arctic Geology and Geophysics: Proceedings of the Third International Symposium on Arctic Geology, Memoir 8, p. 279–295.

MacLean, B., Williams, G., and Zhang, S., 2014. New insights into the stratigraphy and petroleum potential of the Baffin Shelf's Cretaceous rocks; Bulletin of Canadian Petroleum Geology, v. 62, no. 4, p. 289–310. https://doi.org/10.2113/gscpgbull.62.4.289

McWhae, J., Elie, R., Laughton, K., and Gunther, P., 1980. Stratigraphy and petroleum prospects of the Labrador Shelf; Bulletin of Canadian Petroleum Geology, v. 28, no. 4, p. 460–488.

Moir, P.N., Oakey, G.N., Bennett, R., Dickie, K., Williams, G., Budkewitsch, P., Decker, V., Fowler, M.G., Obermajer, M., and Haggart, J.W., 2012. Natural oil seeps on the Baffin Shelf, Nunavut, Canada: geology and geochemistry of the Scott Inlet seep; Geological Survey of Canada, Scientific Presentation 12, 1 p. https://doi.org/10.4095/291575

Najoui, Z., Riazanoff, S., Deffontaines, B., and Xavier, J.-P., 2018. Estimated location of the seafloor sources of marine natural oil seeps from sea surface outbreaks: A new "source path procedure" applied to the northern Gulf of Mexico; Marine and Petroleum Geology, v. 91, p. 190–201. https://doi.org/10.1016/j.marpetgeo.2017.12.035

Nantais, P., 1984. Regional hydrocarbon potential of the Labrador Shelf; Geological Survey of Canada, Open File 1197, 50 p. https://doi.org/10.4095/130015

Nassichuk, W.W., 1983. Petroleum potential in Arctic North America and Greenland; Cold Regions Science and Technology, v. 7, p. 51–88. https://doi.org/10.1016/0165-232X(83)90062-9

Nemčok, M., Rybár, S., Sinha, S.T., Hermeston, S.A., and Ledvényiová, L., 2016. Transform margins: development, controls and petroleum systems – an introduction; Geological Society of London, Special Publications, v. 431, no. 1, p. 1–38. https://doi.org/10.1144/SP431.15

Nøhr-Hansen, H., 2003. Dinoflagellate cyst stratigraphy of the Palaeogene strata from the Hellefisk-1, Ikermiut-1, Kangâmiut-1, Nukik-1, Nukik-2 and Qulleq-1 wells, offshore West Greenland; Marine and Petroleum Geology, v. 20, p. 987–1016. https://doi.org/10.1016/S0264-8172(02)00116-2

Nøhr-Hansen, H., Williams, G., and Fensome, R., 2016. Biostratigraphic correlation of the western and eastern margins of the Labrador–Baffin Seaway and implications for the regional geology; Geological Survey of Denmark and Greenland Bulletin, v. 37, 77 p.

Nøhr-Hansen, H., Pedersen, G.K., Knutz, P., Bojesen-Koefoed, J., Sliwinska, K.K., and Hovikoski, J., 2018. Potential Cretaceous source-rocks from the north-east Baffin Bay, West Greenland; American Association of Petroleum Geologists European Regional Conference, Abstract Volume, p. 29 (abstract).

Normandeau, A., Hayward, S.E., Jarrett, K.A., Jauer, C.D., MacKillop, K., MacIntyre, M., Patton, E., Robertson, A., Thiessen, R., White, M., Faulkner, M., and Wohlgeschaffen, G., 2018. *CCGS Hudson* expedition 2018042: marine geohazards and natural seeps off southeastern Baffin Island, Nunavut; Geological Survey of Canada, Open File 8488, 90 p. https://doi.org/10.4095/313056

Oakey, G.N. and Chalmers, J.A., 2012. A new model for the Paleogene motion of Greenland relative to North America: plate reconstructions of the Davis Strait and Nares Strait regions between Canada and Greenland; Journal of Geophysical Research, Solid Earth, v. 117, no. 10, p. 1–28. https://doi.org/10.1029/2011JB008942

Oakey, G.N., Moir, P.N., Brent, T., Dickie, K., Jauer, C., Bennett, R., Williams, G., MacLean, B., Budkewitsch, P., Haggart, J., and Currie, L., 2012. The Scott Inlet–Buchan Gulf oil seeps: actively venting petroleum systems on the northern Baffin Margin offshore Nunavut, Canada; Proceedings of the Canadian Society of Petroleum Geologists, Calgary, Alberta, May 14–18, 2012; GeoConvention, Abstracts, 3 p.

Pedersen, G.K., Andersen, L.A., Lundsteen, E.B., Petersen, H.I., Bojesen-Koefoed, J.A., and Nytoft, H.P., 2006. Depositional environments, organic maturity and petroleum potential of the Cretaceous coal-bearing Atane Formation at Qullissat, Nuussuaq Basin, West Greenland; Journal of Petroleum Geology, v. 29, p. 3–26. https://doi.org/10.1111/j.1747-5457.2006.00003.x

Punshon, S., Azetsu-Scott, K., and Lee, C.M., 2014. On the distribution of dissolved methane in Davis Strait, North Atlantic Ocean; Marine Chemistry, v. 161, p. 20–25. https://doi.org/10.1016/j.marchem.2014.02.004

Punshon, S., Azetsu-Scott, K., Sherwood, W., and Edinger, E.N., 2019. Bottom water methane sources along the high latitude eastern Canadian continental shelf and their effects on the marine carbonate system; Marine Chemistry, v. 212, p. 83–95. https://doi.org/10.1016/j.marchem.2019.04.004

Rolle, F., 1985. Late Cretaceous–Tertiary sediments offshore central West Greenland: lithostratigraphy, sedimentary evolution, and petroleum potential; Canadian Journal of Earth Sciences, v. 22, p. 1001–1019. https://doi.org/10.1139/e85-105

Schenk, C.J., 2011. Geology and petroleum potential of the West Greenland – East Canada Province; *in* Arctic Petroleum Geology, (ed.) M. Spencer, A.F. Embry, D.L. Gautier, A.V. Stoupakova, and K. Sørensen; Geological Society, London, Memoir 35, p. 627–645. https://doi.org/10.1144/M35.41

Schenk, C.J., 2017. Geology and assessment of undiscovered oil and gas resources of the West Greenland-East Canada Province, 2008; US Geological Survey, Professional Paper, 42 p. https://doi.org/10.3133/pp1824J

Schenk, C.J., Bird, K.J., Brown, P.J., Charpentier, R.R., Gautier, D.L., Houseknecht, D.W., Klett, T.R., Pawlewicz, M.J., Shah, A.K., and Tennyson, M.E., 2008. Assessment of undiscovered oil and gas resources of the West Greenland-East Canada province; U.S. Geological Survey, Fact Sheet 3014, no. 2, 1 p.

Smith, D.R., Gowan, R.J., and McComb, M., 1989. Geology and resource potential of a proposed national marine park, Lancaster Sound, Northwest Territories; Geological Survey of Canada, Open File 2022, 60 p. https://doi.org/10.4095/130762

Sønderholm, M. and Dam, G., 1998. Reservoir characterization of western Nuussuaq, central West Greenland; Danmarks og Grønlands Geologiske Undersøgelse Rapport, v. 1998, no. 6, p. 1–36.

Sønderholm, M., Nøhr-Hansen, H., Bojesen-Koefoed, J.A., Dalhoff, F., and Rasmussen, J.A., 2003. Regional correlation of Mesozoic - Palaeogene sequences across the Greenland-Canada boundary; Danmarks og Grønlands Geologiske Undersøgelse Rapport, 2003/25, 175 p.

Sørensen, A.B., 2006. Stratigraphy, structure and petroleum potential of the Lady Franklin and Maniitsoq Basins, offshore southern West Greenland; Petroleum Geoscience, v. 12, no. 3, p. 221–234. https://doi.org/10.1144/1354-079305-692.

Sørensen, E.V., Hopper, J.R., Pedersen, G.K., Nøhr-Hansen, H., Guarnieri, P., Pedersen, A.K., and Christiansen, F.G., 2017. Inversion structures as potential petroleum exploration targets on Nuussuaq and northern Disko, onshore West Greenland; Geological Survey of Denmark and Greenland Bulletin, v. 38, p. 45–48.

Spencer, A.M., Embry, A.F., Gautier, D.L., Stoupakova, A.V., and Sørensen, K., 2011. An overview of the petroleum geology of the Arctic; Chapter 1 *in* Arctic Petroleum Geology, (ed.) M. Spencer, A.F. Embry, D.L. Gautier, A.V. Stoupakova, and K. Sørensen; Geological Society of London Memoirs, v. 35, p. 1–15.

Wareham, V.E., 2009. Updates on deep-sea coral distributions in the Newfoundland Labrador and Arctic regions, Northwest Atlantic; *in* The Ecology of Deep-Seas Corals of Newfoundland and Labrador Waters: Biogeography, Life History, Biogeochemistry and Relation to Fishes, (ed.) K. Gilkinson and E. Edinger; Canadian Technical Report of Fisheries and Aquatic Sciences, no. 2830, p. 4–22.

Whittaker, J., Goncharov, A., Williams, S., Muller, R.D., and Lietchenkov, G., 2013. Global sediment thickness data set updated for the Australian-Antarctic Southern Ocean; Geochemistry Geophysics Geosystems, v. 14, no. 8, p. 3297–3305. https://doi.org/10.1002/ggge.20181

Wielens, H.J.B.W. and Jauer, C.D., 2009. Saglek Basin: at least ONE petroleum system in an ultra-frontier basin with great potential; *in* Frontiers + Innovation; Canadian Society of Petroleum Geology–Canadian Society of Exploration Geophysicists–Canadian Well Logging Society Convention, Calgary, Alberta, May 4–8, 2009, p. 53–56.

Wilson, R., Klint, K., van Gool, J., McCaffrey, K., Holdsworth, R., and Chalmers, J., 2006. Faults and fractures in central West Greenland: onshore expression of continental break-up and sea-floor spreading in the Labrador–Baffin Bay Sea; Geological Survey of Denmark and Greenland Bulletin, v. 11, p. 185–204.

Zhang, S., 2012. Ordovician stratigraphy and oil shale, southern Baffin Island, Nunavut – preliminary field and post field data; Geological Survey of Canada, Open File 7199, 23 p. https://doi.org/10.4095/291521

Zhang, S., 2013. Rock Eval6 and vitrinite reflectance data from Baffin Island Shelf and Hudson Strait; Geological Survey of Canada, Open File 7341, 32 p. https://doi.org/10.4095/292376

Zhang, S., Creaser, R.A., and Pell, J., 2014. Discovery of organic-rich black shale xenolith from kimberlite on the hall peninsula, Nunavut and its implication for petroleum potential in Cumberland sound; Bulletin of Canadian Petroleum Geology, v. 62, no. 3, p. 125–131.